# SALINE LAKE ICHNOLOGY:

COMPOSITION AND DISTRIBUTION OF CENOZOIC TRACES IN THE SALINE, ALKALINE LAKES OF THE KENYA RIFT VALLEY AND EOCENE GREEN RIVER FORMATION, U.S.A.

A Thesis Submitted to the College of
Graduate Studies and Research
in Partial Fulfillment of the Requirements
for the Degree of Doctor of Philosophy
in the Department of Geological Sciences
University of Saskatchewan
Saskatoon

By
Jennifer Jane Scott

## PERMISSION TO USE

In presenting this dissertation in partial fulfillment of the requirements for a Postgraduate degree from the University of Saskatchewan, I agree that the Libraries of this University may make it freely available for inspection. I further agree that permission for copying of this dissertation in any manner, in whole or in part, for scholarly purposes may be granted by the professors who supervised my dissertation work or, in their absence, by the Head of the Department of Geological Sciences or the Dean of the College of Graduate Studies and Research. It is understood that any copying or publication or use of this dissertation or parts thereof for financial gain shall not be allowed without my written permission. It is also understood that due recognition shall be given to me and to the University of Saskatchewan in any scholarly use which may be made of any material in my dissertation.

Requests for permission to copy or to make other uses of materials in this dissertation in whole or in part should be addressed to:

Head of the Department of Geological Sciences
University of Saskatchewan
114 Science Place
Saskatoon, Saskatchewan S7N 5E2
Canada

OR

Dean
College of Graduate Studies and Research
University of Saskatchewan
107 Administration Place
Saskatoon, Saskatchewan S7N 5A2
Canada

## ABSTRACT

A detailed study was made of the composition and distribution of modern and fossil animal and plant traces around saline, alkaline lakes in tectonically active, closed lake-basins. Modern and Pleistocene traces that were examined in lake basins of the Kenya Rift Valley (Lakes Bogoria, Magadi, and Nasikie Engida) were compared directly with fossil traces from the Eocene Lake Gosiute in the Green River Formation of Wyoming, U.S.A., which had a similar hydrochemistry. Analysis of lithofacies and the stratigraphic packaging of the sediments hosting biogenic structures was undertaken so that their vertical and lateral distribution could be used to interpret lake histories and to help to develop depositional models of enigmatic sedimentary successions. A focus was given to the application of the results for paleoecology and stratigraphy, and a model for predicting the position of different trace associations in vertical successions and in different parts of saline, alkaline lake basins has been developed. Evidence from the Kenyan lakes and Eocene Lake Gosiute shows that (1) sedimentary environments are diverse in underfilled basins, and frequent lake-level fluctuations strongly impact the distribution of sedimentary environments suitable for the production and preservation of biogenic structures; (2) the distribution of biogenic structures in underfilled basins is related to the geomorphological and structural setting, tectonic activity, catchment lithology, the basin margin or basin centre location, climate, and salinity and alkalinity, together with other finer-scale environmental and biological controls; (3) because saline environments are restrictive, sites of relatively dilute inflow (springs, rivers and deltas, ephemeral streams) provide oasis-like habitats for animals and plants, and contribute to the increased diversity and laterally variable distribution of saline-lake trace assemblages; and (4) the vertical distribution of trace fossils in a stratigraphic succession reflects changing environments through time; important stratigraphic surfaces, usually formed during periods of lake-level fall, can be recognized from the overprinting patterns of traces produced under different conditions.

## ACKNOWLEDGEMENTS

I gratefully acknowledge the support and encouragement from my supervisors, Robin Renaut and Luis Buatois (University of Saskatchewan), and committee members: Gabriela Mángano, Jim Basinger, Ernie Walker (University of Saskatchewan) and Phil Currie (University of Alberta). The time and expertise of my external examiner, Sebastian Voigt, are very much appreciated. Alec Aitken (University of Saskatchewan) provided valuable comments on the text. Discussions and fieldwork with Bernie Owen (Hong Kong Baptist University), Alan Carroll and Eric Williams (University of Wisconsin–Madison), Mike E. Smith (Sonoma State University), Leroy Leggitt and Paul Buchheim (Loma Linda University), Kevin Bohacs (ExxonMobil Upstream Research Company), and Tim Lowenstein (Binghamton State University) all contributed to this thesis. Tony Drane (UK) assisted with the identification of insects at Lake Bogoria. Discussions with Terri Graham (University of Saskatchewan) are much appreciated, as well as her research on Eocene vertebrate tracks, which was used in this thesis. Discussions with Warren Fleming (Fiera Biological Consulting) contributed to this thesis. Many other people have also provided encouragement and feedback. Funds for this research were provided by the Natural Sciences and Engineering Research Council of Canada (NSERC) (PGS-D scholarship to J.J.S.; Research Grant RG629-03 to Robin W. Renaut; and Discovery Grant 311726-05 and -08 to Luis A. Buatois) and by the Department of Geological Sciences, University of Saskatchewan. Fieldwork was partially funded by the International Association of Sedimentologists (IAS – Postgraduate Research Grant), the Geological Society of America (GSA – Student Research Grant), and the American Association of Petroleum Geologists (AAPG – Grants-in-Aid Program).

# TABLE OF CONTENTS

## LIST OF TABLES

## LIST OF FIGURES

# CHAPTER 1

## 1. INTRODUCTION

### 1.1. Overview

Organisms respond to the physical and ecological conditions in an environment with a set of evolved behavioural and physiological adaptations that allow them to use water and nutrients, and to successfully reproduce. Together, an assemblage of organisms present in a particular environment reflects the conditions prevalent in that setting, such as its chemistry, the resource availability, oxygen levels, salinity, and whether the setting is subaerial or subaqueous (e.g., Bromley, 1996; Schowalter, 2006). Reconstructions of past environments must rely on clues that provide information about the setting. These clues may be derived from sediments, and from evidence of the way that organisms responded to that setting. Trace fossils are the preserved evidence of animal behaviour in sedimentary rocks, and an assemblage of trace fossils can reflect the set of environmental factors that controlled the presence of animals and their activities in a certain place at a certain time. Trace fossils may also reflect the physical and chemical conditions that led to their preservation (e.g., Bertling, 1999).

The development of ichnology, the study of trace fossils, has been based on these fundamental concepts since the implications of fossil animal traces were recognized by Adolf Seilacher in the 1950s (e.g., Seilacher, 1964), and were even crudely recognized by Leonardo da Vinci in the 16$^{th}$ century (Baucon, 2008). Ichnofacies are assemblages of trace fossils that are recurrent through geological time, and which reflect the general depositional setting and sets of controlling factors in a palaeoenvironment (Seilacher, 1964). The recognition and application of these archetypal assemblages has led to the development of ichnology as an important tool for palaeoecology and stratigraphy (e.g., Seilacher, 1967; Frey, 1975; Ekdale et al., 1984). The discipline is continually being refined, as greater applicability is recognized at a variety of temporal and spatial scales (e.g., Pemberton et al., 2001). Recurrent patterns in the composition, diversity, and distribution of trace fossil assemblages, as well as clues provided by the degree of bioturbation, have widespread applications for palaeoenvironmental reconstructions, particularly when considered together with sedimentological evidence.

Continental and marine environments, and the organisms that have lived within them throughout the Phanerozoic, are inherently different. Although several ichnofacies were defined for the marine realm by Seilacher (1964), only one continental ichnofacies was originally recognized. The development of invertebrate ichnology, in particular, has been focused primarily on marine environments, and continental ichnology has lagged behind, in part due to this historical bias. Presently, three archetypal continental ichnofacies have been widely accepted, which generally reflect the depth of the water table, and whether the setting was subaqueous or subaerial (e.g., Buatois and Mángano, 1998, 2004; Genise et al., 2000; Pemberton et al., 2001). Their refinement continues with more research, as well as with attempts to use an approach that integrates vertebrate trace fossils with invertebrate trace fossils and sedimentology (e.g., R.M.H. Smith, 1993; R.M.H. Smith et al. 1993; R.M.H. Smith and Mason, 1998; Melchor et al., 2006; de Gibert and Saez, 2009; Krapovickas et al., 2009; Scott et al., 2009).

To establish the palaeoenvironmental significance of particular trace fossil assemblages, recurrent associations with particular lithofacies assemblages or with particular environmental controls, such as food source, oxygenation and salinity, must be recognized. Neoichnology, the study of modern animal (and plant) traces, is essential to develop a framework from which to test the findings in the rock record, and has been an integral part of the advancement of marine ichnology (e.g., Basan and Frey, 1977; Wetzel, 2008; Frey et al., 1984; Frey and Pemberton,

1987; Gingras et al., 1999). Similarly, in continental settings, neoichnology has been useful for identification of the types of traces made by non-marine invertebrates (e.g., Chamberlain, 1975; Ratcliffe and Fagerstrom, 1980; Sands, 1987; Metz, 1987, 1990; Hasiotis and Mitchell, 1993; Hasiotis, 2003), and the morphological variants of vertebrate tracks (e.g., Allen, 1997; Marty et al., 2008). Modern traces in subaerially exposed settings have also been studied to better understand their taphonomy, and the spatial significance of invertebrate and vertebrate trace fossil assemblages (e.g., Frey and Pemberton, 1986; Cohen et al., 1991, 1993; Scott, 2005; Scott et al., 2010).

Continental ecosystems and depositional settings differ from those of marine environments in many respects. Perhaps most significantly, sedimentation and the distribution of continental sedimentary environments in time and space are closely related to both the tectonic setting and the prevailing climate. The chemistry of groundwater and lake water can be highly variable, even within a single basin, and can change or fluctuate over relatively short time periods. Additionally, the vertical relationships of lithofacies often reflect abrupt changes in depositional environments. Environments can change drastically in response to rapid changes in climate, for example. Fluctuating water levels in alluvial and lacustrine settings may abruptly affect widespread areas. Successions may contain frequent exposure surfaces that may or may not signify lengthy periods of non-deposition and erosion (e.g., mudflats). In general, the complexities and impacts of environmental changes in continental basins are much greater than in oceanic basins (e.g., Renaut and Gierlowski-Kordesch, in press). Similarly, the variability of organisms and communities living in adjacent environments, and any potential traces that they may create, can lead to extreme lateral heterogeneity in fossilized trace assemblages.

The complexities within continental ichnology are a direct response to the complexities observed in continental environmental settings. Recent advances in continental ichnology have begun to consider more closely the impact of geological processes on plants, animals, and their ecosystems (e.g., Gierlowski-Kordesch, 1991; R.M.H. Smith, 1993; Rodriguez-Aranda and Calvo, 1998; Buatois and Mángano, 2004, 2007; Melchor, 2004; Melchor et al., 2006; Hasiotis, 2007; Voigt and Hoppe, 2010). This thesis applies the fundamental concepts in ichnology in an attempt to characterize the composition and spatial and temporal distribution of both vertebrate and invertebrate traces in several Cenozoic saline, alkaline lake basins of the Kenya Rift Valley and the Eocene Green River Formation of Wyoming, U.S.A. In conjunction with sedimentological and stratigraphic analyses, the relationship between the biological realm and the sedimentary setting at both the basin-wide and local scales were investigated in both modern and ancient environments.

### *1.1.1. Objectives, Hypotheses, and Scope of this Thesis*

This research is exploratory, and seeks to contribute to continental ichnology by recognizing useful, broad patterns in ichno-assemblage composition and the spatial and temporal distribution of continental ichnofacies and suites in relation to environmental factors present in selected Cenozoic saline, alkaline lake basins. The main objectives of this research are to:

1) characterize the composition and spatial distribution of modern invertebrate and vertebrate trace fossils in saline to hypersaline lake basins of the Kenya Rift Valley;
2) compare the findings from the modern setting with Pleistocene deposits in the Kenya Rift Valley and characterize their temporal/vertical distribution; and
3) investigate the applicability of these broad patterns for the stratigraphic and palaeoecological analysis of a much older (Eocene) and very dynamic lake system that had similar water chemistry in Wyoming, United States.

To meet these objectives, several hypotheses were developed and tested. These dealt

mainly with the composition of biogenic structures and their lateral and vertical distribution in saline lake settings, with comparisons between several localities that represent a set of similar modern and ancient environments. These comparisons permitted an assessment of the variability between the different localities investigated, and the effects of preservational biases and early diagenesis on assemblages of fossilized biogenic structures. The following hypotheses were tested:

First, due to the restrictive nature of saline environments on animal diversity in modern environments (e.g., Hammer, 1986; Williams et al., 1990; Williams, 1998), localized areas with relatively freshwater input were expected to have the highest diversity assemblages. To test this hypothesis, environments influenced by springs or fluvial input were compared with shallow lacustrine to lake-marginal areas that were unaffected by these influences.

Second, due to this expected lateral variability the overall diversity of biogenic structures in saline lake basins was predicted to be higher than that shown by previous ichnological research that focused on single localities, and possibly even higher than that in lake basins with fresher lacustrine waters. This was tested by comparing the results of this study with those of other authors.

The third set of hypotheses are related to the vertical distribution of trace fossils in saline lake basins and their potential stratigraphic utility, and are outlined in the following statements: Particular sets of conditions influence the presence of certain trace-types in certain environments. If those conditions change, the types of biogenic structures produced at that locality should also change. Such temporal changes should be shown by the particular chronology of different groups of trace types in a substrate or sedimentary succession. In areas with relatively low sedimentation rates, the different trace types will cross-cut one another, leading to a specific pattern of overprinting that could potentially be used to interpret the changes through time. In cases where the substrate is indurated and subsequently exhumed by erosion of overlying less indurated sediments, biogenic structures will continue to be produced in that substrate following exhumation and should provide evidence that helps to reveal the history of that locality. The recognition of substrates with overprinted traces should be useful as stratigraphic tools because they mark important stratigraphic surfaces. This set of hypotheses was tested by comparing the vertical distribution and/or overprinting patterns of biogenic structures described in this study and by considering their position in well-calibrated sedimentary successions.

Within each basin investigated, this study focused on the zone directly influenced by lake level fluctuations (lacustrine, lake-margin), which in some cases included weakly developed soils (terrestrial). The lateral scale of adjacent lake-margin environments affected by lake level rise and fall varied with the size and tectonic setting of each basin and whether the basin was relatively filled with water or relatively empty, as well as the lake margin slope. Field study focused on discovering repeatable assemblages of biogenic structures and using them as tools for stratigraphical, sedimentological, and paleoecological analyses at local and basin scales. Very detailed lithofacies interpretations, and their positions within a stratigraphic framework, were necessary to establish the sedimentary environments in which the traces were preserved. Exhaustive ichnological analyses of each of the basins or formations considered for comparisons were beyond the scope of this thesis.

### *1.1.2. Organization of this Thesis*

This thesis is organized in chapters that contain rewritten and updated portions of already published material, and results not yet submitted for publication. The published material is referenced throughout the text (Scott et al., 2007, 2008, 2009). This style of organization was chosen in an attempt to reduce repetitiveness, particularly for introductory material, and to allow

the inclusion of case studies that provided useful information, but for which manuscripts have not yet been prepared. All descriptions of lithofacies and modern and fossil traces are provided in table format. A glossary of selected terms used in this thesis is provided in Section 1.4. This thesis partially builds upon the MSc. research of the author (Scott, 2005; Scott et al., 2010).

## 1.2. Background

### *1.2.1. Continental Trace Fossils*

There are fundamental differences between marine trace fossils and ichnofacies, and continental trace fossils and ichnofacies. Importantly, insects, which are primarily air breathers, are the dominant type of animals that produce continental trace fossils. Subaerial exposure of the substrate is frequent, and depending on the distance from a fluvial channel or shoreline, for example, may be the normal condition for the substrate. However, the recognition of traces produced during periods of exposure and their distinction from similar traces that were produced subaqueously can remain a challenge. Clearly defined and exclusive associations between recurrent trace fossil assemblages and certain depositional environments are not always possible, particularly in transitional shoreline or fluvial settings (e.g., *Skolithos*-dominated assemblages) (Buatois and Mángano, in press). The application of ichnofacies without careful consideration of the sedimentary setting will produce unreliable palaeoenvironmental reconstructions. This is especially important in continental settings, particularly at the present level of understanding and agreement among continental ichnologists.

The animals that live in continental environments (e.g., lacustrine, fluvial, terrestrial) differ from marine animals in their composition, behaviour, ecology, and physiology, and have had different evolutionary paths throughout the Phanerozoic (e.g., Buatois et al., 1998). Continental animals have continued to expand into new environments and have penetrated substrates progressively deeper since the latest Silurian (Buatois et al., 1998; Park and Gierlowski-Kordesch, 2007). Some Cambrian and Ordovician examples of marginal lacustrine (e.g., Johnson et al., 1994) and paleosols (e.g., Retallack and Feakes, 1987) have also been reported. The physiological and behavioural evolution of continental organisms coincides with changes in the morphological details of animal traces. The consideration of trace maker identity may greatly improve palaeoecological interpretations based on ichnology, particularly when considering similar traces produced in both subaqueous and subaerial settings (e.g., *Skolithos*). For example, backfilled burrows formed by insects may produce similar trace types to marine examples (e.g., *Taenidium* isp.), but the method of backfilling and the interpreted behaviour may differ greatly (J.J. Smith et al., 2008; cf. Krapovickas et al., 2009). The consideration of modern insect behaviour is very useful for understanding the types of trace fossils found in the Cenozoic (e.g., Ratcliffe and Fagerstrom, 1980; Sands, 1987; Hasiotis, 2003). However, it is important to remember that like trace fossils in marine systems, many different types of organisms can produce similar traces. In these initial steps to characterize and determine the significance of the various trace types found in continental settings, research into the types of trace makers and their particular behaviours is essential.

The temporal overlap of trace fossils formed under different conditions at different times in the same substrate, or the overprinting of traces in palimpsest substrates, is very common in the continental realm (e.g., Zhang et al., 1998; Buatois and Mángano, 2004; Hasiotis, 2007). Recent research into the significance of these overprinting patterns has revealed the potential for applying these patterns for better interpretations of continental sedimentary systems (Uchman and Álvaro, 2000; de Gibert and Saez, 2009; Scott et al., 2009). Deciphering the "taphonomic pathways" of trace fossil assemblages in these frequently changing depositional environments (Zhang et al., 1998; Buatois and Mángano, 2004) is essential for improving the applicability of continental ichnology. The presence of tiering, or the vertical partitioning of traces produced by

trace makers in a single community at a single time, is an important consideration when attempting to determine if environmental conditions changed (Bromley, 1996). True tiering within a single community may be uncommon in continental settings, except in well oxygenated, freshwater lakes and possibly in well developed paleosols with insects that burrow and nest at different depths. In the continental realm, traces that have different relative depths more often reveal changing conditions, such as the lowering of the water table, for example, instead of a community of organisms that lived together and responded to the similar conditions with different behavioural strategies (e.g., Metz, 2000; Uchman and Álvaro, 2000; Keighley and Pickerill, 2003; Kim et al., 2005).

Despite certain difficulties in the application of marine ichnological concepts to continental ichnology, three continental ichnofacies have been widely accepted, namely: 1) Scoyenia (Seilacher, 1967; Frey et al., 1984); 2) Mermia (Buatois and Mángano, 1995, 1998); and, 3) Coprinisphaera (Genise et al., 2000). The significance of these ichnofacies is presently being refined by several workers and much discussion surrounds the meaning of each (e.g., Keighley and Pickerill, 2003; Hasiotis, 2007; Buatois and Mángano, 2009; Voigt and Hoppe, 2010). The Skolithos ichnofacies, for instance, is usually applied with the same significance as the Skolithos ichnofacies in the marine realm, although in continental settings *Skolithos*-dominated trace fossil assemblages often do not necessarily imply high energy shorelines or even subaqueous settings (e.g., Fitzgerald and Barrett, 1986; Netto, 2007; Scott et al., 2007). The presence of *Skolithos*-dominated assemblages may have several different implications for palaeoenvironmental interpretations, depending on the depositional setting. *Skolithos* itself is a "facies-crossing" trace fossil that does not indicate any particular environment (e.g., Schlirf and Uchman, 2005). The consideration of the lithofacies associated with trace fossils is therefore essential when applying ichnofacies.

Several other ichnofacies or sub-ichnofacies for continental trace fossils have been proposed: 1) Termitichnus (R.M.H. Smith et al., 1993); 2) Fuersichnus (Bromley and Asgaard, 1979); 3) Arenicolites (Bromley and Asgaard, 1991); 4) Entradaichnus (Ekdale et al., 2007); 5) Octopodichnus (Hunt and Lucas, 2007a); 6) Celliforma (Genise et al., 2010); and 7) several vertebrate ichnofacies (e.g., Lockley et al., 1994; Lockley, 2007; Hunt and Lucas, 2007a). These remain either controversial or are not yet widely applied in ichnological research. An integrated approach, which includes both invertebrate and vertebrate traces, is presently being developed by some authors (e.g., Melchor et al., 2006; Krapovickas et al., 2009) and is the approach used in this thesis. Other authors use an entirely different approach, by considering only the more local-scale ichnocoenoses for ichnological analysis of terrestrial settings, and have abandoned the ichnofacies concept altogether (e.g., Hasiotis, 2007; J.J. Smith et al., 2008).

The three most commonly recognized continental ichnofacies essentially represent different conditions with respect to the depth of the water table or lake level, or the presence of temporary pools of standing water. The Mermia ichnofacies (Buatois and Mángano, 1995, 1998) comprises simple horizontal trails and tunnels preserved at either upper or lower bedding planes, produced mainly by grazing invertebrates (e.g., nematodes, ostracodes) and larval insects (e.g., beetles, caddisflies, true flies). Branched, shallow-tier burrow networks in sublittoral to profundal zone lacustrine substrates, also assigned to the Mermia ichnofacies, are attributed to the deposit feeding of oligochaetes and/or larval insects (e.g., Voigt and Hoppe, 2010). This recurrent assemblage is associated with shallow to deep, permanently subaqueous fresh water (Buatois and Mángano, 1998) and more rarely saline lakes (Uchman et al., 2007), although it also may be associated with short-lived, freshwater subaqueous to saturated settings in fluvial systems, lake-margin mudflats, or lacustrine shorelines (e.g., Moussa, 1970; Metz, 2000; Buatois and Mángano, 2004). Some examples also preserve the Mermia ichnofacies in settings

influenced by glacial runoff, both in continental (e.g., Benner et al., 2009; Uchman et al., 2009) and freshwater-influenced marginal marine environments (e.g., Pazos, 2002; Buatois et al., 2006, 2010; Netto et al., 2009).

The Scoyenia ichnofacies (Seilacher, 1964; Frey et al., 1984; Buatois and Mángano, 1995, 2007) comprises a variety of horizontal and vertical, open or backfilled, full relief and semi-relief burrows and tunnels, as well as vertebrate footprints and root traces. It is typical of substrates that are frequently inundated and then exposed, and is most common along lacustrine shorelines or in alluvial systems, either near channels or on the floodplain. Several authors have suggested potential sub-divisions of the Scoyenia ichnofacies, including the "shorebird" ichnofacies, for example (Lockley et al., 1994), or trace fossil suites that may be recurrent with particular lithofacies (Melchor et al., 2006). Most of the proposed vertebrate track ichnofacies (e.g., Hunt and Lucas, 2007a) would essentially become sub-divisions of the Scoyenia ichnofacies if implemented. Like the Skolithos and Mermia ichnofacies, as well as marine ichnofacies, the Scoyenia ichnofacies can be found in several different depositional settings (Buatois and Mángano, in press).

The Coprinisphaera ichnofacies (Genise et al., 2000) comprises the nests and burrows of terrestrial animals such as beetles, bees, wasps, termites and ants, and is commonly associated with root traces. It represents stable, pedogenically-altered substrates with relatively deep water tables. Based on examples from South Africa, R.M.H. Smith et al. (1993) suggested the inclusion of the Termitichnus sub-ichnofacies within the Scoyenia ichnofacies. Buatois and Mángano (1995) later included the Termitichnus ichnofacies alongside the Scoyenia and Mermia ichnofacies in their overview of lacustrine trace fossils. However, the subsequently proposed Coprinisphaera ichnofacies (Genise et al., 2000) included termite traces, and the use of the Termitichnus ichnofacies (or sub-ichnofacies) was rejected. Genise et al. (2010) suggested the division of the Coprinisphaera ichnofacies, with the informal definition of the Celliforma ichnofacies as that dominated by the nests of bees and wasps in well drained, often carbonate-rich, paleosols.

The nests of soil organisms typically need specific moisture conditions to be successful, and so the potential exists to use the Coprinisphaera ichnofacies to help interpret the original soil moisture (Genise et al., 2000). Termites, for example, generally require high temperatures (~30° C) and humidities (e.g., Noirot, 1970; Aanen and Eggleton, 2005), but the significance of termite nests in an assemblage may differ depending on the particular type of termite (e.g., African termites vs. South American termites). The understanding of this ichnofacies is strongly linked with neoichnology to interpret the trace fossil assemblages, and is most closely aligned with Cenozoic examples because of the evolutionary history of the trace makers, which diversified mainly throughout the Cenozoic (Genise et al., 2000). The potential does exist for subdivision of the Coprinisphaera ichnofacies to better interpret the moisture conditions that determine the types of traces found in a particular assemblage. For example, the resurrection of the Termitichnus ichnofacies or sub-ichnofacies as part of the Coprinisphaera ichnofacies may be an option for assemblages that include termite nests and galleries, but which do not include the nests of dung beetles or bees (Scott et al., 2009).

The complexities of continental environments and the evolutionary changes in the behavioural exploitation of infaunal resources from the second half of the Paleozoic through the Mesozoic and into the Cenozoic translate into complex ichnological data sets that are available in the continental realm. For instance, the evolution of deeper-tiered terrestrial traces did not occur until the Mesozoic, with traces becoming progressively deeper into the Cenozoic (Buatois et al., 1998). Additionally, each of the three main ichnofacies (Mermia, Scoyenia, and Coprinisphaera) essentially represents different levels of "tiering" from shallowest to deepest, respectively. The

depth of "tiering" in this context is determined by the water table, with Mermia being present in subaqueous settings, Scoyenia being present in settings transitional between subaqueous and subaerial, and the Coprinisphaera ichnofacies present in fully terrestrial settings. The significance of the Skolithos ichnofacies is variable, as stated above. Although some workers dispute the validity of the ichnofacies concept in the continental realm (e.g., Hasiotis, 2007), the recurrent ichnocoenoses recognized by Hasiotis (2007) follow this general spatial distribution of trace assemblages. The ichnofacies concept remains useful as a tool at the broad scale in order to recognize general trends throughout the Phanerozoic that may lead to recognition and prediction of the location of shoreline deposits, for example. In each research study, it will likely be necessary to further subdivide the ichnofacies into smaller units, whether they are ichnocoenoses, ichnofabrics, suites, or sub-ichnofacies, in order to successfully apply trace fossils to the interpretation of a particular sedimentary unit.

Continental lake-basin deposits, and their vertical and lateral distribution, are also complex. Underfilled lake-types (see Section 1.2.2), in particular, show frequent and widespread subaerial exposure surfaces and show changing lake water chemistry with the intercalation of evaporites and fresher water deposits (e.g., oil shale). Although several characteristics of lake-basin sediments can be generalized between similar lake types, each basin is unique (Renaut and Gierlowski-Kordesch, in press). Until the discipline of continental ichnology matures and more case studies are reported, it is necessary to consider the tectonic, climatic, mineralogical, and sedimentological setting in detail. General inferences can be made by using continental ichnofacies, but continental basins are too complex to apply ichnofacies blindly.

### *1.2.2. Lake-Type Basins*

Recent advances in the stratigraphic utility of continental ichnology (e.g., Buatois and Mángano, 2004, 2009; Bohacs et al., 2007a) have built upon the framework of lake-basin types presented by Carroll and Bohacs (1999) and Bohacs et al. (2000, 2007b). Three main types of continental basins that contain lakes can be distinguished by their specific relationship between the supply of water and sediment and the potential accommodation, which results in predictable facies associations and stratal stacking patterns (Carroll and Bohacs, 1999; Bohacs et al., 2000, 2007b). Overfilled basins receive more water and sediment than there is potential accommodation, and are characterized by prograding clastic shorelines into freshwater lakes that overflow the basin-bounding sill and spill into at least one adjacent basin (Carroll and Bohacs, 1999). Balanced-fill lake types, in which the potential accommodation is approximately equal to the sediment and water supply, are characterized by a mix of prograding to aggrading shoreline clastic deposits and lacustrine carbonates and shales in lakes of fluctuating salinities that sometimes spill into an adjacent basin (Carroll and Bohacs, 1999; Carroll et al., 2008). Underfilled basins are typified by saline lakes because the supply of water and sediment is less than the potential accommodation, which results in topographically-closed hydrological systems and frequently fluctuating shorelines (Carroll and Bohacs, 1999). Underfilled basins contain predominantly aggrading evaporitic lacustrine facies (e.g., evaporites, carbonates) mixed with a diverse array of subaerial environments, including dune fields, playas, wetlands, mudflats, alluvial plains with palaeosols and fluvial sedimentation, and both carbonate and clastic shorelines (e.g., Smoot, 1978, 1983; Pietras and Carroll, 2006).

The distribution and characteristic sedimentological features of shoreline, lacustrine, fluvial, and alluvial plain deposits are closely linked to the type of lake basin. In an overfilled basin, for instance, lake level remains relatively stable, and the lateral movement of the shoreline occurs as a result of infilling of the basin with sediment. In balanced-fill and underfilled lake basins, on the other hand, lake level fluctuations tend to have greater impact on the distribution

of shoreline deposits. Lake levels in balanced-fill basins tend to be near or at the spillover point, or lake-bounding sill, and so have relatively more stable shorelines than in underfilled basins. Fine-grained lacustrine deposits in balanced-fill lake basins tend to have a much greater areal extent than in both overfilled and underfilled lake basins. Lakes in underfilled basins are the most sensitive to fluctuations caused by variability in the amount of water input to the basin, as well as the amount of evaporation. Depending on the gradient of the lake margin, even relatively small changes in lake level (e.g., seasonal) can potentially cause great changes in the lateral distribution of shoreline and profundal deposits.

In general, overfilled basins tend to have thick packages of prograding fluvial and shoreline sandstones near the basin margin that eventually may fill the entire lake basin. Balanced fill lakes show aggradational shoreline sandstones and carbonates at the basin margin and aggradational lacustrine mudstones in the basin centre. Underfilled basins, on the other hand, may show extreme lateral displacement of shoreline deposits, which can be found at both the basin margin and basin centre depending on the extent of lake level rise and fall (Bohacs, 2007). Similarly, organic-rich lacustrine deposits in balanced-fill lake basins are found in thicker packages, whereas in underfilled lake-types, organic-rich mudstones tend to be thinner and intercalated with shoreline deposits because of frequent lake-level fluctuations. The lake-type basin model is extremely useful for predicting the distribution of organic-rich source rocks (e.g., oil shale) and potential reservoirs and seals, as well as the type and quality of kerogen (Carroll and Bohacs, 2001) and subsurface petrophysical properties of lacustrine strata (Bohacs, 2007).

### *1.2.3. An Integrated Model*

Environmental factors that impact the distribution and behaviour of organisms are closely related to the depositional setting, particularly in continental settings where even chemical differences between settings exist. The ionic composition and salinity may vary greatly between lakes, rainwater-fed pools on floodplains, or spring-fed lake-margin pools even within the same continental basin, but is more uniform in the oceans. Just as in marine settings, some environmental factors that control both sedimentation and the distribution of trace fossils (e.g., energy) may be partly determined by the proximity to the shoreline. The application of the lake-type basin model to continental ichnology provides a useful framework for understanding the sets of environmental controls prevalent in a basin during a particular time period, and the relationship between lithofacies and trace fossil assemblages (Buatois and Mángano, 2004, 2009; Bohacs et al., 2007a). The lateral and vertical distribution of trace fossils in lacustrine and lake-margin environments may be best understood by considering lake level fluctuations and their impact on the distribution of the controlling environmental factors, including the chemistry of lake and groundwaters. Additionally, the integration of continental ichnology with the lake-type basin model strongly increases the stratigraphic use of trace fossils in lacustrine basins by placing the observed distribution patterns of trace suites, ichnocoenoses, and/or ichnofacies directly into a model of stratal packaging (see Section 1.4.1 for glossary of terms; Buatois and Mángano, 2009).

Buatois and Mángano (2004, 2009) integrated the continental ichnofacies models with lake-type basins, and provided a framework for interpreting the distribution of continental trace assemblages. In overfilled basins with relatively stable shorelines, trace assemblages tend to be dominated by the Skolithos ichnofacies in shoreline deposits, and soft-substrate examples of both the Mermia and Scoyenia ichnofacies (Buatois and Mángano, 2004, 2009; Voigt and Hoppe, 2010). In balanced-fill basins with more frequently fluctuating shorelines, however, trace fossil assemblages comprise the Scoyenia ichnofacies in exposed lake-margin facies, Skolithos ichnofacies in high-energy shorelines, and possibly low-diversity examples of the Mermia

ichnofacies in lacustrine facies (Buatois and Mángano, 2004, 2009). Trace fossils in underfilled basins are characterized by restricted or absent lacustrine suites (Mermia ichnofacies), and overprinted suites or composite ichnofabrics of the Scoyenia ichnofacies in exposed fine-grained littoral sediments that undergo bioturbation in desiccating substrates (Buatois and Mángano (2004, 2009). Laterally restricted examples of the Skolithos ichnofacies may be present (Buatois and Mángano (2004, 2009), and may signify either high energy shorelines, active channels, or low-energy subaerial settings (e.g., Netto, 2007; Hasiotis et al., 2009). This thesis further explores the stratigraphic application of trace fossils in underfilled lake basins of the Kenya Rift Valley and the Eocene Green River Formation of Wyoming, U.S.A., upon which the lake-type basin model of Carroll and Bohacs (1999) and Bohacs et al. (2000) was largely based.

## 1.3. Methods

### *1.3.1. Field*

Two Pleistocene–Recent lake basins in the Kenya Rift Valley (Baringo-Bogoria, Magadi-Nasikie Engida) were investigated to determine general patterns in the composition and distribution of plant and animal traces present around saline to hypersaline alkaline lakes. The underfilled lake-type in the Eocene Green River Formation (Wilkins Peak Member) and correlative Wasatch Formation (Cathedral Bluffs Member) of Wyoming, U.S.A., were also investigated to test and apply the findings from the Kenya Rift. In all cases, the focus of study was on lacustrine, fluvio-lacustrine, deltaic, and alluvial settings in the zone influenced by lake level rise and fall, and not on purely terrestrial settings. Recurrent associations between trace fossil assemblages with lithofacies assemblages were a main topic of consideration. The bulk of research was conducted during three field seasons to Wyoming (July, 2006; June-July 2007; June-July, 2008) and Kenya (August, 2007; August, 2008). Selected data collected during the field seasons of June-July, 2001–2002 in Kenya (during M.Sc. fieldwork) and July 2003 and June, 2004 in Wyoming (as a field assistant to M.E. Smith, Sonoma State University) is included here.

Ancient examples from the central Kenya Rift Valley included the Pleistocene Loboi Silts and the Holocene Bogoria Silts of the Bogoria basin. Emphasis was also placed on the neoichnology of modern Lake Bogoria in the Bogoria basin. In the southern Kenya Rift, late Pleistocene to Holocene saline lake deposits from the Magadi Basin ("Green Beds", High Magadi Beds) were compared with the Pleistocene Loboi Silts of the Bogoria Basin, and with modern environments in the Magadi-Nasikie Engida basin. Neoichnology in the southern rift was focused on the shorelines and areas with hot springs at modern Lake Magadi and Nasikie Engida (Little Magadi). The work in the Kenya Rift Valley builds upon an earlier MSc. study on vertebrate traces and their taphonomy in the Baringo-Bogoria basin in the central rift (Scott, 2005; Scott et al., 2010).

Observations of modern sedimentological processes, environmental factors that influence trace fossil taphonomy, and interactions between trace-making animals and plants in lake margin sediments have been recorded as part of a long-term study of Lake Bogoria (e.g., Tiercelin, 1981; Tiercelin et al., 1981; Renaut, 1982, 1993; Renaut et al., 1986; Tiercelin et al., 1987; Renaut and Owen, 1988, 1991; Renaut and Tiercelin, 1994; R.B. Owen et al., 2004; R.A. Owen et al., 2008). Continuing neo- and paleoichnological investigations were undertaken between June and August of 2001, 2002, 2006, and 2007 (Scott, 2005; Scott et al., 2007, 2009, 2010). Suggestions for tracemakers are based on personal field observations (J.J.S. and R.W.R.), the work of Harper et al. (2003), and on the suggestions by Dr. Tony Drane (UK).

Stratigraphic sections were measured at the decimetre-scale for the Holocene (Bogoria Silts) at Lake Bogoria. Holocene to Pleistocene examples in the Magadi-Nasikie Engida Basin

were placed into the stratigraphic framework of Behr (2002), although a greater level of resolution requires additional fieldwork. Sediment samples were collected where appropriate and feasible, and systematic ichnological descriptions were made of modern and fossil invertebrate traces in the field, from field photographs, and from sediment samples. Where sampling was not possible, photographs are the primary data source.

Eocene examples from Wyoming were focused on lithofacies assemblages most comparable with those of the Kenya Rift. The analysis of trace fossils and their association with different sedimentary facies was undertaken primarily for the underfilled Wilkins Peak Member of the Green River Formation and the correlative Cathedral Bluffs Member of the Wasatch Formation. The Tipton Shale and Laney Members of the Green River Formation, as well as the Wilkins Peak-time "Alkali Creek Member" (Roehler, 1993) or "New Fork Tongue" (M'Gonigle and Dover, 1992) of the Wasatch Formation, were also investigated, but the results will be presented elsewhere. Facies associations show distinct differences between the "basin margin" and the "basin center", and this division has been used here as a framework to compare between the Kenyan rift basins and the Eocene greater Green River basin of southwest Wyoming. Lithofacies descriptions are based on measured stratigraphic sections of exposed outcrops in the Bridger basin of Wyoming, and are compared with the previous work of Pietras and Carroll (2006). Basin-scale stratigraphic correlation of the Wilkins Peak Member, Tipton Shale, and Laney Members of the Green River Formation is based on measured sections from outcrop and core, gamma ray spectra, and tuffs dated by the $^{40}Ar/^{39}Ar$ method (M.E. Smith, 2007; M.E. Smith et al., 2003, 2008b).

Geo-referenced photographs were taken of outcrops, sedimentary structures, and *in situ* trace fossils to aid in the analysis of trace fossil distribution in the Green River Formation. Photo-Link software (Geo-Spatial Experts, Colorado, U.S.A.) was used to link GPS coordinates logged in 2008 with digital photographs using the synchronized time of day. Sediment samples containing trace fossils were collected for further examination of details of trace morphology, as well as sediment mineralogy and textural features. The repository for all of the collected samples that contain vertebrate trace fossils is the Fossil Butte National Monument in Wyoming, U.S.A. Digital photographs recorded the modern traces in the Kenya Rift and trace fossils in all basins. Detailed stratigraphic sections were measured to examine associations between trace fossils and lithofacies, and to reconstruct the sequences of events related to lake-level fluctuations or changes in depositional setting. Sections were measured at the decimetre-scale using a Jacob's staff, and a hand lens was used to estimate sediment grain size. Sediment composition was determined using a hand lens and dilute HCl acid in the field. Colors provided for the stratigraphic sections were named using standard soil color charts, and show general changes in lithology (e.g., carbonate vs. siliciclastic, mudstone vs. sandstone, kerogen-rich vs. kerogen-poor).

### *1.3.2. Laboratory Analyses*

This research was primarily field-based. However, petrographic analysis was used to determine the mineralogy and textural features of some cements to reconstruct the early diagenetic events that led to the preservation of trace-containing units. Kenyan samples were examined by X-ray diffraction (using a Rigaku RU200 X-ray diffractometer), which was used to determine mineralogy in mudstones and sandstones. Backscattered electron images were taken using a JEOL JXA 8600 electron microprobe to investigate the mineralogy and textural relationships of very finely crystalline cements. Oriented bulk samples and oriented clay mineral samples (the < 2μm fraction) were ground by hand and allowed to dry on glass slides for X-ray diffraction. The clay mineral fraction was obtained by gently grinding the samples and using an

ultrasonic bath to separate the clays in Borax-containing water. The samples were centrifuged, first at 700 rpm at 23° C for 3 minutes, and then the fluid remaining was centrifuged at ~2500 rpm at 23° C for 15 minutes to settle the clays in small test tubes. Clays were air-dried on glass slides and then gently ground in ethanol for mounting as oriented slides to be used for analysis. Glycolation for 24 hours was undertaken to determine the presence or absence of swelling clay minerals.

Petrographic studies to characterize sedimentary facies and trace fossils in the Green River Formation were limited (~40 thin sections), but provided valuable information particularly for carbonate facies and spring deposits. No X-ray diffraction was undertaken for the Green River Formation samples. Thin sections were also used for analyzing textures and cements in Pleistocene sediments from Lake Bogoria (~30 thin sections; Scott, 2005). Detailed petrographic studies were beyond the scope of this study.

### *1.3.3. Ichnology*

Trace fossils were identified to the ichnogeneric level where possible, and were grouped into suites (following Bromley, 1996) by the recognition of recurrent associations that may or may not represent true ecological communities (i.e. ichnocoenoses). Trace fossil types preserved on bedding planes (i.e. epichnia, hypichnia) and within beds (i.e. endichnia) were all included in the suites, whether or not they created a recognizable ichnofabric in cross section. In some examples (e.g., *Planolites* ichnofabric), the degree of bioturbation was very high (BI= <5) and did not allow the distinction between different trace types. Estimation of degree of bioturbation within beds (Bioturbation Index = BI) and on bedding planes (Bedding Plane Bioturbation Index = BPBI) was recorded following Droser and Bottjer (1986) and Miller and Smail (1997), respectively. The approach used for this analysis adopts the currently defined ichnofacies in continental settings to recognize broad patterns (i.e. Scoyenia, Mermia, Coprinisphaera, Skolithos), but for more detailed associations with lithofacies, subdivisions (suites) were used. These suites varied in composition between each of the modern and ancient lakes investigated. Binomial ichnotaxonomic nomenclature is provided in italics, whereas the names of ichnofacies are not. Descriptions of the traces are provided in table format. A glossary of selected terms used in this thesis is provided in Section 1.4.

## 1.4. Glossary of Selected Terms and Abbreviations used in this Thesis

### *1.4.1. Glossary of Selected Terms in Alphabetical Order*

The following list defines some of the terms used in this thesis that are not necessarily defined in the text. The definitions were written with reference to: Bromley (1996); Buatois and Mángano (in press); Cohen (2003); Hammer (1986); Renaut and Gierlowski-Kordesch (in press); and Thornwaite (1948).

ARID— A climate characterized by much more evaporation (or potential evapotranspiration) than precipitation, causing an extreme moisture deficiency, or a moisture index of less than -40 (Thornwaite, 1948).
ASSEMBLAGE— A term used loosely to refer to a group of trace fossils (ichnoassemblage), a group of lithofacies, or a group of body fossils.
ASSOCIATION— A term used loosely to refer to ichnological, sedimentological, and/or paleontological features found together in a particular locality or stratigraphic interval.

EULITTORAL— The region where lake-level fluctuations frequently cause both the inundation and the subaerial exposure of sediments on short time scales (from ~daily to ~seasonal). This term may be used interchangeably with shoreline, but was used here mainly to refer to low-gradient areas (e.g., mudflats).
HUMID— A climate characterized by more precipitation than evaporation (or potential evapotranspiration), causing a positive moisture balance, or a moisture index of more than +20 (Thornwaite, 1948).
ICHNOCOENOSIS— A term used to refer to the biogenic structures produced by a biological community, of which the members interact; this term is synonymous with “ichnocommunity”.
ICHNOFABRIC— A term used to refer to any aspect of the texture and internal structure of a substrate resulting from bioturbation and bioerosion at any scale (from Buatois and Mángano, in press).
ICHNOFACIES— A conceptual construct based on the identification of key features shared by different ichnocoenoses of a wide range of ages formed under a similar set of environmental conditions. To avoid confusion with other terms used to group trace fossils at different scales, ichnofacies are commonly referred to as Seilacherian or archetypal ichnofacies. The archetypal nature of ichnofacies relies on a "distillation" process that extracts the key features shared by actual ichnocommunities (from Buatois and Mángano, in press).
ICHNOFAUNA— A very general term to group trace fossils having no scale or genetic connotation (from Buatois and Mángano, in press).
LAKE— A term used to refer to a body of water that is relatively large and stable throughout time (over 100s to 1000s of years or more).
LAKE MARGIN— A term used to refer to the region landward of the shoreline of a lake but lake-ward of fully terrestrial environments, including the eulittoral and supralittoral zones in a variety of settings (e.g., delta-plain, mudflat, beach) without any connotation of gradient.
LITTORAL— The oxygenated, shallow lacustrine region above wave-base where light can penetrate. Macrophyte vegetation also typically characterizes this region, but in saline to hypersaline lakes, vegetation may be absent. This zone may be subaerially exposed on a variety of time scales depending on the gradient and frequency of lake-level fluctuations (~seasonal to ~decadal).
OVERPRINTING (cf. cross-cutting)— A term used here to refer to the superimposition of trace fossil suites within a single bed or bedset, usually representing a change to slightly different environmental conditions through time. In this thesis, the term cross-cutting was used to refer to the superimposition of individual trace fossils within a single bed.
POND— A term used in this thesis to refer to a relatively short-term, relatively small, shallow water body that is not stable over 10s to 100s of years.
POOL— A term used in this thesis to refer to a very short-term, very small body of water that may collect in a variety of environmental settings (e.g., within fluvial channels, on floodplains, delta-plains) and may be stable over days to months (compare with spring pool).
PROFUNDAL— The region within a lake that is below the depth to which light penetrates and it is below storm wave-base. The zone is typically below the chemocline or thermocline and is typically not well-oxygenated or well-mixed in saline lakes.
SEMI-ARID— A climate characterized by greater evaporation (or potential evapotranspiration) than precipitation, causing a moisture deficiency, or a moisture index of -20 – -40 (Thornwaite, 1948).
SHORELINE— A term used loosely to refer to the edge of a lake or pond.
SPRING POOL— A term used to refer to a small body of water that is fed by a point-sourced spring or group of springs; it may or may not be stable over seasons to 10s of years or more.

SUBAQUEOUS— A term used to refer to a sedimentary substrate that is beneath any body of water, which may be very shallow (centimeters) to deep (metres or more).
SUB-HUMID— A climate characterized by approximately the same amount of evaporation (or potential evapotranspiration) as precipitation, causing neither a large excess of moisture or a large moisture deficiency, and having a moisture index of +20 – -20 (Thornwaite, 1948).
SUB-LACUSTRINE— A term used in this thesis to refer to a sedimentary substrate that is subaqueous and specifically within a lake.
SUBLITTORAL— The region within a lake that is below the normal wave-base and is not normally subaerially exposed. Depending on the productivity and salinity within the lake, the sublittoral zone may or may not be well-oxygenated and may or may not receive abundant sunlight.
SUITE—A term used to refer to a group of trace fossils that reflects their (roughly) contemporaneous time of emplacement, and is typically found repeatedly within a particular study area. A suite may or may not be associated with a set of sedimentological features representing a particular depositional environment. A suite may represent a single ichnocoenosis or more than one ichnocoenosis in cases where it is not possible to determine the degree of interaction between the biological communities that produced the trace fossils.
SUPRALITTORAL— The region landward of daily to seasonal flooding by fluctuations in lake level, but it may be inundated by lake waters during storms.
TIERING— A term used to refer to the vertical partitioning of biogenic structures produced by an infaunal biological community, or the vertical partitioning within an ichnocoenosis.

*1.4.2. Abbreviations in Alphabetical Order*

BI— Bioturbation Index
BP— Calibrated years before present (before 1950)
BPBI— Bedding Plane Bioturbation Index
CMM— Cold Mean Month
EARS— East African Rift System
EECO— Early Eocene Climatic Optimum
GRFm.— Green River Formation
ka— Thousands of years before present (BP; 1950)
Ma— Millions of years before present (BP; 1950)
MAP— Mean Annual Precipitation
MAT— Mean Annual Temperature
MATR— Mean Annual Temperature Range
NALMA— North American Land Mammal Ages
O.D.— Ordnance Datum (= Mean Sea Level)
PETM— Paleocene/Eocene Thermal Maximum
POKTZ— Porumbonyanza–Ol Kokwe Transverse Zone (Baringo–Bogoria basin)
T.O.C./O.C.— Total Organic Carbon, Organic Carbon
TDS— Total Dissolved Salts
WMTZ— Waseges–Marmanet Transverse Zone (Baringo–Bogoria basin)

# CHAPTER 2

## 2. FIELD AREAS

### 2.1. Overview

Several field areas were investigated in order to compare both modern traces and trace fossils in lake basins with variable lithologic composition and lake salinity. Most of the lake basins represent underfilled and balanced fill lake-types (e.g., Carroll and Bohacs, 1999; Renaut and Gierlowski-Kordesch, in press), although the Green River Formation also represents overfilled lake-types during its history (e.g., Bohacs et al., 2000; M.E. Smith et al., 2008b). In all cases, the lake basins either are tectonically active (e.g., Lake Bogoria, Lake Magadi), or were tectonically active during the deposition of the trace fossil-bearing strata. Each of the basins preserves spring deposits, either as travertine and tufa in spring mounds formed at spring vents, or as laterally extensive tufa associated with wetlands. Hot springs and their associated pools and outflow channels present around the modern Kenyan lakes investigated are not presently forming travertine or tufa deposits, but have an impact on animal and plant ecology, lake chemistry, and may contribute to the precipitation of sodium carbonate evaporite minerals (Renaut et al., 2000b, 2007). Characterizing the conditions under which the fossil spring deposits formed (e.g., subaerial or subaqueous, temperature) through petrography, scanning electron microscopy, and X-ray diffraction were beyond the scope of this thesis. However, springs were considered when interpreting the sedimentary setting during the periods of biogenic activity.

The modern and ancient lakes also share similar chemistry. In the Kenya Rift Valley, modern lake waters of Lakes Bogoria, Magadi, and Nasikie Engida have Na-$HCO_3$-$CO_3$-Cl composition (e.g., B.F. Jones et al., 1977; Renaut and Tiercelin, 1994; Renaut et al., 2007). All lakes investigated are or were highly alkaline (pH: ~9-10.6), and most were highly saline at some point in their history (e.g., Lake Magadi has up to 330 g $L^{-1}$ Total Dissolved Salts: TDS; B.F. Jones et al., 1977). Although the salinity of the Eocene Wilkins Peak Member of the Green River Formation is unknown, it contains one of the largest concentrations of trona ($NaHCO_3Na_2CO_32H_2O$) worldwide (e.g., Bradley and Eugster, 1969; Wiig et al., 1995). Trona is a highly soluble evaporite mineral formed under alkaline conditions. Halite (NaCl), trona, and other types of sodium-carbonate evaporite minerals including nahcolite ($NaHCO_3$), thermonatrite ($Na_2CO_3H_2O$), gaylussite ($CaCO_3Na_2CO_25H_2O$), and shortite ($2CaCO_2Na_2CO_3$), are present in most of the basins investigated (e.g., Bradley and Eugster, 1969; B.F. Jones et al., 1977; Eugster, 1980; Renaut et al., 1986). Similarly, all of the lake deposits investigated contain zeolites and other authigenic minerals (e.g., opal-A, quartz, magadiite, fluorite), which are typically formed under alkaline conditions and are especially abundant in saline environments (e.g., Goodwin, 1973; Surdam and Eugster, 1976; Renaut, 1993).

There are also some important differences between the Kenya Rift lakes and the Green River Formation (Eugster, 1986). The lake basins of the Kenya Rift are mainly within half grabens or full grabens, and are bounded by normal faults and upthrust horst blocks (e.g., Baker, 1986). In general, spring deposits can be found along normal faults fed by relatively deeply sourced waters (e.g., Lake Bogoria, Nasikie Engida) and also at the bases of alluvial fans, which are fed by young, meteoric waters (e.g., Lake Magadi) (B.F. Jones et al., 1977; Cioni et al., 1992; Renaut et al., 2007). Exposed rocks within the catchments that feed the Kenyan lakes are dominantly composed of Tertiary extrusive volcanic and volcaniclastics which range in lithology from basalt to trachytes and trachyphonolites (e.g., Baker and Wohlenberg, 1971). Mafic

minerals such as olivine and iron- and titanium-rich pyroxenes are common, as well as K-feldspar (e.g., sanidine, anorthoclase) and feldspathoids (e.g., nepheline) (Renaut, 1982). The lakes of the Kenya Rift, in general, lack extensive calcium carbonate deposits (Eugster, 1986) and contain mainly compositionally immature sandstones and Na-, K-, and Mg-rich authigenic clays (e.g., Yuretich and Ervin, 2002; Hover and Ashley, 2003; Deocampo, 2004).

The lacustrine deposits of the Green River Formation, in contrast, are mainly composed of calcite ($CaCO_3$) and dolomite ($Ca\ CO_3MgCO_3$). In the Greater Green River Basin of Wyoming, siliciclastic sediments vary in lithology depending on their position in the basin and location of their source rocks in the surrounding uplifts. The Greater Green River Basin is one of many segmented foreland basins that run in a northwest to south transect from Montana to Colorado along the front range of the Rocky Mountains (Dickinson et al., 1988; DeCelles, 2004). The western margin of the basin is bounded by the thrust faults of the Cretaceous Sevier Orogeny, and the uplifted blocks that form the northeast, southeast, and southern margins of the basin formed during the Laramide Orogeny of the early Cenozoic. Tectonism continued at least until the early Eocene, and directly impacted the lacustrine sediments of the Wilkins Peak Member of the Green River Formation (e.g., Roehler, 1992A; Mederos et al., 2005; M.E. Smith et al., 2008a). Lithologies of catchment rocks included uplifted Mesozoic clastics to Paleozoic carbonates and clastics, to feldspar-rich basement cores of the Laramide uplifts (e.g., Carroll et al., 2006). In general, one of the most important differences in the chemistry of the lakes investigated in this study is that the Green River Formation was partly sourced by Ca-rich sedimentary rocks, whereas the lakes of the Kenya Rift formed in basins without a major Ca source (Eugster, 1986). This difference, together with differences in sedimentation rates and lake-margin gradients, may play an important role in the vertical distribution of preserved trace fossils in the examples examined here. The following sections describe each lake basin investigated in more detail.

## 2.2. Modern Lake Basins, Kenya Rift Valley

The Kenya Rift Valley formed during the Cenozoic as one of two branches of the East African Rift System (EARS), and is connected to the worldwide rift system through Ethiopia to the triple junction at the Red Sea and Gulf of Aden (e.g., Morley et al., 1999; Fig. 2.1). In contrast to the slightly younger western branch of the EARS (Miocene–Recent), in which a series of large half grabens are filled with deep, relatively stable lakes, the eastern branch represents a more advanced and older (Eocene–Recent) branch. It is filled mainly with volcaniclastics and lava flows, as well as a series of shallow, short-lived lakes and their associated deposits (e.g., Baker and Wohlenberg, 1971; Baker, 1986; Morley et al., 1999). The large-scale geometry of both branches of the EARS is controlled by underlying structure in crystalline basement, namely, the position and orientation of the Tanzania Craton, as well as shear zones associated with Precambrian orogenic belts that surround the Tanzania Craton (e.g., Morley, 1999). The large-scale structural features of the Kenya Rift are controlled first by E–W extension, which is possibly due partly to the passive and convective upwelling of the asthenosphere (Morley et al., 1999). Secondly, both large-scale and small-scale features are controlled by the interaction of N–S oriented major normal faults with NW–SE-trending major Precambrian lineaments related to shear zones formed during the Pan African Orogeny that occurred at ~600 Ma (e.g., Le Turdu et al., 1999; Morley, 1999).

**Fig. 2.1.** (Next page) Map of the Kenya Rift Valley.

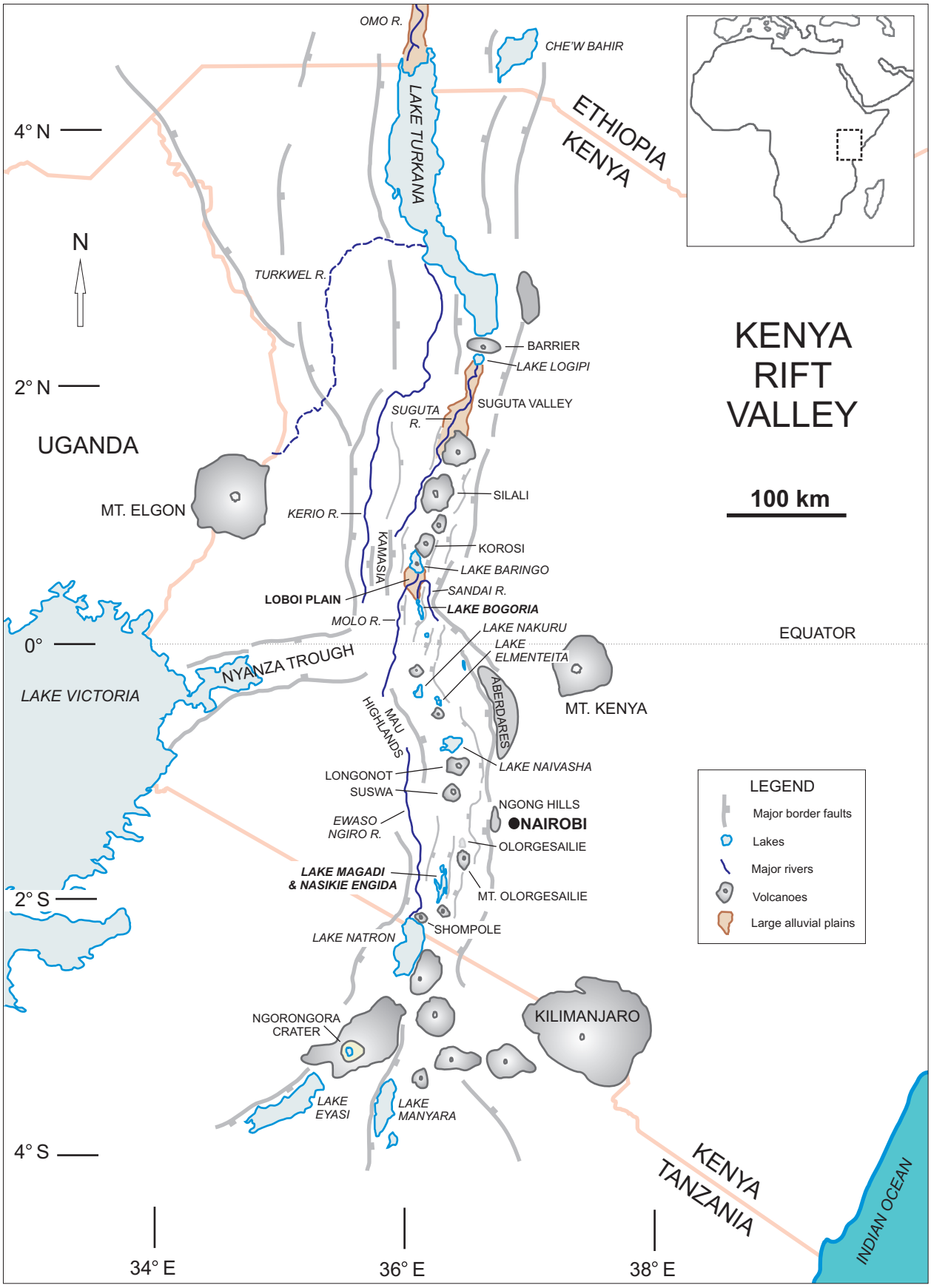
KENYA
RIFT
VALLEY
100 km
OMO R.
CHE'W BAHIR
LAKE TURKANA
ETHIOPIA
KENYA
4° N
N
TURKWEL R.
BARRIER
LAKE LOGIPI
SUGUTA VALLEY
SUGUTA R.
2° N
UGANDA
MT. ELGON
KERIO R.
SILALI
KAMASIA
KOROSI
LAKE BARINGO
SANDAI R.
LOBOI PLAIN
LAKE BOGORIA
MOLO R.
LAKE NAKURU
LAKE ELMENTEITA
EQUATOR
0°
NYANZA TROUGH
LAKE VICTORIA
MT. KENYA
ABERDARES
MAU HIGHLANDS
LAKE NAIVASHA
LONGONOT
SUSWA
NGONG HILLS
NAIROBI
EWASO NGIRO R.
OLORGESAILIE
LAKE MAGADI & NASIKIE ENGIDA
MT. OLORGESAILIE
2° S
SHOMPOLE
LAKE NATRON
NGORONGORA CRATER
KILIMANJARO
LAKE EYASI
LAKE MANYARA
4° S
KENYA
TANZANIA
INDIAN OCEAN
34° E
36° E
38° E
LEGEND
Major border faults
Lakes
Major rivers
Volcanoes
Large alluvial plains

The changing trends in the structural evolution and volcanic history of the Kenya Rift since the early Tertiary have had direct impacts on the basin physiography, drainage systems, and exposed bedrock that contributes to the sedimentary fill, chemistry, and early diagenesis of alluvial and lacustrine deposits (e.g., Baker, 1986; Tiercelin, 1990; Le Turdu et al., 1995; Wescott et al., 1996; Withjack et al., 2002). The resulting chemical and sedimentological characteristics of the lake basins, together with climate and topography, influence the composition and distribution of the fauna and flora (e.g., Anderson and Herlocker, 1973; Bell, 1982).

### *2.2.1. Lake Bogoria*

Lake Bogoria is a small, saline (60–100 $g^{-L}$ TDS), alkaline (pH: ~ 10.3) axial rift lake that lies against the steep Bogoria Fault in an eastwardly dipping axial half graben in the inner rift (Fig. 2.2; Renaut, 1982; Renaut and Tiercelin, 1994; Le Turdu et al., 1995). To the west, the Pleistocene Hannington Trachyphonolites form the Bogoria Plateau, which has been grid-faulted into a series of gently northwestward-dipping, stepped blocks that are buried beneath the sediments of the subsiding Baringo basin to the north (Le Turdu et al., 1995). Both the large-scale and small-scale structural features of the larger Baringo-Bogoria half graben are controlled in part by a series of heterogeneities in the basement oriented at 140–160°, derived from Precambrian shear zones of the Pan African Orogeny (Le Turdu et al., 1995, 1999). Normal faults of the rift are, in general, oriented N–S at ~0–10° as a result of E–W extension, unless they are deflected along inherited basement heterogeneities during their propagation (Morley, 1999; Le Turdu et al., 1999). The significance of the structural controls on the ichnology of the Baringo-Bogoria half graben, as well as the other basins considered in this study, is that they determine the drainage systems and the distribution and chemistry of the sedimentary environments including springs, which impact the local ecology and the formation and preservation of animal and plant traces and trace fossils.

The Baringo-Bogoria basin is transversely dissected in its central part by the Porumbonyanza-Ol Kokwe Transverse Zone (POKTZ) and the Waseges-Marmanet Transverse Zone (WMTZ), upon which the Baringo basin to the north and the Bogoria basin to the south are hinged (Le Turdu et al., 1995, 1999). The central region, the Loboi Plain, is a rapidly subsiding basin that sits between the two basement lineaments, and is filled mainly with siliciclastics up to a kilometer thick that rest upon several km of older sedimentary and volcanic rocks (Hautot et al., 2000; Whaler, 2006). Seismic data suggests that a central rift volcano, once present on the landscape, may have subsided below the present-day surface and is now buried by Pleistocene–Recent sediments (Le Turdu et al., 1995). The Baringo basin is a relatively broad and flat basin, which today contains a shallow lake with fresh waters (~1.5 g $L^{-1}$ TDS) that is filling rapidly with sediment from the Kamasia Range, known also as the Tugen Hills (Renaut et al., 2000a). The Bogoria basin, in contrast, is a narrow, tectonically active half-graben with a steep border fault on its eastern and southern margins, and a more gently dipping grid-faulted half-graben ramp of Pleistocene trachyphonolites in the Maji Moto grid-fault zone. The northern 'hinge-line' along the WMTZ forms the sill between the slightly higher Bogoria basin from the Loboi Plain in the Baringo basin (Le Turdu et al., 1995). The Bogoria basin is both topographically and hydrologically closed, except for infrequent spilling over the northern sill into the Baringo basin during wetter periods (Renaut and Tiercelin, 1994).

Lake basins have been present in the Baringo half-graben since the Miocene (Tiercelin et al., 1987; Renaut et al., 1999). Pleistocene–Miocene lake deposits and lava flows are preserved

**Fig. 2.2.** (Next page) Map of the Lake Bogoria area showing sites investigated for this study.

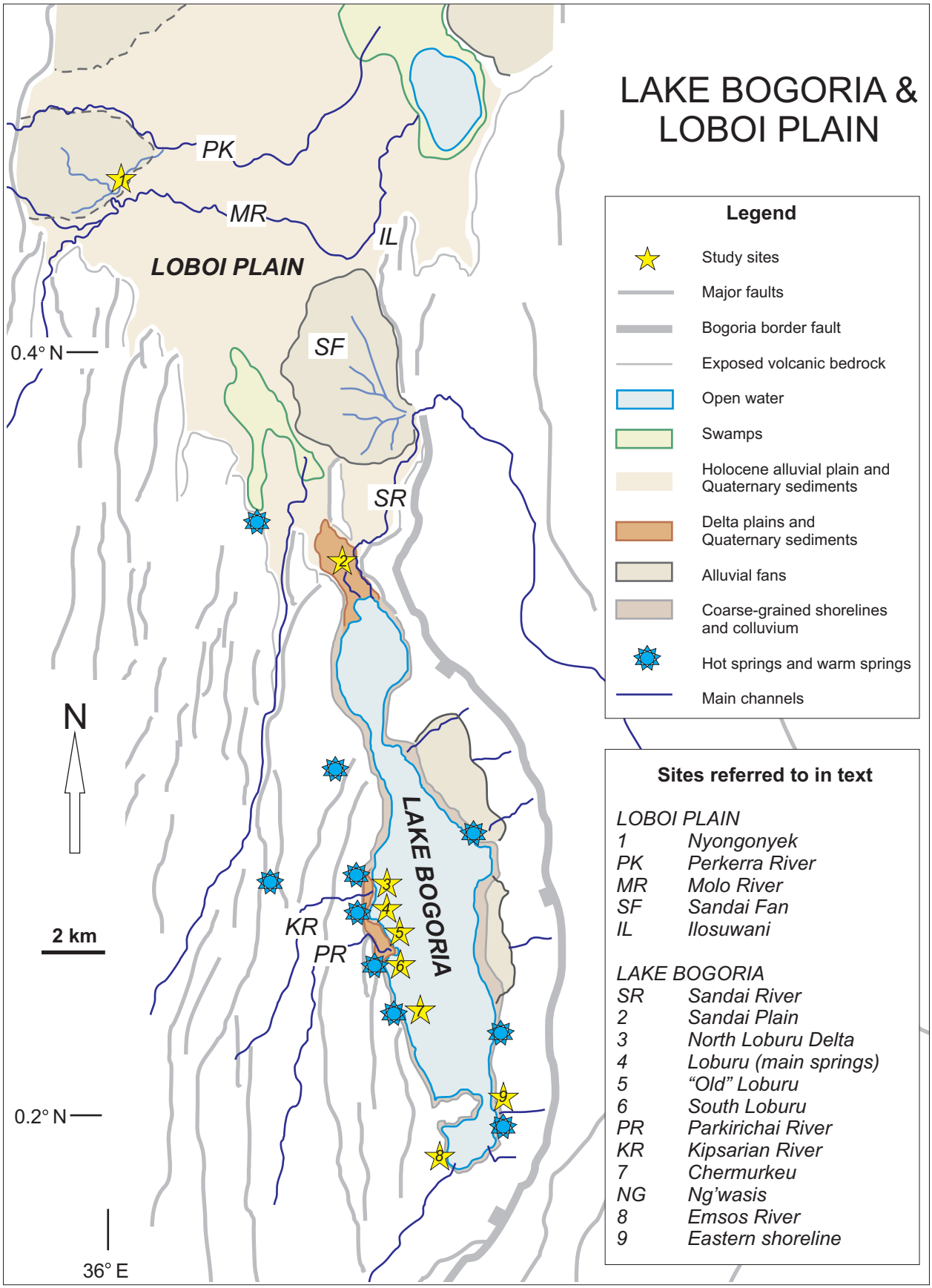
LAKE BOGORIA & LOBOI PLAIN
Legend
Study sites
Major faults
Bogoria border fault
Exposed volcanic bedrock
Open water
Swamps
Holocene alluvial plain and Quaternary sediments
Delta plains and Quaternary sediments
Alluvial fans
Coarse-grained shorelines and colluvium
Hot springs and warm springs
Main channels
Sites referred to in text
LOBOI PLAIN
1 Nyongonyek
PK Perkerra River
MR Molo River
SF Sandai Fan
IL Ilosuwani
LAKE BOGORIA
SR Sandai River
2 Sandai Plain
3 North Loburu Delta
4 Loburu (main springs)
5 "Old" Loburu
6 South Loburu
PR Parkirichai River
KR Kipsarian River
7 Chermurkeu
NG Ng'wasis
8 Emsos River
9 Eastern shoreline
PK
MR
IL
LOBOI PLAIN
SF
SR
LAKE BOGORIA
KR
PR
0.4° N
0.2° N
36° E
N
2 km

in the step-faulted and elevated Tugen Hills, which today form the eastern boundary of the Baringo basin. The Bogoria basin, in contrast, is a relatively young basin formed during the Pleistocene at approximately the same time as extension tectonics in the inner rift caused both the second phase of the Hannington Trachyphonolites (~500 Ka) to be extruded, and their subsequent grid-faulting into a series of connected horsts and small half-grabens and full grabens (Le Turdu et al., 1995, 1999; Clément et al., 2003). Today, the Molo River, which originates in the highlands near Lake Nakuru to the south, bypasses Lake Bogoria along the Molo Graben, and empties water and sediment into the Baringo basin at the Loboi Plain and the Molo delta of Lake Baringo (Fig. 2.2; Renaut and Tiercelin, 1994). The Sandai-Waseges River, which originates south of the Aberdares Range in the high elevation regions of the eastern rift near the Laikipia Plateau, drains into the Bogoria basin through an eroded gorge in the east-bounding Bechot border fault approximately along the WMTZ trend (Le Turdu et al., 1995).

Today, the climate in the Lake Bogoria region is semi-arid due to extreme evaporation, with rainfall of ~900 mm $yr^{-1}$ falling in two rainy seasons between March and August (Renaut and Tiercelin, 1994; Kipkorir, 2002; Ashley et al., 2004). Evaporation is high, at ~2600 mm $yr^{-1}$ (Renaut and Tiercelin, 1994). Lake Bogoria is perennial and relatively deep when compared to the other Kenya Rift lakes (except Lake Turkana) at about 10–12 m depth (Tiercelin et al., 1981, 1987). It is fed by numerous hot-springs that discharge into the lake subaerially via outflow channels on the lake margins, or subaqueously and directly into the more saline bottom waters of the lake (Renaut, 1982; Renaut and Owen, 1988; Renaut and Tiercelin, 1994). The lake is meromictic, with waters < 90 g $L^{-1}$ TDS forming the denser monimolimnion (Renaut and Tiercelin, 1994). Waters have Na–$CO_3$–$HCO_3$–Cl composition (Renaut, 1982). The lake basin is subdivided into three sub-basins by a structural sill that separates the north and central basins, and by Pleistocene volcanic rocks that separate the central from the south basin (Tiercelin et al., 1987). The salinity of both the mixolimnion and the monimolimnion varies between each of the sub-basins depending on the chemistry of the source that feeds them and the amount of inflow. In general, the north sub-basin tends to remain freshest because of the relatively high amount of meteoric inflow from the Sandai River, although in dry years the river may dry up before it reaches the lake (Tiercelin et al., 1987; Renaut and Tiercelin, 1994). The central sub-basin has the highest salinities, and has a proportionately greater amount of inflow from saline hot springs (Cioni et al., 1992; Renaut and Tiercelin, 1994).

The two larger deltas at Lake Bogoria were the main field areas investigated during this study. First, the Sandai delta-plain at the northern end of the lake consists of the southern-most extension of the Pleistocene Loboi Silts, a northward-thinning wedge of the overlying Bogoria Silts, and Holocene shoreline gravels and coarse-grained sands. Modern sedimentation is dominated by clay-rich silts and sands deposited in the channels and mouth of the Sandai River where it enters the lake on the eastern Sandai Plain. Deposition in ephemeral channels activated during the rainy season consists of current-rippled sands with clay-rich drapes that form wavy to flaser bedding. Frequent flooding of the shoreline mudflats during minor fluctuations in lake level leads to the intercalation of channelized and sheetwash delta-plain mud, silt, and sand, with lacustrine mud. Salt efflorescence (trona, thermonatrite) and eolian deflation and deposition contribute to the subaerial reworking of the modern sediments around the lake. Second, the Loburu Delta at the central western shoreline also consists of moderately well indurated Pleistocene sandstones, as well as Holocene lacustrine, shoreline, and delta-plain mud, silt, and sand. Modern littoral processes lead to both the deposition and reworking of fine- to coarse-grained sands, and subaerial exposure leads to the break-up of surficial sediments by salt efflorescence and deflation. Salt tolerant grasses and sedges are present along the shoreline and

around spring-fed pools and channels on the Loburu delta (Onkaware, 2000; R.B. Owen et al., 2004).

The biology of the Bogoria basin, a large part of which is within the Lake Bogoria National Reserve, is relatively well studied when compared with Lake Magadi and Nasikie Engida. The present-day salinity of the lake restricts the lake fauna mainly to cyanobacteria (*Arthrospira*) and chironomid larvae (Insecta: Diptera: Chironomidae), although historical accounts have stated that during fresher times, even hippos were present in the northern part of the lake (Jobe-Akeley, 1929; Tiercelin et al., 1987; Harper et al., 2003). Diatoms are rare in the lake, although they are relatively common in the littoral and spring-fed marshes that surround the lake (Tiercelin et al., 1987; R.B. Owen et al., 2004). Several species of ostracodes were found in cores of Holocene to late Pleistocene lake sapropels deposited during former fresher times, as were the gastropods *Melanoides tuberculata* and bivalves *Corbicula africana* (Tiercelin et al., 1987). Many species of insects, birds, and mammals can be found on the shorelines and lake-margin mudflats, which are present on the two main deltas: the Sandai delta-plain at the north end of the lake, and the Loburu delta on the central western margin (North-Lewis, 1998; Harper et al., 2003). Several other species of insects and mammals that create traces are also found in the slightly topographically higher regions on the alluvial fans and colluvium surrounding the lake. Notably, beetles (Insecta: Coleoptera), earwigs (Insecta: Dermaptera), flies (Insecta: Diptera), termites (Insecta: Isoptera), ants (Insecta: Hymenoptera), and spiders (Arachnida: Araneae) are common in the sediments surrounding Lake Bogoria.

Common mammals present in the Bogoria Reserve today include: zebras, warthogs, Grant's gazelles, impalas, African buffalos, greater kudus, klipspringers, dik-diks, savanna baboons, spotted hyaenas, leopards, mongooses, and hyraxes. Reptiles include four species of venemous snakes, monitor lizards, crocodiles, and tortoises. More than 350 species of birds are present in the region, and several of them nest and feed in the areas surrounding Lake Bogoria (Harper et al., 2003). In particular, flamingos, ostriches, several species of plovers, Marabou storks, yellow-billed storks, little egrets, sacred ibises, eared grebes, and fish eagles are relatively common, with Egyptian geese, teals, crowned cranes, hammerkops, and grey herons visiting ephemeral fresh water pools and the Sandai River (Scott, 2005; pers. obs., 2001, 2001, 2007, 2008). Numerous passerine species can be observed in areas surrounding the lake. For example, kingfishers, several species of weavers, lilac-breasted rollers, swifts, and martins are commonly seen.

### *2.2.2. Lake Magadi*

Lake Magadi lies in a tectonically active region of the southern Kenya Rift at ~600 m above sea level, in a topographically low point within the axial inner graben of the Kenya Rift (Fig. 2.3; Baker, 1986; Hollnack and Stangel, 1998; Behr and Röhricht, 2000). Water collects in the lowest portion of the axial inner rift, which is a complex graben broken up by Pleistocene normal faults and horsts in Pliocene and early Pleistocene trachytic lava flows that divide the Lake Magadi basin into several sub-basins (Baker and Wohlenberg, 1971; Baker, 1986). It is situated in an arid region south of the equator with high evaporation rates (~1.25–2.0° S; ~500 mm rainfall $yr^{-1}$; < 3500 mm $yr^{-1}$ potential evaporation) and presently receives water only from hot springs (< 200) and ephemeral runoff (e.g., Eugster, 1980, 1986; Behr and Röhricht, 2000). Rain water that falls in the western highlands (Mau Range) flows into the rift, but southwards along a step-faulted platform against the western boundary of the rift graben (Nguruman Escarpment) to the Lake Natron basin south of Lake Magadi (Fig. 2.1; Baker, 1986).

**Fig. 2.3.** (Next page) Map of the Magadi area showing sites investigated for this thesis. Drawn from Google Earth.

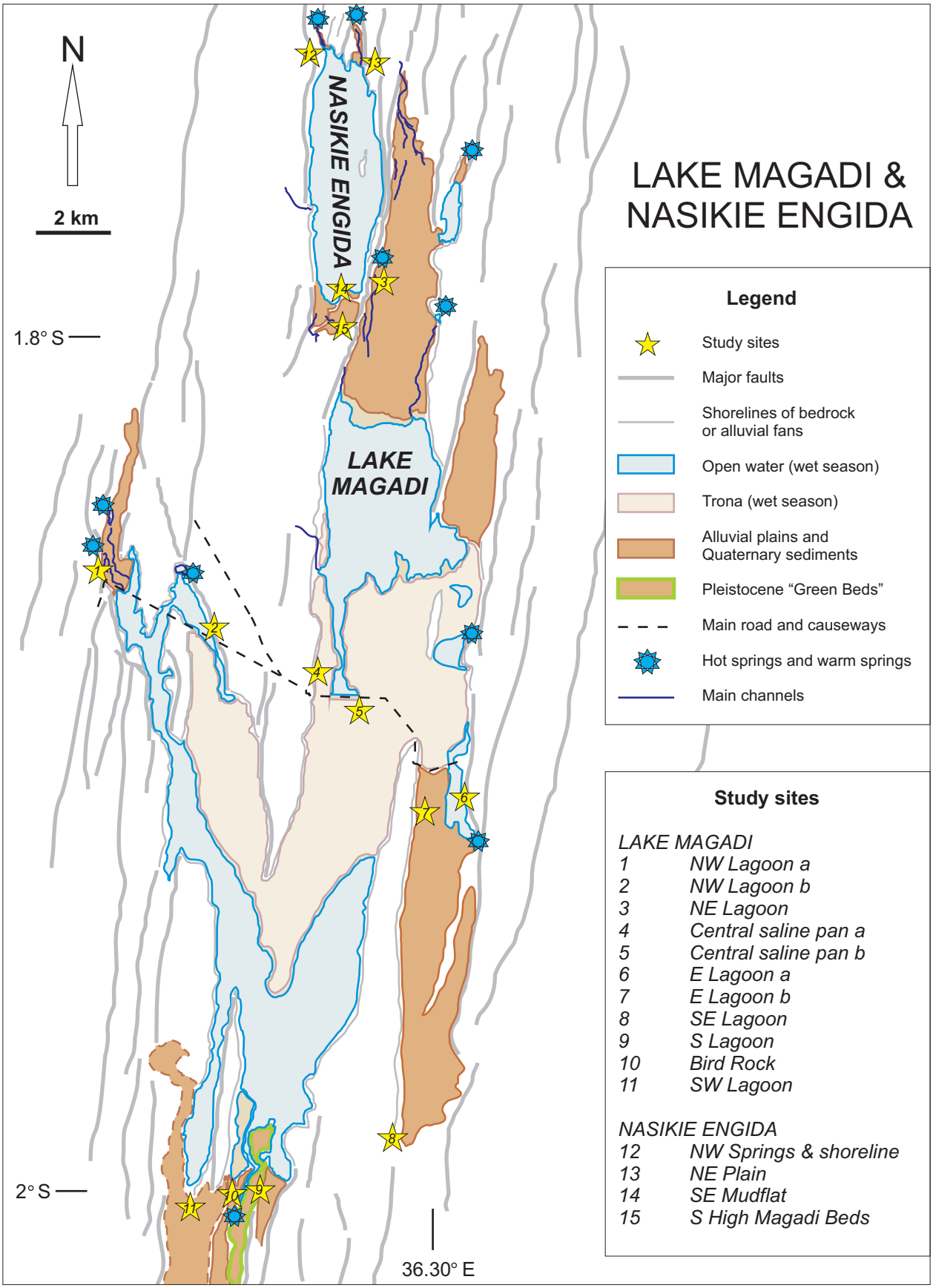
N
2 km
1.8° S
2° S
36.30° E
NASIKIE ENGIDA
LAKE MAGADI
LAKE MAGADI &
NASIKIE ENGIDA
Legend
Study sites
Major faults
Shorelines of bedrock or alluvial fans
Open water (wet season)
Trona (wet season)
Alluvial plains and Quaternary sediments
Pleistocene "Green Beds"
Main road and causeways
Hot springs and warm springs
Main channels
Study sites
LAKE MAGADI
1 NW Lagoon a
2 NW Lagoon b
3 NE Lagoon
4 Central saline pan a
5 Central saline pan b
6 E Lagoon a
7 E Lagoon b
8 SE Lagoon
9 S Lagoon
10 Bird Rock
11 SW Lagoon
NASIKIE ENGIDA
12 NW Springs & shoreline
13 NE Plain
14 SE Mudflat
15 S High Magadi Beds

In the Serengeti region to the southwest of Lake Magadi, rainfall is highest in April and lowest in June–July, with predictable seasonal fluctuations and a predictably wetter climate during El-Niño Southern Oscillations (Wolanski and Gereta, 2001). Very little rain water reaches the rift floor. Historically, rainfall is highest at Lake Magadi from March–May, and averages 472 mm $yr^{-1}$ with ~2500–3500 mm yearly evaporation (Behr and Röhricht, 2000; Becht et al., 2005). Lake water brines are highly saline and alkaline (pH: ~10.5), with Na–$CO_3$–Cl composition, and are derived from the chemical weathering of trachytic lava flows in the catchment (Surdam and Eugster, 1976; B.F. Jones et al., 1977; Eugster, 1980). The highly alkaline waters in Lake Magadi may also be in part due to the leaching of nearby carbonatite lavas (Bell et al., 1973; Baker, 1986). Hot springs, in contrast, vent Na–$HCO_3$–Cl waters with temperatures up to ~82° C (Surdam and Eugster, 1976).

Repeated wetting and drying cycles lead to the precipitation of efflorescent evaporites and their dissolution by meteoric runoff, which increases the evaporative concentration of the lake waters (B.F. Jones et al., 1977; Eugster, 1986). Ephemeral inflow of runoff with Na–Ca–$HCO_3$–Cl composition reaches the lake from the basin margins in part by weakly channelized flow in ephemeral-stream floodplains (Eugster, 1980). The lake brine is also recharged by groundwater-fed springs, which can be relatively fresh (1000–2000 ppm TDS) or highly saline (< 35000 ppm TDS), depending on whether they are sourced by deep, hot water aquifers, or by dilute, cold, shallow groundwater, or by concentrated, alkaline, and cold recirculated lake brine, or a mix (B.F. Jones et al., 1977; Eugster, 1980, 1986). It has also been suggested that hot-spring waters may be sourced from the sub-surface seepage of lake waters at Lake Naivasha (B.F. Jones et al., 1977; Darling et al., 1990; Becht et al., 2005), although this is unsupported by stable isotope analyses (Allen et al., 1989).

The shape of the lake is controlled by three narrow fault-bound grabens, which is crossed by a NW–SE oriented fault zone (Behr and Röhricht, 2000). The shape of the lake basin, the generally steep gradients of the bounding fault blocks, and the location of ephemeral drainage into the lake have a direct impact on sedimentation and the distribution of clastic lithofacies (e.g., Surdam and Eugster, 1976; Baker, 1986; Eugster, 1986). Although there has not yet been a detailed study of clastic sedimentation completed at Lake Magadi, Eugster (1986) summarized the sedimentary facies present in the Magadi basin. Several subfacies commonly found in hydrologically closed basins (Hardie et al., 1978) were recognized at Lake Magadi, including: 1) salt pan; 2) spring marsh and perennial lagoon; 3) saline mudflat; 4) dry sandflat and mudflat (and old lake beds); 5) delta; 6) spring deposit; 7) ephemeral stream floodplain; and, 8) alluvial fan (Eugster, 1986). Behr and Röhricht (2000) and Behr (2002) also recognized several different types of chert in Pleistocene–Holocene deposits of the Magadi basin, some of which show evidence of subaerial exposure (e.g., desiccation cracks), microbial lamination, and trace fossils (Behr, 2002). Casanova (1986) briefly described the formation of disc-like oncolites by microbially mediated low-Mg calcite precipitation on ephemerally wetted floodplains not associated with phases of lacustrine expansion. In contrast, they may signify drier periods with evaporative floodplains (Casanova, 1986).

Biological studies at Lake Magadi have focused on the physiological adaptations that allow teleost fish (*Alcolapia grahami*) to inhabit the highly alkaline and saline spring-fed pools present at various localities along the lake-margin mudflats and lagoons (e.g., Reite et al., 1974; Wood et al., 2002; Bergman et al., 2003). The characterization and identification of novel bacteria and archaea species is also a major area of biological research (e.g., Duckworth et al., 1996; Grant et al., 1999). Microbial ecology has been investigated at Lake Magadi (e.g., Tindall et al., 1980; Tindall, 1988; Dubinin, 1995). Entomological studies at Lake Magadi appear to be

rare, although a new species of water scavenger beetle (Coleoptera: Hydrophilidae) was identified in the shallow pools that surround the lake (Spangler and Steiner, 2003). Spangler and Steiner (2003) also report the identification of wolf spiders (Arachnida: Araneae: Lycosidae: *Wadicosa* sp.), whirligig beetles (Coleoptera: Caraboidea: Gyrinidae: *Orectogyrus* sp. and *Gyrinus* sp.), and the earwig *Labidura riparia* (Dermaptera: Labiduroidea: Labiduridae). Tiger beetles (Coleoptera: Caraboidea: Cicindelidae: *Lophyra pseudodistans*) have also been identified to species (Werner, 1993). Termite (Insects: Isoptera) mounds of fungus-growing termites (e.g., Macrotermitinae, Odontotermitidae) are found in higher, stable slopes surrounding the lake (pers. obs., 2007, 2008).

Published accounts of the vertebrate diversity at Lake Magadi appear to be similarly uncommon, and include brief notes about greater flamingos, avocets, plovers, and other shorebirds. Several bird species were observed during field study. Lesser flamingos (*Phoeniconaias minor*) frequent Lake Magadi, although they only infrequently breed there (Brown and Root, 1971). Predators of flamingos observed at Lake Magadi reported by Brown and Root (1971) include Marabou storks (*Leptoptilos crumeniferus*), tawny eagles (*Aquila rapax*), Egyptian vultures (*Neophron percnopterus*), white-headed vultures (*Trigonoceps occipitalis*), spotted hyenas (*Crocuta crocuta*), jackals (*Canis* sp.), lions (*Panthera leo*), leopards (*Panthera pardus*), and cheetahs (*Acinonyx jubatus*). An African wild cat (*Felis libyca*) was also observed in the northern Magadi basin, just south of lake Nasikie Engida (Aug., 2008, pers. obs.). Large, migratory mammals such as wildebeest (*Connochaetes taurinus*) and zebras (*Equus burchelli*), and their predators (e.g., lions, hyenas), are most abundant in the Serengeti savanna highlands southwest of the Magadi basin in Tanzania, but also use the relatively dry grasslands of the Lake Magadi region during the rainy seasons (e.g., Wolanski and Gereta, 2001). Domestic cattle and goats are also present in the Magadi basin (e.g., Sitters et al., 2009).

Ecological assessments of the Magadi Basin have not yet been completed, to the knowledge of this author. Mammals, in particular, are very poorly known from saline lakes worldwide (Hammer, 1986), and baseline ecological data is lacking for most of the Kenyan saline lakes (Matagi, 2004). Several large mammal species are also known to have occurred in the Magadi region, and include: hunting dog (*Lycaon pictus*), elephant (*Loxodonta africana*), black rhinoceros (*Diceros bicornis*), warthog (*Phacochoerus aethiopicus*), giraffe (*Giraffa* sp.), steenbock (*Raphicerus campestris*), klipspringer (*Oreotragus oreotragus*), impala (*Aepyceros melampus*), Grant's gazelle (*Gazella granti*), gerenuk (*Litocranius walleri*), Coke's hartebeest (*Alcelaphus buselaphus cokii*), and eland (*Taurotragus oryx*) (Stewart and Stewart, 1963). Identifications based on personal observations of vertebrates or invertebrates were made where possible. The photographic data recorded during 2007 and 2008 represents a snapshot view of the ecology and behaviour. This “ad libitum” sampling of the animals present was dictated by logistical constraints, and the sites were not systematically sampled.

### *2.2.3. Lake Nasikie Engida*

Nasikie Engida, commonly known as “Little Magadi”, is a small lake (~0.5 km wide, 6 km long) in a small graben northwest of Lake Magadi, and is separated from the larger lake by a N–S trending horst to the east with relatively low relief (< 100 m) (Fig. 2.3; Renaut et al., 2007). The lake is bounded on the west by the near vertical wall of a N–S trending block of normal-faulted Pleistocene trachyte. Intense faulting of Pliocene basalt and trachyte flows of the interior rift into many isolated grabens and step-faulted platforms occurred during the late Quaternary (Baker and Wohlenberg, 1971; Baker, 1986). The southern margin is relatively gently sloping, contains muddy to sandy shoreline and lacustrine deposits, and is separated from the Lake

Magadi basin to the south by trachytic lava, which appears to not have been downfaulted to the extent of the Nasikie Engida lake basin. The northern margin comprises salt-encrusted mudflats and coarse sand-sized sheetwash, silica-rich organic gels, trachyte boulder colluvium, and a small delta at the northwest margin fed by a group of hot springs along the west-bounding normal fault.

The lake is shallow (< 1.5 m deep), perennial, and is fed almost entirely by the hot springs (Renaut et al., 2007). The spring and lake waters are highly alkaline (pH: ~9.2–9.9; B.F. Jones et al., 1977), and the corrosion of trachyte bedrock and boulders from these waters provides evidence of higher lake levels up to ~1.5 m higher than present (Renaut et al., 2007). Salinity of the lake waters increases southward (< ~134000 ppm; B.F. Jones et al., 1977), with distance from the relatively fresh, alkaline input from the hot springs at the northwest (< ~29000 ppm; B.F. Jones et al., 1977) (Renaut et al., 2007). Hot-spring effluent at the northwest margin of Nasikie Engida is dominated by Na and $HCO_3$ ions, with relatively minor $CO_3$ and Cl, and small amounts of Ca, $SiO_2$, $SO_4$, F, and Br in solution (Surdam and Eugster, 1976). Spring water has a temperature of up to 82°C and contains 26.6 g $kg^{-1}$ TDS (Surdam and Eugster, 1976; B.F. Jones et al., 1977). A fresh, groundwater-fed drinking well in trachytic bedrock just northeast of the lake also contains Na–$HCO_3$–Cl water, but only 0.9 g $kg^{-1}$ TDS and has a pH of 8.0 (Surdam and Eugster, 1976).

Trona efflorescence forms around the lake margin, particularly on the microbe-rich mudflats at the south end of the lake. During times of lower lake levels (e.g., Aug. 2009), euhedral nahcolite crystals precipitate heterogeneously and subaqueously on the lake floor in the shallow Na–$HCO_3$–Cl evaporating brine (Renaut, pers. comm., 2009). Rafts of nahcolite and trona precipitate relatively quickly at the air-water interface in the southern, more saline, part of the lake.

The ecology of the Nasikie Engida area has not yet been assessed, to the knowledge of the author. Mammals reported by Stewart and Stewart (1963) in the Lake Magadi region have been cited above. The results of this study provide a preliminary list of some of the vertebrates and invertebrates that use the area. In particular, several species of insects and spiders, together with birds and mammals, were either directly observed, or evidenced by their tracks. Nasikie Engida, like Lake Magadi, lies in an arid region with relatively lower biological diversity than the neighbouring highlands (e.g., the Serengeti). The hot springs at the north end of Nasikie Engida were briefly investigated to determine whether vertebrate and invertebrate life, and their traces, may be concentrated at this perennial, relatively fresh water source. The mudflats at the south end of the lake were also briefly visited.

## 2.3. Pleistocene–Holocene Lake-margin, Delta, Wetland and Alluvial Plains, Kenya Rift

### *2.3.1. Baringo-Bogoria Basin*

As stated above, the Baringo-Bogoria basin is part of a large half-graben structure in the central Kenya Rift Valley that is subdivided into two sub-basins by transverse basement structures upon which the lake basins are hinged (i.e., the POKTZ and WMTZ; Le Turdu et al., 1995, 1999). The Kamasia Range west of the modern Baringo lake basin (Fig. 2.1) contains Miocene–Pleistocene lacustrine and alluvial sediments deposited before the more recent tectonism in the region that occurred at approximately 300 Ka (Bishop and Chapman, 1970; Bishop et al., 1971; Bishop and Pickford, 1975; Hill et al., 1985; Le Turdu et al., 1995). These sedimentary formations provide evidence of a series of saline, alkaline and freshwater lakes, as well as groundwater-fed spring tufas, that were emplaced syndepositionally with active uplift of the central Kamasia range, and the continuing subsidence of the inner rift (Le Turdu et al., 1999; Renaut et al., 1999, 2000a; R.B. Owen and Renaut, 2000; C.R. Johnson et al., 2009).

The Miocene Ngorora Formation represents the lacustrine and lake-margin deposits of a saline, alkaline lake ponded during the early stages of downfaulting of the inner rift trough, prior to the uplift of the central horst (Kamasia) that later divided the western Elgeyo trough from the Baringo-Bogoria trough (Bishop and Chapman, 1970; Bishop and Pickford, 1975; Tiercelin et al., 1987; Ego, 1994; Renaut et al., 1999). Vertebrate trace fossils (i.e. bird footprints) were reported from wave-rippled sandstones from shoreline sediments of the Ngorora Formation, together with desiccation cracks preserved in clay-rich mudflat deposits (Renaut et al., 1999). An exposed section of the Ngorora Formation near Kapkiamu comprising mainly green-coloured laminated lacustrine strata containing fish fossils and desiccation cracks, and tuffaceous paleosols and sandstones was visited briefly during this study. Renaut and Ego (unpublished; Ego, 1994) investigated the mineralogy of the Ngorora Formation in detail, and presented a measured section of a portion of the formation (Member C) in Renaut et al. (1999). Carbonate root casts and rare burrows were found. Several examples of possible poorly preserved vertebrate tracks were noted, and one sample with fish swimming traces (*Undichna* isp.) was identified.

Following the subsequent extrusion of the Ewalel Phonolites that buried the Ngorora lake deposits and the further uplift of the Kamasia Horst, Lakes Lukeino, Chemeron, and Kapthurin partly filled the subsiding eastern basin at various times during the Pliocene to middle Pleistocene (Bishop et al., 1971; Tiercelin et al., 1987; Renaut et al., 1999, 2000a; R.B. Owen and Renaut, 2000). Sediments of the Kapthurin Formation provide evidence of a lake, or a set of lakes, with fluctuating salinities during the Pleistocene (Renaut et al., 1999, 2000a). Trace fossils including bird and mammal footprints and horizontal invertebrate burrows are preserved in the upper Kapthurin Formation (Bedded Tuff: K4; ~235 Ka; Tryon and McBrearty, 2002) at Rorop Lingop on a step-faulted block west of Lake Baringo (Scott, 2005). Other localities with bioturbated Kapthurin sediments have been reported, but without details of the traces (e.g., C.R. Johnson et al., 2009). The informally named Ilosuwuani formation on the eastern side of the Baringo basin at the Ilosuwuani Horst which may be equivalent to the uppermost Kapthurin Formation (Farrand et al., 1976), also preserves many vertebrate footprints and vertical invertebrate burrows (Scott, 2003, 2005; Scott et al., in prep.).

The stratigraphic nomenclature in place for sedimentary rocks and unlithified sediments deposited after the middle Pleistocene in the Baringo-Bogoria basin remains informal. The correlation of time-equivalent stratigraphic packages has not yet been established, in part due to a lack of absolute dates, and in part due to the complexities of late Pleistocene to Recent grid-faulting and variable rates of subsidence to the north and south of the WMTZ that today divides the Baringo basin from the Bogoria basin. Of particular interest for this study are the middle to late Pleistocene Loboi Silts and the latest Pleistocene–Holocene Bogoria Silts, which are both present in the Bogoria basin.

*2.3.1.1. Loboi Silts*— The Loboi Silts comprise a series of unconsolidated to well cemented alluvial and fluvio-lacustrine siltstones, sandstones, and fluvial volcaniclastics. In general, their colour is reddish brown to brown. They represent a diachronic unit that rests unconformably on the Kapthurin Formation near the eastern boundary of the Loboi Plain at the eastwardly dipping Kapthurin Fault (2–3°), and laterally adjacent to the uppermost Kapthurin further north (K5) (Le Turdu et al., 1995; McBrearty, 1999; Renaut, pers. comm., 2005). At their eastern edge in the Loboi Plain of the Baringo basin, they contain Middle Stone Age artifacts and may be as old as 200 Ka (Farrand et al., 1976). Vertebrate burrows and insect nests and burrows are preserved by carbonate in fine-grained alluvial sediments exposed by badland weathering at

the locality of Nyongonyek (Fig. 2.2). They can be roughly dated to the middle Pleistocene using Middle Stone Age artifacts which appear to be concentrated in several places at a single horizon that overlies the trace-preserving portion of the section (Farrand et al., 1976). A fluvially reworked ash unit will help to constrain the age of these trace fossils and artifacts once it is dated. It has been suggested that the older silts at Nyongonyek and younger Loboi silts may be separated by a fault in the Loboi Plain (Farrand et al., 1976). U-series dating of the carbonate rhizoliths and/or trace fossils preserved as carbonate casts may also be possible, and would help to place the artifacts, trace fossils, and the associated sediments into the improving temporal framework of the basin history. It has also been suggested that a large lake called the "Loboi Lake" may have been present on the eastern side of the Baringo-Bogoria half-graben at some point during the middle to late Pleistocene (McCall, 1967; Farrand et al., 1976), although clear evidence to support this paleolake is lacking.

Towards the southeast, younger alluvial deposits also referred to as the Loboi Silts stretch into the northern axial plain of the Bogoria basin, becoming younger as they approach the modern shoreline of Lake Bogoria. In general, the Loboi Silts show characteristics of increasing influence from the saline, alkaline conditions southward into the Bogoria basin, and an increasing degree of induration by zeolite cements (e.g., Renaut, 1993). It appears, based on stratigraphic relationships and early diagenetic features, that the Loboi Silts were deposited prior to about 20 Ka, and were subsequently cemented by zeolites and calcite during an extended dry period from ~20–12 Ka across the Kenya Rift (Adamson et al., 1980; Hamilton, 1982; Renaut, 1993). The stratigraphy of the Loboi Silts on the Sandai Plain has been discussed in detail by Scott et al. (2008).

Vertebrate (Scott, 2005; Scott et al., 2008) and invertebrate (Scott et al., 2009; this thesis) trace fossils are preserved in the relatively well cemented uppermost beds of the Loboi Silts on Sandai Plain at the north end of Lake Bogoria, as well as in a time-equivalent set of exhumed surfaces on the Loburu delta of the central western shore. The uppermost Loboi Silts comprise a set of poorly to moderately sorted siltstones and K-feldspar sandstones cemented by zeolites, calcite, and Fe- and Mn-oxyhydroxides, with authigenic smectite clay minerals contributing to their relatively high degree of induration (Renaut, 1982, 1993; Scott et al., 2008). Scott et al. (2008) suggested that a spring-fed marsh may have been present on the Sandai Plain during the latest Pleistocene, which contributed to the cementation by zeolites and calcite of root-mats and sediments of the trace-preserving beds. During fieldwork in August, 2008, small travertine and tufa mounds, and stromatolite-coated plant stems formed at spring vents were found on the central and southwestern Sandai Plain. The trace fossils and lithofacies of the exhumed surfaces are described later in this thesis.

*2.3.1.2. Bogoria Silts*— The Bogoria Silts are a northward-thinning wedge of Holocene laminated and unconsolidated lacustrine brown silts that lie disconformably upon the Loboi Silts on Sandai Plain (Farrand et al., 1976; Renaut, 1993). They were deposited solely in the Bogoria basin during a period of higher lake levels, which may have occurred between 12,000 and 6000 years ago (Tiercelin et al., 1981). During the "African Humid Period", which culminated between ~9–6 Ka, several lakes in the Kenya Rift Valley experienced high lake levels, and generally more humid conditions are also evidenced by high lake levels from ~15–5.5 Ka (e.g., Butzer et al., 1972; Street and Grove, 1976; deMenocal et al., 2000; Garcin et al., 2009). This period of overall higher lake levels was briefly interrupted by a dry phase that occurred at ~12–13 Ka (Garcin et al., 2009). Some authors have shown that there was an extended arid period from ~18–12 Ka following the Last Glacial Maximum (Adamson et al., 1980; Hamilton, 1982). More recently, however, other authors have shown that a hyperarid period existed during

the Last Glacial Maximum from ~23–19 Ka, and was followed by the onset of more humid conditions during the latest Pleistocene and early Holocene (Gasse, 2000; Gasse et al., 2008). The post-glacial warming/wetting began ~18–16 Ka in steps of rapid wet/dry oscillations, with two drastic arid-humid transitions occurring at ~15–14.5 Ka and ~11.5–10.5 Ka (Gasse et al., 2008). High lake levels in the Magadi basin in the southern rift are evidenced by the upper High Magadi Beds (discussed below), and may also be attributed to more humid climatic conditions at ~12–9 Ka, followed by drier conditions by ~7 Ka (Butzer et al., 1972; Behr, 2002). Variability in the precise timing of increased rainfall and higher lake levels between the African lake basins may have contributed to the interaction between changes in local climatic conditions and the changing global patterns in the late Pleistocene and Holocene (Garcin et al., 2009).

Today, the Bogoria Silts are patchily distributed across the Sandai Plain due to their erosion by subaerial processes (i.e. eolian deflation, sheetflooding and shallow incision), which expose the underlying and better-cemented Loboi Silts. Delta-plain erosive and depositional processes cause strong lateral variability in the age of the deltaic and delta-plain sediments, so that patches of the Bogoria Silts lay adjacent to later Holocene gravel beach bars and recent alluvial and sheetwash deposits. East of the Sandai River, approximately 800–1000 m from the modern shoreline, sub-fossil flamingo nest mounds are preserved in the Bogoria Silts, although they previously were thought to be older (cf. Scott et al., 2008). Farrand et al. (1976) found a diverse assemblage of vertebrate body fossils (e.g., hippopotamus, crocodile, and fish) that signify relatively freshwater conditions in the lake at that time. The gastropod *Melanoides tuberculata* and the bivalve *Corbicula africana*, also preserved in the Bogoria Silts, aid in this interpretation. These molluscs have been dated to ~10.5 Ka from along the western shore of Lake Bogoria (Young and Renaut, 1979). The relatively high lake levels in the Bogoria basin may correspond roughly to high lake levels in the Baringo basin (e.g., at Ilosuwani), where shells in coquinas of the Kokwob Murren Beds were dated to ~13.7–10 Ka (Young and Renaut, 1979; Tiercelin et al., 1987).

Most of the unconsolidated to weakly cemented Bogoria Silts have either been eroded from steep margins of the lake during subsequent episodes of high lake levels in the middle Holocene (Casanova, 1986; Vincens et al., 1986), or were not originally deposited in those areas, or their distinction from more recent Holocene sediments remains ambiguous. It is unknown if remnants of the Bogoria Silts, or coeval shoreline deposits, are preserved on the eastern margin of the lake. The somewhat indurated reddish silts and interbedded sands of the southern lobe of the Loburu delta on the western margin of the lake, however, may have been deposited during the Bogoria Silts highstand by fine-grained alluvium emptying into the lake where the Parkirichai River enters the lake basin. Until further research is conducted and/or reliable dates are available, it will not be possible to confirm this, although based on observations made during fieldwork and high resolution satellite imagery (Google Earth, 2009) that provides evidence for the development of at least three main delta lobes at Loburu, this suggestion seems reasonable. Similar horizontally bedded reddish buff silts and sands interbedded with colluvial cobbles and gravels are exposed in a section by the ephemeral stream that feeds the smaller delta at north Loburu (Renaut and Tiercelin, 1994).

### *2.3.2 Lake Magadi Basin*

The Lake Magadi basin has contained lakes of variable size and salinities, with corresponding differences in sedimentary deposits, since ~800,000 years ago (e.g., Eugster, 1980; Behr, 2002). The first lake in the history of the basin, Lake Oloronga, was a large, relatively deep and fresh water lake that may have also filled the Lake Natron basin of Tanzania (Eugster, 1980). The Oloronga Beds comprise a series of airfall tuffs, lacustrine carbonates, and

diatomaceous cherts (Eugster, 1980; Behr, 2002) deposited prior to the intense Pleistocene block faulting of trachyte flood lavas that created the series of sub-basins that Lake Magadi now fills (Baker and Wohlenberg, 1971; Baker and Mitchell, 1976; Baker, 1986). A thick and widespread calcrete developed on the Oloronga Beds during an extensive depositional hiatus that may have occurred during a long period of arid conditions that lasted up to ~200,000 years (Eugster, 1980). Other, less well-developed calcretes formed more recently (Behr, 2002). The Oloronga Beds and the calcrete that caps the lake deposits were not examined in this study.

The "Green Beds" directly overly the Oloronga Beds, and comprise up to 30 m thick of green-coloured cherts and their associated deposits (Behr, 2002). Eugster (e.g., 1980) considered these cherts together with the "Magadiite cherts" of the younger High Magadi Beds, although Baker (1958) had originally recognized more than one chert unit. Behr and Röhricht (2000) and Behr (2002) re-examined the Green Beds in greater detail, and with an approach that considered the microbial influence on the formation of cherts at Lake Magadi. The Green Beds were also briefly examined in this study. The ichnofossils reported by Behr and Röhricht (2000) and figured by Behr (2002; his fig. 24) were investigated from the eastern portion of the "SW lagoon", where approximately 10 m of the cherts of the Green Beds are well exposed. Behr (2002) recognized an extensive calcrete above the Green Beds that represents a hiatus in deposition of approximately 20,000 years.

The Pleistocene to early Holocene High Magadi Beds have been dated to 23,700–9310 years B.P. (Behr, 2002), and consist primarily of laminated brown siltstones and fine-grained tuffaceous sediments that contain thin, laterally extensive units of white magadiite chert (Eugster, 1980; Behr, 2002). Discrete ichnofossils and undifferentiated bioturbation were reported from the lower High Magadi Beds by Behr (2002), but no detailed information was provided. A relatively thick chert-rich calcrete unit dated to ~14.5 Ka divides the High Magadi Beds into an older unit and a younger unit. Fish fossils ('*Tilapia*' sp.) are more common in the older, lower, portion of the High Magadi Beds, but also appear at the top of the High Magadi Beds (Behr, 2002). The High Magadi Beds are found around the modern lake in the Magadi Basin, and equivalent brown siltstones to gravels and white chert beds are also found at the southern shoreline of modern lake Nasikie Engida (Renaut, pers. comm., 2007). Just south of the Nasikie Engida basin, an additional small outcrop of the High Magadi Beds preserves trace fossils (Fig. 2.3). The stratigraphic position of these buff-coloured silts and sands is not constrained, although it appears that they are above the magadiite chert layer within the High Magadi Beds, and may be just below the calcrete that divides the High Magadi Beds into two units (cf. Behr, 2002).

Modern trona precipitation began ~7 Ka B.P. in the central Magadi Basin, and has led to the accumulation of up to ~35 m of trona and associated sodium carbonate salt minerals (Butzer et al., 1972). Trona and nahcolite precipitation in an 8 cm-thick bed has been dated to ~9 Ka in Nasikie Engida (Behr, 2002).

## 2.4. Early–Middle Eocene Lake Gosiute, SW Wyoming and NW Colorado, U.S.A.

### *2.4.1. Overview*

The Green River Formation comprises almost 2000 m of siliciclastic, carbonate, and evaporitic (mainly trona) lacustrine and lake-margin strata deposited during the early to middle Eocene (53 Ma–45 Ma) in southwest Wyoming, northwest Colorado, and northeast Utah, U.S.A. (Fig. 2.4; e.g., Bradley, 1964; Roehler, 1992a, 1992b, 1993; M.E. Smith et al., 2008b). Cambrian to Cretaceous carbonates and sandstones of the Cordilleran or Sevier thrust belt (Jurassic–Eocene) formed the western margin of the older Cretaceous foreland basin (e.g., Dickinson et al., 1988; DeCelles, 2004). Movement on the thrust faults continued until ~50 Ma (e.g., DeCelles and Mitra, 1995; Yonkee and Weil, 2010). From the latest Cretaceous to the

middle Eocene, several basement-cored uplifts segmented the foreland and created the ponded and axial lake-basins of SW Wyoming, NE Utah, and NW Colorado, in which the Green River Formation was deposited (e.g., Dickinson et al., 1988; Steidtmann and Middleton, 1991; DeCelles, 2004; Mederos et al., 2005). The basins were bounded by these Laramide uplifts of Precambrian basement (e.g., Wind River Uplift) or Precambrian-Cambrian mudstones (e.g., Uinta Uplift), flanked by Paleozoic and Mesozoic sedimentary rocks (mainly marine carbonates and sandstones) (e.g., Dickinson et al., 1988; DeCelles, 2004; Carroll et al., 2006). Several interbasinal, anticlinal structural sills also related to Laramide tectonics further divided the basins into several sub-basins, which impacted sedimentation and lake salinity (e.g., Roehler, 1992a; M.E. Smith et al., 2008b). The positions of both the basin-bounding Laramide uplifts and the internal sills were influenced by Precambrian faults, suture zones, and possibly by basement lineaments (e.g., Maughan and Perry, 1986; Steidtmann and Middleton, 1991; Marshak et al., 2000; Mederos et al., 2005; Bader, 2008).

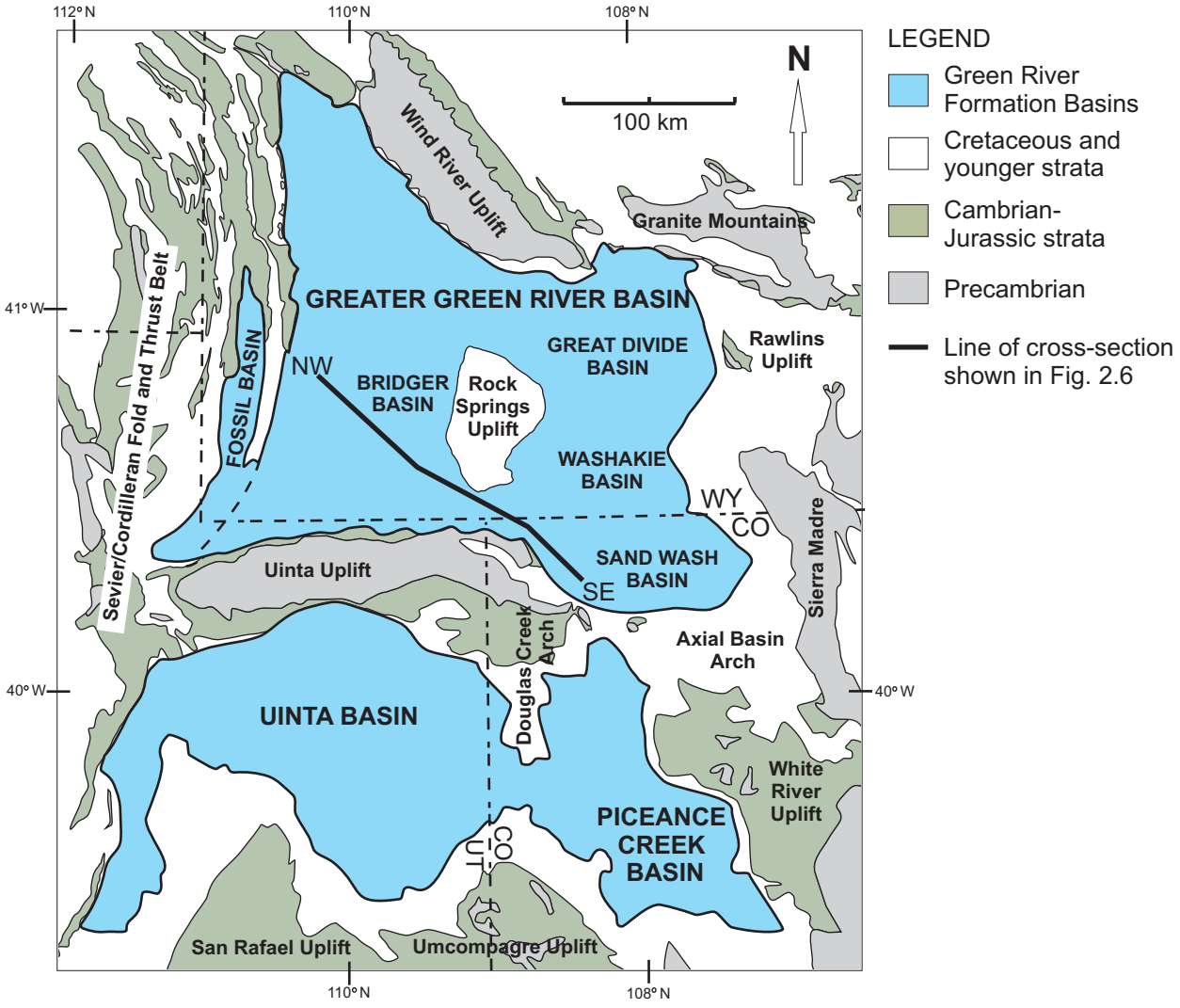


**Fig. 2.4.** Map of the Green River Basins of SW Wyoming, NW Colorado, and NE Utah. Redrawn from M.E. Smith et al. (2008b).

"Lake Gosiute" of the greater Green River basin in Wyoming and Colorado, "Fossil Lake" of the intermontane, axial Fossil basin in SW Wyoming, and "Lake Uinta" of the Piceance Creek basin in Colorado and the Uinta basin in Utah each varied in their salinity, areal extent, and types of sedimentary deposits throughout their history (e.g., M.E. Smith et al., 2008b and references therein). At times, the lakes were interconnected hydrologically, while always interfingering with the surrounding alluvial sediments that comprise the Wasatch, Washakie, Bridger, and Uinta Formations (Roehler, 1992b, 1993). The Green River Formation and its correlative equivalents are rich in oil shale (e.g., Carroll and Bohacs, 2001), coal, uranium, and trona deposits (e.g., Bradley and Eugster, 1969; Wiig et al., 1995), and contain diverse mineral suites (e.g., Surdam and Parker, 1972; Surdam et al., 1972; Goodwin, 1973). Fossil floras and faunas are also exceptionally diverse (e.g., MacGinitie, 1969; Wilson, 1978; Grande, 1984; Wilf, 2000; Zonneveld et al., 2000a; Gunnell and Bartels, 2001). The sediments were deposited in alluvial, fluvio-lacustrine, profundal lacustrine, and evaporitic environments that changed through time according to the tectonic activity and geomorphic evolution of the region, which dictated the amount of inflow and outflow to each of the basins (Carroll and Bohacs, 1999; Bohacs et al., 2000; Carroll et al., 2006, 2008; M.E. Smith et al., 2008b; Doebbert et al., 2010). These lake basins were then overwhelmed in the middle Eocene (~48–47 Ma) by volcaniclastic sedimentation in a series of deltas (e.g., Sand Butte Bed of the Laney Member), terminated by deposition in alluvial plains of volcaniclastics and arkosic siliciclastics (e.g., Bridger and Washakie Formations) (e.g., Roehler, 1993; Buchheim et al., 2000; M.E. Smith et al., 2008b and references therein; Chetel and Carroll, 2010).

### *2.4.2. Climate and Paleobotany*

The Green River Formation and its time-equivalents were deposited during the warmest period of the Cenozoic (the Early Eocene Climatic Optimum, EECO; ~52–50 Ma), a period of high atmospheric $CO_2$ and warm ocean temperatures (< 11°C) (e.g., Zachos et al., 2001, 2008). Based on the $\delta^{18}O$ and $\delta^{13}C$ isotope record from foraminiferans in deep-sea cores, global sea temperatures declined following the EECO, particularly at the poles, until polar ice accumulated in the early Oligocene (e.g., Zachos et al., 2001; Pearson et al., 2007). Overall elevated atmospheric $CO_2$ during the early Eocene has been invoked to explain the extensive sodium carbonate evaporite deposits (e.g., nahcolite) in the Piceance basin of Colorado (Lowenstein and Demicco, 2006). Estimates of the early Eocene atmospheric concentrations of $CO_2$ based on these deposits are between 1125 and 2985 ppm, several times the modern values (Lowenstein and Demicco, 2006). The enormous volumes of trona evaporites in the greater Green River basin were also used to infer that high $[CO_2]_{atm}$ contributed to high weathering rates of the surrounding uplifts, needed to explain the quantity of ions required to produce the trona deposits (M.E. Smith et al., 2008a). The presence of possible (hot?) spring deposits in the basin, however, suggests that extrabasinal or deeply sourced fluids could have supplied some of the Na and $HCO_3$ ions (M.E. Smith et al., 2009). Calculated values based on flow rates and fluid compositions from modern hot springs at Lake Bogoria, Yellowstone, and Thermopolis, WY suggest that hot springs could have provided up to more than four times the amount of the calculated denudation (M.E. Smith, pers. comm., 2009). Similarly, tectonic activity in the Piceance basin at this time also draws into question the factors that led to nahcolite precipitation there, and implies that these evaporites cannot yet be used reliably to discuss climate.

Despite these issues, other data shows that the continental climates in the interior of North America during the Paleocene and early to middle Eocene were generally very warm (mean annual temperature < 25.5°C), humid (mean annual precipitation < 1500 mm), and

experienced relatively less seasonal variation and warmer winter temperatures than today (e.g., Wilf, 2000; Sewell and Sloan, 2006). Calculated temperatures based on fossil plants (e.g., palms) and animals (e.g., crocodilians), as well as $\delta^{18}O$ isotopes (from bivalves), mainly show that in the region of the greater Green River basin, winter temperatures (or coldest mean month) at lower elevations were well above freezing at ~5°C (e.g., Wing and Greenwood, 1993; Greenwood and Wing, 1995; Markwick, 1994; Wilf, 2000; Morrill and Koch, 2002). Low elevations in the Eocene Green River basin centre have been estimated at ~150–300 m above sea level (e.g., Bradley, 1929; Bradley and Eugster, 1969; Wing and Greenwood, 1993). Elevation estimates for the surrounding uplifts range from ~1300–2900 m to more than 3000 m, where snow may have accumulated and periodically supplied runoff to Lake Gosiute (Norris et al., 1996; Wolfe et al., 1998). However, the validity of $\delta^{18}O$ isotope data from laminated carbonates used to suggest that there was alpine snow in the Laramide uplifts (e.g., Norris et al., 1996) has been questioned due to potential diagenetic effects (Morrill and Koch, 2002).

Interestingly, however, the highly negative $\delta^{18}O$ values reported by Norris et al. (1996) from profundal lacustrine facies of the upper Wilkins Peak Member (~51.1–49.6 Ma; M.E. Smith et al., 2008b) approximately correlate with a pulse of siliciclastic sedimentation (the I-Arkose Bed; Culbertson, 1961) associated with abrupt facies changes from lacustrine carbonates to fluvial or deltaic sandstones. Nine main siliciclastic units present within the Wilkins Peak Member (Culberston, 1961) have recently been placed within a geochronological framework that associates them with 100 ka eccentricity cycles (M.E. Smith et al., 2010). Increased amounts of sediment and water input to the Wilkins Peak basin centre from basement-cored uplifts at the basin margins at these times are correlated with eccentricity minima, or periods of lower seasonality, and possibly generally wetter climates (M.E. Smith et al., 2010). Climate-related incision of geomorphic barriers and the sudden capture of the arkose-providing rivers could also explain the abruptness of these siliciclastic units. Similarly, a sudden, > 6 ‰ drop in $\delta^{18}O$ values at ~49 Ma from extremely positive values (< 27 ‰) in the lower Laney Member of the Green River Formation was interpreted as reflecting the possible drainage capture of a large high elevation river (Carroll et al., 2008; Doebbert et al., 2010). Oxygen and carbon isotopes from paleosol carbonates in the northeastern greater Green River basin also provide evidence for 400 ka cycles that may correlate with wet/dry cycles of Lake Gosiute and changes in vegetation related to these cycles (Clyde et al., 2001).

Paleobotanical evidence from taxonomy and morphological features of fossil leaves provides a reliable source of data that provides estimates of mean annual temperatures (MAT), winter temperatures (cold mean month, CMM), mean annual temperature ranges (MATR), and mean annual precipitation (MAP), at least for the sampled environments (e.g., Wing and Greenwood, 1993). Within the greater Green River basin, the evidence provided by leaf morphologies and taxonomic affinities of plant fossil assemblages shows a changing climate from the late Paleocene to the early Eocene (Wilf, 2000). Mean annual temperatures warmed from 12°C–19°C with mean annual precipitation of ~1300–1500 mm in the late Paleocene to 21°C (MAT) and ~1400 mm (MAP) at the Paleocene/Eocene Thermal Maximum at ~55 Ma (Wilf, 2000). Plant diversity also increased, with the influx of tropical plants to the region and about an 80% species turnover (Wilf, 2000). Late Paleocene floras across the Rocky Mountain basins of Wyoming were also relatively homogeneous, with evidence of sharper climatic differences between areas developing in the early Eocene (Wing, 1987). In general, the broad-leaved evergreen forests of the Paleocene and early Eocene gave way to mixed coniferous and broad-leaved deciduous forests during the overall cooling that occurred after the Early Eocene Climatic Optimum (Wing, 1987).

Plant assemblages also reflect a change from relatively wetter to relatively drier and more seasonal climates in the early Eocene, from ~53 Ma (Sourdough flora), to ~52.5 Ma (Niland Tongue flora), to ~50 Ma (Little Mountain flora), with a second species turnover of over 80% in the greater Green River Basin (Wilf, 2000). At this time, mean annual temperatures remained high at ~19.5–23°C, but mean annual precipitation dropped from ~1400 mm to ~760 mm (Wilf, 2000). This shift corresponds to both the onset of the Early Eocene Climatic Optimum and to the change from the wet, coal-producing fluvial facies (Niland Tongue) to the trona evaporites and lacustrine facies of Lake Gosiute (Wilkins Peak) in the greater Green River basin. The slightly younger "Green River" flora (~48–45 Ma) of Wing and Greenwood (1993) postdates the peak temperatures of the EECO, but similarly represents a seasonal climate, with MAT estimates of ~15°C, MAP of ~1160 mm, cold month mean of ~6°C, a warm month mean of ~32°C, and only ~120 mm of precipitation in the three driest months of the year.

Several types of plants preserved in the Green River basin floras likely were present in the sedimentary units investigated in more detail for this thesis, particularly in the fluvio-lacustrine siliciclastic units, and in root-marked lake-margin carbonate facies. The Little Mountain flora, collected from lacustrine facies of the upper Wilkins Peak Member of the Green River Formation (~50 Ma) represents a diverse assemblage in 27 families (Wilf, 2000). It contains horsetails (Equisetaceae: *Equisetum*), birches (Betulaceae: cf. *Alnus*) and other deciduous shrubs and trees (e.g., maples-Arecaceae, oaks-Fagaceae), pines (Pinaceae: *Pinus*) and other gymnosperms, as well as several legumes and other herbs (MacGinitie, 1969; Wilf, 2000). The slightly younger flora from the Bitter Creek delta of the Laney Member contains three main associations: 1) delta wetland plants including horsetails (*Equisetum*), cattails (*Typha*), ferns, and Lauraceae; 2) riparian shrubs and trees including swamp cypress, elm, alder, poplar, willow, and sycamore; and 3) a regional, more upland flora represented by pollen including pine (*Pinus*) (D.J. Scott and Cushman, 2002). Reed impressions preserved in the arkosic siliciclastic units (Chapter 5) possibly represent horsetails (*Equisetum*) and cattails (*Typha*); root-casts and root-marks may represent *Equisetum* as well as willows and other riparian shrubs or trees. Grande (1984) provided a summary of the fossil flora of the Green River Formation and figured numerous species collected from Fossil basin, including a 2 m-high palm frond (*Sabalites*).

### *2.4.3. Fossil Fauna of the Wyoming Green River Basins*

Grande (1984) summarized the Green River Formation fossil flora and fauna, with a focus on the abundant fishes (e.g., rays, gars, perch, dogfish, suckers, catfish, herrings) that were collected from Fossil Lake in Fossil basin, the small, intermontane basin in SW Wyoming. Frogs (*Eopelobates*), snakes (e.g., boa constrictors: *Boavus*), lizards (e.g., varanids?, amphisbaenids), turtles (e.g., soft-shelled: *Trionyx*, pond turtle: *Echmatemys*, snapping turtle: Chelydridae), and crocodilians (e.g., *Leidyosuchus*, *Crocodilus*, *Alligator*) are well represented in the collections from Fossil basin and the greater Green River basin (e.g., Grande, 1984; Grande and Buchheim, 1994; Gunnell and Bartels, 1997; Zonneveld et al., 2000a). Birds of several orders are also preserved in these sediments, including frigatebirds (Pelicaniformes), wading birds (Gruiformes: cranes, rails), grouse-like birds (Galliformes), kingfishers (Coraciiformes), and geese-like birds (Anseriformes: ducks, geese) (Grande, 1984; Gulas-Wroblewski and Wroblewski, 2003; Stidham, 2004; Olson and Matsuoka, 2005). The assemblage includes *Presbyornis*, a goose-like wader that is preserved in high densities in sites interpreted as breeding areas along the margins of the lake (e.g., McGrew and Feduccia, 1973; McGrew, 1980). Flamingo-like birds (Phoenicopteriformes: *Junctitarsus*), although similar to *Presbyornis*, are also represented in Eocene deposits of Wyoming (Olson and Feduccia, 1980; Ericson, 1999). Despite the abundant

shorebird-like footprints preserved in the Green River Formation (Chapter 6), the body fossils of the shorebird order Charadriiformes (plovers, gulls, etc.) are rare (Stidham, 2004). Body fossil records of Ardeiformes (herons) from the Green River Formation are unknown. Most of the orders and some families of modern birds originated during the Paleogene, but modern genera did not appear until the Neogene (after ~23 Ma; James, 2005). An increase in local and global bird diversity occurred following the Paleocene/Eocene Thermal Maximum (PETM) and into the EECO, with increased emigration of European birds into North America (Stidham, 2005). Bird footprints from the Green River Formation (Chapter 6) are probably best attributed to shorebirds (Charadriiformes), cranes (Gruiformes), *Presbyornis* and other duck-like birds (Anseriformes), flamingo-like birds (Phoenicopteriformes), and/or possibly heron-like birds (Ardeiformes).

Most of the collections containing fish, frogs, snakes, birds, and bats were made from profundal lacustrine shales from the relatively freshwater, expanded Lakes Gosiute, Uinta, and Fossil Lake (Grande, 1984). Large reptiles and mammals, in contrast, are best represented in well developed paleosols from alluvial plain deposits (e.g., Honey, 1988; Gunnell and Bartels, 1997; Zonneveld et al., 2000a; Gunnell et al., 2004). No vertebrate fossils have been reported from the lacustrine facies of saline to hypersaline Lake Gosiute (Wilkins Peak Member), and a relatively low diversity assemblage was present in the alluvial facies adjacent to the saline Lake Gosiute in the SW Bridger basin (Zonneveld et al., 2000a). Leggitt (2007a) reported the preservation of turtle and crocodilian scutes, as well as crocodilian and bird eggshell from relatively freshwater facies of the Wilkins Peak Member on the northern margin of the lake near La Barge, Wyoming. The only other known body fossils from the basin centre Wilkins Peak Member are associated with the fluvio-deltaic arkosic siliciclastic units described in Chapter 5. Reptile or mammal bones, bird bones, and possible fish bones were preserved in these facies.

Like the fossil plant assemblages of the late Paleocene to early Eocene, the fossil vertebrate assemblages were also affected by the warm, equable climates, and showed significant species turnover at the onset of the Early Eocene Climatic Optimum, between the North American Land Mammal Ages (NALMA) of the late Wasatchian and early Bridgerian at ~51.5 Ma (Clyde et al., 1997, 2001; M.E. Smith et al., 2010). Mammalian faunas also became more endemic, and the first appearance of several perissodactyls (e.g., Helaletidae (tapirs): *Hyrachyus*; Brontotheriidae: *Palaeosyops*) and primates (e.g., *Omomys*, *Smilodectes*) mark this boundary (Clyde et al., 1997). A list of possible trace making vertebrates present in the Green River basin or Fossil basin during early to middle Eocene time is provided in Table 2.1. Gunnell and Bartels (2001) compared the early Bridgerian faunal lists from the northeastern basin margin localities at South Pass, WY with basin centre localities near Opal, WY, and provided a list of almost 60 species of tetrapods found at these localities. Although the depositional environments were not described in detail, both of these localities were dominated by alluvial facies, with well developed reddish paleosols at the basin margin (Cathedral Bluffs of the Wasatch Formation and the lower Bridger Formation) (Gunnell and Bartels, 2001). This type of comparison is important for the paleoecology of the early to middle Eocene vertebrates and begins to discuss their habitat usage and distribution, a topic to which the correlation between vertebrate trace makers and the environmental distribution of the traces would be a valuable contribution.

Invertebrates preserved in Fossil basin and the greater Green River basin include small crustaceans (e.g., conchostracans, branchiopods, ostracodes), decapod crustaceans (crayfishes: *Procambarus*; prawns: *Bechleja*), bivalves (Unionidae, Pisiidae), gastropods (e.g., *Viviparus*, *Hydrobia*, *Goniabasis*), spiders (Araneae), mites (Acarina), and insects (e.g., Grande, 1984; Hanley, 1976, 1988; Grande and Buchheim, 1994; Yan-Bin et al., 2006; Ingalls and Park, 2010). All of these invertebrates are potential trace makers, particularly in freshwater and fluvio-deltaic

**Table 2.1.** Possible mammalian trace makers known from body fossils in the Green River Formation and equivalents in Wyoming, U.S.A. List compiled with reference to Grande (1984), Clyde et al. (1997), Zonneveld et al. (2000a), and Gunnell and Bartels (2001). References to Eocene vertebrate tracks from other localities that may also be attributable to these trace makers are provided.

| Order | Family | Genus | References of comparable Eocene tracks |
|---|---|---|---|
| Creodonta (extinct) | | | Sarjeant and Wilson, 1988; Sarjeant and Langston, 1994; Lockley et al., 1999; Sarjeant et al. 2002 *in* Hunt and Lucas, 2007b |
| | Hyaenodontidae | *Prolimnocyon* | |
| | | *Prototomus* | |
| | | *Sinopa* | |
| | | *Thinocyon* | |
| | | *Tritemnodon* | |
| | Oxyaenidae | *Patriofelis* | |
| Carnivora (carnivores: cats, dogs, weasels) | | | Sarjeant and Langston, 1994; Lockley et al., 1999 |
| | Miacidae | *Miacis* | |
| | | *Vulpavus* | |
| | | *Uintacyon* | |
| | | *Oodectes* | |
| | Viverravidae | *Viverravus* | |
| | | *Didymictis* | |
| Cete/Mesonychia (tetrapod ancestors to whales, whales) | | | Sarjeant and Langston, 1994; Ataabadi and Sarjeant, 2000 |
| | Hapalodectidae | *Hapalodectes* | |
| | Mesonichidae | *Mesonyx* | |
| Perissodactyla (horses, rhinos, tapirs, brontotheres) | | | Moussa, 1968; Sarjeant and Langston, 1994; Hamblin et al., 1998; Hamblin et al., 1999; Lockley et al., 1999; Mustoe, 2002; Abbassi and Lockley, 2004; Ataabadi and Khazaee, 2004; Mihlbachler et al., 2004; Ataabadi, 2007 |
| | Equidae | *Hyracotherium* | |
| | | *Orohippus* | |
| | Brontotheriidae | *Lambdotherium* | |
| | | *Palaeosyops* | |
| | | *Eotitanops* | |
| | Helaletidae | *Hyrachyrus* | |
| | | *Helaletes* | |
| | | *Dilophodon* | |
| Artiodactyla (suborder Paleodonta; cloven-hooved ungulates) | | | |
| | Dichobunidae | *Bunophorus* | |
| | | *Diacodexis* | |
| | Homacodontidae | *Antiacodon* | |
| | | *Hexacodus* | |
| | | *Microsus* | |
| Rodentia (rodents) | | | Sarjeant and Langston, 1994 |
| | Paramyidae | *Paramys* | |
| | Sciuravidae | *Sciuravus* | |
| | | *Knightomys* | |
| Primates (primates) | | | |
| | Omomyidae | *Omomys* | |
| Cimolesta (extinct) | | | |
| | Pantolestidae | | |
| | Apatemyidae | *Apatemys* | |
| Taeniodonta (extinct) | | | |
| | Stylinodontidae | *Stylinodon* | |
| Tillodontia (extinct) | | | |
| | Esthonychidae | *Esthonyx* | |
| Condylartha (extinct) | | | |
| | Meniscotheriidae | *Meniscotherium* | |
| | Hypsodontidae | *Hyopsodus* | |
| Dinocerata (extinct) | | | |
| | Uintatheriidae | *Bathyopsis* | |

**Table 2.2.** Possible insect trace makers present as body fossils in the Green River Formation of Wyoming, Colorado, and Utah (selected from the lists compiled by Wilson, 1978 and Grande, 1984). Possible trace makers present in Paleocene faunas but not in the Green River Formation are in italics. Possible insect trace makers present as body fossils in the Eocene British Columbia collections but not within the Green River Formation are capitalized (Wilson, 1978).

| Order | Family | Common name | Possible trace making life-stage |
|---|---|---|---|
| Blattodea (cockroaches) | | | |
| | Blattidae | cockroaches | larvae (nymphs?) and adults |
| Orthoptera (grasshoppers, crickets) | | | |
| | Gryllidae | crickets | larvae (nymphs) and adults |
| | Acrididae | short-horned grasshoppers | larvae (nymphs) |
| Ephemeroptera (mayflies) | | | |
| | Baetidae | mayflies | larvae |
| | Ephemeridae | burrowing mayflies | larvae |
| Isoptera (termites) | | | |
| | MASTOTERMITIDAE | MASTOTERMITIDS | LARVAE AND ADULTS |
| Hemiptera (true bugs) | | | |
| | Saldidae | shorebugs | |
| | Cydnidae | burrow bugs | |
| Homoptera (cicadas, hoppers) | | | |
| | *Cicadidae* | *cicadas* | *larvae (nymphs)* |
| Coleoptera (beetles) | | | |
| | Carabidae | ground beetles | larvae and adults |
| | Cicindelidae | tiger beetles | larvae and adults |
| | Dytiscidae | predaceous diving beetles | adults |
| | Staphylinidae | rove beetles | larvae and adults |
| | Scarabidae | scarab beetles | larvae and adults |
| | Elateridae | click beetles | larvae |
| | Cerambycidae | long-horned beetles | larvae |
| | Curculionidae | snout beetles | larvae |
| | *TENEBRIONIDAE* | *DARKLING BEETLES* | *LARVAE AND ADULTS* |
| | Tipulidae | crane flies | larvae |
| Diptera | | | |
| | Chironomidae | midges | larvae |
| | Bibionidae | March flies | larvae |
| | Tabanidae | deer flies | larvae |
| | Stratiomyidae | soldier flies | larvae and adults |
| Trichoptera (caddisflies) | | | |
| | Hydropsychidae | net-spinning caddisflies | larvae |
| | Hydroptilidae | micro-caddisflies | larvae |
| | Limnephilidae | northern caddisflies | larvae |
| | Sericostomatidae | serocostomatids | larvae |
| | *Leptoceridae* | *long-horned caddisflies* | *larvae* |
| Hymenoptera (ants, wasps, bees) | | | |
| | Sphecidae | sphecid wasps | larvae and adults |
| | Formicidae | ants | larvae and adults |
| | VESPIDAE | VESPID WASPS | LARVAE AND ADULTS |

settings of the Green River Formation and surrounding fluvial systems (e.g., Wasatch and Bridger Formations). Insects in the Green River Formation were abundant and well preserved in lacustrine shales, and have been typically found together with plant fossils and vertebrate body fossils of fish, birds, reptiles, and amphibians (Grande, 1984). Most of the insect fossils were collected and described between 1890 (e.g., Scudder, 1890) and about 1950 (e.g., Hull, 1949) (Wilson, 1978 and references therein). Wilson (1978) provided a list of Paleogene insect faunas collected from the Green River basins. Grande (1984) figured numerous species, including larvae. In total, there are ~90 families represented in the Green River collections, with ~300 species described. By the early Eocene, most of the modern families, as well as numerous modern genera, were present (e.g., Staphylinidae: *Bledius*; Fraser et al., 1996). Insect diversity at the familial level increased only slightly within the four major orders represented (Hemiptera, Homoptera, Coleoptera, Diptera) since the middle Eocene (~50 Ma) (Wilson, 1978). The diversity of Lepidoptera and Hymenoptera was relatively low between the middle Eocene and early Oligocene (~35 Ma) (Wilson, 1978). Of the families listed by Wilson (1978) and Grande (1984), several are notable because they are potential trace makers (Table 2.2).

Previous descriptions of trace fossils produced by invertebrates in the Green River Formation and surrounding formations of Wyoming, Colorado, and Utah include: Curry (1957; bird and mammal tracks); Erickson (1967; *Presbyornis* trackway); Moussa (1968; shorebird and perissodactyl footprints); Moussa (1970, nematode or larval insect trails); D'Alessandro et al. (1987; invertebrate traces from fluvial environments); Roehler (1988; bioturbation in fluvio-deltaic environments); Hamblin et al. (1999; bird and mammal footprints); Greben and Lockley (1992; bird footprints); Grande and Buchheim (1994; bioturbation in nearshore environments); Yang et al. (1995; flamingo and duck-like bird tracks); Hasiotis and Honey (2000; crayfish burrows in fluvial/floodplain environments); Zonneveld et al. (2000b; invertebrate traces of several types); Foster (2001; salamander tracks); Leggitt and Cushman, 2001, Leggitt and Loewan, 2002, and Leggitt et al., 2007 (caddisfly cases); Jennings et al. (2002; invertebrate and vertebrate traces); Lamond and Tapanila (2003; borings in stromatolites); Leggitt (2003; flamingo nest-mounds); Hasiotis et al. (2003; arthropod and vertebrate traces); Zonneveld et al. (2006; *Lunulichnus* in fluvial environments); Bohacs et al. (2007a; vertebrate and invertebrate traces); and Martin et al. (2010; fish feeding and swimming traces).

### *2.4.4. Structure and Stratigraphy of the Greater Green River Basin, SW Wyoming and NW Colorado, U.S.A.*

The greater Green River basin is bounded by Laramide uplifts on all sides except the western margin, which is bounded by the Wyoming salient of the Cordilleran or Sevier Fold and Thrust Belt (Fig. 2.5; e.g., DeCelles, 2004; Yonkee and Weil, 2010). All margins of the lake basin were tectonically active during the deposition of the Green River Formation. The changing shape and gradients of the dissected basin influenced sedimentation during the early-middle Eocene (e.g., Roehler, 1992b; Pietras and Carroll, 2006), which was also related to changing climates (e.g., M.E. Smith et al., 2010), lithologies of exposed catchment rocks (Carroll et al., 2006), and input to the basin by various rivers at different times (e.g., Carroll et al., 2008). To the south, the Uinta mountains were uplifted on high-angle thrust faults on both the northern and southern flanks, which were reactivated on Precambrian normal faults that had bounded the

**Fig. 2.5.** (Next page) Map showing study sites in the Wilkins Peak Member of the Green River Formation, Bridger basin, southwestern Wyoming, U.S.A. Compiled from Love and Christiansen (1985), Steidtmann and Middleton (1991), Roehler (1993), Wiig et al. (1995), Sims et al. (2001), Johnston and Yin (2001), Liu and Nummedal (2004), and Yonkee and Weil (2010). Possible spring sites and study sites are discussed in the text.

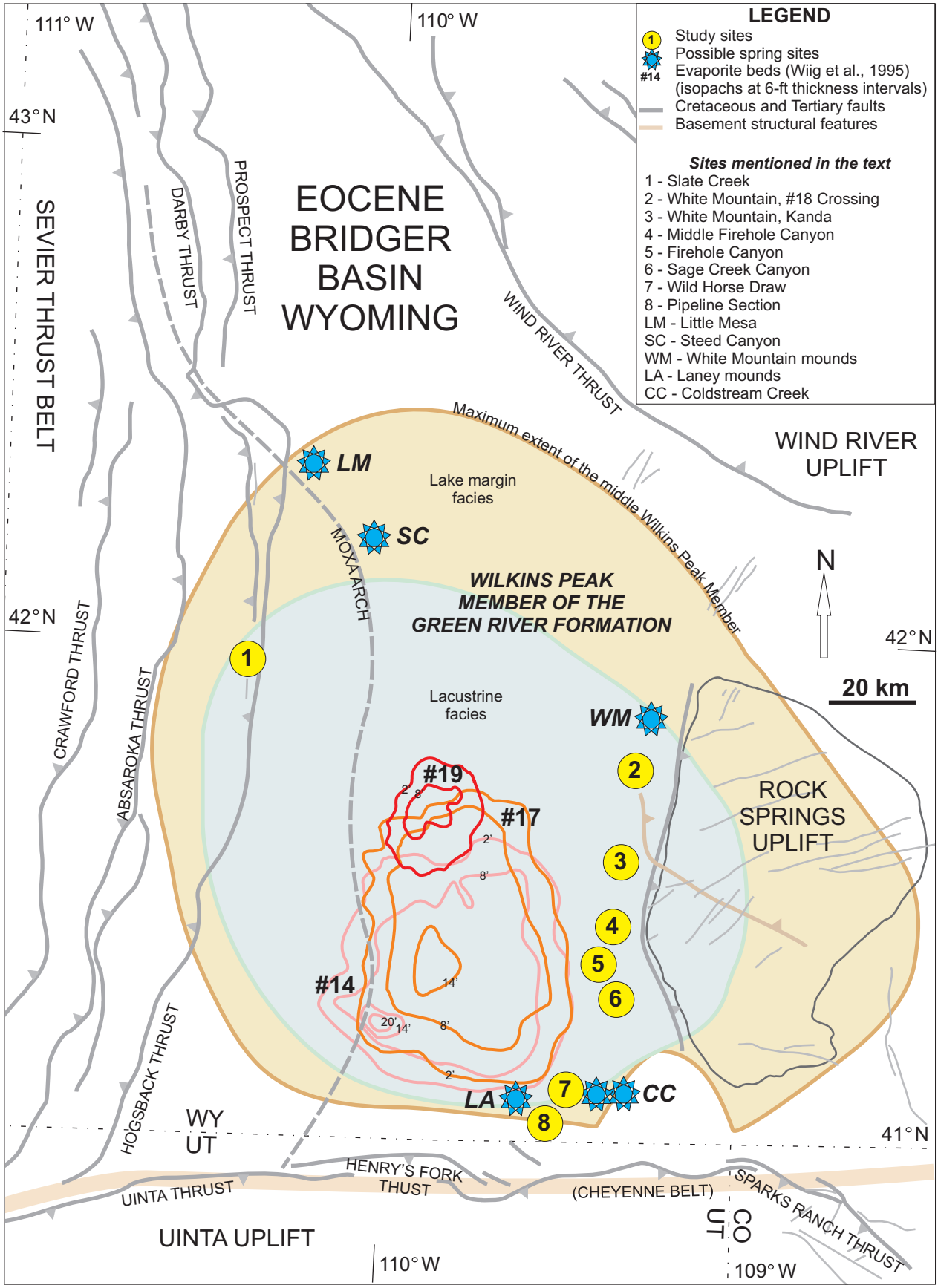
LEGEND
Study sites
Possible spring sites
#14
Evaporite beds (Wiig et al., 1995)
(isopachs at 6-ft thickness intervals)
Cretaceous and Tertiary faults
Basement structural features
Sites mentioned in the text
1 - Slate Creek
2 - White Mountain, #18 Crossing
3 - White Mountain, Kanda
4 - Middle Firehole Canyon
5 - Firehole Canyon
6 - Sage Creek Canyon
7 - Wild Horse Draw
8 - Pipeline Section
LM - Little Mesa
SC - Steed Canyon
WM - White Mountain mounds
LA - Laney mounds
CC - Coldstream Creek
111° W
110° W
43° N
42° N
41° N
109° W
EOCENE
BRIDGER
BASIN
WYOMING
SEVIER THRUST BELT
DARBY THRUST
PROSPECT THRUST
WIND RIVER THRUST
WIND RIVER
UPLIFT
Maximum extent of the middle Wilkins Peak Member
LM
SC
Lake margin
facies
MOXA ARCH
WILKINS PEAK
MEMBER OF THE
GREEN RIVER FORMATION
Lacustrine
facies
WM
#19
#17
#14
2'
8'
14'
20'
N
20 km
ROCK
SPRINGS
UPLIFT
CRAWFORD THRUST
ABSAROKA THRUST
HOGSBACK THRUST
LA
CC
WY
UT
HENRY'S FORK
THUST
UINTA THRUST
(CHEYENNE BELT)
SPARKS RANCH THRUST
UINTA UPLIFT
CO
UT

Uinta graben during Neoproterozoic rifting (e.g., Marshak et al., 2000; Condie et al., 2001; Rybcznski et al., 2008). The general trend of the Uinta Uplift runs E–W, following the Proterozoic Cheyenne Belt Suture Zone which continues eastward of the Uintas to the Cherokee Ridge arch, also an active structure during the Eocene (Bader, 2008). The northernmost mapped fault of the western Uintas is the Henry's Fork Thrust Fault (Johnston and Yin, 2001). Towards the east, the Uinta Uplift trends ESE–WNW, with the Sparks Ranch Thrust Fault forming the margin of the greater Green River basin (Roehler, 1993). The Sand Wash sub-basin of the southeastern corner was bounded on the south by the Axial Basin Arch, the northernmost extension of the White River Uplift in Colorado (Roehler, 1992a). Thrust faults of the basement-cored Laramide Sierra Madre and the Granite Mountains formed the eastern margin of the basin (e.g., Chamberlain et al., 2003), and thrust faults of the Wind River and Gros Ventre Mountains formed the northern boundary (e.g., Steidtmann and Middleton, 1991). Like the Uinta Mountains, the positions of these faults were largely dictated by old structures in the basement (e.g., the southern margin of the Wyoming craton; Steidtmann and Middleton, 1991; Chamberlain et al., 2003). The western margin, formed mainly by thin-skinned thrust faults, was also active during deposition of the Green River Formation (e.g., DeCelles and Mitra, 1995; Zonneveld et al., 2000a; Yonkee and Weil, 2010; this study). The N–S-trending Moxa Arch, an older, thick-skinned thrust fault to the north and anticlinal ridge to the south (e.g. Kraig et al., 1987; Royse, 1993), influenced the thrusting of the younger faults and affected the shape of the western margin (e.g., Becker et al., 2010). This overpressured, natural gas-containing and $CO_2$-rich arch (e.g, Lynds et al., 2010) may have also played a role in the distribution of the trona deposits by forming a sill on the western basin centre of the Bridger basin during Wilkins Peak time (Fig. 2.5). The Moxa Arch continued to develop until at least the early Eocene (Becker et al., 2010).

The Rock Springs Arch, a N–S-trending smaller structure that also influenced the distribution of depositional environments during Wilkins Peak time was an asymmetric block with a Paleocene–Eocene reverse fault along its western flank, which may or may not have formed along a reactivated structure in the basement (Mederos et al., 2005; Johnson and Anderson, 2009). Just north of the Rock Springs Arch, a buried E–W-trending structure evidenced by Bouguer gravity anomaly data (Bankey and Mereweather, 1990; Mederos et al., 2005) may have also influenced the basin shape and sedimentation during Wilkins Peak time (Fig. 2.5; cf. Pietras and Carroll, 2006). Movement of the Wind River Thrust Fault was an important event, marking the base of the Wilkins Peak Member by closing the basin and re-directing a major river that had entered the basin from the north (Steidtmann and Middleton, 1991; Pietras et al., 2003).

The early to middle Eocene sediments deposited in the greater Green River basin from ~53–45 Ma show the variability in lake-types evidenced by the sedimentary package (Fig. 2.6; Carroll and Bohacs, 1999; M.E. Smith et al., 2008b). Roehler (1992b) mapped the various members of the Green River (GRFm.) and Wasatch Formations, and provided several stratigraphic cross-sections of the basin. Roehler (1993) provided paleogeographic maps of each of these members, showing the changing extent of Lake Gosiute through time. At ~53 Ma, a fluvially dominated sediment package, characteristic of the overfilled lake-type, was deposited along the north and northeast flanks of the Uinta Uplift, south of the Rock Springs Uplift, and into the NE–SW-trending depocentre of the Washakie basin (Luman Tongue of the GRFm.; Roehler, 1993; Bohacs et al., 2000; M.E. Smith et al., 2008b). A larger lake followed (~51.5 Ma;

**Fig. 2.6.** Generalized stratigraphy of the greater Green River basin (redrawn from M.E. Smith et al., 2008b and Chetel and Carroll, 2010).

## *SIMPLIFIED EOCENE STRATIGRAPHY OF THE GREATER GREEN RIVER BASIN*

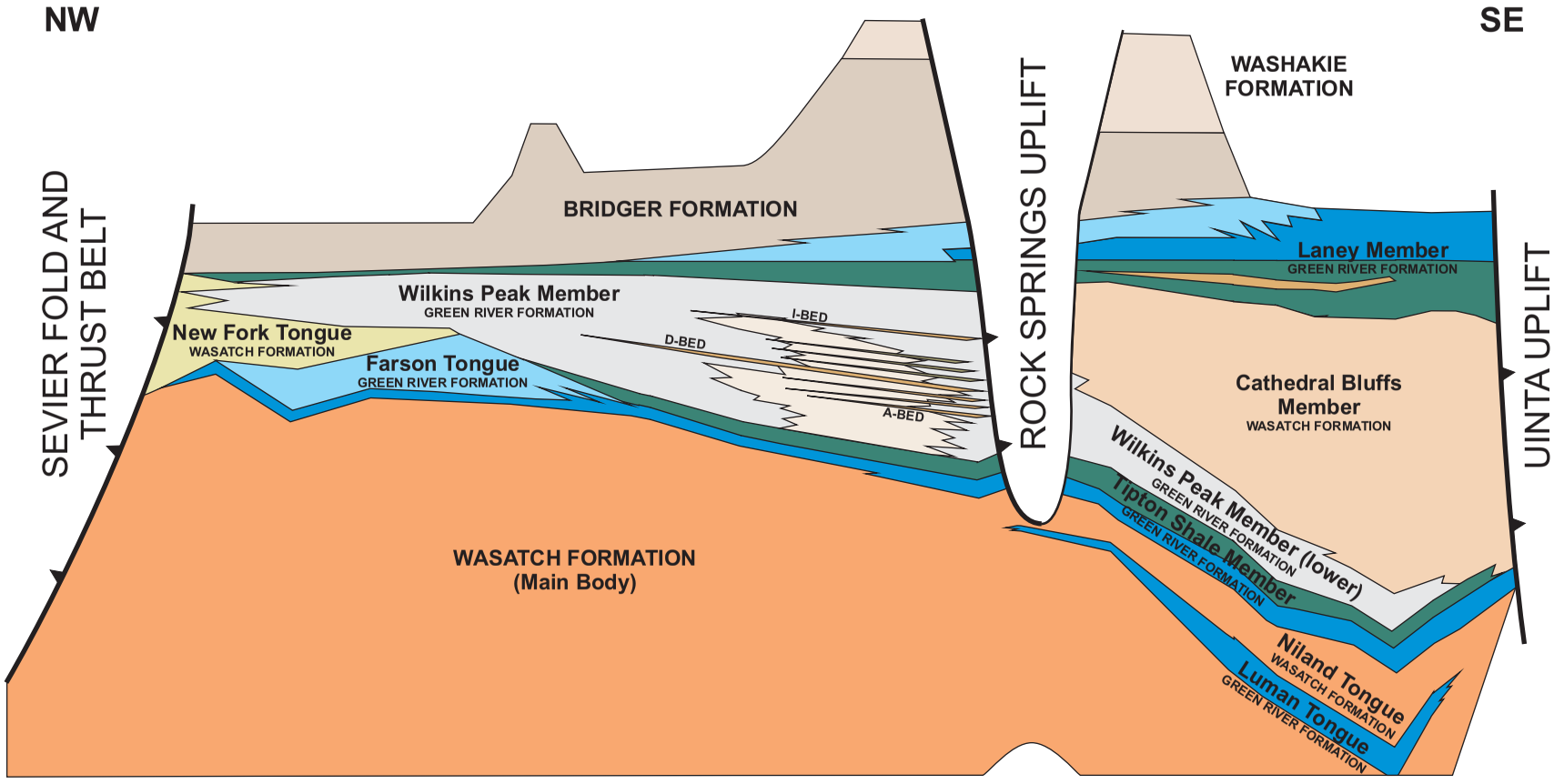


LACUSTRINE UNITS OF THE GREEN RIVER FORMATION

- Overfilled lake-type (Luman Tongue, Scheggs Bed of the Tipton Member, Upper LaClede Bed of the Laney Member)
- Balanced fill lake-type (Rife Bed of the Tipton Member, Lower LaClede Bed of the Laney Member)
- Deltaic units (Farson Tongue, Sand Butte Bed of the Laney Member)
- Fluvio-lacustrine units (A-I Beds of the Wilkins Peak Member, Buff Marker of the Laney Member)
- Underfilled lake-type (evaporative carbonates of the Wilkins Peak Member)
- Underfilled lake-type (evaporites of the Wilkins Peak Member)

ALLUVIAL UNITS

- Main Body of the Wasatch Formation
- Cathedral Bluffs Tongue of the Wasatch Formation
- New Fork Tongue of the Wasatch Formation
- Bridger Formation
- Washakie Formation

M.E. Smith et al., 2008b), representing the transition from an overfilled lake-type to balanced-fill lake-type, with widespread "fluctuating-profundal"lacustrine and deltaic facies across the greater Green River Basin (Tipton Shale Member and the Farson Sandstone of the GRFm.). The thickest accumulation of lacustrine sediments from this time were also deposited along the northern flank of the Uintas, the eastern flank of the Uintas in the Sand Wash basin, and northwestward into the Washakie basin (Roehler, 1992b). Next, the lower Wilkins Peak Member of the GRFm. (~51 Ma; M.E. Smith et al., 2008b), representing an underfilled lake-type basin, also accumulated in these areas, thinning to the north. During deposition of the middle Wilkins Peak and the upper Wilkins Peak (~50.5–49.5 Ma; M.E. Smith et al., 2008b), the depositional centre of the evaporative lacustrine facies shifted westward and northwestward, with sediment thicknesses throughout the Bridger basin becoming more evenly distributed later in time (Roehler, 1992b; Pietras and Carroll, 2006). Fluctuating-profundal facies of the balanced-fill Laney Member of the GRFm. sharply overlie the Wilkins Peak Member (~49.5 Ma; M.E. Smith et al., 2008b), and are associated with a freshening of the lake, and a greater lateral extent of lacustrine facies (Roehler, 1993). The lacustrine facies of the Laney Member are thickest towards the southeast (Roehler, 1992b). The greater Green River basin was then progressively filled from the northwest by volcaniclastic sediments sourced from northwestern Wyoming and Idaho (~49.5–48.5 Ma; Roehler, 1992b; M.E. Smith et al., 2008b; Chetel and Carroll, 2010).

The underfilled lake-type represented by the Wilkins Peak Member of the GRFm. was the main unit investigated for this study. The basin centre facies assemblage, dominated by lacustrine and eulittoral carbonates, sodium carbonate evaporites, and arkosic siliciclastic sediments, are described in detail in Chapter 5. During the evaporative, closed-lake period of Lake Gosiute from ~51.1–49.6 Ma (M.E. Smith et al., 2008b), tectonic activity in the basin is evidenced by unconformities (Pietras et al., 2003) and faults that offset lacustrine sediments (Roehler, 1993; Zonneveld et al., 2000a; this study). Numerous localities where mounds of carbonate and silica travertine, many interpreted as spring deposits, were preserved within Wilkins Peak strata and within the Laney Member (Wiegman, 1965; Bradley and Eugster, 1969; Surdam and Stanley, 1979; Roehler, 1993; M.E. Smith et al., 2009). Additionally, large mounds of silicified mud, fracture-fill travertine, authigenic quartz, and platey calcite crystals representing localized regions of hydrothermal alteration, may have been associated with hot springs at the surface during Wilkins Peak and Laney time (Mayry, 2005), although they may have formed much later (T. Lowenstein, pers. comm., 2010). Considering the abundance of active basement-related structures in the basin during these periods, the distribution of the known mounds and their internal textures, some of the travertine mounds are interpreted as spring deposits that provide part of the paleoecological context of some of the trace fossils and sedimentary features. Strontium isotopes measured in the Laney Member show more radiogenic waters during low lake levels (Rhodes et al., 2002). A relatively higher proportion of spring-fed, deeply sourced waters is one possible mechanism to account for these variations. Strontium isotope data from one carbonate "tufa" mound in the Laney Member also were relatively radiogenic (M. Rhodes, unpublished data; A. Carroll, pers. comm., 2009). The initial investigation of some of these potential spring deposits and their associated sediments (e.g., thick microbial mats) undertaken as part of this study demonstrates that springs likely affected the Eocene ecology of the basin.

# CHAPTER 3

## 3. LITHOFACIES AND DEPOSITIONAL ENVIRONMENTS OF THE KENYA RIFT VALLEY: LAKES BOGORIA, MAGADI, AND NASIKIE ENGIDA

The aim of this chapter is to provide the sedimentological context for the trace fossils that are described in detail in Chapter 4. The saline, alkaline lake basins included in this study share several similarities in the lithology of lacustrine and lake-margin strata. Lakes Bogoria, Magadi, and Nasikie Engida, all of which are located in the inner axial depression of the rift valley, were the focus of this study. In general, the lakes are steep-sided and have only narrow strips of sandy gravel shoreline deposits against bedrock or boulder-sized colluvium. Axial plains, which are fed by rivers running parallel to the main axis of the rift, fan delta-plains, and subaerially exposed deltaic and littoral zones are the most common environmental settings that contain fine-grained sediments for the formation of most of the animal and plant traces in these basins. The deltas and floodplains of ephemeral streams comprise poorly sorted, compositionally immature fine- to coarse-grained sands/sandstones and silts/siltstones sourced from regions dominated by bedrock of trachyte, phonolite, or basalt. Fine-grained sandstones on the lake margins commonly have calcite and zeolite cements (e.g., Surdam and Eugster, 1976; Renaut, 1993). The offshore lacustrine sediments comprise siltstones and mudstones containing predominantly smectitic and/or illitic clay minerals, organic-rich oozes and laminites, sodium carbonate evaporites (mainly trona), chert, and a variety of authigenic Na-rich zeolites (e.g., analcime, erionite) and Na-silicates such as magadiite (e.g., Surdam and Eugster, 1976; Renaut et al., 1986).

Springs are present on the modern lake margins and elsewhere in the Bogoria and Magadi drainage basins. At Bogoria, mounds of travertine and tufa with variable mineralogy (e.g., calcite, aragonite), opaline silica crusts and cements, and microbially influenced textures provide sedimentary evidence of spring discharge (e.g., Renaut, 1982; Renaut et al., 1986; Renaut and Owen, 1988). In some cases, spring fluids may have played an important role in the lake-basin ecology and controlling the mineralogy of lake-margin and lacustrine sediments, although spring deposits may not have formed or been preserved (Renaut et al., 2000b, 2002b, 2007).

All of the lithofacies described may be pedogenically altered, with the degree of pedogenesis increasing towards the basin margins where water tables are typically lower. Common features of siliciclastic sediments that were subaerially exposed for various periods of time include: 1) open root pores and carbonate rhizoliths; 2) carbonate cements and calcrete; 3) bioturbation by terrestrial animals (e.g., termites); 4) weathering and alteration of clasts (e.g., detrital K-feldspar) to clay-minerals; 5) alteration of clays to zeolites (Renaut, 1993); and, 6) the wetting-drying of shrinking and swelling clays to form angular soil peds. Travertine, stromatolitic carbonates, tufa, and chert deposits may also be affected by subaerial exposure, but because of their generally high degree of induration, weathering and pedogenesis are typically weak. In the regions studied, the typical "fluvial" association of meandering channel systems, riverine bars of braided streams, and floodplain and overbank fine-grained sediments is generally poorly developed. However, examples are present in the Loboi Silts of the Baringo basin near Nyongonyek. These types of deposits represent end-members that contain trace fossils typically associated with soils (e.g., Coprinisphaera ichnofacies). In the Kenyan examples studied, as well as in the Green River Formation and correlative members of the Wasatch Formation in the greater Green River basin, the fluvial/floodplain end-members provide important examples that help to distinguish between typical "basin margin" versus "basin centre" trace fossils and sedimentary deposits.

Descriptions of the lithofacies from the localities studied (Figs. 2.2, 2.3) are provided in Table 3.1, with photographs of representative examples. The descriptions are partly based on previously published descriptions together with additional data collected during this study. Some of the lithofacies were present in more than one locality and were grouped according to grain-size and typical sedimentary features in Table 3.1. The following sections summarize the characteristics of the lithofacies and their depositional environments, with discussion of the particular localities where they were best represented and most closely studied. This approach was taken in order to summarize the main lithofacies assemblages of these axial-rift saline lakes as a whole for future comparisons with other saline, alkaline lakes (e.g., the Green River Formation). A closer look at the individual sites is presented with details of the recent traces and trace fossils in Chapter 4.

Dramatic, rapid changes in facies distribution and lake-levels occur in underfilled basins, with subaerially exposed lithofacies common in basin centre areas (Bohacs et al., 2000). However, a broad pattern that characterizes their distribution was recognized, which has been adopted for this study. Certain lithofacies associations were best represented in "basin margin" localities (e.g., conglomerates, gravels, fluvial channels), landward of areas of "frequent" (e.g., seasonal to decadal?) lake-level rise-and-fall. Other lithofacies associations were best represented in "basin centre" localities (e.g., siltstones, mudstones, bedded evaporites), deposited either within the lake or within the zone of frequent lake-level rise-and-fall. Due to the steep lateral margins of the Kenyan fault-bounded lakes and break-up of the inner rift by numerous horsts and grabens, some coarser-grained lithofacies (e.g., gravel beaches) were closely associated with littoral or mudflat finer-grained lithofacies (e.g., laminated siltstones, laminated sandstones). This close association blurred the distinction between the basin margin and basin centre lithofacies at these "coincident margins" (Cohen, 2003). In addition to longer-term changes in lake-levels (100s to 1000s of years), the distinction between the basin margin and basin centre may be comparable to a distinction between highstand and lowstand lithofacies assemblages. "Lake margin" settings are intermediate, and may be dominantly composed of facies typical of basin margin localities (e.g., alluvial plains during low lake levels) or by lithofacies associations typical of basin centre localities (e.g., littoral zone during high lake levels). Nevertheless, certain depositional environments are related to differences in gradients between the basin margin and basin centre (e.g., paleosols and alluvial fans in basin margin localities). This distinction appears to be useful for predicting the distribution of the lithofacies and trace fossil assemblages, as well as assessing their significance.

In general, coarser grain sizes are found in basin margin sites (e.g., coarse sandy or gravelly beach bars) and are associated with relatively high gradient margins ("coincident" fault scarps; Cohen, 2003). Sites with coarse sediments tend to be close to steep basin-bounding faults, even if most deposition occurs within the lake (e.g., fan-deltas, coarse-grained turbidites). In certain relatively low-gradient depositional settings (e.g., fluvial channels of deltas on "non-coincident" margins), however, pockets of relatively coarse-grained material may be isolated within widespread deposits of silts and very fine-grained sands deposited either in the lake or within the zone of frequent lake-level fluctuations. Grain size is, of course, also related to the distance of sediment transport, which also tends to be farthest for rivers that feed the axial plains. The reworking of fine- to coarse-grained sands and gravels by littoral processes (e.g., waves, longshore currents), which can decrease grain size and improve sorting, is more prevalent where the fetch is greater. At Lake Bogoria, for example, this mainly occurs along the hinged, bench-like margin during present-day "intermediate" lake levels (Renaut and Tiercelin, 1994), and to a lesser degree on the lower-gradient, ramp-like axial plain.

**Table 3.1.** Lithofacies of Pleistocene to Recent Lakes Bogoria, Magadi, and Nasikie Engida. Descriptions are based on personal field observations, and published descriptions where necessary (especially Tiercelin et al., 1981; Renaut et al., 1986; Tiercelin et al., 1987; Renaut and Owen, 1988, 1991; Renaut and Tiercelin, 1994; Behr, 2002). Lithofacies are organized by grain size.

| Fig., Sect. | Lithology | Description | Comments; Trace suites (Chapter 4) | Interpretation/modern environment | General distribution | Localities |
|---|---|---|---|---|---|---|
| ***Basin Margin- to Lake Margin-Dominated Lithofacies*** | | | | | | |
| Figs. *3.1*.3A–H, 4C, 8F, 12G; Sect. 3.1.2 | Very poorly to poorly sorted coarse-grained sand- to boulder-sized angular clasts of trachytic, basaltic, or trachyphonolitic lava | Structureless to imbricated deposits of angular, unsorted coarse-grained sand to boulder-sized clasts; clast-supported orthoconglomerate; oligomictic; may be cemented by authigenic zeolites, calcite and/or and clay minerals; clast composition mostly trachyte, trachyphonolite, or basalt, with obsidian flakes; brownish to reddish black and dark brown | Not associated with trace fossils | Colluvium along steep, faulted escarpments; alluvial fans along faulted escarpments | Basin margin to lake margin (high gradient) | Pleistocene to Recent Lake Bogoria; Nasikie Engida, Lake Magadi |
| Fig. *3.1*.1B–D, 1F–G; Sect. 3.1.1 | Very poorly sorted, pebble conglomerate with rounded and subrounded clasts | Very poorly sorted, subrounded to rounded, imbricated pebble conglomerate; matrix-supported paraconglomerate with some clast-supported beds; polymictic; structureless or graded with planar low-angle cross-bedding, or high-angle planar cross-beds; scoured lower contacts | Not associated with trace fossils | Alluvial fan and fluvial channel conglomerates | Basin margin | Late Pleistocene to Holocene ‘Loboi Silts’, Nyongonyek, Baringo basin |
| Fig. *3.1*.6A; Sect. 3.1.2 | Very poorly sorted pebble-conglomerate with subrounded clasts | Weakly horizontal, thickly-bedded pebble-conglomerate with subrounded clasts; fining upwards to poorly sorted silts with pebble clasts; contains thick beds of matrix-supported paraconglomerates and scoured orthoconglomerate lenses; structureless internally; may be cemented by carbonate | Not associated with trace fossils | Fluvial channel lag conglomerate; shallow gradient channel in fan-delta | Basin margin | Pleistocene to Holocene Lake Bogoria; e.g., Parkirichai Section |
| Figs. *3.1*.4E, 6A, 6B; Sect. 3.1.2 | Poorly sorted coarse-grained sand- to pebble-sized subrounded clasts | Weakly horizontally medium-bedded deposits of subrounded clasts with coarse sand-grained to pebble-sized matrix; matrix-supported paraconglomerate; oligomictic; greenish black, dark brown, or gray clasts; may be cemented by carbonate | Not associated with trace fossils | Alluvial fan and/or fluvial channel lag conglomerate | Basin margin | Pleistocene to Holocene Lake Bogoria; reworked in Recent Parkirichai River |
| Fig. *3.1*.1C; Sect. 3.1.1 | Poorly sorted granule- to pebble-orthoconglomerates | Poorly sorted, cross-bedded granule- to pebble-sized orthoconglomerates in medium thick beds and isolated lenses; beds have sharply scoured or undulating bases; grades laterally to very poorly sorted pebble-conglomerates; cross-beds may be draped with fine-grained sediment | Not associated with trace fossils | Braided channels, possibly of distal alluvial fan | Basin margin | Late Pleistocene to Holocene ‘Loboi Silts’, Nyongonyek, Baringo basin |
| Figs. 3.1.4E–H,6A, 6E; Sect. 3.1.2 | Poorly to moderately sorted granule-conglomerate and fine- to coarse-grained sands with clay drapes | Reddish brown, grey, and black poorly to moderately sorted granule-conglomerate/gravel and coarse-grained sands with reddish brown clay drapes; may be present in small, scoured lenses internally imbricated to vaguely low-angle cross-bedded; may preserve horizontal bedding to very low-angle cross-bedding in thick beds with sharp, flat bases; modern point bars may incorporate pebble-sized clasts from older deposits; modern channel meandering at basin margin, straighter towards lake margin; point bars and channel floor near lake margin may contain reddish brown mud drapes; fine-grained sands may be ripple cross-laminated (flaser bedding) with 3D ripple bedforms | Associated with vertebrate footprints (bird and mammal) in modern channel near shoreline; associated with horizontal insect tunnels; Suite LB4 | Fluvial channel point bar and channel thalweg during high flow periods; shallow channels during low flow periods; fan-delta channels | Basin margin to lake margin (low gradient) | Holocene to Recent Lake Bogoria; e.g., Parkirichai Section, modern Parkirichai River |

| | | | | | | |
|---|---|---|---|---|---|---|
| Fig. *3.1.*1A, 1C–F, 1H; Fig. *3.1.*2A–D; Sect. 3.1.1 | Moderately well sorted silt and fine-grained sand (may be interbedded with granule- to pebble-conglomerates) | Reddish tan-coloured, bedded and slightly pedogenically altered moderately sorted silt and fine-grained sand; bioturbated by termite nests and galleries preserved by carbonate; carbonate root casts and crack-filling carbonate are abundant; a massive reworked ash fills an apparently shallow meandering channel that is contemporaneous with the silts and sands; other time-equivalent channel-fill deposits include tangential high-angle planar cross bedded silty sands; interbedded with poorly sorted cross-bedded gravel lenses; intercalated with reworked ash deposited as channel lens | Associated with pedogenic modification and overprinting of fluvial sediments by carbonate roots-casts, bee cells, and termite traces; Suite LB6 | Fluvial channels and overbank deposits; high-angle tangential cross-beds possibly of side bar or lower point bar in channel | Basin margin | Pleistocene Loboi Silts, Nyongonyek, Baringo basin |
| Fig. *3.1.*9A–D; Sect. 3.1.4 | Moderately to poorly sorted coarse-grained sand- to granule-sized clastics | Dark brown to black, clast-supported coarse-grained sand and granule-sized gravels; wide and shallow lenticular channel deposits; presumably associated with planar cross-bedded channel bar gravel sands; microbial mats on surfaces at air-sediment-water interface; may be mud-draped in standing water or in low-energy flow areas | Associated with surface trails and ‘pock mark’ traces; Suites LM1, LM3 | Very shallow braided channel system fed by hot spring effluent | Basin margin to lake margin | Recent Nasikie Engida; e.g., hot-spring effluent channels |
| Fig. *3.1.*7A–G; Sect. 3.1.3 | Moderately sorted coarse-grained sand-granule-sized clastics | Dark brown to brownish black moderately sorted coarse sands and gravels; low- to high-angle planar and non-planar cross-stratified; bed dip directions may be basinward or landward; subrounded to angular clasts; may be weakly cemented by calcite or stabilized by grasses; upper beds may be disrupted by vertebrate footprints; may contain concentrations of reworked mollusc shells | Associated with soft substrate, indistinct mammal footprints and tiger beetle larvae vertical burrows; Suite LB4 | Beach bars, spits, barriers bars, and bedded coarse littoral sands and gravels; may be associated with washover fans and small lagoons | Basin margin to lake margin | Pleistocene to Recent Lake Bogoria |
| Fig. *3.1.*6A, 6D; Sect. 3.1.3 | Moderately to moderately well-sorted medium- to coarse-grained sands | Weakly horizontal-bedded to low-angle planar cross-laminated, subrounded to angular sands; sublitharenite (K-feldspar; aegerine clasts) if cemented; dark brown to brownish black; only small amount of grain-coating silts and clays; may be draped with mud and planktonic cyanobacteria in modern setting | Associated with horizontal tunnels, vertical burrows, and subaqeuous surface trails; Suites LB4, LM3 | Low-gradient littoral sands and gravels, and/or littoral shoal bars on flooded mudflats; or, fluvial point bars | Basin margin to lake margin | Holocene to Recent Lake Bogoria; e.g., Parkirichai Section, Loburu Delta |
| Figs. *3.1.*10A–H, 12A–G; Sect. 3.1.4 | Moderately to poorly sorted fine- to coarse-grained sands and sandstones | Light brown to dark brown moderately to poorly sorted fine- to coarse-grained sands and sandstones; internal structures include: plane bedding (with and without parting lineation), ripple cross-lamination, small-scale trough cross-lamination, and planar cross-bedding; with or without clay drapes; may form wavy to flaser bedding; sedimentary structures and bedforms may be disrupted by salt efflorescence, deflation, and/or vertebrate footprints (e.g., flamingos, wildebeest, gazelles); older examples may be weakly cemented by calcite (geopetal, root-filling, and/or authigenic from altered clays) and zeolites (grain-coating and/or authigenic from altered clays or precursor zeolites) | Associated with vertebrate footprints (mammal and bird), surface trails and tunnels in standing water or low-energy flow channels, and rare vertical burrows; Suites LB4, LM4 | Alluvial and sheetwash deposits on fan-deltas and delta-plains | Basin margin to lake margin | Pleistocene to Recent Lake Bogoria; e.g., Sandai Plain; Pleistocene to Recent Lake Magadi; e.g., NE lagoon |
| Fig. *3.1.*8A–E; Sect. 3.1.3 | Moderately sorted fine- to coarse-grained sands with granules and organic detritus drapes | Dark brown to black fine- to coarse-grained sands with granules and detritus drapes (of planktonic bacteria?); may also be coated by brown-coloured muddy, subaqueous microbial mats | Associated with surface trails and bird footprints; Suites LM2, LM3 | Low-energy saline littoral or flooded alluvial/delta-plain; may be associated with springs | Basin margin to lake margin | Recent Lake Magadi (e.g., NW Lagoon) and Nasikie Engida (e.g., NW shoreline) |

| | | | | | | |
|---|---|---|---|---|---|---|
| Figs. *3.1*.6A, 13A–E, 14E–I; Sects. 3.1.3, 5 | Reddish brown silts and silty very fine-grained sands | Reddish brown silts and silty very fine-grained sands; pedogenically modified and containing termite nests and burrows, roots and root-pores; cemented by zeolites (analcime), calcite, Fe-oxyhydroxides, and Mn-oxyhydroxides; may have isolated pebble-conglomerate lenses (Parkirichai) | Associated with insect nests and mammal burrows; Suite LB5 | Pedogenically modified fluvial/overbank/fan deposits of fan-delta | Basin margin to lake margin | Holocene to Recent Lake Bogoria; e.g., Parkirichai River, "Old" Loburu, Sandai Plain |
| Fig. *3.3*.5A–H; Sect. 3.3.2 | Brown, green, white, and black chert mounds ('pillow-chert' mounds of Behr and Röhricht, 2000; Behr, 2002) | Mounds of chert ~1–2.5 m high and ~1–5 m wide; mounds are made up of smaller 'spheres' draped with vertically and/or horizontally banded or bedded chert, fused to form the mounds (cf. Behr and Röhricht, 2000; Behr, 2002); Behr and Röhricht (2000) interpreted the structures as chert diapirs comprising brecciated and fused microbial chert | Not associated with traces | Possibly hot spring-related chert mounds at spring vents? | Basin margin to lake margin | Pleistocene Lake Magadi: Green Beds; e.g., E lagoon, S lagoon (Bird Rock) |
| Figs. *3.1*.15A, 15C–H, 16A–F; Sects. 3.1.6, 3.3.1 | Coarsely crystalline carbonate travertine mounds | Dominantly whitish grey, large (< several metres diameter, < ~2 m high) irregular mounds of laminated to bedded carbonate; laminae may be pustular and stromatolitic and biogenically controlled; bedding may consist of bladed to fibrous aragonite and calcite precipitated abiogenically; rim, pool, terrace, and micro-terrace features common; may have large (< 4 m wide) internal pool surrounded by precipitates (see Renaut, 1982 and Renaut et al., 1986) | Not associated with traces | Hot spring vent and outflow pools and channels (temperatures < 97° C) | Basin margin to lake margin to shallow lacustrine | Pleistocene to Holocene Lake Bogoria; e.g., Loburu Delta, main site; e.g. Chemurkeu |
| Fig. *3.1*.16G, 16H; Sect. 3.1.6 | Finely crystalline, porous carbonate tufa mounds | Greyish to dark brown, small (< 1 m diameter; < 1 m height) irregular mounds of porous carbonate tufa comprising mainly finely crystalline calcite; abundant reed casts within mounds; associated stromatolitic coatings on plant stems abundant; some dark brown thin laminae preserved as part of tufa mound | Associated with reed stem casts | ?Cool or warm spring-fed wetlands (temperatures < ~40° C) with tufa mounds | Basin margin to lake margin | Pleistocene to Holocene Lake Bogoria; e.g., Sandai Plain |
| ***Lake Margin- to Basin Centre-Dominated Lithofacies*** | | | | | | |
| n/a | Matrix-supported, inversely graded muddy coarse-sands with granules | "Gravelly, black coarse sands; massive but with normal or inversely graded clasts, in units 10–20 cm thick" (from Renaut and Tiercelin, 1994, p. 107) | Traces not investigated | Lacustrine turbidites (Bouma sequence A, B); proximal turbidites | Basin centre (high gradient) | Pleistocene to Recent Lake Bogoria; e.g., eastern central sub-basin |
| n/a | Moderately sorted muddy coarse-grained sands | "Muddy, black to dark brown sands in massive or horizontally stratified beds, 5–200 cm thick" (from Renaut and Tiercelin, 1994, p. 107) | Traces not investigated | Lacustrine turbidites (Bouma sequence C) | Basin centre (high gradient) | Pleistocene to Recent Lake Bogoria; e.g., central sub-basin |
| n/a | Massive silts and silty clays to laminated clay | Reddish brown and grey black silts and clays in units 5–30 cm thick; silts mostly massive; clays may be massive or laminated; may be associated with insect debris and vegetal debris (from Renaut and Tiercelin, 1994, p. 107) | Traces not investigated | Lacustrine turbidites (Bouma sequence D, E); distal turbidites or mud from delta front and prodelta hypopycnal plumes | Basin centre (high gradient) | Pleistocene to Recent Lake Bogoria; e.g., eastern central sub-basin or north sub-basin |
| Fig. *3.1*.13F; Sect. 3.2.2 | Planar cross-stratified silty sands | Reddish brown silty sands and sandstones; reddish brown if cemented (Loboi Silts); planar cross-stratified medium beds dipping basinward at ~5°; beds, 1–3 m thick (Renaut and Tiercelin, 1994, p. 107) | Traces not investigated | Fan-delta foresets; distal alluvial fan | Lake margin to basin centre (high gradient) | Pleistocene to Recent Lake Bogoria; e.g., eastern central sub-basin; north Loburu |

| | | | | | | |
|---|---|---|---|---|---|---|
| Figs. *3.1*.13A–F, 14D–I; Sects. 3.1.5, 3.2.2 | Siltstone and silty fine-grained sandstone with induration and bioturbation increasing upwards | Bioturbated, relatively well indurated siltstone to silty very fine sandstone; bedding biogenically disrupted; degree of induration and bioturbation increases to top of unit; cementation by carbonate and zeolites; at Nasikie Engida, buff-coloured; at Lake Bogoria, reddish buff-coloured; may contain carbonate root molds and/or casts; may contain illuviated clay coatings in pores; may form indurated littoral zone where exposed and flooded by lake; may be coated by thin layer of detritus or sub-littoral microbial mats where shorelines lower energy (e.g., Emsos), which contain surface trails and chironomid tube-structures | Associated with overprinted trace suites during subaerial exposure; Suites LB2, LB4, and LB5; associated with modern examples of low-energy littoral traces, Suites LB1, LB3 | Subaerially exposed littoral and deltaic; littoral to supralittoral in modern setting | Lake margin to basin centre (deposited during higher lake levels, reworked and cemented during low lake levels) | Late Pleistocene to early Holocene Nasikie Engida: High Magadi Beds equivalent?; Pleistocene Loboi Silts, Lake Bogoria |
| Fig. *3.2*.2A–H; Sect. 3.2.1 | Moderately well sorted silts and silty very fine-grained sands | Reddish, planar laminated to lenticular and wavy bedded silts and silty very fine sands with clay drapes and/or thin microbial mats on bedding planes; slightly indurated by ?analcime and stabilized by microbial laminae; bedding may be disrupted by salt efflorescence and bioturbation by insects and grasses and sedges | Associated with abundant insect burrows, root-moulds, and flamingo nests; Suites LB4, LB2 | Low-gradient lower delta-plain supralittoral to eulittoral mudflat; may have hot-spring influence and/or wetland vegetation | Lake margin | Recent Lake Bogoria; e.g., south Loburu Delta |
| Figs., *4.2.2*.1, *4.2.2*.2 Sect. 4.2.2 | Greenish to reddish brown or buff-coloured muddy siltstone to very fine-grained sandstone | Well indurated structureless moderately well sorted brown to buff-coloured muddy siltstone to very fine sandstone that preserves surface mounds interpreted as degraded flamingo nest mounds; cements likely include zeolites, and possibly authigenic clays, iron oxides, carbonate and/or silica; greenish and/or reddish colour may be due to zeolite and/or iron oxyhydroxide cements | Associated with degraded flamingo nest-mounds; Suite LM2 | Eulittoral mudflat to subaerially exposed littoral | Lake margin to basin centre | Late Pleistocene to early Holocene Lake Magadi: High Magadi Beds; e.g., E lagoon, SE lagoon |
| Figs. *3.1*.6C–D, *3.1*.11A–I, *3.2*.1A–H; Sects. 3.1.4, 3.2.1, 3.2.2 | Moderately sorted, coarsening upwards, clay-rich silts to very fine-grained sands | Structureless (flamingo-trampled) to planar-laminated buff-coloured silts and siltstones; may be organic-rich and/or clay-rich; beds may coarsen upwards to reddened silts and silty very fine sands disrupted by efflorescent salts and weakly cemented by analcime; lower bed contacts sharp, upper contacts usually not sharp may contain isolated channel lenses of very fine- to fine-grained sandstones representing channel thalwegs in sub-lacustrine delta-front during higher lake levels and incision of ephemeral channels during lower lake levels; exposed delta-front muddy silts have desiccation crack-polygons and salt efflorescence, and mixed microbial/salt crusts; may contain “trample bubbles” and nest-mounds of flamingos, and/or be bioturbated during exposure | Associated with ‘trample bubbles’, flamingo footprints, degraded flamingo nest-mounds, and vertical and horizontal burrows; Suites LB2 and LB4 | Subaerially exposed delta-front fines and muddy fine-grained littoral to sublittoral lacustrine deposits; subaerially exposed delta-front siltstones form mudflats at Sandai Plain | Lake margin to basin centre | Holocene to Recent Lake Bogoria; e.g., Parkirichai Section (Holocene), Bogoria Silts on Sandai Plain, Recent Sandai Plain |
| Fig. *3.2*.4E, 4F; Sect. 3.2.3 | Laminated to very thinly bedded siltstone | Buff-coloured, well sorted tuffaceous siltstone with horizontal planar lamination to very thin bedding; may preserve fish body fossils; intercalated with white, opaque, magadiite bedded cherts | No trace fossils observed | Sublittoral to profundal lacustrine | Lake margin to basin centre | Late Pleistocene to early Holocene High Magadi Beds; e.g., E lagoon |
| Fig. *3.2*.6A, 6B; Sect. 3.2.4 | Calcareous stromatolitic coating | Laminated, stromatolitic carbonate coating ~3–20 cm thick; internally, laminae are pustular to columnar and show growth of microbes (mainly cyanobacteria) with some filaments preserved; stromatolite coats shorelines of sediments and bedrock, as well as reed stems and shrub or tree branches (see Vincens et al., 1986 and Casanova, 1986); associated with chironomid tube structures (Insecta: Diptera: Chironomidae) | Associated with chironomid pupal cases and plant stem casts; Suite LB1 | Littoral zone to sublittoral lacustrine in freshening lake and springs with Ca input | Basin margin to basin centre | Holocene Lake Bogoria |

| | | | | | | |
|---|---|---|---|---|---|---|
| n/a | Opaline sinter cements and crusts | Opaline, amorphous chert cement and crusts precipitated subaqueously at hot spring vents; diatomaceous, and associated with ostracodes, and molluscs; associated with hydrothermal alteration of bedrock and with fluorite crusts (from Renaut and Owen, 1988) | Associated with branching tunnels at Ol Kokwe, Lake Baringo; Suite LB1 | Subaqueous lacustrine hot spring vents | Basin margin to basin centre (along faults) | Pleistocene to Holocene Lake Bogoria; e.g., south sub-basin; (Lake Baringo: Ol Kokwe) |
| Fig. *3.2.*3E–H; Sect. 3.2.1 | Organic-rich, muddy siliceous gel | Translucent, white, soft and malleable siliceous gel in black, organic-rich muddy matrix; associated with hot spring outflow and evaporative mudflats, microbial mats, lake-margin salt efflorescence, and coarse-grained shoreline sands and gravels | Associated with ?vertical burrows and burrow systems of ?earwigs; Suite LM4 | Eulittoral to littoral zone of saline, alkaline lake; may be associated with hot springs | Lake margin to basin centre | Recent Nasikie Engida; cf. Pleistocene Green Beds, "nodular chert" lithofacies |
| Fig. *3.3.*4H; Sect. 3.3.2 | Massive nodular chert | Greenish grey, massive, nodular chert with grey fine-grained tuffaceous and carbonate muds; chert nodules are white and opaque to translucent and irregular in shape; may be associated with bioherm-like structures (Behr and Röhricht, 2000; Behr, 2002) | Associated with vertical burrows and possible earwig burrow systems; Suite LM4 | Evaporitic, muddy littoral zone; may be associated with hot springs | ?Lake margin to basin centre | Pleistocene Green Beds, Lake Magadi; cf. siliceous gels in organic-rich muds, Nasikie Engida |
| Fig. *3.3.*4A–G; Sect. 3.3.2 | White, green, and black irregularly bedded chert, with silicified carbonate mud interbeds | Thinly bedded (~1–4 cm) green, white, and black chert with irregular upper and lower contacts; may have green or black very thin lenses within white bed; may have pustular laminae; tendency for blackish laminae just below mud laminae; some examples have wind-induced large-scale wrinkle surface features; some examples have large (< 5 cm long), displacive evaporite crystal molds (probably trona or gaylussite? blades); may preserve vertebrate footprints; subaerial to shallow subaqueous insect traces abundant in some horizons; desiccation cracks abundant in some horizons; preserves mat-forming bacteria (see Behr and Röhricht, 2000, Behr, 2002) | Associated with possible vertebrate footprints, vertical burrows, surface trails, and surficial "pock mark" trace fossils; Suites LM 3, LM 4 | Air-sediment-water interface associated with microbial mats and hot-springs; not necessarily related to main central lake; may have been system of spring-fed wetlands and pools | Lake margin to basin centre | Pleistocene Lake Magadi; e.g., Green Beds |
| Fig. *4.2.2.*3; Sect. 4.2.2 | Magadiite chert | White to brownish white, translucent to opaque, very finely crystalline chert; may be found in bedded horizons associated with wet, precursor silica 'gels' (e.g., Eugster, 1967, 1969); may contain ooids, possible root pores, and possible lined and unlined terrestrial invertebrate burrows formed prior to complete desiccation; usually shows desiccation and/or precipitation features like parallel 'micro-fractures' and 'toothpaste' structures | Possible vertical burrows; cf. Suite LM4 | ?Lacustrine to lake-margin wetland? | Lake margin to basin centre | Late Pleistocene to early Holocene Lake Magadi: the High Magadi Beds and equivalents; e.g., S Nasikie Engida; e.g., SE lagoon, Lake Magadi |
| Fig. *3.2.*1C–F, 1H; Sects. 3.2.1, 3 | Black and brown structureless silty clay | Organic-rich silty muds; structureless; with or without air 'bubbles' or gas vesicles; oxidized mud brown, anoxic mud black in colour; typically deposited as delta-front to lacustrine fines and subsequently trampled by flamingos; clay minerals are dominantly smectite, illite, and illite-smectite (I/S) | Associated with flamingo footprints, trampled sediments, and nest-mounds; Suite LB2 | Subaerially exposed muddy littoral to sublittoral lacustrine | Lake margin to basin centre | Recent Lake Bogoria; e.g., shoreline at Sandai Delta Plain |
| cf. Fig. *3.2.*1H; Fig. *3.2.*5; Sect. 3.2.3 | Black organic ooze with bedded and displacive $NaCO_3$ evaporites and other authigenic minerals | Black, organic-rich silty lacustrine mud with authigenic, acicular trona, nahcolite, and thermonatrite; organics are sapropelic and derived from planktonic organisms (e.g., cyanobacteria: *Arthrospira*); horizontal bedding vague if present and disrupted by evaporite precipitation; evaporites may form cohesive beds < 10 cm thick; may contain gaylussite, analcime, fluorite, kanemite, pyrite and siderite (from Tiercelin et al., 1981; Renaut et al., 1986; Tiercelin et al., 1987; Renaut and Tiercelin, 1994) | Not investigated for trace fossils (not expected); note: profundal zone can be found in shallow water where abundant planktonic microbes and shallow chemocline | Sublittoral to profundal lacustrine | Basin centre | Pleistocene to Recent Lake Bogoria; e.g., central sub-basin |

| | | | | | | |
|---|---|---|---|---|---|---|
| Fig. *3.2*.7A–F; Sect. 3.2.5 | Interbedded $NaCO_3$ evaporites and organic-rich mud | Horizons of $NaCO_3$ evaporites (e.g., acicular trona and nahcolite); beds approximately 1–3 cm thick; interbedded evaporite horizons and organic-rich muds; muds may contain displacive evaporites; in the modern setting, muds and salts are associated with pink to salmon-coloured microbes (probably Archaea, Halobacteria); salt teepees developed in ~3 m diameter polygons; finely crystalline surface evaporites may contain wind-induced large-scale 'wrinkle-like' or 'folded' or 'crumpled' bedforms | Not associated with trace fossils | Subaerially exposed basin centre salt pan with seasonal flooding and spring water input | Lake margin to basin centre | Recent Lake Magadi; e.g., NW lagoon |
| Fig. *3.2*.8A–D; Sect. 3.2.5 | Laminated to thinly bedded $NaCO_3$ evaporites | Horizontally laminated to very thinly bedded sodium carbonate evaporites (trona and ?nahcolite); beds ~1–3 cm thick and sometimes in couplets, showing bottom-nucleated acicular trona at base capped with flat, brine surface-nucleated, laminae that settled and rests on acicular crystals of lower, porous bed; may also have transported crystals and/or dissolution/reprecipitation features, including flat, microcrystalline evaporite laminae or beds; salt-induced push-up ridges developed in > 3 m diameter polygons; may contain fine-grained siliciclastics at bedding planes | Not associated with trace fossils | Subaerially exposed basin centre salt pan (with seasonal flooding) | Lake margin to basin centre | Recent Lake Magadi; e.g., central lake |
| Fig. *3.2*.9A–E; Sect. 3.2.5 | Thinly bedded $NaCO_3$ evaporites | Relatively thick, thinly bedded grayish bladed evaporites (mainly trona); sometimes as couplets in beds ~4–7 cm thick with irregular brown silt laminae capping couplet; trona crystals bottom-nucleated with bladed fan-shaped or needle-splay growth; couplets may grade upwards from bottom-nucleated acicular needle-like crystals to very finely crystalline to massive horizon below clastic horizon; clastic horizons may be distinct and continuous (sheetwash?) or vague and lenticular (?eolian); textures may include horizontally oriented recrystallized crystal blades | Not associated with traces | Subaerially exposed basin centre salt pan with clastic horizons deposited by eolian processes or sheetwash | Basin centre | Recent Lake Magadi; e.g.,central lake and brine pools |
| Fig. *3.2*.8E–H; Sect. 3.2.5 | Black to grey, cemented organic-rich mudstone with evaporites | Black to grayish, organic-rich mudstone; well cemented (by zeolites or evaporites?); may be channelized, with channel straight to meandering; large evaporite crystals (trona blades) approximately 5–7 cm in length arranged parallel to sub-parallel to one another and roughly parallel to interpreted current flow; 'flow' crystals may be arranged normal to current direction if there was a 'salt jam' (compare with ice jam); associated with rare vertebrate tracks and dead insects (e.g., grasshoppers, beetles, dragonflies); crystal blades oriented horizontally in black muddy matrix underlie upper salt crust | May be associated with rare vertebrate footprints; Suite LM 4 | Evaporated muddy brine below upper salt crust and evaporated ephemeral channels through salt pan | Lake margin to basin centre | Recent Lake Magadi; e.g., central lake; cf. Holocene basin centre core from Lake Magadi |

### 3.1. Basin Margin to Lake Margin Lithofacies Assemblages

Detrital siliciclastic sediments that are deposited in and around the Kenya Rift lakes studied are derived mainly from Pliocene to Pleistocene lavas of trachyte, basalt, and phonolite composition (e.g., Baker and Wohlenberg, 1971; Baker, 1986). Physically weathered sediment derived from these volcanic rocks is transported to the lake margins by several methods: 1) by gravity, as colluvium against steeply-dipping normal fault scarps; 2) as alluvium transported by ephemeral streams draining very small catchments on escarpments and low-lying plains; 3) as unchanneled sheetwash across deltaic and alluvial plains; 4) by perennial rivers draining larger catchments that include topographically higher areas (e.g., Sandai River, Bogoria drainage); 5) by perennial streams fed by springs (e.g., Nasikie Engida) that acquire sediment from tributaries or other sources; and, 6) by eolian transport of silt- to fine sand-sized particles (e.g., Sandai Plain, Lake Bogoria). The gradient and size of typical basin margin to lake margin depositional settings such as alluvial fans also depend on the tectonic movements of bounding faults, and the relative amount of stability over time (Tiercelin, 1990).

The main depositional environments of the "basin margin" to "lake margin" lithofacies assemblages include: 1) terrestrial floodplains with trunk channels and pedogenically modified overbank deposits; 2) colluvial and alluvial fans; 3) shoreline areas with gravel beach bars, cross-bedded and planar-bedded coarse-grained sands, and small back-barrier lagoons in high-energy shorelines, and muddy detritus-covered coarse-grained sands in lower-energy shorelines; 4) alluvial plains to upper delta-plains with meandering, straight, or anastomosing distributary and terminal distributary channels, sheetflood deposits, eolian deposits, and exposed, old lacustrine or delta-front sediments deposited during highstands; 5) pedogenically modified and indurated delta-plains, mudflats, and shorelines 'abandoned' during lake lowstands; and 6) mainly subaerial, fault-related spring deposits dominated by carbonates and cherts . Lower delta-plain to proximal delta-front and mudflat lithofacies assemblages were grouped with the typical facies of the "basin centre", although they may be closely related to the subaerially exposed upper delta-plain. In general, the modern environments observed at Lake Bogoria, with "intermediate" lake levels, represent a more basin margin-dominated assemblage when compared to Lakes Magadi and Nasikie, which represent a more basin centre-dominated assemblage deposited during present-day low lake levels (cf. Renaut and Tiercelin, 1994).

In the Bogoria basin, the lithofacies of the Loboi Silts, Bogoria Silts, and the modern siliciclastic sediments of the lake and its margins have been previously described by Tiercelin (1981, 1990), Tiercelin et al. (1981), Renaut (1982, 1993), Renaut et al. (1986), Renaut and Owen (1991), and Renaut and Tiercelin (1994). Several analyses and descriptions of the authigenic minerals of the basin as well as hot-spring deposits were given by Renaut et al. (1986, 1998), Renaut and Owen (1988), Renaut (1993), Renaut and Jones (1997), and R.A. Owen et al. (2008). R.B. Owen et al. (2004) described the different types of marshes that surround Lake Bogoria and the composition and environmental significance of the wetland diatom assemblages. Onkaware (2000) investigated the salinity in sediments and the vegetation of the Loburu Delta. In the Magadi basin, Pleistocene to modern lithofacies have been briefly described by Surdam and Eugster (1976) and Eugster (1980). Behr and Röhricht (2000) and Behr (2002) described in detail the chert-containing facies of the Green Beds and High Magadi Beds in the Magadi Basin, and revised the previous interpretations of Eugster and colleagues (e.g., B.F. Jones et al., 1977; Eugster, 1969, 1980). The work presented below benefited from discussions in the field with Bernie Owen (Hong Kong Baptist University) and Robin Renaut (University of Saskatchewan).

### *3.1.1. Bedded and Pedogenically Modified Silts and Sands to Pebble-Sized Channel-Fill Alluvium*

This lithofacies association comprises fluvial floodplain and channel sandstones and gravels with bedded, very fine-grained tuffaceous overbank sands and silts that have been pedogenically modified and bioturbated. Where examined on the southwestern margin of the Baringo basin, the Pleistocene Loboi Silts are being incised by modern ephemeral tributary channels that empty into the Perkerra River, which drains into the southern (Molo) wetlands of Lake Baringo. In the study area, the Loboi Silts correlate with the uppermost Pleistocene Kapthurin Formation of the Baringo basin (K4?, K5?; cf. Tryon and McBrearty, 2006; Tryon, 2006). The sediments appear to represent colluvial and fluvial channel conglomerates, and unchanneled sheetwash and overbank deposits that formed on low-gradient, basin margin, alluvial fan and/or floodplain following a phase of downfaulting (Le Turdu et al., 1995; Renaut, pers. comm., 2001). Near Nyongonyek (Fig. 2.2), these middle Pleistocene (Middle Stone Age; Farrand et al., 1976) deposits are composed of poorly indurated, moderately sorted reddish silts and very fine-grained sands (Figs. *3.1.*1, 2). The sediments retain some planar horizontal bedding, cross-bedding, and cross-lamination, but are generally modified by pedogenesis and bioturbation by termites and other soil-dwelling animals (e.g., mammals, beetles, bees) whose trace fossils are preserved mainly by carbonate cements (see Section 4.1.1). Carbonate root casts and carbonate crack-fill cements are abundant (Le Turdu et al., 1995).

Most of the silts and very fine-grained sands likely represent deposition within shallow channels and overbank deposits onto a flat-lying plain (Figs. *3.1.*1, 2). An ash flow-filled meandering channel is contemporaneous with these trace fossil-preserving fines (Figs. *3.1.*1E, 1F, 2A–D) and with *in situ* and reworked Middle Stone Age stone tools found in gravel lenses in the pedogenically altered silts and sands (Fig. *3.1.*1C). These deposits are best exposed in an < 4 m-deep modern incised gully where a stratigraphic section was measured (0.44°N, 36.00°E; Ashley, Driese, and Owen, 2002, unpublished) and the trace fossils were collected in 2008. Less than ~500 m west of the measured section, fine-grained sands preserved as high-angle accretion surfaces that represent the migration of a channel bar (< ~1.5 m high) are likely time-equivalent to the silts and sands (lower unit) examined in more detail (Fig. *3.1.*1A). Coarser, cross-bedded muddy gravel lenses may represent a braided channel system that is also time-equivalent to the silts and sands (upper unit) that contain trace fossils and root casts (Fig. *3.1.*1C).

Prior to modern incision, the uppermost exposed Loboi Silts were scoured by broad channels that were filled by moderately to poorly sorted, subrounded to rounded pebble-sized polymictic orthoconglomerates (Fig. *3.1.*1C, 1D, 1F, 1G). This unit is likely Late Pleistocene to Holocene in age, and contains Late Stone Age artifacts (Farrand et al., 1976). Beds are normally graded, horizontal to low-angle cross-bedded, and contain some examples of imbricated pebble-sized clasts (Fig. *3.1.*1D, 1G). The uppermost, and *oldest*, conglomerates of this unit may have

**Fig. 3.1.1.** (Next page) Alluvial facies of the Pleistocene Loboi Silts at Nyongonyek, Baringo basin. **(A)** Accretion surfaces in silty fine-grained sands of the lower unit at Nyongonyek. **(B)** Cross-bedded pebble conglomerate of younger gravels. Hammer for scale. **(C)** Channel granule conglomerate lenses and silty fine-grained sands of the Loboi Silts (LS) scoured and overlain by weakly bedded younger (H – Holocene?) pebble conglomerates. **(D)** Pedogenically modified silty fine-grained sands of the Loboi Silts (LS) scoured and overlain by younger, low-angle cross bedded pebble conglomerate and sands (H - Holocene?). Hammer for scale. **(E)** Cross-sectional view of lenticular reworked ash deposit of the Loboi Silts (arrow). Note that the modern channel approximately follows the same course. **(F)** The Loboi Silts in the area where the trace fossils were investigated, showing the laterally equivalent bed to the ash-filled channel (arrow). **(G)** The modern ephemeral channel at Nyongonyek cutting bedded gravels (Holocene?) showing the reuse of the main channel. Hammer for scale. **(H)** The modern ephemeral channel showing the flat, fine-grained beds of a point bar (right). People for scale.

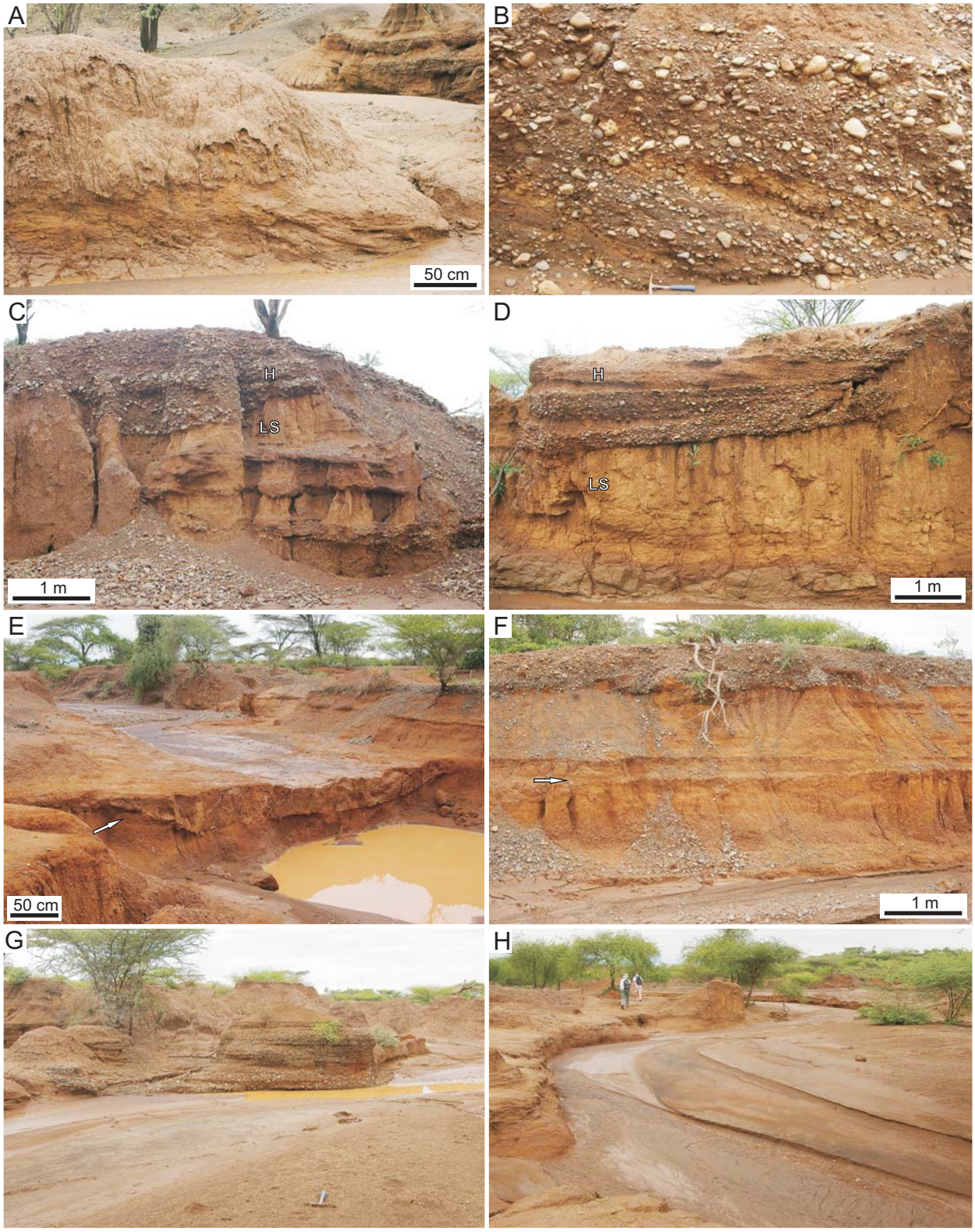
A
50 cm
B
C
H
LS
1 m
D
H
LS
1 m
E
50 cm
F
1 m
G
H

been deposited on an alluvial fan that was built out onto the Pleistocene plain. High-angle planar cross-beds up to 2 m in height are present in a lower unit of imbricated, poorly sorted orthoconglomerates and appear to underlie the uppermost scoured-base conglomerates. They may represent an earlier phase of fan building, or they may represent relatively deep channel flow and the migration of a channel bar (Fig. *3.1.*1B). More fieldwork is required to investigate the timing of these events and for the detailed description of the facies and stratigraphic relationships in this area.

Incision into the distal fan/plain then occurred progressively throughout the deposition of the channel conglomerates. Reddish, indurated termite mounds are preserved on relatively young Late Pleistocene–Holocene terraces within the modern channel system that suggest a period of stability and/or channel abandonment before modern incision (see Section 4.1.1, Fig. *4.1.1.*3A–D). The reconstruction of the relative timing of these conglomerates is complex due to repeated incision events and the deposition of similar sediments. Additionally, the channel systems appear to have been reused during successive periods of incision. For example, the modern channel is presently re-using the Middle Pleistocene ash-filled channel for several hundred metres along its length (Figs. *3.1.*1E, 2A).

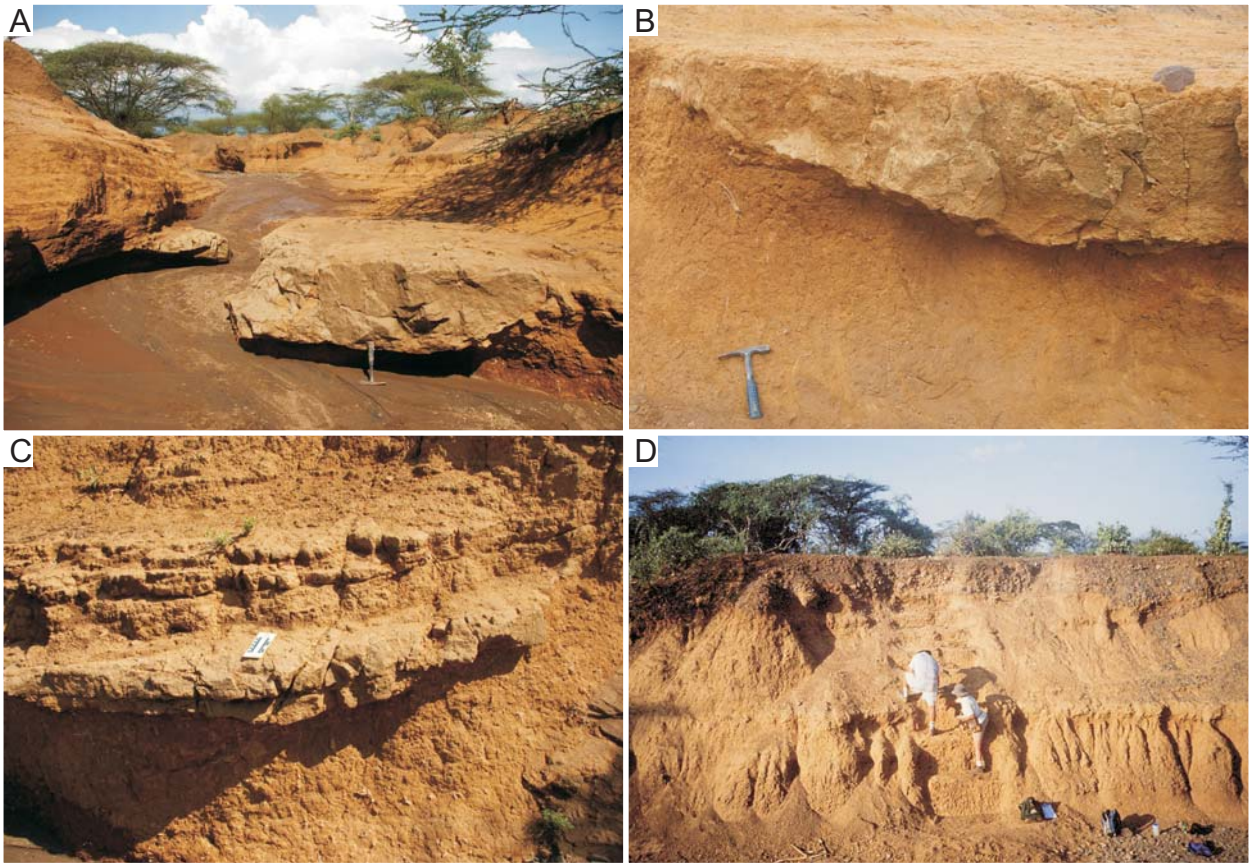


**Fig. 3.1.2.** The trace fossil site in the Loboi Silts at Nyongonyek, Baringo basin. **(A)** Modern channel incising through the Pleistocene ash-filled channel. Hammer for scale. **(B)** The ash-filled channel and the lower unit of the Loboi Silts. Hammer for scale. **(C)** Flat-lying ash beds adjacent to lenticular channel body. Carbonate trace fossils in Loboi Silts below. Ten-cm scale in middle of photograph. **(D)** The measured section of the Loboi Silts at Nyongonyek. People for scale.

*3.1.2. Coarse-Grained Sand- to Boulder-Sized Colluvium and Alluvium*

Along the relatively steep margins of the lakes, particularly if they are basin-bounding normal faults, shorelines may be composed mainly of angular boulders of volcanic rock (Fig. *3.1.*3A–D; Renaut, 1982). These very poorly sorted sediments may contain calcite cements, authigenic smectite and/or illite clay minerals, authigenic zeolites, and, depending on their age, analcime and iron oxide cements (Surdam and Eugster, 1976; Renaut, 1993; Renaut and Tiercelin, 1994; Fig. *3.1.*3C, 3D). Alluvial fans and fan deltas may build out into the lakes or onto the plains of the basin floors, and also contain finer-grained sediments as matrix material (Fig. *3.1.*3D–H; Renaut, 1982). In the Baringo-Bogoria basin, for example, the Pleistocene Sandai-Waseges alluvial fan is relatively large, and formed where the Sandai-Waseges River empties through a narrow gorge onto the rift floor (Fig. *3.1.*3E; Renaut, 1982). The river originates at the eastern rift margin, just west of the Laikipia Highlands north of the Aberdares Ranges, and drains along a series of step-faulted platforms until it finally reaches the rift floor. During the Pleistocene deposition of the fan, the river variably emptied into either the Baringo basin to the north, or into the Bogoria basin to the south (Renaut, 1982). Today, the river flows into the Bogoria basin, and the Sandai-Waseges fan forms a part of the sill separating the Bogoria basin from the lower-lying Baringo basin.

Elsewhere along the high-relief, steep eastern escarpment (boundary fault margin) of the Bogoria basin, alluvial fans fed by very small, local drainages, have coalesced into a series of fan bajadas, which form most of the eastern shoreline of the lake (Fig. *3.1.*3F; Renaut, 1982; Renaut and Tiercelin, 1994). The alluvial fans are incised by channels, contain imbricated cross-bedded gravel lenses (e.g., Renaut, 1982; Renaut and Tiercelin, 1994), and may feed density currents depositing turbidites within the lake (Tiercelin et al., 1987; Tiercelin, 1990; Renaut and Tiercelin, 1994). The toes of these alluvial fans may be reworked to form a coarse-grained shoreline with well developed beaches (Renaut and Owen, 1991). The relief of the western, hinged margin of the Lake Bogoria half-graben basin is relatively low, formed by gently dipping step-faulted Pleistocene trachyphonolites. Trachyphonolite boulders in colluvium may create steep margins of the lake, or small colluvial fans that spread out onto areas where the lake margin has a lower gradient (Figs. *3.1.*3A, 4A–C). Depending on its age and history, the colluvium may be well cemented by calcite or analcime (Fig. *3.1.*3C, 3D). If the colluvium reaches the zone of lake-level rise-and-fall, it may become intercalated with shoreline siltstones and sandstones (Figs. *3.1.*3B, 4C).

Colluvial deposits and small fan deltas are also found along horsts and basin-bounding normal faults at the margins of Lake Magadi and Nasikie Engida. At Lake Magadi (Fig. *3.1.*3G) and Nasikie Engida (Fig. *3.1.*3H), the relief of the basin-bounding faults is much less than the eastern wall of the Bogoria half-graben, and consequently, the size and lateral extent of the colluvial and alluvial fans are generally much less. Similarly, Lakes Magadi and Nasikie Engida are much shallower than Lake Bogoria, so the subaqueous deposition of turbidites has not occurred.

**Fig. 3.1.3.** (Next page) Coarse-grained sands to boulder-sized colluvium and alluvium at Lake Bogoria (A–F), Lake Magadi (G), and Nasikie Engida (H). Photograph shown in (H) courtesy of R.Renaut. **(A)** Trachyphonolite colluvium along the western margin of Lake Bogoria. **(B)** Pebble-sized colluvium at modern shoreline overlying indurated fine-grained sandstones of the Loboi Silts. **(C)** Pleistocene colluvium on the western margin of Lake Bogoria at North Loburu. Hammer for scale. **(D)** Close up of cemented trachyphonolite colluvium at North Loburu. Hammer for scale. **(E)** Google Earth 2009 image of the Pleistocene Sandai Fan on the Loboi Plain north of Lake Bogoria. **(F)** Google Earth 2009 image of coalescing alluvial fans on the eastern, border fault margin of Lake Bogoria. **(G)** Magadi townsite horst forming the margin of the central basin at Lake Magadi. Note small alluvial fan in foreground. **(H)** Alluvial fan with colluvium on the western margin of Nasikie Engida. Note salt efflorescence.

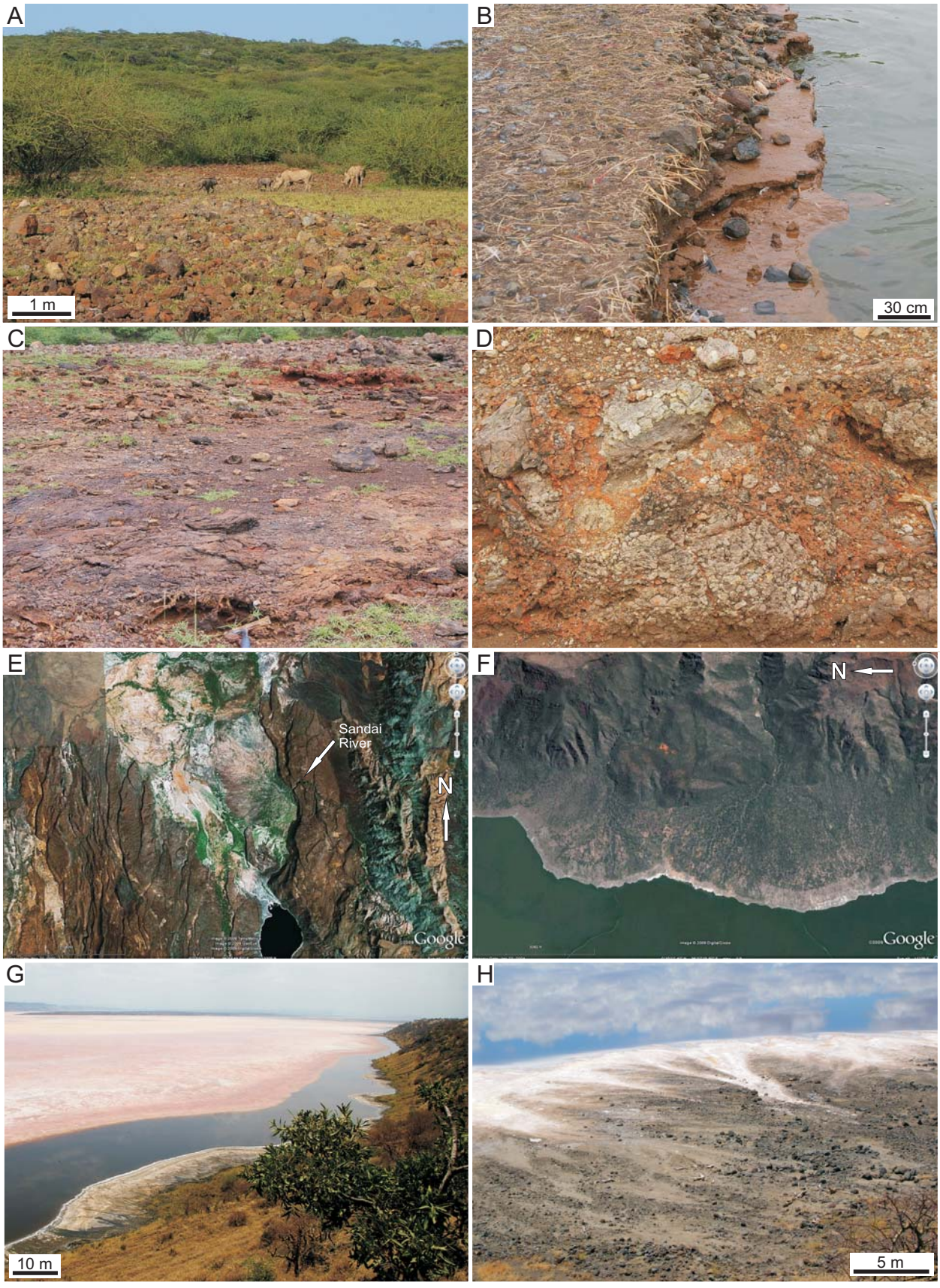
A
1 m
B
30 cm
C
D
E
Sandai
River
N
Google
F
N
Google
G
10 m
H
5 m

Small fan deltas composed of coarse-grained sands to boulder-sized sediments intercalated with fine-grained lake-margin and lacustrine sediments are best developed along the western, hinged margin of Lake Bogoria where ephemeral rivers draining the step-faulted half-grabens enter the basin (Fig. *3.1.*4A–D). A short stratigraphic section was measured where the Parkirichai River enters the Bogoria basin on its western, hinged margin (Figs. *3.1.*4D, 5, 6A), recording mostly coarse-grained fluvial deposits, with a coarsening-upwards unit of silts and fine-grained sands interpreted as delta-front to delta-plain deposits, as well as an uppermost soil that forms the modern land surface adjacent to the incised modern river. The lower unit consists of a very poorly sorted pebble-sized paraconglomerate in a coarse-grained sandy matrix with sub-rounded clasts that may represent deposition of colluvium and alluvium in an alluvial fan/fan delta (Fig. *3.1.*6A, 6B). A sharp, flat contact above this conglomerate is overlain by a bedset with small lenses of poorly sorted granule-sized orthoconglomerates in a matrix of coarse-grained sandstone (Fig. *3.1.*6B). This association is interpreted as a set of shallow channels, representing deposition either in numerous small, shallow channels on the alluvial fan/fan delta, or in a braided channel of the proximal fan delta.

These alluvial facies are sharply overlain by a set of discontinuously laminated and bioturbated siltstones to fine-grained sandstones interpreted as coarsening-upwards beds of delta-front and lacustrine to delta-plain deposits, possibly deposited during the late Pleistocene to early Holocene (Fig. *3.1.*6A, 6C, 6D; see Sections. 3.2.1, 3.2.2). Although these fine-grained facies are typically associated with lake-margin to basin-centre localities, they were overprinted by mammal burrows and possible insect nests that testify to the basin margin location of this site (Fig. *3.1.*6C). Unlike the Nyongonyek paleosols, however, the animal and plant trace fossils at Parkirichai were not preserved by carbonates and only weak pedogenesis affected the silts and fine-grained sands. The unit coarsens upwards and is scoured by a thick bed of horizontal to low-angle cross-bedded coarse-grained sand and granule-sized gravel lenses interpreted as fluvial bars in channels of the fan delta (Fig. *3.1.*6E). These deposits are very similar to those of the modern Parkirichai River, which is presently incising these older alluvial fan to fan delta deposits and feeding the modern delta lobe (Figs. *3.1.*4E–H). The older fluvial channel deposits were scoured into and overlain by pebble-conglomerates and a soil above an erosional contact that may mark the initial incision of the modern channel, and may represent a sequence boundary (Figs. *3.1.*5, *3.1.*6A). The succession recorded in the Parkirichai River section appears to represent the evolution of a fan delta, from: 1) a fining-upwards unit of colluvial and/or alluvial fan deposits; to 2) a coarsening upwards, drowned, prograding fan-delta unit of lacustrine, delta-front, delta-plain, beach(?), and fluvial deposits; to 3) incision and pedogenesis of the present-day proximal upper delta-plain. Today, the incised Parkirichai River is reworking the lower colluvial/alluvial unit and incorporating these older pebble- to boulder-sized clasts into channel deposits close to the lake (Fig. *3.1.*4E, 4F, 4H).

**Fig. 3.1.4.** (Next page) Alluvial fans, fan deltas, and fluvial channels at Lake Bogoria. **(A)** Google Earth 2009 image of the Loburu Delta on the central, western margin of Lake Bogoria. At left is the north Loburu Delta, fed by the Kipsarian River. The two lobes of the delta are fed by the Parkirichai River. **(B)** Google Earth image of the north Loburu Delta showing the flooded main channel (centre) and the wave-influenced coarse-grained shoreline (left). **(C)** Holocene colluvium overlying indurated fine-grained sandstones of the Loboi Silts at north Loburu. **(D)** Google Earth 2009 image of the Loburu Delta showing the older, Pleistocene fan at left and the Holocene to modern lobe (south Loburu) of the Parkirichai River at right. Arrow shows location of measured section shown in Fig. 3.1.5. **(E)** Photograph looking upstream in the Parkirichai River channel showing flat-bedded coarse-grained sands in channel with older, possibly reworked boulders at left. **(F)** The Parkirichai River near the modern shoreline at south Loburu incised into older (Holocene?) conglomerates intercalated with silty sands. **(G)** Parkirichai River looking towards the lake with bird tracks (arrow) and mammal tracks (small pools) in channel. **(H)** The mouth of the Parkirichai River with thousands of lesser flamingos marching up the channel.

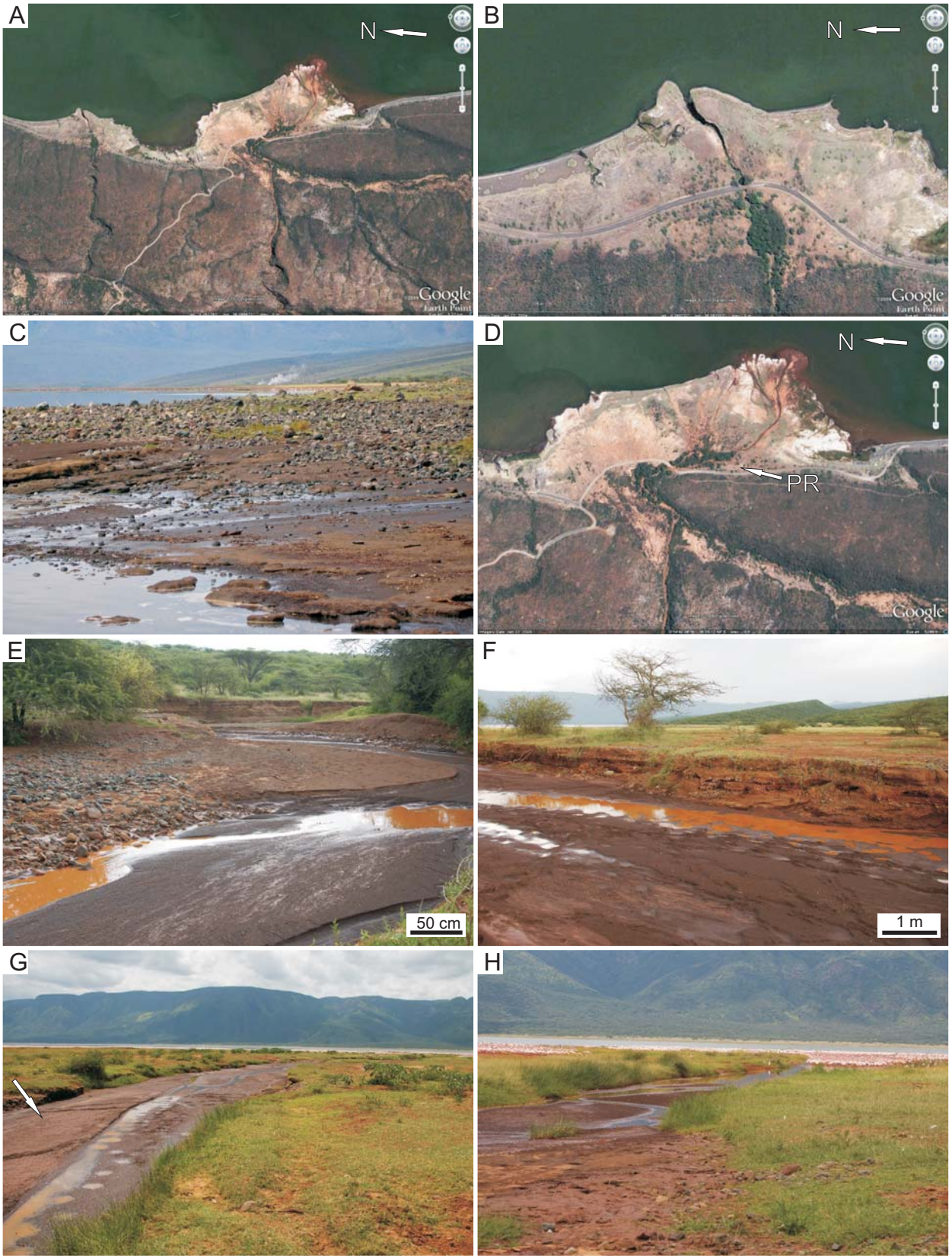
A
N
Google
Earth Point
B
N
Google
Earth Point
C
D
N
PR
Google
E
50 cm
F
1 m
G
H

*3.1.3. Moderately Sorted Coarse-Grained Sand- to Pebble-Sized Shoreline Deposits*

This lithofacies assemblage is best represented at Lake Bogoria, where the lake water is sufficiently deep and there is sufficient fetch for the development of wave-reworked coarse-grained sand and gravel beach deposits. Coarse-grained sand- to pebble-sized clastics derived from trachytic, basaltic, and trachyphonolitic lavas may be reworked into shoreline deposits including: 1) cross-bedded spits and barriers; 2) cross-bedded beach bars; 3) low-angle planar cross-bedded swash zone beach deposits; and, 4) imbricated gravels deposited as lake-shore terraces (Renaut and Owen, 1991). Coarse-grained sand- to granule-sized shoreline terrace deposits stabilized today by grasses represent higher lake levels during the Holocene, and are

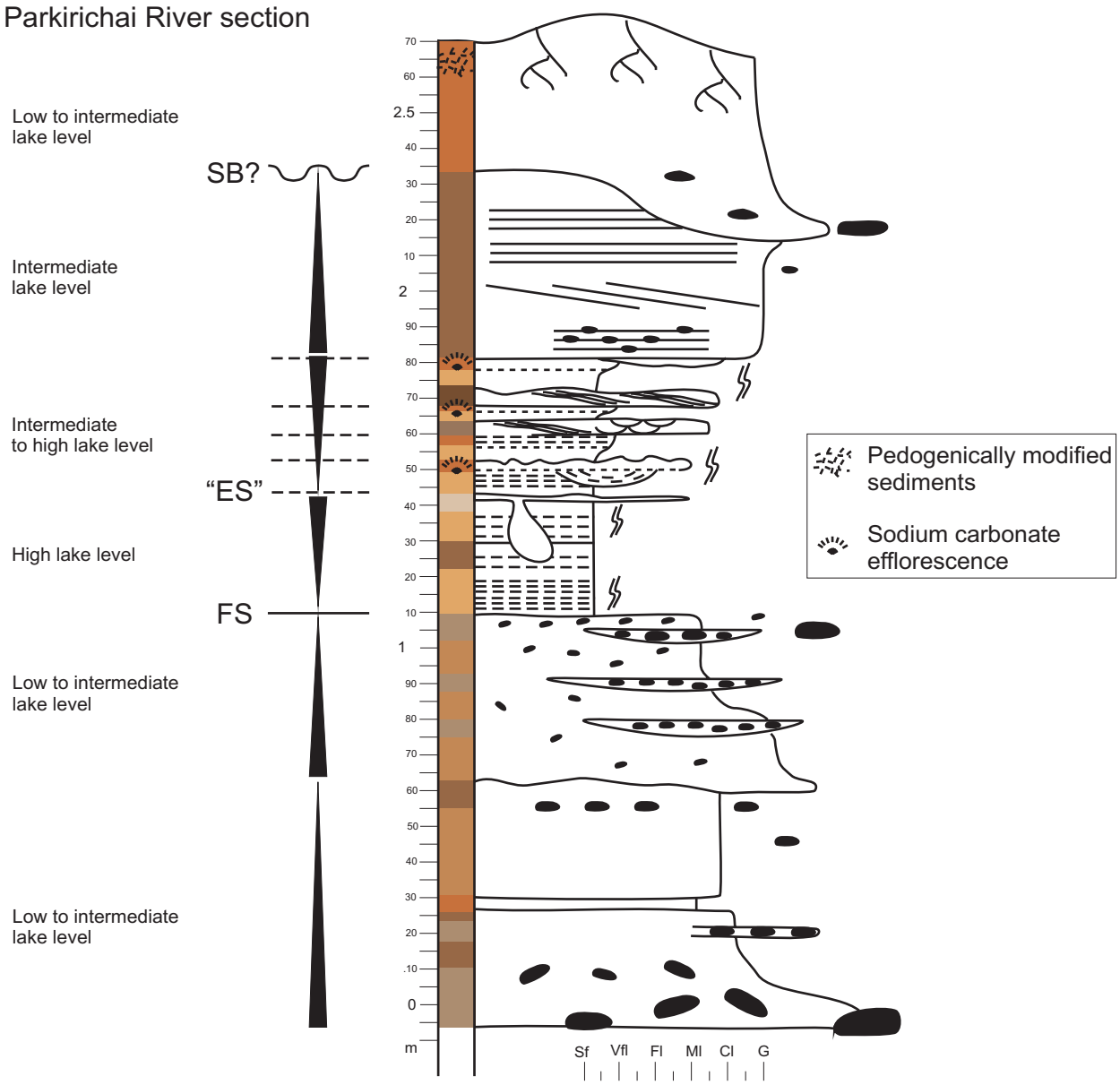


**Fig. 3.1.5.** The measured section from the Parkirichai River showing coarsening upwards and fining upwards cycles. FS: Flooding surface. "ES": Subaerial exposure surface. SB: Sequence boundary. Colours approximate the actual colours of the sediments. See Appendix A for legend.

well exposed on Sandai Plain and locally around the entire lake. These Holocene sediments are transported to the shoreline by ephemeral sheetwash and in shallow channels during rainstorms. The modern shoreline is composed of ~50% beach bars, spits, and barrier bars (Renaut and Owen, 1991). Shallow, narrow, enclosed lagoons containing coarse-grained sand and silt often occur behind the bars, which vary from approximately 5 cm to 30 cm in height and from less

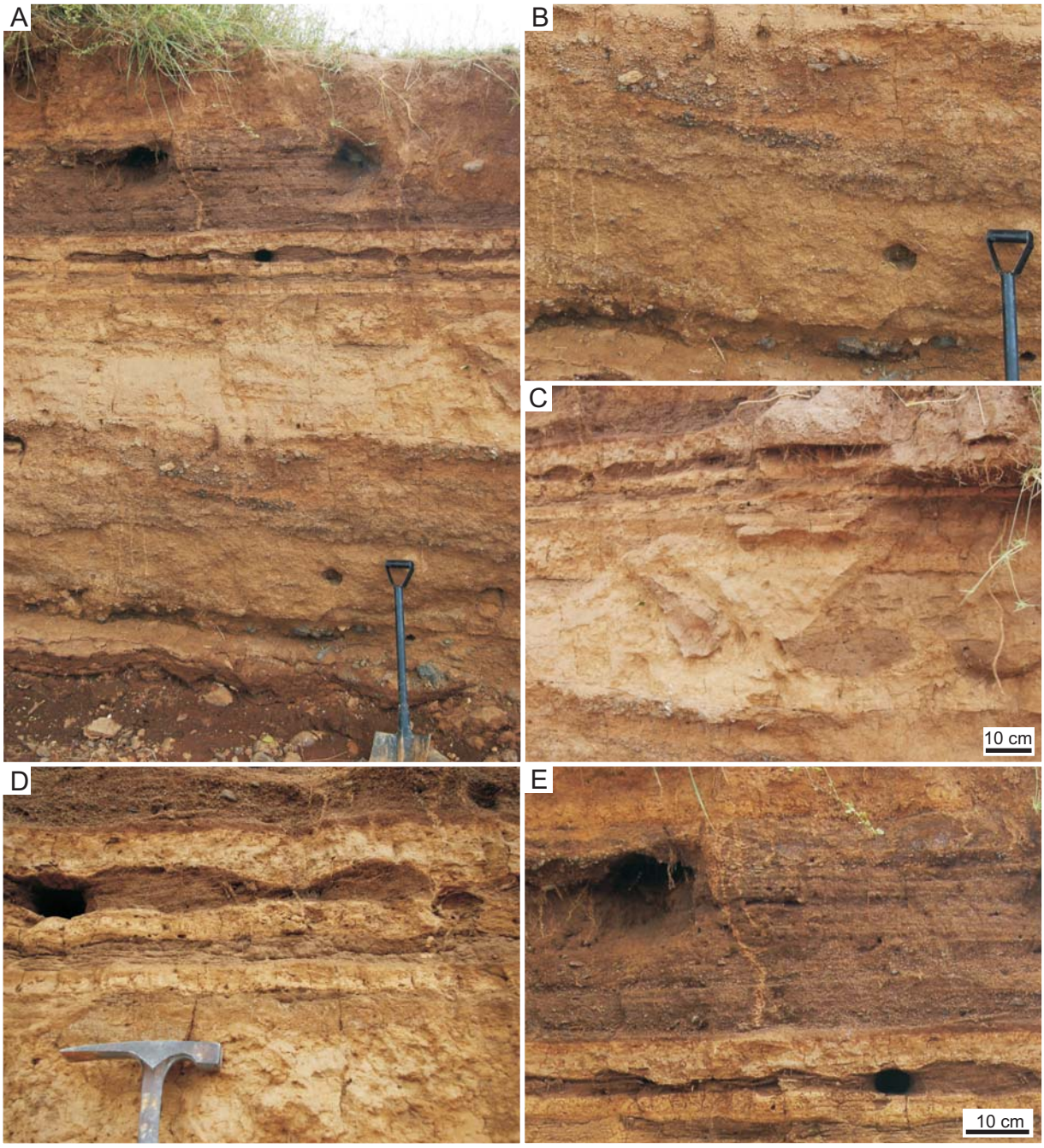


**Fig. 3.1.6.** Photographs showing the measured section from the Parkirichai River. **(A)** Exposed Pleistocene to Holocene sediments. Section is 2.7 m thick. Lower portion shows fining upwards conglomerates **(B, C)**. Middle portion coarsens upwards from buff coloured silts to dark brown bedded coarse-grained sands **(D)**. Upper portion shows bedded coarse-grained sands and granule-sized gravels **(E)** incised and overlain by pedogenically modified silts and gravels. Shovel and hammer for scales.

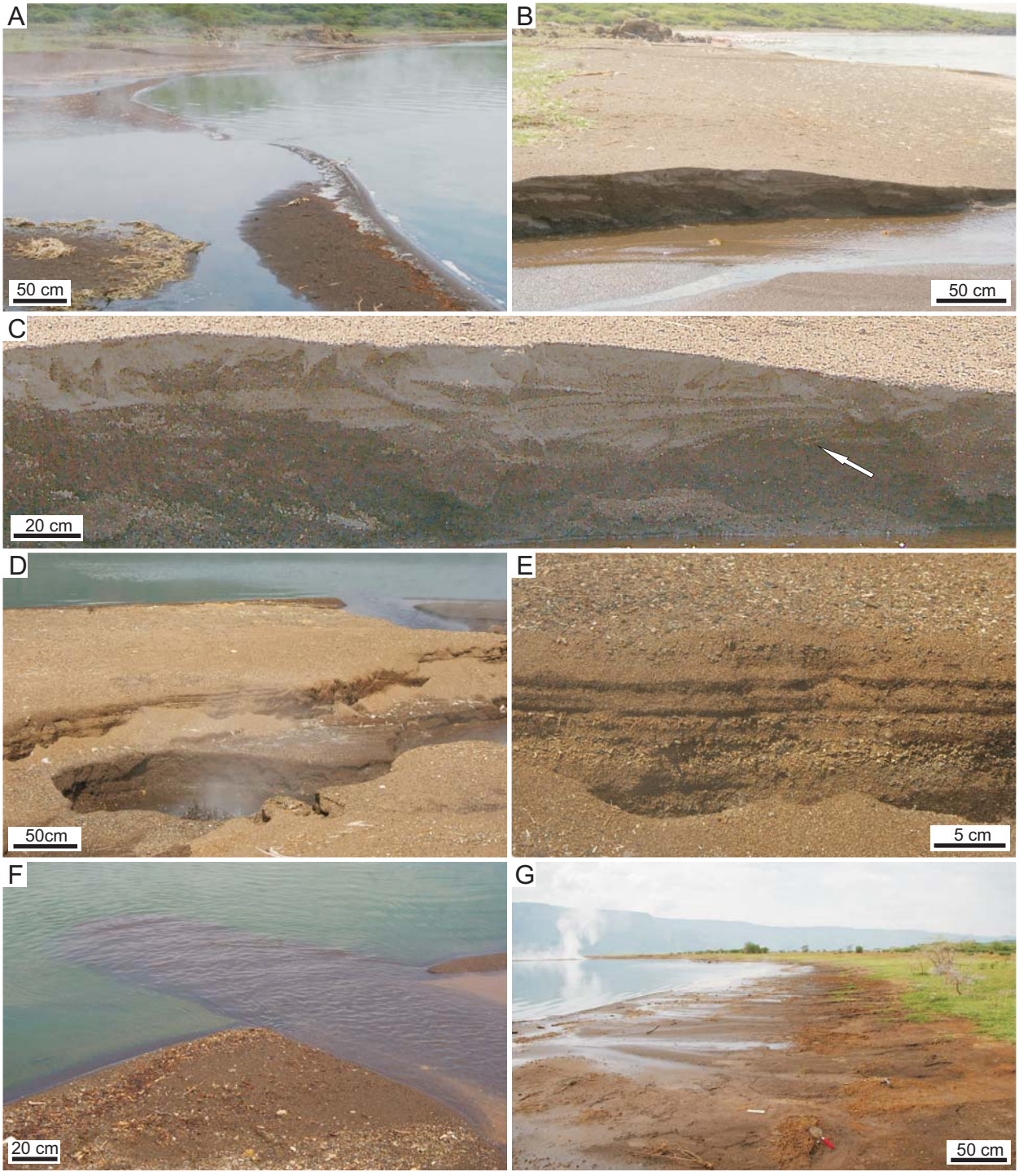


**Fig. 3.1.7.** Coarse-grained sediments of modern shorelines at Lake Bogoria. **(A)** Small spit of western shoreline at north Loburu. Steam is from hot spring outflow. **(B)** Cross-bedded beach bar cut by hot spring outflow channel at north Loburu. **(C)** Beach bar showing convex-up, non-parallel cross-beds dipping away from shoreline (arrow). **(D)** Bedded littoral coarse-grained sands and gravels cut by hot spring near shoreline. **(E)** Close up of (D). **(F)** Mini-delta at shoreline fed by hot spring outflow and reworked littoral sands. **(G)** Shoreline at "old" Loburu showing modern dark brown, coarse-grained littoral sands overlying indurated reddish silty sands of the Loboi Silts.

than 5 cm to 4 m in width (Fig. *3.1.*7A; Renaut and Owen, 1991). The bars comprise non-parallel, convex-up, cross-bedded foresets dipping away from the lake with lakeward dipping planar cross-beds (Fig. *3.1.*7B, 7C).

Planar, parallel, low-angle stratification is present in moderately sorted coarse-grained sands on the relatively low-gradient shoreline (e.g., Loburu Delta, Aug. 2008), which had apparently been reworked and deposited in the littoral zone (above wave base) during high lake levels of the previous rainy season (Fig. *3.1.*7D, 7E). Hot springs easily erode through the


**Fig. 3.1.8.** Coarse-grained sands and gravels of modern shorelines and alluvial flats at Lake Magadi and Nasikie Engida. Photograph shown in (E) courtesy of R.Renaut. **(A)** The South Lagoon at Lake Magadi showing coarse-grained sands, shallow channels, and some colluvial boulders. **(B)** Coarse-grained sands with salt efflorescence along the basin bounding fault of the eastern East Lagoon. **(C)** Close up view of coarse-grained sands with clay drape and salt efflorescence at the eastern margin of the East Lagoon. **(D)** Coarse-grained sands and warm spring outflow at the NW Lagoon at Lake Magadi. **(E)** Close up of coarse-grained sands and detritus in shallow water at the margin of the NW Lagoon. **(F)** Reworked colluvium on the eastern shoreline of Nasikie Engida (looking south).

exposed unconsolidated deposits, creating open pools and redistributing the sands to the new, lower-level shoreline via small outflow channels and very small-scale deltas (Fig. *3.1.*7D, 7F). Shallow incision and sheetwash during rains continually redistribute the sediments to the contemporary shoreline, and exhume the underlying, weakly cemented siltstone and sandstone of older lacustrine and lake-margin deposits (i.e., Bogoria Silts, Loboi Silts). During higher lake levels, waves erode and rework poorly indurated and unconsolidated Pleistocene, Holocene, and recent silts and sands (Fig. *3.1.*7G), and may create steep mini-escarpments around the shoreline.

Lake Bogoria is relatively deep (~10 m) when compared with Lakes Magadi (0–1 m) and Nasikie Engida (< 2 m), and has greater fetch for wind-induced waves to rework colluvial and alluvial sediments into shoreline deposits. These shoreline bar facies were not observed around Lake Magadi or within Pleistocene facies other than those in the Bogoria basin. The eastern shoreline of Nasikie Engida, however, also has well-developed gravel beach terraces. Such deposits might be present in the basin margin siliciclastic lithofacies of the High Magadi Beds and Oloronga Beds that were deposited during higher lake levels in the Magadi basin. At some of the modern coarse-grained sandy shorelines observed at Lake Magadi where water depths were very shallow (< 4 cm), the sand was coated with detritus and/or muddy microbial mats (Fig. *3.1.*8A–E). Where subaerially exposed along coincident margins, the coarse-grained sands may be trampled by flamingos, burrowed by insects, and covered by efflorescent salt crusts (Fig. *3.1.*8A–E). At Nasikie Engida, the supralittoral zone is restricted by the basin bounding horsts and most of the shoreline areas contain thin strands of poorly sorted, angular to subrounded black and dark brown trachytic fine- to coarse-grained sands and granules adjacent to exposed siliceous, organic-rich, muddy ooze from the littoral zone (Fig. *3.1.*8F).

### *3.1.4. Poorly to Moderately Sorted, Muddy Fine- to Coarse-Grained Sand-Sized Delta-Plain Alluvium*

The modern Lakes Bogoria, Magadi, and Nasikie Engida are all oriented N–S in axial basins of the inner rift. Lake Bogoria is relatively deep and fills a half-graben trough. Nasikie Engida is shallow and fills a small full graben, and Lake Magadi is very shallow and fills a series of connected full grabens formed by the uplift of several horsts within the inner rift trough. These lake basins and their Pleistocene precursors contain relatively large and elongate axially oriented alluvial and delta-plains at their northern and southern ends, with fine- to coarse-grained sands and gravels on the upper delta-plains, and silts and fine-grained sands on the lower delta-plains, deposited in channels and as sheetwash. Due to continually changing lake levels, silty muds of the proximal delta-front and organic-rich muddy littoral sediments are closely related to sandy sediments, both laterally and vertically (Section 3.2.1). In contrast, the relatively small fan deltas develop along N–S oriented scarps or hinged margins. Fan deltaic sediments typically include: 1) colluvial and alluvial fan pebble- to boulder-sized clasts (Section 3.1.2); 2) fluvial gravels and coarse-grained sands (Section 3.1.2); 3) beach bars of coarse-grained sands, both stranded from higher lake levels on the upper delta-plain and forming modern shorelines on the lower delta-plain (Section 3.1.3); and 4) muddy silts and fine-grained sands on the low-gradient mudflats of the lower delta-plain (Section 3.2.1). Of the localities investigated, the lower gradient axial plains contain more abundant ephemeral and perennial channels, as well as more extensive sheetwash deposits when compared to the fan deltas, and are expected to leave a more fluvially dominated sedimentary record.

Sediments sourced from small catchments near the lake basin contain coarser grains (e.g., Nasikie Engida; Fig. *3.1.*9), while on the larger, probably older delta-plains, fine-grained sediments deposited during higher lake levels are incised, reworked, and incorporated with sandy alluvial sediments (e.g., Sandai Plain, Lake Bogoria; NE Lagoon, Lake Magadi). At the north

end of Nasikie Engida, for example, hot spring fluids flow into the lake in a perennial channel system of coarse-grained sands and gravels (Fig. *3.1.*9A–D). A weakly channeled supralittoral sandflat with a coarse-grained sandy to gravel surface lag from sheetfloods is also present on the northern lake margin (Fig. *3.1.*9E, 9F). Coarse-grained sands and gravels on the Sandai Plain, in contrast, are locally sourced from older beach bars along its western margin (hinged), and from colluvium along its eastern margin.

Sediments on the delta-plains derive from trachytes, basalts, and trachyphonolites, and in general contain a high proportion of lithic fragments of pyroxenes (e.g., aegerine–augite) and


**Fig. 3.1.9.** Alluvial plains at Nasikie Engida. Photographs shown in (E) and (F) courtesy of R.Renaut. **(A)** Google Earth 2010 image of the northern shoreline of Nasikie Engida showing two spring-fed alluvial plains. **(B)** Hot spring outflow along the steep western border fault of Nasikie Engida. **(C)** Shallow channels with microbial mats and ?chironomid larvae (pink) at the NW hot springs of Nasikie Engida. **(D)** Hot spring outflow near the NW shoreline at Nasikie. Note corrosion on trachytes at right. **(E)** The NE alluvial plain at Nasikie Engida looking north. **(F)** The NE alluvial plain at Nasikie Engida with sheetwash near the shoreline.

minor amounts of olivine, and hematite, ilmenite, magnetite, and Fe-oxides (Surdam and Eugster, 1976; Renaut, 1982; Behr and Röhricht, 2000). Silicates are dominated by sanidine, anorthoclase and nepheline, and minor amounts of plagioclase and quartz (Surdam and Eugster, 1976). These common minerals, together with volcanic glass, weather quickly to clay minerals such as smectite (montmorillonite) and illite, and also alter to authigenic zeolites (e.g., erionite) (e.g., Hay, 1966; Surdam and Eugster, 1976; Renaut, 1993; Deocampo, 2004). Sands and sandstones of this facies assemblage tend to be compositionally and texturally immature, poorly to moderately sorted with angular sand-sized grains, contain a high proportion of detrital clays and silt-sized grains, and may contain early authigenic clays and zeolites. Pleistocene examples of subaerially exposed sandstones at these sites also contain calcite, opal-A, and analcime cements (Surdam and Eugster, 1976; Renaut, 1993; Scott, 2005; Scott et al., 2008). At Lake Bogoria, analcime formed by the alteration of clay minerals and glass in Na-rich groundwaters concentrated by capillary evaporation in an exposed lake-margin pedogenic setting (Renaut, 1993).

The Sandai Plain at the northern end of Lake Bogoria is the only axial alluvial plain in the basin because a flexure in the Lake Bogoria Fault to a NE–SW trend forms the steep southern margin of the lake. Sandai Plain consists of the Late Pleistocene Loboi Silts (fluvio-lacustrine), latest Pleistocene–Holocene Bogoria Silts (lacustrine), and modern moderately to poorly sorted muddy silts and sands. Lithofacies present on the modern upper delta-plain include coarse-grained sands and gravels, partly reworked from Pleistocene beach bars, deposited as unchanneled sheetwash and as small ephemeral channels with unidirectional sedimentary structures and bedforms (Fig. *3.1.*10A–D). Elsewhere on the upper delta-plain, slightly channeled ephemeral sheetwash reworks coarse-grained sands and gravels, and deposits silts and clays within the very small channels (Fig. *3.1.*10F, 10G). Two relatively large (< 4 m wide), incised ephemeral channels are also present on Sandai Plain at Lake Bogoria, which meander slightly upstream (Fig. *3.1.*10E) but become straighter towards the lake. During floods, these channels are active, and the ephemeral flow produces asymmetrical ripple and climbing-ripple cross-lamination to flaser bedding in the confined portions of the channels (Fig. *3.1.*10F). The channels open up into very shallow, but still incised slightly, wide (< 20 m wide) stream mouths where runoff mixes with lake water during the minor rises in lake-level during storms (Fig. *3.1.*10H). The ephemeral channels do not branch into distributaries as they approach the lake on the lower delta-plain. The mouths of the ephemeral streams are slightly lower, incised lacustrine inlets that are regularly flooded by muddy, organic-rich lake waters containing dense populations of planktonic cyanobacteria. Vertebrate tracks are common in the larger inlets of the ephemeral streams, but are not clearly associated with the small, short-lived ephemeral streams.

The seasonal to sometimes perennial Sandai River flows along the east side of the plain along the Bogoria Fault, carrying fresh water and a large fine-grained sediment load. Unlike the ephemeral channels, the single, straight to meandering channel of the river branches into increasingly smaller distributaries where it reaches the very low gradient of the lower delta-plain

**Fig. 3.1.10.** (Next page) Ephemeral channels on the Sandai delta-plain of Lake Bogoria. **(A)** Coarse-grained sands in ephemeral channel reworking Holocene beach deposits near shoreline in 2007. **(B)** Close up of ephemeral channel in (A) showing asymmetrical 3D ripple bedforms and plane bedded sands with parting lineation. Scale at right in cm. **(C)** Close up of asymmetrical 3D bedforms in coarse-grained sands with clay drapes. Scale at lower right in cm. **(D)** Shallow incised channel into the very fine-grained Bogoria Silts. **(E)** Ephemeral channel in flood towards the Loboi Plain. **(F)** Dry, very shallow ephemeral channel with coarse-grained lag towards Loboi Plain. **(G)** Sheetwash and very shallow dry channels at shoreline during higher lake levels in 2007. **(H)** The mouth of Nyoka Donga, the dry, large ephemeral channel on the western Sandai Plain with asymmetrical rippled silty fine- to coarse-grained sands. Note lack of incision. Photo taken during lower lake levels in 2002. Backpack for scale.

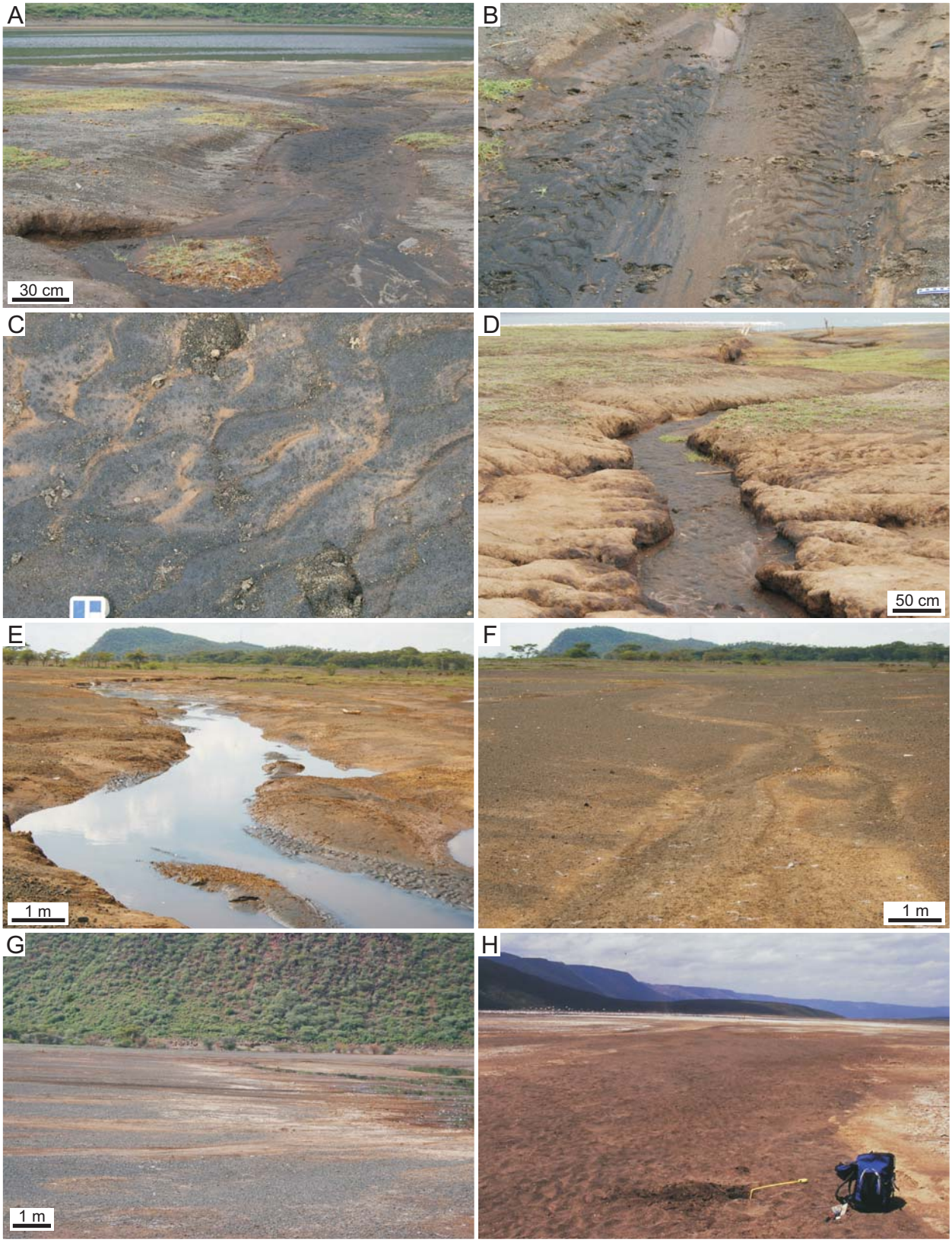
A
30 cm
B
C
D
50 cm
E
1 m
F
1 m
G
1 m
H

near the lake margin (Fig. *3.1.*11A). Within the confined main channels, thalwegs with moderately sorted fine- to coarse-grained sand are present, along with ripple-laminated and planar- to low-angle cross-bedded small point bars (Fig. *3.1.*11C, 11D, 11E). The broad, shallow channel floors may contain current-rippled fine-grained sands with clay drapes (Fig. *3.1.*11D) that would likely be preserved as thin units of flaser to wavy bedding or even climbing ripples, intercalated with lacustrine or delta-front silts and mud. Following heavy rains, the river expands to flood the adjacent delta-plain near the delta mouth with weakly channeled flow that follows slight depressions in the plain surface (older channels filled with lacustrine/delta front sediment?), but typically does not cause much incision (Fig. *3.1.*11A, 11B). These flood-relief 'channels' are evident when dry due to the linear distribution of relatively clay-rich sediments that commonly contain vertebrate footprints formed in wet substrates, desiccation cracks, and a channel-normal zonation of microbial and evaporite efflorescent crusts (Fig. *3.1.*11B; Scott et al., 2010). In general, the centres of the channels contain fewer bird tracks (e.g., flamingo, heron), possibly because the birds use the active to waning-flow channels (e.g., for drinking, bathing), but not the stagnant drying pools that remain following the flood. Any tracks that were formed while water was still standing in the central channel are usually morphologically indistinct in plan view (Scott et al., 2010).

The relatively coarse-grained lithofacies assemblages of the upper and lower delta-plains are transitional with the relatively finer-grained lithofacies of the often subaerially exposed, proximal delta-front. During low lake levels (e.g., 2006; < 1 m lower than 2008 levels), narrow, confined, incised channels within the delta-front of the Sandai River delta that were subaqueous during 2007 and 2008 were exposed (Fig. *3.1.*11E; Renaut, pers. comm., 2006). They cut through buff-coloured deltaic silts as narrow, slightly meandering channels (1–3 m wide) with steep banks and thalwegs that may be flooded by lake water during storms and during lake-level rise, comparable to tidal channels (Fig. *3.1.*11F, 11G). They form linear to sinuous units of dark grey fine-grained lithic silty sands (with asymmetric ripple bedforms and planar cross-beds) isolated within the deltaic silts (Fig. *3.1.*11H), which presumably become interbedded with organic-rich lake mud and deltaic silts deposited when lake levels are higher. Further landward, sheetfloods on the exposed delta flats caused slight incision and irregular topography due to scouring around positive features such as old flamingo nests and stranded pieces of dead trees and shrubs (Fig. *3.1.*11I). In the protected, lakeward side of these features, finer-grained sediments were deposited (and/or were not eroded slightly like the surrounding area). The exposed muddy silts deposited either in the lower delta-plain or subaqueously on the delta-front are typically disrupted by salt efflorescence (Fig. *3.1.*11I), and may be desiccation-cracked where sediments are more clay-rich (Section 3.2.1).

**Fig. 3.1.11.** (Next page) The mouth of the Sandai River at the northern shoreline of Lake Bogoria. Photographs shown in (C–I) all courtesy of R. Renaut. **(A)** The mouth of the Sandai River in flood (2007). View towards south. **(B)** Desiccated clay-rich sediments adjacent to main channel deposited during flood (2007). Scale at bottom centre in cm. **(C)** Dry terminal distributary channel of the Sandai River (2006). Note medium- to coarse-grained sand (dark brown) in channel thalweg isolated in deltaic silts. **(D)** Dry terminal distributary channel of the Sandai River (2006). View towards north. Note asymmetrical 3D ripples draped by clays and coarser sediments towards slightly more incised channel margin at right. **(E)** Dry terminal distributary channel with coarser-grained thalweg at right (2006). View towards south. **(F)** Incised terminal distributary channel flooded by lake waters (2006). View towards south. **(G)** Incised terminal distributary channel flooded by lake waters (2006). View towards north. Note incision of horizontally bedded silts (Holocene Bogoria Silts?). **(H)** Flooded incised channels in deltaic silts in the eastern north sub basin at Lake Bogoria (2006). **(I)** Deltaic silts showing evidence of unconfined flow, with clayey silts deposited downstream of obstacle (2006). Note subsequently formed desiccation cracks and salt efflorescence.


A
1 m
B
C
1 m
D
50 cm
E
1 m
F
50 cm
G
50 cm
H
1 m
I
50 cm

At Lake Magadi, water sourced mostly from springs flows in shallow, anastomosing channels of the axial plains (e.g., NE Lagoon, NW Lagoon; S Lagoon; Fig. *3.1.*12A–G). Modern sediments on the alluvial plain north of Lake Magadi (e.g., the NE lagoon; Fig. *3.1.*12A), for example, form a thin veneer that overlies the late Pleistocene to Holocene High Magadi Beds, and is a few centimeters to a metre in thickness (Surdam and Eugster, 1976). That veneer comprises detrital and pyroclastic sediments slightly coarser than the muddy tuffaceous silts of the High Magadi Beds. Field observations (2007, 2008) of the NE lagoon plain include the anastomosing channeling of modern sediments, the trampling of the upper ~5–15 cm by large vertebrates (e.g., wildebeest), and the formation of efflorescent salts and desiccation cracks (Fig. *3.1.*12B–E). The streams are partly fed by spring waters that flow along the faulted western margin (Fig. *3.1.*12B, 12D). Coarse-grained sediment is derived from the horst that forms the coincident western margin of the axial plain, but in general, the plain appears to consist of muddy fine-grained sediments. The modern muds include unaltered trachytic glass, gaylussite, and erionite, with small amounts of calcite and the zeolites clinoptilolite and chabazite; analcime is lacking (Surdam and Eugster, 1976). The mineral suites of the High Magadi Beds and modern alluvial plain muds at Lake Magadi reflect the mainly glass-rich tuffaceous trachytic clastic source and Na-containing, alkaline brines, with some Ca and K introduced by the weathering of trachytic bedrock and detritus or carbonates (Surdam and Eugster, 1976). Further fieldwork is necessary to characterize the channel system in the alluvial plain of the NE lagoon. In general, it differs from the example at Lake Bogoria because it has a lower gradient, is larger in size, and is fed in part by perennial springs instead of a seasonal river. The lower "delta"-plain of the NE Lagoon does not contain large or small channels emptying into the lake, but instead the small channels appear to grade laterally into a broad, exposed mudflat (Fig. *3.1.*12A).

### *3.1.5. The Exhumed Surfaces at Lake Bogoria, Lake Magadi, and Nasikie Engida*

Several "exhumed surfaces" are present around the margins of Lake Bogoria, and are examples of older, moderately to well cemented lacustrine, littoral, deltaic, and delta-plain sediments that have been exposed by littoral, sheetflood, and eolian processes (Scott et al., 2008, 2009; Figs. *3.1.*13, 14). Modern sedimentation and erosion on the delta-plains at Lake Bogoria is dynamic, and these partially lithified clastic sediments have been buried by younger sediments and then subsequently exhumed by erosion, sometimes on multiple occasions. These surfaces are not necessarily contemporaneous because the processes that led to their cementation may have recurred many times at the same lake level whenever conditions were favourable. These old surfaces are exposed mainly on the Loburu (Fig. *3.1.*13, 14A–D), Sandai (Fig. *3.1.*14E–I), and Emsos delta-plains, and in places along the eastern shoreline (Scott et al., 2009). Although not investigated in detail, a similar surface with increasing induration and bioturbation upwards was identified in the upper High Magadi Beds south of Nasikie Engida (see Section 4.2.3). The reddish brown, indurated High Magadi Beds on the eastern margin of the E lagoon and the southern margin of the SW lagoon may also be comparable to the exhumed surfaces at Lake Bogoria in terms of their genesis and significance as stratigraphic surfaces (see Section 4.2.2).

**Fig. 3.1.12.** (Next page) Alluvial/deltaic plains at Lake Magadi. Photograph shown in (F) courtesy of R.Renaut. **(A)** Google Earth 2010 image of Nasikie Engida (left) and the delta-plain of the NE Lagoon at Lake Magadi. **(B)** View towards north from horst between the NE Lagoon and Nasikie Engida. **(C)** Large desiccation polygons on the delta-plain, with vertebrate footprints at top. **(D)** Shallowly incised, anastomosing distributary channels on the delta-plain of the NE Lagoon. View towards south from horst forming western margin of the plain. **(E)** Close up of area shown in (D). **(F)** The alluvial plain of the NW Lagoon. View towards northwest. Note numerous anastomosing, very shallowly incised channels. **(G)** View towards northwest of the NW Lagoon showing close association with colluvium along a "coincident" margin of the plain.


A
N
1 km
B
5 m
C
1 m
D
5 m
E
3 m
F
G
1 m

The uppermost surface of the Loboi Silts on the Sandai Plain is locally cemented by analcime, clay minerals and calcite (Fig. *3.1.*14G–I); Renaut, 1993; Scott et al., 2008). The zeolites formed mainly through replacement of poorly crystalline smectitic clays and/or volcanic glass that reacted with saline, alkaline pore fluids (Renaut, 1993), and possibly by direct precipitation as a pore-lining cement in subaqueous conditions (Fig. *3.1.*14G; Scott, 2005). Calcite probably precipitated by evaporative concentration of meteoric waters infiltrating the sediments from above and by evapotranspiration of shallow groundwater (Renaut, 1993; R.A. Owen et al., 2008), but may also have been bio-mediated by microbes in the substrate (Scott,

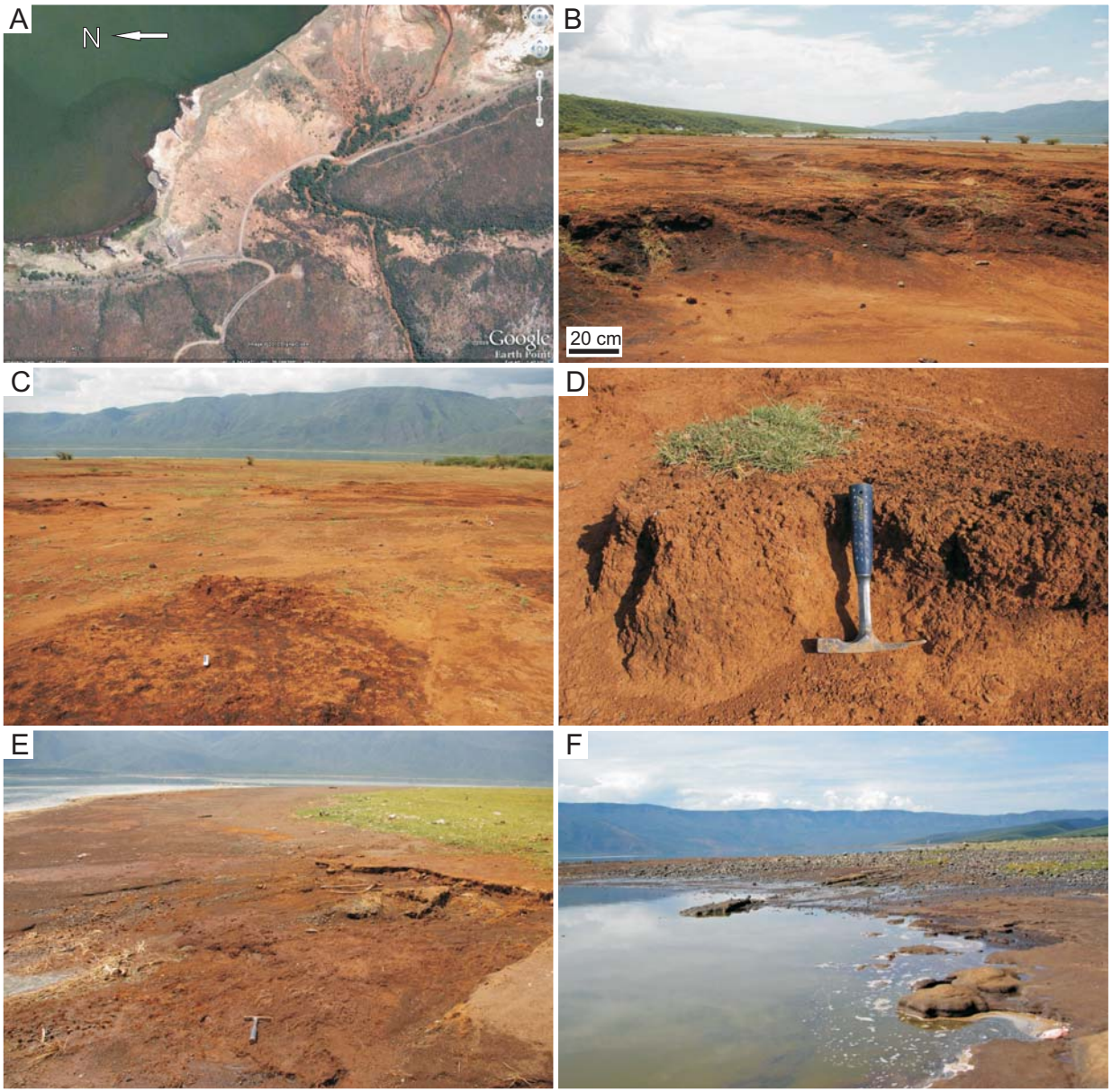


**Fig. 3.1.13.** Pleistocene sediments of the fan delta lobe at "old" Loburu, Lake Bogoria. Photograph shown in (F) courtesy of R.Renaut. **(A)** Google Earth 2009 image of the older, fan delta lobe at Loburu. **(B)** Red- and black-stained silty sandstones of the Loboi Silts at "old" Loburu. **(C)** View towards shoreline of the exposed fan delta sediments. Scale in foreground is 15 cm. **(D)** Close up of pedogenically modified Loboi Silts fan delta sediments. Hammer for scale. **(E)** Loboi Silts fan delta sediments exhumed at present-day shoreline. Hammer for scale. **(F)** Loboi Silts silty sandstones at north Loburu showing fan delta foresets.

2005). At Loburu, hot spring fluids likely influenced the cementation of the older sediments, as well as the preservation of rhizoliths in the 'surfaces' by silica, fluorite, calcite, and zeolites (Fig. *3.1.*14B, 14C; R.A. Owen et al., 2008). Pockets of the exhumed 'surface' have been exposed by erosion of the overlying Bogoria Silts by deflation, fluvial incision and sheet-flooding during lake lowstands (Fig. *3.1.*14E), and by wave erosion during minor lake transgressions (Figs. *3.1.*13E, 14F). Low lake levels also subaerially expose the cemented irregular surfaces normally present within the modern littoral zone (Figs. *3.1.*13F, 14D). The age of the sub-Bogoria Silts disconformity surface is unknown. If the Bogoria Silts are mainly Holocene (cf. Tiercelin et al., 1987), the Loboi Silts, parts of which have been cemented and exhumed, are probably of late Pleistocene age. Renaut (1993) suggested that cementation of the surface might have occurred during an extended dry phase during the late Pleistocene based partly on an association with meter-scale desiccation polygons with cracks also cemented by zeolites, but there is no absolute age for the exhumed Loboi Silts land surface.

On the Sandai Plain, the exhumed "surface" that forms the uppermost Loboi Silts shows a lateral zonation of sedimentary features that is similar to those of the present lake margins around Lake Bogoria (Scott et al., 2009). The surface dips towards the lake at ~2–4° and is a buried platform upon which younger sediments have been deposited (e.g., Bogoria Silts, alluvial fans, etc.). The uppermost Loboi Silts of the Sandai Plain appear to have been deposited in a similar depositional setting to the modern delta (Scott et al., 2008), but some evidence suggests that spring-fed wetlands may also have been present (see Section 3.1.6). For instance, Renaut (1993) described a zeolitic-calcitic root-mat ~1 km north of the present-day shoreline, and small tufa mounds (Late Pleistocene?) with stromatolite-coated reed moulds are also present on the southwestern Sandai Plain (Sect. 3.1.6). Scott et al. (2008) reported vertebrate footprints, including a hominid track, at several sites ~200–800 m landward of the present-day shoreline.

Erosion between 2002 and 2007 exposed a more laterally continuous exhumed surface than was previously recognized (cf. Scott et al., 2008), preserving an assemblage comprising five suites of invertebrate, vertebrate, and plant trace fossils (see Section 4.1.2). Parts of this old surface are exposed in shallow channels near the modern shoreline where they are subject to modification by salt efflorescence and bioturbation by invertebrate burrowers and plant roots where the surface is weakly cemented. The complexity of deltaic sedimentation and concurrent erosion in the littoral zone, as well as by other subaerial processes such as incision and reworking by ephemeral and hot-spring outflow streams, is exemplified on the Loburu Delta by the Loboi Silts, somewhat indurated Bogoria Silts, Holocene littoral and beach granular coarse-grained sands, and modern littoral erosion and re-deposition of granular coarse-grained sands (Fig. *3.1.*13E).

**Fig. 3.1.14.** (Next page) The "exhumed" surfaces at Lake Bogoria. Photographs shown in (B) and (D) courtesy of R.Renaut. **(A)** Exhumed Holocene? lacustrine silts at the main hot spring site at Loburu. Hammer for scale. **(B)** Isolated, exhumed pocket of ?Pleistocene lacustrine silts at the main hot spring site, Loburu, with silica and carbonate rhizoliths. Hammer for scale. **(C)** Well indurated lacustrine silty sands around a hot spring vent at the main site, Loburu. Hammer for scale. **(D)** Exhumed, indurated siltstones (Loboi Silts?) at the main site at Loburu. Mini-topography of surface likely due to modification by flamingos. **(E)** The exhumed Loboi Silts in ephemeral channel on Sandai Plain. Hammer for scale. **(F)** The exhumed Loboi Silts in the littoral zone. Note coarse-grained sands and gravels of modern shoreline deposits. **(G-I)** Photomicrographs of the sandy exhumed Loboi Silts at Sandai, showing grain-coating analcime cement (G), analcime and calcite cements altered from original clayey matrix (H), and microsparite of black-coloured coating (fossil microbial mat?) on sandy exhumed Loboi Silts (I).

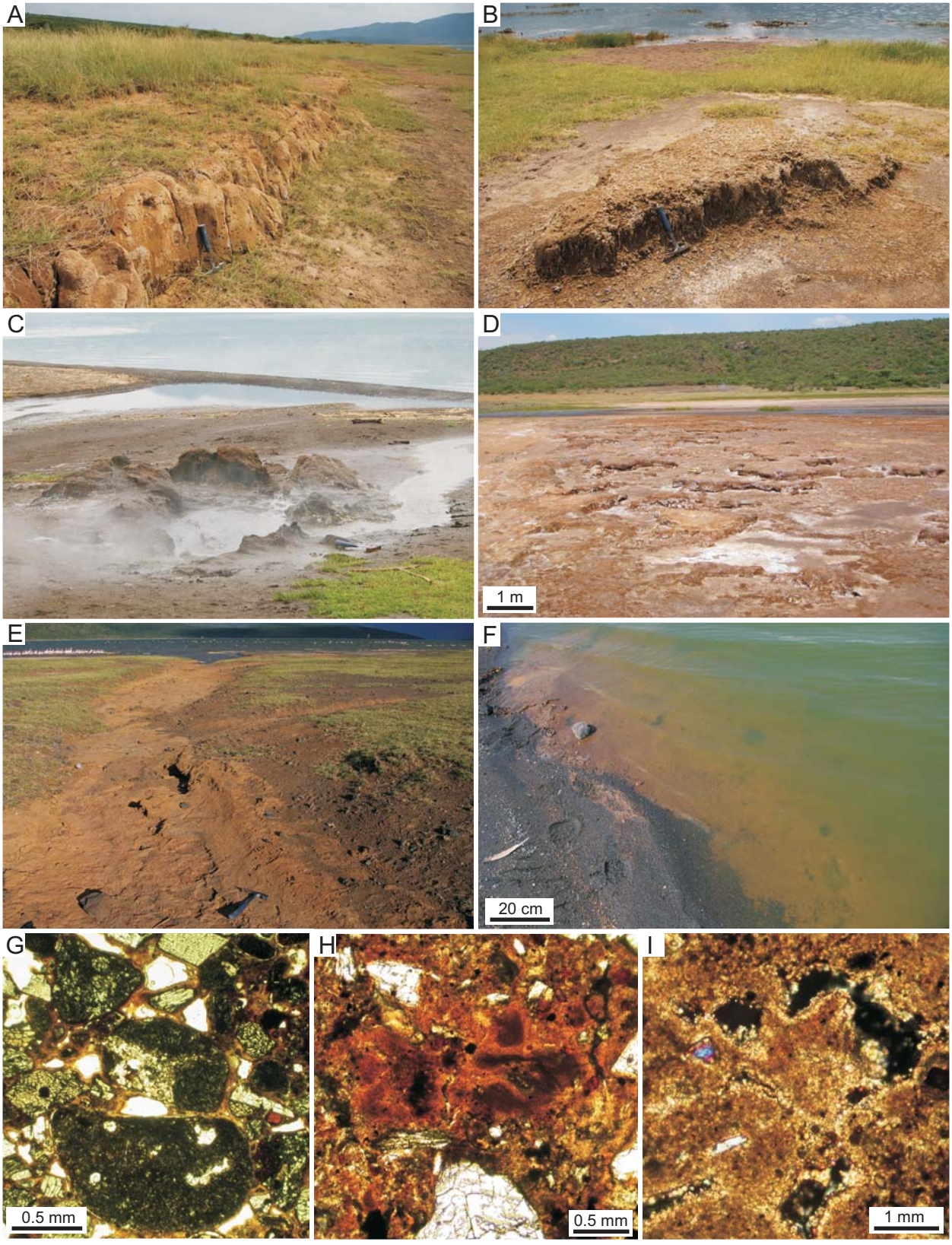
A
B
C
D
1 m
E
F
20 cm
G
0.5 mm
H
0.5 mm
I
1 mm

*3.1.6. Spring-Related Deposits*

The lake basins of the Kenya Rift contain a variety of spring deposits associated with hyperthermal (>75°C), mesothermal (40–75°C), warm (20–40°C), or cool (< 20°C) water (classification of B. Jones and Renaut, 2010). The springs discharge predominantly along axially oriented (N-S) fault systems related to the Neogene extension of the rift and to the interaction of rift-related faulting with inherited (NW-SE) transverse basement structures. Most of the faults along which the spring fluids flow are also the faults that create the margins of the lake basins, and for this reason, spring deposits are included in the basin margin lithofacies assemblage.

Modern springs and/or Pleistocene to Holocene spring deposits are present at Lakes Bogoria (Figs. *3.1.*15, 16), Magadi (Fig. *3.1.*17A–B), and Nasikie Engida (Figs. *3.1.*9B–D, 17C–17D; Surdam and Eugster, 1976; B.F. Jones et al., 1977; Renaut, 1982; Renaut et al., 1986, 1998; Renaut and Jones, 1997). Most of the modern spring waters lack alkaline earths (i.e. $Ca^{2+}$ and $Mg^{2+}$) and few are actively forming travertine or tufa (Fig. *3.1.*15A–C). However, the spring waters: 1) may be an important source of the lake (or wetland) annual recharge; 2) influence or control the chemistry of spring-fed wetlands and lake waters; 3) lead to the sedimentation of opaline silica crusts, gels and cements, fluorite cements, and possibly to sodium carbonate evaporites (especially nahcolite); and, 4) contribute to the weathering and diagenetic alteration of volcanic bedrock (Renaut et al., 1986, 2000b, 2007). The springs may be subaerial on the lake margins or sublacustrine, depending both on the position of the faults along which the hot fluids flow, and the lake level if the springs are located within the zone of lake-level rise-and-fall. Cooler springs fed by meteoric water at Lake Magadi (B.F. Jones et al., 1977) also issue from the base of colluvial fans, which tend to also be aligned along faults (Fig. *3.1.*17A–B).

Travertines, tufas, and sublacustrine opaline silica crusts and cements are associated with hot- and warm-springs at Lake Bogoria (Renaut, 1982; Renaut et al., 1986, 1998; Renaut and Owen, 1988; Renaut and Jones, 1997). Travertine deposits on the Loburu Delta (Fig. *3.1.*15C–H) and at Chemurkeu (Fig. *3.1.*16A–C) are composed mainly of calcite and aragonite, but also contain fluorite, dolomite, opaline silica, and quartz cements (Renaut, 1982; Renaut et al., 1986). Spring-mound facies such as pools, rims, terraces, and miniterraces are all present, together with microbial stromatolitic crusts (Fig. *3.1.*15D–H). Crystal fabrics include dendritic calcite, fibrous to bladed aragonite or calcite, and equant or blocky isopachous and pore-filling cements (Figs. *3.1.*15D, 16B–C; Renaut, 1982; Renaut and Jones, 1997). Oncoids (Fig. *3.1.*15F) and a variety of rhizoliths by silica, calcite, fluorite, or analcime are also formed from the hot-spring fluids (Fig. *3.1.*14B; R.A. Owen et al., 2008). Stromatolitic crusts, some of which formed in the splash zone of spouting spring vents at Loburu, are present in association with the hot springs (Figs. *3.1.*15E, 16E–F). Sublacustrine opaline silica deposits include cements precipitated within trachytic gravels coated and chert crusts < ~5 mm thick, and are also associated with fluorite crusts and stromatolitic carbonate crusts (Renaut and Owen, 1988; cf. Renaut et al., 2002b). Tufa deposits are less common near the lake shores, but comprise porous, finely crystalline, irregular mounds of calcite that preserve the casts of reed stems and other

**Fig. 3.1.15.** (Next page) Hot spring environments at Lake Bogoria. Photographs shown in (B) and (E–H) courtesy of R.Renaut. **(A)** Hot spring vent with fossil travertine mound and modern outflow channels to coarse-grained shoreline at north Loburu (2008). **(B)** Hot spring vent pools near shoreline at south Loburu (2006). Note orange-coloured microbial mats in pools. **(C)** Hot spring vent, outflow channel, and fossil travertine deposits at the main site at Loburu. Arrow showing location of close up photo shown in (D). **(D)** Close up of fossil bedded travertine deposits and modern sediments surrounding modern hot spring vent. **(E)** Spouting spring at the main site at Loburu showing weathered fossil travertine at left and modern/subfossil stromatolitic coating adjacent to spouting spring vent. **(F)** Coated grains (oncoids) in fossil spring mound. Coin for scale. **(G)** Fossil travertine mound at modern shoreline at the main site at Loburu (2006). **(H)** Rims and pools of travertine mound shown in (G).


A
B
C
D
2 cm
E
F
G
H

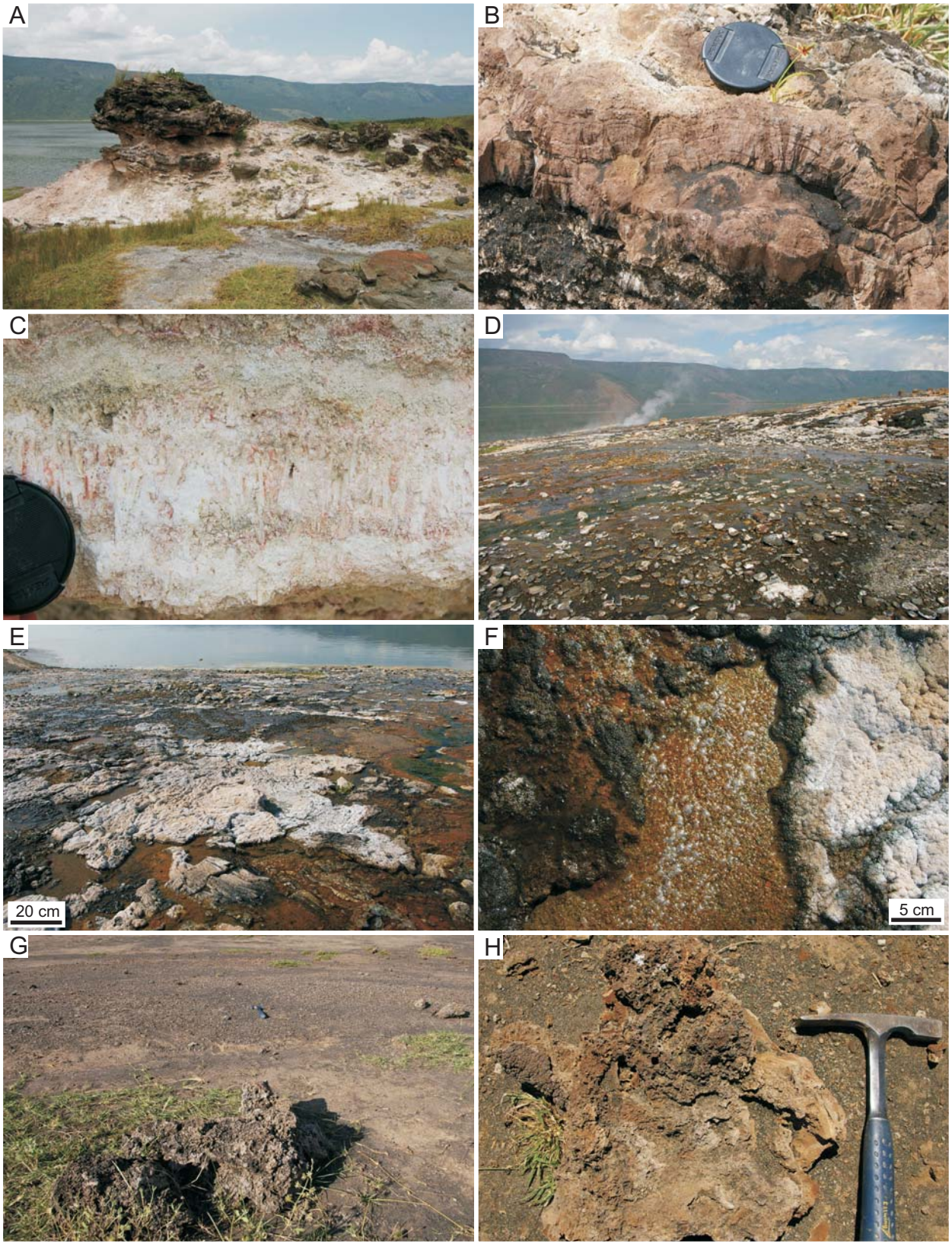
A
B
C
D
E
20 cm
F
5 cm
G
H

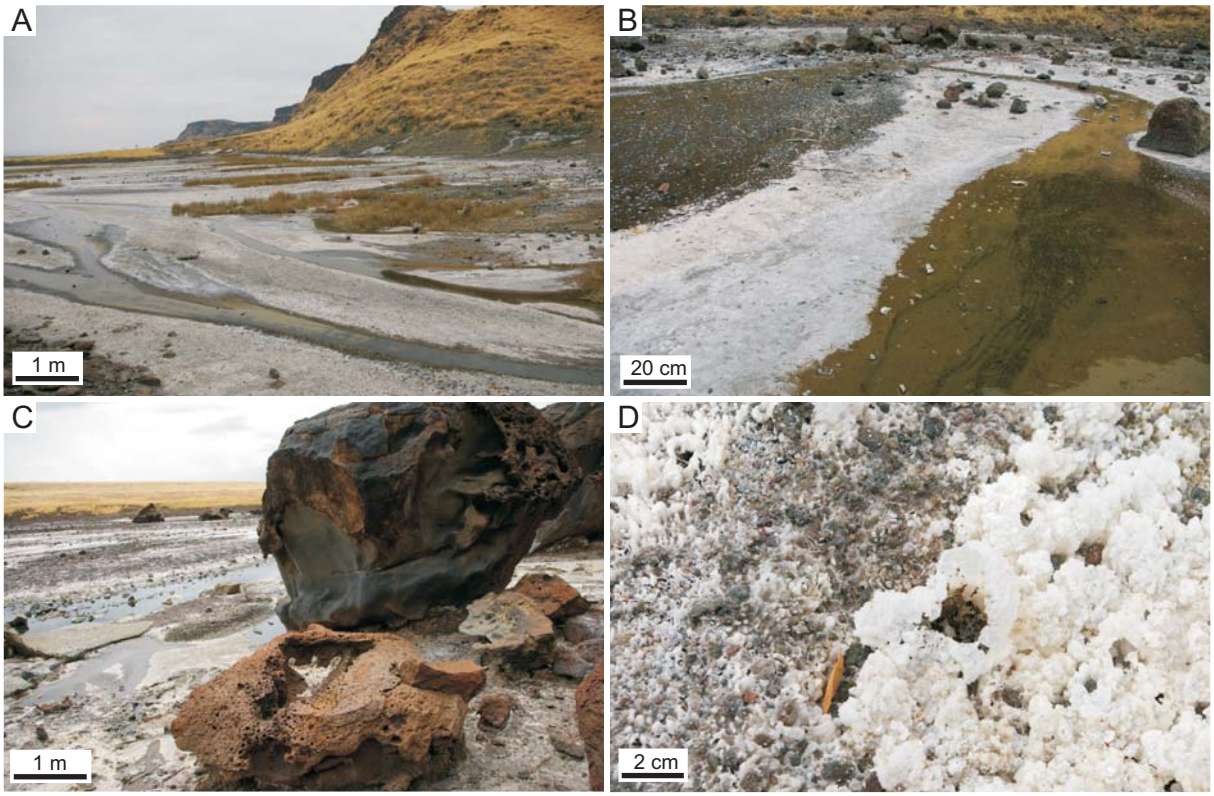


**Fig. 3.1.17.** Modern spring sites at Lake Magadi (A–B) and Nasikie Engida (C–D). Photographs shown in (A) and (B) courtesy of R.Renaut. **(A)** Shallow warm-spring outflow channels at the NW Lagoon at Lake Magadi. **(B)** Close up of shallow channel with spring waters issuing from base of scarp. **(C)** Chemical erosion of trachyte boulders adjacent to hot spring outflow channels at the NW spring site at Nasikie Engida. **(D)** Close up of finely crystalline sodium carbonate and opaline silica? crusts at Nasikie Engida. Note spherical 'popcorn' bubble in crust at centre.

macrovegetation, and are associated with concentrations of individual plant stem and twig moulds preserved as stromatolitic coatings of calcite (Fig. *3.1.*16G–H).

In the Magadi basin, Pleistocene sediments influenced by hot-spring waters may be represented by several facies of the Green Bed cherts (cf. Behr and Röhricht, 2000; Behr, 2002; see Section 3.4.2). Modern springs at Magadi typically issue ambient to warm waters that contribute to the growth of microbial mats in their outflow streams (Fig. *3.1.*17A–B). At northern Nasikie Engida, alkaline hot spring waters flow towards the lake in channels, and have caused the extreme corrosion of trachytes (Fig. *3.1.*17C). The siliceous gels forming along the shorelines of the lake are associated with the evaporitic concentration of alkaline, silica-containing hot-spring waters (Eugster and Jones, 1968). A variety of types of thin, smooth, white crusts form in association with the spring-fed channel system and small fumaroles and vents at Nasikie Engida. They are likely composed of sodium carbonate evaporites, halite and silica, and may form hollow stalagmitic tubes and hollow, spherical 'popcorn', or extensive, flat, smooth surface crusts (Fig. *3.1.*17D).

**Fig. 3.1.16.** (Previous page) Fossil and modern spring deposits at Lake Bogoria. **(A)** Fossil travertine mound at Chemurkeu. **(B)** Close up of bedded travertine deposits forming upper part of mound shown in (A). **(C)** Close up of bedded travertine deposits forming lower part of mound shown in (A). **(D)** Modern spring outflow at Chemurkeu with orange and green microbial mats. **(E)** Modern carbonate deposits in sheetlike outflow at Chemurkeu. **(F)** Modern microbial mats and carbonate deposits at Chemurkeu. **(G)** Pleistocene (?) spring site at Sandai Plain. Tufa/travertine mound in foreground. Hammer for scale in background lying on deposit of stromatolite-coated plant stems associated with tufa/travertine mounds. **(H)** Tufa/travertine mound on Sandai Plain. Hammer for scale.

## 3.2. Lake Margin to Basin Centre Lithofacies Assemblages

Sediments deposited either in the lake (e.g., organic-rich oozes), in the zone of frequent lake-level fluctuations (e.g., mudflats), and those deposited in the central basin during lake lowstands (e.g., bedded evaporites) are included in the basin centre lithofacies assemblages. Like the basin margin assemblage, lake-level fluctuations on several different time scales lead to the intercalation of lithofacies typically found in subaerial settings with those deposited in the lake. As a whole, grain sizes are finer for the basin centre than for the basin margin. Along the coincident margins of fault-escarpments, basin margin lithofacies may be very closely associated with the basin centre lithofacies (e.g., Nasikie Engida; Fig. *3.1.*8F). Coarse-grained turbidites and fan delta sediments are deposited within the lake along steep, border-fault margins (e.g., Renaut and Tiercelin, 1994). Chemical sedimentation (e.g., chert, evaporites) occurs mainly in the basin centre, although hot springs also contribute to locally diverse mineral suites in basin margin to lake-margin sites (e.g., Renaut et al., 1986). Sediments deposited in basin centres during periods of low to intermediate lake levels may be associated with saline to hypersaline conditions that restrict infaunal biogenic activity, whereas those deposited during highstands generally reflect fresher lake waters. In tropical areas, however, the depth of the thermocline is typically shallow, preventing mixing and causing even relatively fresh lake waters to be inhospitable for benthic life due to anoxia (Cohen, 2003). Highstand deposits may be reworked during periods of exposure by the burrowing of terrestrial animals and pedogenesis, providing evidence of lake-level changes, substrate stability, and low sedimentation rates in cases where lowstand sediments were either not deposited or eroded.

The basin centre lithofacies are known from cores taken in the modern lakes (Tiercelin et al., 1987; Behr, 2002), as well as those deposited during higher lake levels, such as the Loboi Silts and Bogoria Silts exposed at the Loburu Delta and Sandai Plain at Lake Bogoria, and the High Magadi Beds at Lake Magadi. Lowstand basin centre deposits, such as the bedded evaporites of the dry saline pan at Lake Magadi, were examined in several places along the basin margins and causeways that cross the lagoons and pan. The main depositional environments of the lake margin to basin centre lithofacies assemblages include: 1) low gradient mudflats of the lower delta-plains, which are frequently flooded and exposed; 2) lacustrine, but sometimes subaerially exposed, delta-front to prodelta muds and fan-delta turbidites; 3) sublittoral to profundal organic-rich muddy oozes and displacive evaporites; 4) sublittoral to littoral stromatolitic carbonates; and 5) interbedded evaporites and organic-rich muddy oozes of salt-pans and lagoons. The following discussion and lithofacies descriptions are supplemented by published and unpublished descriptions by other authors (e.g., Renaut, 1982; Renaut et al., 1986; Tiercelin et al., 1987; Renaut and Tiercelin, 1994; Behr and Röhricht, 2000; Behr, 2002; Owen, pers. comm., 2001–2010; Renaut, pers. comm., 2001–2010).

### *3.2.1. Low-Gradient Littoral and Lower Delta-Plain Mudflat Muddy Silts and Fine-Grained Sands*

Modern examples of deltaic and exposed lacustrine sediments along shorelines are best developed and were investigated in the most detail at Lake Bogoria. Mudflats on the lower delta-plains of the Sandai delta (Fig. *3.2.*1) and southern Loburu Delta (Fig. *3.2.*2) alternate frequently between being flooded and subaerially exposed. Sediments are a mix of exposed muddy lacustrine, delta-front silts, and fine-grained sands deposited on the lake margin as either shoreline or sheetwash deposits. The fine-grained siliciclastic sediments are transported to the lake by perennial and ephemeral rivers that carry silt- and sand-sized clasts weathered from trachytes and trachyphonolites (e.g., K-feldspar laths) and clay minerals (e.g., smectite,

interstratified smectite/illite, kaolinite) from soils and weathered bedrock upstream. Littoral mud at Lake Bogoria is moderately organic-rich (< 0.5–1% O.C.; Tiercelin et al., 1987), and includes many species of Cyanobacteria (e.g., *Arthrospira*), Proteobacteria (e.g., cf. *Aeromonas*/*Vibrio*) and Bacteria (e.g., *Bacillus* spp.) (Tiercelin et al., 1987; Duckworth et al., 1996). Almost certainly, the assemblages of microorganisms present in littoral muds include a mixture of planktonic lacustrine types with those species present in microbial mats associated with hot springs on the Loburu Delta, or with those species present in evaporitic microbial crusts on Sandai Plain. Péniguel (*in* Tiercelin et al., 1987) reported several types of cyanobacteria from the littoral zone at Loburu (i.e. the high temperature form *Synechococcus* cf. *lividus*, *Calothrix* sp., *Oscillatoria neumannii*, *O. willei*, *Pseudanabaena catenta*, and *P. lonchoides*), but subsequent investigations of microbes at Lake Bogoria have not specified the localities from which their samples were taken. No detailed investigations of the crusts on Sandai Plain are known. Dense blooms (> 50% of total phytoplankton) of potentially toxic cyanobacteria (i.e. *Microcystis* spp., *Anabaena* spp.), which have been linked to relatively high lake levels and periods of massive die-offs of lesser flamingos, may settle along the shoreline in 'extensive carpets' that are avoided by the flamingos (Ndetei and Muhandiki, 2005).

Lake level fluctuates seasonally in the semi-arid climate with two rainy seasons at Lake Bogoria. In general, muddy lacustrine and delta-front sediments are deposited during wetter periods when more sediment is brought into the lake and when lake levels are higher (+ ~0.5–2 m). Subsequent shoreline regression during the dry seasons exposes the recently deposited muds, which are then reworked by subaerial and shoreline processes. In particular, the huge populations of lesser flamingos at Lake Bogoria dramatically rework the littoral muds by trampling and churning them in the eulittoral and littoral zones (subaerial to ~1 m depth), and by building their nest-mounds from mud in very shallow water (~0.2–0.5 m depth) (Fig. *3.2.*2A, 2B). These behaviours of the flamingos can cause the destruction of pre-existing sedimentary structures and bedforms, as well as the partial oxygenation of uppermost black subaqueous mud (< depths of ~20 cm). Other subaerial processes that rework the lacustrine muddy sediments include desiccation, break-up by efflorescent salts, deflation, and deposition by eolian processes either on the delta-plain or the lake itself (Scott et al., 2010).

The mouth of the Sandai River (Fig. *3.2.*1A, 1B), the northern shoreline of the lake (Fig. *3.2.*1E, 1F), and the northern sub-basin of Lake Bogoria are especially muddy, due to the dense suspended load of the river and the flocculation of clay aggregates at the delta-front (e.g., Tiercelin et al., 1987). The low-gradient mudflats of the Sandai axial delta-plain are clay-rich, and become desiccation-cracked when exposed (Fig. *3.2.*1C). The desiccation cracks and polygons may follow the abundant tracks of flamingos (Fig. *3.2.*1D). Salt efflorescence develops on the exposed mudflats, forming puffy surface textures and wrinkle-like marks where the crusts are partly due to the desiccation of microbial mats (Fig. *3.2.*1C–F). With gentle slopes, little

**Fig. 3.2.1.** (Next page) Mudflats of the lower Sandai delta-plain at Lake Bogoria. Photographs shown in (B) and (E–F) are courtesy of R.Renaut. **(A)** Shallow lacustrine of the flooded lower delta-plain at the mouth of the Sandai River (2001) with juvenile lesser flamingos in background. **(B)** Exposed silts of the lower delta-plain near the mouth of the Sandai River. Note desiccation polygons and salt efflorescence in slightly lower non-incised channel at centre. **(C)** Eastern shoreline of the northern sub-basin (2002), with coarse-grained sediments (left), desiccated clays with salt efflorescence, and drying clays (right). **(D)** Close up of (C). The rounded, irregular shape of the desiccation polygons is partly dictated by flamingo footprints. Scale is 10 cm. **(E)** Exposed deltaic/lacustrine clayey silts of the northern shoreline (2006) with desiccation polygons and efflorescence forming in cracks. **(F)** Close up (E). Note wrinkled texture in salt crust, which may also be partly due to drying microbial films. **(G)** The lower delta-plain at the mouth of the large ephemeral stream Nyoka Donga in 2001. Note patterned sediments due to weakly channelized sheetwash from previous rain storm. **(H)** The mouth of Nyonka Donga in 2002 showing organic-rich lacustrine muds deposited in lower-lying channel mouth/inlet.


A
B
C
30 cm
D
E
F
10 cm
G
H
20 cm

fetch, and cohesive clays, the mudflat sediments are not typically reworked by waves (Fig. *3.2.*1E); symmetrical ripple bedforms near the shoreline were not observed. During storms, sheetwash and weakly channeled flow on the lower delta-plain dissolve pre-existing salt crusts and deposit fine-grained sands in lower lying areas (Fig. *3.2.*1G). When lake-levels are slightly higher, ephemeral channel mouths on the lower delta-plain are flooded by lake waters and dark brown to black organic-rich muds derived partly from planktonic cyanobacteria are deposited (Fig. *3.2.*1H).

Unlike the lower delta-plain mudflats of Sandai, most of the organic-rich sediments at Loburu are derived from benthic microbial mats. The setting differs from Sandai mainly in that the Loburu mudflats contain numerous hot-spring vents with pools and fumaroles, as well as small seepage pools, probably of mixed lacustrine and hot spring waters (Fig. *3.2.*2A–H). This relatively fresh and perennial water source also contributes to the abundant grasses and sedges in the wetlands of Loburu delta-plain and to more intense infaunal animal activity (Fig. *3.2.*2E, 2F). Sediments of the southern Loburu mudflats are brownish red and moderately indurated; both features may be related to the hot spring fluids though the precipitation of zeolites (analcime) and the chemical weathering of volcanic sediments (Fig. *3.2.*2C, 2D). Like Sandai, the flats at southern Loburu are not typically reworked by oscillatory flow. Ripple marks on the mudflats at the southern Loburu Delta were observed only in sediments that had been stabilized by microbial mats, and appeared to have been wind-generated in a shallow, spring-fed pool. Other textures attributed to benthic microbial mats include wrinkle-like marks and gas-escape bubble-marks (Fig. *3.2.*2G, 2H). Salt efflorescences also develop on the southern Loburu Delta, but are generally patchy (Fig. *3.2.*2H). Desiccation polygons form, but are relatively uncommon (Fig. *3.2.*2G).

Mudflats at Lake Magadi or Nasikie Engida are flat and typically abut against the basin margin horsts (Fig. *3.1.*8B). The mudflat on the lower delta-plain of the NE Lagoon was not investigated, but probably shares some similarities with Sandai Plain (Fig. *3.1.*12A). Black and dark brown fine- to coarse-grained sands and organic-rich muds are common on the shorelines in the very shallow lake waters of the NW lagoon and the E lagoon at Lake Magadi (Fig. *3.1.*8A–E, *3.2.*3A–D). Both lesser and greater flamingos, as well as other wading birds, rework and mix the shoreline sands and organic littoral muds by trampling, feeding, and nest-building (Fig. *3.2.*3C, 3D). Muddy sediment is more abundant between the littoral and supralittoral zones where cool meteoric springs empty onto the lake floor (Fig. *3.2.*3A–D). Desiccation cracks and vertebrate tracks are abundant in these areas (Chapter 4). At Nasikie Engida, a rapid transition from coarse-grained lithofacies to lacustrine facies occurs along the coincident margins that bound the lake (Fig. *3.1.*8F). Organic-rich muddy oozes are deposited in the shallow lake (Fig. *3.2.*3E, 3F), and are covered by thin trona–nahcolite evaporite crusts (< ~1 cm) along the shorelines (Fig. *3.2.*3G,

**Fig. 3.2.2.** (Next page) Mudflats of the southern lobe of the Loburu Delta at Lake Bogoria. Photograph shown in (E) is courtesy of R.Renaut. **(A)** Recently exposed low-gradient mudflat near shoreline (2008). Note flamingo nest mounds and flamingos at shoreline. **(B)** Shoreline of mudflat during regression (2008). Note flamingo nest mounds, likely made prior to regression. Juvenile lesser flamingos in background. **(C)** Reddish cohesive silts of the lower delta-plain mudflat (2008). Note black-coloured anoxic sediments at top (arrow), probably due to microbial metabolism, and oxygenated underlying sediments with weak bedding preserved. Scale in cm. **(D)** Reddish silts showing vague wavy bedding with clay-rich drapes on bedding planes. Scale in cm. **(E)** Shallow pool fed by hot spring with orange and green microbial mats in shallow water. **(F)** Dried pool previously fed by seepage, probably of mixed hot spring and lake waters, onto the mudflat ~50 m from shoreline (2007). Shovel for scale. **(G)** Close up of surface shown in (F). Note narrow desiccation cracks in silts and wrinkle-like marks on surface from thin desiccated microbial mat. Scale is in cm and inches. **(H)** Close up of surface shown in (F). Note probable gas escape bubbles from microbial mats in lower areas and puffy salt efflorescence on slightly higher areas. Scale is in cm and inches.

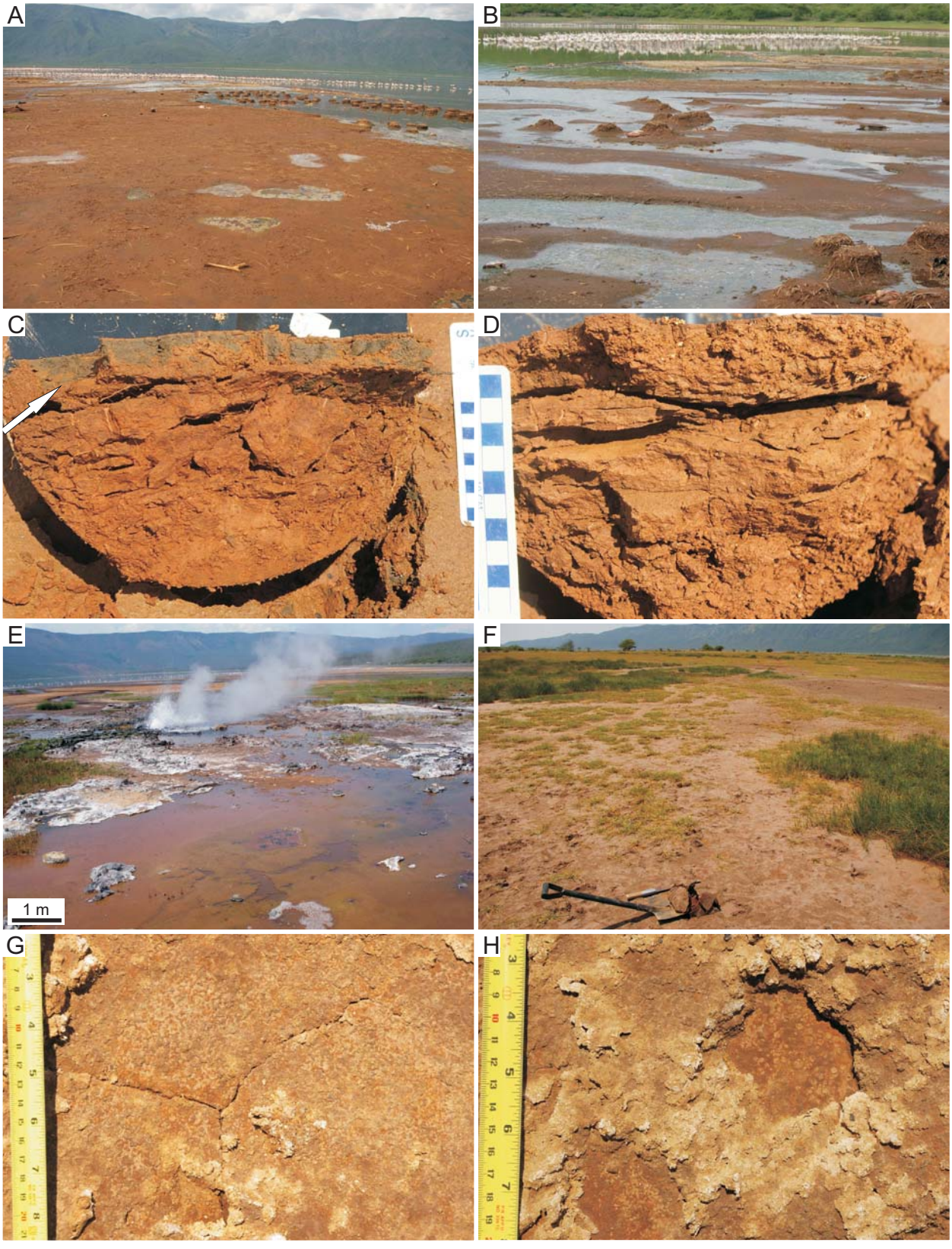
A
B
C
D
E
1 m
F
G
H

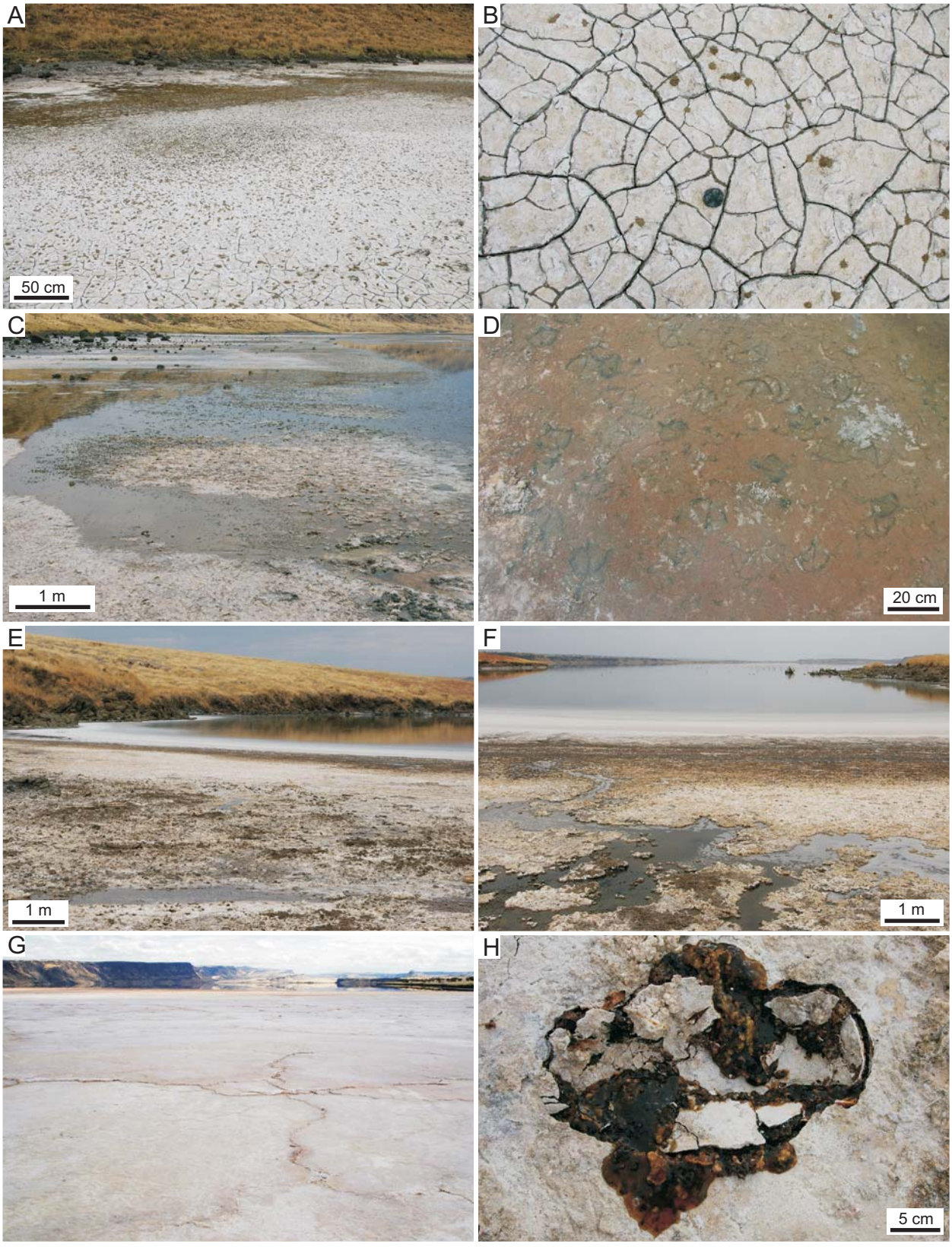
A
50 cm
B
C
1 m
D
20 cm
E
1 m
F
1 m
G
H
5 cm

3H). White, translucent and opaque, siliceous gels are found within the muddy oozes (Fig. *3.2.*3H). Evaporation of the lake waters throughout the dry seasons leads the precipitation of bottom-nucleated and surface-nucleated nahcolite and trona evaporites, especially in the southern, shallower, and more saline part of the lake (Fig. *3.2.*3G).

### *3.2.2. Delta-Front and Organic-Poor Lacustrine Muds, Muddy Sands and Turbidites*

Fine-grained siliciclastic sediments of delta-front, prodelta, and lacustrine environments are deposited in basin centre settings during periods of intermediate to high lake levels (Fig. *3.2.*4). Coarse-grained siliciclastics are deposited as turbidites lakeward of some alluvial fans (Renaut and Tiercelin, 1994). The lake-marginal mudflats and subaerially exposed delta-front lithofacies at the mouth of the Sandai River at Lake Bogoria were described above in Sections 3.1.5 and 3.2.1. Additional lithofacies deposited within the lake, ranging from sandy fan-delta foresets to lacustrine silts, are exposed at Loburu Delta, Sandai Plain, and along the western lake margin. Renaut (1982) previously described the facies from Lake Bogoria, although the following descriptions are mainly based on personal observations (Table 3.1). Lacustrine turbidites that are lakeward of steep alluvial fans were recorded in cores from the eastern margin of the lake, and were described by Renaut and Tiercelin (1994). Tuffaceous, bedded lacustrine silts of the High Magadi Beds are also included in this facies association, although they were not examined in detail (Fig. *3.2.*4E, 4F). The zeolite-rich mineralogy of delta-plain to deltaic facies of the tuffaceous silts of the High Magadi Beds in the NE lagoon was briefly described by Surdam and Eugster (1976).

At Lake Bogoria, most of the siliciclastic sediments deposited within the lake are represented by muddy silts and siltstones deposited from suspension in the delta-front and prodelta as hypopycnal flows (Fig. *3.2.*4A–D). Relative density differences between the sediment-laden river waters and the saline lake waters vary seasonally, with the river waters potentially having greater density during storms and the rainy seasons when the suspended sediment load is high (Fig. *3.2.*4B). Typically, the orange clay-rich suspended load forms surface plumes that float above the denser saline lake water (Fig. *3.2.*4C), but during times of greater amounts of run-off, the denser river waters sink beneath the lake water to form underflows (Renaut and Tiercelin, 1994). Increasing lake salinity away from the mouth of the river may have led to the 'upwelling' of clay-rich water that had apparently been flowing beneath the lake surface in August 2008 (pers. obs., 2008; Fig. *3.2.*4D). Variability in the fluvial sediment load and lake salinity causes variability in the character of the deltaic deposits. They can be structureless due to the settling of flocculated clays, laminated due to the settling of plumes during times of hypopycnal flow, or laminated and cross-stratified due to traction in underflow currents during times of hyperpycnal flow (Renaut and Tiercelin, 1994; Renaut and Gierlowski-Kordesch, in press). Where mixed with the settled blooms of cyanobacteria and heterotrophic bacteria on the lake floor, the mud becomes anoxic and black below the chemocline.

**Fig. 3.2.3.** (Previous page) Mudflats at Lake Magadi and Nasikie Engida. Photograph shown in (G) courtesy of R.Renaut. **(A)** The eastern margin of the E Lagoon at Lake Magadi near a cool water spring issuing from the base of the fault scarp (2007). **(B)** Close up of clay-rich muds with salt efflorescence and desiccation cracks shown in (A). Lens cap for scale is ~5 cm. **(C)** Vertebrate-trampled muddy sediments near the margin of the NW Lagoon (2007). **(D)** Muds and microbial mats with flamingo footprints in shallow water (~5 cm depth) near the margin of the NW Lagoon (2007). **(E)** Northern mudflat at Nasikie Engida where black-coloured muds contain siliceous gels. **(F)** View towards south of northern mudflat at Nasikie Engida. **(G)** View towards north of southern mudflat at Nasikie Engida, with salt crusts and salt-crust push-up ridges forming polygons. **(H)** Black- and dark red-coloured muddy oozes beneath salt crust at the southern mudflat at Nasikie Engida. Note whitish siliceous ooze in muds.

The very fine-grained Holocene Bogoria Silts, deposited as axial delta-front and lacustrine silts in the northern sub-basin, preserve up to 2.2 m of laminated silts on Sandai Plain (Farrand et al., 1976; Renaut, 1993). The beds are nearly horizontal, but dip slightly towards the lake and pinch-out northwards as an onlapping wedge that disconformably overlies the eroded Loboi Silts surface. On Sandai Plain, the Bogoria Silts mainly comprise poorly indurated, buff to

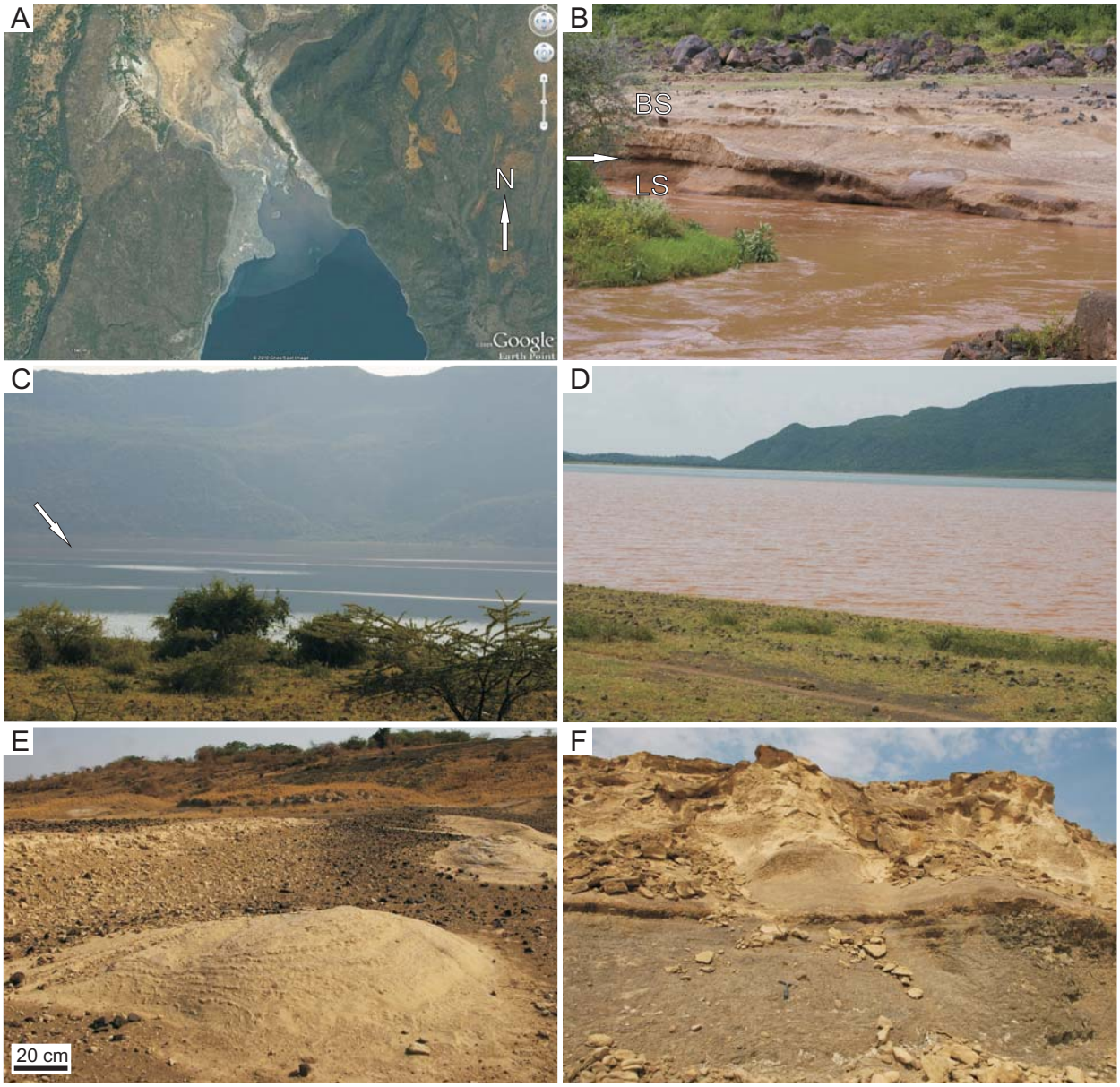


**Fig. 3.2.4.** Fine-grained deltaic and lacustrine environments and sedimentary facies at Lake Bogoria and Lake Magadi. **(A)** Google Earth 2010 image of the northern shoreline of Lake Bogoria with the mouth of the Sandai River at right and plume of fine-grained sediments visible in lake waters. **(B)** Large suspended load of fine-grained sediment in the Sandai River ~500 m from the shoreline (2007). Note the contact (arrow) between the Loboi Silts (LS) and the Bogoria Silts (BS). **(C)** The northern sub-basin at Lake Bogoria in 2007 with sediment plume of overflow on eastern side of basin (arrow). **(D)** The northern sub-basin at Lake Bogoria in 2007 showing upwelling of sediment-laden water at the western margin. Note blue water in background closer to the mouth of the Sandai River, where inflow was apparently denser than the lake water. **(E)** The late Pleistocene to Holocene High Magadi Beds of the western E Lagoon at Lake Magadi. **(F)** The High Magadi Beds in the SE Lagoon at Lake Magadi, showing the tuffaceous upper unit and the darker coloured lower unit containing magadiite chert horizons. Hammer for scale.

pale brown, massive, laminated, or weakly laminated beds (~10–40 cm thick) of clayey silt to very fine-grained sand that contains some ostracods, plant detritus, and other freshwater-indicating fossils (e.g., gastropods and bivalves) (Renaut, 1993). The Bogoria Silts (Fig. *3.2*.4B) share broad similarities with the bedded silts of the High Magadi Beds observed in the E Lagoon and SE Lagoon of Lake Magadi (Fig. *3.2*.4E, 4F) in that they are generally poorly indurated, are horizontally bedded and weakly laminated, and apparently do not preserve lacustrine trace fossils except biogenic structures produced by flamingos.

Lacustrine sediments of fan deltas may be coarser-grained than those of axial deltas (Fig. *3.1*.13). The fine-grained delta-front to lacustrine sediments associated with fan deltas may also be more closely associated with coarser-grained basin margin facies, due in part to the generally higher gradients of fan deltas than those of axial deltas. For example, large-scale, low-angle foresets of the Pleistocene northern Loburu Delta are exposed along the western shoreline of Lake Bogoria (Fig. *3.1*.13F). The sediments, like most of the other exposed Pleistocene Loboi Silts in the Bogoria basin, are reddish brown, are composed of siltstone and very fine-grained sandstone, and are moderately indurated due to cementation by zeolites with some calcite and Fe- and Mn-oxyhydroxides. The foresets dip towards the lake at ~5° and beds are approximately 10–20 cm thick. The unit is overlain by boulder-sized colluvial and alluvial clasts and coarse-grained sands and granules of modern littoral zone. Other older fan-delta silty fine-grained sands at Loburu Delta are also moderately to well indurated, and have been repeatedly buried and exhumed due to changing lake levels since their cementation (Fig. *3.1*.13A–E). Discontinuous horizontal lamination is partially preserved in some examples, but these silty sandstones were mostly bioturbated and pedogenically modified during periods of exposure. These sediments form part of the "exhumed surfaces" discussed in Section 3.1.6.

The southern lobe of the Loburu fan delta preserves a unit of poorly indurated silts that may be time-equivalent to part of the Holocene Bogoria Silts, and are interpreted as delta-front and lacustrine to lower and upper delta-plain sediments. An exposed section in the Parkirichai River was measured at cm-scale resolution, and preserves several lithofacies interpreted to represent a full sequence of lake-level rise-and-fall in a set of fluvial, deltaic, littoral, and lake-margin environments (Fig. *3.1*.5). The delta-front and lacustrine lithofacies present in this section include buff to pale brown massive clayey silts, and weakly horizontal-laminated silty very fine-grained sands (Fig. *3.1*.6A, 6C, 6D). Moving upwards in the section, the fine-grained beds typically have flat bases and coarsen upwards slightly from massive (flamingo-trampled?) and discontinuously planar laminated silts to very fine-grained sand that is reddish towards the top and disrupted by salt efflorescence (Fig. *3.1*.6D). Animal traces nearly identical to the modern southern Loburu delta-plain originate from the tops of the beds. This unit is only ~1 m thick and is sandwiched between two units of fluvial conglomerates and pedogenic silts (Fig. *3.1*.6A).

Alternative interpretations for the genesis of this unit include: 1) the fine-grained unit represents a muddy point bar in an old channel of the Parkirichai River; or, 2) the unit represents overbank fines deposited during floods onto the subaerial delta-plain. Support for the interpretation favoured here includes: 1) the lack of pedogenesis except for the uppermost unit (modern pedogenesis); 2) the moderately well sorted nature of the planar cross-bedded coarse sands, interpreted as beach bars as opposed to fluvial bars; 3) the sharp, flat bases of the transgressive mud beds; and, 4) comparison with the exposed delta-front in the northern sub-basin. The trace (sub-)fossil assemblage is very similar to that on the south Loburu delta-plain, but it is not expected to be substantially different from the assemblage found in the ephemeral muddy channel of the Parkirichai River. Termite traces and mammal burrows suggest a longer period of exposure and probably reflect the position of the deposits within the basin but do not

favour the interpretation of either a fluvial environment or exposed shoreline. The trace fossils are described in Chapter 4. Comparison between the facies in the Loboi Silts at Nyongonyek also supports the lacustrine/delta-front to delta-plain interpretation because of differences in the lithofacies and ichnofossil assemblages.

*3.2.3. Profundal Lacustrine Organic-Rich Oozes and Evaporites*

Lake Bogoria is the deepest and most perennial of the Kenya Rift Valley lakes south of Lake Turkana, and the description and discussion of this lithofacies association focuses on its sublittoral to profundal deposits. The lake is presently less than 12 m deep with lake level at approximately 990 m O.D. (above sea level), but water may spill into the lower-lying Baringo basin to the north if lake levels reach the sill height of ~999 m O.D. Today, at its intermediate level, Lake Bogoria has a distinct, less saline (< 50 g $L^{-}$ TDS) upper mixolimnion, which is separated from the deeper, more saline (< 90 g $L^{-}$ TDS), anoxic monimolimnion by a chemocline at a depth of ~2.5–4 m (Renaut and Tiercelin, 1994; Harper et al., 2003). Saline, sublacustrine hot springs contribute to the higher temperature and salinity in the monimolimnion and help to maintain the meromixis (Renaut and Tiercelin, 1994). The Sandai River at the north end of the lake, the Parkirichai River that feeds the Loburu Delta, and the Emsos River at the south end of the lake contribute fresh water and clays and silts to the less dense mixolimnion (Fig. *3.2*.4C, 4D), unless laden with sufficient sediment to cause hyperpycnal underflows by increasing the density of the inflow waters (Renaut and Tiercelin, 1994; Renaut and Gierlowski-Kordesch, in press).

The productivity of the dominant planktonic cyanobacteria (*Arthrospira fusiformis*) is very high in the surface waters of Lake Bogoria (biomass: 38−365 μg $L^{-1}$ chlorophyll 'a'; individual coils of *Arthrospira*: 3,400–21,000 ml $^{-1}$) (Harper et al., 2003). Also present are the coccoid cyanobacteria *Synechococcus* spp. and *Synechocystis* sp., other filamentous cyanobacteria, namely *Spirulina subsalsa*, *Spirulina subtilissima*, *Phormidium* sp., and *Oscillatoria* sp., and the cyanotoxin-producing planktonic cyanobacteria *Microcystis aeruginosa* (Ballot et al., 2004; Dadheech et al., 2009). The total phytoplankton biomass was measured as up to 777 mg $L^{-1}$ by Ballot et al. (2004), a much greater density than at the fresher, but saline, Lakes Nakuru (104 mg $L^{-1}$) and Elmenteita (202 mg $L^{-1}$). The water temperatures at Lake Bogoria are also higher than the other lakes (25.8–33.7° C), and are closer to the optimal temperature for *Arthrospira* (35–38° C), which makes up ~97% of the total planktonic biomass (Ballot et al., 2004).

The phytoplankton biomass is also characterized by large temporal fluctuations (Oduor and Schagerl, 2007). The primary productivity at Lake Bogoria varies seasonally, with high values in April–May and low values in September–October, and most of the biomass was confined mainly to the upper 35–50 cm of lake water above the light compensation depth in 2004 (Oduor and Schagerl, 2007). Dense blooms coat the lake surface with a green scum (Fig. *3.2*.5A), which settles as detritus at the lower energy shorelines (e.g., Sandai Plain; Fig. *3.2*.5B) and across the lake floor to form sapropelic oozes that are characteristic of the deeper water sediments below the monimolimnion (e.g., Tiercelin et al., 1981; Renaut et al., 1986). Other organisms that contribute to the high amounts of organic matter (up to ~6% T.O.C.) in the profundal muds include rare diatoms of the genus *Nitzschia* sp., six strains of gram-negative alkaliphilic bacteria (e.g., *Vibrio* sp.), the colonies of the coccoid cyanabacterium *Gomphosphaeria aponina*, the chain-like coccoid cyanobacterium *Anabaenopsis arnoldii*, and *Cryptomonas* sp., *Sphaeroeca* sp., and possibly the green algae *Botryococcus braunii* (Renaut et al., 1986; Tiercelin et al., 1987; Harper et al., 2003).

Organic content of the lake muds is highest in the deepest part of the central sub-basin of Lake Bogoria (Tiercelin et al., 1987). Cores of Holocene sediments from the basin-centre organic muds also preserve gastropod shells (*Melanoides tuberculata*), bivalves (*Corbicula africana*), ostracods, and diatom-rich muds (Renaut et al., 1986; Tiercelin et al., 1987). Many species of diatoms (98) in twenty-seven genera were identified from the Bogoria cores, as well as several species of ostracods in the families Darwinulidae, Cyprididae, and Cytheridae (Tiercelin et al., 1987). These organisms imply that much fresher waters existed during the Holocene than those of the modern saline lake.

Clay minerals in the lake are dominated by smectites and interstratified smectite/illite, with some illite, minor amounts of kaolinite (lake margin) and chlorite (deep lake) in both the modern setting and in the Holocene cores (Renaut et al., 1986; Tiercelin et al., 1987). Other authigenic minerals include pyrite, siderite, fluorite, analcime, clinoptilolite, opaline silica, magadiite, kanemite, quartz, and albite (Renaut et al., 1986). Thin beds of white and opaque Magadi-type chert are also found within lacustrine facies of the High Magadi Beds, which were deposited during late Pleistocene to early Holocene highstand of the Magadi lake (e.g., Eugster, 1967; Behr, 2002). At Bogoria, sodium evaporite minerals are common in the cores from the central sub-basin, and may be displacive within muddy units or form discrete beds up to < 50 cm thick of cumulate crystals and fan-shaped bottom-nucleated crystals. Acicular and nodular trona and prismatic nahcolite crystals are the most abundant evaporite minerals in the central sub-basin, together with minor halite and thermonatrite. The latter mineral, which is stable at elevated

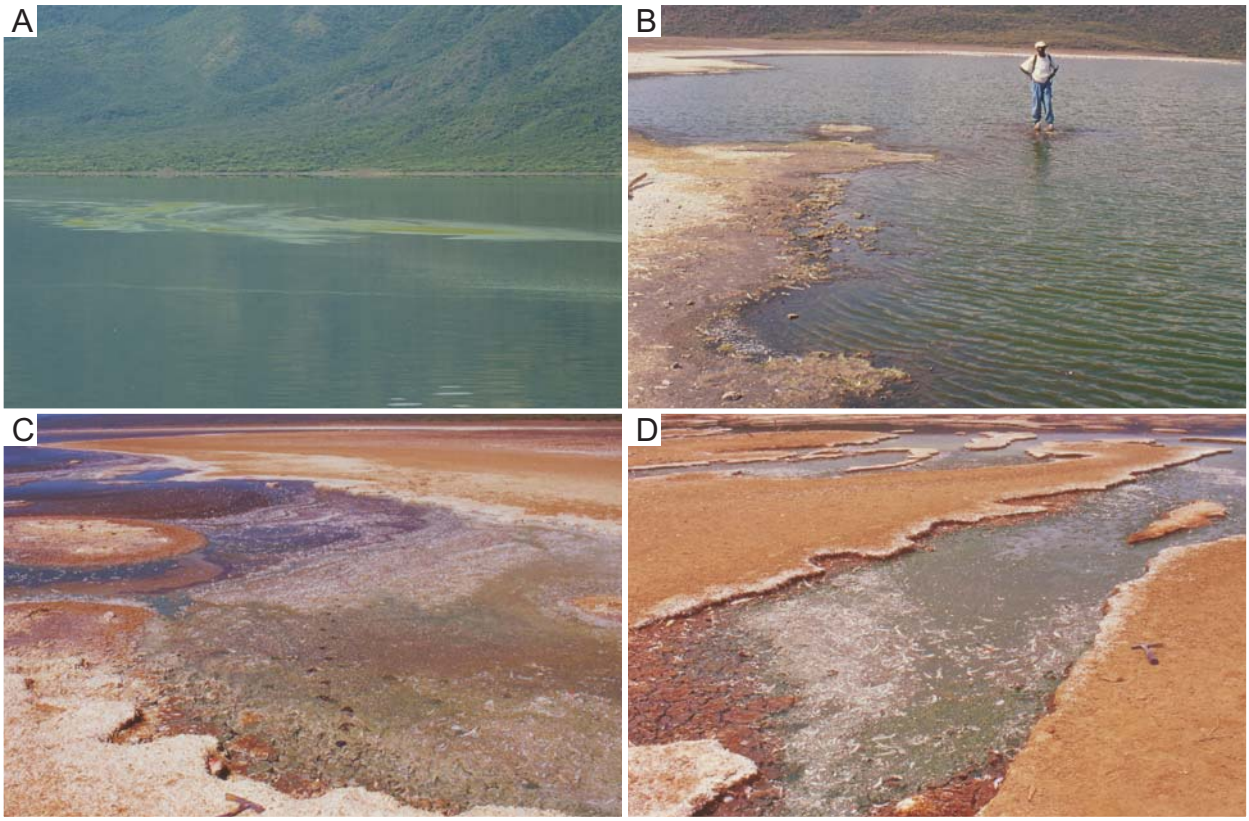


**Fig. 3.2.5.** Blooms of planktonic filamentous cyanobacteria at Lake Bogoria. **(A)** The green-coloured southern central sub-basin with films of cyanobacteria on the lake surface. **(B)** Blooms near the northern shoreline. **(C–D)** Desiccating organic-rich muds (dark brown) and detrital films of planktonic cyanobacteria (green) settled from lake waters that had flooded the terminal distributary channels of the Sandai delta.

temperatures, may be evidence of the influence of sublacustrine hot springs (Renaut et al., 1986). Gaylussite dominates the lacustrine evaporites in the north sub-basin but was not found elsewhere (Renaut et al., 1986). The evaporites likely formed during relatively arid periods when lake levels were low; conversely, the organic muds were likely deposited during wetter periods with higher organic productivity (Renaut and Tiercelin, 1994). Lake Bogoria serves as the best example for the "profundal organic ooze and evaporite" lithofacies because it is relatively deep and perennial when compared with Lakes Magadi and Nasikie Engida.

### *3.2.4. Lacustrine Stromatolitic Carbonates*

Thin beds of stromatolitic carbonates are found throughout the Bogoria basin as discrete lacustrine coatings (< 5 cm thick) on sediments, colluvial boulders, travertine mounds, plant stems, and tree branches (Fig. *3.2.*6A, 6B; Renaut, 1982). Similar stromatolitic coatings have been reported from several other lakes in the Kenya Rift Valley, including the large Pleistocene paleolakes in the Natron–Magadi basin (Casanova, 1986), but were not investigated in this study. These thin coatings also formed on plant stems found in association with small tufa mounds (~0.5 m high) on the Sandai Plain at Lake Bogoria, and suggest that a small spring-fed wetland might have existed there during either the late Pleistocene or Holocene. Although thin stromatolites are also associated with hot spring travertine mounds at Lake Bogoria, the lacustrine examples formed during a humid period of Holocene high lake level (~4500 B.P.; ~999 m O.D.: sill height), an apparent freshening of the lake water, and a greater inflow of Ca-bearing river and groundwater (Vincens et al., 1986).

Internally, the coatings comprise columnar microbial laminae (50–400 μm thick), which alternate between dark, organic-rich layers and layers of carbonate (low-Mg calcite) that preserve the filaments of cyanobacteria (e.g., *Phormidium incrustratum*) (Renaut, 1982; Casanova, 1986; Vincens et al., 1986). According to Casanova (1986), the stromatolite encrustations form in water depths from 0–12 m. The degree of ornamentation (or height of individual columns) is highest for the shallow 0 to -2 m zone, with flattening from -2 to -7 m, and only thin stromatolites without ornamentation at depths from -7 to -11 m. These depth zones vary between lakes, but overall, the presence of the encrustations suggests high lake levels and dilute lake waters (Casanova, 1986). Examples of these widespread lacustrine columnar-laminated encrustations that coat lake-margin bedrock and sediments may specifically indicate a transition from saline waters to fresher waters or from fresh waters to more saline (cf. Icole et al. 1990).

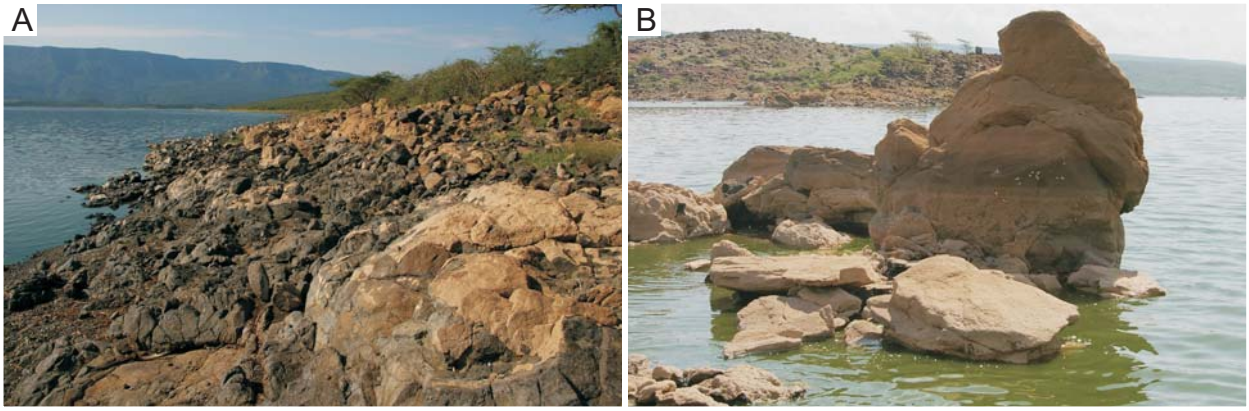


**Fig. 3.2.6.** Stromatolitic coatings formed during higher lake levels at Lake Bogoria. **(A)** The south-central western shoreline of bedrock and colluvium. The coatings are whitish on dark coloured volcanic rocks. **(B)** Stromatolitic coatings on volcanic bedrock at the southeastern shoreline.

*3.2.5. Interbedded Organic Muds and Sodium Carbonate Evaporites*

Interbedded organic-rich muds and evaporites of the basin centre saline-pan is an association observed only at the very shallow Lakes Magadi and Nasikie Engida. During the rainy season, the dried, evaporite pan of Lake Magadi may be almost completely covered with shallow (~15 cm deep), standing rain water (Renaut and Gierlowski-Kordesch, in press). Some of the sodium carbonate salts dissolve, and cyanobacterial blooms occur during this 'productive phase' of the microbial community (Dubinin et al., 1995). As the water evaporates and sodium carbonate salts are re-precipitated in increasingly saline brine, the primary producers become weak and inactive while the decomposing aerobic and anaerobic organotrophs bloom, driving the 'destructive phase' of succession in the microbial ecosystem (Mikhodyuk et al., 2008). Most microbes identified from Lake Magadi are well adapted to the extremely saline and alkaline conditions, including many that are obligately dependent on both $Na^+$ and $HCO_3^-$ ions for their metabolism (Appendix B). Most of the cyanobacteria, bacteria, and archaea have optimal growth conditions within the pH range of ~8.0–11.0, temperatures in the range of ~30–55° C, and salinity ranges from ~1–3% to 10% w/v NaCl. Salinity tolerances may be as high as 20–26% for several species and some species tolerate temperatures up to 60–70° C (Appendix B). For example, the cyanobacterium *Euhalothece* sp. (cf. *Synechocystis salina*), is most productive at salinities of 180 g $L^{-1}$ $Na_2CO_3$, and can even grow in extremely saline conditions up to 230 g $L^{-1}$ $Na_2CO_3$, which is within the range of the extremely haloalkaliphilic anaerobic bacteria that decompose organic matter during the dry season (Mikhodyuk et al., 2008).

The concentrated brines and muddy ooze at Lake Magadi and Nasikie Engida support diverse populations of halophilic and alkaliphilic bacteria and archaea, somewhat different in composition from the bacteria in the soil, water, and sediments around Lake Bogoria (B.E. Jones et al., 1998). More than 100 types have been identified from each of the lakes, with the more extremely alkaliphilic and halophilic types living in Lake Magadi (Duckworth et al., 1996). The photosynthetic primary productivity of cyanobacteria (e.g., *Arthrospira*, *Synechococcus*, *Cyanospira*) presumably supports the rest of the microbial community, although at Lake Magadi cyanobacterial blooms occur only after extensive rainfall (Dubinin et al., 1995; B.E. Jones et al., 1998). The anaerobic microbial communities can decompose most of the organic compounds (e.g., carbohydrates, amino acids) produced by the cyanobacterial blooms (Dubinin et al., 1995; Kevbrin et al., 1998). The red coloration in the modern hypersaline brines is due to the haloalkaliphiles members of halobacterial archaea, which at Lake Magadi are present in densities of $10^7$–$10^8$ $ml^{-1}$ (Mwatha and Grant, 1993). Red-pigmented archaeal colonies collected from littoral muds and salt crusts at Lake Magadi and Nasikie Engida (pH: 10.5–12.5; T: 30–56° C) require high salinity waters (> 15% NaCl w/v) for growth, and have been assigned to various halobacteria genera (e.g., *Natronobacterium*, *Natronococcus*, *Natrialba*) (e.g., Mwatha and Grant, 1993; Duckworth et al., 1996). Like other archaea, halobacteria are remarkably versatile, and can use different methods for obtaining nutrition and energy under adverse conditions (Grant and Ross, 1986). For instance, halobacteria are typically chemoorganotrophs that are light dependent for $CO_2$ fixation, but may also be temporarily able to grow in anaerobic conditions and reduce sulfur compounds (Grant and Ross, 1986). At high salt concentrations, halobacteria are able to outcompete the eubacteria and eukaryotes, although they may be outcompeted themselves by red-coloured anoxygenic phototrophic bacteria (e.g., *Ectothiorhodospira*) under anoxic conditions (Imoff et al., 1981; Grant and Ross, 1986).

The brine at Lake Magadi is extremely saline and alkaline, and fluctuates in these parameters and its depth regularly. The microbial community at Lake Magadi, which is likely very similar to that at Nasikie Engida, reflects these extreme conditions and their fluctuating nature. For example, facultative anaerobic bacteria (*Amphibacillus* spp.) identified from lagoons

at Lake Magadi are adapted to athalassic, frequently drying, soda lakes that require both $Na^+$ and $CO_3^-$ for growth and can tolerate up to 20% Na concentrations (Zhilina et al., 2001). Similarly, the aerobic bacteria *Bacillus alcalophilus* appears to predominate in shoreline muds that are subjected to fluctuating salinities and alkalinities (Duckworth et al., 1996; B.E. Jones et al., 1998). During wet periods, primary production by cyanobacteria is high, and in the following dry periods, most of it is utilized by a variety of heterotrophic anaerobic bacteria, only some of

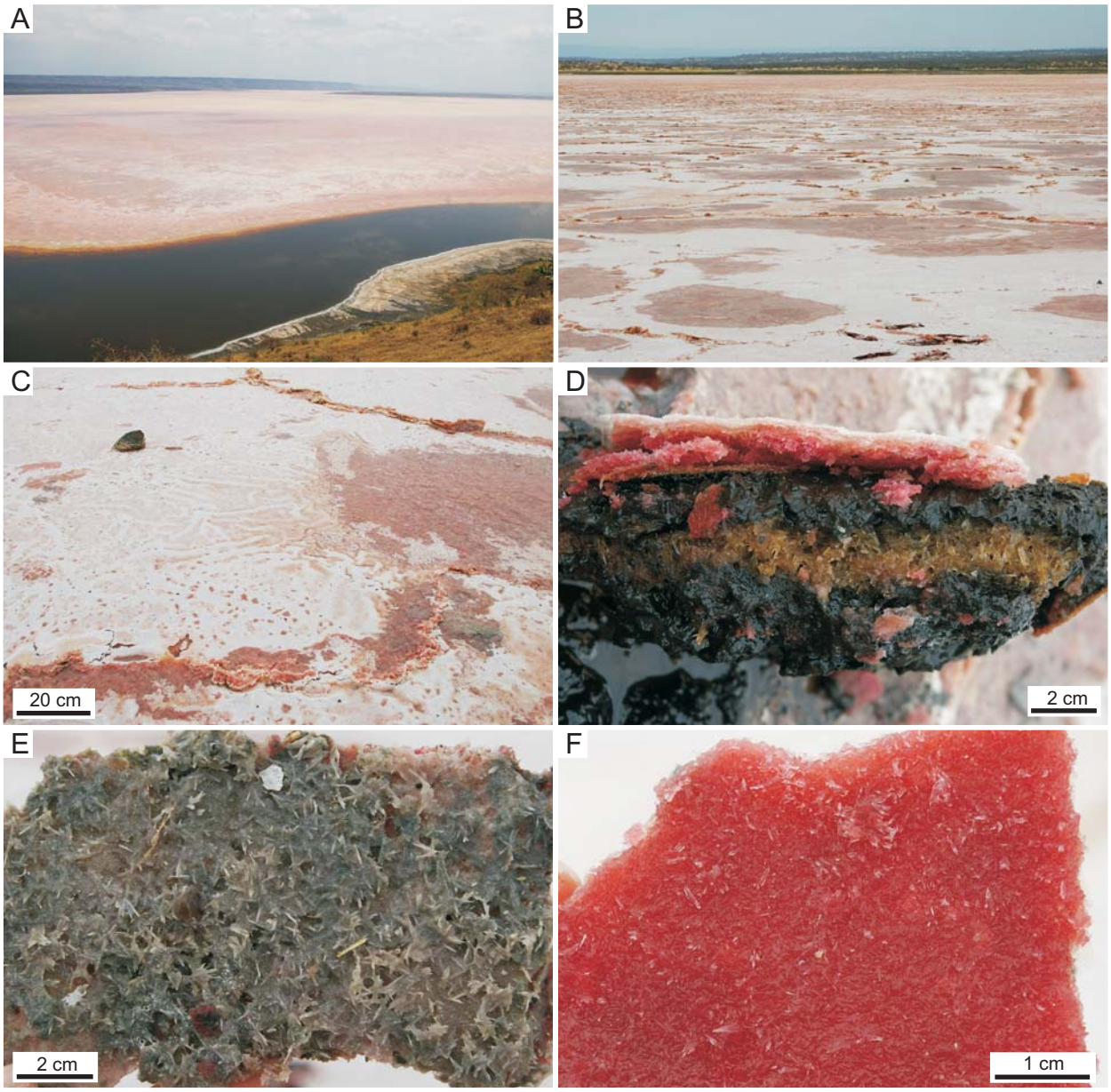


**Fig. 3.2.7.** Interbedded sodium carbonate evaporites and organic-rich muddy oozes of the NW Lagoon at Lake Magadi. **(A)** Salmon-orange coloured sodium evaporite crust on the surface of the central basin. **(B)** Red-coloured sodium carbonate crusts and polygons of push-up ridges due to salt precipitation. Red colour is from halophilic types of Archaea. **(C)** Surface-precipitated salts with wind-induced folding on surface. **(D)** Thin beds of small trona and nahcolite crystal needles interbedded with black-coloured muds. **(E)** Evaporite needles randomly oriented with some clastic sediments forming matrix. **(F)** Close up of red Archaea in trona/nahcolite crust with very small, randomly oriented evaporite crystals.

which are sulfate-reducers (e.g., *Desulfonatronovibrio* sp.) (Zhilina et al., 1997; B.E. Jones et al., 1998). A typical stratification within a trona crust at Lake Magadi reveals an orange-pink area of archaebacterial halophiles in the upper horizon, and several distinct coloured horizons of green, due to cyanobacteria, and purple-red, which contains a number of species of the genus *Ectothiorhodospira* (Grant and Tindall, 1986), with black muds below that contain the low diversity sulfate-reducers.

These fluctuating conditions lead to the genesis of three main evaporite lithofacies observed at Lake Magadi, including the "interbedded organic-rich mud and evaporite" lithofacies observed at the eastern NW lagoon (Table 3.1). In this case, finely crystalline acicular crystal masses, mainly of trona, form hard, dense horizons approximately 1–3 cm thick that are interbedded with horizons of organic ooze derived from the diverse microbial communities described above (Fig. *3.2.*7). Presently forming evaporite horizons at the air-water interface are wet with brine and are salmon-red. The upper horizon is broken up into pressure-ridge polygons up to ~3 m in diameter (Fig. *3.2.*7B). The surface of the finely crystalline evaporite horizon may show the evidence of wind-generated ripples and gentle undulations (Fig. *3.2.*7C).

The second evaporite lithofacies contains much less organic-rich mud in general, and was found along the western margin of the central basin (Fig. *3.2.*8). Like the interbedded mud and evaporites, beds are generally less than 2 cm thick, and also show evidence of fluctuating conditions. This lithofacies comprises horizontally laminated to very thinly bedded evaporites that are sometimes present in couplets. It consists of a lower porous layer of bottom-nucleated acicular trona crystals (< 1 cm length), sometimes in 'crystal bushes', and a very thin drape of very finely crystalline surface-nucleated crystal rafts that settled to rest on the acicular crystal points (Fig. *3.2.*8B, 8C; Renaut, pers. comm., 2007; Renaut and Gierlowski-Kordesch, in press). The salts are whitish to light peach in colour at the surface, but are dark brown to black at depths more than a few centimetres. In this area, polygons are less regular and are generally > 3 m in diameter (Fig. *3.2.*8A). Isolated, meandering channels are filled with extremely dense and well indurated grayish black mud (with silica cement?) with large trona blades showing flow structures (Fig. *3.2.*8E–H). Rare vertebrate tracks may be found in these channels, along with concentrations of dead insects (i.e. grasshoppers, beetles) and transported goat fecal pellets (Fig. *3.2.*8E).

The third main lithofacies of bedded evaporites is found further towards the basin centre (Fig. *3.2.*9A), and consists of bedded trona in beds ~3–7 cm thick with parting horizons of dark-coloured silt and very fine sand that is likely eolian or washed in during floods (Fig. *3.2.*9B–E). The beds are dense, made up of much larger (> 3 cm long), interlocking crystal blades in fans or rosettes that form a solid mass of trona (Fig. *3.2.*9C). The evaporites are greyish white and appear to contain very little organic matter. Of these three main bedded evaporite lithofacies, some notable patterns are observed which may be useful for the interpretation of similar facies in

**Fig. 3.2.8.** (Next page) Very thinly bedded sodium carbonate evaporites near the western margin of the central basin at Lake Magadi. **(A)** View towards the north near the shoreline, showing dry surface and large push-up ridge polygons. **(B)** Needle-like trona (and nahcolite?) crystals both bottom-nucleated (larger upright crystals) and surface-nucleated (thin, finely crystalline crust at top left) crusts. Lens cap for scale is ~5 cm. **(C)** Cross-sectional view of bedded sodium carbonate evaporites showing surface-nucleated needle fans. **(D)** Surface showing larger crystals lying on surface, for both vertically and horizontally oriented crystals. Lens cap for scale is ~5 cm. **(E)** Ephemeral? or excavated? channel in central basin showing black, cemented mud also present beneath the light salmon-coloured crusts. Lens cap at bottom centre is ~5 cm. **(F)** Blocks of thick-bedded bladed evaporites, possibly transported in channel, forming 'salt' jam. Lens cap for scale is ~5 cm. **(G)** Close up of thick-bedded bladed evaporites shown in (F). Lens cap at top right for scale. **(H)** Close up of randomly oriented large crystal blades of trona in black-coloured mud. Lens cap for scale is ~5 cm.

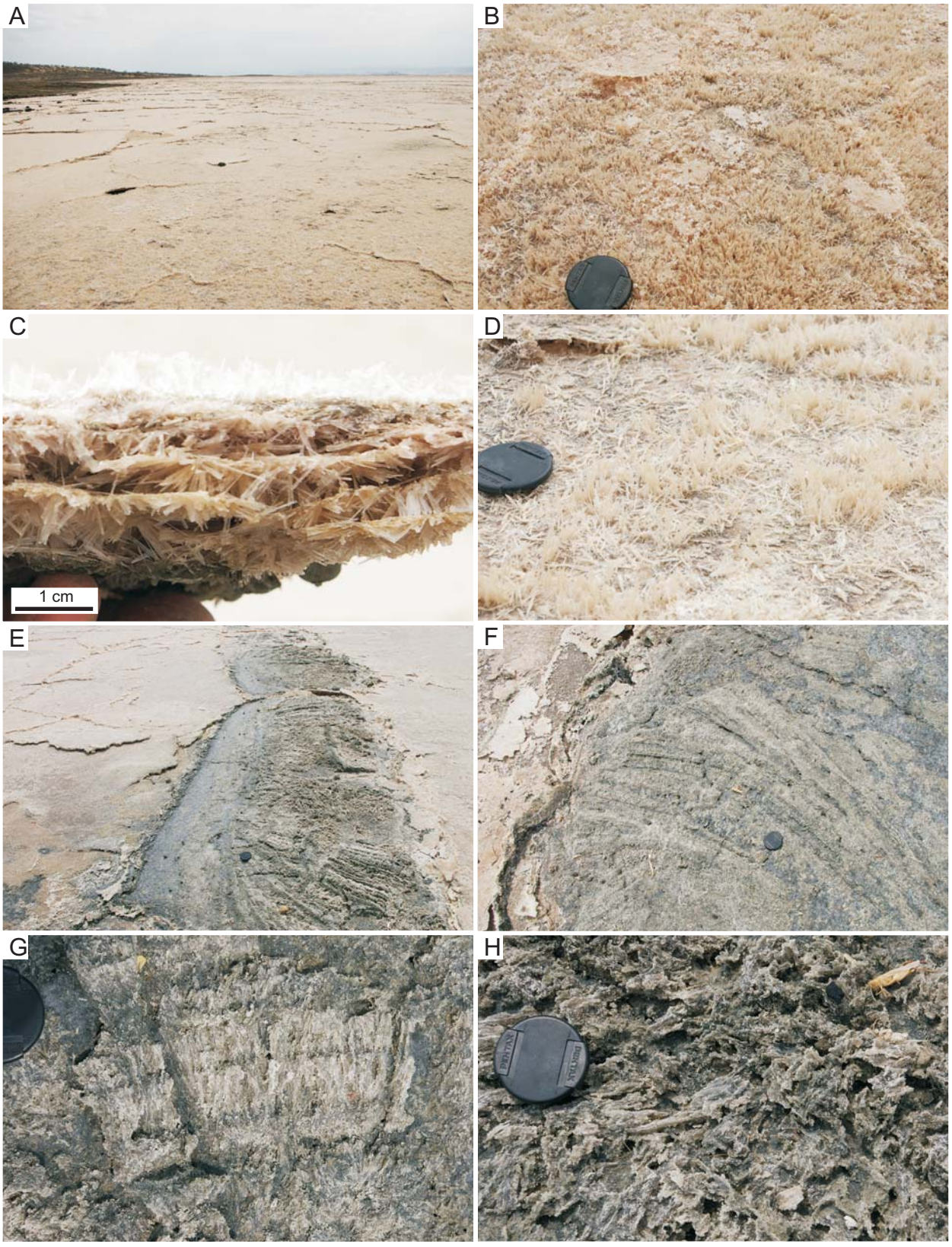
A
B
C
1 cm
D
E
F
G
H

the Green River Formation. Considering their distribution within the top 0.5–1 m of the modern evaporites: 1) there is less organic matter and an increasing amount of silt to fine sand-sized clasts (eolian) towards the basin centre; 2) individual beds tend to be thicker towards the basin centre; 3) there is more open water (spring-fed lagoons) towards the basin margins; 4) polygons are smaller in the wetter areas towards the basin margin; and, 5) evaporite beds are more porous and show more abundant dissolution-reprecipitation features where they were likely in direct contact with water for a shorter amount of time (i.e. margin of the central basin flooded only briefly during rainy season).

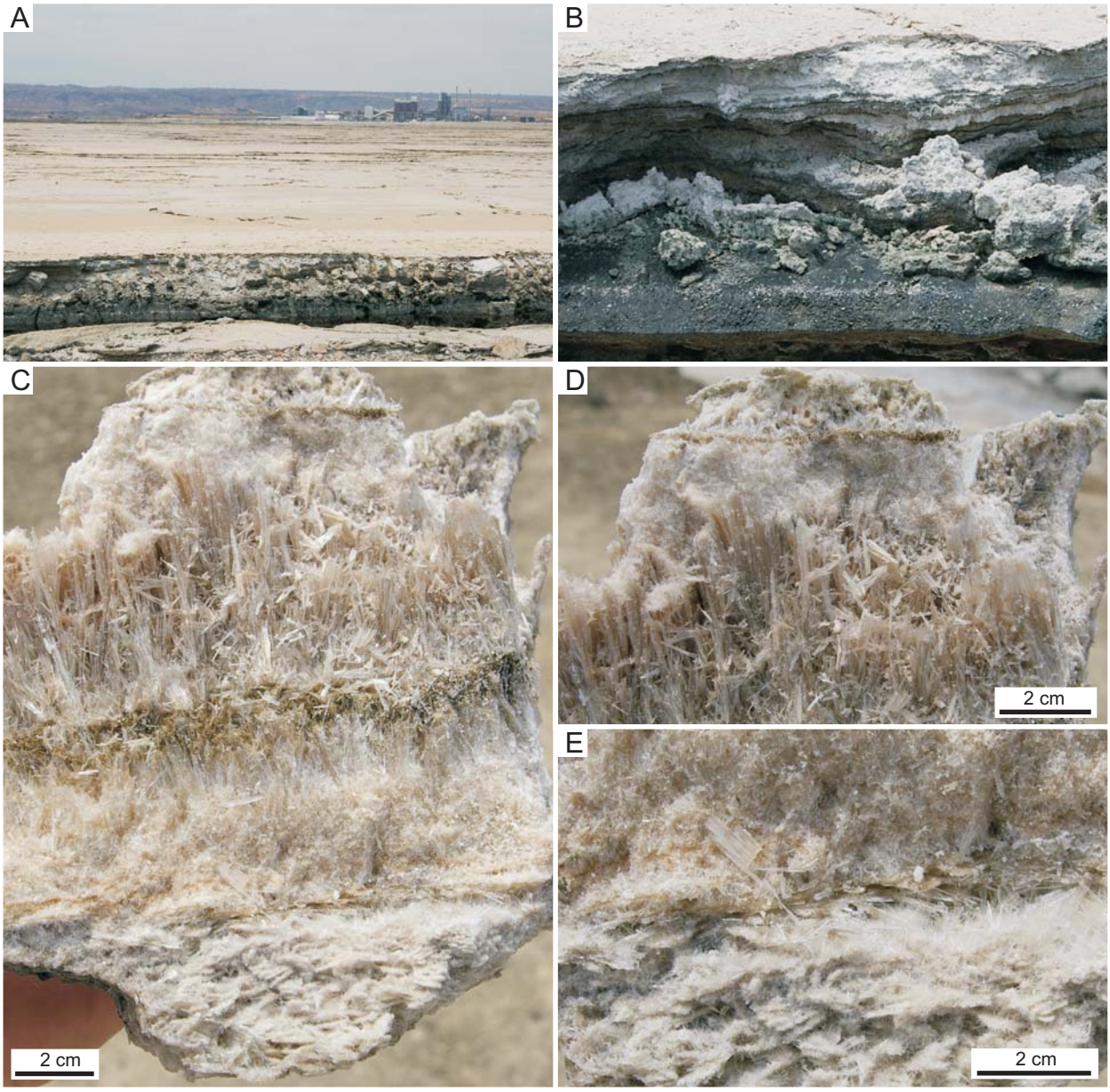


**Fig. 3.2.9.** Thinly bedded sodium carbonate evaporites of the central basin at Lake Magadi. **(A)** Excavated channel in central pan showing bedded evaporites. Note the buildings of the Magadi Soda Company in background. **(B)** Close up of bedded evaporites at channel shown in (A). **(C)** Beds of white needle fans, finely crystalline masses, and small evaporite 'plates' separated by clastics probably derived from eolian and sheetwash processes. **(D)** Close up of upper bedding plane shown in (C). **(E)** Close up of lower bedding plane shown in C.

## 3.3. Hot Springs, Hypersaline Environments, and Microbial Mats

Many of the environments around the tectonically active and closed basins of Lakes Bogoria, Magadi and Nasikie can be considered extreme, from hypersaline brines, highly saline pore-waters and high air temperatures on the lake margins, to hot springs and the environments associated with their outflow. However, spring waters that discharge onto the lake margins can provide oasis-like habitat for a diversity of animals and wetland plants. The springs also provide ions (e.g., Na, Si, F) and gases (e.g., $CO_2$, $H_2S$) that affect the chemistry of surrounding environments and may lead to the preferential cementation of sediments deposited around the spring vents in both subaerial and sublacustrine settings (e.g., Renaut and Owen, 1988; Cioni et al., 1992). High temperatures of the spring waters (e.g., up to 97° C at Lake Bogoria) restrict the types of bacteria, archaea, plants, and animals that can survive in close proximity to the spring vents, with an increasing diversity of life as temperatures cool towards the edges of spring pools and downstream in outflow channels (e.g., Renaut et al., 1998). Microbial mats composed of thermophilic and thermotolerant cyanobacteria, bacteria, and archaea typically grow on substrates associated with the hot spring effluent, where grazing animals cannot survive (e.g., > 50° C; e.g., Brock, 1970; Lamberti and Resh, 1983). Similarly, hypersaline and hyperalkaline environments also limit animal and plant diversity, and may lead to the growth of thick microbial mats on the mudflats that surround a saline lake, for instance, or to the deposition of organic-rich oozes in shallow lake waters. Some of the trace-making organisms (e.g., ephydrid flies, staphylinid beetles) observed at Lakes Bogoria, Magadi, and Nasikie Engida are well adapted for these harsh environments and benefit directly from the growth of the microbial mats, which provide an abundant, stable food source. These types of ecosystems, with simple food chains, depend on the extreme conditions that exclude most plants and animals and limit the number of competitors and predators (e.g., Wiegert and Mitchell, 1973; Mitchell, 1974).

At the same time, the spring discharge provides a relatively freshwater source in an otherwise saline to hypersaline environment, and permits a locally greater diversity of trace-making animals where water temperatures are less than ~40° C. At Lake Magadi, for example, most springs are cooler than those at Lake Bogoria. Where they emerge, an environment with relatively fresh, open water and a microbial food source provides habitat for a diversity of animals dominated by insects, spiders, and birds. Freshwater input to saline lake-margin environments by rivers and their short-lived, overbank pools also creates habitat for a locally greater diversity of plants and animals. These important aspects of saline, alkaline lake settings, especially in tectonically active regions such as the Kenyan Rift and the Eocene greater Green River basin, impact the lake and lake-margin chemistry, sedimentology and stratigraphy, and the ecosystems in which the trace-making animals live. The distribution of trace fossil assemblages in these types of basins (e.g., closed, underfilled) is determined by these factors, particularly during lake lowstands and arid climatic periods. For these reasons, the following sections describe and discuss the springs and spring-related environments, hypersaline environments, and the associated microbes that form the base of the food chain at modern Lakes Bogoria, Magadi, and Nasikie Engida.

### *3.3.1. Lake Bogoria*

Almost 200 hot springs feed Lake Bogoria, which lie mainly along faults and fractures at the western and southeastern edges of the lake (Fig. 2.2; Renaut, 1982; Cioni et al., 1992; Renaut and Tiercelin, 1994; Renaut and Jones, 1997; Renaut et al., 1998). About 60 hot springs with temperatures up to 97° C and brackish (4–6 g $L^{-1}$ TDS), alkaline (pH 7.6–8.4) Na–$HCO_3$ waters discharge along two N–S-trending faults that cross the Loburu Delta. Some springs have small carbonate travertine mounds, most of which are fossil (Figs. *3.1.*15, 16); others discharge from

pools in the delta-plain muds, silts, and sands with no precipitates except minor silica crusts (Figs. *3.1.*15A–C, *3.2.*2E, *3.3.*1A). The spring waters flow lakeward through shallow outflow channels (Figs. *3.1.*15A, *3.1.*15C, *3.3.*1H), or flow into littoral and supralittoral (Cyperus laevigatus) wetlands (Fig. *3.1.*15B, 15G; R.B. Owen et al., 2004). Many springs that discharge onto the Loburu delta-plains lie near the shoreline where their pools may coalesce or mix with lake waters (Figs. *3.1.*15G, *3.2.*2B, *3.3.*1A). Today, hot springs are absent on the Sandai Plain.

Travertine mounds on the western shores of Lake Bogoria were likely formed during the Pleistocene and Holocene, with only minor cementation occurring today (e.g., Renaut, 1982; Renaut and Jones, 1997). The mounds are composed dominantly of calcite and aragonite, and crystals were precipitated both abiogenically and due to the influence of microbial mats depending on the physicochemical conditions (e.g., temperature; $P_{CO_2}$) of hot spring outflow (Figs. *3.1.*15, 16; e.g., Renaut and Jones, 1997). Additional deposits related to the evaporitic concentration of silica-containing hot-spring fluids include silica crusts, silicified microbes, and silica rhizoliths (Renaut et al., 1998; R.A. Owen et al., 2008). Fluorite, calcite, and zeolite cements also preserve rhizoliths of wetland vegetation that grew in the hot-spring influenced Loburu delta-plain (Fig. *3.1.*14B; R.A. Owen et al., 2008). Microstromatolites (< 1 mm diameter) of calcite and silica are formed of laminae that contain coccoid bacteria (and ?archaea) with filamentous cyanobacteria and exopolymers (Fig. *3.1.*16F; Renaut et al., 1998). Some of the travertine precipitation mechanisms were possibly influenced by microbial metabolism and uptake of ions, but most mechanisms were controlled mainly by abiogenic processes (e.g., bladed, fibrous, and platy calcite) (Fig. *3.1.*16B–C; Renaut and Jones, 1997; B. Jones and Renaut, 1998; Renaut et al., 1998; R.A. Owen et al., 2008). Based on comparisons with modern examples, even the dominantly abiogenic deposits were likely closely associated with cyanobacterial and bacterial mats of thermophilic species in cooler (< 70°C) waters, even if the microbes played little direct role in carbonate precipitation.

The thickest, best developed and highest diversity microbial mats at Lake Bogoria, and the most laterally extensive examples of thin, cyanobacterial mats are found both at southern Loburu, where many hot springs vent onto subaerial delta-plain mudflats. The gradient of the lower delta-plain is low (~1–2°), and groundwaters composed of a mixture of saline, lacustrine and fresher, hydrothermal fluids are frequently near (< ~25 cm depth in August, 2007) or at the sediment-air interface depending roughly on the distance from the frequently changing shoreline. Depending on the lake level and the complex interactions, not yet fully understood, between lacustrine-derived and $CO_2$-charged hydrothermal groundwaters, the southern Loburu Delta may be flooded, dry, or it may be partly covered by sodium carbonate efflorescent crusts (Fig. *3.2.*2). The conditions that led to the development of widespread cyanobacterial mats in June-July, 2001 and 2002 were intermediate between these two states, and the delta-plain was partially flooded by numerous shallow pools and partially dry mud with patchy salt crusts (Figs. *3.3.*1E, *3.3.*2A).

**Fig. 3.3.1.** (Next page) Hot-spring environments and microbial mats at Lake Bogoria. **(A)** Shallow hot spring pool on the south Loburu Delta with orange and black microbial mats and white silica and evaporite crusts (2001). Hammer for scale. **(B)** Orange-coloured mat in cooler waters along the margin of the lake at south Loburu (2007). **(C)** Flamingo footprints in thick orangish-brown mat with gas escape bubbles (2001). Scale is in cm. **(D)** Green and black mat at the edge of a seepage pool near the shoreline at south Loburu (2007). The mat overlies muddy coarse-grained sands. Note zebra footprint at top left. **(E)** Thin brown-coloured mat with small gas escape bubbles on the south Loburu mudflat (2001). Note surfacial tunnel traces probably produced by staphylinid beetles feeding on the mat. Scale is in cm. **(F)** Orange and green mat beside boiling spring vent at Chemurkeu. Scale in foreground is ~15 cm long. **(G)** Close up of green and orange mat at Chemurkeu. White crust is probably a mix of opaline silica and sodium carbonate efflorescence. Scale is in cm. **(H)** Bright green filamentous cyanobacterial mat in hot spring outflow channel at the main hot spring site at Loburu.

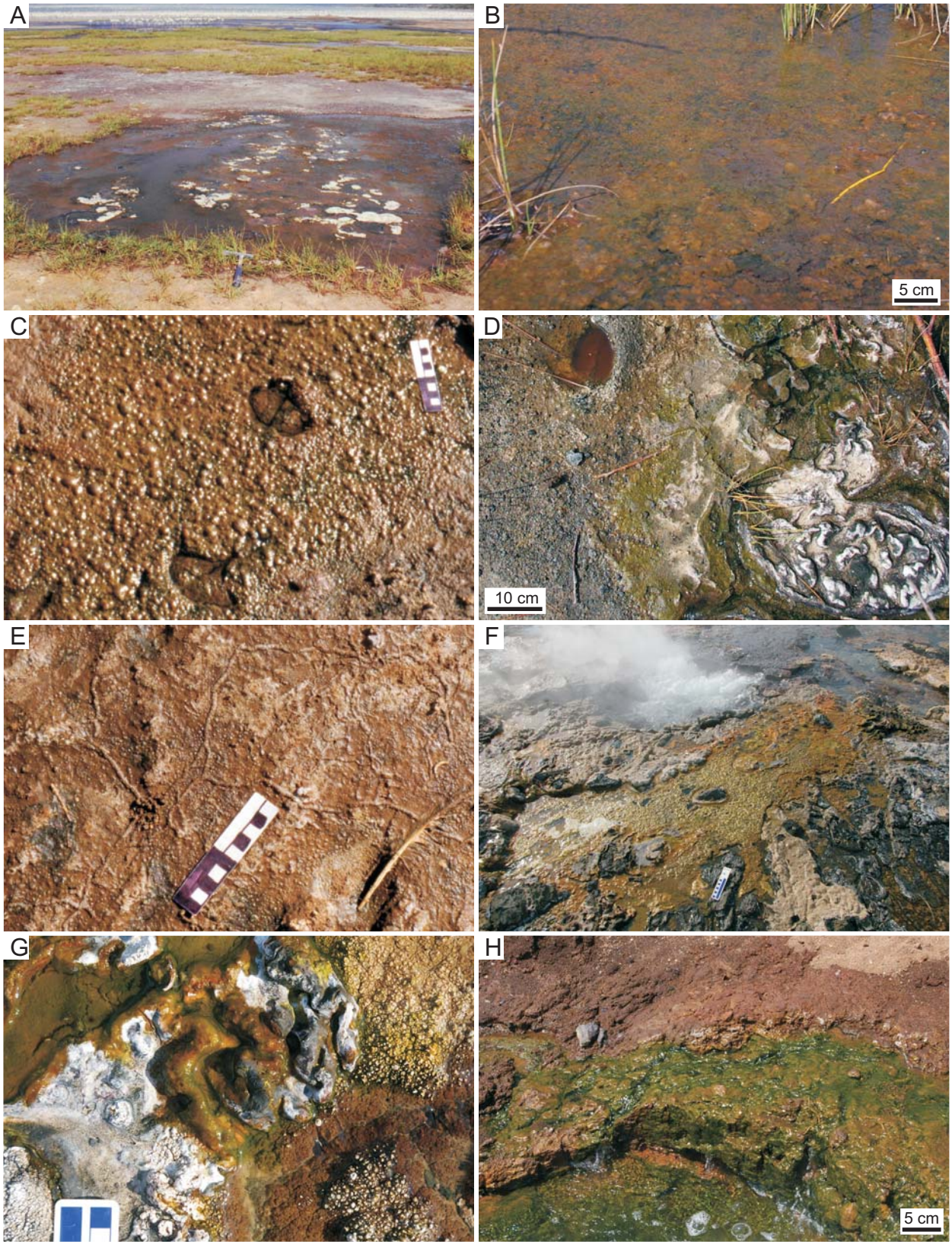
A
B
5 cm
C
D
10 cm
E
F
G
H
5 cm

These same conditions were not observed in August 2007 or 2008 when lake levels were higher (+ ~0.5–0.7 m) and more extensive littoral wetlands had developed. In August 2006, when lake levels were low (- ~0.5–1 m), well developed mats were present around the pools of several recently subaerially exposed spring vents, some of which were active geysers (Fig. *3.2.*2E; Renaut et al., 2008), but thin cyanobacterial mats again were not widespread as in 2001 and 2002.

Holocene, sublacustrine hot-spring deposits at Lake Bogoria comprise pore-filling opaline silica cements in gravels and opaline chert crusts found exposed along the Ng'wasis peninsula and the southern sub-basin of the lake (Renaut and Owen, 1988). The cherts formed subaqueously during periods of higher lake levels in lake waters that were likely relatively fresh (Renaut and Owen, 1988). Silicified ostracod and gastropod shells are preserved with planktonic diatom tests in the Lake Bogoria cherts (Renaut and Owen, 1988). Similar opaline cements and crusts < 5 cm thick on the volcanic island of Ol Kokwe in Lake Baringo, and are also attributed to subaqueous precipitation due to the rapid cooling of silica-containing, hot spring waters (Renaut et al., 2002b). Although the processes involved in the precipitation of these opaline cherts were primarily abiogenic, a cyanobacterial food source for trace-making animals was associated with the hot-spring vents, as shown by stromatolitic laminae and the tunnel networks probably produced by insect larvae (cf. Renaut et al., 2002b).

Other deposits associated with microbial mats, but not necessarily with hot springs, are the stromatolitic calcite coatings described in Section 3.2.4 (Fig. *3.2.*6). In the southern sub-basin of Lake Bogoria, these stromatolites preserve the tube-structures of chironomid (Diptera) larvae, and also possible network-like tunnel systems probably also produced by insect larvae (described in Chapter 4). Chironomid larvae feed on microbial food sources in a wide range of water chemistries (e.g., Cannings and Scudder, 1978). Although cyanobacterial mats are widespread in saline environments without hot-spring inputs (e.g., Bauld, 1981; Stal et al., 1985; Stal, 1995), the best developed examples at Lake Bogoria are directly associated with hot springs (Figs. *3.1.*15B, *3.2.*2E), and only thin, green mats, if any, are present on the shorelines elsewhere. The well drained medium- to coarse-grained sands that form most of the higher-energy shorelines at Lake Bogoria may not be an ideal substrate for the development of microbial mats, unlike the muddy, very low gradient mudflats of southern Loburu (Fig. *3.2.*2). In general, mats are best developed where temperatures and salinities are low enough for cyanobacteria to survive, but high enough to restrict the grazing by animals (e.g., flies, ostracods), and temperatures, salinities, and energy conditions remain relatively stable over sufficient time for the mats to develop (e.g., Brock, 1967; Lamberti and Resh, 1983; Wickstrom and Castenholz, 1985; Stal et al., 1985; Stal, 1995).

*3.3.1.1.* *Microbial Mats*— Thermophilic and thermotolerant microbes at the Loburu hot springs include the mat-building cyanobacteria *Phormidium terebriformis*, *Oscillatoria willei*, *Spirulina subsalsa*, *Synechococcus bigranulatus*, *Pseudanabaena* sp., *Calothrix* sp., and *Chloroflexus* sp., with ~10–20 other coccoid and filamentous cyanobacterial taxa (Appendix B; e.g., Tiercelin et al., 1987; Hindák, 2001; Krienitz et al., 2003; Ballot et al., 2004). Several types of thermophilic bacteria have also been identified from the hot springs at Loburu (e.g., Svetlitshnyi et al., 1996; B.E. Jones et al., 1998; Prowe and Antranikian, 2001), along with many other halotolerant, alkaliphilic, thermotolerant, and/or alkalitolerant species (e.g., Duckworth et al., 1996; Appendix B). Microbial mats built by bacteria and diatoms develop along the margins of most hot-spring pools and their outflow channels, in spring-fed wetlands, and around the edges or slightly higher topographic areas of hydrothermal seepage zones on the mudflats where the waters have cooled to 35–60°C (Figs. *3.2.*2E, *3.3.*1A; Renaut et al., 1998; R.B. Owen et al.,

2004, 2008). On the Sandai delta margin, microbial substrates are limited mainly to detrital cyanobacterial films of *Arthrospira fusiformis* and/or *Microcystis* sp., which are washed ashore from the lake (Fig. *3.2.*5C–D; e.g., Tiercelin et al., 1987; Ndetei and Muhandiki, 2005).

Several species of benthic diatoms can also be abundant in wetlands fed by hot-spring outflow. In contrast, only a few examples are present in the littoral wetlands. Benthic diatoms were not present in the hot spring waters with temperatures > 56° C at Loburu Delta, but a low diversity community commonly sites where waters were 40–56° C, and included *Navicula tenella*, *Navicula cuspidata*, *Anomoeoneis sphaerophora*, *Nitzschia sigma*, *Nitzschia latens*, *Nitzschia elliptica*, and *Nitzschia frustrulum* (R.B. Owen et al., 2004). Benthic diatoms in the hot spring-fed marshes with slightly lower temperatures (~32–50° C) had high diversity, were very abundant, and included *Nitzschia sigma*, *Nitzschia communis*, *Navicula tenelloides*, *Rhopalodia gibberula*, and *Anomoeoneis sphaerophora* (R.B. Owen et al., 2004). Benthic diatoms in the hypersaline littoral zone also associated with cyanobacterial mats, in contrast, showed low diversity and very low abundance, even when compared with the diatom assemblages from proximal hot spring waters (R.B. Owen et al., 2004). Littoral zone temperatures ranged from ~29–32° C and species included *A. sphaerophora*, *N. latens*, *Nitzschia tropica*, together with the planktonic species *Cyclotella meneghiniana* and *Thalassiosira rudolfii* (R.B. Owen et al., 2004).

Relatively thick (< 2 cm) mats of cyanobacteria and bacteria develop in association with the spring waters especially at the water/air interface in pools of hot (< 70° C) standing water at

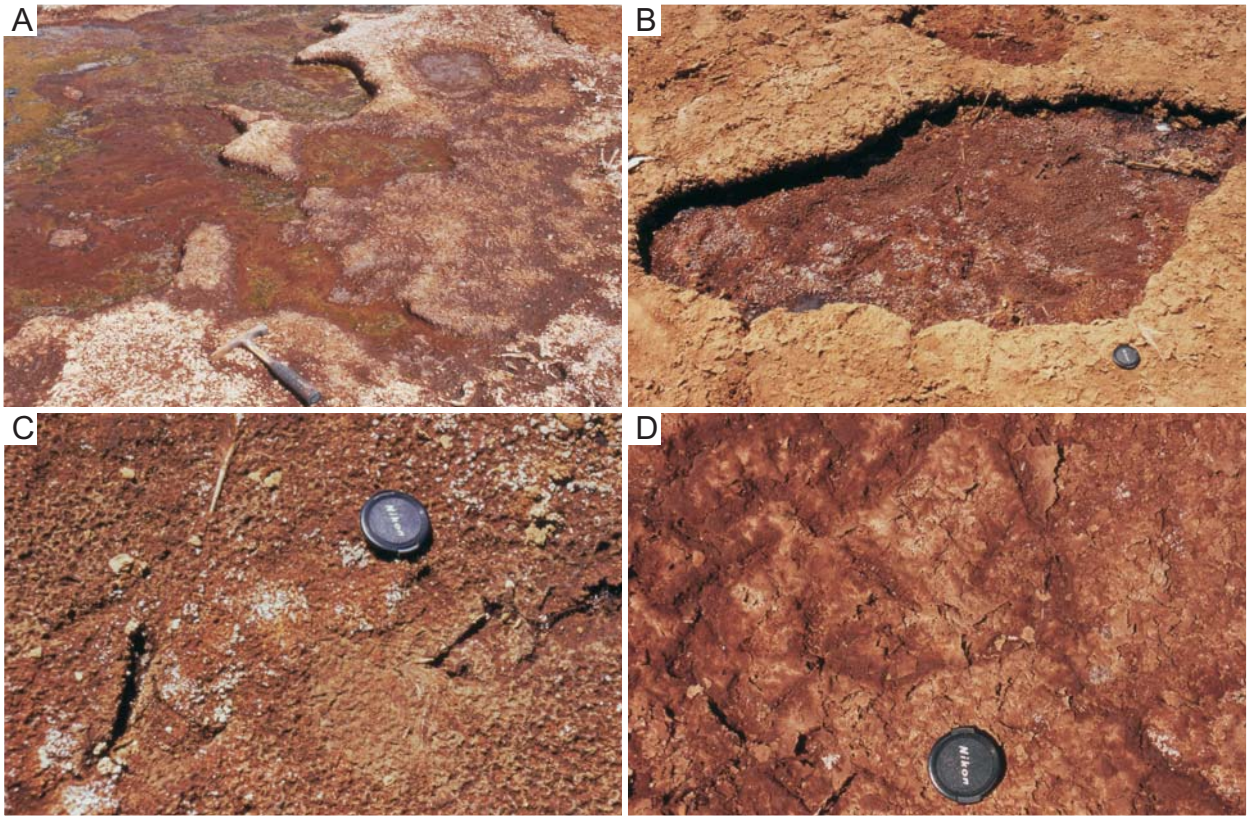


**Fig. 3.3.2.** Desiccated microbial mats on the southern Loburu Delta, Lake Bogoria. **(A)** Flamingo-trampled reddish brown silts coated by orangish-brown and green mats (2002). Hammer for scale. **(B)** Desiccated pool with microbial mats. Lens cap for scale is ~5 cm. **(C)** Close up of desiccated thick (< 2cm) mat in (B) showing well 'preserved' flamingo footprints and wrinkle-like texture of desiccated mat. Lens cap for scale is ~5 cm. **(D)** Mixed crust of desiccated thin (~0.5 cm) microbial mat and sodium carbonate salt efflorescence broken into chips. Lens cap for scale is ~5 cm.

the southern Loburu Delta (Figs. *3.2.*2G, *3.3.*1A; Renaut et al., 1998). Relatively thin mats (< ~0.5 cm thick), mainly of cyanobacteria, are widespread at the sediment/water/air interface on cooler (> 45° C) mudflats, especially where seepage provides low volumes of slowly flowing water (Fig. *3.3.*1E). Mats range from bright green to green-brown to orange to dark green, purple and black, and are often colour-zoned by temperature, both spatially and vertically, depending on species tolerances (Fig. *3.3.*1A–H; e.g., Renaut et al., 1998; Stolz, 2000; Rothschild and Mancinelli, 2001). The colours of mats can also be correlated with the degree of development and age of the mat, which partly determines species composition (e.g., Stal et al., 1985; Stal, 1995; Boomer et al., 2009). For some types of microbes (e.g., cyanobacteria), their colours may change depending on levels of UV light (e.g., Stal, 1995; Frank and Stolz, 2009).

The thicknesses of mats can be related to the age and degree of development of the mat, but also to temperature, because of the interactions with grazing animals at lower temperatures (e.g., Wickstrom and Castenholz, 1985). The upper temperature limits for the larval insects that feed on microbial matter are at most ~45° C, and so it is on the cooler, cyanobacterial-dominated mats that most of the grazing traces are found (Fig. *3.3.*1E). Additionally, because cyanobacteria produce carbohydrates and proteins (in most cases) at the mat surface, they are a suitable food source for animals (Krivosheina, 2008). Most of the other bacteria (e.g., chemotrophic types) are present in the anoxic layers of the mats where concentrations of toxic compounds such as sulfide are higher (e.g., Stal et al., 1985; Stal, 1995; Des Marais, 2003; Frank and Stolz, 2009). However, cyanotoxins produced by some cyanobacteria (e.g., *Microcystis aeruginosa*) are thought to limit the number of animals feeding on them, including insects and flamingos (Kreinitz et al., 2003; Ndetei and Muhundiki, 2005; Krivosheina, 2008).

At Lake Bogoria, cyanobacterial mats and filaments of *Phormidium terebriformis* are characteristically green-brown; *Calothrix* sp. mats are brown or brownish green; *Spirulina subsalsa* filaments are a bright blue-green; *Synechococcus* spp. are a pale to deep blue-green; and *Oscillatoria willei* filaments are grey-green (Fig. *3.3.*1A–H; Renaut et al., 1998; Krienitz et al., 2003; Appendix B). Mats at the Loburu hot springs (Fig. *3.3.*1A–E, 1H) composed of all of these cyanobacterial species were brownish green, whereas the bright blue-green mats were dominated by *S. subsalsa* and *S. bigranulatus*, and brown mats were dominated by *P. terebriformis* and *O. willei* (Krienitz et al., 2003). The green *Synechococcus* mats are found in very hot waters (> 60° C) (Renaut et al., 1998). Green and orange-coloured mats contain *Oscillatoria*, *Phormidium*, *Pseudanabaena*, and possibly *Chloroflexus*, and are found in moderate temperature waters (40–60° C) (Renaut et al., 1998). *Calothrix* mats are common in waters less than ~40° C (Renaut et al., 1998). This community belongs to the most common cyanobacteria in thermal habitats (e.g., Ward et al., 1998). Other colours observed in the mats at Loburu and Chemurkeu (Figs. *3.1.*16D–F, *3.3.*1F–G) include bright orange, purple, and black, which are likely attributable to anaerobic bacteria and archaea, and the production of sulfides (e.g., FeS) by sulfate-reducing types.

When wet, most mats contained gas escape bubbles (~3–20 mm wide; up to ~1 cm high: Fig. *3.3.*1C, 1E). Upon drying, most thick mats developed wrinkle-like structures (Figs. *3.2.*2G–H, *3.3.*2B–C; cf. Hagadorn and Bottjer, 1997, 1999; Porada and Bouougri, 2007) that appear to have formed by surface expansion due to gas pressure and/or by salt crystal growth (cf. Gerdes et al., 1993). Mat desiccation usually leads to fragmentation into chips (cf. Pflüger and Gresse, 1996) or destruction by efflorescent salts (Figs. *3.2.*2H, *3.3.*2D). Other "microbial induced sedimentary structures" (Noffke et al., 2001), including continuous, long, linear, and extremely low-amplitude ripples, were found on the Loburu mudflats where shallow pools that flooded the silty mudflat had recently desiccated.

*3.3.2. Lake Magadi*

Modern Lake Magadi is fed by more than 200 cool, warm, and hot springs that issue from the toes of small colluvial and/or alluvial fans (cool springs) or along faults (warm and hot springs) (e.g., B.F. Jones et al., 1977). Boiling springs like those at Lake Bogoria are not present at Lake Magadi, the hottest group of springs at the northwest margin of Nasikie Engida having temperatures of up to ~86° C (B.F. Jones et al., 1977; Allen et al., 1989). Travertine and tufa are also lacking, except for a large tufa tower (~10 m high) that may have formed subaqueously beneath the Pleistocene Lake Oloronga ~ 15 km northwest of Lake Magadi (Faure et al., 2002; B. Jones and Renaut, 2010). However, Pleistocene cherts (discussed below) preserve evidence of well-developed microbial mats that were likely associated with hot spring fluids. Thick microbial mats like those at the Loburu Delta were not commonly observed in the lagoons during this study. Spring-fed mudflats like those of the southern Loburu lower delta-plain were also not observed. Instead, thin bacterial and cyanobacterial mats (~0.5–1 cm thick) in shallow water (water depth < ~5 cm) were present on the sandy sediments adjacent to warm (~37–42°C) to hot (~66°C) springs issuing from faults in bedrock (Figs. *3.1.*12, *3.3.*3A–G; e.g., NW lagoon, NE lagoon, SW lagoon; B.F. Jones et al., 1977).

The Pleistocene Green Beds comprise a series of cherts deposited in the Lake Magadi Basin at approximately 98–40 Ka (Goetz and Hillaire-Marcel, 1992; Behr, 2002). Several features of the Green Beds suggest that the some of the cherts may be associated with microbial mats and hot spring pools, as well as subaerial exposure (Figs. *3.3.*4, *3.3.*5; Table 3.1). Behr and Röhricht (2000) and Behr (2002) recognized the association between microbes and the chert, and attributed some of the smaller-scale structures to the deformation of microbial mats and siliceous gels (e.g., 'peetees', wind- or desiccation-induced folding; Fig. *3.3.*4C–F). Some of these structures are comparable to the laterally extensive bedded “stromatolites” found in the Green River Formation of Wyoming, which are dominantly composed of carbonates but may also be found in black cherts, and may or may not be associated with spring mounds there (e.g., LaClede Bed, Laney Member, Sand Butte, Wyoming). Other, larger-scale structures at Lake Magadi, such as the “chert dykes” and “pillow cherts” have been attributed to the brecciation, extrusion, and fusion of malleable siliceous gels along contemporaneously active grid-faults (Figs. *3.3.*4A–B, 5A–H; Behr and Röhricht, 2000; Behr, 2002). The “pillow cherts” resemble spring mounds aligned along fissures, and may be comparable to the fissure-ridge travertines from the Lake Turkana region (Renaut et al., 2002a). In the E Lagoon of Lake Magadi alongside the Magadi townsite horst, mounds of chert ~1–2.5 m high and ~1–5 m wide are made up of smaller mounds draped with vertically and/or horizontally banded or bedded chert, fused to form the mounds (Fig. *3.3.*5B–H; cf. Behr and Röhricht, 2000; Behr, 2002). Alternatively, the banding is a result of cementation between fissures and/or fractures in the mounds, which are comparable with the 'fissure-ridge travertine' near Lake Turkana (Renaut et al., 2002a).

Behr and Röhricht (2000) also recognized stromatolitic bioherms < 25 cm in diameter, and preserved by carbonate which was replaced by silica, in the lower, massive cherts of the

**Fig. 3.3.3.** (Next page) Warm-spring environments, microbial mats, and flooded lagoons at Lake Magadi. Photographs shown in (A–B) and (F–H) are courtesy of R.Renaut. **(A)** Warm springs of the NW Lagoon with green mat in shallow outflow stream. **(B)** Red-, orange- and black-coloured mats present where warm springs issue from base of fault scarp at the NW Lagoon. **(C)** Brown-coloured mat in shallow lagoon waters (~3 cm depth) at the NW Lagoon. Note bird footprints (arrow). **(D)** Brownish green-coloured mat with bubble-like texture in very shallow water (~1 cm depth) at the NW Lagoon. **(E)** Bright green mat growing in spring channel at the SW Lagoon. **(F)** Green mat growing around warm spring vent into shallow water (~10 cm depth) at the SW Lagoon. **(G)** Close up of fragmented green-coloured mat adjacent to spring vent in (F). **(H)** The eastern NW Lagoon during the rainy season (2006) showing green cyanobacterial bloom in shallow water (~15–20 cm depth) and several species of wading birds.

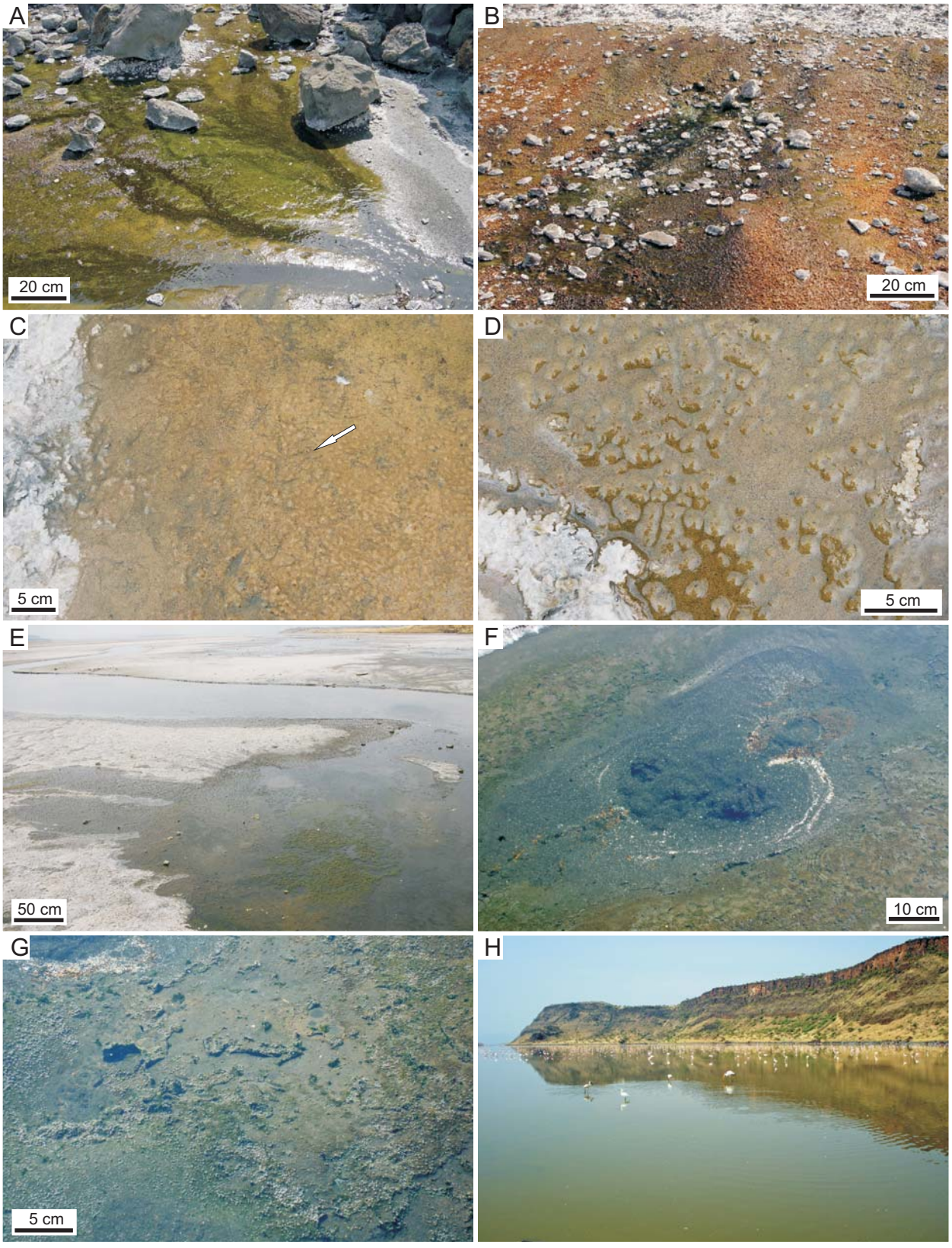
A
20 cm
B
20 cm
C
5 cm
D
5 cm
E
50 cm
F
10 cm
G
5 cm
H

Green Beds (cf. nodular chert; Fig. *3.4*.4H). Other potential spring-related deposits included the "slumped chert", which contains brecciated calcified bacterial stromatolitic bioherms and a later cement with flow structures (Behr, 2002), and may represent part of the downslope 'apron' of a hillside spring vent. Although Behr and Röhricht (2000) recognized the impact of contemporaneous seismotectonic activity on some of the cherts in the Green Beds (e.g., chert dykes; Fig. *3.3*.4A, 4B), they did not find evidence for increased hot-spring activity at that time. Behr (2002), however, attributed the cherts to the formation of colloidal silica gels in spring waters derived from pyroclastic deposits and alkaline groundwater that discharged along faults, in which microbial metabolism might have played an important role in affecting pH and the precipitation of chert. These suggestions for the reinterpretation of some of the features described by Behr and Röhricht (2000) and (Behr, 2002) must be substantiated with more data and the careful study of the internal fabrics, as well as an assessment of the distribution of fabrics and sub-facies within each of the larger mound-like structures.

Behr and Röhricht (2000) and (Behr, 2002) recognized several features that suggest the subaerial exposure of the "bedded cherts" in which the trace fossils they reported (i.e. *Skolithos*) were found. The trace fossils found in the Green Beds during this study were most abundant in this facies (see Sect. 4.2.1). The bedded cherts at the southern margin of modern Lake Magadi preserve deformed beds of microbial and carbonate laminae (Fig. *3.3*.4C–D), gas domes, and calcareous mud drapes, as well as desiccation cracks (Fig. *3.3*.4F) and trona and/or gaylussite pseudomorphs (Fig. *3.3*.4G; Behr and Röhricht, 2000). They are associated with peetee structures in the laminated, siliceous beds that preserve 'pock-mark' traces, probably produced by ephydrid flies feeding on microbial mats (Fig. *3.3*.4E). Behr and Röhricht (2000, p. 273) suggested that the depositional environment for this type of chert might have been "…a broad mudflat with ephemeral channels and solar ponds that were periodically flooded by shallow water comparable to the modern hot-spring mudflats north of [Nasikie Engida] and south of Lake Magadi". Comparisons between the trace fossils in the Green Beds and the area of modern hot-spring outflow at Nasikie Engida supports this interpretation.

Based partly on the presence of microbial mat-forming cyanobacteria (Appendix B) and "abundant ichnofossils", Behr and Röhricht (2000) also interpreted the magadiite cherts of the High Magadi Beds as being precipitated in "solar-like ponds" or shallow lagoons. They emphasize the close resemblance between magadiite lepispheres (bladed crystal spheres) and coated or silicified microbial spheres, possibly of *Gloecapsa*, *Pleurocapsa*, and/or *Entophysalis* (Behr and Röhricht, 2000). Behr (2002) also reported the possible presence of *Chloroflexus* sp., which is present at the hot springs of Lake Bogoria (Hindák, 2001) and is common at other hot spring sites, such as Yellowstone National Park (e.g., Doemel and Brock, 1974; Boomer et al., 2009).

*3.3.2.1.* *Microbial Mats*— Benthic microbial mats at modern Lake Magadi were observed in the outflow channels of warm springs (~37–42°C) that discharge onto the lake margins along horsts, and where the fluids may or may not mix with cooler spring-waters (~30°C) or cool

**Fig. 3.3.4.** (Next page) The bedded chert and nodular chert facies of the Pleistocene Green Beds, southern Lake Magadi. **(A)** The bedded cherts in foreground with chert dykes (see text) in background. Hammer for scale. **(B)** Bedding plane surface of the bedded cherts with large-scale dome structure to right of hammer, possibly due to syn- to post-depositional tectonic activity. **(C–D)** Folded mat surface texture of the bedded cherts. **(E)** Peetee or push-up ridge in the bedded cherts preserving green and orange colour in bioturbated ('pock-marked') carbonates at top surface. **(F)** Desiccation cracks in the bedded cherts. Block at left showing atypical circular polygons, possibly showing shrinkage (arrow). **(G)** Trona or gaylussite? pseudomorphs in bedded chert facies. Lens cap for scale ~5 cm. **(H)** Nodular, massive chert and carbonate. Hammer for scale.

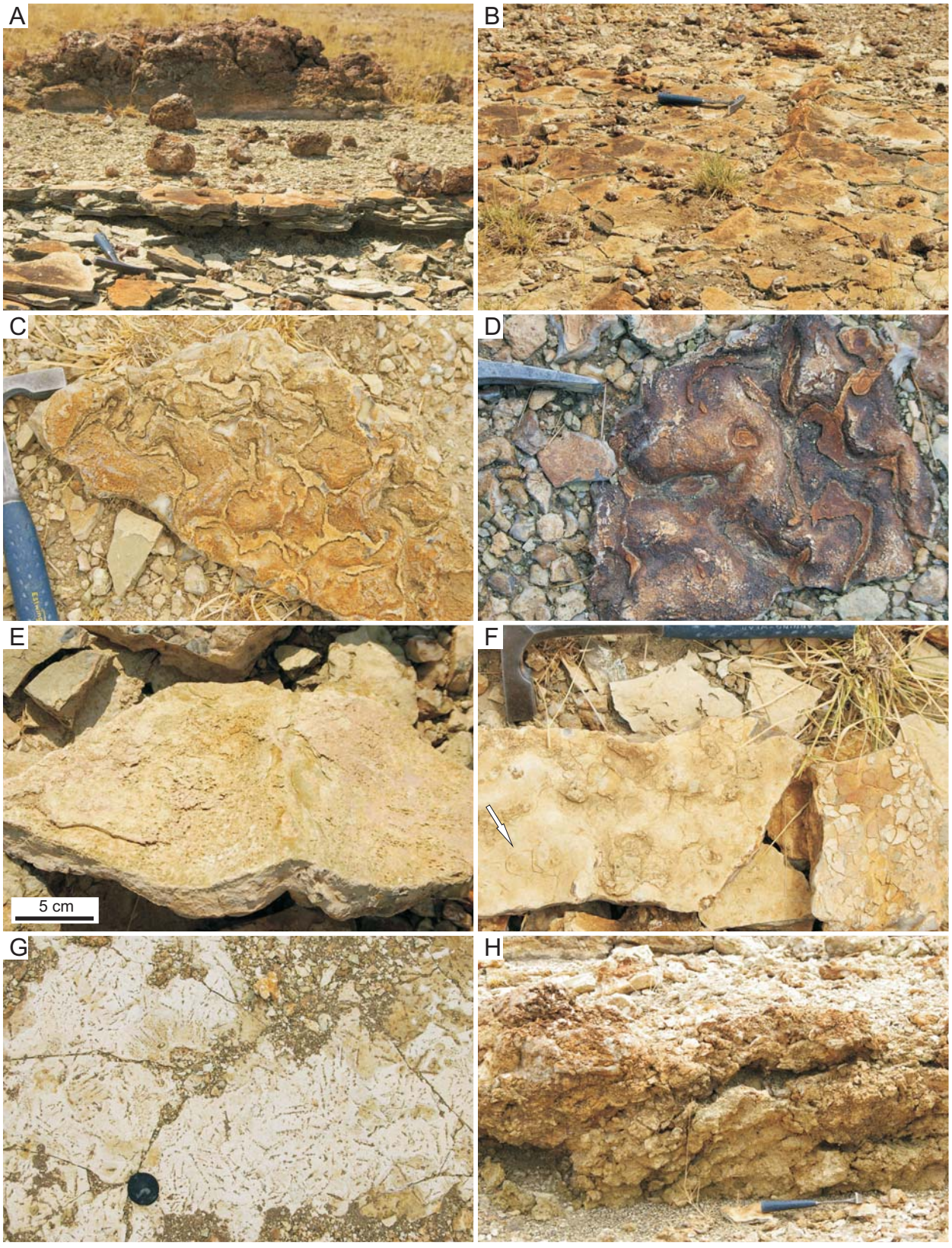
A
B
C
D
E
5 cm
F
G
H

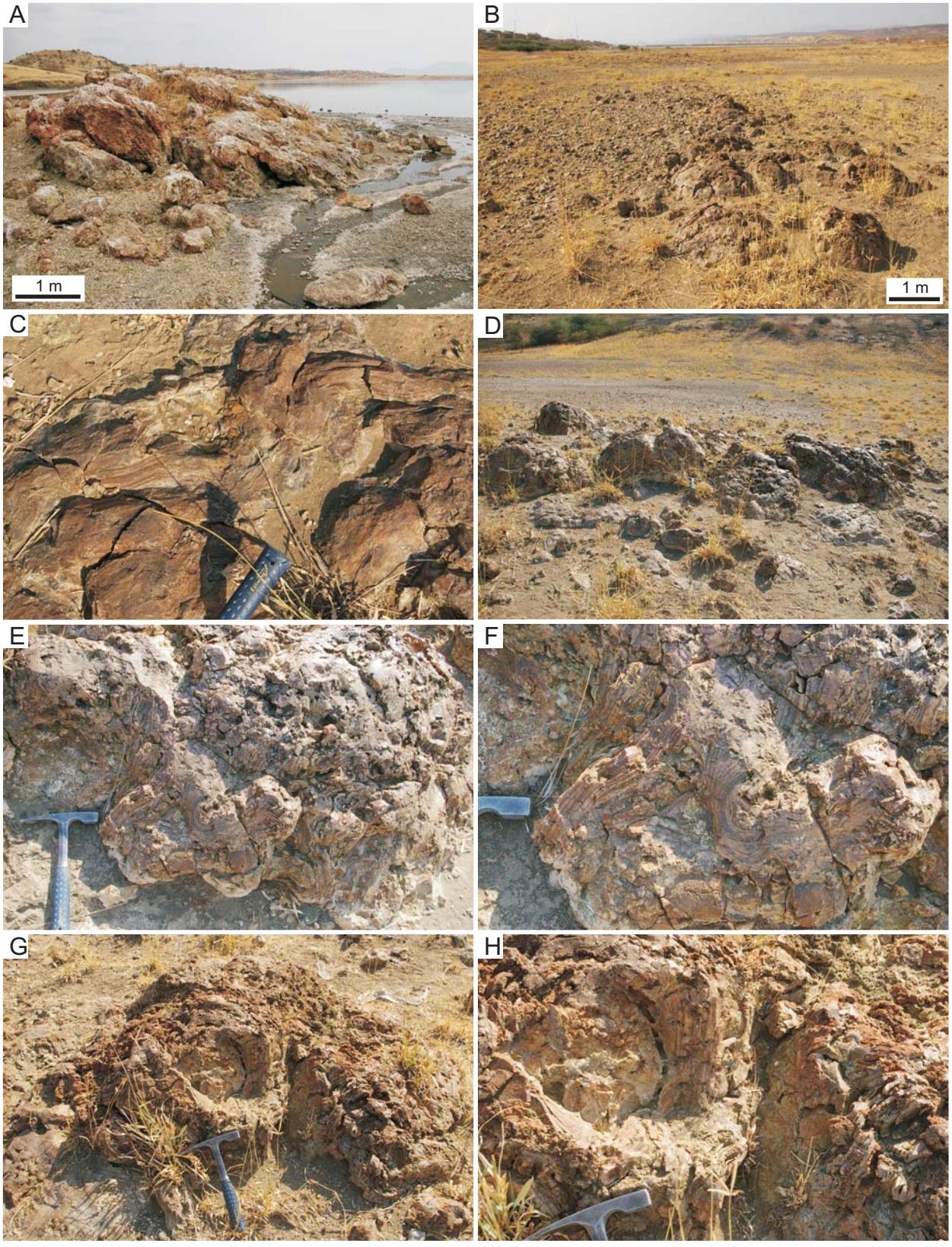
A
1 m
B
1 m
C
D
E
F
G
H

(~25°C), saline surface brines (Figs. *3.2.*3C–D, *3.3.*3A–G; e.g., NW Lagoon, SW Lagoon; cf. B.F. Jones et al., 1977). Colours ranged from dull greenish orange, to dark green, to bright orange and red, to black, and were zoned by species composition, probably according to temperature and salinity (Fig. *3.3.*3A–G; cf. Appendix B). Thin, light green and yellowish white films were observed in the more open, shallow waters of lagoons (e.g., NW lagoon; Fig. *3.1.*8E). Insect traces and bird footprints were observed in association with the benthic mats and films (Fig. *3.3.*3C; see Sect. 4.2.4). In general, planktonic cyanobacteria are common only as blooms during rainy seasons (Fig. *3.3.*4H) and in the cyanobacterial mats developed in warm and/or hot springs at Lake Magadi (B.E. Jones et al., 1998). Together with some bacteria, haloalkaliphilic cyanobacteria may form green and/or orange mats that persist below the trona crusts (e.g., Zhilina et al., 1996).

As described in Section 3.2.5, Lake Magadi hosts a diverse microbial community of halophilic and alkaliphilic cyanobacteria, bacteria, and archaea, with some thermophilic types (e.g., B.E. Jones et al., 1998; Appendix B). Many of these types are common in other extreme environments, including red archaea and orange bacteria such as *Spirochaeta* sp., which has been reported from both marine and continental settings, including cyanobacterial mats in freshwater hot springs, Utah (Zhilina et al., 1996). In general, most of the forms identified at Lake Magadi survive within the trona crusts themselves and partly make up the black organic ooze present within the lake brine (Fig. *3.2.*7). The focus of research to date has been to identify extremophiles for understanding these types of ecosystems and their role in the evolution of life, but not specifically on the biochemistry of a discrete community within one place at one time (e.g., B.E. Jones et al., 1998).

Behr and Röhricht (2000) and (Behr, 2002) investigated the microbial community preserved in the cherts of the Pleistocene Green Beds (Appendix B). Identifications are based on microbe morphology, which is not always a reliable indicator after silicification has occurred (B. Jones et al., 2005). The microbes are dominated by unicellular coccoid cyanobacteria (*Pleurocapsa* sp.) that are preserved as silicified cells with thick calcified mucilaginous capsules, usually found in clusters (Behr, 2002). Other unicellular coccoid cyanobacteria preserved by calcium carbonate and provisionally identified in the Green Beds include *Gloecocapsa polydermatica*, *Entophysalis granulose*, *Chroococcus minor*, and *Synechococcus* sp. (Behr and Röhricht, 2000; Appendix B). The green non-sulfuric bacteria (*Chloroflexus*), which are orange, filamentous, and thermophilic are common in modern neutral to alkaline hot springs, and were found in the "slumped chert" along the Magadi townsite horst in the East Lagoon (Behr, 2002). Similar bacterial communities are present in the hot springs at Yellowstone (Doemel and Brock, 1974). The Yellowstone *Chloroflexus* mats are orange-pink and green (due to *Synechococcus*) when alive, and form "bacterial stromatolites" composed of inter-laminated detrital siliceous sinter with mat laminae and lenses in areas with shallow, gently flowing hot spring effluent (Doemel and Brock, 1974). These motile, photosynthetic autotrophic and sulfide-oxidizing heterotrophic bacteria also move upwards through the layer of overlying cyanobacteria at night, which may contribute to the lamination of the mats (Doemel and Brock, 1974).

Also provisionally identified in the Green Bed cherts are the mat-stabilizing filamentous cyanobacterium *Microcoleus* and the free-floating coccoid cyanobacterium *Microcystis* (Behr,

**Fig. 3.3.5.** (Previous page) Chert mounds ("pillow cherts") at Lake Magadi. **(A)** "Bird Rock" at the S Lagoon. **(B)** Several small mounds of banded cherts with a linear distribution along the Magadi townsite horst. **(C)** Banded layers of the chert mounds. Hammer for scale. **(D)** A group of small chert mounds adjacent to the Magadi townsite horst. **(E)** Close up of one of the mounds shown in (D). Note both banded chert layers and massive chert. Hammer for scale. **(F)** Close up of mound shown in (E). Hammer for scale. **(G)** Chert mound with banding around a circular 'core'. Hammer for scale. **(H)** Close up of circular banding in mound shown in (G). Hammer for scale.

2002). Filamentous cyanobacteria are most numerous in the trace fossil-preserving bedded chert facies and include forms assigned to *Microcoleus*, *Schizothrix* and *Phormidium* (Behr, 2002). Other microbes preserved in the cherts include green algae with reproductive cysts, actinomycete bacteria, and upright, calcareous green algae of Dascladiacea preserved in life position (Behr, 2002).

### *3.3.3. Nasikie Engida*

Hot springs feed Nasikie Engida from the north along the basin bounding fault on the west, and also from along the small horst that separates Nasikie Engida from the alluvial plain the NE lagoon of Lake Magadi. The springs flow from vents north of the lake, and their combined waters discharge into the lake via braided channels that feed sandy flats (Fig. *3.1.*9A–F; *3.3.*6A–G). The springs along the northwest fault are the hottest in the Magadi basin at 86°C (Fig. *3.1.*9B–D; B.F. Jones et al., 1977). Travertine and tufa deposits are not present, but siliceous gels are actively forming from the evaporating hydrothermal fluids in muddy organic oozes along the shorelines (Fig. *3.2.*3E–H). A hypersaline mudflat that is frequently flooded and desiccated lies the south end of the lake is (Fig. *3.3.*6H).

*3.4.3.1. Microbial Mats*— The microbial community at Nasikie Engida is also apparently quite diverse, but no reports specifically on the microorganisms at Nasikie are known. In general, cyanobacterial and bacterial mats were observed in association with the hot springs at the north end of the lake (Fig. *3.3.*6A–G), and bacteria and archaea mats in brine were observed in association with sodium carbonate evaporites at the north end of the lake and on the southern mudflats (Fig. *3.3.*6H). Behr (2002) reported that green algae are predominant in modern Nasikie Engida and in the springs of Lake Magadi. *Bacillus* sp. and two archaea species, *Natronococcus* sp. and *Natrialba magadii* were reported from brine muds and salt crusts at Nasikie Engida (e.g., Duckworth et al., 1996; Grant et al., 1999; Appendix B).

Microbial mats that are associated with hot spring outflow at the north end of the lake cover the subaerially exposed black, organic rich muds and sands within the spring water outflow channels at the air-sediment-water interface and in shallow waters (Figs. *3.1.*9B–D, 3.3.6A–G). The mats range from thin films (< 0.5 cm thick) to thicker mats (< ~1 cm thick), which have large gas escape bubbles (< 3 cm diameter) and/or an irregular, pustular surface texture (Fig. *3.3.*6C–D). They range in colour from green, bright yellow-green, greenish brown, brown, yellowish orange-brown, orange, and black, although colours may change in some types in response to changing levels of UV light (Fig. *3.3.*6A–G; e.g., Franks and Stolz, 2009). The assemblage is probably similar to microbial community associated with hot springs at Lake Bogoria (Appendix B; Fig. *3.3.*6G). The orange, orange-red, pink, dark red, and yellow-brown colours observed from the mudflats at the south end of Nasikie Engida are likely due to the presence of similar types as in the Magadi brines (Appendix B; Fig. *3.3.*6H).

**Fig. 3.3.6.** (Next page) Hot spring environments, microbial mats, and hypersaline mudflat at Nasikie Engida. Photographs shown in (E–H) courtesy of R.Renaut. **(A)** Black, brown, and green mats in outflow channel of hot springs at NW spring site. **(B)** Close up of black mat in shallow hot spring waters. **(C)** Bright green and orange mat along margin of outflow channel with bubble-like texture. Lens cap for scale ~5 cm. **(D)** Orange mat in shallow outflow channel with bubble-like texture. Lens cap for scale ~5 cm. **(E)** Bright light green mat in hot spring outflow channel. **(F)** Green and brown fragmented, leathery mat in outflow channel at NW spring site. **(G)** Creamy yellowish white and red bacteria in hot spring outflow channel. **(H)** Dark red bacteria (probably halophilic Archaea) in shallow lake waters at south end of Nasikie Engida. Note surface nucleation of white sodium carbonate evaporites on lake

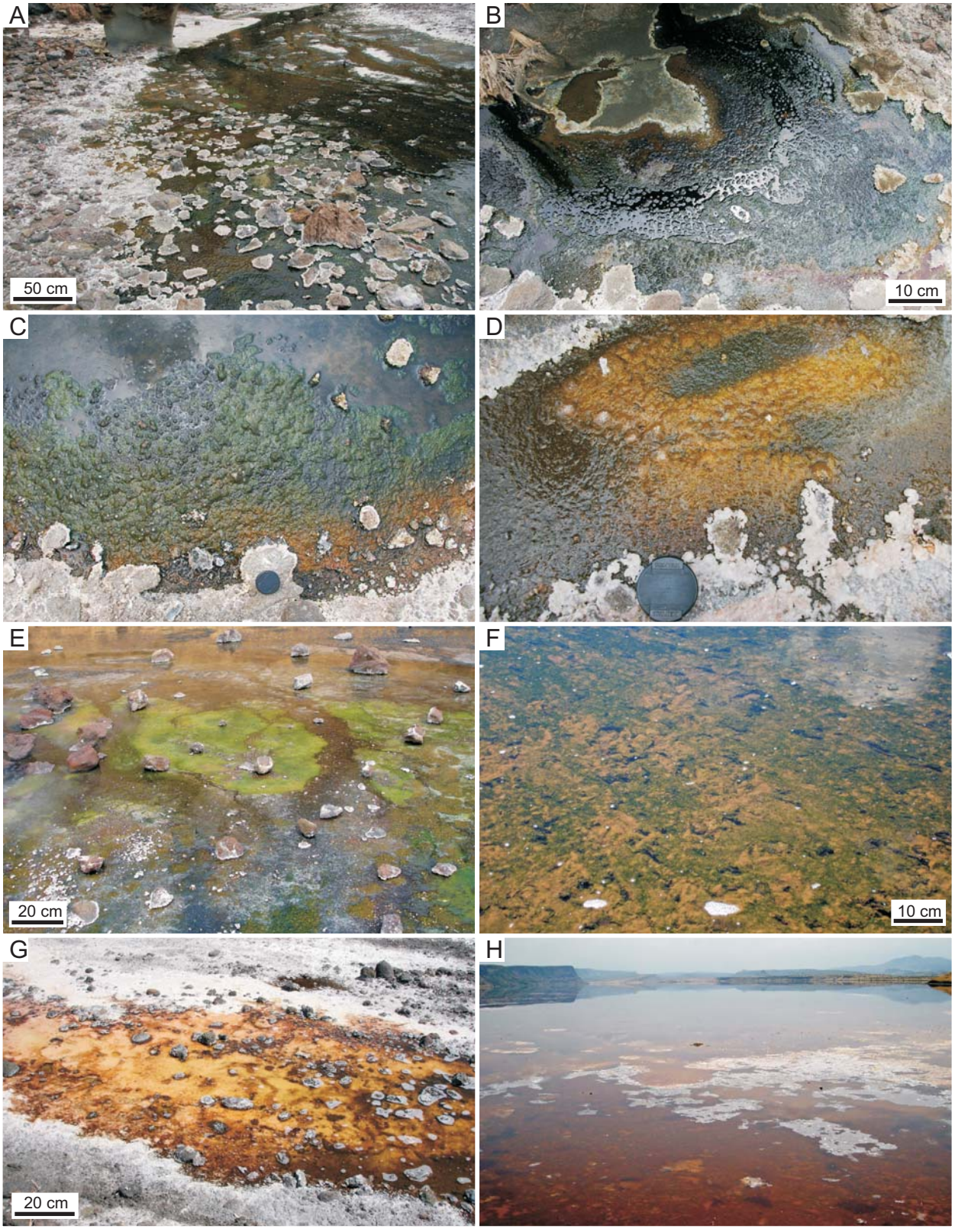
A
50 cm
B
10 cm
C
D
E
20 cm
F
10 cm
G
20 cm
H

# CHAPTER 4

## 4. MODERN TRACES AND TRACE FOSSILS OF THE KENYA RIFT LAKES

Several low to high diversity assemblages of trace fossils and modern plant and animal traces were studied at several localities in the Baringo–Bogoria basin, representing a variety of depositional environments from the "basin margin" to the "basin centre". Insect, mammal, bird, and wetland plant traces in Pleistocene to Recent sediments surrounding Lake Bogoria were studied in greater detail than the localities at Lake Magadi and Nasikie Engida. The evolution of the Lake Bogoria basin and the changing setting of the lake since the Late Pleistocene are relatively well understood, although the chronology is poor. It was possible to place the collection of trace fossils there within a series of short-term stratigraphic contexts. The findings in the Lake Bogoria area provided a framework from which to explore Lakes Magadi and Nasikie Engida, as well as the Eocene Green River and Wasatch Formations of Wyoming.

Four main hypotheses were developed and tested:

1) in saline lake basins, animal and plant traces show greater diversity, greater overall abundance, and have greater preservation potential at sites near fresh water, particularly if they are constant, reliable, and "point-sourced" such as springs;

2) the composition and diversity of the trace assemblages reflect the substrate conditions (i.e. saturation, stability), salinity conditions, proximity to the shoreline, and/or depth of the water table, and may be closely linked to the lithofacies represented from particular depositional environments;

3) trace fossil assemblages in saline lake basins roughly conform to the presently accepted ichnofacies and can be correlated with the position in the basin (i.e. basin margin vs. basin centre), as well as the proximity to the shoreline; and

4) fluctuating shorelines and frequently changing conditions lead to the superposition of different trace fossil suites that reflect these different conditions, particularly on palimpsest substrates that are partly consolidated/indurated and are frequently buried and exhumed where overall sediment aggradation is relatively low.

In general, the dominant trace makers are consistent between the different time periods and localities investigated in the Kenya Rift. Beetles, hymenopterans (i.e. bees, wasps, and ants), earwigs, and termites are the common insect trace makers in modern settings. Burrowing spiders (e.g., wolf spiders/funnel spiders) are also common. Tunnel-producing crickets are present at Lake Bogoria. Shorebirds (e.g., plovers), storks, flamingos, and ostriches are the most common trace-producing birds in modern settings, and common mammals that produce traces include hyaenas, zebras, warthogs, gazelles, wildebeests, and buffaloes. The mammal trace makers differ substantially between the well treed Bogoria basin and the drier savanna of the Magadi–Nasikie Engida basin. The trace fossils and body fossils of hippopotamuses, elephants, and/or giraffes are preserved in some localities (e.g., Loboi Silts, Bogoria basin) and are associated with freshwater wetlands (e.g., Ilosuani Formation, Baringo basin; Scott, 2003). All of these trace makers produce a variety of trace types including 1) vertical, oblique, and horizontal open burrows; 2) vertical, oblique, and horizontal backfilled burrows; 3) nests and cells; and, 4) footprints or "trampled-ground".

The assemblages represent the Mermia, Scoyenia, and Coprinisphaera ichnofacies, as well as the "Termitichnus" sub-ichnofacies and "shorebird" sub-ichnofacies (e.g., Lockley et al., 1994; Buatois and Mángano, 1995; Genise et al., 2000). The Skolithos ichnofacies may be represented by the vertical burrows of tiger beetles, although these traces are produced from subaerially exposed horizons in a range of lake-margin deposits, from low-energy mudflats to

higher-energy sandy shorelines. The informally defined, drier-ground "Celliforma ichnofacies" (Genise et al., 2010) is similar to the Coprinisphaera ichnofacies and may be aligned with the assemblage at Nyongonyek (discussed below), which preserves dominantly bee cells. However, termite nests and tunnels are also abundant there, in contrast to the ichnofacies designations by Genise et al. (2000, 2010) which state that termite traces represent humid, closed forests. The components of the trace assemblages are presented as suites within the more broad ichnofacies and reflect more precisely the interaction between certain trace makers and the environmental conditions to which they responded.

The term "suite" has been chosen to describe the groups of traces recognized because it can include more than one ichnocoenosis (the traces produced by a single "community" of organisms) (cf. McIlroy, 2008). For instance, the Scoyenia-like Suite at Lake Bogoria, described below, may include more than one community of organisms, each responding to a slightly different set of environmental controls. The different trace producers respond to both the lateral variability of conditions, as well as changing conditions through time. As noted by McIlroy (2008), areas with lower sedimentation rates tend to contain trace suites that cannot be divided further into ichnocoenoses because of the close association of traces responding to different conditions (e.g., substrate consistency). Additionally, laterally adjacent areas can vary in the complexity of the interactions between environmental parameters that control the trace assemblage (e.g., Loburu delta: saline mudflat plus hot spring pools vs. western shoreline: saline beach). The area with more than one dominant factor affecting the composition of tracemakers (e.g., fresh water plus saline water) will likely contain a higher diversity of traces, but which cannot be clearly divided into separate ichnocoenoses because the traces were produced in the same substrate at roughly the same time. Descriptions of the trace fossils from each of the localities investigated are presented in table format and are summarized, interpreted, and discussed briefly in the following sections of text.

### 4.1. Modern Traces and Trace Fossils in the Baringo–Bogoria Basin

The trace fossils and modern plant and animal traces in the Baringo–Bogoria basin demonstrate the differences between dominantly "basin margin" trace types, dominantly "lake margin" trace types, and dominantly "basin centre" trace types. Traces formed in wetlands or drying fluvial channels do not reflect these divisions as clearly and may include representative traces from all continental ichnofacies. In all cases, the associated sedimentary evidence was considered in detail and placed into the known basin history and within the context of the basin structure.

#### *4.1.1. Pleistocene Trace Fossils from the Loboi Silts at Nyongonyek, Baringo Basin*

The sedimentary environments and trace fossils preserved in the Loboi Silts at Nyongonyek represent a typical "basin margin" assemblage, which is dominantly composed of traces produced by terrestrial organisms, a lithofacies assemblage that consists of pedogenically altered fluvial and overbank deposits, and is interpreted to have been landward of the zone strongly influenced by lake-level rise-and-fall (Section 3.1.1). The locality itself is relatively near to the basin-bounding faults of the southwestern Baringo basin (Fig. 2.2). Fluvial sediments may contain large clasts (pebble- to cobble-sized) of trachyte, trachyphonolite, and/or basalt in the upper Loboi Silts and ?Holocene channel deposits and are generally poorly to moderately sorted, which coincides with the basin margin position and bedrock lithology in the source area for this locality. The lower, fine-grained Loboi Silts may reflect the reworking of the Kapthurin Formation or other sediments from a distant source prior to faulting of the present-day bounding fault at the southwest Baringo basin. The fine-grained sands are mainly composed of

**Table 4.1.** Trace fossils of the Pleistocene Loboi Silts at Nyongonyek, Baringo Basin.

| Fig. | Trace type | Ichnotaxonomy | Description | Comments | Possible trace maker | Environment |
|---|---|---|---|---|---|---|
| Fig. *4.1.1.* 1A–H | Termite nests | Termite nests A; cf. *Termitichnus* isp. | Roughly spherical to oval-shaped traces ranging in size from ~7 cm diameter up to ~25 cm in diameter; most examples preserved by calcite 'rind' around nest, with some also preserving internal horizontal plates and external, thin, plate-like divisions of the paraecie (external nest); internal morphology shows mensicate-like backfill of some areas; external morphology of some of the nests also includes protrusion-like burrow openings also cemented by calcite | Different sizes of nests may represent different degrees of development | Termites; family unknown; possible that some nests could also be attributed to bees | Paleosol (Pleistocene) |
| Fig. *4.1.1.* 2A–C | Termite nests | Termite nests B; cf. *Termitichnus* isp. | Bioturbated, aggregate-filled oval-shaped nests showing concentric backfill and rind-like packing of aggregates; internal and external structure of nests do not show plate-like divisions of paraecie; external nest may or may not be cemented by calcite; associated with calcite-cemented root moulds and casts; bioturbated areas tend to be reddish in colour and are likely iron-enriched relative to the surrounding sediment | Different in preservation style from Termite nests A & C | Termites; family unknown | Paleosol (Pleistocene) |
| Fig. *4.1.1.* 2E–F | Termite nests | Termite nests C; cf. *Termitichnus* isp. | Small, 'diffuse' nests and associated small burrows (2–4 mm diameter); external portion of nest and burrows preserved by calcite; chambers may be connected by larger tunnels (< ~4 cm diameter); calcite chambers may represent fungus gardens or they may be the paraecie of a nest; plate-like paraecie of Termite nest A not observed with these types; these types of nests tend to be associated with composite rhizolith/termite tunnel traces | These types of nests may represent a different termite taxon; chambers may represent fungus chambers and not the paraecie of the nest | Termites; family unknown | Paleosol (Pleistocene) |
| Fig. *4.1.1.* 1I | Ant nest chambers? | None available | One example of two oval-shaped chambers connected by a straight, circular shaft; all preserved by calcite; chambers < ~12 cm wide by ~8 cm high; shaft between chambers ~1.5 cm diameter and ~15 cm long; external morphology of chambers irregular and due to preservation of short segments of smaller branching burrows < 1 cm diameter near chamber | Compare with modern ant nests figured by Tschinkel, 2004, 2005 | Ants; possibly fungus chambers or small nests of termites | Paleosol (Pleistocene) |
| Fig. *4.1.1.* 3A–D | Ant or termite mounds | None available | Large (< 2 m diameter, ~1 m high), red-brown, indurated mounds of bioturbated silt with branching, open, smooth-walled internal burrows ranging from ~0.5 to 1.5 cm in width; also contains small, straight ?root traces (~2 mm diameter); overall, mound is bioturbated and weathering into irregular pieces; no carbonate cementation | Not preserved by calcite – open burrows remain open; mound red and cemented by iron minerals; mounds are likely Holocene | Ants, possibly termites | Paleosol (?Holocene) |

| | | | | | | |
|---|---|---|---|---|---|---|
| Figs. *4.1.1.* 2D | Termite tunnels | None available; cf. *Palaeophycus*? | Tunnel (~1.2 cm diameter) with external wall of reddish silt and internal fill of calcite cement; internal cemented area roughly circular, porous, and mesh-like; tunnel branches with branches approximately same diameter as main tunnel | Possibly a termite foraging tunnel, kept open and fortified by an external wall of fine-grained sediment | Termites; possibly composite trace with root cast | Paleosol (Pleistocene) |
| Fig. *4.1.1.* 10B | Concentrically backfilled burrows | None available | Dominantly horizontally oriented, pellet/aggregate backfilled burrows; fill is arranged into concentric layers; traces ~2–4 cm wide; usually oval- or circular-shaped in cross section; 'active' portion of burrow not central, but offset towards one wall | The offset, 'active' part of the burrow shows that the concentric fill is towards one side of the burrow, giving it an assymetrical appearance | Termites or ants | Paleosol (Modern) |
| Fig. *4.1.1.* 10A, C | Meniscate backfilled burrows? | cf. *Taenidium* isp. | One example of aggregate-filled burrow with vague meniscate backfill; unwalled; may grade into walled along length; diameter ~7 mm; horizontally oriented; burrow boundary not sharp | Example associated with horizontally oriented cell clusters below tuff bed | Termites, ants, or possibly beetles (dung beetles) | Paleosol (Pleistocene) |
| Fig. *4.1.1.* 10D, E | Pellet-filled burrows | cf. *Planolites* sp. | Vertically, obliquely, or horizontally oriented, pellet/aggregate-filled burrows without lining or constructed wall; burrow boundary is sharp; approximately 0.5–1 cm wide, length unknown; pellets are sediment aggregates 1–2 mm in diameter; may be circular or oval-shaped in cross-section | Unknown insect; possibly termite or ant based on burrow containing variety of sizes of aggregate fill | Termites or ants; may be plugged tunnels of termites used for foraging above ground | Paleosol (Modern) |
| Figs. *4.1.1.* 6F, 8I | Branching burrows | cf. ?*Planolites* isp. | Simple, roughly circular, branched burrows of various diameters, from tiny (1 mm) to medium-sized (<5 mm); oriented in all directions; may be associated with nests or with rhizoliths; most are preserved as calcite casts, while others remain open | Most of the examples are associated with termite nests and/or calcite rhizoliths; open examples are also associated with spherical insect cells | Mainly termites; possibly other insects such as bees and beetles | Paleosol (Pleistocene) |
| Fig. *4.1.1.* 6D, I | Branching burrows | None available | Small to medium-sized (~0.3–1.2 cm diameter) branching burrows with numerous small, knob-like, roughly spherical protrusions along burrow lengths; burrows oriented mainly horizontally and vertically; one example shows upward branching, U-shaped portion of burrow branching with straight, oblique burrow; preserved by carbonate | Roughly spherical 'knobs' on burrows may be small cells of bees along burrow, or small storage pits of termites along foraging tunnels' may be more than one type | Probably bees and/or termites, possibly dung beetles | Palaeosol (Pleistocene) |
| Fig. *4.1.1.* 8B, E, F–I | Composite traces (rhizoliths and termite tunnels) | None available | Dominantly vertically oriented, branching, rhizoliths 'coated' by very small burrows and/or roots; preserved by calcite; most preserved as root moulds with internal root hole filled by silt; if preserved as casts, tend to have constructed wall of reddish silt; burrows oriented in all directions; roots may branch upwards | Most carbonate rhizoliths appear to be composite traces | Shrubs (*Acacia*?) and termites, possibly with other insects | Paleosol (Pleistocene, Modern) |

| | | | | | | |
|---|---|---|---|---|---|---|
| Fig. *4.1.1.* 4H–I | Cell clusters | Indeterminate A | Clusters of small, roughly spherical cells arranged with more cells towards base of cluster, giving “Hershey’s Kiss”-like external morphology; total number of cells variable, ranging from ~4 to ~12; clusters not clearly associated with burrow, but isolated clusters arranged vertically, with larger number of cells in lower cluster, and smallest number of cells in upper cluster; cells < 1 cm in diameter; cells closely placed within cluster; one example associated with carbonate-cemented small burrow (~5 mm diameter) above cluster | Number of cells in clusters difficult to ascertain from external morphology of cluster | Likely bees | Paleosol (Pleistocene) |
| Fig. *4.1.1.* 4A–G, 5A–D, 6A–C, 6E, F | Cell clusters | Indeterminate B | Clusters of small, roughly spherical cells (~0.5–1.5 cm diameter) arranged in various orientations; clusters may be aligned vertically, may show branching, or may be aligned horizontally, apparently along main burrow system of nest; may be associated with small burrows (~3 mm diameter); other clusters may show cells organized irregularly; total number of cells within clusters extremely variable, ranging from 2 to more than ~40; cell sizes also variable within clusters, but typically are ~0.8–1 cm in diameter | Number of cells in clusters may depend on age of nest and degree of sociality of bees, or on taxonomic differences; different sizes of cells within clusters possibly due to amounts of provisions | Likely bees | Paleosol (Pleistocene) |
| Fig. *4.1.1.* 4J | Cell cluster | Indeterminate C | Carbonate-cemented cell cluster within larger excavated area; preserved within tuff bed; excavated area and cluster oriented obliquely; shape and size of individual cells not discernable; associated with small burrows (~3 mm diameter) and possibly with narrow ‘bridges’ (~3 mm diameter) between cell cluster and external margin of excavated area | One example only | Bees or wasps | Paleosol (Pleistocene) |
| Fig. *4.1.1.* 5H | Cell “cap” | Indeterminate D | Convex, thick (~3–4 mm), carbonate-cemented cap; possibly upper wall of a large dung beetle cell?; total width ~3 cm; total height ~1.5 cm | One example only, superficially resembles cap of *Cubitermes* nests | Unknown insect? | Paleosol (Pleistocene) |
| Fig. *4.1.1.* 5D–F | Isolated cells with or without associated burrows | Indeterminate E | Isolated, roughly spherical, cells of various sizes, ranging from ~0.5–1.8 cm diameter; one example within tuff associated with small (4 mm diameter), straight, open burrow; one example with thin wall (~2.5 mm diameter) preserved as carbonate with silt-filled internal chamber; one example with 0.8–1 cm wide vertically oriented burrow or chamber below cell that widened downward | Different sizes may represent different trace makers | Bees or dung beetles | Paleosol (Pleistocene) |
| Fig. *4.1.1.* 6G–J | Cell clusters with burrow | Indeterminate F | Roughly spherical and irregular large cell or cell cluster; 1.5–2 cm diameter; associated with small, straight, short (2–3 cm length) burrows connecting cells; one to several large cells/cell clusters associated with burrow; all preserved by carbonate, suggesting burrow was not backfilled | Sections and petrography required for internal morphology; probably are cell clusters of hymenopterans | Likely bees, possibly wasps or dung beetles | Paleosol (Pleistocene) |

| | | | | | | |
|---|---|---|---|---|---|---|
| Fig. *4.1.1.* 6A–F | Cells with burrow | Indeterminate G | Larger (~1.5–2 cm diameter), roughly spherical cells aligned vertically; may be touching one another, or isolated and separated by short distance (< 4 cm); may be associated with vertical, backfilled burrow (~1.2 cm in diameter), slightly narrow than cells, and with fill different from host; (some associated burrows are obliquely oriented with upward oriented U-shaped branches) | Sections and petrography required for better characterization of internal structure | Dung beetles or bees | Paleosol (Pleistocene) |
| Fig. *4.1.1.* 7A–B | Mammal burrows | Mongoose burrows? | Large burrow or den with expanded chamber at (exposed) terminus; entrance burrow ~15 cm diameter and oval-shaped; entrance burrow oriented horizontally to slightly oblique; chamber oval-shaped and ~20 cm high and ~30 cm wide; length below tuff ~50 cm; unbranched; sharp burrow boundary | Preserved below tuff channel bed; one example only | Likely mammal, possibly mongoose | Paleosol (Pleistocene) |
| Fig. *4.1.1.* 7C | Mammal burrows | Aardvark burrows? | Very large tapered burrow or den; ~40 cm wide towards top (below tuff), tapering gently to ~20 cm wide; unbranched; very sharp burrow boundary; oriented obliquely; length ~ 2 m below tuff | Preserved by tuff below tuff channel; one example only | Likely mammal, possibly aardvark | Paleosol (Pleistocene) |
| Fig. *4.1.1.* 7D–G | Mammal burrows | Rodent or mongoose burrow system? | Medium-sized, dominantly horizontal burrows (~8 cm diameter) in branching burrow system; may branch abruptly from main burrow (8 cm diameter) into several smaller, straight, round-ended burrows (~2.5 cm diameter); one example unbranched and vertical | Preserved by tuff below tuff channel; several examples not examined in detail | Likely mammal, possibly ground squirrels or small mongoose | Paleosol (Pleistocene) |
| Fig. *4.1.1.* 8A–I, 9F | Carbonate rhizoliths | n/a | Branching, roughly circular carbonate root moulds and casts, approximately 6 mm to 2 cm in diameter; some examples show smooth external margins, others have external margins with a pellet-like appearance, particularly if associated with termite traces; some examples have an external network-like morphology, which may be due to root hairs and/or tiny termite burrows; one large example shows downward branching from main root (3 cm diameter); other examples show apparent upward branching; more recent root moulds tend to have smoother external margins | Many examples are composite traces in association with termite nests | Mainly shrubs | Paleosol (Pleistocene, Modern) |
| Fig. *4.1.1.* 10F–I | Mn-oxide lined root pores and root hairs | n/a | Open, vertical root pores with purplish black linings on root-pore wall; dominantly vertically oriented; branching to both roots of same size and to root hairs; abrupt change in diameter from main root to root hairs; root pores are ~3–4 mm wide; root hairs are < 1 mm wide; some examples slightly curved | Dominantly vertically oriented, with horizontal branches and root hairs | Unknown | Paleosol (Pleistocene, ?Holocene) |

volcaniclastic grains (Driese et al., 2002, unpublished).

The trace fossils preserved in the Loboi Silts at Nyongonyek are described in Table 4.1. Micro-scale features of the traces have not yet been examined, and petrography is needed to accurately distinguish between some of the carbonate rhizoliths and the carbonate-filled burrows, to characterize the internal macrostructure and microstructure of the insect cells, and to reconstruct the processes involved in preservation. The key features of this assemblage include: 1) termite and ant nests and tunnels (Figs. *4.1.1.*1–3); 2) the burrows and cells of bees and/or wasps, and possibly dung beetles (Figs. *4.1.1.*4–6); 3) mammal burrows (Fig. *4.1.1.*7); 4) carbonate rhizoliths and other carbonate cements (Figs. *4.1.1.*8, 9); and 5) other traces including backfilled burrows and Mn-oxihydroxide-stained root pores (Fig. *4.1.1.*10). Several criteria were used to preliminarily distinguish between the different types of traces including the orientation, shape, size, and associations between different types of structures (e.g., diffuse burrows + nest with horizontal plates = termites).

First, termite tunnels and nests were recognized if there were small (2–3 mm wide), branching, diffuse burrows in all orientations surrounding a nest (Fig. *4.1.1.*2E–F) or forming a small cluster of diffuse burrows. Many of these small burrows attributed to termites were closely associated with carbonate rhizoliths, and are considered "composite traces" (Fig. *4.1.1.*8F–I). Termite nests were also recognized if they contained smooth, flat horizontal plates within an oval-shaped nest (Fig. *4.1.1.*1E–H), as well as concentrically backfilled oval-shaped burrows/nests (Fig. *4.1.1.*2A–C, 10B). In several cases, only the outside margins of the nests were cemented by carbonate, which suggests that the carbonate formed later and filled open cavities (Fig. *4.1.1.*1A–D). Aggregate-backfilled burrows, including concentrically backfilled tunnels, may be attributable to either termites or ants (Fig. *4.1.1.*10B–E). Other possible ant traces include one example of vertically aligned nest chambers connected by a vertical burrow (Fig. *4.1.1.*1I) and ?Holocene examples of large (< ~2 m diameter), red, iron-enriched mounds with open burrows, not cemented by carbonate (Fig. *4.1.1.*3). Additionally, at least one possible example of a colonial nest of bees was preserved partly by carbonate in the Loboi Silts at Nyongonyek (Fig. *4.1.1.*1C–D). It may be difficult to distinguish between the traces of termite nests and colonial bee nests if the internal structure of the nest is not preserved. The subterranean nests of honey bees (Apidae: Apinae) and stingless bees (Apidae: Meliponinae) are larger nests with a surrounding "involucrum", internal brood combs, and external "storage pots" (see Michener, 1974). As in other bee families, the nests of the eusocial Apidae may be built within already existing structures, including the nests of termites (Michener, 1974).

The clear distinction between wasp and bee nests was not possible with the available data because both construct branching, oblique, vertical, and horizontal burrows with smaller branches that lead to spherical, sub-spherical, or elliptical cells. The cells in the Loboi Silts, however, appear to be mainly spherical to sub-spherical and may be best attributed to solitary or semi-social bee families such as Colletidae, Halictidae, Melittidae, Adrenidae, or Anthophoridae (cf. Michener, 1974). Many examples of oblique burrows with small sub-spherical cells along their lengths were preserved by carbonate, and many other examples consisted of cell clusters of 2–10 cells without an attached burrow (Fig. *4.1.1.*4–6). From the external morphology of the clusters they appear to be comparable to either clumps of cocoons and/or to cell clusters within

**Fig. 4.1.1.1.** (Next page) Insect nests from the Pleistocene Loboi Silts, Nyongonyek, Baringo basin. **(A–B)** Small, spherical termite nest with outer 'wall' preserved by carbonate. **(C–D)** Larger, termite or bee nest with external plates and possibly "food pots" (arrow in C, close-up in D). **(E–F)** Large termite nest with internal horizontal plates and horizontally oriented, meniscate backfilled 'shelves' (close-up in F). **(G–H)** Relatively large termite nest with external plates (arrow in G) preserved by carbonate. **(I)** Possible ant nest with oval-shaped chambers (arrows) connected by vertical burrow. Scales are in cm.

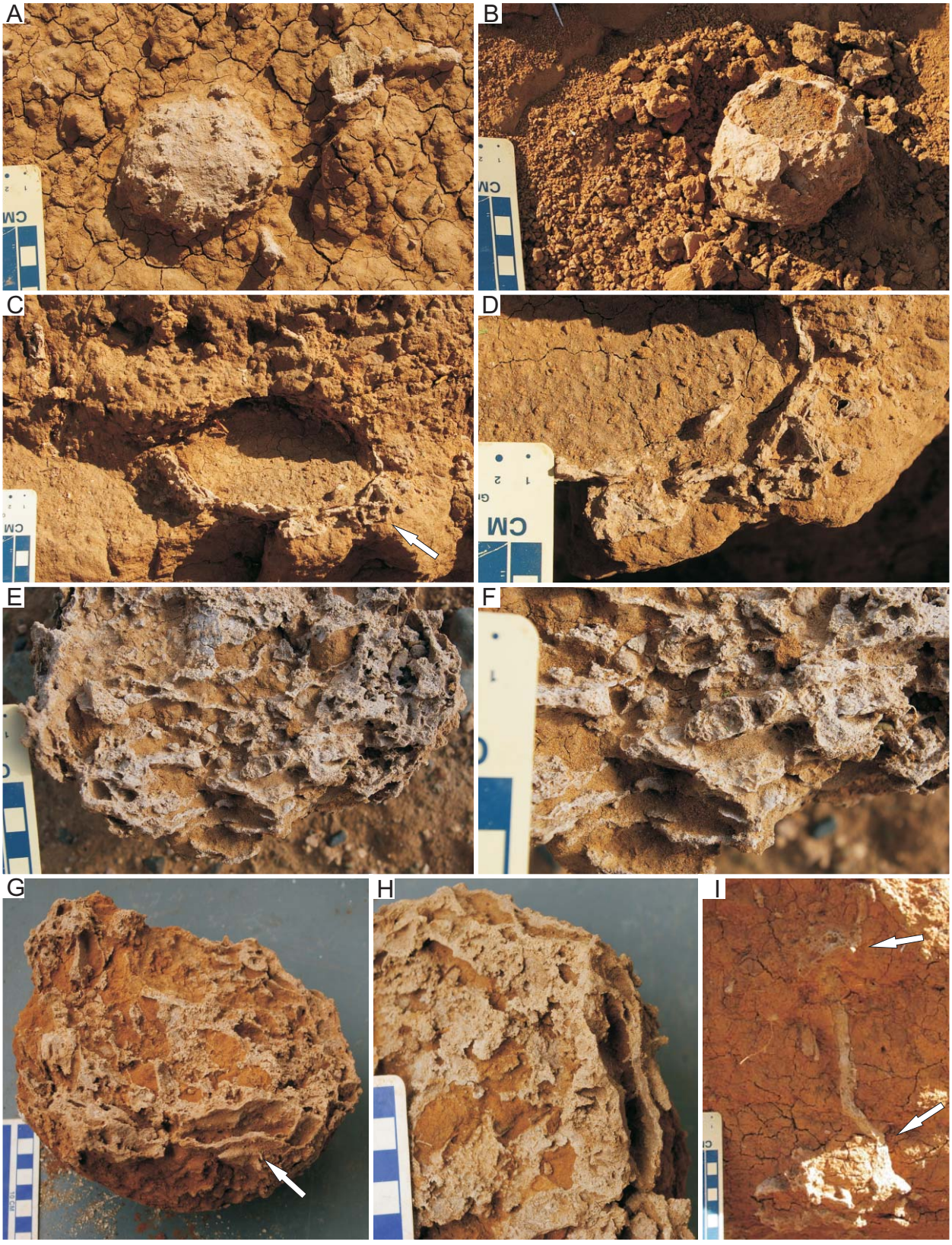
A
B
C
D
E
F
G
H
I

excavated cavities (e.g., in Halictidae) (cf. Michener, 1974). In *Colletes*, for example, cells excavated for either male or female larvae may be a different size, with cells for males being smaller (Alcock, 1999; Rooijakkers and Sommeijer, 2009). If the trace fossils at Nyongonyek consisted of small (0.5–1.5 cm diameter) cells either attached to burrows or clustered in cells they were attributed to bees and/or wasps. Other examples of larger (> 1.5 cm diameter), isolated, spherical to sub-spherical balls may have been produced by dung beetles (e.g., Scarabidae: Scarabaeinae or Geotrupidae; Fig. *4.1.1.*5B, 5D–H, 6G). However. several examples

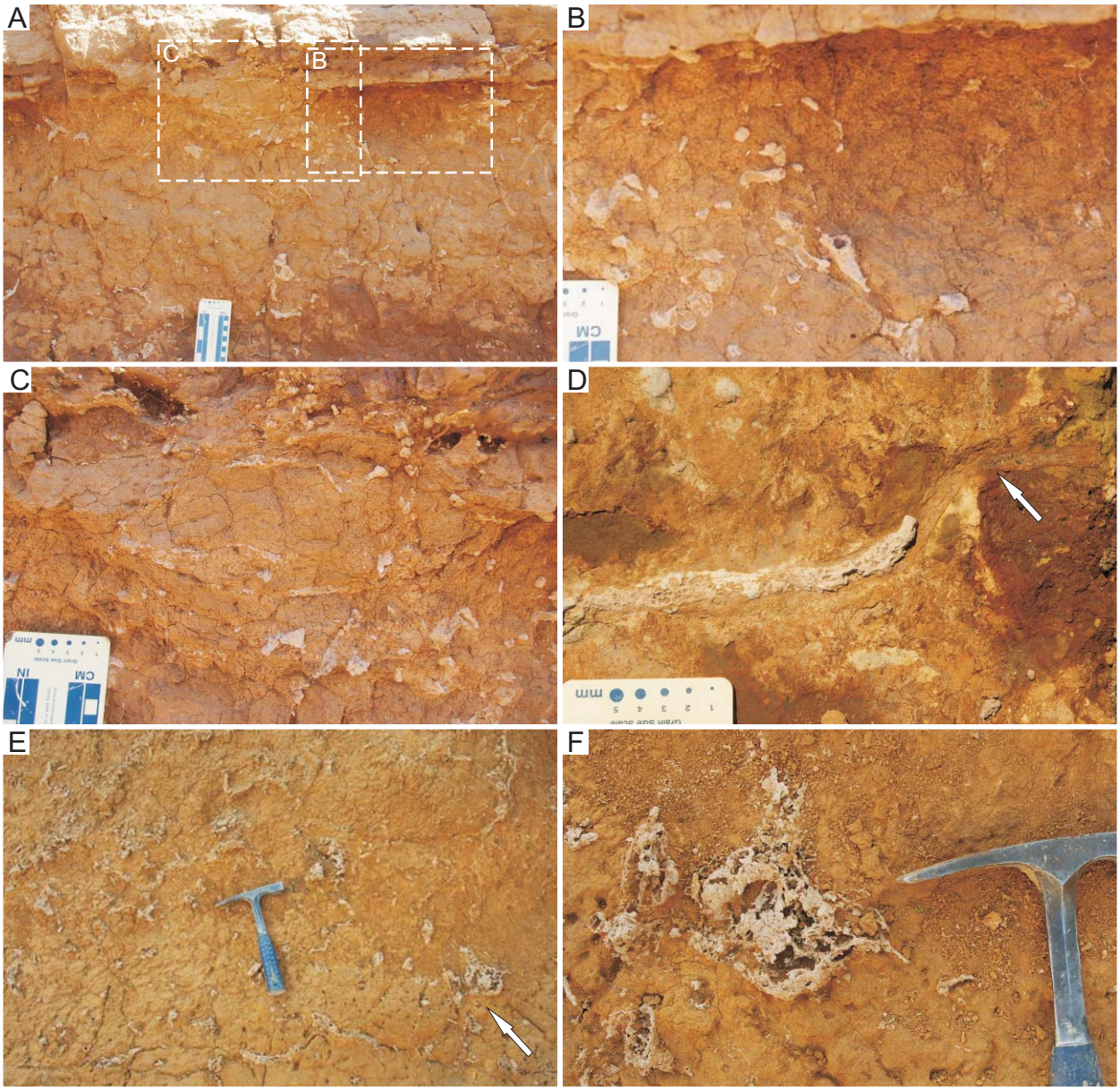


**Fig. 4.1.1.2.** Termite nests and burrows from the Pleistocene Loboi Silts, Nyongonyek, Baringo basin. **(A–C)** Bioturbated area with concentric backfill of pellet-like/sediment aggregate material. Nest is slightly more reddish than host material, with some tunnels and possible root casts preserved by carbonate. **(D)** Horizontally oriented tunnel with wall of host material (arrow) filled with carbonate cement (left). **(E)** The lower unit of the Loboi Silts showing 'network' of small diffuse burrows and small nests preserved by carbonate cements. **(F)** Close up of small nest with diffuse burrows shown by arrow in (E).

of larger spherical balls were attached to small burrows, which suggests that they are also the structures of bees (Fig. *4.1.1.*6H–J; cf. Michener, 1964).

Other trace fossils preserved by carbonate were attributed to roots if they comprised a central open hole and a thin (~1–3 mm thick) wall of carbonate or if they had smaller root hair structures branching from the main structure (Fig. *4.1.1.*8). Clear examples of branching downward root systems were rare (Fig. *4.1.1.*8A). Several examples consisted of carbonate-cemented tubes in various orientations with very small (< 0.5 cm) spherical to sub-spherical protrusions (Fig. *4.1.1.*6I). These structures may represent either rhizocretions along rhizoliths, storage pits along termite tunnels, bee cells in or adjacent to the main burrow, or another unknown structure. Several examples show a composite of several features, and may represent composite trace fossils (e.g., root plus termite tunnels) (Fig. *4.1.1.*8F, 8G, 8I). The carbonate cements also precipitated in other open spaces that were not produced by biogenic activity (e.g., micro-fractures; Fig. *4.1.1.*9). Isolated, small, sub-spherical carbonate structures may also be attributed to the growth of carbonate nodules, but petrography is necessary to confirm this and to better determine the criteria for identification. Most of the field evidence suggests that carbonate precipitated as a pore-filling cement either along fractures, biogenically excavated cavities, or along the outside margins of roots and root pores (Fig. *4.1.1.*9).

Several examples of probable vertebrate burrows were preserved below the reworked channel tuff-bed and are infilled by the tuffaceous sediment. Three main types are recognized here. Future work at Nyongonyek may lead to the recognition of more types and to their better characterization. First, one example of a large, slightly oblique, oval-shaped burrow (~15 cm diameter) opening into an egg-shaped enlarged chamber (~30 cm diameter) was preserved just below the reworked-tuff channel (Fig. *4.1.1.*7A, 7B). Second, one example of a very large,

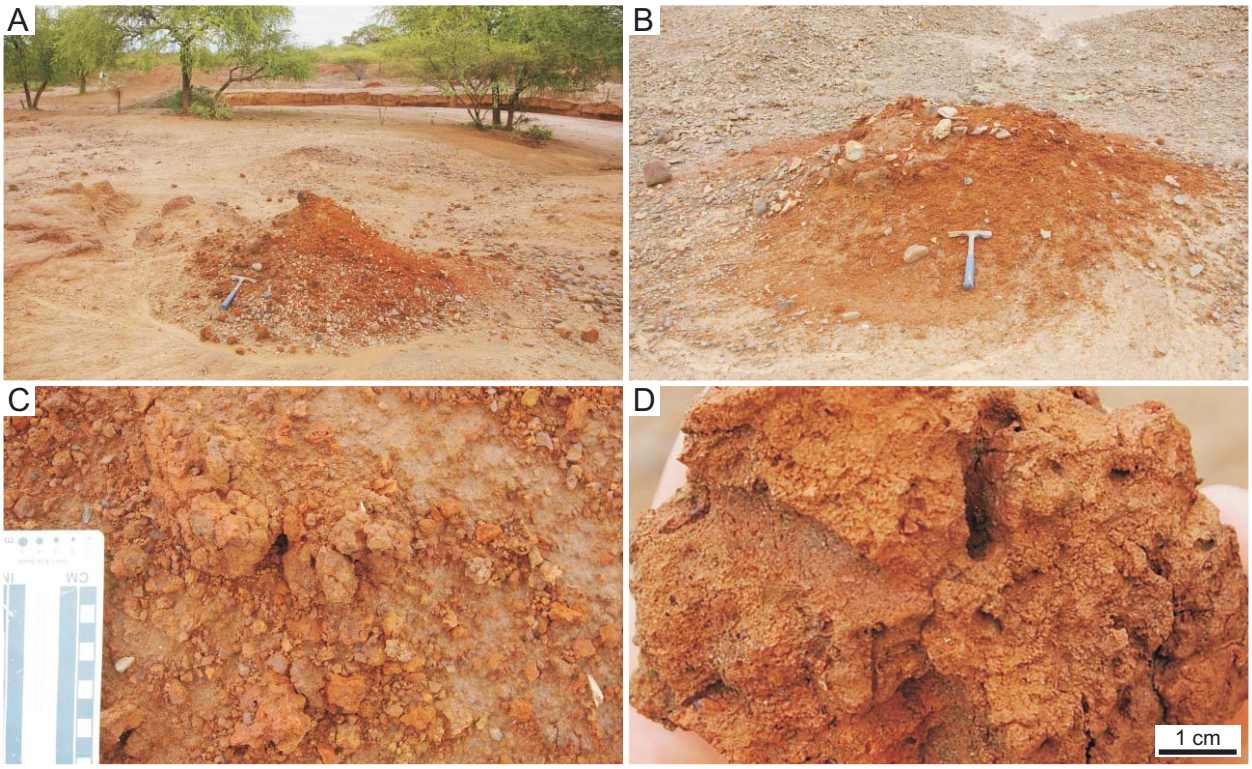


**Fig. 4.1.1.3.** Holocene? ant nests at Nyongonyek, Baringo basin. **(A–B)** Red-stained and cemented mounds in area of modern channel. Hammers for scales. **(C–D)** Close-ups of bioturbated silts within mounds, with open, unwalled burrows. Note lack of carbonate cement.

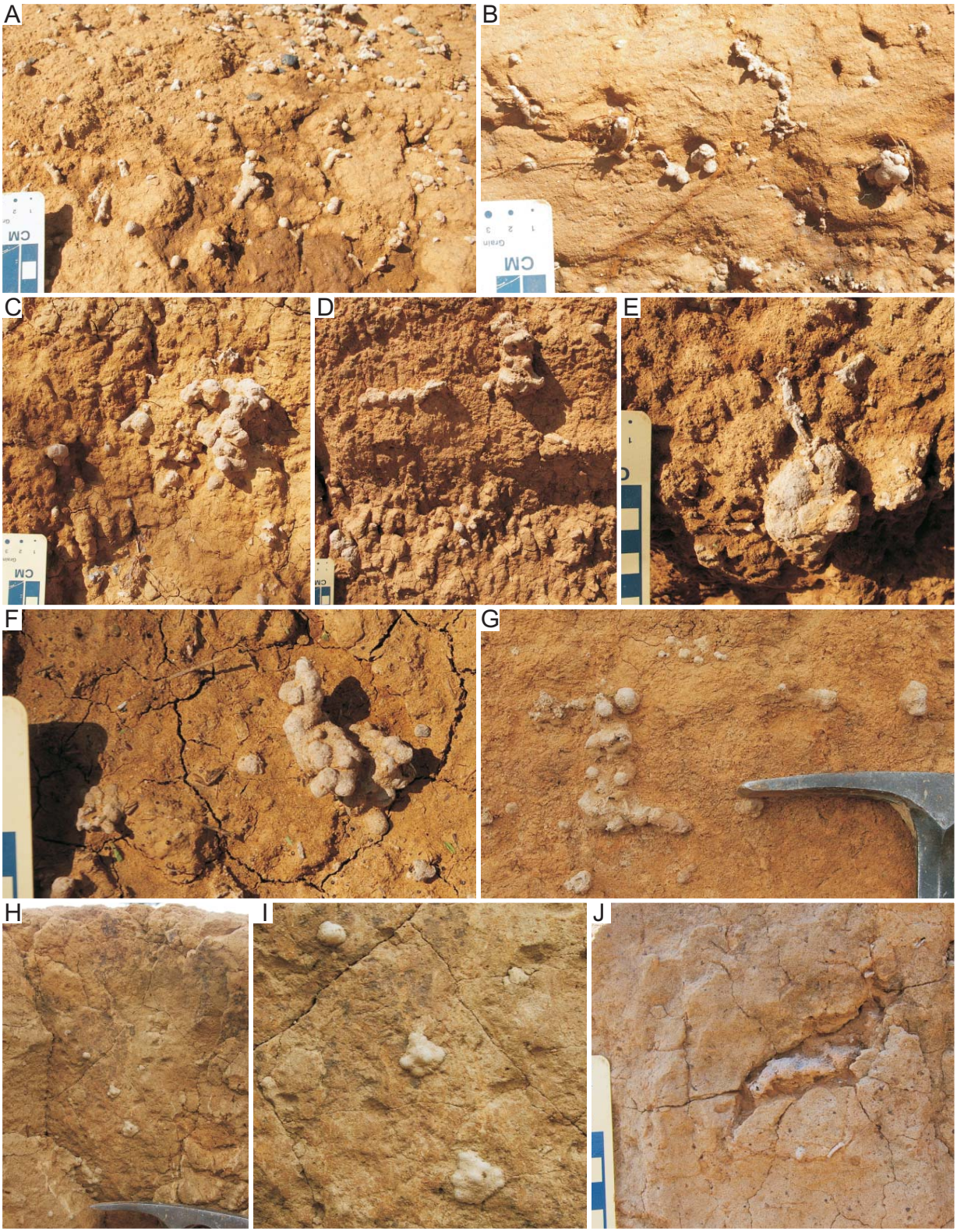


**Fig. 4.1.1.4.** Hymenopteran nests from the Pleistocene Loboi Silts, Nyongonyek, Baringo basin. **(A–I)** Groups of small, spherical cell clumps with or without burrows preserved by carbonate in a silty substrate. The nests and burrows were probably produced by bees. **(H–J)** Hymneopteran nests preserved within the reworked-ash bed. **(H–I)** Vertical arrangement of cell clumps suggests they were part of the same nest. The nests were probably produced by bees. Hammer for scale in (H). **(J)** Possible wasp nest with excavated region surrounding cell clump in centre.

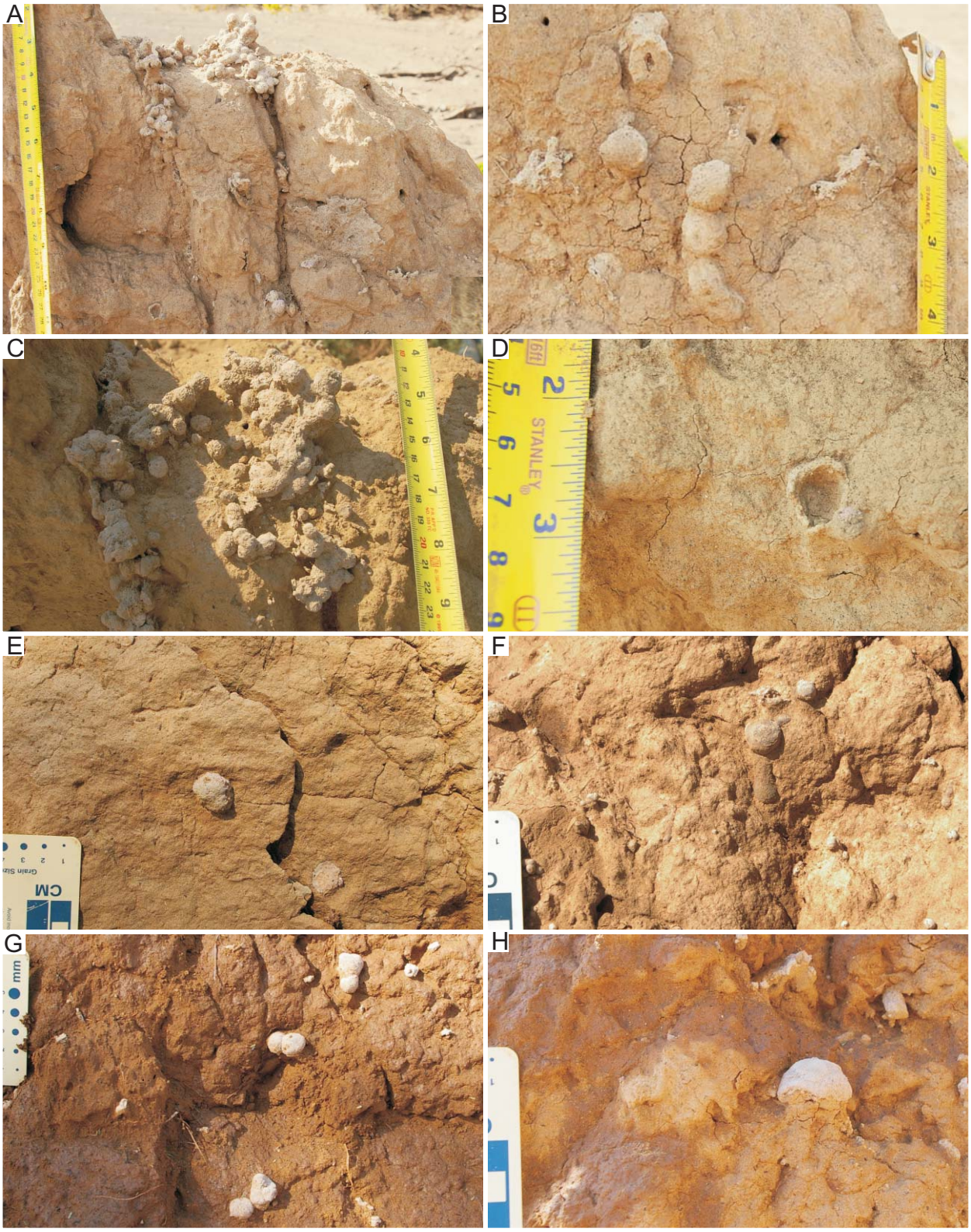


**Fig. 4.1.1.5.** Insect nests from the Pleistocene Loboi Silts, Nyongonyek, Baringo basin. **(A–G)** Randomly and vertically arranged clumps of slightly larger, thick-walled cells than those shown in Fig. *4.1.1.*4. These cells could have been produced by scarabid beetles. Note smaller number of cells in groups shown in (B), (D), and (E–G). **(H)** Cap-like structure preserved by carbonate, similar to the cap-like structures of small *Cubitermes* termite nests.

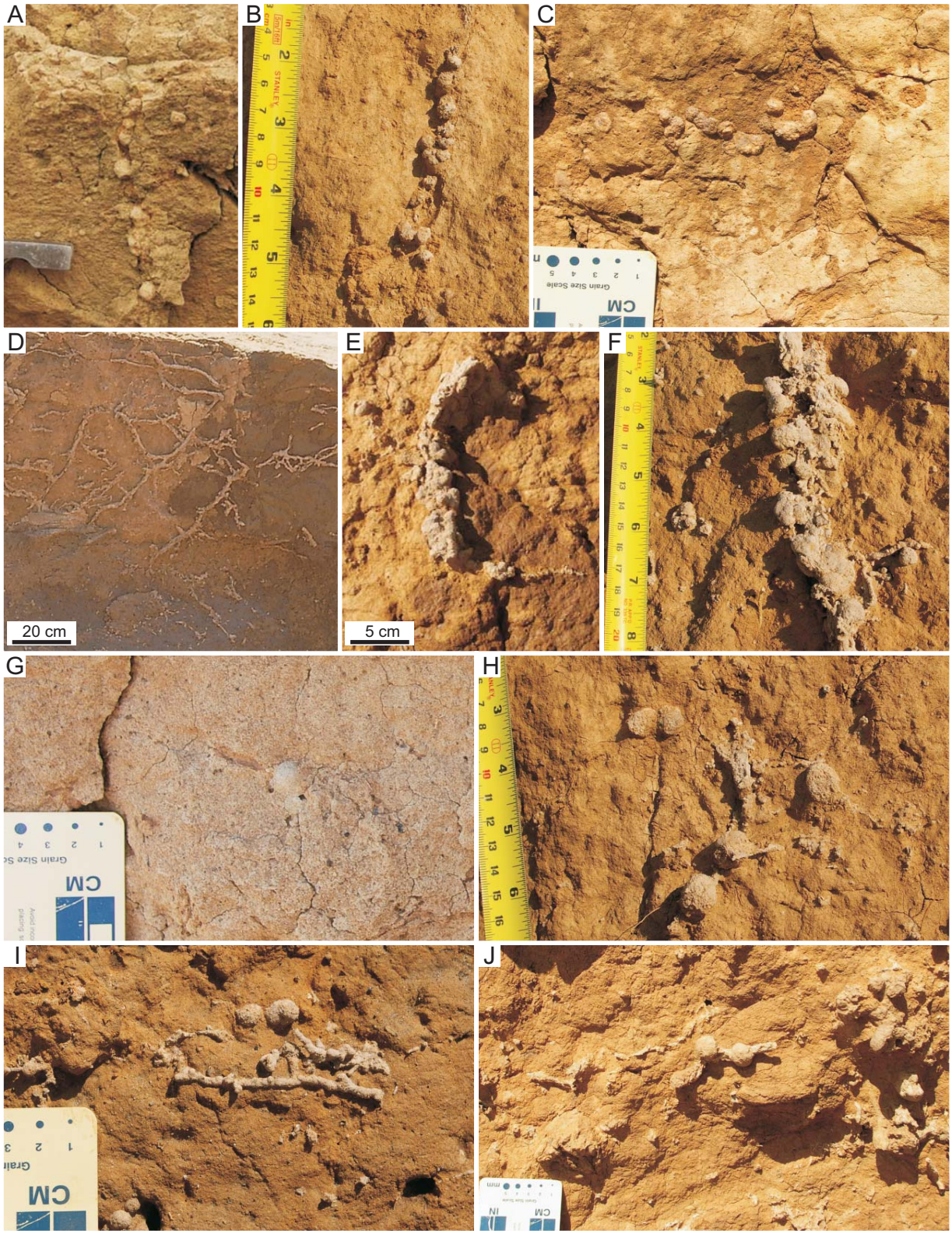


**Fig. 4.1.1.6.** Insect burrows with cells from the Pleistocene Loboi Silts, Nyongonyek, Baringo basin. **(A–C)** Cells preserved by carbonate within burrow partially backfilled with silt in reworked-ash bed. **(D)** Branching burrows with small protrusions or possibly small cells in the reworked-ash bed and preserved by carbonate. **(E–F)** Vertically oriented, possible composite structure of small burrows and cells. **(G)** Isolated, spherical cell attached to open burrow in reworked-ash bed. **(H–J)** Isolated cells attached to burrows. Produced in silts and preserved by carbonate.

obliquely oriented burrow is more than 40 cm wide at the lower contact of the tuff bed, and tapers gently to approximately 20 cm wide, with a length of ~2 m (Fig. *4.1.1.*7C). Lastly, branched, dominantly horizontal networks of smaller burrows were preserved just below the tuff (Fig. *4.1.1.*7F–G). Most of these burrows were ~8 cm in diameter and roughly circular in cross section, but some examples of smaller (~2.5 cm diameter) branches were also preserved. The larger burrows (~15–40 cm diameter) may be attributable to mongoose, aardvark, or possibly other denning mammals, whereas the smaller networks (~2–8 cm diameter) were likely produced by rodents and/or small mongooses.

Other trace fossils or rhizoliths preserved in the Loboi Silts at Nyongonyek include: 1) meniscate backfilled horizontal burrows filled with sediment aggregates (Fig. *4.1.1.*10A, 10C), which may have been produced by termites, ants, or beetles; 2) concentrically backfilled burrows attributed to termites (Fig. *4.1.1.*10B); 3) aggregate-backfilled vertical burrows (Fig. *4.1.1.*10D,

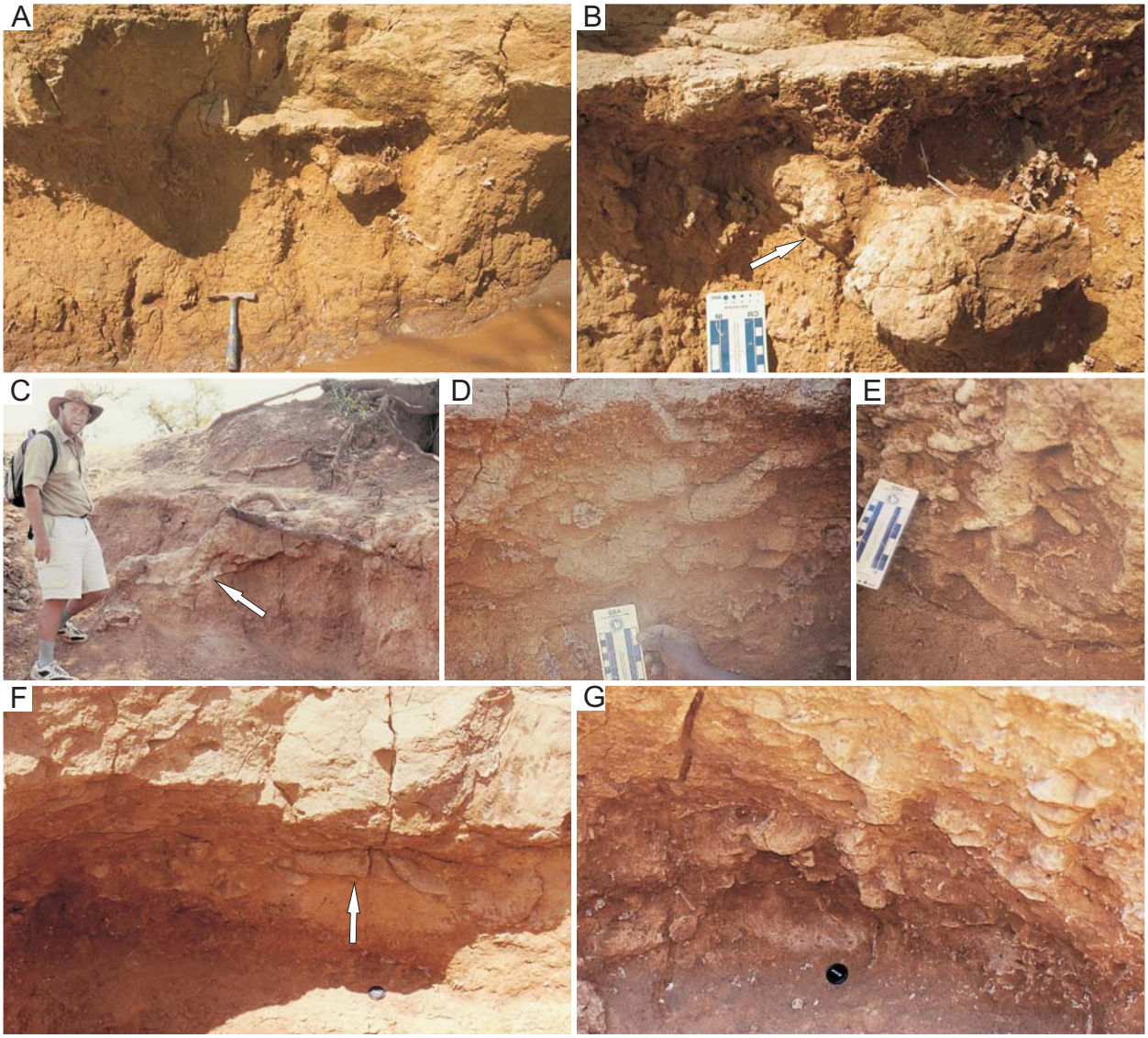


**Fig. 4.1.1.7.** Probable mammal burrows at Nyongonyek, Baringo basin. All examples were produced in the lower unit and preserved by the reworked-ash. **(A–B)** Oval-shaped mongoose? burrow. Note narrow entrance (arrow) to larger chamber. **(C)** Large, obliquely oriented, aardvark? burrow (arrow). **(D–G)** Burrow system of smaller burrows, attributable to ground squirrels? Arrow in (F) points to horizontal, straight branch of the burrow system.

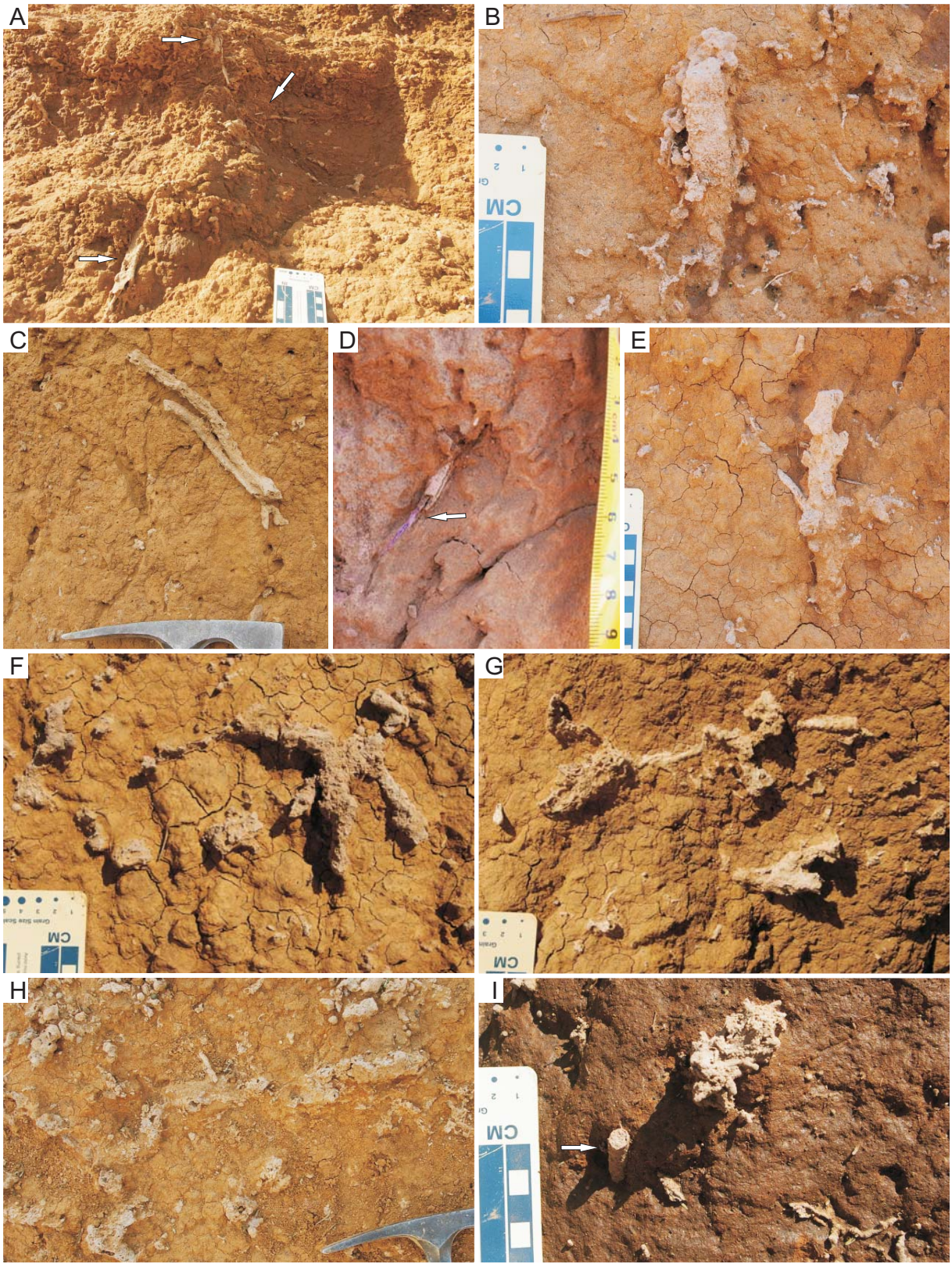


**Fig. 4.1.1.8.** Carbonate rhizoliths and composite burrows in the Loboi Silts at Nyongonyek. **(A)** Downward branching root system (arrows) preserved by carbonate. **(B)** Rhizolith associated with small nodules? and insect burrows?. **(C–D)** Carbonate coated roots of unknown age. Note dead root at centre of rhizolith in (D). **(E–I)** Probable composite structures of rhizoliths associated with small burrows and cells?, possibly produced by termites.

10E); and 4) Mn-oxihydroxide-coated open root holes and root hairs (Fig. *4.1.1.*10F–I). Mn-oxihydroxide root traces are most abundant on the upper reworked channel tuff, and are more abundant in the upper paleosol than in the lower paleosol. One example of a sharp-walled vertical structure in the upper paleosol, which is filled with material different from the host and tapers slightly, may be a fracture or desiccation crack (Fig. *4.1.1.*10J).

Together with the sedimentology, the trace fossils at Nyongonyek represent a flat-lying region with well drained silty soils and abundant vegetation, which is not represented in the lake margin facies of the Loboi Silts within the Lake Bogoria basin. In summary, the preliminary

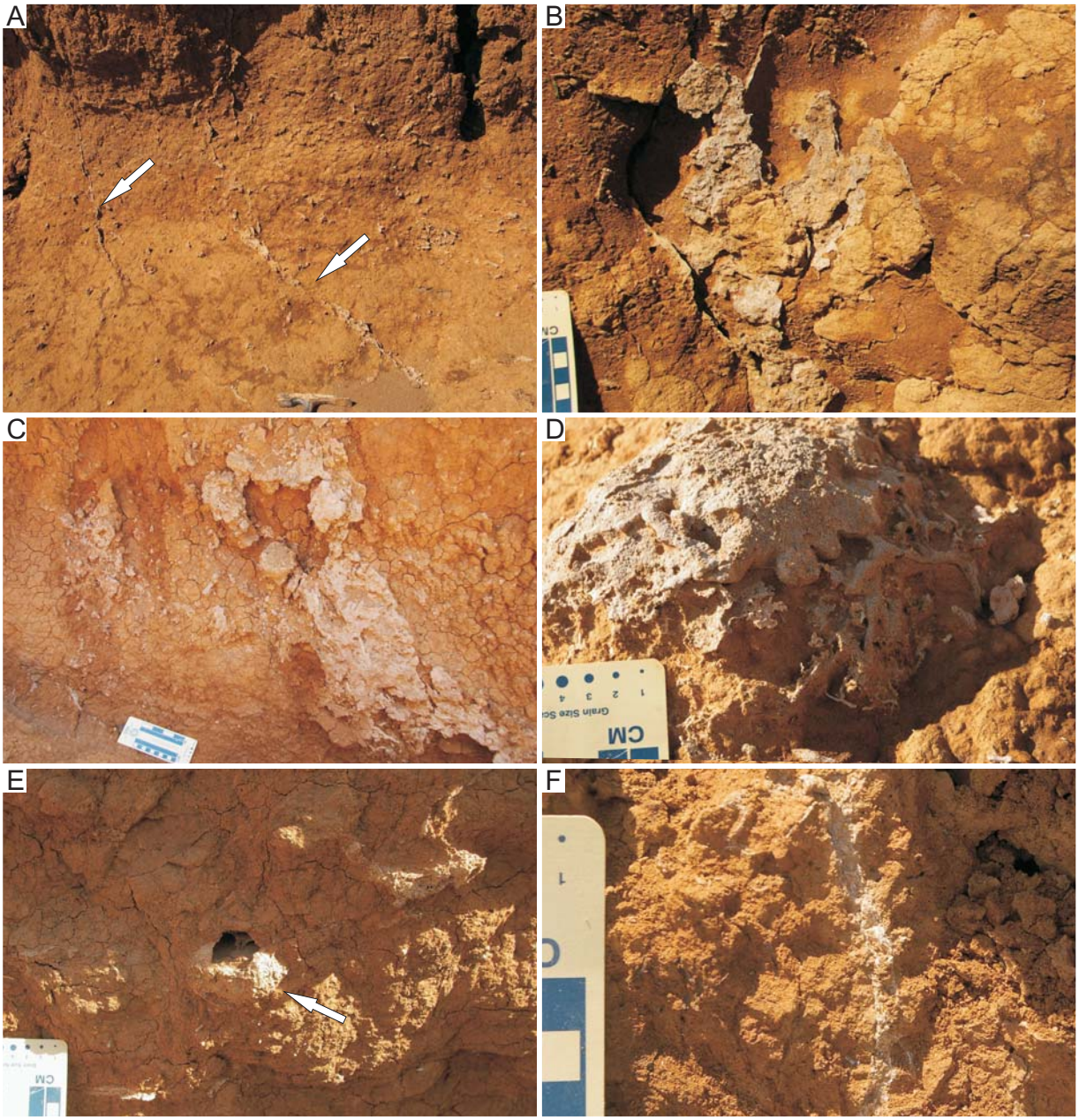


**Fig. 4.1.1.9.** Carbonate cements in the Loboi Silts at Nyongonyek. **(A–B)** Vertically oriented, plate-like fracture-fill carbonates (arrows in A, close-up in B). **(C)** Irregular mass of carbonate within the lower unit of the Loboi Silts. **(D)** Pore-filling carbonate surrounding possible insect nest? **(E)** Accumulation of carbonate at base of open, probably Holocene or Recent large root hole (arrow). **(F)** Modern calcite forming in an open root hole, upper unit, Loboi Silts.

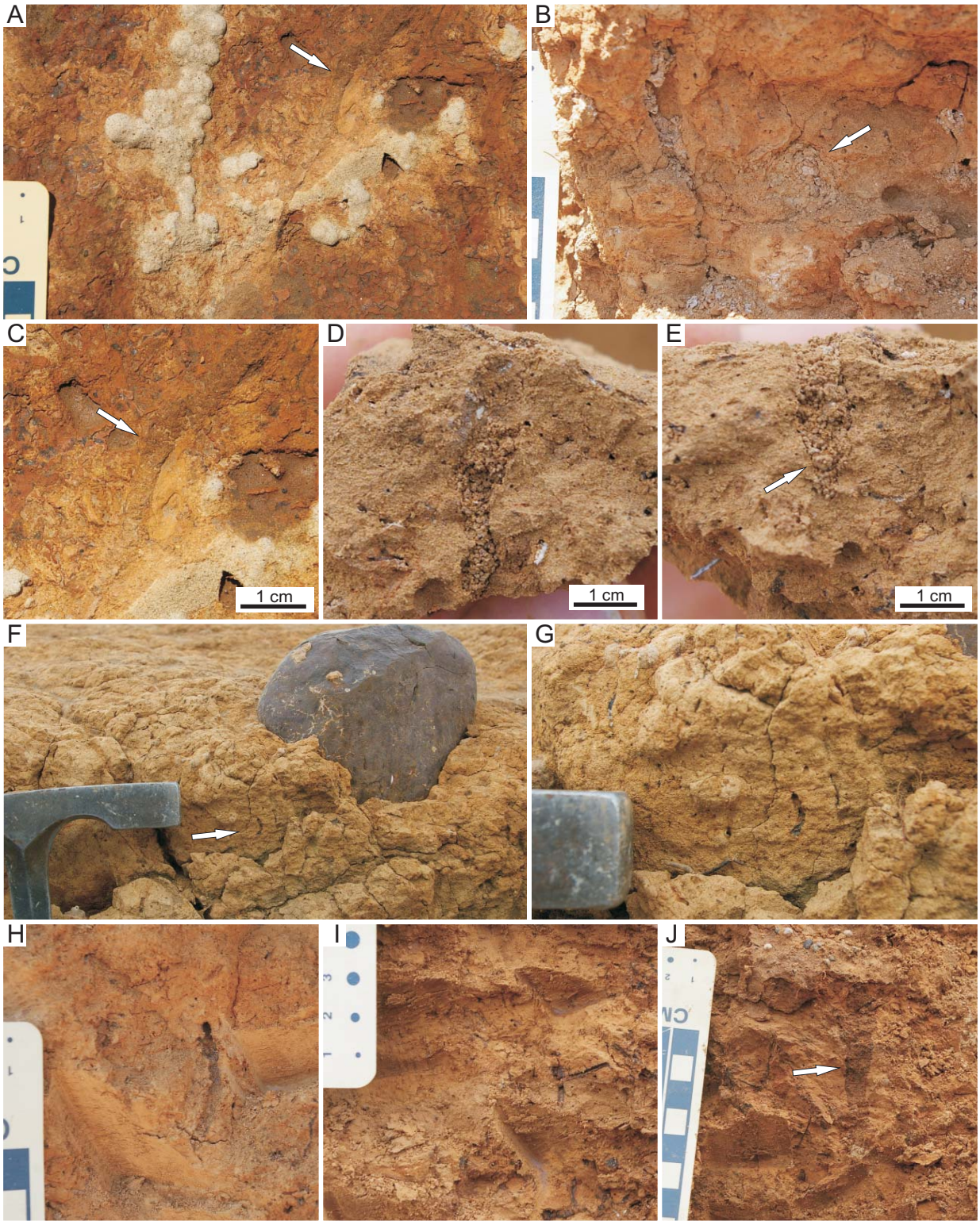


**Fig. 4.1.1.10.** Other traces and structures in the Loboi Silts, Nyongonyek. **(A)** Meniscate backfilled burrow at base of reworked-ash bed (arrow). Fill is sediment aggregates. **(B)** Modern, concentrically backfilled burrow (arrow) filled with sediment aggregates, probably produced by termites. **(C)** Close-up of (A). **(D–E)** Modern, vertically oriented burrows with sediment aggregate backfill; aggregates of various sizes (arrow in E). Possibly produced by termites, ants, or beetles. **(F–G)** Mn-coated burrows or open root holes in the reworked-ash bed (arrow in F). **(H–I)** Modern, open, root holes stained by Mn-oxyhydroxides in (I). **(J)** Possible desiccation crack (arrow) in upper unit.

identification of a suite of terrestrial trace fossils associated with pedogenesis and carbonate cements at Nyongonyek demonstrates two important points: 1) this paleosol/fluvial floodplain assemblage represents an end-member that may be present only in basin margin depositional environments; and, 2) termite trace fossils are associated with both lake margin lithofacies (Section 4.1.2) and with fluvial plains at the basin margin, but the more arid-region bee, wasp, and/or dung beetle trace fossils form an assemblage that was associated only with the basin margin. The preservation of rhizoliths and other structures by carbonate also implies a fresh, meteoric water source of the $Ca^{2+}$, which in closed basins in the modern Kenya Rift is typically precipitated from solution during evaporation shortly after rains or from shallow vadose-zone fluids that still contain $Ca^{2+}$ near the basin margin.

At Nyongonyek, there is a notable lack of well cemented horizons (except the ash) and there was no apparent overprinting of different trace suites that represent different environmental conditions. The traces are interpreted to all reflect similar environmental conditions, were contemporaneous, and are thus included in a single suite, the "Coprinisphaera-like" Suite. This assemblage is comparable to the Coprinisphaera ichnofacies of Genise et al. (2000), but differs from it and the "Celliforma ichnofacies" by containing an abundance of termite nests and tunnels. The presence of termite nests does not reflect a humid climate in this case, but may imply relatively more humid conditions. Based on the trace fossil assemblage, the sedimentary evidence, and the early diagenetic evidence, the environmental conditions that were prevalent in the Nyongonyek area at this time are interpreted to include: 1) low water tables with well drained, low humidity sediments; 2) a fresh, meteoric water source with $Ca^{2+}$; and, 3) a relatively shallow low-energy or ephemeral channel system with abundant fine-grained sediments in the source area (reworked Kapthurin Formation?).

The previous work of S. Driese, G. Ashley, and B. Owen (unpublished, 2002) on the sediments and rhizoliths from the section measured at Nyongonyek reported on the elemental composition of the sediments (from XRF data), pedogenic features, and $\delta^{13}C$ and $\delta^{18}O$ stable isotope analyses of two calcite rhizoliths. They found that the Loboi Silts reflected a constant provenance and suggested that they might be sourced from reworked sediments. The carbon and oxygen isotopes from calcite rhizoliths suggested that the vegetation was dominated by C3 plants (e.g., shrubs) with some C4 plants (e.g., grasses) and that the pedogenic carbonates were precipitated from typical 'tropical' meteoric water. The measured section (3.7 m) consists of a lower paleosol interval (0–1.7 m), the reworked tuff (1.7–1.85 m), a lacustrine interval (~2–3 m), and the upper paleosol interval (3–3.7 m) below the later, incised conglomerate. The unit interpreted by Driese et al. (2002, unpublished) as lacustrine is interpreted here as either: 1) laminated overbank deposits with mud drapes; 2) a flat- to low-angle cross-laminated longitudinal or point bar with a few indicators of higher gradient cross lamination; and/or 3) a flat- to current-ripple-cross-laminated ephemeral channel fill sequence. Many of the laminae are normally graded in thin section, from fine-grained sand to silt with or without a clay drape (thin sections courtesy of S. Driese). The bedding in outcrop is difficult to see in most cases because the very fine-grained nature of the clay-rich silty sediments, pedogenesis, invertebrate bioturbation, and roots have all contributed to the poor exposure of the section, as well as the reworking of the original sedimentary fabric.

A possible reconstruction of the events and environment that led to the preservation of these trace fossils and rhizoliths is as follows. The lower interval represents a paleosol developed on overbank silts that was bioturbated by bees, termites, and roots. The timing of the carbonate precipitation is unknown, but may have occurred shortly after the formation of the traces and prior to the deposition of the reworked tuff, although clear cross-cutting relationships

were not observed. Channel incision occurred prior to the deposition of the reworked tuff and partly exposed the open burrows of mammals (Fig. *4.1.1.*7), which were then filled and preserved by the tuff. The burrows and nests of bees and termites that cross-cut the tuff were formed after deposition of the tuff. However, it is unknown if they formed prior to, during, or after deposition of the ~1 m-thick unit of laminated and cross-stratified fluvial silts and sands that overlies the tuff. Root moulds associated with large termite nests just below the tuff were preserved by carbonate, but the termite nests were not (Fig. *4.1.1.*2A–D). Similarly, the cells of the insects in the tuff were preserved by carbonate, but the burrows associated with them either remained open or the carbonate that filled them had been eroded from the outcrop (Figs. *4.1.1.*6A, 6C, 6G, 4H–J). The processes involved in the carbonate precipitation may have been complex, and may have been influenced by the respiration of plants and/or soil microorganisms that produce $CO_2$. Above the tuff, the same assemblage of trace fossils persists. Vertical Mn-oxihydroxide-lined open root pores or burrows are preserved in the tuff (Fig. *4.1.1.*10F, 10G). Towards the top of the section however, open root pores coated with Mn-oxihydroxides and open or Mn-filled root hair pores are more abundant (Fig. *4.1.1.*10H, 10I), and there are fewer traces preserved by carbonate. Modern dustings of calcite are presently precipitating in some of the root pores and modern termite burrows (Figs. *4.1.1.*9F, 10B).

### *4.1.2. Pleistocene Trace Fossils from the Loboi Silts in the Bogoria Basin*

The trace fossil assemblage preserved in the Pleistocene Loboi Silts within the Bogoria basin represents a complex story of sedimentation, bioturbation, erosion, and then bioturbation again on a relatively well indurated horizon or set of surfaces that are exposed today on the Sandai Plain, Loburu Delta, and at the southern end of the lake near Emsos (Figs. *4.1.2.*1–5; Scott et al., 2009, fig. 3). Descriptions of animal and plant trace fossils preserved in the Loboi Silts in the Bogoria basin have been published by Scott et al. (2008, 2009). The late Pleistocene trace fossils preserved in the Loboi Silts are described here in Table 4.2, and younger trace fossils produced in the firm substrate of the cemented Loboi Silts are described in Tables 4.4 and 4.5. Renaut (1993) described the fossil root mats on Sandai Plain and R.A. Owen et al. (2008a) described the other, likely Pleistocene, fossil rhizoliths preserved at the Loburu Delta (Table 4.3, adapted from Scott et al., 2009).

The Pleistocene Loboi Silts in the Bogoria basin are generally coarser-grained than at Nyongonyek and on the Sandai Plain they are preserved mainly by analcime cements along with some minor calcite and Mn-oxides (Renaut, 1993; Scott et al., 2008, fig. 10). The quantity of analcime increases upwards in the profile of the Loboi Silts on the Sandai Plain (Renaut, 1993). Its formation is attributed to the evaporation of saline pore waters and the authigenic alteration from smectitic clay minerals and glass to analcime (Renaut, 1993). This type of preservation, and the presence of well cemented horizons with induration increasing upwards, was not observed in the older more basin margin-ward Loboi Silts at Nyongonyek. The Loboi Silts are a time-transgressive unit, with the oldest beds in the region of Nyongonyek at ~200 ka and the youngest, Late Pleistocene beds in the Bogoria basin, from ~30–18 ka. The compositionally immature sandy sediments in the Bogoria basin are interpreted to have been deposited in fluvial-deltaic plain and shoreline lithofacies adjacent to a closed basin lake that may have fluctuated in salinity in a very similar way to the modern situation (intermediate lake levels, cf. Renaut and Tiercelin, 1994). Today, sediments transported by the Sandai River into the eastern Loboi Plain and northern Lake Bogoria are sourced mainly from volcanics in the Laikipia Highlands and within the eastern part of the rift, whereas sediments on the western Baringo basin are sourced from sedimentary rocks and volcanics within the rift and the distant highlands south of Lake Nakuru (Fig. 2.1).

**Table 4.2.** Trace fossils preserved in the Pleistocene Loboi Silts in the Bogoria Basin. Trace types marked with an asterix (*) were described by Scott et al. (2009). Trace types marked with a double cross (‡) were also described by Scott et al. (2008). Trace types marked with a section sign (§) have not previously been described from these localities.

| Fig. | Trace type | Ichnotaxonomy | Description | Comments | Possible tracemaker | Interpreted environment | Locality |
|---|---|---|---|---|---|---|---|
| *Trace Fossils of the "Flamingo" Suite* | | | | | | | |
| Fig. *4.1.2.*4B; *4.1.2.*5A, B | (*) Flamingo nest mounds and associated surfaces | None available | Irregular surfaces with undulating margins and weathered, circular mounds ~15–20 cm in diameter at base; height < ~10–15 cm; rounded at top; may have central depression on top of mounds; surfaces may be modified by younger nests; poorly preserved overall; surfaces may be flat with or without nest mounds preserved | Some examples could possibly be intact *Termitichnus* nests not exposed in section | Lesser flamingos, possibly Greater flamingos | Subaerially exposed littoral and/or lake-margin mudflat | Western shoreline north of Loburu, Central Loburu delta, Old Loburu, Emsos |
| Scott et al., 2008, fig. 8F, G | ‡ Trampled surfaces | n/a | Irregular surfaces that appear to have been trampled by flamingos and possibly disrupted by salt efflorescence; also bioturbated with open vertical burrows; compare with modern examples on Sandai Plain in Scott, 2005, fig. 4.7B | Associated with fossil mammal footprints | ? Lesser and/or Greater flamingos | Lake margin near shoreline with muddy low-lying areas | Sandai Plain |
| *Trace Fossils of the "Scoyenia-like Suite"* | | | | | | | |
| Fig. *4.1.2.*1A–F | § Mammal footprints (perissodactyls) | Indeterminate | Roughly circular and fleshy footprints in irregular, trampled substrate; two clear examples show rounded posterior margins and large, rounded displacement rims ~2 cm wide and 1.5 cm high; 1) shows four forward-directed digits reminiscent of hippo footprints; total length ~ 7cm; total width ~9 cm; 2) shows three forward-directed clear digits, with central digit wider than lateral digits, reminiscent of rhino tracks; central digit may be two digits; total width ~7 cm; total length ~8 cm | Comparable morphology and substrate to Ilosuani and Rorop Lingop prints, see Scott, 2005 | Perissodactyls, possibly small hippo or rhino | Saturated sandy substrate, possibly with root mat; possibly marsh (?spring fed) near lake margin | Sandai Plain |
| Scott et al., 2008, fig. 7 | ‡ Mammal footprints (primates) | Indeterminate | Elongate, plantigrade, fleshy footprints with large, oval-shaped digit I, medial concave margin (arch), and posterior rounded margin (heel); total length 20 cm; total width 8.5 cm; lateral margin obscured, possibly due to slippage | One, isolated fossil footprint only; associated with black Mn cement | Human | Lake margin near shoreline with muddy, organic-rich low-lying areas | Sandai Plain |

| | | | | | | | |
|---|---|---|---|---|---|---|---|
| Scott et al., 2008, fig. 8A–I | ‡ Mammal footprints (artiodactyls) | Indeterminate | Several types of hooved footprints preserved mainly in front and hind pairs or in trampled surface, ranging from ~5–12 cm in length and ~5–10 cm in width; medial margins of hooves show different morphologies; most examples shallowly impressed (~1 cm depth) with sharp margins and/or sharp-edged displacement rims ~2–5 mm in width | Several types associated with Mn cement; see Scott, 2005 and Scott et al., 2008 | Suids and bovids (?warthog, ?elands, ?buffalo, ?kudu) | Lake margin near shoreline with muddy, organic-rich low-lying areas | Sandai Plain |
| Fig. *4.1.2.* 4C | * Vertical burrows | *Skolithos* isp. | Vertical, open burrows ~1–1.2 cm in diameter; length less than 10 cm, but not entirely exposed; burrow boundaries sharp and smooth; unlined; unwalled | Also see Scott et al., 2009, fig. 9F | Insects or arachnids: probably beetles or spiders | Stiff to firm subaerial substrate above water table | "Old" Loburu Delta |
| Figs. *4.1.2.*2F; Scott et al. 2009, figs. 11A–C, 12B | * Simple horizontal burrows | *Planolites* isp. | Unlined, horizontal to oblique, straight to curving, endichnial burrows (6–8 mm wide); open, or filled with non-pelletal and/or pelletal material different in colour, but same grain size, as host sediment | May be more than one type | Insects; possibly beetles and/or earwigs | Subaerially exposed moist to wet substrate | Sandai Plain |
| Figs. *4.1.2.* 2H, 3D, 3E | § Vertical burrows | cf. *Skolithos* isp. | Open, vertical to oblique, medium-sized burrows in bioturbated and root-mat containing substrate; burrow boundaries distinct but not sharp; roughly circular cross section; ~4–6 mm diameter | Could possibly be root holes, not examined in detail | ?Insects, possibly beetles; if plants, rhizomatous roots | Wet substrate with vegetation; possibly riparian and/or marshy | Sandai Plain at Sandai River; "Old" Loburu at shoreline |
| *Trace Fossils of the "Termitichnus-like Suite"* | | | | | | | |
| Fig. *4.1.2.*2C; Scott et al., 2009, fig. 11D–E | * Simple horizontal burrows | *Palaeophycus* isp. | Smooth-walled internally, horizontal to oblique, straight to curving, endichnial burrows (< 12 mm wide) that are either open or filled with material similar to the host sediment; lining is fine-grained | Fill may be pellet-like in some examples | Insects; termites, or other insects that use termite nests | Moist to dry substrates | Sandai Plain; "Old" Loburu |
| Fig. *4.1.2.*2D; Scott et al., 2009, fig. 11C, 11F | * Meniscate backfilled burrows | ?*Beaconites* isp. | Thick-walled, meniscate backfilled, straight, unbranched, horizontal burrows preserved as endichnia; are ~8 mm in diameter including the wall; infill is partly pelleted, and partly composed of the poorly sorted host sediment | Directly associated with *Termitichnus* nests | Insects; termites, or other insects (?beetles) using termite nests | Moist to dry substrates | Sandai Plain |
| Scott et al., 2009, fig. 11F, 11G | * Meniscate backfilled burrows | *Taenidium* isp. A | Unwalled, meniscate backfilled, straight to curving horizontal to oblique, unbranched endichnial burrows, from 5–6 mm in diameter to more than 2 cm; infill may be partly pelleted, or of the poorly sorted host sediment | Directly associated with *Termitichnus* nests | Insects; termites, or other insects (?beetles) using termite nests | Moist to dry substrates | Sandai Plain; "Old" Loburu |

| | | | | | | | |
|---|---|---|---|---|---|---|---|
| Fig. *4.1.2*.2D; Scott et al., 2009, fig. 11H | * Concentrically backfilled burrows | ?*Taenidium* isp. B | Concentrically backfilled endichnial burrows composed of adjacent oval-shaped “packets” (i.e. assymetrical groups of thin, indistinct meniscate fill, *sensu* Smith et al., 2008) approximately 2–3 cm in diameter without constructed walls, directly associated with open, unwalled burrows; the meniscate fill is composed of pelletal (~1 mm) and non-pelletal material that is homogeneous with the host sediment | Similar type to concentrically backfilled termite foraging tunnels | Insects; likely termites, but also possibly ants or beetles | Moist to dry stable substrates | Sandai Plain |
| Scott et al., 2009, fig. 11I | * Spreiten-containing burrows | Indeterminate | Open, pellet-walled endichnial burrow ~7 mm in diameter that shows lateral movement of the open burrow and wall, leading to an almost spreiten-containing structure | | Insects; likely termites or ants | Moist to dry substrates | Sandai Plain |
| Fig. *4.1.2*. 2B, 2C, 3A, 3B | [§] Concentrically backfilled burrows | Not previously described | Horizontal, straight to slightly curving tunnels with concentrically backfilled wall structure; tunnels < 4 cm in external diameter with circular to oval cross-section shape; internally smooth-walled | Foraging tunnels of termites; likely produced at depths of < 50 cm | Insects; termites | Moist to dry, well drained, stable substrates | “Old” Loburu |
| Fig. *4.1.2*. 2B, 3C, 4D, 4E; Scott et al., 2009, fig. 12A–E | * Insect nests | cf. *Termitichnus* isp. | Roughly spherical to oval balls (chambers) with concentric fill composed of material similar to the host sediment; chambers range from ~5–25 cm in diameter; some examples show an internal sphere with a smooth lining; the chambers are associated with straight, walled connecting galleries approximately 2–3 cm in diameter; small (5–6 mm diameter), open burrows are directly associated with some chambers | | Insects; termites | Moist to dry, well drained, stable substrates | Sandai Plain; “Old” Loburu |
| Fig. *4.1.2*. 2E, 2F,?2G–H | * Insect nests | Ant nests | Open, three-dimensional burrow networks composed of small, somewhat tabular chambers (< 3 cm diameter) and intersecting branched tunnels of various sizes (~ 3–10 mm diameter) that have smooth burrow margins | May also be associated with pellet-like aggregate fill of burrows | Insects; ants | Moist to dry, well drained, stable substrates | Sandai Plain; Emsos |

**Table 4.3.** Descriptions of modern and fossil plant traces at Lake Bogoria (adapted from Scott et al., 2009). Numbers provided for the corresponding trace suites are as follows: 3 – Mermia-like Suite; 4 – Scoyenia-like Suite; 5 – Termitichnus-like Suite; and 6 – Coprinisphaera-like Suite.

| Type of plant trace | Preserved by | Reference | Localities | Description | Trace suite |
|---|---|---|---|---|---|
| Siliceous vertical rhizoliths | Opaline silica | Owen et al., 2008, fig. 4A | Loburu Delta: lake-marginal plain | White to pale brown, straight, vertically oriented, and generally unbranched, circular and tapering rhizoliths, usually 2-4 mm diameter and up to 20 cm long | 4 |
| Clustered siliceous rhizoliths | Opaline silica, flourite, calcite | Owen et al., 2008, fig. 4B, 4E | Loburu Delta: lake-marginal plain; near hot-springs | White to bluish, dense clusters of siliceous rhizoliths forming irregular, knobby surfaces; individual rhizoliths are ~ 1-4 mm in diameter and ~ 5 cm long | 4 |
| Root and stem moulds in horizontal mats | Open moulds or siliciclastic casts associated with opaline silica mats | Owen et al., 2008, fig. 4G, 4H, 4J | Loburu Delta: lake-marginal plain, near hot-springs; Sandai Plain: fossil tufa mound | Circular and ovoid moulds (5-10 mm diameter) penetrate white to brown siliceous mats, and may be filled with siliciclastics. Also associated with mats are horizontal, reticulate, siliceous rhizoliths that appear to have been rhimzomes (3-10 mm diameter) | 3, 4 |
| Silica-calcite rhizoliths | Calcite and opaline silica | Owen et al., 2008, fig. 4F | Loburu Delta: lake-marginal plain | Calcite-cemented siltstone nodules that form around siliceous vertical rhizoliths ~ 2-4 mm in diameter and 2-5 cm long. | 4 |
| Bulbous fluorite rhizoliths | Fluorite, calcite and opaline silica | Owen et al., 2008, fig. 4D | Loburu Delta: lake-marginal plain | Irregular spheroidal to ovoid flourite-rich knobs ~ 1 cm in diameter and 2 cm long that are associated with silica-calcite rhizoliths | 4 |
| Zeolitic root mats | Analcime, calcite, authigenic clays, Fe-oxihydroxides | Renaut, 1993; Owen et al., 2008, fig. 10A | Loboi Silts, Sandai Plain | Dense networks of hollow tubes ~ 3 mm in diameter and several centimeters long | 5 |
| Calcite root casts | Calcite (micrite and micro-sparite) | Renaut, 1993; Owen et al., 2008 | Loboi Silts, Sandai Plain and Nyongonyek | Sandai: Horizontal and vertical root casts ~ 1-5 cm long and 0.3-1.5 cm in diameter with irregular surface textures; Nyongonyek: Horizontal and vertical, often branching root casts ~ 1-3 cm in diameter and up to 2 m in length | 5 |
| Branching rhizome open networks | Open holes in siliciclastics | Scott et al., 2009 | Loburu Delta; Emsos Delta | Shallow, open branching networks of sedges and grasses in littoral wetlands; rhizome holes may taper and have smooth hole "linings" with no ornamentation; vertical branches (~ 4 mm) are commonly at ~ 90° to horizontal rhizomes (~ 4-6 mm in diameter) | 4 |
| Lined, branching root-hair pores | Open holes in siliciclastics with Mn- and/or Fe-rich linings | Scott et al., 2009 | Loburu Delta; Emsos Delta | 1-3 mm in diameter, these branching networks may branch obliquely upwards or downwards; larger examples tend not to branch and are vertically oriented; all are lined with red to black Mn- and/or Fe-rich linings | 4, 5 |
| Open root-hair pores | Open holes in siliciclastics with no lining | Scott et al., 2009 | Loburu, Emsos, Sandai, and Nyongonyek | 1-2 mm in diameter open, branching root-hair networks with predominantly vertical and oblique orientation of individual root-hair pores | 4, 5, 6? |
| Stromatol-itic stem casts | Calcite | Renaut, 1982 | Sandai Plain: fossil tufa mound; Emsos, Mwanasis | Greyish brown, mammillary, stromatolitic encrustations on plant stems, twigs, and tree stumps; associated with stromatolitic coating around the shoreline and tufa mound on Sandai Plain | 6? |

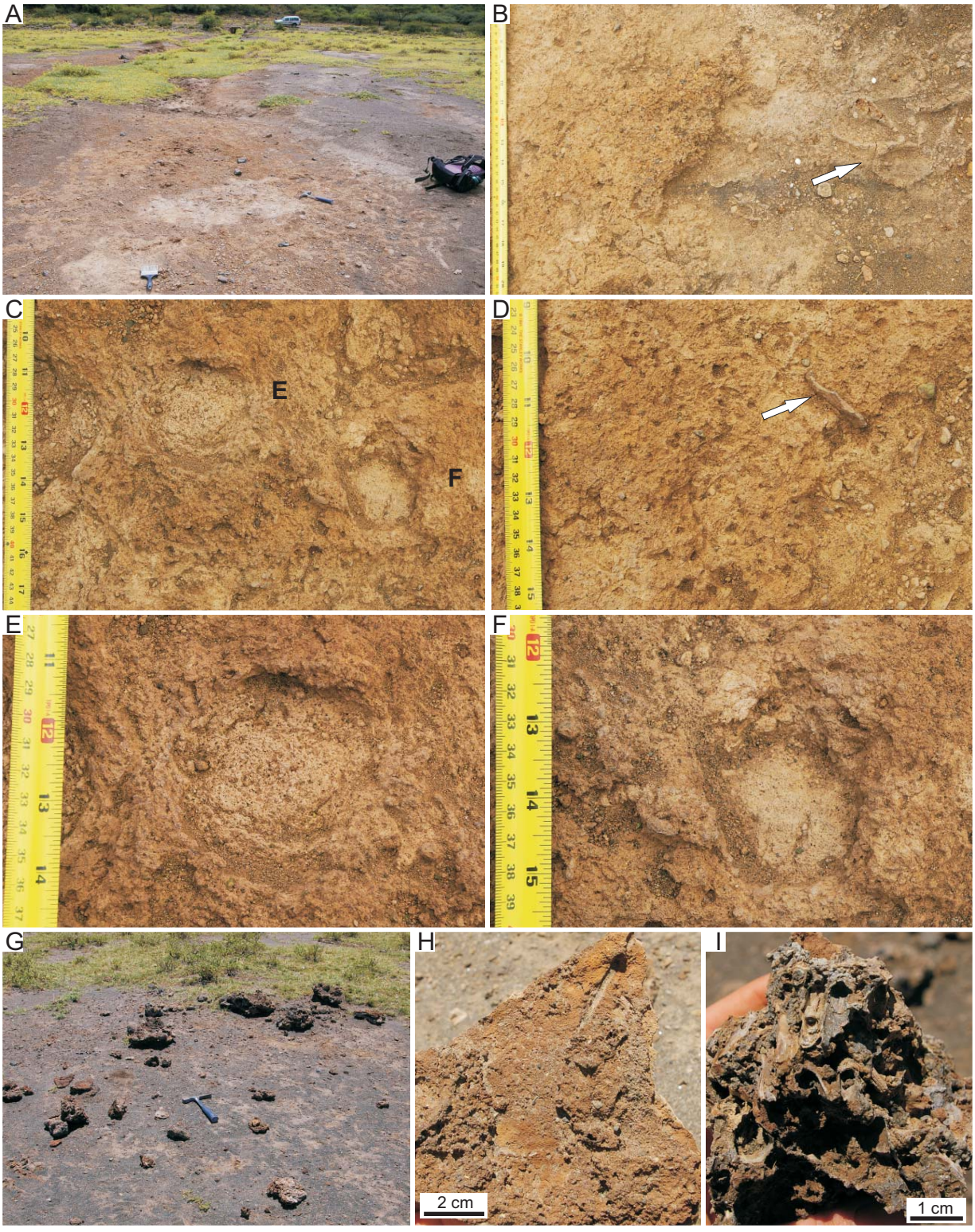


**Fig. 4.1.2.1.** Vertebrate trace fossils and rhizoliths in the Pleistocene Loboi Silts, Bogoria basin. **(A)** Vertebrate trampled surface, southwestern margin of Sandai Plain. Backpack for scale. **(B)** Vertebrate tracks with good preservation of push-up rims (arrow). **(C)** The probably rooted surface with two mammal prints shown in (E) and (F). **(D)** Vertically oriented clast due to vertebrate trampling (arrow). **(E)** Close-up of print, probably produced by a small hippo. **(F)** Close up of vertebrate print, probably produced by a small hippo or rhino. **(G)** Tufa deposits associated with the vertebrate trampled surface. **(H–I)** Close-up of tufa (H) with reed stem casts (I).

The trace fossil assemblages in the Loboi Silts of the Baringo basin and Bogoria basin reflect two different scenarios. In contrast to the paleosol and fluvial plain silty sediments near the basin margin, the trace fossils preserved in the Loboi Silts within ~1 km of the present-day shoreline represent the transition from wet conditions to dry conditions and provide evidence of a relatively long-term regression of the lake during the latest Pleistocene. First, a concentration of dense analcime- and calcite-cemented root mats may provide evidence for spring-fed and/or littoral wetlands on the Sandai Plain approximately 1 km from the present-day shoreline (Renaut, 1993; Scott et al., 2008, fig. 4A). Closer towards the modern shoreline, abundant vertebrate footprints are preserved with a variety of morphologies that suggest saturated to firm but wet substrates (Scott et al., 2008, figs. 7, 8; Fig. *4.1.2.*1). Flamingo nest mounds reported by Scott et al. (2008) from the Loboi Silts ~800 m from the modern shoreline on the eastern side of the Sandai River have been reinterpreted to be preserved in the late Pleistocene–Holocene Bogoria Silts on Sandai Plain instead of the Loboi Silts (Scott et al., 2008, fig. 9; see Section 4.1.3). Poorly preserved, ?flamingo-trampled surfaces, however, are directly associated with the Loboi Silts vertebrate footprints (Scott et al., 2008, fig. 5). These features of the Loboi Silts assemblage provide evidence for an initially saturated substrate that was subaerially exposed for the formation of vertebrate footprints, which form the first suite of traces preserved in the unit. The discovery of preserved remnants of a possible spring vent with rhizoliths, tufa, and microbial laminae on the southwestern Sandai Plain in 2007 (Fig. *4.1.2.*1G–I) suggests that spring waters (?warm) may have influenced the assemblage and preservation of trace fossils on Sandai Plain, as well as at Loburu. These carbonates are associated with vertebrate trampled and rhizo-turbated sands (Fig. *4.1.2.*1A–F). The uppermost Loboi Silts at Sandai on which the footprints were impressed was likely shallowly buried, and then bioturbated by insects prior to cementation.

The second trace fossil suite preserved in this unit on Sandai Plain represents drier conditions and a lower water table, which is attributed to continued lake-level fall. Several types of insect traces are recognized including: 1) horizontal to oblique, open and pellet-filled burrows (cf. *Planolites* isp.; Scott et al., 2009, fig. 11A–B; Fig. *4.1.2.*2F); 2) horizontal, passively silt-filled burrows, with fill different from host material (cf. *Palaeophycus* isp.; Scott et al., 2009, fig. 11D–E); 3) horizontal, meniscate backfilled burrows with and without thick, constructed walls (*Taenidium* ispp. and *Beaconites* isp., respectively; Scott et al., 2009, fig. 11C, 11F–G; Fig. *4.1.2.*2D; 4) open, smooth-walled burrow networks that may represent ant nests (Fig. *4.1.2.*2E–F); 5) concentrically "pellet"-backfilled tunnels (cf. *Taenidium* ispp.; Scott et al., 2009, fig. 11H–I; Fig. *4.1.2.*2B); 6) sub-spherical termite nests with concentric external laminae and open, burrows (*Termitichnus* isp.; Fig. *4.1.2.*2B, 2C; Scott et al., 2009, fig. 12C, 12E); and, 7) carbonate rhizoliths and open root pores. Some examples of *Taenidium* ispp., concentrically backfilled burrows, and *Beaconites* isp. are attributed here to termites, particularly if they contain pellet-like soil aggregates. This suite is composed of trace fossils normally associated with paleosols, but differs in composition from the "Coprinisphaera-like" Suite at Nyongonyek by

**Fig. 4.1.2.2.** (Next page) Trace fossils from the Pleistocene Loboi Silts on the Sandai Plain. **(A)** The Loboi Silts "exhumed surface" in an ephemeral channel. **(B)** Vertical and horizontal burrows, desiccation cracks, and concentrically backfilled traces in the surface shown in (A). **(C)** Concentrically backfilled burrow, probably produced by termites. **(D)** Meniscate/concentrically backfilled burrows with thick walls, probably produced by termites. **(E)** Large-scale desiccation polygon forming positive feature (top left) at Loboi Silts and bioturbation below. **(F)** Close-up of bioturbation of Loboi Silts shown in (E). Most of the traces were likely produced by ants and termites. Pellet-backfilled burrows with infill different from host, possibly produced by eargwigs (arrow), are also present. **(G–H)** The Loboi Silts near Sandai River, preserving root mats and abundant open holes, probably produced mainly by ants and roots (H).

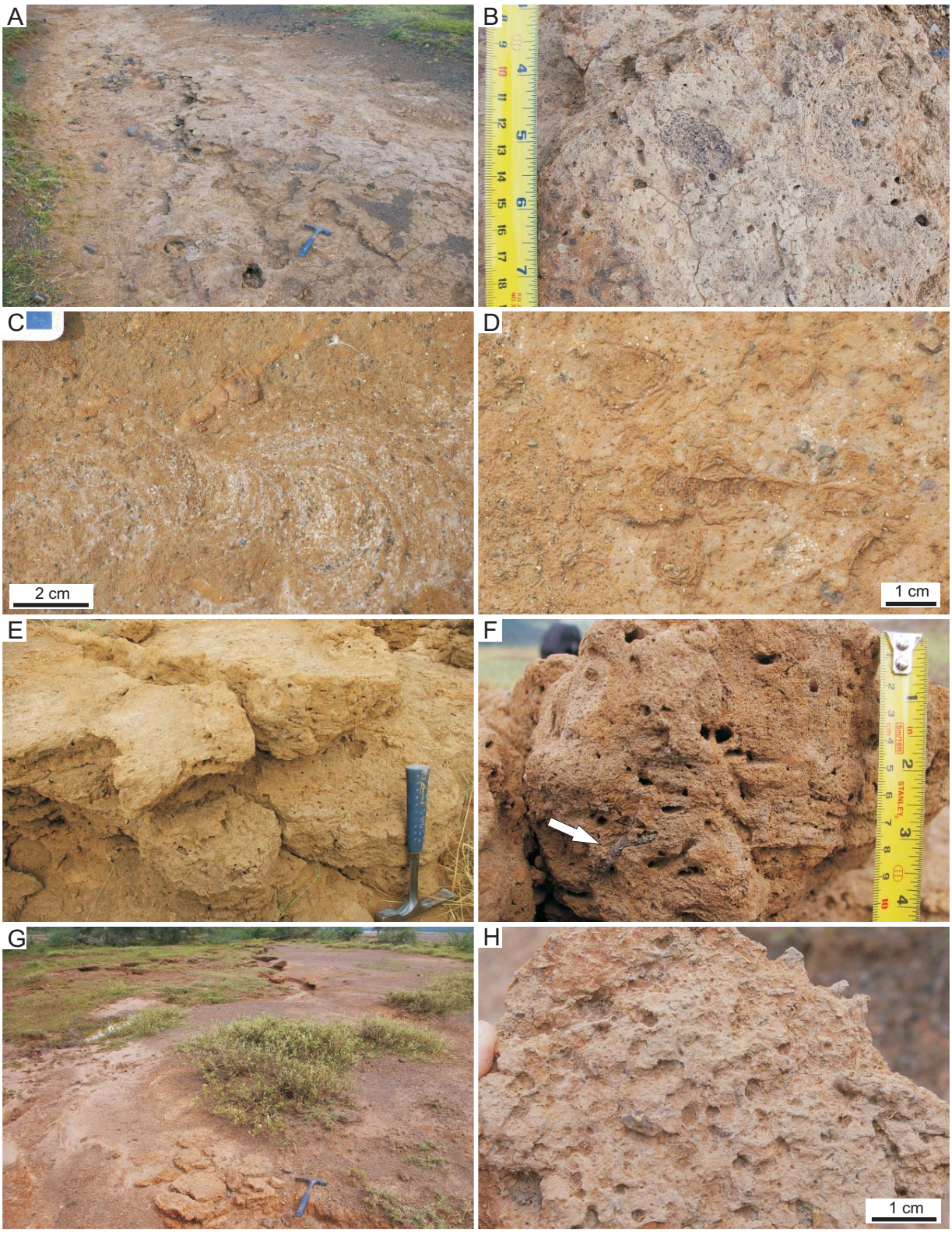
A
B
C
2 cm
D
1 cm
E
F
G
H
1 cm

lacking the presence of brood cells and burrows of bees/wasps and dung beetle brood balls. In the Bogoria basin, this paleosol-like trace assemblage was termed the "Termitichnus-like" Suite by Scott et al. (2009). The red-coloured Loboi Silts exposed along the Sandai River were also bioturbated by abundant, open, medium-sized burrows (not investigated in detail) and preserve root mats (Fig. *4.1.2.*2G–H).

The main, older lobe of the Loburu Delta (Figs. *4.1.2.*3, 4) and the cemented sediments at Emsos (Fig. *4.1.2.*5) also preserve examples of the Termitichnus-like Suite including: 1) concentrically backfilled tunnels attributed to termites (Fig. *4.1.2.*3A–B); 2) small *Termitichnus* isp. nests associated with open burrows (cf. *Planolites* isp.) and open, lined burrows (cf. *Palaeophycus* isp.) (Figs. *4.1.2.*3C, 4D–F; Scott et al., 2009, fig. 12A–B, 12D); along with 3) open, vertical burrows (*Skolithos* isp.) (Fig. *4.1.2.*4C); and 4) eroded and poorly preserved flamingo nest-mounds (Figs. *4.1.2.*4B, 5A–B). The assemblage at Loburu is also associated with several types of rhizoliths, mainly preserving wetland roots and stems that are cemented by opaline silica, fluorite, analcime, and calcite due to the close association of this area with hot springs (R.A. Owen et al., 2008; Table 4.3; Scott et al., 2009, fig. 5). However, due to repeated burial and exhumation of cemented surfaces, particularly near the hot-springs at Loburu, it remains unknown whether the rhizoliths and termite ichnofossils were contemporaneous. In these localities, vertebrate footprints were not preserved as they were on the Sandai Plain.


**Fig. 4.1.2.3.** Trace fossils from the Pleistocene Loboi Silts-equivalent sediments at the shoreline of the Loburu Delta, Bogoria basin. **(A–B)** Relatively well cemented and differentially weathered termite tunnels and nests at the modern shoreline of the "old" Loburu fan delta. **(C)** Concentric rind-like termite nest. Hammer for scale in foreground. **(D)** Bioturbated Loboi Silts-equivalent surface near the modern shoreline. **(E)** Open vertical burrows in the Loboi Silts-equivalent surface.

Two key points can be made from the ichnofossils preserved in the Pleistocene Loboi Silts in the Bogoria basin: 1) a trace fossil assemblage within a single sedimentary unit (or even bed, as at Sandai Plain) may contain two or more suites that represent different conditions – in this case, a drop in lake-level and the water table can be inferred; and 2) the presence or absence of different suites in different localities reflects the lateral variability in depositional and preservational conditions. Although the Loburu Delta and Emsos preserve possible flamingo nest-mounds and the Sandai Delta preserves vertebrate footprints, both of these suites represent wet substrates near the shoreline. In all localities, the lower water-table assemblage of termite and other terrestrial traces is superimposed on these earlier formed suites.

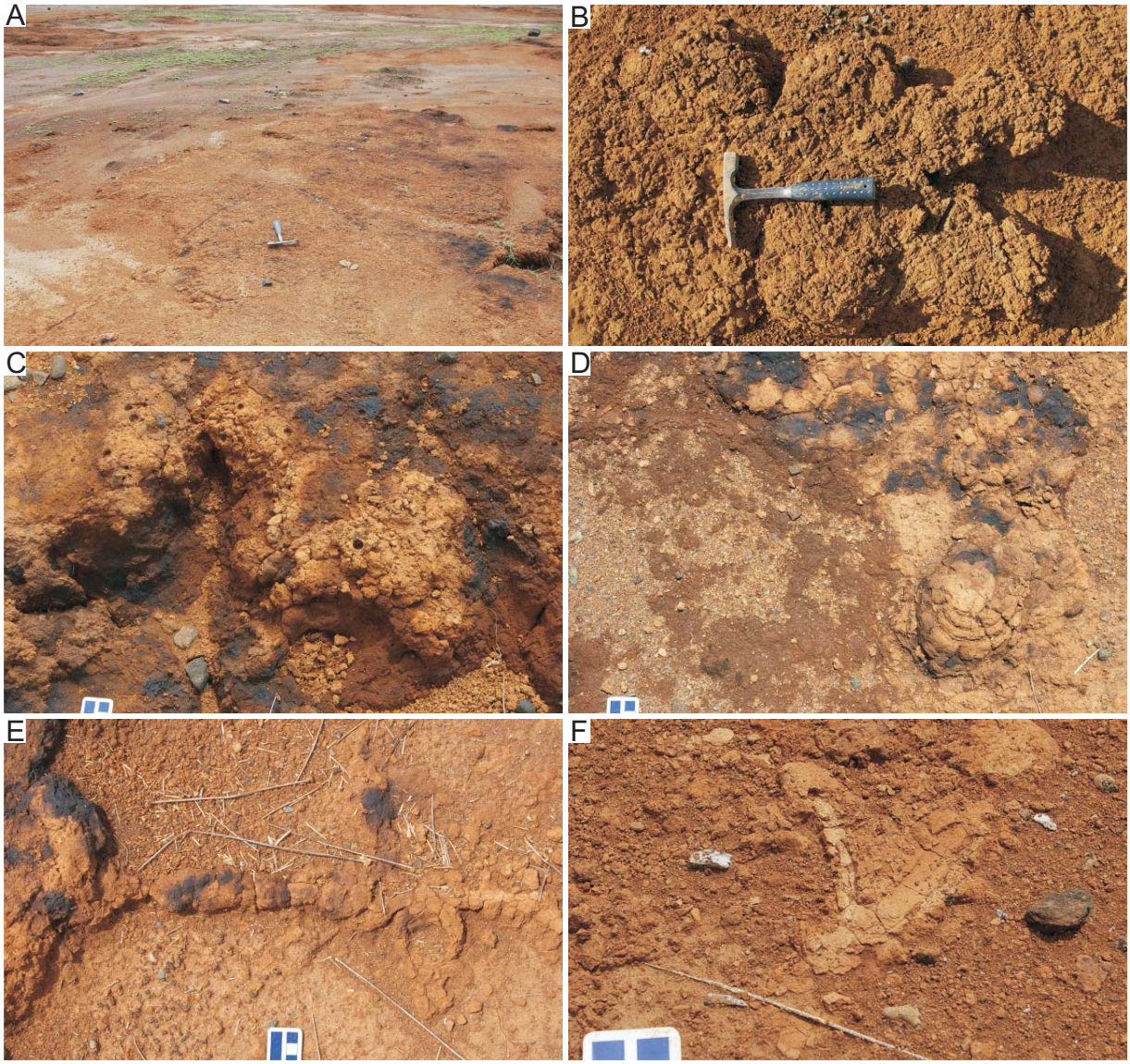


**Fig. 4.1.2.4.** Trace fossils from the Pleistocene Loboi Silts-equivalent sediments on the Loburu Delta, Bogoria basin. **(A)** The cemented, exhumed surface at "old" Loburu. **(B)** Pedogenically modified and bioturbated sediments preserve irregular structures similar to eroded flamingo nests. **(C)** The red- and black-stained bioturbated Loboi Silts-equivalents showing sharp-walled, open vertical burrows. Scale at lower left in cm. **(D)** Cross-section through group of small, spherical termite nests (right) attached to smooth-walled tunnel (top left). Scale at lower left in cm. **(E)** Very small spherical termite nests attached to tunnel. **(F)** Close-up of tunnel, showing smooth internal wall and concentric layering to external part of tunnel.

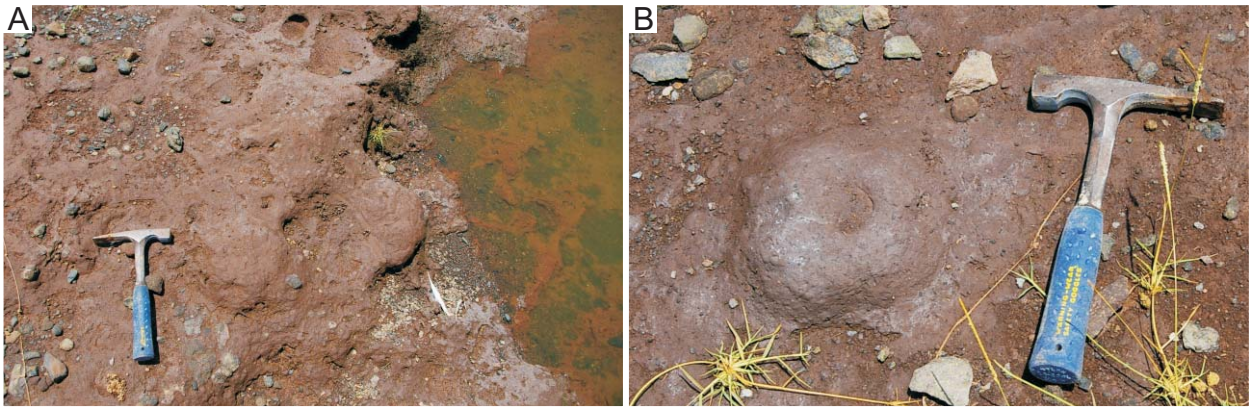


**Fig. 4.1.2.5.** Trace fossils from the Pleistocene Loboi Silts-equivalent sediments at Emsos, Bogoria basin. **(A)** The bioturbated, cemented surface with irregular topography, exhumed at shoreline. **(B)** A "well-preserved" example of a fossil flamingo nest mound.

### *4.1.3. Late Pleistocene–Holocene Trace Fossils from the Bogoria Silts and Other Holocene Deposits in the Bogoria Basin*

The Late Pleistocene to Holocene Bogoria Silts disconformably overlie the Loboi Silts on Sandai Plain, but their stratigraphic position elsewhere is not as clearly observed. At the northern end of the lake on Sandai Plain, the Bogoria Silts comprise an onlapping wedge of buff-coloured lacustrine and deltaic silts with minor sandy units (Farrand et al., 1976; Renaut, 1982, 1993). They are actively being eroded from the Sandai Plain, and exhumed and reburied in some cases, by sheetwash, channelized flow, and wave erosion at the modern shoreline. Pockets of the Bogoria Silts remain, particularly on the eastern side of the Sandai River. Other Holocene sedimentary units around the lake include: 1) dark grey and brown coarse-grained sands and gravel beach terraces stabilized by grasses on the western Sandai Plain; 2) several exhumed yellowish to reddish brown, slightly indurated, and bioturbated silty fine-grained sand units at the main Loburu Delta (Fig. *3.1.*14); 3) dark grey and brown coarse sands, likely littoral, at the "old" Loburu Delta; 4) fluvial conglomerates and lacustrine to deltaic silts preserved in the section measured in the Parkirichai River (Figs. *3.1.*5, 6); and, 5) the mid-Holocene stromatolitic "coating", which is present around the lake but preserved mainly around the southern part of the lake (Fig. *3.2.*6).

The trace fossils preserved in these units help to determine the relative timing of these units by improving the paleoenvironmental interpretations. The stratigraphic position of these units is not well understood, particularly when considering: 1) the frequent fluctuations in lake level which contribute to contemporaneous erosion and exhumation of sediments in some areas, but deposition in other areas; and 2) the initial lateral variability in depositional sub-environments and the lateral variability in authigenic mineral cementation of sediments, which is in part related to fault-aligned, point-sourced hot-spring waters. Absolute dates of ~10 ka were obtained from fossil gastropod and mollusc shells preserved in the Bogoria Silts (Young and Renaut, 1979). Shells of the same types are also preserved in the cemented dark grey and brown sandy gravels on the western margin of the lake and suggest that they may be contemporaneous with the Bogoria Silts, although they may have been reworked into the sandy gravels during later high lake levels. Other units potentially contemporaneous with the Bogoria Silts on Sandai Plain include the fluvial and lacustrine to delta-plain facies preserved in the Parkirichai River section, possibly the silty sands sands stabilized by grasses on "old Loburu" (Fig. *3.1.*13), and possibly some of the slightly indurated silty sand units at "main" Loburu. Additionally, some of the silty

sediments of the subaerially exposed southern Loburu Delta are slightly indurated and may correspond to deposition of the southern lobe of the delta during Bogoria Silts time. The deposition of deltaic, lake-margin, and littoral facies at Lake Bogoria is extremely dynamic and complex, and it is unlikely that the precise timing of these units can be determined.

The trace fossil assemblage present in these Holocene units is comparable to the traces produced by flamingos and insects around the modern shorelines of Lake Bogoria (Section 4.1.4). Because many of these sediments are exposed near the present-day shoreline where insect traces (e.g., beetles) are most abundant, they have been largely overprinted by younger traces.

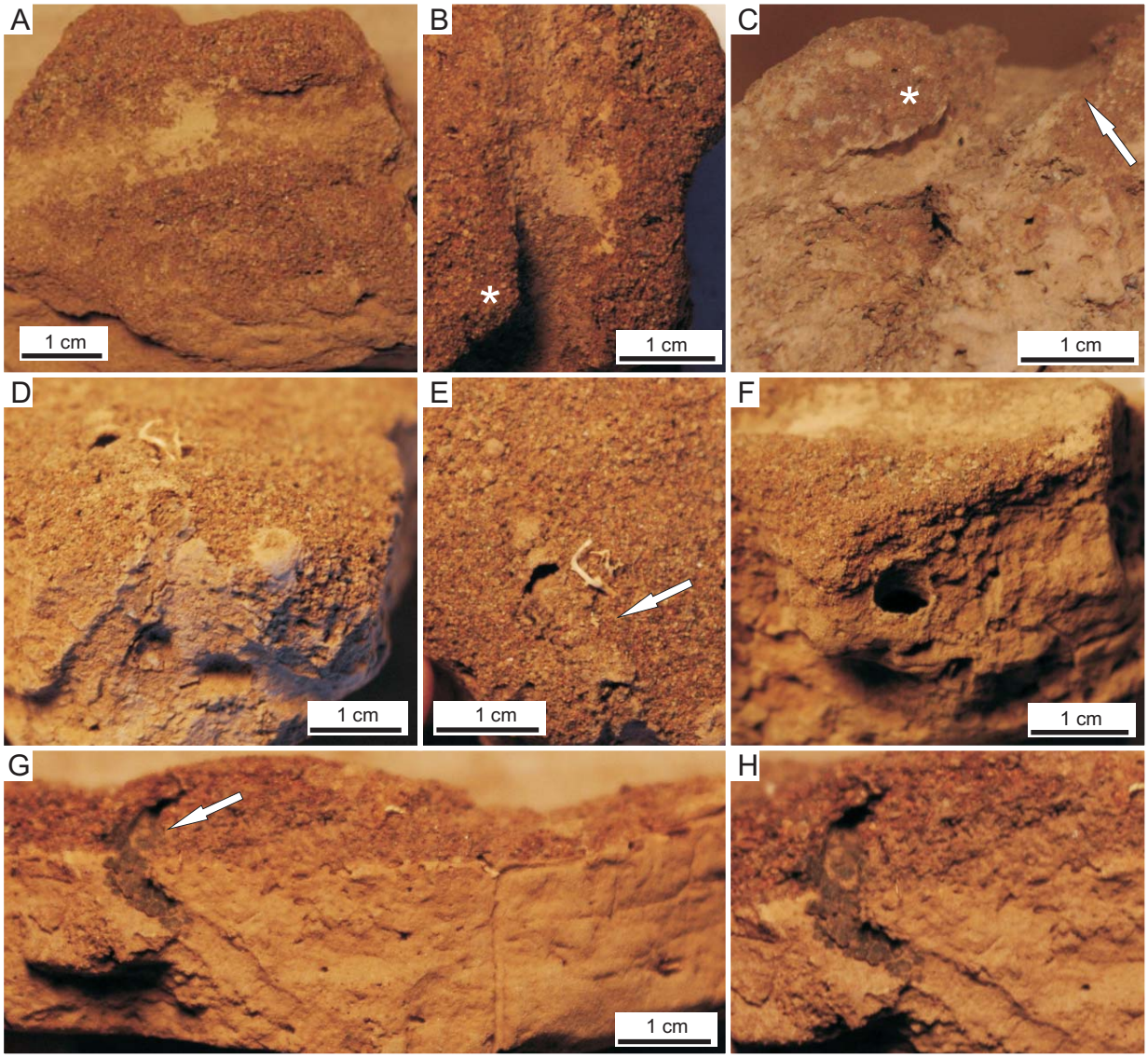


**Fig. 4.1.3.1.** Insect trace fossils from the ?Holocene Bogoria Silts-equivalent sediments exposed in the Parkirichai River, Loburu Delta, Lake Bogoria. All examples are horizontal surface tunnels with vertically oriented branches. **(A–C)** Large horizontal burrow with smooth walls and branch to smaller burrows, possibly produced by crickets. The asterix shown (B) and (C) mark show the same spot in each photo, in a view from above in (B) and from the side in (C). Note different sizes of branches and flattened tunnel of larger, horizontal branch (marked by an arrow in C). **(D–E)** Vertical (D) and horizontally oriented (E) portions of the same tunnel, possibly produced by staphylinid beetles. The roof of the tunnel is not entirely preserved at the top of the bed (arrow in E). **(F)** Close-up of obliquely oriented tunnel with fine-grained burrow lining. **(G–H)** Horizontal surface tunnel (arrow in G) with obliquely oriented vertical portion of same burrow, possibly produced by staphylinid beetles. Note the black-coloured lining.

Two localities preserve Holocene trace fossils that have not been significantly altered by later bioturbation. First, the Bogoria Silts east of the Sandai River on Sandai Plain preserves flamingo nest-mounds (Table 4.4, 4.6; Scott et al., 2008, fig. 9), and second, the lacustrine? and deltaic facies of the Parkirichai River section preserves several types of insect traces (Table 4.4; Figs. *4.1.3*.1–4). Modern traces that obscure the possible Holocene traces in the other units mentioned above are described and discussed in Table 4.5 and Section 4.1.4.

Flamingo nest-mounds are preserved on the uppermost surface of the Bogoria Silts on Sandai Plain (Scott et al., 2008, fig. 9). They were weathered and probably trampled, as well as probably flooded numerous times prior to cementation and exposure. The mounds are low in height relative to modern, freshly made nest-mounds (see Section 4.1.4). In general, they are poorly preserved and difficult to discern from the erosional topography due to modern cattle trails through the area (Scott et al., 2008, fig. 9A). Irregular small-scale topography and undulating mini-escarpments are present along the edges of the nest-mound surfaces (Scott et al., 2008, fig. 9C), which are comparable to the older, trampled, flooded, and eroded modern examples. The precise number of mounds preserved in the Bogoria Silts is unknown, but it may be as many as 40–50. Five, very low-relief mounds are capped with a white crust of unknown mineralogy (Scott et al., 2008, fig. 9C). One of the fossil nest-mounds was sectioned in half to reveal the typical inner structure found in modern flamingo nest-mounds made with muddy sediments: a dense, compacted, inner core with an overlying porous layer (Scott et al., 2008, fig. 9B). Modern flamingo nest-mounds are described in Sections 4.1.4.2 and 4.1.5.1.

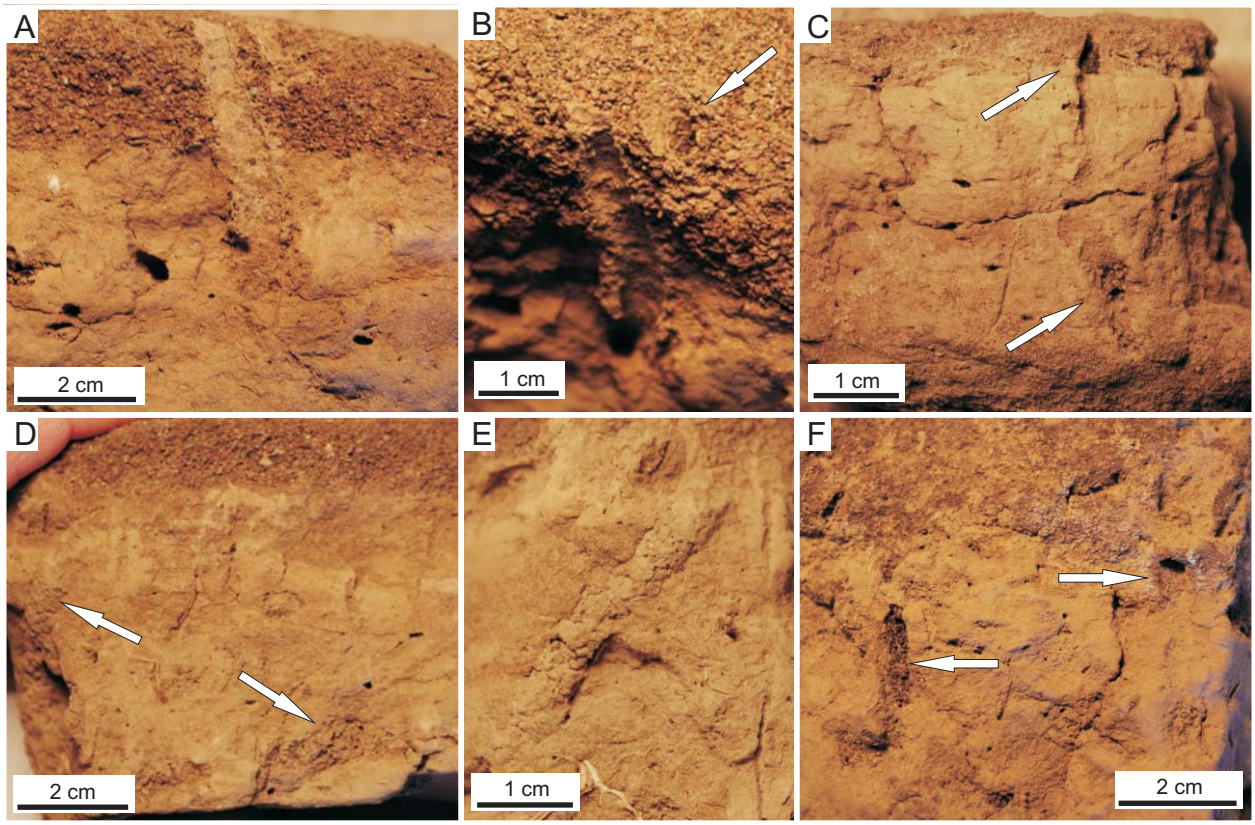


**Fig. 4.1.3.2.** Insect trace fossils from the Parkirichai section, Loburu Delta, Lake Bogoria. All examples are of vertically oriented burrows without evidence of horizontal branches, probably produced by beetles, especially tiger beetles. **(A–C)** Medium-sized vertical burrows with clay-rich lining and partial fill by pelleted/sediment aggregates (C, lower arrow). Burrows may be vertically oriented at surface (arrow in B) and partly constricted in size at the surface (C, upper arrow). **(D–E)** Pellet/aggregate-filled obliquely oriented medium-sized burrows (arrows in D). **(F)** Black lining in vertical burrow at left (left arrow), and open, but partially pellet-filled burrow at right (right arrow).

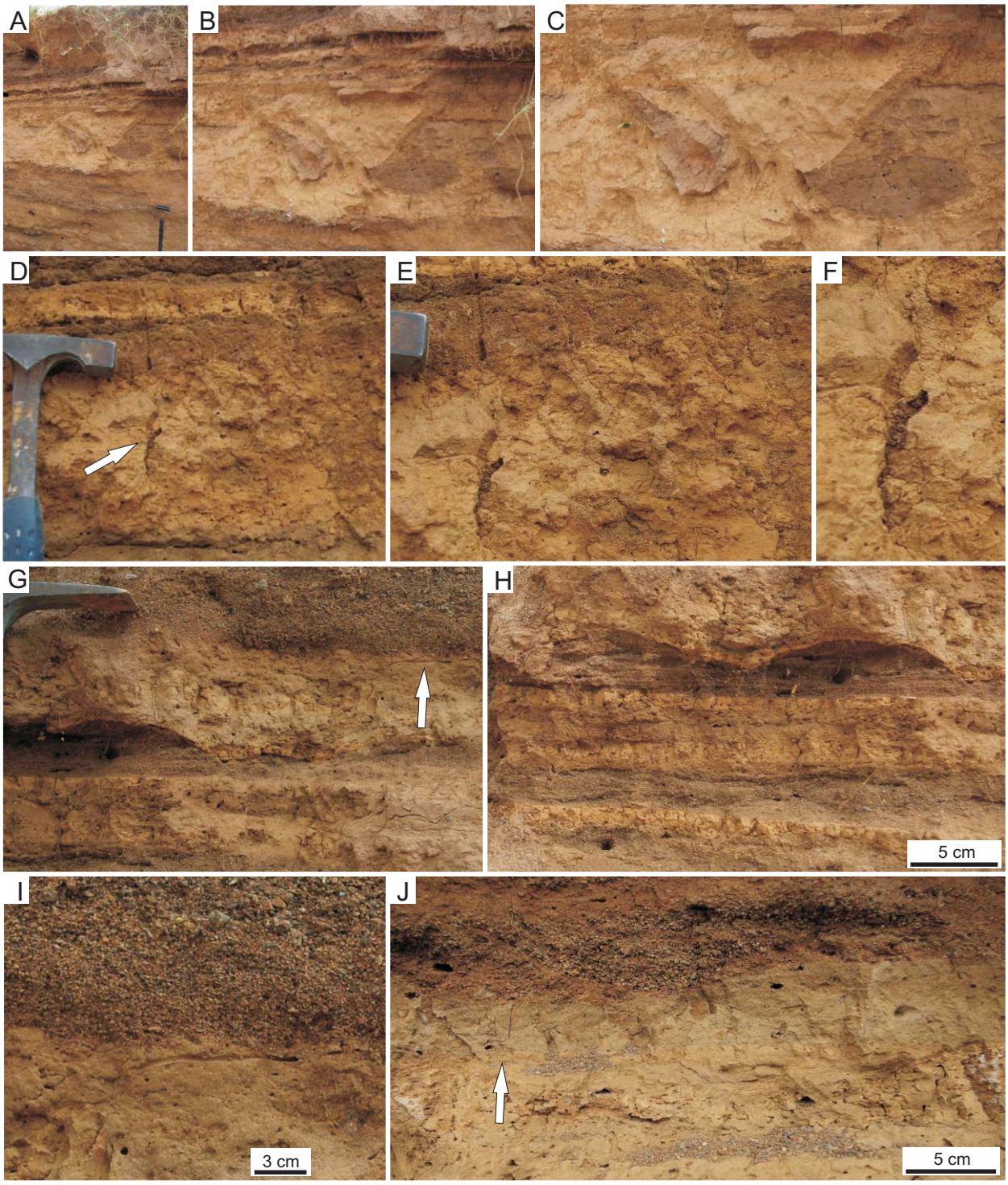


**Fig. 4.1.3.3.** Mammal, insect, and plant traces in the Parkirichai section, Loburu Delta, Lake Bogoria. **(A–C)** Mammal burrow and insect nests? in lower lacustrine silts, originating from sharp contact within silt unit (B, C). Note oblique entrance and spherical chamber of mammal burrow (mongoose?) burrow at left in and termite-like nest at right (B) and (C). **(D–F)** Branched, vertical burrows in upper silt unit showing partial fill of dark-coloured pellet/aggregate material (arrow in D, close ups in E and F). Earwigs are possible producers of these burrows. **(G–J)** the top of the upper silty unit showing bioturbation of silt interbeds (H), horizontal, probable root trace (arrow in G, close up in I), and vertically oriented root trace (arrow in J).

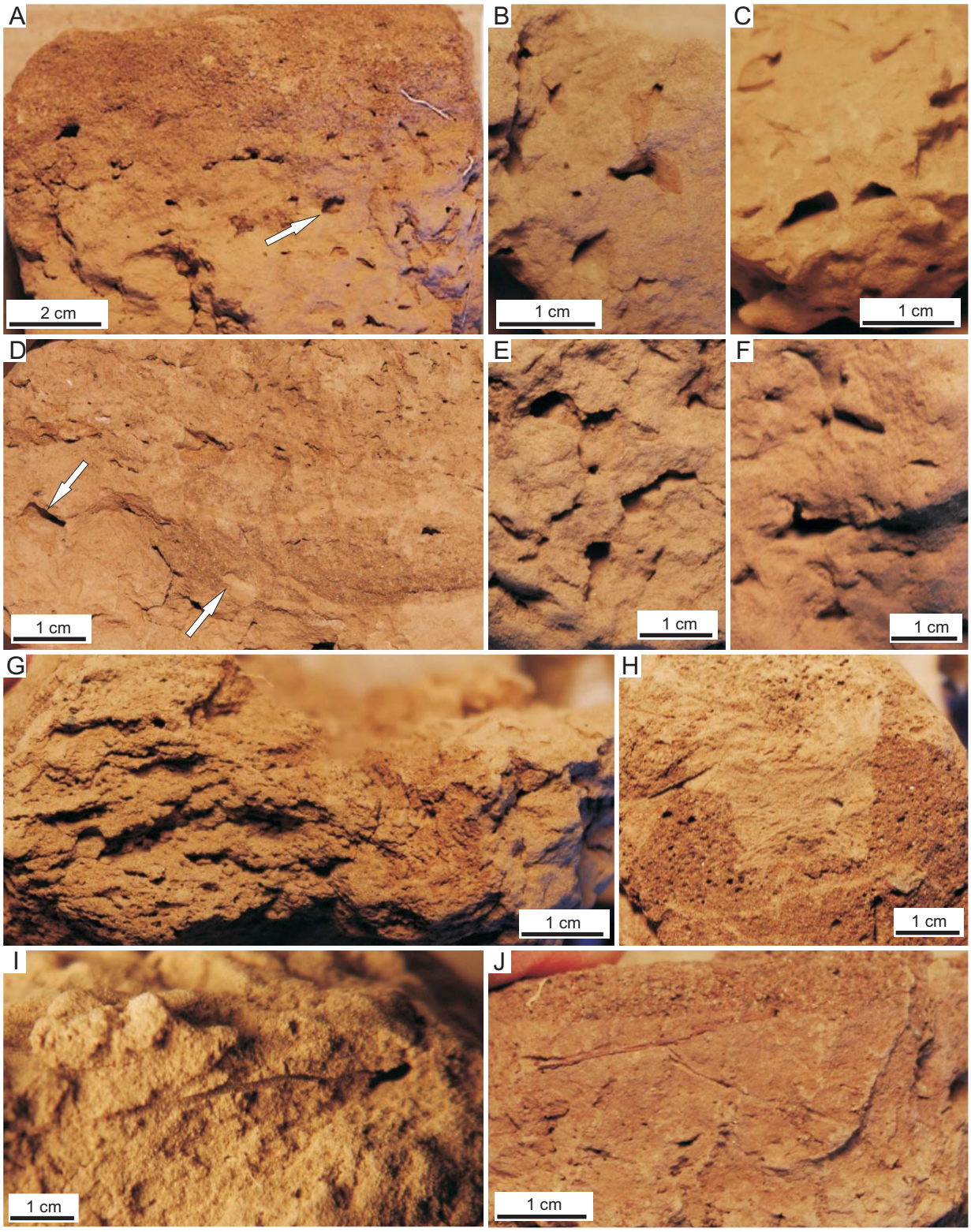


**Fig. 4.1.3.4.** Other biogenic structures in the silty units of the Parkirichai section, Loburu Delta, Lake Bogoria. **(A–F)** Irregularly shaped, open, bubble-like structures with very smooth internal boundaries (arrows in A, D; close-ups in B, C, E, and F). These structures are attributed to the trampling of cohesive sediments by flamingos. **(G–H)** Very small, compressed, bubble-like structures in cross-sectional view (G) and plan view (H). These structures are interpreted as gas escape bubbles from microbial mats. **(I–J)** Small root marks in cross-section (I) and plan view (J).

**Table 4.4.** Trace fossils and associated biogenic-derived structures of the Late Pleistocene–Holocene Bogoria Silts and other Holocene sediments in the Bogoria Basin. Trace types in this table are grouped by locality.

| Fig. | Trace type | Ichnotaxonomy | Description | Comments | Possible tracemaker | Inferred environment | Locality |
|---|---|---|---|---|---|---|---|
| Scott et al., 2008, fig. 9 | Flamingo nest-mounds | none available | Mounds of silty mud with dense internal core and outer, more porous and friable layer; width at base (average: 23 cm) greater than width at top (average: 17 cm); average height: 6 cm; may have slight depression at top and/or whitish crust at top; may be present in groups or linear patterns; associated with irregular, undulating surfaces | Associated with ped-like, non-paleosol fabric in lacustrine silts | Lesser flamingos | Shoreline and exposed littoral/lacustrine | Sandai Plain, east of Sandai River |
| Fig. *4.1.3.* 1A–C | Horizontal tunnels | cf. *Palaeophycus* isp. | Open, large, ?branched, horizontal tunnels with smooth internal margins; internal margins lined with clay; slightly oval-shaped or compressed vertically; approximately 1 cm in width, ~1 cm height; branched into open, smaller (~5 mm diameter) oblique burrow that may have been produced from a different trace maker | Unclear if branching is true branching or secondary from different trace maker (e.g., Heteroceridae) | Likely crickets; modern examples produced by king crickets | Wet to saturated subaerial substrates (modern examples at shoreline) | Parkirichai River section, south Loburu Delta |
| Fig. *4.1.3.* 1C–H | Horizontal tunnels with oblique burrows | cf. *Palaeophycus* isp. | Open, medium-sized horizontal tunnels with an oblique burrow; partially lined by clays; may be lined with Mn-oxihydroxides possibly related to a microbial matter lining; diameter ~4.5 mm | May be associated with oblique vertical burrows | Likely beetles: staphyinids and/or heterocerids | Wet, subaerial substrates | Parkirichai River section, south Loburu Delta |
| Fig. *4.1.3.*3I | Horizontal tunnels (or root trace?) | cf. *Planolites* isp. | Open, unbranched, horizontal tunnels with smooth internal margins; may have clay-rich lining; undulating to perfectly horizontal along bedding planes; tunnels ~4–5 mm in diameter | Very similar to horizontal ‘tunnels’ of plant rhizomes | Insects (e.g., beetle larvae) or roots | Wet, subaerial substrates | Parkirichai River section, south Loburu Delta |
| Fig. *4.1.3.* 2A, B, D–F | Vertical burrows | *Skolithos* isp. | Medium-sized, sometimes lined, vertical to slightly oblique burrows; may be open, or contain clumps of pellet/aggregate fill, or be entirely filled with pellet/aggregates; lining more clay-rich than host; may be slightly narrower at surface; diameter ~4.5 mm at surface, expanding to < 7 mm at ~2 cm depth; fill same as host material or much darker | Likely more than one type included here | Likely tiger beetles, staphylinids, or carabids | Moist, subaerial substrate | Parkirichai River section, south Loburu Delta |

| | | | | | | | |
|---|---|---|---|---|---|---|---|
| Fig. *4.1.3*. 2C | Vertical burrows | cf. *Skolithos* isp. | Small, open, sinuous vertical burrow with constricted, narrow opening to surface and locally concentrated pellet/aggregate fill to side of burrow; walls not sharp; Mn-oxihydroxide lining of burrow opening | Mn-oxihydroxide lining suggests anoxic, saturated conditions | Likely staphylinid beetles | Moist to wet subaerial substrate | Parkirichai River section, south Loburu Delta |
| Fig. *4.1.3*. 3D–F | 3D boxwork burrow system | cf. *Thalassinoides* isp. | Open and pellet-filled, branched burrow system; fill different than host and dark grey brown at Parkirichai; burrows ~1 cm wide; burrow margins unlined and sharp; burrow orientations dominantly vertical and oblique | Greater bioturbation upwards | Insects; possibly earwigs (Dermaptera) | Wet, subaerial, firm substrates | Parkirichai River section, south Loburu Delta |
| Fig. *4.1.3*. 3A–C | Mammal burrows? | None available | Large oblique burrow with expanded oval-shaped terminus; burrow opening ~7 cm wide; width at widest point ~25 cm; burrow margins sharp; unlined/unwalled | Indicates subaerially exposed surface | Unknown mammal?; possibly mongoose | Dry, subaerial, well drained substrate | Parkirichai River section, south Loburu Delta |
| Fig. *4.1.3*. 4A–F | “Trample bubbles” | n/a | Open, isolated, bubble-like pores in clay-rich sediments; most examples oval-shaped; may be compacted; approximately 0.5–1.0 cm wide and ~0.5 cm high; internal margin very smooth, but irregular; may be perforated with small (~2 mm) root pores | Likely only form in clay-rich sediments | Lesser flamingos | Shoreline and exposed littoral/shallow lacustrine | Parkirichai River section, south Loburu Delta |
| Fig. *4.1.3*. 4G, H | Gas escape bubbles | n/a | Very small to small (< 1 mm to ~3 mm diameter), compressed, circular to oval-shaped holes; found in high densities mainly in sandy substrates | Compare with modern examples | Microbial mats | Wet substrates; possibly with hot spring seepage | Parkirichai River section, south Loburu Delta |
| Fig. *4.1.3*.3J | Mn-oxide lined root pores | n/a | Vertically oriented, branched, small root pores lined with Mn-oxides; branching is downwards; ~1–2 mm diameter; length ~5 cm | From upper, eroded surface of lacustrine/deltaic unit | Unknown | Delta plain with salt efflorescence | Parkirichai River section, south Loburu Delta |
| Figs. *4.1.3*. ?3I, 4I–J | Open root pores | n/a | Small (~2 mm diameter), open, vertical and horizontal root traces; may preserve branching of tiny root hairs; root pores may open in to “trample bubbles”; appear lined with clay-rich smooth lining | Roots may be contemporaneous with subaerial animal traces, and/or modern | Unknown | Subaerial substrates | Parkirichai River section, south Loburu Delta |
| Fig. *4.1.3*. 5A–D | Vertical burrows | *Skolithos* isp. | Vertical, apparently passively filled burrows ~4–6 mm in diameter; density is high, creating a *Skolithos* ichnofabric with BI=~4 | Age of burrows unclear; may be recent and/or Holocene | Insects; likely beetles (Cicindelidae: tiger beetles?) and/or spiders | Subaerially exposed lacustrine? | Exhumed surface, Loburu Delta |

| | | | | | | | |
|---|---|---|---|---|---|---|---|
| Fig. *4.1.5*.12 | Open, 3D burrow network | ? cf. *Thalassinoides* isp. | Burrow network with vertical, horizontal and oblique open burrows and expanded areas; walls sharp; burrows ~0.8–1.2 cm in diameter; expanded areas tend to be oriented obliquely and horizontally, and range from 1–2 cm high and 3 cm wide; modern burrows may be formed in old burrow systems; modern burrows are partly actively filled with pelleted sediment aggregates | Age of burrows unclear; may be recent and/or Holocene; burrow system is active today, but may be reusing old network | Insects; likely earwigs, ants, and/or spiders | Subaerially exposed lacustrine? | Exhumed surface, Loburu Delta |
| Fig. *4.1.3*. 6A–D | Chironomid pupal cases | n/a | Small, open pupal cases; attached to a hard substrate; pupal cases are cemented by carbonate, but mainly remain open; internal diameter ~1–1.5 mm; external diameter ~2–2.5 mm; cases < 5 mm long; may be present in clusters of < 50–100 pupal cases; some examples may be tube-structures used by larvae | May possibly be forming today; modern examples are found together with fossil examples | Insects; pupal cases and/or tube-structures of larval Chironomidae | Oxic lacustrine | Stromatolitic coating, south sub-basin, Lake Bogoria |
| Fig. *4.1.3*. 6E, F | ? Branching burrow network | cf. *Labyrintichnus* isp. | Branching network of open tunnels; regular diameter of tunnels, ~1.5 mm; tunnels oriented in all directions and curved, meandering, and straight | May be fluid channels between stromatolite columns | Possibly larval Chironomidae | Oxic lacustrine | Stromatolitic coating, south sub-basin, Lake Bogoria |

Animal trace fossils preserved in the “Bogoria Silts” of the Parkirichai River section include: 1) three types of horizontal tunnels with or without an oblique burrow component, possibly attributable to beetles and crickets (Fig. *4.1.3.*1); 2) open and backfilled vertical and oblique burrows, attributable to tiger beetles, staphylinid beetles, and/or carabid beetles (Fig. *4.1.3.*2); 3) possible mammal burrows (Fig. *4.1.3.*3A–C); and, 4) pellet/aggregate-filled 3D branching burrow network, likely attributable to earwigs (Fig. *4.1.3.*3D–F). Many of the open tunnels may also be attributable to rhizomatous roots, just as in the modern setting on the southern Loburu Delta (Fig. *4.1.3.*3I, 4I–J). Downward-branching, vertical, Mn-oxihydroxide lined vertical roots are also preserved (Fig. *4.1.3.*3J). Modern roots have also bioturbated the unit. Some small, irregular, spherical to oval-shaped structures present within the finer-grained silt beds may be attributable to 'bubbles' formed in modern shoreline and littoral mud by the trampling of flamingos (Fig. *4.1.3.*4A–F). Flamingo trampling may have also contributed to the ped-like, but non-paleosol, fabric of the Bogoria Silts near the Sandai River (S. Driese, pers. comm., 2002; Scott et al., 2008, fig. 9D). Other structures preserved in the Parkirichai section include: 1) sharp-edged structures that may be attributable to mammal footprints (Fig. *4.1.3.*4D); and 2) very small, oval-shaped, smooth-walled holes attributable to gas escape bubbles in microbial mats (Fig. *4.1.3.*4G, 4H).

The trace types listed above are not signatures of lacustrine environments, but together, and with comparison to the modern trace assemblage in the lake-margin zone, they signify repeated changing conditions from wet muddy substrates to drier substrates with lower water tables. Although the interpretation of the finer-grained unit is of fluctuating lake levels and

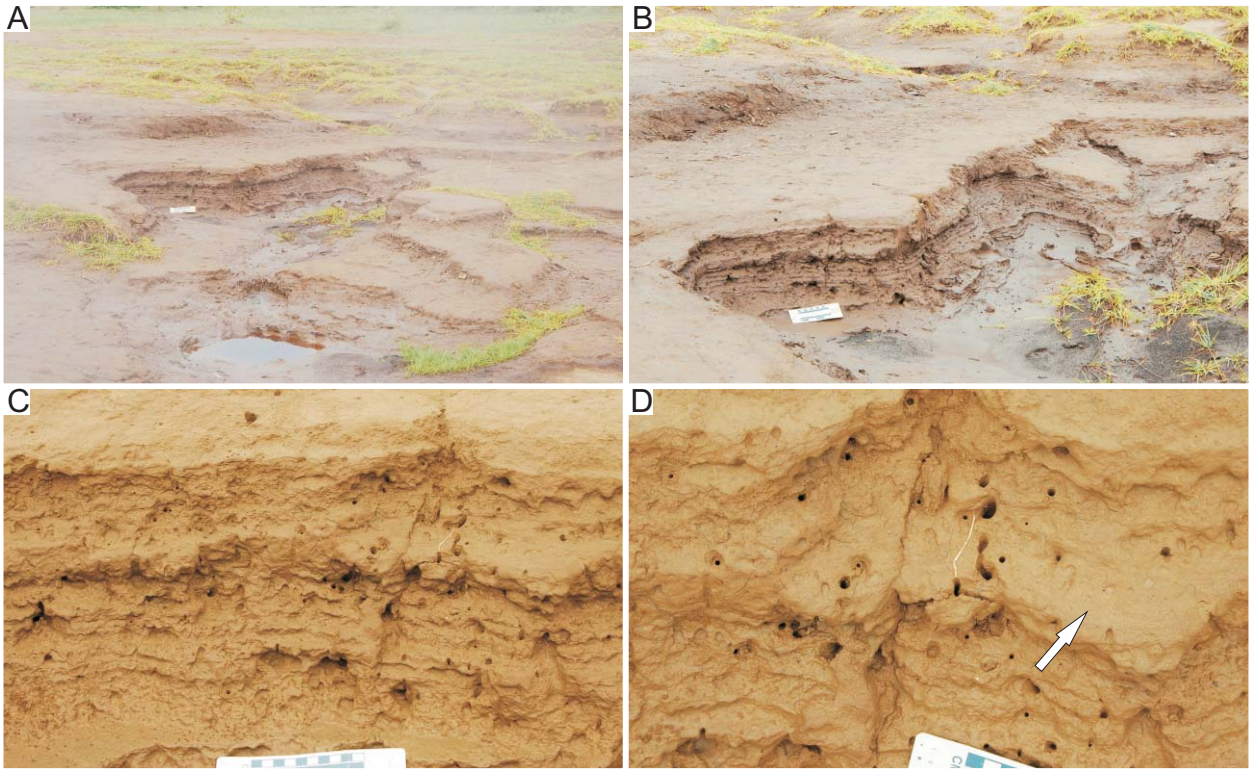


**Fig. 4.1.3.5.** Recent vertical burrows overprinting ?Holocene bedded lacustrine silts at the main site of the Loburu Delta, Lake Bogoria. **(A–B)** These bedded silts (Bogoria Silts equivalents?) have been exhumed and eroded by littoral processes and hot-spring outflow. **(C–D)** Several generations of vertical burrows, probably of tiger beetles, are produced in these “exhumed” surfaces during periods of subaerial exposure. The arrow in (D) is showing a silt-filled, older vertical burrow.

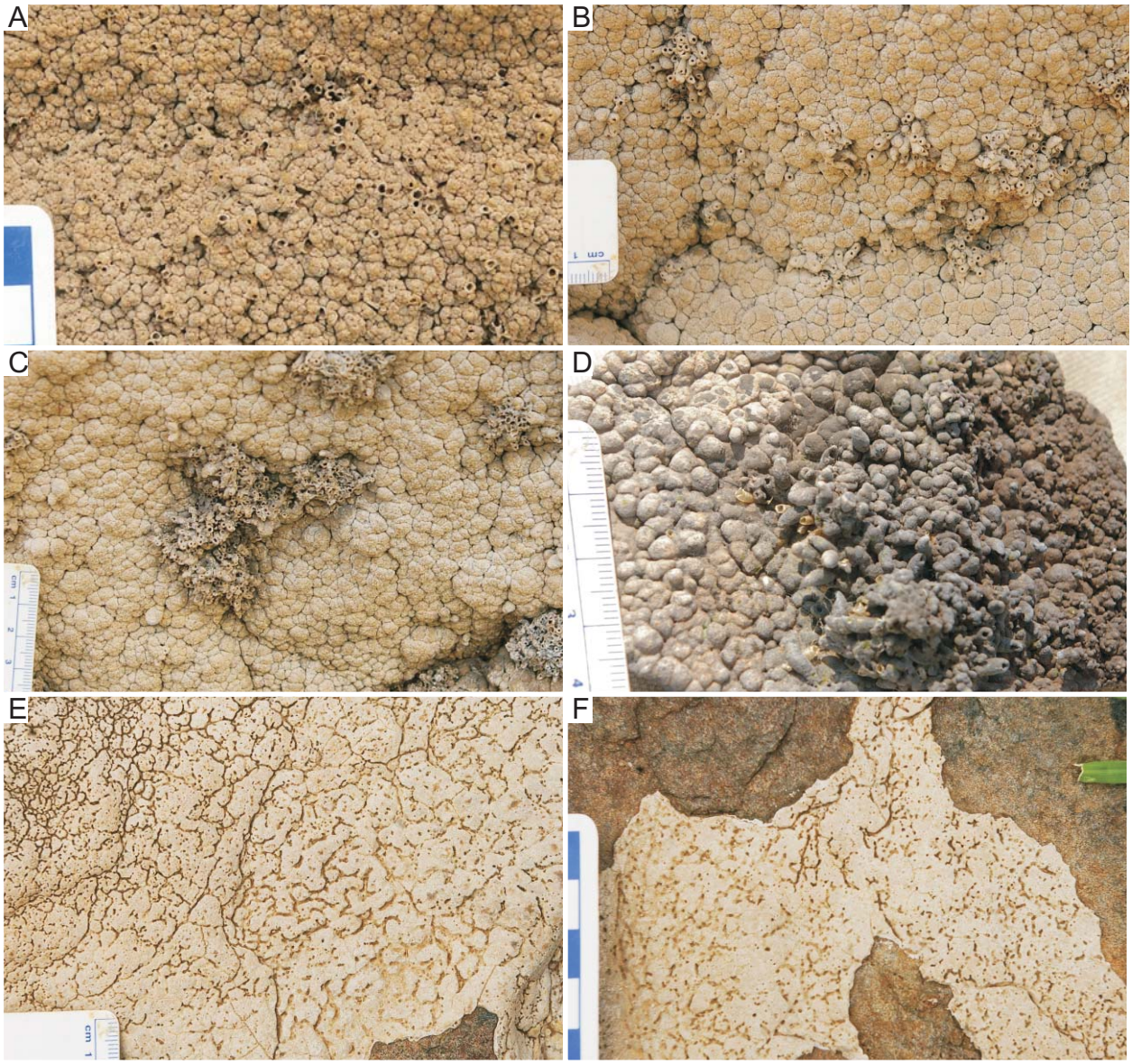


**Fig. 4.1.3.6.** Insect traces in lacustrine stromatolitic coatings, Lake Bogoria. **(A–D)** Chironomid tube-structures and pupal cases preserved in carbonate. Note modern, uncemented pupal cases in (D). **(E–F)** Possible chironomid tunnel networks visible in eroded portions of the stromolitic coating.

repeated regressive successions from lacustrine to subaerially exposed delta-plain facies, the trace fossil assemblage does not unequivocally signify either a lacustrine/delta-plain or ephemeral fluvial setting. If compared with the fluvial succession at Nyongonyek, the traces preserved in the Parkirichai section provide support for wet substrates and a shallow water table. The large horizontal tunnels, comparable to mole cricket tunnels (Fig. *4.1.3.*1A–C), are found today only at the shoreline at Loburu. The lithofacies assemblage at Parkirichai lacks evidence of extensive pedogenesis prior to the modern soil, but does have several thick, discrete beds of clayey silt that coarsen upwards to reddish fine-grained sands that have been disrupted by salt efflorescence. The lacustrine/delta-plain facies in the Parkirichai section appear comparable with the modern south Loburu Delta plain but contain a higher proportion of lacustrine clayey silts.

The slightly indurated silty sands near the hot springs at Loburu also preserve animal and root traces that may or may not be Holocene in age (also see Section 4.1.4). They are described

briefly here. First, several examples of densely bioturbated *Skolithos* isp. ichnofabrics with trace diameters from 4–6 mm are present in an exhumed, indurated surface younger than the Loboi Silts (Fig. *4.1.3*.5A–D). Second, a 3D network of burrows with sharp, irregular walls and variable diameters (0.8–1.2 cm), as well as horizontally and obliquely oriented expanded areas (1–2 cm high, < 3 cm wide), is preserved in another slightly indurated exhumed surface near the present-day shoreline. This network is likely attributable to earwigs (Section 4.1.5.4). Today, these exhumed surfaces and possibly the sub-fossil burrows are being reused by beetles, earwigs, and spiders.

Finally, the mid-Holocene lacustrine stromatolitic coating preserves chironomid pupal cases (Fig. *4.1.3*.6A–D). Network-like tunnels (cf. *Labyrintichnus* isp.) in the stromatolitic coating may also be attributable to chironomid larvae (Fig. *4.1.3*.6E–F). Alternatively, these structures may simply be due to the weathered growth patterns of columnar micro-stromatolites.

### *4.1.4. Modern Traces and Trace-Makers in the Bogoria Basin*

A high diversity assemblage of animal and plant traces is present in the littoral, deltaic, delta-plain, eulittoral to supralittoral, and soil facies assemblages present around modern Lake Bogoria. The main focus of research at Lake Bogoria was on the delta-plains and shorelines at Sandai Plain and Loburu Delta, although several other localities along the western and southern margins of the lake were also investigated (Fig. 2.2). The composition, diversity, and taphonomic signatures of the assemblage vary laterally with changes in substrate characteristics, depth of the water table, proximity to the shoreline, proximity to fresh water, temperature of water source, and the presence of abundant microbial food sources. The various types of invertebrate, vertebrate, and plant traces and trace fossils have been described by Scott et al. (2007, 2009) and are summarized here in Table 4.5. New data obtained in August, 2008 and August, 2006 (courtesy of R. Renaut) is considered in the descriptions and discussions here, and helps to provide a better understanding of some of the invertebrate trace maker identities, as well as the associations with lithofacies. However, no detailed descriptions were made about the vertical and oblique burrows of spiders, which were observed directly in burrows near the shoreline and within the exhumed surfaces at Loburu delta. The traces of flamingos have been previously described in part by Scott et al. (2003, 2007, 2010). Using a combination of both modern and fossil traces from Lake Bogoria, Scott et al. (2009) divided the assemblage into five suites based on observed associations with particular environmental controls and proximity to shoreline. The suites may vary by locality in terms of diversity and may consist of monospecific examples under particular conditions (e.g., high salinity; lack of cyanobacterial mats).

The suites comprise groups of traces that are commonly found together under similar environmental conditions and are roughly correlated to the proximity to the shoreline at Lake Bogoria. Their position relative to the shoreline depends on the lake-margin gradient and depth to the water table. Lateral variability in the composition of each suite depends in part on the proximity to freshwater and microbial food sources, as well as other observed conditions such as substrate grain-size and degree of consolidation or induration. The suites are similar to ichnocoenoses but they also include traces that are present under slightly different conditions, which fluctuate frequently at Lake Bogoria. Together, the assemblage represents the Mermia and Scoyenia ichnofacies, the informal “shore-bird” and “Termitichnus” sub-ichnofacies, and possibly a subaerial example of the Skolithos ichnofacies.

**Table 4.5.** Modern animal traces at Lake Bogoria. Descriptions of trace types marked with an asterix (*) have been taken from Scott et al. (2009). Trace types marked with a cross (†) have also been described by Scott et al. (2007). Trace types marked with a section sign (§) are described from new data obtained in August, 2008 or 2006 (courtesy of R. Renaut). Trace types are organized by the suites used by Scott et al. (2009).

| Fig. | Trace type | Ichnotaxonomy | Description | Comments | Tracemaker | Environment | Localities |
|---|---|---|---|---|---|---|---|
| *Suite 1: "Chironomid" Suite* | | | | | | | |
| Scott et al., 2009, fig. 6A–D | * Tube-structures | None available | Millimeter-sized, straight to curved, non-branching, horizontal tube structures are approximately 0.5 cm to 4 cm in length and comprised of loose detritus and organic material that settled on an exhumed surface. | Associated with benthic microbial mats on firm substrates | Insects; chironomid larvae (Diptera) | Littoral zone with abundant microbial detritus or benthic mats | Western shoreline, north of Loburu |
| Fig. *4.1.3.* 6D | § Pupal cases | n/a | Open tube-like pupal cases; 1.5 mm diameter; < 5 mm long; attached to hard, stromatolitic substrate and found together with fossilized examples cemented by carbonate; may be in clusters of several to tens of pupal cases | Found with fossilized examples in the "stromatolitic coating" | Insects; chironomid pupae (Diptera) | Oxic lacustrine | Southern sub-basin |
| Scott et al., 2009, fig. 6E | * "Pits" | None available | (< 1 cm diameter) shallow, circular- and irregular-shaped "pits" into a moderately indurated substrate; may be connected to vertical burrow | Associated with microbial mats on firm substrates | Insects; chironomid larvae (Diptera) | Littoral zone with abundant microbial detritus or benthic mats | Western shoreline, north of Loburu |
| Scott et al., 2009, fig. 6E–F | * Vertical burrow | Incipient *Skolithos* isp. | Small (~3 mm diameter) vertical burrows into moderately indurated substrate; burrow area brown in colour (oxygenated), in contrast to black, presumably anoxic substrate | Associated with tube-structures and burrows into muddy sediment | Insects; likely chironomid or tiger beetle larvae | Anoxic sediments below oxic littoral zone | Western shoreline, north of Loburu |
| *Suite 2: "Flamingo Nest-Mound" Suite* | | | | | | | |
| Fig. *4.1.5.* 1–4 | † § Nest-mounds | None available | Flattened cone-shaped mounds of mud with slight depressions in centre of upper surface; dimensions vary with age of mound, degree of trampling, and stage of building; base wider than top, and height ~1/3 base width; base width ranges from ~22–39 cm; top width ranges from ~12–28 cm; height varies from ~5–15 cm; has dense internal core at base (~1/2 base width and ~1/2 height) and porous outer layer, thicker at top; materials used vary; old nests may be rebuilt; may include feathers and twigs, and bones in porous layer; may include a thick layer (~ 5 cm) of feathers mixed with mud at top | Morphology is variable depending on age of nest, materials used, and if flooded or rebuilt | Lesser flamingos | Shoreline and subaerially exposed littoral/lacustrine | Mainly at mouth of Sandai River and Loburu Delta area |

| | | | | | | | |
|---|---|---|---|---|---|---|---|
| Scott et al., 2007, figs. 3A, 3B, 6A–G; Fig. *4.1.4.* 10C | † § Footprints (flamingos) | Flamingo footprints | Webbed, 3-toed footprints lacking hallux impression; posterior margin very rounded; ~10 cm wide and ~7 cm long, depending strongly on substrate conditions; third digit longest; digits II and IV same length; divarication angles variable, but range from ~35–70° between digits II and III, and IV and III; webbing to tips of toes; claws often impressed; digits do not show pronounced nodes at tarsal articulations; prints often show skin impressions; morphology strongly dependent on substrate conditions | Morphology is variable depending on substrate; associated with flamingo-trampled surfaces | Flamingos; mainly Lesser Flamingos; similar footprints include Egyptian Geese; other webbed tracks of teals much smaller | Delta-plain, shoreline, and exposed littoral/lacustrine | Mainly at mouth of Sandai River and Loburu Delta area; entire shoreline |
| n/a | † § Footprints (shorebirds) | Shorebird footprints | Small, unwebbed footprints without hallux impressions (plovers), or with hallux impression separated from posterior margin (sandpipers); digits II, III, and IV directed forward, digit III slightly longer; posterior margin pointed; size variable depending on species but range from ~2–4 cm long and ~3–5 cm wide, excluding hallux; tracks wider than long, excluding hallux | The abundance and distribution of bird footprints is necessary to determine their inclusion in this suite | Shorebirds or sandpipers; esp. plovers such as Blacksmith Plover | Delta-plain, shoreline; ephemeral streams and perennial rivers | Mainly at mouth of Sandai River and Loburu Delta area |
| Fig. *4.1.4.* 8A, 8B | † § Footprints (storks) | Stork footprints | Large, thick-toed, clawed bird footprints with three forward facing digits and long, straight pronounced hallux directed towards inside; entire hallux impressed; nodes at tarsal articulation points pronounced; unwebbed; divarication angles ~70–75° on each side; digits I and III ~10–12 cm in length and 2 cm wide; digits II and IV ~9–10 cm in length; dimensions dependent on substrate conditions but typically 20–22 cm long and ~18–20 cm wide; digits may be separated from central metatarsal impression; metatarsal impression circular | The abundance and distribution of bird footprints is necessary to determine their inclusion in this suite; if at shoreline, associated with flamingos footprints | Storks; esp. Marabou stork; similar tracks are those of herons, but they are smaller and more gracile | Delta-plain, shoreline; ephemeral streams and perennial rivers | Mainly at mouth of Sandai River and Loburu Delta area |
| *Suite 3: "Mermia-like" Suite* | | | | | | | |
| Scott et al., 2009, fig. 7A | * † Surface trails | Incipient *Gordia* isp. | Epichnial, horizontal, unbranched, small (1–2 mm), unilobed trails that are self-crossing and looping and were observed to be up to 10 cm in length | Also "preserved" as "salt tracks and trails" | Insects; likely beetle (Coleoptera) or fly larvae (Diptera) | Shallow, subaqueous substrate; associated with hot-springs | "Main" Loburu Delta |
| Fig. *4.1.4.* 2C–H | * † Surface trails | Incipient *Helminthoidichnites* isp. | Epichnial, horizontal, unbranched, small (1–2 mm), unilobed trails up to several centimeters in length that are straight to slightly curved | Also "preserved" as "salt tracks and trails" | Insects; likely beetle (Coleoptera) or fly larvae (Diptera) | Shallow, subaqueous substrate; associated with hot-springs | "Main" Loburu Delta |

| | | | | | | | |
|---|---|---|---|---|---|---|---|
| Fig. *4.1.4.* 2A; Scott et al., 2009, fig. 7C, 7E | * Surface tunnel network | Incipient *Labyrintichnus* isp. | Mainly horizontal, smooth-walled, convex epichnial branched networks comprised of intersecting and crossing, open, straight to curved, and sometimes looping horizontal tunnels in two size modals (1–2 mm wide and 3–4 mm wide); the burrow system is three-dimensional and has oblique to vertical tunnels that connect the horizontal networks which can be up to ~2 m in length; vertical dimensions of the networks were not measured | Unclear if tracemakers of incipient *Labyrintichnus* and incipient *Vagorichnus* are different | Insects; likely beetle larvae and/or certain beetle adults (e.g., Staphylinidae, Heteroceridae, Elateridae, Carabidae); or, fly larvae (Diptera) | Shallow, subaqueous substrate in fresh water; associated with hot-springs | "South" Loburu Delta |
| Figs *4.1.5.* ?10; Scott et al., 2009, fig. 7F, 7I–J | * † Surface tunnel network | Incipient *Vagorichnus* isp. | Lined, three-dimensional, hypichnial and endichnial branched network of straight to slightly curving walled tunnels (4–5 mm width) that are actively filled, commonly with < 1 mm spherical pellets; the pellets appear to be made up of sediment identical to the host substrate; the size of the networks can be up to several meters in horizontal dimensions, and depths of up to 10 cm were observed | Unclear if tracemakers of incipient *Labyrintichnus* and incipient *Vagorichnus* are different | Insects; likely beetle larvae and/or certain beetle adults (e.g., Staphylinidae, Heteroceridae, Elateridae?, Carabidae?) | Wet substrate; associated with hot-springs | "South" Loburu Delta |
| *Suite 4: "Scoyenia-like" Suite* | | | | | | | |
| Figs. *4.1.4.* 5D; *4.1.5.* 8A | * Pellet-filled burrows | "Pellet-filled burrows A" – emended | Unwalled, pellet-filled (pellets are < 1mm), branching endichnial burrow systems composed of horizontal burrows (< 4–5 mm diameter) along buried bedding planes and regular, perpendicular vertical branches less than ~10 cm below the sediment-air interface; pellets are composed of material similar to the host sediment in grain size and colour; these systems are connected with convex epichnial, branching, pellet-walled burrow systems at the surface; burrow boundaries smooth where not filled with pellets | All pellet-filled burrows with pellets of same composition as host material may be produced by same trace maker and found in close association | Insects; possibly larval to adult beetles such as Staphylinidae (e.g., *Bledius*) or Carabidae? | Microbe-rich, subaerially exposed wet substrates; associated with dried pools fed by hot "seepage" springs | "South" Loburu Delta |
| Figs. *4.1.4.* 5E; *4.1.5.* 7E, 7I | * Pellet-filled burrows | "Pellet-filled burrows B" – emended | Unlined/unwalled, vertical and horizontal, unbranched burrows ~4 mm in diameter; partly to completely filled with spherical pellets (~0.5 mm diameter) of material similar to host sediment; may be present in anoxic sediments < 15 cm deep, with oxygenated zone around burrow | One example shows both spherical and elongate pellets in same burrow | Insects; possibly larval to adult beetles such as Staphylinidae (e.g., *Bledius*) | Microbe-rich, subaerially exposed wet substrates; associated with dried pools | "South" Loburu Delta |

| | | | | | | | |
|---|---|---|---|---|---|---|---|
| Fig. *4.1.5.* 8B, 8C | * Pellet-filled burrows | "Pellet-filled burrows C" – emended | Unlined/unwalled, vertical burrows ~4 mm in diameter that are partly filled with elongate fecal pellets (< 0.5 wide, 4–5 mm long) similar in colour and grain size to the host sediment; observed examples were less than 5 cm in length; pellets contain more clay than host | One example shows both spherical and elongate pellets in same burrow | Insects; possibly larval to adult beetles such as Staphylinidae (e.g., *Bledius*) | Microbe-rich, subaerially exposed wet substrates; associated with dried pools | "South" Loburu Delta |
| Figs. *4.1.5.* 7B, 7F–G 8E, 8F | * Larval or pupal cells | "Tear-drop larval burrows" - emended | Vertically oriented, tear drop-shaped, open endichnial burrows up to 5 mm in diameter, with short 1–2 mm wide vertical open burrows that exit to the air-sediment interface; the tear drop may contain ~0.5 mm diameter spherical pellets sub-spherical, and of similar composition to the host substrate, but the exit hole to the surface remains open; bottom of chamber below surface is 1.5–2 cm | May be produced by larvae of other pellet-filled burrow trace maker, or by different species (perhaps also a staphylinid) | Insects; possibly larval to adult beetles such as Staphylinidae (e.g., *Bledius*) | Microbe-rich, subaerially exposed wet substrates; associated with dried pools fed by hot "seepage" springs | "South" Loburu Delta |
| Fig. *4.1.5.* 7H, 7K | § Expanded chambers | cf. "Pellet-filled burrows B" | Obliquely oriented burrows with "wine-bottle"-shaped expanded, chamber-like areas; partially filled with elongate pellets; smooth to slightly ornamented burrow boundary; expanded area attached to burrows ~3–4 mm wide; expanded area < 6–7 mm wide and ~4 cm long | Transitional to "Pellet-filled burrows B" and "tear-drop burrows" | Insects; possibly larval to adult beetles such as Staphylinidae (e.g., *Bledius*) | Wet substrate; high water table; fluctuating lake-levels | "South" Loburu Delta |
| Fig. *4.1.4.* 3D | * Open tunnels | "Upside-down J-shaped burrows" – emended | Small (1–2 mm wide), straight, open, unlined/unwalled tunnels that curve from vertical tunnels onto buried bedding planes, making an upside-down J-shape; internal burrow boundary smooth | Horizontal along bedding planes | Larval insects; possibly beetle or fly larvae | Wet to saturated substrates; microbe-rich sediments | "South" Loburu Delta |
| Fig. *4.1.4.* 3A, 3E | § Open tunnels | Incipient ?*Planolites* isp. | Small (1–2 mm wide), unlined, open horizontal burrows; observed being produced just below subaerially exposed surface | May be transitional with "Upside-down J-shaped burrows" | Larval insects; possibly beetle or fly larvae | Wet to saturated substrates | "South" Loburu Delta |
| Figs. *4.1.4.* 5B–C, 5G–H; *4.1.5.* 6 | * Vertical burrows | Incipient *Skolithos* ispp. | Vertical to oblique, unlined/unwalled, unbranched burrows in three size classes: 1–3 mm, 4–6 mm, and 10–12 mm; burrow depths are ~5–20 cm; burrow margins may be ornamented with "wrinkles" if made in slightly indurated substrates; may or may not be associated with pelleted tumuli at the sediment surface | Ubiquitous around shoreline of entire lake except Sandai Plain | Insects; mainly larval tiger beetles (Cicindelidae) for smaller sizes; larger sizes also possibly spiders and other adult beetles (e.g., Carabidae) | Smaller sizes abundant in wet to damp and firm or cohesive substrates, esp. at shoreline; larger sizes common in slightly higher topographic areas away from shoreline | Shorelines around lake except Sandai Plain; especially abundant at Loburu Delta |

| | | | | | | | |
|---|---|---|---|---|---|---|---|
| Scott et al., 2007, fig. 11E–F; Scott et al., 2009, fig. 9B, 9C | * 3D burrow system | "Boxwork burrow systems" - emended | These burrow systems are primarily made up of horizontal, branching, open, roofed tunnels formed just below the air-sediment interface; internally, the burrow margins are circular and smooth, but the exterior margin is irregular; two size classes (5–6 mm wide and 10–20 mm wide) of burrows in the horizontal branching system; the smaller size class typically branches from the larger burrows; vertical component of this burrow system was also observed in indurated substrates near the present-day shoreline to have depths of up to ~30 cm from the uppermost surface to the base of the burrow system at the water table (pers. obs. J.J.S., 2002) | Common at shoreline at Loburu Delta | Insects; possibly larval and adults of same species; possibly mole crickets (Orthoptera: Gryllotalpidae) or earwigs (Dermaptera)? | Wet to saturated substrates; shoreline | "Main" Loburu Delta |
| Figs. *4.1.5.* 12, 13 | * 3D burrow systems | "Earwig burrow systems" – emended; ? Incipient *Thalassinoides* isp. | Open or pellet-filled, branching three-dimensional burrow systems; unwalled and unlined; burrows range from ~4 to 8 mm up to 1 cm in diameter; portions of the burrows may be backfilled with sub-spherical pellets that tend to be darker than the host sediment; burrow system contains expanded areas for egg-laying (1–2 cm high, < 3 cm wide); expanded areas or "egg chambers" obliquely or horizontally oriented | May reuse and rebuild old burrow systems | Insects; adult and larval earwigs (Dermaptera) | Damp to wet, firm subtrates; may be associated with hot springs and/or with firm, wet substrates with relatively fresh water | Loburu Delta; Emsos area |
| Scott et al., 2009, fig. 10 | * 3D burrow systems | Incipient *Spongeliomorpha* isp. | Unwalled, vertical to oblique, locally branching burrows and burrow systems with ornamented burrow margins that show wrinkle-like transverse patterns; burrows may be open, but are commonly filled with dark pelletal material (< 1 mm) distinctly different from the substrate; the burrows range from 4 mm to 8 mm in diameter | Similar to "Earwig burrow systems" (or Incipient *Thalassinoides* isp.), but not associated with egg chambers | Insects; probably larval earwigs (Dermaptera) | Firm, damp substrates at shoreline | Emsos area |
| Scott et al., 2007, figs. 10A, 11A | † Arthropod trackways | None available; *Sepidium* trackways | Straight to gently curving trackway; 10 mm width; imprints are narrow scratches that are mainly parallel, but sometimes oblique, to the midline; imprint scratches 1 mm wide and 3–8 mm long; stride length of 12–15 mm; track rows are simple; symmetry is generally opposite | Also "preserved" as "salt tracks and trails"; trace maker observed directly | Insects; adult tenebrionid beetles (Coloeptera: Tenebrionidae: *Sepidium*) | Lake margin and mudflat exposed during low lake levels in 1976; subaerial substates | "Main" Loburu Delta |
| Scott et al., 2007, fig. 10B | † Arthropod trackways | Incipient *Siskemia* isp. | Trackways ~5 mm wide with two continuous grooves along the midline (~0.5 mm wide each) and elongate scratch-like imprints oriented obliquely to the midline; track rows simple; trackway is straight to meandering with sharp turns | "Preserved" as "salt tracks and trails" | Insects; adult or sub-adult earwigs; possibly crickets (Orthoptera: Grylloidea) | Mudflat; associated with hot springs; exposed mudflat during low lake levels in 1976 | "Main" Loburu Delta |

| | | | | | | | |
|---|---|---|---|---|---|---|---|
| Scott et al., 2007, fig. 10C | † Arthropod trackways | Indeterminate trackways | Trackways of groups of imprints with alternate symmetry; three circular imprints per group; trackway external width 4–6 mm; spacing between imprint groups < 2 mm; individual imprints < 1 mm in diameter; trackways frequently cross-cut one another and are generally straight but show angular changes of path direction | "Preserved" as "salt tracks and trails" | Insects | Mudflat; associated with hot springs; exposed mudflat during low lake levels in 1976 | "Main" Loburu Delta |
| Scott et al., 2007, fig. 10D | † Arthropod trackways | Incipient *Diplichnites* isp. A | Trackways are straight to gently curving; imprints are not grouped and are opposite across the midline; imprints perpendicular to the midline; imprints ellipsoidal to circular in shape; three size classes: 1) 1–2 mm; 2) 2–3 mm; 3) 3–4 mm maximum external widths | "Preserved" as "salt tracks and trails"; type is transitional with incipient *Diplopodichnus* isp. | Probably insects; size classes may correspond to sub-adult stages of development | Mudflat; associated with hot springs; exposed mudflat during low lake levels in 1976 | "Main" Loburu |
| Scott et al., 2007, fig. 10F–G | † Arthropod trackways | Incipient *Diplopodichnus* isp. | Straight to gently curving, locally looping or meandering bilobed trails; 1–4 mm wide; transitional to uni-lobed examples; width of median longitudinal furrow is < 0.5 mm; imprints are very closely spaced, perpendicular to the midline and ellipsoidal; imprints opposite; commonly cross-cut one another and other trackways and trails | "Preserved" as "salt tracks and trails"; type is transitional with incipient *Diplichnites* isp. | Probably insects | Mudflat; associated with hot springs; exposed mudflat during low lake levels in 1976 | "Main" Loburu |
| Fig. *4.1.4.* 4A–D | § Arthropod trackways | Incipient *Diplichnites* isp. B | Large arthropod trackways < 2 cm external width; trackways straight to gently curving; individual imprints not observed; groups of imprints are alternate across the midline; midline is ~0.5 cm wide; material does not show details well, and may be sub-fossil; trackways very dense and cross-cut frequently | Similar "preservation" to "salt tracks and trails"; exposed "omission surface"? | Large insects | Exposed mudflat during low lake levels in 2006 | "Main" Loburu |
| Scott et al., 2007, fig. 7E, 7F | † § Footprints (ostriches) | Ostrich footprints | Two-toed large footprints; toes directed forward, digit II sometimes splayed; divarication < 40°; central toe (digit III) with large claw; digit III typically impressed more deeply than digit II; total length ~16 cm; total width ~8 cm; digits massive; impressions oval-shaped with bulbous areas at tarsal articulations; trackway very narrow; juvenile footprints smaller (~10 cm length) | Also produce shallow 'bathing wallows' in dry silt and sand | Birds; ostriches | Open areas; dry to damp substrates, includes delta-plain away from shoreline; occasionally near shoreline | Sandai Plain; Loboi Plain; Loburu Delta |

| | | | | | | | |
|---|---|---|---|---|---|---|---|
| Scott et al., 2007, fig. 7A, 7B | † § Footprints (storks)<br><br>Note: also included in the "Flamingo Nest-Mound" Suite | Stork footprints | Large, thick-toed, clawed bird footprints with three forward facing digits and long, straight pronounced hallux directed towards inside; entire hallux impressed; nodes at tarsal articulation points pronounced; unwebbed; divarication angles usually ~70–75° on each side; digits I and III ~10–12 cm in length and 2 cm wide; digits II and IV ~9–10 cm in length; dimensions dependent on substrate conditions; typically 20–22 cm long and ~18–20 cm wide; digits may be separated from central metatarsal impression, if so, metatarsal impression circular | The abundance and distribution of bird footprints is necessary to determine their inclusion in this suite | Birds; storks; esp. Marabou stork; similar tracks are those of herons, but herons are smaller and more gracile | Delta-plain, hot-spring pools, ephemeral streams and perennial rivers | Mainly at mouth of Sandai River and Loburu Delta area |
| n/a | § Footprints (doves) | Mourning dove trackways | Small, four-toed footprints with hallux directed towards midline; trackways with footprints angled towards centre ("pigeon-toed"); short stride length; back claw may drag | Preservation only expected if in wetter substrates | Birds; doves | Terrestrial; dry substrates away from lake margin | Western margin |
| e.g., Scott et al., 2007, fig. 10C, 10D | † § Footprints (other birds) | Yellow-billed stork; Grey heron; Sacred ibis; Cattle egret; Hammerkop; Egyptian geese; teal | Note: measurements taken from Stuart and Stuart (1994) and photographs; Unwebbed footprints with hallux impressions include Yellow-billed stork (~12 cm total length), Grey heron (~12 cm total length), Sacred Ibis (~11.5 total length), and Cattle egret; Hammerkop tracks not observed; Webbed footprints include Egyptian Goose (~8 cm total length) and teals (~4.5 cm total length) | Typically in wet substrates near sites of fresh water | Birds; several types of non-passerine birds observed | Riparian; associated with hot-springs | Sandai River; Parkirichai River; "South" Loburu |
| Fig. *4.1.4.* 7C, 7D | † § Footprints (bovids) | African buffalo footprints | Very large, rounded double hoof prints; length ~12 cm; front feet more rounded and larger than hind feet; medial gap between hooves on front feet extends entire length of track and may be curved; on front foot, medial gap may be wider towards front of track; tips of hooves directed towards centre; overall shape is circular for front, oval for hind; outside track margins sharp | Preservation only expected if in wetter substrates | Mammals; African buffalo | Terrestrial; dry substrates, includes delta-plain away from shoreline; may be associated with riparian zone | Sandai Plain east of Sandai River; southern western margin |
| Fig. *4.1.4.* 7A–B | † § Footprints (bovids) | Greater kudu footprints | Large, oval-shaped double hoof prints; length ~8 cm; front feet slightly wider than hind; hoof margins rounded with gentle slope towards back of prints; medial gap straight and narrow; tips of hooves directed slightly medially and rounded | Preservation only expected if in wetter substrates | Mammals; Greater kudu | Normally terrestrial; associated with hot springs | Chemerkoi; "South" Loburu; southern margin |
| Figs. *4.1.4.* 7F?, 9E, 9F | † § Footprints (bovids) | Grant's gazelle footprints | Medium-sized (< 6 cm length), tear-drop to heart-shaped double hoof prints; front foot slightly wider than hind towards back of print; if unsplayed, medial gap straight and very narrow and is entire length of track; margins of hooves | Very similar to impala tracks | Mammals; Grant's gazelle | Delta-plain to terrestrial; associated with fresh water and shrubby | Sandai Plain; "South" Loburu |

| | | | | | | | |
|---|---|---|---|---|---|---|---|
| | | | sharp; tips of hooves pointed forward and pointed; outside margins of front hooves have slight inward indentations; back margins very rounded, giving tracks heart shape | | | vegetation | |
| Fig. *4.1.4.* 7F? | †§ Footprints (bovids) | Impala footprints | Medium-sized (< 5 cm length), heart-shaped double hoof prints; front feet slightly larger than hind; outside margins of front hooves are not indented; back margins of hooves are rounded, and tracks appear more heart-shaped than Grant's gazelles; tips of hooves pointed forward and very pointed | Very similar to Grant's gazelle tracks | Mammals; impalas | Delta-plain to terrestrial; associated with fresh water and shrubby vegetation | "South" Loburu; western margin |
| Fig. *4.1.4.* 8C | †§ Footprints (suids) | Warthog footprints | Small-sized (< 4 cm length), rounded double hoof-prints with overall square shape; medial gap is wider towards front and does not continue through the back of the foot; back margins square to rounded; tips of hooves rounded and directed forward; margins of tracks not sharp | Associated with grasses and sedges; tracks often in very wet substrates | Mammals; warthogs or bushbuck | Lake margin and delta-plain; associated with hot-spring and littoral wetlands | mainly "South" Loburu Delta |
| Fig. *4.1.4.* 7I | †§ Footprints (equids) | Zebra footprints | Large (~10 cm length) single hoof prints with very rounded front margins and flat to concave and indented back margins; front foot wider and more rounded than hind; margins of tracks very sharp at sides and front, and gradually sloping at back; may show "triangular frog" mark at back centre from fleshy pad on back centre of hoof; overall shape of front foot is round, back foot is oval | Also produce shallow 'bathing' wallows in dry areas; associated with grasses and sedges; tracks often in very wet substrates | Mammals; zebras (*Equus burchelli*) | Lake margin and delta-plain; associated with hot-spring and littoral wetlands | mainly Loburu Delta |
| Scott et al., 2007, fig. 5G | †§ Footprints (hyaenas) | Spotted hyaena footprints | Large (< 9 cm length) footprints with four toes on front and hind feet; may have claw impressions; digits crowded and large, with impressions of digits sometimes overlapping; front foot larger than hind; digits on back feet slightly more pointed; digits on front feet very rounded; metatarsal pad large and very little space between it and toes; back margin of metatarsal pad has two lobes; front margin of metatarsal pad with one, flat lobe; overall shape of tracks is oval | Associated with flamingos near shoreline | Mammals; spotted hyanea | Shoreline to terrestrial | Sandai Plain; "South" Loburu Delta |
| Scott et al., 2007, fig. 5F | †§ Footprints (felids) | Leopard footprints | Large (< 8 cm length) footprints with four toes on front and hind feet; no claw impressions; digits very rounded on front foot and oval on hind; digits separated; front foot larger than | Associated with ostrich tracks on Sandai Plain; preservation only | Mammals; leopards | Terrestrial; dry substrates, includes delta-plain away from | Sandai Plain; western margin |

| | | | | | | | |
|---|---|---|---|---|---|---|---|
| | | | hind; metatarsal pad very large with two lobes at front and three lobes at back; very little space between metatarsal pad and digits | expected if associated with wetter substrates | | shoreline | |
| Fig. *4.1.4.* 8D, 8E | [§] Footprints (? felids) | ?Serval footprints | Medium-sized (< 4.5 cm length) footprints with four toes on front and hind feet; digits round to oval-shaped and separated; no claw impressions; small gap between digits and metatarsal pad; front margin of metatarsal pad flat; hind margin of metartarsal pad indistinct; digits II,V set back from digits III, IV; digits directed outwards | Possibly a different mongoose species | Mammals; serval cat or caracal? | Delta plain to shoreline | "South" Loburu Delta |
| Fig. *4.1.4.* 8D–G | [§] Footprints (mongoose) | Mongoose footprints | Medium-sized (< 4 cm length) footprints with four toes on front and hind feet; claw impressions may be very clear; digits oval-shaped and separated from one another, with two central digits closer together; gap between digits and metatarsal pad; digits II and V are set back from front toes, which are even; all toes directed forward; metatarsal pad has flat to convex front margin and indistinct double-lobed back margin | In one case, found together with similar tracks of different individual, possibly different species | Mammals; mongoose; possibly Large grey mongoose? | Delta plain to shoreline | "South" and "Main" Loburu Delta |
| Scott et al., 2007, fig. 5I | [† §] Footprints (primates) | Baboon footprints | Large, elongate hind footprint (< 14 cm length) with medium-sized hand-like front footprint (< 8 cm length); hind foot has prominent heel, wide metatarsal impression, and circular thumb metatarsal impression on medial side of track; digits in hind feed have circular impressions, with digit I offset towards inside and other four digits crowded and forward facing; front foot shows a wide metatarsal impression with four, long toes directed forward and a circular digit I set back behind the metatarsal pad and offset towards the inside | Preservation only expected if associated with wetter substrates | Mammals; Olive baboons | Terrestrial; dry substrates, includes delta-plain away from shoreline | Western margin |
| Scott et al., 2007, fig. 5E | [† §] Footprints (aardvarks) | Aardvark footprints | Medium-sized (< 8 cm) three-toed footprints with long, wide, blunt claws; feet have 4 (front) or 5 (hind) digits, but only 3 are impressed; all toes directed forward | Also produce burrows; may be associated with termite mounds | Mammals; aardvark | Dry substrates, includes delta-plain away from shoreline | Sandai Plain |
| Scott et al., 2007, fig. 7G | [† §] Footprints (reptiles) | Crocodile trackways | Large, elongate hind footprint (< 13 cm length) with medium-sized front foot (< 7 cm length); all toes clawed and claw impressions clear; three digits (I, II, III) impressed more deeply on both hind and front feet; usually deepest towards inside; digit IV may or may not be impressed, but if not, outside margin of track is not sharp; if so, digit impression is directed towards the back; | Variable morphology depending on behaviour (e.g., crawling, walking, swimming) | Reptiles; Nile crocodile | Riparian – fluvial ; (shoreline at Lake Baringo) | Sandai River |

| | | | | | | | |
|---|---|---|---|---|---|---|---|
| | | | hind print may have deeply impressed heel and is flat and wide; digit lengths increase slightly from digit I to II to III; trackway is slightly sinuous, often with sinuous tail drag and sometimes with wide, slightly sinuous belly drag | | | | |
| Scott et al., 2007, fig. 7H | † § Footprints (tortoise) | Tortoise trackways | Trackway consists of two, widely separated lines of footprints and drag marks of feet; individual tracks usually unclear; width of trackway < 40 cm, width of prints + drag < 10 cm | Preservation only expected if associated with wetter substrates | Reptiles; Hump-backed tortoise | Dry substrates, includes delta-plain away from shoreline | Dry lake margin, Lake Bogoria |
| n/a | † § Excavated ground | Warthog bathing pits | Large, irregular, excavated pits in sandy gravels adjacent to hot-springs; may be ~1–2 m in diameter; deepest part of pit in centre; depth < ~1 m | Likely would be not possibly to identify in fossil record if preserved | Warthogs; adults and juveniles | Delta-plain; associated with hot springs; sandy substrates | "South Loburu" |
| *Suite 5: "Termitichnus-like" Suite* | | | | | | | |
| Fig. *4.1.4.* 11B–D | § Pellet-walled tunnels | ? cf. *Palaeophycus* isp. | Open, straight to curving tunnels (~1–2 cm internal diameter) with constructed walls of sediment aggregates with surrounding sediment (~3–4 cm external diameter); smooth internal walls; horizontal and branching above ground; sometimes connected to open, vertical burrows of same diameter and with smooth internal walls | May be protective subaerial tunnels for above-ground foraging or incipient nests of winged adults | Insects; termites | Terrestrial, alluvial fan and delta-plain above zone of lake-level rise | Western margin, north of Loburu |
| Fig. *4.1.4.* 11A | § Termite mounds | None available | Description of external morphology only: large, above-ground mounds with chimneys; mounds < 2 m high and wide with chimneys < 2 m above mounds; constructed of a variety of materials including masticated sediment aggregates, sediment clasts, plant material, and insect exoskeletons; material cemented together in layers, sometimes concentric layers; normally have several large (< 10 cm wide) open passages at top of mounds | Mounds vary in dimensions depending on the age of the colony | Insects; termites (Macrotermitinae) | Terrestrial, alluvial fan and delta-plain above zone of lake-level rise | Western margin, north of Loburu; "Old" Loburu; "South" Loburu |
| n/a | § Mammal burrows | Indeterminate | Includes burrows of aardvarks, warthogs, hyaenas (not observed), mongoose (not observed), ground squirrels (not observed) | Variety of burrow types not investigated in detail | Various burrowing mammals | Terrestrial, alluvial fan and delta-plain above zone of lake-level rise | Western basin margin |

*4.1.4.1. Suite 1: The "Chironomid" Suite*— The "Chironomid" Suite is composed of traces and structures produced by larval and pupal chironomids (Insecta: Diptera: Chironomidae) (Table 4.5). *Paratendipes* sp. is the only animal living in the saline waters of modern Lake Bogoria (Harper et al., 2003). Chironomids are well known to live in hypersaline conditions (e.g., Hammer, 1986), they prefer microbe-rich substrates (e.g., Edgar and Meadows, 1969), and their dominant food source is cyanobacteria or other organic detritus (e.g., Oliver, 1971), which is usually abundant in these settings. The suite includes: 1) tube-structures produced by larvae from microbial and organic detritus for their protection (Brennan and McLachlan, 1979; Scott et al., 2009, fig. 6A–D); 2) shallow, circular pits into indurated substrates < ~1 cm in diameter that may represent their "feeding territories" on microbial mats (cf. Chaloner and Wotton, 1996) or areas excavated for the formation of the tube-structures (Òlafsson and Paterson, 2004; Scott et al., 2009, fig. 6E); 3) vertical burrows < 2 mm in diameter (Scott et al., 2009, fig. 6F); and, 4) their pupal cases, which are attached to solid substrates, and may be preserved by carbonate as in the examples from the Holocene stromatolitic coating at the southern sub-basin of Lake Bogoria (Fig. *4.1.3*.6D).

Based on the conditions under which chironomids live at Lake Bogoria, the "Chironomid" Suite represents a saline lacustrine environment above the chemocline in oxygenated waters with an abundant microbial food source, although their vertical burrows may penetrate through anoxic sediments. Other structures that would fit into this suite are the U-, Y-, or J-shaped branching vertical burrows (e.g., *Polykladichnus*) described by other authors from other settings (e.g., Uchman and Álvaro, 2000; Gingras et al., 2007). These structures are normally formed in soft substrates greater than 10 mm in thickness (McLachlan and Cantrell, 1976), and at Lake Bogoria, trampling of shallow lacustrine soft substrates with abundant cyanobacteria by flamingos is expected to reduce their preservation potential substantially.

*4.1.4.2. Suite 2: The "Flamingo Nest-Mound" Suite*— The second suite observed at Lake Bogoria comprise mainly the traces of flamingos and characterizes the flooded delta-plain or lake-margin and subaerially exposed littoral and lacustrine muddy sediments (Scott et al., 2009, fig. 13). The "Flamingo Nest-Mound" Suite is found in very wet to shallowly submerged substrates (Scott et al., 2009). Lesser and greater flamingos (*Phoeniconaias minor* and *Phoenicopterus ruber*) are normally very abundant at Lake Bogoria. Lesser flamingos, in particular, may be present in huge concentrations (up to 1–2 million birds) because their main food source, the planktonic cyanobacterium *Arthrospira*, is also usually very abundant at Lake Bogoria (Harper et al., 2003). The types of traces included in this suite are described in Table 4.5 and discussed in greater detail in Section 4.1.5.1.

Several behaviours of flamingos produce discrete traces or biogenically produced structures (e.g., Scott et al., 2003, 2007). The birds walk in littoral muds while feeding from shallow lake waters or drinking and bathing from areas with relatively freshwater input to the lake, and consequently completely churn and partly oxygenate the sediments with their "trampling" (Scott et al., 2007, fig. 6). Many bubble-like structures, interpreted to have been produced during trampling of littoral mud by flamingos, were observed at Loburu delta (Fig. *4.1.4*.1A). These structures are also preserved in the ?Bogoria Silts of the Parkirichai River (Section 4.1.3, Fig. *4.1.3*.4).

Flamingos build their nest-mounds in exposed littoral muds, normally in areas near fresh or brackish water (e.g., hot springs at Loburu, the mouth of Sandai River). Nests are built in clusters or linear arrangements during periods of lake-level fall, with progressively younger nests lake-ward (Scott et al., 2007, fig. 6). The flamingos display in large "armies" on the exposed

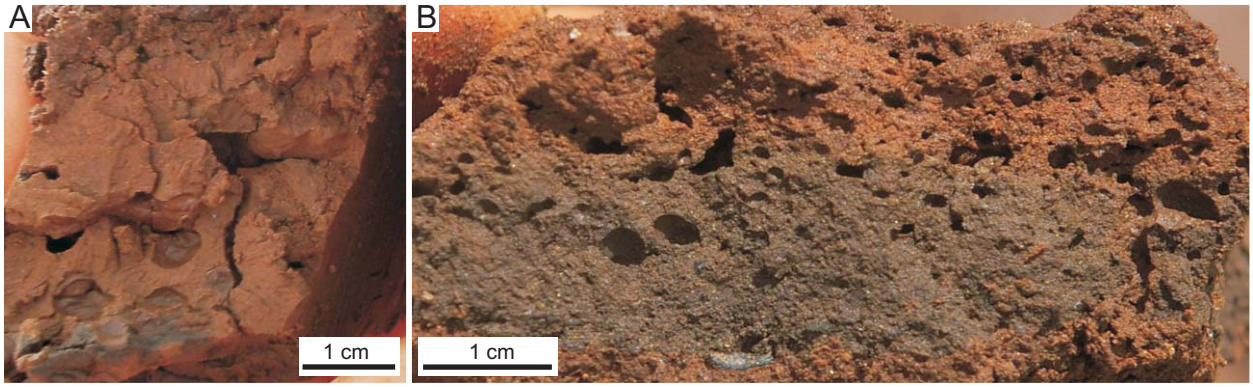


**Fig. 4.1.4.1.** Modern biogenic structures at shoreline of Lake Bogoria. **(A)** Irregular bubble-like structures with very smooth internal margins, attributed to flamingo trampling of clay-rich substrate. **(B)** Bubble-like structures of various sizes in sandy substrate, mainly oval-shaped or spherical and attributed mainly to gas-escape in microbe-rich sediments. Some were probably produced by insect larvae and roots.

delta-plain near the shoreline, and may walk to the relatively fresh water sources in large groups. They create thousands of new footprints each day which can produce "flamingo-trampled surfaces" in which discrete footprints may be difficult to discern (Scott et al., 2007, fig. 6). Some other bird footprints may be associated with the muddy substrates at the shoreline, including Marabou storks and Blacksmith plovers. This suite is similar to the "shore-bird ichnofacies" of Lockley et al. (1994). Its consistent association with the "Scoyenia suite" at Lake Bogoria supports the notion that it may be best considered as a sub-ichnofacies of the Scoyenia ichnofacies (Melchor et al., 2006).

*4.1.4.3. Suite 3: The "Mermia-like" Suite*— The "Mermia-like" Suite consists mainly of simple surface trails and dominantly horizontal, branching surface tunnels that were associated with very shallow subaqueous (< ~3 cm depth) and water-saturated cyanobacteria-rich substrates at the air/water/sediment interface (Scott et al., 2009, fig. 7). Spherical structures associated with this suite and microbial mats are interpreted as gas-escape bubbles (Fig. *4.1.4.*1B). Simple, straight or curving to gently meandering trails were assigned to Incipient *Gordia* isp. and Incipient *Helminthoidichnites* isp. (Scott et al., 2009, fig. 7A,B). They were observed along the margins of drying, spring-fed pools on the southern Loburu delta, along the shoreline at Loburu, and in quiet, very shallow lake waters at Emsos (Fig. *4.1.4.*2A–H). Other examples were 'preserved' as 'salt trails' at the main Loburu delta, which may represent sub-fossil traces in shallow buried substrates (see Scott et al., 2007, figs. 8, 10). The trace makers of these trails were not directly observed at Lake Bogoria, but observations of small dipteran larvae tunneling just below the sediment surface at south Loburu, and comparisons with similar trails at Lake Magadi and Nasikie Engida, suggest that they were produced by dipteran and/or coleopteran larvae. Only chironomid (Diptera) larvae are known to live within the lacustrine benthos (Harper et al., 2003), and accordingly, no simple trails are expected to be produced in the deeper lake waters. Although not studied, it is possible that simple trails and possibly branched tunnels associated with sublacustrine springs may be produced by other organisms, such as ostracods, which are preserved in Holocene sediments retrieved as core (Tiercelin et al., 1987).

Incipient *Labyrintichnus* isp. and incipient *Vagorichnus* isp. represent the small (2–4 mm diameter), lined and unlined (respectively), open and backfilled (respectively), dominantly horizontal, branching tunnel systems of insects at Lake Bogoria (Scott et al., 2009, fig. 7C–J). Seen from the surface, the tunnels are consistent in diameter, with two size classes (~2 mm and ~3.5 mm diameter). They are most abundant in association with shallow films of spring-fed

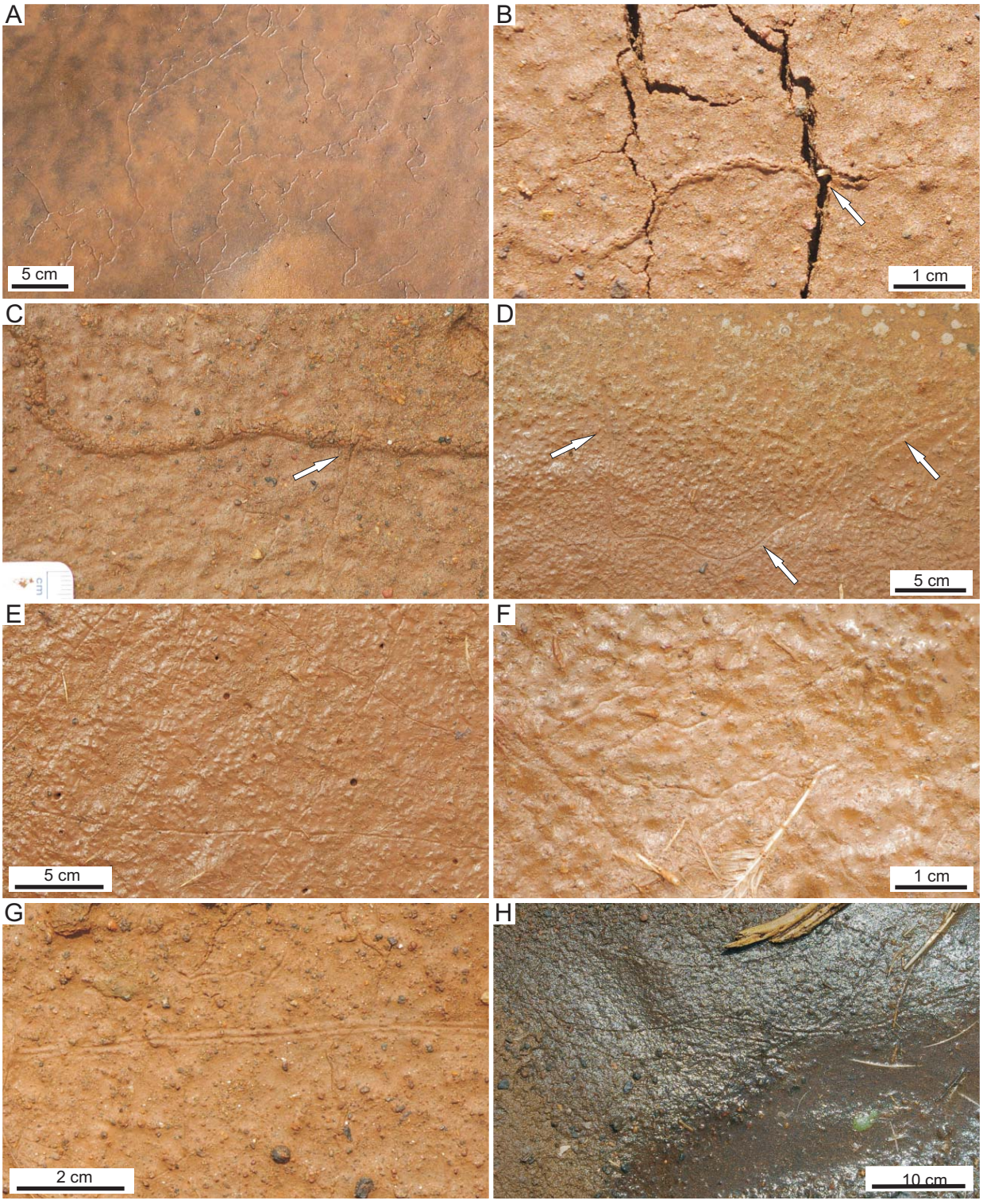


**Fig. 4.1.4.2.** Modern insect traces on the mudflat at the south Loburu Delta, Lake Bogoria. All examples are included in the "Mermia-like" suite. Photograph shown in (A) courtesy of R.Renaut. **(A)** Branched surface tunnels formed in very shallow water on mudflat (Incipient *Labyrintichnus*). **(B)** Insect larvae producing surface tunnel (arrow). **(C)** Very small-sized suface trail (arrow; Incipient *Helminthoidichnites*) cross-cutting surface tunnel. **(D)** Surface trail (arrows) at edge of drying pool. **(E)** Cross-cutting straight to slightly sinuous surface trails (Incipient *Helminthoidichnites*). **(F)** Irregularly sinuous surface trails (Incipient *Helminthoidichnites*). **(G)** Straight surface trail with lateral ridges (Incipient *Archaeonassa*). **(H)** Gently curving trails (Incipient *Archaeonassa*) at shoreline.

pools (e.g., 2006, 2007) and with widespread cyanobacterial mats (e.g., 2001, 2002). The distinction between the two incipient ichnogenera in the modern examples from Lake Bogoria is not reliable, because the two types appear to be transitional with one another. The larger examples are best associated with *Vagorichnus* isp. and may be backfilled with pelletal material. The open tunnels (*Labyrintichnus* isp.) show the excavation of material from within the tunnels as small tumuli at the 'nodes' from which the tunnels branch. The surface tunnels in microbial mats remained open and based on branching patterns were apparently reused, showing "true branching" in a system or network of tunnels. These dominantly horizontal tunnel networks are

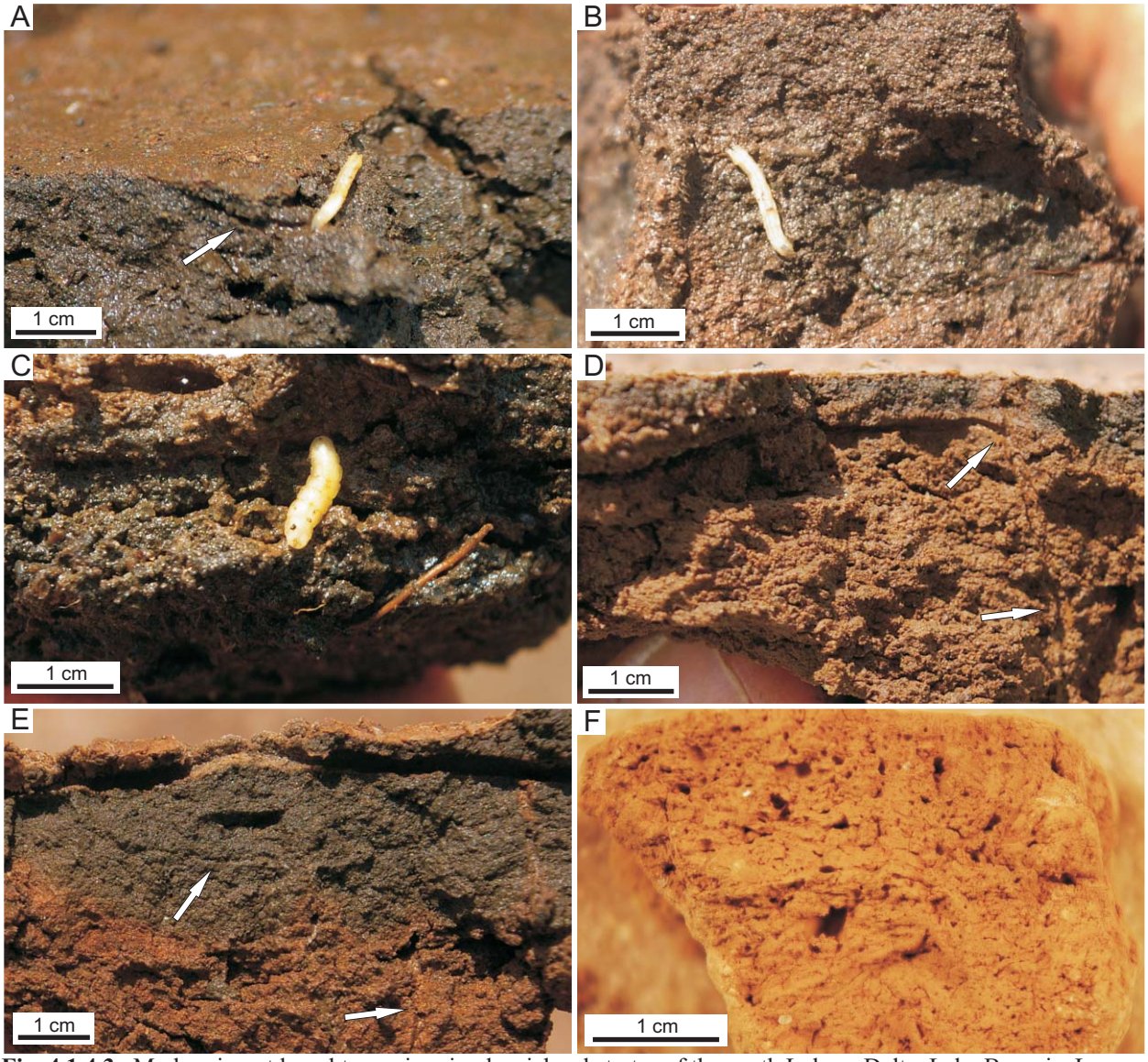


**Fig. 4.1.4.3.** Modern insect larval traces in microbe-rich substrates of the south Loburu Delta, Lake Bogoria. Larvae are probably dipteran (fly, A, B) and coleopteran (beetle, C). **(A)** Small-sized open tunnel in cohesive substrate just below air/sediment surface. Dark colour in substrate is partly due to microbial metabolism. **(B–C)** Larvae burrowing in microbe-rich substrate. Note sedge root at right in (C). **(D)** Small-sized "Upside-down J-shaped burrow" (arrows) with horizontal portion below dark-coloured microbe-rich substrate near surface. **(E)** Small-sized open burrow (arrows) in microbe-rich substrate (Incipient *Planolites*). Note horizontal tunnel just below air/sediment surface. **(F)** Dried modern silts from south Loburu showing numerous open burrows and root holes.

discussed in further detail with other traces produced by staphylinid and heterocerid beetles in Section 4.1.5.3.

Scott et al. (2009) also included vertebrate footprints (flamingo and mammal) impressed within microbial mats, and plant (sedge) roots that produce open holes in microbial mats as part of this suite.

*4.1.4.4. Suite 4: The "Scoyenia-like" Suite*— The "Scoyenia-like" Suite comprises the vertical burrows, 3D burrow systems, and trackways of insects and spiders, as well as the footprints of vertebrates including mammals, reptiles, and some birds. It is the most diverse of the suites at Lake Bogoria, and is comparable to the Scoyenia ichnofacies as defined by Frey et al. (1984) and Buatois and Mángano (e.g., 1998). The dominant insect tracemakers include beetles (Coleoptera: e.g., Tenebrionidae, Carabidae, Staphylinidae, Cicindelidae, Heteroceridae) and earwigs (Dermaptera: Labiduridae). Ants (Hymenoptera: Formicidae) were observed together with earwigs, spiders (unidentified), and mites (Hydracarina: red water mites) in supralittoral indurated substrates of the Loburu Delta. Spiders were also observed in wet silty sand and within vertical burrows in coarse sandy gravel at the southern Loburu Delta. Crickets (Orthoptera: Grylloidea) and their horizontal tunnels were also observed in the supralittoral zone on the Loburu Delta (see Section 4.1.5.3).

Detailed descriptions of the trace types observed are provided in Table 4.5. Photographs of the traces were provided by Scott et al. (2007, figs. 5, 7, 8, 10, 11) and Scott et al. (2009, figs. 8, 9, 10). New figures are presented here (Figs. *4.1.4.*3–6 and in Sections 4.1.5.2, 4.1.5.3, and 4.1.5.4), which discuss forms included in the "Scoyenia-like" Suite. Several types of traces are

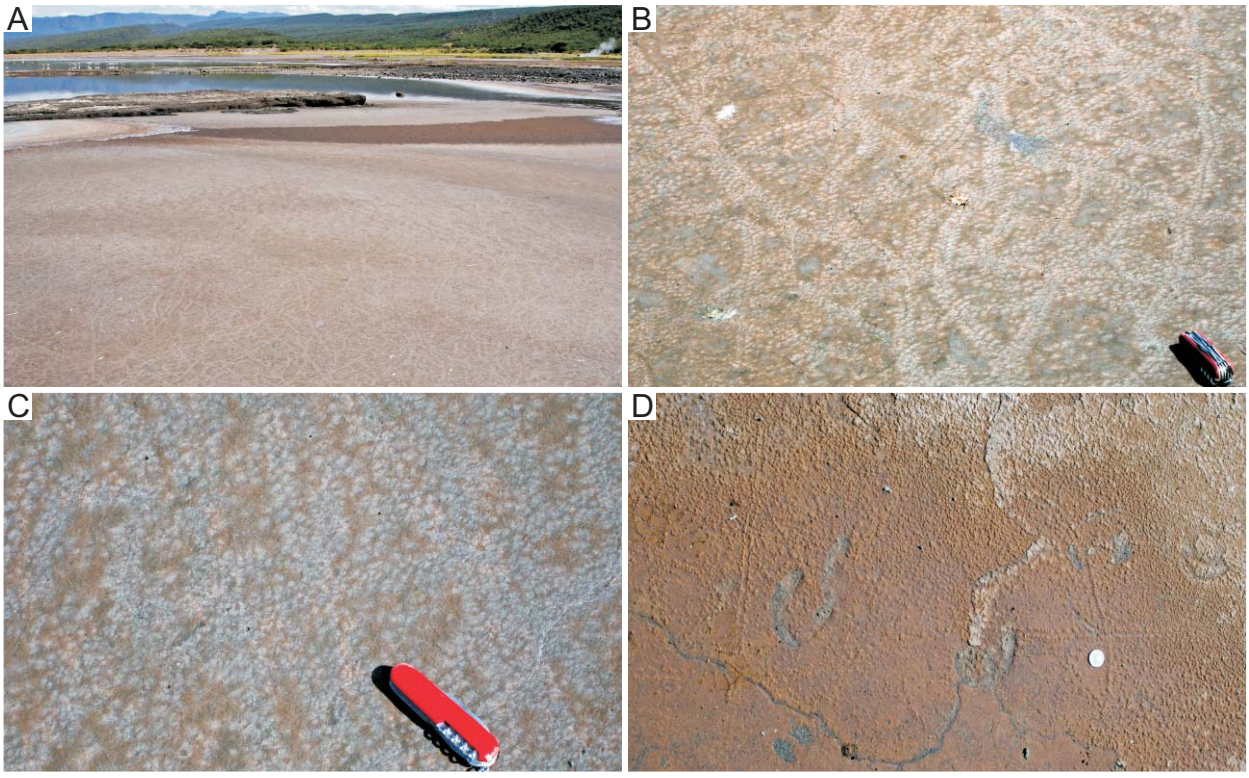


**Fig. 4.1.4.4.** Sub-fossil arthropod trackways at the main hot-spring site at Loburu Delta, Lake Bogoria. Trackways are in exposed, slightly indurated shallow littoral lacustrine muds. The age of the traces and their trace makers are unknown. All photographs are courtesy of R.Renaut.

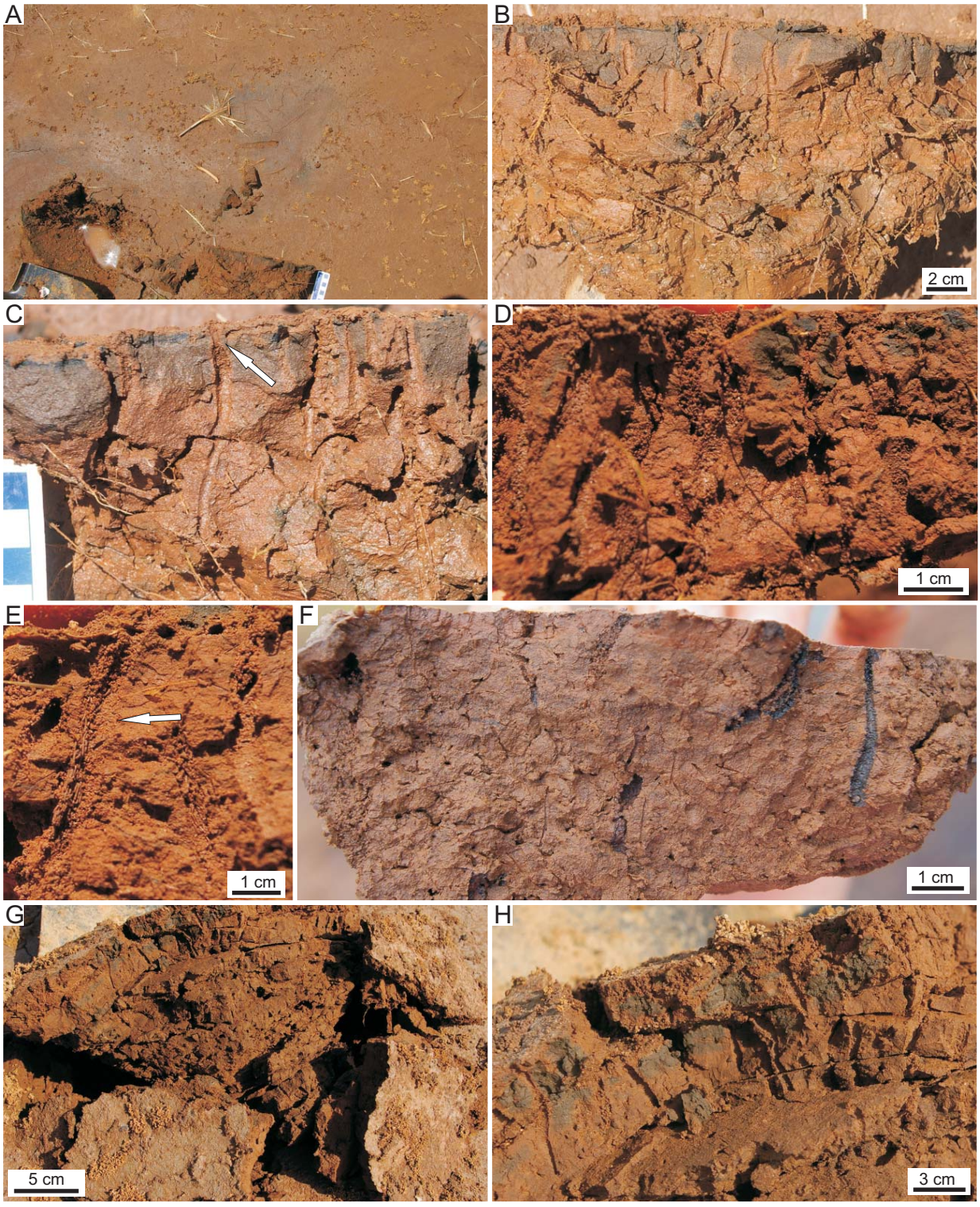


**Fig. 4.1.4.5.** Modern vertical burrows in slightly indurated or cohesive mudflat sediments at Lake Bogoria. **(A)** Mudflat surface at south Loburu showing shallow depth of water table where vertical burrows shown in (B–E) were found. **(B–E)** Vertical burrows, some filled with spherical and elongate pellets/sediment aggregates (D, E). Note constriction of top of open burrow in (C) (arrow). **(F)** Pellet-filled burrows and black-lined burrows in slightly indurated silts at Emsos. **(G–H)** Vertical burrows associated with "pellet-roofed" horizontal tunnels in microbe-rich silts from south Loburu. (G) shows broken salt-enrusted surface with pellet-tunnels (lower centre, right). Numerous vertical burrows associated with these pellets in (H).

representative examples of the incipient forms of defined ichnotaxa, including Incipient *Skolithos* ispp., Incipient *Vagorichnus* isp., Incipient *Diplichnites* isp., Incipient *Diplodichnus* isp., Incipient *Planolites* isp., Incipient *Spongeliomorpha* isp., and Incipient *Siskemia* isp. Other traces observed such as the *Sepidium* (Tenebrionidae) trackways, upside-down J-shaped burrows, tear-drop burrows, pellet-filled burrows A, B, and C, and 3D boxwork burrow systems have not been formally described by other authors. The 3D boxwork burrow systems of earwigs are likely comparable to *Thalassinoides* isp., but future research should focus on the branching patterns of

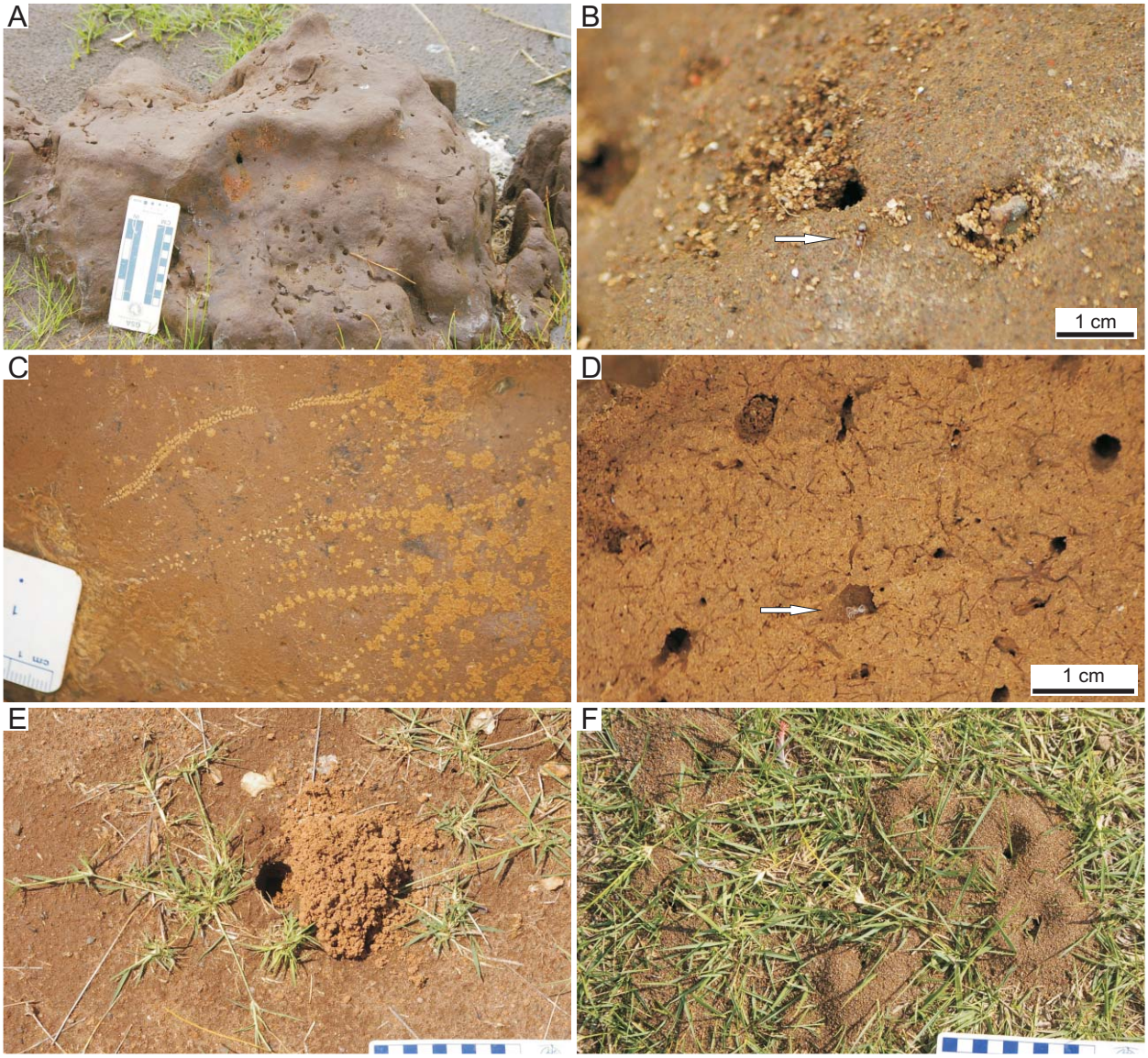


**Fig. 4.1.4.6.** Modern arthropod traces at the main site at Loburu, Lake Bogoria. The water table is relatively lower in these substrates (ranges from ~30 cm to ~1 m). **(A–B)** Open burrows of insects in indurated substrate near hot spring. The arrow in (B) is pointing to an ant. **(C)** Arthropod trackways? possibly produced by mites on vertical surface of an indurated "exhumed" surface. The trackways are visible in sodium carbonate salt efflorescence forming on drying sediments. **(D)** Open and pellet-filled burrows and root traces in slightly indurated "exhumed" surface substrate. Arrow is pointing to a spider, but the burrows were probably produced by earwigs, ants, and spiders. **(E)** Large vertical to oblique open burrow with excavated sediment aggregates piled as tumuli at surface. Burrow probably produced by a spider or beetle. **(F)** Group of burrow openings in sandy substrate (~1m water table depth). Burrows probably produced by ants.


**Fig. 4.1.4.7.** Modern vertebrate footprints at Lake Bogoria. **(A–B)** Numerous tracks of greater kudus at the hot spring site of Chemurkeu. **(C–D)** African buffalo trackway in sandy substrate at SE shoreline. **(E–G)** Vertebrate tracks in subaqueous and subaerial microbe-rich substrate at south Loburu. Tracks produced by impalas/Grant's gazelles (top in F) and zebras (G; arrows). **(H–I)** Vertebrate trampled surface in desiccated spring/seepage pool at south Loburu. Zebra tracks in (I) indistinct due to puffy salt efflorescence.

their burrows to confirm this (see Section 4.1.5.4). *Spongeliomorpha* isp., *Skolithos* ispp., and boxwork burrow systems with ornamented burrow margins represent the bioturbation of drying, firmer, and slightly indurated, or clay-rich cohesive substrates. Vertebrate tracks (e.g., mammals, some birds) are also included in the "Scoyenia-like" suite (Figs. *4.1.4.*7, 8).

Several types of rhizoliths are also included in this suite because of their growth and preservation under the same set of environmental variables as the different trace types (i.e. wet, soft to cohesive, fine-grained substrates, and relatively fresh water). They are described in Table 4.3 (adapted from Scott et al., 2009). The Pleistocene–Holocene rhizoliths at Loburu were preserved by a variety of authigenic minerals (e.g., opaline silica, fluorite, analcime) precipitated under geochemical conditions determined mainly by the composition and temperature of hot-spring fluids in association with the evapotranspiration by the plants themselves (R.A. Owen et

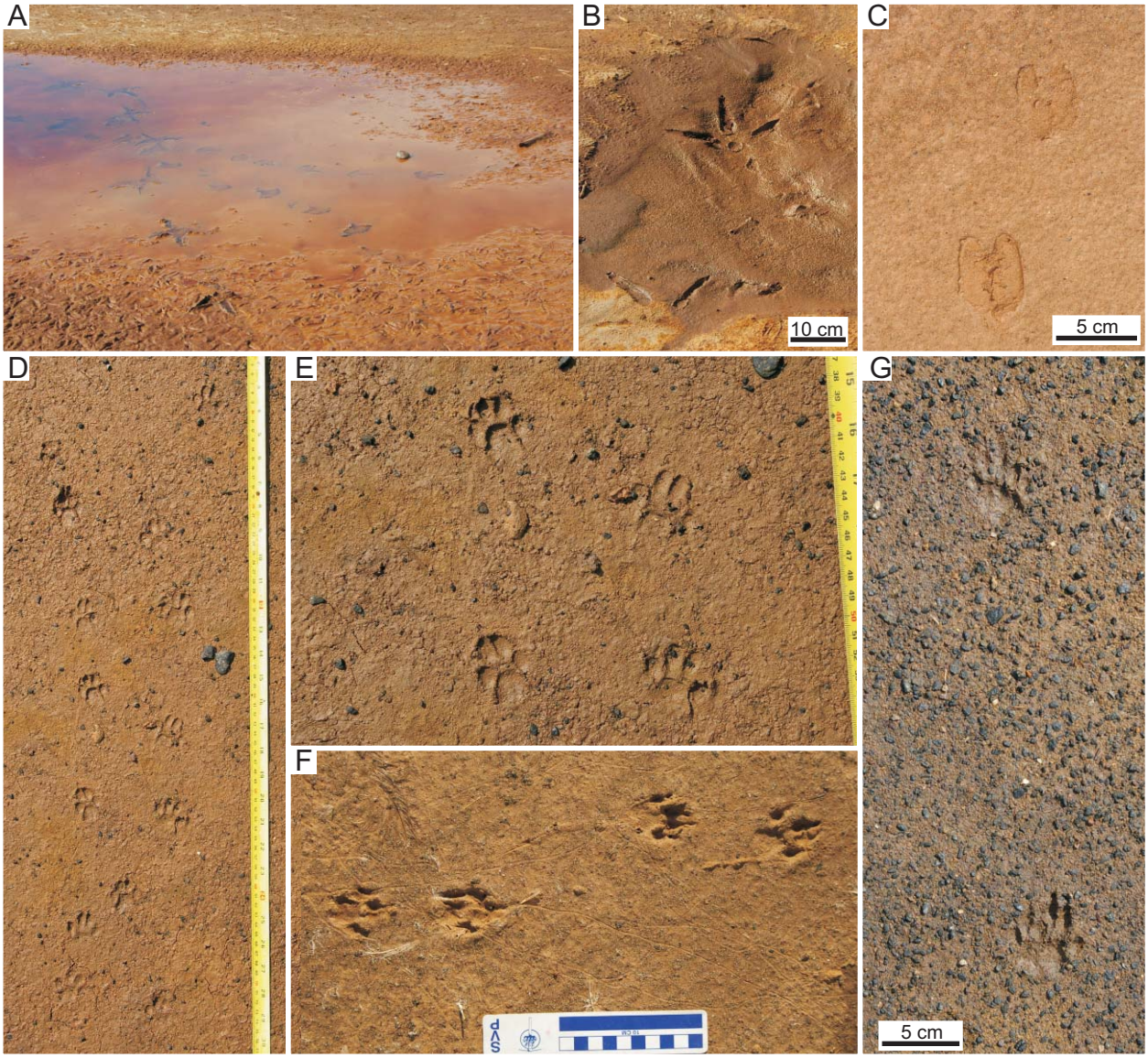


**Fig. 4.1.4.8.** Modern vertebrate tracks near shoreline of the Loburu Delta, Lake Bogoria. **(A–B)** Marabou stork tracks in desiccating pools on lower delta-plain. **(C)** Warthog tracks on wet, slightly firm mudflat substrate. **(D–G)** Mongoose trackways in muddy and sandy substrates at Loburu. Trackway on right in (D) and (E) may have been produced by a serval cat, or similar small felid.

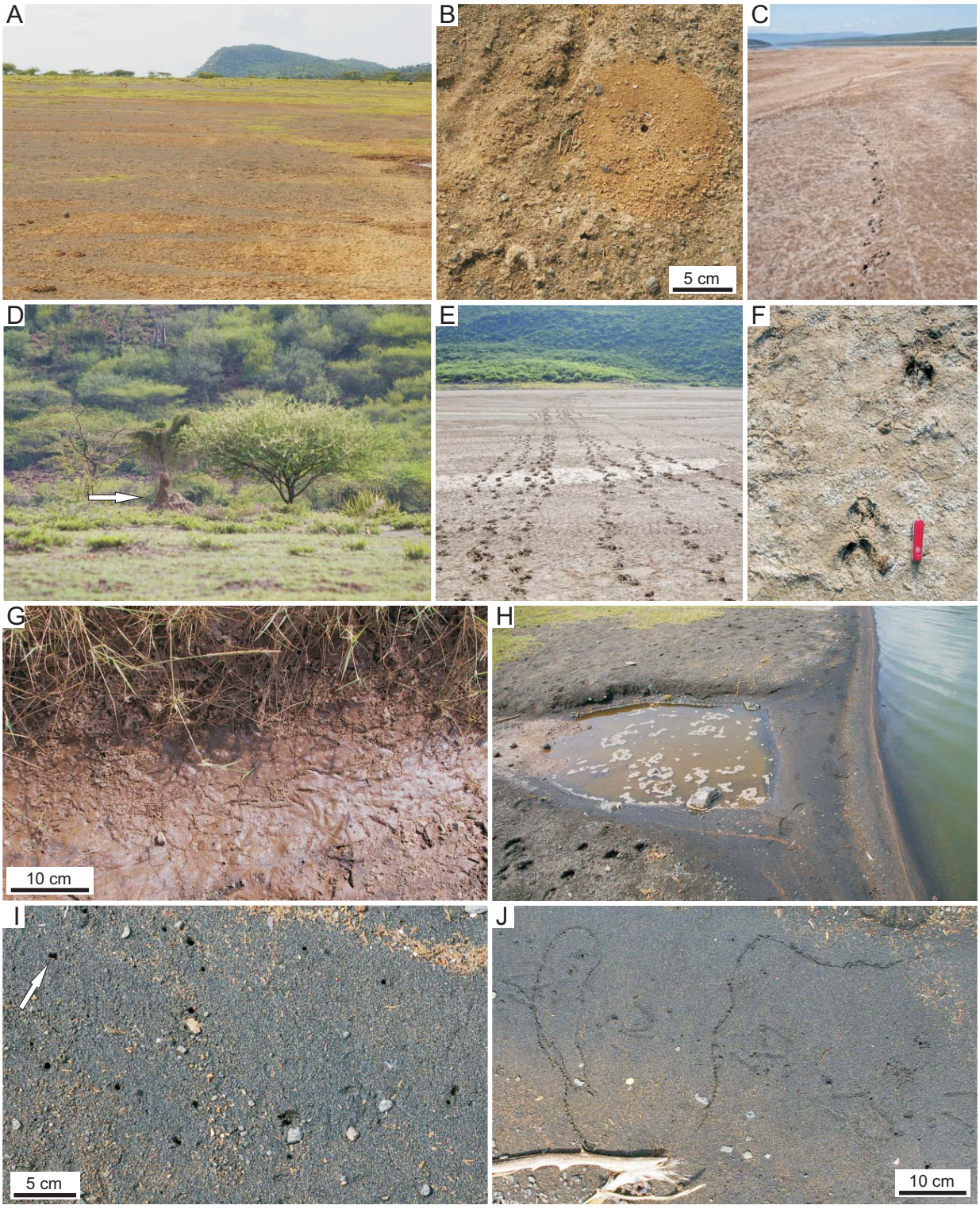


**Fig. 4.1.4.9.** Modern traces on the Sandai Plain, Lake Bogoria. Photographs shown in (C), (E), and (F) courtesy of R.Renaut. **(A)** The dry Sandai Plain in 2007. **(B)** Burrow opening with excavated material, probably produced by ants. **(C)** Bovid trackway near shoreline in 2006. **(D)** Termite mound (arrow) of Macrotermitinae towards the wooded boundary to Sandai Plain. **(E–F)** Grant's gazelle trackways crossing the Sandai Plain. **(G)** Bioturbated mud in temporarily wet substrate. **(H)** Vertebrate trampled (goats?) coarse-grained sandy shoreline at the southwestern margin of the Sandai Plain. **(I)** Feeding probe marks of shorebirds (arrow) and open vertical burrows of tiger beetles? at shoreline. **(J)** Insect trail and bird tracks (unknown producer) on sandy substrate at shoreline.

al., 2008). Plant traces associated with the Scoyenia-like Suite include branching, dark, organic-lined root-hair pores and open holes from rhizomous wetland sedges and grasses (R.A. Owen et al., 2008; Scott et al., 2009, fig. 5H–L).

The greatest diversity of animals, and the variety of trace types they produced, was observed on the Loburu Delta in moist to wet, and soft to firm, substrates. Lower diversity examples of this suite were observed on the Sandai Plain and along the shorelines of the western lake margin. Overall, this assemblage was associated with moist to wet substrates in areas with high water tables and cohesive substrates, and was concentrated near fresh and brackish water sources including hot-springs and rivers. Animal and plant traces from this suite may be found around the entire lake, but environmental factors that restrict biodiversity, such as increased salinity, strongly affect the precise make-up of the suite in the modern setting. The Loburu delta contains all of the trace types described in Table 4.5, whereas the Sandai Plain, which does not have hot springs, contains a much less diverse assemblage of vertebrate footprints and rare invertebrate burrows (Figs. *4.1.4.*9, 10). Incipient *Skolithos* isp. formed by tiger beetle adults and larvae are widespread around the lake and often comprise a monospecific example of this trace suite. Because tiger beetles are likely responding to a different set of environmental conditions (see Section 4.1.5.2), the vertical burrows of tiger beetles should probably be distinguished from the Scoyenia-like Suite and instead be considered as a representative of a "Skolithos" Suite at Lake Bogoria.

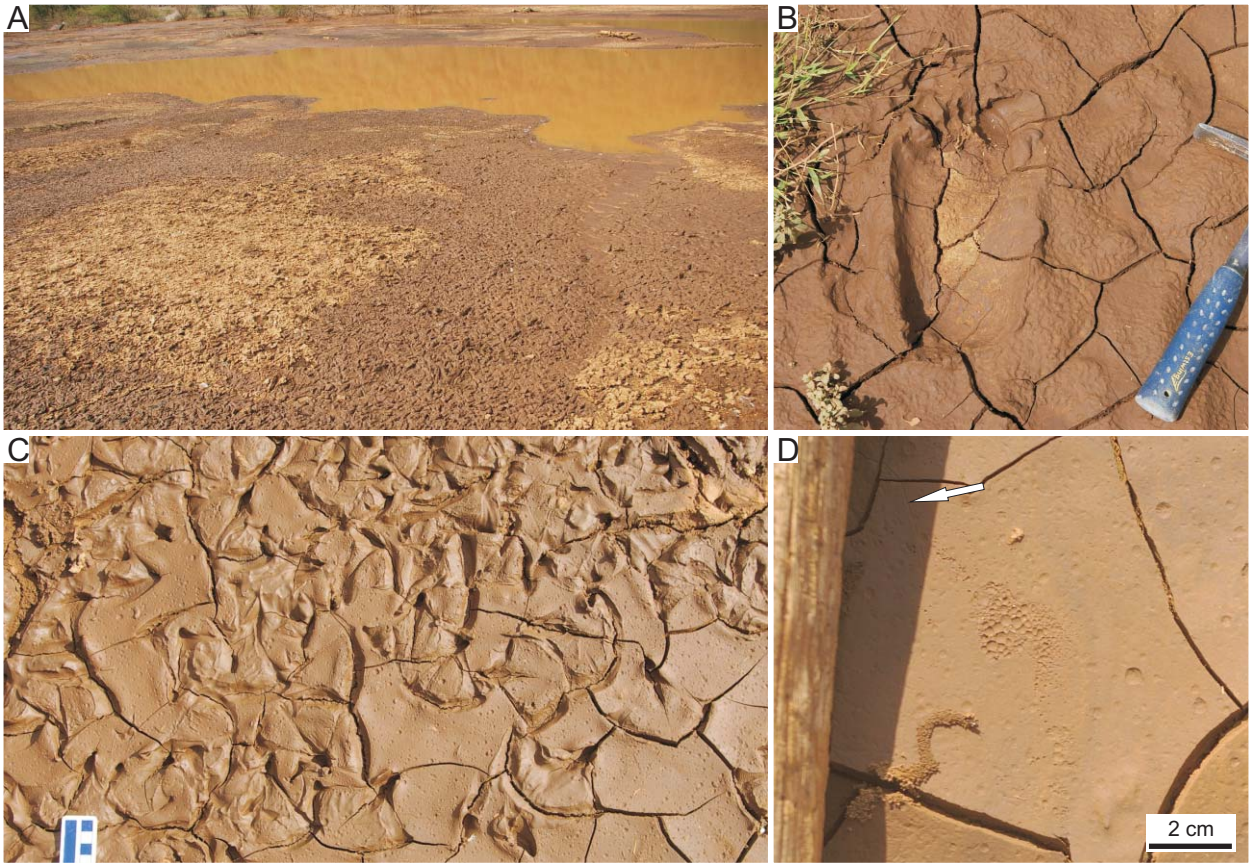


**Fig. 4.1.4.10.** Modern traces near the Sandai River, Lake Bogoria. **(A)** Ephemeral flood pools of the Sandai River in 2007. Note flamingo-trampled surface in foreground. **(B)** Human footprint in desiccating mud. Note wide width due to slipping towards left. **(C)** Flamingo tracks and track-dictated morphology of desiccation cracks. **(D)** Pellet-roofed tunnel (lower left), tiny simple surface trail (arrow), bubble-marks, and raindrop imprints on clay-rich substrate.

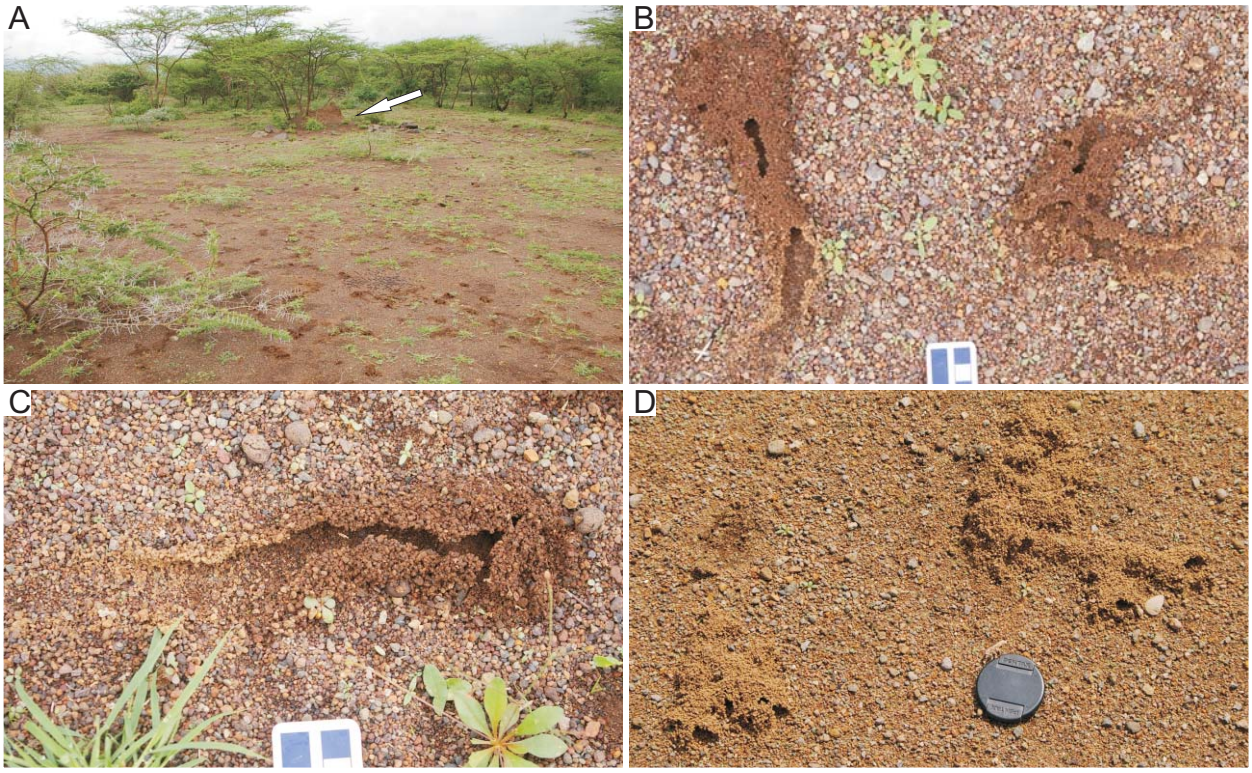


**Fig. 4.1.4.11.** Modern termite traces ~100 m from the western shoreline at north Loburu. **(A)** Coarse-grained sand and gravel surface covered by tunnels shown in (B–D). Note old termite mound in background (arrow). **(B–D)** Examples of partially collapsed surface tunnels of termites produced with coarse-grained sand and mud.

*4.1.4.5. Suite 5: The "Termitichnus-like" Suite*— The "Termitichnus-like" Suite was recognized by Scott et al. (2009) from fossil examples in the Loboi Silts and equivalent units exposed around the margins of Lake Bogoria. The traces that comprise this suite (*Planolites* isp., *Palaeophycus* isp., *Beaconites* isp., *Taenidium* ispp., *Termitichnus* isp., and ant nests) were observed only in the fossil examples and not the modern lake-margin and delta-plain sediments. However, large termite mounds built by fungus-growing species of the subfamily Macrotermitinae (Insecta: Isoptera: Termitidae) are present around the shorelines of Lake Bogoria where the lake-margin slopes are relatively steep, and presumably, water tables are relatively deep and substrates are well drained. The mounds were observed in terrestrial sites, outside of the range of typical present-day lake-level rise, and in close association with *Acacia* trees (Fig. *4.1.4.*11A). The mounds were not studied in detail, but they show several typical features of fungus-growing termite mounds of the Macrotermitinae, including: 1) large mounds < 2 m in height, taller than wide; 2) tall, narrow "chimneys" rising < 2 m above the mound; and 3) numerous large (< 8 cm diameter), open passages with smooth internal walls towards the tops of the mounds (air exchange passages). Other traces of modern termites observed include small (1.5–2 cm internal diameter; 3–4 cm external diameter), open tunnels built above the ground surface with masticated sediment aggregates and surrounding sediment forming the tunnel walls and roofs (Fig. *4.1.4.*11B–D). They sometimes branch, are smooth internally, and are sometimes connected to subterranean tunnels. These structures may be either subaerial foraging tunnels built to protect the termites from low humidities and light while feeding subaerially.

*4.1.5. Common Trace Makers at Lake Bogoria*

Several large mammals and birds frequent the shoreline and delta-plain areas at Lake Bogoria. Lesser flamingos, in particular, have a dramatic impact on shoreline and shallow lacustrine sediments by trampling subaqueous and subaerial substrates, producing millions of footprints, and through their excavation of mud, construction of nest mounds, and compaction of sediments near nesting areas. The most abundant invertebrate trace makers in wet, cohesive substrates of the supralittoral zone included the larvae and adults of tiger beetles (Coleoptera: Cicindelidae), the larvae and adults of rove beetles (Coleoptera: Staphylinidae), and the larvae and adults of earwigs (Dermaptera: Labiduridae). Other trace makers include the larvae and/or adults of other insects such as dipteran flies, carabid beetles, heterocerid beetles, unidentified beetle larvae, crickets, and spiders. The types of traces produced by these insects were included in the Scoyenia-like Suite and in some cases it was possible to observe these trace makers directly within their burrows. This section briefly describes some important behavioural and ecological aspects of some trace makers and discusses the observations made at Lake Bogoria, as well as the potential significance of their life-history and distribution for ichnology.

*4.1.5.1. Flamingos (Ciconiiformes: Phoenicopteridae)*— Flamingo-like gregarious birds are known from rocks as old as the Eocene of southwest Wyoming (McGrew and Feduccia, 1973, 1980; McGrew, 1980; Ericson, 1999), and the flamingo family Phoenicopteridae was present in Kenya by at least the Miocene (Dyke and Walker, 2008). Today, flamingos are found at tropical and subtropical saline lakes and inland salt pans, as well as marine saline lagoons and deltas (e.g., Allen, 1956; Kear and Duplaix-Hall, 1975; Ogilvie and Ogilvie, 1986; Caziani et al., 2007). They extensively modify delta-plain, sandy shoreline, mudflat, and shallow littoral sediments. Flamingos congregate at suitable breeding and feeding sites, which are typically inaccessible saline mudflats that predators are unable to reach in areas where there is an abundant food supply of microorganisms in the water or sediment (e.g., Allen, 1956; Brown and Root, 1971). They also require freshwater for drinking and bathing (e.g., Brown, 1973). Thus, breeding areas tend to be concentrated near fresh water sources if possible (cf. Berry, 1971; Brown and Root, 1971). At Lakes Bogoria, Magadi, Nasikie Engida, and at Lake Natron (Brown and Root, 1971) these fresher, open water areas may be fed directly by hot springs and/or by meteoric water at delta mouths.

Two species are present at Lake Bogoria and elsewhere in Africa: Lesser flamingos (*Phoeniconais minor*) and Greater flamingos (*Phoenicopterus ruber*), which differ in food source because of differences in their bill structures (e.g., Jenkin, 1957; Ogilvie and Ogilvie, 1986). Greater flamingos feed on larger items including insect larvae and other small invertebrates (e.g., brine shrimp) that may be filtered directly from soupy mud (e.g., Gallet, 1950). Lesser flamingos filter much smaller food items such as spiral-shaped cyanobacteria (e.g., *Arthrospira*, *Anabaena*), diatoms, and tiny insect larvae smaller than 1.0 x 0.4 mm (Jenkin, 1957; Vareschi, 1978). Both species feed while walking through shallow water, but only Lesser flamingos feed from lake water while swimming in deeper areas that have abundant films of cyanobacteria on the surface of the lake. During the field seasons of 2001, 2002, 2007, and 2008, Lesser flamingos were more abundant at the relatively deep, steep-sided Lake Bogoria, whereas Greater flamingos were more common at lakes with more extensive low-gradient mudflats (e.g., Nasikie Engida, Lake Magadi).

Flamingos dramatically impact their sedimentary environments as a result of their life-history. They congregate in such huge numbers (< 2 million at Lake Bogoria) and feed, display, bathe, and "march" in shoreline areas. They not only trample and churn sediments, but they also greatly contribute to the compaction of subaerially exposed surfaces. Their nest-building


**Fig. 4.1.5.1.** Modern flamingo nests at the south Loburu Delta. Photographs shown in (F–H) courtesy of R.Renaut. **(A–E)** Freshly made nest mounds. Note feathers in top and outer parts of nests. **(F–H)** Freshly made nest mounds on older surface exposed during August, 2006. Note reddish, oxygenated sediments of outer nest.

activities are both constructive and destructive, by building nest-mounds from mud excavated from around the nest if available (Fig. *4.1.5.*1). Normally, flamingos that live in lacustrine settings choose low-gradient saline mudflats during periods (seasonal) of lake-level fall for their breeding sites, when exposed shallow littoral areas provide an increasing amount of suitably wet, muddy nest-building sediments and protection from predators (e.g., Allen, 1956). The breeding areas are extensively trampled, forming compacted sedimentary surfaces that are resistant to erosion and may preserve the irregular micro-topography formed by concentrations of degraded nest mounds. Old nest mounds may even serve as sediment baffles on delta-plains, where they may withstand erosion by lake flooding, deltaic underflows, and/or subaerial sheetflows (Fig. *4.1.5.*2A–D).

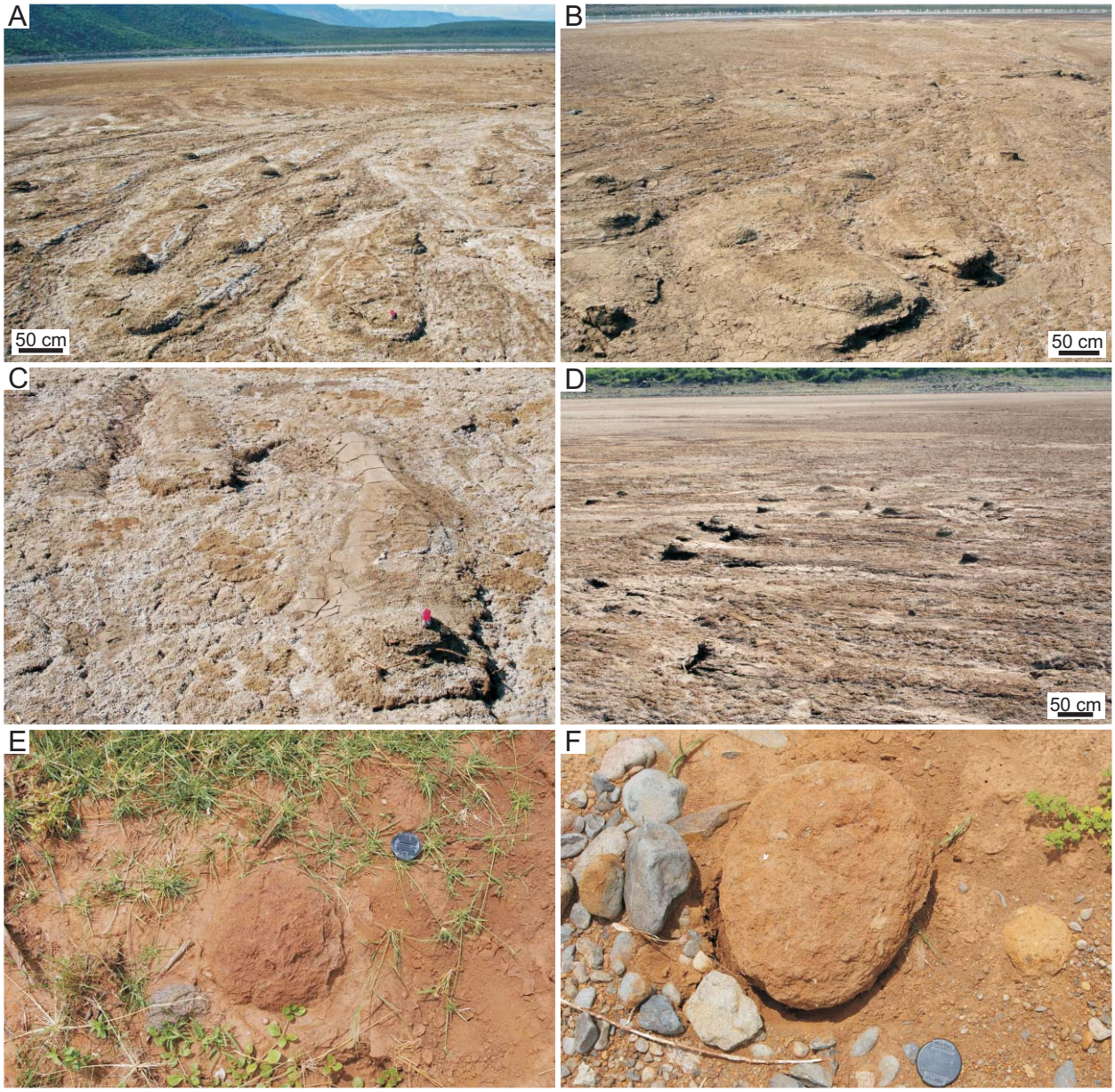


**Fig. 4.1.5.2.** Degraded flamingo nest mounds at Lake Bogoria. Photographs shown in (A–D) courtesy of R.Renaut. **(A–D)** Old flamingo nests mounds at the mouth of the Sandai River. Erosion during flood due to weakly channelized flow around nest-mound obstacles. **(E–F)** Possible internal core of flamingo mound or large, cemented siltstone clast adjacent to modern Parkirichai River.

Modern and fossil flamingo traces are described from Lake Bogoria in Tables 4.2, 4.4, 4.5, and from Lake Magadi in Tables 4.8 and 4.9. The morphology of flamingo footprints is extremely variable depending on substrate conditions and whether or not the sedimentary surface has been trampled by many birds (Scott et al., 2007, fig. 6; Scott et al., 2010). Nest mounds also vary in morphology and size depending on substrate conditions (e.g., wet fresh mud or compacted surface), the stage of nest-building, and the degree of erosion of abandoned nests (Figs. *4.1.5*.1, 3). Weathered and fossilized examples of flamingo nest mounds and associated structures may be reduced to minor, irregular or circular lumps on irregular surfaces, or they may be isolated, oval-shaped mud mounds, potentially transported as very large clasts during floods (Fig. *4.1.5*.2E, 2F). Old, abandoned nest mounds may be flooded and exposed by fluctuating lake levels (Fig. *4.1.5*.3A–H), they may be bioturbated by the roots of salt-tolerant sedges and grasses (Fig. *4.1.5*.3B), they may be colonized by burrowing insects (Fig. *4.1.5*.3C), or they may be trampled when exposed by mammals and birds, including flamingos. Other structures produced by flamingos include large, circular moat-like depressions with slightly raised areas in the centre: these are produced by (Greater) flamingos feeding from soupy mud around them while standing in one place (See Section 4.2.4, Fig. *4.2.4*.9C, 9D; cf. Gallet, 1950, pp. 39–40)

Table 4.6 provides some measurements of flamingo nests from Lake Bogoria, ranging from fresh, large nests at Sandai Plain, to weathered and abandoned nests at south Loburu, to fossilized nests in the Bogoria Silts of Sandai Plain. Nests are normally built by a flamingo straddling the nest site and using its bill to pull the mud towards itself to form a mound of mud between its legs, or by collecting the mud within the bill and squirting it onto the mound (e.g., Brown, 1973; Ogilvie and Ogilvie, 1986). The mud mound is then compacted with the bill and feet, forming an internal, more-compacted core (Fig. *4.1.5*.4). The nest mound is gradually enlarged with the addition of more mud along the sides of the mound, reinforcing and thickening the base of the mound (Gallet, 1950; Allen, 1956; Ogilvie and O.gilvie, 1986). When the time of egg-laying approaches, the flamingos fervently add mud to the mound to increase its height, which forms an outer, more porous layer of less-trampled clumps of mud (Fig. *4.1.5*.4; Ogilvie and Ogilvie, 1986). At the top, a circular depression is made for the egg. In general, the nests are widest at the base and the width at the top of the nest is greater than the nest height (Fig. *4.1.5*.5).

As flamingos pull mud up onto the nest-mounds during the nest-building process, they create muddy depressions in the substrate (Figs. *4.1.5*.1, 3). Where nest-mounds are built together in “clumps” or “strings”, as is the case in most colonies, the lower-lying areas created eventually coalesce and the surface on which the nest-mounds are built becomes an area of increased positive relief with vertical margins, here termed “mini-escarpments”. The shape of such surfaces and mini-escarpments tends to be curvilinear, and in cases where the nest-mounds have been destroyed by erosion, the curves of the mini-escarpment correspond to the original position of an associated nest-mound. If the nest is permitted to dry and bake beneath the sun, it can last many months or even years after use (Berry, 1971; Brown, 1973). When old colony sites are revisited, flamingos commonly add to preexisting nests by using fresh mud to rebuild the nest-mound and increase its height for further use (Allen, 1956; Ogilvie and Ogilvie, 1986).

Many flamingo behaviours, including feeding and displaying, involve the trampling and compaction of substrates. At the mouth of the Sandai River, for example, trampling by flamingos helps to maintain the position of established channels, which are often also associated with nests. At the Loburu Delta in June 2002, previously flooded flamingo-trampled surfaces < 30 cm above lake level were exposed due to lake level drop. These “mini-escarpments” formed along the shoreline as a result of flamingo activity and its interaction with erosion by waves. The

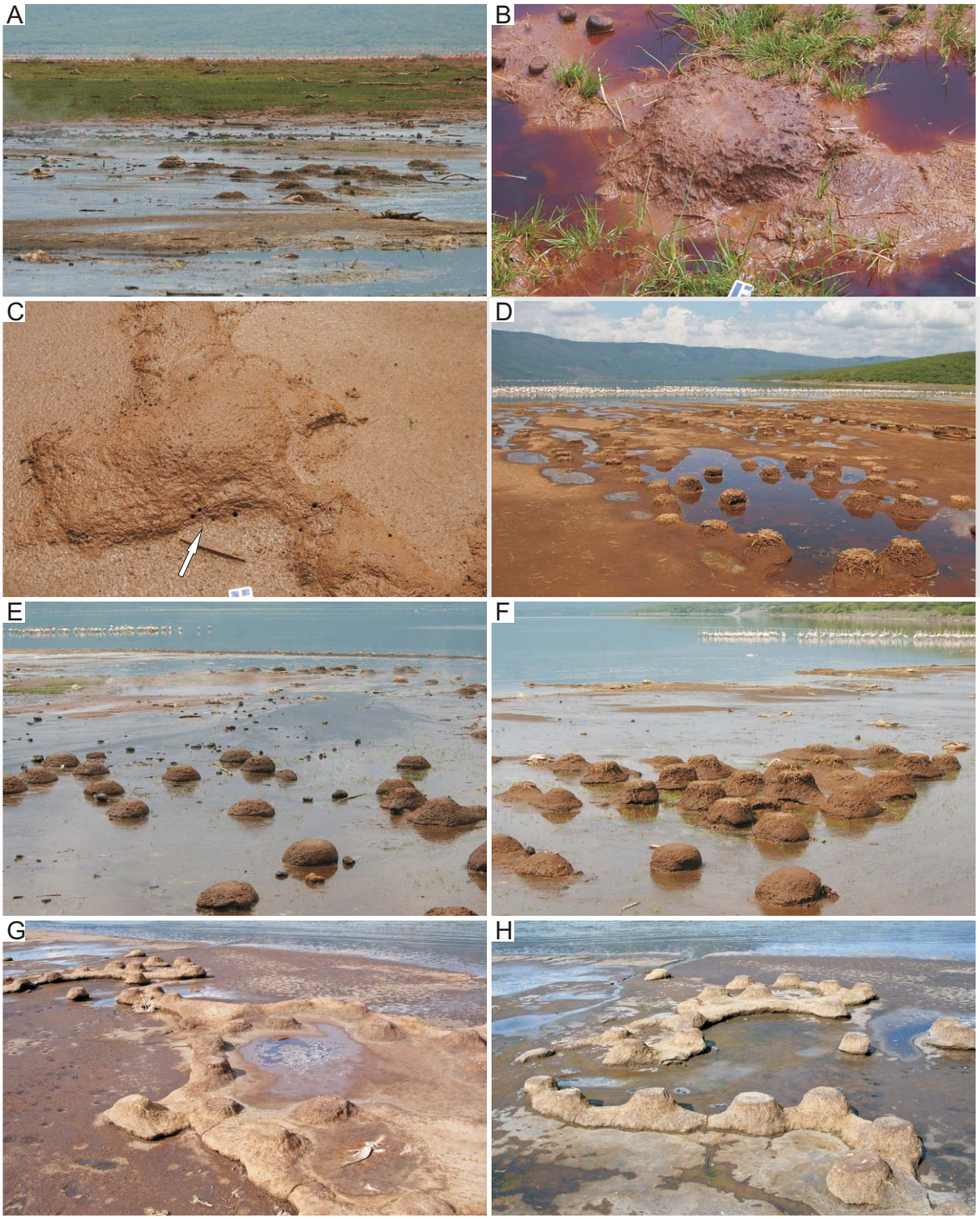


**Fig. 4.1.5.3.** Degraded flamingo nest mounds at south Loburu, Lake Bogoria. Photographs shown in (G) and (H) courtesy of R.Renaut. **(A–F)** In August, 2007. Arrow in (C) showing insect burrows into nest surface. **(G–H)** Drying nest mounds during lake level fall showing linear arrangement.

preservation potential of flamingo-generated or modified structures and surfaces may be especially high in rift valley lakes, due to the rapid cementation of glass-rich, compositionally immature sediments by zeolites such as analcime.

The recognition of structures produced by flamingos in the Cenozoic rock record can potentially be used to: 1) recognize subaerially exposed sediments; 2) help to identify regressive surfaces, sequence boundaries, and co-planar (regression + flooding) surfaces; 3) help to identify shorelines and low-gradient areas, depending on the distribution of nest-mounds; 4) help to distinguish between saline and freshwater mudflats; and 5) help to interpret structureless sediments or units with ped-like textures but which are not paleosols. Applications of vertebrate footprints in general also apply to flamingo footprints, including: 1) the recognition of different substrate characteristics (e.g., consistency, water content); 2) using footprint densities to help identify shorelines (e.g., "shore-bird ichnofacies"); and 3) using taphonomic features of the fossil prints to help interpret environmental conditions (cf. Scott et al., in press). The preservation of these traces is expected to be more prevalent where the preservation potential of vertebrate bones

**Table 4.6.** Measurements of modern and fossil flamingo nest-mounds at Lake Bogoria. Measured in July, 2002.

| | Width at top (cm) | Width at base (cm) | Height (cm) |
|---|---|---|---|
| **Fossil flamingo nest-mounds in the Bogoria Silts, Sandai Plain, July 2002.** | | | |
| 1. | 18 | 25 | 9 |
| 2. | 16 | 25 | 7 |
| 3. | 24 | 24 | 6 |
| 4. | 16 | 16 | 9 |
| 5. | 15 | 23 | 5 |
| 6. | 14 | 28 | 3 |
| 7. | 14 | 24 | 3 |
| 8. | 23 | 27 | 8 |
| 9. | 18 | 18 | 1 |
| 10. | 15 | 21 | 5 |
| ***Average:*** | ***17*** | ***23*** | ***6*** |
| **Modern flamingo nest-mounds at the mouth of Sandai River, July 2002.** | | | |
| 1. | 24 | 35 | 12 |
| 2. | 27 | 34 | 8 |
| 3. | 28 | 37 | 12 |
| 4. | 26 | 28 | 8 |
| 5. | 28 | 34 | 13 |
| 6. | 23 | 29 | 11 |
| 7. | 33 | 36 | 11 |
| 8. | 28 | 39 | 13 |
| 9. | 21 | 37 | 15 |
| 10. | 28 | 32 | 12 |
| ***Average:*** | ***27*** | ***34*** | ***12*** |
| **Modern flamingo nest-mounds at South Loburu, July 2002.** | | | |
| 1. | 19 | 34 | 10 |
| 2. | 22 | 39 | 10 |
| 3. | 16 | 20 | 9 |
| 4. | 21 | 29 | 11 |
| 5. | 26 | 26 | 10 |
| 6. | 22 | 22 | 11 |
| 7. | 12 | 24 | 12 |
| 8. | 17 | 26 | 5 |
| 9. | 17 | 27 | 11 |
| ***Average:*** | ***19*** | ***27*** | ***10*** |

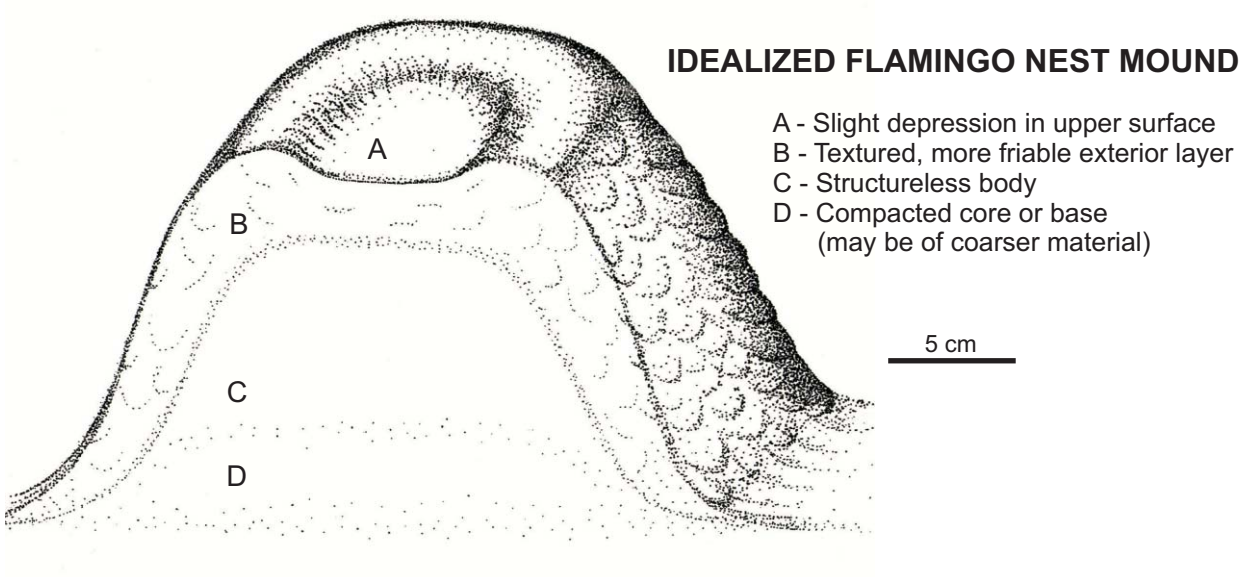


**Fig. 4.1.5.4.** Schematic diagram of an idealized nest mound.

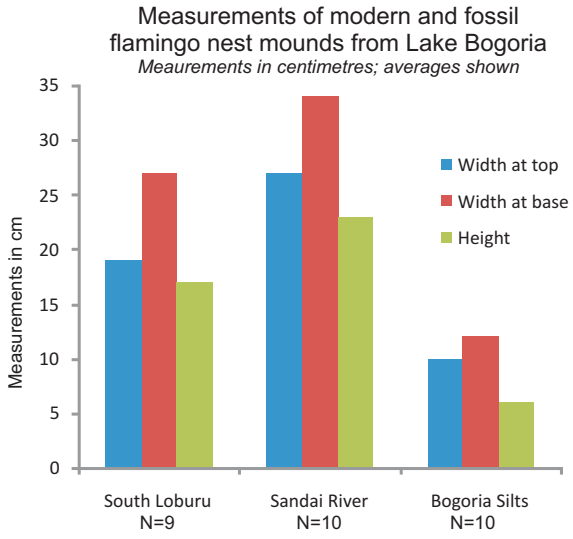


**Fig. 4.1.5.5.** Bar graph showing nest mound dimensions from different sites at Lake Bogoria in 2002.

is limited (e.g., saline flats). Thus the recognition of fossil flamingo traces may also contribute to the paleobiological and paleoecological understanding of flamingos and extinct flamingo-like birds (e.g., *Presbyornis*, *Juncitarsus*).

*4.1.5.2. Tiger Beetles (Coleoptera: Cicindelidae)*— Predaceous beetles of the suborder Adephaga, tiger beetles are closely related to the ground beetles (Carabidae), but an important difference between them in ichnological terms is the burrow-dwelling habits of tiger beetle larvae. Tiger beetles are well known to produce simple, vertical and oblique burrows during all stages of their life cycle (e.g., Criddle, 1907; Stanley and Fagerstrom, 1974; Dreisig, 1980; Pearson, 1988). They hunt by "sitting and waiting" near the surface, using their characteristic dorsal abdominal protrusion with "hooks" to maintain their position in the burrow in a small indent in the burrow wall until prey passes near the burrow opening (e.g., Pearson, 1988). They grab the prey with their large mandibles and pull it into the burrow. The burrows of adults and

larvae may be distinguishable from one another, but the distinction between the burrows of different genera of tiger beetles is likely impossible, particularly if dealing with fossil material. However, it may be possible to recognize their burrows to family (Cicindelidae) if certain features are preserved in their burrows (e.g., Netto, 2007). Namely, a "screw-like" ornamentation on the internal burrow boundary may be produced by the thoracic protrusion on the larvae, which is used for stabilizing the larvae near the top of their burrows when hunting (Fig. *4.1.5*.6). In most cases, however, these structures are not produced even in the modern setting and likely are produced only in very cohesive or slightly indurated substrates.

Larval tiger beetles excavate small to medium-sized, vertical, open burrows that may bend slightly, becoming oblique, and may contain a slightly enlarged chamber at the base of the burrow. The burrows are circular, and range in size depending on the larval instar and also by species. Typically, burrows of the first instar are ~2 mm in diameter, second instar burrows range from ~2–4 mm, third instar burrows are ~3–5 mm, and adult burrows are ~4–10 mm in diameter (e.g., Bauer, 1991; Takeuchi and Hori, 2007; Mawsdley and Sithole, 2009). The third instar excavates a slightly enlarged pupal chamber at either the base or side of the burrow. Adults emerge by using the third instars burrow or occasionally by excavating an emergence burrow (Bauer, 1991). This behaviour may lead to the presence of occasional U-shaped burrow in association with the dominantly vertical burrows (cf. Netto, 2007). The depths of the burrows are extremely variable, are shallowest for first instars, and typically range from ~5 cm to 45 cm deep (e.g., Bauer, 1991; Knisley, 1984; Knisley and Juliano, 1988). Both larvae and adults may plug their burrows at the top with sub-spherical excavated sediment aggregates during certain parts of the day and/or year, depending on their pattern of activity (nocturnal or diurnal), life history (timing of developmental phases), the climatic zone within which they live (tropical or temperate), and whether or not their habitat is flooded (closed) or exposed (opened) during seasonal rains or by high tides (e.g., Criddle, 1907; Dreisig, 1980; Guppy et al., 1993; Satoh et al., 2006).

Adult tiger beetles may also excavate burrows in order to escape temperature conditions outside their preferred range. In hot, arid settings, adults excavate shallow, oblique burrows to escape temperatures more than ~36° C during the hottest times of day and retreat to burrows to spend the night when temperatures are lower than ~20° C (e.g., Dreisig, 1980). They may reuse old burrows or excavate a new burrow each time they need to escape (Dreisig, 1980). Adult daily shelter burrows in dune sands have been recorded with depths < 9 cm and lengths < 16 cm (Knisley and Hill, 2001), but vary depending on temperature and soil moisture (Guppy et al., 1983). In hot environments where access to shade or wet substrates is available, adults may simply just relocate to areas with more suitable temperatures, or excavate very shallow (< 1 cm depth) oblique burrows in moist to wet substrates (Guppy et al., 1983). The depths of adult tiger beetle burrows may also be related to the moisture requirements of larvae. In dune sands, for example, it has been suggested that the adults dig deep burrows for oviposition in moist sediments (e.g., Knisley and Hill, 2001). In climatic zones with cold winters, both adults and larvae excavate deep (< 2 m) vertical to oblique burrows which are plugged by excavated sediment (e.g., Criddle, 1907).

In modern settings, tiger beetles are present in many different environments in both tropical and temperate zones worldwide, including: dune sands (e.g., Pineda and Kondratieff, 2003); riverine habitats in humid and semi-arid climates (e.g., Zerm and Adis, 2001; Mawdsley and Sithole, 2007); saline lagoons (e.g., Eusebi et al., 1989) and lakes (e.g., Willis, 1967; Hoback et al., 2000); intertidal to supratidal zones (e.g., Satoh and Hori, 2005); and even within montane or semi-open forested areas (e.g., Knisley, 1984; Schultz, 1989). Temporal and micro-habitat segregation between species living in the same localities has been well studied (e.g., Ganeshaiah

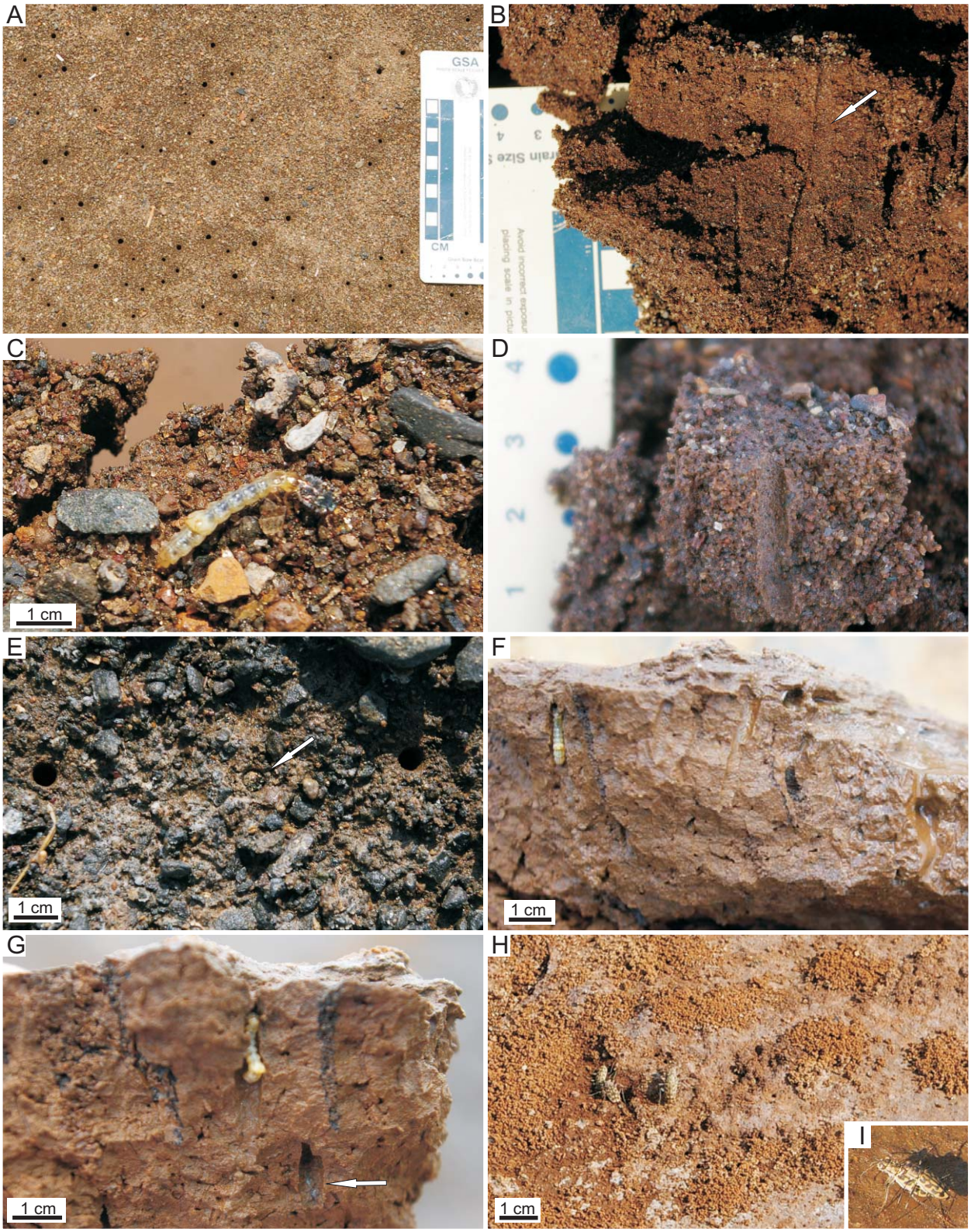


**Fig. 4.1.5.6.** Modern tiger beetle burrows and tiger beetle larvae in shoreline sediments at Lake Bogoria. **(A–E)** Coarse-grained sand of shoreline at "old" Loburu. Arrow in (E) showing head of tiger beetle larvae at burrow opening. **(F–G)** Muddy cohesive and slightly indurated muds at Emsos. Note black lining of vertical burrows. Arrow in (G) showing expanded, rounded terminus of burrow. **(H–I)** Adult tiger beetles mating at south Loburu.

and Belavadi, 1986; Schultz and Hadley, 1987), showing that within a suitable environment, one species or another will occupy certain areas during times of the year that are both warm enough and humid/wet enough. Several factors have been cited as being the most important controls on their habitat usage, which differ slightly between the fossorial adults and the usually sedentary larvae. Adults and larvae generally occupy the same or slightly different micro-habitats within the same area (e.g., Knisley, 1987).

All tiger beetles require open, warm, sunny areas, and sandy substrates in general, even within forests (e.g., Schultz, 1989; Hadley et al., 1990). Water availability is especially important for larvae in order to prevent desiccation (Knisley and Juliano, 1988; Hadley et al., 1990), but also plays a role in adult behaviour (Guppy et al., 1983). Oviposition sites are carefully chosen near water or moist sediments by adults because of the sedentary behaviour of the larvae (e.g., Knisley and Hill, 2001; Zerm and Adis, 2001). Food availability is clearly a limiting resource for sedentary larval tiger beetles (e.g., Pearson and Knisley, 1985).

Temperatures of air and substrates control the micro-habitat utilization and behaviour (e.g., finding shade, burrowing) of adults (e.g., Dreisig, 1980; Eusebi et al., 1989), especially in dry, hot environments (Guppy et al., 1983). However, tiger beetles endemic to dune fields prefer areas with only very sparse vegetation and shifting sands, where larvae remain in their closed burrows until moisture levels increase due to rainfall directly on the dunes (Pineda and Kondratieff, 2003). In the more typical environments used by tiger beetles, such as inland salt flats, shady oviposition sites are chosen by some adults in order to protect their larvae from high temperatures and desiccation (e.g., Hoback et al., 2000).

Salinity has rarely been measured during ecological studies of tiger beetles, and the upper limits that tiger beetles can withstand are unknown. Some species prefer saline habitats and may be segregated from other species in the same habitat depending on salinity (Hoback et al., 2000). Hoback et al. (2000) reported oviposition in substrates with up to ~12 g $L^{-1}$ TDS. The salinity tolerances of *Cicindela* species utilizing saline playa habitats in New Mexico and Arizona have not been reported, although several species were observed on saline flats with < ~22 g $L^{-1}$ TDS (Knisley, 1984). The presence of many species in coastal habitats worldwide suggests that as a group, they can tolerate salinities at least as high as sea water (~35 g $L^{-1}$ TDS). Those in saline lagoons must survive fluctuating salinity levels, from ~4–16 g $L^{-1}$ TDS during wet seasons, to more than that of sea water during evaporative periods (Eusebi et al., 1989). Satoh and Hori (2005) reported one species, capable of living in habitats flooded bimonthly by spring tides, in substrates with salinities up to 5% (or 50 g $L^{-1}$ TDS).

Most, but not all, cicindelid larvae do not leave their burrow during development, and some have evolved physiological and/or behavioural adaptations to survive flooding and anoxia (e.g., Zerm and Adis, 2003; Satoh et al., 2006). Other species are able to leave their burrows and excavate new burrows nearby if the micro-habitat conditions change (e.g., flooding; Brust et al., 2006). Larval burrows are unlined, and developmental success depends on the larvae being able to live protected within their burrows, stay moist and at the right temperature, as well as to have access to a food source that does not require them to leave their burrows. Ideal places for larvae are those with relatively wet and stable moisture conditions within sandy burrowing substrates (e.g., shorelines, fluvial bars). These also tend to be places that are suitable habitat for other insect adults and larvae (e.g., dipterans, staphylinids, tenebrionids) upon which the tiger beetles prey (e.g., Knisley and Juliano, 1988). Even during the dry season of semi-arid South Africa, riverine species of tiger beetles are active along perennial rivers up to ~15 m distance from the water's edge (Mawdsley and Sithole, 2007).

The sandy, vegetation-free shorelines that surround Lake Bogoria are another example of this ideal environment. However, there is a general lack of tiger beetle burrows at Sandai Plain

when compared to the rest of the shoreline, which may be related to: 1) muddier sediments along the shoreline; 2) trampling of the plain near the shoreline by flamingos; 3) the total lack of shade and very high surface temperatures; 4) thick salt crusts; and/or 5) a lower density of other insects that could provide food for larvae (e.g., diptera). Very few tiger beetle burrows were observed at Lake Magadi and none were observed at Nasikie Engida, although this may be due to a lack of intensive sampling and/or beetle inactivity during August. The examples observed at Magadi were associated with spring-fed inflow to the NW Lagoon (Site 1) in wet substrates above the observed water level in the lagoon (see Section 4.2.4.1). Although the eastern shoreline of the E Lagoon was heavily bioturbated by insects, only the burrows of staphylinid beetles and spiders were identified when the area was visited during August 2007 and 2008. The shoreline there is similar to that of Sandai Plain in that salinity is very high and flamingos trample on and build nests from the substrate, but daily surface temperatures are likely even higher at Magadi. More data is required to explain the apparently lower abundance of tiger beetles at Magadi.

The overall consistent association between larvae and wet, usually sandy, shorelines that are subaerially exposed for at least part of the year may emerge as a valuable tool for the reconstruction of various sedimentary parameters within lacustrine and fluvial environments. For example, sedimentation rate, seasonal sedimentation, and seasonal exposure of the substrate may be gleaned by using the vertical burrows of tiger beetles in active fluvial environments. Tiger beetle burrows in estuaries (e.g., Satoh et al., 2006), intertidal sandflats, salt marshes, and marine beaches (e.g., Fenster et al., 2006) may also be important for recognizing subaerially exposed substrates with vertical burrows (*Skolithos* isp.) in these transitional environments between the continental and marine realms. They may form a previously unrecognized part of the supratidal community that produces burrows of the Psilonichnus and/or Skolithos ichnofacies in marine strata.

On a landscape scale, the relative density of burrows is expected to be highest along stable shorelines or at the position where a changing shoreline is most typically present during the "summer" when the larvae are active. In order to use the density of the vertical burrows of larval tiger beetles as a mapping tool, it may be necessary to distinguish them from other vertical burrows. The typical distribution of tiger beetle larval burrows is along shorelines in both lacustrine and fluvial settings, so that this type of distribution, together with morphological features, could potentially be used to recognize them. Other high densities of simple, unbranched vertical burrows in similar places could be produced by spiders. No studies of tiger beetles using barrier bars and spits in either marine or lacustrine settings are known to this author, but it is expected that they do, provided that the bars remain subaerially exposed and are stable for a sufficient period of time for larval development.

Potentially, the highest densities of tiger beetle larval burrows could be used for mapping moisture conditions of subaerially exposed suitable substrates — mainly shorelines — with lower densities on both the subaqueous side and subaerial side of the shoreline. In a study of tiger beetle species habitat distribution in New Mexico, Knisley (1984) found that densities were highest in the freshwater river-edge or lake-edge habitats (~3.3 g $L^{-1}$ TDS) when compared with grasslands, sand flats, or saline flats (~22 g $L^{-1}$ TDS) and were very low in montane grassland habitats. Although the density between individual species sharing the river-edge or lake-edge habitats varied from low to high, because a larger number of species was present in this habitat type, they showed the overall highest density (Knisley, 1984). Frequently fluctuating lake levels in closed lake basins, for example, may 'spread out' this roughly linear distribution throughout the year in tropical regions where tiger beetles are active year-round, or it may be 'spread out' by the movement of the larvae and reestablishment of burrows in other sites during higher water levels (cf. Brust et al. 2006). Alternatively, the possibility exists that larval tiger beetles may

plug their burrows when the habitat is flooded regularly, as in the examples from intertidal sites in Japan (Satoh et al., 2006).

The burrows of tiger beetles whose primary habitat is active dune fields show a different distribution from shoreline examples, but one which also reflects moisture conditions. Populations of *Cicindela limbata*, endemic to the Coral Pink Sand Dunes of Utah, were most abundant at transition areas between active, shifting dunes with very little vegetation and more stabilized and more vegetated dunes (Knisley and Hill, 2001). More specifically, both adults and larvae were most abundant in the interdune swales of transverse dunes away from the slipface, where the sandy substrates were relatively moist and had some sparse vegetation, and on the non-vegetated stoss-side lower slopes of the adjacent dune (Knisley and Hill, 2001). Larvae were most active following rains and were also observed on the mid- and upper stoss-side of the slopes, as well as at the bases of some slipfaces, during wetter periods (Knisley and Hill, 2001). Overall, burrows of *C. limbata* were concentrated within interdune swales and low slopes (66%), and became progressively fewer from the mid-slope (24%) to the upper dune crest (10%) (Knisley and Hill, 2001). A small population of *C. tranquebarica*, the only other tiger beetle species inhabiting the dune field, was also present in some interdune swales but only where the substrate contained more clay and wetter substrates (Knisley and Hill, 2001). This study by Knisley and Hill (2001) provides evidence that within dune fields the density of tiger beetle burrows is also highest in areas with more moisture. If preserved, examples of high-density vertical and oblique burrows in this type of setting can also show a distinct distribution, which as in this case may reflect the linear interdune swales of transverse dunes.

The diversity of environments in which tiger beetles are presently found worldwide may limit the applicability of their burrows as a tool. However, in sedimentological terms, three main aspects of their ecology may be reflected in the rock record. First, they all require open areas during all stages of the life cycle, and second, these open areas tend to be sandy overall. There are exceptions to this, however, particularly in saline playas (e.g., Knisley, 1984). What does tie together their habitats is that they are all areas that experience frequent disturbances, by erosion, by sedimentation, and/or by regular flooding. Active dune fields, for example, are continually shifting, which maintains the generally open, vegetation-free suitability of the environment for tiger beetles. Third, tiger beetles are also typically closely associated with water bodies of various salinities. In riverine settings, for example, both larvae and adults produce burrows within channel sands, on point bars, on shorelines, and on floodplains during periods of subaerial exposure (e.g., Zerm and Adis, 2001; Mawdsley, 2009; Mawdsley and Sithole, 2009). Many species are able to survive periods of flooding (hours to months) by either simply plugging their burrows, or by altering their heart rate and respiration (e.g., Zerm et al., 2004). Thus, tiger beetles can produce vertical burrows from subaerially exposed surfaces within active channel systems. Similarly, other depositional environments such as lacustrine and playa-lake shorelines, the upper reaches of tidal flats and marine beaches, which are frequently flooded, may produce a close association with subaqueous sedimentation and the vertical burrows of tiger beetles.

*4.1.5.3. Rove Beetles (Coleoptera: Staphylinidae), with Discussion of Similar Burrows of Beetles (Coleoptera: Heteroceridae, Carabidae) and Crickets (Orthoptera: Anostostomatidae)* — Staphylinid beetles are diverse and extremely abundant (> 40,000 described species) worldwide (Grimaldi and Engel, 2005). Burrowing types live primarily in transitional zones of fluvial (e.g., Smith and Hein, 1971), lake margin (e.g., Silvey, 1936; Garcia and Neill, 1991), intertidal (e.g., Griffiths and Griffiths, 1983), salt marsh (e.g., Wyatt and Foster, 1988), sabkha and lagoon settings (e.g., Gerdes et al., 1985). Staphylinids are the oldest members of the suborder Polyphaga, with fossil examples from marginal environments of meromictic lakes in the

Triassic rifts of eastern North America (~220 Ma; Fraser et al., 1996; Grimaldi and Engel, 2005). Subsequent records include the first appearance of the genus *Bledius* in the Eocene from the Green River Formation (Scudder, 1890 *in* Herman, 1986). Staphylinids may be predaceous (e.g., *Thinopinus* spp.), scavengers or parasites, or they may feed exclusively on diatoms and cyanobacteria (e.g., *Bledius* spp.) (Richards, 1983; Herman, 1986). Intertidal, salt marsh, lagoon, and lake-margin species are typically found in vegetation-free, wet, well-drained subaerial substrates (e.g., Craig, 1970; Gerdes et al., 1985; Wyatt and Foster, 1988), but can survive periods of immersion (several hours to several days) by waters with various salinities (e.g., Wong and Chan, 1977; Griffiths and Griffiths, 1983; Wyatt, 1986; Herman, 1986; Topp and Ring, 1988). Adult beetles that are caught outside of their burrows during floods can fly directly from the water surface to dry ground (Herman, 1986). Some species may relocate their burrows to higher ground during long term or seasonal floods (Herman, 1986). Burrows help staphylinids survive periods of flooding, desiccation, extreme temperatures, and help protect them from predators and parasites (Herman, 1986).

Staphylinids (*Bledius* spp.; possibly *Paederus* sp.) are abundant at the southern Loburu Delta at Lake Bogoria, where they produce several types of burrows in both the adult and larval stages (Figs. *4.1.5.*7, 8). The genus *Bledius* is well known as a subsocial, burrowing, microbe-feeding beetle in marine intertidal environments and salt lakes (e.g., Herman, 1986; Garcia and Neill, 1991). Characteristically, members of this genus excavate "wine bottle-shaped" dwelling burrows with narrow (~2–3 mm) vertical openings to the surface and larger expansions of the burrows below (< ~7 mm diameter) where larval and adult individuals live (Griffiths and Griffiths, 1983; Herman, 1986). These burrows typically open at the surface into branched networks of roofed horizontal feeding tunnels where the adults and larvae graze on diatoms and other microbes. The larval burrows of first instars are the shallowest (< 3 cm), with the expanded wine-bottle chamber becoming progressively deeper throughout their life cycle (Griffiths and Griffiths, 1983; Wyatt, 1986). Brooding adult females construct special "maternal burrows" where eggs are laid in individual chambers adjacent to a large living chamber (Bro Larsen, 1950 *in* Foster and Treherne, 1976; Griffiths and Griffiths, 1983; Wyatt, 1986). Hatched larvae congregate in the maternal burrow until about two-thirds of the way through the first instar, where they are protected from predators, parasites, and flooding, as well as fed algal material brought to the burrow by the mother from her surface galleries (Wyatt, 1986; Wyatt and Foster, 1989).

Simpler burrows are also excavated by *Bledius*, which usually have a horizontal component just below the sediment surface, often forked or branched, and a vertical component that extends to depths of 2 cm up to 40 cm for overwintering adults of temperate climates (Herman, 1986). The burrows may be lined with excavated sediment pressed against the burrow wall, or they may be lined with food storage caches of microbes pressed against the burrow walls (Herman, 1986). Flooded burrows may show a concentration of fine-grained sediment at the base of the burrow (Herman, 1986). Burrows of adults and larvae are constructed by excavating material with the mandibles and pressing it against the tunnel or burrow walls while stabilizing the body with the spine-like setae on the forelegs (Herman, 1986). *Bledius* spp. start their burrows by digging a trench and placing the excavated material to the margins, forming two parallel walls. They then press their heads against the end of the trench to raise an arch over the gallery, which is then roofed over with sediment excavated from within the tunnel (Herman, 1986).

At Lake Bogoria, burrows recognized as "tear drop-shaped burrows", "pellet-filled burrows", Incipient *Vagorichnus* isp., and possibly also Incipient *Labyrintichnus* isp. are attributed to the various burrows constructed by *Bledius*, although other beetles such as carabids

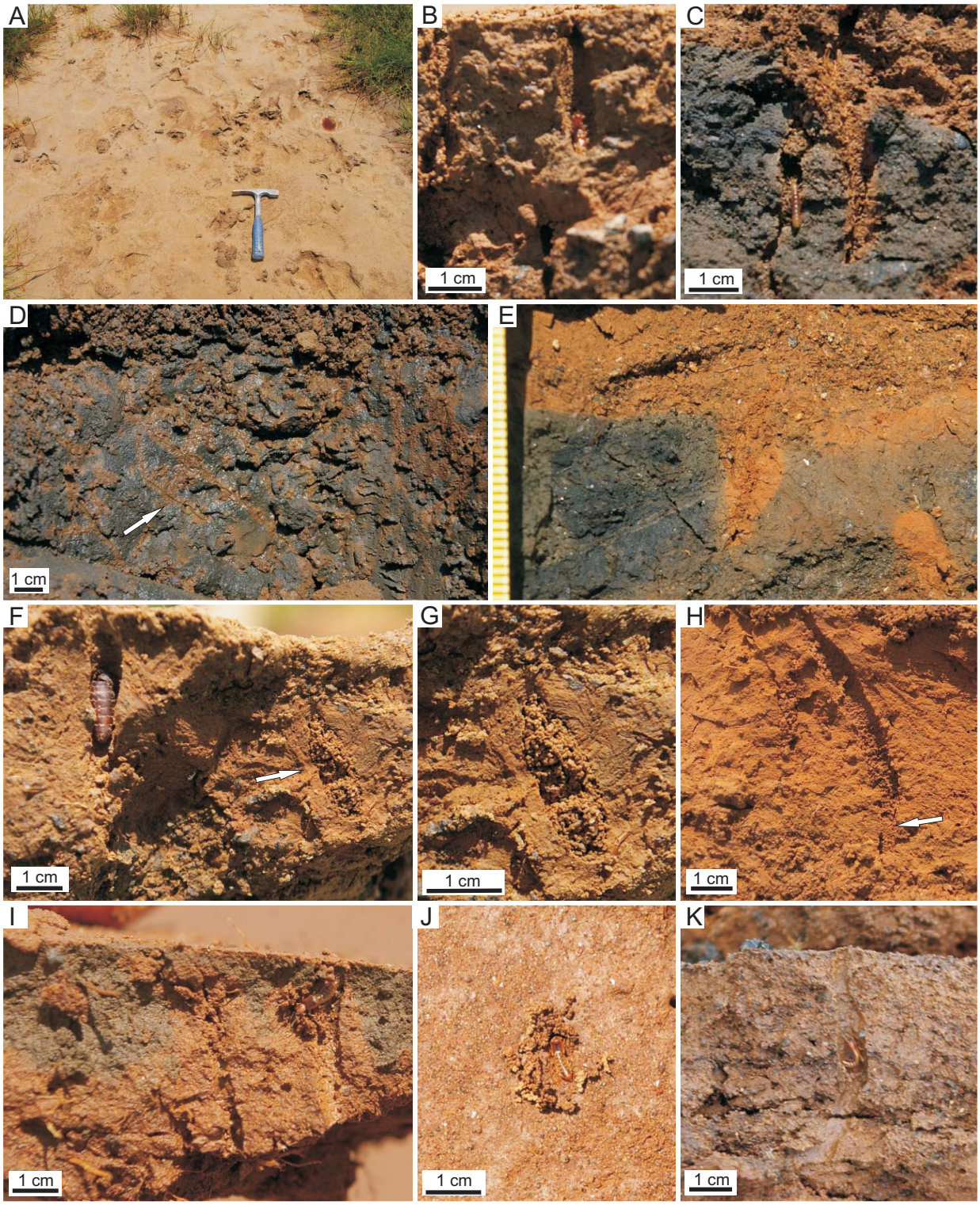


**Fig. 4.1.5.7.** Rove beetle (Coleoptera: Staphylinidae) burrows at south Loburu, Lake Bogoria. **(A)** Substrate surface of dried seepage/spring pool. **(B–C)** Staphylinid burrows in black, anoxic substrate. **(D)** Oxygenation of clayey sediment along sedge roots (arrow). **(E)** Oxygenation of sandy substrate along pellet-filled burrows. **(F–H)** Pellet-filled expanded larval burrows. Arrow in (H) showing vertical burrow continuing below the expanded chamber. **(I)** Adult? staphylinid at right had been within vertical burrow. **(J)** Adult? staphylinid burrowing into sediment with excavated sediment aggregates. **(K)** Staphylinid within expanded chamber. Note vertical burrow continuous below chamber.

or heterocerids may have also produced pellet-filled burrows and surface tunnels (Table 4.5; Fig. *4.1.5.*7). In several examples from Lake Bogoria, "tear drop-shaped" and "wine bottle-shaped" burrows, as well as segments of the vertical burrows, are partly or entirely filled with sub-spherical pellet-like sediment aggregates and/or elongate, very narrow pellets interpreted as fecal pellets (Figs. *4.1.5.*8B–C). In intertidal environments, the beetles plug their burrows during submersion by tides with sediment excavated from within the enlarged chamber, and reopen the burrow to the surface once the tide has retreated (Wyatt, 1986). The complete filling of chambers at Bogoria is not well understood, although they may simply be abandoned burrows that are filled during the excavation of new burrows. Endichnial *Bledius* burrows at south Loburu were observed in wet, silty sand and gravel of recently exposed areas that had been flooded by either hot spring-fed seepage pools (Fig. *4.1.5.*7A) or by lake transgressions during the previous rainy season. It is unknown whether the beetles remain within their burrows during periods of flooding, which is unlikely for longer term flooding events (cf. Wong and Chan, 1977; cf. Wyatt, 1986), or whether they migrate to nearby unflooded areas with wet substrates.

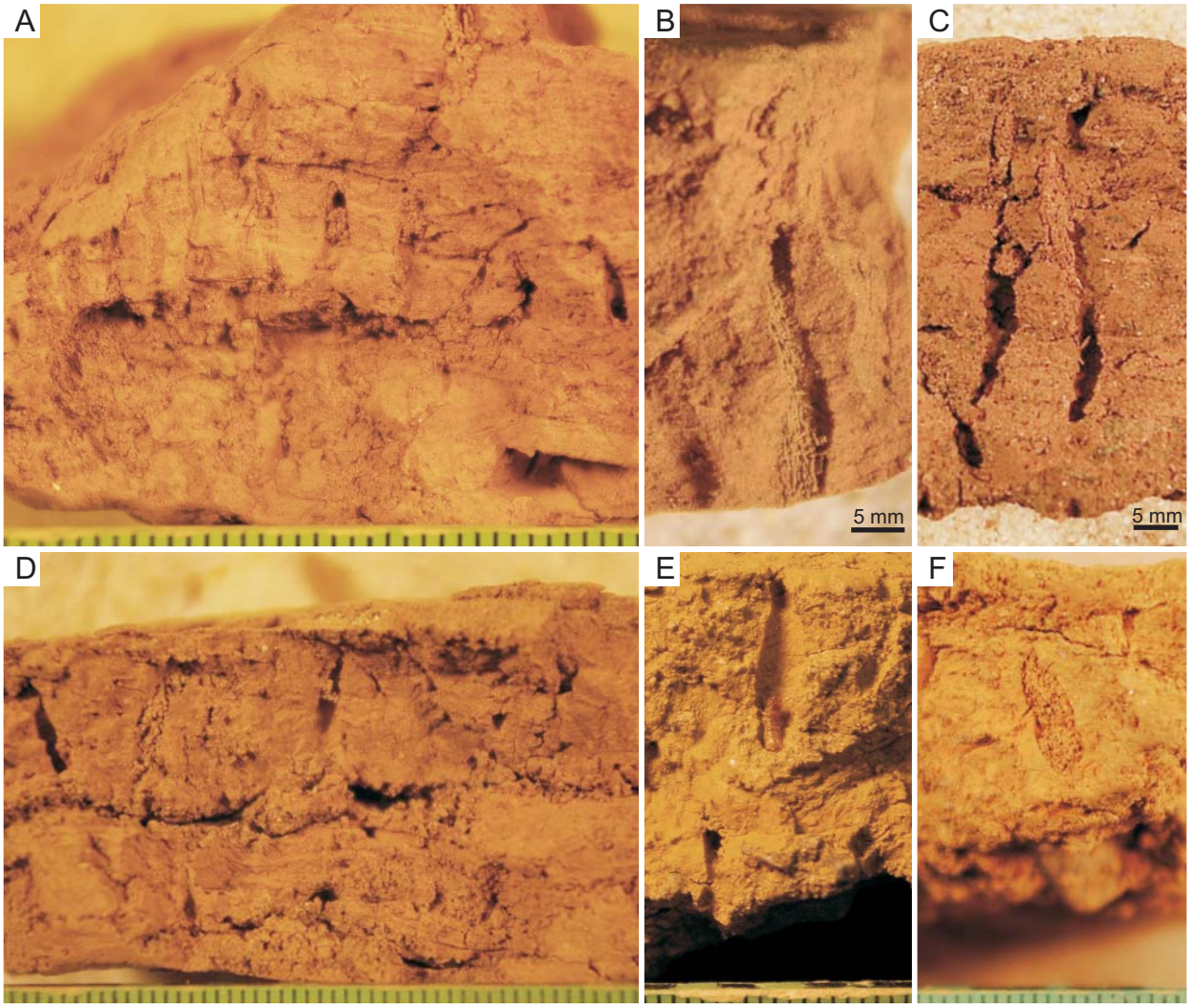


**Fig. 4.1.5.8.** Rove beetle burrows in dried sediment from south Loburu. **(A)** Probable maternal nest with vertically oriented branches where eggs are laid. **(B–C)** Elongate pellets along the side of vertical burrow, probably produced by staphylinids. **(D)** Pellet-filled ?maternal nest. **(E)** Tear-drop-shaped larval chamber. **(F)** Pellet-filled larval chamber.

It is very likely that at least some, if not most, of the Incipient *Vagorichnus* isp./Incipient *Labyrintichnus* isp. tunnel networks on the surface of wet cyanobacterial mat substrates observed at south Loburu in 2001 and 2002 were produced by *Bledius* larvae and adults (Fig. *4.1.5*.9). The branching horizontal tunnels of *Bledius* are kept open, and may anastomose with the tunnels of other individuals (Herman, 1986). However, the burrows produced by *Heterocerus* (Polyphaga: Heteroceridae), also present at Lake Bogoria, are very similar to those of *Bledius* (Silvey, 1936; Wyatt, 1986). *Heterocerus* also produces shallow, branching, horizontal, open tunnel systems for feeding on microbial substrates (Silvey, 1936; Clarke and Ratcliffe, 1989), as well as subsurface burrows with narrow, vertical necks and enlarged, spherical chambers below (Claycomb, 1919; Wyatt, 1986) (not observed at Lake Bogoria). In *Heterocerus*, the larger burrows of adults (~6 mm outside diameter), which show an almost meniscate-like packing of the tunnel roof ("compaction units" *sensu* Clarke and Ratcliffe, 1989), were not observed in association with the cyanobacterial mats in 2001 or 2002. Surface tunnels with these features, however, were present in association with smaller, smoother larval tunnels along the shorelines at Loburu and Emsos in 2007 (Fig. *4.1.5*.10). Many examples of branching horizontal tunnels near the hot springs at Loburu and on drying hot spring pools on south Loburu are roofed by loose, sub-spherical sediment aggregates (Fig. *4.1.5*.9). It seems likely that the pellet-roofed examples are produced by staphylinid adults due to their association with tumuli, whereas the more irregularly-roofed, ploughing-like tunnels are those of heterocerid adults, due to the close proximity of *Heterocerus* to these types of tunnels. Clarke and Ratcliffe (1991) noted that adults of *Heterocerus* do not excavate the tunnels, but instead push the sediment upwards and then behind the body with the legs. This behaviour is evidenced by the tunnel roof morphology (Fig. *4.1.5*.10G–I).

Large, horizontal, branching, open burrows of crickets (possibly king crickets; Orthoptera: Anostostomatidae), also present along the shoreline at Loburu, are similarly mole-like tunnels just below the sediment surface (Fig. *4.1.5*.11). They are distinguishable mainly by their large size (1 cm diameter), their undulating pattern in plan view (Fig. *4.1.5*.11H–I), the general lack of a vertical component to the burrow system, and a lack of associated tumuli of excavated material. These tunnel systems are produced in a similar manner as *Heterocerus* (Clarke and Ratcliffe, 1991) and also were not observed to be constructed of excavated sediment. Orthopteran nymphs increase in size until the adult stage is reached, and it is possible that some of the smaller mole-like horizontal tunnels (Scott et al., 2007, fig. 11F), especially near the shoreline, may be produced by these insects.

Other potential makers of small, branched, shallow tunnels include "minute mud-loving beetles", which were not identified at Bogoria but are possibly there (Georyssidae; Tony Drane, pers. comm., 2007), and the larvae of ground beetles (Carabidae; cf. Silvey, 1936). A very diverse family with more than 40,000 described species, the oldest fossils of carabids are also from the late Triassic of Virginia (Grimaldi and Engel, 2005). Silvey (1936) described the shallow, horizontal, oblique, and vertical subsurface burrows and tunnels of several species of carabids from the sandy substrates of wet, inner beach, bars, and spits of freshwater lakes in the Great Lakes region. Most carabid habitats are closely associated with wet to saturated substrates along shorelines, and some (e.g., *Bembidion*) even oviposit in flooded areas where the larvae hatch subaqueously (Kleinwächter and Bürkel, 2008). Immature forms are able to survive submergence for at least a couple of hours (Silvey, 1936).

The burrows studied by Silvey (1936) had depths ranging from ~4 cm to just below the sediment surface, and most of the forms did not branch, but those of *Omophron* spp. did. Carabids are present at the Loburu delta at Lake Bogoria (*Bembidion* spp., *Trechus* spp., *Tachys* spp.: Tony Drane, pers. comm., 2007; pers. obs., 2008). Carabids (e.g., *Dyschirius* spp.) are often found in association with *Bledius*, upon which they prey within the *Bledius* burrows

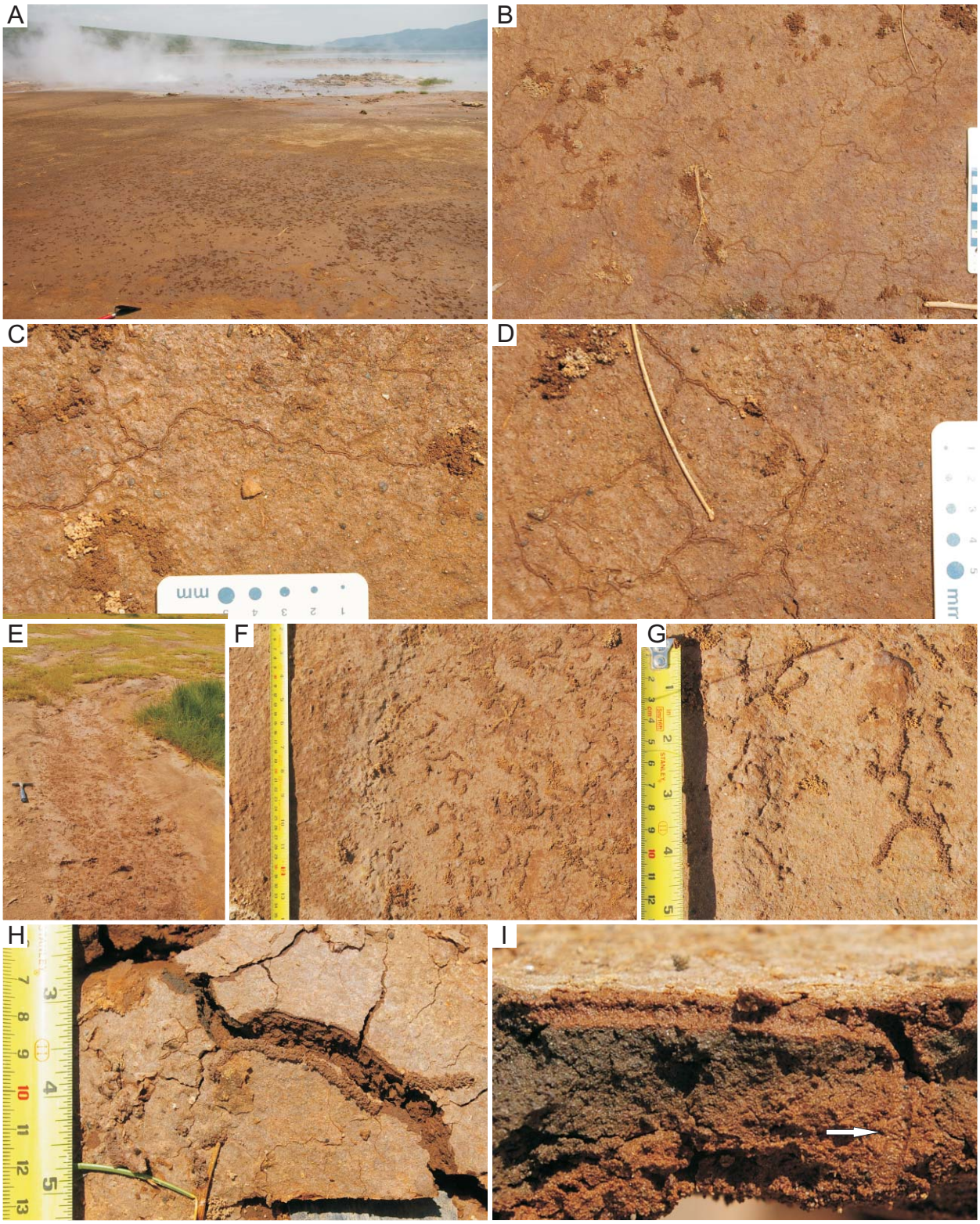


**Fig. 4.1.5.9.** Probable staphylinid burrows on the mudflats at Lake Bogoria. (A–D) are at the main hot-spring site of the Loburu Delta. **(A)** Mudflat with thousands of tumuli of excavated material **(B–D)** Small-sized, branched surface tunnels associated with tumuli. **(E–I)** are at the south Loburu Delta. Note pellet-like sediment aggregates forming tunnel roofs in (F–H) and sharp turn from vertical burrow at the surface (arrow in I).

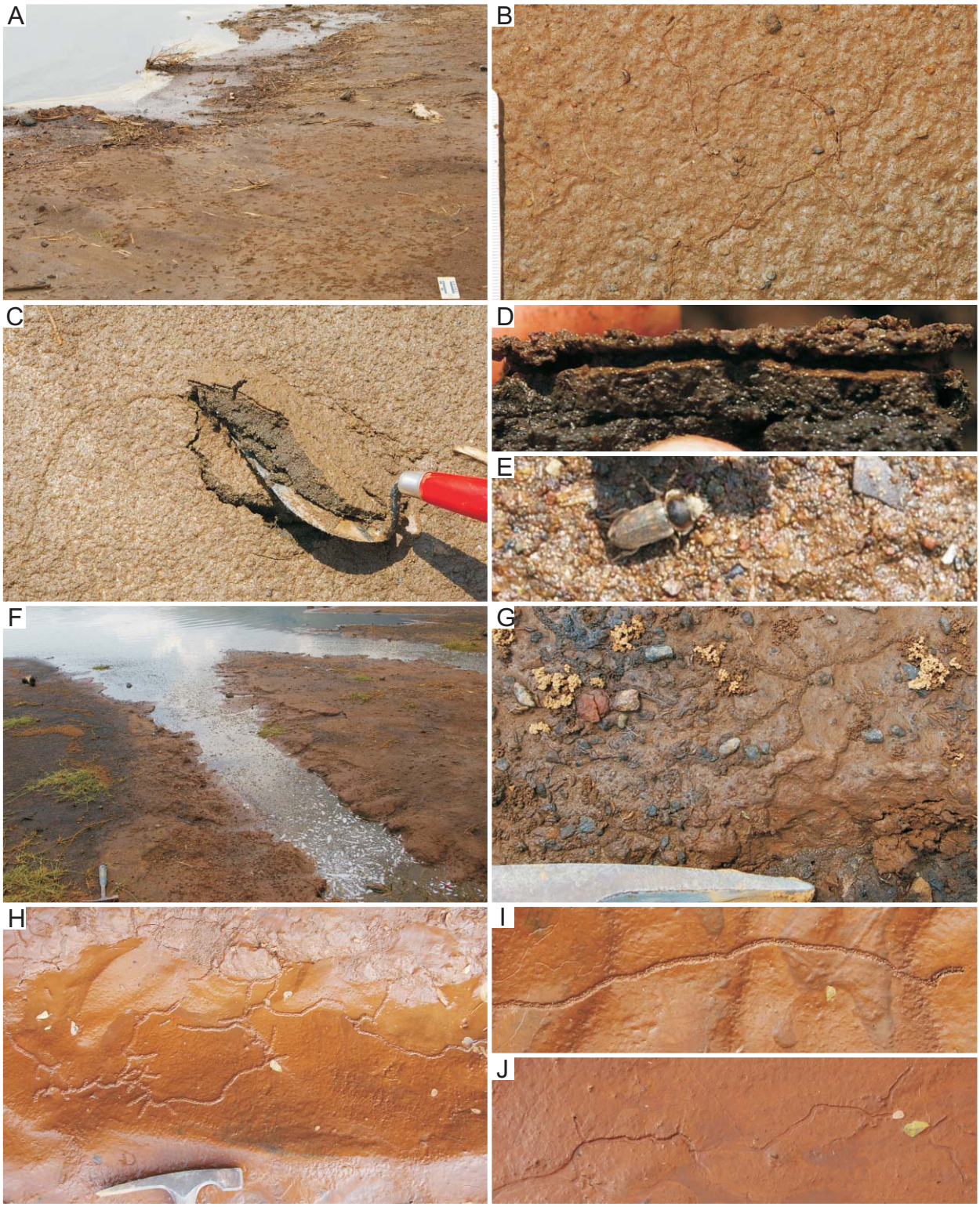


**Fig. 4.1.5.10.** Surface tunnels at the shorelines of Lake Bogoria. (A–E) are at south Loburu. **(A)** Shoreline with strands of sedges and other detritus. **(B–E)** Surface tunnels in upper layer of sediment. Adult heterocerid beetle in (E) was found in close proximity to these tunnels. **(F–G)** The shoreline at Emsos (F) with textured, probable heterocerid adult surface tunnels in (G). **(H–J)** Branched network of textured surface tunnels possibly produced by heterocerid adults in clay drape in the modern channel of the Parkirichai River.

(Herman, 1986). They may be responsible for the burrows assigned to the very small incipient *Labyrintichnus* isp. by Scott et al. (2009). Although carabid adults and larvae were observed at south Loburu, they were not observed within burrows. Most carabids are predators (Lövei and Sunderland, 1996) and most of carabids in Silvey's study (1936) fed on settled zooplankton (e.g., copepods, crustacean larvae) within unbranched burrows. Some others also fed on phytoplankton. The burrow systems of the phytoplankton-eating examples (i.e. *Dyschirius* sp.) studied by Silvey (1936), suggest that these types of horizontal, branching, shallow sub-surface tunnels may represent a behaviour closely related to their food source. Together, they represent the types of shallow subsurface tunnels formed by insects feeding on microorganisms that have either settled on the surface, live interstitially, or grow as interstitial and surficial microbial films and mats.

The distribution of *Bledius* adults and larvae, as well as their burrows, is typically in moist to wet, well drained, lower energy, vegetation-free substrates along shorelines with an abundant microbial food source (e.g., Griffiths and Griffiths, 1983; Gerdes et al., 1985; Wyatt and Foster, 1988; Garcia and Neill, 1991). Both adults and larvae feed on green algae, cyanobacteria such as *Oscillatoria* and *Anaebaena*, and diatoms (Herman, 1986). The distribution of intertidal *Psamathobledius* and their burrows is dictated by substrate hardness and the presence of a diatom-rich food source (Griffiths and Griffiths, 1983). In areas with suitable substrate penetrability, *Psamathobledius* burrows were concentrated in quieter areas with high chlorophyll *a* concentrations (2 mg $m^{-2}$) in the upper 4 mm of sediment, so that their distribution was very locally concentrated (Griffiths and Griffiths, 1983).

Salinity does not appear to be a major control on the distribution of staphylinid burrows; they are tolerant of saline conditions up to at least 70 g $L^{-1}$ (Gerdes et al., 1985). They may prefer saline habitats as a strategy of predator avoidance (Herman, 1986). Most species of *Bledius* select microbial food sources with lower salinities (< 4% salt content in *B. spectabilis*), and may avoid a high salt content in their food by gathering it following rains and storing it within their burrows (Larsen, 1952 *in* Herman, 1986). At Lake Bogoria, this may help to explain the apparent association between high concentrations of horizontal tunnel networks and microbial mats adjacent to relatively freshwater hot springs. In intertidal salt marshes, densities are greatest in "edge" regions along channels (< 4000 individuals $m^{-2}$) where water will not pool (Wyatt and Foster, 1988). Disperal of larvae into marginal habitats extends the range for burrows into less well drained areas (e.g., salt flats flooded by the spring tide), but their landward limit appears to be strictly controlled by the presence of vegetation (Wyatt and Foster, 1988). When in use, the burrows may be restricted to narrow ribbons along shorelines with steep gradients, or if shoreline gradients are lower, their roughly linear distribution is widened normal to the water body (e.g., Craig, 1970). In intertidal settings, they range seaward up to ~12 m below the high water mark, but not seaward of the mid-tidal range (Griffiths and Griffiths, 1983). At Gavish Sabkha, the "*Bledius* zone" represents a relatively narrow band along the margins of protected lagoons, in "wetlands" with water tables 0–30 cm below the surface (Gerdes et al., 1985). At Solar Lake, a deep and perennial backshore lagoon, *Bledius* was restricted to fringing wetlands above the high water mark, and during summer periods when lake levels were lower, extended its range onto littoral flats to the low water line (Gerdes et al., 1985).

On lake-marginal salt flats in Spain, *Bledius* burrows and their associated tumuli of excavated material were found ~10–25 m landward of the shoreline, between saturated substrates at the shoreline and the landward extension of vegetation (Garcia and Neill, 1991). More than 2500 individuals $m^{-2}$ (< 35000 $m^{-2}$) were found in substrates with ~15% moisture content, but were much less concentrated in very wet (17.3% moisture; ~550 individuals $m^{-2}$) and in drier substrates (12.3% moisture; ~122 individuals $m^{-2}$) (Garcia and Neill, 1991). In dry sandy

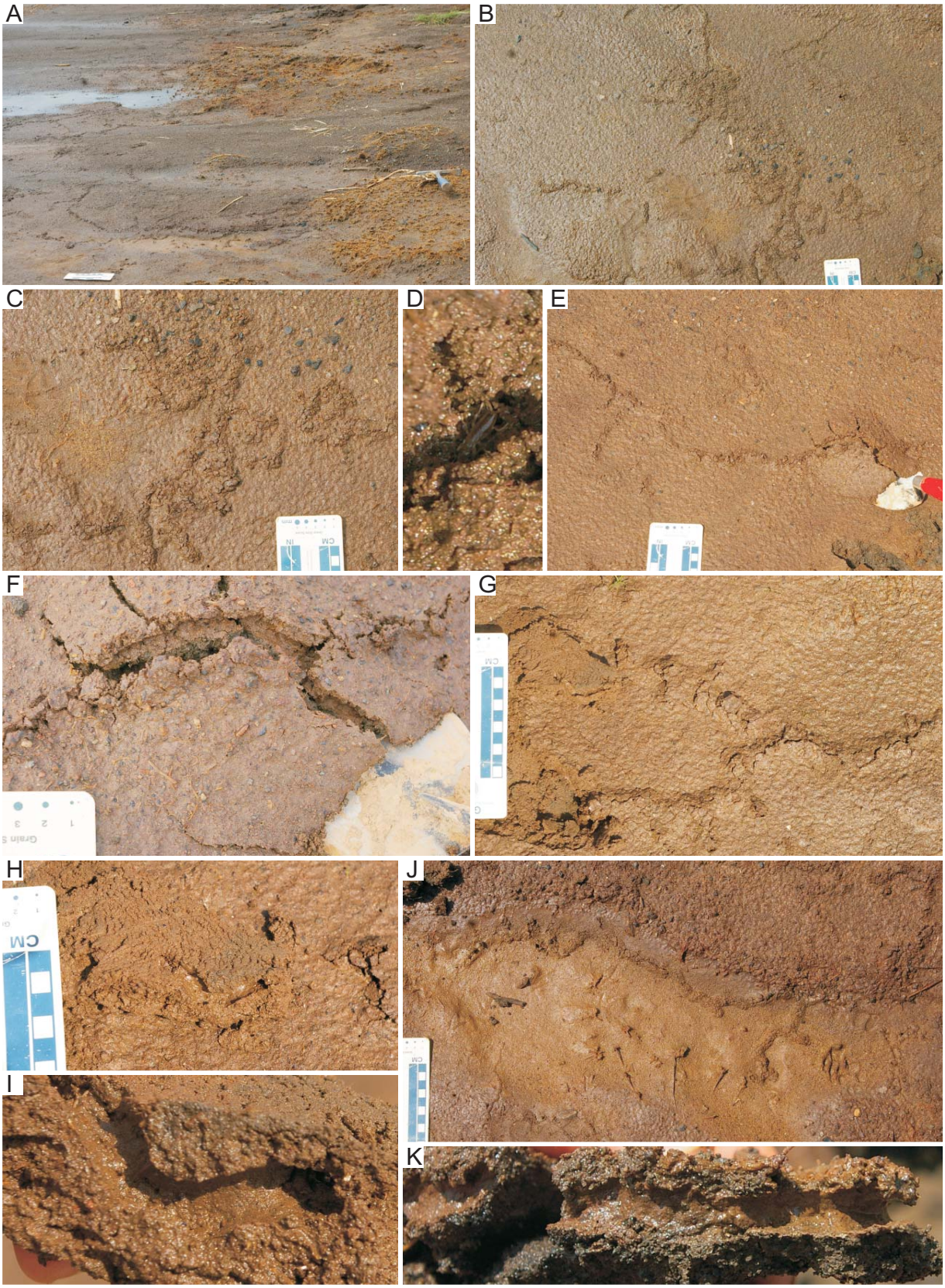


**Fig. 4.1.5.11.** Large surface tunnels at Loburu Delta, Lake Bogoria. **(A)** Sandy swash-zone sediments. **(B–K)** Large sized, branched surface tunnels probably produced by crickets (in D). Note smooth internal lining in (H) and (I–K).

substrates (8.7% moisture) the burrows of *Bledius bicornis* were not found (Garcia and Neill, 1991). At Bogoria, the burrows of staphylinids were found in silty substrates across the exposed low gradient southern Loburu Delta where it is frequently flooded by the lake during seasonal high lake levels and by seepage pools of hot spring effluent that is probably mixed with lake water. *Bledius* spp. are found only in permanently wet areas, and both adults and larvae remain close to their food source (Herman, 1986). Herman (1986) suggests that understanding the distribution of salt lakes should help locate the past and present populations of *Bledius*. The evidence from Lake Bogoria and the presence of *Bledius* in the Green River Formation support the idea that the evolution of inland *Bledius* and other arthropods with a similar life style (e.g., *Heterocerus*) may be linked to tectonically active areas that contain saline lakes in closed basins that are fed in part by hot springs.

Other staphylinids also burrow, including predatory and saprozoic species along the marine beaches (e.g., Craig, 1970; Wong and Chan, 1977; Topp and Ring, 1988). The range of predatory staphylinids (e.g., *Thinopinus pictus*) burrowing in intertidal beaches of North America was restricted to areas with wet, uncompacted sandy substrates (Craig, 1970). Moisture contents dictated the landward range to a couple of metres landward of the high water wave mark, and substrate hardness restricted their seaward range to above the high water mark of the neap tide, beyond which the substrate was siltier and more well packed (Craig, 1970). Topp and Ring (1988) found that *Thinopinus* preferred fine-grained sand substrates, where they burrowed as deep as 40 cm in uncompacted sediments. Saprozoic, intertidal staphylinids of the genus *Bryothinusa* in Hong Kong feed on microbes as well as interstitial meiofauna (e.g., collebolans, larval crustaceans). They were most abundant in the mid-intertidal zone, flooded twice daily, where they were concentrated in the upper 15 cm, with a few examples of burrows as deep as 20 cm. The animals are tiny (2 mm) and were not reported to block their burrows during submergence (Wong and Chan, 1977), possibly because of effective trapping of air within vertical burrow less than 3 mm in diameter (Maitland and Maitland, 1994).

In fluvial settings, *Bledius* spp. burrows and tumuli were abundant on the moist, soft, freshly exposed sand bars that lacked vegetation (Smith and Hein, 1971). Burrowing activity was greatest during warmer temperatures (~35° C) (Smith and Hein, 1971). The densest concentrations of burrows were found where mud drapes covered loose fine- to medium-grained sand, providing some cohesiveness to the substrate (Smith and Hein, 1971). The burrows extended vertically only to the depths of underlying compact layers, where the burrowing continued horizontally along bedding planes (Smith and Hein, 1971). The burrows figured by Smith and Hein (1971) do not share the characteristic "wine bottle-shaped" expansions of *Bledius* burrows observed at Lake Bogoria and in intertidal regions. The difference in burrow morphology may be due to life history-related, species-specific differences, as well as substrate moisture and hardness conditions. Unfortunately, Craig (1970) did not describe the burrows of predatory intertidal staphylinids in detail for comparison. Garcia and Neill (1991) provided a drawing of the *Bledius* burrows, which showed branching, vertical and horizontal burrows concentrated in the upper 3.5 cm of the substrate, but did not mention or show the expanded dwelling chambers characteristic of *Bledius* burrows in intertidal areas and at Lake Bogoria.

*4.1.5.4. Earwigs (Dermaptera: Labiduridae)*— The earwigs (Dermaptera) comprise a monophyletic lineage of the basal neopteran orthropteroid group of hemimetabolous insects that were present by the Jurassic and may have originated as early as the Carboniferous (Gullan and Cranston, 2000; Haas and Kukalová-Peck, 2001). Their bodies are flattened dorso-ventrally, they may or may not have small wings that fold back against the abdomen, and they all possess two large, distinctive abdominal forceps that are used during aggressive and/or predaceous

behaviour for foraging, defense, and courtship (e.g., Styrsky and Van Rhein, 1999; Walker and Fell, 2001; Matzke and Klass, 2005). They are nocturnal and dominantly cursorial, typically taking shelter in burrows or under stones and leaf litter during the day and feeding on plants and/or animals at night (e.g., Lamb, 1975). Earwigs are subsocial and in most taxa exhibit maternal care of the eggs and nymphs in burrows excavated by the mother, where she protects the nest and continually cleans the eggs from fungus (e.g., Radl and Linsenmair, 1991; Rankin et al., 1996; Matzke and Klass, 2005). Together with nymphs and males, foraging females also take refuge in burrow systems that contain aggregations of earwigs, concentrated especially near food sources (e.g., Lamb, 1975; Sauphanor and Sureau, 1993). Earwigs are attracted by pheromones to areas where other earwigs burrow, in some genera (e.g., *Forficula*) because they are gregarious, and in others (e.g., *Labidura*) because they reuse the burrows of other earwigs for shelter (Sauphanor and Sureau, 1993). Foraging females use pheromones to relocate their brood chambers (Radl and Linsenmair, 1991).

Earwigs are most abundant in the tropics, in regions with high, consistent temperatures and in areas with high humidities or soil moisture where they are able to breed throughout the year (e.g., Guillet and Vancassel, 2001; Haas et al., 2005). Soil moisture (e.g., optimum for *Nala lividipes*: 5–20% in sand, 20–50% in clay) and temperature (e.g., optimum for *N. lividipes*: 22–32.5° C) are important for the hatching of eggs, survival of nymphs and adults, as well as the burrowing activities of nymphs and ovipositing females (e.g., Simpson, 1991; Simpson, 1993). The diversity of earwigs in Kenya (46 species) is lower than in neighboring countries with generally higher humidity and lower elevations (e.g., Congo, Tanzania, Uganda), but higher than the drier and/or more mountainous areas (e.g., Ethiopia, Somalia) (Haas et al., 2005). In temperate regions (mainly Palaearctic), earwigs are less diverse, raise young only during the summer, and retreat to their burrows throughout the winter (e.g., Guillet and Vancassel, 2001). They are found in both continental and marginal marine settings, such as the intertidal to supratidal zone of the Mediterranean region and Atlantic coasts of northern Africa and southern Europe (e.g., Colombini et al., 1996; Popham, 2000), and the west coast of North America (Lamb, 1975, 1976a).

The burrows of earwigs have only rarely been described in detail (e.g., Fulton, 1924; Lamb, 1976b), although several studies have investigated the maternal behaviour within the burrows (e.g., Radl and Linsenmair, 1991; Kölliker and Vancassel, 2007) and the environmental distribution of their burrows as it relates to foraging behaviour and activity (e.g., Lamb, 1975; Colombini et al., 1996). Earwigs use burrows for shelter from predators and adverse environmental conditions (e.g., heat, sun) at all stages of their life cycle (e.g., Lamb, 1975; Colombini et al., 1996), but descriptions of these non-maternal burrows have not been found in the literature. Simpson (1991) noted that earwig nymphs of *Nala lividipes* (Labiduridae) do not burrow unless the substrate is suitably moist (in sand: 20%). Female earwigs also excavate and maintain nests in "suitable substrates" (Radl and Linsenmair, 1991), where they oviposit clutches of eggs. Gullan and Cranston (2000) figured the nest of a labidurid as a short, vertical tunnel, approximately the width of the mother, which opened into an oval-shaped, horizontally oriented chamber just below the soil surface, approximately the length of the mother. A video of a female earwig (Forficulidae: *Forficula auricularia*) provided online by ARKive – Images of Life on Earth (www.arkive.org) shows the female excavating the burrow by removing sediment and transporting it as roughly sub-spherical aggregates to the burrow margin with her mandibles and maxillae.

Fulton (1924, p. 360) briefly described some burrowing habits of earwigs: 1) female earwigs closed the entrances to their burrows with sediment; 2) female earwigs used their mandibles to loosen sediment particles, worked the loose sediment under their thoraxes with their

heads and forefeet until a small pellet was formed, and then either removed the pellet from the chamber or used it to close cracks into the burrow; 3) pellets were used to keep the egg chambers tightly closed to prevent the escape of young nymphs and were later opened the chambers to permit the nymphs to disperse. Within the more derived Forficulina (including Labiduridae and Forficulidae), mothers excavate either shallow depressions, tunnels, or a system of tunnels and chambers for laying eggs within a nest (Matzke and Klass, 2005). Females of the more basal earwig species *Tagalina papau* (Pygidicranidae) dig troughs about body length using the mandibles, and fresh eggs are attached to the smooth internal wall of the burrow (Matzke and Klass, 2005). During the day, nymphs of *T. papau* dig tunnels with inclinations of ~30–40° and depths approximately equal to body length (Matzke and Klass, 2005).

At Lake Bogoria, the nests and burrows of earwigs were abundant in: 1) slightly firm, moist substrates of muddy to silty fine-grained sand on the Loburu delta; 2) firm, partly cemented substrates adjacent to hot spring vents; and 3) slightly cohesive, wet sandy substrates along the modern shoreline at Loburu (Figs. *4.1.5.*12, 13). Although no specimens were collected, it was possible to tentatively identify most of the photographed earwigs as *Labidura riparia* (Labiduridae), a cosmopolitan earwig found worldwide in the tropics and in intertidal areas of the Atlantic African and Mediterranean coasts (Popham, 2000). Females were observed protecting their nests and eggs (Fig. *4.1.5.*12C). Ants were observed stealing the eggs of earwigs from a bioturbated exhumed surface (Fig. *4.1.5.*12I). Males were observed in tunnels near hot springs (Fig. *4.1.5.*12K–L). Earwig nymphs were observed within an abandoned, old flamingo nest and other sediments at south Loburu (Fig. *4.1.5.*13E), but their burrows were not identified in this case. Earwigs were also observed burrowing in firm, moist substrates at Emsos.

The burrow systems of these earwigs were described in Table 4.5, and may possibly represent incipient forms of cf. *Thalassinoides* isp. and *Spongeliomorpha* isp., although the branching patterns were not examined in detail. Large, dominantly horizontal, branching tunnel systems present in wet substrates along the shoreline ("boxwork burrow systems") may also be attributed to either earwigs or crickets, although the animals were not directly observed in association with these forms (Table 4.5; Scott et al., 2009, fig. 9B, C). In general, the burrows: 1) are medium- to large-sized (4–6 mm and 8–12 mm) in diameter; 2) are present in horizontal, vertical, and oblique orientations; 3) branch frequently; 4) may be partly backfilled with sub-spherical pellet-like aggregates that tend to be a darker colour than the substrate; 5) may show wrinkle-like ornamentations on the internal burrow margin in firm substrates; 6) may be associated with expanded chambers (1–2 cm high, < 3 cm wide); and 7) do not have constructed walls or linings.

More fieldwork and experimentation with the burrowing behaviours of earwigs is necessary in order to characterize these burrow systems. Examples of *Thalassinoides* ispp. in lacustrine environments reported by other authors (e.g., Schlüter and Kohring, 1992; Keighley and Pickerill, 1997; Kim et al., 2002) may possibly be attributable to the work of earwigs and/or crickets, which also exhibit similar burrowing and nesting behaviours (e.g., West and Alexander, 1963). In particular, small forms of *Thalassinoides suevicus* reported by Keighley and Pickerill (1997) from the Carboniferous continental rift strata of eastern Canada contain chamber-like swellings that are proportionately larger than the swellings at T- or Y-branches of typical *Thalassinoides*. Similarly, the examples of Schlüter and Kohring (1992) reported from ?Pleistocene lake beds in the Lake Manyara half-graben (Tanzania) are open, branching burrow systems with swellings, but they also have some burrows with "agglutinated" burrow walls of apparently pellet-like material. The site at Lake Manyara may possibly be comparable to the Loburu Delta at Lake Bogoria based on the trace fossils, high fluorine levels, horizons of chert nodules, and calcareous algal concretions (cf. Schlüter and Kohring, 1992, 2002). The 3D

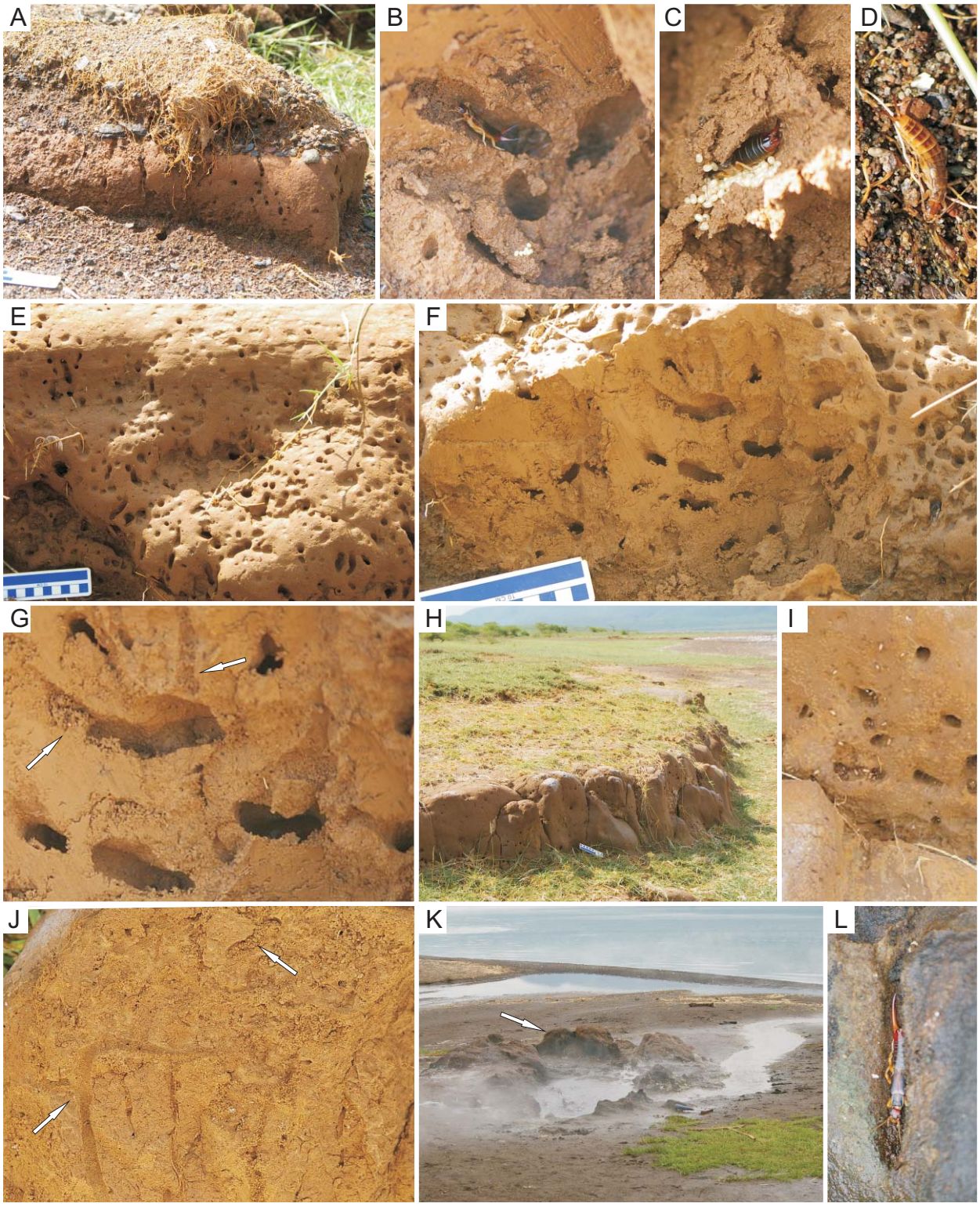


**Fig. 4.1.5.12.** Earwig burrows in firm substrates at the main hot-spring site at the Loburu Delta, Lake Bogoria. **(A)** An exhumed surface with burrows in silt below gravels. **(B–D)** Adult female earwigs. **(E)** Burrows in the exhumed surface. Multiple generations of open and filled burrows. **(F–G)** Within the substrate shown in (E) are large-sized oblique and vertical branching burrows of different diameters (arrow at right in G), with sharp walls, and partial pellet/sediment aggregate fill (arrow at left in G). **(H–J)** Ants stealing earwig eggs (I) from earwig burrows (J) in an exhumed surface. **(K–L)** Earwig burrows in firm substrate adjacent to hot spring vent.

architecture of the open burrow systems observed at Lake Bogoria is also superficially similar to that of ant nests (cf. Halfen and Hasiotis, 2010). Earwigs should be considered as the possible trace makers of such fossil burrow systems younger than the Jurassic, and possibly as old as the Carboniferous (cf. Haas and Kukalová-Peck, 2001).

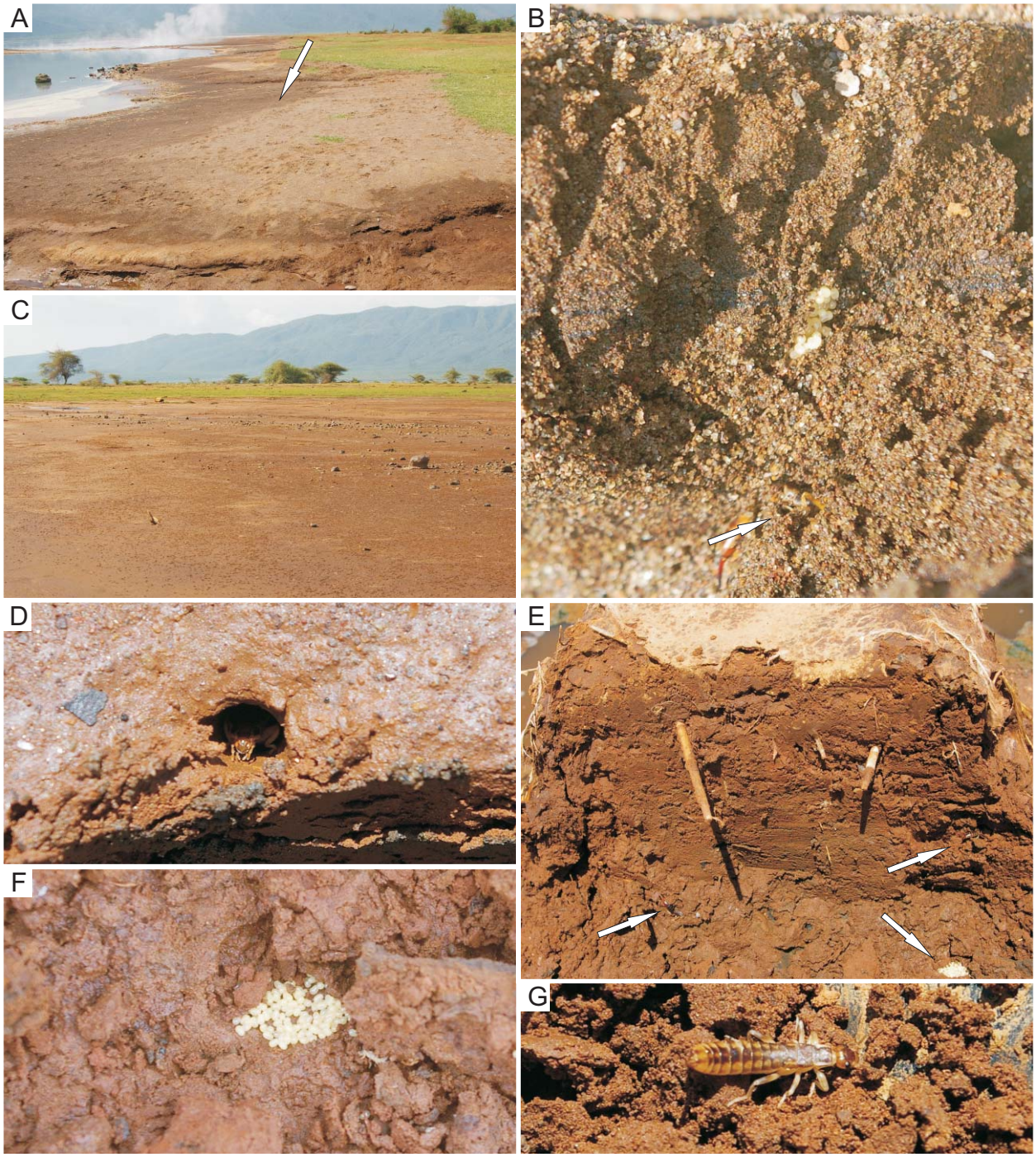


**Fig. 4.1.5.13.** Earwig burrows in soft and cohesive substrates at Loburu, Lake Bogoria. **(A)** Sandy shoreline at Loburu. Arrow showing site where burrows were found. **(B)** Branched and mainly vertically oriented earwig burrows in soft sandy substrate. **(C–G)** Earwig burrows and nests in muddy sediments at south Loburu. Arrows in (E) pointing to earwig nymphs escaping from the sectioned flamingo nest mound.

*4.1.6. Trace Fossils in the Exhumed Surfaces of the Bogoria Basin*

Several exhumed surfaces of relatively well indurated silts and sands, cemented by zeolites, calcite, iron- and manganese-oxihydroxides, form a large portion of the western margin of Lake Bogoria. Analcime is an abundant, pervasive cement in these sediments, and is likely a product of the highly saline and alkaline lake waters reacting with compositionally immature sediments under high evaporation rates (Renaut, 1993). In areas along normal faults with hot springs (e.g., Loburu Delta), high temperature waters are enriched in silica, fluorine, $CO_2$, and sometimes calcium, which leads to the additional cementation of sediments, rhizoliths, and trace fossils by opaline silica and fluorite (e.g., Renaut et al., 1986; R.A. Owen et al., 2008). Induration of the lake-margin sediments appears to occur particularly during arid climatic periods, when lake levels remain low for extended periods. Early diagenetic processes, in conjunction with climate-influenced changes in lake levels due to either greater or lower input of sediment + water sourced within the catchment, leads to the complex interplay between deposition, induration, and erosion. The affect of this interaction differs laterally depending on the depositional environment (e.g., delta vs. fault-controlled shoreline) and whether there was input of hot-spring fluids.

The set of erosion-resistant surfaces are exposed on Sandai Plain, Loburu delta, Emsos, and along large parts of the western shoreline during low-intermediate lake levels (cf. Renaut and Tiercelin, 1994; e.g., 2006). The uppermost surface(s) of the Pleistocene Loboi Silts within the Bogoria basin, in particular, are laterally extensive due in part to their relatively high degree of induration and survival through possibly several episodes of deposition and exhumation. Trace fossils preserved in the Loboi Silts (Section 4.1.2) reflect the initial substrate conditions during deposition and subaerial exposure, a subsequent period of burial, relatively lower water tables, bioturbation by termites, and cementation, as well as the exhumation of the cemented surface and present-day bioturbation by plants and animals. The trace fossils in the Loboi Silts were grouped in trace suites based on comparison with groups of modern animal and plant traces that can be found together in different sub-environments of the lake-margin at Lake Bogoria (see Section 4.1.4; Fig. *4.1.6.*1). The suites differ slightly from the presently accepted ichnofacies models, but are generally very similar. The Loboi Silts 'surface' preserves different suites, which are overprinted upon one another and show cross-cutting relationships that reflect changing conditions that broadly coincide with changing lake levels through time (Fig. *4.1.6.*2). The trace fossil assemblage, if considered in suites, shows overprinting patterns that are in general accordance with the present understanding of lake-level rise-and-fall from the Late Pleistocene to Recent (Fig. *4.1.6.*3). This approach has the potential to provide evidence of changing environmental conditions represented by a single surface (or set of surfaces) in other saline lake basins, and can be used as a sequence stratigraphic tool that marks combined regressive and flooding surfaces. In the case of the Loboi Silts, the uppermost surface is interpreted as a sequence boundary overlain by sediments deposited during lake highstand(s).

The Loburu Delta also preserves other bioturbated, younger, “exhumed surfaces” that are less indurated than the Loboi Silts, but which are also undergoing present-day bioturbation. Some of these sediments are likely equivalent to the Bogoria Silts, whereas others may have been deposited during Holocene highstands. The greater abundance of these types of units and a higher number of surfaces at Loburu are attributed to the influence of hot-spring fluids in their

**Fig. 4.1.6.1.** (Next page) Map showing the localities of the trace fossil suites recognized at Lake Bogoria. The trace types included in each suite (boxes at left) are listed by suite in the boxes at right. This figure was adapted from Scott et al. (2009, fig. 2).

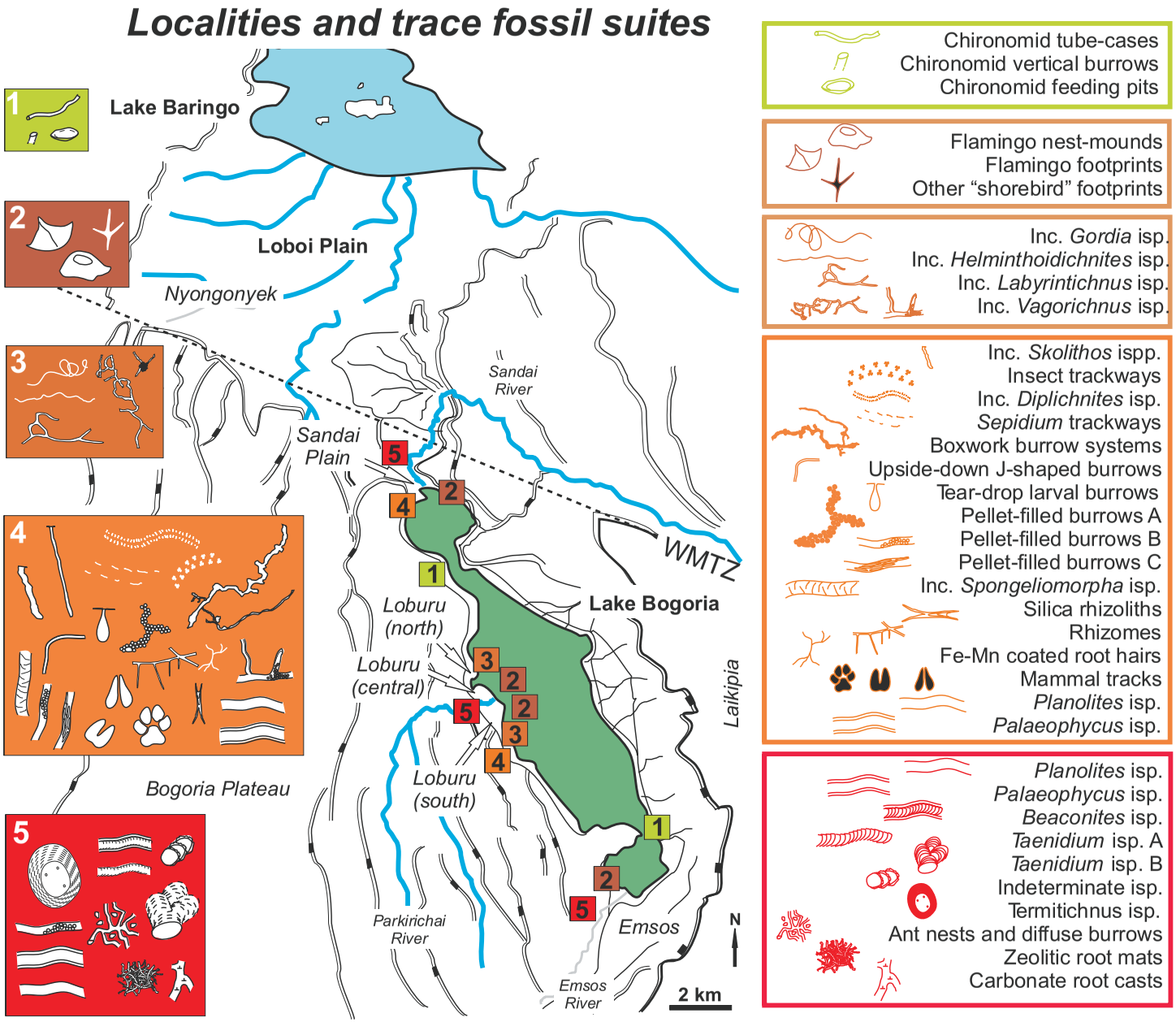
Localities and trace fossil suites
1
Lake Baringo
2
Loboi Plain
Nyongonyek
3
Sandai Plain
Sandai River
4
Bogoria Plateau
5
WMTZ
Lake Bogoria
Loburu (north)
Loburu (central)
Loburu (south)
Laikipia
Parkirichai River
Emsos
Emsos River
N
2 km
Chironomid tube-cases
Chironomid vertical burrows
Chironomid feeding pits
Flamingo nest-mounds
Flamingo footprints
Other “shorebird” footprints
Inc. Gordia isp.
Inc. Helminthoidichnites isp.
Inc. Labyrintichnus isp.
Inc. Vagorichnus isp.
Inc. Skolithos ispp.
Insect trackways
Inc. Diplichnites isp.
Sepidium trackways
Boxwork burrow systems
Upside-down J-shaped burrows
Tear-drop larval burrows
Pellet-filled burrows A
Pellet-filled burrows B
Pellet-filled burrows C
Inc. Spongeliomorpha isp.
Silica rhizoliths
Rhizomes
Fe-Mn coated root hairs
Mammal tracks
Planolites isp.
Palaeophycus isp.
Planolites isp.
Palaeophycus isp.
Beaconites isp.
Taenidium isp. A
Taenidium isp. B
Indeterminate isp.
Termitichnus isp.
Ant nests and diffuse burrows
Zeolitic root mats
Carbonate root casts

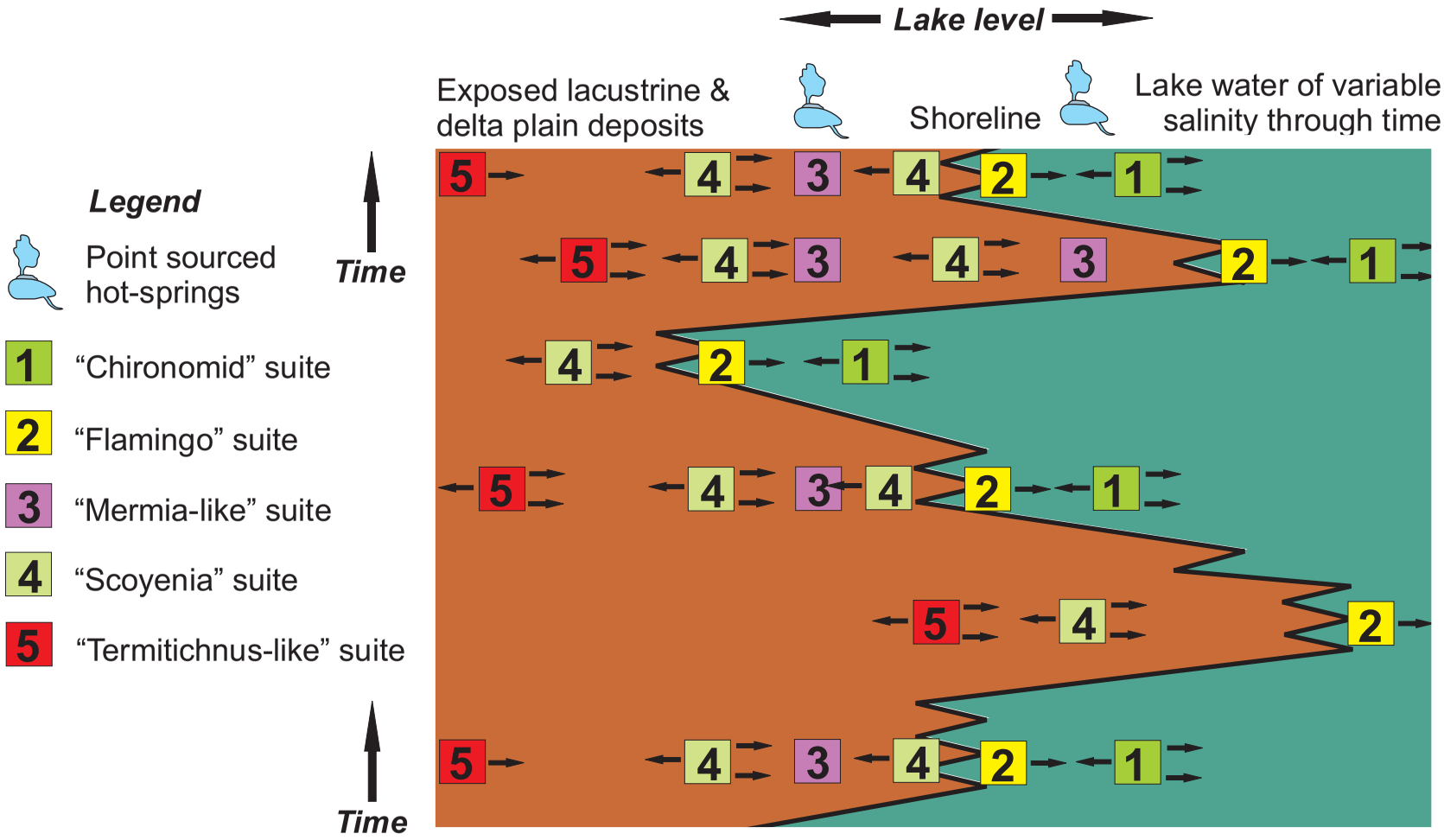


**Fig. 4.1.6.2.** Schematic model of the lateral and vertical distribution of the trace suites recognized at Lake Bogoria, which track changing lake levels through time.

cementation. Additionally, due to differences in the lake-boundary gradients between the axial and hinged-margin deltas, aggradation of delta lobes is more prevalent at Loburu, whereas the delta at Sandai presumably undergoes relatively greater progradation with fewer cemented horizons or surfaces. Present-day animal and plant bioturbation that overprints the older trace fossils is much more abundant and diverse at Loburu than at Sandai, due primarily to the presence of hot springs at Loburu. If observed in the rock record, a delta similar to Loburu (hinged margin) might show overall greater bioturbation and greater diversity of trace fossils associated with aggradational packaging of delta lobes and a higher abundance of preserved subaerially exposed surfaces. A delta similar to Sandai (axial margin), in contrast, might show an overall lower diversity of traces concentrated onto fewer regressive surfaces and dominantly progradational sediment packaging.

*4.1.6.1. Preservation and Representation of Trace Suites in the Exhumed Surfaces at Lake Bogoria*— The preserved sub-fossil and fossil traces in the exhumed surfaces, together with the modern traces that further bioturbate the surfaces, form a set of suites (Fig. *4.1.6.*1) that can be placed within the stratigraphic and environmental context of the basin to better understand their distribution (Figs. *4.1.6.*2, 3). Taphonomic processes (discussed below) and the sites of biogenic activity where the traces were formed are both related to the history of changing lake levels, as well as the positions of rivers and springs, which are relatively static in comparison. The major known depositional events in the Bogoria basin can be roughly correlated with the composition and distribution of the trace suites. A model considering these points was constructed to place the trace fossils into the stratigraphic context of the basin (Fig. *4.1.6.*3).

The following is a summary and brief discussion of the taphonomic factors involved in the preservation of trace suites preserved in the exhumed surfaces, including both the Loboi Silts and Bogoria Silts. The surfaces apparently do not preserve evidence of the Mermia-like Suite, of which the delicate surficial traces were likely destroyed by vertebrate trampling, bioturbation, and/or the formation and deflation of efflorescent salts. Similarly, the fragile chironomid tube structures of the Chironomid Suite were not preserved in the surfaces, but modern-day traces attributed to chironomids (e.g., pits) rework the cemented substrate. In contrast, trampled and compacted flamingo nest mounds of the Flamingo Suite are relatively resistant to modification by further trampling and salt efflorescence. Poorly preserved examples of these mounds in the exhumed surfaces survive at Loburu, Emsos, and were observed in the extensive cemented mudflat deposits exposed north of Loburu during low lake levels of 2006. Footprints of the ?Flamingo Suite and the Scoyenia-like Suite were not preserved outside of Sandai Plain (see Scott et al., 2008), which may be attributed to an overall lower degree of invertebrate bioturbation and vertebrate trampling.

Several types of invertebrate burrows included in the Scoyenia-like Suite were preserved in the exhumed surfaces around the lake. Plant trace fossils included in the Scoyenia-like Suite were preserved at Loburu; these rhizoliths are associated with hot-spring fluids (R.A. Owen et al., 2008). Invertebrate trace fossils of the Termitichnus-like Suite, likely produced after shallow burial of the surfaces, were preserved in all of the Loboi Silts exhumed surfaces, but not in the younger, ?Bogoria Silts equivalent surfaces. Their formation and preservation is related to an extended period of lower lake levels. The exhumed surfaces also contained some modern traces from the Chironomid Suite (i.e. pits), flamingo nest mounds of the Flamingo Suite, and many

**Fig. 4.1.6.3.** (Next page) Diagram showing the trace suite distribution related to the general sequence of known depositional and exposure events in the Bogoria basin since the Pleistocene. This figure was adapted from Scott et al. (2009, fig. 14).

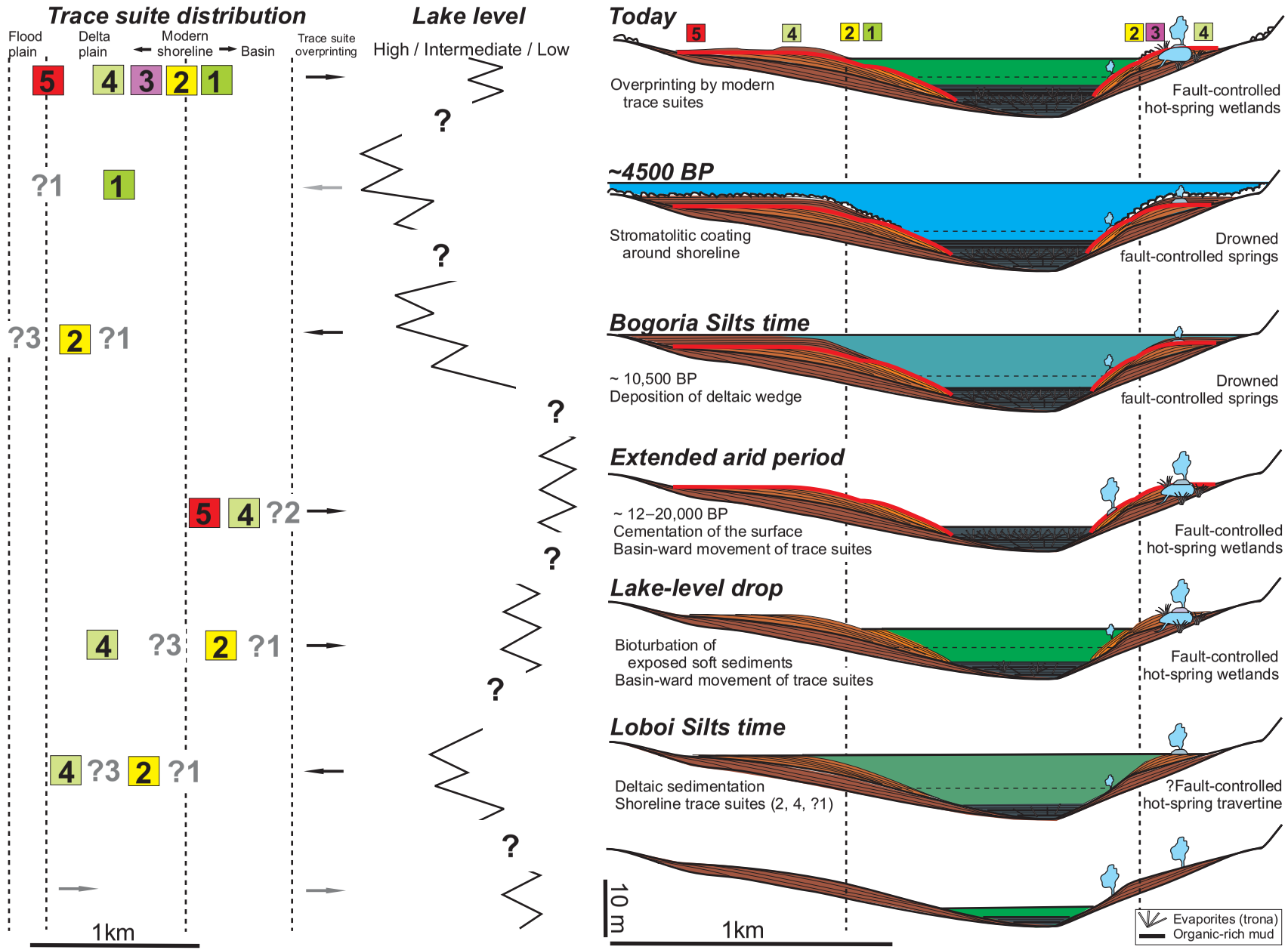
Trace suite distribution
Lake level
Flood plain
Delta plain
Modern shoreline
Basin
Trace suite overprinting
High / Intermediate / Low
1km
Today
Overprinting by modern trace suites
Fault-controlled hot-spring wetlands
~4500 BP
Stromatolitic coating around shoreline
Drowned fault-controlled springs
Bogoria Silts time
~ 10,500 BP
Deposition of deltaic wedge
Drowned fault-controlled springs
Extended arid period
~ 12–20,000 BP
Cementation of the surface
Basin-ward movement of trace suites
Fault-controlled hot-spring wetlands
Lake-level drop
Bioturbation of exposed soft sediments
Basin-ward movement of trace suites
Fault-controlled hot-spring wetlands
Loboi Silts time
Deltaic sedimentation
Shoreline trace suites (2, 4, ?1)
?Fault-controlled hot-spring travertine
10 m
1km
Evaporites (trona)
Organic-rich mud

burrows and plant traces of the Scoyenia-like Suite which are presently bioturbating the exposed and shallowly buried surfaces. The greatest density of modern traces is near the present-day shoreline in the area seasonally affected by lake-level rise-and-fall.

Modern processes that affect the exposed exhumed surfaces are primarily destructive and cause the disintegration of the surface by efflorescent salt crystallization near the shoreline where there is capillary evaporation of saline pore-waters, and by the continued trampling by flamingos and other vertebrates such as bovids. Pedogenic processes, including destruction by roots and the wetting and drying of the surface, lead to the formation of peds and the break-up of the surface. Wave erosion along the shoreline has greatly contributed to exposing the surface, but has also led to the destruction of the uppermost and possibly most delicate portions of it. Processes that continue to indurate the surface include local cementation by calcite precipitated subaerial portions of the surface by evaporation of meteoric waters (Renaut, 1993; Scott, 2005). Cementation of the surface by zeolites (analcime) may be ongoing, but very slow (Renaut, 1993).

## 4.2. Modern Traces and Trace Fossils in the Magadi–Nasikie Engida Basin

Several modern sites were visited in the Magadi–Nasikie basin to investigate the composition of the animal and plant traces under different salinities in a variety of depositional environments. Cool, warm, and hot springs, together with small amounts of seasonal rain, provide the lakes with areas of open water that support a diverse assemblage of animal and plant life. The animal trace data presented here will be complemented by the geochemical work of R. Renaut (in prep.), who measured various aspects of the water geochemistry (e.g., salinity, temperature) at each of the modern sites. In addition to the modern sites, the Pleistocene Green Beds and the Late Pleistocene–Holocene High Magadi Beds were investigated at five sites. The dominant trace makers in the zone of lake-level rise-and-fall were: flamingos and other birds; mammals; and spiders, earwigs, dipteran flies, and beetles (e.g., staphylinids). Several trace makers were photographed within their burrows, and other insects (wasps, beetles, orthopterans) were photographed alive and dead at certain localities but without any association to burrows. Figure 2.3 shows the locations of the sites.

### *4.2.1. Pleistocene Trace Fossils of the Green Beds, Magadi Basin*

Behr and Röhricht (2000) briefly described ichnofossils preserved in the Magadi "Green Beds", which comprise laminated, microbially mediated chert and calcite, as well as a more massive and bioturbated "nodular chert" facies. Behr (2002) reported that the trace fossils could be identified as *Skolithos*, together with "bioturbation" in the Green Beds. As part of this study, trace fossils were briefly investigated from these two main facies at the southern margin of Lake Magadi. Two sites were visited: 1) the SW Lagoon, which mainly preserved a unit of coarse-grained cemented tuff with or without irregular chert nodules capped by a desiccation-cracked flat-bedded cherty surface (Fig. *4.2.1.*1); and 2) the S Lagoon, where nodular cherts within fine-grained tuffaceous and carbonate mud sediments, as well as abundant microbially mediated laminated cherts and calcite, were the two main facies observed (Figs. *4.2.1.*2–3). The stratigraphic relationship between these two sites was not studied. Trace fossils from these sites are described in Table 4.7. The sites were investigated only briefly and it is expected that more trace types and better examples in the Green Beds will be discovered with future fieldwork.

The upper, flat chert capping the tuffaceous and carbonate-containing cherts in the SW Lagoon preserves shallow irregular depressions that are interpreted as poorly preserved mammal footprints (canid and ?rhino), although future fieldwork is needed to confirm this (Fig. *4.2.1.*1B, 1C). The chert preserving the shallow canid prints also preserves very fine surface textures (mm-scale) interpreted as a surface crust of finely crystalline sodium carbonate efflorescence on a

**Table 4.7.** Trace fossils in the Pleistocene Green Beds, S and SW Lagoon areas, Lake Magadi basin.

| Fig. | Trace type | Ichnotaxonomy | Description | Comments | Possible tracemaker | Interpreted environment | Locality |
|---|---|---|---|---|---|---|---|
| Fig. *4.2.1.* 2A–C, 2F, 2G | 'Pock marks' | None available | Small, shallow, roughly circular depressions with or without slightly raised rims which may be only on one side; preserved in epirelief; may be irregular in shape; range from < 2 mm diameter to ~4 mm; depth < 1 mm; boundaries of depressions slightly sloped towards centre in apparently soft original substrate; other examples with sharp, more vertical boundaries may have been formed in more cohesive substrate; sharp-walled examples cross-cut soft-walled examples; sharp-walled examples may be filled with material same as substrate; appear to be several 'generations' of depressions, sometimes with several 'pock marks' superimposed and slightly offset | Interpreted as feeding pits of adult ephydrids; compare with modern examples from hot springs at Nasikie Engida | Diptera: Ephydridae | Wet, cyanobacterial mat at air/water/sediment interface, possibly in hot spring-fed channels and/or pools | S Lagoon area, Pleistocene Lake Magadi |
| Fig. *4.2.1.* 2D, 2H | 'Pock marks' | None available; compare with plug-shaped burrows? | Medium-sized, shallow, roughly circular and irregular depressions preserved in epirelief; may have raised ridges apparently 'pushed' to one side of depression; examples with sharp margins ~5 mm in diameter; more irregular examples < 1 cm in diameter | Larger than 'pock marks' of dipterans; compare with spiders on mats at Nasikie | Spiders? | Wet soft substrate and/or cyanobacterial mat | S Lagoon area, Pleistocene Lake Magadi |
| Fig. *4.2.1.* 2C | 'Pock marks' with horizontal burrows | Indeterminate | Small, sharp-walled 'pock mark' depressions or shallow burrows connected with meandering burrows; 'pock marks' roughly circular or irregular, and < 3 mm diameter; connecting burrows , < ~2 mm diameter | Compare with 'bird probe marks' from Nasikie Engida | Diptera: Ephydridae larvae? | Wet, cohesive microbial mat | S Lagoon area, Pleistocene Lake Magadi |
| Fig. *4.2.1.* 2F, 2H | Surface trails | *Helminthoidichnites* isp. | Small, straight to curving or gently meandering trails preserved in concave epirelief; ~3 mm in diameter (range 2–4 mm); variable preservation, typically with indistinct, irregular trail boundaries; may change direction at sharp angles; one example appears transitional with shallow tunnel just below surface | Compare with modern examples from E Lagoon and Nasikie Engida | Insects; probably larvae of dipterans or water beetles | Wet soft substrate and/or cyanobacterial mat | S Lagoon area, Pleistocene Lake Magadi |
| Fig. *4.2.1.* 2I | Horizontal burrows | ?*Planolites* isp. | Small, straight horizontal tunnels terminating at open, vertical burrow of same diameter; preserved in epirelief; cross-cut one another; may branch, but unclear from example | | Probably insects, possibly very small arachnids (mites) | Wet, cohesive muddy substrate and/or microbial mat | S and SW Lagoon, Pleistocene Lake Magadi |

| | | | | | | | |
|---|---|---|---|---|---|---|---|
| Figs. *4.2.1.* 1D, 1F, 3B–C | Vertical burrows | *Skolithos* isp. A | Small, sharp-walled, unlined, circular, open, vertical burrows; diameter ~3–4 mm; burrows appear straight and not oblique within top 1 cm; depths > 1 cm (only observed from top); no raised ridges surrounding burrows preserved | Not associated with microbial mat features | Possibly tiger beetle larvae (Coleoptera: Cicindelidae) | Cohesive fine-grained substrate | S and SW Lagoon areas, Pleistocene Lake Magadi |
| Figs. *4.2.1.* 1F, 3C | Vertical burrows | *Skolithos* isp. B | Medium-sized, sharp-walled, unlined, circular to oval, open vertical and oblique burrows; diameter < 1 cm; depths > 1 cm, but only observed from top; no raised ridges surrounding burrows preserved | Not associated with microbial mat features | Spiders or insects (beetles?) | Cohesive fine-grained substrate | S and SW Lagoon area, Pleistocene Lake Magadi |
| Fig. *4.2.1.* 1G, 1H | ?3D burrow system | Indeterminate | Small and medium-sized, sharp-walled, open burrows; close association of smaller oblique and horizontal burrow (~4 mm diameter), which may branch from strongly oblique larger burrow (~1 cm diameter); example from SW Lagoon also shows possible horizontally oriented chamber (~3 cm wide, ~1.5 cm high) | Not associated with microbial mat features | Possibly earwigs (Dermaptera) | Cohesive fine-grained substrate at S Lagoon; Fine-grained substrate with chert nodules at SW Lagoon | S and SW Lagoon areas, Pleistocene Lake Magadi |
| Figs. *4.2.1.* 3B, 3E | ?3D burrow system | Indeterminate | Small (< 4 mm diameter) and medium-sized burrows (< 1 cm diameter) in horizontal, oblique, and vertical orientations; burrow boundaries irregular (and compacted?) or sharp and circular; branching not observed in cross-section view; bioturbated unit ~50 cm thick | Not associated with microbial mat features | Possibly earwigs (Dermaptera) and spiders | Bioturbated, porous substrate of carbonate with irregular chert nodules | S Lagoon area, Pleistocene Lake Magadi |
| Fig. *4.2.1.* 1E | Bioturbated | Indeterminate | Very small (< 2 mm) roughly circular and irregular backfilled and open ‘burrows’ in bioturbated tuffaceous substrate; all orientations; preserved as endichnia; sample not collected | May be simply holes remaining after chemical weathering | Unknown; roots?; small insect larvae or arachnids (mites)? | Fine-grained tuffaceous substrate with chert nodules | SW Lagoon area, Pleistocene Lake Magadi |
| Fig. *4.2.1.* 1B | Vertebrate footprints (canid) | Indeterminate | Medium-sized shallow depression that may be attributable to two footprints of a canid or hyaena (double register); total length of ‘hind’ impression ~6.5 cm including claw marks; total width ~4.5 cm; claw marks show tips of both front and hind impressions; preserved in concave epirelief | Possible, very shallow footprint; compare with Nasikie Engida | Possibly Wild dog or hyaena | Bedded chert capping nodular chert unit; surface texture looks like microbial/salt crust | SW Lagoon area, Pleistocene Lake Magadi |
| Fig. *4.2.1.* 1C | Vertebrate footprints (perissodactyl) | Indeterminate | Large shallow depression that may be a partially exposed rhino footprint; total length ~15 cm; total (extrapolated) width ~18 cm; if footprint, only digit III and II or IV exposed; digits broad and very rounded with digit III much wider; impression margins rounded; preserved in concave epirelief | Possible, shallow footprint; different surface texture within depression | Possibly rhino | Bedded chert with sodium carbonate (trona) pseudomorphs | SW Lagoon area, Pleistocene Lake Magadi |

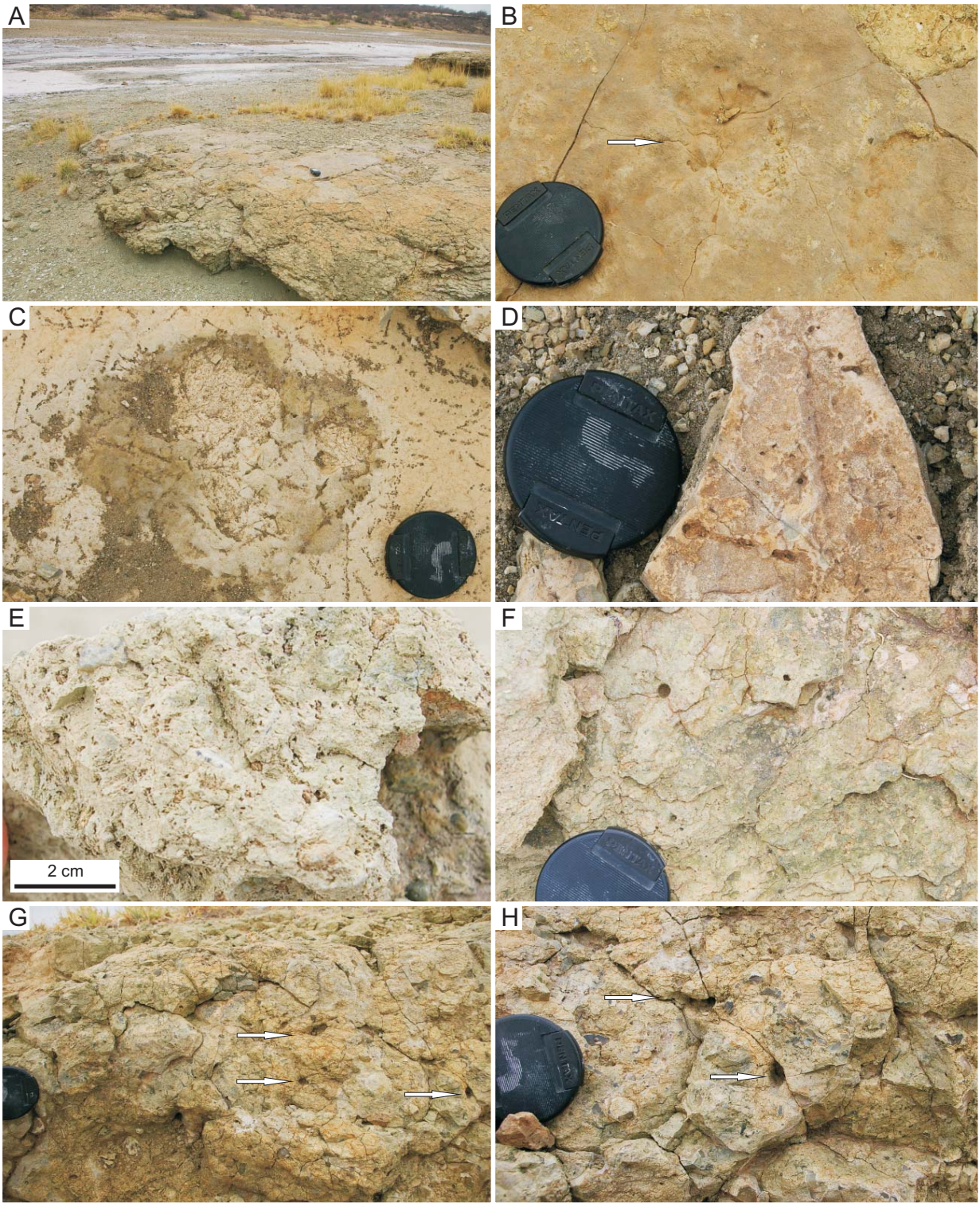


**Fig. 4.2.1.1.** Trace fossils in the Pleistocene cherts of the "Green Beds" in the SW Lagoon, Lake Magadi. **(A)** Exposure of the Green Beds in the SW Lagoon (foreground). GPS for scale. **(B)** Possible shallow canid footprint (arrow) preserved on upper surface of Green Beds shown in (A). **(C)** Possible shallow perissodactyl (rhino?) footprint preserved on upper surface of Green Beds with sodium carbonate evaporite pseudomorphs. Lens cap for scale is ~5 cm. **(D)** Horizontal tunnel and small open burrows. **(E)** Bioturbated carbonate with very small, backfilled burrows. **(F)** Openings of circular, open, vertical burrows. **(G)** The massive nodular chert facies with possible earwig burrow system (arrows). **(H)** Close-up of burrows shown in (G).

muddy substrate based on observations at Lake Bogoria and Nasikie Engida (Fig. *4.2.1.*1B). Large pseudomorphs of sodium carbonate (trona) crystal blades (< 7 cm length) are present within a substrate that possibly preserves a large (< 18 cm width) footprint of a rhino (Fig. *4.2.1.*1C). Other trace fossils preserved in this unit include: 1) a horizontal tunnel (Fig. *4.2.1.*1D); 2) small, open vertical burrows (Fig. *4.2.1.*1D); 3) small, partly backfilled, irregular ?burrows preserved as endichnia in a bioturbated fine-grained tuffaceous substrate (Fig. *4.2.1.*1E); 4) medium-sized, open vertical burrows (Fig. *4.2.1.*1F); and, 5) the larger, open burrows and ?chambers of a possible 3D burrow network in a fine-grained substrate with nodular chert (Fig. *4.2.1.*1G, 1H). In general, this assemblage of traces suggests subaerial exposure of the substrates, and together with the lithofacies, appears comparable to the associations present along the shorelines and mudflats of Nasikie Engida.

The bedded chert facies present at the S Lagoon locality preserves an additional suite of trace fossils that compares well with the modern examples observed at the NW hot springs at Nasikie Engida. Together with desiccation-cracked carbonate mud drapes, as well as heaved, domed, and cracked thick microbial mats, the traces appear to have been formed in very shallow subaqueous substrates or at the sediment/water/microbial mat/air interface (Fig. *3.3*.4). Behr and Röhricht (2000) and Behr (2002) described the trace fossils from the bedded chert facies of the Green Beds as open, vertical, ~1 mm in diameter, < 1 cm in depth, excavation pellets of beetle larvae and creeping traces on the mat surfaces. The burrows may occupy < 50% of the chert (Behr and Röhricht, 2000). Behr and Röhricht (2000) also recognized the desiccation cracks in support of their view that these cherts were subaerially exposed prior to lithification.

Thousands of small (~2–4 mm), very shallow (< 2 mm depth), roughly circular depressions covered the upper calcitic laminae of the bedded cherts at the southern S Lagoon (Fig. *4.2.1.*2A–I), which Behr (2002) associated with cyanobacterial mats. The depressions are interpreted as the "pock mark"-like feeding pits of adult, air-breathing, dipteran flies (likely Ephydridae) in a setting very similar to the subaerially exposed cyanobacterial mats at the northwestern hot springs at Nasikie Engida (see Section 4.3). Several generations of these pits are superimposed upon one another, showing slightly different substrate consistencies, from soft-walled, very shallow (~1 mm), irregular and circular pits (Fig. *4.2.1.*2A–C, 2F–G), to sharp-walled, deeper (~2 mm), more circular pits (Fig. *4.2.1.*2D). Slightly deeper circular pits (~2–3 mm depth) were associated with shallow horizontal tunnels (Fig. *4.2.1.*2C); these traces may have been produced by the larvae of ephydrid flies, which are known to also burrow in cyanobacterial mats (Simpson, 1979). Larger (5–6 mm), shallow, circular pits with more prominently raised ridges (< 1 mm high) surrounding the pits were also preserved in the bedded cherts (Fig. *4.2.1.*2D). The trace makers of these structures are not known, but comparison with Nasikie Engida suggests that they may have been produced by spiders that also inhabit the mats. Small (~3 mm width), shallow, simple horizontal trails (*Helminthoidichnites* isp.) are also preserved in association with the pock marks (Figs. *4.2.1.*2F). Some examples lead to circular burrows (Fig. *4.2.1.*2I), others show false branching (Fig. *4.2.1.*2H), and others may have led to

**Fig. 4.2.1.2.** (Next page) Trace fossils preserved in the bedded chert facies of the Pleistocene "Green Beds" east of the SW Lagoon, Lake Magadi. **(A–D)** "Pock-mark" traces preserved on upper bedding plane. Note multiple generations of marks in (A) and (B), small horizontal burrows in pock-marked surface (arrow in C) and larger-sized surface holes with well preserved rims (arrow in D). **(E)** Side view of bedded chert showing finely interbedded chert (greenish grey) with ?organic rich laminae (dark green to black) and carbonate mudstone (whitish laminae). **(F)** Horizontal trail on pock-marked surface (arrow). **(G)** Possible horizontal trails partly controlling desiccation crack patterns on pock-marked surface. Tip of hammer at right for scale. **(H)** Surface trails or tunnels on upper bedding plane. Arrow is showing possible tunnel roof. **(I)** Horizontal trails terminating at small holes (vertical burrow openings?) on upper bedding plane.

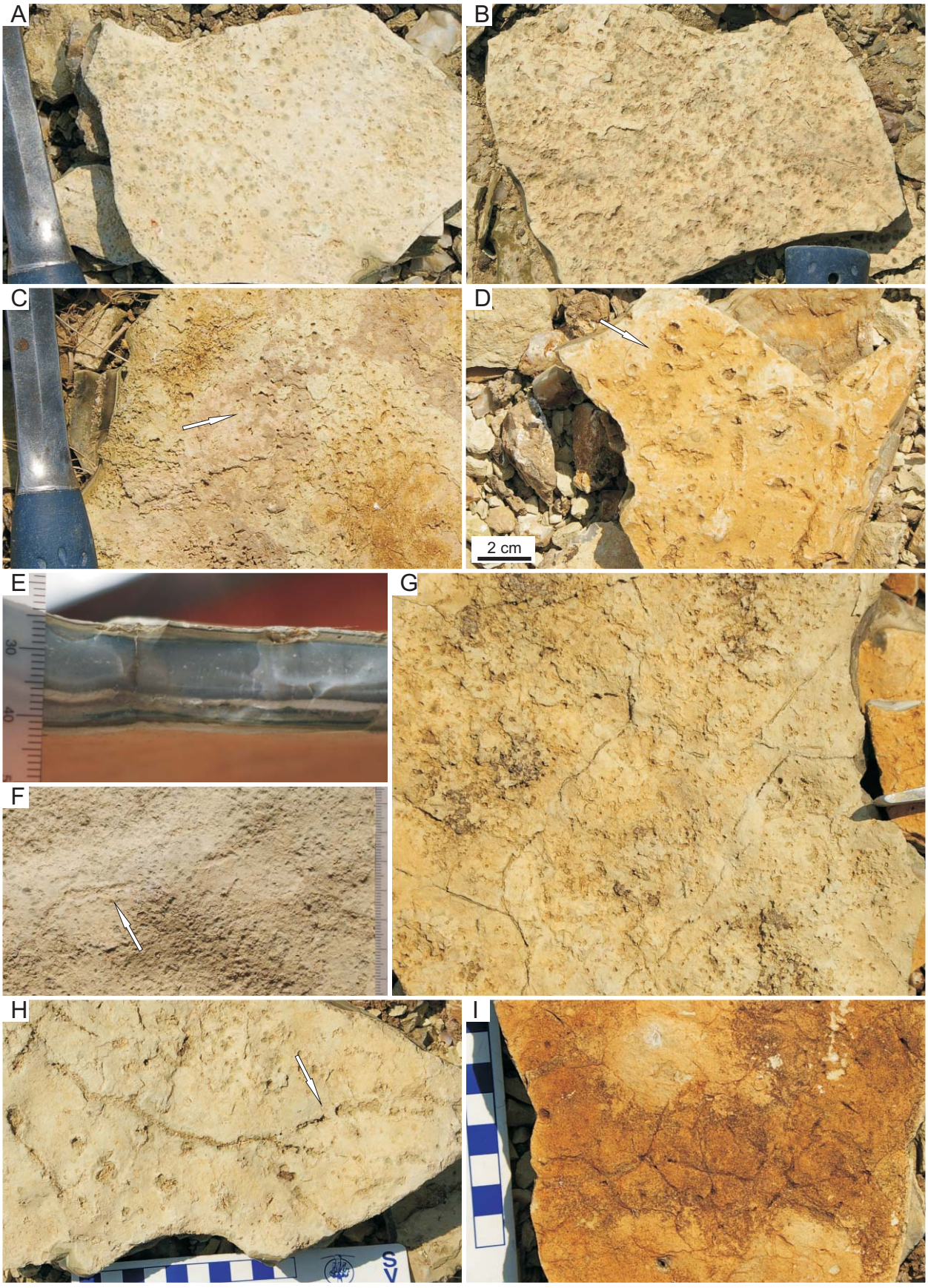
A
B
C
D
2 cm
E
30
40
G
F
H
I

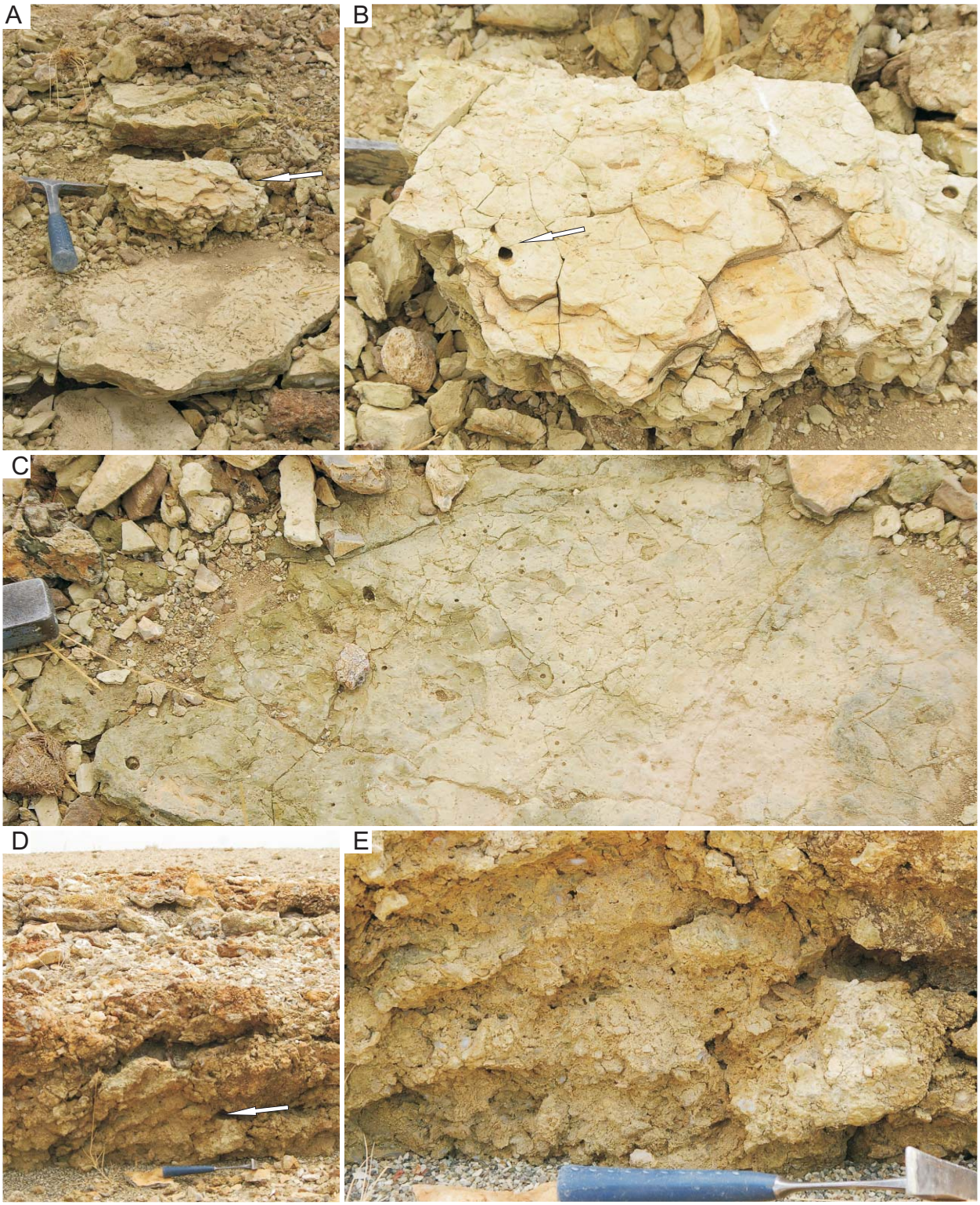


**Fig. 4.2.1.3.** Trace fossils preserved in the Pleistocene "Green Beds" east of the SW Lagoon, Lake Magadi. **(A–C)** Vertical to oblique burrows in carbonates of the bedded chert facies. Arrow in (A) showing position of sediments in (B). Arrow in (B) showing branched oblique burrows of two sizes, possibly produced by earwigs. (C) Two size classes of vertical, open burrows. Note larger burrow (~8 mm diameter) at lower left and smaller burrows (~3 mm diameter). **(D–E)** Bioturbated massive, nodular chert facies with arrow in (D) showing position of photograph in (E). Note massive, nodular texture of substrate and numerous open holes in different orientations in (E).

the formation of meander-like desiccation cracks (Fig. *4.2.1.*2G).

Other traces preserved in this locality include vertical and oblique burrows, and possibly 3D burrow systems (Fig. *4.2.1.*3). In a bed of laminated silt that overlies a bed of laminated chert with sodium carbonate crystal pseudomorphs, oblique, sharp-walled burrows ~1 cm in diameter branch into smaller (~4 mm) horizontal and oblique burrows (Fig. *4.2.1.*3A–B). These traces may have been produced by earwig adults and nymphs, and compare well to the examples observed at Lake Bogoria and Nasikie Engida. Other fine-grained bedding planes preserve dense concentrations of small (3–4 mm) and medium-sized (< 1 cm) vertical burrows that may have been produced by beetles, earwigs, and/or spiders (Fig. *4.2.1.*3C). Finally, a fine-grained, bioturbated substrate with nodular chert preserves many irregular, medium-sized horizontal, vertical, and oblique burrows (Fig. *4.2.1.*3D–E), which may represent the activities of earwigs and/or beetles in a setting similar to the southern mudflats at Nasikie Engida.

*4.2.2. Late Pleistocene–Holocene Trace Fossils in the High Magadi Beds*

The High Magadi Beds are exposed around the margins of modern Lake Magadi in several places, including the eastern and southern lagoons. They are flat-lying and partially covered by modern sediment, with some thick (< 10 m) remnants forming isolated 'islands' or terraces against steep-sided basin-bounding slopes. Three main facies preserve trace fossils: 1) zeolite-cemented red-brown tuffaceous silt; 2) weakly cemented buff-coloured silts; and 3) white chert and carbonate. During the preliminary survey of trace fossils around Lake Magadi conducted for this study, several sites were visited, including: 1) the north-eastern shoreline of the E Lagoon (Fig. *4.2.2.*1); 2) the north-western margin of the E Lagoon; 3) the southern E Lagoon (Fig. *4.2.2.*2); 4) the southern SW lagoon (Fig. *4.2.2.*3); and 5) the south margin of Nasikie Engida (Fig. *4.2.2.*4). The trace fossils are described in Table 4.8.

The most abundant trace fossils observed were more than one hundred degraded flamingo nest mounds and their associated, often strangely shaped, substrate-modified surface structures preserved in zeolite-cemented red-brown tuffaceous silt (Figs. *4.2.2.*1–3). Recognized as irregular and rounded protrusions of salt-encrusted, cemented silts through thin veneers of modern sediments, they were best observed along the eastern shoreline of the E Lagoon (Fig. *4.2.2.*1) and southern margin of the SW Lagoon (Fig. *4.2.2.*3). In most cases, a dense, thick (~5 mm) crust of very finely crystalline efflorescence of sodium carbonate coated the exposed portions of the mounds, and likely contributed to their roundedness by salt-weathering (Figs. *4.2.2.*1B, 3). The mounds are poorly preserved and appear to have undergone extensive weathering. One rounded example measured ~15 cm diameter and ~8 cm high (Fig. *4.2.2.*1C–D), but the sizes of the mounds and related structures were quite variable. The “salt weathering phenomena” observed in the High Magadi Beds by Eugster (1980, p. 215) are reinterpreted here as salt-weathered fossil flamingo nests. Smith and McAllister (1986) examined salt weathering features near Lake Magadi in detail and reported on the formation of tafoni and honeycomb weathering features in the High Magadi Beds, but none of the features they described appear to be related to the strange structures produced by flamingos.

The rounded mounds and their associated linear and/or strangely shaped surfaces compare well with the old, degraded, flooded, and weathered nest mounds and surfaces observed at Lake Bogoria and in recent examples at Lake Magadi. Based on comparisons with excavated modern and fossil flamingo nest mounds at Lake Bogoria, the fossil examples at Lake Magadi are interpreted as the internal, dense cores of nest mounds, along with the trampled and compacted surfaces on which they were built. Just as at Lake Bogoria, some of the strange shapes (e.g., large circular pits) are attributed to the excavation of soupy mud for the initial building of the nest mounds (Fig. *4.2.2.*1E).

**Table 4.8.** Trace fossils in the Late Pleistocene–Holocene High Magadi Beds, Lake Magadi Basin and ?High Magadi Beds south of Nasikie Engida. Trace types are grouped by locality in this table.

| Fig. | Trace type | Ichnotaxonomy | Description | Comments | Possible tracemaker | Interpreted environment | Locality |
|---|---|---|---|---|---|---|---|
| Figs. *4.2.2.* 1, 2C, 3 | Flamingo nest-mounds (and flamingo-modified surfaces) | None available | Circular mounds, irregularly shaped mounds, and linear to irregular, flamingo-modified surfaces in indurated reddish-brown silts; mounds very degraded and rounded at top; vary from ~10 cm to 20 cm diameter at top, from ~15 cm to 30 cm at base, and from 5 to 15 cm high; linear surfaces variable, but commonly ~15 cm in diameter | Compare with degraded nests at Lake Bogoria, and fossil examples from Bogoria Silts and Loboi Silts | Flamingos; unknown if Greater or Lesser flamingos | Low gradient muddy shoreline and exposed littoral | High Magadi Beds, Magadi Basin; E Lagoon, SW Lagoon, ?SE Lagoon |
| Fig. *4.2.2.* 2G | Vertical burrows | *Skolithos* isp. | Straight, medium-sized vertical burrows; partly filled with sub-spherical pellet-like aggregates; 4 mm diameter; sample does not show entire length of burrow, but is at least 10 cm long; burrow boundary sharp and unornamented; unlined/unwalled | Compare with pellet-filled burrows from Lake Bogoria | Insect; likely beetle (e.g., Coleoptera: Cicindelidae) | Moist, somewhat cohesive substrate | High Magadi Beds, Magadi Basin, SE Lagoon |
| Fig. *4.2.2.* 2E | Branching open burrows | Indeterminate | Downward branching, open burrow system; main burrow vertical and < 2 cm in diameter with smaller burrows branching outward from upper part of burrow system; smaller burrows 6 –9 mm in diameter; dominant orientations vertical and horizontal; unlined/unwalled; burrow boundaries defined but not sharp | Composite trace fossil? | Unknown insect (?Dermaptera) | Moist, somewhat cohesive substrate | High Magadi Beds, Magadi Basin, SE Lagoon |
| Fig. *4.2.2.* 2F | Horizontal burrows | cf. *Planolites* isp. | Straight, open, horizontal burrows ~8 mm in diameter; unlined/unwalled; burrow boundary not sharp | | Insect; possibly earwig or cricket? | Unknown | High Magadi Beds, SE Lagoon |
| Fig. *4.2.2.* 4B, 4C | ? Root hairs | None available | Sub-millimeter holes in various orientations; branching?; may be filled with carbonate | May be evidence of palustrine environment | Plants; probably grasses or sedges | Cohesive, wet carbonate and opaline silica substrate | High Magadi Beds, Nasikie Engida south |
| Fig. *4.2.2.* 4E | ? Vertical burrows | cf. *Skolithos* isp. | Medium-sized (4 mm diameter), sub-circular, vertically oriented open holes; appear to have been formed prior to desiccation of cherty-gel substrate | Evidence of subaerial exposure prior to lithification of chert | Insects or arachnids, or even grasses or sedges | Cohesive carbonate and opaline silica substrate (Magadiite?) | High Magadi Beds, Nasikie Engida, southern margin |
| Fig. *4.2.2.* 4B–C | Tapered vertical burrow | Indeterminate | Partially lined, sharp-walled, tapered vertical burrow to rounded base; diameter at top ~ 1cm; diameter at base ~ 6 mm; apparently | Evidence of subaerial exposure prior | Insects or arachnids; possibly funnel | Cohesive carbonate and opaline silica | High Magadi Beds, Nasikie Engida, |

| | | | | | | | |
|---|---|---|---|---|---|---|---|
| | | | formed prior to complete desiccation of silica gel substrate; well cemented lining different material than host (buff-coloured carbonate and clay?); small holes (? root hairs) penetrate lining and burrow boundary | to lithification of chert | or wolf spider? | substrate (Magadiite?) | southern margin |
| Fig. *4.2.3.* 1D–H | 3D burrow systems | *Thalassinoides* isp. | Open, unlined/unwalled burrow system with sharp burrow boundaries; burrows of horizontal, vertical, and oblique orientations; branching shows T- and Y-junctions, and multiple burrows branching from enlarged chambers; burrows variable in size, from 8–10 mm diameter to < 2.5 cm diameter for enlarged areas; one example of an oval-shaped chamber was 2 cm in height and ~2.8 cm wide; no evidence of pellet-like fill | Compare with earwig burrow system in exhumed surfaces at Lake Bogoria and Schlūter and Kohring (1992) | Insects; likely earwigs (Insecta: Dermaptera); possibly Orthopterans (i.e. crickets), termites, or ants | Firm substrate at wet lake margin developed on tuffaceous, weakly developed paleosol | ?High Magadi Beds, S of Nasikie Engida |
| Fig. *4.2.3.* 1C | Walled cells | Indeterminate | Thick-walled, oval-shaped ?cell (one specimen, in situ, cross-section only); constructed wall of material similar to host; wall ~3 mm in diameter; internal material similar to host | Similar types in the Olorgesailie Formation, M13–14 | Insects; possibly dung beetle nest or pupal chamber of other beetles | Tuffaceous, weakly developed paleosol | ?High Magadi Beds, S of Nasikie Engida |
| Fig. *4.2.3.* 1I | Meniscate backfilled burrows | cf. *Beaconites* isp. | Thick-walled, meniscate backfilled burrow; constructed wall approximately 2 mm in diameter; total burrow diameter ~1.8 cm; internal margin of constructed wall sharp on one side only; meniscae may extend into wall | Similar to cf. *Beaconites* isp. in the Loboi Silts, Bogoria basin | Insects; unknown, possibly termites | Tuffaceous, weakly developed paleosol | ?High Magadi Beds, S of Nasikie Engida |
| Fig. *4.2.3.* 2A, 2C | Open tunnel network (termite nest?) | Indeterminate | Large (< 2.5 cm diameter), passively filled, branched tunnel network with U-shaped orientation; attached to large (< 15 cm diameter), passively filled, vertically oriented open chamber | Similar to some termite nests in Olorgesailie Fm. (e.g., M14, B4) | Likely termites (e.g., Odontotermes) | Tuffaceous, weakly developed paleosol | Overprinted on ?High Magadi Beds, S of Nasikie, (Holocene) |
| Fig. *4.2.3.* 2A | Termite nest | cf. *Termitichnus* isp. | Large, roughly oval-shaped nest with horizontal plates; nest ~35 cm wide and ~20 cm high; plates 2–3 cm high; associated with large, open vertical passages ~5 cm in diameter; nest material and tunnel fill is pinkish in colour; host material is greenish tuffaceous silt of ?High Magadi Beds | Compare with termite nests of the Ol Tepesi Beds, western Olorgesailie Fm. | Termites (e.g., Insecta: Termitidae: Macrotermitinae) | Tuffaceous, weakly developed paleosol | Overprinted on ?High Magadi Beds, S of Nasikie, (Holocene) |
| Fig. *4.2.3.* 2B | Vertical burrow | *Skolithos* isp. | Large (2.5 cm diameter) vertical burrow with sharp burrow boundaries; unlined/unwalled; passively filled | | Unknown; possibly spiders or beetles | Tuffaceous, weakly developed paleosol | Overprinted on ?High Magadi Beds, S of Nasikie |


**Fig. 4.2.2.1.** Fossil flamingo nest mounds of the High Magadi Beds, eastern shoreline of the E Lagoon, Lake Magadi. **(A)** View of mudflat with irregular topography due to underlying, well indurated High Magadi Beds. **(B)** An irregular surface of the High Magadi Beds forming positive topography at modern mudflat. Lens cap for scale at lower left ~5 cm. **(C–D)** Fossil nest mounds and surface uncovered from beneath modern coarse-grained sands. **(E–F)** Examples showing variable shapes of flamingo-modified surface. **(G–H)** Remnant of the High Magadi Beds at the E Lagoon. (H) shows irregular surface, attributable to multiple, overlying layers of nest mounds.

Two sites visited at Lake Magadi (eastern shoreline of the E Lagoon and the southern E Lagoon) also preserve 'islands' of well-cemented, thicker packages (2–3 m) of the High Magadi Beds that may show the salt-weathering phenomena referred to by Eugster (1980) (Figs. *4.2.2.*1G, 1H, 2A–C). Alternatively, or additionally, the irregular weathering of these strata may possibly be due to the weathering of several overlying beds that all preserve flamingo nest mounds. Supporting evidence for this interpretation includes the location of these islands adjacent to steep lake-bounding faults, which suggests that the position of the lake margin

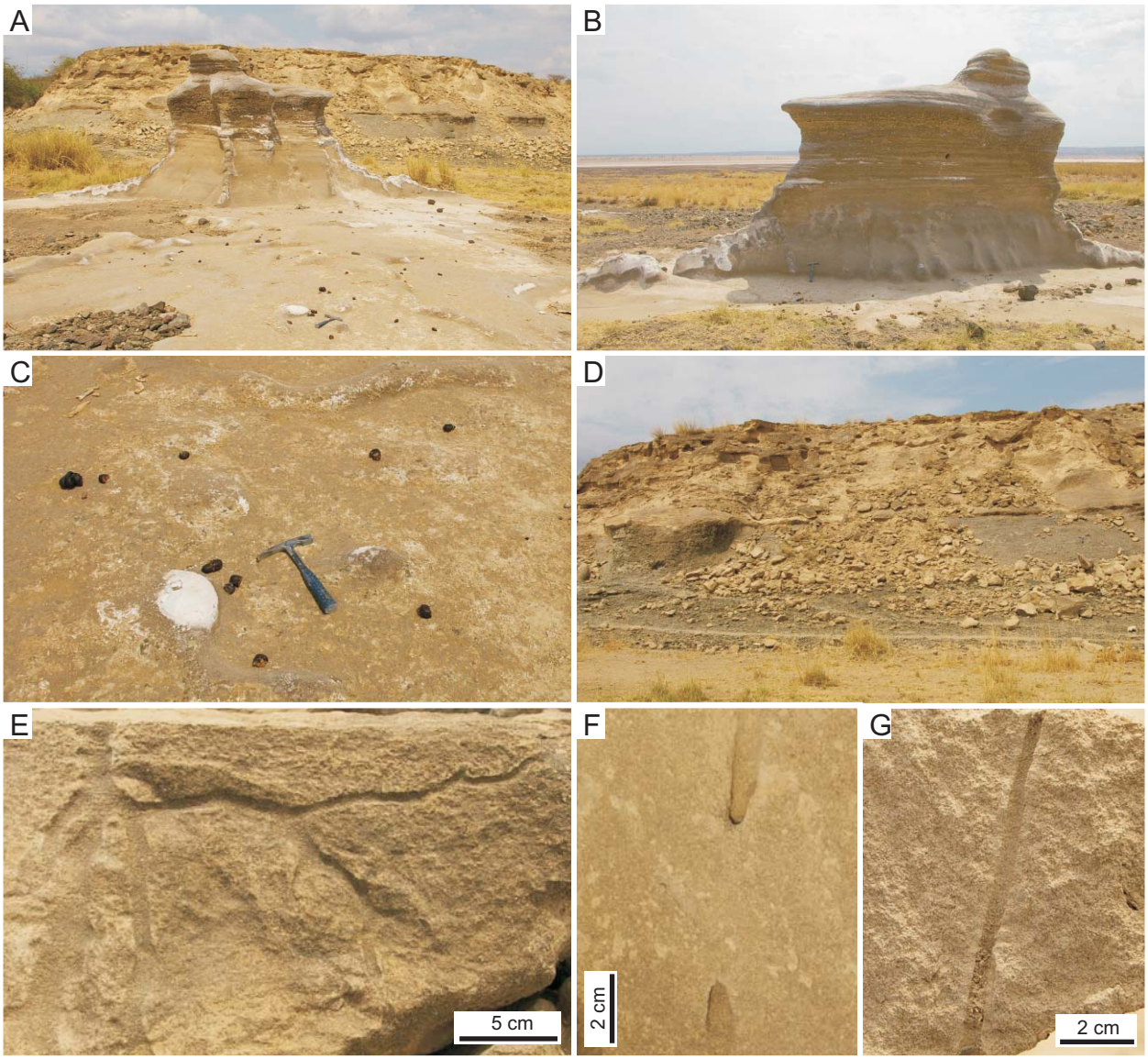


**Fig. 4.2.2.2.** The High Magadi Beds at the SE Lagoon, Lake Magadi. **(A)** Remnant of the High Magadi Beds in foreground with irregular surface at base. In background is the magadiite chert unit (lower) and the tuffaceous silts of the upper unit. Hammer for scale at bottom centre. **(B)** The remnant of the High Magadi Beds shown in (A). The laminated upper part is equivalent to the magadiite chert unit-containing lower unit in (A). Note irregular weathering similar to remnant in E Lagoon. **(C)** The irregular "exhumed" lower surface shown in (A) and (B). The topography is interpreted to be due to degraded fossil flamingo nest mounds. Hammer for scale between two mounds. **(D)** Exposure of the magadiite chert unit and the upper tuffaceous unit. **(E–G)** Trace fossils in the tuffaceous unit of the High Magadi Beds. (E) Root or insect trace? (F) Open horizontal burrow just below bedding plane. (G) Vertical burrow partially filled with spherical pellet/aggregate material.

mudflats of the High Magadi Lake were likely static through time. Today, modern flamingo nests built along the eastern margin of the E Lagoon at Lake Magadi are built from the thin layer of muddy sands that overly the High Magadi Beds. The more precise stratigraphic position of this unit within the High Magadi Beds is unknown, but it is suspected to be below the laminated tuffaceous silts (?Upper High Magadi Beds) on the western margin of the E Lagoon, which may make it equivalent to the Middle High Magadi Beds (Eugster, 1980; Behr, 2002).

Observations from the Loburu Delta at Lake Bogoria of modern nests being built upon older exhumed, cemented surfaces with nest mounds and irregular surfaces, supports the idea that these types of surfaces could be superimposed. Berry (1971) also reported the re-use of older, degraded nest mounds from the Etosha Pan, Namibia. Nest mounds in one of the colonies examined there were built upon a 'platform' of older, compacted, closely grouped nests about 30–40 cm higher than the surrounding pan. There, excavations showed at least six layers of previous nests, distinguished by levels of concentrated egg-shell fragments and feathers (Berry, 1971). Similar excavations at Lake Magadi may support this interpretation and provide more evidence for establishing criteria to recognize nest mounds in cross-section.

Other trace fossils are preserved in the poorly indurated, buff-coloured tuffaceous silts of the High Magadi Beds in the southern E Lagoon area (SE Lagoon) at the type locality for magadiite chert. This unit overlies the indurated red-brown silts that preserve flamingo-modified surfaces and weathered nests (?Middle High Magadi Beds), as well as the horizon that contains magadiite. The trace fossils from this unit include a partially pellet-backfilled example of *Skolithos* isp., an open horizontal burrow (*Palaeophycus* isp.), and a unidentified downward branching, vertical and horizontal, open trace fossil that may be attributable to either a large root

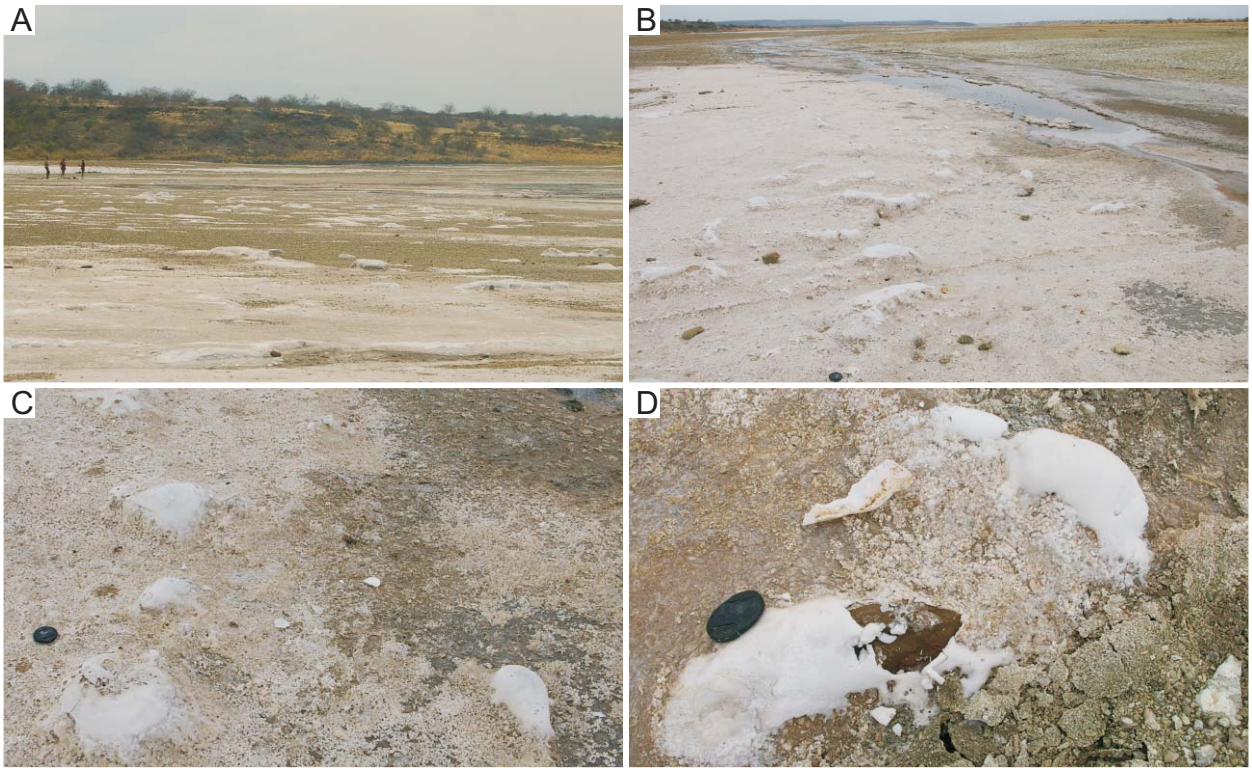


**Fig. 4.2.2.3.** The “exhumed” High Magadi Beds in the SW Lagoon, Lake Magadi. **(A–D)** Irregular topography of High Magadi Beds overlain by thin veneer of modern sediments. Bright white efflorescence marking very fine-grained sediments of the High Magadi Beds (shown in D).

or perhaps the burrows of earwigs in a soft, fine-grained substrate (Fig. *4.2.2.*2D–G). No trace fossils were observed during a brief visit to the laminated, buff tuffaceous lacustrine silts of the High Magadi Beds on the western margin of the E Lagoon.

A small exposure of the High Magadi Beds is also present along the southern margin of Nasikie Engida and includes: 1) tuffaceous, laminated buff silt; 2) white magadiite and carbonate mud; 3) horizontal and cross-bedded conglomerate; and 4) calcrete (Fig. *4.2.2.*4). Within the white magadiite and carbonate mud unit, several examples of trace fossils likely produced subaerially were discovered. First, medium-sized (5 mm), roughly circular, vertically oriented open holes penetrated a thin bed (< 1cm) of chert and may be comparable to the open holes through the siliceous salt crust at the southern margin of Nasikie Engida (Fig. *4.2.2.*4E). Second, a large (>1 cm diameter), tapered, and lined 'burrow' was preserved within a sample of magadiite chert mixed with yellowish carbonate mud that also contained numerous very small holes possibly formed by roots and root hairs (Fig. *4.2.2.*4B–C). These small holes penetrate the burrow lining. Another example of a vertical burrow (~5 mm diameter) was preserved in a sample of chert with dark brown material that appears organic-rich (Fig. *4.2.2.*4D). These initial few observations of traces in magadiite may have implications for the interpretation of the genesis of the cherts at Lake Magadi, and suggest that magadiite-type cherts should be investigated for other evidence of subaerial exposure prior to their lithification. With the limited evidence presented here, it is unclear if a soft magadiite precursor-gel was bioturbated while buried beneath younger sediments, although the irregular margins of the open holes suggest that it may have been burrowed into during its initial genesis within a wet, soupy but cohesive, organic-rich mud substrate.

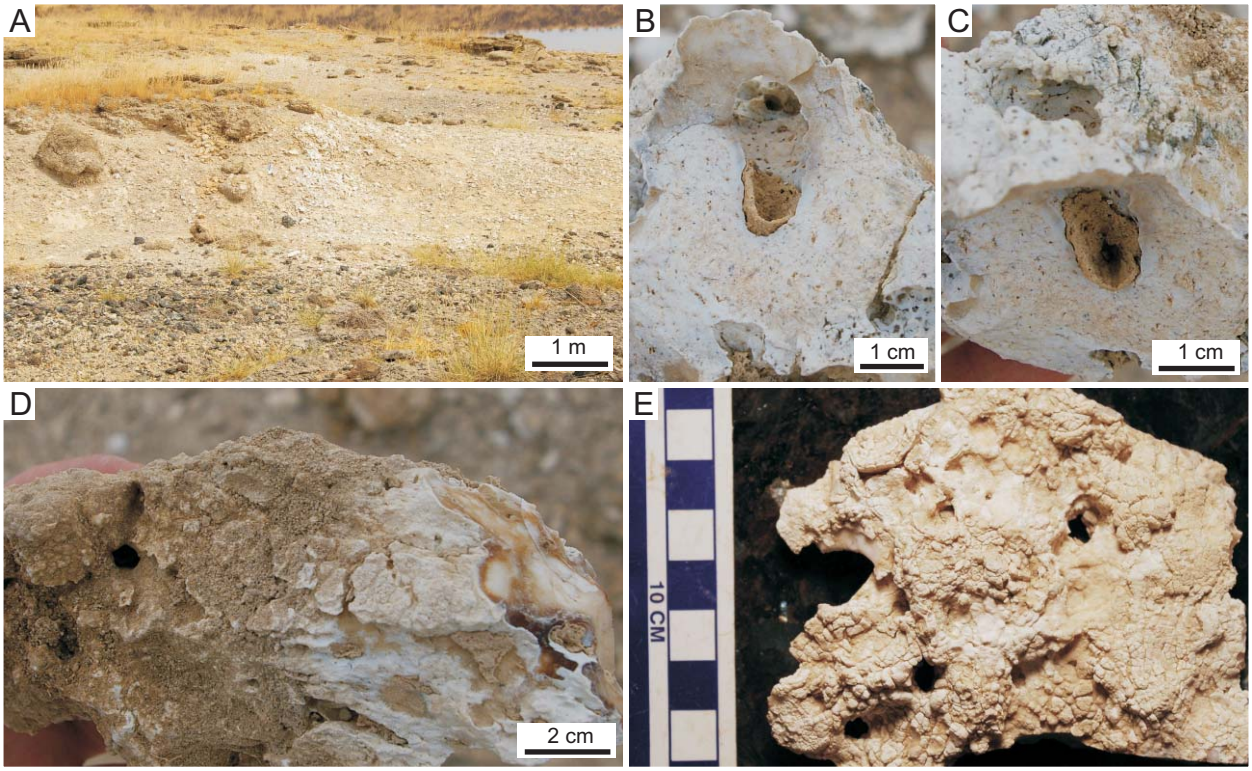


**Fig. 4.2.2.4.** The High Magadi Beds at the southern shoreline of Nasikie Engida. **(A)** Outcrop of laminated silts (light buff), white magadiite layer, and caliche at top of unit. **(B–C)** Fossil tapered vertical burrow with cemented silt lining in magadiite. Numerous tiny holes likely due to roots. **(D)** Vertical burrows in magadiite chert. Far right showing preserved dark brown organic matter, burrow hole at left. **(E)** Vertical burrow holes in thin magadiite bed.

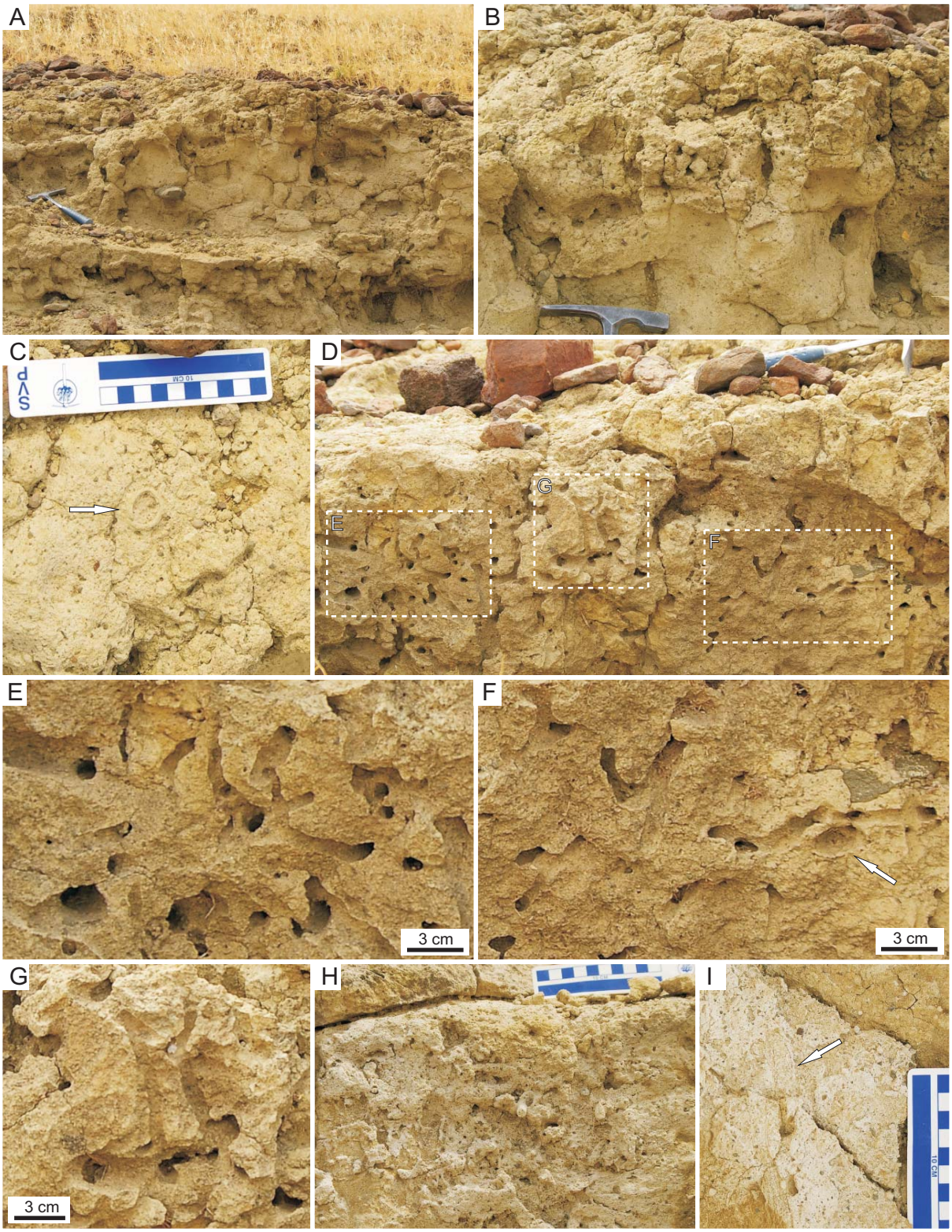


**Fig. 4.2.3.1.** The "exhumed" High Magadi Beds south of Nasikie Engida. **(A–B)** The High Magadi Beds showing increasing bioturbation and pedogenesis upwards. **(C)** A thick-walled trace, possibly of a scarabid beetle (arrow). **(D–H)** Possible earwig burrow system (*Thalassinoides*). Boxes in (D) show positions of (E–G). Note sharp, smooth walls, variable burrow diameters and chambers at branching points. Arrow in (F) showing an oval-shaped chamber. Burrows in (H) preserved by carbonate. **(I)** Walled meniscate-backfilled burrow attributed to termites (arrow).

*4.2.3. Trace Fossils in the "Exhumed Surfaces" Around Nasikie Engida*

South of Nasikie Engida, a small outcrop area exposes up to 3 m of light-coloured fine-grained sediments possibly equivalent to the High Magadi Beds, as well as a pocket of the older Oloronga Beds (Figs. *4.2.3.*1, 2). During reconnaissance, the ?High Magadi Beds in this locality were found to preserve many trace fossils, which are described in Table 4.8. The unit shares several features with the exhumed surfaces of the ?Bogoria Silts on the Loburu Delta at Lake Bogoria, which suggests that these beds may also represent the superposition of trace fossil suites formed under different environmental conditions on a single, stratigraphically important surface. A small pocket of ?High Magadi Beds-equivalent strata exposed in the NE delta plain of Nasikie Engida also appears to be relatively more indurated upwards, and should be investigated during future fieldwork to determine if the upper unit also represents an "exhumed" surface (Fig. *4.2.3.*3).

The degree of induration and intensity of bioturbation increase upwards from white, massive siltstone to buff siltstone containing thousands of small burrows and/or root pores (Fig. *4.2.3.*1A–B). Within the lower whitish silt, several large (~2.5 cm diameter) vertical burrows are preserved that are passively filled with coarse grained material different from the host (Fig. *4.2.3.*2B). These burrows may be more recent, along with several apparently Holocene termite nests and associated passages (Fig. *4.2.3.*2A, 2C). A single, thick-walled possible brood ball of a dung beetle is preserved within the silt and is filled with the same material as the host substrate (Fig. *4.2.3.*1C). Within the upper, more indurated buff silt, a 3D burrow system assigned to *Thalassinoides* isp. is also preserved, with several features very well exposed (Fig. *4.2.3.*1D–G). The burrows are open, ~1–2 cm in diameter, have sharp burrow boundaries, smooth internal walls, and branch in all orientations from enlarged chambers that may be oval-shaped or irregular. This burrow system is attributed to earwigs, and is remarkably similar the burrow network with egg chambers observed at Lake Bogoria within which the adult females of

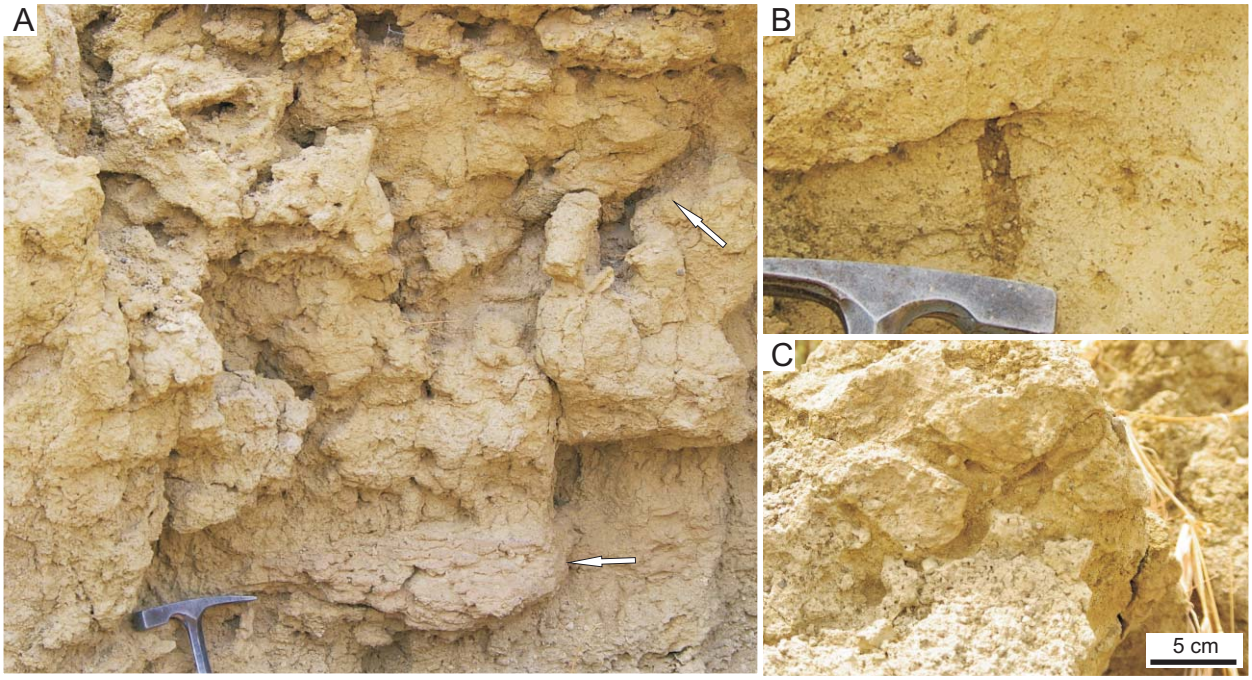


**Fig. 4.2.3.2.** Holocene trace fossils overprinting the High Magadi Beds south of Nasikie Engida. **(A)** Large termite nest showing main, horizontally layered nest (lower arrow) and large ventilation pipes (upper arrow). **(B)** Large burrow filled passively with coarse-grained sediment. **(C)** Branched large burrows filled with recent sediment.

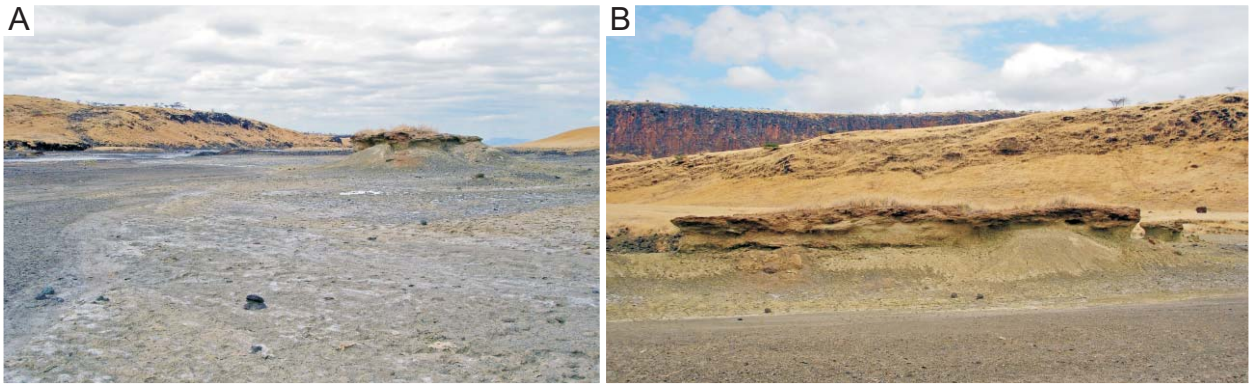


**Fig. 4.2.3.3.** A possible "exhumed" surface at the NE alluvial plain at Nasikie Engida. Photographs are courtesty of R.Renaut. **(A)** View of the plain looking north and showing remnant, older sediments possibly equivalent to the High Magadi Beds. **(B)** View of remnant sediments with apparently increasing induration towards the top.

*Labidura* were directly observed (see Section 4.1.5.4). In some places, the burrow system is filled with carbonate cement (Fig. *4.2.3.*1H). Lastly, thick-walled, meniscate backfilled examples cf. *Beaconites* isp. are very similar to those attributed to termites (foraging tunnels) in the exhumed surfaces (Loboi Silts) at Lake Bogoria (Fig. *4.2.3.*1I). With further work, the investigation of the relative timing of trace fossils preserved in the ?High Magadi Beds south of Nasikie Engida may also show the superposition of trace fossils associated with a moist, firm substrate near the shoreline substrate overprinting a older, more terrestrial suite.

### *4.2.4. Modern Animal Traces around Lake Magadi*

Most of the sites investigated along the shorelines of Lake Magadi had some influence of spring-fed, relatively fresh water. The trace types and general characteristics of each site are described separately below. Table 4.9 provides descriptions of each of the types recognized.

*4.2.4.1. Northwest (NW) Lagoon 1*— The site lies adjacent to a steep, faulted western border of the NW Lagoon where warm springs (~35–45°C) issue at ground level from the base of the escarpment (Fig. *4.2.4.*1A). Green and orange cyanobacterial mats grow at the water/sediment/air interface along the coarse sand and gravel shoreline. No examples of the feeding traces of adult ephydrid flies (brine flies) were observed at the time the site was visited, but shallow, indistinct vertebrate footprints covered the mats. Adult flies and pupal cases (probably both ephydrids) were abundant along the shoreline. Thin, flat, sodium carbonate crusts were present on exposed sediments at the shoreline. Very little vegetation was observed, although there were small areas with sedges near the spring pools and grasses up the slope of the escarpment. Towards the lagoon, substrates in the very shallow subaqueous zone were either black and dark brown sands or organic-rich mud with blackish, thick, subaqueous microbial mats.

**Fig. 4.2.4.1.** (Next page) Modern animal traces at the NW Lagoon (west), Lake Magadi. Photographs shown in (A) and (B) are courtesy of R.Renaut. **(A)** Shallow water along the margins of the NW Lagoon. **(B)** Straight to gently curving trails produced subaqueously in detritus. Salt crust at left. Trace makers are probably fly larvae (e.g., Stratiomyidae). **(C–D)** Shorebird footprints with feeding traces along trackway (semi-circle marks). Produced subaqueously in coarse-grained sand and infilled by detritus. **(E–F)** Vertebrate tracks in cohesive, organic rich muds. Tracks produced subaqueously. (E) Trampled sediments. (F) Clearly impressed and stabilized flamingo footprints. **(G–H)** Bird probe-mark feeding traces in cohesive muds. Note lunate shape to impressions and groups of two to three.

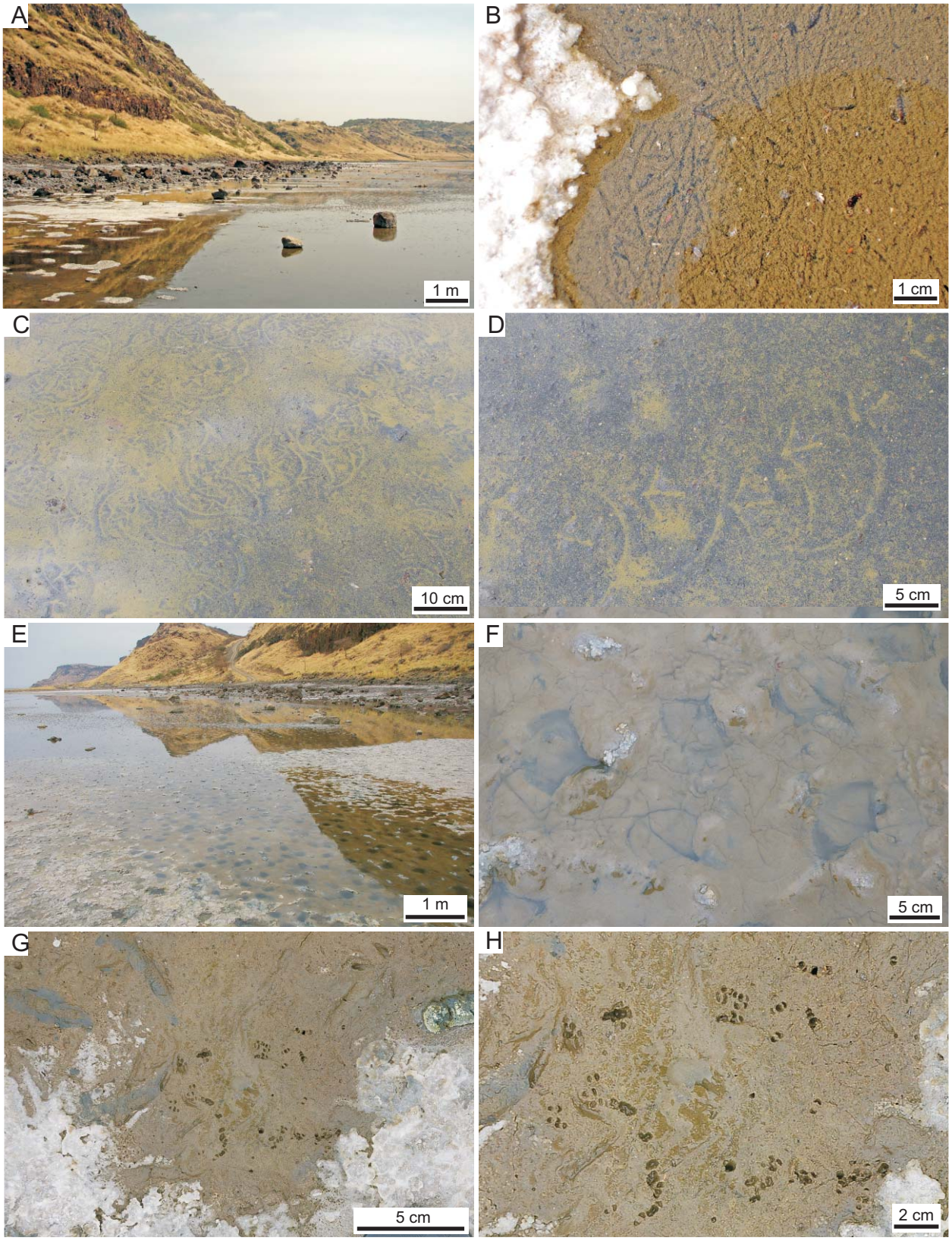
A
1 m
B
1 cm
C
10 cm
D
5 cm
E
1 m
F
5 cm
G
5 cm
H
2 cm

**Table 4.9.** Modern animal traces at Lake Magadi observed in August 2007 and 2008. Supplementary photos of traces in August 2005 and 2006 were provided by R. Renaut. Division of trace types into suites follows that of Scott et al. (2009).

| Fig. | Trace type | Ichnotaxonomy | Description | Comments | Tracemaker | Environment | Localities |
|---|---|---|---|---|---|---|---|
| *Suite 1: "Chironomid" Suite* | | | | | | | |
| Fig. *4.2.4.* 7B | Vertical burrows | cf. incipient *Polykladichnus* isp. | Small open burrows; diameter variable, ~2–3 mm; burrow openings irregular and roughly circular or oval-shaped; examined only in plan view | Irregular margins to burrows due to medium grain-sized sand | Insects (Diptera); chironomid larvae? | Cyanobacterial mat on wet, cohesive sand below salt crust | E Lagoon |
| Fig. *4.2.4.* 3E, 3F | Chironomid tube structures | None available | Small, open, vertically oriented tube structures of organic material; ~3 mm external diameter, ~1 mm internal diameter; approximately 2–3 cm long; tubes were present in dense concentrations and supported one another to remain vertical | Present in extremely dense concentration | Insects (Diptera); likely chironomid larvae | Shallow subaqueous in microbe-rich water | NW Lagoon |
| *Suite 2: "Flamingo Nest-Mound" Suite* | | | | | | | |
| Figs. *4.2.4.* 2E–G, 9A, 9B | Flamingo nest-mounds & associated surfaces | None available | Large mounds of organic-rich mud; wider at base than top with either flat top surface or with central depression (< 4 cm deep); external portion of mounds porous and made of irregular lumps of mud; tops of mounds may have a smooth surface crust, likely of sodium evaporites and flamingo waste; may be associated with linear to irregular raised surfaces of muddy sediment with rounded margins, < 40 cm diameter | Observed in different degrees of degradation at different sites | Flamingos; unknown if Lesser or Greater flamingos | Wet, muddy substrate in saline mudflat or exposed low-gradient littoral | NW Lagoon; E Lagoon |
| Fig. *4.2.4.* 9C, 9D | Feeding structures (flamingos) | None available | Very large (< 75 cm diameter), shallow, circular depressions usually with central, circular, rounded raised area (< 30 cm diameter); depth of depressions ~5 cm; margins of depressions have slightly raised rims (~3 cm | Structures may be the beginnings of nest-mounds | Flamingos; probably Greater flamingos | Wet, muddy substrate in saline mudflat | E Lagoon |
| Figs. *4.2.4.* 1E–F, 2A–D, 9E, 11B | Footprints (flamingo) | Flamingo footprints | Large, three-toed, webbed footprints with rounded posterior margins; webbing to tips of digits; claws extend beyond webbing; tips of digits face only slightly outward; webbing not always impressed depending on substrate; total length ~7–8 cm; total width ~11 cm; examples in subaqueous substrates may be circular depressions in a line (trackway) | Footprint morphology extremely variable depending on substrate | Flamingos; unknown if Lesser or Greater flamingos | Wet, exposed saline mudflat to shallow subaqueous | NW Lagoon; NE Lagoon; E Lagoon, SW Lagoon |
| Fig. *4.2.4.* 7E | Footprints (storks) | Stork footprints | Large, unwebbed, four-toed footprints; total length including hallux ~18 cm; total width ~15 cm; metatarsal impression star-like due to wet substrate and impression of metatarsal area | Morphology altered by salt efflorescence | Marabou stork | Saline mudflat with salt crust over wet mud | E Lagoon |

*Suite 3: "Mermia-like" Suite – Shallow Subaqueous Suite*

| | | | | | | | |
|---|---|---|---|---|---|---|---|
| Figs. *4.2.4.* 1B, 4C–E | Horizontal trails | Incipient *Helminthoidichnites* isp. | Small surface trails (2–2.5 mm diameter); straight to gently curving or looping; some examples of sharp turns (~120°); examples of cross-cutting same and other trails; margins of trails may be irregular in cyanobacterial mat and loose organic substrates | Associated with adult dipterans (chironomids) and discarded pupal cases | Insects (Diptera); pupating chironomid adults? | Very shallow subaqueous with fresher water influence and microbial substrate | NW Lagoon; NE Lagoon |
| Figs. *4.2.4.* 1C, 1D, 11C | Footprints (shorebirds) | | Medium-sized, three-toed footprints without webbing; digits straight and directed outward from metatarsal; posterior margin of prints triangular; total length ~3.5–4 cm; total width ~6 cm | Associated with 'swinging' feeding structures | Birds; shorebirds (possibly Black-winged stilts) | Very shallow subaqueous with fresher water influence; microbe-rich sandy substrate | NW Lagoon; (NE Lagoon); SW Lagoon |
| Fig. *4.2.4.* 1C, 1D | Feeding structures (shorebirds) | None available | Surface 'trails' apparently produced by shorebirds swinging narrow bill along substrate; 'trails' are gently curved into semi-circles; ~12–16 cm in length and ~5 mm diameter | Associated with shorebird footprints | Birds; shorebirds (possibly Black-winged stilts) | Very shallow subaqueous with fresher water influence | NW Lagoon |
| Figs. *4.2.4.* 1G–H, 11C, 11D | Feeding structures (shorebirds) | cf. *Skolithos* isp. | Small (2–3 mm) holes with distinct margins; irregular and roughly circular to oval-shaped; some clear examples of crescent-shaped holes, usually in pairs with concave margins of crescents facing towards one another; often in groups of < 10 holes | Associated with shorebird footprints | Birds; shorebirds | Very shallow subaqueous with fresher water influence; microbe-rich sandy substrate | NW Lagoon |
| *Suite 4: "Scoyenia-like" Suite* | | | | | | | |
| Figs. *4.2.4.* 2H, 2I, 8C | Vertical burrows | Incipient *Skolithos* isp. | Small to medium-sized (~2–4 mm diameter), straight, circular, open vertical burrows with sharp burrow boundaries; unlined/unwalled; slight, circular depression (~ 1mm depth) around burrow opening | | Insects (Coleoptera); likely Cicindelidae and Staphylinidae | Clay-rich, cohesive, wet, substrate; substrate may be anoxic | E Lagoon; NW Lagoon |
| Fig. *4.2.4.* 8C, 8D | Vertical burrows | Pellet-filled burrows | Medium-sized (4–6 mm diameter), open or pellet-filled, oblique and vertical burrows; pellets are elongate and tiny (< 1 mm diameter, < 3 mm long); burrow boundaries sharp; unlined, unwalled; associated with excavated pellet-like aggregates in tumuli surrounding burrow opening | Compare with pellet-filled burrows at South Loburu, Lake Bogoria | Insects (Coleoptera); staphylinids directly observed at site | Clay-rich, cohesive, wet, anoxic substrate | E Lagoon |
| Figs. *4.2.4.* 3D, 7H | Vertical burrows | ? Incipient *Skolithos* isp. | Large (1.5–2 cm diameter), circular, open burrows with large circular tumuli (< 2 cm high) of excavated material surrounding burrow opening; burrow boundaries not sharp; may have web covering burrow opening | | Spiders; web observed at burrow opening | Moist to wet, muddy to sandy subaerial substrates | NW Lagoon; E Lagoon |

| | | | | | | | |
|---|---|---|---|---|---|---|---|
| Fig. *4.2.4.* 9F | Bird nests (scrape) | None available | Large (< 30 cm outside diameter; ~20 cm diameter at top), circular, bird nest built from dried salt crust chips, gravel, and twigs; < 5 cm high, with shallow depression over most of top surface (~15 cm diameter) | Built after substrate dried; no eggs in nest | Birds; shorebirds, probably black-winged stilt or large plover | Dried salt crust near shoreline on saline mudflat | E Lagoon |
| Fig. *4.2.4.* 11C | Footprints (long-legged waders) | Wading bird footprints | Medium-sized, unwebbed four-toed footprints (but hallux not impressed in this example); nodes along digits clearly impressed; claw impressions prominent; digits straight and ~6 mm in diameter; total length ~6.5–7 cm excluding hallux; total width ~7 cm; digits directed forward or outward | Hallux not impressed | Little egret | Wet, muddy shoreline | SW Lagoon; (NW Lagoon) |
| Figs. *4.2.4.* 4F, 5A–D, 12A | Footprints (bovids) | Wildebeest footprints | Medium-sized hoof prints; hind foot total length ~8.5 cm; hind foot total width ~6.5 cm; tracks narrower at anterior than posterior; tips of hooves slightly pointed; outside margins slightly concave towards anterior; posterior margins of hooves rounded; medial gap straight and continues through track, widening slightly (< 1 cm) at back | Measurements made from perfect tracks in loose silt; morphology variable with substrate | Mammals (Bovidae); Blue wildebeest | Wet to soupy, channelized low gradient alluvial/delta-plain | NE Lagoon; SW Lagoon |
| Fig. *4.2.4.* 6B, 6C | Footprints (bovids) | Cattle footprints | Medium-sized, poorly impressed hoof prints in slightly indurated substrate; only anterior margins and outside margin impressed; overall shape circular; total width ~5 cm; total length ~6–7 cm; rounded anterior margin and tips of hooves; outside edge convex; medial gap straight were visible | Not clear if bovids salt pan and tracks only preserved in channel mud, or if preferentially visiting channels | Domestic cattle | Cemented muddy, organic rich ephemeral channel | Central lake |
| Figs. *4.2.4.* 3B, 3C, 8B | Footprints (bovids) | Goat footprints | Medium-sized hoof prints; total length ~4–5 cm; total width ~3–4 cm; front print narrower and more pointed than hind print; tips of front prints pointed; tips of hind prints blunt; splayed in wet clay; overall shape of hind print square; overall shape of front print triangular to heart-shaped | Tracks through crust into underlying mud appear as holes with sharp margins | Domestic goats | Salt crust covering soupy microbe-rich mud near relatively fresh water source | E Lagoon; NW Lagoon |
| Fig. *4.2.4.* 7G, 12B | Footprints (hyaenid) | Hyaena footprints | Medium-sized four-toed canid-like footprints; small interdigital space; digit pads large and crowded; metatarsal pad large and circular, with one anterior lobe and broad, rounded single-lobed posterior margin; claws not impressed; total length ~7–7.5 cm; total width ~5.5 cm | | Mammals (Hyaenidae); probably Spotted hyaena | Saline mudflat and dry lake-margin silt | SW Lagoon; E Lagoon |

Simple horizontal trails of insect larvae (ephydrid fly larvae?) were observed near the shoreline in very shallow water with an organic detritus substrate (Fig. *4.2.4.*1B). Also present in this shallow subaqueous zone were the shallowly impressed footprints of shorebirds (probably stilts) into a sandy substrate that was covered with yellow-green-coloured bacterial colonies that filled the footprint depressions. Associated with the shorebird trackways were their semi-circular feeding traces formed as they presumably swung their bills back and forth on the sediment surface while slowly walking (Fig. *4.2.4.*1C, 1D). Other feeding signs of shorebirds included the distinct, crescent-shaped bill probe marks, which were present in pairs or in groups up to approximately ten (Fig. *4.2.4.*1G, 1H).

Domestic goats trampled the salt-encrusted shorelines near the spring pools and outflow channels, and shorebirds and flamingos trampled and fed from the muddy substrates within the lagoon (Figs. *4.2.4.*1E, 1F, 2A–D). Exposed, trampled surfaces were covered by sodium carbonate crusts (Fig. *4.2.4.*2A–D). The morphology of flamingo footprints and trampled surfaces was extremely variable depending on the substrate and its subsequent preservational history (e.g., exposure, growth of microbial mat). Flamingo nest-mounds and their associated raised surfaces near the shoreline appeared to have been built when water levels were slightly higher (Fig. *4.2.4.*2E–G), and were burrowed by the vertical, open, and pellet-filled burrows of beetles (likely tiger beetles) (Fig. *4.2.4.*2H, 2I). In the middle of the lagoon, about 100 m from the shoreline, Greater and Lesser flamingos were observed feeding in shallow water (~30 cm depth), and a few large, old nest mounds protruded above the present water level.

*4.2.4.2. Northwest (NW) Lagoon 2*— This site, where some animal traces were observed and photographed was along the eastern margin of the northern NW Lagoon (Fig. *4.2.4.*3), flanks the more central part of the eastern NW Lagoon where bedded trona and organic-rich mud was observed in 2007 (Fig. *3.2.*7). The lagoon floods during the rainy season, and the very shallow water (~10–15 cm depth) covering the cemented crusts below supports cyanobacterial blooms. Several bird species visit the lagoon during these times, including Great White pelicans, African spoonbills, Yellow-billed storks, Little egrets, and flamingos (identified from photos courtesy of R. Renaut, taken in July 2006). During the drier seasons (e.g., August, 2007), areas with narrow strips of water remain open adjacent to the fault scarps bounding the lagoon. There, pockets of sedges were abundant (at a spring vent?), and egrets (Little egret?) were observed within the vegetation. Very high densities of vertically oriented chironomid tube structures were observed just below the water/air interface amongst green, filamentous cyanobacteria (Fig. *4.2.4.*3E, 3F). Spiders were observed walking on this 'substrate' and small amounts of web lay across the water surface.

Subaerially exposed, drying, organic-rich mud was covered in a thin salt crust through which domestic goats produced punch-like oval-shaped footprints into the mud (Fig. *4.2.4.*3A–C). Large spider burrows with large, circular piles of excavated material and web covering the burrow entrances were observed (Fig. *4.2.4.*3D). Several types of dead insects covered the crusted mud, but no other animal traces were present. The adult carcasses of very large beetles (~4 cm body length: probably either Carabidae or Tenebrionidae), small beetles (~1 cm body length: ?Scarabidae), wasps (~2.5 cm body length), and medium-sized orthopterans (~3 cm body length: grasshoppers or locusts: Family Acrididae) were photographed.

*4.2.4.3. Northeast (NE) Lagoon*— The NE Lagoon is the alluvial plain north of the central lake and was observed from just east of Nasikie Engida (Fig. *4.2.4.*4). Fresh water flows slowly along the base of the western scarp that separates the Lake Magadi Basin from Nasikie Engida and in small, shallow channels on the western side of the plain (Figs. *4.2.4.*4A, 5A, 5B). The

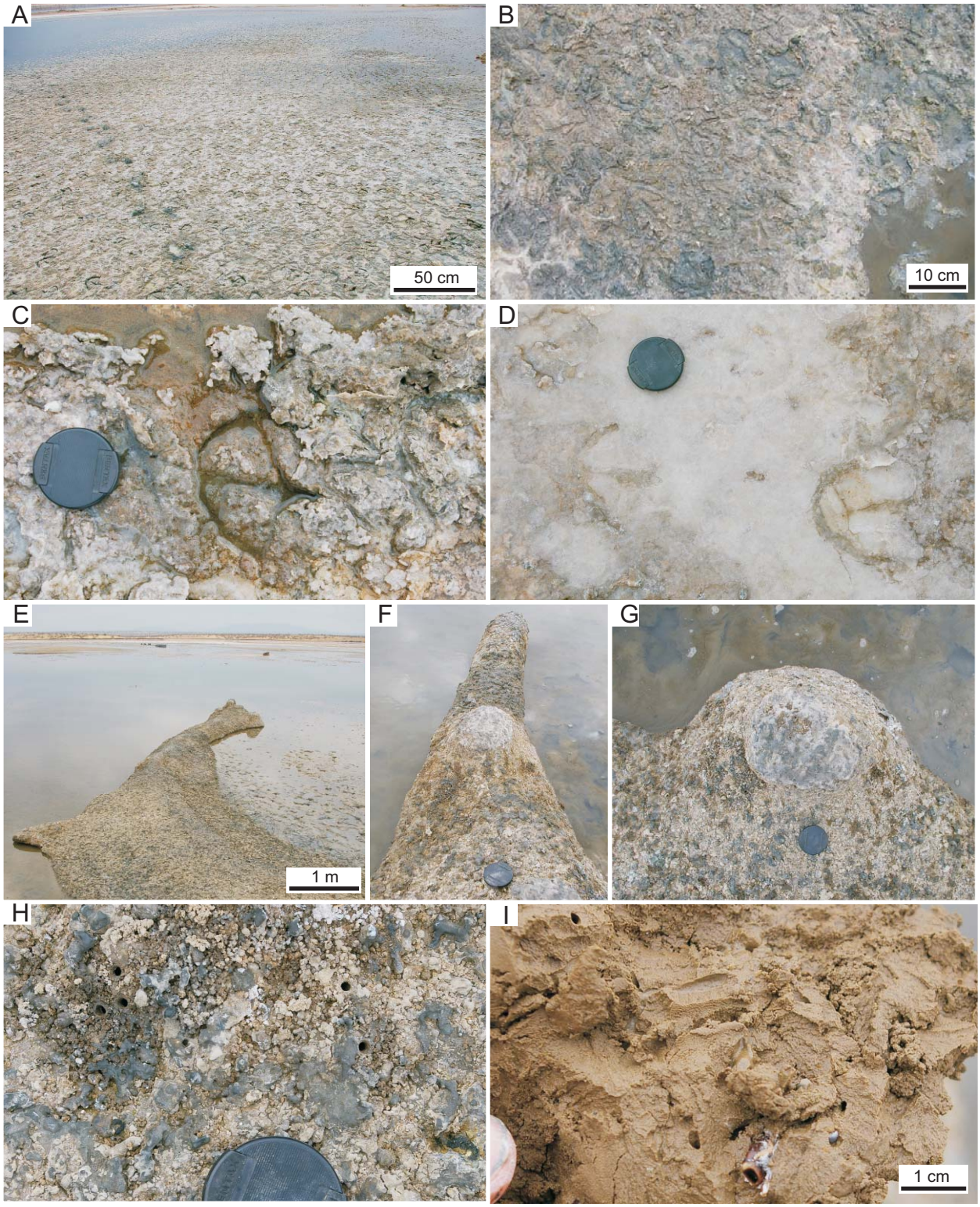


**Fig. 4.2.4.2.** Modern animal traces at the NW Lagoon (west), Lake Magadi. **(A–D)** Flamingo-trampled, salt-encrusted wet, cohesive muds. Tracks in (D) probably produced after salts precipitated. **(E–G)** Modern, degraded, flamingo nest mounds and associated surface above present water levels. **(H–I)** Open insect burrows in nest-mound surface, probably produced by tiger beeltes. Note pupal case (lower centre) and pellet-filled pupal chamber (right) in (I).

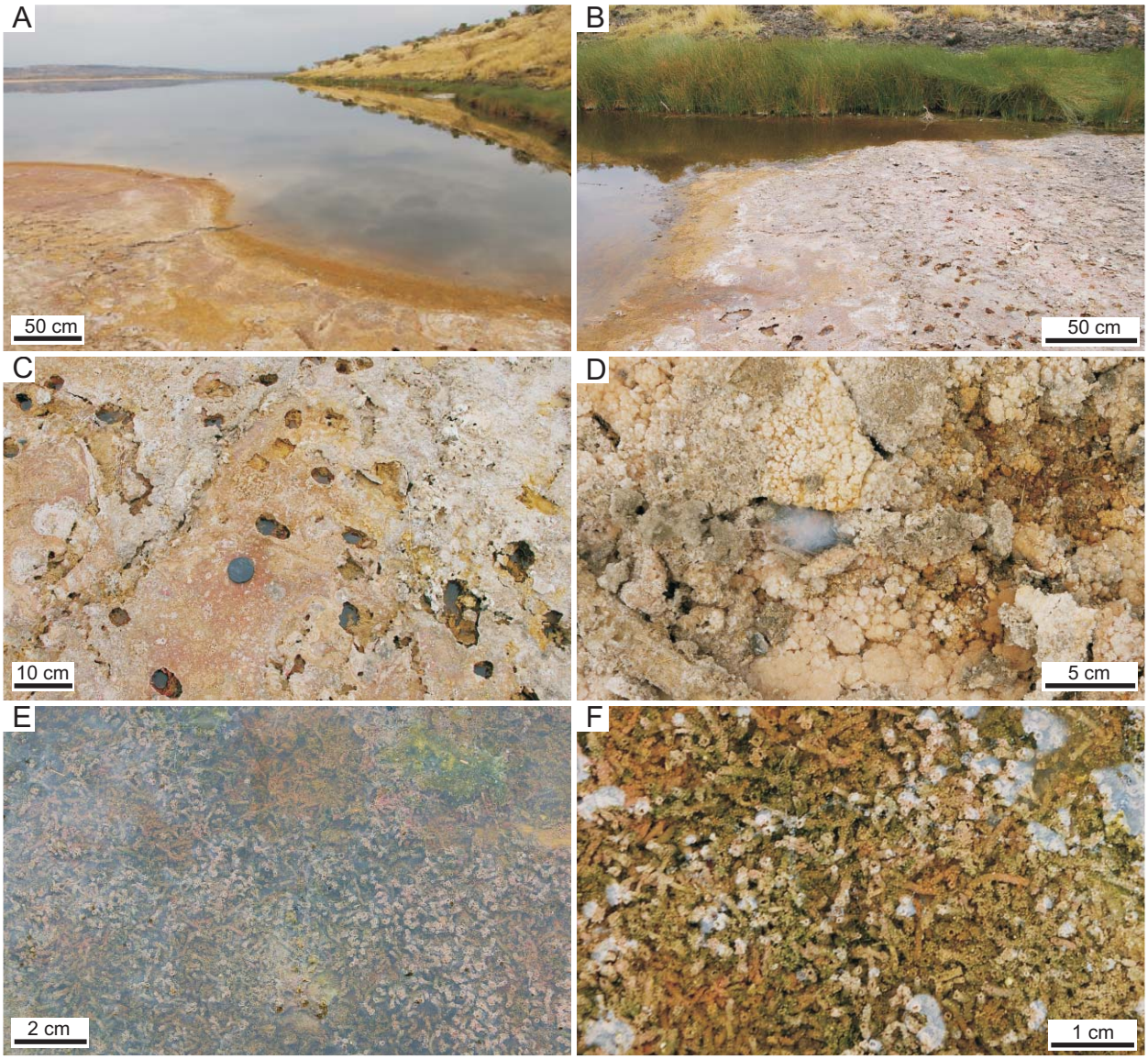


**Fig. 4.2.4.3.** Modern animal traces at the NW Lagoon (east), Lake Magadi. **(A)** Salt-encrusted mudflat at the eastern margin of the NW Lagoon. **(B)** Vertebrate-trampled mudflat. Note sedges in background growing in relatively fresh water. **(C)** Vertebrate tracks (goats?) "punched" through salt crust. Lens cap for scale in centre ~5 cm. **(D)** Spider burrow in salt crust with web covering burrow entrance. **(E–F)** Thousands of chironomid larval tube- structures.

faulted escarpment is very steep and abuts sharply with the floor of the plain. Coarse sand is present in a narrow strip along the escarpment, but quickly grades into silts of the alluvial plain. No plants were observed except grasses that covered the escarpment. Strandlines of dipteran pupal cases (ephydrid and chironomid?) coated the sandy shoreline and adult flies (ephydrids and possibly chironomids) were abundant (Fig. *4.2.4.*4C, 4D). In very shallow water along the escarpment, simple, small horizontal trails (~2–3 mm diameter), assigned to Incipient *Helminthoidichnites* isp. and attributed to ephydrid larvae were abundant in detritus and microbial mats that coated the sandy shoreline (Fig. *4.2.4.*4C–E). The margins of the trails were not smooth in many examples and showed irregular and regular markings that may be due to the movement of the larvae by ventral prolegs with well-developed claws, which characterize ephydrid larvae in flowing water habitats with microbial substrates (Simpson, 1979).

In slightly deeper water (~15 cm), indistinct, deep impressions of bird footprints (flamingos) produced in soupy mud were abundant (Fig. *4.2.4.*4A–B). A Black-winged stilt was observed within one of the small channels near the escarpment, and likely produced some of the prints in the soupy substrate (Fig. *4.2.4.*5B). Blue wildebeest trackways were numerous, and crossed the plain from west to east in August of 2007 and 2008 (Figs. *4.2.4.*4F, 5A–D). The morphology of their footprints was extremely variable as they crossed in and out of the channels and depended on the saturation and grain size of the substrate. Wildebeest were observed standing together on the open plain. Human footprints were also observed along the muddy edge of the most quickly flowing channel along the escarpment (Fig. *4.2.4.*5D).

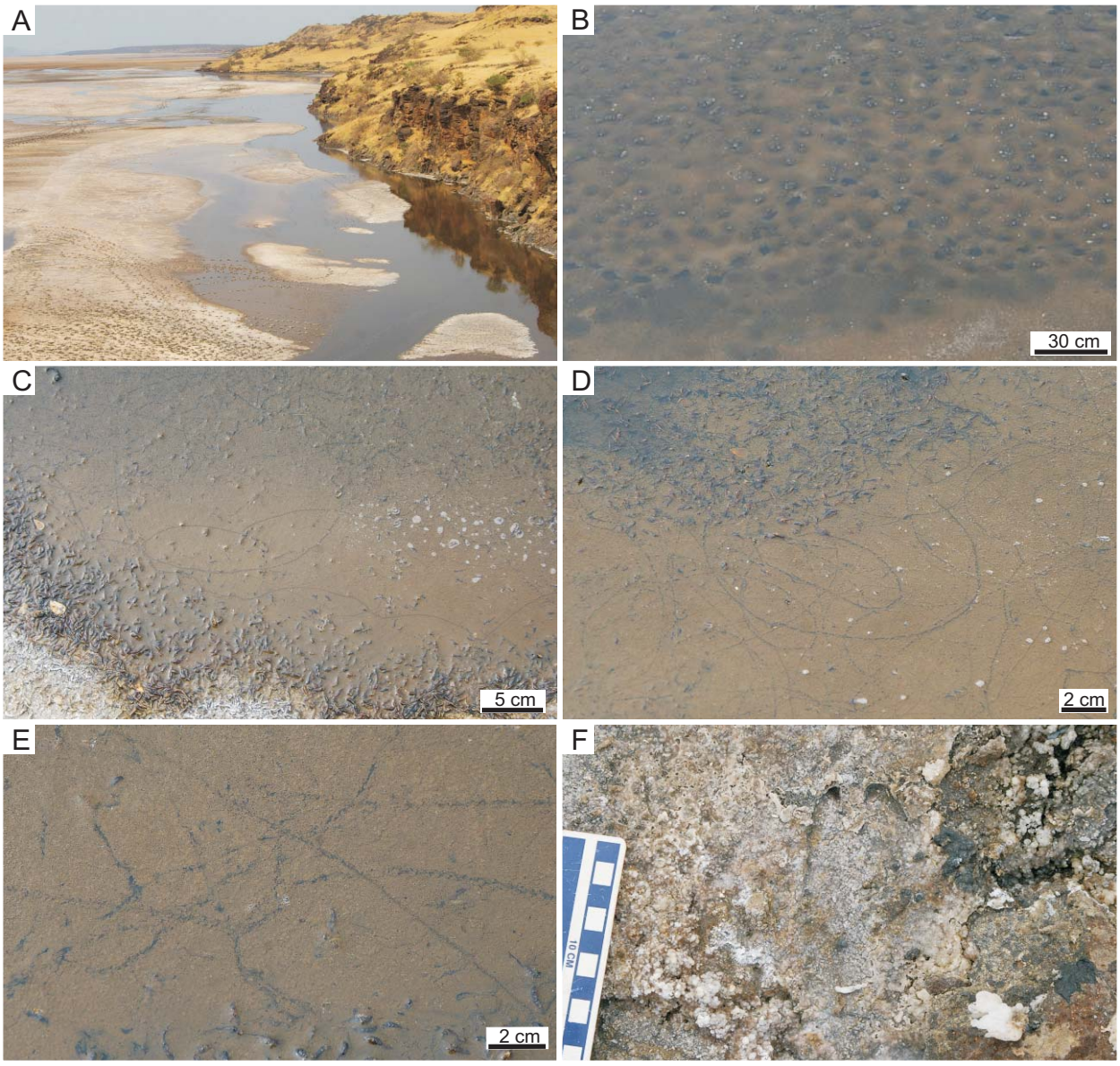


**Fig. 4.2.4.4.** Modern animal traces at the NE Lagoon, Lake Magadi. **(A)** Numerous vertebrate trackways (wildebeest) crossing the NE Lagoon form west to east. **(B)** Vertebrate-trampled shallow subaqueous muds, probably produced by wildebeest and possibly birds. **(C–E)** Straight to curving trails produced in shallow subaqueous cohesive substrate. Trails cross-cut one another, self-cross (in D, Incipient *Gordia*), and show sharp turns. Note that the trail margins are irregular, possibly from appendage markings of ephydrid fly larvae. **(F)** Shallowly impressed wildebeest footprint (centre) in salt crust at margin of NE Lagoon.

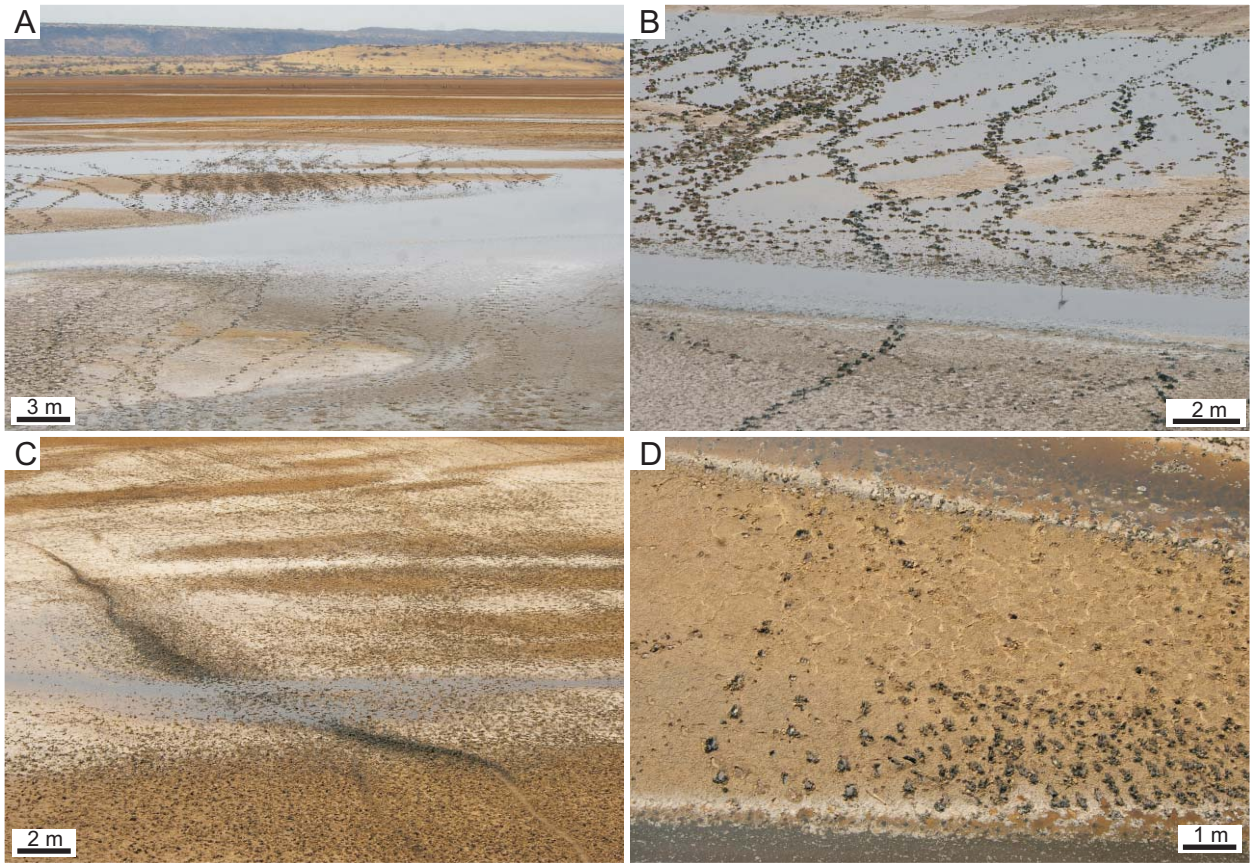


**Fig. 4.2.4.5.** Wildebeest trackways crossing the NE Lagoon, Lake Magadi. **(A)** Trackways oriented from west to east. Note how morphology changes depending on weather they were produced in shallow water **(B)**, drier alluvial plain sediments **(C)**, or through wet, salt-encrusted muds **(D)**.

*4.2.4.4.* *Central Lake (Saline Pan)*— The central lake pan was visited only during the dry season, when bedded coarsely crystalline sodium carbonate evaporites had precipitated from the brine that had previously covered the pan. Along the western margin of the central lake basin, the bedded salts were nearly dry at the surface, no live animals were observed either moving on them or burrowing into them, and no plants were observed. However, vertebrate footprints were found approximately 100 m from the lake margin within black, cemented mud of an ephemeral channel that remained just slightly moist, but was indurated at the surface (Fig. *4.2.4.*6A). The footprints were not well impressed into the substrate, but the tips of hooves and the outside margins cut through the cemented substrate (Fig. *4.2.4.*6B, 6C). They are attributed to medium-sized bovids, probably domestic cattle. Many carcasses of large insects (e.g., dragonflies, grasshoppers) were concentrated near the ephemeral channels, and were found either laying on the surface or cemented within the blackish mud and trona.

*4.2.4.5.* *East (E) Lagoon*— The E Lagoon of Lake Magadi is eastward of the small horst that divides it from the central lake. The silts and sands of the High Magadi Beds are well exposed along the western margin of the E Lagoon, and they underlie the thin shoreline/mudflat sediments (~5–20 cm thickness) on the eastern margin. Modern sediments along the eastern shoreline were mainly silty black and brown fine- to medium-grained sands covered by thick crusts of coarsely crystalline sodium carbonate efflorescent salt crusts (Fig. *4.2.4.*7A). Small

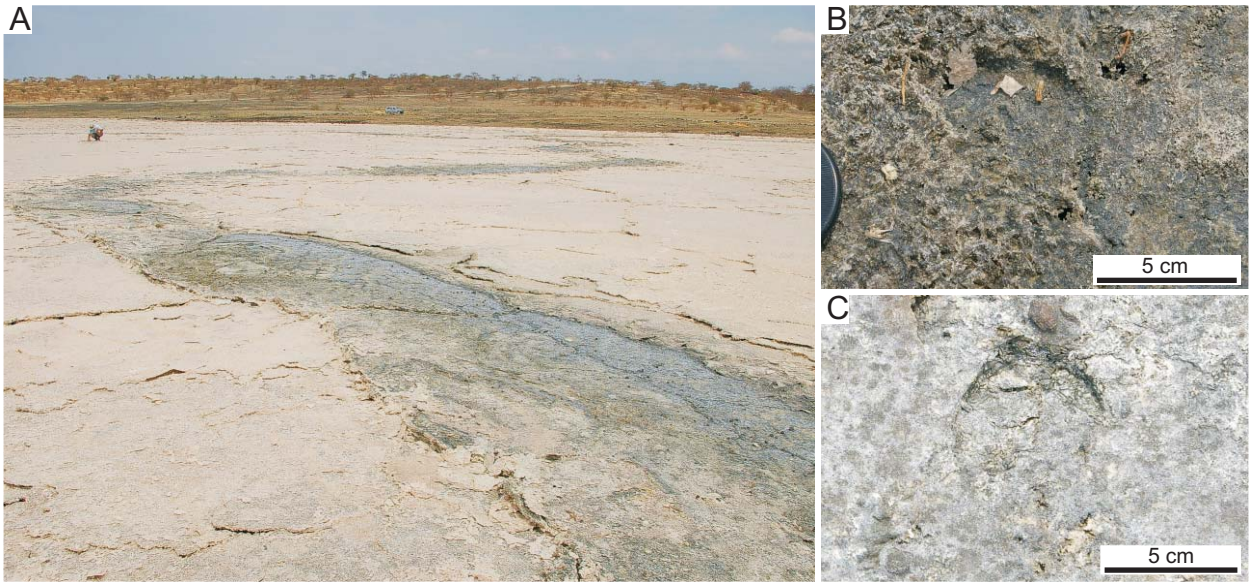


**Fig. 4.2.4.6.** Vertebrate tracks in the central saline pan, Lake Magadi. **(A)** Ephemeral? or excavated? channel through bedded evaporites. **(B–C)** Shallowly impressed bovid tracks in black muds of the channel shown in (A).

springs issued from the base of the scarp and clayey sediments were abundant in this area (Fig. *4.2.4.*8A). No vegetation was observed except grasses on the lake-bounding escarpment. Fossil degraded flamingo nests and associated structures preserved in the High Magadi Beds were exposed along the shoreline as small, rounded protuberances coated with very finely crystalline sodium carbonate salt crusts (Fig. *4.2.4.*9A, 9B). The timing of trace formation at this site could be observed as either "pre-salt crust" or "post-salt crust".

The first group of traces, the "pre-salt crust" traces, was produced mainly by the activities of flamingos. First, nest mounds of various sizes and states of degradation were observed (Fig. *4.2.4.*9A, 9B). Fresh nests showed typical features of flamingo nest-mounds, including: 1) large size (< 40 cm diameter at the base, < 25 cm diameter at the top, and < 20 cm high); 2) an external coating of sediment 'spit' onto the mound as porous clumps of mud; and 3) a central circular depression in the top surface up to 3–4 cm deep. Degraded, but apparently modern, nest mounds were abundant and much smaller and rounded (< 10 cm high, < 25 cm wide at the base) (Fig. *4.2.4.*7A). These degraded nests may represent the remaining internal cores of dense, compacted material as observed in modern nests at Lake Bogoria. Flamingo footprints and flamingo-trampled areas were everywhere along the shoreline (Figs. *4.2.4.*7D, 9E), with some Marabou stork trackways (Fig. *4.2.4.*7E). Additionally, very large circular depressions (< 75 cm diameter) interpreted as the feeding/trampling structures of flamingos (more likely Greater flamingos), formed part of this group (cf. Gallet, 1950, p. 39–40) (Fig. *4.2.4.*9C, 9D). The depressions were shallow (< 5 cm depth), had slight rims at their outside margins, and some had raised circular areas (< 30 cm diameter) in the centre of the depression. An alternative interpretation of these structures is that they are the beginnings of new nest mounds that were abandoned. All of these structures were then modified and covered by sodium carbonate efflorescence as the substrates dried. Small, irregular, soft-walled open burrows, presumably feeding burrows of insects (likely Diptera or Coleoptera), were produced below the salt crust (Fig. *4.2.4.*7B). It is unknown whether these burrows were produced prior to or after formation of the salt crust. A surface scraped nest mound of a bird, likely of a Black-winged stilt, was constructed from dried salt crust fragments and other clasts (Fig. *4.2.4.*9F).

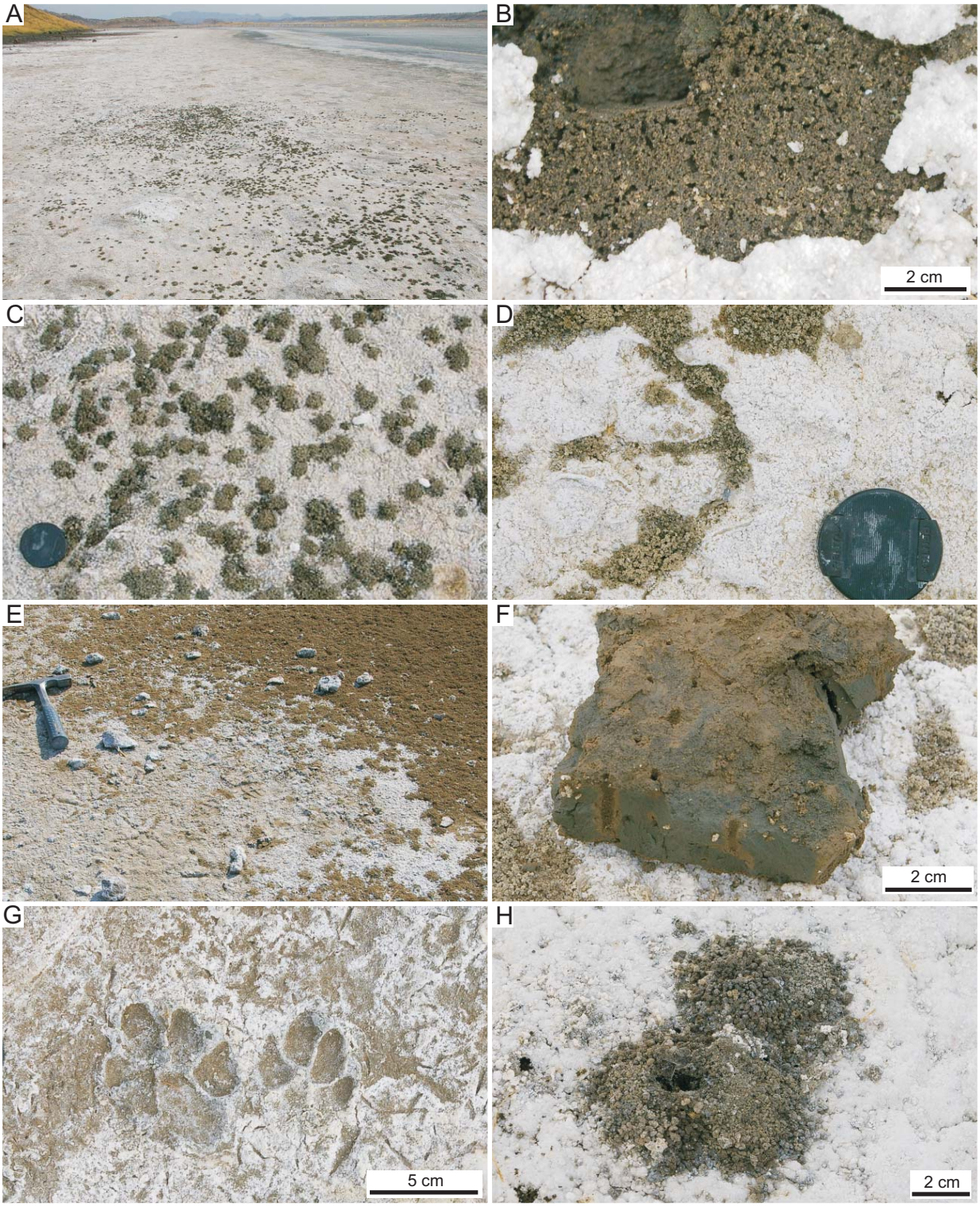


**Fig. 4.2.4.7.** Modern animal traces on the eastern margin of the E Lagoon, Lake Magadi. **(A)** The sandy mudflat at the E Lagoon, showing salt-encrusted surface with tumuli of excavated material from insect burrows. **(B)** Small open burrows beneath the salt crust, possibly produced by fly larvae. **(C)** Close-up of tumuli of sediment aggregates shown in (A). **(D)** Excavated material from insect burrow accumulating in flamingo footprint formed prior to the development of the salt efflorescence. **(E)** Marabou stork trackway (lower left) produced before salt crust and excavated material from insect burrows at top. **(F)** Vertical burrows in sandy mud substrate showing oxygenation of grey sediment. **(G)** Hyaena tracks produced in muddy substrate prior to salts. **(H)** Large open burrows of spiders.

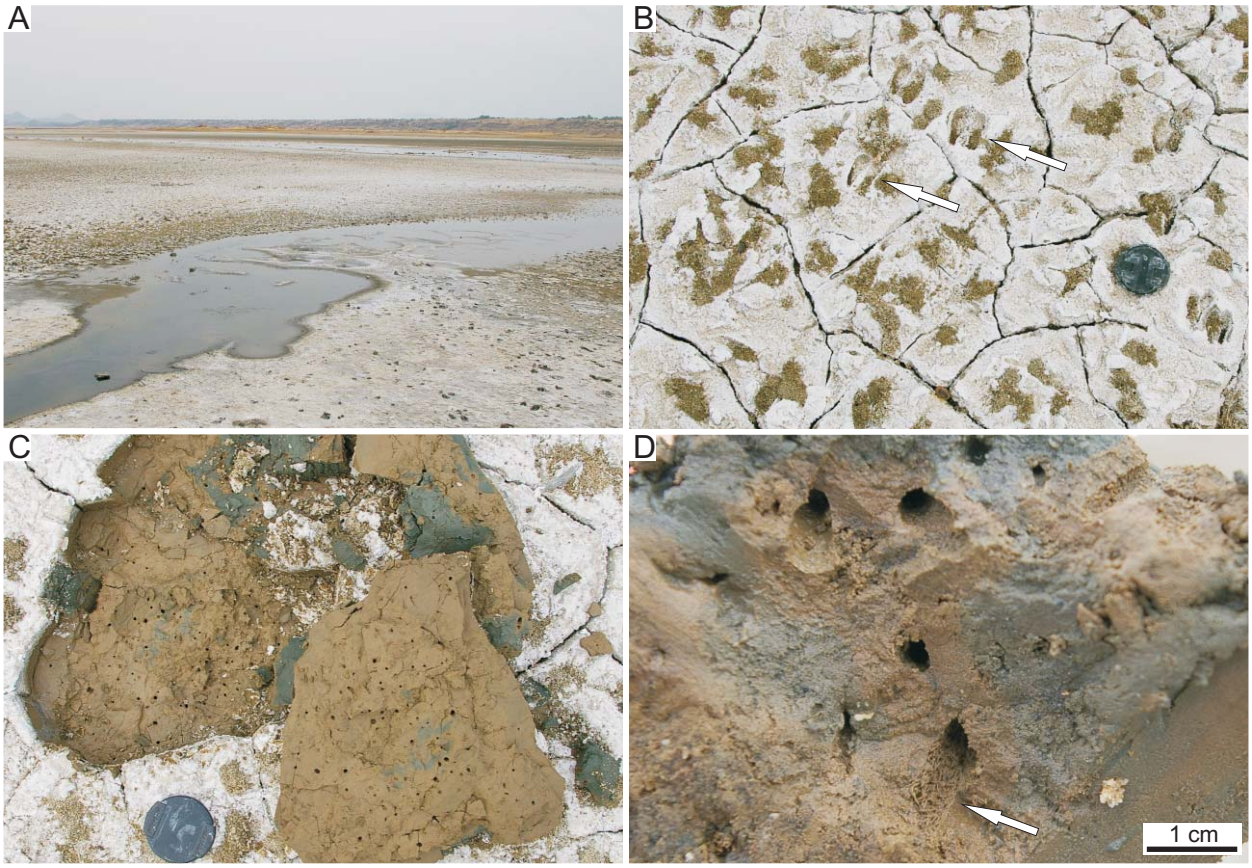


**Fig. 4.2.4.8.** Modern animal traces on the eastern margin of the E Lagoon, Lake Magadi. **(A)** Site of cool-spring outflow on to mudflat. **(B)** Vertebrate tracks (goats; arrows), desiccation cracks, and excavated material in clay-rich sediment. **(C–D)** Vertical burrows of several sizes produced by beetles (tiger beetles? staphylinids? carabids?). Close-up in (D) shows elongate pellet-fill in some examples (arrow).

Following the formation of the salt efflorescence and partial drying, the mudflat sediments were bioturbated by beetles and spiders and visited by mammals (Fig. *4.2.4.*7). The footprints of hyaenas, domestic goats, and domestic cattle were produced on the drying substrate (Figs. *4.2.4.*7G, 8B). Dense concentrations of the vertical burrows of beetles were present everywhere along the shoreline (Fig. *4.2.4.*7A, 7C, 7E). Sub-spherical aggregates of excavated material formed tumuli at the burrow openings, completely covered the salt crusts in some places, and were transported as clasts into depressions on the flats, including flamingo footprints (Fig. *4.2.4.*7D). Most of these short (< 5 cm depth), vertical and slightly oblique, open and pellet-filled burrows were attributed to staphylinid beetles (Figs. *4.2.4.*7F, 8C, 8D). An adult staphylinid was photographed in association with the burrows, and the elongate pellet-fill of the burrows was also associated with staphylinids at the southern Loburu Delta at Lake Bogoria. Other small vertical burrows may have been produced by tiger beetles although none were observed. Larger vertical burrows with large piles of excavated material and web were attributed to spiders (Fig. *4.2.4.*7H). Where exposed, the well indurated High Magadi Beds have apparently not been burrowed into by these trace makers.

*4.2.4.6. South (S) Lagoon*— The S Lagoon is a spring-fed lagoon at the southern end of the central basin. Several types of wading birds including Yellow-billed stork, Lesser flamingos, Greater flamingos, Little egret, and Black-winged Stilt were observed in the shallow water (Fig.


**Fig. 4.2.4.9.** Modern bird traces on the eastern margin of the E Lagoon, Lake Magadi. **(A–B)** Freshly made flamingo nest mounds. Note central depression in mounds in (B). Lens cap for scale in (B) is ~5 cm. **(C–D)** Large circular depressions with central mound, produced either by feeding activities of greater flamingos, or by the incipient building of nest mounds. **(E)** Flamingo trampled substrate with subsequent salt efflorescence. **(F)** Mound-like bird nest of gravel-sized clasts and salt-crust chips. Probably produced by a black-winged stilt.

*4.2.4.*10). Spring water flows towards the central lake in very shallow, flat channels through silty sediment (Fig. *4.2.4.*11A). Along the eastern margin of the lagoon, black and dark brown coarse sand and gravel form the shoreline near Bird Rock. Red, green, and orange cyanobacterial mats coated the sandy substrates where the springs emptied onto the lake plain. Dipteran adults and pupal cases were abundant around the mats, but no horizontal trails of their larvae were observed at this site. Flamingo footprints, Little egret footprints, and shorebird footprints were observed in the muddy sand along the shoreline (Fig. *4.2.4.*11B, 11C). Small holes in the substrate appear to have been made as probe marks of the shorebirds and/or egrets (Fig. *4.2.4.*11C, 11D). The

**Fig. 4.2.4.10.** Wading birds near "Bird Rock", S Lagoon, Lake Magadi. Water depth is ~5–10 cm (in August, 2007). Several species of wading birds are present: yellow-billed storks, black-winged stilts, little egrets (all in foreground), and lesser and greater flamingos (background).

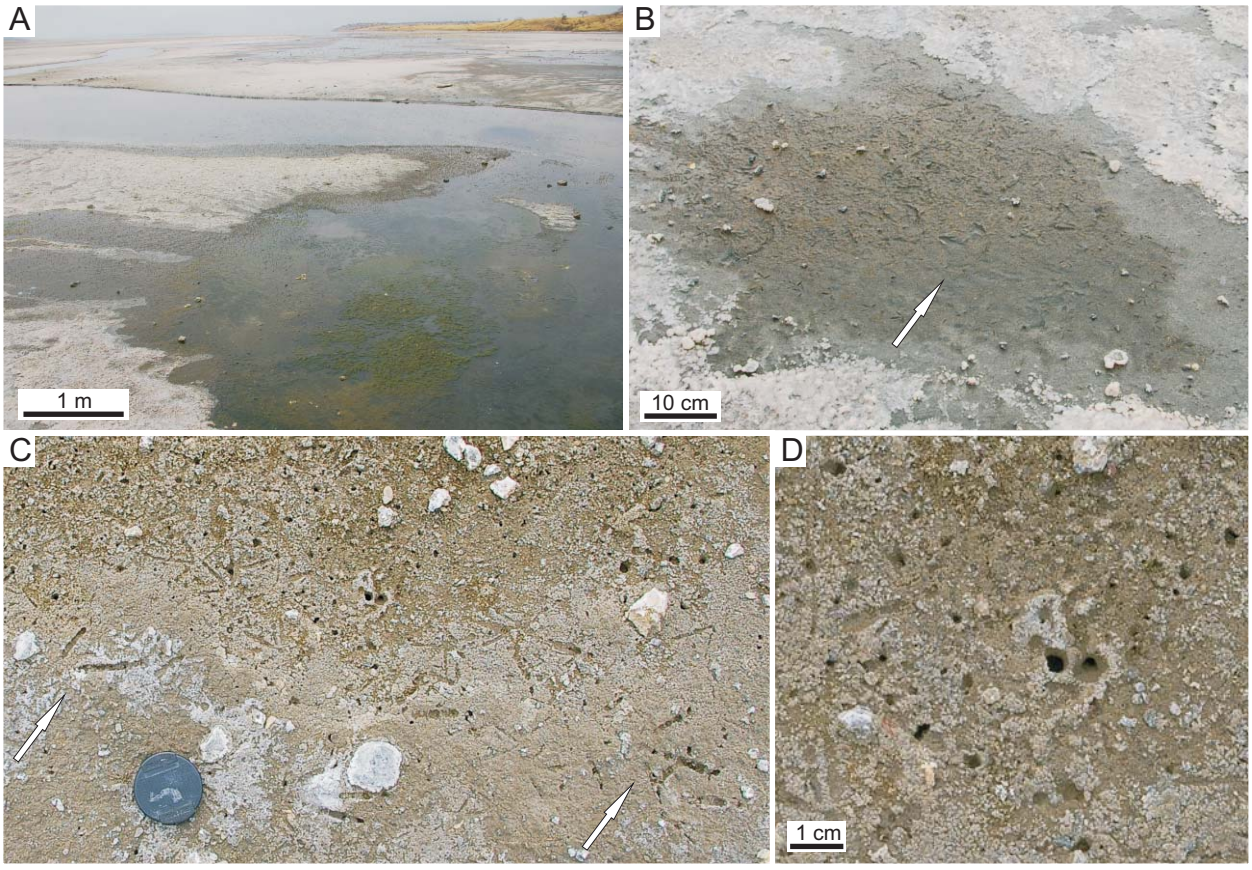


**Fig. 4.2.4.11.** Modern animal traces near "Bird Rock" at the S Lagoon, Lake Magadi. **(A)** Very shallow, partly spring-fed channel on the alluvial plain. **(B)** Bird tracks in wet substrate. Arrow is pointing to a flamingo track. **(C–D)** Bird tracks (probably lesser egret; arrows) and numerous holes at water's edge. Open holes are a mix of burrow openings and the probe-marks of feeding birds (close-up in D).

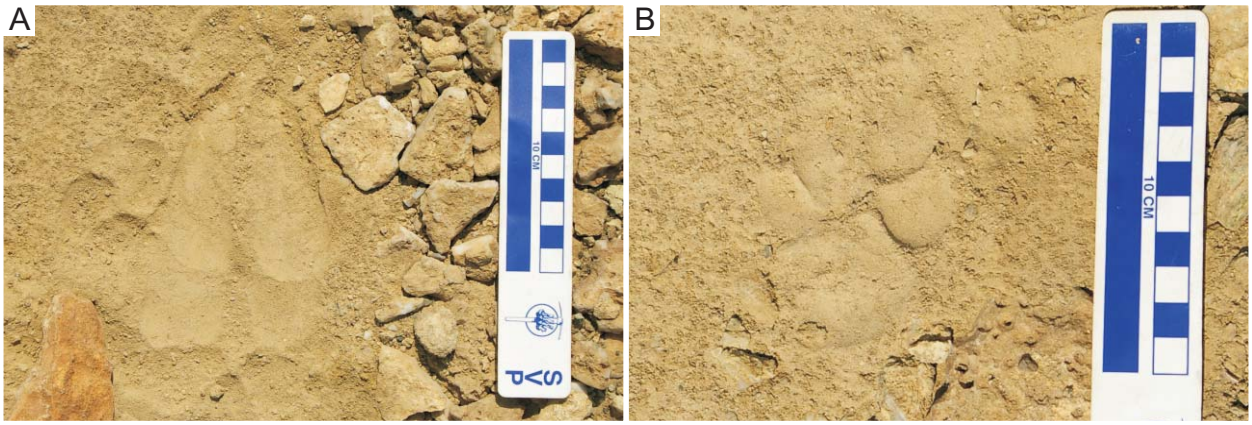


**Fig. 4.2.4.12.** (Below) Modern vertebrate tracks east of the S Lagoon, Lake Magadi. **(A)** Wildebeest tracks (double register) in soft, dry silt. **(B)** Hyaena track in soft, dry silt.

subaerially exposed bars between channels were trampled by bird footprints. Footprints of wildebeests and hyaenas were observed in the higher, dry areas near the springs at the S Lagoon (Fig. *4.2.4.*12). Zebras were seen towards the lake on dry substrates.

### *4.2.5. Modern Animal Traces around Nasikie Engida*

Modern animal traces were investigated at the hot springs near the northwest shoreline of Nasikie Engida. The southern mudflat was briefly visited. Along the horst between the NW Lagoon of Lake Magadi and Nasikie Engida, a dead termite mound of a Macrotermitinae colony that showed some internal structures was photographed. The trace types are described in Table 4.10.

*4.2.5.1. Northern Hot Springs and Northwestern Shoreline*— The hot springs north of Nasikie Engida are the hottest in the Magadi area (B.F. Jones et al., 1977) and provide the main input of water to the lake (Fig. *4.2.5.*1). The spring water temperature and flow volume remains relatively constant, so that the site and its subenvironments are relatively perennial when compared to the more seasonal and ephemeral subenvironments around Lake Magadi. The greatest diversity of animal traces at any site investigated in the Magadi–Nasikie Engida area was observed here (e.g., Fig. *4.2.5.*2). Most of the traces were observed along the edges of the hot water pools and channels, on subaerial, wet cyanobacterial mats, and on the very finely crystalline sodium carbonate (and opaline silica?) crusts (Figs. *4.2.5.*1, 3). In coarse sandy substrates along the shoreline just east of the hot spring outflow channels, simple, subaqueous, horizontal trails (Fig. *4.2.5.*4) were observed and more terrestrial trace types were observed in subaerial substrates (Fig. *4.2.5.*5).

Thousands of small "pock marks", interpreted as the feeding pits of dipteran larvae and adults (Ephydridae; possibly soldier fly Stratiomyidae larvae), covered the green and orange-coloured cyanobacterial mats at the mat/sediment/air interface (Fig. *4.2.5.*1D–G). They were < 2 mm deep, roughly circular to slightly oval-shaped, and ~3–4 mm in diameter. Both adult and larval ephydrid flies (e.g., *Scatella* spp.) adapted to hot spring environments feed on cyanobacterial mats (e.g., Wirth and Mathis, 1979). Adults graze on the mats by rasping, and larvae pull fragments of the mat with their specially adapted mouthparts (e.g., Simpson, 1979). An adult stratiomyid fly (Diptera) was also photographed on the mats, but their traces were not identified. These flies also feed on microbial mats and are abundant at hot spring sites in Yellowstone (Brues, 1924). Thousands of very small, white, elliptical eggs were embedded within the cyanobacterial mat.

**Table 4.10.** Modern animal traces observed at Nasikie Engida. Traces are grouped into suites following those at Lake Bogoria.

| Fig. | Trace type | Ichnotaxonomy | Description | Comments | Tracemaker | Environment | Locality |
|---|---|---|---|---|---|---|---|
| *Suite 1/3A – Chironomid/"Mermia-like" Suite* | | | | | | | |
| Fig. *4.2.5.* 4E, 4F | Chironomid tube structures | None available | Very small (~2 mm external diameter) tube structures constructed of organic detritus; < ~1 cm in length; concentrations of reworked tube structures oriented horizontally on organic detritus substrate; in situ tubes vertically oriented with open central holes of sub-millimetre diameter | Tube structures laying horizontally and loose on organic substrate, as well as vertical and in situ | Probably chironomids (Diptera) | Shallow subaqueous shoreline with detritus | NW shoreline near NW hot springs, Nasikie Engida |
| Fig. *4.2.5.* 4A–C | Surface trails | Incipient *Helminthoidichnites* isp. | Small (~2–3 mm diameter), straight to slightly curving, simple horizontal trails; may cross-over other trails, but do not branch | Dipteran pupal cases observed within trails | Diptera larvae (Stratiomyidae) and/or pupae (Ephydridae); also, water beetle larvae (e.g. Dytiscidae, Hydrophilidae) | Shallow subaqueous shoreline with detritus | NW shoreline near NW hot springs, Nasikie Engida |
| Fig. *4.2.5.* 1C | Surface trails | Incipient cf. *Archaeonassa* isp. (or Incipient *Helminthoidichnites* isp.) | Small, unbranched, straight to gently meandering or curving surface trails with slightly raised lateral ridges; internal diameter ~2 mm; external diameter ~4 mm; different trails cross-cut one another | Larvae observed tunneling in soupy mud, just below sediment-air/water interface | Insect larvae, likely beetles (Coleoptera) | Very shallow subaqueous littoral and hot spring effluent pool | NW hot springs |
| *Suite 3B? – Hot Spring Effluent/Microbial Mat Suite* | | | | | | | |
| Fig. *4.2.5.* 1D–G | 'Pock marks' (feeding pits) | None available; compare with plug-shaped burrows? | Small, circular to oval-shaped, shallow, open depressions in cyanobacterial mat; width ~2–3 mm; depth ~1–2 mm; margins of structure not sharp, and may be slightly raised surrounding depression | Feeding structures/pits of adult brine flies and possibly larvae | Brine flies (Insecta: Diptera: Ephydridae) (directly observed) | Wet, subaerial cyanobacterial mat in hot spring effluent channels | NW hot springs, Nasikie Engida |
| Fig. *4.2.5.* 1E | Bird probe marks | None available | Small, open vertical holes frequently in sets of two or as individual burrow openings; diameter ~3–4 mm; unlined/unwalled; roughly circular to oval-shaped holes | Could be confused with *Arenicolites* isp. or *Polykladichnus* isp. if only observed from above | Shorebirds (plovers) | Wet to soupy, subaerial cyanobacterial mat in hot spring effluent channels | NW hot springs, Nasikie Engida |

*Suite 4 – "Scoyenia-like" Suite*

| | | | | | | | |
|---|---|---|---|---|---|---|---|
| Fig. *4.2.5.* 8B | Vertical burrows | Incipient ? *Skolithos* isp. (observed from surface only) | Small-sized, open vertical burrows observed as irregular, circular holes through efflorescent crust; diameter ~4 mm | Compare with open holes in High Magadi Beds chert | Insects or arachnids | Drying, muddy substrate with salt crust on surface | SE shoreline mudflat, Nasikie Engida |
| Fig. *4.2.5.* 5B, 5C | 3D burrow networks | Indeterminate; cf. incipient *Planolites* isp. or cf. Incipient *Thalassinoides* isp. | 3D burrow system of earwig adults and nymphs; burrows open, unlined/unwalled; orientations vertical, horizontal, and oblique; in this example, burrows dominantly horizontal; variable diameters, but constant diameter along length of individual branches; larger branches (adult) ~8 mm diameter; smaller branches (nymphs) ~3–4 mm wide | Compare with branching open burrows in High Magadi Beds, SE Lagoon | Earwigs (Insecta: Dermaptera) (observed directly within burrows) | Wet, soft, sandy lake margin/shoreline near hot springs | NW shoreline, Nasikie Engida |
| Fig. *4.2.5.* 5B?, 6A | Open burrows | Indeterminate; ?Incipient *Planolites* isp. | Small, open burrows, mainly horizontally oriented; branching unknown; diameter ~2–3 mm | Not examined in detail | Small infaunal arthropods, including water mites | Wet, soft, sandy shoreline near hot springs | NW shoreline, Nasikie Engida |
| Fig. *4.2.5.* 3G | Bird footprints (plovers) | Shorebird footprints | Three-toed, medium-sized, unwebbed bird footprints; total length ~3.5–4 cm; total width ~6.5 cm; posterior margin triangular; digits straight and directed outwards | | Shorebirds, likely large-sized plover (e.g., Blacksmith plover) | Drying sodium carbonate crust on moist sandy gravel | NW shoreline, near hot springs at Nasikie Engida |
| Fig. *4.2.5.* 3F | Bird footprints (storks) | Stork footprints | Large, four-toed, unwebbed bird footprints with backward directed hallux (digit I); length of digit III ~8–9 cm; total length of footprints ~15 cm; total width ~12 cm; claws not observed | Digits look more gracile than Marabou stork | Storks or herons, possibly Yellow-billed Stork | Sodium evaporite crust substrate on moist sand | NW shoreline, near hot springs at Nasikie Engida |
| Fig. *4.2.5.* 3A | Bird footprints (geese) | Geese footprints | Large, three-toed, bird footprints with slightly triangular posterior margin and wide digits; webbing and claw impressions not observed; digit lengths similar; digits II and IV directed forward | Very similar footprints to flamingos | Egyptian goose (observed directly in area) | Subaerial, wet, muddy sand; drying with sodium evaporite crust | NW hot springs, Nasikie Engida |
| Fig. *4.2.5.* 3C, 3D | Mammal footprints (mongooses : Carnivora: Viverridae) | Mongoose footprints | Small, four-toed footprints with clear claw impressions; measurements and description from hind footprint: total length ~3.5 cm; length without claws ~2.8 cm; total width ~2 cm; four digits impressed, all directed forward and well separated; interdigital space large; metatarsal pad chevron-shaped; all digits anterior to metatarsal pad; width of metatarsal pad almost as wide as all digits together | Two dead mongooses were found in hot-spring channels; one banded mongoose because of long legs; other may be slender mongoose | Medium-sized mongoose, probably banded mongoose and/or slender mongoose | Moist, very finely crystalline, subaerial sodium carbonate crust | NW hot springs, Nasikie Engida |

| | | | | | | | |
|---|---|---|---|---|---|---|---|
| Fig. *4.2.5.* 3E | Mammal footprints (canid) | Dog footprints | Medium-sized, canid footprints with four oval-shaped, forward-directed digit impressions; digits II and V set back from digits III and IV; digits III and IV even at anterior edge; large space between metatarsal pad and digits III and IV in hind footprint; metatarsal pad with two lobes at posterior and one lobe anterior; claw impressions not observed; length of hind footprint ~7 cm, width ~5.5 cm | | Wild dog or medium- to large-sized domestic dog | Moist, very finely crystalline, subaerial sodium carbonate crust | NW hot springs, Nasikie Engida |
| Fig. *4.2.5.* 3C | Mammal footprints (bovids) | Small bovid footprints | Small-sized bovid footprints in moist, finely crystalline salt crust; anterior margin rounded but narrower than posterior margin; medial gap very narrow towards anterior, wider towards posterior but still narrow; length ~5–7 cm, width ~4–5 cm | | Small-sized bovid, possibly common duiker or domestic goat or sheep | Moist, very finely crystalline, subaerial sodium carbonate crust | NW hot springs, Nasikie Engida |
| Fig. *4.2.5.* 3B | Mammal footprints (bovids) | Large bovid footprints | Large bovid footprints in wet mud; impressions likely look larger due to soft, wet, muddy substrate; hooves rounded at anterior margin; large, sinuous medial gap between hooves; hind foot ~15 cm length and ~10 cm wide; front foot ~13 cm length and < 10 cm wide | | Large bovids, probably buffalo (possibly eland or sable) | Drying, muddy pool with microbial mat and salt crust | NW hot springs, Nasikie Engida |
| Fig. *4.2.5.* 3B | Mammal footprints (bovids) | Medium-sized bovid footprints | Medium sized bovid footprints in moist mud with salt crust; footprint very heart-shaped with wide, rounded posterior margins to hooves, and very pointy anterior margins; medial gap narrow, and complete from anterior to posterior, but wider towards anterior and posterior; front and hind not distinguished; length ~7 cm, width ~ 5.5 cm | Size may be slightly larger due to moist mud substrate | Medium-sized bovids (probably Grant's gazelle or impala) | Drying, muddy pool with microbial mat and salt crust | NW hot springs, Nasikie Engida; SW mudflat, Nasikie Engida |
| Fig. *4.2.5.* 6D, 6E | Funnel-shaped vertical burrows | Indeterminate; ? cf. plug-shaped burrow types | Large, shallow, funnel-shaped vertical burrows; width at surface < 5 cm; width at base ~ 1.5–2 cm; depth ~3 cm; one example is covered with web | Observed in groups > 10 | Spiders (Arachnida: wolf or funnel spiders) | Wet, coarse sandy shoreline near hot springs with salt efflorescence | NW shoreline, Nasikie Engida |
| Fig. *4.2.5.* 6H | ? Tapered vertical burrows | Indeterminate; incipient *Skolithos* isp. | Large, shallow, circular, vertical, open burrow with small amount of excavated material surrounding burrow, but not in tumulus; no web observed; diameter ~3 cm; appears to taper to rounded base at depth of 3–4 cm | Observed from surface only | Spiders (Arachnida: wolf or funnel spiders) | Wet, sandy shoreline near hot springs with salt efflorescence | NW shoreline, Nasikie Engida |

| | | | | | | | |
|---|---|---|---|---|---|---|---|
| Fig. *4.2.5.* 6F | Vertical burrows | Incipient ? *Skolithos* isp. (observed from surface only) | Large, circular, oblique, open burrow; length unknown, width ~3 cm; burrow opening surrounded by even, circular ring of pellet-like excavated material approximately 0.5 cm above the surface; spider web remnants around edges of burrow | | Spiders (web present around burrow opening) | Moist to wet, sandy shoreline near hot springs with salt efflorescence on surface | NW shoreline, Nasikie Engida |
| Fig. *4.2.5.* 6C | Vertical burrows | Incipient ? *Skolithos* isp. | Medium-sized, circular, open burrows without tumuli; diameter ~1 cm | Observed from surface only | Spiders or insects such as beetles | Moist to wet, sandy shoreline with salt efflorescence | NW shoreline, Nasikie Engida |
| Fig. *4.2.5.* 6B | Vertical burrows | Indeterminate | Large, slit-like or elliptical-shaped, oblique, open burrow; length unknown; width ~4 cm, height ~1.5 cm; tumulus not present in example, excavated material may have been incorporated into salt efflorescence; web present around burrow opening | May be earwig burrow reused by spider | Spiders (observed directly within burrow) | Moist to wet, sandy shoreline near hot springs with salt efflorescence on surface | NW shoreline, Nasikie Engida |
| *Suite 5 – Dry Substrate Suite – cf. "Termitichnus-like" Suite* | | | | | | | |
| Fig. *4.2.5.* 6G | ? 3D burrow network | Indeterminate (observed from surface only) | Large mounds of excavated, dry, pellet-like material; two adjacent cone-shaped mounds with one open, burrow (1 cm in diameter) in centre of depression in centre of mound; width of smaller mound ~10 cm, larger mound ~30 cm wide | Not excavated; only observed from surface | Probably ants | Slightly moist to dry, sandy lake-margin colluvium near hot springs | NW shoreline, Nasikie Engida |
| Fig. *4.2.5.* 9 | Termite nests and mounds | None available | Large, degraded, constructed mound around a shrub; ~2 m in height and 1.5 m in diameter; no chimney, but many large (~4–15 cm diameter), roughly circular to oval-shaped open, branching passages to outer mound (ventilation system); within 'passages' are open 'galleries' (~1 cm diameter); many horizontally oriented, flat to oval-shaped chambers (~4–6 cm wide and ~2–4 cm high towards outside of mound, separated by thin (~3–5 mm) 'plates' of fine-grained material; chamber walls/plates appear concentrically laminated; building materials include pellet-like sediment aggregates (~1–3 mm diameter) and dead termite exoskeletons; exterior of mound shows zones of concentrically laminated pellet-like material in some areas where old passages were filled | Some chambers very similar to fossil 3D burrow system in High Magadi Beds, south of Nasikie Engida | Termites (Insecta: Isoptera: Termitidae: Macrotermitinae) | Terrestrial soil on bedrock; well above lake level at margin of Nasikie Engida basin | East basin margin horst, Nasikie Engida |

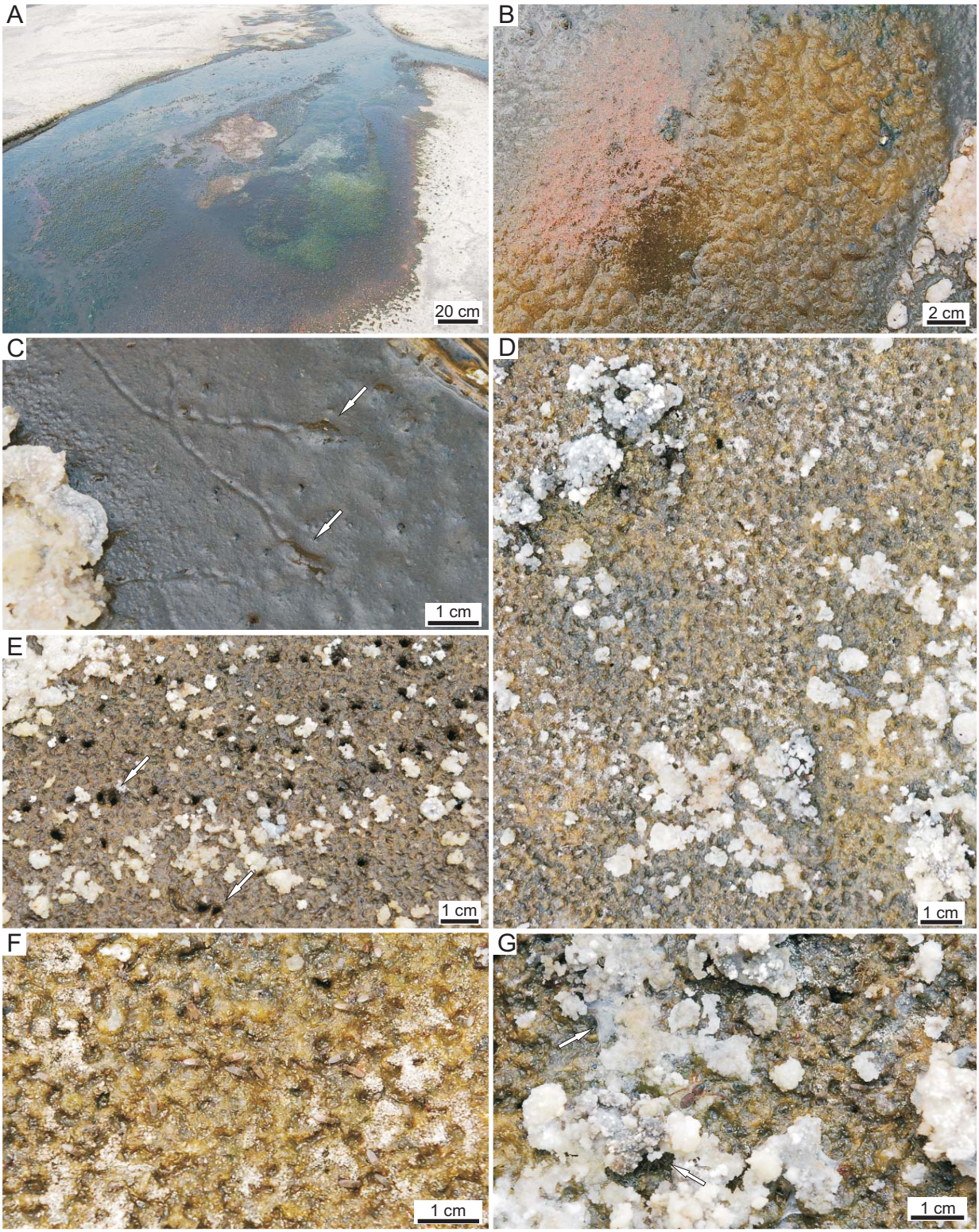


**Fig. 4.2.5.1.** Modern animal traces at the NW hot-spring site at Nasikie Engida. **(A)** Shallow hot-spring outflow channel with cyanobacterial mats on small subaerially exposed channel bars. **(B)** Close-up of orangish brown cyanobacterial mat and pinkish chironomid larvae? **(C)** Insect larvae (arrows; beetle?) producing straight to gently curving trails (Incipient *Archaeonassa*) in soupy mud. **(D–G)** "Pock-mark" traces on cyanobacterial mats. Note crescent-like possible bird probe-marks (arrows in E). Note dipteran (ephydrid) adults feeding on mat in (F) and spider webs on salt efflorescence in (G; top arrow). The lower arrow in (G) points to a spider beneath the salt crust.

Within the mats, several examples of deeper, vertical holes ~4 mm in diameter were recognized as the probe marks of shorebirds (compare with NW Lagoon 1) (Fig. *4.2.5.*1E), although some of these holes may be attributable to the shallow burrows of small spiders. Many species of spiders were observed on the mats, with webs spun on the newly forming salt crusts above the mats (Fig. *4.2.5.*1G). Wasps were also observed in this setting, and were apparently feeding on green cyanobacterial mats, but no traces were observed (Fig. *4.2.5.*2A). Simple horizontal trails of insect larvae (beetles or dipterans) with raised lateral ridges (cf. Incipient *Archaeonassa* isp.) were produced as the larvae tunneled just below the sediment/air interface in wet mud at the edges of very shallow hot spring pools (Fig. *4.2.5.*1C). Two dead mongooses (Viverridae; probably banded mongooses, possibly slender mongooses) were also found at the edges of the hot spring pools, along with dense concentrations of bright pink egg masses of chironomid flies that settled there (Fig. *4.2.5.*1B).


**Fig. 4.2.5.2.** Insects at the NW hot-spring site at Nasikie Engida. **(A)** Wasp feeding on cyanobacterial mat. **(B)** Dead adult beetles (probably a dysticid water beetle at left; scarabid dung beetle at right) on salt crust. **(C)** Dead snout beetle (Circulionidae) on salt crust. **(D)** Live tenebrionid beetle in dry sediments a few metres from the shoreline. **(E)** Large, dead scarabid beetle. **(F)** Leg parts of dead grasshoppers (Orthoptera, probably Acrididae).

Very finely crystalline sodium carbonate (and opaline silica?) crusts formed on subaerially exposed sandy and muddy substrates along the edges of the hot spring channel area (Fig. *4.2.5.*3). Many vertebrate tracks were produced on this substrate after precipitation of the crust. In wet muddy substrates, the tracks of Egyptian geese (Fig. *4.2.5.*3A) and a large bovid (buffalo, eland, or possibly sable) (Fig. *4.2.5.*3B) were observed. Also present were the footprints of mongooses (banded and/or slender) (Fig. *4.2.5.*3C, 3D), domestic goats (Fig., *4.2.5.*3C), and canids (either Wild dog or domestic dog) (Fig. *4.2.5.*3E). The tracks of a medium-sized bovid (Grant's gazelle?) (Fig. *4.2.5.*3B), a stork (probably Yellow-billed stork) (Fig. *4.2.5.*3F), and a shorebird (Fig. *4.2.5.*3G) were impressed into desiccating substrates with more

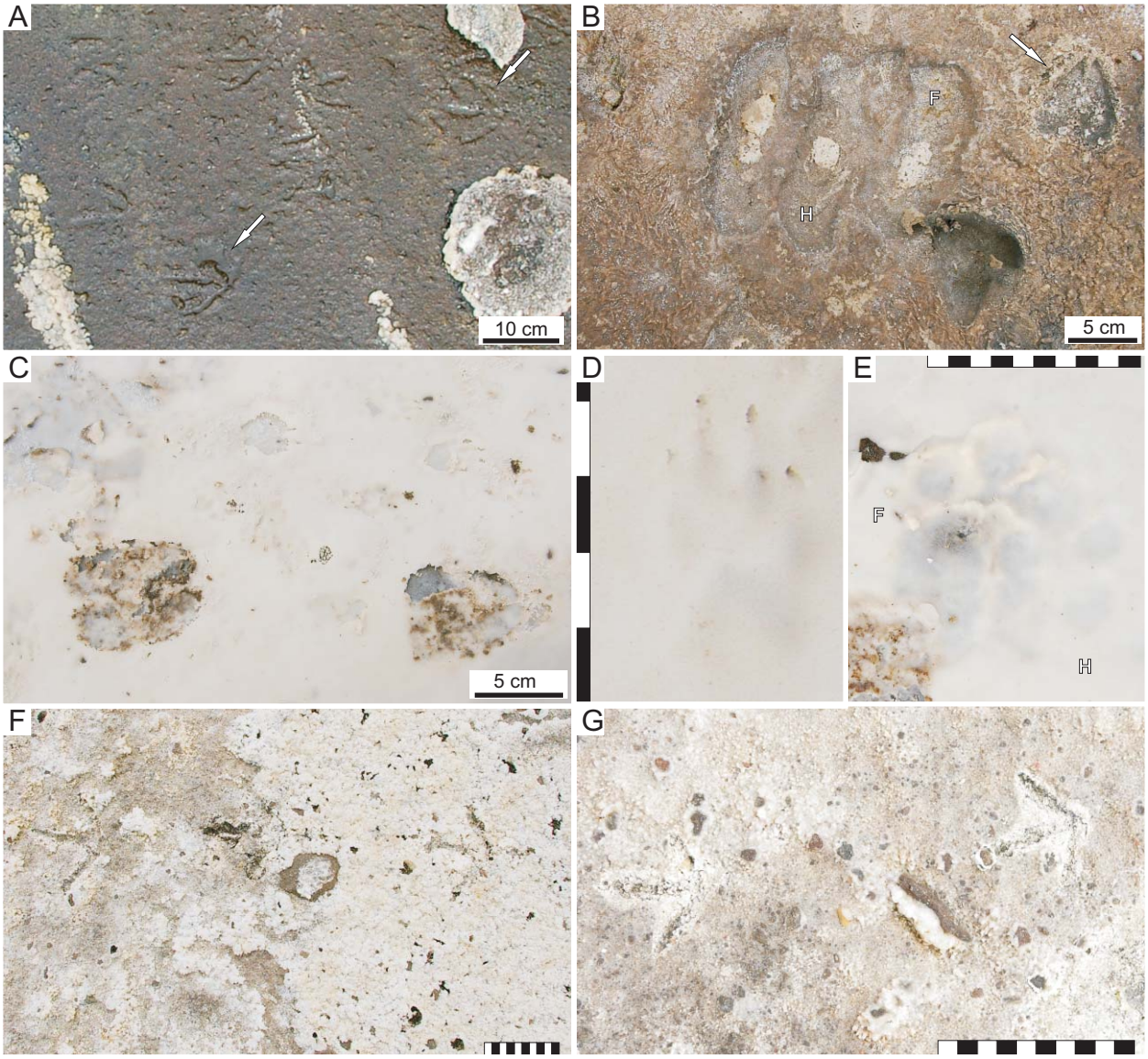


**Fig. 4.2.5.3.** Vertebrate tracks at the NW hot-spring site at Nasikie Engida. **(A)** Webbed bird tracks (arrows point to best examples). **(B)** Large bovid front (F) and hind (H) tracks at centre produced in subaqueous substrate and smaller bovid tracks (arrow) produced after subaerial exposure. **(C)** Goat tracks (bottom) and mongoose (top) trackway produced on finely crystalline salt efflorescence (with opaline silica?). **(D)** Close up of shallowly impressed mongoose footprint. Note claw impressions at tips of digits. **(E)** Canid tracks produced in wet finely crystalline salt/silica effloresence. **(F–G)** Bird tracks produced in drying salt crust. Tracks in (F) possibly of a yellow-billed stork. Shorebird tracks in (G).

coarsely crystalline sodium carbonate crusts. During the visit to the area in August, 2007, Lesser and Greater flamingos, Egyptian geese, Yellow-billed stork, pelicans, Black-winged stilt, Blacksmith plover, Cattle egrets, Hammerkop, an unidentified dark-coloured shorebird, and Grey-headed gulls were observed in this area.

Just eastward of the hot spring outflow delta area, simple horizontal trails in very shallow water were observed in subaqueous organic detritus substrates (Incipient *Helminthoidichnites* isp.) (Fig. *4.2.5.*4A–C). Some of the pupal cases of ephydrid flies were within the trails, suggesting that the trails may be made by mobile pupae. In a few cases, insect larvae (possibly

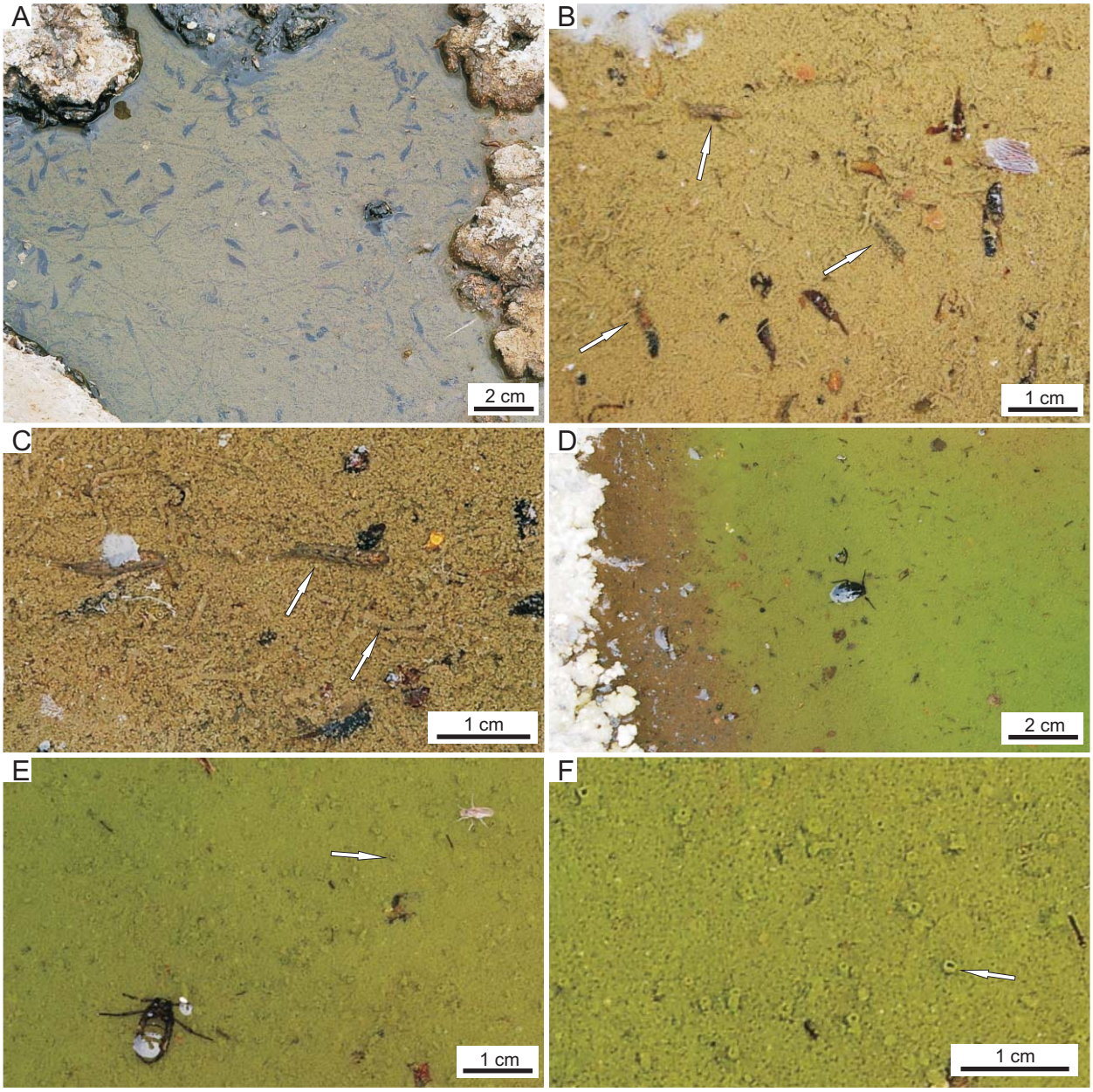


**Fig. 4.2.5.4.** Modern insect traces at the NW shoreline of Nasikie Engida. **(A–C)** Pupal cases and trails of dipteran larvae in shallow subaqueous substrate of organic detritus. Arrows in (B) point to larvae making the trails. Note that two larvae are using the same trail in (B). Arrows in (C) showing larvae (top arrow; stratiomyid?) and chironomid larval tube-structure (lower arrow). **(D–F)** Adult water beetle and *in situ* chironomid tube-structures (arrows in E and F).

either Diptera: Stratiomyidae or Coleoptera: Dysticidae or Hydrophilidae) were observed directly within their simple, horizontal trails, and appeared to be following one another and reusing the same trail (Fig. *4.2.5.*4B, 4C). Thousands of apparently reworked, horizontally oriented, loose tube structures of chironomid larvae built from the organic detritus partly formed the substrate through which the larger larvae were feeding along trails. In a nearby area along the shoreline with bright green cyanobacteria- and/or green algal-coated substrates, hundreds of in situ, vertically oriented, open tubes of the chironomid larvae were observed in a clear-water, shallow, subaqueous setting (Fig. *4.2.5.*4D–F). Adult water beetles (Coleoptera: Dysticidae and/or Hydrophilidae?) swam in the shallow water (Fig. *4.2.5.*4D, 4E).

The traces of earwigs and spiders were abundant in wet, loose, subaerially exposed sandy substrates with thin salt efflorescent crusts along the shoreline (Figs. *4.2.5.*5). Adult earwigs (probably *Labidura* sp.), eggs, and nymphs were observed within their burrow networks in close association with spiders, red water mites (Arachnida: Hydracarina), and an unidentified dipteran? larvae. The burrow systems consisted of branching, unlined/unwalled burrows of different diameters (adults: ~7 mm and nymphs: ~4 mm) in various orientations, but were dominantly horizontal. The burrow diameters were consistent along their lengths, with smaller burrows typically branching from larger burrows. No fill was observed within the burrows in these

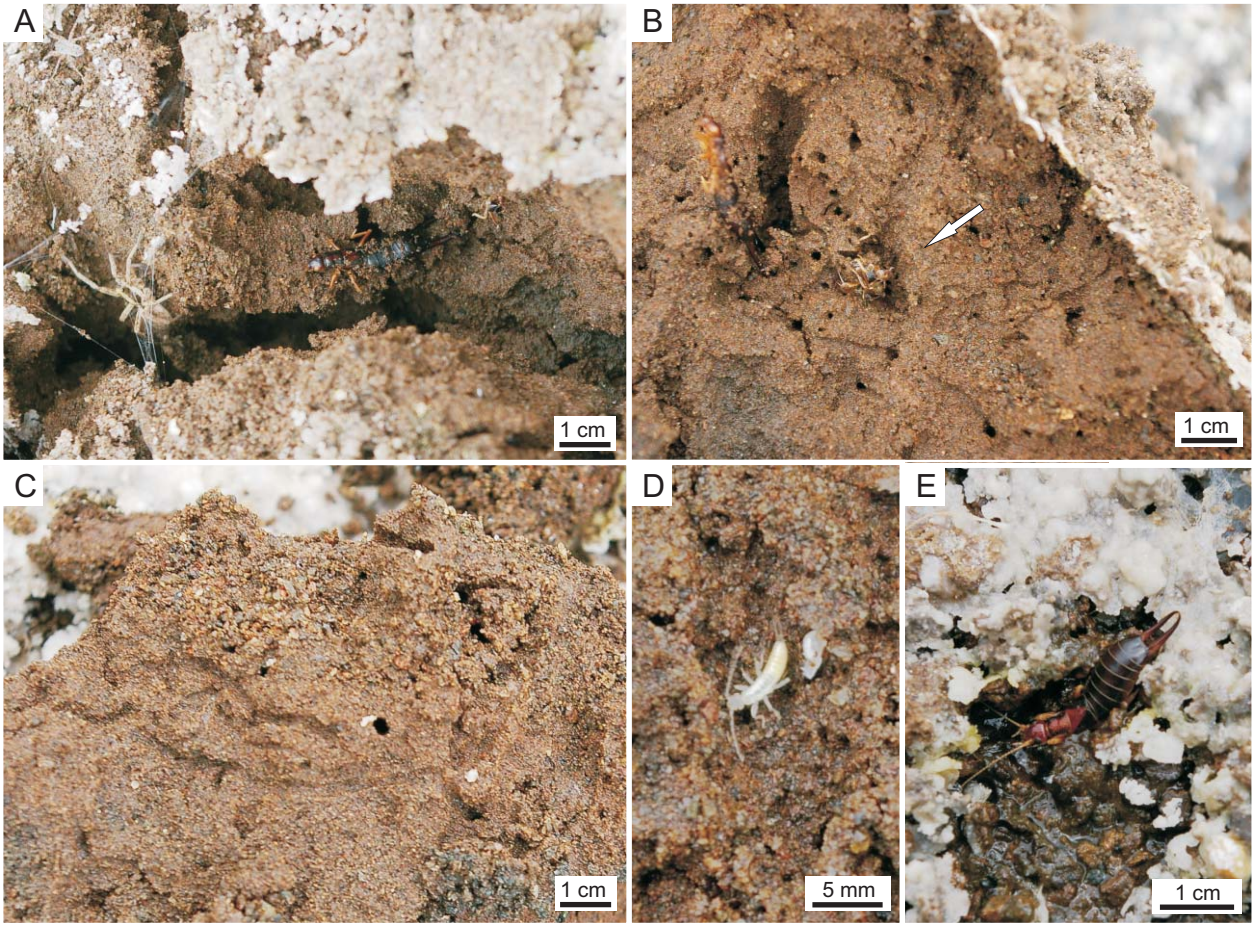


**Fig. 4.2.5.5.** Earwig traces in soft substrate at the NW shoreline of Nasikie Engida. **(A)** Photograph showing adult earwig (centre) and spider (left), both living within the wet, sandy shoreline substrate. **(B)** Earwig nest showing adult burrow (larger, left) and smaller burrows of the nymphs (arrow is pointing to a group of nymphs). **(C)** Horizontally oriented branched burrows of earwigs produced within the bed. **(D)** Close-up of earwig nymph. **(E)** Close-up of adult female earwig.

examples. Some of the smaller burrows (< 3 mm) may by attributable also to mites (Fig. *4.2.5.*5B, 6A).

Burrows attributed to spiders were typically large, oblique, open, unlined/unwalled, and roughly circular or oval (Fig. *4.2.5.*6C–F), although one example observed was slit-like in cross-section (Figs. *4.2.5.*6B). Burrow diameters were approximately 1.5–3 cm at their openings with sometimes large, circular piles of sub-spherical pellet-like excavated material around the burrow openings. The depths of the burrows is unknown, except for several examples of shallow, funnel-shaped burrows < 5 cm deep and < 5 cm across at the widest, uppermost part of the funnel (Fig. *4.2.5.*6E). The larger burrows (2–3 cm diameter) were found in concentrations of several burrows within ~1 $m^2$ in drier, sandy substrates along the lake margin (Fig. *4.2.5.*6D). Large mounds of dry, excavated material (< 30 cm diameter) were also found further from the shoreline and were attributed to ants (Fig. *4.2.5.*6G), which were observed directly. Several dead carcasses

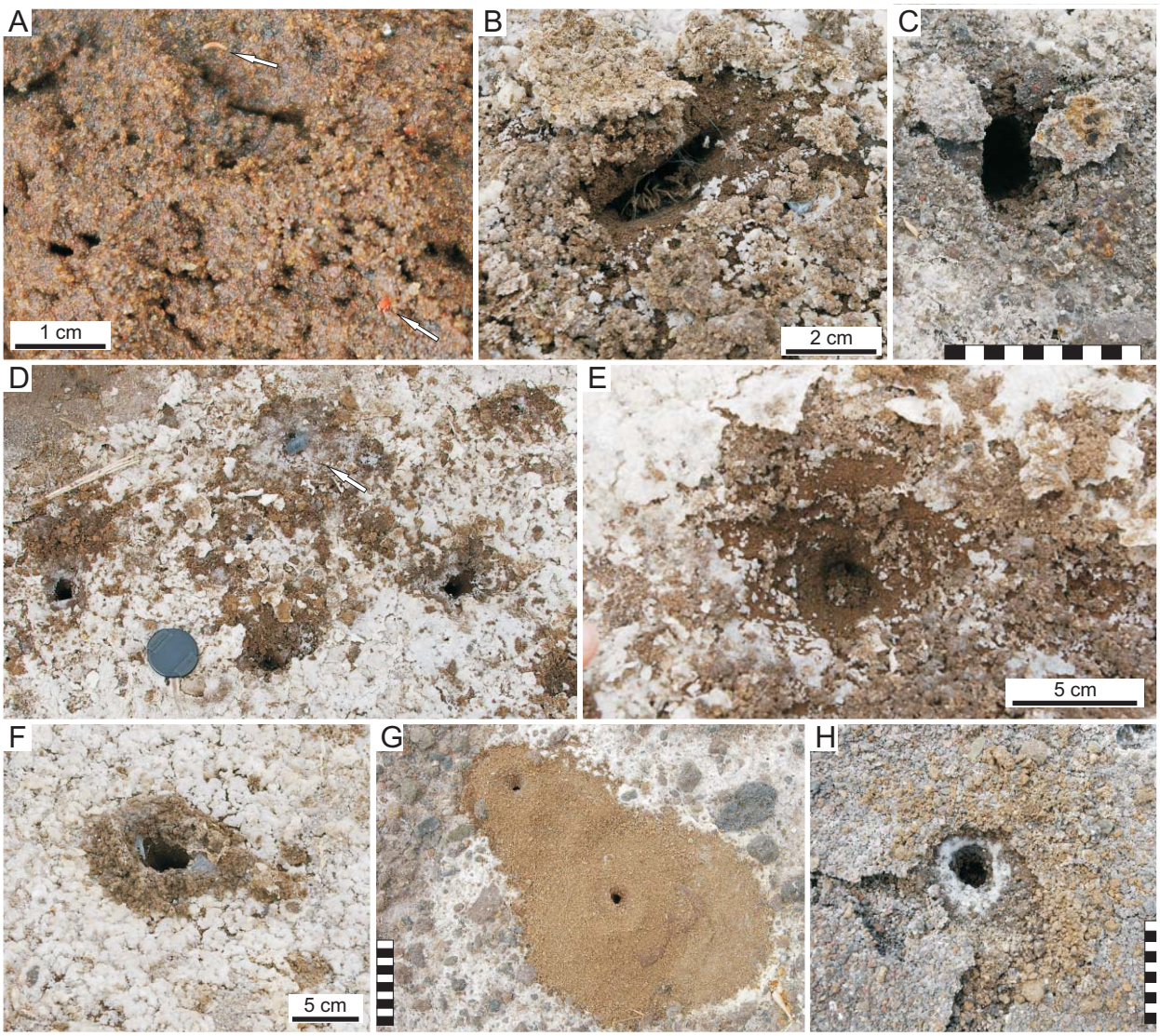


**Fig. 4.2.5.6.** Modern arthropod burrows at the NW shoreline of Nasikie Engida. **(A)** Top arrow pointing to unknown insect larvae or possibly an oligochaete. Lower arrow pointing to a mite (Acarina). **(B)** Slit-like spider burrow with spider. **(C)** Oval-shaped oblique burrow of spider. **(D)** Group of spider burrows. Note burrow opening covered by web (arrow). **(E)** Shallow, funnel-shaped burrow of spider. **(F)** Circular burrow of spider with web around opening. **(G)** Excavated material and openings of an ant nest. **(H)** Circular open burrow of a beetle or spider.

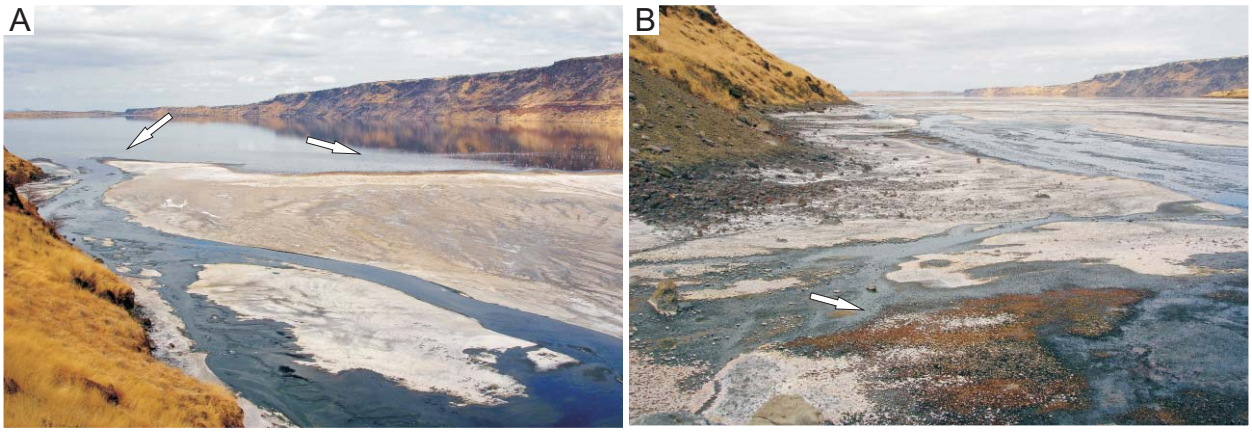


**Fig. 4.2.5.7.** Modern environments at the NE alluvial plain at Nasikie Engida. Photographs shown in (A) and (B) courtesy of R.Renaut. **(A)** Flamingos and other birds (arrows) along shoreline of NE alluvial plain. **(B)** Microbial mats near shallow channels, probably bioturbated by ephydrid flies.

of insects lying on salt crusts were photographed along the lake margin, including: large dung beetles (Scarabidae) (Fig. *4.2.5.*2F), a smaller scarabid (Fig., *4.2.5.*2B), grasshoppers/locusts (Orthoptera: probably Acrididae) (Fig. *4.2.5.*2E), a weevil (Coleoptera: Ciculionidae) (Fig. *4.2.5.*2C), and a water beetle (?Dysticidae) (Fig. *4.2.5.*2B). An alive tenebrionid beetle (Tenebrionidae: ?Tentyriinae: *Zophosis* sp.) was observed on dry sandy gravel substrates near the steep-sided shoreline east of the hot springs area (Fig. *4.2.5.*2D).

*4.2.5.2. Northeastern Delta Plain*— The northeastern delta plain at Nasikie Engida was only very briefly investigated. A gravel plain with very shallow, broad channels fed by hot spring outflow, the facies observed there were similar to the northwestern outflow plain described above (Fig. *4.2.5.*7). Noteworthy observations include the abundant footprints of birds and domestic goats in salt-encrusted sandy gravel and wet, soft muddy sand substrates. Sandy gravel channel margins coated by green and orange cyanobacterial mats were covered by adult dipterans (probably ephydrids), and presumably also contained their pock mark feeding pits, although they were not directly observed at this locality (Fig. *4.2.5.*7B).

*4.2.5.3. Southern Mudflats*— Brief investigation of the southern mudflats at Nasikie Engida showed a mix of sandy gravel fan deposits adjacent to salt-encrusted organic-rich black lacustrine muds at the SW mudflat in 2006 (photos courtesy of R.Renaut) (Fig. *4.2.5.*8). At the southeastern shoreline in 2007, soupy black and red-coloured organic lacustrine mud covered with sodium carbonate crusts contained irregular masses of siliceous gels (Fig. *4.2.5.*8A–D). Animal traces in these substrates included abundant mammal tracks (bovids; SW flats) (Fig. *4.2.5.*8E, 8F) and roughly circular to oval-shaped holes through salt crusts (SE flats) (Fig. *4.2.5.*8B). Earwigs and tenebrionid beetles were observed under and on the salt crust. The vertical 'burrows' are thus likely best attributed to earwigs or beetles, but may also have been produced by spiders based on observations at the NW shoreline of Nasikie Engida. This facies and trace fossil association may be comparable to the nodular chert facies of the Green Beds south of Lake Magadi.

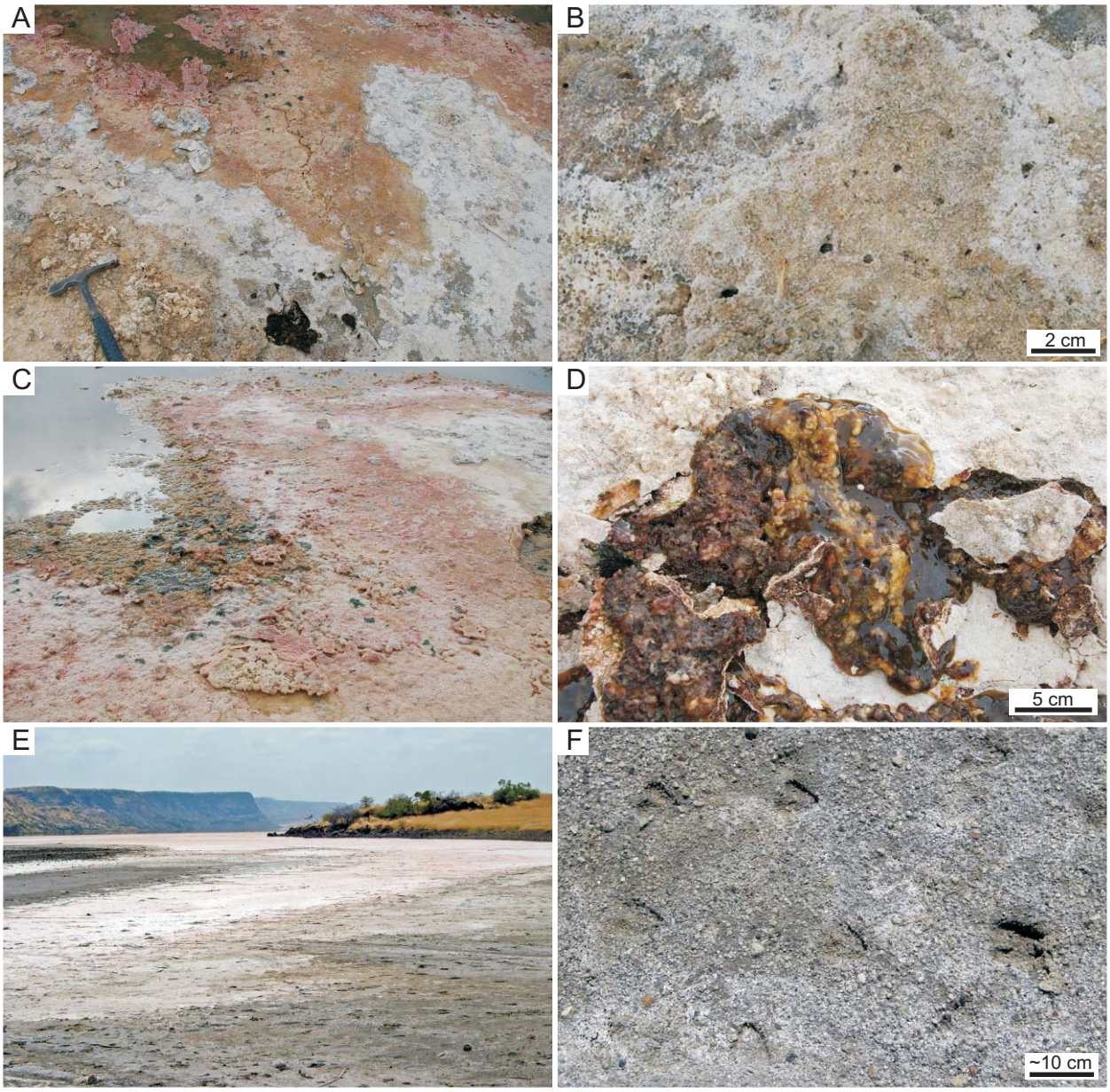


**Fig. 4.2.5.8.** Modern animal traces at the southern mudflats at Nasikie Engida. Photographs shown in (E) and (F) courtesy of R.Renaut. **(A–D)** Salt encrusted flats of the SE shoreline at Nasikie Engida. Note open burrow holes in (B) and whitish siliceous gels in (D). **(E–F)** Vertebrate footprints on sandy substrates of the SW mudflat.

*4.2.5.4. Terrestrial "Basin Margin"*— The lake margin of Nasikie Engida is generally steep and consists of volcanic bedrock, colluvium, and reworked gravel- to cobble-sized clasts along shorelines. Above the level of typical lake-level rise, thin soils have developed on the bedrock or colluvium. Animal traces in this terrestrial zone were not investigated, but they are likely produced by dung beetles, other beetles, ants, and possibly wasps and bees. Additionally, the large mounds of fungus-growing termites (e.g., Macrotermitinae) are a conspicuous feature on the dominantly grassy, savannah landscape (Fig. *4.2.5.*9A). Several observations were made of a degraded termite mound from a "basin margin" terrestrial site on the westward-dipping ridge that separates Nasikie Engida from the NW Lagoon of Lake Magadi.

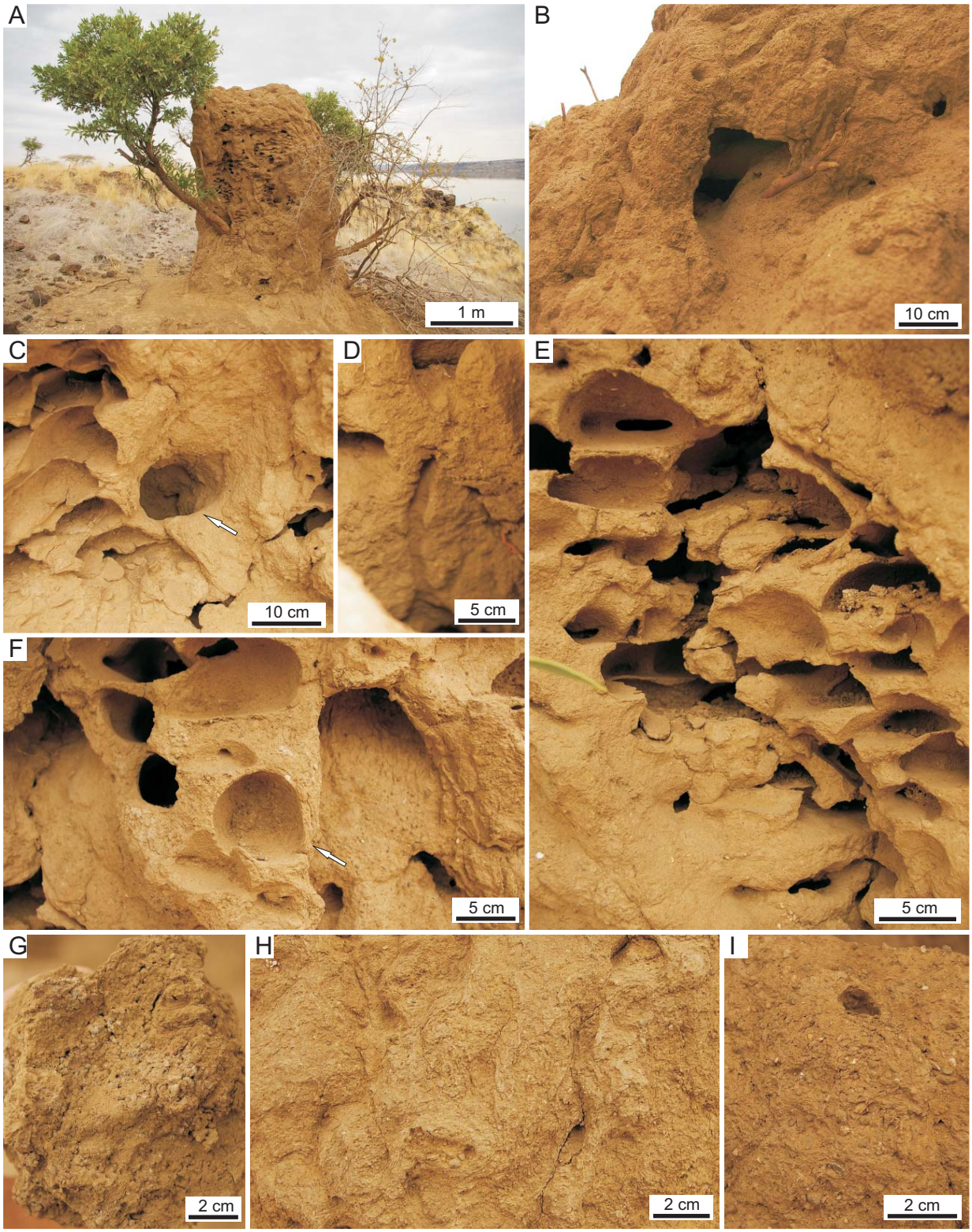


**Fig. 4.2.5.9.** Internal structures of an abandoned termite (Macrotermitinae) mound at Nasikie Engida. **(A)** Broken mound on shallow soils of horst between Nasikie Engida and Lake Magadi. **(B–C)** Ventilation pipes exiting mound (arrow in C). **(D)** Small tunnel along pipe shown in (C). **(E–F)** Fungus gardens and chambers of internal nest. Note rind-like concentric layers around chamber in (F) (arrow). **(G–I)** External textures of the mound. Note pellet-like sediment aggregates in (G), and concentrically 'backfilled' areas with aggregates and insect body parts in (H) and (I).

The large (~2 m high, ~1.5 m diameter), constructed mound likely contained most of the nest above ground because the soil depth is very shallow (cf. Sands, 1987). The entire mound was constructed of fine-grained aggregated sediment, plant fragments, and insect carcasses cemented together with clay and likely with a salivary secretion. Portions of the exterior 'wall' had broken from the mound, revealing some of the internal structure. Large (~4–15 cm diameter), open, passages with smooth internal walls opened to the exterior of the mound, and are interpreted as passages for ventilation of the mound (Fig. *4.2.5.*9B, 9C). Smaller tunnels (~1.5 cm diameter) were constructed along the walls of the passageways (Fig. *4.2.5.*9D). Numerous horizontally oriented, circular and oval-shaped, open areas interpreted as fungus-garden chambers were separated by thin, horizontal floors of very fine-grained materials, and were connected to neighbouring chambers by slit-like or elliptical-shaped passages (Fig. *4.2.5.*9E, 9F). The walls of these chambers were smooth, finely laminated, and appeared to have been built with concentric layers around the chambers (Fig. *4.2.5.*9F). The external mound layer of the mound was porous, and consisted mainly of pellet-like, sub-spherical sediment aggregates (Fig. *4.2.5.*9G–I). Several areas showed the concentric layered pattern of construction, and the infilling of old passages by concentrically laminated aggregates (Fig. *4.2.5.*9I). These 'concentric' laminae were superficially very similar to the meniscate backfill produced by soil-dwelling arthropods (cf. Smith et a., 2008).

*4.2.6. Trace Suites in the Magadi–Nasikie Engida Basins*

The assemblage of modern, sub-fossil, and fossil animal and plant traces in the Bogoria basin was grouped into suites according to the observed sets of limnological and ecological environmental factors that appeared to control their distribution. The most important factors observed and interpreted at Lake Bogoria included: 1) whether the substrate was subaqueous or subaerial; 2) substrate water content; 3) water salinity; 4) water temperature; 5) degree of substrate induration; 6) substrate cohesiveness; 7) substrate grain size; 8) availability of food source; 9) temperature of substrate; 10) depth to water table; and 11) possibly air temperature. These factors are strongly controlled by the: 1) climate and lake level changes; 2) the proximity to the shoreline; 3) the proximity to hot springs; and 4) the gradient of the lake margin; as well as the 5) tectonic setting; and 6) structural controls on sedimentation. These environmental factors controlled the trace assemblage composition, as well as the lateral, ecology-related distribution of the trace making animals and the different types of traces those animals produced. The vertical distribution of traces in a locality is also related to the: 1) gradient of the lake-bounding features (e.g., axial plain, alluvial fan, normal fault); 2) sedimentation rate; and 3) the rate of sediment cementation and degree of induration.

A similar assemblage of modern and fossil trace suites was observed at Lake Magadi and Nasikie Engida as at Lake Bogoria. In modern examples that represented approximately a few weeks time, the relative timing of trace formation could be interpreted by using clues to substrate saturation provided by trace morphology (vertebrate and invertebrate) and whether the traces had been formed prior to, during, or following the development of salt crusts. Similar clues to the timing of trace formation could also be drawn from microbial mat features (e.g., desiccation features, wrinkle marks) and minor depositional or erosional features (e.g., thin clay drapes). Groups of traces formed at the same time may represent true ichnocoenoses formed under a particular set of conditions. However, in some cases these groups are equivalent to the undividable trace suites, which probably include more than one ichnocoenose.

At Lake Magadi and at Nasikie Engida, the “Chironomid” Suite (Suite LM1) differed from that at Lake Bogoria because the subaqueous tube-structures of chironomid larvae were also closely associated to simple, subaqueous surface trails produced by insect larvae (e.g., Incipient

*Helminthoidichnites* isp., Incipient *Archaeonassa* isp.). In the Magadi–Nasikie basins, these subaqueous trails were observed in water up to ~20 cm deep at shorelines near spring-fed or meteoric water input (e.g., NW Lagoon, NE Lagoon). Wet, subaerially exposed mudflats with relatively freshwater pools where the "Mermia-like" Suite (LB3) was observed at Lake Bogoria were not observed at Magadi or Nasikie. Surficial, horizontal tunnels (e.g., Incipient *Vagorichnus* isp., Incipient *Labyrintichnus* isp.) of microbe-feeding insects (e.g., staphylinids and heterocerid beetles, crickets) were similarly not observed at Magadi, although the vertical and oblique burrows of staphylinid beetles were observed on the drying mudflats of the E Lagoon. Another major difference between Lake Bogoria and Magadi–Nasikie was the presence of a "hot spring assemblage",that included the pock mark feeding structures (Suite LM3) of adult dipterans and an abundance of spider burrows at NW Nasikie Engida, as well as the trace fossils in the Green Beds at the S Lagoon of Lake Magadi. The development of hot spring ecosystems that include these same animal members as those at other hot spring localities (e.g., Yellowstone) represent relatively competition- and predator-free high-temperature areas with flowing, channelized hot-spring outflow (e.g.,Brues, 1924; Brock et al., 1969; Wiegert and Mitchell, 1973; Collins et al., 1976). South Loburu at Lake Bogoria is characterized by seepage vents and standing water on a low-gradient mudflat flooded seasonally by lacustrine waters. Microbial mats containing the horizontal surface tunnels at South Loburu appear to be associated with these features. The lack of the 'pock mark' traces at Bogoria may be associated with the relatively high diversity of predators there, and/or the relatively higher stability of substrates influenced by hot spring water when compared to the channelized flow at Nasikie Engida.

The "Flamingo" Suite (LM2) consisted of essentially the same set of traces as at Bogoria: flamingo nests-mounds, flamingo footprints, and other subaqueous or saturated shoreline shorebird and stork footprints. Similar to the distribution at Bogoria, nest mounds were observed in muddy, flat-lying substrates near fresh water sources (e.g., E Lagoon, NW Lagoon). Footprints were also observed near spring-fed channelized flow in the S Lagoon, but nest mounds were not seen in the coarse-grained sand and gravel substrates there.

The diversity of the "Scoyenia-like" Suite (Suite LM4) at Lake Magadi and Nasikie was lower overall than at Lake Bogoria, and with a slightly different composition of traces. The traces of modern earwigs were also common near hot springs at Nasikie, but were not observed elsewhere in the Magadi–Nasikie basin. The vertical and oblique burrows of spiders were much more common along the shoreline and hot-spring outflow channels at Nasikie than at Bogoria. Small to medium-sized vertical burrows were much less widespread at Magadi–Nasikie than at Bogoria, and very few tiger beetle vertical burrows were observed, which may possibly be related to higher air temperatures at Magadi. Horizontal tunnels and boxwork-like burrows of crickets were lacking at Magadi–Nasikie, as were the horizontal, branched tunnels of heterocerid beetles, and the horizontal tunnel networks of staphylinids in microbial mats. Pellet/aggregate backfilled vertical and oblique burrows were observed at the E Lagoon at Magadi, but the tear-drop- and wine-bottle-shaped dwelling burrows of *Bledius* sp. were not seen. However, it is likely that these types of burrows are present at the E Lagoon and would be discovered with more fieldwork.

More terrestrial suite(s) at Magadi–Nasikie also consisted of the nests and foraging tunnels and burrows of termites (e.g., Termitidae: Macrotermitinae). Terrestrial areas were not investigated in detail at Magadi–Nasikie, but it is expected that the relative proportion of dung beetle burrows and brood chambers would be higher in the Magadi area, due to the abundance of dung beetle carcasses found on dried substrates that had been flooded during the previous rainy season (e.g., NW Lagoon 2, Central lake). The "Termitichnus-like" Suite at Bogoria was associated with exposed delta-plains near the lake, whereas the "Coprinisphaera-like" Suite was

further towards the basin boundaries and associated with the fluvial Loboi Silts at Nyongonyek. It is unknown whether the "Termitichnus-like suite", which lacked bee cells and dung beetle brood chambers and burrows at Bogoria, is present at Lake Magadi. If so, it may be found towards the basin margins, and possibly on the low-lying delta plains that surround the lake (e.g., NE Lagoon).

Overall, the trace suites observed at Lake Bogoria, Lake Magadi, and Nasikie Engida were broadly consistent. Simple, horizontal, subaqueous trails appeared to be more abundant at Lake Magadi and Nasikie Engida than at Bogoria. In all cases they were associated with localities having: 1) soft, fine-grained, subaqueous substrates; 2) standing water; and 3) relatively freshwater input from springs (e.g., Magadi: NW Lagoon) and streams (e.g., Bogoria: Emsos), when compared with hypersaline lake waters. The diversity of the Scoyenia-like Suite was higher at Bogoria than at Magadi and Nasikie Engida. This may have been due to: 1) lower lacustrine salinities at Bogoria; 2) relatively lower air temperatures at Bogoria; and 3) a more abundant cyanobacterial food source associated with spring pools on mudflats at Bogoria. These important factors are closely related to other factors such as the more widespread and greater development of salt efflorescences at Magadi. The different trace assemblages associated with hot springs at the different lake basins appears to be mainly associated with: 1) greater amounts of cyanobacterial mats at Bogoria as a food source, which is important for the horizontal feeding networks produced by staphylinid (*Bledius*) and heterocerid beetles; 2) the stability of the environment with suitable substrates (e.g., Loburu vs. fluvial channels at NW Nasikie Engida); and 3) the relative contrast between the hot-spring setting and the surrounding environments and the ecological isolation of the hot-spring setting, which are both higher at NW Nasikie than at Loburu.

# CHAPTER 5

## 5. LITHOFACIES OF THE WILKINS PEAK MEMBER AND CORRELATIVE UNITS, BRIDGER BASIN, WYOMING

Several localities in the Bridger basin of Wyoming were investigated in order to (i) determine the composition and distribution of trace fossils; (ii) place the trace fossil assemblages within their stratigraphic and sedimentological contexts; (iii) assess the environmental controls on their distribution, and (iv) assess their utility for stratigraphy. The basin-scale stratigraphy of the Green River Formation in the Bridger basin is well known, and the general facies associations of the different members have been described (e.g., Roehler, 1992b; Bohacs et al., 2000; Carroll and Bohacs, 2001; M.E. Smith et al., 2008b). The focus of this thesis is underfilled basins, so the Wilkins Peak Member was most thoroughly investigated. Previous accounts of the stratigraphy and sedimentology of the Wilkins Peak Member (e.g., Culbertson, 1961; Smoot, 1978, 1983; Roehler, 1993; Pietras and Carroll, 2006; M.E. Smith, unpublished data) provided the framework for this study. Relatively small packages of sediments within this framework that preserved trace fossils were studied in detail, including bed-by-bed analysis of the relationship between lithofacies and trace fossil assemblages.

The Wilkins Peak Member preserves several lithofacies assemblages that differ depending on their position within the basin because of the basin physiography and variety of sediment source areas, both which changed through time in this tectonically active region. In general, coarser-grained, dominantly siliciclastic sediments deposited in terrestrial and lake-margin environments are more abundant towards the basin margins, and finer-grained carbonate sediments were deposited nearer the basin centre. However, because the basin was closed to surface outflow during Wilkins Peak time, changes in sediment input, water input, and local accommodation caused widespread lake-level changes that operated on a variety of time-scales and which differed in lateral extent. As such, lacustrine and shoreline facies can be found at the basin margin, in the basin centre, and in all positions between. Fluvial and sheetflood facies can also be found throughout the basin, although they are lacking in cores from the basin depocentre (Pietras and Carroll, 2006). This important characteristic distinguishes underfilled basins and affects the distribution of trace fossils due to their close association with sedimentary facies. Nevertheless, basin centre and basin margin lithofacies assemblages differ in lithology and in gradient- and base-level-related features such as the degree of pedogenic modification of sediments, inferred water-table depths, and the types of fluvial and lacustrine depositional environments represented.

This chapter focuses on the description and interpretation of the basin centre lithofacies, with consideration of their stratigraphic packaging and lateral variability. The findings at the basin margin localities are briefly described.

### 5.1. Description of the Basin Centre Lithofacies

The basin centre of the Wilkins Peak Member within the Bridger basin is defined by the area containing oil shale, lacustrine dolomitic mud, bedded evaporites, and evaporative and desiccated carbonates of the littoral to eulittoral zones. Nine main arkosic siliciclastic units (Culbertson, 1961) interfinger with the lacustrine deposits and are included as part of the basin centre assemblages of the Wilkins Peak Member, although they are present mainly on the eastern side of the Bridger basin. Several localities were investigated as part of this study, and stratigraphic sections of (i) the lowermost, lower Wilkins Peak-time, arkosic unit (the A-Bed), (ii) the thickest, late lower Wilkins Peak-time, arkosic unit (the D-Bed), and (iii) the early middle

Wilkins Peak-time E-Bed were measured at the decimeter-scale. Carbonate units containing: evaporite pseudomorphs; sublittoral, littoral, to eulittoral; and subaerially exposed lake-plain deposits were included in the measured sections below and above the D-Bed, above the E-Bed, and within the D-Bed and A-Bed in Middle Firehole Canyon (A-Bed), Firehole Canyon (A-, D-, and E-Beds), and Sage Creek Canyon (A-Bed). Other localities investigated included the carbonate units above and/or below the D-Bed and the D-Bed siliciclastics towards the low-gradient northern basin margin, exposed on White Mountain at Kanda and at the #18 Crossing (Fig. 2.5).

Roehler (1992b, 1993) provided a framework for the distribution of lithofacies associations for the Green River Formation. Smoot (1978, 1983) described the main lithofacies of the Wilkins Peak Member in the southern and central Bridger basin. Pietras and Carroll (2006) previously described the lithofacies of the Wilkins Peak Member exposed on White Mountain and from cores in the basin centre. M.E. Smith (unpublished data) provided a more chronologically precise stratigraphy of the southern basin margin to basin centre.

The lithofacies observed in lacustrine to eulittoral carbonates, the lowermost arkosic interval (A-Bed), and the middle arkosic intervals (D-Bed, E-Bed) are described by locality in Tables 5.1, 5. 2, and 5. 3, and are accompanied by figures of representative examples. The figures are grouped according to this division so that the facies preserved in these different sedimentary units can be compared between localities. The descriptions are based primarily on field observations supported by some petrographic examination. Stratigraphic sections are presented in Figures 5.1 (FC, D1), 5.2 (FC, D2), 5.3 (MFC, A), 5.4 (FC, A), and 5.5 (SCC, A).

**Fig. 5.1.** (Next page) The measured section of the middle Wilkins Peak Member from below the D-Bed to above the D-Bed in Firehole Canyon (Section FC, D1). The stratigraphic divisions referred to in the text are shown at left. Note that the depositional cycles shown represent fining-upwards or coarsening-upwards, but also show "landward-upwards" cycles where fine-grained paleosol or overbank facies were part of the succession. A legend for the measured sections is provided in Appendix A.

**Fig. 5.2.** (Two pages ahead) The measured section of the middle Wilkins Peak Member from the second unit of the D-Bed to above the E-Bed in Firehole Canyon (Section FC, D2). See notes provided in the caption for Fig. 5.1. A legend is provided in Appendix A

D-Bed - Firehole Canyon, Section FC, D1

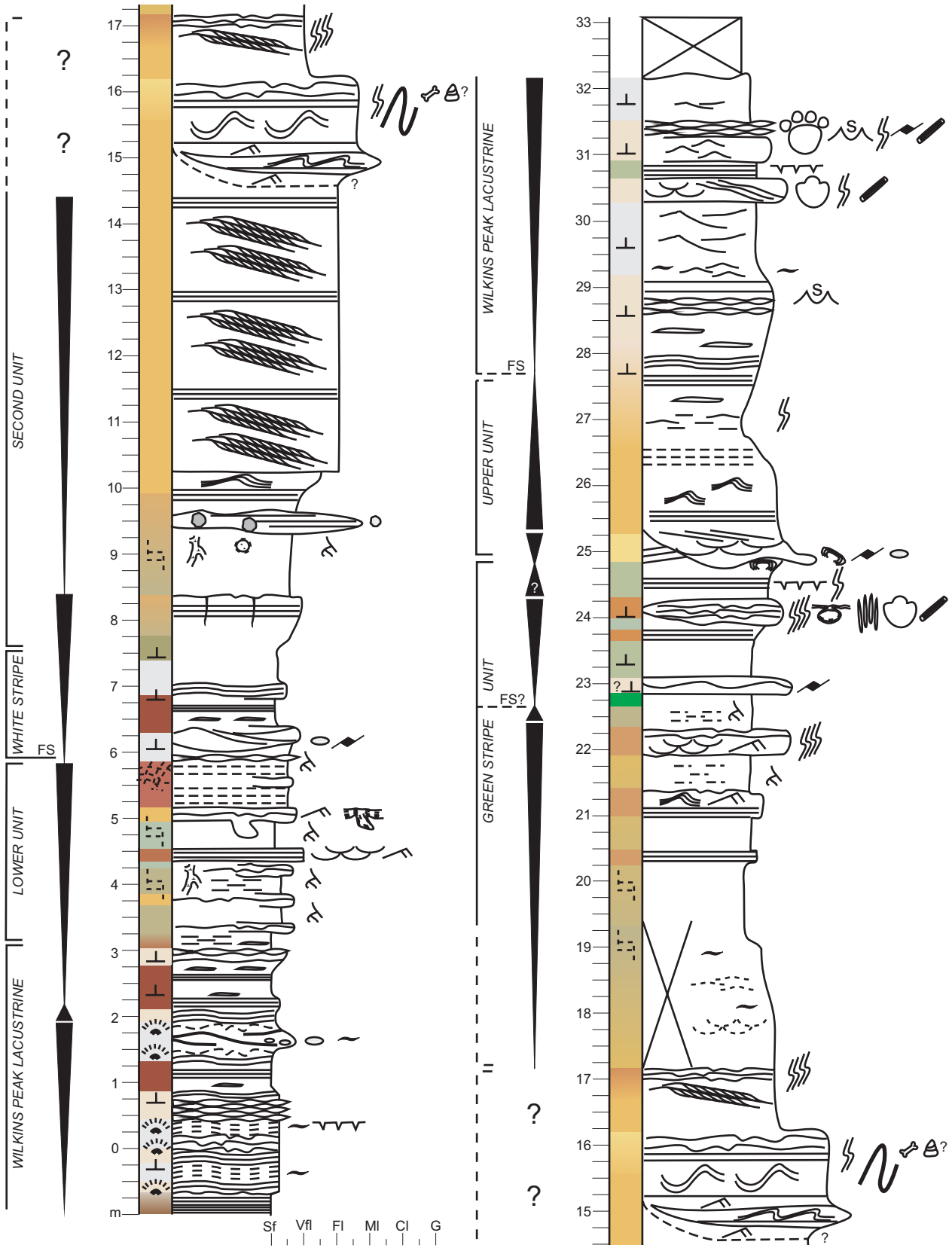

D-Bed - Firehole Canyon, Section FC, D2

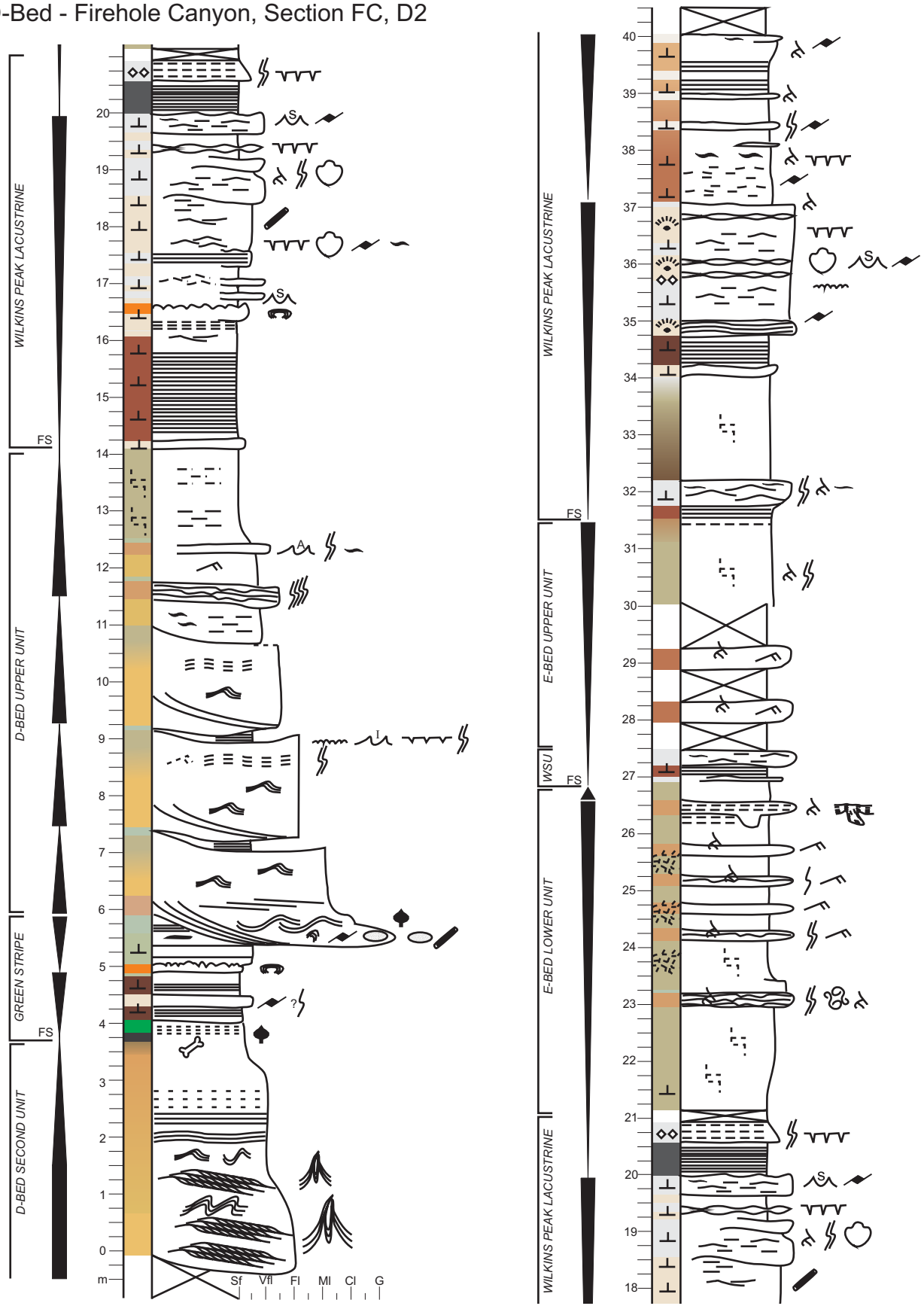

A-Bed
Middle Firehole Canyon

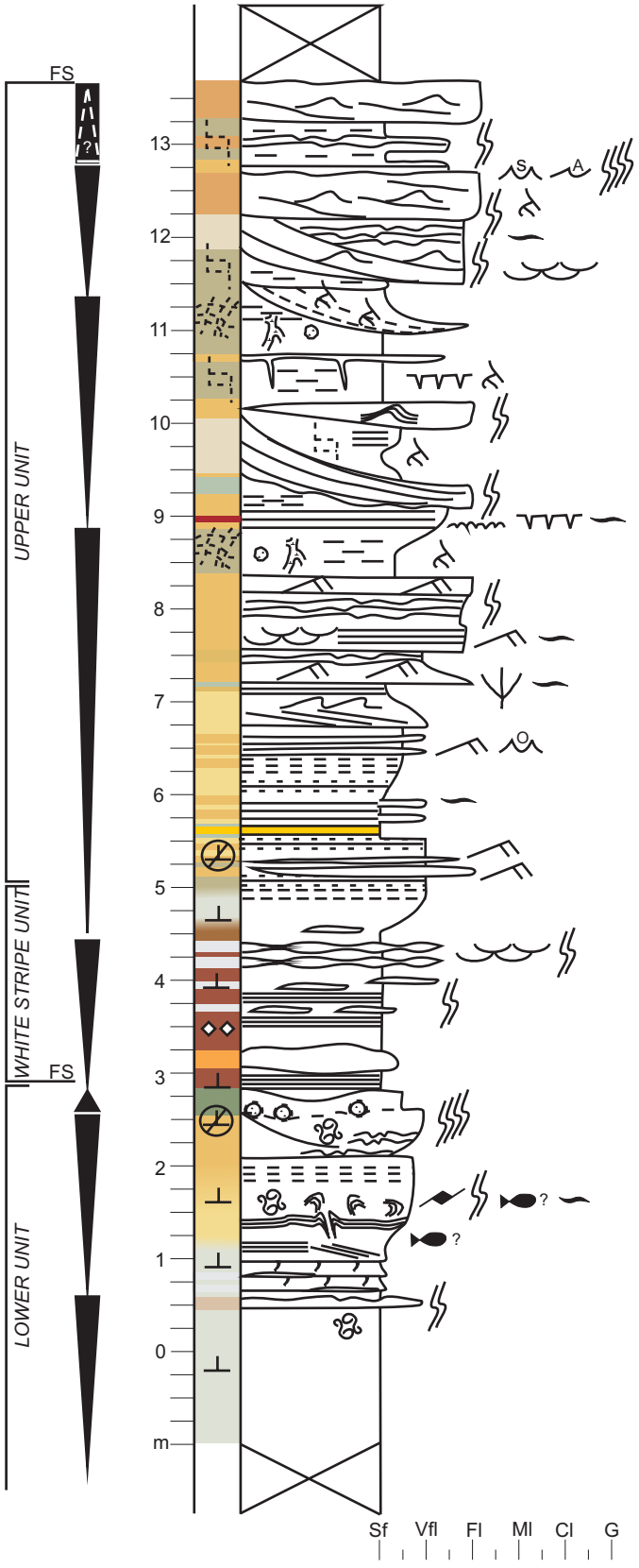


**Fig. 5.3.** The measured section of the A-Bed in Middle Firehole Canyon. See notes provided in the caption for Fig. 5.1. See Appendix A for legend.

A-Bed
Firehole Canyon

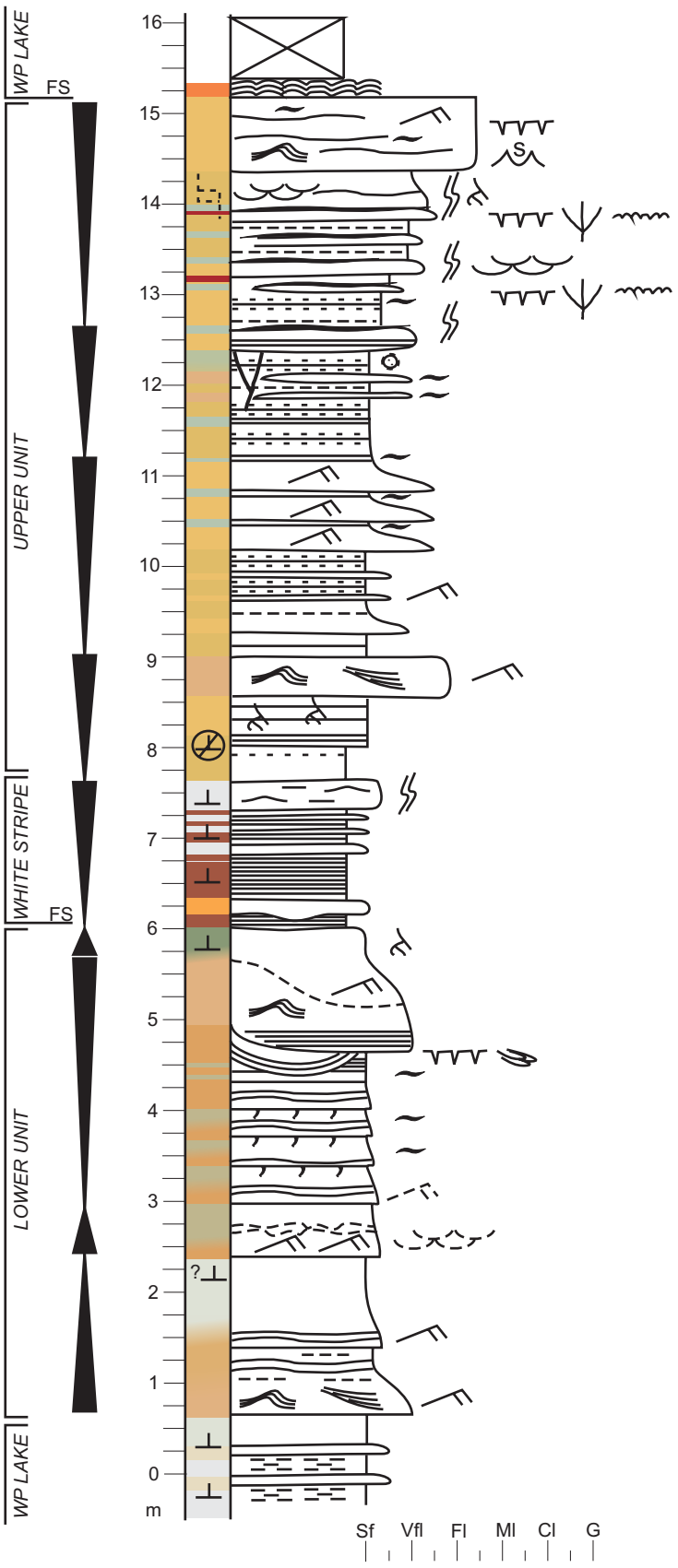


**Fig. 5.4.** The measured section of the A-Bed in Firehole Canyon. See notes provided in the caption for Fig. 5.1. See Appendix A for legend.

A-Bed
Sage Creek Canyon

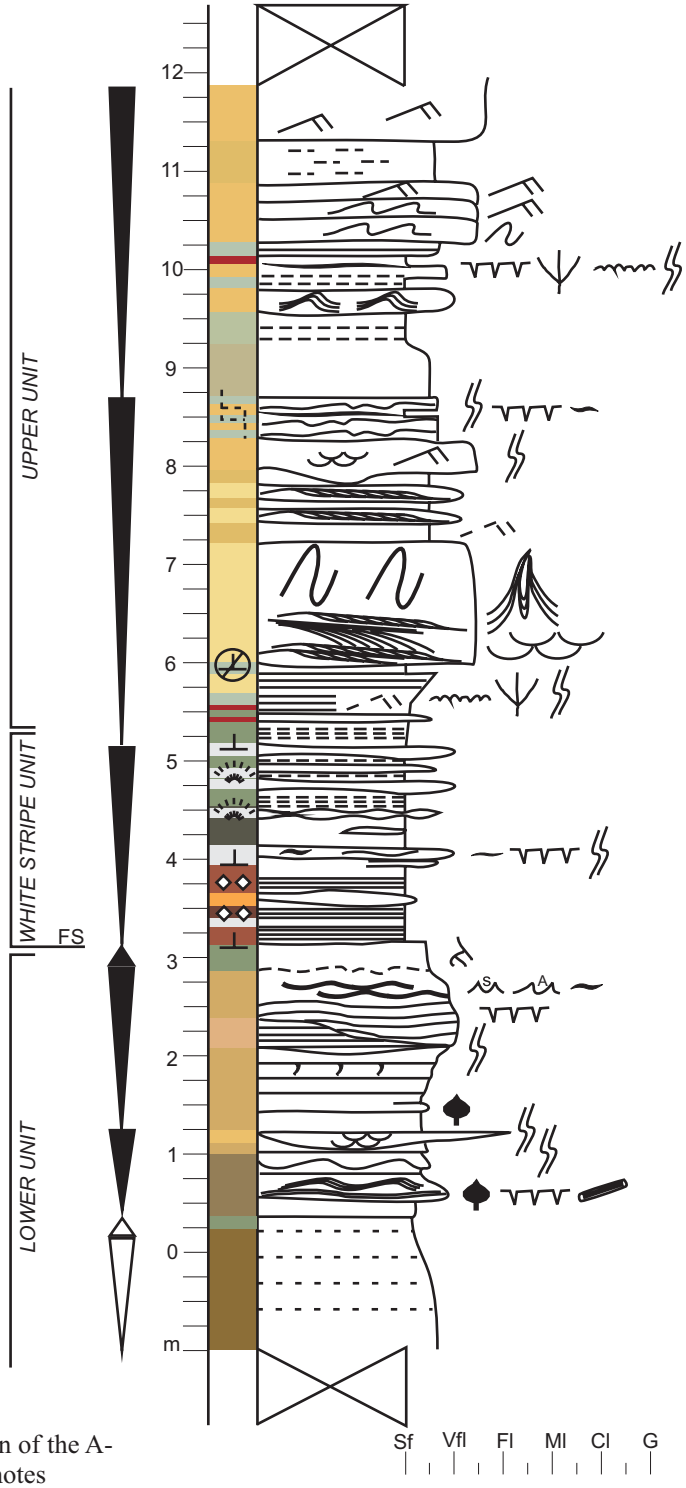


**Fig. 5.5.** The measured section of the A-Bed in Firehole Canyon. See notes provided in the caption for Fig. 5.1. See Appendix A for legend.

*5.1.1. Descriptions of the Carbonate Lithofacies of the Basin Centre Wilkins Peak Member*

Lithofacies of the carbonate units are described in detail in Table 5.1. The lacustrine carbonates units interfinger with the arkosic siliciclastic units and are included in the measured sections from Firehole Canyon (Fig. 5.1, 5.2). The numbers of the figures showing these facies begin with "*5.1.1.*", and were grouped together so that the carbonates could be more easily compared between localities. Carbonates comprise the majority of profundal to sublittoral, littoral, and eulittoral facies of Lake Gosiute. Only a small portion of the carbonates were investigated because the associations of trace fossils with different basin centre lithofacies were consistent and recurrent, with most traces preserved in wave-rippled littoral to eulittoral calciclastic siltstones and sandstones. The term calciclastic is used following Pietras and Carroll (2006), and is used to refer to reworked fragments of partly consolidated carbonate sediments derived from the reworking of local carbonates (intraclasts) and/or regional carbonates (extraclasts; Tucker and Wright, 1990). The term calciclastic refers to siltstones and sandstones containing "lime-clasts" of Tucker and Wright (1990). This study focused on well exposed carbonates above and below the D-Bed in different localities (e.g., White Mountain, Firehole Canyon), and on lacustrine carbonates contained within the A-Bed and D-Bed.

**Table 5.1.** Lithofacies descriptions from the basin centre carbonate units of the Wilkins Peak Member. Localities include: 1) White Mountain Kanda, above and below the D-Arkose Bed; 2) White Mountain #18 Crossing, below the D-Bed; 3) Firehole Canyon, above and below the D-Bed; and 4) above the E-Bed in Firehole Canyon. Also included are the carbonate units within the A-Arkose Bed in Sage Creek Canyon, Firehole Canyon, and Middle Firehole Canyon, as well as within the D-Bed in Firehole Canyon.

| Fig. | Lithology | Description | Comments; Trace suites (Chapter 6) | Interpreted Environment | Locality | Section, Metre |
|---|---|---|---|---|---|---|
| ***White Mountain, Kanda, above D-Bed and carbonate bench below D-Bed*** | | | | | | |
| Fig. *5.1.1.* 1B | Orangish white granule conglomerate | Clast-supported, orangish white granule conglomerate; matrix material orangish calcareous siltstone; clast material rounded carbonate intraclasts; internally discontinuous wavy-bedded | No trace fossils observed | Sheetflood granule-conglomerate; reworked in littoral zone | White Mountain, Kanda, below D | n/a |
| Fig. *5.1.1.* 1C | Grey coarse-grained calcareous sandstone with intraclasts | Grey coarse-grained calcareous sandstone; bed ~10 cm thick; internally massive to vaguely hummocky to very low amplitude oscillation-rippled; preserves isolated mudstone drape lenses on hummocks and in swales; base of bed may fill small-scale 'ripple'-troughs in underlying white mudstone; base of bed may contain randomly and vertically oriented carbonate crust intraclasts | No trace fossils observed | Eolian and/or sheetflood sandstone filling efflorescent crust at base, reworked by littoral processes in subaerially exposed lake-margin | White Mountain, Kanda, below D | n/a |
| Fig. *5.1.1.* 1A, 1D, 1F | Graded greyish white and orangish white calcareous sandstone | Normal-graded greyish white medium-grained calcareous sandstone, fining to orangish white calcareous siltstone; may contain orangish white siltstone or mudstone drape; bedding ~1–2 cm thick and gently undulating | No trace fossils observed | Sheetflood deposits into littoral zone | White Mountain, Kanda, below D | n/a |
| Figs. *5.1.1.* 1E; *6.1.1.*1E–H | Greyish white muddy calcareous sandstone | White calcareous sandstone; discontinuously flat-bedded, with beds ~3 cm thick; beds internally massive; grey mudstone partings may preserve iron-stains representing root-marks | Associated with vertebrate footprints; Suite BC2B | Subaerially exposed swash zone, possibly with fringing marsh | White Mountain, Kanda, below D | n/a |
| Fig. *5.1.1.* 1F | White mudstone | White calcareous or dolomitic mudstone; internal structure preserving isolated 'ripple'-troughs filled with coarser calcareous material; upper contact irregular with coarse-grained calcareous sandstone | No trace fossils observed | Carbonate mudflat mudstone possibly reworked by efflorescent salt crust | White Mountain, Kanda, below D | n/a |
| Figs. *5.1.1.* 1A, 1D, 1F, 1G; *6.1.1.*1A–D | Orangish white calcareous siltstone and greyish white mudstone | Interbedded orangish white calcareous siltstone and greyish white mudstone; bedding continuous and flat to slightly undulating; may preserve very low amplitude and rounded symmetrical, interference ripple crests on bedding planes; mudstone laminae < ~0.5 cm thick; sandstone beds internally flat- to slightly wavy-laminated; upper bedding | Associated with vertebrate footprints produced on firm substrate; Suite BC2B | Subaerially exposed, flat-lying eulittoral carbonate mudflat with carbonate crust, efflorescent salt crusts, and/or mixed | White Mountain, Kanda, below D | n/a |

| | | | | | | |
|---|---|---|---|---|---|---|
| | | planes may preserve irregular, bubbly lamination | | microbial/salt crusts | | |
| n/a | Light grey mudstone | Light grey mudstone; lenticular- to wavy- bedded with grey calcareous sandstone | No trace fossils observed | Sand-starved littoral carbonate mudflat | WM, Kanda, below D | n/a |
| Fig. *5.1.1*.1H | Grey and white dolomitic mudstone | Grey and white dolomitic mudstone; may be internally massive with platy breakage; may be vaguely interbedded with grey mudstone and white and orangish white mudstone drapes; desiccation cracks common | No trace fossils observed | Saline, sand-starved, littoral to eulittoral dolomitic mudflat | White Mountain, Kanda, above D | n/a |
| Fig. *5.1.1*.1H | Grey dolomitic mudstone | Grey dolomitic mudstone; internally discontinuous laminated; preserves orange-stained horizons; beds ~1–2 cm thick | No trace fossils observed | Sublittoral to littoral shallow lacustrine, possibly with detritus-rich horizons | White Mountain, Kanda, above D | n/a |
| ***White Mountain #18 Crossing, carbonate bench above the D-Bed (note: no carbonate bench below D-Bed at this site)*** | | | | | | |
| Fig. *5.1.1.* 2A, 2B, 2C | Orangish white calcareous sandstone | White to orangish white calcareous sandstone; may preserve indistinct, discontinuous horizontal lamination internally; beds typically ~2–4 cm thick; may preserve desiccation cracks and contain greyish white mudstone drapes; may be coarser and base; may preserve ripples on lower bedding plane | Associated with ?horizontal trails that may dictate desiccation crack morphology; Suite BC2A | Swash zone at shoreline of very low gradient lake-margin; may be subaerially exposed | White Mountain, #18 crossing, above D | n/a |
| Fig. *5.1.1.* 2D, 2E | Orangish white calcareous sandstone and olive-grey siltstone | Orangish white, lenticular- to wavy- to flaser-bedded calcareous sandstone with olive grey siltstone; ripple crests rounded and symmetrical; beds typically ~1–2 cm thick with wavy lower and upper contacts; ripples as bedforms preserve low-amplitude assymetrical (combined flow?), parallel, sinuous ripple crests | Rippled bedding planes preserve small surface tunnels and trails; Suite BC2A | Littoral zone of very low gradient lake margin; regressive succession | White Mountain, #18 crossing, above D | n/a |
| Fig. *5.1.1*.2F | Greyish and orangish white calcareous siltstone | Orangish and greyish white calcareous siltstone with silty and muddy drapes on undulating, irregular bedding planes; undulating beds massive internally and churned appearance (possibly trampled by mammals); may locally preserve ripple bedforms; high density of surface trails suggests quiet water and stable substrate | Not associated with iron-stained root marks; preserves small surface trails and desiccation cracks; Suite BC2A | Muddy littoral to eulittoral flats; subaerially exposed and desiccated | White Mountain, #18 crossing, above D | n/a |
| Fig. *5.1.1.* 2G, 2H | Grey, greyish white to pink calcareous and dolomitic mudstone and siltstone | Grey, greyish white to pink calcareous and dolomitic siltstone; internally massive or preserving discontinuous, non-parallel, wavy bedding with overall “churned” appearance; may preserve rare, small, discrete burrows and indistinct, probable mammal tracks; rarely preserves minute desiccation cracks (?shrinkage cracks) in grey-coloured mud drapes; may preserve iron-stained possible plant material or root-marks; may preserve intraclasts below upper grey mud drape | Associated with poorly preserved mammal tracks and occasional small burrows, iron-stains, desiccation (?shrinkage) cracks, and intraclasts; Suite BC2B | Paludal, marshy and muddy littoral areas of very low gradient lake margin; may be subaerially exposed | White Mountain, #18 crossing, above D | n/a |

| | | | | | | |
|---|---|---|---|---|---|---|
| Fig. *5.1.1*.2D | Greyish green siltstone | Greyish green siltstone with red-stained horizons; discontinuously laminated to continuously laminated; may grade upwards to lenticular bedding with orange-white calcareous siltstone and sandstone | Not associated with animal or plant traces | Sublittoral lacustrine | WM, #18C, above D | n/a |
| Fig. *5.1.1*. 2A, 2C | Olive grey dolomitic siltstone and white calcareous siltstone | Olive grey dolomitic siltstone with white calcareous siltstone interbeds; laminated, but may be broken up by desiccation; forms drapes on sandstone beds; grades upwards to lenticular bedded grey siltstone with isolated sandstone lenses; unit capped by sheet-like white calcareous sandstone | No trace fossil observed | Sublittoral to littoral lacustrine to swash zone with subaerial exposure | White Mountain, #18 crossing, above D | n/a |
| ***Firehole Canyon, below the D-Bed, Section FC, D1*** | | | | | | |
| Fig. *5.1.1*. 3B, 3D | Orangish white calcareous sandstone | Orangish white calcareous sandstone; very thinly bedded, with beds ~0.5–2 cm thick; wavy- to flaser-bedded, with flat to slightly undulating, to oscillation-rippled internal lamination; mudstone drapes are grey mudstone | Not associated with plant or animal trace fossils | Littoral carbonate sandstone | Firehole Canyon, below D1 | e.g., FC, D1, m ~2 |
| Fig. *5.1.1*.3E | Orangish pinkish white calcareous siltstone and sandstone with evaporite pseudomorphs and carbonate intraclasts | Orangish pinkish white calcareous siltstone to sandstone; thinly bedded, with beds ~3–5 cm thick; beds irregular and discontinuous, containing isolated lenses of carbonate mudstone (disrupted wavy to flaser bedding) and discontinuous horizons of broken carbonate crusts; sandstone beds may contain rounded carbonate mudstone intraclasts; evaporite pseudomorphs randomly oriented in carbonate siltstone matrix; disrupted bedding primary feature | Not associated with plant or animal trace fossils; facies not observed at Lake Magadi, but may form in NE lagoon | Littoral to lake-margin mudflat around trona pan; flooded by sheetfloods; contains oscillation ripples; evaporite pseudomorphs transported and/or formed interstitially by capillary evaporation | Firehole Canyon, below D1 | e.g., FC, D1, m ~1.5 |
| Fig. *5.1.1*. 3C, 3D, 3F, 3F, 3G, 3H, 3I | Bedded orangish pinkish white calcareous siltstone with evaporite pseudomorphs | Orangish pink-white calcareous siltstone; bedded with evaporite (probably trona) pseudomorphs; very thinly bedded with beds ~1–3 cm thick; beds often draped with grey mudstone; bedding ranges from undulating, horizontal bedding with drapes, to wavy and flaser bedding; grey dolomitic drapes may preserve desiccation cracks on bedding planes; bedding planes may preserve very low amplitude, round-crested oscillatory interference ripples; trona blades small (< 1 cm length) and oriented mainly horizontally; trona blades typically do not disrupt mud drapes; bedding primary; thicker beds contain larger evaporite pseudomorphs | Not associated with plant or animal trace fossils; compare with Lake Magadi, central basin margin | Frequently flooded and exposed trona pan towards basin centre; pan flooded from above with very shallow water only | Firehole Canyon, below D1 | e.g., FC, D1, m ~0.5 |
| Fig. *5.1.1*.3I | Grey dolomitic mudstone | Thinly bedded grey dolomitic mudstone; internally discontinuously to continuously laminated; beds ~2 cm thick | Not associated with trace fossils | Sublittoral lacustrine to “flooded pan” lacustrine | Firehole Canyon, below D1 | e.g., FC, D1, m ~ -0.5 |

***Firehole Canyon, above the D-Bed, Sections FC, D1 and FC, D2***

| | | | | | | |
|---|---|---|---|---|---|---|
| Fig. *5.1.1.* 4A, 4B | White calcareous sandstone with intraclasts | White, graded calcareous sandstone with granule-sized flat and rounded intraclasts; slightly scoured base; internally planar laminated with flat-lying intraclasts; oscillation-ripple reworking of upper laminae; overlain by black and reddish brown organic-rich mudstone | No trace fossils observed | Swash zone to littoral carbonate lacustrine; possibly reworked storm bed | Firehole Canyon, above D2 | e.g., FC, D2, m ~20 |
| Fig. *5.1.1.*4C | Orangish white calcareous sandstone | Orangish white calcareous sandstone with small-scale trough cross-lamination and very low-angle cross-lamination; preserves branched, vertical burrows preserved as endichnia; unit preserves reed casts, desiccation cracks, and vertebrate footprints | Bioturbated by endichnia; bedding plane preserves vertebrate tracks; Suite BC1, BC2B | Subaerially exposed littoral to swash zone beach carbonate | Firehole Canyon, above D1 | e.g., FC, D1, m ~30.5 |
| Fig. *5.1.1.* 4F, 4G | Orangish white calcareous sandstone | Thinly bedded orangish white calcareous sandstone; beds ~2–5 cm thick; continuous, wavy to flat contacts; internally contains very low-angle lamination and small-scale trough cross-lamination; may contain thicker beds with very rounded ripple crests, or small-scale hummocks and swales (~20 cm wavelength, ~2 cm amplitude); may be interbedded with grey mudstone | No trace fossils observed | Littoral to swash zone beach carbonate sandstones with storm beds | Firehole Canyon, above D1 | e.g., FC, D1, m ~30 |
| Fig. *5.1.1.* 4D, 4E | Orangish white calcareous sandstone | Wavy- to flaser-bedded orangish white calcareous sandstone; beds ~1.5–2 cm thick; symmetrical-rippled and planar-laminated horizontal beds with drapes; some small desiccation cracks | No trace fossils observed | Littoral carbonate lacustrine | Firehole Canyon, above D1 | e.g., FC, D1, m ~29 |
| Fig. *5.1.1.* 5A, 5B, 5C, 5D | Greyish white and orangish white muddy calcareous siltstone and sandstone | Greyish white dolomitic mudstone and orangish white calcareous siltstone to very fine-grained sandstone; preserves large desiccation polygons and possible vertebrate footprints; upper bedding planes may contain large carbonate crust fragments and carbonate mudstone intraclasts; greyish white muddy siltstone may be vaguely ripple-laminated or flat-bedded | Associated with horizontal burrows and desiccation cracks; Suite BC2A | Subaerially exposed and desiccated carbonate mudflat | Firehole Canyon, above D2 | e.g., FC, D2, m ~17.5 |
| Fig. *5.1.1.* 5E, 5F, 5G, 5H | Greyish white, orangish white, and white muddy carbonate siltstone and sandstone | Greyish and orangish white carbonate siltstone and sandstone; irregular bedding planes with occasional desiccation cracks; internally massive; may preserve fragments of original carbonate crust with carbonate intraclasts; top bedding plane may have been altered by salt efflorescence; preserves reed casts and vertebrate footprints; may preserve evidence of desiccated microbial mats (‘laminated’ and irregular cracks) | Associated with vertebrate footprints and reed casts; preserves microbial mat features associated with small burrows; Suite BC2A, BC2B | Subaerially exposed, carbonate littoral to eulittoral saturated mudflat and/or marsh | Firehole Canyon, above D1, above D2 | e.g., FC, D1, m ~31.5<br>e.g., FC, D2, m ~19.5 |
| Fig. *5.1.1.*4H | White calcareous sandstone and greyish light brown mudstone | Interbedded wavy-bedded white calcareous sandstone and greyish light brown mudstone; mudstone beds < 4 cm thick; sandstone beds ~1–2 cm thick; unit coarsens upwards | No trace fossils observed | Sublittoral to littoral lacustrine without signs of desiccation | Firehole Canyon, above D1 | e.g., FC, D1, m ~28.5 |

| | | | | | | |
|---|---|---|---|---|---|---|
| Fig. *5.1.1*.6F | Greyish white and orangish white muddy calcareous siltstone | Interbedded greyish white dolomitic mudstone and orangish white calcareous siltstone; flat beds with slightly irregular contacts; no evidence of desiccation | Possibly associated with mammal track underprints; cf. BC2A | Littoral carbonate mudflat | Firehole Canyon, above D2 | e.g., FC, D2, m ~17.3 |
| Fig. *5.1.1*.6A | Tan white calcareous siltstone and sandstone | Very thinly bedded tan white calcareous very fine sandstone; bedding ~0.5–1 cm thick; bedding continuous, and parallel, with wavy to irregular bed contacts; grades transitionally upwards to lenticular-bedded siltstone with sandstone lenses; lithology mixed arkosic siliciclastics and carbonate | No trace fossils observed | Sublittoral to littoral lacustrine; transition from fresher/siliciclastic lake deposits to saline/carbonate lake deposits | Firehole Canyon, above D1 | e.g., FC, D1, m ~27.5 |
| Fig. *5.1.1*.6H | Greyish green mudstone and tan siltstone | Interbedded greyish green mudstone and tan arkosic siltstone; preserves desiccation cracks in cross-section, ~20 cm deep; internally, beds are discontinuously laminated; preserves iron-stained root-marks | Associated with iron-stained root-marks, but not with animal traces | Subaerially exposed siliciclastic mudflat; represents lake-level drop | Firehole Canyon, above D1 | e.g., FC, D1, m ~31 |
| Fig. *5.1.1*.6B –D | Light brown carbonate mudstone | Light brown carbonate mudstone with horizontal, parallel, discontinuous lamination | Not associated with trace fossils | Sublittoral to muddy littoral lacustrine | Firehole Canyon, above D2 | e.g., FC, D2, m ~19.5 |
| Fig. *5.1.1*.6B, 6E | Bluish dark grey to black laminated mudstone | Bluish dark grey and black organic-rich laminated dolomitic mudstone; contains many small black plant fragments | Not associated with animal traces | Sublittoral lacustrine | Firehole Canyon, above D2 | e.g., FC, D2, m ~20.5 |
| Fig. *5.1.1*.6G | Black and reddish brown mudstone | Black and reddish brown organic-rich carbonate mudstone; black and reddish brown colours interbedded, possibly due to fluctuating conditions of oxidation; internally discontinuously laminated | Not associated with animal traces | Sublittoral lacustrine | Firehole Canyon, above D2 | e.g., FC, D2, m ~20.2 |
| ***Firehole Canyon, above the E-Bed*** | | | | | | |
| Fig. *5.1.1*. 8A, 8C, 8D | Orangish white calcareous sandstone and mudstone | Orangish white calcareous sandstone in discontinuous, 2–6 cm thick beds; internally, may preserve oscillation ripple cross-lamination; wavy- to flaser-bedded, with some irregular bedding planes; may also preserve spherical, open or filled, holes possibly representing evaporite (?shortite) dissolution; some beds preserve randomly oriented carbonate crust intraclasts in upper < 2 cm, likely representing subaerially exposed evaporite crust; bedding planes may preserve 'bubbly texture' attributed to gas escape bubbles in microbial mats; beds may contain irregular, evaporite (trona) pseudomorphs with larger bladed fan pseudomorphs | Associated with mammal footprints and tiny surface trails; bench may represent shallowing upwards from shallow saline lacustrine, becoming subaerially exposed upwards; Suite BC2A, BC2B | Hypersaline evaporitic littoral and eulittoral mudflat carbonates | Firehole Canyon, above E1, above E2 | e.g., FC, E2, m ~35.5 |
| Fig. *5.1.1*. 8A, 8E | Pinkish white calcareous sandstone mudstone drapes | Pinkish white calcareous sandstone with well preserved wavy- and flaser-bedding with greyish white mudstone drapes; bedding not disrupted by evaporites or bioturbation | No trace fossils observed in cross section; cf. Suite BC2 | Littoral lacustrine | Firehole Canyon, above E2 | e.g., FC, E2, m ~36 |

| | | | | | | |
|---|---|---|---|---|---|---|
| Fig. *5.1.1*.8G | Tan white calcareous sandstone and greyish white mudstone interbeds with evaporite pseudomorphs | Tan to orangish white, thinly bedded (~2–4 cm), calcareous siltstone with large (< 3 cm length), bladed, displacive, random to vertically oriented evaporite pseudomorphs; slightly smaller (~2 cm length) bladed evaporite pseudomorphs oriented horizontally; beds part of wavy- to flaser-bedded carbonate unit, with greyish white drapes; evaporite beds contain horizontally to randomly oriented carbonate drape intraclasts | Compare with evaporite facies from Lake Magadi; no trace fossils observed | Littoral to eulittoral mudflat or pan with sodium carbonate brine | Firehole Canyon, above E1 | e.g., cf. FC, E2, m ~34.8 |
| Fig. *5.1.1*.8F | Tan white calcareous sandstone with evaporite pseudomorphs | Tan to orangish white, very thinly bedded (~0.5–2 cm) calcareous siltstone with large (~2 cm length) bladed evaporite pseudomorphs; occasional greyish white carbonate mudstone drapes; beds flat to very gently undulating | Compare with evaporite facies from Lake Magadi; no trace fossils observed | Sublittoral to littoral mudflat or pan with sodium carbonate brine | Firehole Canyon, above E1 | e.g., cf. FC, E2, m ~35 |
| Fig. *5.1.1*. 8A, 8B | Orangish white calcareous sandstone with evaporite pseudomorphs | Orangish white calcareous sandstone preserving evaporite blade pseudomorphs with random orientation; single sandstone bed ~10 cm thick, internally massive; overlies organic-rich carbonate mudstone; upper and lower contacts irregular | Not associated with trace fossils | Hypersaline sublittoral | Firehole Canyon, above E2 | e.g., FC, E2, m ~34.8 |
| Fig. *5.1.1*.7D | Orange-pinkish white calcareous sandstone with greyish white carbonate mudstone interbeds | Orangish and pinkish white calcareous sandstone with grey and white mudstone drapes; bedding includes discontinuous, parallel, horizontal lamination to flaser bedding; some beds preserve carbonate mudstone drape intraclasts at base, grading upwards to horizontal bedding and small-scale hummocks upper surfaces; some units show wavy bedding with broken-up greyish white calcite/dolomitic mudstone drapes and orangish white calcareous sandstone | Associated with high densities of small surface tunnels and trails and rare vertebrate footprints; Suites BC2A, BC2B | Carbonate mudflat and beach showing some exposure; preserves possible storm beds | Firehole Canyon, above E1 | e.g., cf. FC, E2, m ~32.5 |
| Fig. *5.1.1*. 7D, 7E | Greyish to orangish white calcareous siltstone and grey mudstone | Light grey to orangish white carbonate siltstone; preserves very low amplitude, round-crested symmetrical ripple bedforms; some remnants of the uppermost laminae show signs of subaerial exposure including crusts of carbonate mudstone intracasts; preserves very small surface trails; preserves reed impressions; possible, poorly preserved vertebrate footprints are preserved in siltstone below original surface crust | Associated with surface trails in remnants of original surface crust and reed impressions; Suite BC2A; Suite BC2B? | Littoral to eulittoral carbonate mudflat near marshy area | Firehole Canyon, above E1 | e.g., cf. FC, E2, m ~32.3 |
| Fig. *5.1.1*.9E –H | Light grey to orangish grey carbonate muddy siltstone | Light grey muddy calcareous and dolomitic siltstone; internally massive with platy breakage or flat- to flaser-bedded with very slightly undulating bed contacts; occasionally preserves very low amplitude, round-crested symmetrical ripple bedforms; may preserve desiccation cracks and vertebrate footprints and small surface trails in surface crust laminae | Associated with poorly preserved vertebrate footprints and small surface trails; Suites BC2A, BC2B | Littoral to eulittoral lake-margin mudflat; may be marshy | Firehole Canyon, above E1, above E2 | e.g., FC, E2, m ~37, m ~40 |

| | | | | | | |
|---|---|---|---|---|---|---|
| Fig. *5.1.1.* 9B, 9C | Orangish white and grey calcareous siltstone and brown mudstone | Orangish white and grey calcareous siltstone and brown to grey mudstone; wavy bedded or massive internally; preserves iron-stained circular root-marks; individual beds discontinuous and thin (~0.5–2 cm); may be intercalated with brown lacustrine mudstone | Compare with grey carbonate facies at #18 Crossing; no trace fossils observed | Littoral to lake-margin marsh | Firehole Canyon, above E2 | e.g., FC, E2, m ~37, m ~38.5 |
| Fig. *5.1.1.* 7D, 7F, 7G | Olive-grey and white dolomitic and calcareous mudstone and siltstone | Olive grey dolomitic mudstone finely interbedded with greyish white carbonate siltstone and mudstone drapes; drapes < 1 – ~3 mm thickness; bedding planes may be irregular and iron-stained, possibly representing organic detritus on irregular surface | Associated with high densities of small surface trails in drapes; Suite BC2A | Littoral carbonate mudflat | Firehole Canyon, above E1 | e.g., cf. FC, E2, m ~32 |
| Fig. *5.1.1.* 7A, 7B | Olive-grey mudstone | Olive-grey dolomitic mudstone; discontinuously laminated or internally massive | No trace fossils observed | Sublittoral to muddy littoral | Firehole Canyon, above E1, above E2 | e.g., FC, E2, m ~31.8 |
| Fig. *5.1.1.* 9A, 9B, 9D | Light brown carbonate mudstone | Light brown carbonate mudstone; weakly bedded with irregular bedding contacts; intercalated with discontinuous, flat-bedded calcareous siltstone thin beds; grades upwards into flaser-bedded calcareous siltstone and sandstone; preserves plant fragments including pine needles and fruit | No trace fossils observed | Organic sublittoral to littoral marsh carbonate mudstone | Firehole Canyon, above E2 | e.g., FC, E2, m ~39.5 |
| Fig. *5.1.1.*7 B, 8A, 8B | Brown to dark brown carbonate mudstone | Brown to dark brown carbonate mudstone; massive or laminated internally; weathers greyish white | No trace fossils observed | Organic-rich sublittoral lacustrine | Firehole Canyon, above E2 | e.g., FC, E2, m ~34.5 |
| ***"White Stripe" Carbonate Unit within the D-Bed at Firehole Canyon*** | | | | | | |
| Fig. *5.1.1.* 10C | Light grey and orangish grey muddy intraclast conglomerate | Light grey muddy carbonate intraclast conglomerate with well rounded pebble-size intraclasts; bed < 20 cm thick; discontinuous non-parallel cross bedding present, with beds < 5 cm thick; internally appears churned and massive | No trace fossils observed | Possibly transgressive lag conglomerate, partially reworked into littoral bar | Firehole Canyon, within D | e.g., FC, D1, m ~6.2 |
| Fig. *5.1.1.* 10C–D | Greyish white calcareous sandstone | Flaser- to wavy-bedded orangish white calcareous sandstone; internally, laminations wavy to undulating and continuous | No trace fossils observed | Littoral lacustrine | Firehole Canyon, within D | e.g., FC, D1, m ~6.4 |
| Fig. *5.1.1.* 10C | Orangish white calcareous sandstone and grey mudstone | Lenticular- to wavy-bedded orangish white calcareous sandstone and grey mudstone; sandstone lenses isolated within mudstone; lower contact erosional into siliciclastic siltstones | No trace fossils observed | Littoral lacustrine; base of transgressive lake carbonate | Firehole Canyon, within D | e.g., FC, D1, m ~6 |
| Fig. *5.1.1.* 10C | Brown mudstone and orangish white calcareous sandstone | Lenticular-bedded brown, organic-rich mudstone with isolated calcareous sandstone lenses | No trace fossils observed | Sublittoral to littoral lacustrine | Firehole Canyon, within D | e.g., FC, D1, m ~6.5 |

| | | | | | | |
|---|---|---|---|---|---|---|
| Fig. *5.1.1.* 10C–D | Brown mudstone | Brown, laminated and massive organic-rich mudstone | No trace fossils observed | Sublittoral lacustrine | Firehole Canyon, within D | e.g., FC, D1, m ~6.5 |
| Fig. *5.1.1.* 10E | Greenish grey mudstone | Calcareous, greenish grey, massive mudstone; organic-poor | No trace fossils observed; consider density contrasts of inflow vs. lacustrine | Sublittoral lacustrine; hypopycnal prodelta? and transition to arkosic unit above | Firehole Canyon, within D | e.g., FC, D1, m ~7.5 |
| Fig. *5.1.1.* 10E | Olive green siltstone | Olive green massive siltstone; siliciclastic and organic-poor | No trace fossils observed | Sublittoral lacustrine; may represent hypopycnal delta-front of arkosic unit | Firehole Canyon, within D | e.g., FC, D1, m ~7.8 |
| ***"White Stripe" Carbonate Unit within the A-Bed at Middle Firehole Canyon, Firehole Canyon, and Sage Creek Canyon*** | | | | | | |
| Fig. *5.1.1.*11 A–B, 12A, 12C | Porphyritic or pyroclastic orange tuff | Orange tuff with granule-sized white crystals distributed throughout tuff; up to ~30 cm thick, as thin as ~5 cm; reworked into a laterally continuous bed with undulating or lenticular geometry; typically no internal structure but may preserve vague non-parallel cross-beds | Helps to demonstrate topography of upper contact of lower siliciclastic units; no trace fossil observed | Reworked sublittoral tuff bed; possibly reworked into sublittoral bars and/or lenticular channel fill | Middle Firehole, Sage Creek, and Firehole Canyons | e.g., SCC, m 3.5; FC, m 0.2; MFC, m 3.2 |
| Fig. *5.1.1.*11 C | Orangish grey-white calcareous sandstone | Orangish grey-white calcareous sandstone; discontinuous and continuous, planar parallel bedded; beds form ~0.5–1.5 cm thick; lenticular geometry to bed, < ~30 cm thick; preserved at base of carbonate unit in shallow channel of lower siliciclastic unit | No trace fossils observed | Swash zone carbonate sandstone, forming base of transgressive lacustrine unit in abandoned channel | Firehole Canyon, A (N) | e.g., cf. FC, m 0.0 |
| Fig. *5.1.1.* 11E, 12F | Orangish white and pinkish grey calcareous sandstone | Orangish white and pinkish grey calcareous sandstone; sandstone beds may be wavy- to flaser-bedded or interbedded with light brown mudstone and greyish green mudstone; sandstone beds ~1–3 cm thick and may have continuous wavy to undulating bedding contacts; may preserve low amplitude symmetrical ripple bedforms; some beds preserve simple burrows; internally may preserve small-scale cross-lamination | Associated with simple burrows (*Planolites* isp.); Suite BC1 | Occasionally subaerially exposed littoral lacustrine or relatively freshwater littoral lacustrine | Firehole Canyon, A (N); Middle Firehole Canyon, A | e.g., cf. FC, m 1.3–1.6<br>e.g., MFC, m ~4.4 |
| Fig. *5.1.1.* 13B, 13C | Greyish and orangish white calcareous sandstone | Greyish and orangish white and white calcareous sandstone; wavy- to flaser-bedded with both greyish green and brown to light brown mudstone interbeds and drapes; may be interbedded with brown to light brown carbonate mudstone, with sandstone beds may be massive internally with irregular lower and upper contacts; sandstone beds may contain large (< 2 cm height), bladed trona fan pseudomorphs, oriented upwards | Not associated with trace fossils | Littoral saline lacustrine | Sage Creek Canyon, A; Firehole Canyon, A (N) | e.g., SCC, m ~4.6–4.8<br>e.g., cf. FC, m ~1.2 |

| | | | | | | |
|---|---|---|---|---|---|---|
| Fig. *5.1.1.* 11F, 11G | Dark brownish green mudstone | Massive dark greenish brown mudstone; may be interbedded with wavy-bedded calcareous sandstone | Not associated with trace fossils | Littoral to sublittoral or lagoonal; possibly represents hypopycnal delta front or prodelta | Firehole Canyon, A (N) | e.g., cf. FC, m ~1.8 |
| Fig. *5.1.1.* 12E | Pinkish light grey siltstone to sandstone and brown mudstone | Pinkish light grey muddy carbonate siltstone to sandstone; interbedded and wavy-bedded with organic-rich brown mudstone and white carbonate sandstone; upper bedding planes preserve animal trace fossils produced in wet to soupy substrate | Preserves trace fossils (*Planolites* isp. and cf. *Beaconites* isp.); Suites BC1, BC2A | Littoral lacustrine with occasional subaerial exposure | Middle Firehole Canyon, A | e.g., MFC, m ~4.3 |
| Fig. *5.1.1.* 12C, 12G | Greyish green to greyish and greenish tan marl mudstone | Greyish to greenish tan marl mudstone; internally massive to discontinuously laminated; not associated with trace fossils except occasional iron-stained root-hair marks towards top of unit; colour change occurs gradually upwards from greyish green to greyish tan to greenish tan, likely due to increasing siliciclastic input | Greenish tan-coloured mudstone may be associated with iron-stained root-hair marks; not associated with animal traces | Muddy sublittoral to littoral | Middle Firehole Canyon, A | e.g., MFC, m ~4.5–5 |
| Fig. *5.1.1.* 13D, 13E | Greyish green marl mudstone | Greyish green mudstone; discontinuously laminated; mixed siliciclastic and carbonate mudstone lithology; may be lenticular- to wavy-bedded, or interbedded with greyish and orangish white carbonate sandstone lenses and interbeds; shallow (< 1 cm) desiccation cracks into mudstone preserved as casts by carbonate sandstone beds above; sandstone beds have irregular upper contacts and may be bioturbated | Associated with shallow desiccation cracks; sandstone beds may be slightly bioturbated | Littoral to eulittoral mudflat representing initial deposition of upper siliciclastic unit | Sage Creek Canyon, A; Firehole Canyon, A (N) | e.g., SCC, m ~5–5.5<br>e.g., cf. FC, m ~1.3 |
| Fig. *5.1.1.* 12D | Brown to light brown mudstone | Brown mudstone containing organics; laminated to massive; may be lenticular-bedded with grey or greyish brown carbonate sandstone lenses; lenses are isolated and connected; associated with simple burrows at Middle Firehole Canyon where interbedded with wavy-bedded calcareous sandstone | Not associated with trace fossils except at Middle Firehole Canyon; Suite BC1 | Sublittoral to littoral carbonate lacustrine | Middle Firehole, Sage Creek, and Firehole (N) Canyons | e.g., SCC, m ~4.2–4.5; cf. FC, m 1.1; MFC, m ~3.8 |
| Fig. *5.1.1.* 11I, 12B, 13A | Dark brown laminated mudstone | Dark brown, organic-rich, laminated to massive, carbonate mudstone; may contain small, white, dispersed shortite crystals, especially above the reworked tuff; in Firehole Canyon, lake muds show lower contact erosional, filling channel topography | Not associated with trace fossils | Sublittoral lacustrine | Middle Firehole, Sage Creek, and Firehole Canyons | e.g., SCC, m ~3.3; FC, m ~0.5; MFC, m ~3.5 |

## Figure captions for photographic plates, Section 5.1.1.

**Fig. 5.1.1.1.** Carbonate lithofacies from below the D-Bed at White Mountain, Kanda. **(A)** The carbonate bench below the D-Bed at Kanda. Block at left contains well preserved mammal footprint. **(B)** Intraclast conglomerate and bedded calciclastic sandstones. Arrow is showing a possible vertical burrow. **(C)** Bedded carbonates showing irregular, continuous lamination possibly attributable to microbial mats. **(D)** Bedded carbonates. **(E)** Calcareous sandstone with reddish marks, possibly representing root marks. **(F)** Bedded carbonates. Arrow is showing bed with isolated "ripple-troughs" possibly due to efflorescent salt crust. **(G)** Typical carbonate sandstone outcrop. Note symmetrical ripple bedforms on block at top left. **(H)** Structureless grey dolomitic mudstone with orange-weathering, desiccation-cracked beds.

**Fig. 5.1.1.2.** Carbonate lithofacies from above the D-Bed at White Mountain, #18 Crossing site. **(A)** The carbonate bench above the D-Bed at #18 Crossing. **(B)** Thick carbonate sandstone bed with rippled base and planar lamination. **(C)** White mudstone drape on sandstone. **(D)** Shallowing upwards succession from olive green shales to ripple-laminated carbonate sandstones. **(E)** Asymmetrical ripple bedforms on upper bedding plane of sandstones. Lens cap for scale is ~5 cm. **(F)** "Irregular" bedding planes in carbonate siltstones, possibly due to bioturbation. Flat bedding plane below lens cap contains numerous surface trails. **(G)** Light grey dolomitic mudstone with possible vertebrate tracks. **(H)** Grey dolomitic mudstone with flat-lying carbonate crust intraclasts.

**Fig. 5.1.1.3.** Carbonate lithofacies below the D-Bed in Firehole Canyon (Section FC, D1). **(A)** Bedded evaporites (lower, pinkish) and carbonate mudstones (white) below arkosic siliciclastics of the D-Bed (top). **(B)** Interbedded calciclastic sandstones and laminated mudstones. **(C)** Bedded evaporites with carbonate pseudomorphs. **(D)** Bedded evaporites with carbonate pseudomorphs (below) and bedded carbonates (above). **(E)** Intraclast conglomerate horizon (arrow) within bedded evaporite unit. **(F)** Bedded evaporites with carbonate pseudomorphs. **(G)** Bedding plane of very thinly bedded evaporites with carbonate pseudomorphs. Note very low amplitude bedforms. **(H)** Close-up of bedding plane shown in (G). **(I)** Laminated dark brown shales (weather grey) below bedded evaporite unit.

**Fig. 5.1.1.4.** Carbonate lithofacies above the D-Bed in Firehole Canyon (Sections FC, D1 and FC, D2). **(A)** Above the D-Bed in FC, D2, m ~20. **(B)** Close-up of calciclastic sandstone bed in (A) showing flat-lying intraclasts and planar-lamination. **(C)** Above the D-bed in FC, D1, m ~30.5. Bed preserves planar- to low-angle cross-lamination and full relief burrows. **(D)** Wavy- to flaser-bedded carbonates in FC, D1. **(E)** Low-amplitude symmetrical ripple bedforms above FC, D1. **(F)** Coarsening-upwards succession at the top of the D-Bed (FC, D1, m ~31.5). **(G)** Bedded carbonates at top of FC, D1 (m ~30). **(H)** Lenticular- and wavy-bedded carbonates near top of FC, D1 (m ~28.5).

**Fig. 5.1.1.5.** Carbonate lithofacies above the D-Bed in Firehole Canyon (Sections FC, D1 and FC, D2). **(A)** Bedding planes of bedded carbonates above FC, D1 (m ~30.5). **(B)** Desiccation cracks in carbonate sandstone. **(C)** Linear shrinkage-crack-like markings in carbonate sandstone above FC, D1. **(D)** Flat-lying carbonate intraclasts in bedded siltstone. **(E)** Cracked and bioturbated carboante siltstones. Arrow is showing portion of crack polygon with linear ridges. **(F)** Randomly oriented carbonate crust fragments, possibly disrupted by salt efflorescence. **(G)** Bedded siltstone with irregular bedding planes, possibly due to bioturbation. **(H)** Siltstone with reed impressions on upper bedding plane.

**Fig. 5.1.1.6.** Carbonate lithofacies above the D-Bed in Firehole Canyon (Sections FC, D1 and FC, D2). **(A)** Lenticular- and horizontal-bedded siltstones in FC, D1 (m ~27.5). **(B)** Thinly bedded carbonates above FC, D2 (m ~19.5). **(C)** Close-up of siltstones shown in (B). **(D)** Bedding plane of siltstones shown in (C). **(E)** Black, organic rich shale with black, possibly plant, fragments. **(F)** Interbedded mudstones and siltstones in FC, D2 (m ~17.3). **(G)** Interbedded black and dark reddish brown oil shale in FC, D2 (m ~20.2). **(H)** Mudstone and very fine-grained siliciclastic sandstones with desiccation cracks intercalated with wavy-bedded carbonates at top of FC, D1 (m ~31).

**Fig. 5.1.1.7.** Carbonate lithofacies above the E-Bed in Firehole Canyon. **(A)** The carbonate bench above the E-Bed (FC, E2, m ~32). **(B)** Close-up of contact between olive green mudstone and brown organic-rich mudstone (weathers white). **(C)** Surface texture on bedding plane of carbonate siltstone showing either 'bubble-like' texture or rounded crust fragments. **(D)** The carbonate bench above the E-Bed (FC, E1). **(E)** Low amplitude rounded symmetrical ripple beforms in thinly bedded siltstones. **(F)** Siltstone bedding plane with reddish possible organic detritus and reed impressions. **(G)** Dark grey and white mudstone with surface trails in white drape.

**Fig. 5.1.1.8.** Carbonate lithofacies with evaporite pseudomorphs above the E-Bed in Firehole Canyon. **(A)** Carbonate bench with evaporite pseudomorphs above FC, E2 (m ~34.5–37). **(B)** Close-up of light brown mudstone (m ~34.5). **(C)** Close-up of spherical structures (possible evaporite pseudomorphs) in sandstone. **(D)** Close-up of bedded carbonates with trona fan pseudomorphs. **(E)** Wavy-bedded calciclastic siltstones with drapes towards top of bench. **(F–G)** Thinly bedded evaporites with carbonate pseudomorphs at base of bench (m ~35).

**Fig. 5.1.1.9.** Carbonate lithofacies above the E-Bed in Firehole Canyon. **(A)** Grey-weathering dolomitic mudstones with whitish siltstones, possibly showing shallowing-upwards lake-cycles (FC, D2, m ~37–40). **(B)** Close-up of mudstones in lake-cycles. **(C)** Close-up of red-stained white mudstone. **(D)** Close-up of possible gymnosperm leaf (needle) impressions on light brown mudstone. **(E)** Top of the bench at FC, D2, m ~40. **(F)** Close-up of symmetrical ripple bedforms from FC, D2, m ~40. **(G)** Desiccation cracks in white drape. (H) Bubble-like texture preserved as positive features on upper bedding plane.

**Fig. 5.1.1.10.** The "white stripe" carbonate unit in the D-Bed at Firehole Canyon. **(A)** Outcrop view of the FC, D1 section showing carbonates below D at base, and the "white stripe" sandwiched between the sandstone units. **(B)** The "white stripe" unit in D1 showing sharp lower contact and gradational upper contact. **(C)** The lower contact of the "white stripe" in D1 with intraclast conglomerate at base. **(D)** Lacustrine carbonates of the "white stripe" and the upper contact with arkosic facies of D1. **(E)** The transition from lacustrine carbonates to massive siliciclastic mudstones to desiccation cracked mudstones (arrow).

**Fig. 5.1.1.11.** The "white stripe" carbonate unit in the A-Bed at Firehole Canyon (N). Refer to Table 5.1 for descriptions of the lithofacies shown. **(A)** The "white stripe" in the A-Bed. Note thickening at centre where deposited in shallow channel. Person for scale at left. **(B)** Close-up of the lower contact of the carbonate unit showing underlying topography in arkosic mudstones (dashed line). **(C)** Coal bed (dark brown) underlying bedded carbonate sandstones in shallow channel at base of "white stripe" unit. **(D)** Lacustrine carbonates and the upper contact of the "white stripe" unit. **(E)** Close-up of interbedded lacustrine mudstones and siltstones. **(F)** Close-up of transition to olive green marlstones. **(G)** Brownish olive green marlstones (at top) showing actual colour of rocks. **(H)** The upper contact of the "white stripe" in a laterally adjacent site. **(I)** Brown lacustrine carbonates of the "white stripe" with white shortite crystals.

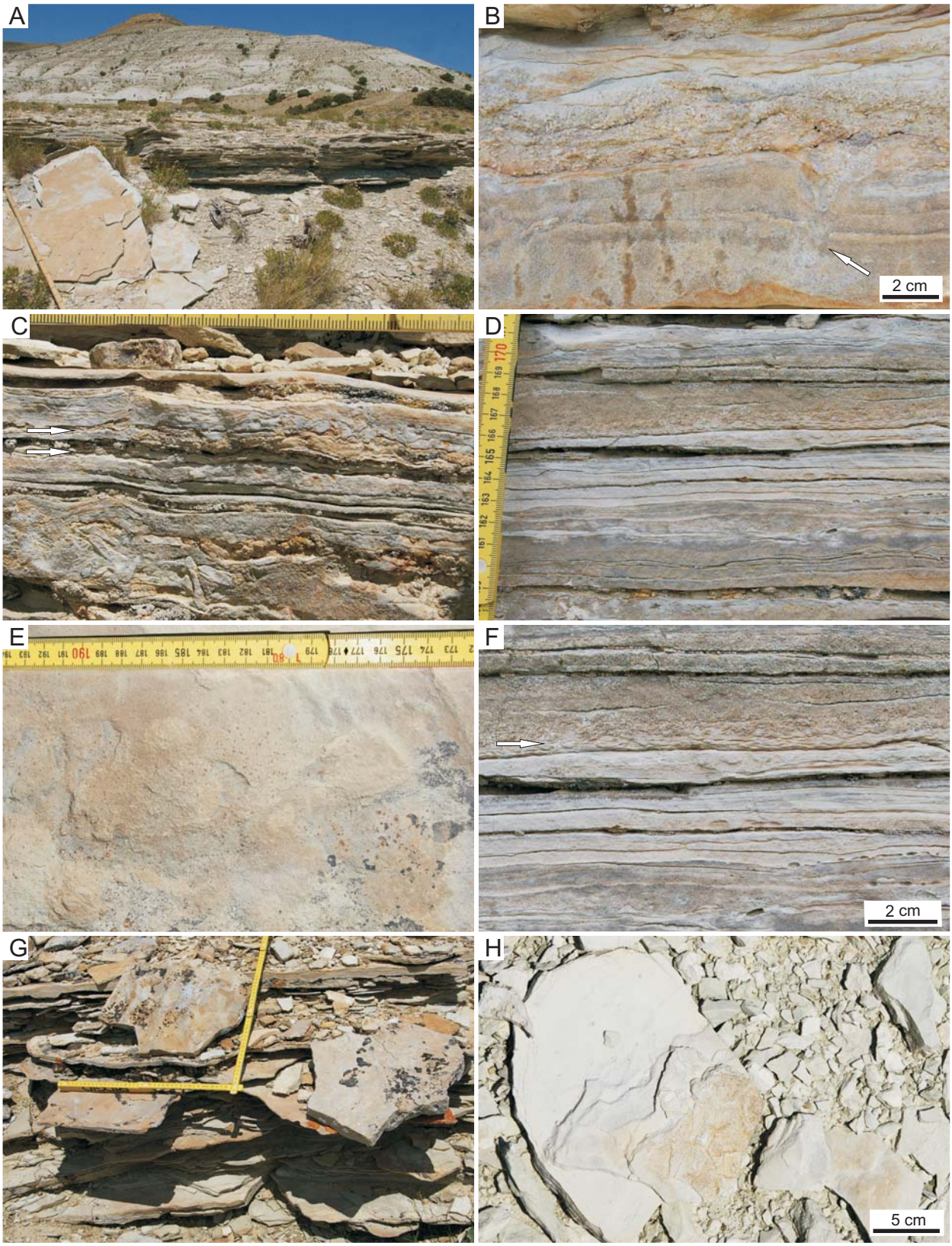


**Fig. 5.1.1.1.** Carbonate lithofacies from below the D-Bed at White Mountain, Kanda. Refer to Table 5.1 for descriptions of the lithofacies shown. See above for full caption.

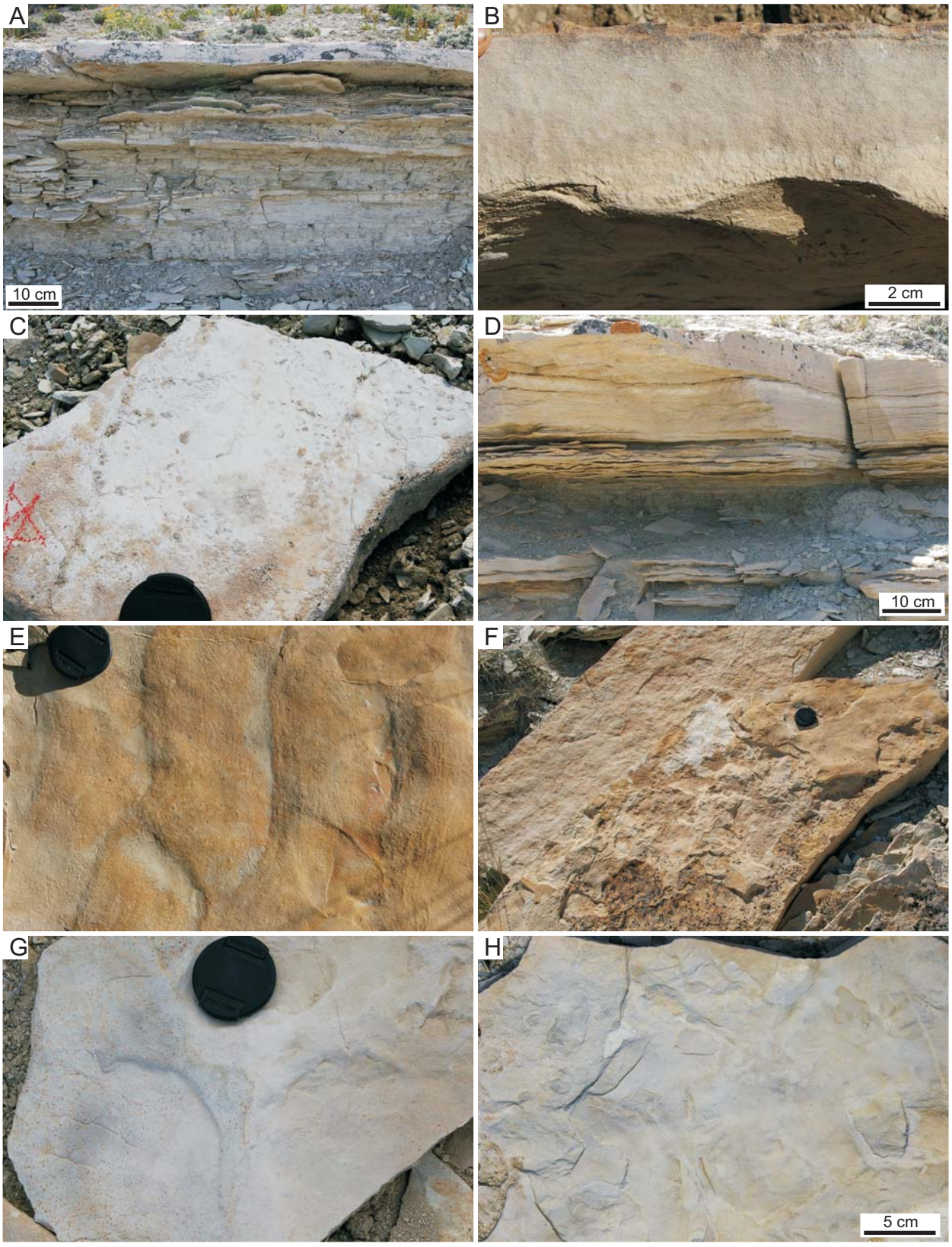


**Fig. 5.1.1.2.** Carbonate lithofacies from above the D-Bed at White Mountain, #18 Crossing site.
**Fig. 5.1.1.3.** (Next page) Carbonate lithofacies below the D-Bed in Firehole Canyon (Section FC, D1).

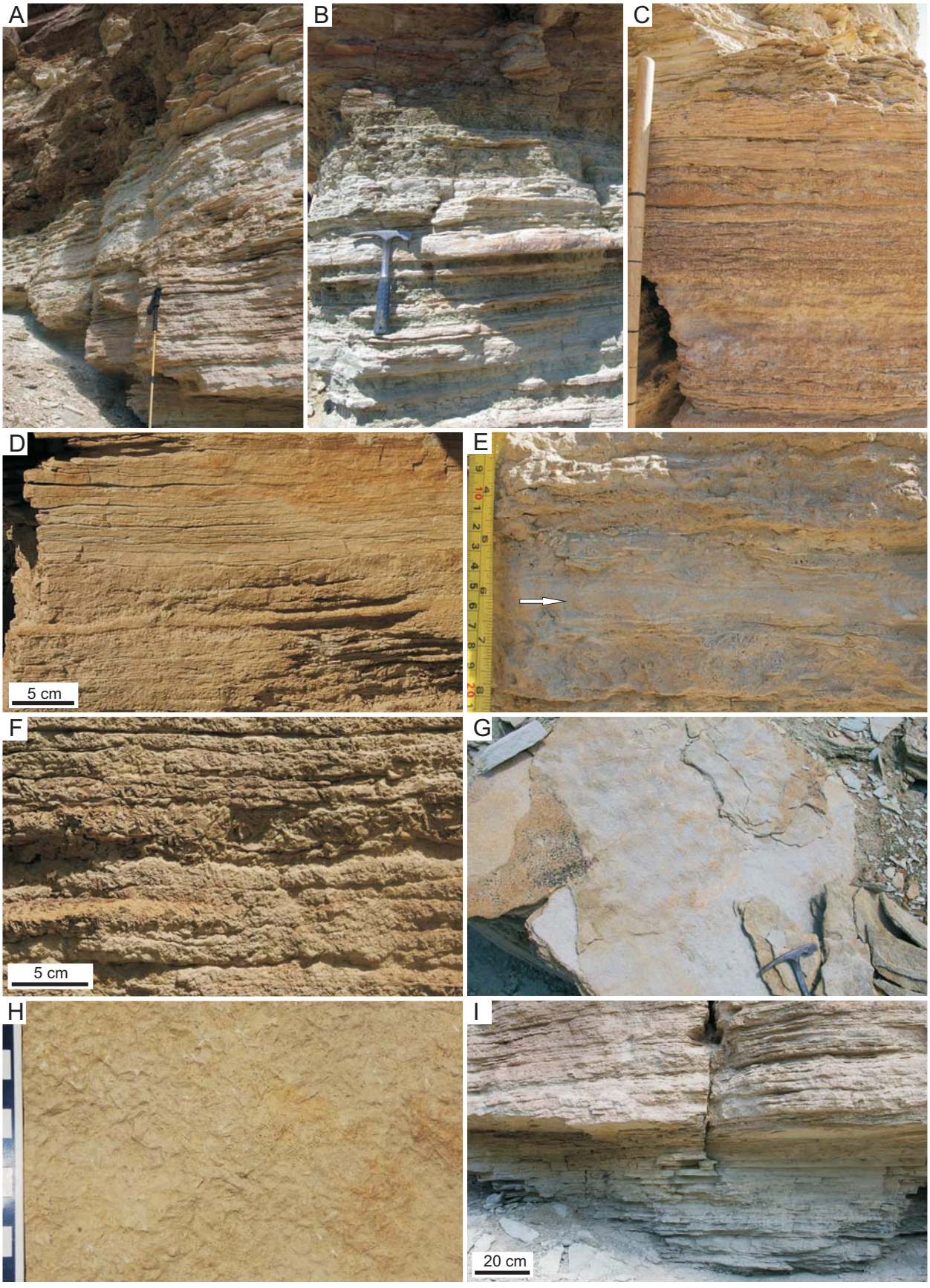
A
B
C
D
5 cm
E
F
5 cm
G
H
I
20 cm

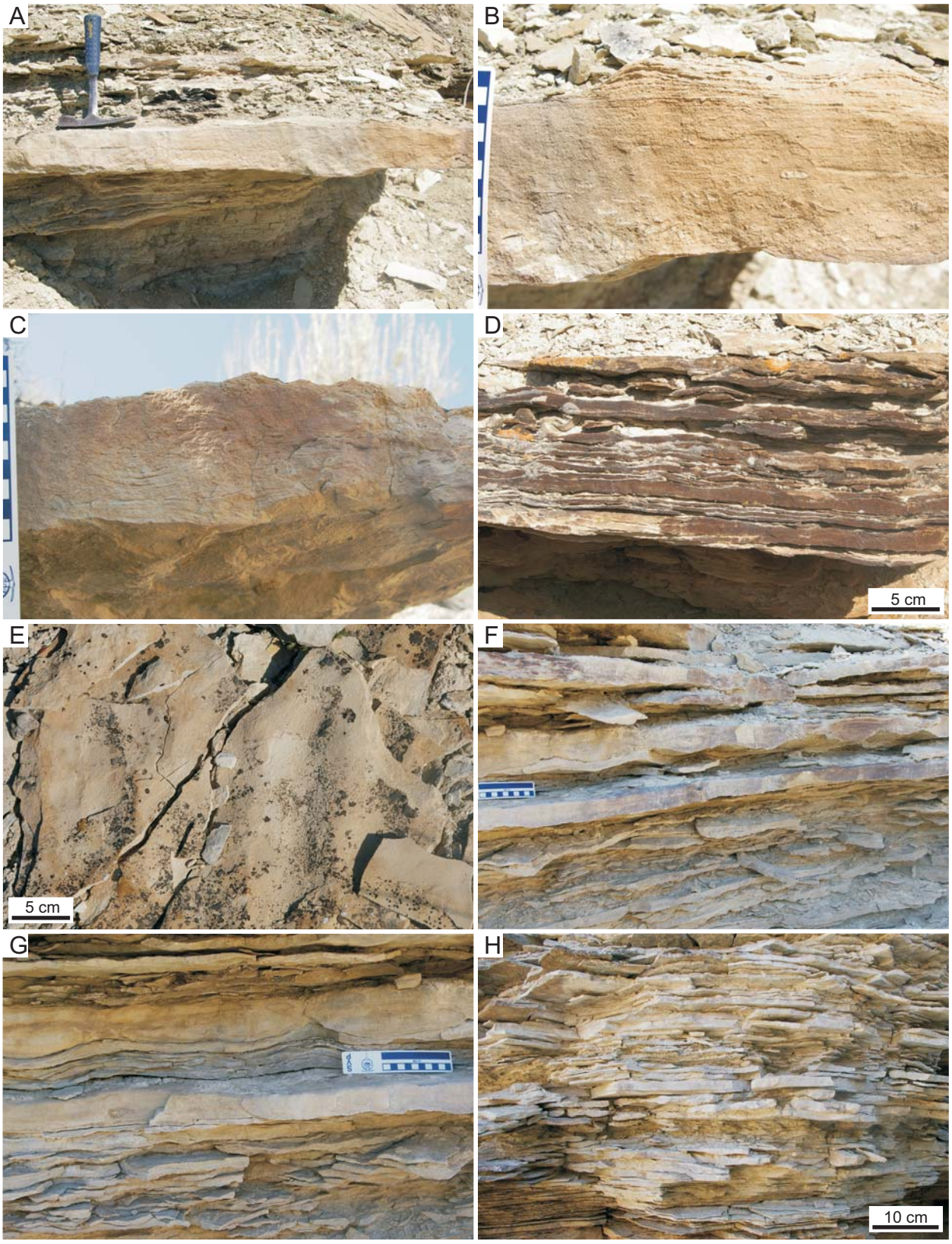


**Fig. 5.1.1.4.** Carbonate lithofacies above the D-Bed in Firehole Canyon (Sections FC, D1 and FC, D2). Refer to Table 5.1 for descriptions of the lithofacies shown. See above for full caption.

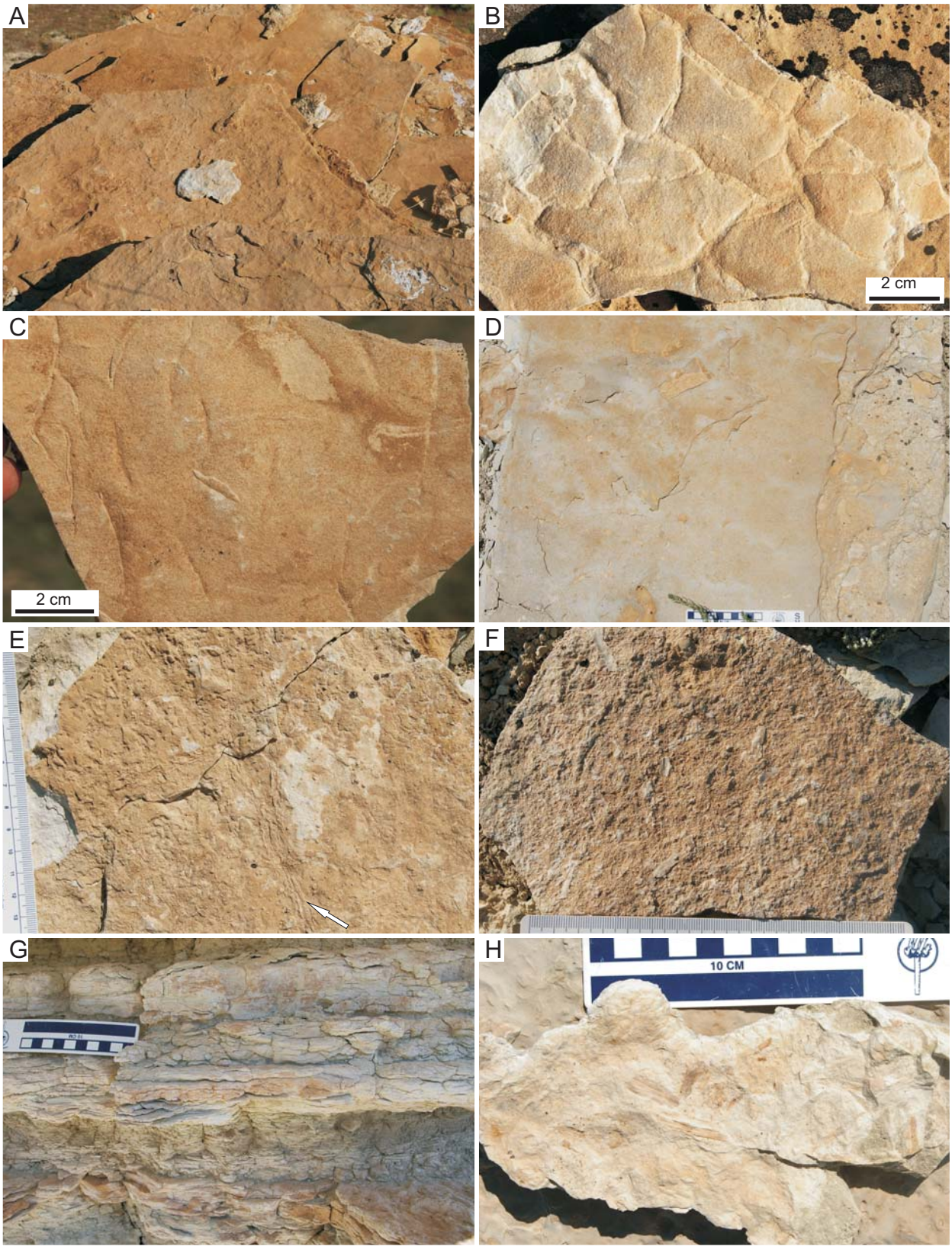


**Fig. 5.1.1.5.** Carbonate lithofacies above the D-Bed in Firehole Canyon (Sections FC, D1 and FC, D2). Refer to Table 5.1 for descriptions of the lithofacies shown. See above for full caption.

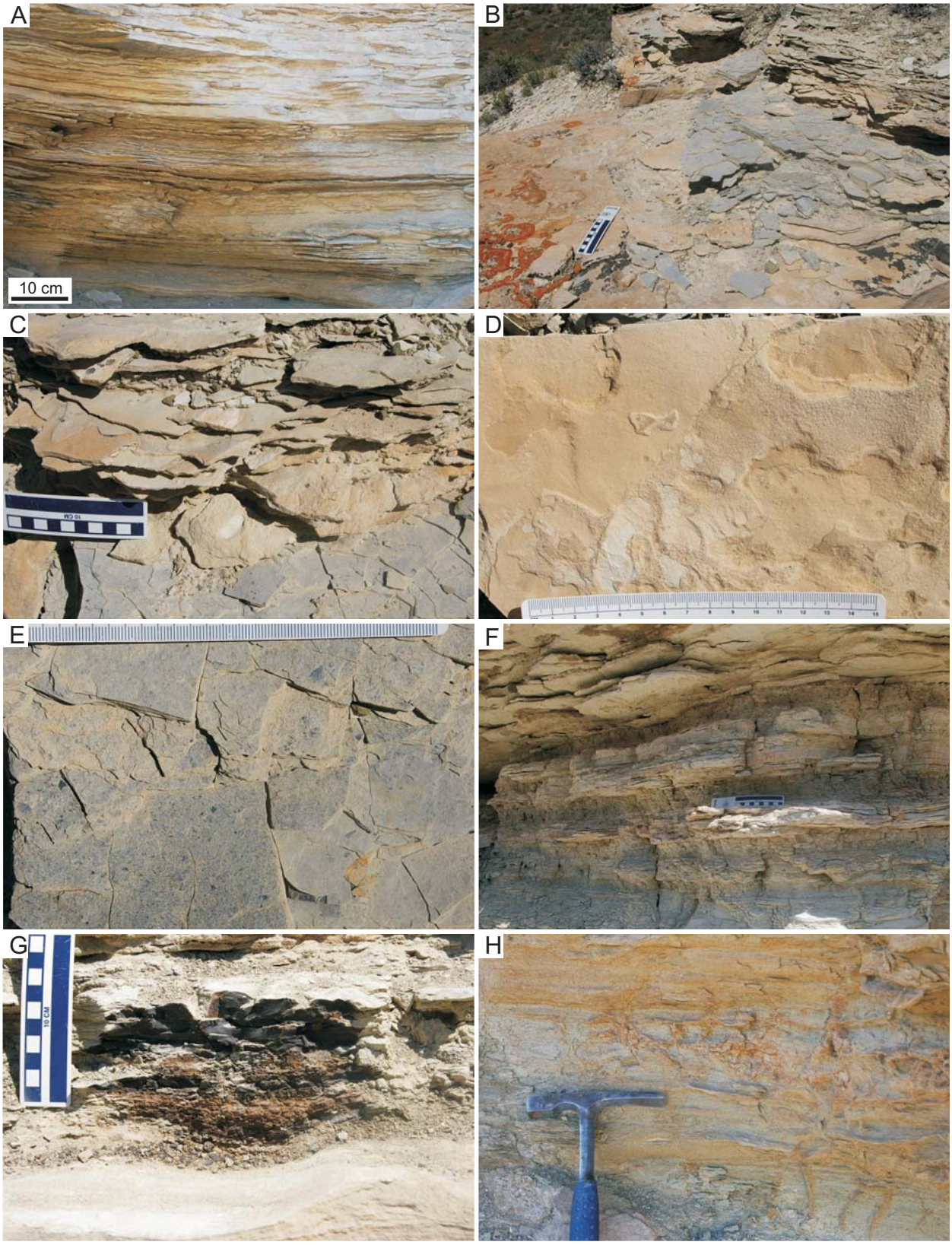


**Fig. 5.1.1.6.** Carbonate lithofacies above the D-Bed in Firehole Canyon (Sections FC, D1 and FC, D2). Refer to Table 5.1 for descriptions of the lithofacies shown. See above for full caption.

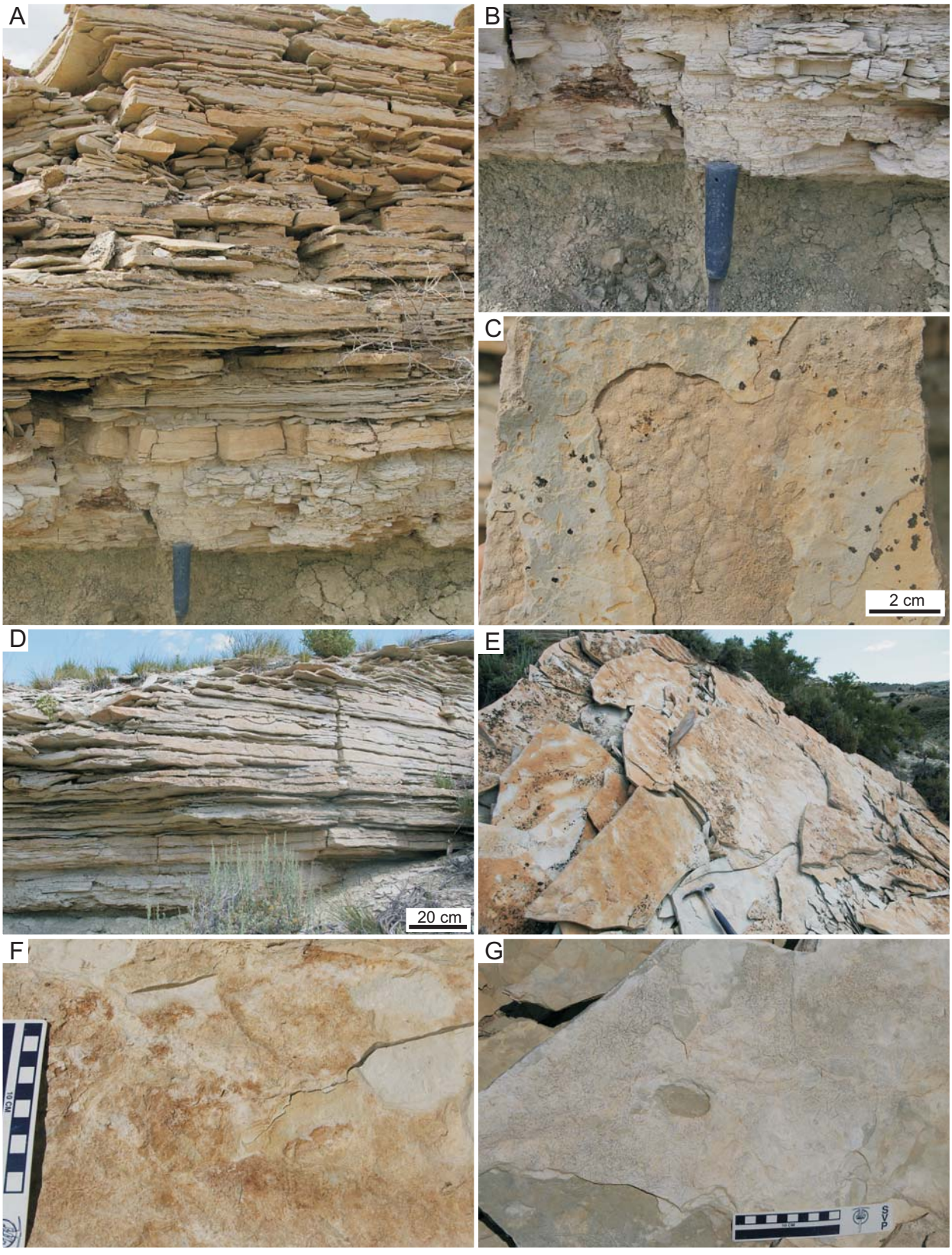


**Fig. 5.1.1.7.** Carbonate lithofacies above the E-Bed in Firehole Canyon. Refer to Table 5.1 for descriptions of the lithofacies shown. See above for full caption.

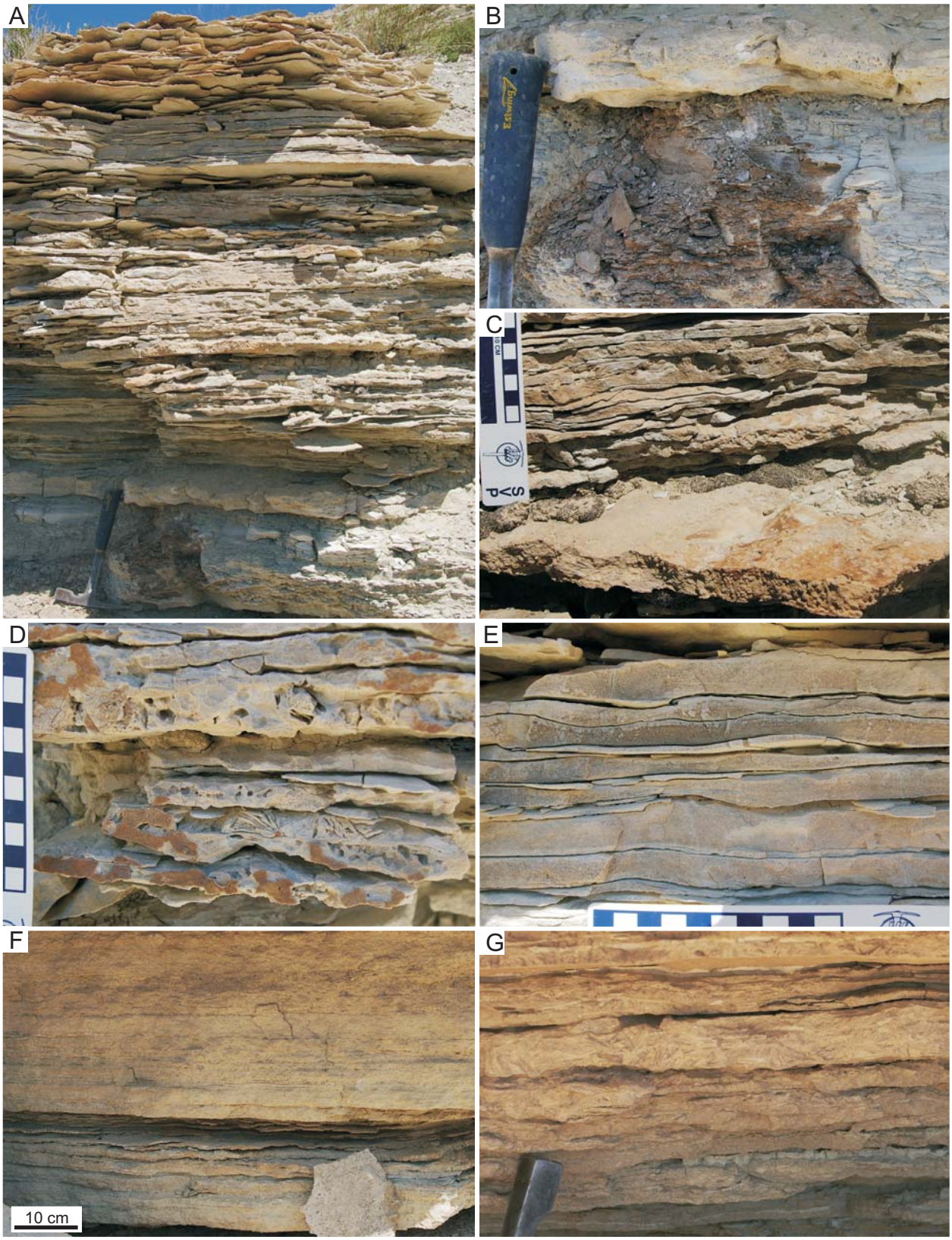


**Fig. 5.1.1.8.** Carbonate lithofacies with evaporite pseudomorphs above the E-Bed in Firehole Canyon. Refer to Table 5.1 for descriptions of the lithofacies shown. See above for full caption.

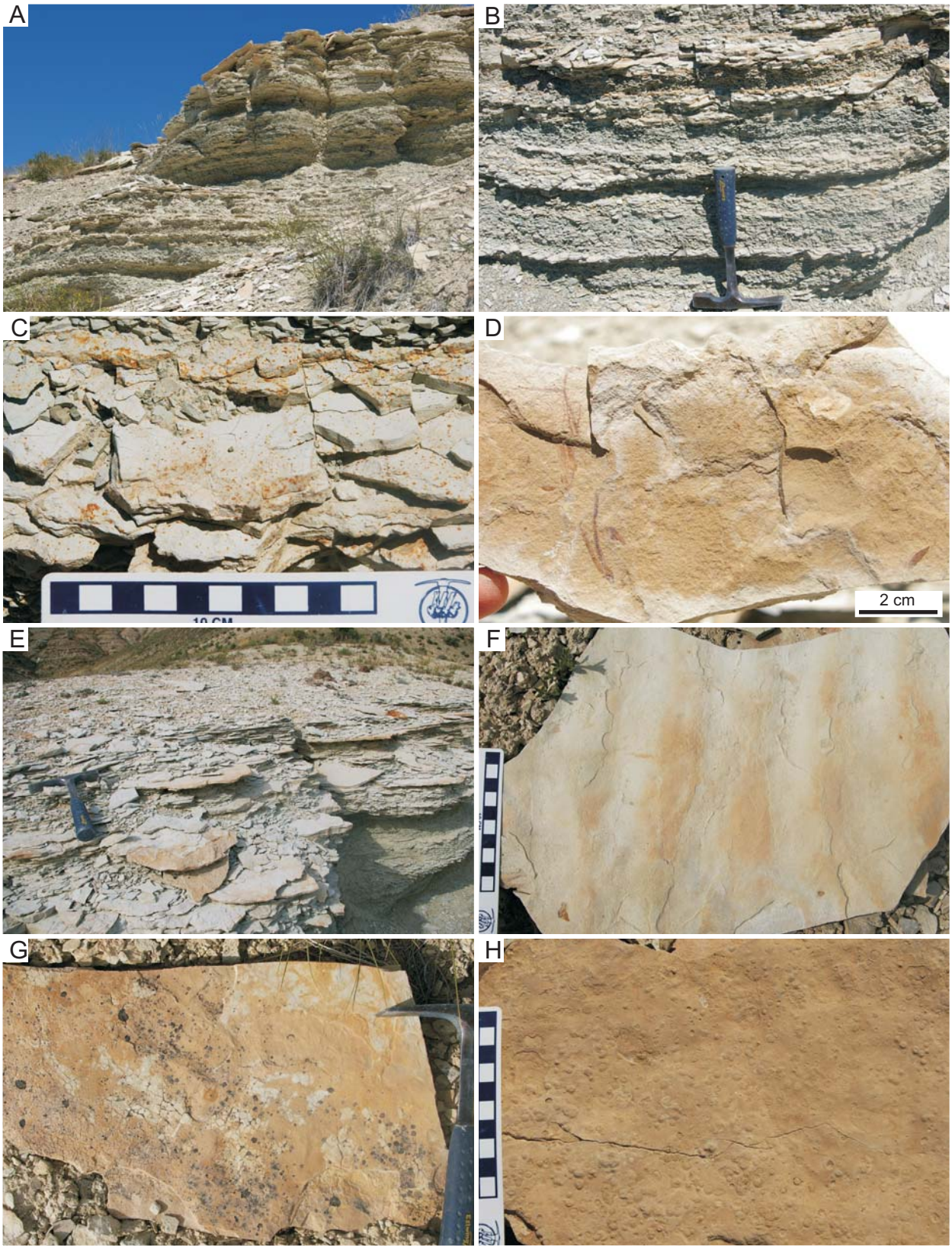


**Fig. 5.1.1.9.** Carbonate lithofacies above the E-Bed in Firehole Canyon. Refer to Table 5.1 for descriptions of the lithofacies shown. See above for full caption.

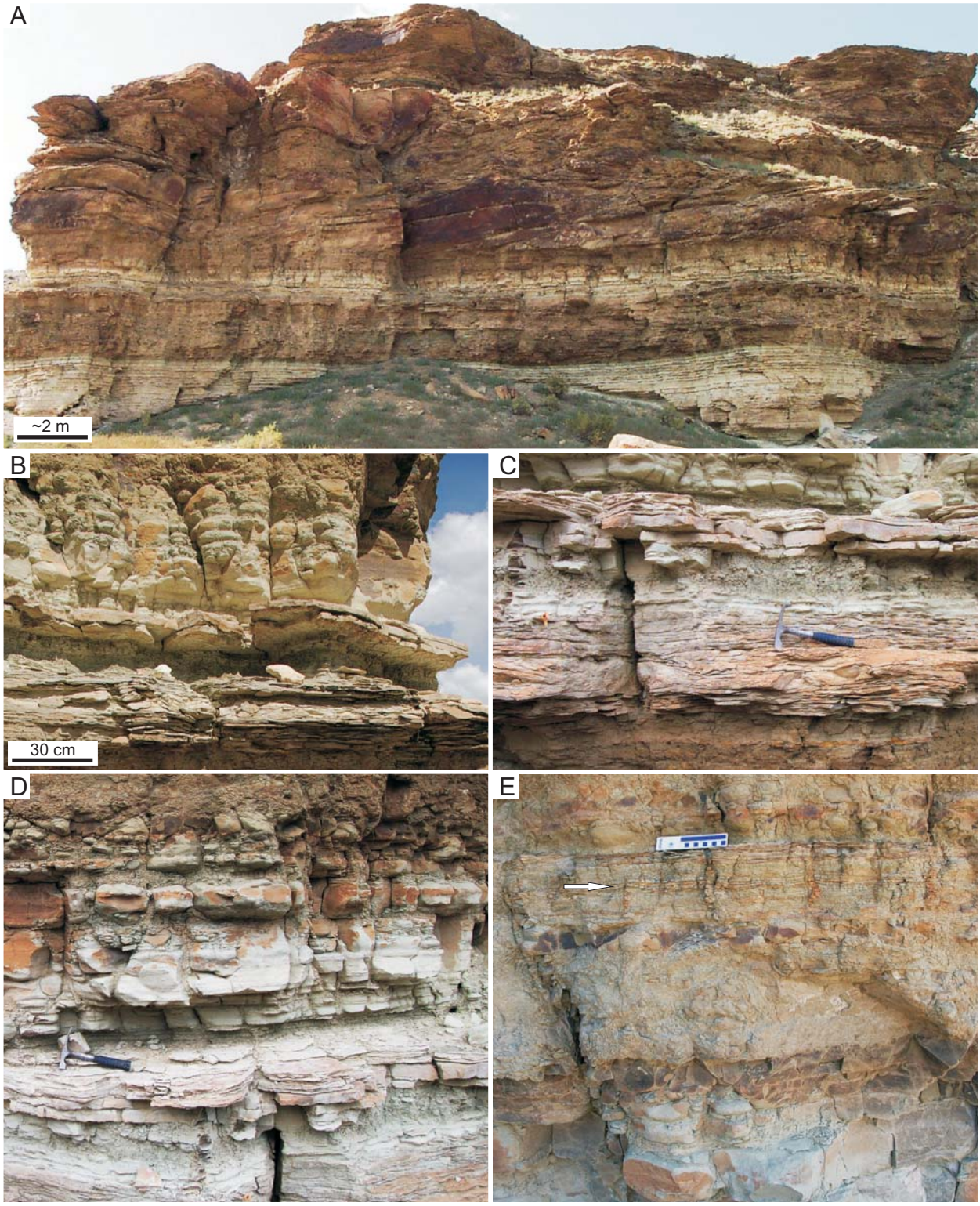


**Fig. 5.1.1.10.** The “white stripe” carbonate unit in the D-Bed at Firehole Canyon. Refer to Table 5.1 for descriptions of the lithofacies shown. See above for full caption.

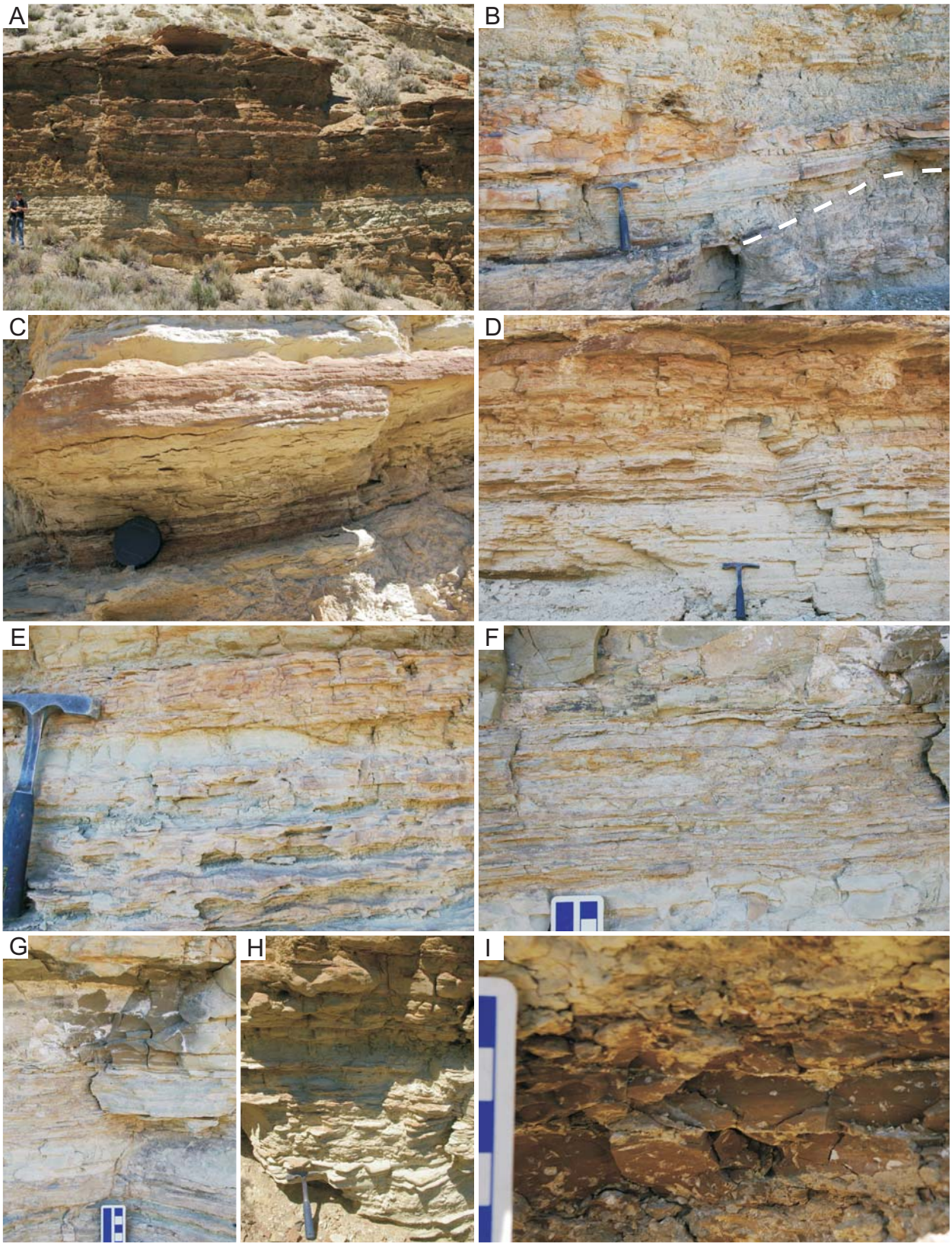


**Fig. 5.1.1.11.** The "white stripe" carbonate unit in the A-Bed at Firehole Canyon (N). Refer to Table 5.1 for descriptions of the lithofacies shown. See above for full caption.

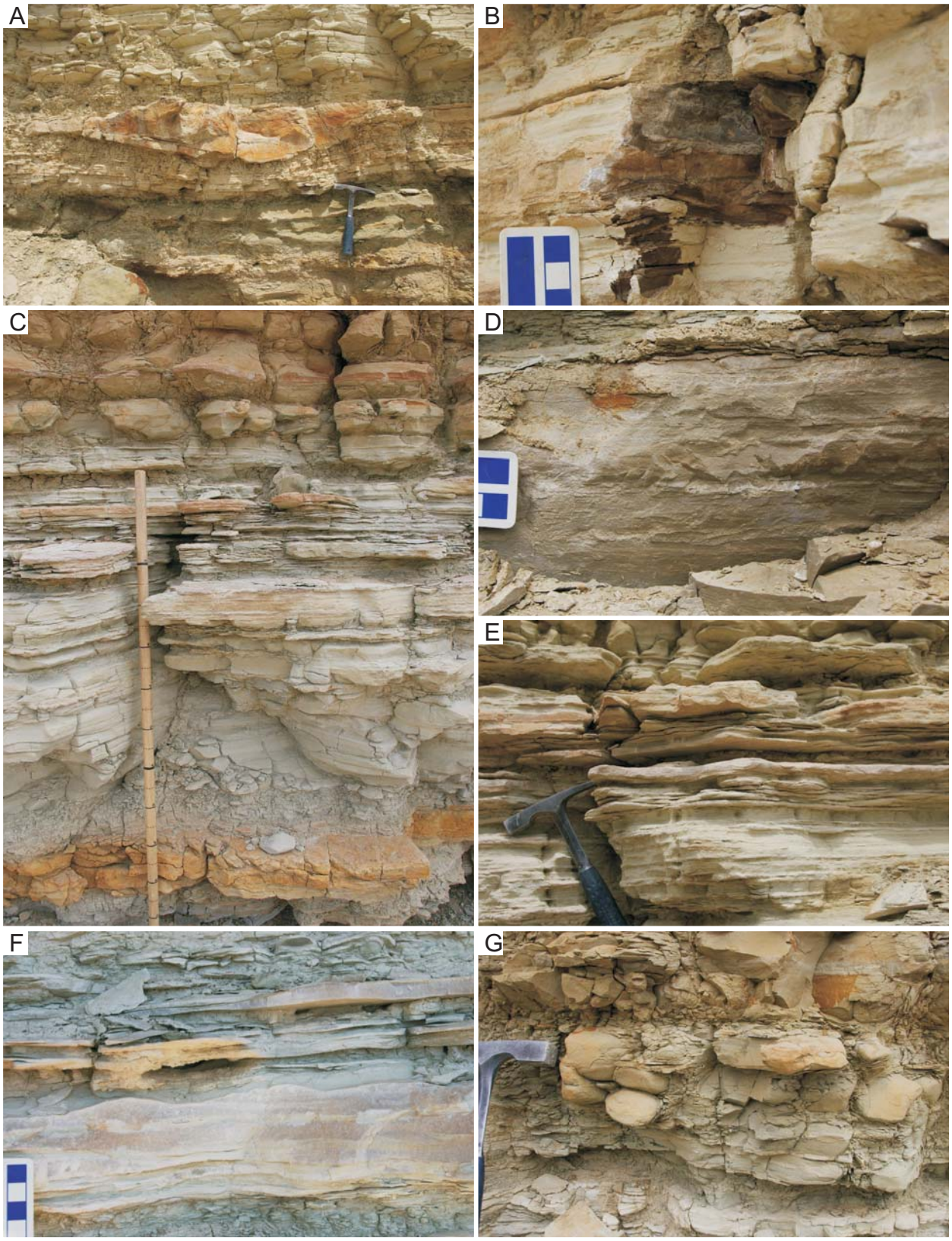


**Fig. 5.1.1.12.** The "white stripe" carbonate unit in the A-Bed at Middle Firehole Canyon. Refer to Table 5.1 for descriptions of the lithofacies shown. See next page for full caption.

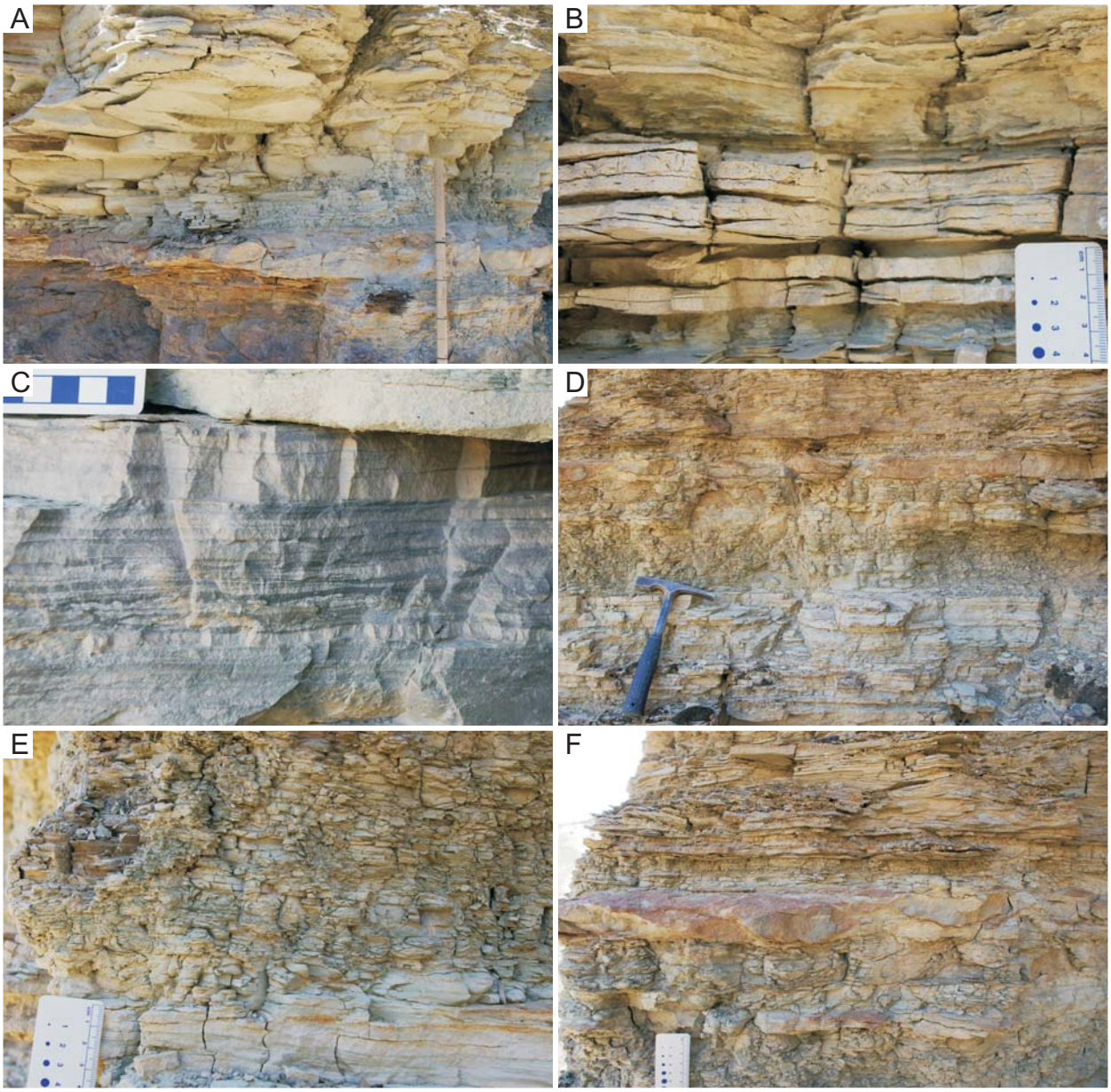


**Fig. 5.1.1.13.** The "white stripe" carbonate unit in the A-Bed at Sage Creek Canyon. Refer to Table 5.1 for descriptions of the lithofacies shown. **(A)** The lower contact of the "white stripe" showing dark brown laminated oil shale below and above the Second Tuff, grading upwards to light brown, massive mudstone. **(B)** Bedded siltstones with dissolved trona fans. **(C)** Close-up of wavy-bedded pink sandstones and grey siltstones. **(D)** The upper contact of the "white stripe" showing bedded marlstones. **(E)** Brown marlstones. **(F)** Interbedded marlstones and sandstones.

**Fig. 5.1.1.12.** (Previous page) The "white stripe" carbonate unit in the A-Bed at Middle Firehole Canyon. Refer to Table 5.1 for descriptions of the lithofacies shown. **(A)** The lower "white stripe" unit showing lens of the yellow-orange Second Tuff. **(B)** Close-up of dark brown organic-rich oil shale. **(C)** Coarsening upwards succession of the "white stripe" with bedded carbonates and marlstones at transitional upper contact. **(D)** Close-up of light brown bedded lacustrine carbonates at MFC, A, m ~4.2. **(E)** Lenticular- to wavy-bedded calcareous siltstone. Lower portion adjacent to hammer preserves burrows. **(F)** Close-up of calciclastic sandstones with oscillation ripple structures. **(G)** Transitional upper contact of the "white stripe" showing change in colour to marlstone.

*5.1.2. Descriptions of the Arkosic Siliciclastic Lithofacies of the A-Arkose Bed*

Lithofacies of the lowermost arkosic interval (the A-Bed) are described in Table 5.2. The figures that accompany the table are grouped together so that they can more easily be compared with lithofacies of the D-Bed (below). The numbers of the figures for A-Bed lithofacies begin with "*5.1.2.*". Stratigraphic sections of the A-Bed were measured in three localities: Middle Firehole Canyon (Fig. 5.3), Firehole Canyon (Fig. 5.4), and Sage Creek Canyon (Fig. 5.5). Arkosic mudstones, siltstones, and sandstones, and marl mudstones and siltstones dominate the lithofacies preserved in A-Arkose Bed (Table 5.2). Two main packages of siliciclastic sediments (~5–7 m thick) separated by thin packages of lacustrine carbonates (~1.5 m thick) that contain an orange-coloured tuff (the Second Tuff) were present in the three localities investigated. These The sections were divided into the lower unit, the "white stripe" unit, and the upper unit of the A-Bed for descriptive and comparative purposes. Each of the siliciclastic units contains smaller coarsening-upwards, regressive cycles. Lake-level changes operated on several time-scales due to changing climates and tectonic activity, leading to minor to major transgressions. Frequent transgressive/regressive cycles and difficulties in distinguishing between transgressions due to relatively short-term climate changes, longer-term climate changes, or tectonically controlled transgressions make it difficult to use sequence stratigraphic terminology to describe the cycles. Nevertheless, it appears that the A-Arkose Bed consists of two upward-shallowing, internally conformable, parasequences bounded by flooding surfaces that show a progradational stacking. The base of the "white stripe" unit is the flooding surface of the second parasequence. The contact between the top of the A-Bed and the overlying Wilkins Peak Member may represent a paraconformity in Middle Firehole Canyon with the hiatus represented by terrestrial bioturbation, and may be considered a sequence boundary that is overlain by lacustrine facies of a relatively major transgression of the lake.

**Table 5.2.** Lithofacies descriptions of arkosic sediments from the A-Arkose Bed, Basin Centre. Localities include Middle Firehole Canyon (MFC), Firehole Canyon (FC), and Sage Creek Canyon (SCC). The sections were divided into a lower unit, "white stripe" unit, and upper unit.

| Fig. | Lithology | Description | Comments; Trace suites (Chapter 6) | Interpreted Environment | Locality | Section, Metre |
|---|---|---|---|---|---|---|
| ***Lithofacies from the A-Bed, Middle Firehole Canyon*** | | | | | | |
| Fig. *5.1.2.*4C | Reddish buff granule-conglomerate | Reddish buff intraclastic granule-conglomerate preserved at base of scoured channel sandstone unit; oligomictic with mudstone intraclasts; geometry of conglomerate beds from wedge-shaped toes to lenticular-shaped cross-beds | Not associated with trace fossils | Distributary channel thalweg | Middle Firehole Canyon, A (E), upper unit | e.g., cf. MFC, A, m ~6.8 |
| Fig. *5.1.2.* 5G, 5H | Greyish buff fine-grained sandstone | Greyish buff-coloured fine-grained arkosic sandstone; internally climbing ripple-laminated and small-scale trough cross-laminated; preserves vertical burrows; upper unit of coarsening upwards channel deposits; upper bedding plane preserves sharp-crested, sinuous, low-amplitude asymmetrical ripple bedforms; bioturbated on upper bedding plane | Associated with insect appendage scratch-marks, meniscate backfilled burrows; Suites BC7, BC8A | Flat channel floor deposits of shallow distributary channel on delta-plain/floodplain | Middle Firehole Canyon, A, upper unit | e.g., MFC, A, m ~12.2–12.8 |
| Fig. *5.1.2.* 5D, 5E | Reddish buff fine-grained sandstone | Reddish buff fine-grained sandstone with light greyish blue mudstone drapes; internally small-scale trough cross-laminated, flaser bedded, and irregularly bedded due to bioturbation; preserves indistinct bioturbation and sharp-walled insect nest | Associated with insect nest, likely produced by ants; Suite BC8B | Subaerially exposed channel fill deposits | Middle Firehole Canyon, A, upper unit | e.g., MFC, A, m ~12 |
| Fig. *5.1.2.* 4D–F, 5A, 5F | Buff fine-grained sandstone | Buff-coloured fine-grained arkosic sandstone; internally ripple-laminated in very thin low-angle cross-beds; may preserve ripple-lamination, subcritical climbing ripple-lamination, and small-scale trough cross-lamination in inclined and horizontal bedsets; ripple lee-face dip direction downstream and perpendicular to dip of inclined accretion surfaces; lower contact slightly scoured into plane-bedded very fine-grained sandstone and laminated siltstones; some load structures; intercalated with pedogenically modified siltstones; east of section, channel scour cuts deeper, with conglomerate | Associated with vertical burrows originating from top bedding planes; top bed preserves iron-stained bunch-like root-marks; Suite BC3B | Point bar and channel fill deposits of shallow distributary channel on delta-plain/floodplain | Middle Firehole Canyon, A, upper unit | e.g., MFC, A, m ~9.5–10, m ~11.5–12 |
| Fig. *6.2.* 4A–C | Greyish buff silty very fine-grained sandstone | Greyish buff silty very fine-grained sandstone; wedge-shaped geometry; internally preserves ripple lamination at base and low-angle planar cross-lamination at top of wedge; bioturbated by the *Planolites* ichnofabric with surface trails on top laminated surface | Associated with *Planolites* ichnofabric and surface trails; Suites BC5A, 7 | Levee deposit of distributary channel | Middle Firehole Canyon, A (E), upper unit | e.g., cf. MFC, A, m ~10 |
| Fig. *5.1.2.* 2C, 2D, 2E | Buff very fine-grained sandstone | Light buff-coloured very fine-grained arkosic sandstone; gently climbing ripple-laminated, and flat beds internally ripple-laminated; frequently with siltstone, mudstone, or organic detritus drapes on bed tops; preserves deep vertical burrows and escape traces; fines upwards with upper contact transitional to | Associated with *Skolithos* ispp. and escape traces; Suite BC3A | Unconfined flow or weakly channeled flow on lower delta-plain | Middle Firehole Canyon, A (E), lower unit | e.g., cf. MFC, A, m ~1.5–2.5 |

| | | | | | | |
|---|---|---|---|---|---|---|
| | | structureless tan siltstone without reactivation surface; laterally, unit pinches out to greenish tan siltstone with desiccation cracks and dewatering structures; lower contact flat and slightly irregular, but not scoured, with underlying buff siltstone | | | | |
| Fig. *5.1.2.* 4F–H | Grey very fine-grained sandstone | Heterolithic grey very fine-grained mica-rich arkosic sandstone with buff-coloured mudstone drapes that weather red; preserves planar lamination and draped ribs-and-furrows of very low amplitude 3D ripple-lamination; coarsens upwards from dark greyish green pedogenically modified siltstone; plane beds preserve red- and black-stained bedding planes with bubbly, microbial mat texture | Preserves *Steinichnus* isp. on clay-draped bedding plane; associated with microbial mat textures; Suites BC7, BC8A | Distal to more proximal crevasse deposits on upper delta-plain/floodplain | Middle Firehole Canyon, A, upper unit | e.g., MFC, A, m ~8.7–9.5 |
| Fig. *5.1.2.* 3E–G | Light tan very fine-grained sandstone | Light tan-coloured very fine-grained arkosic sandstone; internal structures dominantly planar lamination, planar-cross lamination and ripple cross-lamination; contains minor tan siltstone interbeds; coarsens upwards from heterolithic facies below; overlain by dark greyish green pedogenically modified siltstone; preserves isolated set of relatively high angle lateral accretion surfaces that scour into and pinch out laterally to horizontal bedding; preserves deep desiccation cracks (~20 cm depth) | Associated with iron-stained, pellet-filled vertical burrows, irregular bedding due to bioturbation, and escape traces; Suites BC3, BC5B | Lower delta-plain with sedimentation from distal sheetfloods and/or distal crevasse deposits | Middle Firehole Canyon, A, upper unit | e.g., MFC, A, m ~6.8–8.3 |
| Fig. *5.1.2.* 3A–D | Tan siltstone and very fine-grained sandstone | Heterolithic, interbedded tan siltstone and silty very fine-grained sandstone; horizontally bedded; beds thin, ~0.5–4 cm thick; intercalated sandstone bedsets < ~15 cm thick preserve ripple- and planar-lamination and may have a lenticular geometry (~2 m width); siltstones laminated with iron-stained horizons; some horizons preserve graded beds with bluish light buff-coloured mudstone and iron-stained horizons; some beds preserve wavy bedding with bluish buff-coloured drapes; some sandstones preserve evidence of oscillatory flow, but ripple-lamination dominantly unidirectional; some ripple-laminae show swollen lens-sets and chevron upbuilding; lower contact gradational with interbedded and lenticular-bedded marl siltstone and calciclastic sandstone; unit coarsens upwards | Trace fossils not observed, bedding planes not visible | Wet lower delta-plain with standing water pools, sheetflood or distal crevasse sandstones, and thin lenticular channel sandstones | Middle Firehole Canyon, A, upper unit | e.g., MFC, A, m ~5–6.8 |
| Fig. *5.1.2.* 4D, 4F, 5A–C, 5H | Greenish light brown to bluish green siltstone | Greenish light brown to bluish green siltstone; horizontally bedded with vague discontinuous lamination and blocky breakage due to pedogenic modification; preserves horizons of carbonate root casts or nodules with iron-stained rinds; contains iron-stained horizons; may preserve desiccation cracks; intercalated with ripple- and planar-laminated channel sandstone bedsets; may be cross-bedded in abandoned channel fill deposit with scoured base | No trace fossils observed except root casts | Paleosol developed on upper delta-plain/floodplain overbank and abandoned channel deposits | Middle Firehole Canyon, A, upper unit | e.g., MFC, A, m ~8.5–8.8, m ~10.2–11.7 |
| Fig. *5.1.2.* 1E, 1G, 2B–C, | Tan siltstone | Tan-coloured arkosic siltstone (upper); internally structureless, discontinuously horizontally bedded, or laminated; totally bioturbated (BI=5) in places; some discrete burrows preserved in bioturbated horizon; appears mottled; laminated horizon preserves | Some discrete burrows in bioturbated unit; contains escape | Suspended load deposits on lower delta-plain to proximal delta- | Middle Firehole Canyon, A, lower and upper units | e.g., MFC, A, m ~2.2–2.8 |

| | | | | | | |
|---|---|---|---|---|---|---|
| 2F | | possible escape traces or bird tracks in cross-section; preserves scoured contact within siltstone, filled with vague trough cross-stratification; also grades upwards from climbing rippled very fine-grained sandstone east of measured section | traces and full relief burrows; Suite BC1 | front; associated with broad channel or sheetflood sandstones | | |
| Fig. *5.1.2.* 1A, 2F | Bluish green siltstone | Bluish green siltstone; internally massive with a mottled appearance; lower contact with tan siltstone irregular; lowest horizon of bed preserves carbonate nodules or root casts with iron-stained rinds; upper contact sharp with lacustrine carbonate mudstones | May be bioturbated; indistinct discrete burrow fills observed; Suite BC1 | Flooded delta-plain, possibly wetland; may signify first unit of lake transgression | Middle Firehole Canyon, A, lower unit | e.g., MFC, A, m ~2.6–2.9 |
| Fig. *5.1.2.* 4H | Bluish light green mudstone | Bluish light green mudstone, present as thin laminae and drapes on planar-laminated very fine-grained sandstones; preserves desiccation cracks in thin, graded beds | Associated with probable bird tracks; Suite BC5B | Distal sheetfloods or distal crevasse splays on delta-plain | Middle Firehole Canyon, A, upper unit | e.g., MFC, A, m ~7.2, m ~9.3 |
| Fig. *5.1.2.* 1C–G, 2A, 3A | Olive greenish tan marlstone | Olive greenish tan marlstone; internally structureless or laminated, lenticular-bedded, or low-angle planar cross-laminated; thinly (~3 cm thick) horizontally bedded with desiccation cracks < 5 cm deep; beds graded and laminated at bases; contains laminated crust-like (microbially stabilized?) horizons that preserve dewatering structures; brecciated horizons likely bioturbated; also preserves blackish small bones of fish (or gastropod radulae?); underlies and is adjacent (basinward) to climbing-rippled very fine-grained sandstone | Possibly preserves escape traces and bioturbation; associated with fish bones; Suite BC1 | Relatively freshwater littoral mudflat to lower delta-plain suspended load deposits | Middle Firehole Canyon, A, lower and upper units | e.g., MFC, A, m ~1–2.2, m ~4.8–5 |
| Fig. *5.1.2.* 1B, 1C, 3A | Light greyish green marlstone | Light greyish green marlstone; may be internally structureless with slightly mottled texture towards top; upper contact of lower structureless unit sharp and capped by thin bed of bioturbated pinkish grey siltstone | Associated with indistinct burrows and mottled texture; Suite BC1 | Muddy sublittoral to littoral lacustrine | Middle Firehole Canyon, A, lower and upper units | e.g., MFC, A, m ~ -1–1, m ~4.6–4.8 |
| ***Lithofacies from the A-Bed, Firehole Canyon; descriptions below include exposures from Firehole Canyon (North)*** | | | | | | |
| n/a | Orangish tan fine-grained sandstone | Orangish tan fine-grained arkosic sandstone forming channel sandstone body with scoured lower contact; contains large-scale tangential lateral accretion surfaces | Not investigated for trace fossils | Distributary channel on delta-plain | Firehole Canyon, A (N), upper unit | e.g., cf. FC, A, m ~14–15 |
| Fig. *5.1.2.* 8A | Greyish buff fine-grained sandstone | Greyish buff fine-grained sandstone that weathers red; internally ripple-laminated to climbing ripple-laminated; internal geometry of bedsets may show lateral accretion surfaces; bed contacts sharp with scoured bases; bed geometry shows isolated and connected lenses ~30–70 cm thick and ~2–6 m wide, with lateral sandstone beds ~10 cm thick; intercalated with laminated siltstone | Not investigated for trace fossils | Shallow distributary channels on delta-plain | Firehole Canyon, A, upper unit; also at FC, A (N) | e.g., FC, A, m ~9<br><br>e.g., cf. FC, A, m ~8.5–15 |
| Fig. *5.1.2.* 8D | Reddish and greyish buff fine-grained sandstone | Reddish and greyish buff-coloured, micaceous, fine-grained arkosic sandstone; thinly bedded (~3–5 cm thick); some individual beds with lenticular geometry; adjacent to and interbedded with laminated light tan siltstones; beds may fine upwards to light tan mudstone drapes < 1 cm thick | | Weakly channelized flow on lower delta-plain; possibly represents distal crevasse | Firehole Canyon, A, upper unit | e.g., FC, A, m ~12–12.4 |

| | | | | | | |
|---|---|---|---|---|---|---|
| Fig. *5.1.2.* 7B–H | Greyish buff very fine-grained sandstone | Greyish buff very fine-grained arkosic sandstone that weathers red; internally ripple-laminated and climbing ripple-laminated; lowermost unit of the A-Bed; lower contact sharp and horizontal, not scoured; unit sits directly on massive, greyish light green mudstone of main lake carbonates without evidence of exposure; ripple-laminated sandstone ~30 cm thick; unit fines upwards to massive and discontinuously laminated light buff-coloured very fine-grained sandstone and finally to massive greyish light green massive marl mudstone; lateral variation of this unit may include lenticular sandstones with decimetre-scale cross-lamination and concave-up scours downstream | Not associated with trace fossils | Possibly underflow deposits of delta front; fines upwards to massive marl mudstone | Firehole Canyon, A (N), lower unit | e.g., cf. FC, A, m ~1, m ~2.5 |
| Fig. *5.1.2.* 8G | Orangish tan very fine-grained sandstone | Tan to orangish tan very fine-grained arkosic sandstone; internal structure variable, from poorly bedded with irregular bedded to ripple cross-laminated; preserves iron-stained root marks; bedding planes may preserve flat-topped symmetrical ripple bedforms that are straight to slightly sinuous, parallel, and not bifurcated; forms upper facies of coarsening upwards successions; bedding planes may preserve very thin mudstone drapes with desiccation cracks | Possibly bioturbated but no discrete burrows observed | Crevasse deposits or distal sheetfloods into freshwater ponds on delta-plain | Firehole Canyon, A, upper unit | e.g., FC, A, m ~14.0–15.2, m ~10.5–11.2 |
| Fig. *5.1.2.* 9F–H | Buff very fine-grained sandstone | Buff-coloured very fine-grained arkosic sandstone; preserves large-scale trough cross-stratification; internally, trough cross-stratified bedsets may grade upwards from planar laminated to ripple-cross laminated; adjacent wedge-shaped bedset with flat base onto desiccated mudstone fines upwards from low-angle cross-laminated very fine-grained sandstones to climbing-rippled very fine-grained sandstones with dark-coloured ripple drapes | Possibly associated with indistinct simple burrows of Suite BC1 or BC5A; similar facies with channel sandstone at top of lower unit of FC, A | Channel cut and fill and overbank deposits on lower delta-plain; shows lateral differences with measured section | Firehole Canyon, A (N), upper unit | e.g., cf. FC, A, m ~8.5–10.5 |
| Fig. *5.1.2.* 8B, 8D, 8E, 8F | Light tan very fine-grained sandstone | Light tan-coloured very fine-grained to fine-grained arkosic sandstone; flat beds ~2–5 cm thick; may preserve planar lamination internally; beds horizontal with flat bases and often irregular upper contacts; may contain irregular, bioturbated laminae towards tops of beds; may be interbedded with flat, laminated beds of bluish green mudstone or contain bluish green mudstone drapes on bedtops; may contain iron-stained root marks and reddish black stained bedding planes; drapes may be gently undulating to wavy; may preserve flute marks on lower bedding planes and flow-scoured bird footprints | May be bioturbated by the *Planolites* ichnofabric; associated with desiccation cracks and bird footprints; Suites BC5A, BC5B | Crevasse deposits or distal sheetfloods onto freshwater mudflat with standing water or pond on delta-plain; frequently desiccated | Firehole Canyon, A, upper unit | e.g., FC, A, m ~12.5–13.9 |
| Fig. *5.1.2.* 6E–H | Light buff very fine-grained sandstone | Light buff-coloured very fine-grained arkosic sandstone; internally planar-laminated at base, grading upwards to to ripple-laminated, grading to climbing ripples and brownish olive to bright green siltstone; lower contact sharp and scoured, preserving tool marks and desiccation cracks as casts; bed geometry “lunate sigmoidal”, with gently curved channel margin scour and dominantly flat, horizontal to slightly dipping base; | Possibly preserves horizontal traces in convex hyporelief on bottom contact; similar facies to upper unit of FC, A (N) | Terminal distributary channel of proximal delta front or lower delta-plain | Firehole Canyon, A, lower unit | e.g., cf. FC, A, m ~4–6 |

| | | | | | | |
|---|---|---|---|---|---|---|
| | | thickness of bedset < 2 m; > 20 m wide; upper contact of green siltstone with sublittoral lacustrine mudstones | | | | |
| Fig. *5.1.2.* 9A–D | Olive greenish buff muddy very fine-grained sandstone and greyish olive green siltstone | Olive greenish buff-coloured muddy very fine-grained sandstone; lowermost sandstone unit of upper unit in FC (N); flat base; overlies greyish olive green mudstones that overly lake carbonate unit; sandstones pinch out laterally with wedge-shaped geometry; bottomsets ripple-laminated or climbing ripple-laminated, grading to convolute lamination with flame structures and massive topsets; bedsets fine upwards slightly; unit fines upwards to bedded brownish olive green siltstones; lower contact preserves desiccation crack casts | Associated with "open spheres", representing dissolved shortite; lower contact preserves possible *Planolites* of ?Suite BC1 | Distal sheetflood or crevasse sandstone into shallow muddy marginal lacustrine (of main lake); could be considered proximal delta-front | Firehole Canyon, A (N), upper unit | e.g., cf. FC, A, m ~8.2 |
| Fig. *5.1.2.* 8B, 8C | Light tan muddy siltstone (with bluish light green mudstone) | Light tan-coloured, massive to laminated muddy siltstone; may contain laterally continuous iron-stained horizons; interbedded with lenticular beds of fine-grained mica-rich arkosic sandstones; beds fine upwards slightly to bluish light green mudstone; fining upwards beds may preserve laminated, brown, very fine-grained (lower) sandstone; units may preserve deep iron-stained fractures (< ~50 cm) | Bedding well preserved, not bioturbated; preserves deep desiccation fractures | Distal sheetfloods or crevasse splays into flooded freshwater mudflat or pond on delta-plain | Firehole Canyon, A, upper unit | e.g., FC, A, m ~11.4–12.4 |
| Fig. *5.1.2.* 9A, 9B, 9E, 9F | Brownish green to buff-coloured siltstone | Brownish green to buff-coloured siltstone in thin (~3–12 cm thick), flat horizontal beds that are graded from discontinuously laminated or ripple-laminated buff siltstone and very fine-grained sandstone; within bedset, ~2 m thick, beds fine upwards and become thinner upwards; top of bedset desiccated, with large cracks preserved as casts on base of overlying sandstone; lower contact of unit both transitional with massive greyish olive green mudstone overlying lake beds; also overlies climbing-rippled very fine-grained sandstone | No trace fossils observed; facies also preserved in lower A-Bed at Sage Creek Canyon; facies directly overlies transitional greyish olive green mudstone | Deposition from pulses of waning flow and suspension; may represent delta-top mudflat to delta-front | Firehole Canyon, A (N), upper unit | e.g., cf. FC, A, m ~8–9 |
| Figs. *5.1.2.* 8B, 8C | Olive green mudstone and very fine-grained sandstone | Massive olive green arkosic mudstone with very thin (~1 cm thick) very fine-grained arkosic sandstone interbeds; sandstone beds internally ripple-laminated; sandstone beds preserve iron-stained marks; carbonate root cast with iron-stained rind preserved within massive muddy siltstone; facies coarsens upwards to poorly bedded very fine-grained sandstone | No trace fossils observed | Muddy shallow lake or interdistributary pond on delta-plain with distal sheetflood or crevasse deposits | Firehole Canyon, A, upper unit | e.g., FC, A, m ~9.5–10.2 |
| Fig. *5.1.2.* 6C | Brownish olive to bright green siltstone | Massive brownish olive siltstone changing upwards to bright green siltstone; uppermost siltstone of lower unit; may preserve iron-stained possible root-marks; bed may fine upwards to green silt from climbing-rippled very fine-grained sandstone at base of bedset | May preserve iron-stained root marks | Wet delta-plain flooded by main lake; wetland siltstones of lower delta-plain | Firehole Canyon, A, lower unit; FC, A (N) lower unit | e.g., cf. FC, A, m ~5.5–6 |
| Fig. *5.1.2.* 9B; *5.1.1.* 11D–H | Brownish and greyish olive green mudstone | Massive to vaguely horizontally bedded brownish and greyish olive green mudstone; transitional lower contact with "white stripe" carbonate unit of main lake; lower portion lenticular bedded with calciclastic sandstone lenses or interbedded with ripple-laminated calciclastic sandstones; lower contact may be | Not associated with trace fossils | Shallow muddy littoral to eulittoral with arkosic input; may be lateral to channel or | Firehole Canyon, A (N), upper unit | e.g., cf. FC, A, m ~7.8–8.4 |

| | | | | | | |
|---|---|---|---|---|---|---|
| | | sharp and sit directly on calciclastic sandstones; upper contact with brownish green bedded siltstone | | basinward of channel mouth | | |
| Fig. *5.1.2.* 8B–E | Bluish light green mudstone | Laminated bluish light green arkosic mudstone; may form flat, continuous beds ~1–1.5 cm thick or form thin to thick drapes (0.2–0.5) on very fine-grained sandstones; interbedded with very fine-grained to fine-grained arkosic sandstones; typically preserves desiccation cracks and bird footprints; may preserve bubbly, likely microbial, surface textures and horizontal traces | Associated with shorebird footprints, horizontal trails and tunnels, and desiccation cracks; Suite BC5B | Suspension fall-out deposits of freshwater mudflat with standing water or interdistributary pond on delta-plain | Firehole Canyon, A, upper unit | e.g., FC, A, m ~12.5–13.9 |
| Fig. *5.1.2.* 6B–F | Brownish green to light green and light tan siltstone and mudstone | Light green and light tan mudstone and siltstone; forms medium-thickness (~30–40 cm), horizontal to slightly dipping, parallel, graded beds from laminated siltstone in lower ~10 cm, to massive mudstone, to desiccated uppermost contact; desiccation cracks ~5 cm deep and filled with siltstone from overlying bed; scoured by lenticular channel at towards top of unit, ~50 cm depth, ~3 m width; channel fill of fining upwards thin beds of laminated mudstone and siltstone; upper contact laterally variable, may be sharp and flat planar-laminated channel sandstone or may be irregular with green siltstone | No trace fossils observed, but upper contact of unit preserves possible horizontal burrows preserved in convex hyporelief; very similar facies in lower MFC, A and SCC, A | Distal delta front deposits with subaerially exposed bedset tops; preserves siltstone-filled sub-lacustrine delta-front channel; part of coarsening upwards prograding delta-front | Firehole Canyon, A, lower unit | e.g., FC, A, m ~1–5.5 |
| Fig. *5.1.2.* 7D, 7E, 7G. 7H | Greyish light green mudstone | Massive greyish light green mudstone; may be marlstone, but not tested for carbonate content; present in fining-upwards thick beds of discontinuously laminated to ripple-laminated light buff muddy very fine-grained arkosic sandstone or ripple-laminated and climbing-rippled sandstone that sits sharply on massive greyish light green mudstone of main lake | No trace fossils observed | Possibly represents prodeltaic lacustrine, or sublittoral lacustrine lateral to terminal distributary channel | Firehole Canyon, A (N), lower unit | e.g., cf. FC, A, m ~ 1.5–2.3 |
| Fig. *5.1.1.* 11B–C | Dark brown to black silty coal | Dark brown to blackish brown laminated silty coal horizon ~5 cm thick; preserved as thin lens within shallow channel scour at top of lower unit | No trace fossils observed | Coaly layer in low lying channel of delta-plain | Firehole Canyon, A (N), lower unit | e.g., cf. FC, A, m ~5.5 |
| ***Lithofacies from the A-Bed, Sage Creek Canyon*** | | | | | | |
| Fig. *5.1.2.* 11A | Orangish tan fine-grained sandstone | Orangish tan fine-grained arkosic sandstone; internally ripple-laminated; lower contact scoured; correlative unit shows deep scour and high angle cross-bedded lateral accretion surfaces | No trace fossils observed | Proximal overbank deposits | Sage Creek Canyon, A, upper unit | e.g., SCC, A, m ~11.5–12 |
| Fig. *5.1.2.* 11A, 11C–D | Light buff fine-grained sandstone | Light buff-coloured fine-grained arkosic sandstone; forms thick bed with ripple lamination and trough cross-stratification at base; large-scale convolutions at top that do not affect overlying siltstone and sandstones; lower part preserves medium-thick stacked bedsets of downstream-dipping dune-scale cross-lamination as bottomsets, slightly downward dipping ripple cross-lamination and planar lamination as topsets; internal structure oriented perpendicular to lateral accretion surfaces of sandstone; lower contact slightly scoured to flat and overlies planar-laminated very fine-grained sandstones; preserves small holes, possibly bioturbation, eroded mudballs/pellets?, or shortite molds | Associated with “small holes” bioturbation or shortite molds; cf. Suite BC3A | Rapid deposition of channel bars in possible terminal distributary channel; syndepositional convolute bedding | Sage Creek Canyon, A, upper unit | e.g., SCC, A, m ~6–7.2 |

| | | | | | | |
|---|---|---|---|---|---|---|
| Fig. *5.1.2.* 10E | Orangish buff fine-grained sandstone | Orangish buff-coloured fine-grained arkosic sandstone; weathers dark red; bed geometry lenticular with low-angle accretion surfaces; scoured lower contact into buff-coloured siltstone; internally preserves planar-cross lamination in opposite directions, small-scale trough cross-lamination, planar-lamination, and may be bioturbated with vague irregular bedding; preserves trace fossils originating from upper surface of bed | Associated with pellet-filled *Skolithos* and cf. *Thalassinoides* isp. B in firm substrate; Suites BC3A, BC3B | Exposed shallow channel on lower delta-plain | Sage Creek Canyon, A, lower unit | e.g., SCC, A, m ~1.2 |
| Figs. *5.1.2.* 11E; *6.2.* 16A–B | Light buff very fine-grained sandstone | Light buff-coloured very fine-grained arkosic sandstone; internally preserves ripple-lamination in slightly downward-dipping thin cross-beds and small-scale trough cross-lamination; interbedded with flaser-bedded muddy very fine-grained sandstone; preserves small open holes | Associated with “small holes” bioturbation or shortite molds; cf. BC3A | Levees or channel bars of distributary channel | Sage Creek Canyon, A, upper unit | e.g., SCC, A, m ~7.6–8.2 |
| Fig. *5.1.2.* 11F–H | Light buff very fine-grained sandstone and silty very fine-grained sandstone | Light buff-coloured very fine-grained arkosic sandstone; coarsening upwards unit; finely interbedded with bluish green mudstone and buff-coloured siltstone; internally planar- and discontinuously cross-laminated; may be climbing-rippled; may preserve desiccation cracks and bird footprints on base in convex hyporelief if interbedded with bluish light green mudstone; bedding planes may be red-stained; upper sandstone beds grade upwards internally from planar laminated to sheared and convoluted planar lamination | Associated with bioturbation preserved in convex hyporelief and bird footprints, meniscate backfilled burrows, and desiccation cracks; Suite BC5A | Crevasse deposits into standing water (crevasse pool?) on delta-plain; desiccated at least occasionally | Sage Creek Canyon, A, upper unit | e.g., SCC, A, m ~9.7–10.5 |
| Fig. *5.1.2.* 10G, 10H | Light buff very fine-grained sandstone | Light buff-coloured very fine-grained arkosic sandstone with buff-coloured siltstone drapes;wavy-bedded to flaser-bedded with vague small-scale trough cross-lamination; preserves sharp-crested asymmetrical and symmetrical ripples with drapes and desiccation cracks; fines upwards to bright green siltstone; unit has scoured base and vague (lateral) accretion surfaces | No trace fossils observed | Flooded terminal distributary channel of lower delta-plain with unidirectional and oscillatory flow | Sage Creek Canyon, A, lower unit | e.g., SCC, A, m ~2.1–3 |
| Fig. *5.1.2.* 11B | Light tan silty very fine-grained sandstone and bluish tan siltstone | Light tan-coloured silty very fine-grained arkosic sandstone; preserves planar lamination with red-stained bedding planes; fines upwards to discontinuously laminated or massive bluish tan siltstone; lower contact transitional with interbedded mudstones and sandstones above carbonate lake muds; upper contact sharp and slightly scoured by channel sandstone | Associated with bird trampled and small burrows on sandstone bedding planes; Suites BC5A, BC5B | Possibly mouth bar deposits of terminal distributary channel or distal levee deposits of channel | Sage Creek Canyon, A, upper unit | e.g., SCC, A, m ~5.7–6 |
| cf. Fig. *5.1.2.*11 E; Fig. *6.2.* 16C–D | Light buff muddy very fine-grained sandstone | Light buff to brownish buff-coloured muddy very fine-grained arkosic sandstone with bluish light green muddy bedding plane drapes; ripple-laminated to flaser-bedded and wavy-bedded with irregular bedding planes due to bioturbation, desiccation, and weak pedogenic modification; interbedded with ripple-laminated very fine-grained sandstones and siltstone beds | Associated with bioturbation and weak pedogenesis; Suite BC9 | Subaerially exposed proximal overbank (?levees) or channel bars | Sage Creek Canyon, A, upper unit | e.g., SCC, A, m ~7.5–8.6 |
| Fig. *5.1.2.* 11D–E | Brown silty very fine-grained | Light brown silty very fine-grained sandstone; internally preserves discontinuous ripple-lamination; intercalated with ripple-laminated and convoluted buff sandstones; not disturbed by | Not associated with trace fossils | Possibly represents waning flow or drowning of | Sage Creek Canyon, A, upper unit | e.g., SCC, A, m ~7.3 |

| | | | | | | |
|---|---|---|---|---|---|---|
| | sandstone | large-scale convolutions in bed below | | channel | | |
| Fig. *5.1.2.* 10A, 10G | Greenish brown siltstone | Massive greenish brown siltstone; scoured slightly by small lenticular channel with low-angle lateral accretion surfaces; siltstone preserves burrows possibly attributable to lacustrine decapods crustaceans | Associated with *Thalassinoides* isp. A and large backfilled burrows; Suite BC1 | Subaerially exposed lower delta-plain or muddy littoral | Sage Creek Canyon, A, lower unit | e.g., SCC, A, m ~1–1.5 |
| Fig. *5.1.2.* 11A | Green silty very fine-grained sandstone | Massive to vaguely horizontally bedded green silty very fine-grained sandstone; may be slightly pedogenically modified; upper contact sharp with orangish tan overbank sandstone | No trace fossils observed, but bioturbated? | Possibly incipient paleosol on upper delta plain | Sage Creek Canyon, A, upper unit | e.g., SCC, A, m ~11–11.5 |
| Fig. *5.1.2.* 10A, 10C, 10D, 10F | Dark greenish brown siltstone | Dark greenish brown siltstone; fining upwards horizontal beds ~10–15 cm thick; internally planar-laminated with some wavy laminae towards tops of beds, and small-scale trough cross-laminated at base; preserves laminated hummocks and swales (wavelength ~20 cm, amplitude ~4 cm), as well as erosional unidirectional ripples preserved on lower bedding plane (interpreted as storm beds); upper bed of bedset preserves possible vertical burrows; may preserve small desiccation cracks in upper laminae of beds; bedding planes red-stained and may preserve reed impressions | May be associated with possible vertical burrows and desiccation cracks; not associated with root-marks | Occasionally subaerially exposed muddy littoral to eulittoral mudflat that preserves some storm beds | Sage Creek Canyon, A, lower unit | e.g., SCC, A, m ~0.5–2; lateral to measured section may form entire lower unit |
| Fig. *5.1.2.* 11B | Brownish green mudstone and very fine-grained sandstone | Finely interbedded brownish green mudstone and very fine-grained arkosic sandstone; may preserve red- or black-stained bedding planes, bird trampled bedding planes, and bioturbation; lower contact grades transitional upwards from marlstone; upper contact sharp with planar-laminated silty very fine-grained arkosic sandstone; mudstones organic-rich | Associated with bird trampled surface and bioturbation; Suites BC5A, BC5B | Distal deposits of terminal distributary channel (either downstream or lateral) into lagoon or main lake | Sage Creek Canyon, A, upper unit | e.g., SCC, A, m ~5.5–5.8 |
| Fig. *5.1.2.* 10A–B | Brownish green siltstone | Thick bed of massive to discontinuously laminated dark brownish green siltstone; brighter green at top of bed; lower contact not exposed | Not associated with trace fossils | Muddy littoral or sublittoral | Sage Creek Canyon, A, lower unit | e.g., SCC, A, m ~ -1–0.5 |
| Fig. *5.1.2.* 10G | Green siltstone | Massive green arkosic siltstone; preserves iron-stained root-marks; lower contact gradational with very fine-grained sandstone, in fining upwards unit ~0.8 m thick; upper contact sharp and irregular with lake beds above | Not associated with trace fossils except iron-stained root-marks | Wet delta-plain; possibly flooded lake-fringing wetland | Sage Creek Canyon, A, lower unit | e.g., SCC, A, m ~2.9–3.1 |
| Fig. *5.1.2.* 11F | Light brownish olive green siltstone | Light brownish and light bluish olive green arkosic siltstone; internally massive; fines upwards to massive bluish light green mudstone below climbing-rippled very fine-grained sandstone bed; conchoidal-weathered outcrop surfaces | Not associated with trace fossils | May represent flooded overbank siltstones or distal crevasse into pond | Sage Creek Canyon, A, upper unit | e.g., SCC, A, m ~8.6–9.2 |
| Fig. *5.1.2.* 11F, 11H | Bluish light green mudstone | Bluish light green mudstone; internally discontinuously laminated or massive; may be interbedded with light buff-coloured silty very fine-grained arkosic sandstone; preserved with desiccation cracks and bird footprints if bedded | Associated with bird tracks, backfilled burrows, and desiccation cracks; Suite BC5B | Standing water on delta-plain, possibly interdistributary pond; occasionally desiccated | Sage Creek Canyon, A, upper unit | e.g., SCC, A, m ~9.3–10 |

## Figure captions for photographic plates, Section 5.1.2.

**Fig. 5.1.2.1.** The A-Bed at Middle Firehole Canyon (lower unit). **(A)** The lower A-Bed at Middle Firehole Canyon. **(B)** Massive to bedded marlstones of the lower unit. Arrow showing possibly subaerially exposed bed with lowermost burrows in the section. **(C)** Close-up of greyish green marlstone (MFC, A, m ~0.5). **(D)** Close-up of olive greenish tan marlstone. **(E)** Tan siltstone with increasing bioturbation upwards. **(F)** Bedded olive greenish tan marlstone with desiccation crack. **(G)** Water escape structure? (arrow) in laminated tan siltstone.

**Fig. 5.1.2.2.** The A-Bed at Middle Firehole Canyon (lower unit). **(A)** Water escape structure? (arrow) in tan siltstone. Note small black flecks are possible fish bones or gastropod radulae. **(B)** Trough cross-bedding in bioturbated tan siltstone. **(C)** Pinching out of ripple-laminated sandstone to tan siltstone. **(D)** Ripple-laminated sandstone adjacent to section at m ~1.5–2.5. **(E)** Ripple-laminated sandstone shown in (D). **(F)** Upper contact of the lower arkosic unit showing bright green siltstone below lacustrine facies and orange-stained horizon (arrow).

**Fig. 5.1.2.3.** The A-Bed at Middle Firehole Canyon (upper unit). **(A)** The lower portion of the upper unit (m ~5–6.8), gradually coarsening upwards and transitional with underlying lacustrine facies. **(B)** Heterolithic facies with reddish iron-stained horizons and sandstone interbeds with mudstone drapes (arrow). **(C)** Close-up of laminated heterolithic facies at m ~6. **(D)** Close-up of possible oscillation ripple structures with chevron upbuilding within swollen lens set. **(E)** The middle portion of the upper unit (m ~6.8–10). Note pedogenically modified siltstones below cross-bedded sands at top. **(F)** Laminated and "irregular"-bedded sandstones at top of first coarsening-upwards cycle of upper unit (m ~8). **(G)** Isolated cross-beds within "irregular"-bedded sandstones.

**Fig. 5.1.2.4.** The A-Bed at Middle Firehole Canyon (upper unit). **(A)** The upper unit just east of the measured section showing isolated thin channel lenses in lower portion and amalgamated sandstones at top. **(B)** Scoured base of channel east of measured section. **(C)** Intraclast conglomerates of channel lags. **(D)** The upper portion of the upper unit (m ~8–10 in foreground). **(E)** Vertical burrows in ripple-laminated accretionary sandstones. **(F)** A green, relatively well developed paleosol (m ~8.8). **(G)** Heterolithic facies above paleosol that preserves ornamented backfilled burrows. **(H)** Bluish green laminated mudstone with desiccation cracks below channel sandstones at m ~9.5.

**Fig. 5.1.2.5.** The top of the A-Bed at Middle Firehole Canyon (upper unit). **(A)** Amalgamated channel sandstones and siltstones preserving horizontal and cross-bedding (m ~10–12.5). **(B)** A green-coloured, weakly developed paleosol (m ~11). **(C)** Close-up of weakly developed paleosol on bedded heterolithic facies. **(D)** Small-scale trough cross-laminated sandstone (m ~12.5). **(E)** Close-up of flaser-bedded sandstone with insect nest at left. **(F)** Downstream-dipping ripple laminae in sandstone at m ~12.5. **(G)** Sharp-crested sinuous asymmetrical ripple bedforms at top of section (m ~12.7). **(H)** Bedded siltstones and ripple-laminated sandstone at top of section (m ~12.7–13.5), overlying bioturbated sandstone (with hammer).

**Fig. 5.1.2.6.** The A-Bed at Firehole Canyon (lower unit). **(A)** The lower contact of the lower unit west of the measured section, showing sharp base of unit overlying lacustrine facies, but little change in grain size. **(B)** The bedded marly siltstones of the lower unit (m ~2–5). **(C)** The upper contact of the lower unit showing bedded siltstone facies below the orange-coloured Second Tuff. **(D)** The thick bedded siltstone facies with desiccation cracks at the top of a bed (arrow). **(E)** The A-Bed, showing the sharp contact of the channel sandstone below the "white stripe" unit. **(F)** The lower unit, showing the bedded siltstone facies filling a trough-shaped channel scour (dotted line), and cut by the sandstone channel above. **(G)** Desiccation-crack polygons on the base of the scoured channel shown at top in (F). **(H)** Planar lamination in channel sandstone.

**Fig. 5.1.2.7.** The A-Bed at Firehole Canyon (lower unit). **(A)** The A-Bed near the measured section (landward of photos shown in Fig. *5.1.2.*6), showing sharp contact with the lacustrine unit below and a change in grain size at the contact. **(B)** Close-up of the lower contact. **(C)** Ripple-lamination in the lowermost sandstone of the A-Bed. **(D)** Greyish green marlstone overlying the sandy lowermost bed (m ~1–2). **(E)** Sandstones intercalated with massive siltstones in the lower unit (m ~2–3). **(F)** Close-up of climbing ripple lamination in sandstones at m ~2.5. **(G)** Fining upwards cycles in lower unit at Firehole Canyon (N). **(H)** Cross-bedded sandstone at base of fining upwards cycle in lower unit at Firehole Canyon (N).

**Fig. 5.1.2.8.** The A-Bed at Firehole Canyon (upper unit). **(A)** The upper unit of the A-Bed. **(B)** A coarsening upwards cycle with the heterolithic facies (m ~11–12.5). **(C)** Close-up of the heterolithic facies with laminated siltstones, mud drapes, and reddish iron-stained horizons. **(D)** Close-up of the bedded sandstone facies preserving the *Planolites* ichnofabric (m ~12.5). **(E)** Close-up of bioturbated sandstone bed at m ~13. **(F)** Desiccation-cracked mud-drape on sandstone at m ~13. **(G)** Flat-topped symmetrical ripple bedforms at m ~14.5.

**Fig. 5.1.2.9.** The A-Bed at Firehole Canyon (N) (upper unit). **(A)** The upper unit of the A-Bed showing overall coarsening upwards from lacustrine facies at base to thick sandstone beds at top. **(B)** Sharp lower contact of fining-upwards sandstone wedges above lacustrine facies of "white stripe" unit. **(C)** Fining-upwards in sandstone shown in (B), with ripple-lamination at base, convolute bedding, and structureless upper portion. **(D)** Close-up of flame-like convolutions. **(E)** Bedded siltstone facies above wedge-shaped sandstone bodies at base of upper unit. **(F)** Bedded siltstone facies overlain by ripple-laminated sandstone with desiccation cracks preserved at base (compare with upper portion of lower unit of A-Bed at Firehole Canyon in Fig. *5.1.2.*6. **(G)** Desiccation-crack polygons at base of sandstone in (F). **(H)** Large-scale trough cross-stratification in lower portion of upper unit at Firehole Canyon (N).

**Fig. 5.1.2.10.** The A-Bed at Sage Creek Canyon (lower unit). **(A)** The lower unit at Sage Creek showing dark greenish brown bedded siltstone facies coarsening upwards to very fine-grained sandstone (m ~0.5–2). **(B)** Dark greenish brown marlstone at base of lower unit. **(C)** Bedded siltstone facies with unidirectional ripples at base of bed at top. **(D)** Planar- and in-phase symmetrical ripple lamination in bedded siltstone facies. **(E)** Massive tan siltstone and shallow channel facies at m ~1.2. Arrow is showing location of vertical burrows preserved in sandstone. **(F)** Desiccation crack in marly bedded siltstone facies. **(G)** Upper contact of lower unit showing fining upwards to green siltstone below lacustrine facies. **(H)** Small-scale, sharp-crested symmetrical ripples in sandstone near top of lower unit (m ~2.8).

**Fig. 5.1.2.11.** The A-Bed at Sage Creek Canyon (upper unit). **(A)** The outcrop at Sage Creek Canyon showing sandstones of upper A-Bed overlain by lacustrine facies below the B-Bed (top). **(B)** Transitional lower contact of the upper unit, with planar-laminated sandstones interbedded with dark brown mudstones. **(C)** Channel sandstone in lower portion of upper unit with medium-scale trough cross-stratification, ripple-lamination, and planar cross-lamination. **(D)** Large-scale convolutions at top of channel sandstone (m ~6.5–7). **(E)** Small scale trough cross-lamination in sandstone at m ~7.5. **(F)** Massive tan siltstone and greenish blue mudstone at base of coarsening upwards cycle (m ~8.5–9.2). **(G)** Ripple-laminated sandstones in coarsening upwards cycle at m ~9.8. **(H)** Heterolithic facies that preserves bird footprints (arrow).

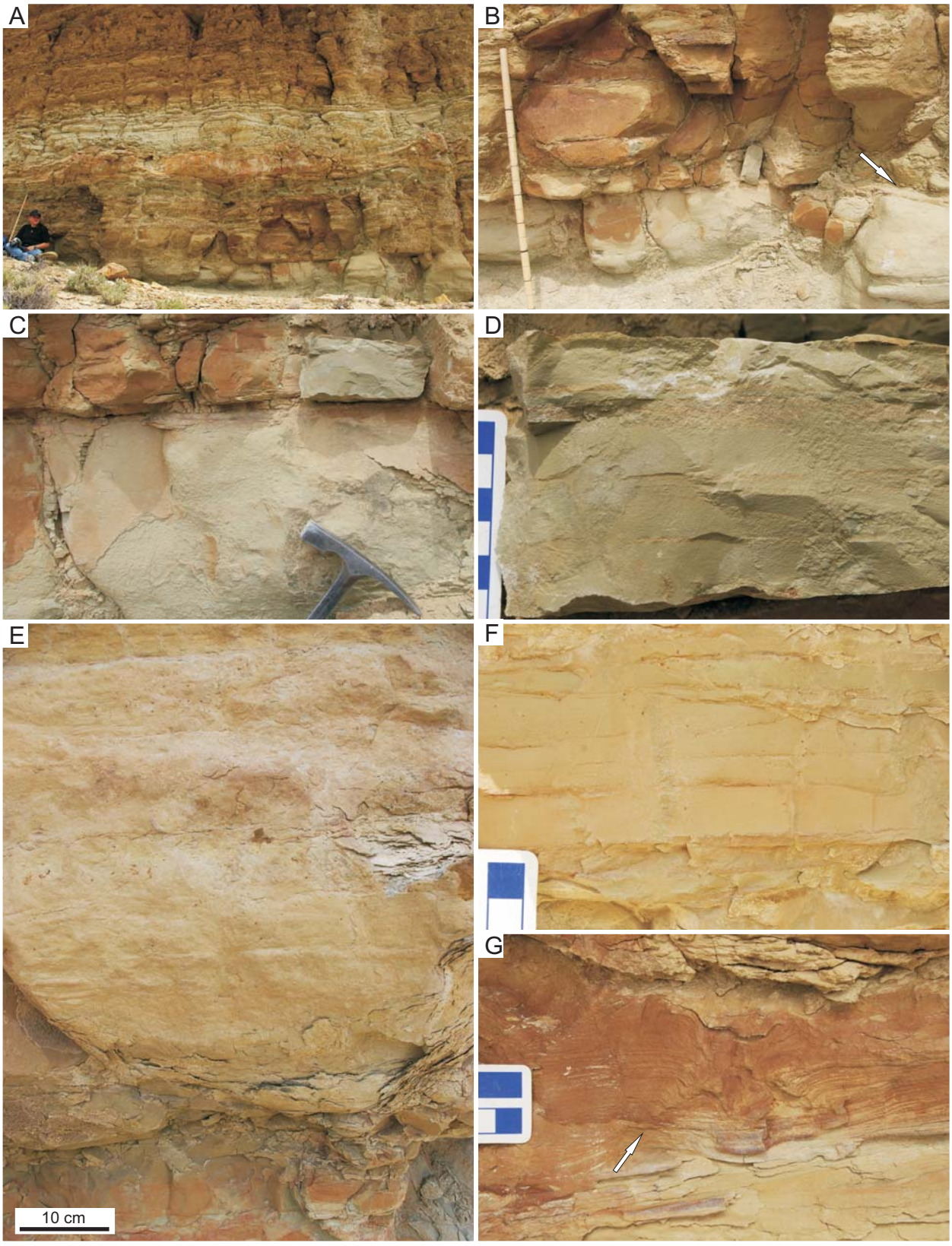


**Fig. 5.1.2.1.** The A-Bed at Middle Firehole Canyon (lower unit). Refer to Table 5.2 for descriptions of the lithofacies shown. See above for full caption.

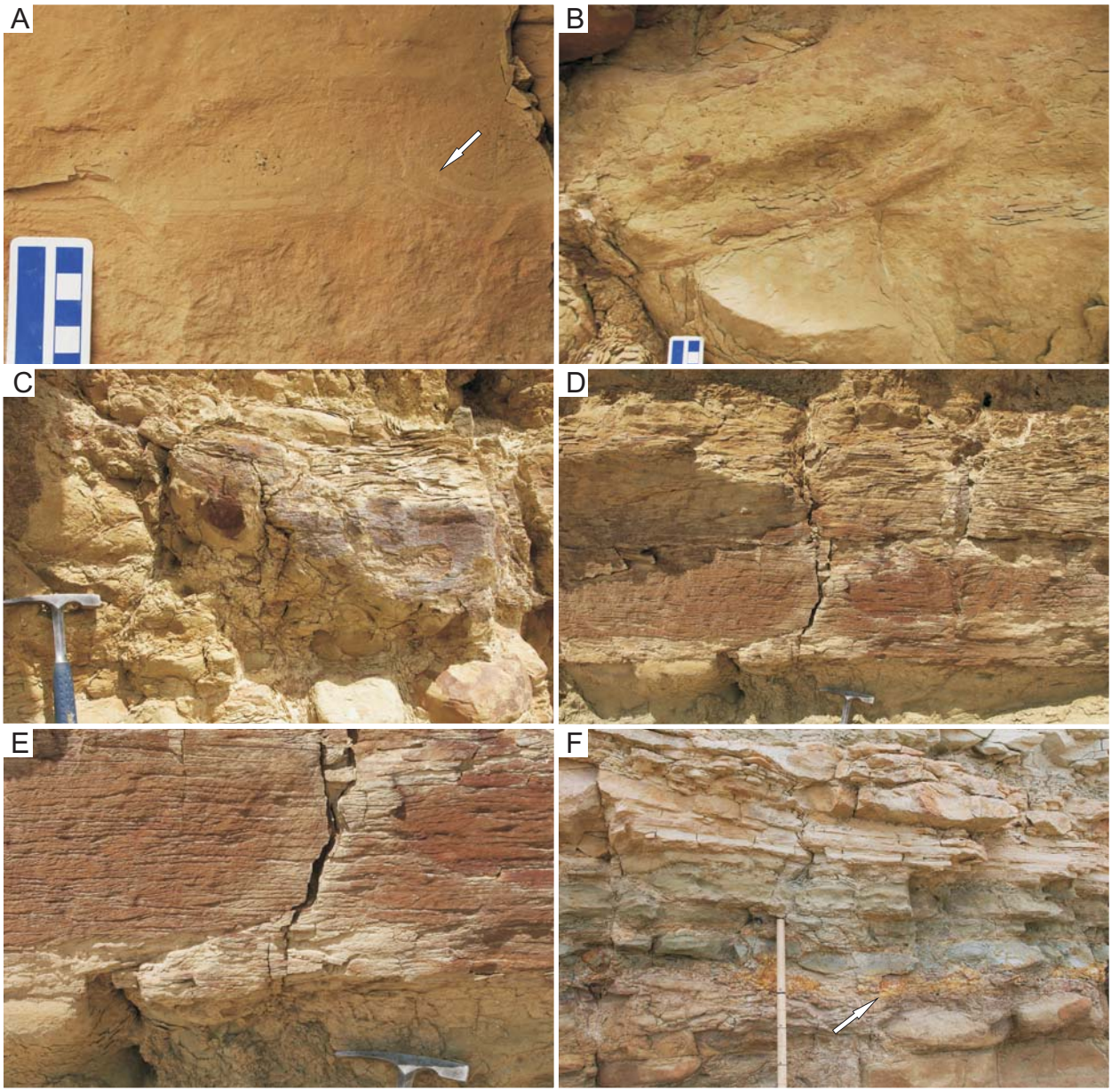


**Fig. 5.1.2.2.** The A-Bed at Middle Firehole Canyon (lower unit). Refer to Table 5.2 for descriptions of the lithofacies shown. See above for full caption.

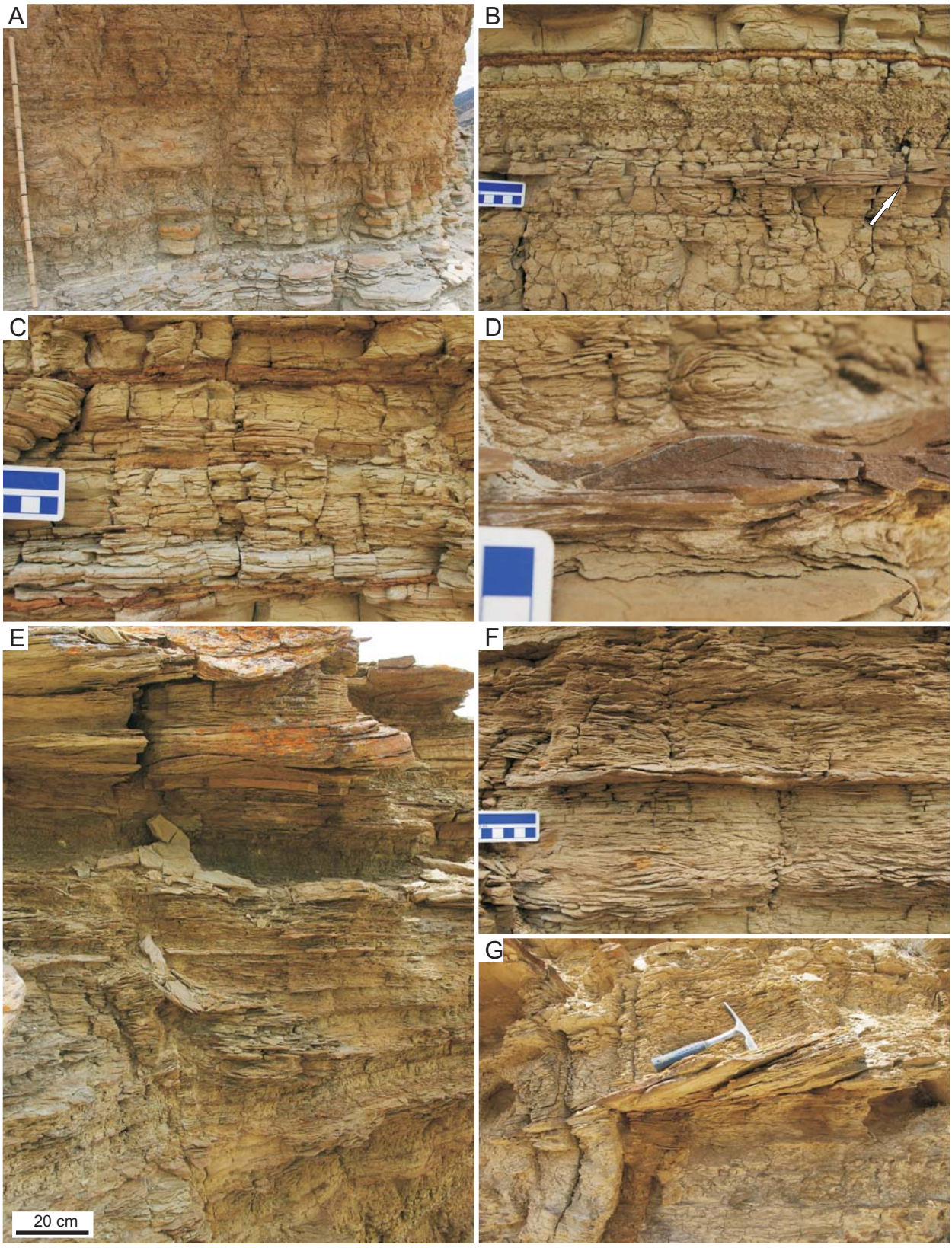


**Fig. 5.1.2.3.** The A-Bed at Middle Firehole Canyon (upper unit). Refer to Table 5.2 for descriptions of the lithofacies shown. See above for full caption.

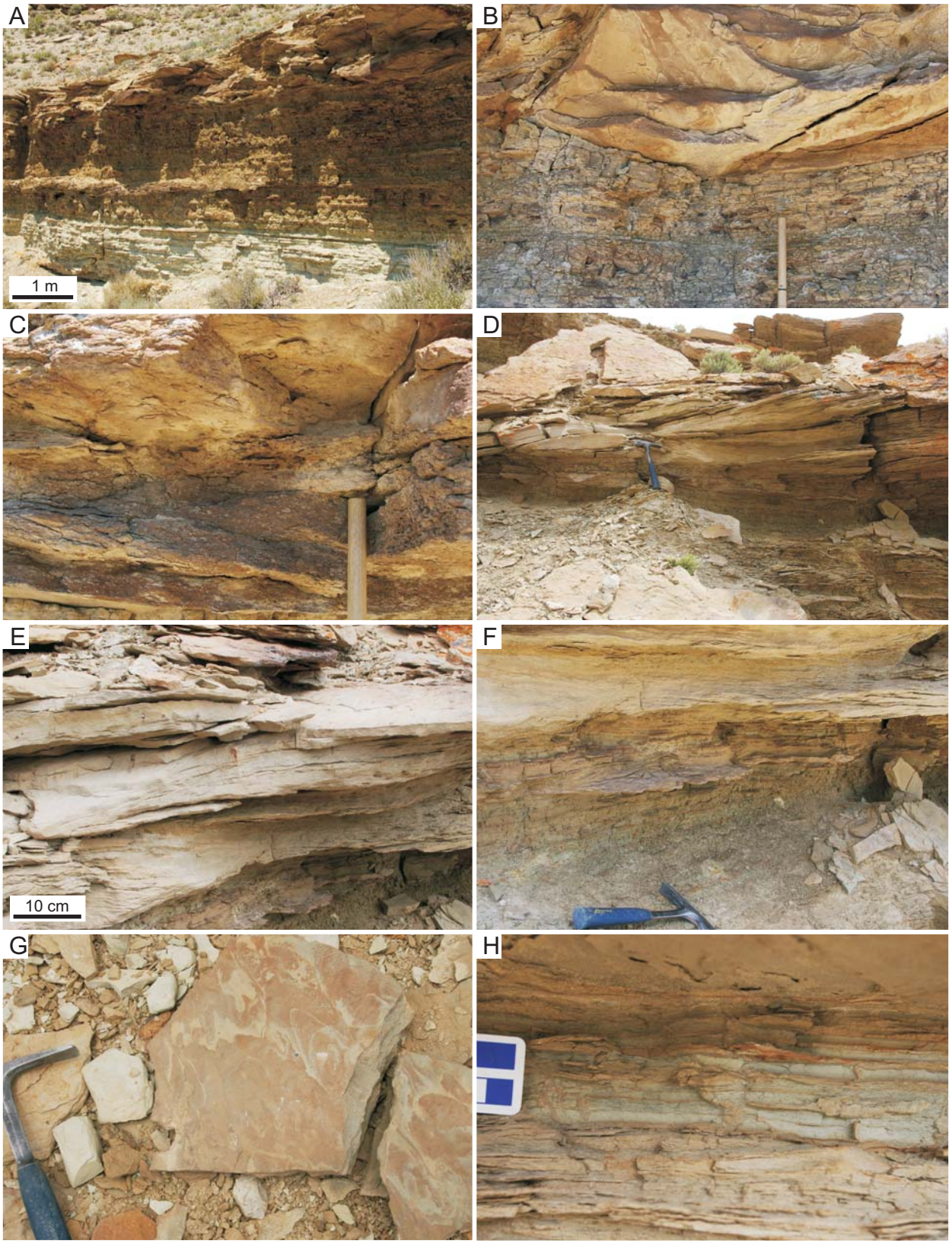


**Fig. 5.1.2.4.** The A-Bed at Middle Firehole Canyon (upper unit). Refer to Table 5.2 for descriptions of the lithofacies shown. See above for full caption.

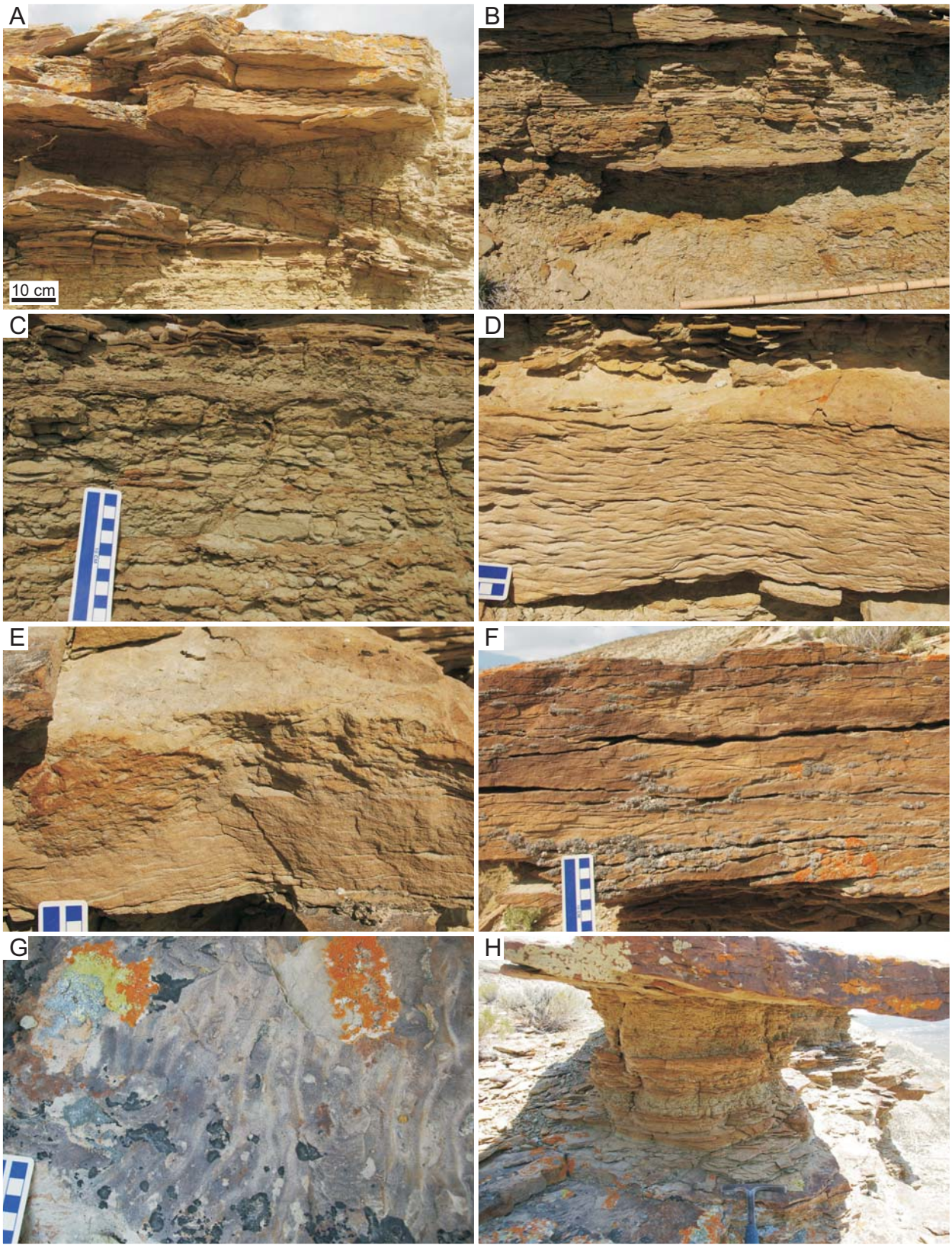


**Fig. 5.1.2.5.** The top of the A-Bed at Middle Firehole Canyon (upper unit). Refer to Table 5.2 for descriptions of the lithofacies shown. See above for full caption.

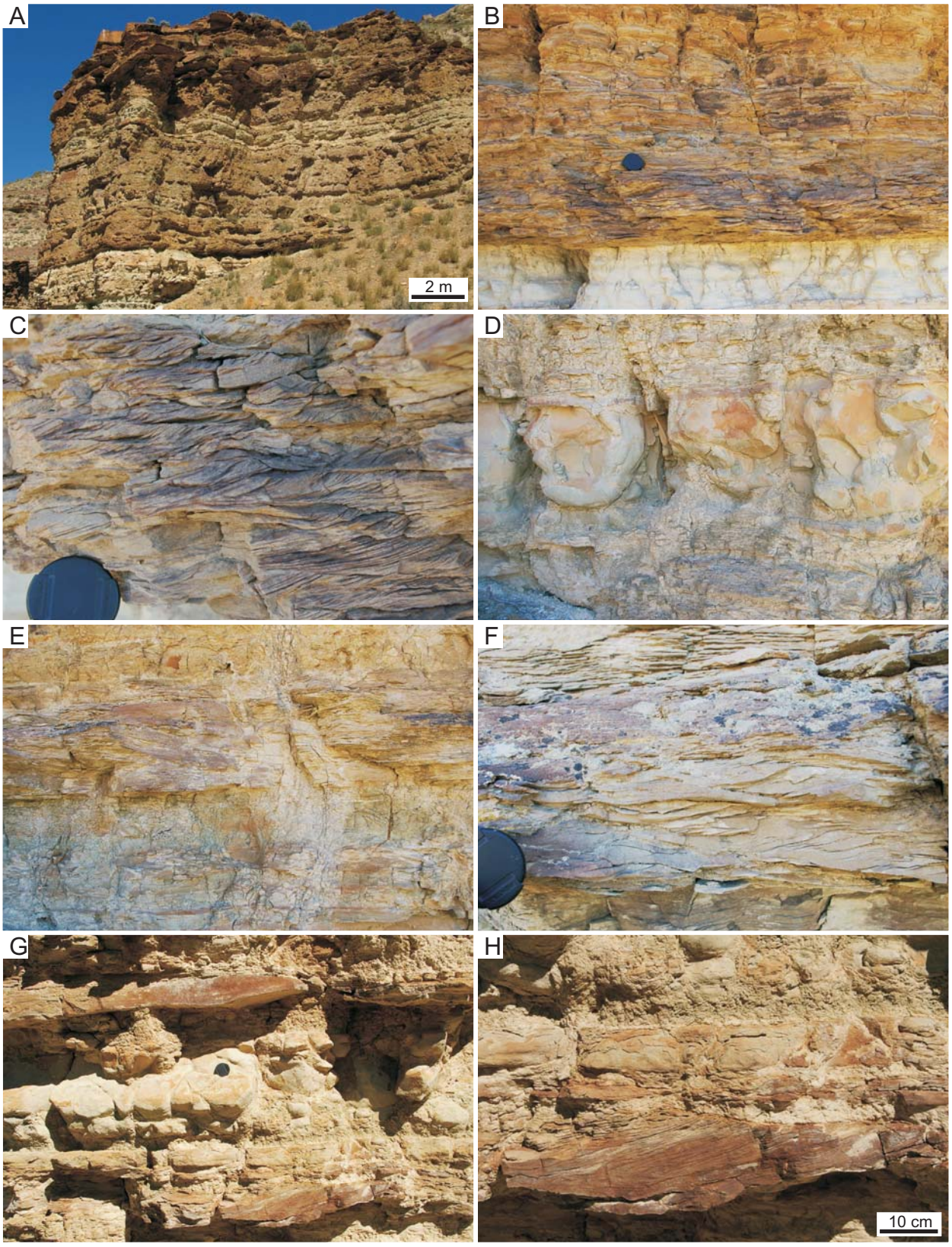


**Fig. 5.1.2.6.** The A-Bed at Firehole Canyon (lower unit). Refer to Table 5.2 for descriptions of the lithofacies shown.

**Fig. 5.1.2.7.** (Next page) The A-Bed at Firehole Canyon (lower unit). See above for full caption.

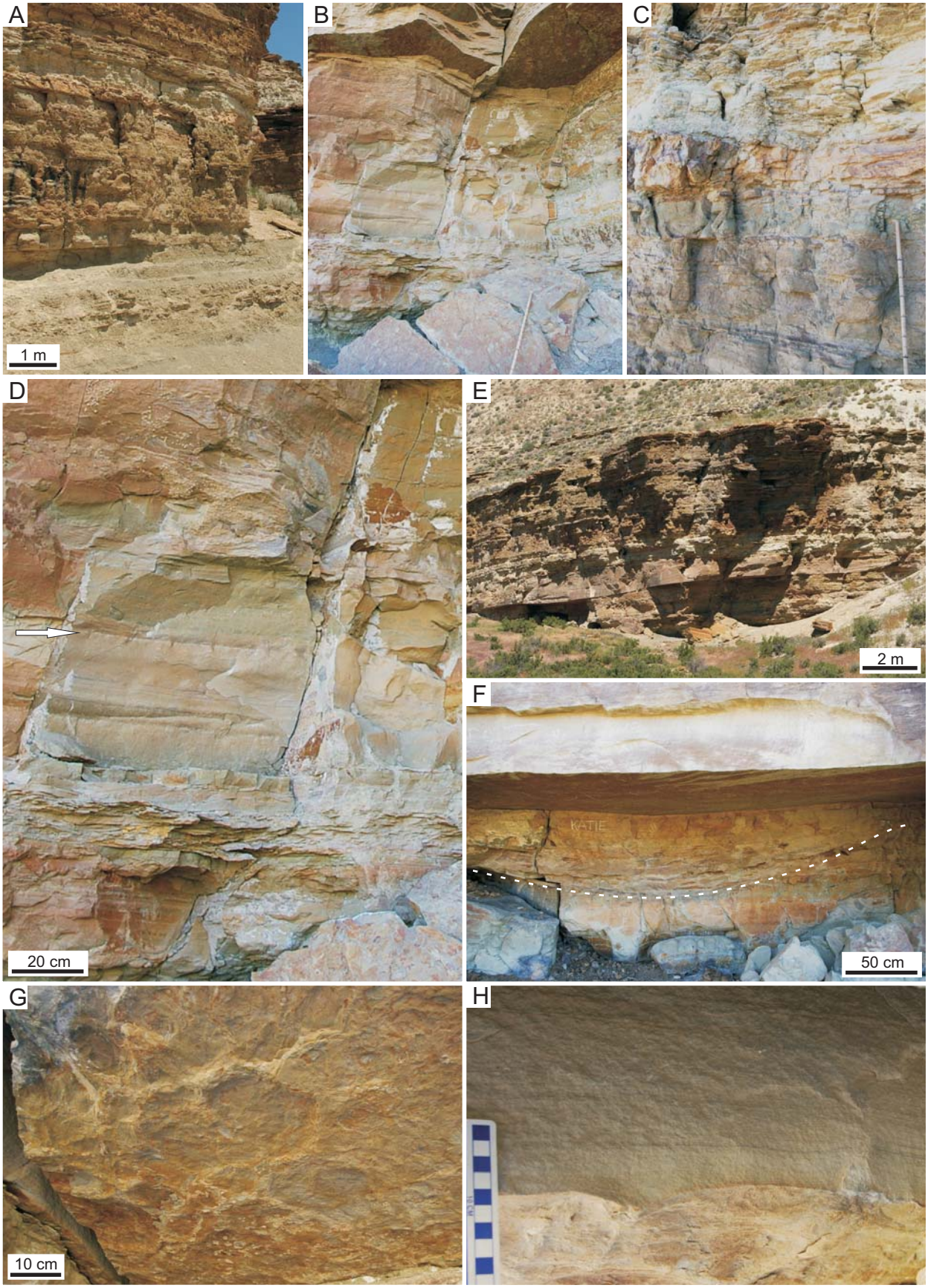
A
1 m
B
C
D
20 cm
E
2 m
F
50 cm
G
10 cm
H

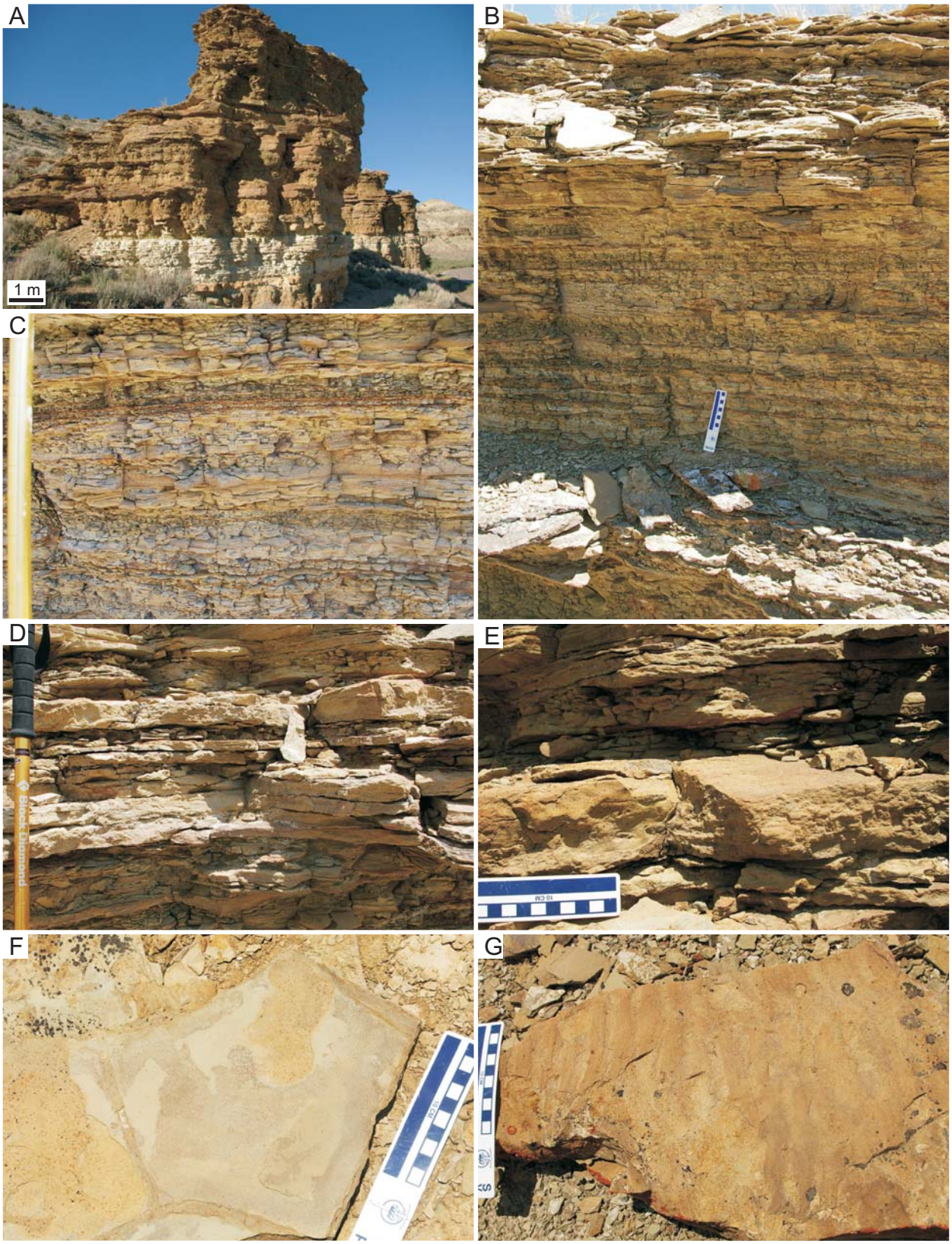


**Fig. 5.1.2.8.** The A-Bed at Firehole Canyon (upper unit). Refer to Table 5.2 for descriptions of the lithofacies shown. See above for full caption.

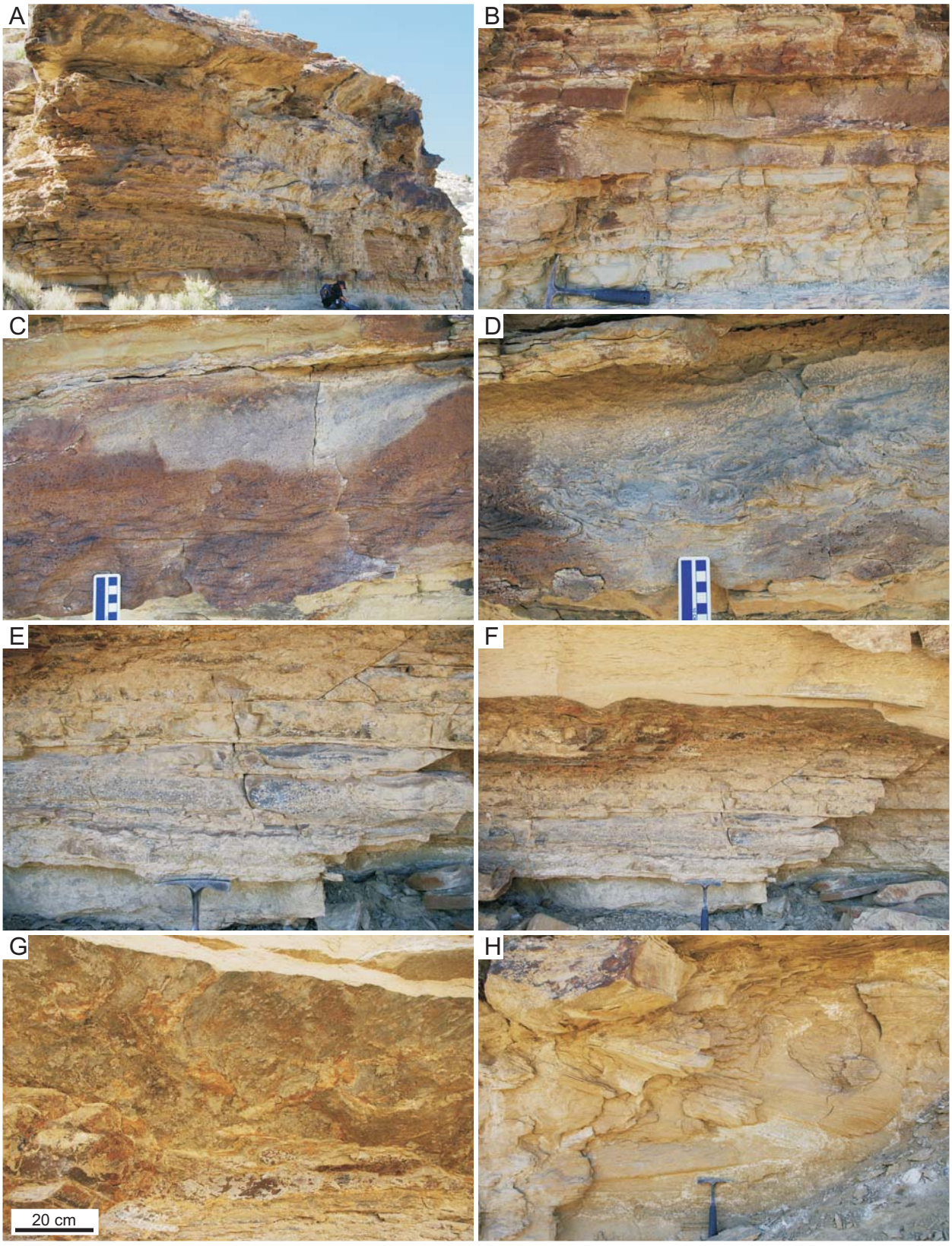


**Fig. 5.1.2.9.** The A-Bed at Firehole Canyon (N) (upper unit). Refer to Table 5.2 for descriptions of the lithofacies shown. See above for full caption.

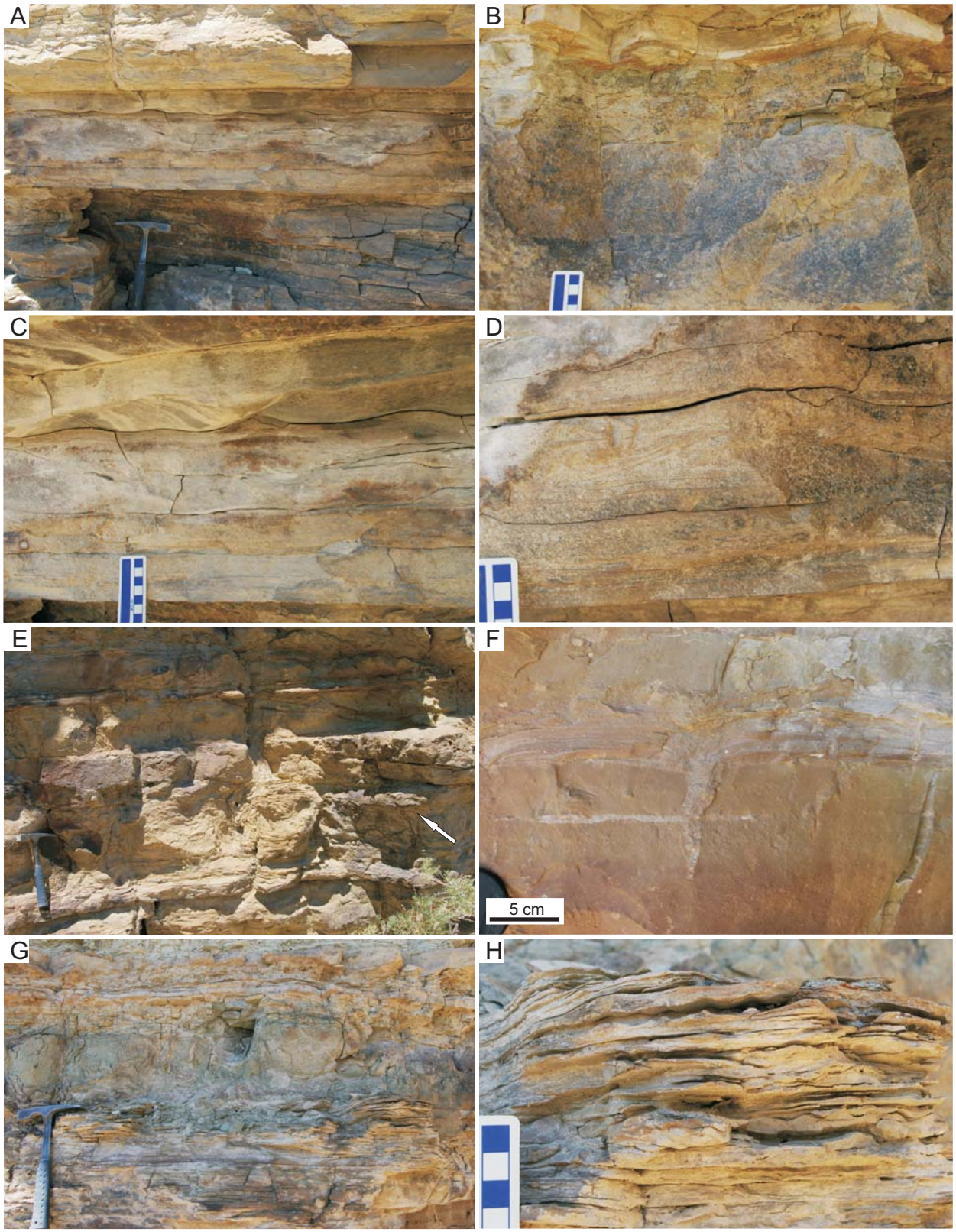


**Fig. 5.1.2.10.** The A-Bed at Sage Creek Canyon (lower unit). Refer to Table 5.2 for descriptions of the lithofacies shown. See above for full caption.

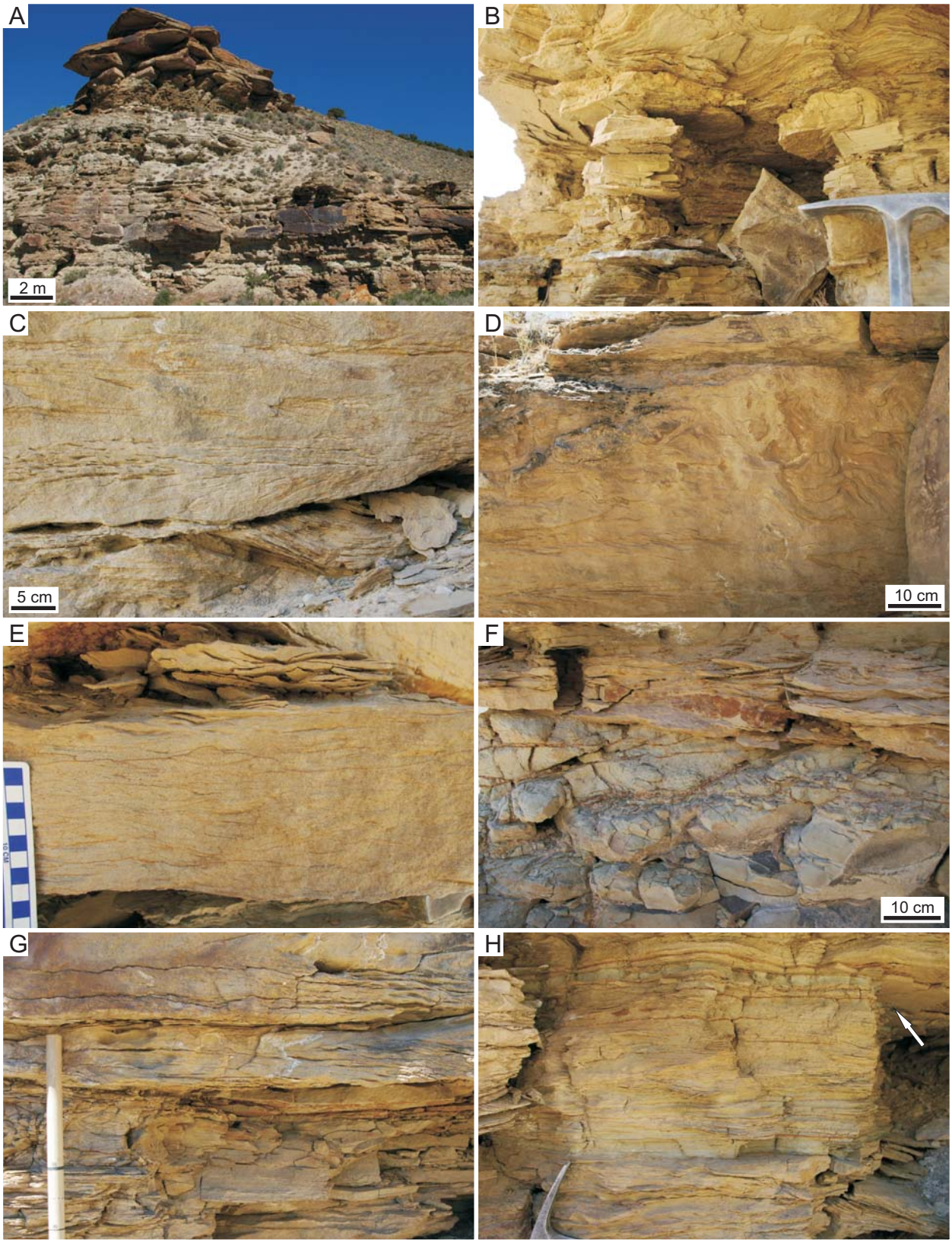


**Fig. 5.1.2.11.** The A-Bed at Sage Creek Canyon (upper unit). Refer to Table 5.2 for descriptions of the lithofacies shown. See above for full caption.

*5.1.3. Descriptions of the Arkosic Siliciclastic Lithofacies of the D- and E-Arkose Beds*

Lithofacies of the middle arkosic siliciclastic intervals (the D-Bed and E-Bed) are described in Table 5.3. Two stratigraphic sections of the middle Wilkins Peak Member were measured in Firehole Canyon, referred to here as FC, D1 (Fig. 5.1) and FC, D2 (Fig. 5.2). The figure numbers that refer to these lithofacies begin with "*5.1.3.*". The lithofacies of the D-Arkose Bed are similar to those of the A-Bed, but comprise proportionately more sandstones. The D-Bed in Firehole Canyon is much thicker than the A-Bed, and was informally divided into a lower unit, a "white stripe" unit, a second unit, a "green stripe" unit, and an upper unit. A portion of the middle Wilkins Peak Member in Firehole Canyon was measured in two sections, separated laterally by about 500 m E–W (FC, D1: Fig. 5.1; FC, D2: Fig. 5.2). The D-Bed was also briefly investigated on White Mountain at Kanda, where it was divided into a lower unit, white stripe unit, and an upper unit. The D-Bed, like the A-Bed, shows an overall "shallowing-upwards" succession, with facies becoming more landward and subaerial, with more deeply scoured channels, towards the top of the unit. In Firehole Canyon, two transgressions may have taken place within the D-Bed, represented by the lacustrine "white stripe" and "green stripe" units, although it is not clear if the "green stripe" represents deposition related to a transgression of the main lake. If so, the D-Bed in Firehole Canyon may represent three parasequences that record progradation of a fluvio-deltaic system. The upper contact of the D-Bed varies laterally depending on whether active channels, abandoned channels, or pedogenically modified subaerial sediments were flooded during the next major transgression of Lake Gosiute. The E-Bed consists mainly of terrestrial and fluvial facies within Firehole Canyon, although it also contains a thin package of lacustrine carbonates and could be divided into a lower unit, white stripe unit, and upper unit (Fig. 5.2).

**Table 5.3.** Lithofacies descriptions from the basin centre arkosic siliciclastic units, D-Arkose Bed and E-Arkose Bed. Localities include Firehole Canyon (FC, D1; FC, D2-E2) and White Mountain at Kanda (WM, K) and the #18 Crossing (WM, #18C).

| Fig. | Lithology | Description | Comments; Trace suites (Chapter 6) | Interpreted Environment | Locality | Section, Metre |
|---|---|---|---|---|---|---|
| ***Lithofacies of the D-Bed, White Mountain, Kanda (divided into lower, "white stripe", and upper units; lower unit not investigated)*** | | | | | | |
| Fig. *5.1.3.* 1C | Greyish tan fine-grained sandstone and intraclast pebble-conglomerate | Greyish tan fine-grained arkosic sandstone preserving weak horizontal to slightly inclined bedding; contains oriented, well rounded, pebble-sized carbonate mudstone intraclasts in bedded sandstone; coarsens upwards to matrix-supported intraclast conglomerate with plant fragments, fining to bedded fine sandstone with oriented intraclasts; lower contact transitional with greenish buff-coloured siltstone | Not associated with trace fossils | Initial deposition of the upper unit into sublittoral lake downstream of terminal distributary channel | White Mountain, Kanda, D, upper unit | n/a |
| Fig. *5.1.3.* 1D | Greyish buff fine-grained sandstone | Greyish buff-coloured fine-grained arkosic sandstone with scoured base; internal structures include plane-bedding, ripple cross-lamination, planar lamination, low angle trough cross-lamination, and convolute bedding (sheared); preserves planar cross-lamination in wedge-shaped lateral accretion bedsets with in-phase decimetre-scale undulations; lower contact scoured into grey carbonate siltstones | Some vertical burrows observed; Suite BC3A; compare with first channel sandstone of upper A in SCC | Channel bars (point bar) with lateral accretion and convolute bedding | White Mountain, Kanda, D, upper unit | n/a |
| Fig. *5.1.3.* 1E; *6.1.3.* 3A | Greyish tan fine-grained sandstone | Greyish-tan fine-grained arkosic sandstone with large-scale lateral accretion surfaces; lateral accretion surfaces < 2 m high; internally, preserves plane-bedding with parting lineation and ripple-lamination in thin cross-beds; may be present in large-scale trough cross-stratified bedsets | Associated with *Ancorichnus* isp.; Suite BC7? | Distributary channel bars (side bars?) and channel floor | White Mountain, Kanda, D, upper unit | n/a |
| Fig. *5.1.3.* 1F | Reddish tan very fine-grained sandstone | Slightly reddish tan very fine-grained arkosic sandstone with very small amplitude and wavelength symmetrical ripple bedforms capping unit of climbing-rippled and ripple cross-laminated sandstone; no desiccation cracks; no clay drape; ripple reworking also affected underlying greenish silty very fine-grained sandstone, suggesting stabilization of sediment prior to wind-induced ripple formation, possibly by a microbial mat | Associated with soft but slightly cohesive substrate horizontal trails; Suite BC7 | Abandoned channel deposits or exposed channel bar | White Mountain, Kanda, D, upper unit | n/a |
| Fig. *6.1.3.* 2A–H | Tan-coloured fine-grained sandstone | Tan-coloured very fine-grained to fine-grained arkosic sandstone; planar-laminated, irregular-bedded, and 3D ripple-laminated; preserves very thin partings in flaser-bedded bedsets | Associated with vertebrate footprints in cross-section; Suite BC4 | Proximal, wet overbank deposits | White Mountain, Kanda, D, upper unit | n/a |
| Fig. *5.1.3.* 1A–B, 1H; | Tan fine-grained sandstone with clay drapes | Fine-grained tan arkosic sandstone with planar-lamination, parting lineation and clay drapes; plant fragments present on bedding planes; top of beds preserve possible rain-drop impressions; wide desiccation cracks in clay drapes filled with | Associated with bird tracks, desiccation cracks, and cf. | Overbank deposits into very shallow water (desiccated overbank) | White Mountain, Kanda, D, upper unit | |

| | | | | | | |
|---|---|---|---|---|---|---|
| Fig. *6.1.3.* 1A–H | | arkosic sand from above; small load structures with irregular shapes common; possible, circular rain-drop impressions or microbial mat bubble texture preserved on base of sandstones | *Vagorichnus* isp.; Suite BC5B | | | |
| Fig. *5.1.3.* 1A, 1B, 1H | Tan to brown very fine-grained sandstone and greenish-buff and brown siltstone | Tan to brown arkosic very fine-grained sandstone and greenish-buff siltstone; beds ~10–20 cm thick; some beds normally graded and fine upwards; some beds more discretely interbedded; sand-sized horizons with planar-lamination and ripple cross-lamination; sand beds ~5 cm thick with undulating bases and bed-tops, associated with churned siltstone and sandstone that may preserve iron-stained root-marks; some beds inversely graded from plane bedded very fine-grained sandstone to churned, ?bioturbated fine-grained sandstone | Associated with vertebrate footprints in cross-section and "churned" beds, produced in soupy substrates; Suite BC4 | Proximal, wet overbank (overfilled), probably into shallow standing water | White Mountain, Kanda, D, upper unit | n/a |
| Fig. *5.1.3.* 1B, 1G | Greenish buff-coloured siltstone | Massive and weakly pedogenically modified greenish buff-coloured siliciclastic siltstone; preserves iron-stained root marks, carbonate root-casts and deep, iron-stained fractures (< 50 cm long) | Not associated with animal traces; preserves root casts | Incipient overbank paleosol with high water table | White Mountain, Kanda, D, upper unit | n/a |
| Fig. *5.1.3.* 1C | Greenish brown marl siltstone | Weakly bedded to massive greenish tan-brown siliciclastic siltstone; no evidence of pedogenesis; grades transitionally into weakly horizontally bedded light tan-coloured very fine-grained arkosic sandstone to grayish tan fine-grained sandstone with large mud clasts and plant fragments | Not associated with animal traces | Sublittoral lacustrine; prodelta, distal delta front or hypopycnal delta-front | White Mountain, Kanda, D, upper unit | n/a |
| Fig. *5.1.3.* 1A–D | Olive greenish light brown carbonate siltstone | Olive greenish light brown carbonate siltstone; internally discontinuously laminated to massive; horizontally bedded in thin beds | Not associated with animal traces | Sublittoral lacustrine | White Mountain, Kanda, D, white stripe | n/a |
| ***Lithofacies of the D-Arkose Bed, White Mountain, #18 Crossing*** | | | | | | |
| n/a | Olive-tan very-fine grained arkosic sandstone | Olive-tan, very fine-grained arkosic sandstone preserving climbing ripples and flaser bedding; climbing-ripple beds may be draped by ~1 cm thick undulating drapes of silty very fine-grained sandstone; intercalated with brecciated olive-tan siltstone beds with signs of desiccation | Note that climbing ripples show flow from the north to north-east | Sheetflood or unconfined flow deposits on delta-plain | White Mountain, #18 crossing | n/a |
| n/a | Tan siltstone and mudstone | Tan coloured siltstone and mudstone; appears to have been pedogenically modified; recessive unit; poorly exposed | Not investigated in detail | Desiccated mudflat and overbank deposits | White Mountain, #18 crossing | n/a |
| ***Lithofacies of the D-Bed, Firehole Canyon, Section D1 (divided into lower unit, second unit, "green stripe" unit, and upper unit)*** | | | | | | |
| Fig. *5.1.3.* 7D | Intraclast conglomerate in grey fine-grained sandstone | Clast-supported intraclast conglomerate with grey fine-grained arkosic sandstone matrix; intraclasts rounded mudstones and stromatolitic crust fragments; small lateral extent; pinches out laterally; forms part of base of upper unit trough cross-stratified sandstone | Not associated with trace fossils | Channel thalweg in terminal distributary channel | Firehole Canyon, D1, upper unit | e.g., FC, D1, m ~25 |

| | | | | | | |
|---|---|---|---|---|---|---|
| Fig. *5.1.3.* 5A, 5E, 5G, 5H | Carbonate mudstone intraclast conglomerate in greyish green siltstone | Intraclast conglomerate with granule-sized, moderately rounded carbonate mudstone intraclasts and greyish green siltstone matrix; bed forms an orange-weathered marker bed (~10 cm thick) with sharp lower and upper contacts; intraclast conglomerate pinches out within bed; internally, preserves asymmetrical ripple crests; lower contact rests sharply on “green stripe” mudstone | Not associated with trace fossils | Trangressive lag or storm deposit in interdistributary bay | Firehole Canyon, D1, green stripe unit | e.g., FC, D1, m ~23 |
| Fig. *5.1.3.* 3B, 3D, 3E, 4E | Grey fine-grained sandstone | Grey fine-grained arkosic sandstone; internally plane-bedded of upper flow regime; may preserve sheared plane beds; may contain pebble-sized mudstone and bedded sandstone intraclasts in thin bed with scoured base (m ~9.5); interbedded with ripple-laminated very fine-grained sandstone (m ~14.5) | Not associated with trace fossils | Possibly down-dip “chute” of downstream accreting sandstones | Firehole Canyon, D1, second unit | e.g., FC, D1, m ~9.5, m ~14.5 |
| Fig. *5.1.3.* 7C, 7D | Tan silty fine-grained sandstone | Tan-coloured, silty fine-grained arkosic sandstone; internally massive or weakly bedded with wavy, parallel, continuous laminae; lower contact sharp but not erosional; sandstone covers underlying thin stromatolitic horizon with little disruption in places; lateral to intraclast conglomerate | Forms lower contact of upper unit | Crevasse or basinward splay of terminal distributary channel | Firehole Canyon, D1, upper unit | e.g., FC, D1, m ~25 |
| Fig. *5.1.3.* 6A–D, 6H | Reddish grey and reddish orange fine-grained sandstone | Reddish grey and reddish orange fine-grained arkosic lenticular sandstones; variable within unit; sandstones pinches out laterally; preserves rounded load structures and/or vertebrate footprints in cross-section within bed; internally, may preserve irregular bedding, may be entirely bioturbated, or preserve planar bedding; preserves palm frond and reed impressions on lower contact, as well as vertebrate and invertebrate trace fossils; upper contact irregular with light buff-coloured muddy very fine-grained sandstone that preserves sharp-walled, pellet-filled burrows; upper contact of sandstone beds may preserve symmetrical, straight ripple bedforms | Associated with mammal and reptile tracks and abundant small *Planolites* isp. at base, Suite BC6; preserves vertebrate tracks in cross-section, Suite BC4, and full relief burrows, Suite BC9 | Crevasse and shallow channel sandstones on very wet delta-plain with standing water | Firehole Canyon, D1, green stripe unit | e.g., FC, D1, m ~24 |
| Fig. *6.1.3.* 5E | Reddish buff fine-grained sandstone | Red-stained buff-coloured fine-grained arkosic sandstone; may preserve ripple cross-lamination in planar cross-beds and irregular bedding in buff coloured sandstone, grading upwards to massive and intensely bioturbated reddish buff sandstone; uppermost surfaces may preserve yellow-tan clay drapes with cf. *Palaeophycus* isp. cross-cutting *Planolites* ichnofabric | Associated with *Planolites* ichnofabric; Suite BC5A | Possibly subaqueous levee or lower channel bar | Firehole Canyon, D1, second unit | e.g., FC, D1, m ~17 |
| Fig. *5.1.3.* 4F, 4G | Light buff fine-grained sandstone | Buff-coloured fine-grained arkosic sandstone; internally plane-bedded with soft sediment deformation; geometry of sand bed may show evidence of slumping, pinching out; preserves medium-grained sandstone rounded intraclasts; also preserves bone fragments (long bones of birds?) and possibly casts of gastropods; contains iron-stained mudstone intraclasts horizontally oriented in plane beds | Bioturbated in soft substrate with bioturbation increasing upwards to bed-top; Suite BC1 | Possibly slumped channel bar or subaqueous and/or unstable levee | Firehole Canyon, D1, second unit | e.g., FC, D1, m ~15–16? |

| | | | | | | |
|---|---|---|---|---|---|---|
| Fig. *5.1.3.* 4A–D | Tan very fine-grained sandstone | Tan-coloured very fine-grained sandstone; large-scale geometry of flat-based accretion surfaces interpreted as downstream accretion; internally preserves downward-dipping thin (< 2 cm thick) beds of ripple cross-lamination in planar cross-beds; only lee side preserved; flow direction evidenced by ripple lees and foresets oblique and parallel to accretion surfaces; bedsets ~1.5 m-thick bounded by planar laminated beds ~10–20 cm thick; bedsets pinch out down-dip and may fine upwards to brown siltstone; lower contact may be very slightly scoured, and coarsens upwards rapidly from planar-laminated silty very fine-grained sandstone and climbing ripple-laminated very fine-grained sandstone; underlying siltstone facies progressively thicker down-dip of accretion surfaces; unit may be scoured above by large-scale trough cross-stratified sandstones | No trace fossils observed | Downstream accretion of terminal distributary channel onto eulittoral mudflat or within shallow lake; possibly subaqueous mouth bar, hyperpycnal delta front, or possibly alluvial fan toe near shoreline | Firehole Canyon, D1, second unit | e.g., FC, D1, m ~10–14 |
| Fig. *5.1.3.* 7E, 7F | Light buff muddy very fine-grained sandstone | Light buff-coloured, muddy very fine-grained sandstone; internally massive or with irregular, weak bedding; lower contact irregular with red-orange and red-grey sandstone; preserves large-sized full relief burrows with sharp walls | Associated with large *Planolites* isp. and pellet-filled burrows; Suite BC9 | Bioturbated, well drained overbank deposits | Firehole Canyon, D1, upper unit? | e.g., FC, D1, m ~24.5 |
| Fig. *5.1.3.* 2A, 2C, 2D | Tan silty very fine-grained sandstone | Tan-coloured, silty very fine-grained arkosic sandstone; typically intercalated with green mudstone; internally, bedding may be disrupted, likely by vertebrate trampling; internal structures preserved include plane to wavy very thin beds (~1 cm thick), flaser bedding, and vague small-scale cross-stratification; preserves iron-stained root marks | Associated with vertebrate footprints produced in wet to soupy substrates; Suite BC4 | Distal crevasse splay or sheetflood deposits into floodplain or lake-margin marsh | Firehole Canyon, D1, lower unit | e.g., FC, D1, m ~3.5–5 |
| Fig. *5.1.3.* 5A–D | Reddish grey very fine-grained arkosic sandstone | Reddish grey silty very fine-grained arkosic sandstone; intercalated with olive tan siltstone; internally preserves planar lamination, climbing ripple-lamination and small-scale trough cross-lamination; may be pedogenically modified towards top, with irregular upper contacts; top surface bioturbated and preserves reddish surface crust | Preserves large vertical cf. *Taenidium barretti* and *Skolithos* isp.; Suites BC3, BC9 | Well-drained crevasse deposits onto floodplain siltstone | Firehole Canyon, D1, green stripe unit | e.g., FC, D1, m ~22 |
| Fig. *5.1.3.* 7A, 7B, 7F | Buff very fine-grained sandstone | Buff- to greyish buff-coloured, very fine-grained (lower) arkosic sandstone; medium- and large-scale trough cross-stratified; scoured trough fill includes internally ripple-laminated planar cross-beds; climbing ripples with internally graded laminae to dark-coloured (organic detritus) drapes form majority of unit; also preserves flaser bedding with whitish mudstone drapes; grades upwards to muddy tan siltstone | Not associated with trace fossils | Terminal distributary scour and fill channel deposits | Firehole Canyon, D1, upper unit | e.g., FC, D1, m ~25–26 |
| Fig. *5.1.3.* 7G | Buff-coloured muddy very fine-grained sandstone | Buff-coloured muddy very fine-grained arkosic sandstone; planar-bedded with muddy drapes to very thinly wavy bedded and lenticular bedded; upper contact gradational with oscillation-rippled, wavy- and flaser- bedded carbonate unit above D | Not associated with trace fossils | Flooded terminal distributary channel at delta front | Firehole Canyon, D1, upper unit | e.g., FC, D1, m ~27–28 |

| | | | | | | |
|---|---|---|---|---|---|---|
| Fig. *5.1.3.* 3A–H | Olive tan muddy siltstone and silty tan very fine-grained sandstone with bluish green mudstone | Olive tan arkosic siltstone and silty tan very fine-grained sandstone with bluish green mudstone drapes; two cycles represented with slightly different facies; 1) siltstone grades upwards from massive to discontinuously laminated to interbedded or draped with bluish green mudstone; laminated horizon preserves large desiccation cracks with heaved laminae; 2) massive to discontinuously laminated siltstone becomes greener towards top and preserves iron-stains and carbonate root-casts with iron-stains; at top of first coarsening upwards cycle silty sandstone beds are planar laminated and small-scale, low-amplitude trough-cross-laminated; second cycle intercalated with and scoured by thin bed of plane-bedded grey fine-grained sandstone with pebble-sized, rounded mudstone and sandstone intraclasts; upper contact coarsens rapidly to planar-laminated and climbing ripple-laminated; fine-grained sandstone; sandstone interbeds may be distal toes of downstream-accreted sandstones | Not associated with trace fossils; associated with desiccation features, root casts, and/or iron-stained root-marks towards tops of cycles | Exposed hypopycnal delta-front to saturated mudflat; coarsening upwards cycles capped by sheetflood sandstones or distal toes of downstream-accreting sandstones (clinothems?) | Firehole Canyon, D1, second unit | e.g., FC, D1, m ~8.5–9.5 |
| Fig. *5.1.3.* 5A, 5B, 5D, 5F | Olive tan siltstone and reddish grey very fine-grained sandstone | Olive tan siltstone intercalated with red-grey very fine-grained sandstone; siltstone internally massive with conchoidal weathering; lower contact transitional with olive green muddy siltstone; sandstone beds internally very low-angle cross-laminated and climbing-rippled | Not associated with trace fossils | Distal crevasse or overbank siltstones with crevasse sandstones; siltstones possibly deposited in overbank ponds | Firehole Canyon, D1, second unit to green stripe unit | e.g., FC, D1, m ~20–21 |
| Fig. *5.1.3.* 3A | Olive tan siltstone | Olive tan-coloured arkosic siltstone; internally massive with conchoidal weathering; may preserve vague discontinuous lamination; lower contact gradational with lake mudstone | Not associated with animal trace fossils | Shallowing upwards hypopycnal delta front or muddy sublittoral | Firehole Canyon, D1, second unit | e.g., FC, D1, m ~7.5–8.5 |
| Fig. *5.1.3.* 7G; Fig. *6.1.3.* 10F | Tan muddy siltstone | Tan muddy siltstone; poorly bedded in lower portion; very thinly bedded upwards with very small horizontal traces on lower bedding plane; grading upwards to planar-bedded silty very fine sandstone; lower part of unit grades upwards from trough cross-stratified and climbing-rippled buff sandstone | Associated with possible very small horizontal traces; Suite BC7 | Flooded terminal distributary channel during transgression | Firehole Canyon, D1, upper unit | e.g., FC, D1, m ~26–27.5 |
| cf. Fig. *5.1.3.* 5A | Olive green muddy siltstone | Olive green muddy siltstone; internally massive with vague discontinuous lamination; breakage platy; forms top of second unit | Not well exposed; no trace fossils observed | Overbank muddy siltstones | Firehole Canyon, D1, second unit | e.g., FC, D1, m ~19–20 |
| Fig. *5.1.3.* | Light greyish green muddy | Light greyish green muddy siltstone; internally laminated within thin beds ~3 cm thick, becoming massive towards top; parting | Not associated with trace fossils | Relatively freshwater to | Firehole Canyon, D1, | e.g., FC, D1, m |

| | | | | | | |
|---|---|---|---|---|---|---|
| 6A–G | siltstone | planes between laminae are darker in colour, and may represent the settling of organics; signs of exposure within unit include tiny desiccation cracks; upper surface of this unit capped by and orange, thin stromatolitic layer on sandstone filling desiccation cracks | | brackish lake or interdistributary bay | green stripe unit | ~23–23.8, m ~24.3–25 |
| Fig. *5.1.3.* 5A, 5E, 5F | Brown to black mudstone (weathers bright green) | Dark brown to black discontinuously laminated mudstone; weathers bright green; lower contact not sharp, unit appears to have settled onto to underlying olive tan siltstone; upper contact sharp with intraclast carbonate bed | Forms the "green stripe"; compare with green in lower unit of the A-Bed | Organic-rich lake deposits; possibly an interdistributary bay or lagoon fed by seepage? | Firehole Canyon, D1, green stripe unit | e.g., FC, D1, m ~22.8 |
| Fig. *5.1.3.* 2A, 2B | Reddish tan and light green mudstone | Reddish tan and green mudstone; discontinuously laminated; pedogenically altered; preserves iron-stained root-marks and carbonate root casts with iron-mineral rinds; upper contact irregularly eroded and overlain by wavy-bedded calciclastic sandstones and intraclast conglomerates | No trace fossils observed | Subaerially exposed and pedogenically modified overbank deposits | Firehole Canyon, D1, lower unit | e.g., FC, D1, m ~5–6 |
| Fig. *5.1.3.* 2A, 2C, 2D, 2E | Light green mudstone | Green mudstone, massive or broken into weakly developed peds; associated with iron-stained root-marks signifying wet sediments; may be intercalated with thin, rippled, tan-coloured, silty very fine-grained sandstone beds; contains red-stained horizons ~2 cm thick; lower contact appears gradational with lake beds below | Associated with vertebrate footprints produced in wet to soupy substrates; Suite BC4 | Relatively fresh water overbank deposits near lake; may represent riparian to lake-margin marsh; eventually desiccated | Firehole Canyon, D1, lower unit | e.g., FC, D1, m ~3.5–5 |

***Lithofacies of the D-Bed, Firehole Canyon, Section D2 (divided into second unit, "green stripe" unit, and upper unit)***

| | | | | | | |
|---|---|---|---|---|---|---|
| Fig. *5.1.3.* 9B | Greyish buff pebble-conglomerate | Clast-supported greyish buff, poorly sorted, polymictic, pebble-conglomerate with medium- to coarse-grained grey arkosic sandstone matrix; clasts oriented in all directions; clasts rounded and composed of orange-tan mudstone, reddish grey medium-grained sandstone, coated mudstone, green mudstone, buff very fine-grained sandstone, and possibly coarsely crystalline tuff; facies pinches out laterally to grey coarse-grained sandstone | Not associated with trace fossils; clasts probably derived from older Green River Formation and Wasatch Formation | Channel thalweg of large terminal distributary channel | Firehole Canyon, D2, upper unit | e.g., FC, D2, m ~6 |
| Fig. *5.1.3.* 9A, 9C, 9D | Grey and tan coarse-grained sandstone | Grey and tan coarse-grained sandstone; structures include slightly convolute plane-beds along lower contact, and non-parallel large-scale cross-stratification; also preserves numerous reed and leaf impressions in lower part of unit | Not associated with trace fossils | Channel deposits; possibly lower side bar and channel thalweg | Firehole Canyon, D2, upper unit | e.g., FC, D2, m ~6, |

| | | | | | | |
|---|---|---|---|---|---|---|
| Fig. *5.1.3.* 8B | Greyish tan fine-grained sandstone | Greyish tan fine-grained arkosic sandstone; internal structure includes plane-beds and ripple-lamination within low angle cross-beds; some laminae show soft sediment deformation due to shear; unit also preserves large-scale dewatering structure within plane-bedded and ripple cross-laminated sandstone | Not associated with trace fossils; large-scale dewatering structure may possibly be due to tectonic activity | Rapid deposition of channel or delta front sandstones | Firehole Canyon, D2, second unit | e.g., FC, D2, m ~1 |
| Fig. *5.1.3.* 8C, 8D | Light buff very fine-grained sandstone | Light buff very fine-grained arkosic sandstone; internal structure includes critical climbing ripple-lamination, with sheared or supercritical climbing ripple-lamination; may preserve black drapes on parting planes; unit fines upwards | Not associated with trace fossils | Rapid deposition, possibly of delta front sandstones | Firehole Canyon, D2, second unit | e.g., FC, D2, m ~1.5 |
| Fig. *5.1.3.* 8A | Light brown/tan very fine-grained sandstone | Light brown to tan very fine-grained arkosic silty sandstone with internal parallel, continuous, wavy lamination and planar lamination | Not associated with trace fossils | Overbank deposits on delta-plain | Firehole Canyon, D2, second unit | e.g., FC, D2, m ~2–3 |
| Fig. *5.1.3.* 9E | Greenish light buff muddy very fine-grained sandstone | Greenish light buff muddy very fine-grained arkosic sandstone; internally laminated with low angle cross-lamination at base, grading to climbing ripples, to discontinuously, parallel wavy- and planar-laminated very fine-grained sandstone; bedding planes may contain green mudstone drapes; units capped by green, laminated muddy siltstone; lower contacts sharp but not scoured | Associated with small *Planolites* isp. on mud-draped planar to wavy beds in upper part of sandstone unit; Suite BC7 | Waning flow in flood channel, possibly in wet delta-plain anastomosed system | Firehole Canyon, D2, upper unit | e.g., FC, D2, m 7–11 |
| Fig. *5.1.3.* 9H | Light greenish tan very fine-grained sandstone and green mudstone | Light greenish tan very fine-grained mica-rich arkosic sandstone with green mudstone drapes; sandstone beds irregularly planar laminated and bioturbated; may preserve low-amplitude, straight, sharp-crested ripple bedforms | Associated with indistinct *Planolites* isp.; Suite BC7, BC8A | Distal and/or waning crevasse splay | Firehole Canyon, D2, upper unit | e.g., FC, D2, m ~12.5 |
| Fig. *5.1.3.* 9G, 9H | Brownish green muddy siltstone, reddish tan very fine-grained sandstone | Brownish green muddy siltstone intercalated with reddish tan very fine-grained sandstone; siltstones are discontinuous laminated and massive with platy to blocky breakage; sandstones are planar laminated or irregularly bedded; bioturbation may have disrupted all bedding | Associated with vertical and horizontal full relief burrows; Suite BC8A | Pedogenically altered overbank deposits | Firehole Canyon, D2, upper unit | e.g., FC, D2, m ~11.5–13 |
| Fig. *5.1.3.* 9A | Green mudstone and buff siltstone | Lenticular-bedded and interbedded green mudstone with buff arkosic siltstone; lower contact gradational with greyish green and tan marl; upper contact sharp, flat, and erosional with coarse-grained arkosic channel sandstone or scoured by arkosic intraclast conglomerate | Not associated with trace fossils | Possibly interdistributary bay or main lake with arkosic input | Firehole Canyon, D2, green stripe unit | e.g., FC, D2, m ~5.8 |
| Fig. *5.1.3.* 9E, 9F | Greenish tan muddy siltstone | Greenish tan muddy arkosic siltstone; discontinuously ripple laminated; laminae fine upwards to muddy drapes on bedding planes; preserves very low amplitude interference ripple | Preserves very small surface tunnels; Suite BC7 | Abandoned flood channel pools, possibly in wet | Firehole Canyon, D2, upper unit | e.g., FC, D2, m ~9 |

| | | | | | | |
|---|---|---|---|---|---|---|
| | | bedforms;‘bubble texture’ on surface attributed to gas-escape bubbles of microbial mats, and narrow, shallow, desiccation cracks; also preserves very small horizontal surface tunnels preserved in concave and convex epirelief | | delta-plain anastomosed system | | |
| Fig. *5.1.3.* 8A | Brownish olive siltstone | Brownish olive-green arkosic siltstone; internally massive; lower and upper contacts gradational; transition to green stripe unit | Not associated with trace fossils | Distal overbank fines | Firehole Canyon, D2, second unit | e.g., FC, D2, m ~3 |
| Fig. *5.1.3.* 8E, 8F | Dark brownish olive siltstone | Dark brownish olive-green arkosic siltstone; internally preserves discontinuous lamination; preserves plant material and large bone fragments, probably mammal, possibly reptile; lower and upper contacts gradational | Not associated with trace fossils | Distal overbank fines into interdistributary bay or delta-plain lake | Firehole Canyon, D2, green stripe unit | e.g., FC, D2, m ~3.7–3.9 |
| Fig. *5.1.3.* 9A | Mixed tan and greyish green to dark brown marly muddy siltstone | Mixed tan and greyish green muddy siltstone to dark brown mudstone; internally laminated to massive and thinly bedded, with horizontal beds ~4–5 cm thick; lower contact gradational with dark brown mudstone within intraclast bed; upper contact scoured by channel conglomerate; unit preserves a stromatolitic horizon and plant fragments | Not associated with trace fossils | Freshwater or brackish lake, with mixed siliciclastic and carbonate sediments | Firehole Canyon, D2, green stripe unit | e.g., FC, D2, m ~4.5–6 |
| Fig. *5.1.3.* 8E, 8F | Blackish dark green muddy siltstone | Blackish dark green muddy siltstone; internally massive and discontinuously laminated with platy breakage; lower contact gradational; upper contact sharp with carbonate mud and intraclast conglomerate above | Not associated with trace fossils; the “green stripe” bed | Interdistributary bay or lagoon | Firehole Canyon, D2, green stripe unit | e.g., FC, D2, m ~4.2 |
| Fig. *5.1.3.* 8E, 8F | Dark brown to black mudstone | Dark brown to black laminated and discontinuously laminated mudstone; weathers bright green; lower and upper contacts gradational | Not associated with trace fossils; the “green stripe” bed | Interdistributary bay or lagoon | Firehole Canyon, D2, green stripe | e.g., FC, D2, m ~3.9–4.1 |
| Fig. *5.1.3.* 8A, 8E; Fig. *6.1.3.* 11A | Brown and orange muddy intraclast conglomerate | Distinct orange-weathering marker bed with sharp lower contact and gradational upper contact; internally, divisible into three beds, with the lower and upper beds composed of dark brown mudstone (carbonate?) and the middle bed an intraclast conglomerate; total bed thickness ~15 cm; lower mudstone bed contains possible invertebrate burrows filled with intraclast mudstone material | May be associated with trace fossils associated with conglomerate; Suite BC1? | May represent a transgressive lag | Firehole Canyon, D2, green stripe unit | e.g., FC, D2, m ~4.4 |
| ***Lithofacies of the E-Arkose Bed, Firehole Canyon, Section D2-E2 (divided into a lower unit, the ‘white stripe’ unit, and an upper unit)*** | | | | | | |
| Fig. *5.1.3.* 10E, 10F | White calciclastic sandstone | Greyish white calciclastic sandstone; lower contact with siliciclastic mudstone preserves parallel, continuous planar lamination; upper contact with siliciclastic mudstone above thinly bedded (< 5 cm), internally massive to wavy bedded calciclastic sandstone with draped bedding planes | No trace fossils observed | Littoral lacustrine; represents brief lake expansion | Firehole Canyon, E2, white stripe unit | e.g., FC,D2, m ~27–27.5 |

| | | | | | | |
|---|---|---|---|---|---|---|
| Fig. *5.1.3.* 10F | Tan very fine-grained sandstone | Tan-coloured very fine-grained sandstone; trough cross-bedded with scoured base; internally preserves vague ripple laminae in cross-beds; bedset ~2 m thick; laterally adjacent to greenish brown siltstone | No trace ofssils observed | Shallow channel on floodplain | Firehole Canyon, E2, upper unit | e.g., cf. FC, D2, m ~27.8 |
| Fig. *5.1.3.* 10D | Greyish tan silty very fine-grained sandstone | Greyish tan silty very fine-grained arkosic sandstone; internally 'parallel', irregular laminated; may preserve discontinuous ripple-lamination; irregular bedding likely due to bioturbation; preserves iron-stained root-marks | Associated with large, vertically oriented cf. *Taenidium barretti*; Suite BC9 | Crevasse deposits onto floodplain | Firehole Canyon, E2, lower unit | e.g., FC, D2, m ~23 |
| Fig. *5.1.3.* 10C | Tan very fine-grained sandstone | Tan very fine-grained arkosic sandstone; internally massive and vaguely ripple-laminated; likely bioturbated; preserves iron-stained root-marks; preserves possible vertebrate footprint in cross-section; poorly exposed | Likely bioturbated; associated with possible mammal footprint; Suite BC4 | Crevasse deposits onto floodplain; may be close to lake | Firehole Canyon, E2, upper unit | e.g., FC, D2, m ~26.5, ~28, ~29 |
| Fig. *5.1.3.* 10B–C, 10G | Greenish brown siltstone | Greenish brown siltstone; massive to irregularly bedded, with platy to blocky breakage; may preserve discontinuous, but irregular, very thin horizontal bedding; likely intensely bioturbated, with mottled texture | Associated with *Planolites*; Suite BC9 | Floodplain deposits | Firehole Canyon, E2, lower unit | e.g., FC, D2, m ~23–26, m 27.5–33 |
| Fig. *5.1.3.* 10C | Tan to greyish green siltstone and mudstone | Tan very fine-grained arkosic sandstone, greyish green siltstone, with green mud drapes; discontinuous ripple-laminated to planar-laminated very fine-grained sandstone with mudstone drape; preserves very low amplitude vague interference ripple bedforms on upper bedding plane | Associated with small- to medium-sized *Planolites* isp.; Suite BC9 | Distal or waning crevasse splay deposits onto floodplain | Firehole Canyon, E2, lower unit | e.g., FC, D2, m ~23.2 |
| Fig. *5.1.3.* 10E, 10H | Brownish green mudstone | Brownish green mudstone; massive internally; no trace fossils observed; upper contact sharp with calciclastic sandstone and lacustrine mudstones | Associated with the thin 'white stripe' in E2 | Wet floodplain flooded by lake | Firehole Canyon, E2, lower unit, upper unit | e.g., FC, D2, m ~26.7, m ~33.8 |

## Figure captions for the photographic plates, Section 5.1.3.

**Fig. 5.1.3.1.** The D-Bed on White Mountain at Kanda (upper unit). **(A)** Outcrop view showing reddish brown siltstones overlying lacustrine mudstones, and coarsening upwards to the bedded sandstones that preserve trace fossils. **(B)** The siltstone and bedded sandstone units shown in (A). **(C)** The base of the upper unit, showing gradual coarsening upwards from lacustrine mudstones at base to sandstones with matrix supported pebble-conglomerate (arrow). **(D)** Sandstone scoured into underlying lacustrine mudstones. **(E)** Large-scale lateral accretion surfaces of channel sandstone in upper unit. **(F)** Sharp-crested asymmetrical ripple bedforms at top of sandstone in (E). **(G)** Weakly developed paleosol of upper unit. Fractured mudstone and siltstone in lower part of photo overlain by laminated heterolithic facies. **(H)** Interbedded sandstones and siltstones near top of D-Bed. This facies preserves bird tracks.

**Fig. 5.1.3.2.** The D-Bed at Firehole Canyon (Section FC, D1; lower unit). **(A)** The lower unit at FC, D1. **(B)** The upper contact of the lower unit, sharply overlain by lacustrine carbonate sandstones. **(C)** The heterolithic facies of the lower unit (m ~5). **(D)** Close-up of the vertebrate track-preserving sandstones at m ~5. **(E)** The massive siltstones of the lower portion of the lower unit (m ~4).

**Fig. 5.1.3.3.** The D-Bed at Firehole Canyon (Section FC, D1; lower portion of the second unit). **(A)** Coarsening upwards cycle with siltstones and heterolithic facies above the "white stripe" unit (m ~6.8–8.5). **(B)** Coarsening upwards of the massive siltstone facies to planar-laminated sandstones. Note medium-grained sandstone horizon with rounded intraclasts just below hammer. **(C)** Close-up of the laminated heterolithic facies with deep desiccation cracks at m ~8.3. **(D)** Close-up of the plane-bedded medium sandstone with rounded intraclasts (m ~ 9.5). **(E)** Close-up of the internally laminated sandstone balls shown in (D). **(F)** Siltstones with possible carbonate root casts at m ~9.

**Fig. 5.1.3.4.** The D-Bed at Firehole Canyon (Section FC, D1; middle portion of the second unit). **(A)** Outcrop view showing large-scale accretion surfaces above the "white stripe" unit (middle of photograph). **(B)** Outcrop view showing the pinching out of accreting sandstones into siltstones shown in Fig. *5.1.3.*3. **(C)** The lower portion of the thick sandstone beds a m ~10–11. **(D)** Internally ripple-laminated downstream-dipping cross-beds. **(E)** Sheared planar beds at ~ m 15. **(F)** Possible levee deposit with internal slumping. **(G)** Close-up of upper part of sandstone shown in (F), with plane-beds and soft substrate bioturbation.

**Fig. 5.1.3.5.** The D-Bed at Firehole Canyon (Section FC, D1; the "green stripe" unit, lower part). **(A)** Outcrop view showing the "green stripe" in the middle of the photograph. **(B)** Ripple-laminated and bioturbated siltstones and sandstones of coarsening upwards unit below the "green stripe". **(C)** Close-up of sandstone shown in (B). **(D)** Close-up of sandstone shown in (B). **(E)** Close-up of the "green stripe" overlying olive green siltstones. **(F)** Close-up of the "green stripe". **(G)** The carbonate horizon with internal intraclast conglomerate and unidirectional ripples (arrow). **(H)** Close-up of the intraclast conglomerate within the carbonate horizon above the "green stripe".

**Fig. 5.1.3.6.** The D-Bed at Firehole Canyon (Section FC, D1; the "green stripe" unit, upper part). **(A)** Outcrop view showing bedded marlstones and orange-coloured sandstone unit at m ~23–24.5. **(B)** The bedded green marlstone facies sharply overlain by a thick sandstone lens. **(C)** Probable vertebrate tracks in cross-section within the sandstone lens. **(D)** Bedded green marlstone facies above the sandstone lens, and scoured into from above by sandstones of the upper unit. **(E)** Close-up of the laminated green marlstone facies. **(F)** Close-up of an orange, laminated stromatolitic horizon above a desiccation-cracked lower bedding plane. **(G)** Close-up of the desiccation cracks below the stromatolitic horizon. **(H)** Straight, symmetrical ripple bedforms in sandstone in float, from m ~25.

**Fig. 5.1.3.7.** The D-Bed at Firehole Canyon (Section FC, D1; the upper unit). **(A–B)** The lower contact of the upper unit at m ~25, showing large-scale trough cross-stratification. **(C)** Close-up of a stromatolitic horizon overlain by sandstone of the upper unit. **(D)** Intraclast conglomerate at the base of the upper sandstone, containing fragments of the stromatolitic horizon. **(E)** Thin, lenticular beds of cross-bedded sandstone of the lower upper unit. **(F)** Ripple lamination in the lower upper unit. **(G)** The transition from the upper unit to wavy-bedded carbonates at the top of the D-Bed.

**Fig. 5.1.3.8.** The D-Bed at Firehole Canyon (Section FC, D2); the lower unit and "green stripe" unit). **(A)** Outcrop view of the second unit, green stripe unit, and upper unit in Section FC, D2. Note overall fining upwards to the green stripe unit in lower part of photograph. **(B)** Metre-scale and decimeter-scale (arrow) water escape structures in the second unit (m ~0–1.5). **(C)** Ripple-laminated sandstone with supercritical climbing ripples (arrow). **(D)** Supercritical climbing ripples with stoss-side preserved and black drapes. **(E)** The "green stripe" unit showing black actual colouring of the sediments. Note siltstones below also dark in colour. **(F)** Olive siltstones below the "green stripe" preserving bone of reptile or mammal (centre of photo).

**Fig. 5.1.3.9.** The D-Bed at Firehole Canyon (Section FC, D2; the upper unit). **(A)** Outcrop view showing bedded siltstone facies above the green stripe scoured into and overlain by large-scale fining upwards cycles in lateral accretion surfaces. **(B)** Channel lag conglomerate with pebble-sized clasts possibly of older Wilkins Peak sediments and the sandstones of the Wasatch Formation. **(C)** Coarse-grained cross-bedded sandstone of upper unit. **(D)** Reed impression and plant material at base of coarse-grained sandstone. **(E)** Fining-upwards cycle within channel. Green mudstone at top of cycle. **(F)** Ripple bedforms and bubble-like texture in heterolithic facies near top of fining upwards cycle. **(G)** Greenish brown pedogenically modified overbank sediments (m ~12). **(H)** Greenish brown sandstones with ripple bedforms on upper bedding plane (top of photograph).

**Fig. 5.1.3.10.** The E-Bed at Firehole Canyon (Section FC, D2). **(A)** Outcrop view showing the top of the D-Bed, lacustrine facies, and the greenish brown E-Bed towards top. **(B)** The greenish brown E-Bed at the site of the FC, D2 section. **(C)** Close-up of greenish brown silty sandstones of the E-Bed. **(D)** "Irregularly"-bedded and bioturbated sandstones of the E-Bed (m ~23). **(E)** Massive greenish brown siltstones overlain by the "white stripe"of the E-Bed (m ~27). **(F)** Cross-bedded sandstone of the upper E-Bed scouring in lacustrine mudstones of the "white stripe" shown in (E). **(G)** Laminated silty sandstones of the upper E-Bed. **(H)** The upper contact of the E-Bed with the overlying lacustrine facies.

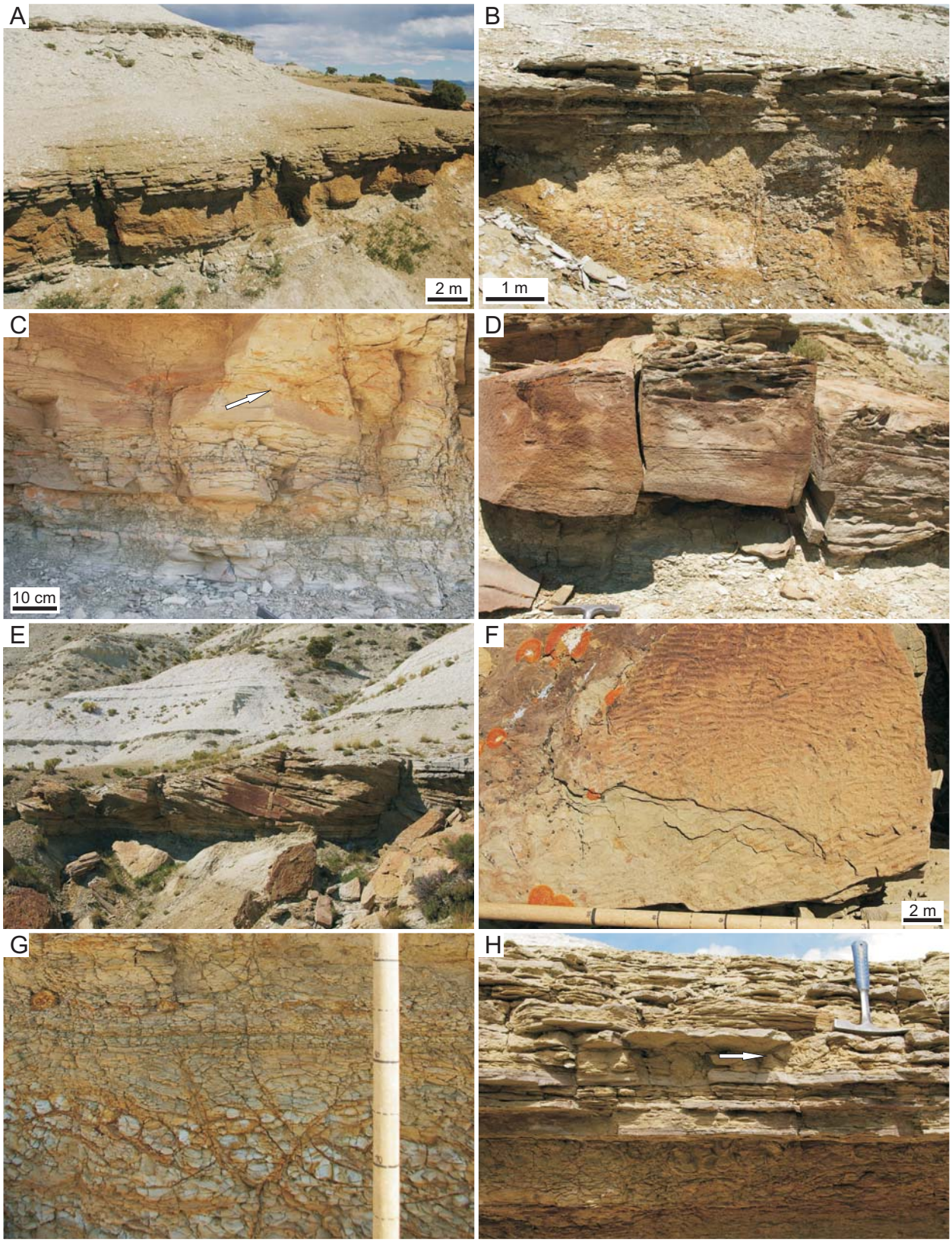


**Fig. 5.1.3.1.** The D-Bed on White Mountain at Kanda (upper unit). Refer to Table 5.3 for descriptions of the lithofacies shown. See full caption above.

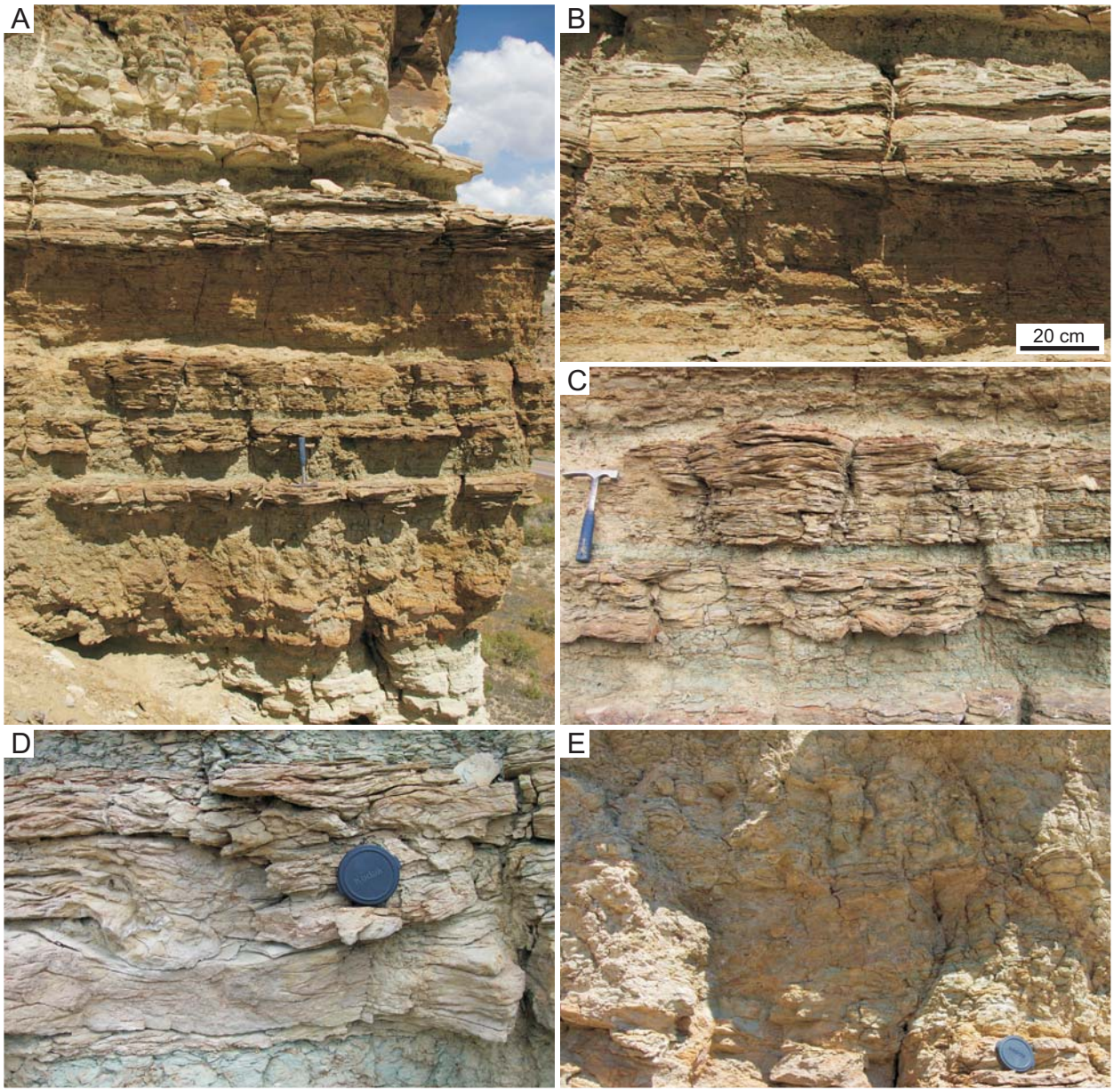


**Fig. 5.1.3.2.** The D-Bed at Firehole Canyon (Section FC, D1; lower unit). Refer to Table 5.3 for descriptions of the lithofacies shown. See full caption above.

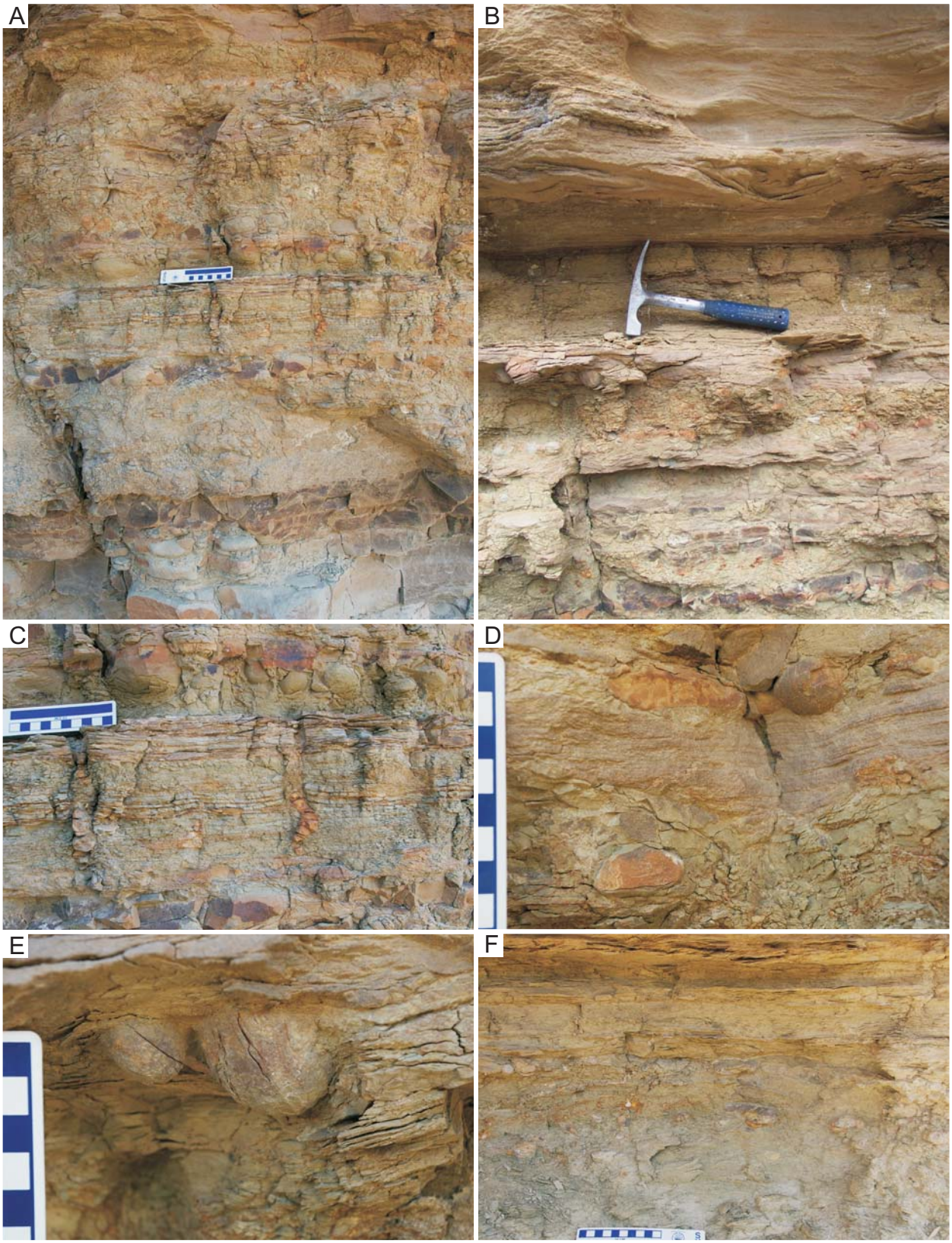


**Fig. 5.1.3.3.** The D-Bed at Firehole Canyon (Section FC, D1; lower portion of the second unit). Refer to Table 5.3 for descriptions of the lithofacies shown. See full caption above.

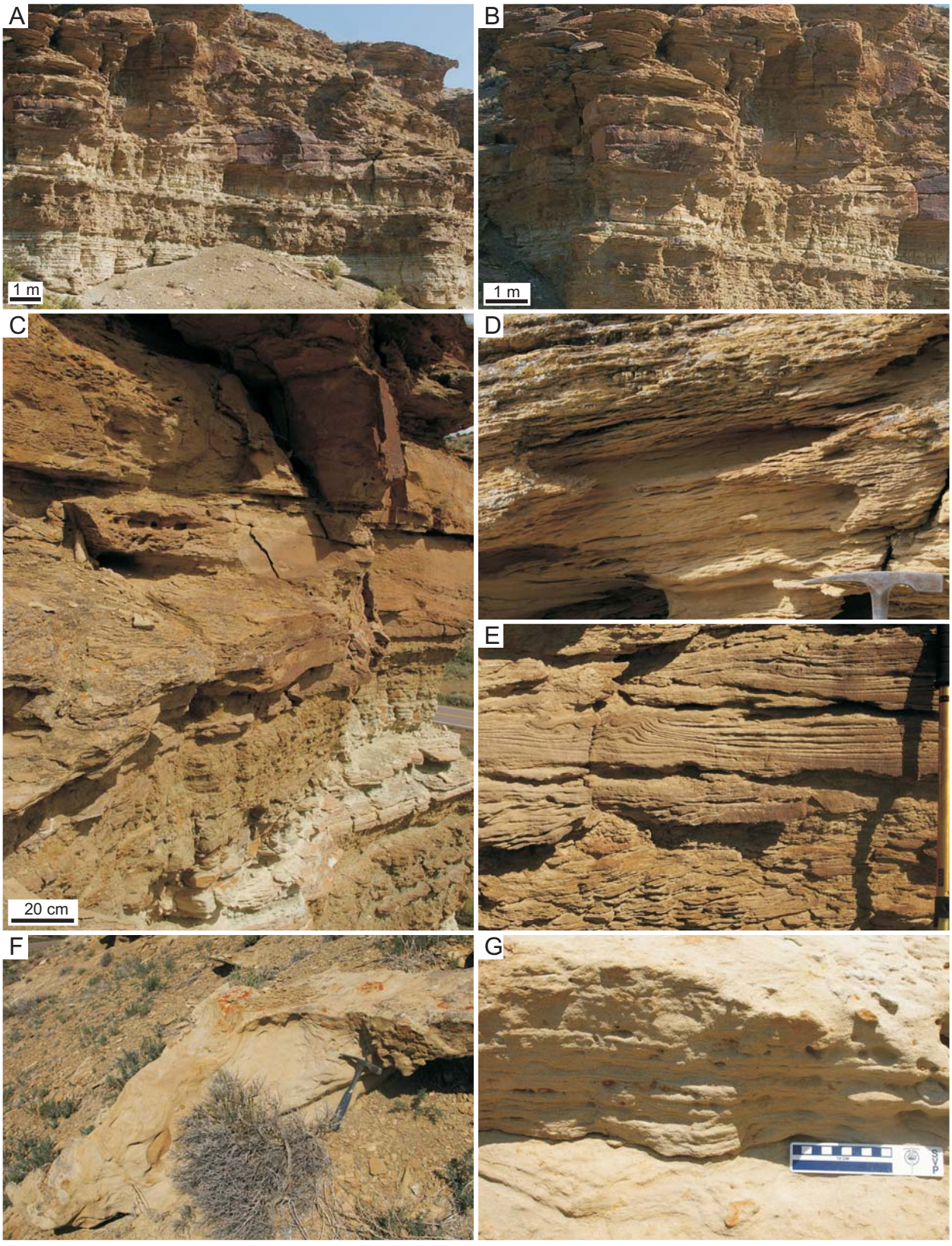


**Fig. 5.1.3.4.** The D-Bed at Firehole Canyon (Section FC, D1; middle portion of the second unit). Refer to Table 5.3 for descriptions of the lithofacies shown. See full caption above.

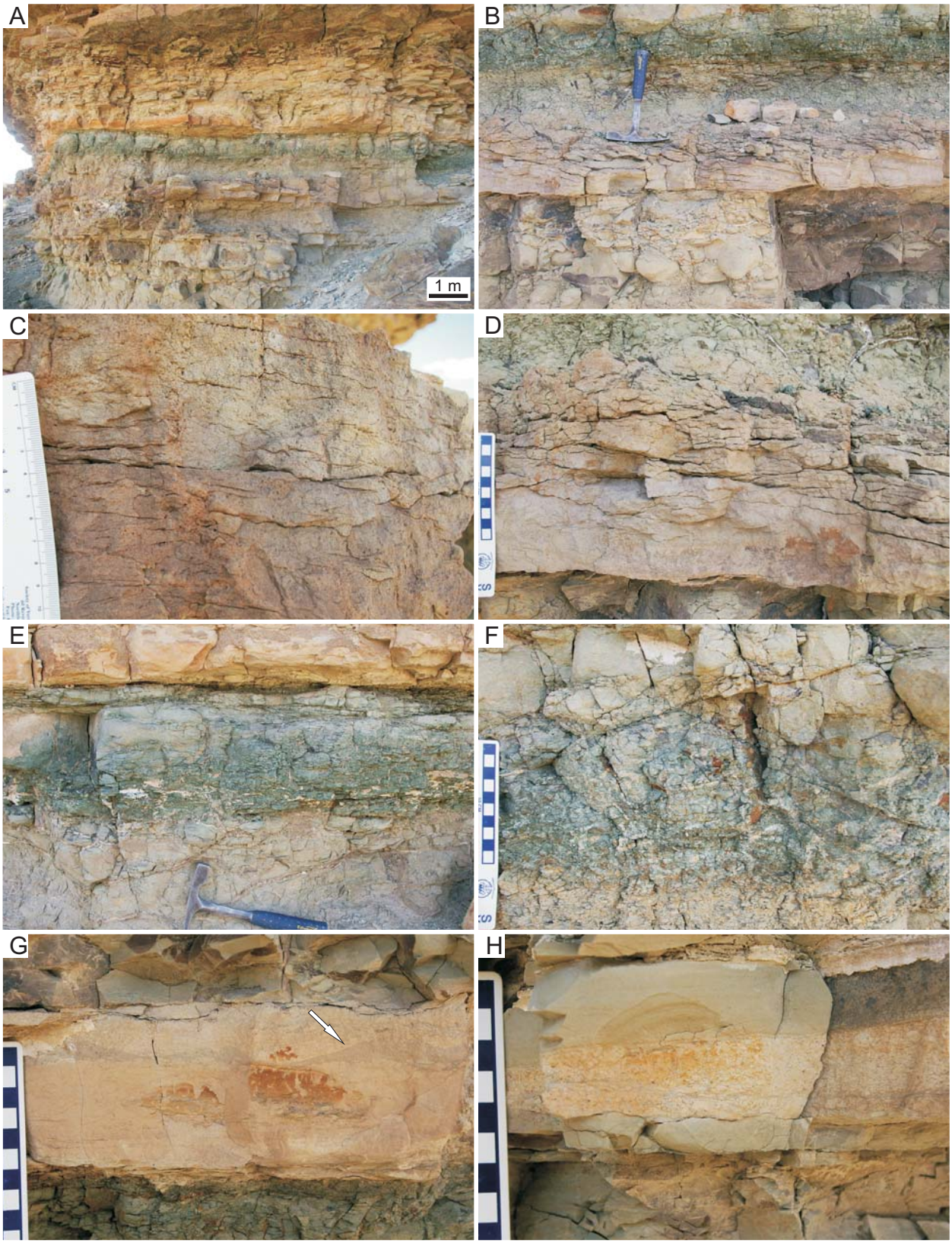


**Fig. 5.1.3.5.** The D-Bed at Firehole Canyon (Section FC, D1; the "green stripe" unit, lower part). Refer to Table 5.3 for descriptions of the lithofacies shown. See full caption above.

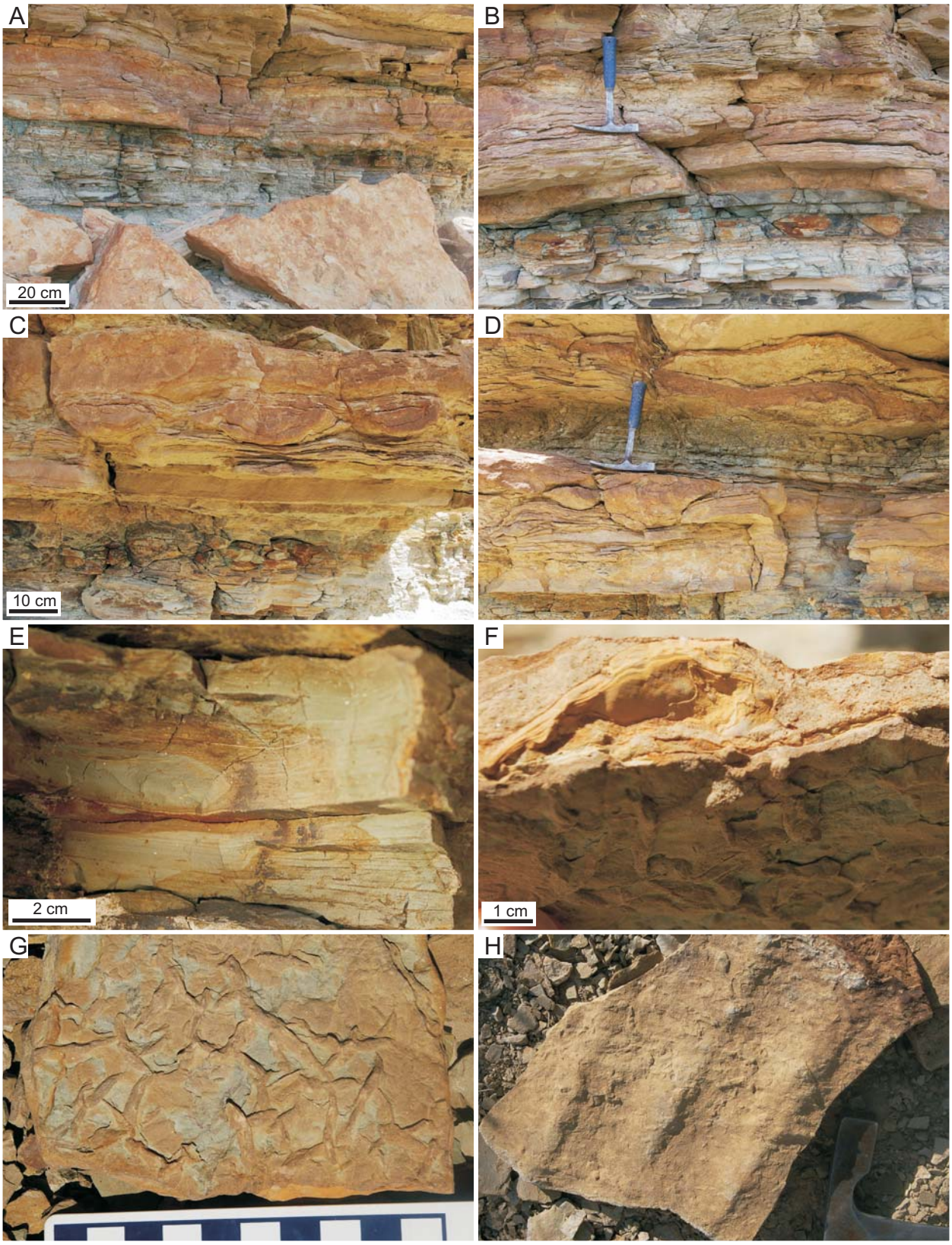


**Fig. 5.1.3.6.** The D-Bed at Firehole Canyon (Section FC, D1; the "green stripe" unit, upper part). Refer to Table 5.3 for descriptions of the lithofacies shown. See full caption above.

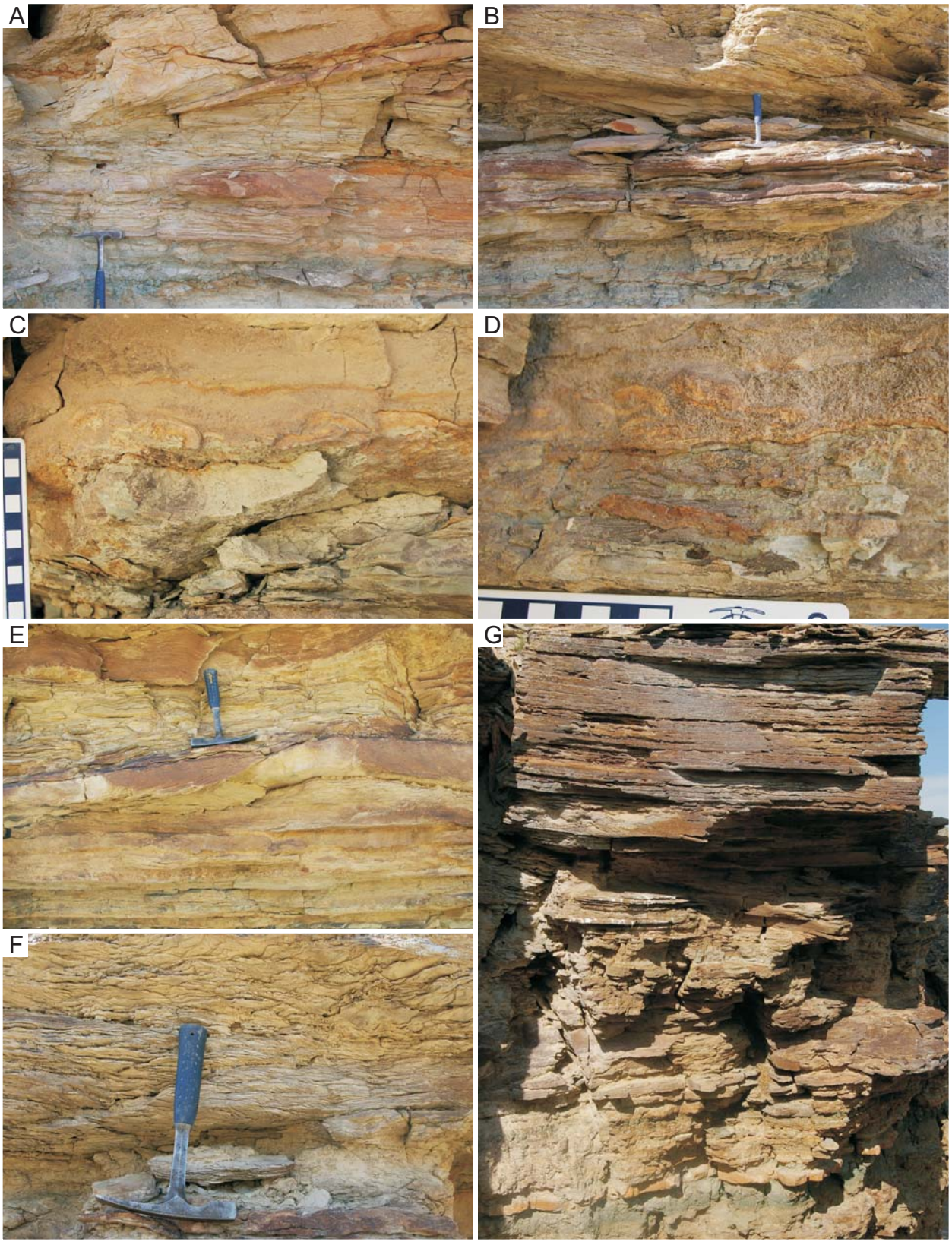


**Fig. 5.1.3.7.** The D-Bed at Firehole Canyon (Section FC, D1; the upper unit).
**Fig. 5.1.3.8.** (Next page) The D-Bed at Firehole Canyon (Section FC, D2); the lower unit and "green stripe" unit)

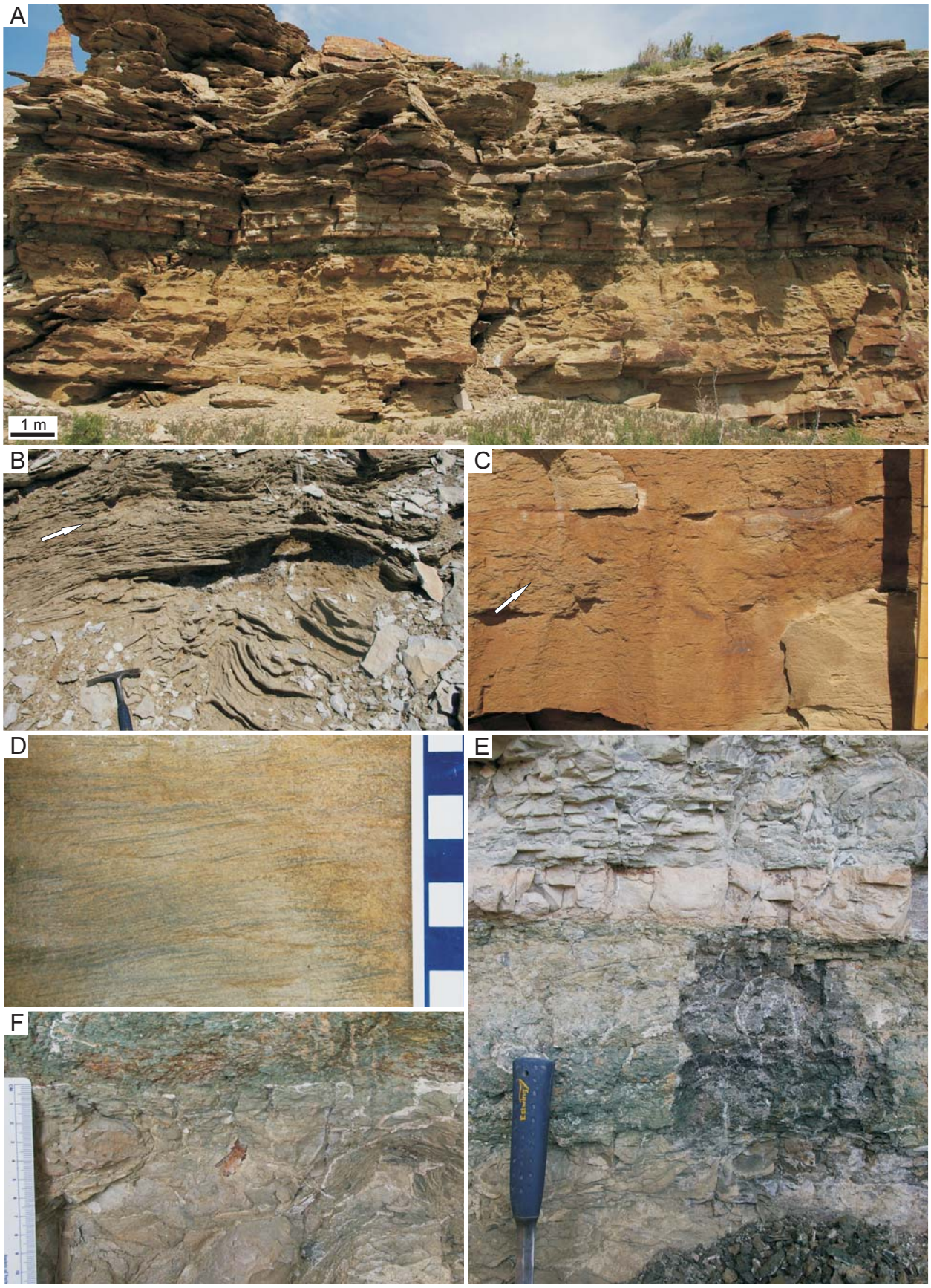
A
1 m
B
C
D
E
F

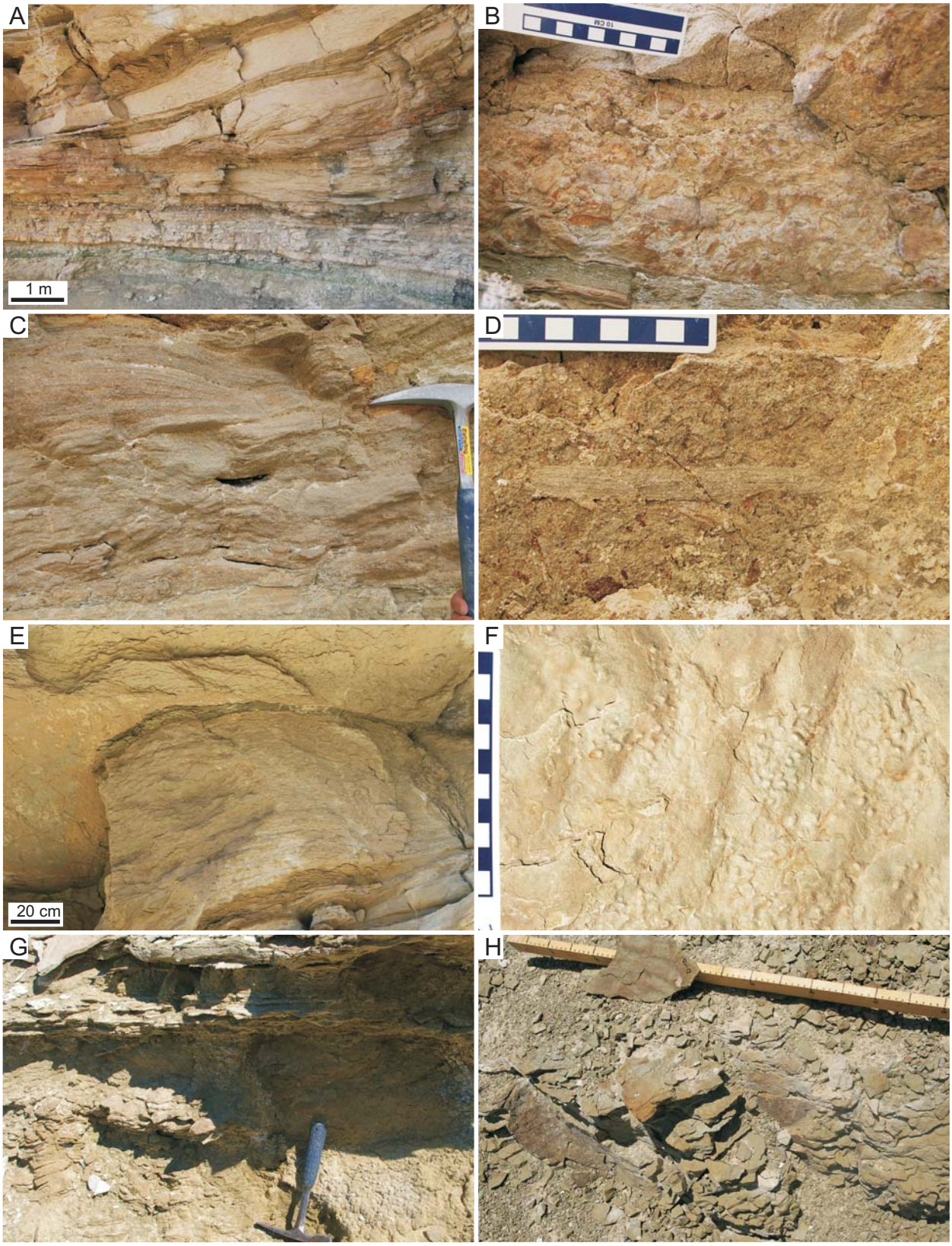


**Fig. 5.1.3.9.** The D-Bed at Firehole Canyon (Section FC, D2; the upper unit). Refer to Table 5.3 for descriptions of the lithofacies shown. See full caption above.

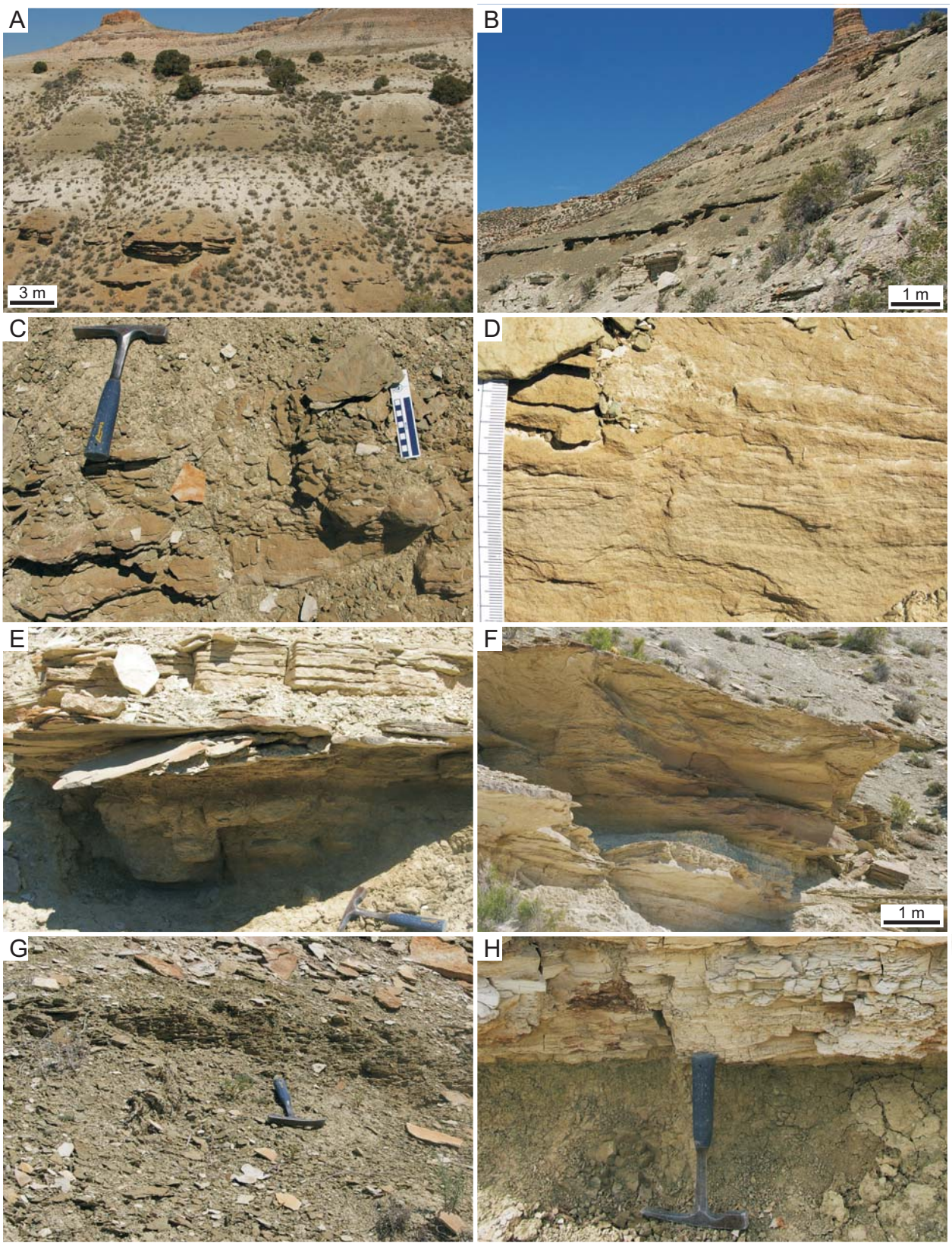


**Fig. 5.1.3.10.** The E-Bed at Firehole Canyon (Section FC, D2). Refer to Table 5.3 for descriptions of the lithofacies shown. See full caption above.

## 5.2. Summary of Lithofacies Associations in the Basin Centre

The following sections of text summarize the facies associations at the basin centre localities (described in Tables 5.1, 5.2, and 5.3) and discuss their interpreted sedimentary environments. Trace fossils were a valuable tool in the interpretation of the sedimentary environments and are briefly mentioned in the following text. Detailed descriptions and discussion of the trace fossils are presented in Chapter 6.

Two main groups of interrelated facies assemblages are present in the basin centre of the Wilkins Peak Member, divisible by lithology into: 1) evaporative carbonates; and 2) arkosic siliciclastics. In general, the carbonate units represent littoral, mudflat, and saline pan deposits of Lake Gosiute. The arkosic units are dominated by alluvial deposits, including channel sandstones, crevasse splay and levee sandstones, and overbank siltstones and mudstones. Several lithofacies recognized in this study represent areas intermediate between the carbonate-lake facies and alluvial-floodplain facies, including: 1) rippled sandstones that may have been deposited as bars at mouths of distributary channels; 2) plane-bedded, cross-stratified, and convoluted sandstones that may represent subaqueous levees; 3) massive arkosic siltstones interpreted as being deposited from hypopycnal flows in the prodelta or distal delta front of the main lake; 4) heterolithic lenticular-bedded mixed arkosic siltstone, calcareous marlstones, and calciclastic siltstones and sandstones; and, 5) massive marlstones. Additionally, massive to laminated organic-rich siliciclastic mudstones and siltstones may represent a relatively freshwater lake or interdistributary bay facies association atypical of the Wilkins Peak Member sediments (e.g., the "green stripe"). The term "marl" is used here to refer to mixed carbonate and siliciclastic lithologies; because some of these mixed sediments contain silt-sized siliclastics better referred to as siltstones mixed with carbonate mudstone, "marl" is used as a qualifier to describe both mudstones and siltstones to reflect these differences in grain-size. The term "marlstone" is also used to refer only to marl mudstones of mixed carbonate and arkosic siliciclastic lithologies.

Many of the lithofacies described here do not preserve trace fossils. However, to place the trace fossils within a stratigraphically relevant context and to determine the sedimentary environments with which they were associated, they were considered as elements within stratigraphic packages. The sedimentology and local-scale stratigraphy of the units in which the traces were preserved were used to recognize the lithofacies-related distribution of the traces.

### *5.2A. Basin Centre Carbonates and Evaporites*

#### *5.2.1. Intraclastic Calcareous Conglomerates*

Carbonate deposits in the Wilkins Peak Member may be composed of coarse-grained calciclastics of reworked carbonates, including intraclastic carbonate conglomerates containing reworked carbonate mudstone intraclasts derived from desiccated carbonate crusts. This is the "Littoral Association" of Pietras and Carroll (2006), who divided it into the "Intraclastic Conglomerate Lithofacies" and the "Calcareous Sandstone Lithofacies". These coarse-grained carbonates are typically white or slightly orangish to pinkish white. Lower bed contacts may be scoured, undulating to wavy, or flat, and upper bed contacts often preserve symmetrical ripple bedforms ranging from low amplitude (< 1 cm) to moderate amplitude (< 4 cm), or they may possibly be disrupted by salt efflorescence. The intraclastic carbonate sandstones and conglomerates are interpreted to have formed in two main sedimentary environments.

First, they may have been produced within the lake and represent storm beds or transgressive lags. Three examples of this facies were recognized. Examples from the measured sections provided throughout the text are referred to first by the section locality (e.g., FC, D1), followed by a reference to the metre-number where the facies can be found in the section (e.g., m

~6.2). First, the basal "white stripe" unit in the D-Bed in Firehole Canyon (e.g., FC, D1, m ~6.2; Fig. *5.1.1.*10C) is scoured at the base, cross-bedded, and contains pebble-sized rounded clasts. Second, the enigmatic, orangish white and brown, granule-sized carbonate intraclast bed that lies abruptly over the "green stripe" within the D-Bed of Firehole Canyon (e.g., FC, D1, m ~23; FC, D2, m ~4.4; Figs. *5.1.3.*5G–H, 8E), is sandwiched between an upper and lower carbonate mudstone within the same bed, and pinches out laterally. Possible trace fossils are preserved below the conglomerate in Section FC, D2. The upper portion of this bed in Section FC, D1 preserves unidirectional ripples that are directed eastward, or landward. The third example is from the carbonate bench above the D-Bed in Section FC, D2 (e.g., FC, D2, m ~20). In this case, a white carbonate bed preserves flat-lying carbonate mudstone intraclasts at its base, fines upwards to discontinuously planar-laminated and small-scale trough cross-laminated calcareous sandstone, and preserves relatively high amplitude (~4 cm) symmetrical ripple crests on its upper surface (Fig. *5.1.1.*4A, 4B). Black oil shale overlies the carbonate.

The second setting where carbonate intraclast conglomerates were formed is on the subaerially exposed eulittoral "lake-plain", which represents the flat-lying region that experiences frequent flooding by the lake followed by subaerial exposure. Desiccated carbonate mudstone fragments were reworked by both littoral and sheetflood processes, and incorporated into white to orangish white calcareous sandstones. Two examples of this facies are provided. First, the carbonate bench below the D-Bed on White Mountain at Kanda is dominated by wavy-bedding and wave-rippled or flat flaser-bedding in calcareous siltstones and sandstones, but also contains intraclast conglomerates and coarse-grained calcareous sandstones. The intraclasts may be flat-pebble and or edge-wise breccias with either flat-lying or randomly oriented intraclasts (terminology following Tucker and Wright, 1990) (Fig. *5.1.1.*1C). The intraclast horizon lies at the base of a thin bed (~10 cm thick) that grades upwards to a coarse calcareous sandstone with very small (~1 cm width), isolated "ripple troughs", which may represent the disruption of the carbonate sediments by efflorescent salt crusts and/or "adhesion ripples" (Fig. *5.1.1.*1C, 1F; cf. Smoot and Castens-Seidell, 1994). A second type of intraclast conglomerate, also found in this bench, consists of a matrix-supported, rounded-clast, granule-conglomerate (Fig. *5.1.1.*1B). Discontinuous wavy-lamination is preserved within the siltstone matrix. The lamination is interpreted as being derived from sheetfloods, which transported the clasts to the littoral zone where the deposit was reworked by littoral processes.

### *5.2.2. Massive and Ripple-Laminated Calcareous Siltstones and Sandstones*

Calcareous siltstones and fine-grained sandstones that are wavy-bedded, flaser-bedded, finely interbedded, or preserve small-scale cross-lamination and low-angle cross-lamination are the dominant types of carbonates easily observed from well exposed carbonate benches. Some examples of internally massive calcareous siltstones and sandstones are weakly subparallel, discontinuous, planar-laminated. Finer-grained carbonate facies are typically well exposed only if they underlie these more resistant beds. The upper bedding planes of the calciclastic sandstones commonly preserve small desiccation cracks (Fig. *5.1.1.*5B, 5C), remnants of carbonate mudstone drapes (Fig. *5.1.1.*5F) sometimes preserved as flat-lying intraclasts (Fig. *5.1.1.*5D), and poorly preserved mammal footprints and/or horizontal surface traces (e.g., FC, above D1, above D2, above E2). Bird footprints were not observed in this facies. In a few places, surface textures that appear to have been formed by salt efflorescence and/or microbial crusts are preserved on the upper bedding planes (e.g., WM, K, below D, Fig. *5.1.1.*1C, 1D, 1F; FC, above D2, Fig. *5.1.1.*5E). Efflorescent salt crusts likely contributed to the poor preservation of most of the mammal footprints, which typically were only impressed to shallow depths in stiff substrates. In some cases, large bladed-fan pseudomorphs of trona crystals are preserved within

the substrates (e.g., FC, above D2 or E2). In other examples, this facies preserves no evidence of subaerial exposure.

This facies corresponds to the "Palustrine Association" of Pietras and Carroll (2006), representing the littoral to eulittoral zone with deposition of carbonates in frequently flooded and exposed areas. The interpreted sedimentary environments include mudflats with little wave energy (planar-interlaminated, wavy-laminated), as well as higher energy littoral areas (wavy-bedded, flaser-bedded) (e.g., Figs. *5.1.1.*1, 2, 4, 8). Less commonly, calciclastic sandstones preserve small-scale trough cross-stratification and low-angle planar cross-lamination and are interpreted to represent the swash zone of a beach (e.g., FC, D1, m ~30.5, Fig. *5.1.1.*4C; WM, #18C, above D, Fig. *5.1.1.*2A, 2B). This facies, observed above the D-Bed in Firehole Canyon, is the only example observed of a basin centre carbonate littoral zone sandstone facies that preserves dominantly vertical, full-relief backfilled burrows to depths of ~8 cm from the upper bedding plane.

Some of the calcareous sandstones preserve impressions of reeds on the upper bedding planes (e.g., FC, D1, m ~31.5), as well as red-coloured iron-stained root marks (e.g., WM, #18C, above D; Fig. *5.1.1.*2G). These are typically beds that are internally massive, have irregular upper and lower bedding planes (e.g., Fig. *5.1.1.*5G), and may preserve desiccation cracks, as well as indistinct possible mammal footprints. These beds are interpreted to represent a paludal setting, or shallow lake-fringing wetland that was subaerially exposed. Other examples from this locality (e.g., WM, #18C, above D) of thin-bedded (~2 cm thick), massive calcareous sandstones without root marks or reed impressions preserve possible fish swimming trails and possible snake locomotion traces.

The carbonate unit preserved within the A-Arkose Bed also preserves examples of the calciclastic siltstone and sandstone facies association. They may be wavy-bedded, flaser-bedded, or horizontally bedded, with flat, undulating, or rippled bed contacts, and grade upwards from lenticular-bedded mudstones with calciclastic sandstone lenses (e.g., MFC, A, m ~4; Fig. *5.1.1.*12C–F). Rare, small-scale trough cross-lamination is present, associated with low-amplitude, rounded, symmetrical ripple crests on upper bedding planes (e.g., MFC, A, m ~4.5). This facies preserves horizontally and vertically oriented trace fossils produced in cohesive substrates. Desiccation cracks were not associated with this particular example.

Flaser-bedded white calcareous siltstones of this facies are also present below the D-Arkose Bed in Firehole Canyon (e.g., FC, below D1, m ~0.5), where they abruptly overlie the bedded evaporites with wavy lower contacts (Fig. *5.1.1.*3B–D). Laminae and very thin beds (< 2 cm thick) are continuous, with flat, gently undulating, wavy, or symmetrical ripple-crested bed contacts. Very few mudstone interbeds are present. Lenticular-bedded carbonate mudstones and siltstones are absent in this transition, supporting the interpretation that these bedded evaporites were not formed in a sublittoral deep lake setting. Instead, the flaser-bedded siltstones help to demonstrate that the evaporites likely formed adjacent (basinward) to shallow littoral waters, where oscillatory flow contributed to the internal structures preserved. [In places, some of the upper bed contacts of the evaporites are wavy, with evidence of oscillatory reworking.] Vertically, the siltstone facies grades upwards to light brown and brown, massive to discontinuously laminated oil shale, marking the transition from the evaporite pan to open water and a rise in lake level (e.g., FC, below D1, m ~0.2–1.2; Fig. *5.1.1.*3A, 3B).

### *5.2.3. Lenticular- to Wavy-Bedded Carbonate Mudstones, Siltstones, and Marlstones*

The lenticular- and wavy-bedded carbonate mudstone and siltstone facies was also observed in the prominent carbonate benches within Firehole Canyon (e.g., FC, above D1; FC, above D2; FC, above E2) and on White Mountain (e.g., WM, K, below D; WM, #18C, above D),

and in the carbonate units within the arkose beds (e.g., MFC, A; SCC, A; FC, D1). It was encountered in both coarsening upwards and fining upwards successions, and is transitional between wavy- to flaser-bedded calcareous sandstones or laminated mudstones (Figs. *5.1.1*.2A, 2D, 6A). It is also present in transitional facies between carbonate units and arkosic or marl mudstones and siltstones (e.g., MFC, A, m ~4.6; SCC, A, m ~5–5.5; Figs. *5.1.1*.12D–12E, 13C–D). Massive siltstones interbedded with laminated grey to brown carbonate mudstone are found within this facies; the siltstones typically have flat to slightly undulating upper and lower bed contacts. Displacive trona-fan pseudomorphs are preserved in some siltstone beds (e.g., SCC, A, m ~4.5–5; Fig. *5.1.1*.13B). These pseudomorphs are associated with small desiccation cracks and full-relief burrows (e.g., *Planolites* isp.) into mudstone that are filled with calcareous siltstone (e.g., MFC, A, m ~3.8–4.1; SCC, A, m ~5). The vertically oriented burrows in this facies imply that the lake waters and mudstone pore-waters were not hypersaline, and the traces might have been produced in more dilute lake waters associated with freshwater inflow from the fluvial-deltaic system.

Orangish white and light grey or white calcareous siltstone and dolomitic mudstones are commonly wavy-bedded, flaser-bedded, or finely interbedded, and have flat to undulating laminae. This facies was encountered only within the carbonate units of the typical Wilkins Peak Member (Figs. *5.1.1*.1, 6) and not within the arkosic units. Bedding planes preserve extremely low amplitude (< 5 mm), rounded, symmetrical or interference ripple bedforms produced in the orangish white siltstone, which were draped with light grey to white mudstone (Fig. *5.1.1*.2E, 7E–G). High density surface trails and tunnels may be preserved within the mudstone drapes, producing concave epirelief trails along the siltstone bedding planes. The density and the preservation of sharp burrow boundaries or tunnel walls suggests that thin microbial mats may formerly have covered the siltstones. This facies locally preserves small desiccation cracks. It is interpreted to represent deposition in low-gradient, littoral to eulittoral mudflats with little wave energy. Shallow impressions of mammal footprints are preserved in this facies, and were discovered on a siltstone bedding plane coated with a laminated siltstone and mudstone surface crust, possibly with a mixed microbial and efflorescent salt origin (e.g., WM, K, below D). Where this facies was associated with bedded evaporite pseudomorphs (e.g., FC, below D1, m ~0–0.5, m ~1.5; Fig. *5.1.1*.3G, 3H), no trace fossils were found.

### *5.2.4. Laminated or Massive to Poorly Bedded Carbonate Mudstones and Siltstones*

Massive to poorly bedded orangish white siltstones and dominantly grey mudstones are preserved in two main types. First, they may be vaguely bedded (~2–3 cm thick), preserve reddish, iron-stained root marks, and exhibit an overall "churned" internal texture (mammal-trampled?), with platey to irregular fracture (e.g., WM, #18C, above D; Fig. *5.1.1*.2F–H). Very poorly preserved possible mammal footprints and reed casts are locally preserved on the upper surfaces (e.g., FC, above D1 and D2 or E2; Fig. *5.1.1*.5H). They are interpreted to represent marshy and muddy littoral areas with occasional subaerial exposure. Very small desiccation (shrinkage?) cracks and flat-lying mudstone intraclasts are preserved on some upper bedding planes (Fig. *5.1.1*.2H).

The second expression of this facies dominantly consists of organic-poor, light brownish grey, olive grey, greyish green, or greyish white dolomitic and calcareous mudstone that is (i) discontinuously laminated, (ii) massive with irregular to platy fracture surfaces, or (iii) laminated but desiccated. It forms monotonous units of the Wilkins Peak Member several metres thick, in which trace fossils were not observed (e.g., FC, above E2, m ~38–39; Fig. *5.1.1*.9A–D). The grey mudstones may be interbedded or intercalated with orangish white calcareous siltstones that preserve desiccation cracks on bedding planes (e.g., WM, K, above D; Fig. *5.1.1*.1H). They are

interpreted to have been deposited in sublittoral and shallow saline lacustrine waters, possibly protected from winds, and which were occasionally subaerially exposed. This facies corresponds to the "Brecciated Carbonate Mudstone–Siltstone Lithofacies" of the "Palustrine Association" of Pietras and Carroll (2006), who recognized the additional local preservation of wavy laminae.

*5.2.5. Interbedded Evaporite Pseudomorphs and Carbonate Mudstones or Siltstones*

Pietras and Carroll (2006) included this facies within their "Salt Pan Association", composed of the "Displacive Evaporite Lithofacies" and the "Bedded Evaporite Lithofacies". In the deeper, buried portions of the Bridger Basin, sodium carbonate salts (mainly trona) were deposited in thick light brown to brown bedsets, from ~2 m to ~24 m thick, throughout the deposition of the Wilkins Peak Member (e.g., Deardorff and Mannion, 1971; Wiig et al., 1995). They are thickest and most numerous in the lower part of the Wilkins Peak Member (below the D-Bed) of the southern part of the basin, and become thinner, fewer, less extensive, and deposited further northward during middle and upper Wilkins Peak time (Culbertson, 1971; Wiig et al., 1995). Shifting loci of trona deposition, shown by thickness isopach maps of the ~25 individual beds (Wiig et al., 1995), appear to reflect tectonic events and differential subsidence in different parts of the basin throughout Wilkins Peak time. They may also provide information about the underlying topography and smaller areas within the basin where non-deposition or dissolution occurred. These thick trona units are preserved only in the subsurface; no cores were examined during this study. Trona fabrics are typically either: 1) massive to coarsely crystalline and contain interlocking bladed or rosette crystal fabrics with fractures filled by vertically oriented layers of evaporites; 2) finely crystalline and interbedded with carbonate mudstone; or 3) coarsely crystalline with disrupted carbonate mudstone partings (Deardorff and Mannion, 1971). Halite, natron, and shortite may be associated with trona, but almost always in small quantities except for Bed #14, which underlies the A-Arkose Bed and contains up to 25% halite (Culbertson, 1971; Wiig et al., 1995). Pyrite is typically present in the trona beds (Deardorff and Mannion, 1971). In modern brine samples, by-products of trona mining, B.E. Jones et al. (1998) found alkaliphilic and haloalkaliphilic Bacteria and Archaea, similar to those from Lake Magadi.

Relatively thin bedded trona units (< 2 m thickness) are also present in outcrop where they are exposed as interbedded orangish white to light grey carbonates with beds of trona blade pseudomorphs draped by carbonate mudstone (Fig. *5.1.1.*3, 8). Many of the beds are not interbedded with mudstone, but are coated only by very thin mudstone partings. Bed contacts range from flat to irregular (due to the evaporite crystals) to wavy, providing evidence of oscillatory flow and slight reworking of the evaporite horizons. The lower contact of the bedded evaporites below the D-Bed is undulatory to rippled, and overlies light grey laminated lacustrine dolomitic mudstones above oil shale (e.g., FC, D1, m -0.5; Fig. *5.1.1.*3I). Below the D-Bed, individual carbonate beds with trona pseudomorphs (e.g., FC, D1, m ~0–2; cf. Bed #17 or #18, Culbertson, 1971) are typically ~0.5 cm to ~2 cm in thickness. Trona crystal pseudomorph lengths are about the same as the thickness of the bed in which they are contained. The pseudomorphs are randomly oriented, suggesting some minor transport. Some thicker beds (~3 cm thick) contain isolated, trona blades that are orthogonal-shaped, and may have been dissolved and reprecipitated in their primary depositional settings. Most crystal pseudomorphs do not penetrate the carbonate mudstone interbeds, suggesting that the trona fabrics and bedded nature of the deposits are primary rather than due to intrasedimentary growth. In other cases, where mudstone partings are absent or extremely thin (< 0.5 mm), bedding contacts are irregular and disrupted by the growth of the trona crystals (Fig. *5.1.1.*3G, 3H). Some larger bladed pseudomorphs (~2 cm length) are arranged in vague fans that cross-cut bedding planes, and appear to have grown later within the bedded deposits.

Small desiccation cracks are preserved on some bedding planes, but evidence for large-scale polygons with deep fractures was not seen in outcrop. No trace fossils were observed in this facies. It is comparable to the finely interbedded organic-rich muds and trona facies present at the NW Lagoon of Lake Magadi, which experiences seasonal flooding by shallow water that supports the cyanobacterial blooms. Additional evidence that supports subaerial exposure of the bedded evaporites includes an intraclastic (pebble-size) calcareous conglomerate bed with normal grading and undulating upper contact that is sandwiched between the thicker-bedded evaporites beds (Fig. *5.1.1.*3E). This association is interpreted to represent a subenvironment located slightly landward of the more thinly bedded salt-pan, in which the trona crystals grew from saline pore waters in mudflat sediments to form efflorescences, and which was occasionally flooded by both sheetfloods and the lake. The setting may be comparable to zones where puffy efflorescences form on the Sandai Plain at Lake Bogoria.

Other examples of evaporite pseudomorphs in outcrop include thickly bedded carbonate mudstones that contain large (< 5 cm length) trona pseudomorph fans, which appear to have grown within the bed but do not disrupt the overlying mudstone drape (e.g., FC, above E1; Fig. *5.1.1.*8D, 8G). This facies is associated with a possible large mammal footprint and the intraclasts of a desiccated carbonate mudstone drape (e.g., FC, above E2), which suggests that the trona fan may have precipitated before subaerial exposure. In another outcrop example (FC, above E1; Fig. *5.1.1.*8C), there are both open and filled matrix-supported spheres that may represent the dissolution of shortite crystals, or their repeated dissolution and reprecipitation before outcrop exposure (Deidre LaClair, pers. comm., 2008).

### *5.2.6. Very Thinly Laminated to Massive Organic-Rich Micrite (Oil Shale)*

Kerogen-rich, calcareous lacustrine mudstones are very finely laminated (sub-millimetre scale), massive, or contain thin lenses of calcareous siltstone in lenticular-bedded examples (e.g., Figs. *5.1.1.*6G, 11I, 12B, 12D). This facies corresponds to the "Profundal–Sublittoral Association" of Pietras and Carroll (2006). Colour variations from black, dark brown, brown, to light brown, generally reflect the organic content (T.O.C. up to 18%; Carroll and Bohacs, 2001) and the inclusion of greyish coarser-grained or more coarsely crystalline calcite. Most of the organic matter was derived from cyanobacteria and bacteria (Carroll and Bohacs, 2001). B.E. Jones et al. (1998) suggested that sulfides, which are common in the oil shales, provide evidence for the presence of sulfate-reducing bacteria in the anaerobic muds.

These brown to black micritic mudstones are interpreted to have been deposited in sublittoral to profundal, anoxic, saline to hypersaline lake waters. No trace fossils were preserved with this facies. The water depths under which they were deposited are unknown, although the often close stratigraphic association with subaerially exposed littoral facies (e.g., FC, above D2, m ~20) suggests that water was likely shallow (but more than ~5 m?). Saline lakes that contain abundant microbial communities, such as Lake Bogoria, have chemoclines at relatively shallow depths, with anoxic waters and laminated sediments below (e.g., Renaut and Tiercelin, 1994; Harper et al., 2003). High-temperature lake waters in areas without cold winters can also develop a shallow anoxic hypolimnion due to the presence of the thermocline and inhibition of lake water-mixing (e.g., Cohen, 2003).

Of the localities investigated, this facies was present within the "white stripe" carbonate units of the arkose beds in the Firehole Canyon area (Figs. *5.1.1.*10–13), as well as below and above the arkose beds. Notably, it was also present below the D-Bed in Firehole Canyon (e.g., FC, D1, m ~1–3), underlain by interbedded evaporite (trona) pseudomorph-containing beds with organic-poor carbonate mudstones that preserve desiccation cracks, and conformably overlain by greyish green, discontinuously laminated, arkosic mudstones. Brownish, dark grey laminated

mudstones are also preserved below the bedded evaporite interval at the base of Section FC, D1 (Fig. *5.1.1.*3I). They contain progressively less organic matter upwards, becoming light grey below the rippled, undulating contact with the bedded evaporites. In other examples, this facies grades transitionally upwards to massive greyish green arkosic mudstones (e.g., FC, D1, m ~7.3; Fig. *5.1.1.*10D) and massive greyish green and olive green siltstones (e.g., MFC, A, m ~4.8; Fig. *5.1.1.*12G). The massive or discontinuously laminated arkosic mudstones and siltstones facies that overlie organic-rich lacustrine facies may reflect density contrasts between the saline lake waters and the freshwater fluvial input, and may have been deposited by suspension fall-out from overflows or interflows (cf. Renaut and Gierlowski-Kordesch, 2010). Within the A-Bed, laminated dark brown oil shale contains disseminated, euhedral, shortite crystals (e.g., MFC, A, m ~3.5; SCC, A, m ~3.3–3.8; Fig. *5.1.1.*11I), attesting to the saline nature of the pore-fluids.

*5.2.7. Stromatolitic, Laminated Horizons of Carbonate Mudstones*

Laminated stromatolitic horizons are another facies associated with lacustrine deposition in the Wilkins Peak Member, although they are much more abundant in the overlying Laney Member (Roehler, 1993). They are typically ~2–4 cm in thickness, orange, and preserve continuous slightly pinching and swelling laminae, with irregular to convex-upward bulbous expansions along the horizons. The horizons are commonly fragmented, and clasts may be incorporated into intraclast conglomerates of overlying beds (e.g., FC, D1, m ~25; Fig. *5.1.3.*6F, 7C, 7D). Similar to the "stromatolitic coatings" in the Bogoria basin, these horizons may be evidence of chemical changes in the lake waters associated with an increased influx of freshwater, and they appear to be associated with lake transgressions (e.g., FC, A, m ~9.2). For this reason, stromatolitic horizons may represent flooding surfaces of the transgressing lake (Leroy Leggitt, pers. comm., 2007) at different scales, marking minor to major transgressions (e.g., just below the Wilkins Peak/Laney contact). Thin stromatolitic beds, however, may be only locally preserved as fragmented horizons that do not crop out well (e.g., above the A-Bed, FC).

***5.2B. Arkosic Siliciclastics of the Basin Centre***

*5.2.8. Intraformational Intraclast Conglomerates*

Conglomerates are relatively uncommon in the basin centre. However, they may be preserved in units interpreted as fluvial channel deposits and as transgressive lacustrine lags. Arkosic siliciclastic conglomerates have been identified in both the A-Bed and the D-Bed. Most examples are clast-supported and non-imbricated. However, two examples of matrix-supported pebble-conglomerates were associated with the transition from lacustrine to fluvial facies, including the lower part of the upper unit of the D-Bed at Kanda (e.g., Fig. *5.1.3.*1C). Section FC, D1 ("second" unit) in Firehole Canyon also preserves a small lens-shaped bed of an oligomictic, matrix-supported, intraformational pebble-conglomerate with grey fine-grained arkosic sandstone matrix that may represent the initial "chute" of the overlying ripple-laminated sandstones that are interpreted here to be mouth bar deposits (FC, D1, m ~9.5; Fig. *5.1.3.*3B, 3D, 3E). Wedge-shaped and lenticular beds of clast-supported oligomictic intraclastic granule-conglomerates in the upper A-Bed at Middle Firehole Canyon are interpreted as lags in the thalweg of a distributary channel (e.g., cf. MFC, A, m ~9.5; Fig. *5.1.2.*4C). The base of the upper unit in Section FC, D1 preserves a pebble-sized, polymictic, intraclastic conglomerate with a buff, fine-grained arkosic sandstone matrix. This conglomerate is present at the partially scoured base of the overlaying unit of large-scale trough cross-stratified channel sandstones. Intraclasts include broken stromatolitic carbonate mudstones from the underlying bed (Figs. *5.1.3.*7C, 7D). Section FC, D2 (upper unit) preserves a polymictic pebble-conglomerate with coarse-grained arkosic sandstone matrix (e.g., FC, D2, m ~5.5). Clast compositions include grey

sandstone, possibly derived from the Wasatch Formation, as well as green mudstones and carbonate mudstones (Fig. *5.1.3*.9B). This conglomerate is interpreted as a channel lag and is overlain by channel-fill sandstones.

*5.2.9. Medium- to Coarse-Grained Cross-Bedded Sandstones*

Most arkosic sandstones in the basin centre are fine-grained or very fine-grained. Medium- to coarse-grained sandstones are uncommon, and were identified only in the upper unit of Section FC, D2 in Firehole Canyon (FC, D2, m ~6). This grey, coarse-grained arkosic sandstone has slightly convoluted plane-beds along its lower contact and large-scale non-parallel cross-stratification. It is associated with the pebble-conglomerate that is interpreted as a channel lag. The cross-strata are interpreted as channel fill and lateral accretion deposits of a channel bar (Fig. *5.1.3*.9A–D).

*5.2.10. Very Fine- to Fine-Grained Planar- and Cross-Bedded Sandstones*

Most basin-centre arkosic sandstones are very fine-grained to fine-grained and preserve internal structures including: 1) large-scale trough cross-stratification; 2) non-planar, epsilon cross-bedding; 3) planar lamination; 4) graded plane-bedding; 5) ripple-lamination; 6) small-scale trough cross-lamination; and 7) horizontal beds with irregular upper and lower contacts, probably due to biotubation. Based on their stratigraphic context, sedimentary structures and trace fossils, these sandstones are interpreted to represent a variety of depositional environments, including: 1) channel bars; 2) channel floors and fill; 3) crevasse splays; 4) levees; 5) distributary mouth bars; and, 6) either unchanneled sheetfloods or deposition within broad shallow channels on the lower delta-plain.

Thin plane-beds (~1 cm) of graded, fine-grained (upper) sandstones are typically greyish buff and represent upper flow regime deposits. The beds may have scoured bases and be associated with pebble-sized intraclast conglomerates (e.g., FC, D1, m ~9.5; Fig. *5.1.3*.3). Some consist of sheared plane-beds closely associated with ripple-laminated accretionary beds (e.g., FC, D1, m ~14.7; Fig. *5.1.3*.4E). Other examples were found in bioturbated sandstones (e.g., FC, D1, m ~16). Convolutions within the bioturbated bedset provide possible evidence of slumping and rapid deposition. This association is tentatively interpreted to represent deposition possibly in a subaqueous levee of a terminal distributary channel (e.g., FC, D1, m ~16; Fig. *5.1.4*.4F, 4G), but more fieldwork is required to confirm this interpretation.

Ripple cross-laminated fine-grained (lower) sandstones are typically light buff- or tan-coloured, and represent a variety of depositional environments. In the second unit of the D-bed in Firehole Canyon, for example, ~1 m- to 1.5 m-thick bedsets contain ripple-lamination in ~1.5 cm-thick cross-beds separated by planar-laminated topsets of very fine-grained (lower) sandstones (e.g., FC, D1, m ~10–14). These bedsets dip towards the basin, are flat-based, and rest on siltstones that grade upwards from sublittoral lacustrine carbonates to siliciclastic muddy units interpreted as mudflat deposits. The ripple-flow direction is oblique to parallel to the basinward dip of the accretion surfaces, which are interpreted to represent downstream accretion. The toes of the accretionary bedsets fine upwards to siltstones, and also pinch out to siltstones. Unlike typical fluvial channels, the sandstones do not scour progressively deeper into underlying sediments down-dip of the accretion surfaces, but instead appear to build upon the adjacent siltstones which were deposited at their toes. The lower contact of the sandstones in the measured section is gradational, with a coarsening-upwards set of planar-laminated, silty, very fine-grained sandstones that rest on greenish tan siltstones (Figs. *5.1.3*.3A–H, 4A–D). Within these siltstones, a small scoured bed of grey fine-grained sandstone with pebble-sized mudstone and sandstone intraclasts precedes a transition to the accreting sandstones downstream (Fig.

*5.1.3*.3B, 3D, 3E). Based on their structures, lack of trace fossils, bedset geometry, and their stratigraphic context, these sandstones are interpreted as progradational mouth-bar deposits of a terminal distributary channel (cf. Schomaker et al., 2010).

The second unit in Section FC, D2 is also composed of plane-bedded and ripple-laminated fine-grained sandstones at its base (Fig. *5.1.3*.8A–D). These sandstones grade upwards into climbing-rippled very fine-grained sandstones (e.g., FC, D2, m ~1.8), in which the climbing-ripple laminae are draped by blackish detritus, implying fluxes in energy. They fine upwards to olive tan siltstones that, in turn, were draped by black laminated mudstones interpreted as an interdistributary bay, lagoon, or small lake on the delta-plain (Fig. *5.1.3*.8E–F). A similar scenario is present in the upper unit of FC, D1 (e.g., FC, D1, m ~25.5–28), with the rippled channel deposits fining-upwards to slightly undulating discontinuous planar lamination, then to discontinuous oscillation ripple-lamination, and on to lenticular-bedded siltstone and mudstone (Fig. *5.1.1*.6A). The base of this unit is also composed of very fine-grained sandstone, which preserves planar lamination and large-scale trough cross-stratification, as well as a scoured bed with an intraclast conglomerate at its base (e.g., FC, D1, m ~25–26; Fig. *5.1.3*.7).

Other examples of climbing-rippled or ripple-laminated very fine-grained sandstones are interpreted to represent channel fill deposits (point bars, channel floor), crevasse splays, unconfined flow deposits, or sediments within a broad shallow channel on the lower delta-plain (e.g., MFC, A, lower unit). Climbing-ripple cross-lamination is usually associated with planar- and ripple-lamination, and individual beds may be draped with siltstone, mudstone, or organic detritus (Fig. *5.1.2*.2E, *5.1.3*.8C, 8D). Channel-fill successions typically fine-upwards, from scoured bases with large-scale cross-stratification upwards to heterolithic facies, to laminated mudstones (e.g., FC, D2, m ~6–11; Fig. *5.1.3*.9A–F). Trace fossils may be preserved in the heterolithic facies (e.g., *Helminthoidichnites* isp.). Crevasse splay sandstones may also preserve small-scale trough cross-stratification, ripple-lamination in flat beds, and irregular bioturbated bedding. The successions typically coarsen upwards, and may be intercalated with massive siltstones (e.g., FC, D1, m ~20–22.5; Fig. *5.1.3*.5A–C), pedogenically altered siltstones (e.g., FC, E2, m ~22–26; Fig. *5.1.3*.10D), or with massive to laminated mudstones (e.g., FC, D1, m ~23.5–24.5; Fig. *5.1.3*.6). Trace fossils are preserved in all of these examples, and show pre-depositional suites (e.g., vertebrate footprint casts, *Planolites* isp.), syndepositional suites (e.g., *Skolithos* ispp.), and post-depositional suites (e.g., pellet-filled burrows, cf. *Taenidium barretti*/ cf. *Lunulichnus*).

The climbing-rippled and ripple-laminated sandstones in the lower unit of the A-Bed in Middle Firehole Canyon contain abundant vertical burrows of *Skolithos* ispp., commonly to depths of more than 0.3 m (see Chapter 6). This sandstone unit, possibly representing unconfined flow (sheetfloods) or flow within a broad shallow channel on the lower delta-plain, abruptly abuts with mudstones that are interpreted as an occasionally desiccated mudflat to muddy littoral zone (e.g., MFC, A, m ~1–2; Fig. *5.1.2*.2B–E). A similar scenario is envisaged for the relatively thin D-Bed towards the northern White Mountain (#18 crossing), which preserves climbing-rippled muddy very fine-grained sandstones with current flow southwards towards the basin.

The ripple-laminated and planar-laminated, very fine-grained sandstones may also be intercalated and interbedded with massive or laminated light green mudstones that preserve reddish, iron-stained root marks, vertebrate footprints produced in formerly soupy substrates, and/or deep desiccation cracks. This facies association is preserved in the lower unit and in the lower second unit of the D-Bed in Firehole Canyon (Fig. *5.1.3*.2, 3A, 3C). The sandstones are interpreted as distal sheetflood or splay deposits that were deposited on subaerially exposed but wet mudflats. A similar facies association occurs in the upper unit of the D-Bed on White

Mountain at Kanda (Fig. *5.1.3.*1A, 1B, 1H). The ripple-laminated and planar-laminated sandstones in this case coarsen upwards and are deeply scoured by a sandstone bedset that preserves large-scale lateral accretion surfaces. The succession represents relatively distal to more proximal overbank deposits onto a wet delta-plain.

*5.2.11. Heterolithic Very Fine-Grained Silty Sandstones and Mudstones*

Heterolithic facies observed in the basin centre are of three main types. The first is typically composed of tan very fine-grained (lower) arkosic sandstones finely interlaminated with or draped by greenish tan to green muddy siltstone and mudstone. Internally, they preserve thin beds (~1 cm-thick) of ripple cross-lamination, slightly undulating to wavy parallel laminae, flaser lamination, and planar lamination, all of which usually preserve mud drapes on bedding planes or mud lenses in ripple troughs. Low amplitude combined-flow or asymmetrical ripple bedforms may be preserved. Some have "bubble" textures attributed to microbial mats, desiccation cracks, and dominantly horizontal trace fossils (e.g., *Helminthoidichnites* isp., *Planolites* isp., *Steinichnus* isp.). This facies association is interpreted as either: 1) channel-fill deposits towards the top of upward-fining beds (e.g., FC, D2, m ~8.8; Fig. *5.1.3.*9A, 9E, 9F); or, 2) distal overbank/levee or distal crevasse-splay deposits (e.g., WM, K, upper unit; e.g., MFC, A, m ~9; Fig. *5.1.2.*4G). In both cases, they are interpreted to represent lower flow regime conditions with some deposition from suspension.

The second type of heterolithic facies consists of thin (~1–2 cm-thick) horizontal beds of tan siltstones or silty very fine-grained sandstones, finely interbedded with bluish green clay-rich mudstone or ripple-laminated, very fine-grained sandstones (e.g., MFC, A, m ~5–7.5; Fig. *5.1.2.*3; FC, A, m ~11–14, Fig. *5.1.2.*8). Internally, the coarser-grained beds may be horizontally laminated, unidirectional or oscillation ripple cross-laminated, flaser- to wavy-bedded, or preserve convoluted unidirectional ripple cross-lamination. The finer-grained beds are typically laminated in thin beds or form wavy to undulating drapes on the underlying sandstone beds. Reddish iron-stained root marks are commonly preserved in the siltstone and sandstone beds, and desiccation cracks, shorebird and wading bird footprints, and horizontal invertebrate trace fossils (e.g., *Vagorichnus* isp., *Helminthoidichnites* isp.) may be preserved in the bluish green clay-rich mudstone laminae. Both the sandstone and siltstone interbeds contain abundant reddish, iron-stained horizons, which in this case suggests an environment with fluctuating redox conditions and shallow water tables. Thicker interbeds of very fine-grained sandstone (~2–5 cm-thick) may preserve the *Planolites* ichnofabric, comprising intensely bioturbated sandstones with indistinct burrows preserved in full-relief. This facies is present in coarsening-upwards units with transitional lower contacts and more sandstone beds towards the top (e.g., MFC, A, m ~5–8; SCC, A, m ~10; Fig. *5.1.2.*11H).

The environment of this heterolithic facies is interpreted as either: 1) the lower delta-plain, with sediment and water input from distal unconfined flow/sheetfloods or distal overbank deposits (e.g., MFC, A, m ~5–8); or 2) a flooded overbank setting, with sediment and water input from distal crevasse splays (e.g., SCC, A, m ~10). Another example is provided by the lowermost "second" unit of the D-Bed in Firehole Canyon (e.g., FC, D1, m ~7.5–9.5; Fig. *5.1.3.*3A, 3C). The bed coarsens upwards from massive green siltstones conformably overlying carbonate lacustrine mudstones, and is preserved as bluish green mudstones finely interbedded with very fine-grained planar-laminated sandstones, which were subsequently desiccated. This facies is interpreted as the distal mudflat of the lower delta-plain, capped by distal sheetflood- or splay-derived heterolithic facies.

The third type of heterolithic facies also coarsens upwards from a transitional lower contact with carbonate lacustrine facies, and is also interpreted to have been deposited on the lower delta-plain (e.g., SCC, A, m ~5.5–6; Figs. *5.1.1.*13F; *5.1.2.*11B). In this example, laminated very fine-grained sandstones are finely interbedded with dark brown marl and dark brown and blackish green siliciclastic mudstones. Sandstone interbeds preserve bubble-textures and a bird-trampled texture. They are black-, purple-, and red-stained, which is interpreted to represent organic matter, possibly of both plant and microbial origin. The facies coarsens upwards to a planar-laminated, very fine-grained sandstone that may represent distal terminal distributary mouth-bar deposits. The main difference between this facies in Sage Creek Canyon and Middle Firehole Canyon is the more common association with lacustrine facies, a higher amount of organics, and the coarsening upwards to terminal (?) distributary-channel facies in Sage Creek Canyon. The Sage Creek Canyon area might have been slightly lower than Middle Firehole Canyon (cf. trona bed #14 isopach, Wiig et al., 1995), and/or the blackish mudstones might have been deposited in a lake-margin lagoon or embayment.

*5.2.12. Massive to Poorly Bedded and Bioturbated Siltstones*

Massive and poorly bedded or discontinuously laminated siliciclastic siltstones within the basin centre are mainly either tan, greenish tan, bluish green, olive green, brownish green, or dark brownish green. These colour differences apparently represent slight variations in grain size, proportions of arkosic siliciclastics (either sand or clay) and carbonates, and the quantity of organic matter. In general, the tan-coloured massive to discontinuously laminated siltstones are slightly coarser-grained and better sorted. They may be intercalated with sandstone facies interpreted as crevasse splays and which are associated with more terrestrial trace fossils (e.g., cf. *Taenidium barretti*/cf. *Lunulichnus* isp.) (e.g., FC, D1, m ~19–22; Fig. *5.1.3.*5A, 5B). In this setting, they are interpreted as distal overbank fines derived from either crevasse splays or distributary channel floods onto well drained upper delta-plains or floodplains. In the lower unit of the A-Bed at Middle Firehole Canyon however, tan-coloured siltstones are cemented with carbonate (e.g., MFC, A, m ~2.2–2.8) and overlie olive greenish tan marlstones (Fig. *5.1.2.*1). In this case, they preserve a mottled texture due to complete bioturbation, vague irregular bedding, and some discrete full-relief burrows. Laminated horizons within the poorly bedded unit preserve escape traces, and many of the laminated horizons are brecciated, probably due to bioturbation. These siltstones also preserve black disseminated fish bones (or possibly gastropod radulae). This facies grades laterally to a climbing-ripple-laminated sandstone unit interpreted as either sheetflood deposits or a broad shallow channel emptying directly into the lake (Fig. *5.1.2.*2). The colour of the siltstones in these examples appears to be reflecting the coarser grain sizes, and does not indicate the depositional environment.

Greenish tan massive siltstones tend to be present between tan massive siltstones and olive to dark green siltstones, or brownish green siltstone or mudstone (e.g., FC, D1, m ~22.5; Fig. *5.1.3.*5A–E). The colour change may represent proportionately more clay than tan-coloured siltstones, proportionately more organic matter, and/or less well drained conditions. An increase in the amount of clay, organic matter, and/or water table level is interpreted to be responsible for transitional changes from olive green, to brownish green, to dark brownish green siltstones (e.g., FC, D1 and D2, below the "green stripe"; Fig. *5.1.3.*8E, 8F). Bright green siltstones form a laterally extensive bed that directly underlies the lacustrine carbonate mudstones in the A-Bed at Middle Firehole Canyon, Firehole Canyon, and Sage Creek Canyon. That bed preserves carbonate nodules or root casts with reddish, iron-stained rinds in discrete horizons at the base of the green siltstone (e.g., MFC, A, m ~2.7; Fig. *5.1.2.*2F), and locally preserves reddish, iron-stained root marks. In these examples, the colour change may be related to the transgressing

lake, and could possibly signify increased reducing conditions.

Brownish green and green siltstones that preserve vague discontinuous lamination and have blocky to platey breakage are also present in units intercalated with thin beds of ripple-laminated or irregular-bedded very fine-grained sandstones (e.g., FC, E2, lower and upper units; FC, D2, m ~12.5–14; Figs. *5.1.3.*9G–H, 10B–C, 10G). The sandstones associated with these siltstones preserve horizontally dominated, backfilled burrows, and may be bioturbated to the point of preserving only irregular bedding planes. These siltstones are interpreted as pedogenically modified and bioturbated incipient paleosols on the upper delta-plain to floodplain. The colour may be due to the presence of arkose-derived clays, organic matter, and/or may be evidence of high water tables when compared to typically red floodplain paleosols, present in the Cathedral Bluffs Member of the Wasatch Formation/Wilkins Peak Member at the southern basin margin. Siltstones interpreted as weakly developed paleosols within the A-Bed (e.g., MFC, A, m ~8.7, m ~10.2–11.5; Figs. *5.1.2.*4D, 4F, 5A–C) range in colour from greenish light brown in better-developed soils, to bluish green siltstones that retain discontinuous laminae. The colour is attributed to the abundance of bluish light green mudstone in the parent material. Both examples preserve carbonate root casts/nodules with reddish, iron-stained rinds.

*5.2.13. Massive to Laminated Dark Green, Brown, and Black Mudstones and Siltstones*

Dark green and brown to black non-carbonate mudstones were observed in two main facies associations. First, dark brownish green to black laminated mudstones, which weather to bright green, form the "green stripe" unit of the D-Bed in Firehole Canyon (Figs. *5.1.3.*5, 8). They are interpreted to represent organic-rich deposits of a freshwater to brackish lake. Whether it was an interdistributary bay or a lagoon of the main lake, or an isolated lake on the upper delta-plain is unknown.

Dark greenish brown non-carbonate siltstones are also preserved in the lower A-Bed of Sage Creek Canyon (e.g., SCC, A, m ~ -1–2). The lower part of the unit (e.g., SCC, A, m ~-1–0.5) consists of structureless, but vaguely horizontally bedded, dark brownish green mudstones (Fig. *5.1.2.*10B). No trace fossils or other features were observed. The lower part may represent a low salinity area of the main lake, possibly in the muddy sublittoral to littoral zone with abundant non-carbonate muds. Upwards (e.g., SCC, A, m ~0.5–1.5), very fine planar laminae and undulating to wavy laminae are present in graded beds (< 10 cm thick) with desiccation cracks at the top of the bedset (Fig. *5.1.2.*10A, 10C, 10D). Together with relatively high amplitude (~5 cm) in-phase ripple-lamination and erosional unidirectional current ripples (possibly landward flow), the sedimentological features and lack of trace fossils suggest that these dark greenish brown siltstones may represent the muddy sublittoral to littoral zones with some possible storm-generated unidirectional structures. Plant material may be preserved on lower bedding planes. The dark siltstones coarsen from massive greenish brown siltstones to cross-laminated very fine-grained sandstones that preserve pellet-filled vertical burrows with sharp walls (e.g., SCC, A, m ~1.5–2; Fig. *5.1.2.*10E), suggesting shallowing upwards and subaerial exposure of the muddy littoral to channelized lower delta-plain. Correlative exposures preserve desiccation cracks < 5 cm deep and possible prawn burrows (cf. *Thalassinoides* isp.) in muddy beds of this facies (Fig. *5.1.2.*10F).

*5.2.14. Massive, Laminated, and Lenticular-Bedded Marlstones*

Mudstones with mixed carbonate and arkosic lithology tend to be greyish green, and may be brownish or dark green if they are organic-rich. They are typically massive, lenticular-bedded, or laminated, and are best represented in transitional contacts with lacustrine carbonate

mudstones below, and either green mudstones and greenish tan arkosic siltstones above (e.g., FC, D1, m ~3; FC, D1, m ~7.5, Fig. *5.1.1.*10D–E; MFC, A, m ~4.5–5, Fig. *5.1.1.*12G; SCC, A, m ~5.5, Fig. *5.1.1.*13D–E). The massive mudstones may be hypopycnal flow deposits, deposited lakeward of terminal distributary channels carrying fresh water into the saline lake (e.g., FC, D1, m ~7.5). This facies is also present in the uppermost D-Bed in Section FC, D1 (e.g., FC, D1, m ~27), where it records the gradual flooding of an active channel during a major lake transgression.

Laminated greyish green marlstones are also preserved above the "green stripe" in the D-Bed in Firehole Canyon (e.g., FC, D1, m ~24.5, Fig. *5.1.3.*6A–G; FC, D2, m ~5.5, Fig. *5.1.3.*9A). They may preserve dark detrital drapes on laminae and very small desiccation (or shrinkage?) cracks. This facies is interpreted to represent the evaporation of an interdistributary bay, lagoon, or small lake on the delta-plain, and/or the seepage of saline ground water onto the delta-plain. Similarly, marlstones in the lower unit of the A-Bed (e.g., MFC, A, m ~ -1–2; Fig. *5.1.2.*1) represent mixed siliciclastic and carbonate lithologies, and likely represent "mixed" salinities as well, with presumably freshwater input from rivers entering the saline lake. Extensive bioturbation in both greyish light green marlstone and tan-coloured marly siltstone facies are interpreted as relatively fresh water indicators here, supported by the presence of fossil fish bones or gastropod radulae (e.g., MFC, A, m ~1.5–1.8). These facies, like the massive and graded muddy siltstone beds in the lower A-Bed of Firehole Canyon (e.g., FC, A, m ~1.5–2.2, Fig. *5.1.2.*6D, 6G–H; m ~3–4.5, Fig. *5.1.2.*7A–D) and Sage Creek Canyon (e.g., FC, A, m ~0.5–1.5; Fig. *5.1.2.*10), are interpreted as being deposited in muddy, low-energy littoral zone of the main lake, with freshwater and siliciclastic sediment input from terminal distributary channels.

## 5.3. Interpretation of the Basin Centre Deposits

### *5.3.1. Lacustrine Carbonates and Evaporites of the Shifting Basin Centre*

Climate and tectonics, both within and external to the basin, influenced the extremely variable areal extent of Lake Gosiute, its depth, chemistry, sediment input, and subsequently its deposits and paleoecology. Tectonics and geomorphology dictated the basin physiography and accommodation, as well as changing amounts of input from freshwater sources (e.g., fluvial systems and possibly hot- and cool-water springs). Most of the Wilkins Peak Member in the basin centre is composed of carbonate sublittoral to profundal lacustrine mudstones and littoral calcareous siltstones and sandstones that are variably intercalated with either bedded evaporite units or fluvial or fluvio-deltaic sandstones and siltstones (e.g., Culbertson, 1961; Smoot, 1983; Roehler, 1992b, 1993; Pietras and Carroll, 2006; Figs. *5.1.1.*1–13). Depending mainly on the depth of the lake and/or whether the carbonate mudstones were deposited below a chemocline, the profundal to sublittoral deposits range from finely laminated dark brown to black oil shale (e.g., Fig. *5.1.1.*6G), to massive brown micritic mudstones (e.g., Fig. *5.1.1.*12B), to light brown and grey dolomitic and calcareous mudstones (e.g., Fig. *5.1.1.*12D). Gradational colour changes occur within the lake beds, some in parallel with changing internal structures (e.g., presence of lenticular bedding). The colour changes may signify differences in the oxygen content in the sediments, possibly related to fluctuating lake levels, changing depths of the chemocline, changing overall salinity and evaporation rates, or fetch-related variable depths of wind-sourced energy. Only rarely do sublittoral deposits or lenticular-bedded mudstones preserve trace fossils, which may have been during periods of lower salinity and/or brief periods of subaerial exposure (e.g., the "white stripe" unit of the A-Arkose Bed in Middle Firehole Canyon; Figs. *5.1.1.*12, *6.1.1.*11).

Littoral calcareous siltstones and sandstones, which range from poorly bedded to planar-interbedded, to wavy- and flaser-bedded internally, are the best exposed carbonate units in the basin centre, typically forming orangish-white resistant benches (e.g., Figs. *5.1.1*.1, 7). Most of the littoral facies are closely interbedded with eulittoral, or subaerially exposed, deposits. They preserve evidence of frequent flooding and exposure, including: symmetrical ripple bedforms; carbonate crust intraclasts; possible microbial and/or efflorescent salt crust surface textures; desiccation cracks; and mammal footprints and horizontal invertebrate traces produced in wet to firm substrates (e.g., Fig. *5.1.1*.5A–F). Other lake-margin facies, including poorly bedded calcareous siltstones and grey mudstones, preserve reddish, iron-stained marks of small roots and reed impressions, together with desiccation cracks and possible mammal footprints (e.g., *5.1.1*.5G, 5H). This association provides evidence of lake-fringing wetlands that were occasionally desiccated. The littoral carbonate facies also preserve displacive evaporite pseudomorphs (e.g., trona fans), that are evidence for evaporative concentration of saline pore waters in very shallow water to subaerially exposed sediments (e.g., Fig. *5.1.1*.3, 8).

Pietras and Carroll (2006) recognized a recurrent facies association that typifies the minor, and frequent, lake expansion and contraction cycles within the basin centre Wilkins Peak carbonate units. Ranging from ~0.1–6 m in thickness, the cycle consists of littoral intraclastic and wavy-bedded calcareous sandstones at its transgressive base overlain by laminated organic-rich shales of the profundal-sublittoral association, coarsening slightly to the dolomitic and calcareous mudstones and siltstones of the palustrine association, and may be capped by bedded evaporites of the salt-pan association (Pietras and Carroll, 2006). Many more of these cycles were identified from cores in the basin centre than towards the northern basin margin (on White Mountain). They demonstrate the relatively greater accommodation towards the deeper basin that preserves the trona beds, as well as the pinching out of lacustrine facies laterally to more mudflat and sheetflood facies towards the northern basin margin (Pietras and Carroll, 2006).

Roehler (1993) divided the Wilkins Peak Member in to three parts: the lower Wilkins Peak, which includes most of the trona units and arkosic sediments (including the D-Bed) deposited mainly in the south-southeast portions of the basin; the middle Wilkins Peak, which refers to the deposits above the D-Bed and below the I-Bed; and, the upper Wilkins Peak, from just below the I-Bed to the upper contact with the Laney Member. Pietras and Carroll (2006) illustrated N-S cross-sections of the basin at these three intervals, showing the gradual flattening of the sedimentary basin fill upwards. The lower Wilkins Peak Member was deposited mainly in the southern Bridger Basin, in an area confined between the Uinta Mountains to the south, the Wyoming Thrust Belt to the west, and the Rock Springs Uplift to the east. A large proportion of the mineable trona was deposited in this basin before deposition of the first arkosic interval (Beds #1–#14) (e.g., Culbertson, 1971; Wiig et al., 1995). Much greater accommodation was available towards the southern margin along the Uinta Uplift than the ramp-style northern margin, as shown by the overall thickness of the southern basin margin deposits (Roehler, 1992b). The deposits there are composed mainly of quartzose siliciclastic alluvial facies thickly intercalated with lacustrine carbonate units that indicate large expansions of the lake (Smoot, 1983). Together with the isopach thickness maps of the trona intervals (Wiig et al., 1995), changing positions of the trona basins (Culbertson, 1971), and correlation with age-dated tuffs and the arkosic "marker" units (Pietras and Carroll, 2006; M.E. Smith, 2007; M.E. Smith et al., 2008b), the overall thickness of the Wilkins Peak Member makes it possible to infer the impact of tectonics on the distribution of sedimentary facies. Conversely, the lateral and vertical distribution of sedimentary facies (e.g., trona, oil shale) helps to demonstrate tectonic movements in the basin.

During middle Wilkins Peak time, movement of the Darby Thrust Fault of the Wyoming Thrust Belt at Slate Creek on the western margin may have occurred between deposition of Trona Beds #18 and #19, which was approximately during the deposition of the D-Bed (see Section 5.4). Oil shale, carbonates, minor evaporite beds (pirsonnite? Tim Lowenstein, pers. comm., 2010), and lithic sandstones comprise the majority of the section. A northwestward shift in the basin centre marks the beginning of the middle Wilkins Peak Member. Trona-bed-thickness isopach maps (Wiig et al., 1995) suggest that the deeper basin then moved progressively eastward with the Bridger basin during middle Wilkins Peak time. The movement of the Sparks Ranch Thrust Fault on the eastern Uinta Uplift during the last stages of the lower Wilkins Peak (Roehler, 1993) also likely affected the basin physiography during middle Wilkins Peak time. Pietras and Carroll (2006) showed thicker sediment packages both south and north of the Breathing Gulch locality on White Mountain during middle Wilkins Peak time. This possible hinge-line is also the location of the large, hydrothermally altered carbonate mounds on White Mountain described by Mayry (2005), and may correspond to an E-W oriented buried uplift recognized from gravity anomaly data by Bankey and Merewether (1990).

Carbonate facies deposited at the beginning of middle Wilkins Peak time and which overlie the D-Bed in Firehole Canyon comprise mostly laminated dark brown oil shale, brownish grey discontinuously laminated mudstones, and poorly bedded to wavy-bedded and discontinuously ripple-laminated calcareous sandstones with carbonate crusts and intraclasts and evaporite pseudomorphs (Figs. *5.1.1.*4–6). The lake cycles of Pietras and Carroll (2006) can be recognized in the vertical associations of the facies. As in the other localities investigated (e.g., WM, #18C, above D), the littoral facies association preserves horizontal burrows, trails, and tunnels and poorly preserved mammal footprints (e.g., FC, D2, m ~17.8–19). Bird footprints are notably lacking in this facies association. Above these carbonates, the E-Bed is poorly exposed and consists mainly of pedogenically modified and bioturbated brownish green arkosic siltstones, intercalated with thin beds of ripple-laminated very fine-grained sandstones that preserve discrete full-relief burrows (e.g., *Planolites* ispp., cf. *Taenidium barsretti*/cf. *Lunulichnus* isp.). The E-Bed in Firehole Canyon preserves a more terrestrial facies association and ichnological signature than any of the lower arkose beds, but similarly contains a thin, internal "white stripe" lake cycle carbonate unit (e.g., FC, E2, m ~27).

Above the E-Bed, typical carbonate facies of the Wilkins Peak persist, preserving mammal footprints and horizontal trails in littoral to eulittoral facies (Figs. *5.1.1.*7–9). Large trona-fan pseudomorphs formed within a thin carbonate bed (~5 cm thick), and possible dissolved shortite 'spheres', suggest that the lake had a higher salinity in this locality above the E-Bed than above the D-Bed. The F-Bed is poorly exposed, preserving channel sandstones and green siltstones, and was not investigated in detail. The rest of the Wilkins Peak Member in Firehole Canyon is also poorly exposed and was not measured. The upper arkose beds (G to I) are present, but consist mainly of poorly exposed green siltstones that likely represent terrestrial deposition.

The upper Wilkins Peak Member consists mainly of a thick succession of oil shale in the basin centre (e.g., Tollgate Rock, near Green River), contains only two trona beds (Beds #24 and #25) that were deposited towards the northeast of the trona basin (Culberston, 1971; Wiig et al.,1995), and contains the final arkosic interval, the I-Bed. The I-Bed at Tollgate Rock coarsens upwards from bluish green laminated mudstones, to planar-laminated heterolithic arkosic siltstones with some sheared horizons, to climbing-ripple-laminated very fine-grained sandstones with medium-scale trough cross-stratification and locally scoured bases. This lithofacies association is very similar to portions of the arkose beds in the Firehole Canyon area (e.g., FC, A, m ~12.5–15), which contain abundant bird footprints and horizontal burrows likely produced by

air-breathing insects. However, the Tollgate Rock I-Bed succession does not preserve trace fossils, and was most likely deposited below the chemocline in relatively deep saline lake waters. This example shows the utility of recognizing lithofacies associated trace fossil assemblages, and their absence, for interpreting depositional environments. The characteristics of this unit at Tollgate Rock provide additional support for a deltaic origin of the arkose beds (discussed below). More specifically, this succession is interpreted as a distal prodeltaic setting, coarsening upwards to underflow deposits of the distal delta-front.

*5.3.2. Depositional Environments of the Arkose Beds*

The arkosic units are interpreted to represent fluvially dominated deltas with numerous distributary and terminal distributary channels that prograded across the flat basin floor and into the shallow saline lake following periods of low lake levels. The system may have been similar to the Volga Delta into the northern Caspian Sea (Kroonenberg et al., 1997; Overeem et al., 2003; Li et al., 2004), an example which has not previously been described from ancient deposits. The descriptions, measured sections, and discussion of the arkose beds in this thesis present a testable model for their deposition, their interaction with lacustrine deposits, and their stratigraphic packaging. The trace fossils provide evidence to support the model, and in turn, the stratigraphic packaging of the sediments helps to better place the trace fossils associations within their paleoenvironmental contexts. The system is complex, with fluvial facies and lacustrine facies closely intercalated. To better understand the distribution of trace fossils in underfilled basins, and their applicability to paleoenvironmental reconstructions and stratigraphy, this example of a basin centre, low-gradient, saline lacustrine fluvio-deltaic system has been described in detail. With future work (e.g., petrography, X-ray diffraction), the lake- and groundwater chemistry of the changing environments should provide valuable evidence for the improvement of the model. Paleocurrent measurements and a closer look at the sedimentology of the sandstones will also greatly improve the understanding of the system. The following discussion mainly focuses on the D-Bed; a more detailed discussion of the A-Bed is presented in Chapter 6 to show the use of trace fossils, placed within their sedimentological and stratigraphic context, to improve understanding of the system.

The river that fed the system likely entered the basin from the southeast and may have been sourced from the Sierra Madre Uplift in the southeastern Washakie Basin (Smoot, 1983; Mike Smith, pers. comm., 2010), where typical alluvial facies (e.g., ribbon channel bodies, channel sheet sandstones, well developed red and grey paleosols) of the Cathedral Bluffs Member of the Wasatch Formation were deposited. Several facies associations near the terminus of the paleoriver in the Bridger basin are similar to crevasse-splay and distributary channel deposits described from the Cumberland Marshes, a frequently avulsing distributary system fed by the Saskatchewan River onto the Lake Agassiz plain at the Saskatchewan/Manitoba border (e.g., Farrell, 2001). The "Arkose Beds" may mark the climatic transitions from arid, highly seasonal periods (high eccentricity) to generally more wet, less seasonal periods (low eccentricity) (cf. M.E. Smith et al., 2010). Still, lake-level fluctuations were frequent, and lake levels probably responded quickly to changes in sediment and water input. The exposures in the Firehole Canyon area may more closely record the interaction between the lake and the siliciclastic units because the region was lower lying (a possible sub-basin) when compared with the White Mountain area (cf. Deardorff and Mannion, 1971; cf. Wiig et al., 1995). The inflow supplied from the river-delta system may have caused initial transgressions that led to formation of the oil shale that conformably overlies some of the bedded evaporites (e.g., Section FC, D1, m ~2–3).

Sandstones and siltstones that were deposited in channels are present in the top portions of the lower units (e.g., A-Bed at MFC, FC, and SCC), and although some of these channels are interpreted as being on the lower delta-plain or within shallow lake waters, the lower units of both the D-Bed and A-Bed preserve fewer indicators of subaerial exposure and more lacustrine indicators than do the upper units. The arkose beds studied here show an overall coarsening-upwards succession, with progressively more deeply incised channel bodies, and more abundant landward lithofacies (e.g., paleosols) and trace fossils towards the tops of the units. Of the localities investigated, channel sandstone bodies were only infrequently observed to scour into the underlying lacustrine carbonate units. For example, a cross-bedded channel of the lower E-Bed scours into the underlying lacustrine carbonates. This association may be evidence of a relatively lower, possibly shifted, base level in the area when compared with the D-Bed and lower Wilkins Peak arkosic deposits in Firehole Canyon. [The upper unit of the D-Bed at Kanda also preserves channel sandstones scoured into lacustrine mudstones, which could be evidence that the basin slope was relatively steeper there than in Firehole Canyon during the time of the upper D-Bed (cf. Schumm, 1993).] Deeply scoured channels with large-scale lateral accretion surfaces were present only in the upper portions of the upper units of the arkose beds. The tops of the arkose beds preserve indicators of active channels flooded by the transgressing main lake (e.g., FC, D1, m ~25–30), as well as channel sandstones and paleosols that experienced relatively slow sedimentation rates and possibly abandonment, represented by greater bioturbation and more terrestrial trace fossils, before the unit was drowned by the main lake (e.g., MFC, A, m ~12–13.5).

The lower contacts of the arkosic mudstones, siltstones, and marlstones are generally conformable and gradational with the underlying carbonate lacustrine facies, in both the base of the lower units, as well as the base of the upper units. Climbing-rippled arkosic sandstones of the lower A-Bed in Firehole Canyon sit directly on lacustrine carbonate mudstones, but fine upwards to light greyish green mudstones that are interpreted as being deposited within the main lake (e.g., FC, A, m ~0.7–3; Fig. *5.1.2*.6A–H). The lower arkosic units represent the more distal portions of the "delta", whether they were basinward of (e.g., FC, A, lower unit; Fig. *5.1.2*.6) or marginal to the terminal distributary channels (e.g., ?FC, D1; Fig. *5.1.3*.2). The lower units grade upwards to more subaerially exposed facies, which are interpreted as briefly exposed mudflats or wetlands. Reddish, iron-stained root marks preserved in both siliciclastic and carbonate mudstones and siltstones provide evidence of lake-fringing or riparian wetlands with shallow water tables. Siliciclastic and marl siltstones containing these root marks cap the lower A-Bed and also preserve horizons of carbonate root-casts/nodules with reddish, iron-stained rinds, and may represent shallowing of the water table due to the transgressing lake represented by the lacustrine carbonates above (e.g., MFC, A; Fig. *5.1.2*.2F). The D-Bed preserves vertebrate footprints produced in wet-soupy substrates together with root marks, with pedogenic modification and desiccation features towards the top of the lower unit (Fig. *5.1.3*.2). In both cases, the lower units are considered as the first of the set of progradational parasequences that make up the arkose beds in the Firehole Canyon area, with the most landward facies at the tops of the units (Figs. 5.1–5).

Both the A-Bed and D-Bed in the Firehole Canyon area contain carbonate lacustrine units, called here the "white stripe units", which visually divide the lower arkosic units from the upper arkosic units. The lower contacts of these lacustrine carbonates are sharp and locally erosive, and can be called flooding surfaces. Section FC, D1 preserves a calciclastic intraclast conglomerate with a scoured base, which is interpreted as a transgressive lag (FC, D1, m ~6; Fig. *5.1.1*.10C). The A-Bed, however, shows laminated organic-rich micritic shales directly above an erosional surface, which demonstrates the gently undulating surficial topography of the

underlying unit in Firehole Canyon (N), probably partly produced during the transgression (Fig. *5.1.1.*11A–C). These minor transgressions within the arkose beds may be a response to the filling of the low-accommodation shallow lake with siliciclastics and even further flattening of the basin floor. Alternatively, the minor lake expansions that interfingered with the arkose-beds may be due to background, climate-related, changes in precipitation. The upper 'contacts' of the lacustrine carbonates with the second siliciclastic units in both the A-Bed and D-Bed are conformable and transitional. Lithofacies change gradually upwards and include: 1) lenticular-bedded, wavy-bedded, and interbedded marl to siliclastic mudstones with calciclastic and siliciclastic siltstones and sandstones (e.g., SCC, A; Fig. *5.1.1.*13D–F); and, 2) massive siltstones, changing in colour upwards from greyish green to olive green (e.g., MFC, A; FC, D1; Figs. *5.1.1.* 10D, 10E, 12C, 12G). Lithological differences between the marl mudstones and siltstones, and the siliciclastic siltstones are shown by colour changes typically from brown or greyish green carbonate-containing sediments to olive green, with proportionately more arkosic lithology.

In the lower "second unit" of the D-Bed (FC, D1), the massive greyish green marlstone to olive green siltstone coarsens upwards to planar-laminated very fine-grained arkosic sandstone, which was then exposed, as shown by 20 cm-deep desiccation cracks and an irregular upper surface (Fig. *5.1.3.*3A, 3C). The overlying discontinuously laminated olive-tan siltstone also coarsens to planar-laminated to planar-laminated very fine-grained arkosic sandstone with reddish, iron-stained root marks and possible carbonate root casts. Together, these two coarsening-upwards cycles are interpreted to represent distal mudflat to fringing wetland facies basinward of a terminal distributary channel, which are scoured into by the possible initial incision "chute" facies of the downstream-accreting channel or mouth bar sandstones. The scour-fill consists of a thin unit (~30 cm thick) of upper flow regime plane-bedded and ripple-laminated fine-grained sandstone that may represent incipient mouth bar deposits (cf. Farrell, 2001; Fig. *5.1.3.*3B, 3D).

Three flat-based, stacked, ~1.5 m-thick, basinward-dipping, downlapping accretionary fine-grained sandstones with internal downstream-dipping, ripple-laminated cross-beds are interpreted to represent the subsequent progradation and aggradation of a distributary mouth bar (Section 5.2.10; Fig. *5.1.3.*4A–D). The ripple-laminated bedsets are each capped by plane-bedded fine-grained (lower) sandstone topsets that may represent a decrease in flow velocity. Trace fossils are lacking from this portion of the section. Numerous other accretion surfaces, or clinoforms, within this unit are present up to at least 100 m up-dip (eastward) from the position of the measured section. Down-dip (westward), the clinoforms terminate with a large concave-upwards scour into massive tan siltstones and thin cross-laminated sandstones. Laterally (southward), the bedsets may represent the more marginal portions of the bar. The measured section appears to be right in the middle of the delta-front feeder channel (terminal distributary). Alternatively, these bedsets represent downstream accretion confined within a terminal distributary channel that scoured only slightly into the underlying mudflat facies. Similar deposits were recently described from a deltaic succession in the Green River Formation of Utah (Schomacker et al., 2010).

Above the accretionary sandstones, the unit coarsens slightly to a fine-grained (upper) sandstone, ~1 m-thick with plane-beds, convoluted plane-beds and large-scale convolutions (~0.5 m), and at the top of the bedset, irregular bedding planes that were bioturbated (e.g., FC, D1, m ~16; Fig. *5.1.3.*4F, 4G). This sandstone may represent a levee with internal slumping. The bioturbation appears to have been produced subaqueously in a soupy substrate. This facies marks the upper surface of the coarsening upwards succession. It may overlie a large scour surface that cuts into the underlying downstream-accreting sandstones, but more fieldwork is required to place this unit within the stratigraphy of the second unit. In nearby areas of the

outcrop, the clinoform unit is overlain by sandstones with large-scale cross-stratification that appear to represent channel bars.

Above the thick sandstone unit, approximately 3 m of poorly exposed greenish mudstones and siltstones are intercalated with very fine-grained reddish grey sandstones that coarsen upwards. This part of the succession is interpreted as overbank/floodplain or floodplain pond siltstones with progressively more proximal crevasse sandstones, considered as the lower part of the "green stripe" unit. Internally, these sandstones contain planar lamination in the lower bed, planar lamination with climbing-ripples in the second bed, and small-scale trough cross-lamination in the upper bed. The upper sandstone in this succession is bioturbated with traces that are interpreted to represent fluvial and terrestrial environments (e.g., *Skolithos* ispp., cf. *Taenidium barretti* isp./cf. *Lunulichnus* isp.) and provide evidence of subaerial exposure, draining of the substrate, and stability of the substrate (e.g., FC, D1, m ~22; Fig. *5.1.3*.5B–D). Together, these intercalated siltstones and cross-laminated sandstones represent progressively more landward, or more terrestrial, facies that overlie the terminal distributary deltaic sandstones below.

In Section FC, D2, the roughly time-equivalent deposits instead preserve facies similar to those interpreted as mouth bar and levee sandstones in FC, D1. Internally, these fine-grained arkosic sandstones preserve undulating plane beds, non-climbing-ripple-lamination, and supercritical climbing-ripple-lamination (Fig. *5.1.3*.8A–D). The lowest exposed fine-grained sandstones in this section also preserve metre-scale and decimetre-scale dewatering structures (Fig. *5.1.3*.8B). They may represent slumping of mouth bar and/or subaqueous levee deposits, or they may represent tectonic movement in the basin. The sandstone units at the base of Section FC, D2 fine-upwards to undulating and flat planar-laminated very fine-grained sandstones possibly deposited in the distal delta-front, or distributary mouth bar area. Above this, the siltstones that mark the upper "second" unit in FC, D2 lie conformably above the distal sandstones. They are ~0.7 m-thick, grading transitionally from dark brownish olive green siltstone with discontinuous lamination, to blackish dark green discontinuously laminated siltstone containing mammal bones, to a black mudstone that weathers bright green (the "green stripe"; Fig. *5.1.3*.8E, 8F). Based on these facies associations, it is possible that these siltstones may have been deposited by hypopycnal flows within the lake. Alternatively, if the sandstones represent deposition within channels, the fining upwards succession may represent channel migration, avulsion, and/or filling with fine-grained sediments, which were then flooded by the main lake, lagoon, or interdistributary lake on the delta-plain.

The "green stripe unit" overlies massive olive-tan siltstones in Section FC, D1. As an alternative interpretation to that given above, the "green stripe" lake may might been situated on the upper delta-plain, possibly within or adjacent to a channel system, which contained pinching-out crevasse splay sandstones. However, a gamma ray spike present within the "green stripe", as well as all other basal lacustrine units (M.E. Smith, pers. comm., 2010), supports the interpretation that it was an interdistributary bay or lagoon of the main lake. The sediments themselves are a ~1.5 m-thick unit of bright green-weathering dark brown and black mudstone to greyish green laminated mudstone that conformably overlies brownish olive green siltstones (e.g., FC, D1, m ~22.5; Fig. *5.1.3*.5). Above the "green stripe" in both FC, D1 and FC, D2, a carbonate, intraclastic conglomerate-containing bed ~15 cm thick may represent a transgressive lag or storm bed generated from the main lake (Fig. *5.1.3*.5G–H). Above the intraclast bed, massive to laminated greyish green mudstones with dark, detritus-rich parting planes are interpreted to represent the filling of the interdistributary bay/lake (e.g., FC, D1, m ~24–25; Fig. *5.1.3*.6A–G). Stromatolitic horizons and small desiccation cracks are preserved in the laminated upper portion of the unit.

In Section FC, D1, the laminated greyish green mudstone unit contains locally scoured reddish-orangish grey fine-grained arkosic sandstones that pinch out laterally. Local, lateral facies changes are extreme within this unit. Internally, the lower portion may be planar-bedded or it may preserve bulbous load structures (ball and pillow) and/or mammal footprints preserved in cross-section (e.g., FC, D1, m ~24; Fig. *5.1.3.*6A–D). The bottom bedding plane preserves abundant trace fossils as casts, including vertebrate footprints (crocodilian, mammal?) and medium-sized *Planolites* with sharp burrow boundaries. Vertical *Skolithos* burrows in the sandstone originate from the upper bedding plane. These sandstones are interpreted to represent crevasse-splay and/or crevasse channel deposits that filled in the small lake/bay in places, while adjacent laminated mudstones persist upwards for another ~0.5 metre. The uppermost portion of the "green stripe" unit in FC, D1 preserves a thin orange stromatolitic horizon with tan fine-grained sandstone of the upper unit abruptly overlying it; laterally, the unit was both scoured by the tan fine-grained sandstone containing stromatolite intraclasts and gradational with light buff, very fine-grained planar-laminated sandstone that preserved subaerial, terrestrial trace fossils (Fig. *5.1.3.*7A–F).

The lower contact of the upper unit in FC, D1 is complex. The gradational planar-laminated sandstone may represent the distal mouth bar of the overlying, scour-based, channel deposits. Large-scale, trough cross-stratified, very fine-grained sandstone grades upwards to planar-laminated and climbing-ripple cross-laminated sandstones (e.g., FC, D1, m ~25–26; Fig. *5.1.3.*7). These fluvial deposits quickly fine upwards to weakly planar-laminated, muddy, very fine-grained sandstones that preserve possible very small horizontal burrows on the lower bedding planes. Upwards, a transition to lenticular-bedded tan mudstones with calciclastic siltstone lenses signifies the flooding of the channel by the main lake. For this reason, these channel deposits also represent a terminal distributary. The arkosic material gradually passes upwards to lenticular-bedded greyish green carbonate or marlstone, to plane-bedded carbonates, to littoral carbonate calciclastic sandstones (e.g., FC, D1, m ~26.5–29; Figs. *5.1.1.*6A, *5.1.3.*7H). This succession records the gradual transition to the next major carbonate lake unit above the D-Arkose Bed.

In Section FC, D2, however, a more channel-dominated upper unit is preserved. The "green stripe" unit is essentially the same as in Section FC, D1, with an intraclast conglomerate above the bright green-weathering mudstone, greyish green laminated mudstones, and a stromatolitic horizon. The uppermost ~0.5 m of this unit here also preserves massive greyish green mudstones and a lenticular-bedded thin unit, which was later incised by channel deposits of the overlying sediments. Approximately five metres of section then preserves three fining-upwards successions of mainly coarse-grained to muddy very fine-grained arkosic sandstones (e.g., FC, D2, m ~6–11; Figs. *5.1.3.*8A, 9A–F). The lowermost fining-upwards unit preserves a pebble-conglomerate that contains rounded clasts of older Wilkins Peak mudstones and sandstone clasts that possibly were derived from the underlying Wasatch Formation. The scoured-base also preserves large reed impressions, and reddish to black plant material is found throughout the lowest 30 cm. Internal structures in the lowest unit include: 1) large-scale cross-beds with tangential bases; 2) sheared, plane-bedded coarse sandstones; and 3) plane-bedded to climbing-rippled fine-grained sandstones. Laminated green mudstones separate the fining-upwards sandstone bedsets. The second unit and third bedsets have scoured bases with large-scale cross-beds with tangential bases, grading upwards to climbing-rippled sandstones and heterolithic, slightly undulating, ripple-laminated, very fine-grained sandstones with green mudstone drapes. Bedding planes of these greenish, muddy very fine-grained sandstones preserve very low-amplitude interference-ripple bedforms, a bubble-like texture attributed to microbial mats, very small surface tunnels and trails and small desiccation cracks. These three

units are interpreted as distributary channel cut and fill.

The upper unit in FC, D2 continues to fine-upwards with the deposition of brownish olive green muddy siltstone, intercalated with reddish tan very fine-grained sandstone beds (e.g., FC, D2, m ~11–14; Fig. *5.1.3.*9G–H). Similar facies dominate the E-Bed (Fig. *5.1.3.*10). The siltstones are discontinuously laminated or massive with platy to blocky breakage and are interpreted as overbank deposits. The sandstone interbeds are internally bedded with irregular bedding planes, attributable to a high degree of bioturbation in wet substrates overprinted by traces representing drained, subaerial substrates, and are interpreted to represent subaerially exposed levee or splay deposits, becoming more distal to the main channel upwards. The upper contact of the D-Arkose Bed in Section FC, D2 with the lacustrine carbonates above the D-Bed is sharp, in contrast to Section FC, D1. In FC, D2, the carbonate unit preserves a thin, sharp-based basal calciclastic sandstone bed, overlain by sublittoral to profundal laminated, organic-rich, micritic carbonate mudstone (oil shale).

On White Mountain at Kanda, the D-Bed is ~15 m thick and overall more fine-grained and more poorly exposed, but coarsens upwards to very fine-grained and fine-grained channel sandstones with a deeply scoured base and large-scale accretion surfaces (Fig. *5.1.3.*1). The lower contact of the upper D-Bed at Kanda appears to be gradational, from massive to discontinuously laminated grey mudstones of the lacustrine facies below ("white stripe" unit), to weakly bedded to massive greenish tan-brown siltstone without signs of subaerial exposure. The siltstones grade transitionally upwards into weakly laminated light tan, very fine-grained arkosic sandstone that continues to coarsen upwards, to greyish tan fine-grained sandstone and a matrix-supported, pebble-conglomerate with carbonate intraclasts. No sharp contacts are present within this succession, which is interpreted to be the initial sublacustrine deposition from the dilute fluvial system into the saline lake, becoming more proximal to the feeder channel upwards. The conglomerate grades upwards to greyish tan fine-grained sandstone with flat-lying intraclasts along low-angle, planar cross-beds. Upwards, a scoured sandstone incises the lower intraclastic sandstone, contains plane-beds, sheared plane-beds, and large-scale planar cross-lamination with internal ripple-lamination.

The lower portion of the upper unit at Kanda also partly consists of a deeply fractured greenish buff siltstone preserving abundant reddish, iron-stained root marks, interpreted as an incipient palaeosol developed on distal overbank deposits with a shallow water table (Fig. *5.1.3.*1A–B, 1G). No trace fossils are preserved within it. The upper contact of this siltstone is flat, and the fracture-tops are abruptly overlain by the flat-lying greenish siltstones of the subsequent coarsening-upwards cycle (cf. Pietras and Carroll, 2006). Above the relatively thin upper unit at Kanda, dolomitic, organic-poor, shallow sublittoral to littoral lacustrine mudstones of Lake Gosiute were deposited. The "green stripe" unit is lacking at Kanda, as well as the littoral and eulittoral carbonate facies above the D-Bed present in Firehole Canyon.

The heterolithic facies of the upper unit at Kanda are similar to the lower unit of Section FC, D1 in Firehole Canyon, preserving vertebrate footprints produced in soupy, sandy substrates internally ripple cross-laminated and wavy-bedded with mud-drapes. Very fine-grained sandstones also preserve desiccation cracks and bubbly microbial-mat-like textures, together with bird footprints, cf. *Vagorichnus* isp. horizontal tunnels, and pellet-filled horizontal burrows. The depositional environment is interpreted as an overbank-fed mudflat to proximal overbank area, finally cut by the distributary channel that provided the sediment and freshwater. Within the channel fill deposits, climbing-ripple-lamination, ripple cross-lamination, oriented perpendicular to the (lateral?) accretion surfaces, and plane-beds with parting lineation and rare trace fossils (*Ancorichnus* isp.) are preserved. The uppermost sandstones of the upper unit appear to have undergone a brief period of stability and abandonment, with bioturbation and

possible stabilization by microbial mats, prior to the deposition of the overlying, shallow lacustrine dolomitic mudstones.

### *5.3.3. Summary of the Depositional Model for the A- and D-Arkose Beds*

In summary, the A-Bed and D-Bed represent the progradation of a sandy fluvial system into the flat-lying, littoral to lake-marginal regions of Lake Gosiute following lacustrine lowstands during periods of aridity. The progradation may have occurred during the transition from high-eccentricity climatic periods to low-eccentricity climatic periods (cf. M.E. Smith et al., 2010), when more water and sediment, sourced from an area with exposed basement, was available. Autogenic processes, such as incision through a sedimentary or uplifted barrier to the basin, may have been involved in the sudden appearance of the arkosic sediments at possible climate-related periods during Wilkins Peak time (Alan Carroll, pers. comm., 2008). Most of the arkosic sediments are concentrated on the eastern margin of the Bridger basin, thinning northwards and thickening towards the southeast (Culbertson, 1961), but remaining north of the quartzose siliciclastics sourced in the Uinta Uplift of the southern margin. The lateral facies relationships between the quartzose siliciclastic alluvial and the arkosic alluvial systems are as yet unknown.

The terms “delta” and “delta-plain” have been used here to describe the general setting of the arkosic units. The system is envisaged as a fluvially-dominated delta formed where multiple terminal distributary channels emptied into the eastern central basin of Lake Gosiute, with increasingly more typical floodplain facies associations being deposited on the subaerial delta-plain. Because of the eastern barrier formed by the Rock Springs Uplift, together with the arkosic materials possibly being sourced from the eastern margin of the Greater Green River Basin > ~150 km away, the system was likely fed by a single river, or a few smaller rivers. The arkosic sheetflood sediments in the northern lake-margins on White Mountain may have been sourced from elsewhere. The combination of a very low-gradient (~1–2°) basin “floor” and a shallow, closed lake played an important role in the vertical packaging of the sediments and the lithofacies preserved, by determining the low amounts of available 'vertical' accommodation within the lake itself and the splay-like spreading of sediments on the delta-plain. In most cases, even sediments interpreted as being basinward of terminal distributary channels showed evidence of frequent flooding and exposure. Coupled with frequent lake-level rise-and-fall and rapid facies changes, these features presumably ensured that the “delta” did not necessarily assume a typical triangular-shaped geometry. Sublacustrine facies normally preserved in deltas of deep lakes present (e.g., Gilbert-type delta-front foresets, Bitter Creek Delta of the Laney Member in the Washakie Basin) were not present. During lake lowstands, the shoreline may have been finger-like (webbed bird-foot?), where terminal distributary channels extended basinward, building up the lake-margin area with fluvial and overbank facies intercalated with littoral lacustrine and mudflat facies. During periods of higher lake-levels, the shape of the shoreline on the delta-plain may have been straight or gently curved, similar to a typical wave-dominated delta planform, with facies association more similar laterally (e.g., the lower unit of A-Bed at MFC, FC, and SCC).

The depositional cycles within these arkose beds are comparable to the “lake cycles” of Pietras and Carroll (2006), with transgressive shallow lacustrine facies abruptly resting on the underlying sediments, followed by sublittoral organic-rich lacustrine mudstones that shallow upwards, culminating in subaerially exposed, sometimes fully terrestrial, facies. Progradational stacking within the arkose beds was observed in two to three main cycles bounded by flooding surfaces (cf. parasequences), each with at least two smaller-scale depositional cycles that typically coarsen upwards (Figs. 5.1–5.5). These smaller-scale cycles (cf. parasequences *sensu*

Bohacs et al., 2007b?) were not bound by flooding surfaces, but typically surfaces of relatively more stable, landward facies and trace fossils in their uppermost beds. These cycle-bounding "surfaces" were sharply overlain by coarsening-upwards successions of either more basinward lithofacies and trace fossils, or were scoured by overlying fining-upwards fluvial successions. These cycles may be comparable in scale to those outlined by Farrell (2001), who recognized paleosols as parasequence-bounding 'surfaces' and coarsening-upwards successions (e.g., crevasse splay progradation and abandonment) as parasequences. Retrogradational, small-scale cycles may be observed towards the tops of the parasequences by facies associations that provide evidence of initial rises in water tables or early flooding by the expanding lake (e.g., the green siltstone at the top of the lower unit, A-Bed; the fining-upwards succession observed in FC, D2 below the "green stripe"; the fining-upwards succession within the flooded active channel at the top of FC, D1). Fining-upwards bedsets were also recognized in the lower A-Bed of Firehole Canyon, but formed an overall coarsening-upwards trend within the lower unit.

Trace fossils are especially important for recognizing subaerial exposure surfaces and periods of substrate stability, and helped to reconstruct the environments represented by ambiguous lithofacies associations by signifying changing, relative water table depths, the depths of standing water, substrate consistency, and broadly, the relative salinity of pore- or lake-waters (see Chapter 6). X-ray diffraction (preferably quantitative) and petrography of the transitional marl mudstone and siltstone facies might provide valuable insights to whether the sediments were deposited in the lake or on the lake-plain. Paleocurrent measurements and mapping are necessary to better understand the geometry of the system. A consideration of whether the paleocurrent measurements were taken from the lower, second, or upper units of the D-Bed could possibly show any tectonic shifting of the basin centre that might have occurred during or shortly after the deposition of the D-Bed. To test and improve this model, several points should be addressed: 1) which of the other arkose beds also have "white stripe" units, in what regions can they be observed, and if they lack the white stripe units, is there a sharp contact between a lower and upper unit? 2) does the stratigraphic packaging of the other arkose beds differ from the A- and D-Bed? 3) do the paleocurrents show a change from lower Wilkins Peak to middle Wilkins Peak to upper Wilkins Peak time, and if so, does this correlate with changes in the depositional centre of the trona beds or known tectonic movements in the basin? 4) do the degree and lateral distribution of incised large channel sandstones into lacustrine facies indicate the shifting of the basin centre and base-level through time, or is this a more local, autogenic feature? and 5) what is the lateral relationship between the quartzose siliciclastic facies of the southern margin and the arkosic siliciclastic facies on the eastern margin?

## 5.4. Basin Margin Lithofacies Assemblages

Trace fossils and lithofacies assemblages at several "basin margin" localities were also investigated as part of this study (Fig. 2.5). Detailed description and discussion of these sites is beyond the scope of this thesis, but the main features of these areas are briefly summarized below.

### *5.4.1. The Southern Basin Margin*

Lithofacies of the southern margin, next to the Uinta Uplift, are dominated by sedimentary rocks derived from Mesozoic quartzose siliciclastics and Paleozoic carbonates, deposited in fluvio-deltaic environments (Cathedral Bluffs Tongue of the Wasatch Formation) that interfinger with lacustrine carbonates of the Green River Formation. Due to the close association of the alluvial depositional settings with lake-margin and lacustrine settings, the basin margin strata are discussed together. Wiegman (1964, 1965), Smoot (1983), and M.E. Smith

(unpublished data) investigated the stratigraphy and sedimentary environments of the southern basin margin. Fluvio-lacustrine/deltaic and lacustrine strata of the balanced-fill Tipton Shale Member preserve abundant trace fossils in several paleoenvironments, including: 1) soft sediment vertical burrows and full-relief burrows in fluvio-lacustrine siliciclastic sediments; 2) simple horizontal burrows overprinted by meniscate burrows in lake-margin strata deposited in the littoral zone and subsequently subaerially exposed; 3) mottled and bioturbated oolitic carbonates, vertical burrows in cross-bedded calciclastic sandstones, and horizontal burrows in shales associated with tufa deposits, interpreted as a shoal and backshore lagoon environment with seepage springs; and 4) soft-substrate bioturbation of littoral siliciclastic sediments with branched backfilled burrows, small horizontal burrows, and vertebrate footprints on subaerially exposed, bedded, mixed siliciclastic and calciclastic sandstones of the lake-margin.

The Wilkins Peak Member at the same locality preserves: 1) alluvial fan conglomerates and sandstones, and green calcareous paleosols preserving probable crayfish burrows; 2) horizontal burrows in probable small playa-like settings; and 3) heavily bioturbated lacustrine siliciclastic sediments cemented with carbonate, possibly representing a bench-like environment; and 4) lacustrine to lake-margin siliciclastic sediments overprinted by small and large meniscate backfilled burrows in subaerial exposure surfaces. A heavily bioturbated, subaerially exposed surface with large-sized backfilled burrows can be traced laterally towards the basin centre (~500 m) where large and small vertebrate footprints are preserved, together with a possible bird-trampled soupy substrate preserving a texture remarkably similar to the shallow subaqueous mudflat at Sandai Plain, Lake Bogoria (Fig. 5.4.1). Higher in the section, a site preserving ~40 possible hot-spring mounds also preserves a thick, desiccated microbial mat just above the mound horizon, pellet-backfilled branching horizontal burrows in siliciclastic sandstones, and vertical and horizontal burrows in calciclastic sandstones adjacent to the carbonate mounds. This site is described in more detail below (Section 5.4.1.1). Upwards in the section, the Laney Member at the southern margin consists of bedded buff carbonates with subaerial exposure features (e.g., desiccation cracks), horizontal trails, and possible vertebrate footprints.

*5.4.1.1. Spring (?) Mounds and Associated Facies*— A full assessment of the geochemical, mineralogical, and petrographical features preserved in the many possible spring deposits within the greater Green River basin is beyond the scope of this thesis. The purpose of including this preliminary work here is to establish that the input of spring water into the greater Green River Basin may have influenced the chemistry and $CO_2$ content of lake waters, encouraged the growth of microbial mats in lacustrine and lake-margin environments, and contributed to authigenic mineral precipitation. These types of factors also influence the composition and distribution of animal and plant communities, as well as infaunal and epifaunal biogenic activity in these substrates.

Most of the possible spring sites appear to have been structurally controlled, in areas where they may have formed an important part of the local- to basin-scale paleoecology, at least during the time of the Wilkins Peak and Laney Members of the Green River Formation. Several

**Fig. 5.4.1.** (Next page) The Wilkins Peak Member at the southern margin of the Bridger basin. **(A)** Outcrop view of lacustrine carbonates and siliciclastic sandstones showing bioturbated exposure surfaces (arrows). **(B)** The uppermost unit in (A), showing heterolithic wavy- and flaser-bedded sandstones with carbonate drapes and interbeds, with burrows originating from the top surface (line at right), becoming less abundant downwards. **(C)** Close-up of large meniscate backfilled burrows in (B). **(D)** View from top of bed in (A–C) towards the basin centre. Arrow shows location of (E–G). **(E)** Large mammal footprints on wave-rippled surface. **(F)** Textured calciclastic siltstone surface with wave-ripple bedforms. **(G)** Textured surface shown in (F), with parallel linear markings preserved as positive features. Compare with flamingo-tracked texture in Scott et al. (2007, fig. 6G).


A
B
C
D
E
F
G

groups of possible spring mounds are exposed north of the Henry's Fork Fault of the Uinta Uplift in a WSW–ENE-trending alignment (Fig. 2.5; Wiegman, 1965; Surdam and Stanley, 1979). The mounds vary in size and detail, and first appear in the middle Wilkins Peak Member in Coldstream Creek (between strata correlated with the arkosic "F-Bed" and "G-Bed"; M.E. Smith, unpublished data). This group of at least four mounds is characterized here as mounds with stromatolitic laminae, having a dominantly micritic peloidal fabric with fenestral porosity, aggregations of spherical, micritic "coated grains", tubules, or possibly brine-shrimp egg cysts, and a lack of silica cement or silica replacement of carbonate (Fig. 5.4.2A–C). The Coldstream Creek mounds are bounded above and below by massive, micritic lacustrine calcite that shows irregular to platy breakage, but are laterally adjacent to, and apparently contemporary with, a ~ 0.5 m-thick bed of thinly laminated micritic carbonate that contains numerous microfaults, ostracodes, and rare mm-scale surface trails (Fig. 5.4.2D). These mounds may have formed subaqueously.

Further west, and towards the top of the Wilkins Peak Member at Wild Horse Draw, two different types of spring mounds are preserved. First, two large, brecciated and partially silicified, carbonate mudstone mounds up to 30 m high are exposed in Wild Horse Draw and eastward towards Little Mountain (Fig. 5.4.3). These mounds resemble in size, shape, texture, and mineralogy the three large mounds exposed along the northern White Mountain, which were reported and analyzed by Mayry (2007) and Mayry and Buchheim (2004, 2005). Those mounds

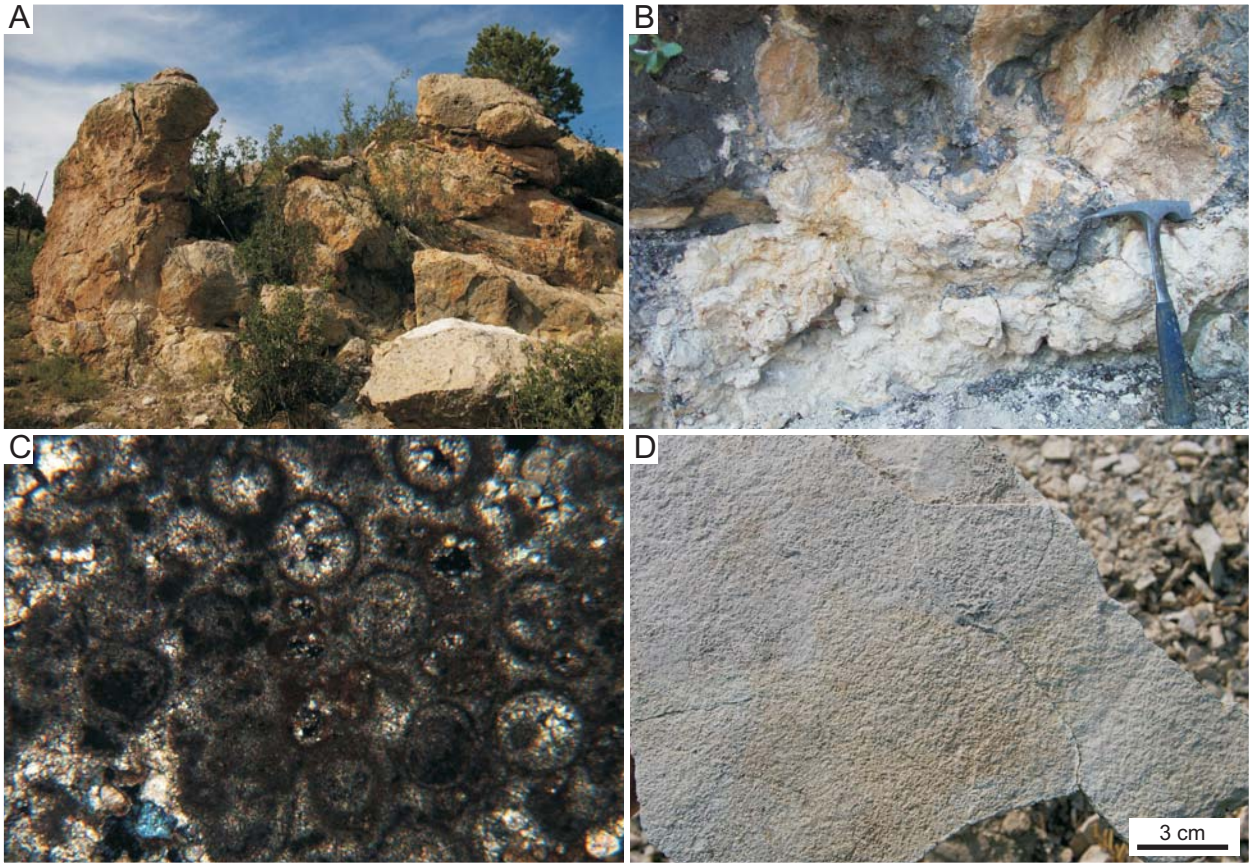


**Fig. 5.4.2.** Carbonate mounds at Coldstream Creek. **(A)** View of carbonate mound, approximately 4 m across. **(B)** Unbedded internal texture of mound. Fenestral porosity along laminae is visible in thin section (not shown). **(C)** Photomicrograph (cross-polars) of micritic carbonate with circular tubules? or ooids? Field of view 1 mm. **(D)** Upper bedding plane of laminated carbonate adjacent to mound. Ostracodes on surface, with possible surface trails.

appear to have been periodically active throughout the latest Tipton to latest Wilkins Peak time (Mayry, 2007), and are roughly aligned along the western blind thrust fault of the Rock Springs Uplift, which had its latest movement during the late Paleocene to early Eocene (Fig. 2.5; Mederos et al., 2005).

Although detailed stratigraphic correlation of the large mound in Wild Horse Draw was not undertaken, field relationships show that it may have been active before and possibly during the deposition of the I-Bed of the Wilkins Peak Member to just below the contact between the Wilkins Peak and the Laney Members (Fig. 5.4.3). Key textural characteristics of the Wild Horse "Mother" mound include brecciated mudstone, laminae building towards open channel porosity, and quartz precipitation in channels and small fractures, with some replacement of calcite by silica (Fig. 5.4.3). Like the large mounds present on White Mountain and at Little Mesa on the La Barge Platform (Fig. 2.5), the large mounds at the southern margin could represent the later brecciation and silicification of lacustrine mudstone that is relatively resistant to weathering (T. Lowenstein, pers. comm., 2010). However, the preservation of unaltered lacustrine sediments of the Laney Member that overlie the large mound at Wild Horse Draw does not seem to support that interpretation unless the 'mounds' formed during Laney time.

Approximately 40 smaller mounds concentrated along the roughly E–W line north of the Henry's Fork Fault form the second group at Wild Horse Draw, and are present at the transition between the Wilkins Peak Member and the Laney Member of the Green River Formation (Fig.

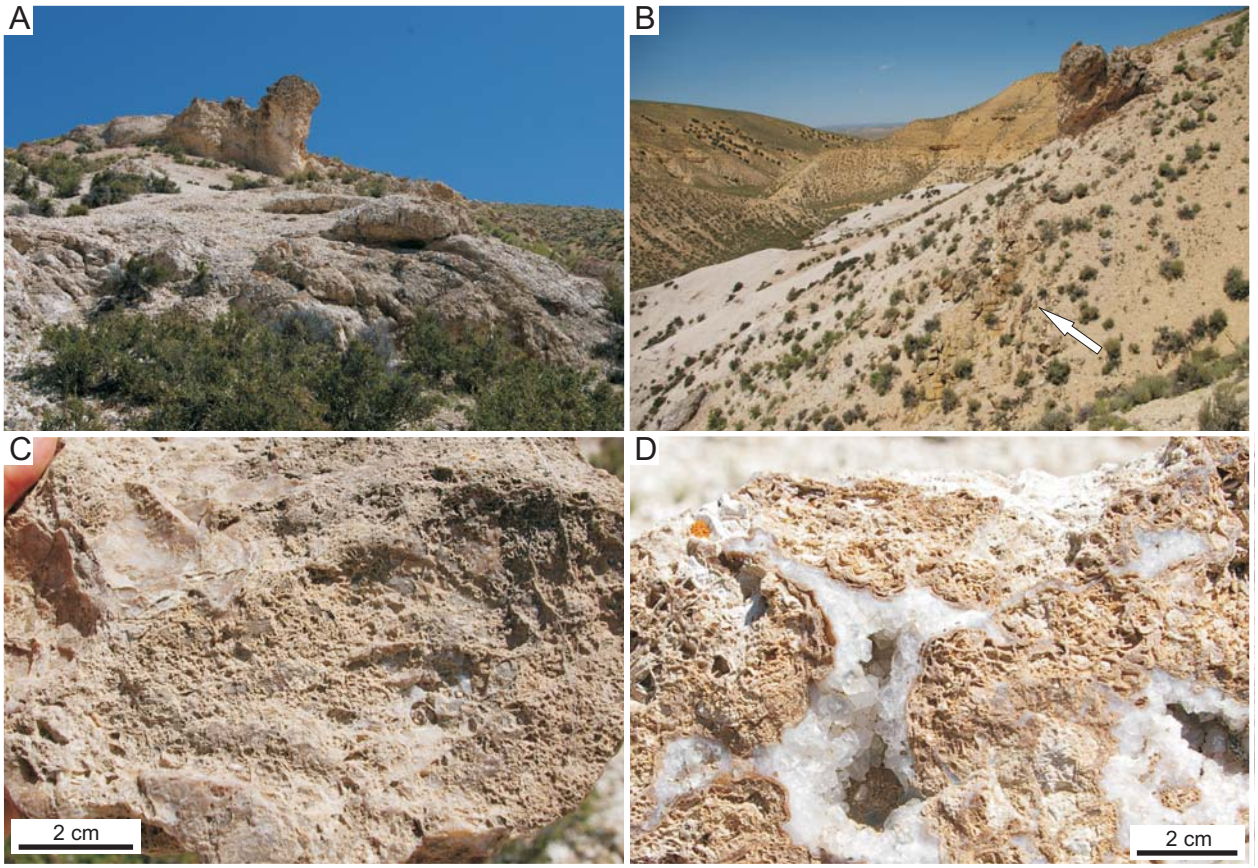


**Fig. 5.4.3.** The large carbonate mound at Wild Horse Draw. **(A)** View showing white, silicified carbonate mudstone mound. Field of view about 10 m in foreground. **(B)** View towards the west of the carbonate mound. Arrow showing possible fault associated with mound. Note the buff Laney Member in background. **(C–D)** Hand samples of mound carbonates showing silicified mudstone, laminae along large-scale porosity, and megaquartz filling porosity.

5.4.4). The mounds are approximately 2–3 m in height and are roughly spherical to cone-shaped, with diameters from 2–5 m. Macro-scale textures include vertical and horizontal layered bands that coat carbonate build-ups with vague internal laminae, which are amalgamated to form the mounds (Fig. 5.4.4), and are similar in this way to the Pleistocene chert "pillow mounds" east of Magadi townsite in the Magadi Basin. Adjacent and contemporary deposits include: 1) laminated carbonate mudstone with or without ostracodes; 2) peloidal micrite forming thick microbial mats that have internal and surficial mat textures and features (Fig. 5.4.5); 3) carbonate siltstones with desiccation features and trace fossils (Fig. 5.4.5H); and, 4) wave-rippled sandstones with ripple amplitudes of < 2 cm. Some fragments of possible silica crusts were


**Fig. 5.4.4.** The smaller carbonate mounds at Wild Horse Draw. **(A)** View of grey mound with the Laney Member above. Dozens of small mounds are found along this horizon. **(B)** Close-up showing travertine laminae filling vertical and horizontal fractures in mudstone mound. **(C)** Carbonate mound buried by siliciclastic sandstones of the Wilkins Peak Member. **(D–E)** Mound with travertine laminae draping carbonate mound at several horizons. **(F)** Internal view of a small mound showing breccia-filled possible vent pipe within mound (arrow at right of structure).

preserved on wave-rippled sandstones, and could show that at least some of the silica formed contemporaneously with the small mounds (Fig. 5.4.5G). Silica cementation and replacement of micritic and dolomitic carbonate mudstone is widespread above the spring-mound level. Deposits in the lower Laney Member at this locality include: 1) stromatolites with silica cement; 2) desiccated mudstones with vertebrate footprints and invertebrate surface trails; 3) silicified microbial mats?; and, 4) extensive and sheet-like peloidal micrite travertine with fenestral porosity, together with 5) buff carbonate mudstone that is poorly exposed.

Lastly, a group of four large spring mounds are preserved along the same line west of the Flaming Gorge reservoir, which are well within the Laney Member (Fig. 5.4.6). The mounds are up to 40 m high and more than about 50 m in diameter, and contain large (0.5 m), open conduits and a variety of spring-like facies. Peloidal micrite forms microbial shrubs, and the shrub-channel porosity is filled with finely-crystalline silica cement. Below the mounds at this site (at the same horizon as the Wild Horse Draw mounds?), an extensive unit up to 3 m thick preserves numerous small mounds that are exposed only at their upper surface, together with many stromatolite-coated logs (Fig. 5.4.6C, 6D). This unit was not investigated in detail.

Other possible spring mound localities in the greater Green River basin include: 1) North Barrel Springs, within the Laney Member; 2) possibly along the Spark's Ranch Thrust Fault on the eastern margin of the Uinta Uplift, within the lower Wilkins Peak (cf. Roehler, 1993, figs. 78–80); 3) Little Mesa area (Leggitt, 2007a); and, 4) Steed Canyon near La Barge, which preserves mounds similar to the small mounds at Wild Horse Draw near the top of the Wilkins Peak Member (Leggitt, 2007b). Structurally, the La Barge area is approximately at the junction of the Hogsback Thrust Fault and the Moxa Arch (e.g., Kraig et al., 1987; Becker et al., 2010). Stromatolitic microbial buildups that include layers of encrusted caddisfly cases are preserved along the northern margin of Lake Gosiute during the time of the Laney Member (Leggitt and Cushman, 2001; Leggitt and Loewan, 2002). These mounds were not attributed to spring input or to sublacustrine seeps, but they are also preserved near La Barge, and along the northern shoreline of the Laney Lake Gosiute (Leggitt and Cushman, 2001).

Other potential spring mounds in the Green River Formation include the huge stromatolitic mounds of the West Willow Creek Field and the Willow Creek Algal Mound in the Uinta Basin, Utah (cf. Osmond, 2000). The mounds consist of stromatolitic and skeletal (ostracode-dominated) carbonates with vuggy porosity that are more than 30 m in height, and are surrounded by onlapping lacustrine black shales (Osmond, 2000). The mineralogy of the mounds includes calcite, dolomite, pyrite, and chert and quartz cements, with pore-filling sparry calcite, dolomitization of carbonate matrix, and pore-filling and grain-replacing silica (Osmond, 2000). The West Willow Creek mound is on a NW–SE trending fault just SW of a steeply dipping NW–SE trending syncline, and although the Willow Creek Algal mound is directly SE of the West Willow Creek mound, no faults have been recognized at that locality (cf. Osmond, 2000). The faults and syncline present at the West Willow Creek mound were interpreted to have been active after the deposition of the mounds and laterally adjacent shales by Osmond (2000). The similarities with the spring mounds in the Greater Green River Basin include size, stromatolitic fabric, ostracods, their diagenetic history and authigenic mineral suite, and an association with faults. Osmond (2000) also reported the occurrence of several other similar mounds in the Uinta Basin.

**Fig. 5.4.5.** (Next page) Microbial mat features at Wild Horse Draw. **(A–E)** Surface textures of ~5 cm-thick, laterally continuous bed above small carbonate mound horizon. (A–C) Desiccation features of blackish crust like surface. Burrows (?) at left in (C). (D–E) Possible animal trails on surface where blackish crust not preserved. **(F)** Bubble-like texture, possibly attributable to a cyanobacterial mat. **(G)** Portion of siliceous crust on surface of sandstone. **(H)** Pellet-filled horizontal burrow in sandstone below small mound horizon.

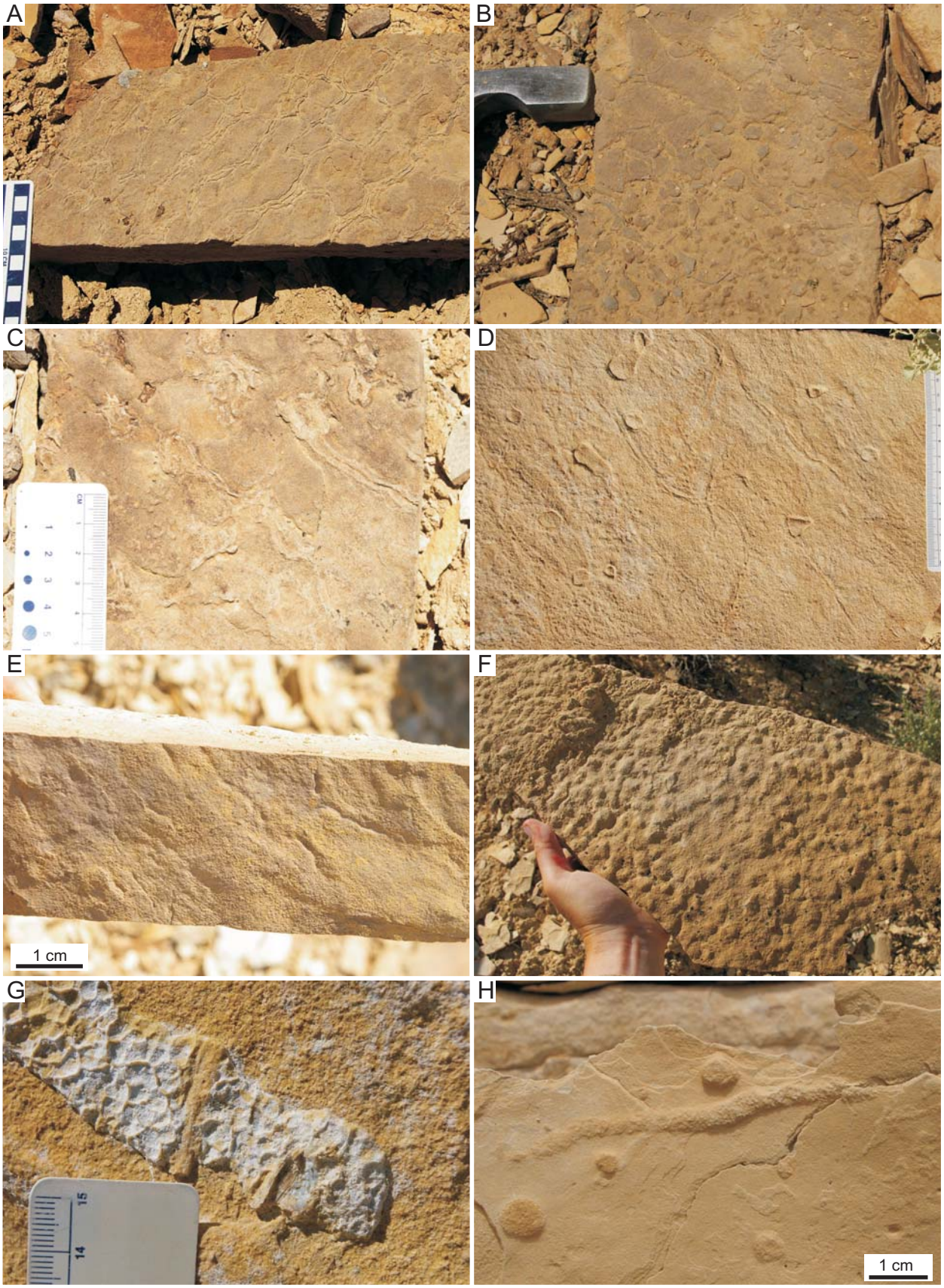
A
B
C
D
E
1 cm
F
G
H
1 cm

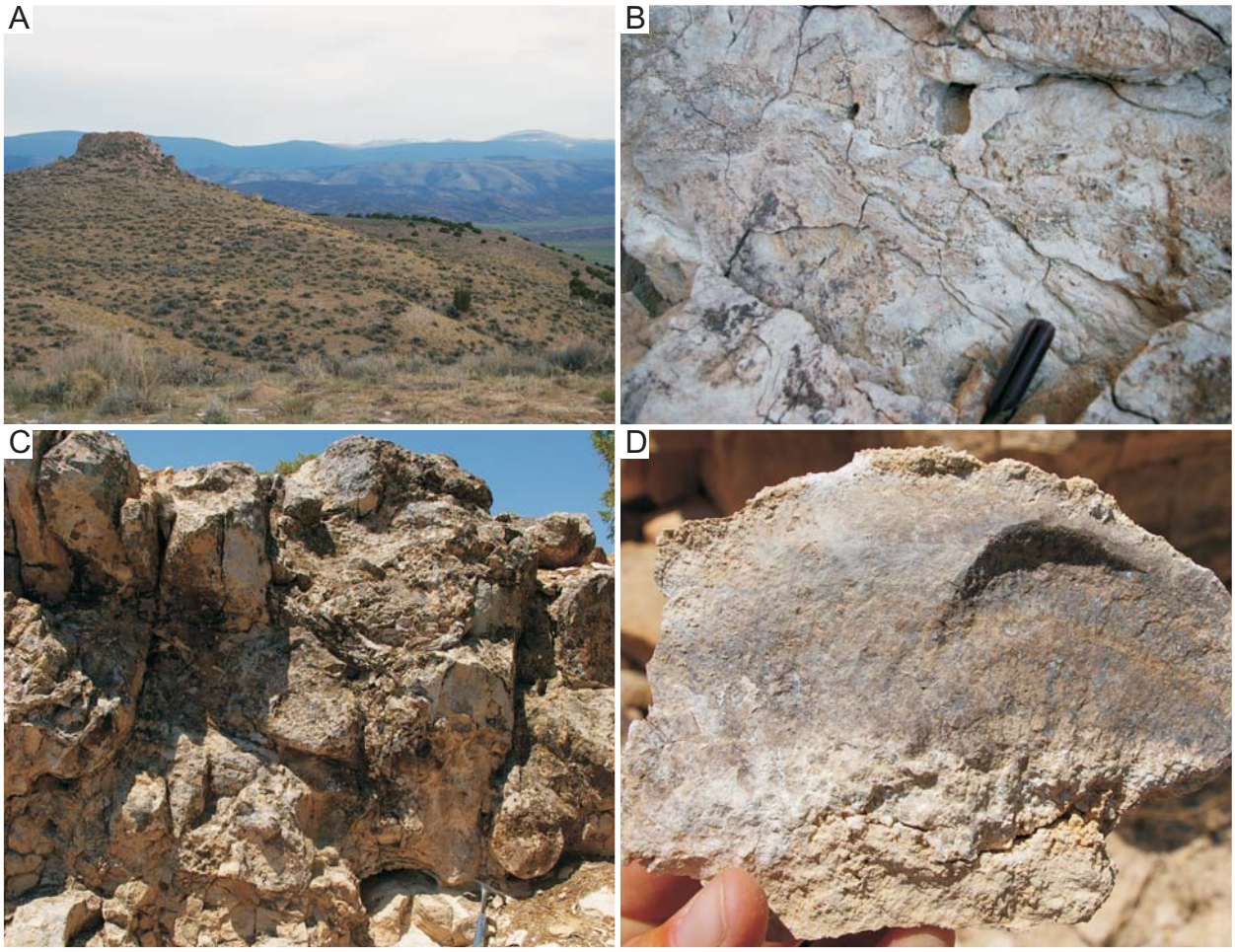


**Fig. 5.4.6.** The "Laney" mounds on the west side of Flaming Gorge Reservoir. **(A)** View towards south of very large mound in the Laney Member with the Uinta Mountains in background. **(B)** Laminated texture of the mound. **(C)** Horizon of small mounds lower in the section, showing coated logs (lower right). **(D)** Close-up of silicified, stromatolite-coated log.

### *5.4.2. The Western Basin Margin*

One locality on the western basin margin was also investigated as part of this study. At Slate Creek, adjacent to the thrust belt, siliciclastic sediments including quartzose and lithic sandstones sourced from the west and northeast represent: 1) deltaic depositional environments (Farson Tongue); 2) fluvio-deltaic or delta-plain environments (New Fork Tongue or "Alkali Creek Member" of the Wasatch Formation; M'Gonigle and Dover, 1992; Roehler, 1992a); and 3) fluvial environments. Carbonates of the Wilkins Peak Member represent sublittoral lacustrine and lake margin environments. The Wilkins Peak Member in this area unconformably overlies the green mudstones and channel sandstones of the lower New Fork Tongue with a basal conglomerate containing pebble-sized clasts of laminated stromatolitic beds, clasts of digitate travertine, and other carbonate clasts (Figs. 5.4.7, 5.4.8A). Light brown shales, kerogen-rich dark brown oil shales, grey dolomitic mudstones, and evaporite horizons (?pirsonnite; T. Lowenstein, pers. comm., 2010) are present above the conglomerate at the base. The lacustrine

**Fig. 5.4.7.** (Next page) A measured section at Slate Creek, western margin, Bridger basin. Colours approximate actual colour of rocks in the field. Lower star at right showing marker bed with meniscate burrows (Fig. 5.4.8B, 8C). Upper star at right showing stratigraphic position of photographs shown in Fig. 5.4.8D–F.

Slate Creek, western Bridger basin

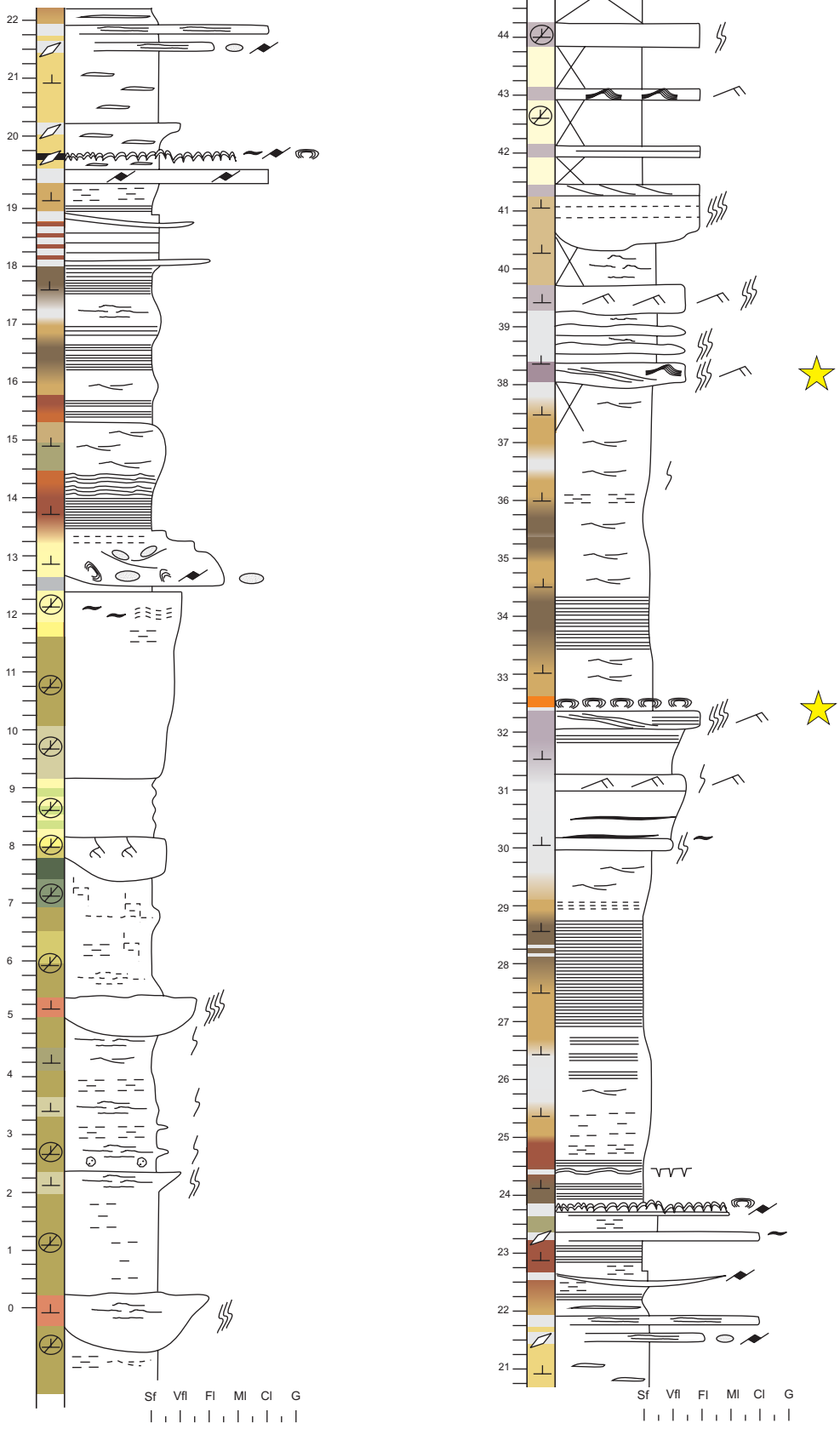

facies of the Wilkins Peak pinch out to the steeply dipping conglomerate, which represents a "progressive unconformity" with growth strata deposited in the Wilkins Peak lake (Fig. 5.4.8A). Trace fossils are abundant in the underlying channel sandstones of the New Fork Tongue, but were not found within the lacustrine shales. Higher in the section, a stratigraphically important, very fine-grained sandstone bed marks the first deposits westward of the fault conglomerate and preserves abundant meniscate backfilled burrows, as well as small vertical burrows in laterally adjacent shallow channel deposits (Fig. 5.4.8B, 8C). Fluvial and delta-plain sandstones above these lake-margin beds preserve abundant large-sized backfilled burrows that provide evidence of lower water tables (Fig. 5.4.8D–F).

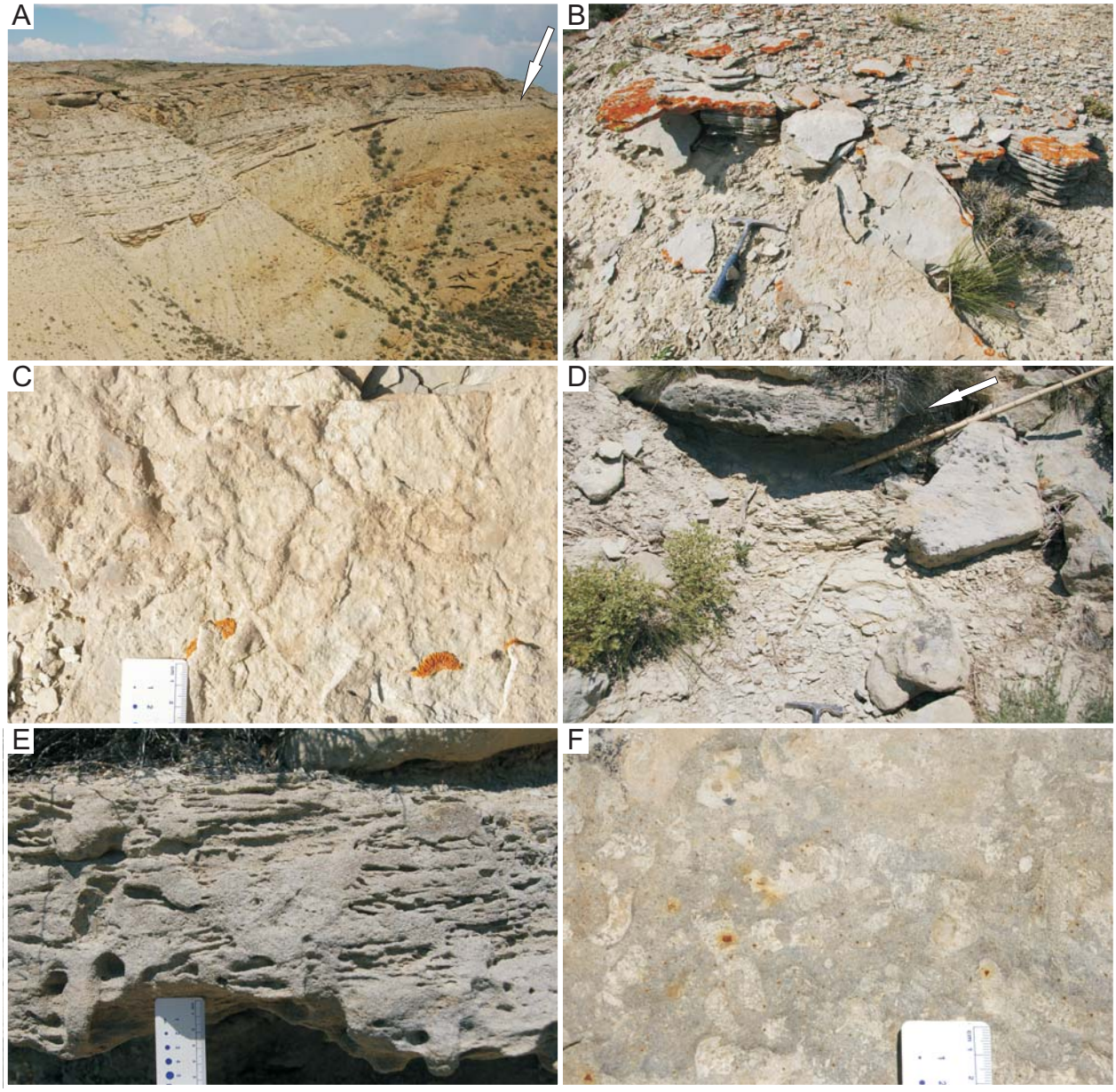


**Fig. 5.4.8.** Slate Creek on the western margin of the Bridger basin. **(A)** Growth strata of the Wilkins Peak Member overlying the Wasatch Formation, with conglomerate at base (resistant bed at left). Arrow showing the marker bed in (B–C). **(B)** The marker bed shown by arrow in (A). Note bioturbated bed in foreground. **(C)** Close-up of bioturbated horizon in (B). **(D–F)** Fluvial sandstones overlying lacustrine carbonates (arrow in D) preserve large, meniscate backfilled burrows (cf. *Taenidium barretti*). Cross-sectional view in (E), bedding plane view in (F).

# CHAPTER 6

## 6. TRACE FOSSILS OF THE WILKINS PEAK MEMBER AND CORRELATIVE UNITS, BRIDGER BASIN, WYOMING

Vertebrate and invertebrate trace fossils are abundant in siliciclastic shoreline sandstones, fluvio-deltaic sandstones, and calciclastic littoral siltstones and sandstones of the Green River Formation in both basin centre and basin margin localities, as well as within the correlative Cathedral Bluffs Member of the southern margin. Few workers have previously studied the trace fossils of the Green River Formation, although much is known of its paleontology. Paleontology in the Green River Formation, Wasatch Formation, and the Bridger Formation, Wyoming is primarily focused on fish, birds, and mammals (e.g., McGrew, 1980; Grande, 1984; Zonneveld et al., 2000a). Insect fossils are common in lacustrine carbonates, and gastropods and bivalves are preserved mainly in nearshore and shoreline sandstones and siltstones of freshwater lacustrine deposits (e.g., Wilson, 1978; Hanley, 1988). Previous work on trace fossils in the Green River Formation of Wyoming, Utah, and Colorado comprises a small set of references (Erickson, 1967; Moussa, 1968, 1970; D'Alessandro et al., 1987; Greben and Lockley, 1992; Foster, 2001; Jennings et al., 2002; Hasiotis et al., 2003; Lamond and Tapanila, 2003; Bohacs et al., 2007a), and occasional passing remarks in geology-focused papers (e.g., Roehler, 1988). Bohacs et al. (2007a) used insect and vertebrate traces to make inferences about the paleogroundwater table and lake-level in different lake-types of the greater Green River basin, represented by the Tipton, Wilkins Peak, and Laney Members.

Trace fossils preserved in the Wilkins Peak Member (underfilled lake-type) in the Bridger Basin of Wyoming are described and interpreted in this chapter. As described in Chapter 5, lithofacies of the Wilkins Peak Member can be grouped into associations that partly reflect their position within the basin (e.g., bedded evaporites, arkosic sandstones sourced from the southeast). Similarly, trace fossils can be grouped into assemblages that also reflect their position within the basin, due to major differences in water table depths (e.g., generally shallow in the basin centre), and the often close association between trace types and lithofacies characteristic of the basin centre. This chapter focuses on the detailed descriptions of traces in the basin centre. Due to the diversity of sedimentary environments within the basin centre, including saline lake-margins and freshwater fluvio-deltaic systems, many of the hypotheses and interpretations from the Kenya Rift Valley are applied to the examples from these depositional settings. Detailed descriptions and interpretations of the basin-margin measured sections and their trace fossils will be prepared for publication elsewhere.

### 6.1. Descriptions of the Basin Centre Trace Fossils

Several localities within the basin centre of the Bridger basin that preserve trace fossils were investigated in order to recognize the main associations between trace fossil types and their sedimentary environments. Many more localities preserve trace fossils than those that were studied, although reconnaissance of additional localities suggests that the majority of trace types, and their inclusion within the recognized trace suites, is consistent with the findings from the better studied sites. To determine their paleoenvironmental significance, several sedimentary units that preserve the traces were described in detail (Chapter 5) so that any lithofacies-related and/or environmentally related trace assemblages could be identified. Within the basin centre area of the Wilkins Peak Member, trace fossils were preserved in nine main lithofacies-related suites that represent: 1) fluctuating lake salinities; 2) transitions from subaqueous to subaerial settings in lacustrine to fluvio-deltaic and alluvial plain environments with variable water table

depths; 3) variable sedimentation rates; and 4) variable degrees of pedogenic modification. In this chapter, trace fossil descriptions (Section 6.1), their groupings into trace suites (Section 6.2), and interpretations of their significance by locality (Section 6.3) are provided. The trace fossils preserved in several examples of the basin centre carbonate facies, as well as within the A-Arkose Bed and the D-Arkose Bed in the Firehole Canyon area, are described in three tables, divided on their presence in carbonate or arkosic sandstone lithofacies. Traces preserved in carbonate facies of the Wilkins Peak Member and in the arkose beds are described in Table 6.1, with references to figures provided in the table. Traces preserved in the A-Bed are described in Table 6.2, and those preserved in the D-Bed are described in Table 6.3.

### *6.1.1. Trace Fossils from the Carbonate Facies of the Wilkins Peak Member*

The carbonate facies of the basin centre of the Wilkins Peak Member preserve trace fossils produced primarily in littoral to eulittoral depositional settings that were flooded frequently with saline lake waters and subaerially exposed (Table 6.1). Presumably, some of the traces produced in these environments were also produced in relatively freshwater pools with input from direct precipitation onto the lake-plain and/or pools remaining following sheetfloods. The localities investigated include: 1) below the D-Bed on White Mountain at Kanda (WM, K); 2) above the D-Bed on White Mountain at the #18 Crossing (WM, #18C); 3) below and above the D-Bed in Firehole Canyon (FC, D1 and D2); and 4) above the E-Bed in Firehole Canyon (FC, E2). Lacustrine carbonate and littoral facies also form a portion of the arkose beds, and their trace fossils were investigated at: 1) Middle Firehole Canyon (A-Bed) (MFC, A); and 2) Sage Creek Canyon (A-Bed) (SCC, A).

**Table 6.1.** Trace fossils preserved in the basin centre carbonate facies above and below the D-Bed and E-Bed of the Wilkins Peak Member. Localities include Firehole Canyon (FC, A; FC, D1; FC, D2; FC, E2), White Mountain (Kanda, #18 crossing), Middle Firehole Canyon (MFC, A), and Sage Creek Canyon (SCC, A).

| Fig. | Trace type; Trace suite | Ichnotaxonomy | Description | Comments | Tracemaker | Interpreted Environment | Locality | Section, metre |
|---|---|---|---|---|---|---|---|---|
| ***White Mountain, Kanda, above and below the D-arkose Bed*** | | | | | | | | |
| Fig. *6.1.1.* 1E, 1F | Vertebrate footprints (mammal) (Suite BC2B) | Indeterminate | Small possible footprint; ~4 cm total length, ~3 cm width; posterior margin rounded to slightly pointed; digits poorly impressed, but appears to be 4–5; possibly associated with two same-sized footprints (gait could be lope?); preserved in concave epirelief | Compare with small prints in D-Bed arkose at Kanda | Small mammal, possibly small creodont or carnivore | Subaerially exposed carbonate eulittoral mudflat; firm substrate | White Mountain, Kanda, below D | n/a |
| Fig. *6.1.1.* 1A–D | Vertebrate footprints (mammal) (Suite BC2B) | Indeterminate | Medium large mammal footprint with three digits and rounded posterior margin; possible fourth digit not visible; fleshy pad at base of foot; shallowly impressed; preserved as a mould in concave epirelief beneath 1 cm-thick carbonate crust; total length ~12 cm, total width unclear but ~9–10 cm; one digit preserves hoof-like impression at anterior margin | Mainly preserved in plan view; not discernable in cross-section; firm substrate | Medium-large mammal, possibly rhino-like perissodactyl | Subaerially exposed carbonate eulittoral mudflat; firm substrate | White Mountain, Kanda, below D | n/a |
| Fig. *6.1.1.* 1G | Vertebrate footprints (mammal) (Suite BC2B) | Indeterminate | Medium-sized possible mammal footprint preserving four, well-separated, rounded digit impressions; total width ~7 cm; metatarsal impression not preserved | Associated with possible claw scratch marks and hoof-like impressions | Medium-sized mammal, possibly felid-like carnivore | Subaerially exposed carbonate eulittoral mudflat; firm substrate | White Mountain, Kanda, below D | n/a |
| Fig. *6.1.1.* 1G | Vertebrate footprints (mammal) (Suite BC2B) | Indeterminate | Medium-sized possible mammal footprint consisting of two, parallel, elongate impressions; length ~2.5 cm, width of both impressions ~3 cm | Associated with possible claw marks and cat-like digits | Medium-sized mammal, possibly artiodactyl | Subaerially exposed carbonate mudflat; firm substrate | White Mountain, Kanda, below D | n/a |
| Fig. *6.1.1.* 1H | Vertebrate footprints (mammal) (Suite BC2B) | Indeterminate | Large possible mammal footprint; wider than long; ~12 cm length, ~16 cm width; posterior margin rounded with small central cleft; poorly preserved but digits look well separated; preserved in concave epirelief | Shallowly impressed, but deeper than medium-sized track | Large mammal; possibly uintathere or hippo-like perissodactyl | Subaerially exposed carbonate eulittoral mudflat | White Mountain, Kanda, below D | n/a |

Note: No trace fossils were observed in the dolomitic mudstones above the D-arkose Bed at Kanda.

***Mountain #18 crossing, carbonate benches above the D-arkose Bed***

| | | | | | | | | |
|---|---|---|---|---|---|---|---|---|
| Fig. *6.1.1.* 2A, 2B, 2C | Horizontal surface trails (Suite BC2A) | cf. *Archaeonassa* isp. | Small (~3 mm diameter), unbranched, straight to curving to sinuous, horizontal surface trails preserved in concave epirelief; appear to have walls in uppermost dolomitic mud drape, but likely just due to cohesive substrate; frequently cross-cut one another; present in high densities (BPBI=5) | Traces made in drape but are impressed into underlying surface as trails; produced subaqueously | Possibly insect larvae, such as dipteran or coleopteran larvae | Very shallow subaqueous carbonate mudflat; wet but cohesive substrate | White Mountain, #18 Crossing, above D | n/a |
| Fig. *6.1.1.* 2D | Horizontal tunnels (Suite BC2A) | cf. *Planolites* isp. | Small (~2 mm diameter), unbranched, unwalled, straight to curving horizontal tunnels preserved in convex epirelief; fill same as host; appear to have been actively filled | Associated with combined flow ripple bedforms | Possibly insect larvae, such as dipteran or coleopteran larvae | Shallow subaqueous littoral to eulittoral carbonate lake-margin | White Mountain, #18 Crossing, above D | n/a |
| Fig. *6.1.1.* 2E, 2F | Horizontal burrows (Suite BC2A) | *Helminthoidichnites* isp. | Medium-sized (~4–6 mm), straight to sinuous, possible horizontal burrows preserved in convex epirelief; unclear if just desiccation cracks but sinuous pattern suggests that they are traces, or cracks formed along traces | Associated with desiccation cracks | Unknown invertebrate; possibly large insect larvae or adult | Subaerially exposed swash zone carbonate sandstone on very low gradient lake margin | White Mountain, #18 Crossing, above D | n/a |
| Fig. *6.1.1.* 2G, 2H | Simple burrows (Suite BC2A) | cf. *Planolites* isp; cf. *Fuersichnus* isp. ? | Medium-sized (3–6 mm diameter), dominantly horizontal burrows with elongate, rhomb-like morphology where traces move in and out of interbed plane; vertically oriented associated traces are circular in cross-section and are present in closely spaced pairs; fill is same as host; unknown if preserved in convex epirelief or convex hyporelief; burrow boundaries may be sharp and/or irregular | Burrows may not be made by same trace maker; rhomb-shaped morphology similar to oriented shrinkage cracks | Unknown invertebrate; possibly oligochaete? | Subaqueous muddy littoral with cohesive carbonate siltstone substrate | White Mountain, #18 Crossing, above D | n/a |
| Fig. *6.1.1.* 3A, 3B | Surface marks (Suite BC2A) | cf. *Undichna* isp. | Parallel, narrow scratch marks with external diameter of both marks from ~0.5–2 cm; scratch marks remain parallel around sharp curve, but become further apart; another example shows straight, parallel scratch marks with external diameter of ~1.2 cm | Possibly just tool marks | Medium-sized fish | Subaqueous swash zone carbonate sandstone on very low gradient lake margin | White Mountain, #18 Crossing, above D | n/a |

| | | | | | | | | |
|---|---|---|---|---|---|---|---|---|
| Fig. *6.1.1.* 3C | Surface marks (Suite BC2A) | Indeterminate; cf. *Helminthoidichnites* isp. | Irregularly sinuous surface markings preserved in concave and convex epirelief; concave central trail ~0.5–1 cm in diameter; convex, possible 'push-up' or sediment displacement ~1–1.5 cm in diameter | Appears to be locomotion trace of a small snake in wet, cohesive substrate | Possibly small snake | Subaqueous swash zone carbonate sandstone on very low gradient lake margin | White Mountain, #18 Crossing, above D | n/a |
| Fig. *6.1.1.* 3D | Vertebrate footprints (mammal) (Suite BC2B) | Indeterminate | Small possible mammal footprints; ~5 cm length, ~4 cm total width; posterior margin rounded but triangular; digits not well impressed but likely 4–5; poorly preserved; preserved as moulds in concave epirelief | Compare with small possible footprints from Kanda | Small mammal, possibly small creodont or carnivore | Very shallow to subaerially exposed marshy mudflat | White Mountain, #18 Crossing, above D | n/a |
| Fig. *6.1.1.* 3E–I | Vertebrate footprints (mammal) (Suite BC2B) | Indeterminate | Medium-sized possible mammal footprints; possibly showing elongate 'heel' impression; total length ~12 cm, total width ~9 cm; posterior margin much narrower than anterior and rounded; appears to be three, hooved digit impressions; may be present in adjacent or offset pairs | Three digits suggest hind foot of perissodactyl | Medium-sized mammal, possibly brontothere such as *Lambdotherium* | Subaerially exposed carbonate mudflat | White Mountain, #18 Crossing, above D | n/a |
| Fig. *6.1.1.* 3D, 3I | Iron-stained root marks (cf. Suite BC2B) | n/a | Sub-millimeter, circular, iron-stained marks | Only present in dolomitic mudstone facies at this locality | Marsh plants such as cattails and other reeds | Muddy, dolomitic, paludal marsh | White Mountain, #18 Crossing, above D | n/a |
| ***Firehole Canyon, above and below the D-arkose Bed*** | | | | | | | | |
| Fig. *6.1.1.* 4A, 4B | Horizontal trails and tunnels (Suite BC2A) | *Helminthoidichnites* isp. | Small (~2 mm diameter), straight to curving to looping, surface trails preserved in concave epirelief | Looping example may be *Gordia* isp. | Likely insect larvae, such as coleoptera or diptera | Eulittoral carbonate mudflat | Firehole Canyon, in float above D2 | n/a |
| Fig. *6.1.1.* 4C, 4D | Horizontal trails and tunnels (Suite BC2A) | *Helminthoidichnites* isp. | Small (~3 mm diameter), slightly sinuous surface tunnel preserved in epirelief; burrow boundaries not sharp, but distinct; fill same as host; tunnel apparently produced below upper mud drape | Could also be assigned to *Planolites* isp. | Unknown invertebrate; possibly insect larvae | Subaerially exposed carbonate lake-plain | Firehole Canyon, above D1 | e.g., FC, D1, m ~31.5 |
| Fig. *6.1.1.* 5C, 5D, 5E | Vertical burrows (Suite BC2A) | cf. *Polykladichnus* isp.; cf. *Arenicolites* isp. | Very small (~1–2 mm diameter), open burrows; orientation vertical, oblique, and horizontal; burrow boundaries sharp; unwalled/unlined; possibly some; observed in plan view only | | Invertebrate, possibly chironomid larvae or oligochaetes | Subaerially exposed carbonate eulittoral mudflat | Firehole Canyon, in float, above D2 | n/a |

| | | | | | | | | |
|---|---|---|---|---|---|---|---|---|
| Fig. *6.1.1.* 5G | Vertical burrows (Suite BC2B) | *Skolithos* isp. | Small- to medium-sized (~3–4 mm diameter), open, possible vertical burrows; sharp burrow boundaries in carbonate siltstone; unwalled, unlined; observed from bedding plane only | Associated with trona fan pseudomorph, desiccation cracks, and possible vertebrate footprints | Likely insects, possibly tiger beetles or staphylinids | Subaerially exposed evaporitic mudflat | Firehole Canyon, in float above D2 | n/a |
| Fig. *6.1.1.* 5A, 5B | Simple burrows (Suite BC2A) | cf. *Palaeophycus* isp. | Small (~1.5–2 mm diameter) vertical, oblique, and horizontal burrows; burrow boundaries sharp; unlined/unwalled; fill same as host; interpreted as passively filled; unbranched; BPBI=2–3 | Associated with possible vertebrate tracks and microbial mat features (‘laminated’, irregular, desiccation polygons) | Small invertebrate, possibly chironomid larvae or oligochaetes | Subaerially exposed carbonate mudflat; intercalated with light brown mudstone | Firehole Canyon, above D2 | e.g., FC, D2, m ~19 |
| Fig. *6.1.1.* 4G | Horizontal burrows (Suite BC2A) | cf. *Planolites* isp.; cf. *Fuersichnus* isp.? | Medium-sized (~3–6 mm diameter), straight to slightly curving, dominantly horizontal burrows; burrow boundaries irregular and diameter variable; horizontal burrows appear to be moving in and out of bedding plane horizon – “terminations” are rounded to pointed | Compare with similar types at White Mountain, #18C; produced in soupy but cohesive mud | Unknown invertebrate | Littoral to lake-margin marsh carbonate siltstone | Firehole Canyon, in float above D2 | n/a |
| Fig. *6.1.1.* 4H | Horizontal tunnels and/or burrows (Suite BC2B) | cf. *Vagorichnus* isp. | Medium-sized (~5 mm diameter), branching horizontal tunnels and/or burrows; some branches smaller (~2.5 mm diameter); preserved in convex epirelief and full relief; burrows straight to gently curving to slightly sinuous; branches at several different angles; some examples of cross-cutting instead of branching | Some examples appear to be desiccation cracks, but if cracks, likely followed burrows | Likely insect larvae and adults; possibly beetles, such as heteroceridae or staphylinidae | Subaerially exposed carbonate mudflat | Firehole Canyon, above D2 | e.g., FC, D2, m ~17.5, m ~20 |
| Fig. *6.1.1.* 6C, 6D | Horizontal burrows (Suite BC2B) | None available; compare with ‘boxwork’ burrows from Lake Bogoria | Medium-large, straight to curving, branching burrows preserved as convex hypichnia; smaller diameter burrows (~6 mm diameter) branch from larger burrows (~1.2 cm diameter) without enlargement of main burrow; burrow boundaries indistinct and irregular, possibly influenced by salt efflorescence; fill same as host | | Possibly insect adult, such as beetle or cricket | Subaerially exposed carbonate mudflat | Firehole Canyon, in float, above D2 (East) | n/a |

| | | | | | | | | |
|---|---|---|---|---|---|---|---|---|
| Fig. *6.1.1.* 6E, 6F, 6G | Horizontal burrows (Suite BC2B) | None available; compare with 'boxwork' burrows from Lake Bogoria | Large, straight, branching burrows preserved in full relief on upper bedding plane; ~1–2 cm diameter of burrows, with enlarged, bioturbated areas off of main burrow and enlarged branching nodes; unwalled, unlined; fill different from host; calcareous sandstone fill appears to be passive; burrow boundaries not sharp, but distinct; may represent original horizontal surface tunnels without convex tunnel roof preserved | Host material carbonate mudstone drape with oriented shrinkage cracks | Possibly insect adult, such as beetle or cricket | Subaerially exposed carbonate mudflat | Firehole Canyon, above D1 | e.g., FC, D1, m ~31.5 |
| Fig. *6.1.1.* 6H | Backfilled burrows (Suite BC2B) | *Beaconites* isp. | Medium-sized (~6–8 mm diameter), meniscate-backfilled burrow with sharp burrow boundaries and distinct 'walled' region where meniscae do not reach burrow boundary; meniscae well-separated; preserved in full relief, observed from upper bedding plane | | Insect larvae or adults, possibly beetles | Subaerially exposed carbonate lake-plain | Firehole Canyon, above D1 | e.g., FC, D1, m ~31.5 |
| Fig. *6.1.1.* 6B | Backfilled burrows (Suite BC2B) | Indeterminate; compare with pellet-filled burrows from Lake Bogoria | Medium-sized (< 8 mm diameter), backfilled burrows with sediment aggregate fill; burrow boundaries distinct but not sharp; burrow fill slightly darker than host; preserved in full relief, observed from upper bedding plane; horizontally dominated orientation | Compare with vertical and horizontal burrows from FC, D1, m ~30 | Likely insect adults such as beetles | Subaerially exposed muddy carbonate littoral to eulittoral marsh | Firehole Canyon, above D2 | e.g., FC, D2, m ~20.8 |
| Fig. *6.1.1.* 6A | Vertical to horizontal burrows (Suite BC1) | cf. *Planolites* isp. | Medium-sized (~6–10 mm diameter), vertical and horizontal burrows; preserved in full relief; may be branched; burrow boundaries very irregular and may be indistinct; fill same as host; appears to be active backfill because fill different from host and burrows are horizontally oriented; overall bioturbated appearance; BI=2–3; depth of burrows ~8 cm | Associated with desiccation cracks, vertebrate tracks, and reed casts on upper bedding plane | Likely insect adults; possibly beetles, earwigs, or crickets | Subaerially exposed carbonate beach | Firehole Canyon, above D1 | e.g., FC, D1, m ~30.5 |
| Fig. *6.1.1.* 7A | Vertebrate footprints (mammal) (Suite BC2B) | Indeterminate | Small (~6 cm length) mammal footprint; three digits clearly impressed; from symmetry, probably had four digits; wider than long; posterior margin concave; example may possibly preserve hind foot impression with three digits as direct register on forefoot | | Unknown mammal, possibly small rhino-like perissodactyl such as *Hyracodon* | Marshy eulittoral mudflat | Firehole Canyon, in float above D2 | n/a |

| | | | | | | | | |
|---|---|---|---|---|---|---|---|---|
| Fig. *6.1.1.* 7B | Vertebrate footprints (mammal) (Suite BC2B) | Indeterminate | Small, possible mammal footprints preserved in concave epirelief; double register, with hind foot slightly ahead of front foot; tracks circular shape; ~4 cm in total length and ~4 cm total width; digits not clearly visible | Associated with possible chironomid larvae open burrows | Unknown mammal; possibly small perissodactyl such as *Heptodon* | Evaporitic littoral to eulittoral carbonate mudflat | Firehole Canyon, in float above D2 | n/a |
| Fig. *6.1.1.* 7C | Vertebrate footprints (mammal) (Suite BC2B) | Indeterminate | Small mammal footprint; overall shape circular; slightly wider than long; posterior margin very rounded; total length ~3.5 cm; total width ~4 cm; digits unclear but probably four | Associated with carbonate crust intraclasts and possibly with salt efflorescence | Small mammal; possibly small perissodactyl, such as *Heptodon* | Desiccated subaerially exposed carbonate lake-plain | Firehole Canyon, above D1 | e.g., FC, D1, m ~31.5 |
| Fig. *6.1.1.* 7D | Vertebrate footprints (mammal) (Suite BC2B) | Indeterminate | Small mammal footprint; longer than wide; ~5 cm long, ~4 cm wide; posterior margin narrower than anterior; may preserve claw marks; number of toes not clear, but likely 4 or 5 | Associated with endichnial burrows, desiccation cracks, and reed casts | Small- to medium-sized mammal; possibly a dog-like carnivore, creodont, or pantolestid | Subaerially exposed carbonate beach | Firehole Canyon, above D1 | e.g., FC, D1, m ~30.5 |
| Fig. *6.1.1.* 7E | Vertebrate footprints (mammal) (Suite BC2B) | Indeterminate | Medium-sized, elongate, possible mammal footprint; total length ~7.5 cm; total width ~6 cm; appears very baboon-like, with three to four, circular impressions anteriorly, one circular digit offset medially, and an elongate, rounded heel | May be regressive surface, capped by siliciclastic mudflat mudstone | Medium-sized mammal; possibly a primate such as *Smilodectes* | Subaerially exposed muddy littoral; orangish grey carbonate siltstone | Firehole Canyon, above D1 | e.g., FC, D1, m ~31 |
| Fig. *6.1.1.* 7F, 7G | Vertebrate footprints (mammal) (Suite BC2B) | Indeterminate | Medium-sized, circular-shaped mammal footprints preserved in concave epirelief; preserves oval-shaped metatarsal pad (wider than long) and four, widely separated, circular digit impressions; total length ~6.5 cm; total width ~6 cm; another example is ~7.5 cm in length, ~9 cm in width, with widely splayed digits | Footprints clearly impressed, but do not preserve fine details | Medium-sized mammal; possibly tillodont such as *Esthonyx*, cimolesta, condylarth, or cat-like carnivore | Subaerially exposed littoral to eulittoral marshy lake-plain | Firehole Canyon, above D1 | e.g., FC, D1, m ~31.5 |
| Fig. *6.1.1.* 7H | Vertebrate footprints (mammal) (Suite BC2B) | Indeterminate | Medium-sized mammal footprint; total length ~6 cm; total width ~5 cm; print preserves metatarsal pad impression with flat-rounded anterior margin, and elongate, forward-directed digit impressions, possibly with claws; number of digits either 4 or 5 | | Medium-sized mammal; possibly creodont, or hyaena-like mesonychid or carnivore | Subaerially exposed littoral to eulittoral marshy lake-plain, possibly with salt effloresence | Firehole Canyon, above D1 | e.g., FC, D1, m ~31.5 |

| | | | | | | | | |
|---|---|---|---|---|---|---|---|---|
| Fig. *6.1.1.* 8A | Vertebrate footprints (mammal) (Suite BC2B) | Indeterminate | Medium-sized mammal footprint; overall circular-shaped; wider than long, with broad, rounded posterior margin; four clearly impressed digits with hooves; two central digits closer together and further forward than lateral digits | May represent front foot, with four digits | Medium- to medium-large sized mammal; possibly rhino-like perissodactyl | Subaerially exposed littoral to eulittoral marshy lake-plain | Firehole Canyon, above D1 | e.g., FC, D1, m ~31.5 |
| Fig. *6.1.1.* 8B | Vertebrate footprints (mammal) (Suite BC2B) | Indeterminate | Medium-large, circular-shaped, mammal footprint preserved in concave epirelief; wider than long; posterior margin very broad and rounded; appears to be three digits, with central digit wider than slightly laterally directed outer digits; possibly hooved; total length ~10 cm; total width ~12 cm | May represent hind foot, with three digits | Unknown mammal; possibly hippo- or rhino-like perissodactyl; possibly Amynodontid like *Amynodon* | Desiccated carbonate mudflat with intraclasts of carbonate crusts on track surface | Firehole Canyon, in float above D2 | n/a |
| Fig. *6.1.1.* 8C | Vertebrate footprints (mammal) (Suite BC2B) | Indeterminate | Medium- to medium-large mammal footprint; longer than wide with rounded heel; number of digits likely 5; anterior margin wider than posterior; ~11 cm long; ~9 cm wide | May be direct register | Medium- to medium-large mammal; possibly pantolestid, condylarth, or creodont | Subaerially exposed littoral to eulittoral marshy lake-plain | Firehole Canyon, above D1 | e.g., FC, D1, m ~31.5 |
| Fig. *6.1.1.* 8D | Vertebrate footprints (mammal) (Suite BC2B) | Indeterminate | Large possible mammal footprint with rounded, bulbous digits; overall shape circular; total width ~13 cm; total length unclear, but ~12–14 cm; appears to be four widely spaced digits; posterior margin broad and very rounded | | Large mammal, possibly hippo-like perissodactyl like *Amynodon* | Subaerially exposed littoral to eulittoral marshy lake-plain | Firehole Canyon, above D1 | e.g., FC, D1, m ~31.5 |
| Fig. *6.1.1.* 8E | Vertebrate footprints (mammal) (Suite BC2B) | Indeterminate | Very large possible mammal footprint; total width < ~25 cm; total length < ~22 cm; two of digits more clearly impressed, with anterior push-up ridges; digits possibly hooved | Compare with very large footprint from Firehole Canyon, above E2 | Large mammal, possibly uintathere such as *Bathyopsis* | Subaerially exposed littoral to eulittoral marshy lake-plain | Firehole Canyon, above D1 | e.g., FC, D1, m ~31.5 |
| Fig. *6.1.1.* 8F, 8G, 8H | Vertebrate footprints (mammal) (Suite BC2B) | Indeterminate | Very large mammal footprint; total length ~32 cm, total width unknown, but ~28 cm; slightly longer than wide; two clearly impressed digits slightly triangular and may preserve hoof impressions; number of digits 4 or 5; posterior margin tapered but rounded | | Large mammal, possibly pantodont such as *Coryphodon* or uintathere such as *Bathyopsis* | Subaerially exposed littoral to eulittoral marshy lake-plain | Firehole Canyon, above D1 | e.g., FC, D1, m ~31.5 |

Note: no trace fossils were observed in the bedded evaporite facies below the D-Bed in Firehole Canyon

***Firehole Canyon, carbonate benches above E (EV-evaporite-containing bench; N-EV-bench without evaporites)***

| | | | | | | | | |
|---|---|---|---|---|---|---|---|---|
| Fig. *6.1.1.* 9A, 9B | Surface trails (Suite BC2A) | *Helminthoidichnites* isp. | Very small (~1.5–2 mm diameter), straight and gently curving surface trails preserved in concave epirelief; trails produced through carbonate mud drape, which preserves wall-like trail boundaries | Sometimes reserved in very high densities: BPBI=<6; compare with White Mountain, #18 Crossing | Likely insect larvae such as coleoptera or diptera | Littoral carbonate mudflat; preserved in grey and white dolomitic carbonate mudstones | Firehole Canyon, above E1 (N-EV), above E2 (EV, N-EV) | e.g., FC, E2, m ~37, m ~40 |
| Fig. *6.1.1.* 9C | Surface trails or tunnels (Suite BC2A) | *Helminthoidichnites* isp. | Small (~3–4 mm diameter), straight to sinuous surface trails preserved in concave and convex epirelief; may dictate orientation of desiccation cracks; some examples branched, probably false branching | Associated with vertebrate footprints, desiccation cracks, and raindrop impressions | Likely insect larvae such as coleoptera | Eulittoral carbonate mudflat; also, microbial and/or evaporite crust on mudflat | Firehole Canyon, above E2 (EV, N-EV) | e.g., FC, E2, m ~36.5, m ~40 |
| Fig. *6.1.1.* 9D | Horizontal tunnels (Suite BC2A) | cf. *Labyrintichnus* isp. | Small (~2.5 mm diameter), possible horizontal tunnel; preserved in concave epichnia in possible microbial/evaporite crust; trace is branched and open | Only one example; possible tunnel through microbial crust | Possible insect larvae and/or adults of coleopteran, such as Staphylinidae | Subaerially exposed microbial and/or evaporite crust in carbonate sandstone; lake-margin | Firehole Canyon, above E2 (EV) | e.g., FC, E2, m ~35.8 |
| Fig. *6.1.1.* 9E, F | Horizontal burrows (Suite BC2B) | cf. *Planolites* isp. or cf. *Thalassinoides* isp.? | Medium-sized (~4–6 mm diameter), dominantly horizontal, slightly curving, branching burrows with fill different from host (coarser); unwalled, unlined; burrow boundaries indistinct and/or poorly preserved; fill may be slightly more organic-rich than host, with small iron-stained spots; likely backfilled | Appear to have been produced in soft to soupy substrate | Likely insect adults such as coleoptera or orthoptera (crickets) | Subaerially exposed eulittoral very fine-grained mudflat with saturated to soupy substrate | Firehole Canyon, above E2 (EV) | e.g., FC, E2, m ~35.5 |
| Fig. *6.1.1.* 10A | Vertebrate footprints (mammal) (Suite BC2B) | Indeterminate | Small vertebrate footprint preserved as mould in concave epirelief; overall shape is circular with wide, rounded posterior margin; digits not clear but appear to be 3–4; overall length ~4 cm; overall width ~4 cm | | Unknown mammal; possibly small brontothere such as *Heptodon* | Eulittoral carbonate mudflat | Firehole Canyon, above E2 (N-EV) | e.g., FC, E2, m ~40 |
| Fig. *6.1.1.* 10B | Vertebrate footprints (mammal) (Suite BC2B) | Indeterminate | Small vertebrate footprints preserved in carbonate siltstone with remnants of subaerially exposed crusts with carbonate intraclasts | Associated with small surface trails preserved in | Mammals | Littoral to eulittoral carbonate mudflat; may be | Firehole Canyon, above E1 (N-EV) | n/a |

| | | | | | | | | |
|---|---|---|---|---|---|---|---|---|
| | | | | remnants of surface crusts | | marshy | | |
| Fig. *6.1.1.* 10C | Vertebrate footprints (mammal) (Suite BC2B) | Indeterminate | Medium-sized vertebrate footprint preserved as a mould in concave epirelief; overall shape is wider anteriorly with elongate, rounded heel; much wider anteriorly than in posterior half; total length ~9 cm, total width ~6 cm; width at heel ~4 cm; number of digits not clear, possibly 3–4; has 'ball'-like feature on human-like plantigrade track | Compare with elongate track from #18 Crossing | Unknown mammal; possibly perissodactyl brontothere such as *Lambdotherium* | Eulittoral carbonate mudflat | Firehole Canyon, above E2 (N-EV) | e.g., FC, E2, m ~40 |
| Fig. *6.1.1.* 10D | Vertebrate footprints (mammal) (Suite BC2B) | Indeterminate | Very large, overall circular shaped, possible vertebrate footprint; slightly wider than long; total width ~25 cm, total length ~22 cm; broad, plantigrade print; digits not clearly preserved but appear to be 4 (possibly 5); digits likely hooved | ?Compare with WP higher in section from Eagle? | Unknown large mammal; possibly pantodont like *Coryphodon*, uintathere like *Bathyopsis*, or large hippo-like perissodactyl | Desiccated, evaporitic, eulittoral carbonate mudflat | Firehole Canyon, in float above D2, likely from E2 (EV) | FC, E2, likely from m ~36 |



***"White Stripe" carbonate unit within the D-arkose Bed at Firehole Canyon (note: the "white stripe" is not present within the D-Bed on White Mountain)***

Note: No trace fossils were observed within the 'white stripe' carbonate unit within Section D1; this unit is not exposed in Section D2

***"White Stripe" carbonate unit within the A-arkose Bed at Middle Firehole Canyon, Firehole Canyon, and Sage Creek Canyon***

| | | | | | | | | |
|---|---|---|---|---|---|---|---|---|
| Fig. *6.1.1.* 12B | Horizontal trails (Suite BC2A) | cf. *Helminthoidichnites* isp. | Small (~3 mm diameter), possible surface trails; preserved in concave epirelief; curving to sinuous; burrow boundaries distinct but appear collapsed | If trails, produced in wet, cohesive substrate | Unknown invertebrate; possibly insect larvae | Occasionally subaerially exposed littoral lacustrine | Middle Firehole Canyon | e.g., MFC, m~4.4 |
| Fig. *6.1.1.* 12F | Surface traces (Suite BC2A) | cf. *Labyrintichnus* isp. | Small (~2–3 mm diameter), branched, possible burrow preserved in concave epirelief; open; burrow boundaries sharp but not straight | Compare with similar trace above E2, Fig. 9D | Unknown invertebrate; possibly insect larvae | Occasionally subaerially exposed littoral lacustrine | Middle Firehole Canyon | e.g., MFC, m~4.4 |
| Fig. *6.1.1.* 11A–D, 11F | Horizontal burrows (Suite BC1) | cf. *Palaeophcys* isp.<br>cf. *Taenidium* isp. | Small (~3–4 mm diameter) burrows oriented mainly vertically, but also obliquely and horizontally; preserved in full relief; unwalled/unlined; burrow boundaries distinct; burrows appear to be originating in calcareous sandstone lenses or wavy-beds and burrowing into organic-rich muds; fill is calcareous sandstone; appear meniscate backfilled | Probably same traces as *Planolites* isp. from Firehole Canyon (N) | Unknown invertebrate; possibly oligochaete or semi-aquatic to aquatic insect | Occasionally subaerially exposed littoral lacustrine with organic-rich muds | Middle Firehole Canyon | e.g., MFC, m ~4.2<br>e.g., SCC, m ~4 |

| | | | | | | | | |
|---|---|---|---|---|---|---|---|---|
| Fig. *6.1.1.* 11E | Simple burrows (Suite BC2A) | *Planolites* isp. | Small (~3 mm diameter), simple burrows preserved in convex epirelief in carbonate sandstone beds interbedded with light brown mudstone; unwalled/unlined; burrow boundaries distinct but not sharp; fill same as host | Preserved in carbonate sandstone towards top of white stripe unit | Unknown invertebrate; possibly oligochaete or insect | Occasionally subaerially exposed littoral lacustrine | Firehole Canyon (N) | e.g., cf. FC, m ~1.8 |
| Fig. *6.1.1.* 12A, 12C, 12D, 12G | Horizontal traces (Suite BC2A; cf. Suite BC7) | Indeterminate surface bioturbation cf. *Beaconites* isp. | Medium to large (~6 mm to ~1.2 cm in diameter), dominantly horizontal traces; preserved in epirelief; trace margins not sharp or distinct, but backfill-like internal structure shows disruption of sediment; some examples show almost meniscate backfill; curving to looping to just general bioturbation of surface layer | Substrate not desiccated; substrate soupy when traces produced | Possibly adult insect; possibly detritus-feeder; possibly gastropod | Occasionally subaerially exposed littoral lacustrine | Middle Firehole Canyon | e.g., MFC, m ~4.4 |
| Fig. *6.1.1.* 12E | Vertebrate footprints (bird) | Indeterminate | Possible shorebird footprints preserved in concave epirelief; if so, preserve claw impressions; total length ~2 cm | Produced in soupy substrate | Small shorebird | Occasionally subaerially exposed littoral lacustrine | Middle Firehole Canyon | e.g., MFC, m ~4.4 |

## Figure captions for the photographic plates, Section 6.1.1.

**Fig. 6.1.1.1.** Animal trace fossils in carbonate facies below the D-Bed on White Mountain, Kanda (Suite BC2B). **(A–C)** Relatively well preserved, shallowly impressed medium-sized mammal footprint with remnant of overlying crust preserved. **(D)** Close-up of the surface texture of crust shown in (A–C). **(E)** Possible vertebrate footprints (arrows) of small mammal. **(F)** Close-up of lowermost track shown in (E). **(G)** Possible poorly preserved vertebrate footprints (arrows). **(H)** Possible large vertebrate footprint. Note rounded posterior margin of impression at lower left.

**Fig. 6.1.1.2.** Animal trace fossils in carbonate facies above the D-Bed on White Mountain, #18 Crossing (Suite BC2A). **(A–C)** High density surface trails preserved on upper bedding plane of carbonate siltstone. Note remnants of white crust in (C). **(D)** Surface trails and horizontal burrow (arrow) on surface preserving unidirectional ripple bedforms and grey mudstone crust. **(E)** Meandering horizontal burrow at centre, possibly controlling mud-crack morphology. **(F)** Gently curving horizontal burrows. **(G–H)** High density burrows (cf. *Planolites*?) on upper bedding planes of carbonate siltstone.

**Fig. 6.1.1.3.** Animal trace fossils in carbonate facies above the D-Bed on White Mountain, #18 Crossing (Suite BC2). **(A)** Possible fish swimming trace (arrow). Note sharp bend in trace, with grooves more widely spaced around bend (arrow). **(B)** Possible fish swimming trace or tool marks? **(C)** Large sinuous surface trace, possibly produced by a snake. **(D)** Small mammal footprints (centre of photograph) in structureless siltstone with red iron-stained possible root marks. **(E)** Medium-large mammal footprints (arrows) with wide anterior portion. Gait is possibly a lope. **(F)** Close-up of mammal track shown at lower left in (E). **(G)** Close-up of shallowly impressed mammal track onto surface with flat-lying carbonate crust clasts. **(H–I)** Medium-large possible mammal footprints (side by side in centres of photographs; lope?).

**Fig. 6.1.1.4.** Animal trace fossils in carbonate facies above the D-Bed in Firehole Canyon (Suite BC2A). **(A)** Surface trails (*Helminthoidichnites*) on upper bedding plane. Arrow showing loop in one of the trails (cf. *Gordia*). **(B)** Surface trails showing false branching (lower arrow) and lateral ridges (arrow at right). **(C)** Sinuous surface trail (arrow). **(D)** Slightly sinuous surface burrow. **(E)** Horizontal burrow with fill same as host. **(F)** Shallow surface trails (arrows). **(G)** Relatively high density burrows (cf. *Planolites*?). **(H)** Branched burrows preserved as positive epirelief.

**Fig. 6.1.1.5.** Animal trace fossils in carbonate facies above the D-Bed in Firehole Canyon (Suite BC2). **(A)** Very small open vertical burrows associated with possible small mammal footprint (arrow). **(B)** Very small open vertical burrows associated with crack-like polygon with linear ridges (arrow), interpreted as microbial mat features. **(C)** Close-up of very small open burrows associated with small mammal footprint. **(D)** Close-up of small open burrows. **(E)** Small open burrows (horizontal and vertical) produced in cohesive substrate. **(F)** Medium-sized open vertical burrows.

**Fig. 6.1.1.6.** Animal trace fossils in carbonate facies above the D-Bed in Firehole Canyon (Suites BC1? and BC2B). **(A)** Vertical and horizontally oriented full-relief burrows with indistinct burrow boundaries. **(B)** Large full-relief burrows with fill slightly different than host. **(C)** Large horizontal, branched surface burrows. **(D)** Close-up of node-like structure on burrow shown at left in (C). **(E)** Branched full-relief burrows with fill different from host. **(F)** Close-up of burrows in (E) showing circular cross-section of vertically oriented branch (arrow). **(G)** Close-up of burrows in (E) showing sharp burrow boundaries and fill different from host. **(H)** Meniscate-backfilled, walled burrow.

**Fig. 6.1.1.7.** Mammal footprints in carbonate facies above the D-Bed in Firehole Canyon (Suite BC2B). Outline drawings at right show interpretation of impressions (arrows show same position on photo and drawing). **(A–C)** Small mammal footprints, possibly produced by perissodactyls. **(D)** Small footprint possibly produced by a creodont or dog-like mammal. **(E)** Medium-sized footprint possibly produced by a primate. **(F–H)** Medium-sized footprints possibly produced by carnivore-like mammals.

**Fig. 6.1.1.8.** Mammal footprints in carbonate facies above the D-Bed in Firehole Canyon (Suite BC2B). Outline drawings at right show interpretation of impressions (arrows show same position on photo and drawing). **(A–B)** Medium-sized footprints possibly produced by perissodactyls. **(C)** Medium-large mammal footprint. **(D)** Large mammal footprint possibly produced by hippo-like perissodactyl. **(E–H)** Very large mammal footprints possibly produced by uintatheres. (G) Close-up of digit impressions in (F). (H) Close-up of posterior margin in (F).

**Fig. 6.1.1.9.** Animal trace fossils in carbonate facies above the E-Bed in Firehole Canyon (Suite BC2). **(A–B)** High density surface trails. Sharp burrow boundaries in (B) suggest soupy, cohesive substrate. **(C)** Surface trails that may dictate morphology of desiccation cracks. **(D)** Branched, open surface tunnel (arrow at right) on surface with bubble-like texture and sodium-carbonate evaporite pseuodomorphs (arrow at left). **(E–F)** High density branched burrows with fill different from host.

**Fig. 6.1.1.10.** Mammal footprints in carbonate facies above the E-Bed in Firehole Canyon (Suite BC2B). Outline drawings at right show interpretation of impressions (arrows show same position on photo and drawing). **(A–B)** Small footprints possibly produced by perissodactyls. **(C)** Medium-sized footprint possibly produced by a perissodactyl. **(D)** Very large footprint possibly produced by a uintathere.

**Fig. 6.1.1.11.** Animal traces in lacustrine carbonates of the "white stripe" units in the Firehole Canyon area (Suite BC1). **(A–C)** Small burrows filled with material different from host at Middle Firehole Canyon. Arrow in (C) showing circular cross-section of burrow. **(D)** Open burrows on bedding plane above bioturbated unit shown in (A–C). **(E)** Filled burrows in same facies of Firehole Canyon (N). **(F)** Small burrows (lower arrow) associated with possible desiccation cracks (upper arrow) at Sage Creek Canyon.

**Fig. 6.1.1.12.** Animal traces in carbonate facies of the "white stripe" unit at Middle Firehole Canyon (Suite Bc2). **(A)** Probable subaerial exposed surface with surface bioturbation (arrow). **(B)** Surface trails (arrow) on surface shown in (A). **(C)** Possible meniscate backfill of burrow (arrow) on surface shown in (A). **(D)** Surficial trail or burrow (arrow ) with indistinct boundaries on same surface shown in (A). **(E)** Possible bird tracks (arrows) on same surface shown in (A). **(F)** Branched open surface tunnel (arrow) on same surface shown in (A). **(G)** Surficial bioturbation (arrow). **(H)** Unusual texture (due to salt efflorescence?) on same surface shown in (A).

**Fig. 6.1.1.1.** (Next page) Animal trace fossils in carbonate facies below the D-Bed on White Mountain, Kanda (Suite BC2B). Refer to Table 6.1 for descriptions of the traces shown. See full caption above.

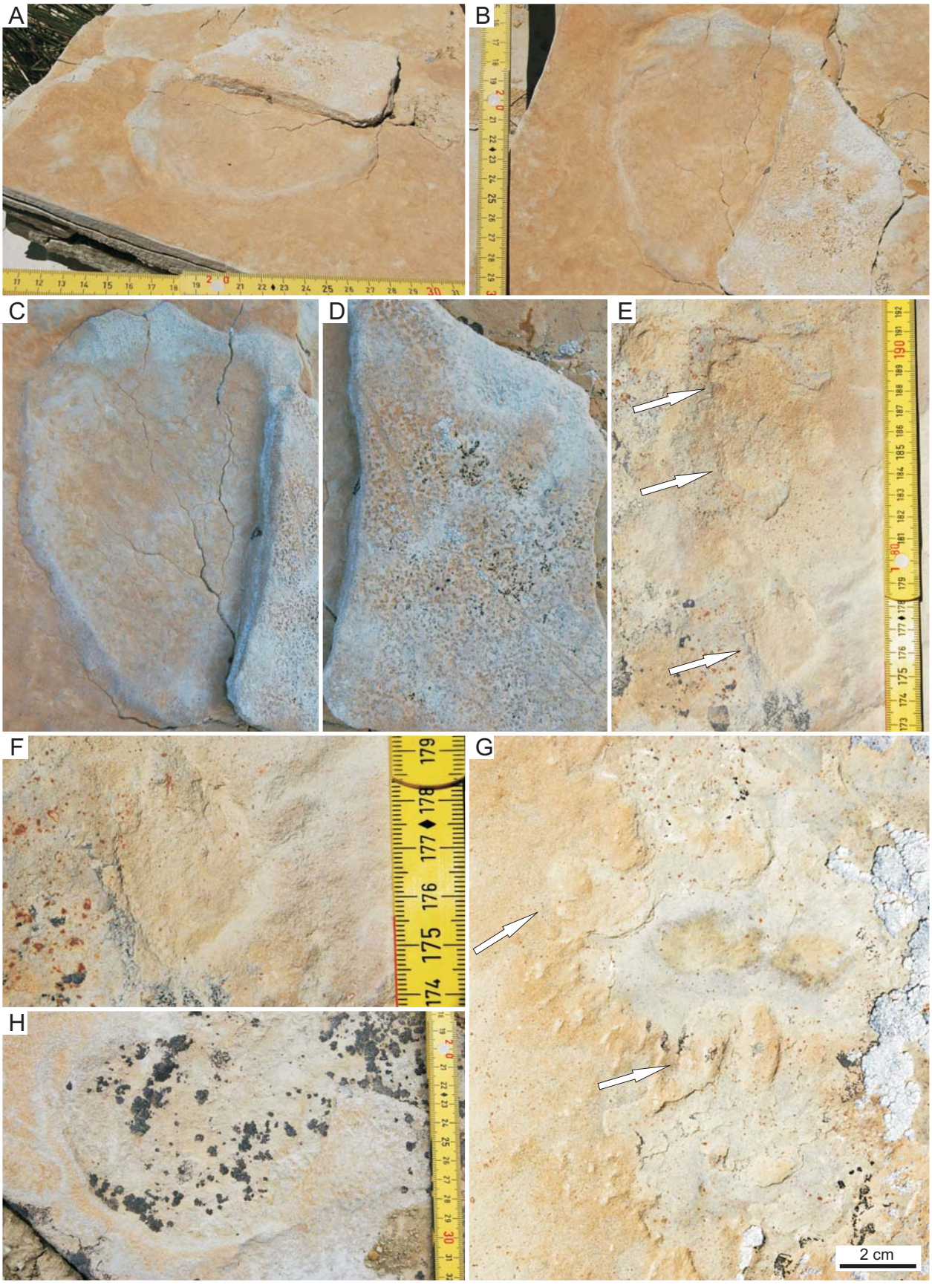
A
B
C
D
E
F
G
H
2 cm

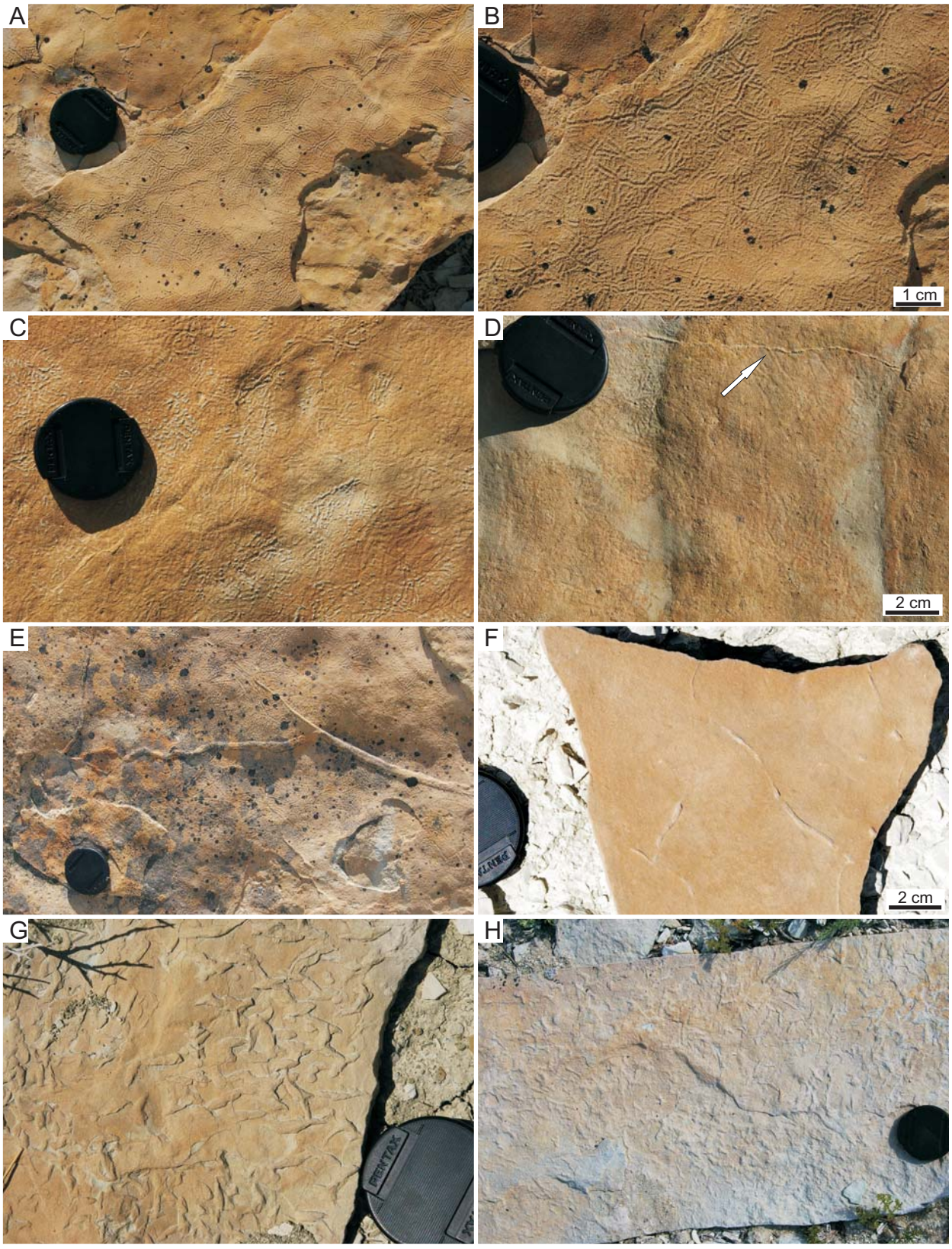


**Fig. 6.1.1.2.** Animal trace fossils in carbonate facies above the D-Bed on White Mountain, #18 Crossing (Suite BC2A). Refer to Table 6.1 for descriptions of the traces shown. See full caption above.

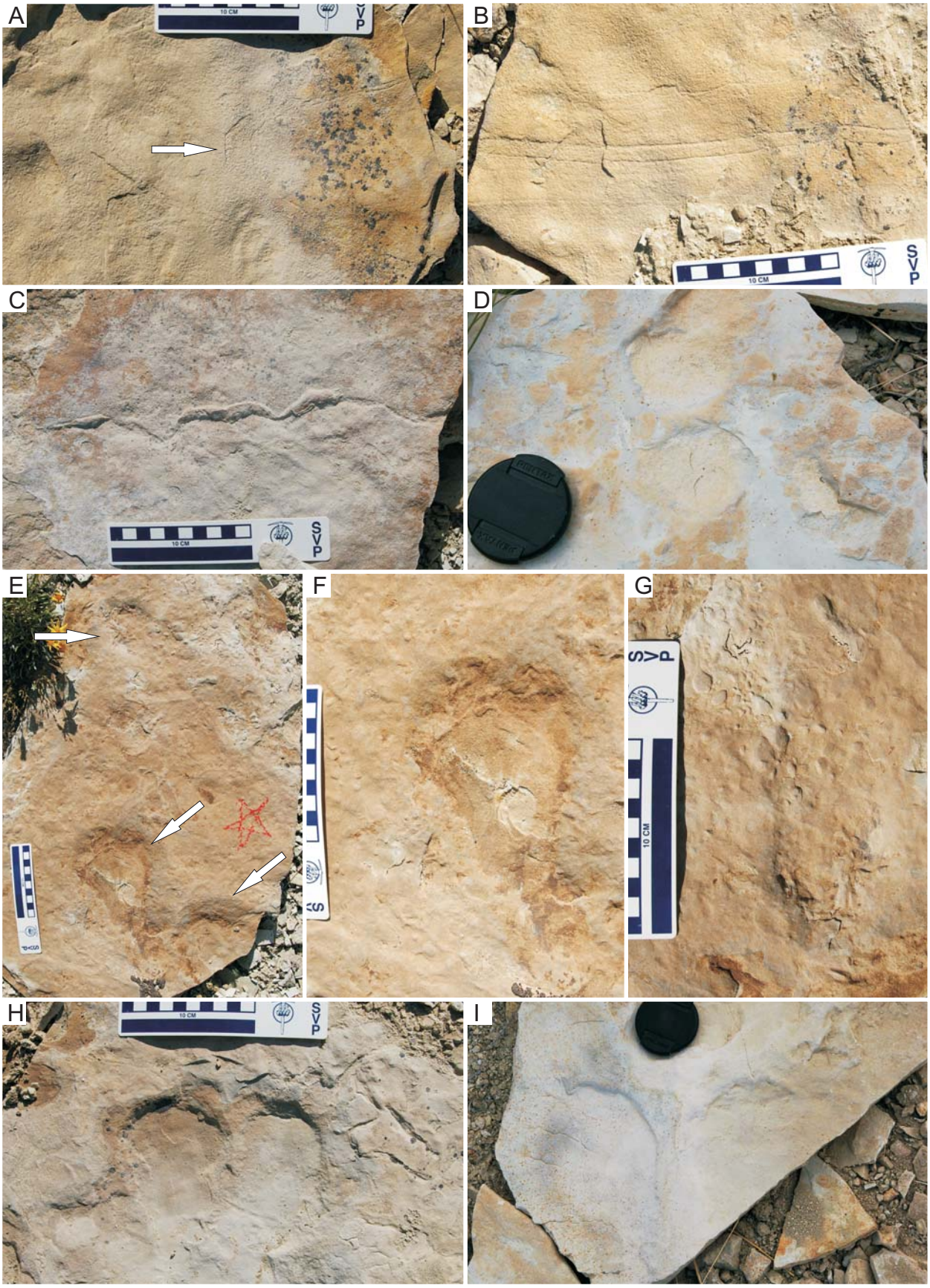
A
B
C
D
E
F
G
H
I

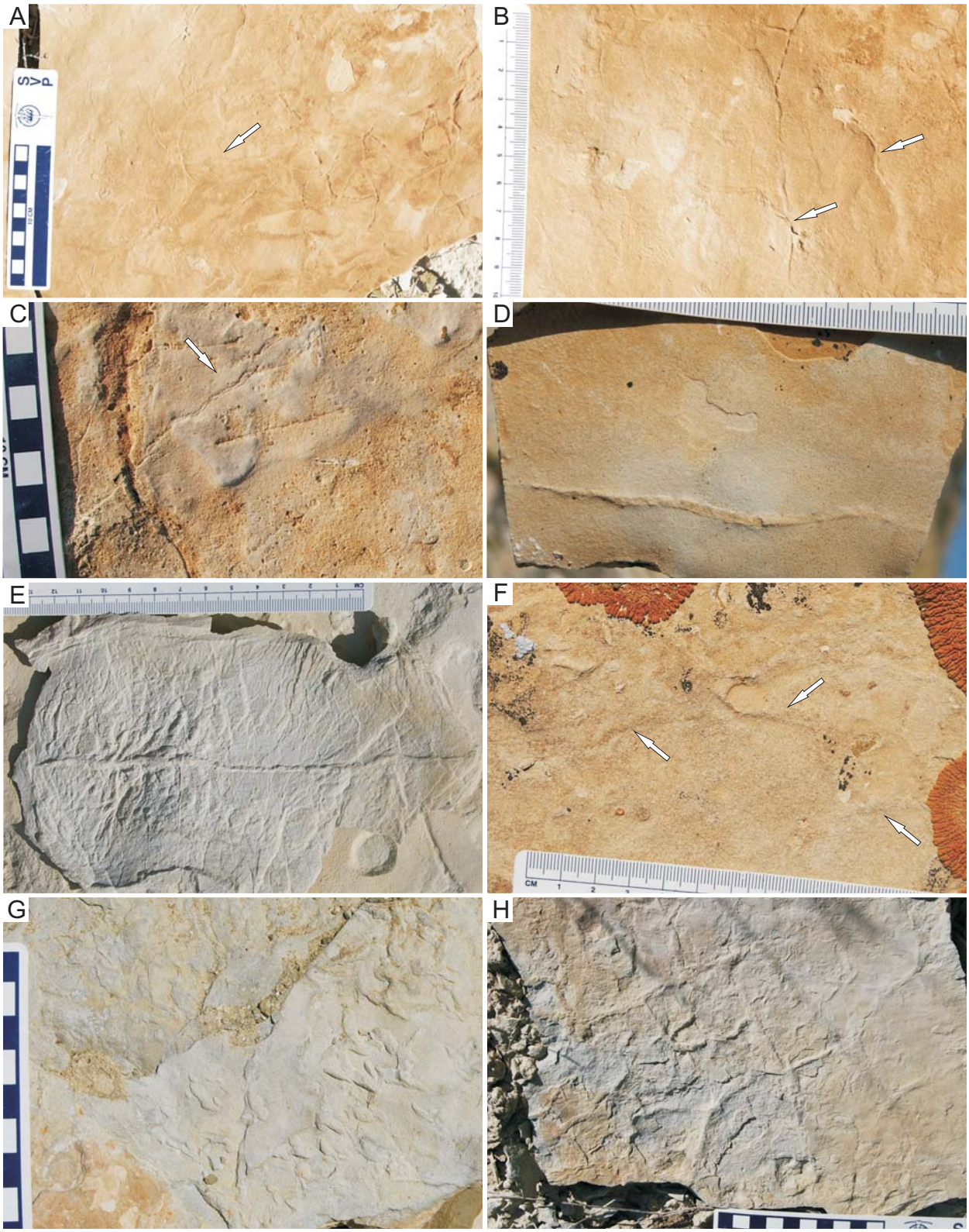


**Fig. 6.1.1.4.** Animal trace fossils in carbonate facies above the D-Bed in Firehole Canyon (Suite BC2A).

**Fig. 6.1.1.3.** (Previous page) Animal trace fossils in carbonate facies above the D-Bed on White Mountain, #18 Crossing (Suite BC2). Refer to Table 6.1 for descriptions of the traces shown. See full caption above.

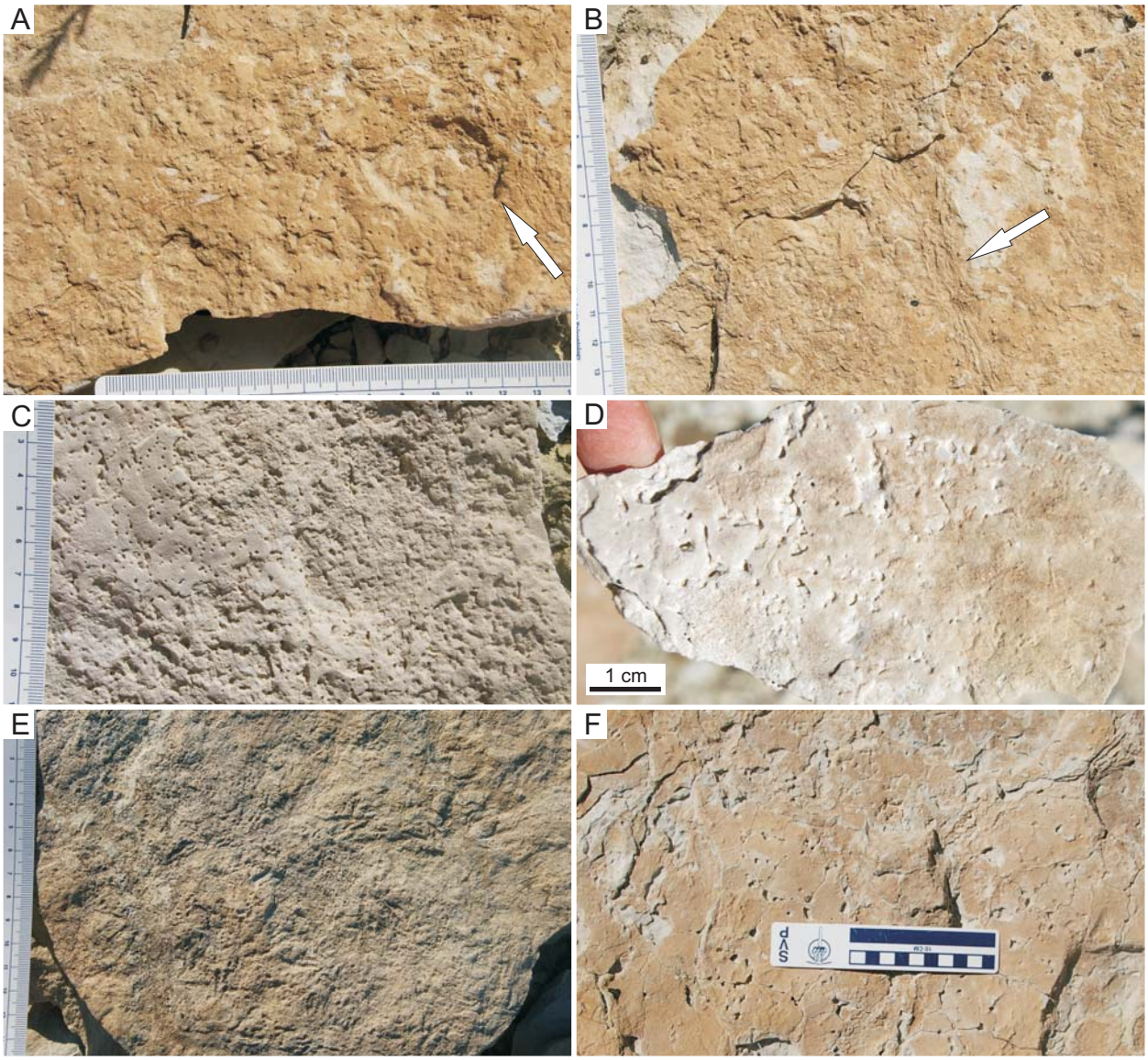


**Fig. 6.1.1.5.** Animal trace fossils in carbonate facies above the D-Bed in Firehole Canyon (Suite BC2). Refer to Table 6.1 for descriptions of traces shown. See full caption above.

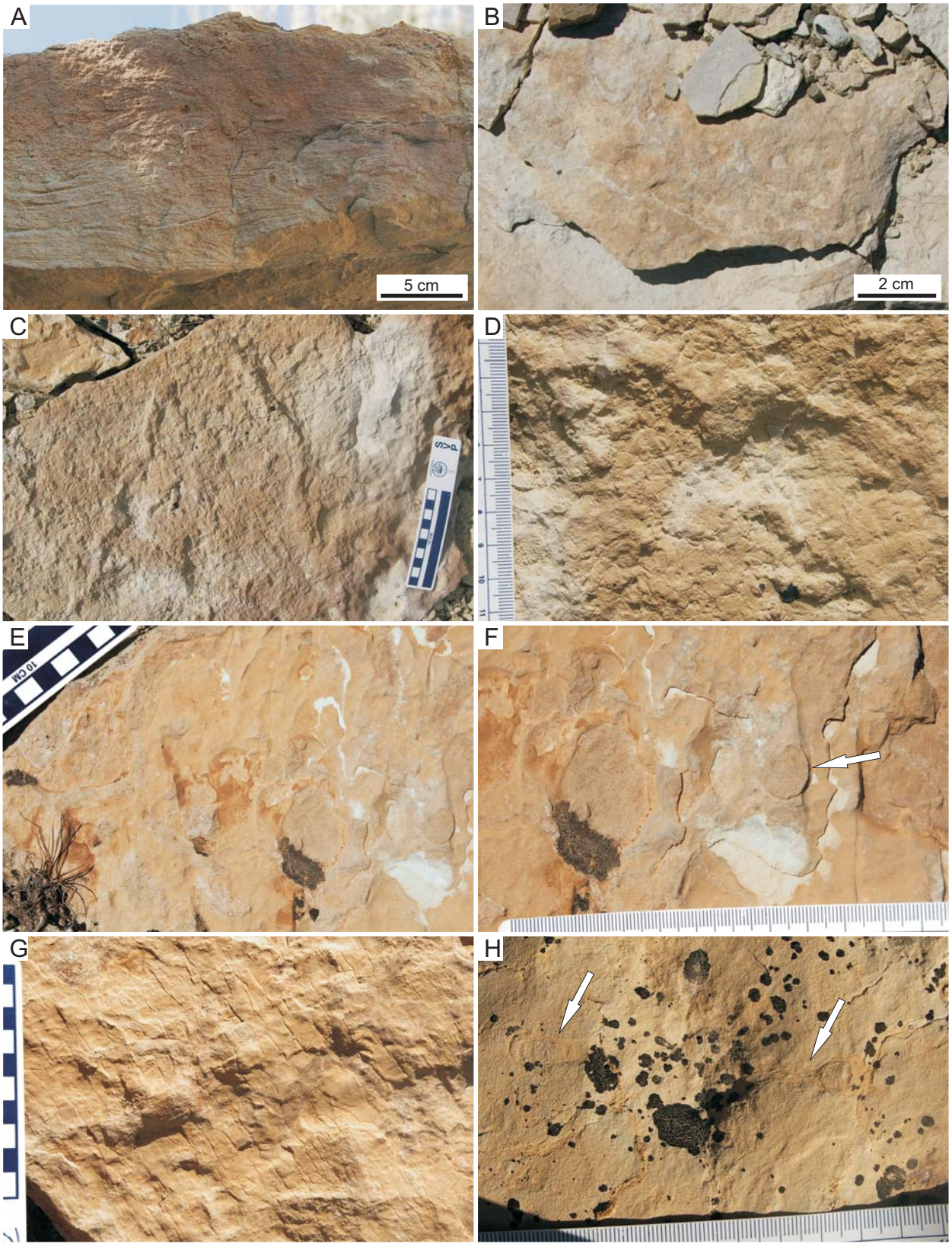


**Fig. 6.1.1.6.** Animal trace fossils in carbonate facies above the D-Bed in Firehole Canyon (Suites BC1? and BC2B). Refer to Table 6.1 for descriptions of traces shown. See full caption above.

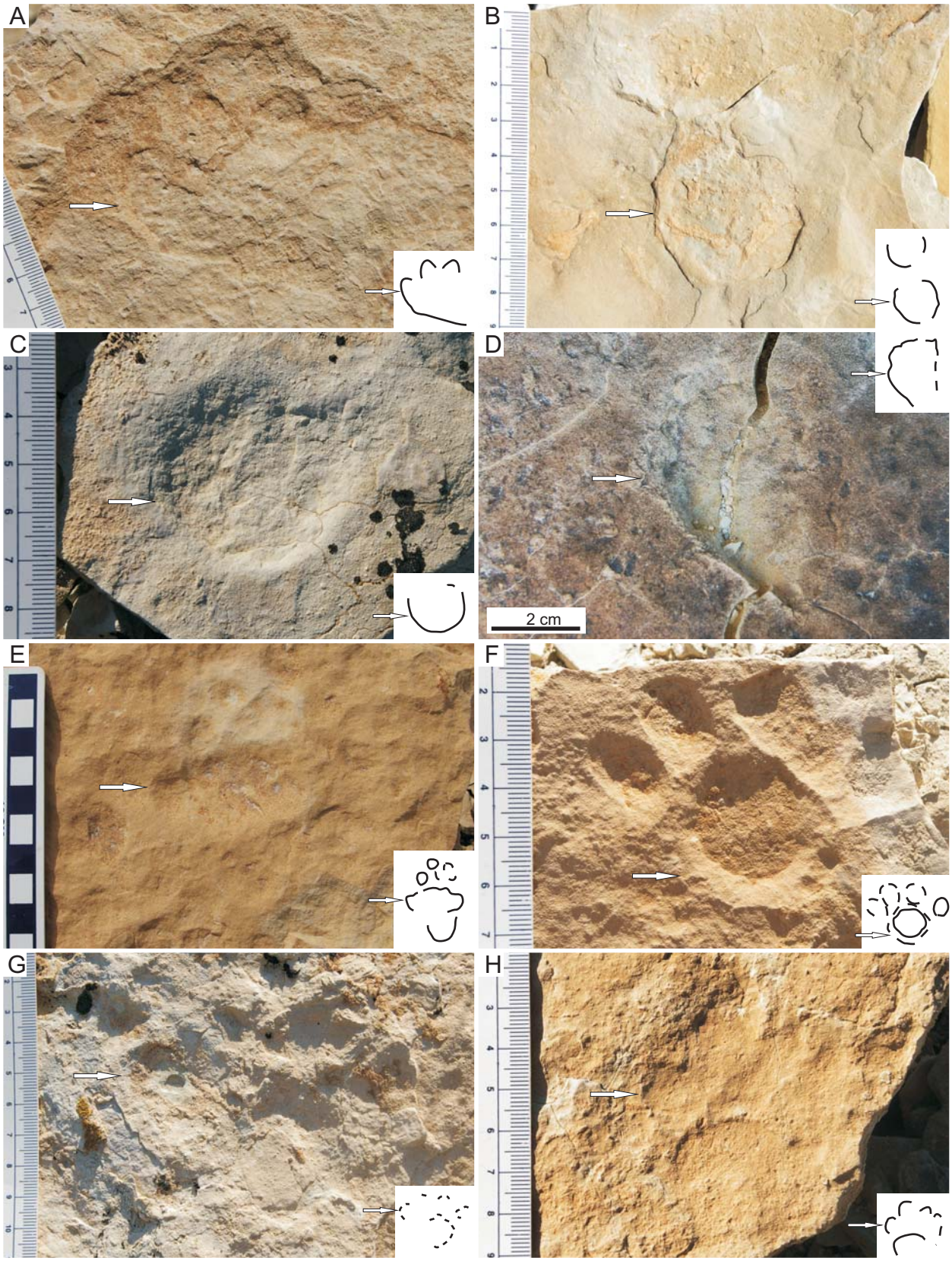


**Fig. 6.1.1.7.** Mammal footprints in carbonate facies above the D-Bed in Firehole Canyon (Suite BC2B).Refer to Table 6.1 for descriptions of traces shown. See full caption above.

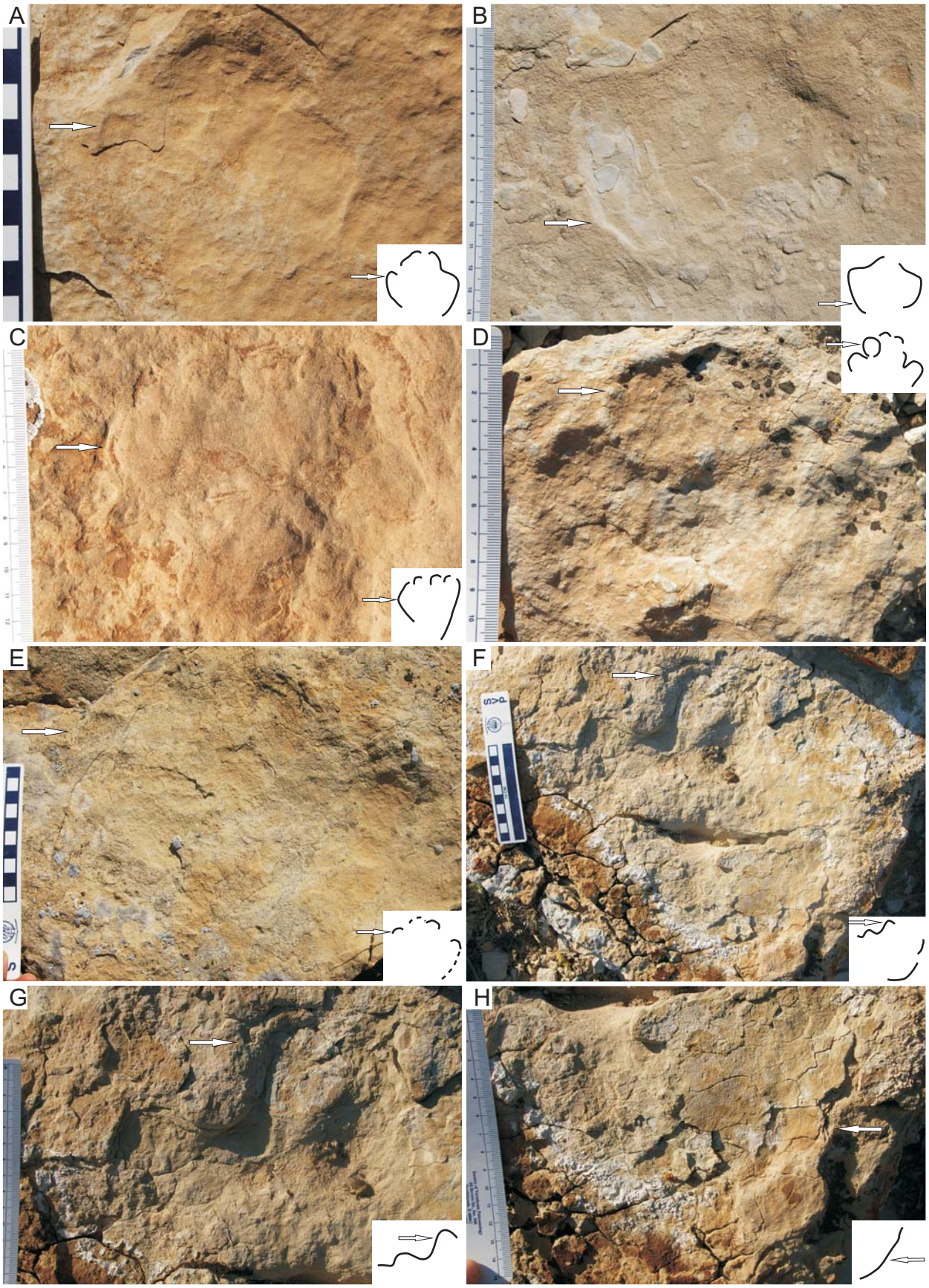
A
B
C
D
E
F
G
H

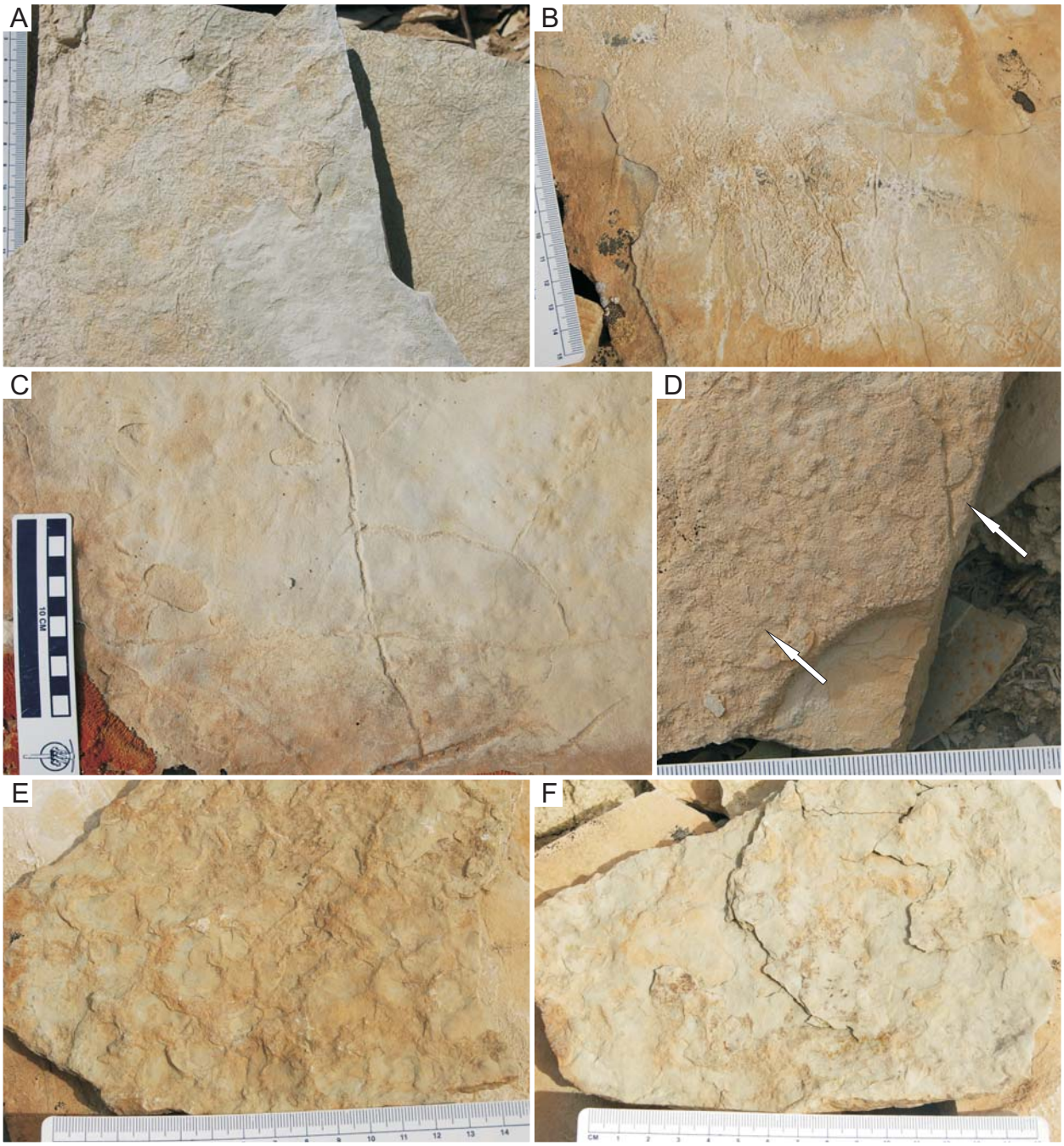


**Fig. 6.1.1.9.** Animal trace fossils in carbonate facies above the E-Bed in Firehole Canyon (Suite BC2). Refer to Table 6.1 for descriptions of traces shown. See full caption above.

**Fig. 6.1.1.8.** (Previous page) Mammal footprints in carbonate facies above the D-Bed in Firehole Canyon (Suite BC2B). Outline drawings at right show interpretation of impressions (arrows show same position on photo and drawing). Refer to Table 6.1 for descriptions of traces shown. See full caption above.

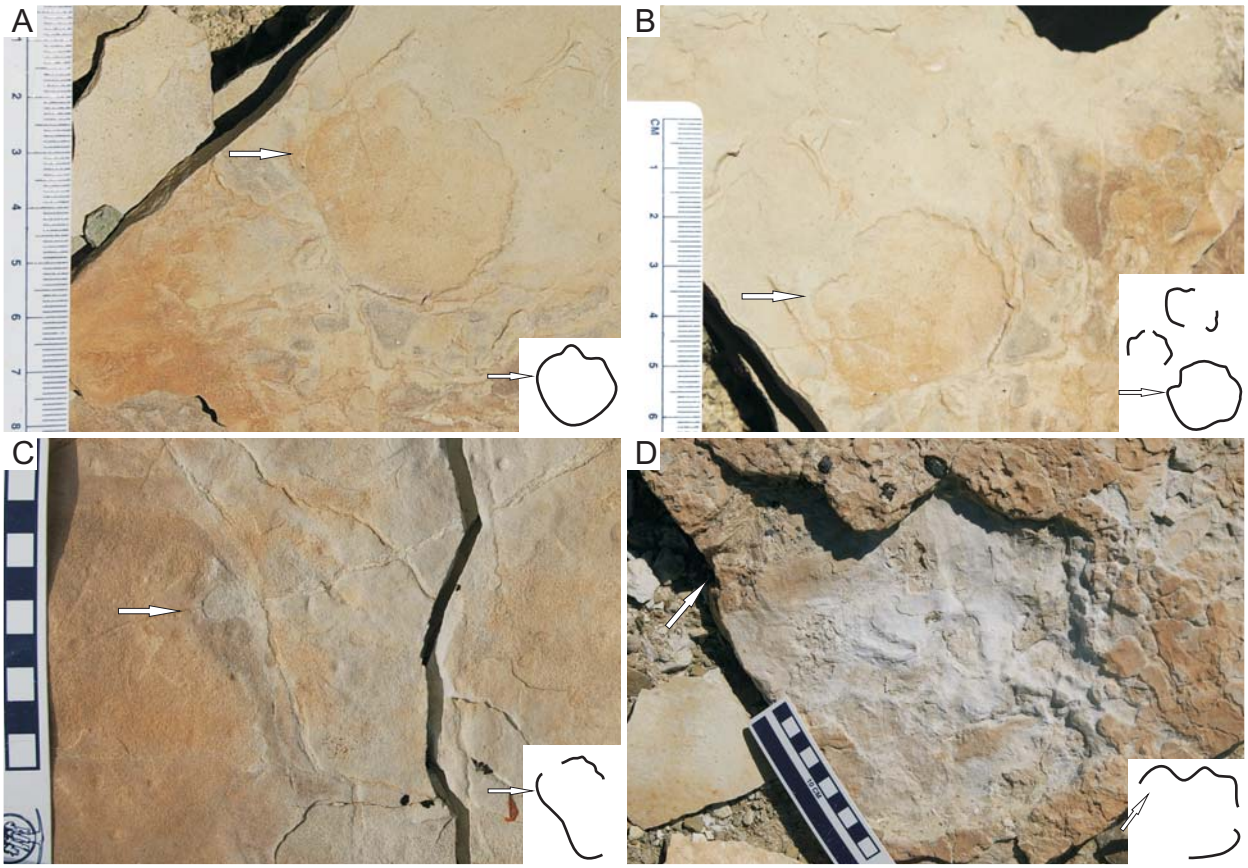


**Fig. 6.1.1.10.** Mammal footprints in carbonate facies above the E-Bed in Firehole Canyon (Suite BC2B). Outline drawings at right show interpretation of impressions (arrows show same position on photo and drawing). Refer to Table 6.1 for descriptions of traces shown. See full caption above.

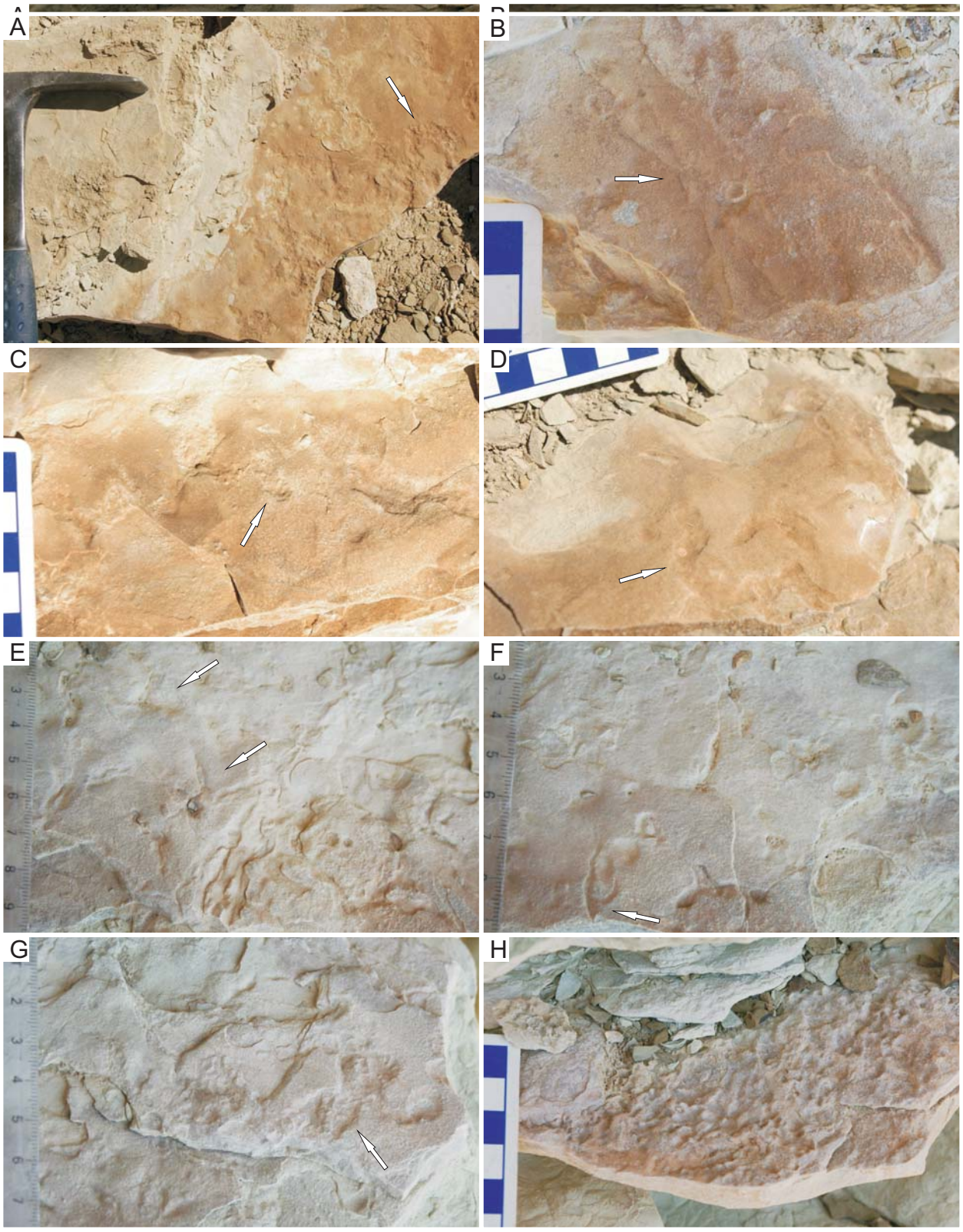


**Fig. 6.1.1.11.** Animal traces in lacustrine carbonates of the "white stripe" units in the Firehole Canyon area (Suite BC1). Refer to Table 6.1 for descriptions of traces shown. See full caption above.

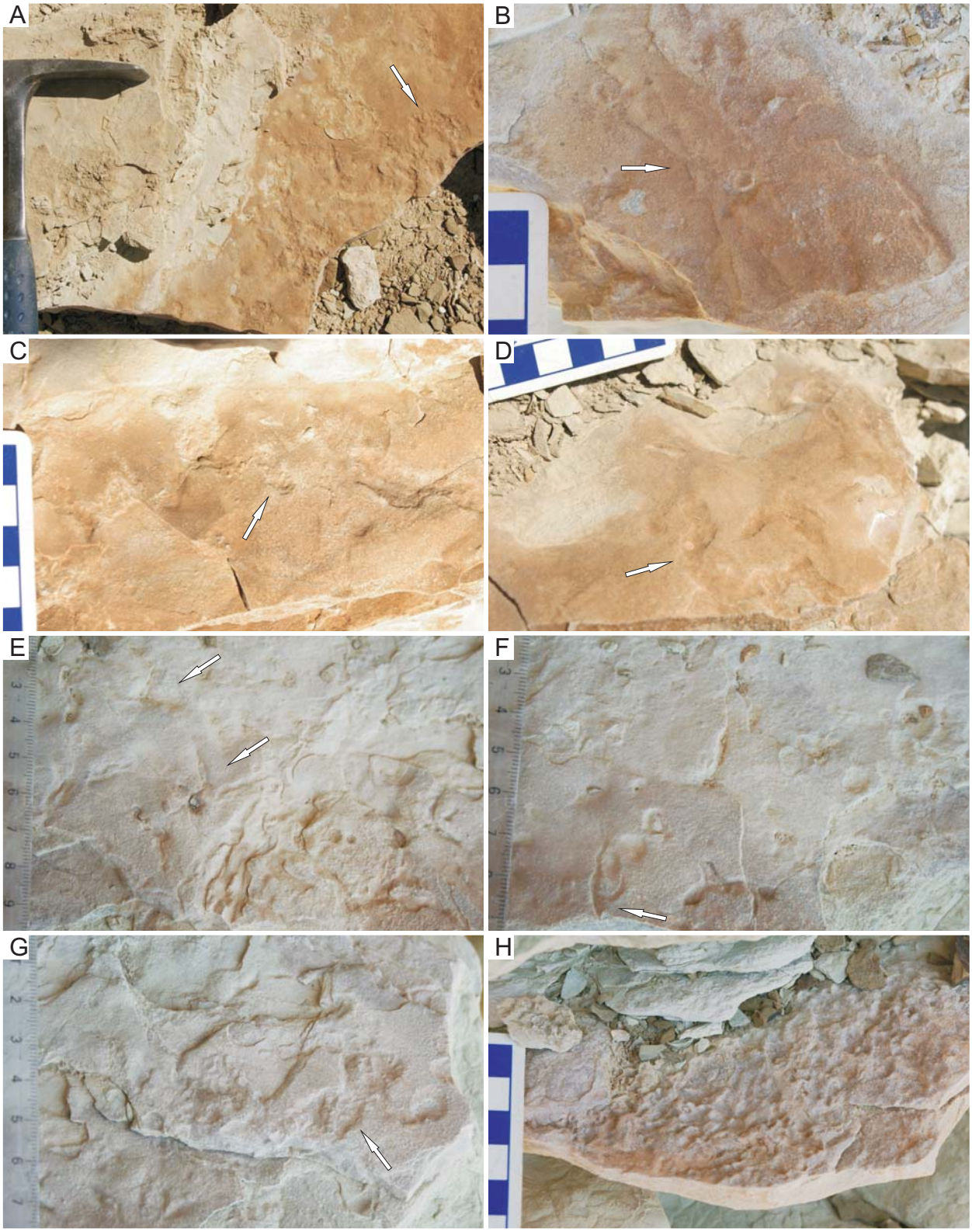


**Fig. 6.1.1.12.** Animal traces in carbonate facies of the "white stripe" unit at Middle Firehole Canyon (Suite BC2). Refer to Table 6.1 for descriptions of traces shown. See full caption above.

### *6.1.2. Trace Fossils Preserved in the Arkosic Facies of the A-Bed*

Trace fossils preserved in the A-Bed were studied at Middle Firehole Canyon (MFC), Firehole Canyon (FC), and Sage Creek Canyon (SCC). The traces were mainly produced in settings associated with fluvial input and freshwater, although some examples are interpreted as being produced in or near the carbonate lake, which may have become locally fresher due to fluvial input to the lake. Some of the traces provide evidence of lower water tables towards the tops of the A-Bed, although in contrast with the basin margin, water tables appear to have been consistently higher. Traces were produced in "sub-lacustrine" subaqueous settings, subaqueous settings on the fluvio-delta plain or within channels, and in subaerially exposed substrates (Table 6.2).

**Table 6.2.** Trace fossils preserved in the siliciclastic facies of the A-Arkose Bed at Middle Firehole Canyon, Firehole Canyon, and Sage Creek Canyon.

| Fig. | Trace type; Trace suite | Ichnotaxonomy | Description | Comments | Tracemaker | Interpreted Environment | Localities | Section, metre |
|---|---|---|---|---|---|---|---|---|
| ***Trace Fossils in the A-Bed at Middle Firehole Canyon (divided into the "lower unit" and "upper unit", separated by carbonates of the "white stripe unit")*** | | | | | | | | |
| Fig. *6.1.2.* 5B, 5C, 7A | Simple surface trails and tunnels (Suite BC7) | cf. *Helminthoidichnites* isp. | Very small (~1–2 mm diameter), straight, unbranched, very shallow tunnels preserved in convex epirelief; also preserved as surface trails without tunnel, as concave epirelief | Cross-cut by meniscate burrows; associated with insect or arachnid scratch marks; substrate probably wet and cohesive | Insect larvae; possibly dipteran or coleopteran | Exposed ripple-laminated channel fill deposits on upper delta-plain | Middle Firehole Canyon, A, upper unit | e.g., MFC, A, m ~9, m ~12.5–12.7 |
| Fig. *6.1.2.* 4B | Simple surface trails and tunnels (Suite BC7) | *Helminthoidichnites* isp. | Medium-sized (3 mm diameter), slightly curved, unbranched surface trail; sample preserved in concave epirelief on capping laminated sandstone above bioturbated, wedge-shaped sandstone | Unclear if backfilled or filled passively | Invertebrate; insect larvae or gastropod | Exposed upper surface of possible levee sandstone | Middle Firehole Canyon, A, upper unit | e.g., cf. MFC, A, m ~10.5 |
| Fig. *6.1.2.* 7B, 7C | Simple burrows (Suite BC8A) | *Planolites* isp. | Small to medium-sized (~3–4 mm diameter) unlined burrows preserved as concave epirelief; may be partly filled and preserved as convex epirelief; unwalled, unlined, but burrow boundaries distinct; burrows oriented dominantly horizontal but also have vertical component; no branching observed | Also associated with insect nest | Insects; possibly beetles, ants, or termites | Subaerially exposed delta-plain | Middle Firehole Canyon, A, upper unit | e.g., MFC, A, m ~12.5–12.7 |
| Fig. *6.1.2.* 1A, 1B, 1D, 1E | Simple burrows (Suite BC1) | cf. *Planolites* isp. | Small- (~3 mm) to medium-sized (~5–6 mm) full relief burrows; unwalled, unlined; burrows in all orientations into brown siltstone; fill different from host and probably active fill | May have formed after exposure; texture appears mottled | Unknown arthropod or annelid | Exposed littoral lacustrine/carbonate mudflat | Middle Firehole Canyon, A, lower unit? | e.g., MFC, A, m ~0.5–2.5 |
| Fig. *6.1.2.* 4A, 4C, 4E, 4F | Simple burrows (Suite BC5A) | *Planolites* isp. | Medium-sized (~4–6) full relief burrows with indistinct burrow boundaries in bioturbated sandstone substrate; unwalled/unlined | Forms the softground *Planolites* ichnofabric | Unknown arthropod or annelid | Freshwater saturated sheetflood and/or levee sandstones | Middle Firehole Canyon, A, upper unit | e.g., MFC, A, m ~8; cf. MFC, A, m ~10.5 |

| | | | | | | | | |
|---|---|---|---|---|---|---|---|---|
| Fig. *6.1.2.* 7C, 7D, 7E | Backfilled burrows (Suite BC8A) | cf. *Planolites* isp. | Medium large (~7 mm diameter), unlined, unwalled, branched, backfilled burrows; preserved in concave and convex epirelief; fill not meniscate; fill material same as host, but broken into large chips; mainly horizontal, but also with vertical component; bioturbated areas along burows; burrow boundaries clear but not sharp; fill appears disorganized, not meniscate, not aggregate-filled | Moderately high diversity bioturbated surface suggests low sedimentation rate and channel abandonment | Insects; possibly beetles or crickets | Exposed channel sandstones on upper delta-plain | Middle Firehole Canyon, A, upper unit | e.g., MFC, A, m ~12.5–12.7 |
| Fig. *6.1.2.* 3H | Horizontal burrows (Suite BC5B) | *Planolites* isp. | Medium-large (~8–11 mm diameter), horizontal burrows filled with material slightly different from host; burrow boundaries not sharp and burrow widths variable; may show external ornamentation or longitudinal markings | Associated with irregular bedding (BI=2), vertical burrows, and possible bird tracks in cross-section; substrate likely wet | Probably adult insects such as beetles or crickets | Distal crevasse or sheetflood sandstones on delta-plain | Middle Firehole Canyon, A, upper unit | e.g., MFC, A, m ~8 |
| Fig. *6.1.2.* 5C, 5D | Backfilled burrows (Suite BC8A) | *Spongeliomorpha* isp.) | Horizontal, unbranched, unlined, unwalled backfilled burrows with scratch marks oriented in all directions and cutting into substrate; preserved in convex hyporelief | Preserved in clay-draped fine-grained sandstone; cohesive substrate | Insects; possibly beetles or crickets | Subaerially exposed plane-bedded sandstones (overbank) on upper delta-plain | Middle Firehole Canyon, A, upper unit | e.g., MFC, A, m ~9.5–10 |
| Fig. *6.1.2.* 7A, 7F, 7G?, 7H | Meniscate backfilled burrows (Suite BC8A) | *Taenidium barretti* | Small to medium-sized (~3–5 mm diameter), unwalled, meniscate backfilled burrows; burrow margins clear but not sharp; may show branching and cross-cutting; dominantly horizontally oriented but associated with some vertically oriented burrows | Traces likely produced after exposure of sandy substrate; cross-cut very small surface tunnels | Insect (beetle?) or oligochaete | Exposed channel sandstones on upper delta-plain | Middle Firehole Canyon, A, upper unit | e.g., MFC, A, m ~12.5–12.7 |
| Fig. *6.1.2.* 2A–D, 2F–H, 6E, 6F | Vertical burrows (Suite BC3A) | *Skolithos* ispp. | Small- and medium-sized (~1–2 mm and 3–5 mm diameter), unlined, unwalled, vertical and oblique burrows; often very long (> 1 m length); may show movement of traces upwards (escape traces) during deposition of next bed; some preserve blackish aggregate-like fill; burrow boundaries sharp; some examples are partly passively filled | May be partly escape traces; associated with climbing ripples | Arthropod; possibly tiger beetle larvae | Climbing-rippled very fine-grained arkosic sandstone representing sheetflood or broad channel deposits on lower delta-plain | Middle Firehole Canyon, A, lower unit, east of measured section | e.g., cf. MFC, A, m ~1.5–2<br>e.g., MFC, A, m ~8, m ~12 |

| | | | | | | | | |
|---|---|---|---|---|---|---|---|---|
| Fig. *6.1.2.* 6A–D | Vertical burrows (Suite BC3B) | *Skolithos* isp. | Medium-large (~6–7 mm diameter), unlined, unwalled vertical burrows; depth often shallow (~3 cm); some examples preserve blackish aggregate-like fill | Trace produced from top of point bar, likely subaerially | Arthropod such as spider or beetle (e.g., tiger beetle adults) | Point bar in shallow active stream; low angle cross-stratification | Middle Firehole Canyon, A, upper unit | e.g., MFC, A, m ~9.5–10 |
| Fig. *6.1.2.* 7A | Insect trackways (Suite BC7) | Indeterminate | Possible scratch marks from insect or arachnid; scratches clear, but not associated with trackway | | Arthropod; likely insect or arachnid | Exposed channel sandstones on upper delta-plain | Middle Firehole Canyon, A, upper unit | e.g., MFC, A, m ~12.5–12.7 |
| Fig. *6.1.2.* 1F | Full relief burrows (Suite BC1) | Indeterminate | Large (< ~4 cm diameter) branching burrow system with small (~4 mm), vertically oriented, branches; burrow fill is composed of brecciated sediment, slightly darker than host; burrow boundaries sharp and distinct, but slightly irregular | Compare with large burrow from Suite BC1 at Sage Creek Canyon | Possibly larger crustacean such as crayfish or crab? | Mudflat near freshwater channel or sheetflood sandstones | Middle Firehole Canyon, A, lower unit | e.g., MFC, A, m ~1.2 |
| Fig. *6.1.2.* 8A, 8B, 8C, 8D, 8E, 8F | Excavated insect nest (Suite BC8B) | Indeterminate | Possible insect nest, most closely resembles ant nests, but could be termite nest; excavated into sandstone; red-stained, subspherical bioturbated structure with abundant unbranched simple burrows (*Planolites* isp.); nest structure ~14 cm wide by ~8 cm high | Associated with bioturbated surface (BI=4–6), suggesting substrate stability and low sedimentation rate | Insects; possibly ants | Exposed channel sandstones on upper delta-plain | Middle Firehole Canyon, A, upper unit | e.g., MFC, A, m ~12.5–12.7 |
| Fig. *6.1.2.* 2, A, 2E, 3D?, 3F | Escape traces (Suite BC3A) | None available | ~Medium-sized escape traces associated with medium-sized (~4 mm diameter) vertical burrows; disrupted laminae are downward-directed | Directly associated with vertical burrows | Insects; possibly tiger beetle larvae | Rapid and/or renewed sheetflood, crevasse, or channel fill sedimentation on lower delta-plain | Middle Firehole A, upper and lower units | e.g., cf. MFC, A, m ~1.3<br>e.g., MFC, A, m 7.5–8 |
| Fig. *6.1.2.* 3B, 3C, 3D? | Footprints of wading birds or escape traces? (Suite BC1, Suite BC5B) | None available | Possible bird footprints preserved in cross section; sandstone laminae are displaced downwards by narrow depression; only single depressions, do not appear three-toed; depth of impressions approximately 5 cm; depressions from several horizons | Possibly escape trace of invertebrates or water escape structures | Medium-sized wading bird or shorebird | Saturated littoral to eulittoral mudflat | Middle Firehole Canyon, A, lower unit | e.g., MFC, a, m ~1.5, m ~8 |
| Fig. *6.1.2.* 3A | Vertebrate footprints (shorebirds) (Suite BC5B) | Indeterminate | Possible bird footprints preserved as casts in convex hyporelief on slightly trampled surface; digit impression straight, narrow, ~4 mm wide and ~4–5 cm long | Do not appear to be tool marks – other options? | Medium-sized shorebird or wading bird | Distal levee, crevasse splay, or sheetflood into shallow water | Middle Firehole Canyon, A, upper unit | e.g., MFC, A, m ~7.2 |

| | | | | | | | | |
|---|---|---|---|---|---|---|---|---|
| Fig. *6.1.2.* 9A, 9B, 9C, 9D | Root marks (cf. Suite BC8B; cf. Suite BC3B) | n/a | Open, bunch-shaped root marks; each ~4 mm in diameter; expanding outwards at depth of ~10 cm; mainly unbranched | Associated with insect nest in stable substrate | Unknown plants; possibly bunched-root marsh plants | Exposed channel sandstones on upper delta-plain | Middle Firehole Canyon, A, upper unit | e.g., MFC, A, m ~9.5–10, m ~12.5 |
| Fig. *6.1.2.* 9E | Root casts | n/a | Circular, white root casts; ranging in diameter from ~1 cm to 3 cm; typically with yellow-orange iron-stained 'rind' (goethite?); preserved together with iron-stained root marks | Associated with pedogenically modified greenish clastic siltstone | Unknown plants; possibly shrubs such as willows | Subaerially exposed delta-plain with high water table | Middle Firehole Canyon, A, lower and upper units | e.g., MFC, A, m ~2.8, m ~8.8, m ~10.9 |
| Fig. *6.1.2.* 9F | Iron-stained root-marks? (cf. Suites BC4, BC5) | n/a | Millimetre-sized, circular, open iron-stained marks; may be abundant in distinct horizons, where not necessarily representing roots | Associated with laminated siltstones and mudstones | Unknown plants; possibly marsh plants such as horsetails | Subaerially exposed but waterlogged lower delta-plain | Middle Firehole Canyon, A, upper unit | e.g., MFC, A, m ~5–6 |
| ***Trace Fossils in the A-Bed of Firehole Canyon (divided into the "lower unit" and "upper unit", separated by carbonates of the "white stripe unit")*** | | | | | | | | |
| Fig. *6.1.2.* 10A | Horizontal branching tunnels (Suite BC5B) | cf. *Labyrintichnus* isp. | Small (~ 2.5 mm diameter), horizontal, branching tunnels; high density in small area; cross-cut one another; preserved as positive epirelief; one example shows collapsed tunnel roof | Associated with bird tracks, microbial mat bubble texture, clay drapes, and desiccation cracks | Insect larvae and/or adults; possibly staphylinids | Ephemeral freshwater pool fed by crevasses or sheetfloods on delta-plain | Firehole Canyon, A, upper unit | e.g., FC, A, m ~12.5–14 |
| Fig. *6.1.2.* 10B | Horizontal branching tunnels (Suite BC5B) | cf. *Vagorichnus* isp. | Small (~2.5 mm diameter), horizontal burrows preserved in convex epirelief; backfilled, possibly with slightly meniscate fill; frequently cross-cutting one another, and possibly branched; fill slightly different from host | May be same type as cf. *Labyrintichnus* isp. | Insect larvae or adults, probably beetle | Ephemeral freshwater pool fed by crevasses or sheetfloods on delta-plain | Firehole Canyon, A, upper unit | e.g., FC, A, m ~12.5–14 |
| Fig. *6.1.2.* 10C, 10D | Horizontal branching tunnels (Suite BC5B) | *Vagorichnus* isp. | Medium-sized (~4–5 mm diameter), horizontal, branching tunnels preserved as concave hyporelief at base of beds; fill and lining not preserved; burrow boundaries smooth | Produced in muddy substrate, possibly subaqueous or on mudflat near shoreline | Insect larvae and/or adults; possibly staphylinids, heterocerids | Wet muddy substrates on lower delta-plain buried by waning flow sandstones (crevasse, sheetflood , or terminal distributary mouth) | Firehole Canyon, A(N), upper unit | e.g., cf. FC, A, m ~8.8 |

| | | | | | | | | |
|---|---|---|---|---|---|---|---|---|
| Fig. *6.1.2.* 12D, 12E, 12F | Full relief burrows? (cf. Suite BC3) | cf. *Planolites* isp. | Very small to small sized (1–1.5 mm and ~3 mm diameter) indistinct burrows preserved as endichnia within fine-grained arkosic sand, along bedding planes with tool marks and parting lineation, as well as within sandstone units preserving convolute and ripple cross-lamination; many examples are open holes within sandstone, others are filled with host material | If burrows, animals possibly living subaqueously and transported with bedload; if not burrows, possibly pellets or clay clasts; more abundant at bases of beds | Arthropods; possibly chironomids or other dipteran larvae; possibly oligochaetes; possibly brine shrimp | Active channels; associated with fine-grained sandstones with convolute bedding or horizontal lamination with parting lineation | Firehole Canyon, A, upper unit<br><br>Firehole Canyon, A(N), upper unit | e.g., FC, A, m ~12.5–14.3<br><br>e.g., cf. FC, A, m ~9? |
| Fig. *6.1.2.* 12A, 12B, 12C | Simple burrows (Suite BC5A) | *Planolites* isp. | Medium-sized (~4–5 mm diameter) unlined burrows preserved in full relief within very fine- to fine-grained arkosic sandstone; burrows cross-cut one another; branching not observed; typically preserved in high density fabrics; typically monospecific | Typically preserved in bioturbated beds (BI =4–6), termed *Planolites* Ichnofabric; substrate may have been soupy and/or shallow subaqueous | Unknown invertebrate; possibly oligochaetes or insect larvae | Saturated crevasse splay or levee sandstones into shallow overbank ponds | Firehole Canyon, A, upper unit | e.g., FC, A, m ~12.5–14.3 |
| Fig. *6.1.2.* 10F | ? ‘Pock mark’ traces (Suite BC5B) | none available | Small (~3 mm diameter), circular to oval-shaped, shallow depressions, typically with one margin steeper and more sharp-walled; preserved as concave epichnia; BPBI = 3 | Compare with ‘pock mark’ traces from Nasikie Engida | Arthropods; possibly dipteran adults | Ephemeral freshwater pool fed by crevasses or sheetfloods on delta-plain | Firehole Canyon, A, upper unit, in float | e.g., cf. FC, A, m ~12.5–14.3 |
| Fig. *6.1.2.*10 E | Invertebrate trackway (Suite BC5B) | cf. “Furrow-shaped traces” (Bohacs et al., 2007) | Large (~12 mm outside diameter) trackway in soupy, clay-draped substrate; medial furrow (~2–3 mm) with lateral push-up mounds; preserved in concave and convex epirelief | Shown by Bohacs et al. (2007) from Kanda, D-Bed | Probably insect adult | Ephemeral freshwater pool fed by crevasses or sheetfloods on delta-plain | Firehole Canyon, A, upper unit | e.g., FC, A, m ~12.5–14 |
| Fig. *6.1.2.* 11A–F | Footprints (shorebirds) (Suite BC5B) | Indeterminate | Three- or four-toed, medium-sized (~3 cm width, 2.5–3 cm length), unwebbed bird footprints; usually preserves hallux, directed medially; claw impressions typically preserved; preserved in concave epirelief and convex hyporelief | Possible example of shorebird ichnofacies?; associated with tool marks and desiccation cracks | Medium-sized shorebirds | Desiccated ephemeral freshwater pool fed by crevasses or sheetfloods on delta-plain | Firehole Canyon, A, upper unit | e.g., FC, A, m ~12.5–14 |
| Fig. *6.1.2.* 11G | Vertebrate footprints (shorebirds) (Suite BC5A) | Indeterminate | Medium-sized, unwebbed bird footprint with four digits; hallux short and directed towards side; total length ~6 cm; total width ~7–8 cm; digits very narrow and may not | Produced in wet to soupy substrate | Medium to large shorebird | Ephemeral freshwater pool fed by crevasses or sheetfloods on delta-plain | Firehole Canyon, A, upper unit | e.g., FC, A, m ~12.5–14 |

| | | | | | | | | |
|---|---|---|---|---|---|---|---|---|
| | | | represent the base of a true track, but instead were produced as the foot penetrated the substrate; preserved in epirelief | | | | | |
| Fig. *6.1.2*.11 H | Vertebrate footprints (wading birds) (Suite BC5B) | Indeterminate | Three-toed, , partially webbed bird footprint; possibly preserves hallux; total width ~13.5 cm; total length ~10 cm without hallux; total length including possible hallux ~14 cm; three digits directed outwards; preserved as a cast in convex hyporelief | Produced in wet substrate | Large crane-like or egret-like wading bird | Ephemeral freshwater pool fed by crevasses or sheetfloods on delta-plain | Firehole Canyon, A, upper unit | e.g., FC, A, m ~12.5–14 |
| n/a | Root casts (cf. Suites BC4, BC5) | n/a | Circular, white root casts; ranging in diameter from ~1 cm to 3 cm; typically with yellow-orange iron-stained 'rind' | Associated with iron-stained horizons in laminated siltstones | Unknown plants; possibly shrubs such as willows | Subaerially exposed lower delta-plain with fluctuating water table | Firehole Canyon, A, upper unit | e.g., FC, A, m ~12.4 |
| n/a | Iron-stained root-marks? (cf. Suites BC4, BC5) | n/a | Millimetre-sized, circular, open iron-stained marks; may be abundant in distinct horizons, where not necessarily representing roots | Associated with laminated siltstones and mudstones | Unknown plants; possibly marsh plants such as horsetails | Subaerially exposed but wet and/or waterlogged delta-plain mudstones, siltstones, and sandstones | Firehole Canyon, A, upper unit | e.g., FC, A, m ~9.8–12.8, m ~14.2 |
| ***Trace Fossils in the A-Bed of Sage Creek Canyon (divided into the "lower unit" and "upper unit", separated by carbonates of the "white stripe unit")*** | | | | | | | | |
| Fig. *6.1.2*.15 F, 15G, 16A, 16B, 16C | Full relief burrows? (cf. Suite BC3) | cf. *Planolites* isp. | Very small to small sized (1–1.5 mm and ~3 mm diameter) indistinct burrows preserved as endichnia within fine-grained arkosic sand, along bedding planes with tool marks and parting lineation, as well as within sandstone units preserving convolute and ripple cross-lamination; many examples are open holes within sandstone, others are filled with host material | If burrows, animals possibly living subaqueously and transported with bedload; if not burrows, possibly pellets or clay clasts | Arthropods; possibly chironomids or other dipteran larvae; possibly oligochaetes; possibly brine shrimp | Active channels; fine-grained sandstones with convolute bedding or horizontal lamination with parting lineation | Sage Creek Canyon, A, upper unit | e.g., SCC, A, m ~5.8, m ~6–7.8 |
| Fig. *6.1.2*.16 D | Full relief burrows (Suite BC9?) | Indeterminate | Small (~3 mm diameter) and medium-large (~10 cm diameter) burrows preserved in full relief; burrow boundaries irregular but distinct; burrow fill different from host; circular in cross section | Present in pedogenically altered heterolithic channel deposits | Unknown invertebrates; likely insects | Abandoned channel and/or waning flow channel deposits | Sage Creek Canyon, A, upper unit | e.g., SCC, A, m ~8.4 |

| | | | | | | | | |
|---|---|---|---|---|---|---|---|---|
| Fig. *6.1.2*.15 A, 15B, 15D | Horizontal burrows (Suite BC5A) | *Planolites* isp. | Medium-sized (~4–6 mm diameter), horizontally oriented burrows preserved in convex hyporelief; burrow boundaries irregular but may be distinct; burrow widths variable | Associated with bird-trampled surface and possible microbial mat features on bedding plane; substrate wet to soupy | Unknown invertebrates | Mudflat or shallow lagoon on lower delta-plain | Sage Creek Canyon, A, upper unit | e.g., SCC, A, m ~5.8 |
| Fig. *6.1.2*. 17A, 17B | Full relief burrows (cf. Suite BC5A) | cf. *Palaeophycus* isp. | Small (4 mm diameter) and medium-sized (~6–7 mm diameter) full relief burrows in bioturbated sandstone; lining not preserved in medium-sized traces but sample shows differential weathering around burrow fill, same as host material; lining preserved in smaller example, preserved as convex epichnia | Preserved in bioturbated sandstone; compare with *Planolites* ichnofabric at South Margin, Tipton section | Invertebrate | Bioturbated sandstone | Sage Creek Canyon, A, upper unit, north of measured section | n/a |
| Fig. *6.1.2*.16 H, 16I, 17C | High density hypichnia (Suite BC5B) | cf. *Fuersichnus* isp. | Medium-sized (~6 mm diameter), unwalled burrows preserved as convex hypichnia; may possibly be bilobed and may preserve longitudinal ornamentation; tapered on both ends, but not banana-shaped | Preserved in locally moderately high density (BPBI=~3–4) | Unknown invertebrate | Base of fluvial sandstone | Sage Creek Canyon, A, upper unit; SCC, A (N) upper unit | e.g., SCC, A, m ~10.2 |
| Fig. *6.1.2*.16 G | Meniscate backfilled burrows (Suite BC5B) | *Taenidium barretti* | Very small (~1.5 mm diameter), unwalled, meniscate backfilled horizontal burrows; preserved in semi-relief at base of bed | Associated with bird track in soupy, desiccated substrate | Possibly insect larvae or oligochaete | Desiccated ephemeral standing water on delta-plain or crevasse pool | Sage Creek Canyon, A, upper unit | e.g., SCC, A, m ~10 |
| Fig. *6.1.2*.17 D, 17E, 17F | Full relief burrows (cf. Suite BC9) | cf. *Taenidium barretti*<br>cf. *Lunulichnus* isp. | Large (1.5 cm diameter), circular, slightly curving, open and backfilled horizontally and vertically oriented full relief burrows; preserved as endichnia and convex hypichnia; one example shows lining; may preserve external ornamentation | May have come up into sandstone bed from below | Probably insect; possibly large beetle | Base of fluvial sandstone | Sage Creek Canyon, A, upper unit, north of measured section | n/a |
| Fig. *6.1.2*.13 C, 13D | Branching burrow system (Suite BC1) | *Thalassinoides* isp. A | Overall U-shaped burrow system with medium- and large burrow branches (~4 mm and < 1.2 cm); fill different from host and passive; sharp burrow boundaries; unwalled and unlined; branches are T-shaped; burrow branches taper downwards | Fossil prawns (*Bechleja rostrata*) are known from Fossil Basin | Probably crustacean; possibly prawns | Littoral briefly exposed eulittoral mudflat; associated with thin siltstone beds showing fining upwards; preserved in marlstone | Sage Creek Canyon, A, lower unit, east of measured section | e.g., SCC, A, m ~1 |

| | | | | | | | | |
|---|---|---|---|---|---|---|---|---|
| Fig. *6.1.2*. 14G, 14H | Branching burrow system (Suite BC3B) | *Thalassinoides* isp. B | Branching burrow system with oval-shaped expanded chambers; chambers ~1.5–2.5 cm across, ~1–1.5 cm high; burrows ~8 mm diameter; burrows and chamber with sharp burrow boundaries, but unlined and unwalled | Associated with pellet-filled vertical burrows; substrate may have been firm | Arthropod; very similar to earwig nests and burrows; possibly prawns | Abandoned small, shallow channel on lower delta-plain | Sage Creek Canyon, A, lower unit | e.g., SCC, A, m ~1.2 |
| Fig. *6.1.2*.14 C | Vertical burrows (Suite BC3B) | *Skolithos* isp.; cf. *Polykladichnus* isp. | Small (~1.5–2 mm diameter), straight or slightly curved, vertical and oblique burrows with sharp burrow boundaries; up to ~5 cm deep with rounded base to burrow; may branch upwards | Substrate cohesive, and may have been firm; traces could possibly be root marks | Probably insect larvae; possibly tiger beetle larvae | Abandoned small, shallow channel on lower delta-plain | Sage Creek Canyon, A, lower unit | e.g., SCC, A, m ~1.2 |
| Fig. *6.1.2*. 14A, 14D, 14E, 14F | Vertical burrows (Suite BC3) | *Skolithos* isp.; cf. *Macanopsis* isp. | Medium-sized (4–6 mm diameter) vertical to slightly oblique burrows with very sharp walls preserved in full relief; some examples become wider downwards; burrow straight and unbranched; unlined/unwalled, but burrow boundary appears textured from pellet-like fill; partly or totally filled with pellet-like sediment aggregates; traces originate from top of bed and extend to depths of ~15 cm; some examples ~5 cm deep terminate in oval-shaped chambers, ~1 cm wide by 7 mm high | Substrate cohesive, and may have been firm; associated with escape burrows in trough cross-stratified sandstone bed | Insect, possibly tiger beetle larvae or staphylinid beetles | Abandoned small, shallow channel on lower delta-plain | Sage Creek Canyon, A, lower unit | e.g., SCC, A, m ~1.2 |
| Fig. *6.1.2*.13 A | Escape traces or bird tracks? (Suite BC1) | None available | Deformed-downwards laminae to depths of ~2.5 cm; width ~0.3 cm at bed top, and ~0.1 cm wide at bottom of trace; two traces are within 2 cm of one another (possibly bird digits?) | Associated with small *Planolites* isp. and irregular bedding | Either arthropod or bird (probably shorebird) | Possibly represents distal sheetflood on lower delta-plain; shallow water or soupy subaerially exposed substrate | Sage Creek Canyon, A, lower unit | e.g., SCC, A, m ~0.7 |
| Fig. *6.1.2*.14 B | Escape traces (Suite BC3A) | None available | Vertically to obliquely oriented, medium-sized escape traces preserved in trough cross-stratified sandstone; indistinct | Overprinted by Suite BC3; produced in soupy substrate | Possibly insect, such as tiger beetles | Active, small, shallow channel on lower delta-plain | Sage Creek Canyon, A, lower unit | e.g., SCC, A, m ~1.2 |
| Fig. *6.1.2*.13 B | Full relief burrow? (Suite BC1) | Indeterminate; *Thalassinoides* isp. A? | Irregular, large (< 3 cm diameter) possible branching burrow associated with smaller cracks or burrows (~4 mm diameter); fill different from host; burrow boundaries sharp but irregular | Compare with *Thalassinoides* isp. A and large burrows from MFC, A, Suite BC1, lower unit | Possibly decapod crustacean such as crayfish or prawns | Shallow littoral zone? | Sage Creek Canyon, A, lower unit | e.g., SCC, A, m ~1 |

| | | | | | | | | |
|---|---|---|---|---|---|---|---|---|
| Fig. *6.1.2.* 17G, 17H | Arthropod nest cell? (Basin margin suite?) | cf. *Coprinisphaera* isp. | Spherical structure with internal burrows?; ~2.5 cm diameter; internal burrow-like structures ~4 mm diameter; stained reddish | Not clearly a trace fossil; one sample only; possibly a mud ball | Arthropod; probably insect, but possibly earthworm | Channel lag at base of active channel sandstone; transported | Sage Creek Canyon, A, upper unit, north of section | n/a |
| Fig. *6.1.2.* 16E, 16F | Vertebrate footprints (bird) (Suite BC5B) | Indeterminate | Medium-sized (~6 cm width), four-toed, webbed bird footprint preserved as a cast in convex hyporelief; digit impressions associated with mudcracks | Associated with *Taenidium barretti* | Probably gull-like or duck-like bird | Desiccated ephemeral pool, possibly on upper delta-plain | Sage Creek Canyon, A, upper unit | e.g., SCC, A, m ~10 |
| Fig. *6.1.2.* 15E | Vertebrate footprints (bird) (Suite BC5B) | Indeterminate | Probable bird-trampled surface preserving distinct digit impressions of unwebbed bird footprints; lengths of digits < ~5 cm | Associated with *Planolites* isp.; produced in cohesive, soupy, and subaqueous substrate | Probably shorebirds | Mudflat or shallow lagoon on lower delta-plain | Sage Creek Canyon, A, upper unit | e.g., SCC, A, m ~5.8 |
| n/a | Iron-stained root-marks | n/a | Very small (1 mm diameter), circular, iron-stained root-hairs; iron staining like outside rind; internal area same material as host | Iron-stained horizons not preserved | Unknown plants; shrubs such as willows | Subaerially exposed lower delta-plain siltstones with shallow water table | Sage Creek Canyon, A, lower unit | e.g., SCC, A, m ~3 |

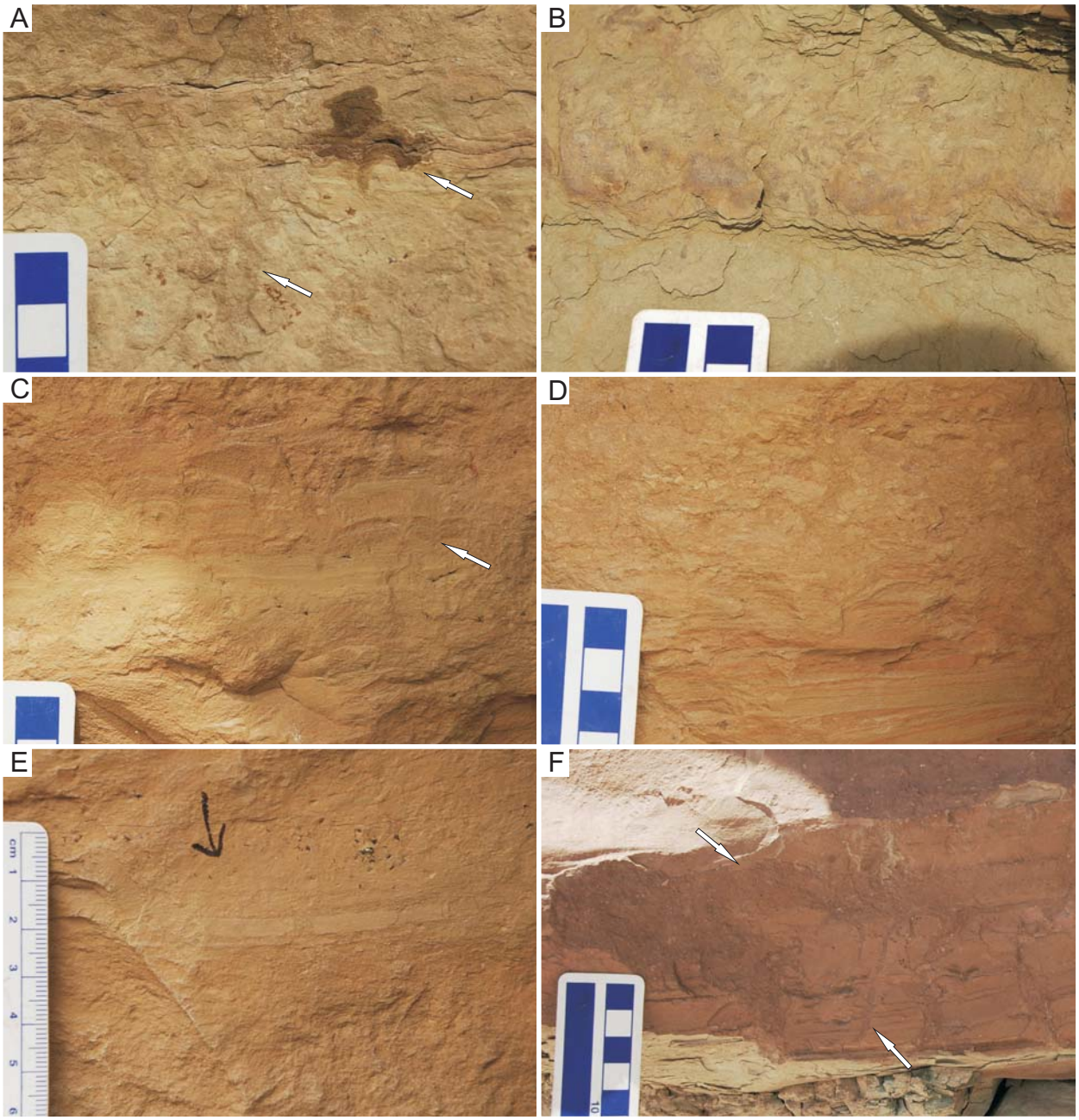


**Fig. 6.1.2.1.** Animal traces in the A-Arkose Bed (lower unit) at Middle Firehole Canyon (Suite BC1). Refer to Table 6.2 for descriptions of traces shown. **(A)** Mottled, bioturbated siltstone showing rare, distinct burrow boundary (lower arrow) and possible bird tracks in cross-section (upper arrow). **(B)** Mottled, bioturbated siltstone of possibly subaerially exposed substrate. Note burrow fill slightly different from host. **(C)** Laminated siltstones showing possible escape traces (left) and/or bird tracks in cross section (arrow). **(D)** Brecciated laminated siltstone possibly due to bioturbation. **(E)** Close-up of thick mudstone laminae, showing crack or sharp-walled burrow. Horizon with black arrow preserves possible fish bones or gastropod radulae. **(F)** Large branched burrows (upper arrow) with small vertical branches (lower arrow), possibly produced by a crustacean.

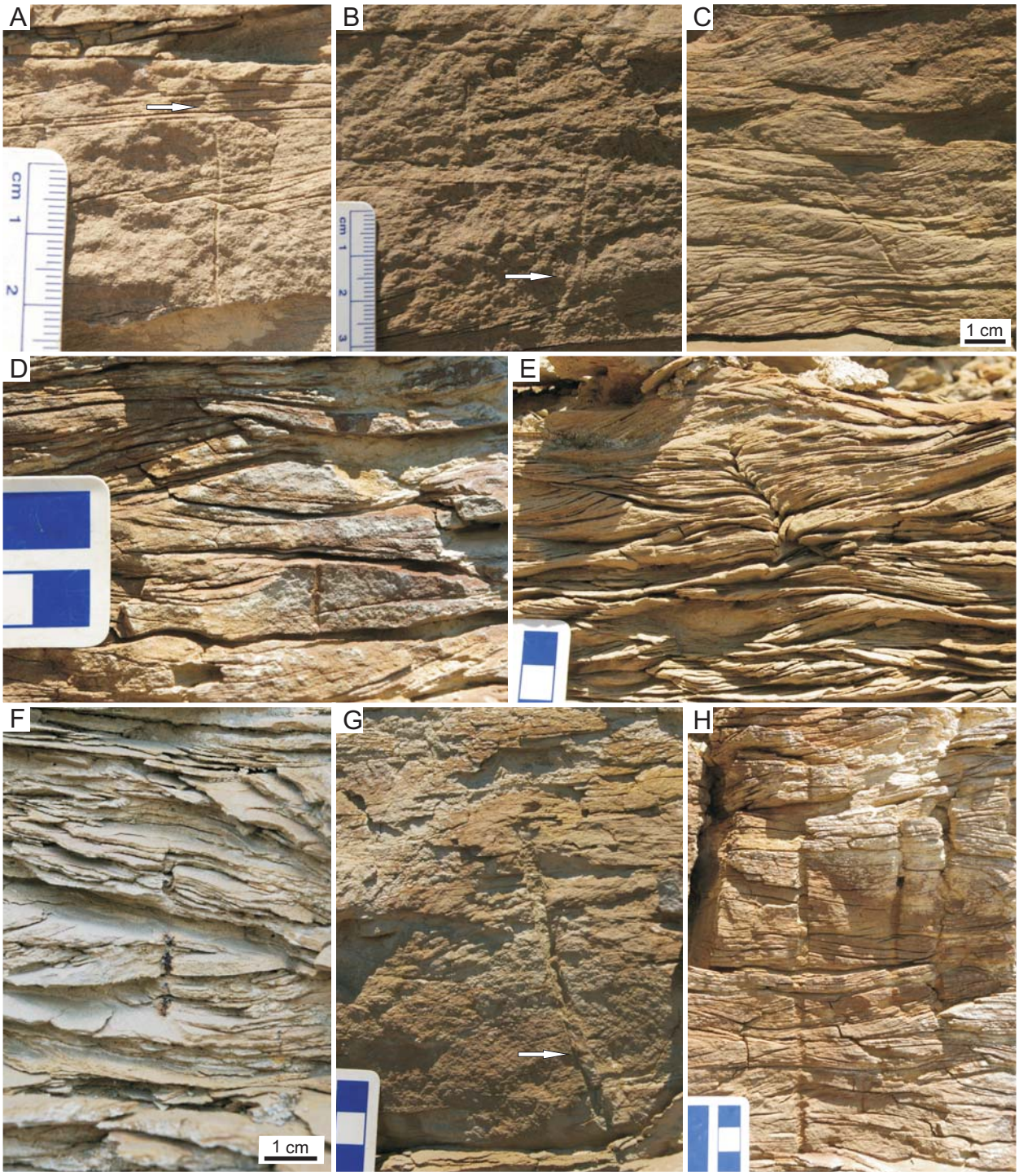


**Fig. 6.1.2.2.** Vertical burrows in the A-Arkose Bed at Middle Firehole Canyon (lower unit) (Suite BC3). Refer to Table 6.2 for descriptions of traces shown. **(A)** Small vertical burrow with escape trace at top (arrow). **(B)** Small vertical burrows (arrow) that originate from several different surfaces. **(C)** Oblique, partly filled vertical burrow. **(D)** Small vertical burrow originating from bedding plane in small-scale trough cross-laminated sandstone. **(E)** Escape trace with downward-directed laminae. **(F)** Medium-sized vertical burrow with black lining. **(G)** Partially filled (passive fill) medium-sized vertical burrow. **(H)** Sharp-walled open vertical burrows.

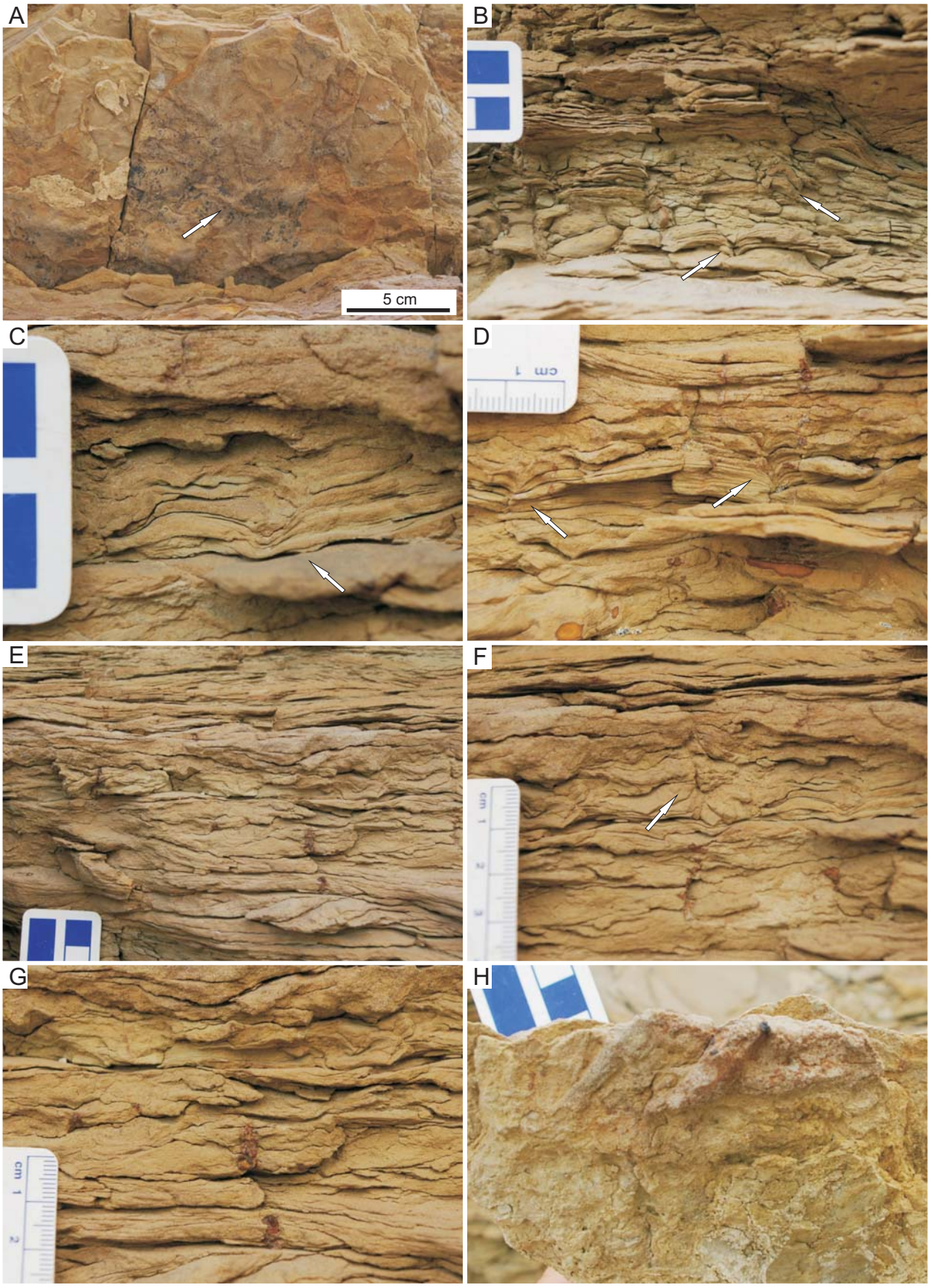
A
5 cm
B
C
D
E
F
G
H

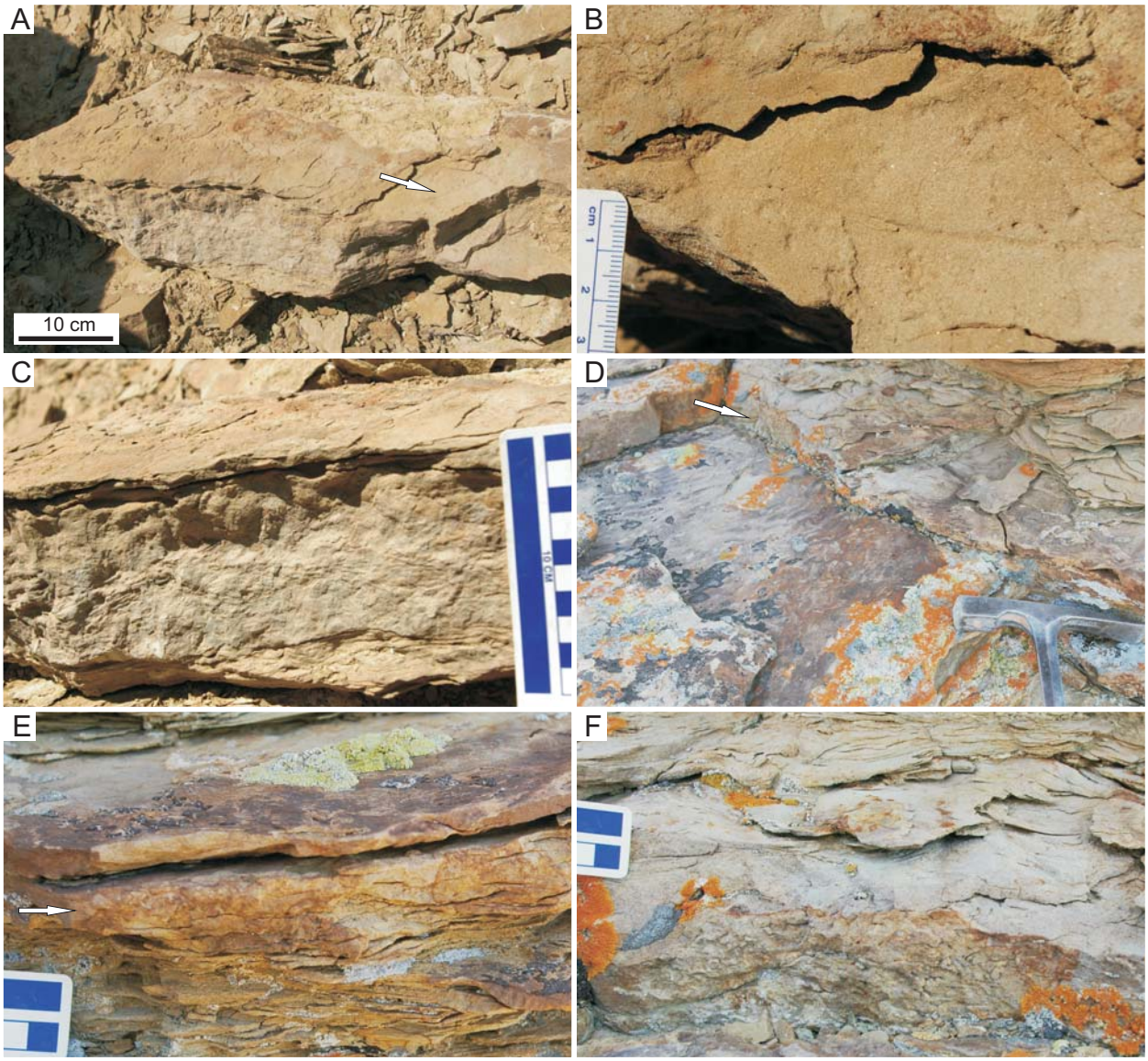


**Fig. 6.1.2.4.** Animal traces in the A-Arkose Bed at Middle Firehole Canyon (upper unit) (Suites BC5A and BC7). Refer to Table 6.2 for descriptions of traces shown. **(A)** Bioturbated wedge-shaped sandstone with surface trail on upper bedding plane (arrow). **(B)** Close-up of surface trail on surface shown in (A). **(C)** Close-up of bioturbated wedge-shaped sandstone in (A). **(D–E)** Upper sandstones preserving bioturbated horizon (arrows in D and E, close-up in F).

**Fig. 6.1.2.3.** (Previous page) Animal traces in the A-Arkose Bed at Middle Firehole Canyon (upper unit) (Suites BC3 and BC5). Refer to Table 6.2 for descriptions of traces shown. **(A)** Bird track (arrow) preserved as cast on lower bedding plane. **(B)** Possible bird tracks in cross-section (upper arrow) and/or escape traces (lower arrow). **(C)** Probable bird track in cross-section (arrow). **(D)** Escape traces or bird tracks in cross-section (arrows). **(E)** Vertical burrows with reddish black fill and "irregular" bedding or bioturbated or trampled substrate. **(F)** Vertical burrow and escape trace (arrow) in irregularly bedded sandstone. **(G)** Close-up of vertical burrow with reddish black fill shown in (E). **(H)** Large horizontal burrows with fill different from host.

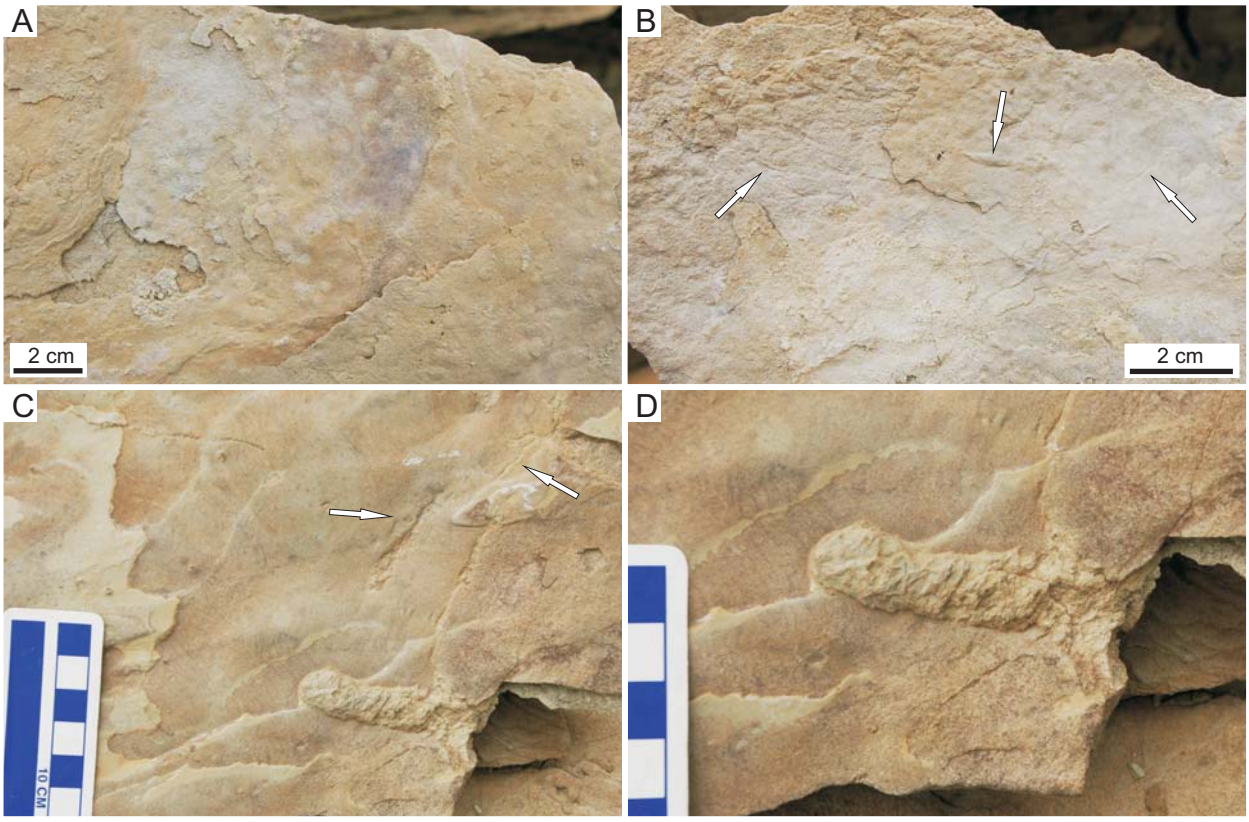


**Fig. 6.1.2.5.** Animal traces in the A-Arkose Bed at Middle Firehole Canyon (upper unit) (Suite BC5B or BC7 and BC8). Refer to Table 6.2 for descriptions of traces shown. **(A)** Bubble-texture in purple-stained mudstone laminae. **(B)** Horizontal trails and burrow (arrows) on surface shown in (A). **(C–D)** Ornamented backfilled burrow (*Spongeliomorpha*) and surface trails (arrows in C).

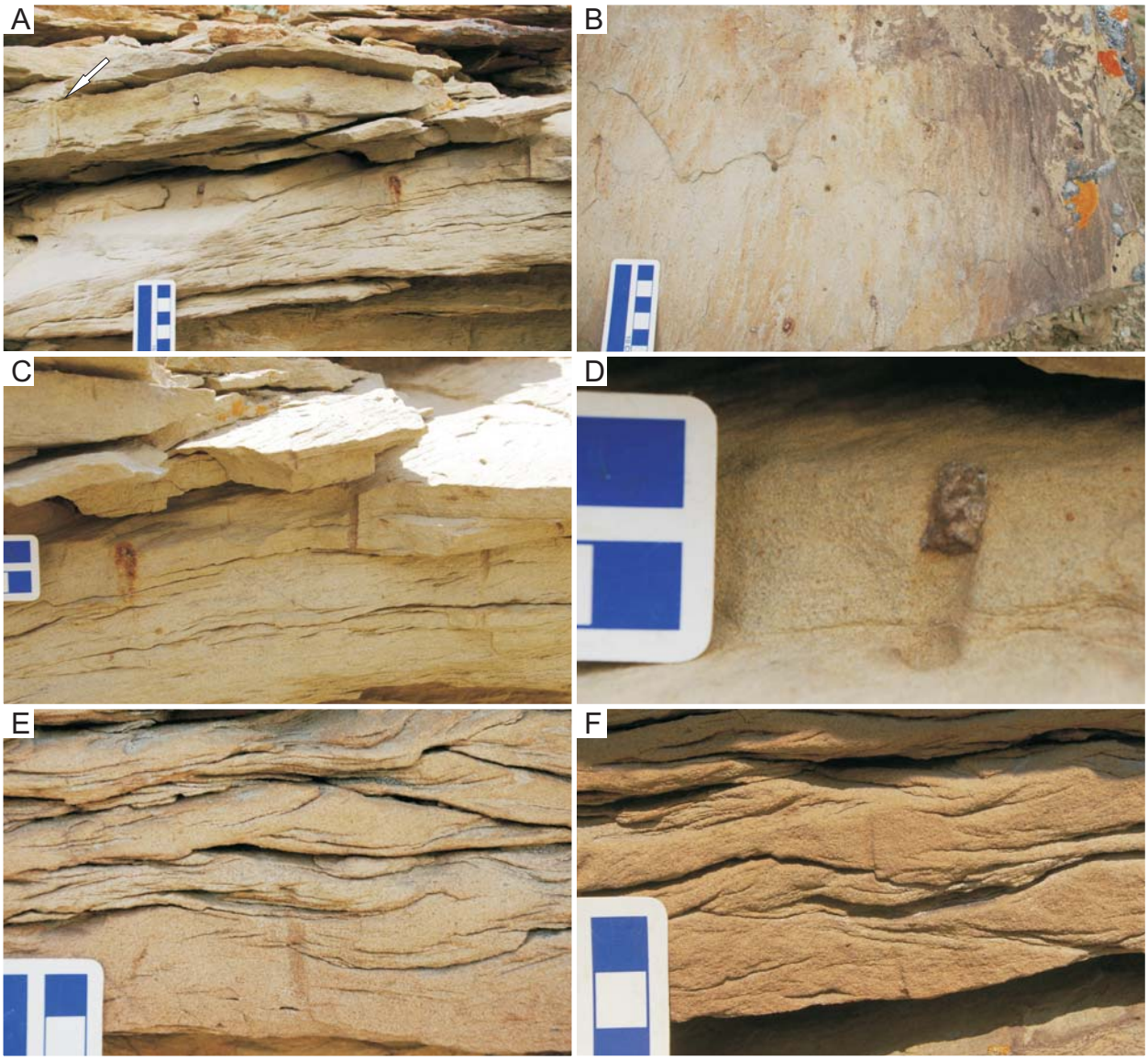


**Fig. 6.1.2.6.** Animal traces in the A-Arkose Bed at Middle Firehole Canyon (upper unit) (Suite BC3). Refer to Table 6.2 for descriptions of traces shown. **(A–F)** Vertical burrows in ripple-laminated sandstones interpreted as point-bar and shallow channel deposits. Note pellet-like backfill in (D).

**Fig. 6.1.2.7.** (Next page) Animal traces in the uppermost A-Arkose Bed at Middle Firehole Canyon (Suites BC7 and BC8A). Refer to Table 6.2 for descriptions of traces shown. **(A)** Black-stained surface with surface trails (arrow at top right) and appendage scratchmarks (arrows) of Suite BC7 and burrows of Suite BC8A. **(B)** Top surface with horizontal burrow (arrow) and other sharp-walled burrows. **(C–D)** Top surface, with trails and pellet-backfilled burrows (arrow in C). **(E)** Pellet-backfilled burrows and bioturbated area near burrow (arrow) on top surface. **(F–H)** Meniscate backfilled branching burrows (arrow in F, G, arrow at right in H), and lined burrow (*Palaeophycus*?, lower arrow in H).

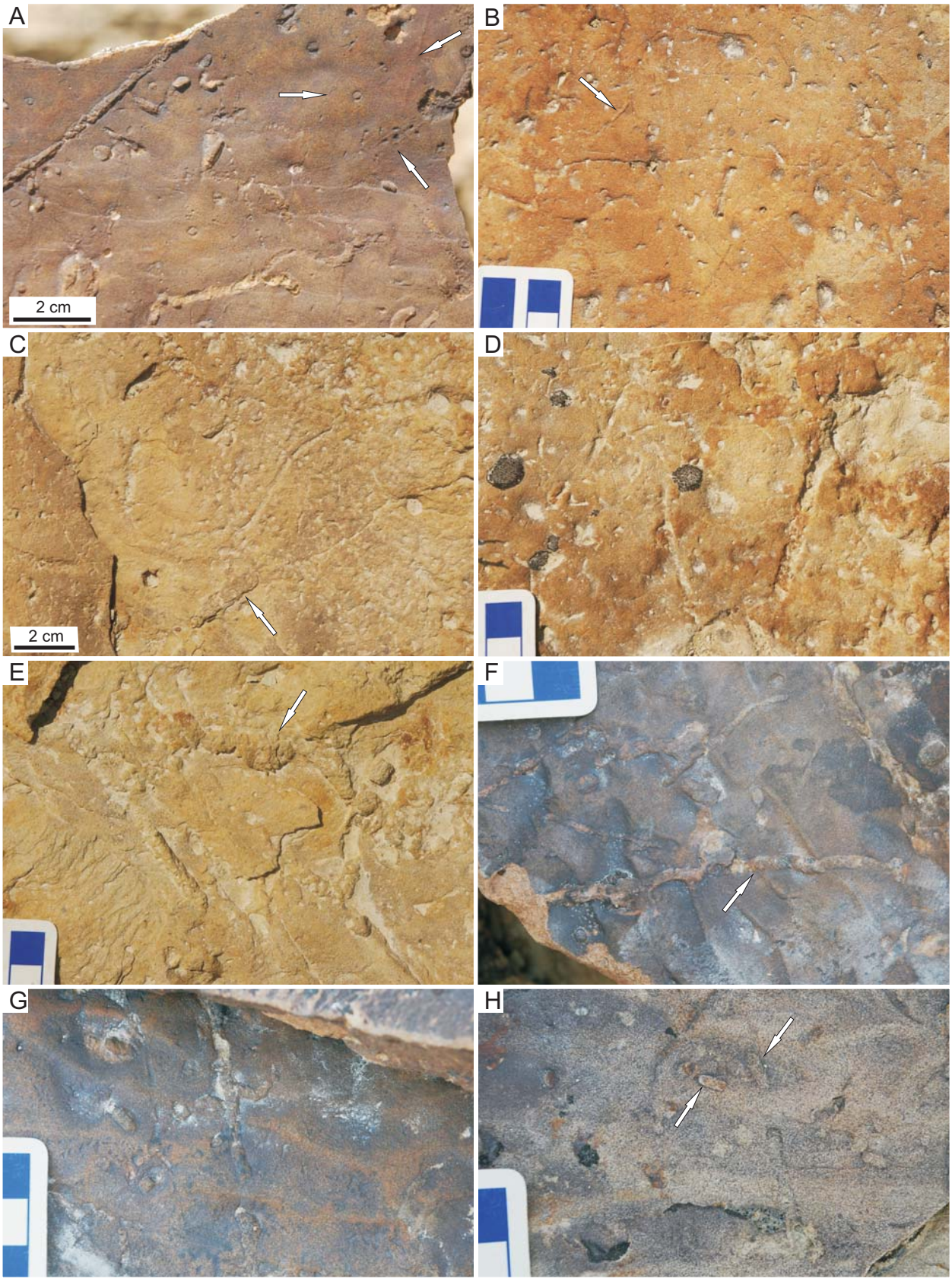
A
2 cm
B
C
2 cm
D
E
F
G
H

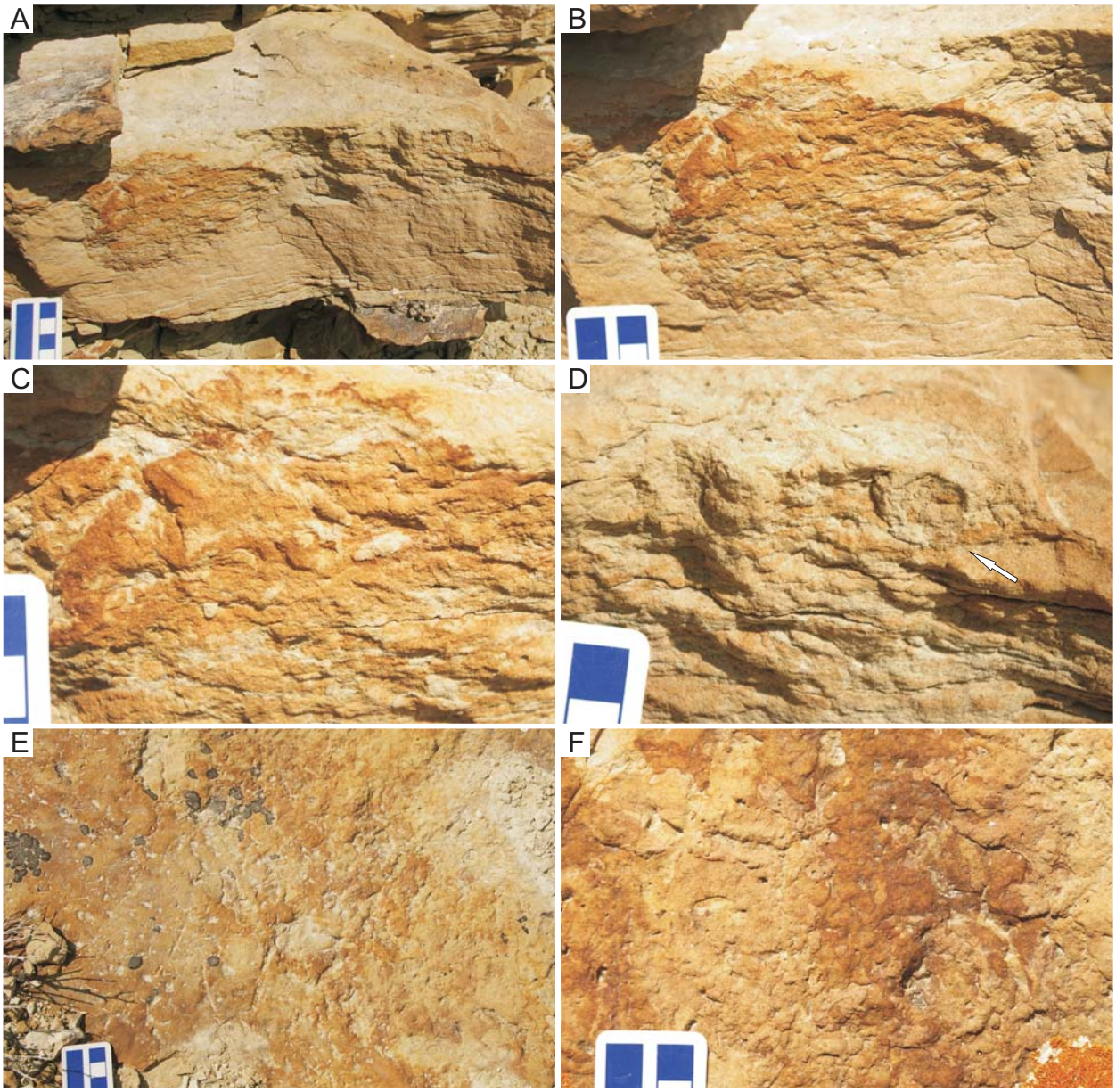


**Fig. 6.1.2.8.** Animal traces in the uppermost A-Arkose Bed at Middle Firehole Canyon (Suites BC8B). Refer to Table 6.2 for descriptions of traces shown. **(A–C)** Insect nest in flaser-bedded sandstone. Note sharp boundary to bioturbated area and simple backfilled burrow in nest area. **(D)** Thick-walled tunnel associated with nest (arrow). **(E–F)** Bioturbated region on top surface associated with nest (right in E, close-up in F).

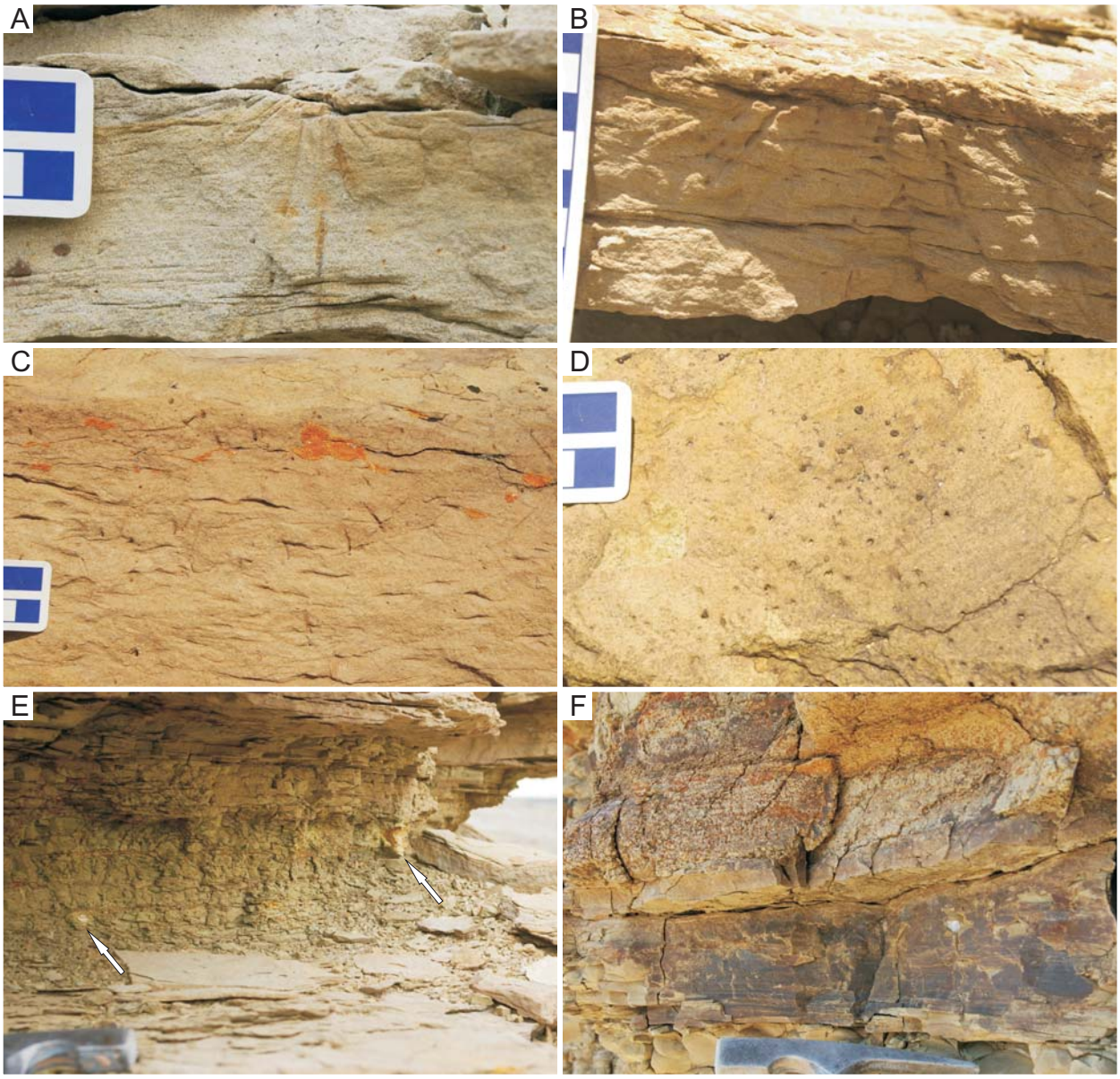


**Fig. 6.1.2.9.** Plant traces in the A-Arkose Bed at Middle Firehole Canyon (upper unit). Refer to Table 6.2 for descriptions of traces shown. **(A–D)** Bunch-like root traces in the uppermost upper unit. (D) shows bedding plane view. **(E)** Carbonate root casts (arrows) in weakly developed paleosol in middle portion of upper unit. **(F)** Red iron-stained horizon, possibly with abundant root-hair marks in lower portion of upper unit.


**Fig. 6.1.2.10.** Animal traces in the A-Arkose Bed at Firehole Canyon (upper unit) (Suite BC5B). Refer to Table 6.2 for descriptions of traces shown. **(A)** Branched surface tunnels preserved in convex epirelief. **(B)** Backfilled, branched surface tunnels preserved in convex epirelief. **(C–D)** Open branched burrow network preserved in concave hyporelief at base of sandstone at Firehole Canyon (N). **(E)** Furrow-shaped traces on upper bedding plane (arrow). **(F)** Pock-mark-like traces preserved on upper bedding plane.

**Fig. 6.1.2.11.** (Next page) Bird tracks in the A-Arkose Bed at Firehole Canyon (upper unit) (Suite BC5B). Refer to Table 6.2 for descriptions of traces shown. **(A–D)** Shorebird trackways preserved as moulds on upper bedding planes. **(E)** Shorebird tracks preserved as casts. Note extension of digits into desiccation crack (upper left, arrows) and alteration of track morphology by unidirectional flow (lower arrow). **(F)** Shorebird track preserved as cast, showing slippage marks in skin texture (arrow). **(G)** Medium-sized wading bird footprint. **(H)** Large wading bird footprint preserved as a cast on lower bedding plane. Note possible impression of hallux (arrow).

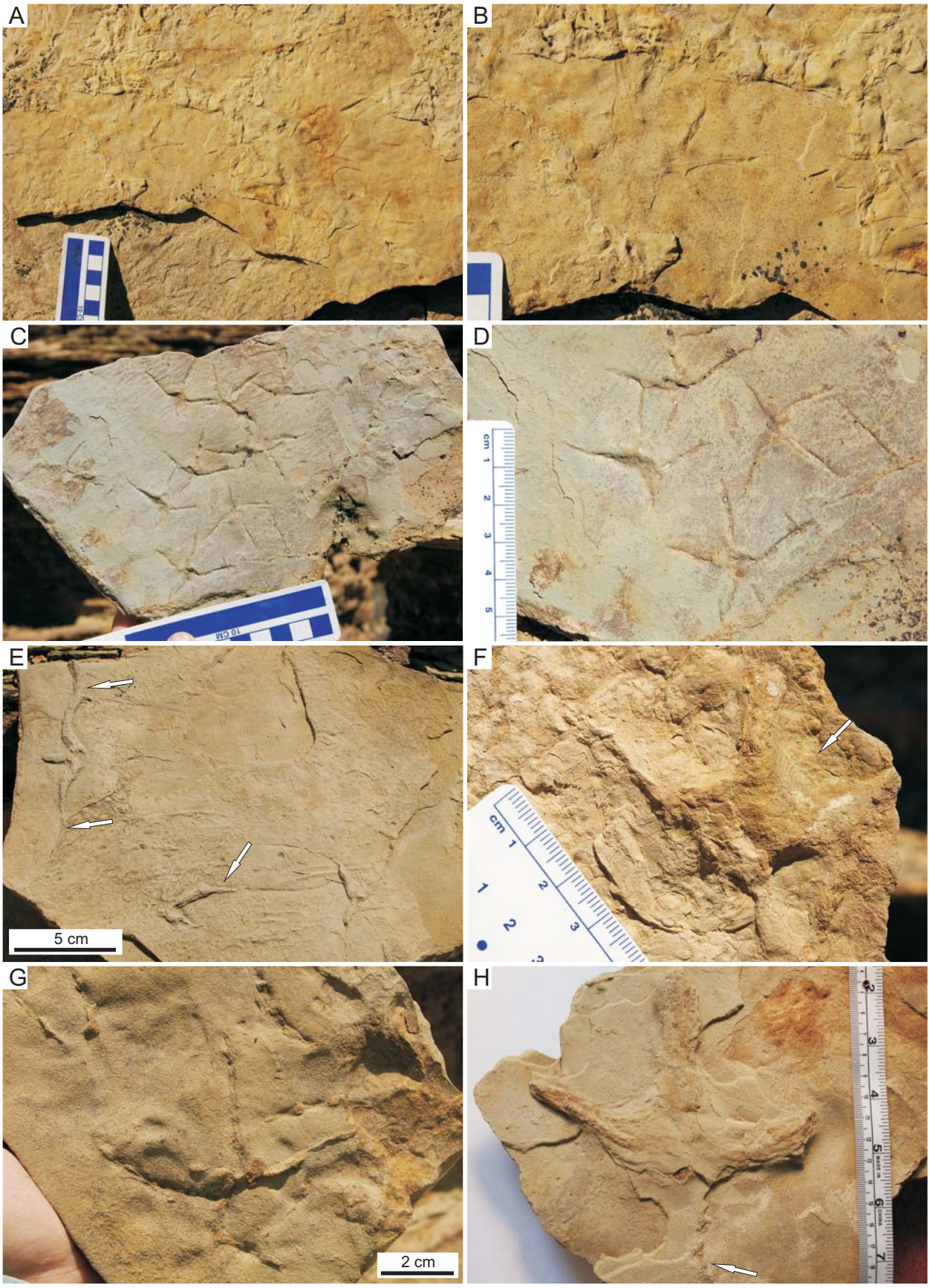
A
B
C
D
E
F
G
H
5 cm
2 cm

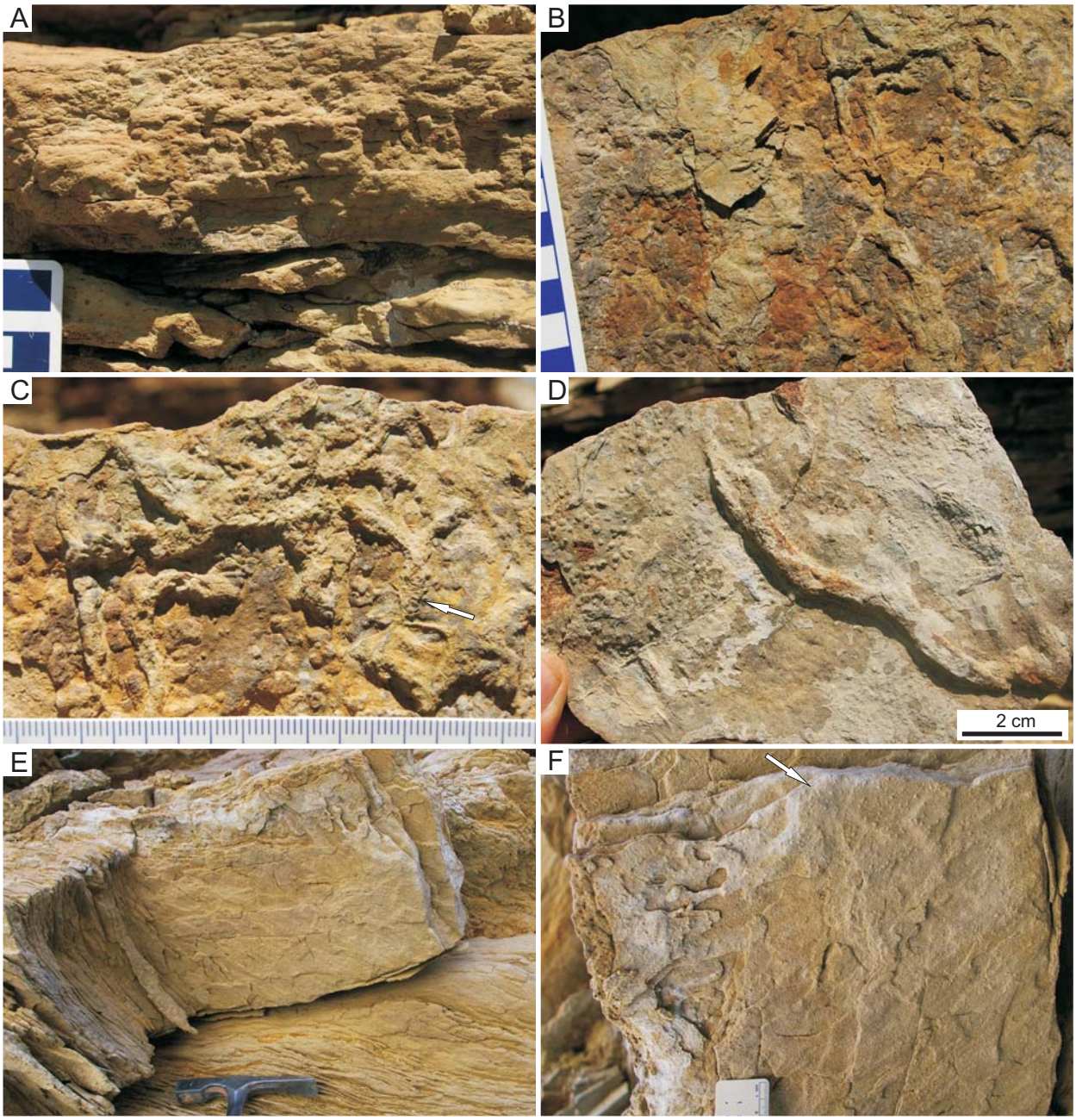


**Fig. 6.1.2.12.** Simple burrows in the A-Arkose Bed at Firehole Canyon (upper unit) (Suite BC5A). Refer to Table 6.2 for descriptions of traces shown. **(A)** The *Planolites* ichnofabric – bioturbated sandstone of simple burrows. **(B–C)** Red- and purple-stained bedding plane with horizontal burrows. Arrow in (C) showing possible meniscate fill. **(D)** Very small burrows on bedding plane (left side of photograph). **(E–F)** Very small burrows on lower bedding plane of cross-laminated sandstone in upper unit at Firehole Canyon (N). Arrow in (F) pointing to small burrows.

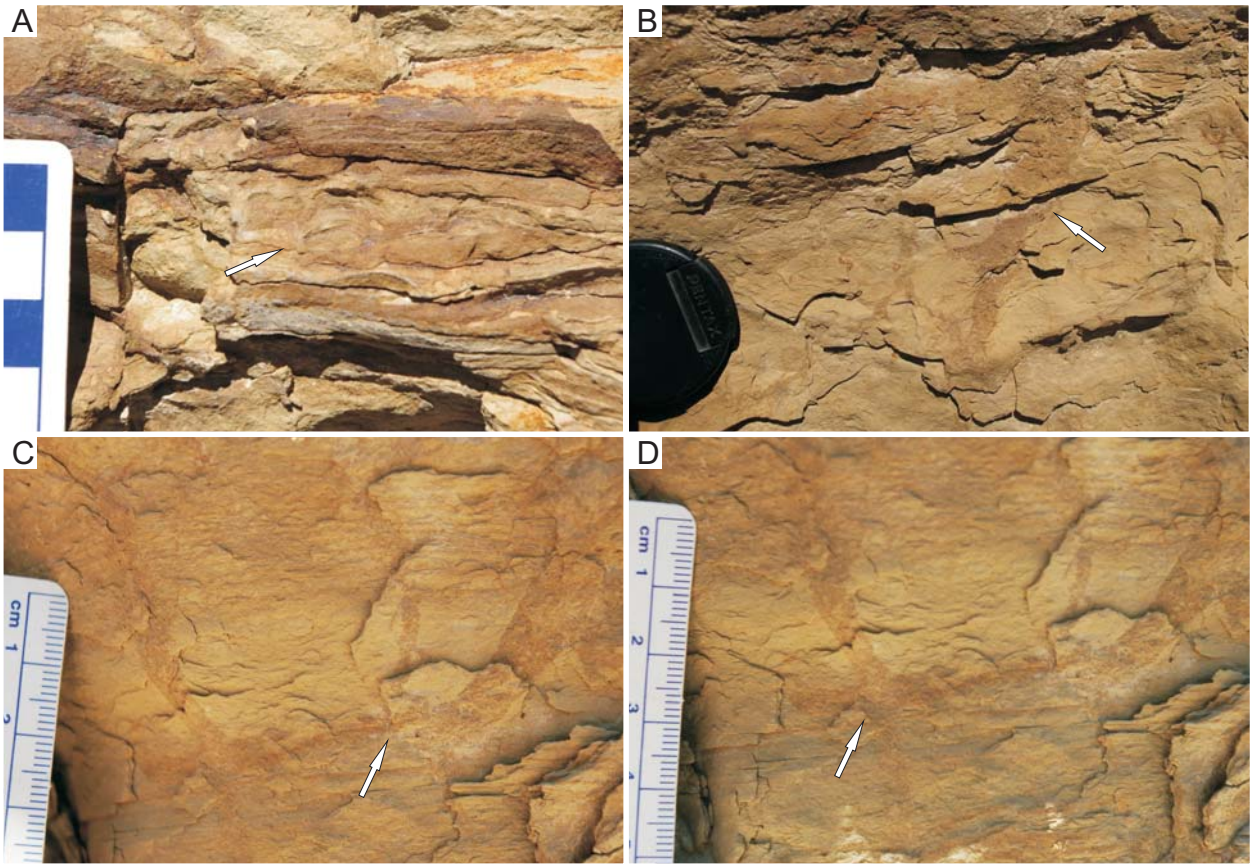


**Fig. 6.1.2.13.** Animal traces in the A-Arkose Bed at Sage Creek Canyon (lower unit) (Suite BC1). Refer to Table 6.2 for descriptions of traces shown. **(A)** Escape trace or possible bird track in cross-section (arrow) in laminated siltstone. **(B)** Large, sharp-walled burrow (arrow) possibly produced by a crustacean. **(C–D)** Branched, U-shaped burrows (arrows) possibly produced by prawns.

**Fig. 6.1.2.14.** (Next page) Animal traces in the A-Arkose Bed at Sage Creek Canyon (lower unit) (Suite BC3). Refer to Table 6.2 for descriptions of traces shown. **(A)** Sandstone bed with sharp-walled vertical burrows. **(B)** Escape traces/vertical burrows (arrows) in cross-bedded sandstone. **(C)** Very small sharp-walled vertical burrows. **(D)** Sharp-walled and pellet-backfilled vertical burrow. **(E)** Sharp-walled open vertical burrow. **(F)** Vertical burrows with oval-shaped chambers at burrow endings (arrows). **(G–H)** Possible earwig or ant nest or crustacean burrow system showing oval-shaped chambers. Note vertical burrow in (H).

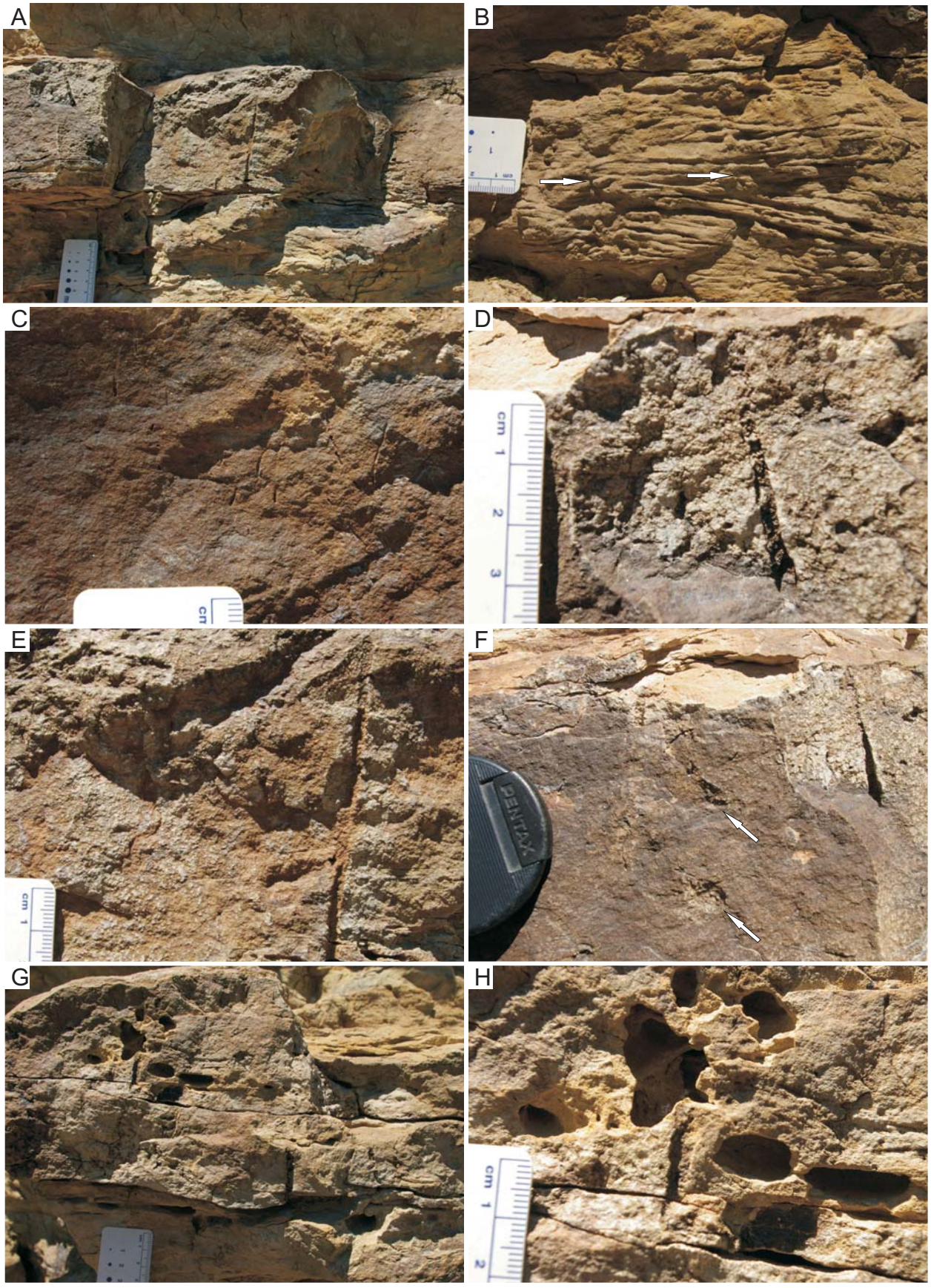
A
B
C
D
E
F
G
H
PENTAX


**Fig. 6.1.2.15.** Animal traces in the A-Arkose Bed at Sage Creek Canyon (lower portion of upper unit) (Suite BC5). Refer to Table 6.2 for descriptions of traces shown. **(A–D)** Horizontal burrows on red- to purple-stained horizons. **(E)** Bird-trampled surface. **(F–G)** Small burrows? on lower bedding plane of planar-laminated sandstone.

**Fig. 6.1.2.16.** (Next page) Animal traces in the A-Arkose Bed at Sage Creek Canyon (upper unit) (Suites BC3?, BC9, and BC5). Refer to Table 6.2 for descriptions of traces shown. **(A–C)** Very small possible "circle" burrows in cross-laminated sandstone. Note possible vertical burrow in middle of (A). **(D)** Weakly pedogenically modified sandstone with clay drape showing large backfilled burrows (arrow) and small backfilled burrows. **(E–F)** Webbed bird footprint associated with desiccation cracks. Preserved as cast on lower bedding plane. **(G)** Very small meniscate burrow next to bird track in (E) and (F). **(H–I)** High density burrows preserved on lower bedding plane above bird-track horizon. (cf. *Planolites*?, cf. *Fuersichnus*?).

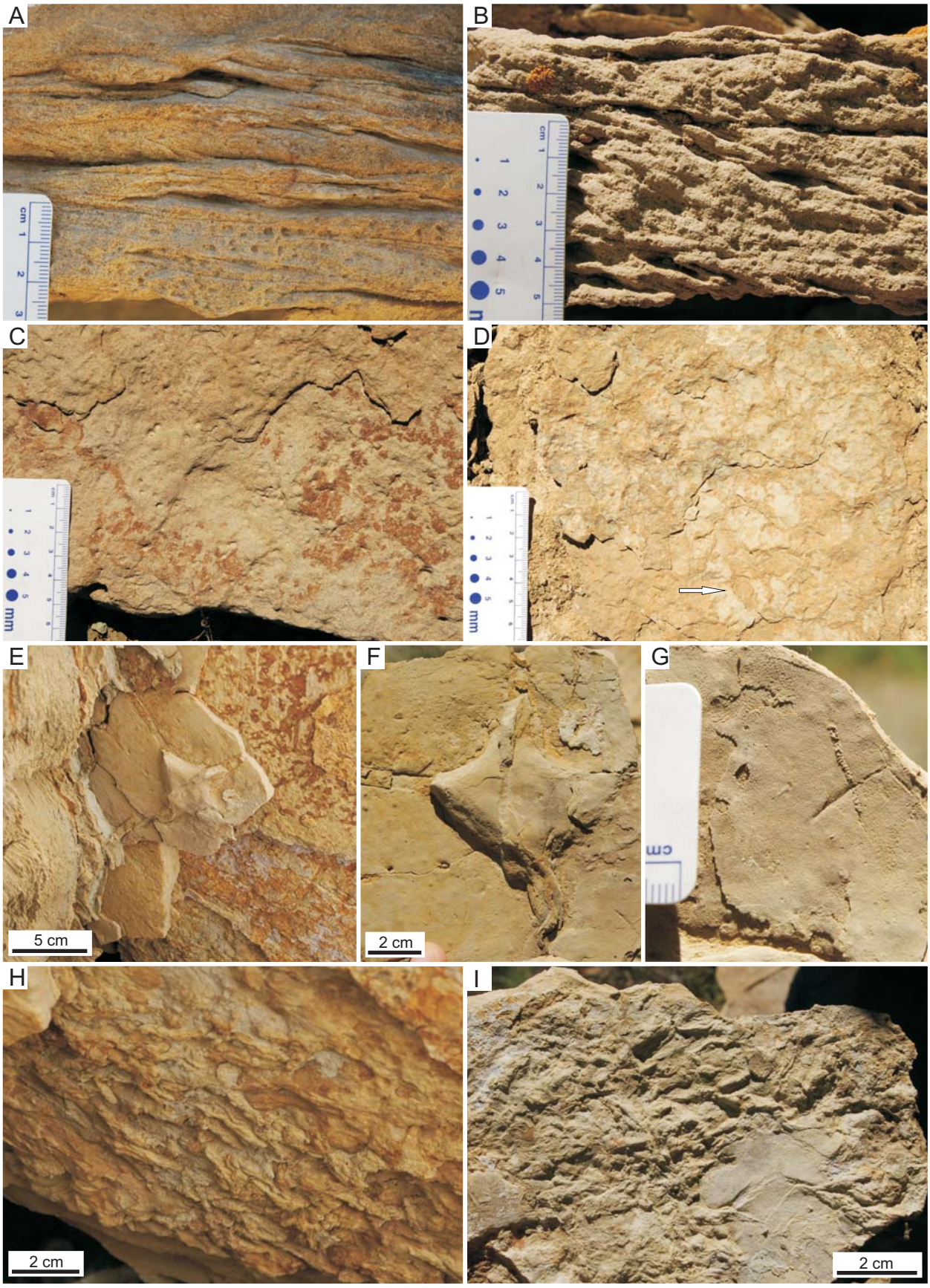
A
B
C
D
E
5 cm
F
2 cm
G
H
2 cm
I
2 cm

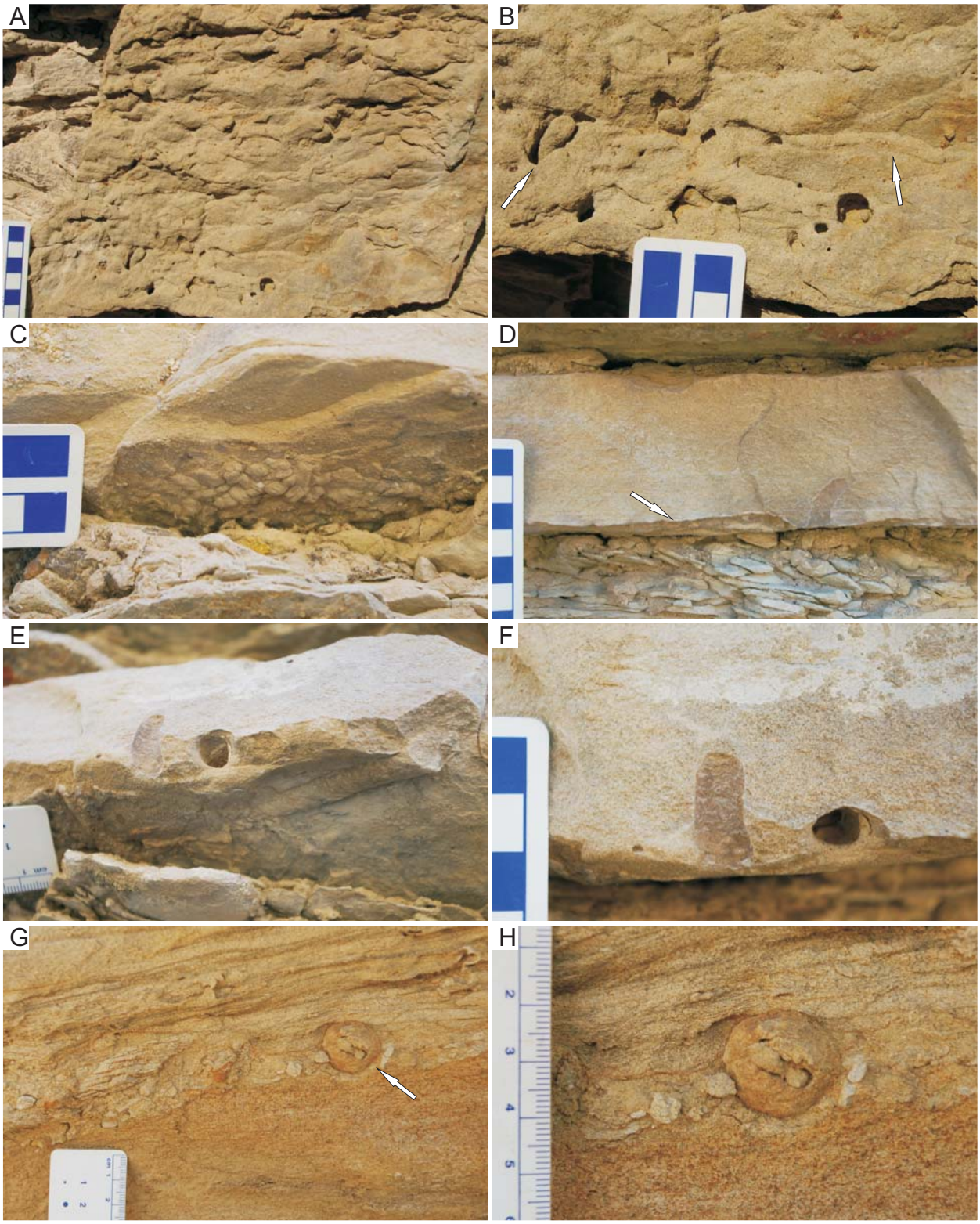


**Fig. 6.1.2.17.** Animal traces in the A-Arkose Bed at Sage Creek Canyon (N) (upper unit). Refer to Table 6.2 for descriptions of traces shown. **(A–B)** Bioturbated sandstone with medium-sized and large burrows with walls (arrows in B). **(C)** High density traces on lower bedding plane (cf. *Fuersichnus*?). **(D–F)** Large backfilled and partially walled horizontal burrows at base of fluvial sandstone. Note lining in open burrow at right in (F). **(G–H)** Possible insect nest (earthworm?) or beetle brood cell preserved in channel lag (arrow in G, close-up in H).

*6.1.3. Trace Fossils Preserved in the Arkosic Facies of the D-Bed and E-Bed*

Trace fossils preserved in the D-Bed and E-Bed (Table 6.3) were studied primarily in Firehole Canyon, in two stratigraphic sections separated by ~500 m (FC, D1; FC, D2). An interesting assemblage of trace fossils is also preserved in the D-Bed on White Mountain at Kanda (WM, K), which are also described in Table 6.3. Abundant traces were preserved within the channel sandstones of the D-Bed at Logan Draw, although that locality was only briefly visited and is not included here.

**Table 6.3.** Trace fossils preserved in the basin centre siliciclastic unit, the D-Arkose Bed and E-Arkose Bed at Firehole Canyon (Sections D1 and D2-E2) and White Mountain (Kanda).

| Fig. | Trace type; Trace suite | Ichnotaxonomy | Description | Comments | Tracemaker | Interpreted Environment | Locality | Section, metre |
|---|---|---|---|---|---|---|---|---|
| ***Trace fossils from the D-Arkose Bed, White Mountain, Kanda*** | | | | | | | | |
| Fig. *6.1.3.* 3A | Horizontal burrow (Suite BC7?) | cf. *Taenidium* isp. | Large (~2 cm diameter) horizontal burrow without fill; preserved in concave epirelief; side burrow margin preserves obliquely oriented 'wrinkles'; lower burrow margin preserves non-planar, meniscate-like, 'wrinkles' oriented roughly perpendicular to direction of motion; burrow boundaries not sharp | Tracemaker may have used peristaltic motion; alternatively, arthropod appendage impressions form oblique striations in burrow wall | Possibly large annelid or arthropod | Active channel or crevasse splay; planar lamination in very fine-grained arkosic sand with parallel current lineation (low flow regime) | White Mountain, Kanda, upper unit | n/a |
| Fig. *6.1.3.* 1H | Simple burrows (BC5A) | *Planolites* isp. | Medium-sized (~5mm diameter), indistinct burrows in bioturbated substrate; fill same as host; appear to have been actively filled; unlined, unwalled; dominantly horizontally oriented; BI=3; preserved in full relief | Example of *Planolites* ichnofabric | Unknown invertebrate | Bioturbated crevasse sandstone | White Mountain, Kanda, upper unit | n/a |
| Fig. *6.1.3.* 1A, 1B | Horizontal burrows (Suite BC5B) | cf. *Vagorichnus* isp. | Medium-sized (~3–4 mm diameter), branching, horizontal tunnels preserved in convex hyporelief; appear to be backfilled with sediment aggregates in places | Associated with bird footprints and raindrop/microbial ? texture and desiccation cracks | Unknown invertebrate; possibly staphylinid, carabid, or heterocerid beetles | Subaerially exposed cohesive to saturated substrates; distal, desiccated crevasse-splay sandstones with clay drapes | White Mountain, Kanda, upper unit | n/a |
| Fig. *6.1.3.* 1C, 1F | Horizontal burrows (Suite BC5B) | *Planolites* isp. | Medium-sized (~4 mm diameter), unbranched, slightly curving, horizontal tunnels preserved in convex hyporelief; fill is same as host; not walled or lined | Associated with bird footprints and raindrop/microbial ? texture and desiccation cracks | Unknown invertebrate | Subaerially exposed cohesive to saturated substrates; distal, desiccated crevasse-splay sandstones with clay drapes | White Mountain, Kanda, upper unit | n/a |
| Fig. *6.1.3.* 3B, 3C, 3D | Horizontal surface bioturbation (Suite BC7) | Indeterminate | Medium-sized (~5–7 mm diameter), curved, unbranched, horizontal trails/burrows preserved in concave epirelief; lateral margins of trails slightly pushed up; associated with indistinct ploughing/burrowing structures on indeterminate affinity | Associated with very low amplitude, wind-induced wave ripples | Unknown invertebrate; possibly gastropod or beetles | Shallow overbank pool or pool within channel | White Mountain, Kanda, upper unit | n/a |

| | | | | | | | | |
|---|---|---|---|---|---|---|---|---|
| Fig. *6.1.3.* 2D | Vertebrate footprints (mammal) (Suite BC5B) | Indeterminate | Small possible mammal tracks in plan view; pair preserved, likely front and hind, approximately same size; ~3 cm length, ~2 cm width; digits not clearly impressed but appear to be unclawed, possibly with hoof-like claws; number of digits likely 4 or 5 on front and hind; posterior margins rounded to slightly pointed | Total of three tracks on same surface; associated with fine-scale desiccation features and iron-stained root marks | Small mammal; possibly hyaenodont (Creodont), carnivore, or condylarth | Subaerially exposed and partially dried, churned crevasse-splay very fine-grained sandstone, possibly into floodplain pool | White Mountain, Kanda, upper unit | n/a |
| Fig. *6.1.3.* 2A, 2B, 2C, 2E, 2H | Vertebrate footprints (mammal) (Suite BC4) | Indeterminate | Medium-sized mammal tracks in cross-section; typically ~5 cm depth and ~5 cm wide; depths up to ~20 cm; frequently shows asymmetrical profile, with one side more pointed, perhaps the front of the foot; rare examples of tracks in plan view show ~6 cm length and ~4 cm width, with splayed non-hoofed digits; number of digits unknown; laminations normally deformed but preserved | Preserved in cross-section and produced during deposition; rare examples in plan view; morphology suggests saturated to soupy or subaqueous substrates | Medium-sized mammal; possibly creodont, condylarth, or smaller perissodactyl such as *Hyrocotherium* | Shallow-water or subaerially exposed fluvial (mainly crevasse) fine-grained arkosic sandstones; high water table, saturated to soupy substrates | White Mountain, Kanda, upper unit | n/a |
| Fig. *6.1.3.* 1G | Vertebrate footprints (mammal) (Suite BC5B) | Indeterminate | Medium-sized mammal tracks preserved as casts in convex hyporelief; ~5–6 cm length, ~5 cm width; best example shows two smaller lateral digits offset towards sides; large, wider and longer central digit; central digit possibly two 'fused' digits; posterior margin slightly pointed; looks digitigrade | Associated with *Planolites* isp., medium-sized wading bird tracks, raindrop impressions/microbial texture, and desiccation cracks | Medium-sized mammal; likely perissodactyl such as *Hyracotherium* | Distal, desiccated crevasse-splay deposits into shallow pools | White Mountain, Kanda, upper unit | n/a |
| Fig. *6.1.3.* 1D, 1E, 1F | Vertebrate footprints (wading bird) (Suite BC5B) | Indeterminate | Medium-sized, four-toed, unwebbed bird footprints with slender, clawed digits; three forward-directed digits with short hallux directed straight backwards or medially; total length ~8 cm, total width ~10 cm; trackway preserved: stride narrow and short, ~11 cm pace length, inside straddle ~3 cm; feet directed forward in trackway, no signs of "waddling"; preserved in convex hyporelief | Associated with microbial mat-like textures, *Vagorichnus* isp., and desiccation cracks | Medium-sized wading bird or larger shorebird | Distal, desiccated crevasse-splay deposits into shallow pools | White Mountain, Kanda, upper unit | n/a |
| n/a | Root casts | n/a | Iron oxide and carbonate casts of roots; typically preserved in cross-section with carbonate internally and yellow and orange iron mineral | | Shrubs or trees | Incipient paleosols in calcareous soils with shallow water tables | White Mountain, Kanda, upper unit | n/a |

| | | | | | | | | |
|---|---|---|---|---|---|---|---|---|
| | | | "rinds"; typically ~2–4 cm diameter and flattened vertically | | | | | |
| Fig. *6.1.3.* 2E, 2F | Iron-stained root-marks (cf. Suite BC4) | n/a | Small, iron-stained root marks consisting of circular iron "rinds" < 2 mm diameter or as irregular, iron-stained "flecks" | Not associated with animal traces except vertebrate tracks in cross-section | Wetland plants | Rooted wetland siltstones and incipient paleosols | White Mountain, Kanda, upper unit | n/a |
| ***Trace fossils from the D-Arkose Bed, Firehole Canyon, Section D1 (divided into lower unit, second unit, "green stripe" unit, and upper unit)*** | | | | | | | | |
| Fig. *6.1.3.* 10F | Simple burrows (Suite BC7?) | Indeterminate | Small (~1–2 mm diameter), short, trail-like traces preserved as hyporelief; appear open | Produced in soupy substrate; possibly just shrinkage marks? | Unknown invertebrate | Delta front at feeder channel during transgression | Firehole Canyon, D1, upper unit | e.g., FC, D1, m ~27.5 |
| Fig. *6.1.3.* 5F, 5G, 5H, 6B, 6C, 8A, 8B | Simple burrows (Suite BC5A) | cf. *Planolites* isp. | Small- to medium-sized (3–5 mm diameter), simple burrows oriented horizontally and vertically; unbranched; unlined/unwalled; fill same as host but appears to be active fill; burrow boundaries distinct but not sharp in some substrates; frequently cross-cutting; preserved in full relief, convex hyporelief, and convex epirelief | Might signify fresh standing water conditions; may have very indistinct burrow boundaries in sandy, soupy substrates; may form *Planolites* ichnofabric | Unknown invertebrate; possibly insect larvae | Preserved in many sandstone facies; associated with delta top, crevasse, or channel sandstones; often interbedded with mudstones | Firehole Canyon, D1, second unit, green stripe unit | e.g., FC, D1, m ~17, m ~24 |
| Fig. *6.1.3.* 5G, 5H | Simple burrows (Suite BC5A) | *Palaeophycus* isp. | Medium-sized (4–5 mm diameter), burrows preserved in full relief; observed from upper bedding plane; dominantly vertically oriented; have dark linings; fill same as host | Cross-cut the *Planolites* ichnofabric | Unknown invertebrate; possibly oligochaetes | Exposed or stable non-deposition surfaces at top of rippled sandstones representing crevasse or levee | Firehole Canyon, D1, second unit | e.g., FC, D1, m ~17 |
| Fig. *6.1.3.* 6C | Simple burrows (Suite BC5B) | cf. *Planolites* isp. | Medium-large (~7–10 mm) simple, unbranched burrows; oriented horizontally and vertically; fill may be same as host (if sandstone) or different from host (if siltstone or mudstone); fill typically sandstone; burrow boundaries sharp; unlined, unwalled | May be associated with large cf. *Taenidium barretti* that cross-cuts *Planolites* ichnofabric | Unknown invertebrate | Crevasse splay or levee sandstone | Firehole Canyon, D1, second unit, green stripe unit | e.g., FC, D1, m ~17, m ~24.5 |
| Fig. *6.1.3.* 5A, 5B, 5D | Full relief burrows (Suite BC1?) | *Planolites* isp. | Medium-large (~7–8 mm diameter) full relief burrows with very indistinct burrow boundaries; fill slightly different colour from host; oriented in all directions | Forms example of larger-sized *Planolites* ichnofabric | Unknown invertebrate | Possibly subaqueous, levee sandstones of distributary (terminal?) channel | Firehole Canyon, D1, second unit | e.g., FC, D1, m ~16 |
| Fig. *6.1.3.* 5A, 5B, | Full relief burrows (Suite BC1?) | Indeterminate | Large (~1–2 cm diameter) full relief burrows with sharp burrow boundaries; may have had burrow lining that eroded differentially; fill | Shares some similarities with Indeterminate horizontal traces | Unknown invertebrate | Possibly subaqueous, levee sandstones of distributary | Firehole Canyon, D1, second | e.g., FC, D1, m ~16 |

| | | | | | | | | |
|---|---|---|---|---|---|---|---|---|
| 5C | | | different from host (coarser) and passive; slightly curved burrows (~1 cm diameter) may expand into circular structures (~2 cm diameter) | from m ~24 (Fig. 9C–E), described below | | (terminal?) channel | unit | |
| Fig. *6.1.3.* 9C, 9D, 9E | Horizontal traces (Suite BC6) | Indeterminate | Medium-large (~8–10 mm diameter) surface traces with expanded (< ~1.5 cm across) circular areas; also associated with circular areas not connected to tunnel-like traces; very smooth boundaries; preserved as casts in convex hyporelief | Could be load structures; associated with desiccation cracks preserved as casts in bed above trace-preserving bed | Unknown; if traces, could be tadpole traces or frog 'nests' | Crevasse sandstone into freshwater delta-plain/floodplain lake | Firehole Canyon, D1, green stripe unit | e.g., FC, D1, m ~24 |
| Fig. *6.1.3.* 9F | Horizontal traces (Suite BC5B) | cf. *Vagorichnus* isp.? | Medium-sized (~5 mm diameter), slightly curving and branched (secondary successive) burrows or surface trails or tunnels; preserved as casts in convex hyporelief; burrow boundaries indistinct; unlined/unwalled; fill same as casting host; burrows/tunnels appear to have been produced in green mudstone | Sample in float from upper part of "green stripe unit" | Unknown invertebrate | Probably crevasse sandstone; sample in float, unknown if into floodplain lake or onto floodplain siltstone | Firehole Canyon, D1, green stripe unit | e.g., FC, D1, m ~24.5+? |
| Fig. *6.1.3.* 9G, 9H | Horizontal traces (Suite BC7?) | Indeterminate | Medium-large (~11 mm diameter) burrows with non-discrete areas of bioturbation; bioturbated area preserves 'sun ray-like' or 'probe-like' traces ~6 mm in diameter); preserved in convex semi-relief (unknown if epirelief or hyporelief) | | Unknown invertebrate; possibly a gastropod | Probably crevasse sandstone; sample in float, unknown if into floodplain lake or onto floodplain siltstone | Firehole Canyon, D1, green stripe unit | e.g., FC, D1, m ~24.5+? |
| Fig. *6.1.3.* 10C, 10D | Backfilled burrows (Suite BC9) | Pellet-filled burrows | Large (~1.2 cm diameter), backfilled burrows with sharp, irregular burrow boundaries; unwalled/unlined; fill appears to be sediment aggregates and may be same as host or darker than host; straight, unbranched, and oriented vertically and horizontally | May be just different preservation of cf. *Taenidium barretti*, but slightly smaller | Unknown invertebrate; possibly adult insect (beetle) | Crevasse sandstones and floodplain siltstones | Firehole Canyon, D1, green stripe unit | e.g., FC, D1, m ~24–25 |
| Fig. *6.1.3.* 7A, 7B, 10E | Bioturbation (Suite BC9) | Indeterminate | Discrete but irregular areas of bioturbation possibly produced by same trace maker as pellet-filled burrows; preserved as convex epirelief; may contain sediment aggregates as 'fill'; associated with pellet-filled burrow ~1.2 cm diameter | Compare with "Irregularly clustered tunnels" of de Gibert and Sáez (2009) | Unknown; possibly adult insects or root structure | Planar bedded crevasse sandstones | Firehole Canyon, D1, green stripe unit | e.g., FC, D1, m ~24–25 |
| Fig. *6.1.3.* 7C, | Backfilled burrows (Suite BC9) | cf. *Taenidium barretti* | Large (~1.5–2 cm diameter), backfilled burrows; may be preserved open with irregular burrow | Associated with basin margin fluvial | Unknown invertebrate; possibly large | Originates from rippled proximal crevasse-splay | Firehole Canyon, D1, green | e.g., FC, D1, m ~24.5, |

| | | | | | | | | |
|---|---|---|---|---|---|---|---|---|
| 7D, 7E, 7F, 10A, 10B | | cf. *Lunulichnus* isp. | boundaries; dominantly oriented vertically and horizontally, occasionally obliquely; may branch; preserved in full relief and as convex hyporelief and convex epirelief; burrow boundaries distinct to sharp; burrow boundary may appear textured due to chippy burrow fill; fill sometimes preserves meniscae and is typically composed of large, angular, sediment-aggregates including mud-chips; fill sometimes may just appear as ~2 cm or more across of bioturbated sandstone without distinct burrow boundaries | environments; appears to signify lower water tables; always last cross-cutting suite where preserved; deepest tier trace observed in entire Formation; in Firehole D1, maximum depth ~0.5 m | adult insect (beetle?), frog, or crustacean | sandstones within floodplain siltstone unit | stripe unit | m ~22.3 and lower; m ~17 |
| Fig. *6.1.3.* 5E | Escape traces (Suite BC5A) | n/a | Medium-sized, straight to curved, vertically oriented escape traces causing bedding to be 'pulled' upwards | Associated with *Planolites* ichnofabric and cf. *Palaeophycus* isp. in upper beds | Unknown invertebrate; possibly oligochaetes | Rippled delta top sandstone | Firehole Canyon, D1, second unit | e.g., FC, D1, m ~17 |
| Fig. *6.1.3.* 7A, 7C | Vertical burrows (Suite BC3A) | *Skolithos* isp. | Very small (~1 mm diameter, < 2 cm depth), straight, unbranched, vertical and oblique burrows preserved in full relief; originate from rippled "pause planes" within sandstone bed; open, but red-stained relative to host rock, possibly clay-lined | Traces appear to have been produced during deposition; cross-cut by large vertical cf. *Taenidium barretti* | Very small invertebrate; possibly chironomid larvae or oligochaetes | Rippled proximal crevasse-splay or channel sandstone | Firehole Canyon, D1, green stripe unit | e.g., FC, D1, m ~22.3 |
| Fig. *6.1.3.* 7B, 7D | Vertical burrows (Suite BC3A) | *Skolithos* isp. | Small-medium-sized (~3–5 mm diameter), open, straight, vertical burrows with distinct burrow boundaries; originated from top of crevasse or channel sandstone unit | | Likely insect, possibly tiger beetle | Rippled proximal crevasse-splay or exposed channel sandstone | Firehole Canyon, D1, green stripe unit | e.g., FC, D1, m ~22.3 |
| Fig. *6.1.3.* 7B | Vertical burrows (Suite BC9) | *Skolithos* isp. | Medium-sized (~7–8 mm diameter) vertical burrows; preserved in full relief, observed from top bedding plane; walls distinct but not sharp; open and passively filled with sediment different from host; may taper downwards from ~1.2 cm wide | | Likely insect or spider | Rippled proximal crevasse-splay or exposed channel sandstone | Firehole Canyon, D1, green stripe unit | e.g., FC, D1, m ~22.3, ~24 |
| Fig. *6.1.3.* 4A | Vertebrate footprints (mammal) (Suite BC4) | Indeterminate | Medium-sized mammal footprints preserved in cross-section; footprints may preserve clear anterior and posterior margins; in best example, total length ~7 cm; total depth ~5 cm | Show wet to soupy substrate; associated with iron-stained root marks | Medium-sized mammal, possibly perissodactyl, e.g., *Hyracotherium* | Freshwater overbank deposits near lake; high water table | Firehole Canyon, D1, lower unit | e.g., FC, D1, m ~5 |

| | | | | | | | | |
|---|---|---|---|---|---|---|---|---|
| Fig. *6.1.3.* 4B, 4C, 4D, 9A, 9B | Vertebrate footprints (mammal) (Suite BC4) | Indeterminate | Medium-large mammal footprints preserved in cross section; indistinct track margins; possibly viewed from anterior or posterior, not side-view; total depth > 12 cm; total width > 10 cm; may be preserved as isolated, irregular, sandstone plugs into mudstone | Associated with greater depths and more disruption of bedding than medium-sized prints in cross-section; depth reflecting substrate conditions | Unknown medium-large sized mammal, possibly hippo-like perissodactyl | Freshwater overbank deposits near lake; high water table | Firehole Canyon, D1, lower unit, green stripe unit | e.g., FC, D1, m ~5, m ~24 |
| Fig. *6.1.3.* 8A–F | Vertebrate footprints (reptile) (Suite BC6) | Indeterminate | Medium-sized reptile footprints preserved as casts in convex hyporelief; both front and hind footprints preserved, as well as elongate, parallel, scratch-marks in groups of three or four; front footprints wider than long, ~6–7 cm wide and ~4 cm long, and may be associated with three clear scratch-marks; hind footprints longer than wide with four digits, ~7 cm wide, ~6–8 cm long | Cross-cut by small *Planolites* isp.; tracks indicate swimming and walking behaviours | Medium-sized crocodilian; some scratch-marks could be from turtles | Freshwater floodplain lake filled with proximal crevasse or channel sandstone | Firehole Canyon, D1, green stripe unit | e.g., FC, D1, m ~24 |
| Fig. *6.1.3.* 8G | Vertebrate footprints (mammal) (Suite BC6) | Indeterminate | Medium-large ?mammal or crocodilian footprint preserved as cast in convex hyporelief; three to four overall rounded digits, but may preserve claw impressions; rounded triangular overall shape; posterior margin rounded but tapered; total length ~13 cm, total width ~10 cm | Could potentially be a large crocodilian hind footprint; cross-cut by small *Planolites* isp., and may also cross-cut *Planolites* isp. | Medium-sized mammal, possibly rhino-like perissodactyl | Freshwater floodplain lake filled with proximal crevasse or channel sandstone | Firehole Canyon, D1, green stripe unit | e.g., FC, D1, m ~24 |
| n/a | Root casts | n/a | Medium-sized (~2–3 cm), roughly circular-shaped carbonate and iron root casts; internally, circle of white carbonate; external rind of iron minerals coloured red, orange, and bright yellow | Associated with carbonate ?nodules, iron-stained root marks, soil peds, and desiccation fractures | Shrubby riparian vegetation | Wet floodplain to riparian areas | Firehole Canyon, D1, second unit | e.g., FC, D1, m ~9 |
| Fig. *6.1.3.* 4A | Iron-stained root-marks (cf. Suite BC4) | n/a | Small (~1–2 mm), circular to irregular-shaped, iron-stained root marks; iron stains similar to rinds; internal circle just host material; always cross-cut original deposition | Associated with vertebrate tracks in cross-section and with larger carbonate root casts | Wetland vegetation, possibly *Equisetum* or similar plants | Wet floodplain marsh, lake-fringing marsh, and/or riparian marsh | Firehole Canyon, D1, lower unit, second unit | e.g., FC, D1, m ~4 |

***Trace fossils from the D-Arkose Bed, Firehole Canyon, Section D2 (divided into second unit, "green stripe" unit, and upper unit)***

| | | | | | | | | |
|---|---|---|---|---|---|---|---|---|
| Fig. *6.1.3.* 11D, 12C, 12E, 12F | Horizontal trails (Suite BC7) | *Helminthoidichnites* isp. | Very small (1–2 mm diameter), straight to gently curving, unbranched trails or tunnels preserved in concave and convex epirelief | Associated with backfilled burrows, and with microbial 'bubble' texture and desiccation cracks | Possibly oligochaete or insect larvae (e.g., dipteral) | Desiccated overbank deposits and abandoned channel tops | Firehole Canyon, D2, upper unit | e.g., FC, D2, m ~8.8, m ~12.5 |
| Fig. *6.1.3.* 11B, 11C | Horizontal burrows (Suite BC6) | *Planolites* isp. | Small (~2–4 mm diameter) vertically and horizontally oriented burrows preserved as casts in convex hyporelief; burrow boundaries distinct; burrows produced in green mudstone, filled by buff very fine-grained sandstone | Not associated with desiccation features | Possibly oligochaete or insect larvae | Waning flow or standing water deposits in channel | Firehole Canyon, D2, upper unit | e.g., FC, D2, m ~8.5 |
| Fig. *6.1.3.* 11C, 11D, 11E, 12F | Horizontal burrows (Suite BC8A) | *Planolites* isp. | Small (~3 mm diameter), horizontal and vertical burrows; straight to slightly curving; fill same as host; preserved in convex epirelief and full relief; burrow boundaries distinct but not sharp; unwalled/unlined; appear to have been actively filled | Associated with backfilled burrows | Unknown invertebrate; possibly oligochaete, probably insect | Desiccated overbank deposits; may be associated with weakly developed paleosol | Firehole Canyon, D2, upper unit | e.g., FC, D2, m ~11.5, m ~12.5 |
| Fig. *6.1.3.* 12C, 12E | Meniscate backfilled burrows (Suite BC8A) | ? *Taenidium* isp. | Small (~3 mm diameter), dominantly horizontal, backfilled burrows preserved in epirelief; fill possibly meniscate, but not well preserved; burrow boundaries distinct and may be sharp; unbranched; may cross-cut | Traces preserved on sandstone interbed within pedogenically modified green siltstone | Unknown invertebrate; possibly oligochaete or insect | Desiccated overbank deposits; may be associated with weakly developed paleosol | Firehole Canyon, D2, upper unit | e.g., FC, D2, m ~11.5 |
| Fig. *6.1.3.* 12B | Ornamented full relief burrows (Suite BC8A) | cf. *Scoyenia* isp. | Medium-large (~8 mm diameter) full relief burrow with longitudinal scratch-like ornamentation; 'scratches' near parallel and < 2 cm long; fill same as host; unwalled/unlined | May possibly be a cast of a reed with longitudinal ribs | Unknown; probably adult insect, possibly a reed cast | Desiccated overbank deposits; may be associated with weakly developed paleosol | Firehole Canyon, D2, upper unit | e.g., FC, D2, m ~11.5 |
| Fig. *6.1.3.* 12C, 12E | Backfilled burrows (Suite BC8A) | Pellet-filled burrows | Small- to medium-sized (~3–4 mm diameter) backfilled, dominantly horizontal burrows; fill composed of sediment aggregates; straight to slightly curving; burrows full relief; preserved in convex epirelief; burrow boundaries distinct and may be sharp; unbranched but may cross-cut | Just slightly smaller version of pellet-filled burrows | Likely insect, possibly beetle | Desiccated overbank deposits; may be associated with weakly developed paleosol | Firehole Canyon, D2, upper unit | e.g., FC, D2, m ~11.5 |
| Fig. *6.1.3.* 12D, 12E | Backfilled burrows (Suite BC8A) | Pellet-filled burrows | Medium-sized (~5–6 mm diameter), backfilled, dominantly horizontal burrows; fill composed of sediment aggregates; straight to slightly | Just slightly larger version of pellet-filled burrows | Likely insect, possibly beetle | Desiccated overbank deposits; associated with weakly developed paleosol | Firehole Canyon, D2, upper unit | e.g., FC, D2, m ~11.5 |

| | | | | | | | | |
|---|---|---|---|---|---|---|---|---|
| | | | curving; moving in and out of bedding plane; burrows full relief; preserved in convex epirelief; burrow boundaries distinct and may be sharp; unbranched but may cross-cut | | | | | |
| Fig. *6.1.3.* 11A | Passively filled burrows (Suite BC1?) | Indeterminate | Medium-sized (~3–7 mm diameter), vertically oriented and compacted burrows with variable diameter into organic-rich mudstone; fill passive with carbonate matrix mudstone from intraclast conglomerate; burrows extend from bottom contact of intraclast conglomerate bed; burrows may have an expanded circular termination ~1.2 cm wide | Associated with an event-bed intraclast conglomerate | Unknown invertebrate | Intraclast conglomerate event-bed possibly representing a transgressive lag | Firehole Canyon, D2, green stripe unit | e.g., FC, D2, m ~4.4 |
| ***Trace fossils from the E-Arkose Bed, Firehole Canyon, Section D2-E2*** | | | | | | | | |
| Fig. *6.1.3.* 12H | Horizontal trails (Suite BC7) | cf. *Helminthoidichnites* isp. | Medium-sized (~4 mm diameter), horizontal, unbranched, trail or tunnel preserved in concave epirelief; burrow boundaries irregular | Associated with *Planolites* burrows; possibly produced by gastropod; wet to soupy substrate | Unknown invertebrate; possibly insect larvae or adult | Distal or waning crevasse-splay deposits onto floodplain | Firehole Canyon, E2 | e.g., FC, D2, m ~23.2 |
| Fig. *6.1.3.* 12H | Simple burrows (Suite BC7) | *Planolites* isp. | Small-medium-sized (~3.5 mm diameter), horizontal and vertically oriented, unbranched burrows; preserved in epirelief; filled with sandy host material; burrow boundaries distinct but not sharp; appear to have been actively filled | Associated with extremely low amplitude ripple bedforms | Unknown invertebrate; likely insect larvae or adult | Distal or waning crevasse-splay deposits onto floodplain | Firehole Canyon, E2 | e.g., FC, D2, m ~23.2 |
| Fig. *6.1.3.* 12H | Backfilled burrows (Suite BC9) | cf. Pellet-filled burrows | Medium-sized (~6 mm diameter), vertically oriented backfilled burrow; burrow boundaries distinct but irregular; fill of host material and appears to be of sediment aggregates | | Unknown invertebrate; likely insect larvae or adult | Desiccated distal crevasse-splay deposits onto floodplain | Firehole Canyon, E2 | e.g., FC, D2, m ~23.2 |
| Fig. *6.1.3.* 12G | Backfilled burrows (Suite BC9) | cf. *Taenidium barretti* | Large (~1.5 cm diameter), vertically oriented, open burrow with ‘lumpy’, irregular internal burrow boundary texture; burrow boundary clear, but slightly indistinct | | Unknown invertebrate; possibly large adult insect (beetle?), frog, or crustacean | Crevasse sandstones onto floodplain | Firehole Canyon, E2 | e.g., FC, D2, m ~23 |
| n/a | Vertebrate footprints (mammals) (Suite BC4) | Indeterminate | Medium-sized (~5 cm width), possible mammal footprint preserved in cross-section | Overlies discontinuously laminated greenish brown siltstone | Unknown medium-sized mammal | Crevasse sandstones onto wet floodplain near lake | Firehole Canyon, E2 | e.g., FC, D2, m ~26.5 |

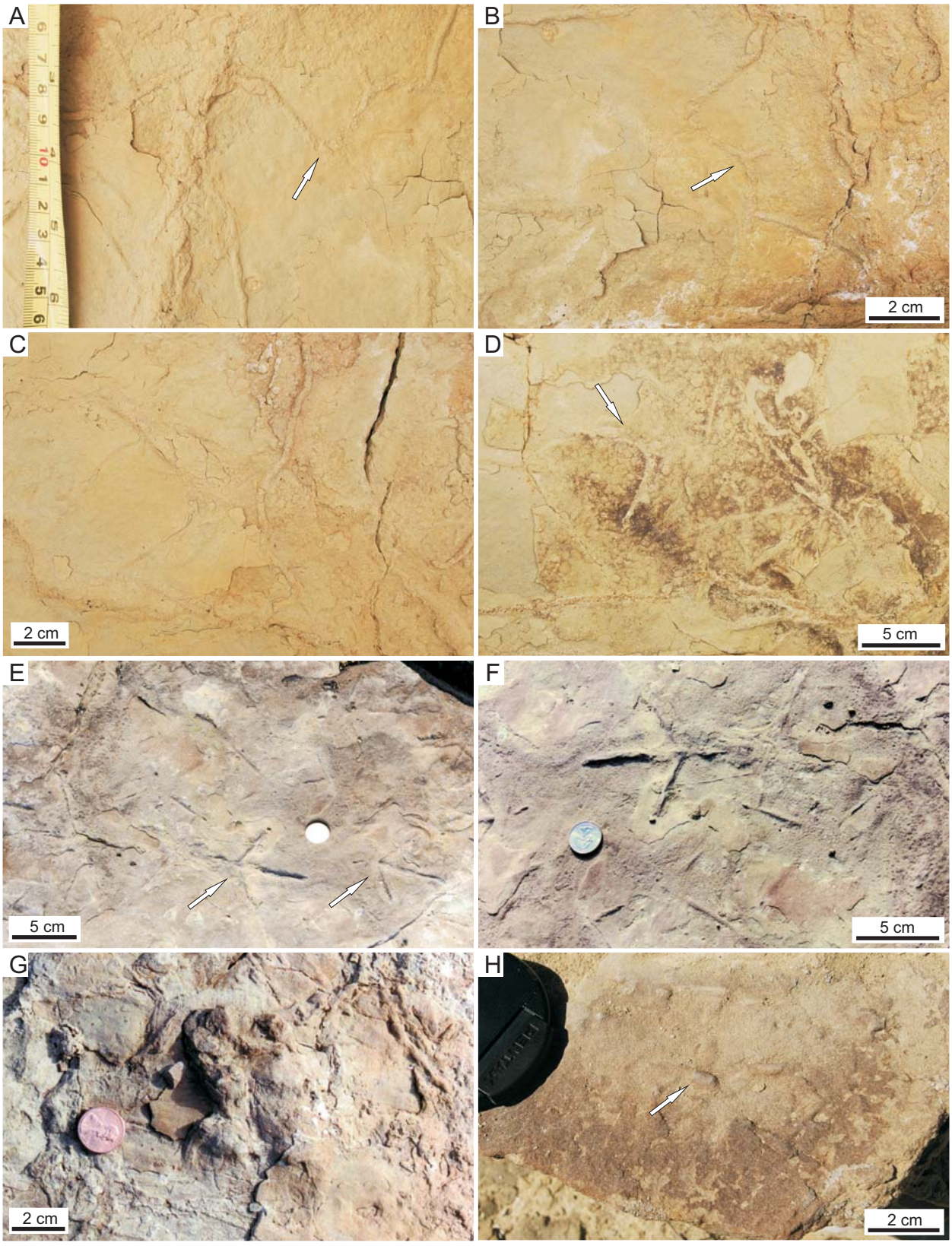


**Fig. 6.1.3.1.** Animal traces in the D-Arkose Bed at White Mountain, Kanda (upper unit) (Suite BC5). Refer to Table 6.3 for descriptions of traces shown. See caption two pages ahead.

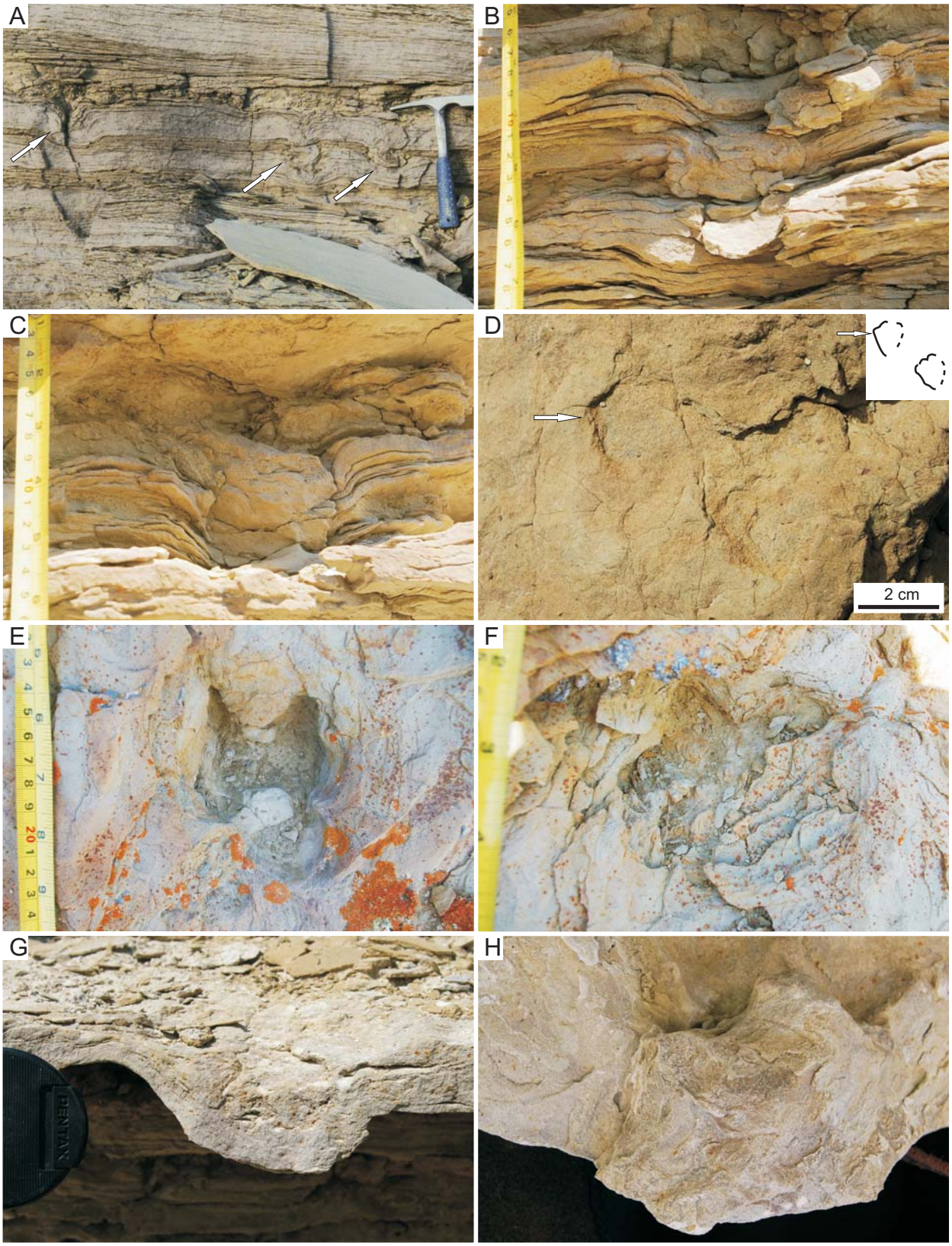


**Fig. 6.1.3.2.** Mammal footprints in the D-Arkose Bed at White Mountain, Kanda (upper unit) (Suites BC4 and BC5B). Refer to Table 6.3 for descriptions of traces shown. See caption on next page.

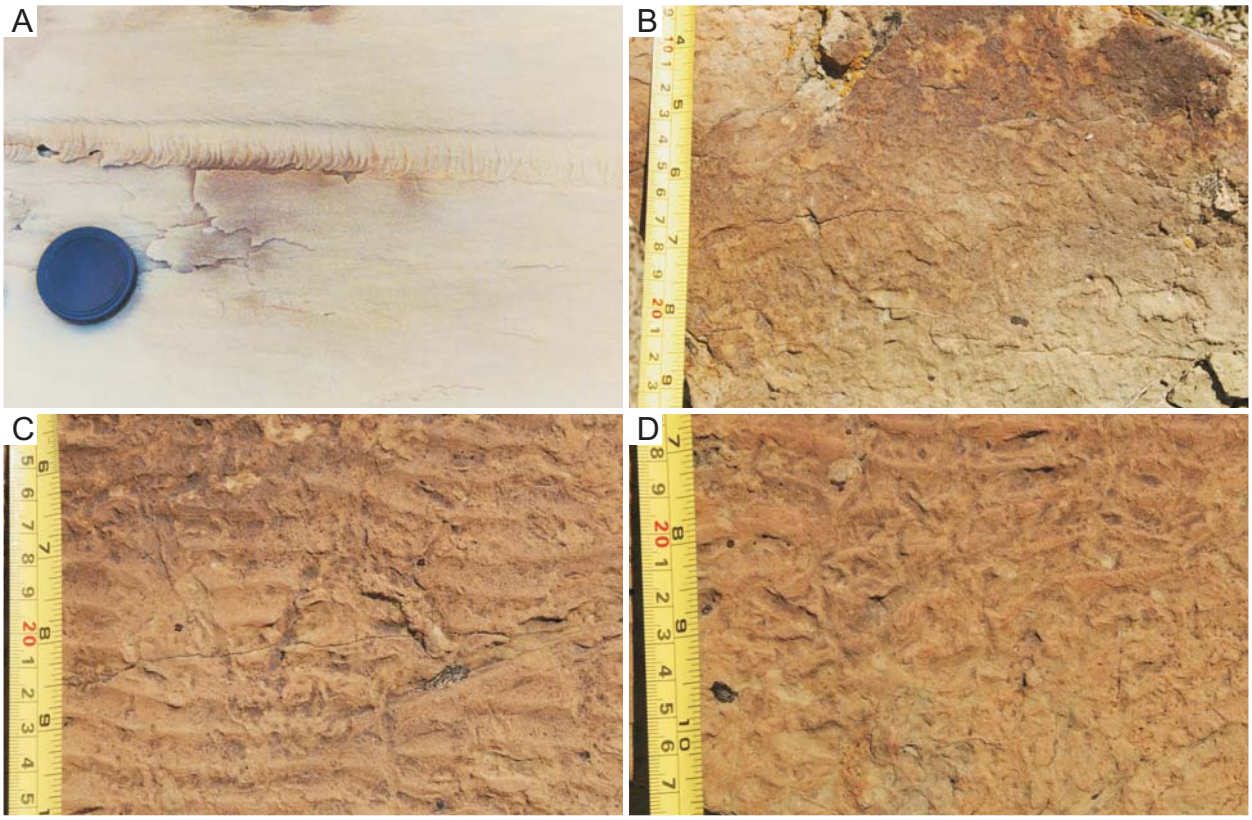


**Fig. 6.1.3.3.** Animal traces in the D-Arkose Bed at White Mountain, Kanda (upper unit) (Suite BC7). Refer to Table 6.3 for descriptions of traces shown. **(A)** Horizontal meniscate backfilled burrow with appendage scratch-like marks along burrow boundary. **(B–D)** Bioturbation of upper surface of rippled channel sandstone with some discrete burrows with indistinct burrow boundaries.

**Fig. 6.1.3.1.** (Two pages back) Animal traces in the D-Arkose Bed at White Mountain, Kanda (upper unit) (Suite BC5). (A–C) Partially pellet-backfilled, branching burrows preserved in convex hyporelief. (D) Bird tracks (arrow) and bubble-like surface texture preserved on base of bed. (E–F) Heron-like bird trackway (arrows in E) preserved as casts on base of bed. (G) Mammal footprint preserved as cast on base of bed, possibly produced by horse-like perissodactyl. (H) Simple burrows (arrow) on upper bedding plane.

**Fig. 6.1.3.2.** (Previous page) Mammal footprints in the D-Arkose Bed at White Mountain, Kanda (upper unit) (Suites BC4 and BC5B). Refer to Table 6.3 for descriptions of traces shown. **(A)** Disrupted planar beds due to mammal trackway (arrows). **(B–C)** Mammal footprints in cross section showing sharp boundaries to disrupted area and slight push-up rims at edges of tracks. **(D)** Shallowly impressed small mammal footprints on bedding plane. **(E–F)** Mammal footprints in plan view, produced in soupy substrate. Note splay of digits in (E). **(G–H)** Mammal footprint in cross-section (G) and from below (H).

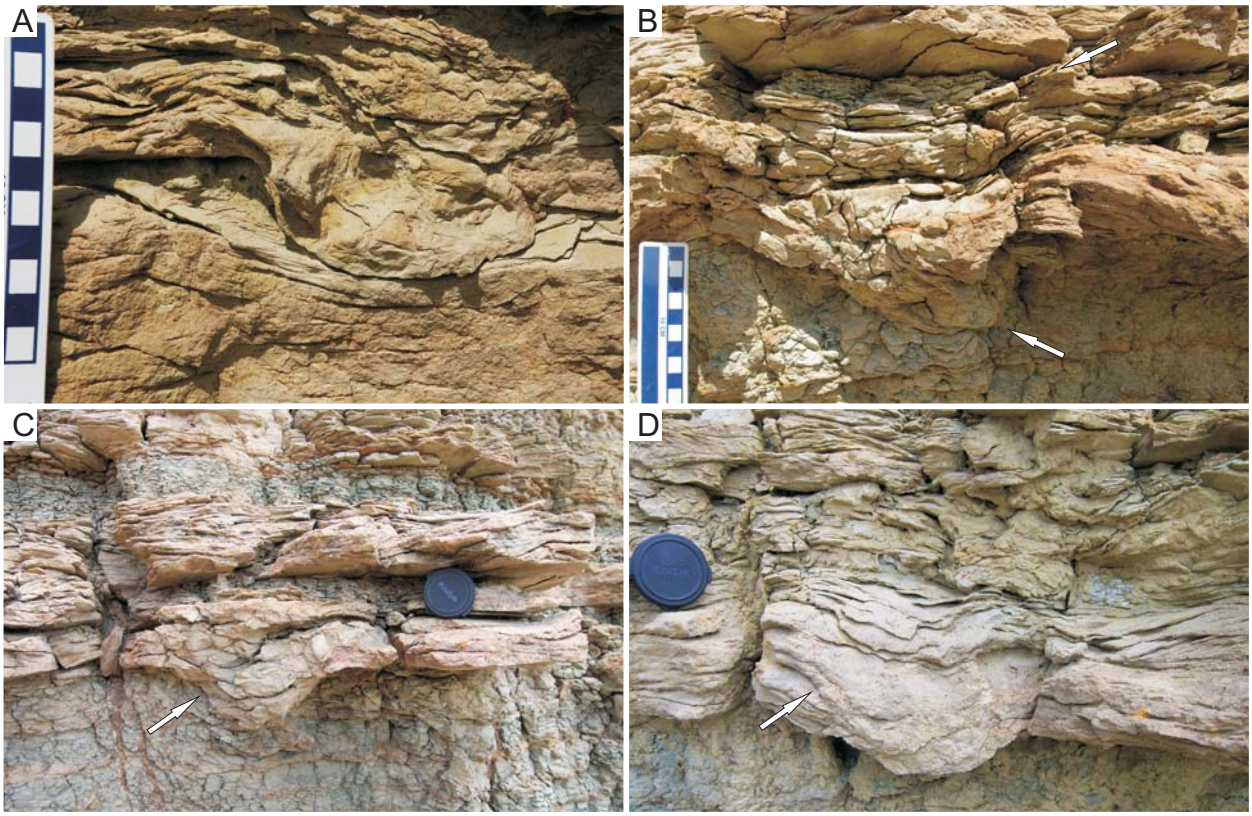


**Fig. 6.1.3.4.** Mammal tracks in the D-Arkose Bed at Firehole Canyon (FC, D1) (lower unit) (Suite BC4). Refer to Table 6.3 for descriptions of traces shown. **(A–D)** Footprints in cross-section (arrows) in heterolithic facies of the lower

**Fig. 6.1.3.5.** (Next page) Animal traces in the D-Arkose Bed at Firehole Canyon (FC, D1) (second unit) (Suites BC1 and BC5A). **(A–D)** Soft-substrate burrows and bioturbation in possible levee sandstone unit. (E) Escape traces (arrows) in cross-bedded sandstone. **(F–H)** Soft-substrate *Planolites* ichnofabric with some lined *Palaeophycus* (G, H) visible on upper bedding plane.

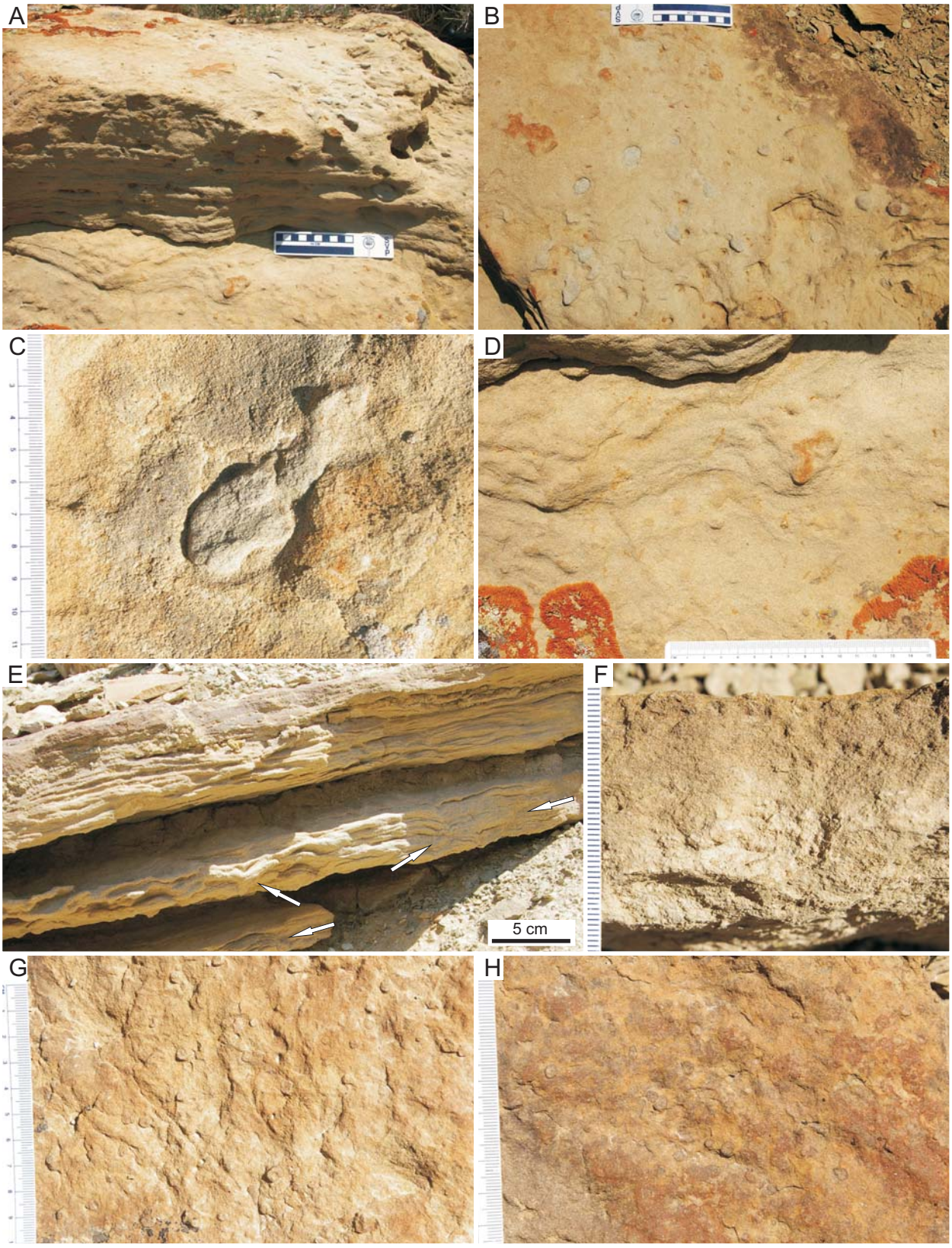


**Fig. 6.1.3.5.** Animal traces in the D-Arkose Bed at Firehole Canyon (FC, D1) (second unit) (Suites BC1 and BC5A). Refer to Table 6.3 for descriptions of traces shown. See full caption previous page.

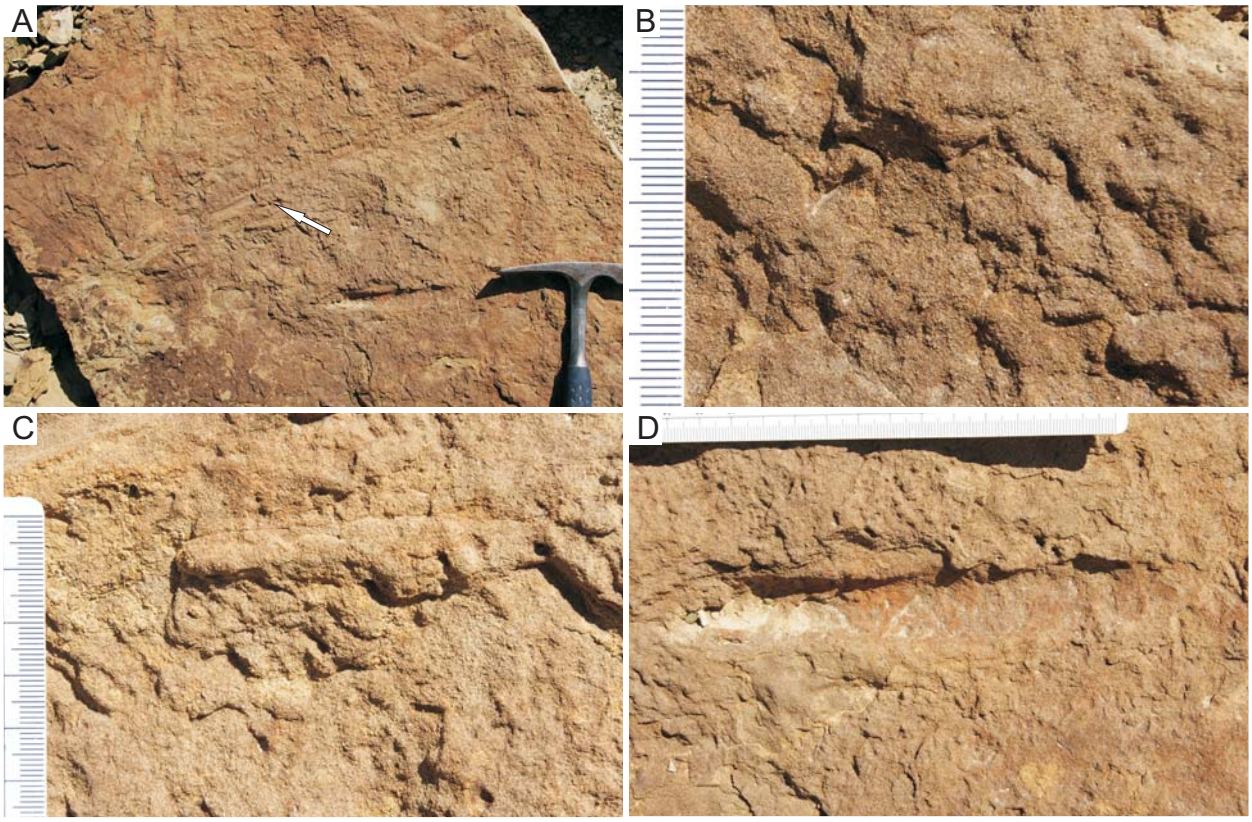


**Fig. 6.1.3.6.** Animal traces in the D-Arkose Bed at Firehole Canyon (FC, D1) (second unit) (Suites BC5A and BC9). Refer to Table 6.3 for descriptions of traces shown. **(A–D)** Bioturbated sandstone (*Planolites* ichnofabric) with large *Palaeophycus* (C), and large plant impressions (arrow in A) and horizontal, sharp-walled, large open burrows (close-up in D).

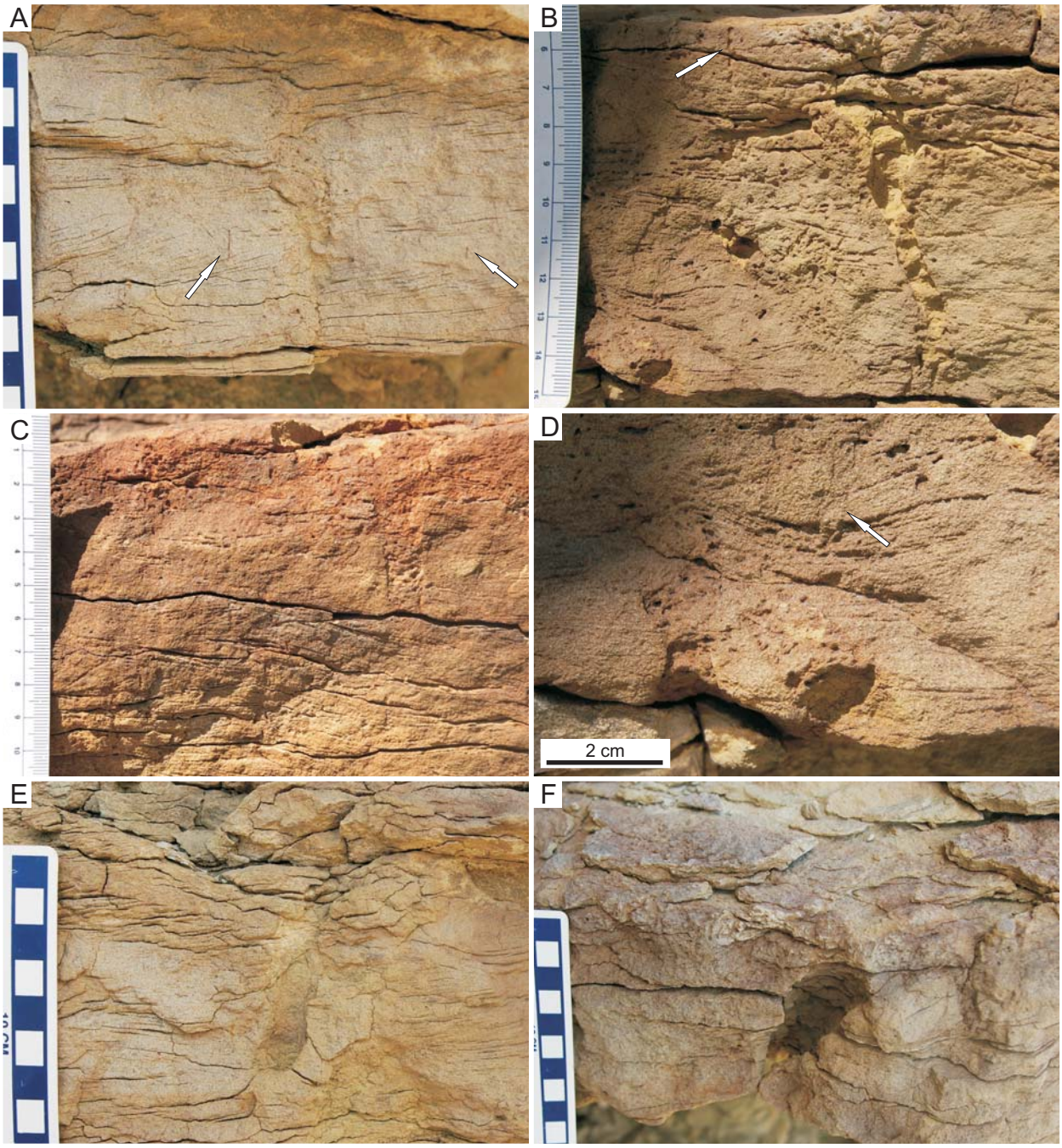


**Fig. 6.1.3.7.** Animal traces in the D-Arkose Bed at Firehole Canyon (FC, D1) (green stripe unit, lower) (Suites BC3 and BC9). Refer to Table 6.3 for descriptions of traces shown. **(A–F)** Cross-laminated sandstone with very small, small, and medium-sized vertical burrows originating from several bedding planes (arrows), cross-cut by root-like "clustered tunnels" (in A and B), large vertical burrows (B), and large backfilled and open burrows (C–F).

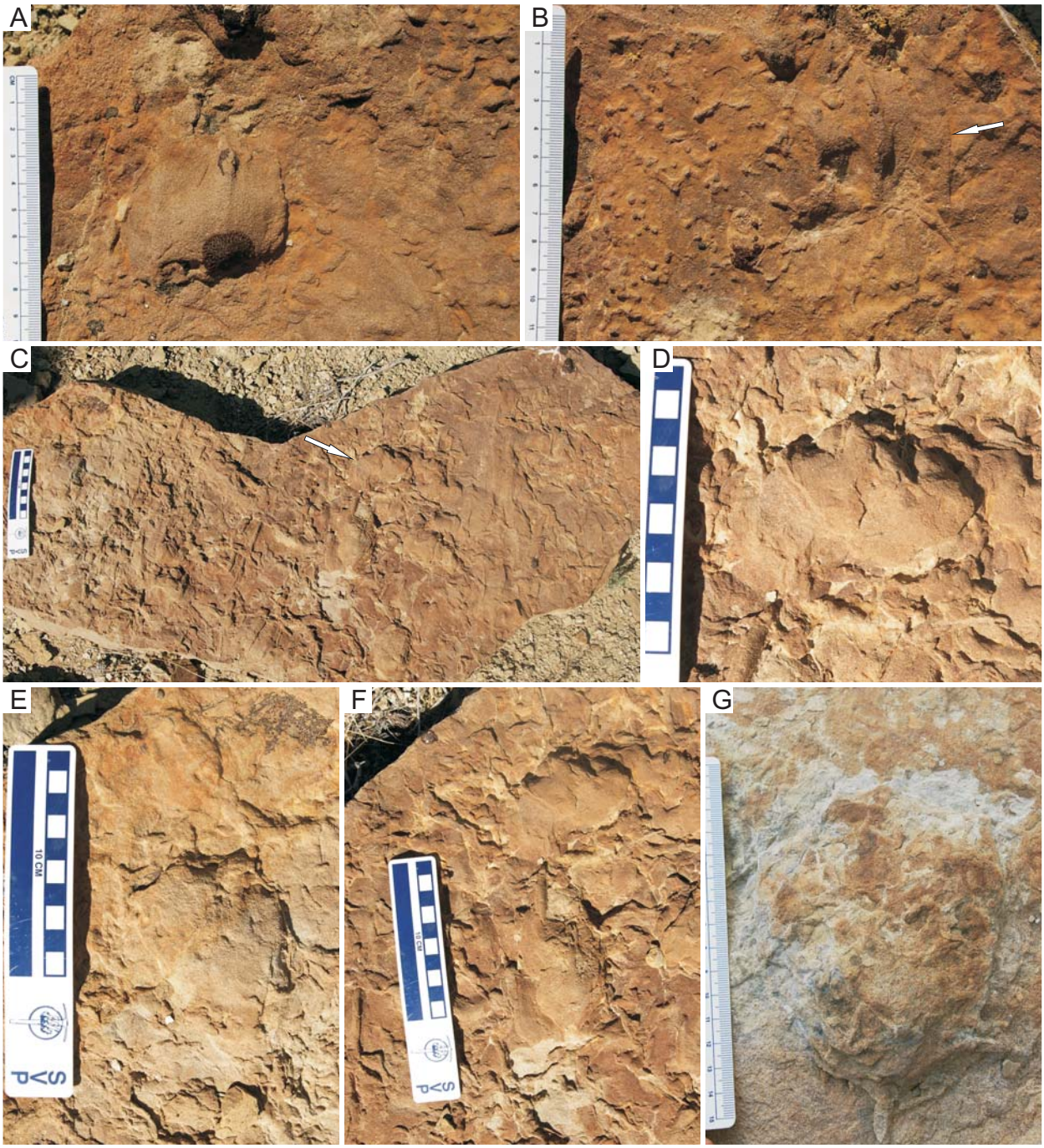


**Fig. 6.1.3.8.** Animal traces in the D-Arkose Bed at Firehole Canyon (FC, D1) (green stripe unit, upper) (Suite BC6). Refer to Table 6.3 for descriptions of traces shown. **(A–F)** Vertebrate tracks attributed crocodilians preserved as casts (arrows in B and C, close-ups in A, D, E, and F), with simple burrows with sharp burrow boundaries. **(G)** Vertebrate track produced by a mammal or crocodilian.

**Fig. 6.1.3.9.** (Next page) Animal traces in the D-Arkose Bed at Firehole Canyon (FC, D1) (green stripe unit, upper) (Suite BC4, BC6, and BC5B). **(A–B)** Large mammal footprints in cross-section (arrows). **(C–E)** Indeterminate traces preserved on lower bedding plane (arrow in C), with circular expanded areas and smooth burrow boundaries. **(F)** Branched, horizontal burrows preserved in convex hyporelief. **(G–H)** Ray-like (G) traces and surface bioturbation (H) on bedding plane.

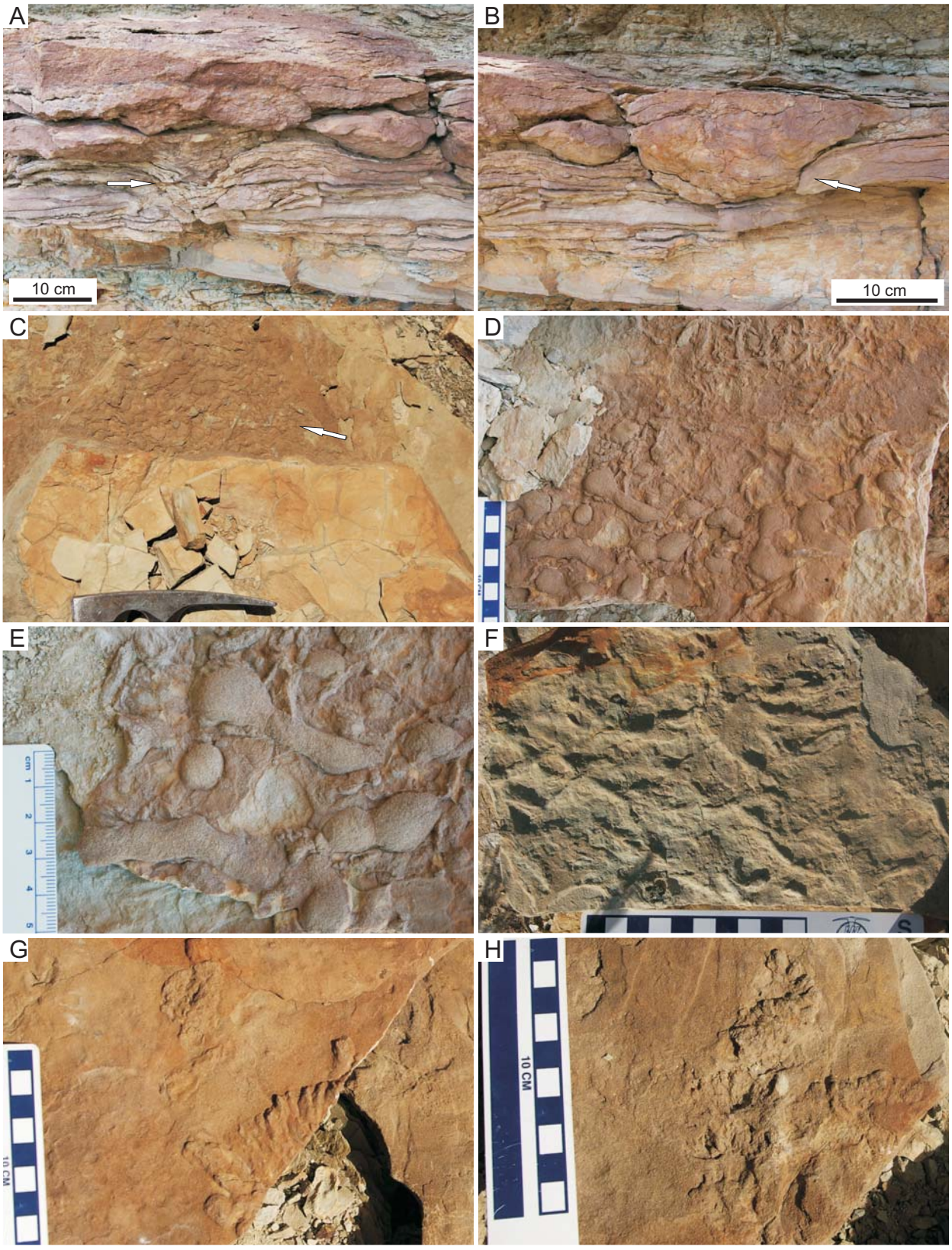


**Fig. 6.1.3.9.** Animal traces in the D-Arkose Bed at Firehole Canyon (FC, D1) (green stripe unit, upper) (Suite BC4, BC6, and BC5B). Refer to Table 6.3 for descriptions of traces shown. See full caption previous page.

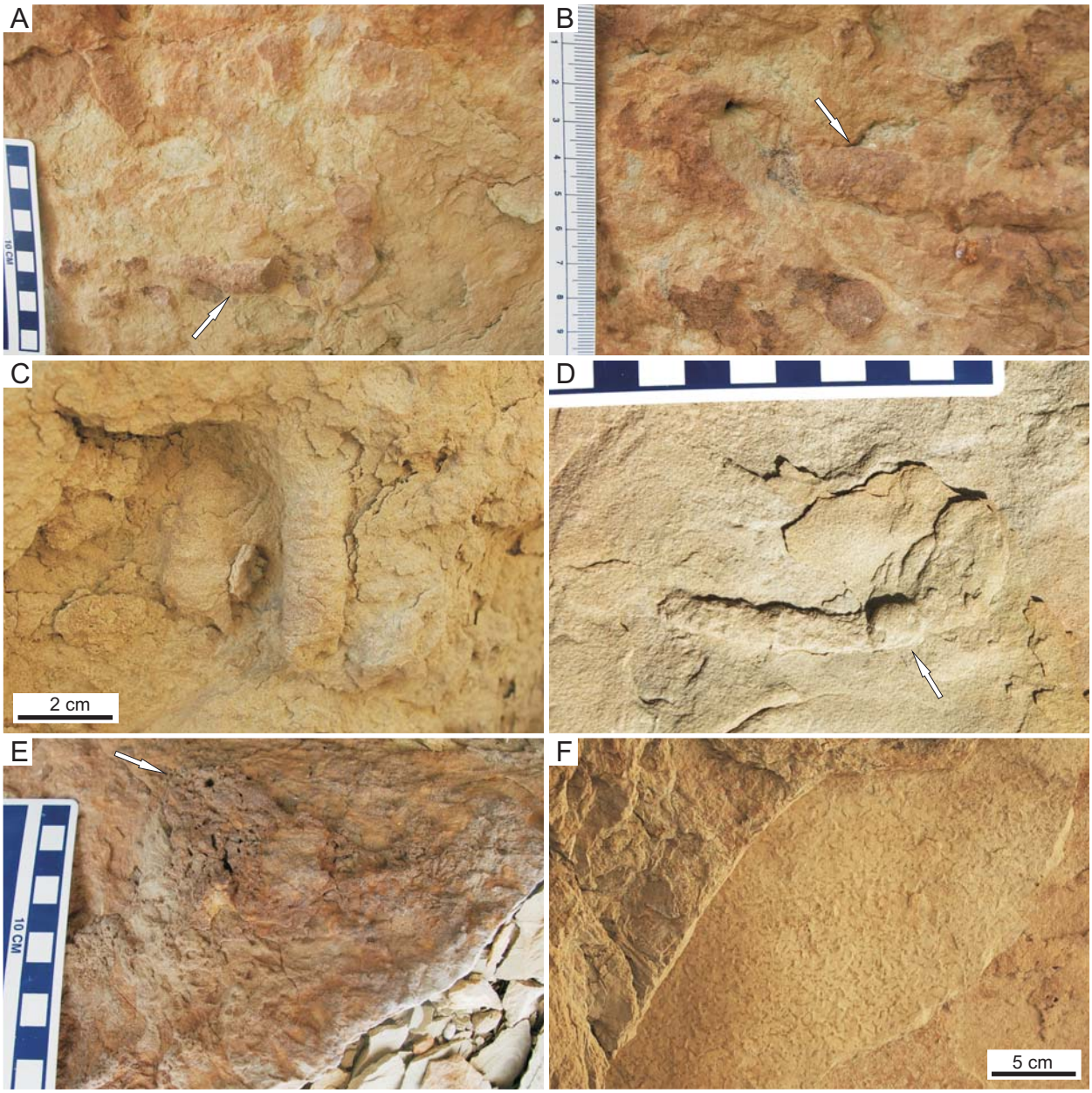


**Fig. 6.1.3.10.** Animal traces in the D-Arkose Bed at Firehole Canyon (FC, D1) (upper unit) (Suites BC9 and BC7?). Refer to Table 6.3 for descriptions of traces shown. **(A–B)** Large, pellet-backfilled horizontal burrows (arrows). **(C)** Vertically oriented pellet-backfilled burrow. **(D)** Vertical branch of horizontally oriented pellet-backfilled burrow with circular cross-section (arrow). **(E)** Root "cluster" open burrows (arrow). **(F)** Very small horizontal traces on lower bedding plane.

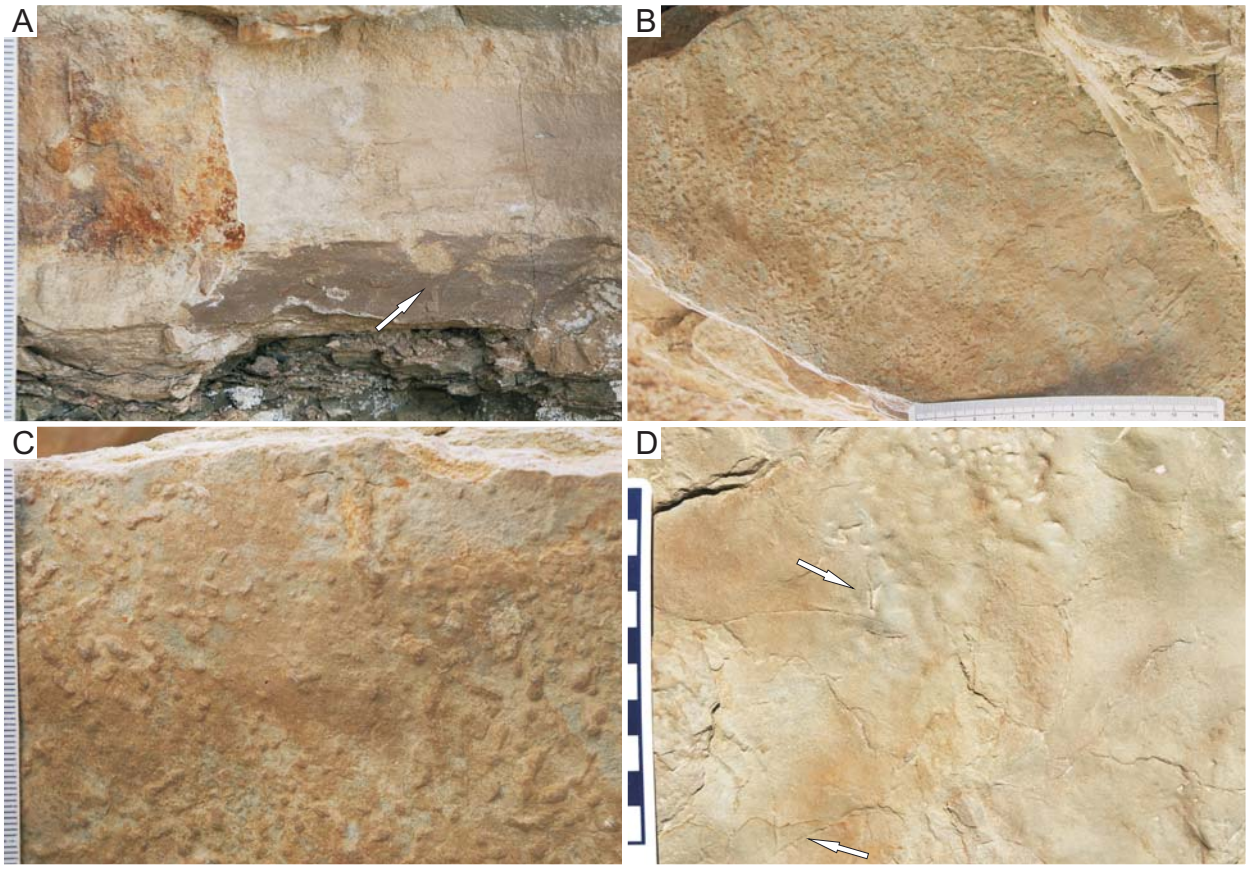


**Fig. 6.1.3.11.** Animal traces in the D-Arkose Bed at Firehole Canyon (FC, D2) (green stripe and upper units) (Suites BC1?, BC6, and BC7). Refer to Table 6.3 for descriptions of traces shown. **(A)** Possible burrow (arrow) in organic-rich lacustrine mudstone below carbonate intraclast conglomerate horizon in the "green stripe" unit. **(B–C)** Simple burrows with sharp burrow boundaries preserved at base of sandstone beds. **(D)** Surface trails preserved on upper bedding plane of heterolithic facies.

**Fig. 6.1.3.12.** (Next page) Animal traces in the D-Arkose Bed and the E-Arkose Bed at Firehole Canyon (FC, D2) (upper unit of D-Bed and E-Bed) (Suites BC7, BC8, and BC9). Refer to Table 6.3 for descriptions of traces shown. **(A)** Weakly pedogenically modified and bioturbated sandstone of the upper D-Bed (m ~11.5). **(B)** Close-up of bioturbated sandstone in upper unit with larger burrow preserving longitudinal ornamentation (cf. *Scoyenia*) (arrow). **(C–E)** Horizontally oriented small backfilled burrows on sandstone bedding plane of upper, pedogenically modified D-Bed (P=pellet-fille burrows; Pl=*Planolites*, ?T=?*Taenidium*). **(F)** Surface trails (arrows) on rippled upper bedding plane in the upper D-Bed (m ~12.5). **(G–H)** Burrows in the E-Bed. (G) shows large vertical burrow cross-cutting irregularly-bedded sandstone. (H) shows vertically oriented., pellet-backfilled burrow (arrow) in laminated siltstone.

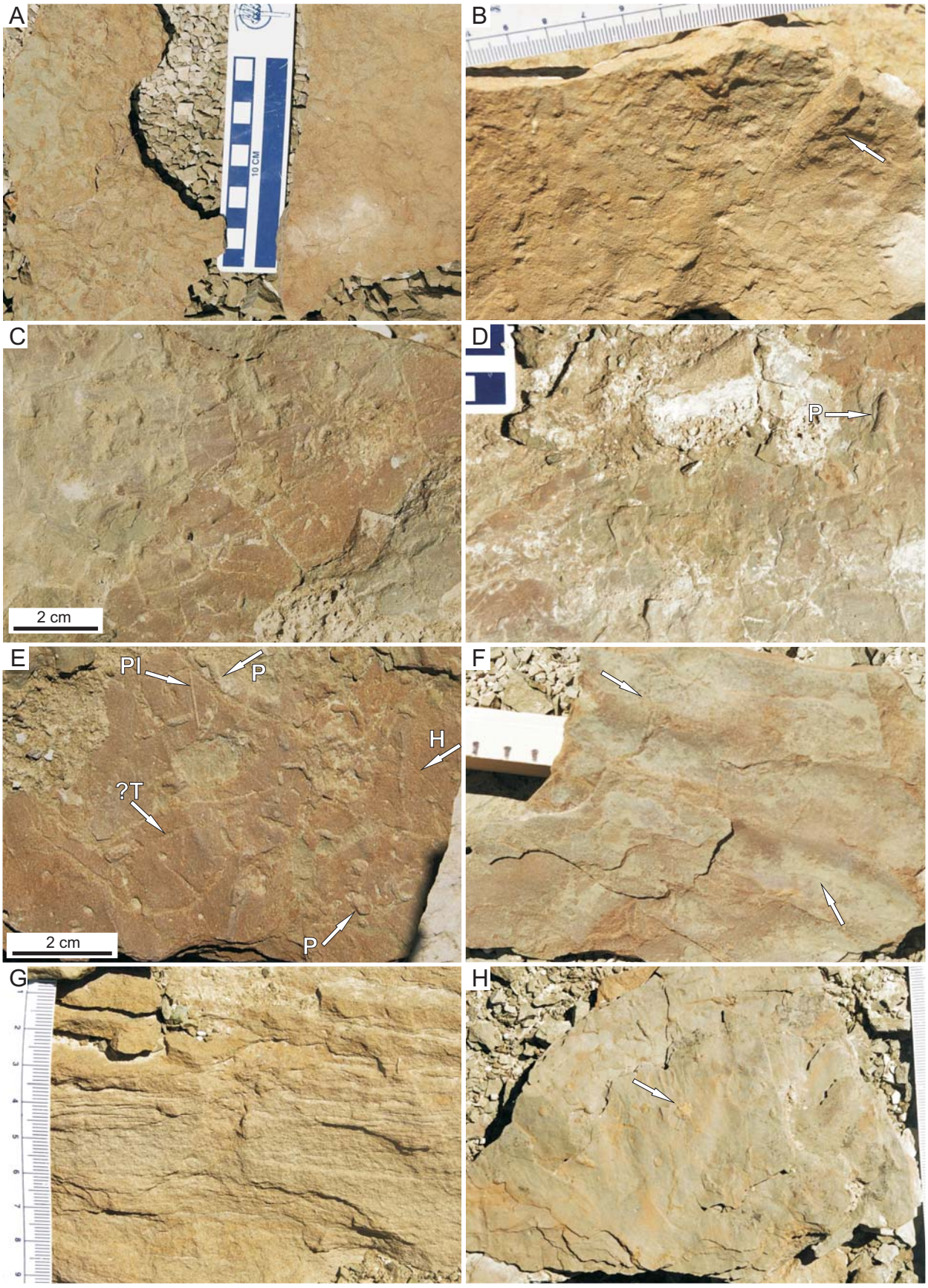
A
10 CM
B
C
2 cm
D
P
E
Pl
P
H
?T
2 cm
P
F
G
H

## 6.2. Basin Centre Trace Fossil Suites

Table 6.4 summarizes the main features of the basin centre trace fossil suites and their associated lithofacies. Nine suites of trace fossils were recognized from the basin centre localities investigated, representing a variety of environmental conditions (e.g., salinity, subaerial exposure, water table depth) and depositional settings (e.g., mudflats, ephemeral pools, fluvial channels). Some of the suites were divided into pre-desiccation and post-desiccation sub-suites based on differences in environmental conditions represented by associated desiccation features (e.g., desiccation cracks, carbonate crusts, interpreted lower water table). Non-distinct ichnotaxa were present in several assemblages. For instance, simple full-relief burrows (*Planolites* isp.) were included in several of the suites, and probably represent traces formed by several different animals (e.g., oligochaetes, insect larvae). Where abundant and forming a high density *Planolites* ichnofabric (BI=3–6) in soft substrates (e.g., Suites BC1, BC5A, BC6), they are interpreted as representing relatively freshwater conditions, and were likely produced subaqueously and/or in saturated substrates. Other examples of *Planolites* isp., formed in subaerial and desiccating, firmer substrates, probably also represent areas with relatively fresh pore-waters (e.g., Suites BC7, 8, 9). The following sections summarize and discuss the significance of each of the trace suites.

### *6.2.1. Suite 1 (BC1): Littoral to Eulittoral Full-relief Burrows*

Bioturbation of lacustrine carbonates is uncommon, particularly within the more typical Wilkins Peak saline lake facies. However, full-relief burrows were produced in sediments interpreted as representing relatively freshwater areas of Lake Gosiute or the lower delta-plain where fluvial facies are closely associated with lacustrine facies. Examples of Suite BC1 were preserved in a few different lithofacies of the A-Arkose Bed and the D-Arkose Bed, all interpreted as being near the shoreline, sub-lacustrine, or in fluvial facies that were closely associated with the main lake. The full-relief traces included in this suite were vertically oriented, and showed both indistinct burrow boundaries in soft sandstone substrates and distinct burrow boundaries in finer-grained or heterolithic facies. Total bioturbation of soft substrates produced mottled textures with rare discrete burrows. Examples of Suite BC1 are described below.

In lacustrine facies most similar to the typical Wilkins Peak within the A-Bed (the "white stripe" unit), discrete full-relief burrows (*Planolites* isp.) were preserved in wavy- and lenticular-bedded carbonate mudstones and calciclastic siltstones (e.g., MFC, A, m ~3.7–4; Fig. *6.1.1.*11A–D). The burrows were produced into carbonate mudstones and were filled from overlying interbeds that had been briefly subaerially exposed, evidenced by their association with desiccation cracks (e.g., SCC, A, m ~4.0; Fig. *6.1.1.*11F). The burrows are small (~3 mm diameter), have sharp burrow boundaries but are unwalled/unlined, and were filled by calciclastic siltstone. It is unknown whether they were filled passively or actively into the mudstone from the overlying siltstone. The presence of these burrows implies lower salinities of the lake and substrate pore waters. Lithofacies indicators, such as interbedded arkosic mudstones or marls with calciclastic siltstones also suggest that there was freshwater input to the lake, or nearby freshwater environments, during these intervals. However, the close association of trona fan evaporite moulds in the calciclastic siltstone interbeds (e.g., SCC, A, m ~4–5) shows that the pore waters were likely at least hyposaline (3–20 g $L^{-1}$) or mesosaline (20–50 g $L^{-1}$), following the terminology of Hammer (1986), and may have undergone evaporative concentration during subaerial exposure.

This trace suite is also represented in the lower unit of the A-Bed in Middle Firehole Canyon (e.g., MFC, A, m ~0.3–2.4; Fig. *6.1.2.*1A–E), where it is represented mainly by

**Table 6.4.** Summary of trace fossil assemblages in the "Basin Centre" of the Wilkins Peak Member, Green River Formation, Bridger basin, Wyoming.

| Trace Suite # | Trace fossil assemblage summary | Key associated sedimentary features | Lithofacies association | Interpretation | Examples |
|---|---|---|---|---|---|
| Suite BC1 *Relatively Freshwater Littoral to Eulittoral Full Relief Burrows* | – Full relief burrows with indistinct burrow boundaries oriented in all directions, may totally bioturbate horizons within substrate<br>– Examples of simple full relief burrows with distinct, but not sharp, burrow boundaries are small to medium-sized (~3–5 mm and 6–10 mm diameter)<br>– Two morphotypes of *Planolites* isp. (indistinct or distinct) dependant on substrate: distinct burrow boundaries in heterolithic facies (cf. *Palaeophycus*); indistinct burrow boundaries in sandy facies<br>– Includes possible *Thalassinoides* isp. A burrow attributed to prawns and large (< 4cm) branching burrows with small (~4 mm) branches<br>– May be associated with escape burrows and/or bird footprints? in cross section<br>– Traces within this suite may be vertically oriented<br>– No overprinting of trace fossil suites observed, except for presence of mammal tracks (BC2) on desiccated bed top of carbonate beach facies | – Highly bioturbated examples produces 'mottled' texture<br>– Irregular, vague bedding due to bioturbation<br>– Brecciation of laminated substrate due to bioturbation<br>– Desiccation cracks<br>– Small-scale dewatering structures<br>– Close lateral or vertical association between carbonate lake facies and freshwater fluvial or sheetflood facies | – Greyish green marlstone to light greenish tan arkosic siltstone; internally massive, weakly bedded, or horizontally bedded<br>– Bioturbated laminated facies appear brecciated<br>– Associated with fining upwards beds of siltstone and mudstone, with planar to slightly inclined laminae in siltstone at base, to structureless mudstone with narrow desiccation cracks at bed tops<br>– One example in small-scale trough cross-laminated and low-angle planar cross-laminated calciclastic sandstone<br>– May be associated with plane-bedded and convoluted fine-grained sandstone | – Shallow muddy lacustrine that may undergo brief periods of subaerial exposure<br>– Close association between carbonate lake facies and fluvial/sheetflood arkosic siltstones and sandstones suggests mixed chemistry and relatively fresh lake waters<br>– Traces observed in facies representing initial progradation of arkosic fluvial system into saline carbonate lake<br>– Also observed in carbonate lake beach facies during lake transgression and flooding of fluvial channel<br>– May be preserved in subaqueous levee deposits; traces produced in soupy substrate | – MFC, A, m ~0.5–2.5<br>– MFC, A, m ~4.2–4.4<br>–SCC, A, m ~0.7–1<br>– SCC, A, m ~4.0–5<br>– FC, D1, m ~16<br>– FC, D1, m ~30.5 |
| Suite BC2 *Evaporitic Eulittoral Mammal Footprints and Simple Surficial Traces* | – Can be divided into Suite BC2A (pre-desiccation, probable subaqueous substrate) and Suite BC2B (post-exposure, probable subaerial substrate)<br>– Suite BC2A consists mainly of: 1) simple, horizontal trails and tunnels and burrows on bedding planes; 2) includes very small vertical burrows (e.g., *Polykladichnus* isp.); 3) possible cf. *Fuersichnus* isp. preserved in convex hyporelief; and 4) possible fish (*Undichna* isp.) and snake locomotion traces<br>– Suite BC2B consists mainly of: 1) poorly preserved, small to large mammal | – Mud drapes<br>– Symmetrical ripple bedforms<br>– Bubbly microbial textures<br>– Sodium carbonate evaporite pseudomorphs<br>– Desiccation cracks<br>– Carbonate chips (broken and desiccated carbonate crusts)<br>– Reed impressions and iron-stained root-marks | – Evaporative carbonates<br>– Greyish white and orangish white calciclastic siltstones and fine sandstones with lenticular-, flaser- and wavy-bedding, and planar to slightly undulating laminae<br>– Calciclastic siltstones and sandstones may preserve trona fan evaporite pseudomorphs or spherical ?shortite pseudomorphs and molds | – Littoral to eulittoral carbonate mudflats with oscillatory flow, frequently flooded with very shallow saline lake waters, then exposed and desiccated, sometimes with development of efflorescent salt crusts and microbial crusts<br>– Littoral to eulittoral dolomitic and carbonate fringing marshes that were frequently desiccated | – FC, above D1, m ~ 29–32<br>– FC, above D2, m ~17–20<br>– FC, above E2, m ~35–37<br>– WM, K, below D<br>– WM, #18C, above D |

| | | | | | |
|---|---|---|---|---|---|
| | footprints (e.g., small rhino-like mammal, cat-like mammal tracks); 2) large (~1 cm diameter) full relief burrows with indistinct walls; 3) includes medium-sized to large, mainly horizontal branching burrow networks with poorly preserved burrow boundaries (possibly disrupted by salt efflorescence); and 4) small vertical burrows (*Skolithos* isp.)<br>– Preserved primarily as concave and convex epichnia<br>– No overprinting of trace fossil suites observed except by iron-stained root-marks (cf. Suite BC2B) | | – Light grey and orangish white mudstones and siltstones may be structureless internally with poorly preserved mammal tracks and iron-stained root-marks | – Possible fresh water influence at White Mountain, #18 Crossing suggested by possible cf. *Fuersichnus* isp. (BPBI=6), *Undichna* isp., possible snake trace, and high density of surface tunnels in mudstone drape (BPBI=5–6) | |
| Suite BC3<br>*Delta-Plain Sandstone Vertical Burrows* | – Mainly comprised of vertical burrows, and can be divided into two sub-suites depending on whether the traces were produced during sedimentation (Suite BC3A) or during a period of substrate stability (Suite BC3B)<br>– Suite BC3A includes: 1) small (2–3 mm) to medium-sized (4–7 mm diameter), straight to slightly curved, vertical to oblique burrows (*Skolithos* isp.) with sharp burrow boundaries, partially filled with pellet-like aggregate fill; depths variable, from ~15 cm to > 30 cm; 2) very small (~1.5–2 mm diameter) straight to slightly curved vertical burrows (*Skolithos* isp.) with sharp burrow boundaries; may branch upwards (*Polykladichnus* isp.)<br>– *Skolithos* isp. may grade upwards into escape burrows<br>– Suite BC3B includes: 1) medium-sized vertical burrows that may expand gradually downwards but remain straight, or terminate in expanded oval-shaped chambers (*Macanopsis* isp.); 2) *Thalassinoides* isp. B consisting of expanded, horizontally oriented, connected oval-shaped chambers < 2.5 cm across, possibly earwig nests and burrows<br>– Burrows originate from top of bed (Suite BC3B) or from draped horizons in ripple- | – Associated mainly with ripple-lamination, small-scale trough cross-lamination, or climbing-ripple lamination with draped beds<br>– Close lateral or vertical association with fining-upwards horizontal beds of greenish tan marlstone or arkosic siltstone (mudflat facies)<br>– May be present in irregularly bedded sandstones if associated with bioturbation from Suite BC5A | – Climbing ripple-laminated buff very fine-grained sandstone in thick bed that pinches out laterally to horizontally bedded greenish tan siltstone that contains Suite BC1<br>– Cross-laminated and small-scale trough cross-laminated orangish buff very fine-grained arkosic sandstone in thin bed with lenticular geometry, overlies greenish tan siltstone with horizontal bedding and contains Suite BC1<br>– Irregularly bedded and ripple-laminated very fine-grained arkosic sandstones in coarsening upwards succession, associated with bird footprints and *Planolites* isp. of Suite BC5 | – Distal sheetflood sandstones or broad, shallow channel fill on lower delta-plain, adjacent to mudflat with fining upwards horizontal bedding<br>– Small lenticular channel on lower delta-plain, closely associated with horizontally bedded fining upwards siltstones and marlstones representing mudflat facies<br>– Traces produced in cohesive to firm, probably wet but not subaqueous substrates<br>– Represents subaerial exposure and brief periods of substrate stability; traces produced during brief pauses in sedimentation (Suite BC3A), or following sedimentation (Suite BC3B) | – cf. MFC, A, m ~1-2<br>– MFC, A, m ~7–8<br>– MFC, A, m ~9.5–10<br>– MFC, A, m ~12<br>– SCC, A, m ~1.2<br>– SCC, A, m ~6–8<br>– FC, A (N): cf. FC, A, m ~3?<br>– FC, D1, m ~22 |

| | | | | | |
|---|---|---|---|---|---|
| | laminated or irregularly bedded substrates (Suite BC3A)<br>– May include possible escape-like traces that are very small (~1–2.5 mm diameter) open “circles” preserved in active channel deposits,may be more abundant at the base of beds (cf. Suite BC3A)<br>– Suite BC3B may be associated with open, bunch-shaped root molds<br>– Very closely associated with Suite BC5 in MFC, A, m ~7–8<br>– Cross-cut by Suite BC9 in FC, D1, m ~22 | | | | |
| Suite BC4<br>*Lower Delta-Plain/Wet Floodplain Mammal Footprints* | – Deeply impressed mammal footprints preserved in cross section, recognized by deformed sandstone laminae and ‘churned’ appearance to mudstone or siltstone<br>– Some examples very similar to load structures (ball and pillow)<br>– May be closely associated with bird footprints and simple surface traces (Suite BC5B) and the *Planolites* ichnofabric (BI= <4) in sandstones (Suite BC5A)<br>– No overprinting of trace suites | – Very weak pedogenesis in light greenish tan siltstones that may be laminated or structureless with blocky breakage<br>– Iron-stained root-marks and carbonate root casts with iron-stained rinds<br>–Planar-lamination, ripple cross-lamination and/or climbing ripple-lamination in very fine-grained arkosic sandstones<br>– Produced during sediment deposition | – Interbedded light greenish tan siliciclastic mudstones, siltstones, and light orangish buff, ripple- or planar-laminated very fine arkosic sandstones<br>– Ripple-laminated and climbing ripple-laminated orangish buff very fine-grained arkosic sandstones | – Wet to saturated, or possibly very shallow subaqueous, substrates on lower delta-plain mudflat with frequent distal sheetflood, crevasse-splay, and/or levee overbank sandstone deposition<br>– Crevasse-splay deposits into shallow standing water<br>– Wet to saturated, or possibly very shallow subaqueous, substrates on floodplain with frequent overbank deposition | – FC, D1, m ~5<br>– FC, D1, m ~24.5<br>– FC, D2, m ~26.5<br>– WM, K, D, upper unit |
| Suite BC5<br>*Delta-Plain/Floodplain Ephemeral Pool Footprints, Surface and Subsurface Burrows*, | – Can be divided into two sub-suites: Suite BC5A (pre-desiccation in wet to soupy substrates) and Suite BC5B (subaerially exposed, during desiccation)<br>– Suite BC5A consists of: 1) indistinct medium-sized (~4–6 mm diameteR) *Planolites* isp., and includes the *Planolites* ichnofabric (BI= 3–6), preserved in full relief in very fine-grained thin sandstones beds; 2) medium-sized *Palaeophycus* isp. in more heterolithic facies; and may include 3) escape burrows in underlying beds<br>– Suite BC5B consists of: 1) small to medium-sized shorebird, wading bird, and goose-like footprints, without webbing; 2) isolated bird footprints or trampled | – Light bluish green mudstone drapes<br>– Desiccation cracks<br>– Bubbly microbial surface texture<br>– Carbonaceous material and leaves<br>– Red- and black-stained bedding planes<br>– Iron-stained root-marks<br>– Produced following sediment deposition and during sediment desiccation and/or draining | – Buff very fine-grained sandstones with buff siltstone or light bluish green mudstone drapes, with planar-lamination or bioturbated<br>– Interbedded thin beds of laminated buff siltstones and laminated light bluish green mudstones with planar- to ripple-laminated buff sandstones<br>– Interbedded dark brown to black mudstones with planar-laminated light tan very fine-grained sandstones | – Ephemeral freshwater ponds on delta-plain, with frequent input of very fine-grained sandy sediment as distal crevasse-splay, levee/ overbank, or sheetflood deposits<br>– Desiccated lagoon or standing water on mudflat at shoreline, or even shallow lacustrine, with distal sheetflood or distal terminal distributary mouth bar deposits, with presumably ‘mixed’ salinity (subsaline to hyposaline) | – MFC, A, m ~7–8.2<br>– FC (N), A, upper unit: cf. MFC, A, m ~2.2<br>– FC, A, m ~6.5–8.4<br>– SCC, A, m ~5.8<br>– SCC, A, m ~10<br>– FC, D1, m ~17 |

| | | | | | |
|---|---|---|---|---|---|
| | surfaces; 3) bedding-plane traces such as *Labyrintichnus* isp., *Vagorichnus* isp., *Planolites* isp., tiny *Taenidium barretti*, and arthropod trackways preserved as concave and convex epirelief and hyporelief; 4) full relief, medium-large (~6–9 mm diameter) *Planolites* isp; and 5) may include rare mammal footprints preserved in semi-relief<br>– May be closely associated with deeply impressed mammal tracks (Suite BC4)<br>– May be overprinted by Suite BC9 | | | | |
| Suite BC6<br>*Standing (Relatively)Fresh water Lake or Channel Footprints and Burrows* | – Vertebrate footprints (crocodilian and possibly perissodactyl) and vertebrate scratch-marks (swimming traces of crocodilians) preserved as casts in convex hyporelief<br>– Abundant, distinct *Planolites* isp. preserved as casts in convex hyporelief, which may be cross-cut by vertebrate tracks and/or cross-cutting the vertebrate tracks<br>– Also includes Indeterminate traces with circular expanded areas attached to medium-sized burrows, very smooth burrow boundaries, preserved in convex hyporelief (FC, D1, m ~25)<br>– Suite may be overprinted by full relief burrows of Suite BC9 | – Structureless to laminated greenish tan siltstones buried by ripple-laminated, lenticular-shaped fine-grained sandstone bed with load casts (balls) on lower contact<br>– Carbonaceous material, including leaves and reed impressions<br>– No desiccation cracks | – Red-stained, grey fine-grained arkosic sandstone overlying structureless to laminated greenish tan siltstones and green mudstone<br>– Heterolithic, wavy-laminated to undulating bedded facies of very fine-grained arkosic sandstone and green arkosic mudstone<br>– Planar laminated very fine-grained arkosic sandstones in close vertical association with desiccation-cracked bed with mud-drape | – Standing (relatively) freshwater, either in shallow small lake or within channel<br>– Relatively long-lived, shallow, fresher water lake on delta-plain, possibly an interdistributary bay, or possibly a large water-hole within channel system on delta-plain<br>– Traces preserved by sandstone bed interpreted as crevasse-splay/channel sandstone into standing shallow water | – FC, D1, m ~24, m ~25<br>– FC, D2, m ~8.6 |
| BC7<br>*Freshwater Waning Flow Simple Surface Traces* | – Simple horizontal trails (*Helminthoidichnites*) and small (~2–4 mm diameter) simple burrows (*Planolites*) preserved in epirelief<br>– Includes rare arthropod (insect or spider?) scratch-marks and partial trackways<br>– Includes indistinct surface trails and bioturbation preserved as in concave epirelief with lateral push-up ridges, possibly produced by gastropods<br>– Compare with indistinct surface bioturbation in “white stripe” unit of MFC, A-Bed, m ~4.4 – relatively freshwater?<br>– May be overprinted by Suite BC8 or BC9 | – Very narrow desiccation cracks<br>– Very low amplitude interference ripple bedforms and asymmetrical ripple bedforms<br>– Planar lamination<br>– Bubbly surface texture, attributed to microbial mats | – Fining upwards units of climbing-rippled greyish buff fine- and very fine-grained arkosic sandstone to heterolithic undulating interlaminated very fine-grained sandstone with green siltstone and mudstone to laminated green mudstone<br>– Traces preserved in heterolithic facies<br>– Indistinct bioturbation preserved on rippled and plane-bedded sandstones | – Waning flow channel fill deposits during flood events, possibly in frequently avulsing channels<br>– Distal crevasse-splay deposits onto floodplain<br>– Laminated silty very fine-grained sandstone of waning flow levee-top deposits<br>– Freshwater shallow films on subaerially exposed substrates that preserve asymmetrical ripple bedforms | – FC, D2, m ~8.8<br>– FC, D2, m ~12.5<br>– FC, E2, m ~23.2<br>– cf. MFC, A, m ~10.5<br>– MFC, A, m ~12.7<br>– WM, K, D<br>– FC, D1, m ~25? |

| | | | | | |
|---|---|---|---|---|---|
| BC8<br>*Stable, Subaerial Substrates with Lower Water Table Backfilled Burrows and Nests* | – Traces are dominantly horizontally oriented, small (~3 mm diameter), medium-sized (4–5 mm diameter), and medium-large (~7 mm diameter) backfilled burrows<br>– Can be divided into Suite BC8A and Suite BC8B, with Suite BC8B signifying slightly lower water tables and more stable substrates<br>– Suite BC8A includes small *Taenidium barretti*, branched *Planolites* isp., aggregate-filled horizontal burrows, and *Steinichnus* isp. preserved in concave and convex epirelief and in convex hyporelief<br>– Suite BC8B includes excavated, spherical insect nests, ~20 cm diameter, with simple *Planolites* burrows; associated with bioturbated substrates with abundant *Planolites*; probably produced by ants, possibly termites<br>– May cross-cut Suite BC7 | – Associated with black-stained sandstones (Mn-coated?) with sharp-crested asymmetrical ripple bedforms<br>– May be associated with weakly developed paleosols<br>– Associated with open, “bunched” root-molds<br>– May be associated with clay drapes and cohesive, moist to wet substrates | – Ripple-laminated planar cross-bedded and horizontally bedded greyish buff fine-grained sandstones<br>– Red-stained bioturbated sandstones with irregular bedding in bed preserving insect nest<br>– Very fine-grained sandstones intercalated with brownish green, pedogenically modified arkosic siltstones<br>– Ripple-laminated sandstones with clay drapes overlying a paleosol | – Emergent to subaerially exposed, stable fluvial or crevasse-splay sandstone and heterolithic substrates<br>– Traces produced on emergent abandoned shallow channel sandstones on upper delta-plain, and may be associated with freshwater<br>– High bioturbation indices (BI=3–5) and terrestrial trace types suggest low sedimentation rates, and/or abandonment of channel with sediment bypass<br>– Substrates not necessarily well drained, but in setting with relatively low water tables | – MFC, A, m ~9.5<br>– MFC, A, m ~12–12.7<br>– FC, D2, m ~11.5<br>– Note: this suite is also present in basin margin localities |
| BC9<br>*Well Drained, Subaerial Substrates with Lower Water Table Full Relief Burrows* | – Includes vertical, oblique, and horizontal full relief burrows<br>– Most burrows medium-sized or large (< 2 cm diameter); may include some small *Planolites* isp.<br>– Includes: branched, backfilled *Planolites* ispp.; unbranched, sometimes filled, large cf. *Taenidium barretti*; large, open or passively filled *Skolithos* isp. from tops of beds; and, vertically oriented, large, open clustered-burrow structures (or root molds?)<br>– Burrows usually with distinct burrow boundaries, but typically only sharp boundaries in more cohesive, finer-grained substrates<br>– Burrows may be dominantly horizontally oriented if cross-cutting Suite BC6 or produced within finer-grained substrates<br>– This suite may cross-cut Suites BC3, BC5A, BC6, and BC8 | – Associated with a variety of features, depending on depositional environment of subaerially exposed sediments<br>– Associated with irregular bedding attributed to bioturbation<br>– Not typically associated with desiccation cracks | – Grey fine-grained arkosic sandstone and buff very fine-grained arkosic sandstone intercalated with olive greenish tan arkosic siltstones or brownish green arkosic siltstones with pedogenic modification<br>– Internal structures of sandstone substrates typically ripple-laminated, small-scale trough cross-laminated, planar cross-laminated, or irregularly bedded | – Typically produced in sandstones deposited as distal to proximal crevasse splays<br>– Appears to be associated with well drained, subaerial substrates, with more vertically oriented examples in depositional environments with lower water tables<br>– Dominantly horizontally oriented examples may have been produced in areas with higher water tables (e.g., FC, D1, m ~17, m ~24.5) when compared to vertically oriented examples (e.g., FC, E2, m ~23) | – FC, D1, m ~17<br>– FC, D1, m ~22.3<br>– FC, D1, m ~24.5<br>– FC, E2, m ~23<br>– SCC, A, m ~8<br>–Note: this suite is also present in basin margin localities |

bioturbated substrates (BI=3–6). Some medium (~5 mm) discrete burrows visible within "brecciated" siltstones (MFC, A, m ~1.5; Fig. *6.1.2.*1E) also show sharp burrow boundaries. Here, this suite is associated with structureless light greyish green marl mudstone and laminated, brecciated, or irregularly bedded and structureless tan-coloured marl siltstone. Desiccation features are present at the tops of fining upwards beds of siltstones and marl mudstones. The tan-coloured siltstones also preserve possible disseminated fish bones (or gastropod radulae; Fig. *6.1.2.*1E), and are laterally adjacent to climbing-rippled sandstones that represent either sheetfloods or deposition within a broad shallow channel. This association is interpreted as being produced in a relatively freshwater (hyposaline?) muddy littoral to eulittoral mudflat to lower delta-plain setting that became progressively more landward and subaerially exposed upwards. The trace maker(s) of these simple full-relief burrows is unknown, and could possibly have been oligochaete annelids, small crustaceans such as prawns, or semi-aquatic insects such as beetles or even earwigs.

Other trace fossils included in this suite are escape traces produced through laminated horizons in marl mudstone and siltstone in the lower A-Bed of Middle Firehole Canyon and Sage Creek Canyon (e.g., MFC, A, m ~1.5, Fig. *6.1.2.*1C; SCC, A, m ~1, Fig. *6.1.2.*13A), which may have been produced by the same trace maker that bioturbated the structureless and brecciated marl siltstones. Alternatively, some of these "escape traces" could be interpreted as bird footprints produced in a soupy, possibly shallow subaqueous substrate and preserved in cross-section. Additionally, a single example of a branched, U-shaped burrow (*Thalassinoides* isp. A) preserved in the lower A-Bed of Sage Creek Canyon (e.g., SCC, A, m ~1; Fig. *6.1.2.*13C, 13D) was observed in fining-upwards beds of marl mudstones with desiccation cracks at the bed tops. The branched U-shaped burrow is most comparable to those produced by small prawns in marginal marine, intertidal environments (e.g., northern Gulf of California, pers. obs., 2009). Fossil prawns (*Bechleja rostrata*) are known from the Green River Formation of Fossil Basin (Grande, 1984). Other large (< 4 cm diameter) branching, full-relief burrow systems of indeterminate affinity may also have been produced by crustaceans (e.g., SCC, A, m ~1, Fig. *6.1.2.*13B; MFC, A, m ~1.2, Fig. *6.1.2.*1F).

In calciclastic marginal lacustrine facies just above the D-Bed in Firehole Canyon, medium (~6–10 mm diameter) full-relief burrows assigned to *Planolites* isp. were preserved in low-angle cross-laminated and small-scale trough cross-laminated calciclastic sandstones (e.g., FC, D1, m ~30.5; Fig. *6.1.1.*6A). This sandstone is interpreted as subaerially exposed beach deposits and represents the first exposed bed of the transgressing main lake, after flooding an active fluvial channel carrying arkosic sediment and presumably freshwater. Although these traces are closely associated with mammal footprints and other indicators of subaerial exposure, they are included in Suite BC1 because they are unique within the calciclastic facies investigated, and appear to be closely associated with the shoreline. They are preserved in sediments that may have been deposited in relatively fresh lacustrine setting (hyposaline to mesosaline?) in close association with fluvial input. Like the other examples of this suite, the traces are vertically oriented, unlike the full-relief burrows included in Suite BC2.

Within the second unit of the D-Bed in Firehole Canyon (FC, D1, m ~16), a bioturbated sandstone bed with large-scale convoluted plane-beds preserves indistinct, medium-large (~7–8 mm) *Planolites* isp. that were produced in a soft, soupy, possibly subaqueous sandy substrate (Fig. *6.1.3.*5A–D). Additionally, large (~1–2 cm diameter) burrows of indeterminate affinity that preserve expanded, circular areas attached to burrows also bioturbated this substrate (Fig. *6.1.3.*5B, 5C). The depositional environment of the sandstone lithofacies in which these traces were preserved is not well understood. Possible settings include a subaqueous/sub-lacustrine levee of a terminal distributary channel or channel bars within a freshwater fluvial channel on the

delta-plain. This example is included in Suite BC1 because of morphological similarities with the other bioturbated units described above (e.g., mottled texture), the relatively deep-tier nature of the traces (~40 cm depth from the uppermost bedding plane), and the formation of the traces in a soupy substrate, interpreted as representing a depositional environment near the main lake.

### *6.2.2. Suite 2 (BC2A, BC2B): Evaporitic Littoral and Eulittoral Mammal Footprints and Simple Surficial Traces*

Most trace fossils preserved in the basin centre carbonate facies of the Wilkins Peak Member are preserved in subaerially exposed wavy-bedded calciclastic siltstones and sandstones with mudstone drapes or carbonate crusts. Structureless to poorly bedded dolomitic mudstones interbedded with calcitic siltstones and mudstones that preserve iron-stained root-marks and desiccation cracks are closely associated with the calciclastic littoral to eulittoral facies, and preserve the same suite of trace fossils. Both lithofacies associations also preserve reed impressions. Locally preserved bubbly surface textures are interpreted as evidence of microbial mats. Calcite mudstone crusts may also have been stabilized by or produced in association with microbial mats. Other crust textures appear to have been produced by the reworking of carbonate mudstones by salt efflorescence, and may represent mixed salt/microbial crusts in some examples (e.g., White Mountain, Kanda, below D). Evaporite pseudomorphs (e.g., trona fans) are common within these exposed lake-plain facies. The sedimentary features of the evaporitic littoral to eulittoral zones indicate frequent flooding and exposure by fluctuating lake levels of a saline (mesosaline) to hypersaline (> 50 g $L^{-1}$) lake. No trace fossils were observed in the bedded evaporites interpreted as salt-pan deposits.

The trace fossils of this suite consist mainly of poorly preserved mammal footprints preserved as moulds in concave epirelief and simple, unbranched horizontal surface trails (e.g., *Helminthoidichnites* isp., *Archaeonassa* isp.) produced in carbonate mudstone drapes. The vertebrate footprints range from small- to large, and were produced by several types of mammals (see Table 6.1; Figs. *6.1.1.*1A–G, 3D–I, 7A–H, 8A–H). In most cases, they do not preserve fine details, likely due to: 1) their modification by salt efflorescence or break-up of the carbonate surface crust; 2) initially being produced in firm substrates; and/or 3) initially being produced in subaqueous substrates. Although they are generally poorly preserved, the mammal tracks are described in order to begin a database of the types preserved in this seemingly harsh, saline environment. With future research, it may be possible to better recognize distinctive features of the tracks and begin to interpret the paleoecology of these Eocene mammals through their association with particular sedimentary environments. Bird footprints are notably absent in this trace suite, possibly due to their destruction by taphonomic processes (cf. Scott et al., 2010). Other trace types in this suite, all preserved in epirelief, include: 1) medium-large-sized branched, horizontal surface tunnels (e.g., FC, above D2, Fig. *6.1.1.*6C, 6D); 2) medium-sized branching horizontal tunnels (cf. *Vagorichnus* isp.) (e.g., FC, above D2, Fig. *6.1.1.*4H); 3) simple, horizontally oriented burrows (cf. *Planolites* isp.) (e.g., WM, #18C, above D, Fig. *6.1.1.*2D); and 4) possible fish swimming traces (*Undichna* isp.) and snake locomotion traces (e.g., WM, #18C, above D, Figs. *6.1.1.*3A–C). Full-relief burrows of this suite are dominantly horizontally oriented, and include: 5) branched full-relief burrows with indistinct burrow boundaries, expanded areas, and fill different from host material (e.g., FC, above D1, Fig. *6.1.1.*6E–G); 6) backfilled, horizontally oriented burrows (e.g., FC, above D2, Fig. *6.1.1.*6B); 7) a medium-sized meniscate backfilled burrow (*Beaconites* isp.) (e.g., FC, above D1, Fig. *6.1.1.*6H); and 8) very small- to small-sized vertical burrows (cf. *Polykladichnus* isp., cf. *Arenicolites* isp., *Skolithos* isp.) (e.g., FC, above D2, Fig. *6.1.1.*5C–E). Trace makers of the invertebrate traces in this suite were likely all produced by the larvae and adults of semi-aquatic

(e.g., chironomid larvae, beetle larvae) and air-breathing insects (e.g., beetles, crickets).

This suite is divided into two sub-suites that represent slightly different substrate conditions. First, the simple horizontal trails (*Helminthoidichnites* isp., *Archaeonassa* isp.) were likely produced by aquatic to semi-aquatic insect larvae in shallow water or within saturated 'films' on the exposed sediment surface (Suite BC2A). Second, although some of the mammal tracks may have been produced subaqueously in very shallow water, they represent exposure of the substrate (Suite BC2B). The other traces included (e.g., cf. *Vagorichnus* isp., *Beaconites* isp.) are considered as part of the same sub-suite as the mammal tracks (Suite BC2B), because they also represent exposed, wet substrates. They could, however, be considered as a separate ichnocoenosis because it is arguable whether they were part of the same "community" as the mammals. Due to ambiguities in the relative timing of the different trace types, and precise differences in water depth when the traces were produced, this association remains considered as a single suite of traces found recurrently together.

### *6.2.3. Suite 3 (BC3A, BC3B): Delta-Plain Sandstone Vertical Burrows*

Suite BC3 is found in very fine-grained, ripple-laminated arkosic sandstone facies that are interpreted to represent shallow channels, point bars within larger shallow channels, or unconfined flow (sheetfloods, crevasse splays) on the delta-plain. All examples of this suite, mainly composed of vertical burrows, are associated with small- to medium-scale trough cross-lamination, ripple lamination, climbing-ripple lamination, or ripple-laminated planar cross-beds. The traces were produced either during deposition, from bedding planes during pauses in sedimentation, or from the tops of small lenticular channel and point bar sandstones. This suite includes small- (~1–2 mm diameter) to medium (~4–7 mm) vertical burrows, many of which contain a reddish black pellet-like backfill. This suite excludes large (> 1 cm diameter) vertical burrows that are associated with other large, vertically oriented burrows (e.g., cf. *Taenidium barretti*) that appear to be linked to a drop in water tables (Suite BC9). Many of the vertical burrows in Suite BC3 may have been produced by tiger beetle larvae, as well as other beetles (e.g., carabids?, staphylinids?), whereas the larger vertical burrows (Suite BC9) may have been produced by adult beetles or spiders. Suite BC3 can be divided into BC3A, which contains traces produced during deposition or brief pauses in sedimentation, and BC3B, which contains traces produced from the tops of beds during relatively longer periods of substrate stability.

In the lower A-Bed of Sage Creek Canyon (e.g., SCC, A, m ~1.2), small lenticular channel bodies with internal cross-laminae in opposing directions and small-scale trough cross-lamination are interpreted as short-lived terminal distributary channels on the lower delta-plain. One example of a lenticular sandstone preserves escape traces (Suite BC3A), as well as vertical burrows and possible earwig nests and burrows (Suite BC3B), produced from the upper, subaerially exposed surface of the bed (Fig. *6.1.2.*14A–H). In contrast, climbing ripple-laminated very fine-grained buff arkosic sandstones in the lower A-Bed of Middle Firehole Canyon, interpreted as sheetfloods or deposition within a broad shallow channel on the lower delta-plain, preserve vertical burrows originating from siltstone-draped bedding planes that represent pauses in sedimentation within the sandstone body (Fig. *6.1.2.*2A–H). Upward movement of the trace makers occurred when sedimentation resumed, as shown by escape or possibly equilibrium burrows in close association with the vertical burrows (Fig. *6.1.2.*2E). The sandstones are laterally associated with thin beds (~5–30 cm thick) of fining-upwards laminated siltstones to structureless mudstones that preserve examples of Suite BC1 and are interpreted as having been deposited in the shallow muddy littoral zone with brief periods of subaerial exposure.

Very small- (~1.5–2 mm diameter), small- (~2–3 mm diameter), and medium (~4–7 mm diameter) vertical burrows (*Skolithos* ispp.) with sharp walls and pellet-like sediment aggregate fill mainly comprise most of this suite in the lower unit of SCC, A (Suite BC3B; Fig. *6.1.2.*14A–F). The burrows are slightly curved or obliquely oriented, and some medium-sized examples may become expanded downwards, or terminate in oval-shaped chambers (*Macanopsis* isp.; Fig. *6.1.2.*14F), interpreted as insect pupal chambers produced possibly by beetles (e.g., tiger beetles). Depths range from ~2 cm for very small burrows, to ~15– > 30 cm for medium-sized burrows, apparently depending in part on the thickness of the sandy substrate. Additionally, one example of an open, branched burrow system with horizontally oriented oval-shaped chambers (*Thalassinoides* isp. B) was also preserved in the lower A-Bed at Sage Creek Canyon (e.g., SCC, A, m ~1.2; Fig. *6.1.2.*14G, 14H). It cross-cuts a medium-sized vertical burrow, which may or may not be associated with the *Thalassinoides* burrow system. The size and shape of the oval-shaped chambers are remarkably similar to earwig nests and burrows observed at Lake Bogoria. The A-Bed example may have been produced by earwigs (possibly Forficulidae, known from Florissant, CO; Wilson, 1978), or possibly by prawns. Together, this assemblage is interpreted to represent probably wet, cohesive to firm, subaerially exposed sandy substrates near the lake shoreline in an area near freshwater input.

In the upper unit of the A-Bed at Middle Firehole Canyon (e.g., MFC, A, m ~7-8; Fig. *6.1.2.*3A–H), Suite BC3A was observed in close association with bird footprints and large (~8–11 mm diameter) *Planolites* isp. (Suite BC5B; Fig. *6.1.2.*3A, 3H). There, Suite BC3A is represented by medium-sized vertical burrows with blackish-reddish aggregate fill and escape traces, preserved in irregularly bedded and ripple-laminated very fine-grained arkosic sandstones at the top of a coarsening upwards succession (Fig. *6.1.2.*3B–G). The traces were produced from bedding planes in the sandstone bed or during active sedimentation if they are escape traces. This assemblage is interpreted to have been produced in wet substrates on the lower delta-plain, with sedimentation and water input from unconfined flows/sheetfloods or from a coarsening-upwards crevasse-splay succession. Medium-sized vertical burrows were preserved in the cross-bedded point bar deposits of the overlying, more landward succession (Suite BC3B; e.g., MFC, A, m ~9.5–10; Fig. *6.1.2.*6A–D), as well as in small-scale trough cross-laminated sandstones towards the top of the unit (Suite BC3A; e.g., MFC, A, m ~12; Fig. *6.1.2.*6E–F).

Very small vertical burrows (~1 mm diameter) preserved in small-scale trough cross-laminated fine-grained arkosic sandstones (e.g., FC, D1, m ~22; Fig. *6.1.3.*7A) that are interpreted as crevasse-splay deposits on the (upper?) delta-plain, are included in Suite BC3A. They may have been produced by aquatic suspension feeders such as chironomid (Diptera) larvae or detritus feeders such as oligochaetes. These traces were apparently produced during very brief pauses in sedimentation, while other, small- to medium-sized examples were produced following sedimentation of the bed (Fig. *6.1.3.*7B, 7D). Several examples of very small and circular possible escape-like traces preserved in active fluvial channel deposits (e.g., SCC, A, m ~6–7, Fig. *6.1.2.*16A–C; cf. FC (N), A, m ~9, Fig. *6.1.2.*12E, 12F) are also tentatively included in Suite BC3 because of their association with active sedimentation. These 'circle' traces tend to be more abundant at the bases of channel sandstone beds, becoming less abundant upwards, and may possibly have been produced by aquatic insect larvae (e.g., chironomids) or oligochaetes. Alternatively, these structures could be open shortite moulds or differentially weathered-out mud clasts or fecal pellets incorporated from the bed below.

*6.2.4. Suite 4 (BC4): Lower Delta-Plain/Wet Floodplain Footprints*

Mammal footprints seen mainly in cross-section comprise this suite. They were deeply impressed (~3–15 cm) into muddy to sandy substrates of heterolithic and ripple-laminated sandstone facies that preserve iron-stained root-marks, and signify wet to soupy substrates in areas with shallow water tables. The tracks are medium (~5 cm length/width) to large in size (< ~15 cm length/width), and are recognized by deformed sandstone laminae that pinch out towards the impressions or by a plug-shaped feature that contains churned and otherwise structureless mudstone or siltstone. Footprints of this suite were rarely observed in plan view, but some were probably produced by gracile perissodactyls (e.g., *Hyracotherium* sp.). The larger footprints may have been produced by rhino-like or hippo-like perissodactyls.

Mammal tracks of this suite were present in four main lithofacies associations, interpreted as areas with shallow water tables on lake-fringing mudflats and/or wet to saturated or shallow subaqueous substrates near distributary channels. First, the lower unit of the D-Arkose Bed (e.g., FC, D1, m ~3–6; Fig. *6.1.3*.4A–D), consists of greyish green mudstones and ripple-laminated very fine-grained arkosic sandstones. The unit coarsens upwards from carbonate lake facies, and preserves iron-stained root-marks. Weakly developed paleosols cap the unit. Together, these features suggest that the mammal tracks were produced in wet to saturated substrates on the lower delta-plain, at the transition from mudflat facies to distal sheetflood or crevasse splays, with subaerial exposure becoming more frequent upwards.

Mammal tracks of this suite were also preserved in the upper unit of the D-Bed on White Mountain at Kanda (Fig. *6.1.3*.2A–H). Again, they are distinguished by sharply deformed sandstone laminae and churned siltstones. In this case, they are more closely associated with fluvial channel facies, but are also preserved in interbedded siltstones and very fine-grained sandstones to ripple-laminated very fine-grained sandstones. These sediments are interpreted as proximal to medial overbank deposits, either crevasse splays or levee deposits of distributary channels on the delta-plain. There, this suite was preserved in close association with Suite BC5, which is characterized by bird footprints and horizontal trails and tunnels. Planar-laminated sandstones (within channel?) at this locality preserve horizontal traces (cf. *Taenidium* isp.) (Suite BC7?; Fig. *6.1.3*.3A). Horizontal grazing (?) traces of indeterminate affinity in ripple-laminated sandstones (within channel (?), levee?) are preserved towards the top of the unit (Suite BC7? Fig. *6.1.3*.3B–D).

Other examples of this suite are present in the “green stripe” unit of the D-Bed in Firehole Canyon (e.g., FC, D1, m ~24; Fig. *6.1.3*.9A, 9B), preserved in a sandstone unit interpreted as a crevasse channel into a shallow interdistributary bay or small lake on the delta-plain. In the E-Bed of Firehole Canyon (e.g., FC, E2, m ~26.5), mammal tracks in cross-section were preserved in thin ripple-laminated very fine-grained sandstone beds intercalated with brownish green siltstones that may be distal crevasse splays onto weakly developed paleosols on the upper delta-plain or floodplain. This suite appears to represent wet to saturated or shallow subaqueous substrates (long-lived or temporary) with freshwater input from overbank floods or sheetfloods.

*6.2.5. Suite 5 (BC5A, BC5B): Delta-Plain/Floodplain Ephemeral Pool Footprints and Surface and Subsurface Burrows*

Suite BC5 is associated mainly with heterolithic lithofacies of very fine-grained arkosic sandstone beds with bluish green mud drapes, desiccation cracks, and bubbly bedding-plane textures attributed to microbial mats, interpreted as ephemeral ponds fed by pulses of overbank freshwater and arkosic sediments. The suite can be divided into: 1) a 'pre-desiccation' suite (Suite BC5A), which consists of bioturbated sandstones with indistinct simple burrows produced in soupy substrates; and 2) a subaerial, 'desiccation' suite (Suite BC5B), which consists of bird

tracks and horizontal surface burrows. Suite BC5A may be comparable to the "overfilled overbank" trace association of Buatois and Mángano (2004, 2007), and BC5B may be similar to the "desiccated overbank" setting, although the sandstones were also often desiccated and are in close association with the bird-tracked, desiccated mudstones.

Suite BC5A is typically found in thin (3–7 cm thick) sandstone beds interbedded with light bluish green mudstones that preserve bird footprints (e.g., FC, A, m ~6.5–8.2; Fig. *6.1.2.*12A–D). Internally, these beds are planar-laminated to discontinuously laminated or structureless, and typically are draped by siltstone or mudstone drapes. Some are bioturbated (BI=3–6), with greater bioturbation towards the tops of the beds including some discrete burrows (Fig. *6.1.2.*12A). The burrows are medium-sized (~4 mm diameter), dominantly horizontally oriented, unwalled with indistinct burrow boundaries, and filled with the host sandstone. They are attributed to *Planolites* isp., and highly bioturbated examples are referred to as the "*Planolites* Ichnofabric". This association comprises Suite BC5A, which is interpreted to represent bioturbation in soft, saturated, probably shallow subaqueous sandstone substrates deposited into very shallow overbank freshwater ponds, either as levee sandstones or crevasse splays from shallow channels onto the lower or upper delta-plain. Other examples of the *Planolites* ichnofabric are preserved in a wedge-shaped, possible levee sandstone (e.g., cf. MFC, A, m ~10.5; Fig. *6.1.2.*4A, 4C), and in ripple-laminated shallow channel deposits (e.g., MFC, A, m ~12; Fig. *6.1.2.*4D–F). In another possible levee deposit (e.g., FC, D1, m ~17), high density *Planolites* isp. are associated with high density *Palaeophycus* isp. with clay-rich burrow linings, as well as escape traces in the underlying ripple-laminated sandstone bed (Fig. *6.1.3.*5E–H). These examples are all interpreted as being produced in freshwater, with soupy and possibly subaqueous substrates.

Suite BC5B represents the traces produced during desiccation of freshwater shallow ponds. It is characterized by bird footprints and small surface trails and tunnels on desiccated bedding planes that may be interbedded with bioturbated sandstones (e.g., FC, A, m ~6.5–8.2; SCC, A, m ~10; WM, K, D, upper unit). The bird footprints are mainly small (~3 cm length) and were produced by shorebirds, although some larger examples (< 7 cm length) present may have been produced by medium-sized wading birds (e.g., egrets) (e.g., FC, A, m ~6.5–8.2; Fig. *6.1.2.*11A–H). The traces are preserved as moulds in concave epirelief or casts in convex hyporelief. Most of the bird-footprinted horizons consist of very fine-grained arkosic sandstones with thin muddy siltstone or thin to thick bluish green mudstone drapes, or the bird tracks were impressed into bluish green mudstone beds that were buried by very fine-grained sandstone. Desiccation cracks are common, as are bubbly surface textures attributed to microbial mats.

This association also includes several types of surficial traces (Fig. *6.1.2.*10A–F), including simple trails (*Helminthoidichnites*), arthropod trackways produced in saturated substrates ("furrow-shaped traces"; cf. Bohacs et al., 2007a), and small, branching tunnels preserved in convex epirelief (e.g., cf. *Labyrintichnus* isp.) and convex hyporelief (e.g., cf. *Vagorichnus* isp.). All of these invertebrate traces were likely produced by insects such as beetle larvae and adults. One example of a small meniscate-backfilled burrow (*Taenidium barretti*) preserved in epirelief was associated with bird tracks (e.g., SCC, A, m ~10; Fig. *6.1.2.*16E–G). Where substrates were cohesive, Suite BC5B is represented by high-density simple burrows preserved as convex hyporelief on the bases of sandstone beds (e.g., cf. *Fuersichnus* isp., SCC, A, m ~10, Fig. *6.1.2.*16H, 16I). The sedimentary environment is interpreted as very shallow, frequently desiccated, ephemeral ponds on the delta-plain, with sediment and freshwater input from overbank floods (crevasse or levee) and possibly sheetfloods.

Another expression of Suite BC5B is preserved in the lowermost upper unit of the A-Bed in Sage Creek Canyon (e.g., SCC, A, m ~5.5–5.8; Fig. *6.1.2.*15A–E). In this case, planar- to

ripple-laminated very fine-grained sandstones are finely interbedded with brownish to blackish green arkosic mudstones and preserve black- and red-stained bedding planes attributed to drapes of organic matter and possibly microbial mats. This facies conformably overlies carbonate mudstones and calciclastic siltstones of the main lake ("white stripe" unit). One example of a bird-trampled sandstone bed was observed, in association with medium-sized (~6 mm diameter), horizontally oriented, full-relief burrows (*Planolites* isp.) and very small (~3 mm diameter), possible full-relief burrows (cf. *Planolites* isp.; Fig. *6.1.2.*16F, 16G) assigned to cf. Suite BC3A. Both are filled with host material and possess indistinct burrow boundaries. In this case, the setting is interpreted as a shallow lagoon or mudflat lake-ward of the prograding fluvial system, as shown by the inferred terminal distributary mouth bar and channel sandstones that overlie the sandstone. This association of bird tracks and larger, full-relief but horizontally oriented examples of *Planolites* isp. was also seen in the upper unit of the A-Bed of Middle Firehole Canyon (e.g., MFC, A, m ~7–8; Fig. *6.1.2.*3A, 3H) where Suite BC5B was closely associated with vertical burrows and escape traces of Suite BC3A. Together the assemblage represents wet to saturated relatively freshwater substrates in an area with frequent flooding and subaerial exposure, interpreted as distal sheetfloods or crevasse splays on the lower delta-plain.

### *6.2.6. Suite 6 (BC6): Standing Water (Relatively) Freshwater Lake or Channel Footprints and Bioturbation*

This suite is represented by: 1) vertebrate footprints and vertebrate scratch marks interpreted as the swimming and walking traces of crocodilians and mammals (Fig. *6.1.3.*8A–G); 2) small *Planolites* isp. (~4 mm diameter) with distinct burrow boundaries and the *Planolites* ichnofabric (BPBI=3–4) (Fig. *6.1.3.*8A, 8B); and 3) unusual surface traces with expanded circular areas and very smooth burrow boundaries (Fig. *6.1.3.*9C–E). These traces were preserved in convex hyporelief at the base of an irregularly bedded, lenticular sandstone with a locally scoured base that overlies a laminated light greyish green siltstone (marl?) and which preserves load-like structures attributed to mammal footprints of Suite BC4 (e.g., FC, D1, m ~24.5). Clayey material at the base of the lenticular sandstone is red-stained, which may represent plant-derived detritus. Although this unit (the "green stripe" unit, FC, D1) is not clearly understood and shows complex facies relationships, the interpretation is that this association represents a relatively long-lived interdistributary bay or relatively freshwater lake on the delta-plain. The sandstone is interpreted as a lenticular crevasse-splay deposit that terminated subaqueously in shallow water. The traces preserved on the base of the bed are interpreted as having been produced subaqueously in relatively freshwater (fresh: < 0.5 g $L^{-1}$, subsaline: 0.5–3 g $L^{-1}$, or hyposaline: 3–20 g $L^{-1}$?). The underlying laminated marl (?) siltstone lies conformably above the "green stripe", which is an organic-rich, laminated mudstone interpreted as interdistributary bay suspension-fallout deposits (e.g., FC, D1, m ~22.8–23.8). The sandstone was then bioturbated with some distinct examples of medium-sized *Planolites* isp., pellet-filled burrows, and vertical burrows (*Skolithos* isp.) included in Suite BC9, indicative of subaerial exposure.

The simple *Planolites* isp. burrows included in this suite differ from those included in Suite BC5A mainly by their preservation. In this case, small-medium-sized *Planolites* isp. are preserved in convex hyporelief, and many preserve sharp burrow boundaries, probably due to the presence of more cohesive, clayey or organic material in the substrate. Due to this style of preservation, *Planolites* isp., which are preserved in the heterolithic channel fill sandstones and siltstones in the upper unit of FC, D2 (Fig. *6.1.3.*11B, 11C), are included in Suite BC6. This suite apparently signifies standing freshwater in either a shallow lake (FC, D1, green stripe unit) or within an abandoned channel (FC, D2, upper unit).

### *6.2.7. Suite 7 (BC7): Freshwater Waning Flow Simple Surface Traces*

A low diversity, low density suite of horizontal surface trails (*Helminthoidichnites* isp.) and horizontal burrows (*Planolites* isp.) was preserved in convex and concave epirelief in heterolithic arkosic sandstone and mudstone facies. Together with the associated lithofacies, they are interpreted to represent waning flow conditions within: 1) distributary channels (e.g., FC, D2, m ~8.5–9); 2) in distal levee or crevasse-splay deposits (e.g., FC, D2, m ~12.5; FC, E2, m ~23); and 3) in uppermost levee-wedge sandstones (e.g., cf. MFC, A, m ~10.5). *Helminthoidichnites* isp. was preserved on mud-draped, silty very fine-grained sandstones that also preserved very low amplitude interference-ripple bedforms and incipient desiccation cracks (FC, D2, m ~8.8; Fig. *6.1.3.*11D). *Helminthoidichnites* and small, surficial *Planolites* were also preserved on the upper surfaces of overbank sandstones interpreted as distal levee or crevasse-splay deposits (e.g., FC, D2, m ~12.5, Fig. *6.1.3.*12E; FC, E2, m ~23.2, Fig. *6.1.3.*12F, 12H). In the upper A-Bed at Middle Firehole Canyon (e.g., cf. MFC, A, m ~10.5), a wedge-shaped arkosic sandstone bed interpreted as a levee deposit (Eric Williams, pers. comm., 2008) preserves *Helminthoidichnites* isp. on its upper, laminated surface (Fig. *6.1.2.*4B). This example is also interpreted to represent waning flow and production of the trace in very shallow subaqueous freshwaters on the desiccating substrate. Clay-draped very fine-grained sandstones interpreted as abandoned shallow channel deposits at the top of the A-Bed in Middle Firehole Canyon also preserve *Helminthoidichnites* as well as arthropod scratch-marks that were probably produced in a shallow film of water before the bioturbation of the unit by Suite BC8 (Fig. *6.1.2.*7A).

The top of the D-Bed at Kanda also preserves surficial trails that were likely produced in a shallow film of water and may have been produced during the waning stages of unidirectional flow within a delta-plain channel (Fig. *6.1.3.*3B–D). These traces are of indeterminate ichnotaxonomic affinity, but may possibly be attributable to the locomotion traces of gastropods. They are unbranched shallow trails of medium size (~5–7 mm diameter) preserved in concave epirelief with the lateral margins of the trails pushed up slightly. They are associated with indistinct ploughing or burrowing structures that are very similar to the features left by gastropod locomotion in modern settings. Similar traces were preserved in association with sun-ray-like or probe-like traces in the D-Bed of Firehole Canyon (e.g., FC, D1, m ~25?; Fig. *6.1.3.*9G, 9H), as well as in oscillation-rippled calciclastic siltstones of the "white stripe" unit of the A-Bed at Middle Firehole Canyon (Suite BC2A; MFC, A, m ~4.4; Fig. *6.1.1.*12A, 12C, 12D, 12G).

### *6.2.8. Suite 8 (BC8A, BC8B): Stable, Subaerial Substrates with Lower Water Table Backfilled Burrows and Nests*

The trace fossils included in Suite BC8 represent subaerially exposed settings associated with incipient paleosols and stable, probably moist to wet, substrates. The suite can be divided into two sub-suites: 1) Suite BC8A, with small- to medium-sized, full-relief, dominantly horizontally oriented meniscate- and sediment aggregate-backfilled burrows; and 2) Suite BC8B, represented by concentrated areas of simple backfilled burrows and excavated, bioturbated areas interpreted as insect nests and their associated, diffuse burrow system (probably ants). The traces were preserved in channel sandstones capped by incipient paleosols developed on bluish green siltstones (e.g., MFC, A, m ~12.7; Fig. *6.1.2.*7A–H), in ripple-laminated very fine-grained sandstones overlying a paleosol (e.g., MFC, A, m ~9.5; Fig. *6.1.2.*5C, 5D), and in very fine-grained sandstones interbedded with brownish green siltstones interpreted as incipient paleosols (e.g., FC, D2, m ~11.5; Fig. *6.1.3.*12A–E). This suite, one of two "terrestrial" suites in the basin centre localities, this suite is interpreted to represent bioturbation by air-breathing invertebrates, probably insects and oligochaetes, in moist to wet but relatively well drained, stable substrates,

such as abandoned channel sandstone deposits. Although the traces are preserved in sandstone beds, it is likely that the organisms that produced them were also living and feeding within the surrounding siltstones. There is overlap between this suite and Suite BC9. With more data, it may be possible to improve interpretation of these traces and determine if the two suites should be joined or reorganized. Suite BC8 is distinguished here by the 1) presence and dominance of small meniscate-backfilled burrows (*Taenidium barretti*), which are rare in Suite BC9; 2) the lack of large cf. *Taenidium barretti* and large vertical burrows; 3) overall smaller burrows (e.g., small- to medium-sized *Planolites* isp.); and 4) the presence of an excavated insect nest associated with abundant *Planolites* isp. and *Palaeophycus* isp. burrows that are present within the nest structure and which bioturbated the surrounding sediment.

The lack of large cf. *Taenidium barretti* (Suite BC9) and the presence of an insect nest within this suite at the top of the A-Bed in Middle Firehole Canyon is not easily be explained because both of these trace types are interpreted to be indicators of relatively lower water tables. However, the abundant small meniscate burrows, which are dominantly horizontally oriented, implies more poorly drained substrates and their initial production in wet sandstones (in substrates with freshwater). For comparison, small *Taenidium barretti* are abundant within planar-laminated channel sandstones of the upper G-Bed in Sage Creek Canyon, and were also preserved in association with bird footprints in the upper A-Bed of Sage Creek Canyon (e.g., SCC, A, m ~10; Suite BC5B). A potential explanation for the setting at Middle Firehole Canyon (MFC, A, m ~12.7) is as follows: 1) small *Taenidium barretti* burrows, possibly feeding burrows, were produced in wet but not saturated, freshwater, sandy substrates with detritus or clay drapes; 2) the abandonment of the channel provided a stable substrate with a low sedimentation rate, permitting the high degree of bioturbation; and 3) the stable substrate was the more important environmental factor for the development of the insect nest when compared to well drained substrates or low water tables, which apparently are important controls for the production of large cf. *Taenidium barretti*. Additionally, or alternatively, the large cf. *Taenidium barretti* burrows may need easily burrowed sandy substrates that are moist but not wet. This is supported by the deep burrows observed in basin margin localities such as Slate Creek and "the Eagle" at the Southern Margin, which appear to have been produced by a trace maker (frog?, crustacean?, beetle?) that aestivated.

### *6.2.9. Suite 9 (BC9): Well Drained, Subaerial Substrates with Lower Water Table Full-Relief Burrows*

Trace fossils indicating slightly lower water tables (> ~20 cm depth?) in apparently well drained sandy substrates are included in Suite BC9, which was observed to cross-cut Suites BC3, BC5A, BC6, and BC8. All the traces included in this suite were preserved in full-relief, and may be vertically oriented, or vertically and horizontally oriented. Examples with more vertically oriented traces are interpreted to represent relatively deeper water tables (e.g., FC, E2, m ~23; Fig. *6.1.3.*12G) than those with more horizontally oriented traces (e.g., FC, D1, m ~17; Fig. *6.1.3.*6A, 6C, 6D). The suite is characterized by: 1) sediment aggregate/pellet-backfilled burrows (e.g., FC, D1, m ~24–25; Fig. *6.1.3.*10C, 10D); 2) large, vertically and horizontally oriented cf. *Taenidium barretti* burrows (e.g., FC, D1, m ~22.3, m ~24–25; Figs. *6.1.3.*7C–F, *6.1.3.*10A, 10B); 3) large vertical *Skolithos* isp. burrows originating from the upper surfaces of sandstone beds (e.g., FC, D1, m ~22.3; Fig. *6.1.3.*7B); and 4) vertically oriented clustered-burrow structures or composite traces of roots and burrows (e.g., FC, D1, m ~22.3, m ~24.5; Fig. *6.1.3.*7A, 7B, *6.1.3.*10E). Monospecific examples of large cf. *Taenidium barretti* full-relief burrows are especially indicative of relatively low water tables, easily burrowed substrates, and/or well drained substrates, and were also observed in basin margin localities (e.g., Slate

Creek, Southern Margin). The inclusion of this trace fossil in this suite is tentative because of its often monospecific occurrence and its common presence in basin margin localities. It may signify slightly better drained substrates or slightly deeper water tables than the other trace fossils included in this suite.

In the basin centre, this suite was observed in the second unit of the D-Bed (FC, D1, m ~17, m ~22.3), the "green stripe" unit of the D-Bed (FC, D1, m ~24.5), and in the lower E-Bed (FC, E2, m ~23). Vertically oriented cf. *Taenidium barretti* burrows are present in the proximal crevasse sandstone bed below the interdistributary bay (?) "green stripe" unit (FC, D1, m ~22.3; Fig. *6.1.3.*7C–F). In contrast, dominantly horizontally oriented, slightly smaller, aggregate-filled burrows were preserved within a proximal crevasse sandstone bed that was interpreted as being originally deposited into standing water (FC, D1, m ~24; Fig. *6.1.3.*10A–D). Large cf. *Taenidium barretti* were also preserved in a relatively thick, irregularly bedded (bioturbated) crevasse-splay sandstone in the E-Bed (FC, E2, m ~23; Fig. *6.1.3.*12G), but were not observed in thinner, ripple-laminated (more distal?) crevasse-splay deposits that contained aggregate-filled burrows (Fig. *6.1.3.*12H).

## 6.3. Comparison between the Archetypal Ichnofacies and the Basin Centre Trace Suites

The trace fossil suites recognized in the basin centre of the Wilkins Peak Member in the Bridger basin, and their interpreted significances broadly agree with the ichnofacies model of Buatois and Mángano (2004, 2007, in press). The Mermia ichnofacies is well represented by simple, horizontal trails and burrows in Suites BC2A and BC7. These are interpreted to have been produced in shallow subaqueous substrates, both in the lake waters of the littoral to eulittoral zone (Suite BC2A), as well as in heterolithic facies representing waning unidirectional flow in fluvial channels, levee deposits, and/or distal crevasse splays (Suite BC7). Salinities probably ranged from freshwater (< 0.5 g $L^{-1}$) in the fluvial environments to hyposaline (3–20 g $L^{-1}$) or mesosaline (20–50 g $L^{-1}$) in the littoral to eulittoral saline lake carbonate facies. No trace fossils were observed in the sublittoral or profundal carbonate lake facies of the typical Wilkins Peak Member, but simple *Planolites* burrows were preserved in sublittoral carbonate mudstones that are interbedded with calciclastic siltstones of the "white stripe" carbonate units of the A-Arkose Bed (Suite BC1). Bioturbation by small- to medium-sized, indistinct *Planolites* full-relief burrows was present in facies interpreted as being deposited in the main lake, but at sites with close association to freshwater fluvial input (Suite BC1). Suite BC1 also includes possible prawn and other crustacean burrows, which are excluded from the Mermia ichnofacies but are comparable to the Psilonichnus ichnofacies characteristic of marine backshore environments.

Other examples of the "*Planolites* ichnofabric" (Suite BC5A) were preserved in thin sandstone beds interpreted as crevasse-splay deposits in shallow freshwater ponds, fitting well with the interpreted significance of the Mermia ichnofacies (Buatois and Mángano, 2004). These sandstones are interbedded with or draped by arkosic mudstones that preserve horizontal, surface burrows (e.g., cf. *Labyrintichnus*, cf. *Vagorichnus*) that may correspond to the Mermia ichnofacies or be included in the Scoyenia ichnofacies because of their association with bird footprints and desiccation cracks (Suite BC5B). In summary, trace fossils typically assigned to the Mermia ichnofacies (e.g., *Helminthoidichnites*, *Planolites*) are preserved in several depositional settings of the basin centre, ranging from somewhat saline to freshwater environments. In all cases, the traces are interpreted as being formed in shallow subaqueous to saturated substrates. *Planolites* in particular, appears to be associated with fresh, subsaline (0.5–3 g $L^{-1}$), or possibly hyposaline (3–20 g $L^{-1}$) waters, while *Helminthoidichnites* is present in substrates that probably represent greater variability in salinity. Suite BC6 also includes high density examples of *Planolites*, and although their occurrence in BC6 is interpreted to represent

freshwater subaqueous conditions, the suite is not directly compatible with the Mermia ichnofacies because of the association of these burrows with vertebrate footprints and swim traces attributed to crocodilians and/or turtles.

The Scoyenia ichnofacies, characteristic of frequently flooded and exposed substrates, is represented by Suites BC2B, BC4, BC5B, BC8A, and BC9. Mammal footprints, horizontally oriented burrows, and rare meniscate-backfilled burrows of Suite BC2B that were produced in eulittoral carbonate mudflats are a good example of the typical Scoyenia ichnofacies. The lack of meniscate-backfilled burrows and shorebird footprints, and poor preservation of the mammal footprints may be indicators of the Scoyenia ichnofacies in an evaporative saline environment. Mammal footprints of Suite BC4 may be laterally associated with bird footprints, horizontal tunnels (e.g., cf. *Vagorichnus*, pellet-filled burrows), or small backfilled burrows (*Taenidium barretti*) of Suite BC5B, or they may be found without other traces. Both suites represent the Scoyenia ichnofacies, but show differences in substrate conditions, from soupy to shallow subaqueous substrates in settings with active sedimentation (Suite BC4) to desiccating, wet to saturated substrates during periods of non-deposition or suspension fall-out sedimentation (Suite BC5B).

The more terrestrial, stable and/or well drained substrates with relatively (slightly) lower water tables represented by Suites BC8 and BC9 are dominated by meniscate-backfilled and aggregate-backfilled burrows, which is typical of the Scoyenia ichnofacies. However, elements of each of these suites that represent lower water tables (e.g., insect nests and burrows of Suite BC8B, vertically oriented large cf. *Taenidium barrettii* of Suite BC9) are somewhat more closely aligned with the Coprinisphaera ichnofacies although the typical elements of this ichnofacies were not present. In general, Suites BC2B, BC4, and BC5B represent environments either closer to the lake margin or closer to fluvial channels on the delta-plain that undergo frequent overtopping of their banks than Suites BC8 and BC9. Suite BC8A represents lake margin or delta-plain settings further from the lake shoreline and/or fluvial channels than Suites BC2B, BC4, and BC5B. Suites BC8B and BC9 may represent more landward facies and/or the draining of the same substrates in which other trace suites were previously produced (e.g., Suites BC3, BC7, BC8A). In the basin centre, even these 'terrestrial' suites were produced in substrates with shallow water tables, corresponding to the lack of more terrestrial lithofacies, such as the better developed, red paleosols and isolated ribbon-like channel bodies present in basin margin localities.

The Skolithos ichnofacies is represented mainly by vertical burrows produced approximately during sedimentation, as well as vertical burrows produced from subaerially exposed substrates. Suite BC2 preserves examples of very small vertical burrows in saline, evaporitic carbonate substrates, which were likely produced in very shallow subaqueous substrates by organisms such as chironomid larvae (Suite BC2A; e.g., *Polykladichnus* isp.) or in wet, subaerially exposed substrates near the shoreline (Suite BC2B; e.g., *Skolithos* isp.). Suite BC3 was designated for the very small-, small-, and medium-sized (< 7 mm diameter) vertical burrows and their accompanying escape traces and full-relief burrows (*Thalassinoides* isp. B) observed in the (relatively) freshwater substrates of the A-Arkose Bed and D-Arkose Bed. Some of the vertical burrows may have been produced from subaqueous substrates during brief pauses in sedimentation, as shown by their initiation from ripple-laminae bedding planes and association with escape traces (Suite BC3A), while others were produced from bed-tops of small, shallow lenticular channels or from cross-bedded point-bar deposits (Suite BC3B). Other occurrences of larger (~1 mm diameter) vertical burrows that are interpreted to represent lower water tables and/or well drained sandy substrates were included as part of Suite BC9. Overall, the vertical burrows in BC2, BC3, and BC9 were associated with either lake-margin sheetflood deposits or

delta-plain fluvial channels and crevasse splays, with examples produced 'during' sedimentation (i.e. syndepositional) and following sedimentation preserved in close association with one another.

## 6.4. Application of the Basin Centre Trace Fossil Suites for Paleoenvironmental Reconstructions

Trace fossils provide valuable evidence for the interpretation of the diverse depositional settings in the basin centre of the Wilkins Peak Member in the Bridger Basin. Many of the trace fossils preserved are closely associated with certain lithofacies or lithofacies associations (e.g., bird tracks in bluish green laminated mudstones, Suite BC5B), while others (e.g., large cf. *Taenidium barretti*) are associated with a variety of substrates but provide information related to environmental factors such as water table depths. The presence or absence of a particular trace suite within lithofacies with which they are typically related also provide information about the sedimentary environments. For example, the *lack* of Suite BC5B in bluish green laminated mudstones that coarsen upwards to ripple-laminated very fine-grained arkosic sandstones in the I-Bed at Tollgate Rock, suggests that there, the sediments were deposited subaqueously by similar processes as were the subaerially exposed lithofacies association in the upper A-Bed of the Firehole Canyon area. Additionally, some trace fossils (e.g., *Planolites* isp.) were typically found in lithofacies associated with soupy to shallow subaqueous substrates with freshwater fluvial input (e.g., Suite BC5A). Their presence in more ambiguous lithofacies (e.g., green or tan siltstones and marlstones, A-Bed; Suite BC1) suggests relatively freshwater conditions, even in facies interpreted as being deposited in littoral or eulittoral zones of saline Lake Gosiute.

The following sections focus on the application of the trace fossils for interpretations of depositional settings of the Wilkins Peak basin centre. Sedimentological features and stratigraphic relationships of different lithofacies have also helped to determine the significance of the trace fossils. Stratigraphic sections of the middle Wilkins Peak carbonates below the D-Bed to above the E-Bed in Firehole Canyon (Figs. 6.4.1–2) show the vertical distribution of the associated trace fossil suites. Trace fossil suites preserved within the arkose beds are also referenced in the stratigraphic sections provided of the A-Bed (Figs. 6.4.3–5) and D-Bed (Figs. 6.4.1–2).

### *6.4.1. Interpretation of the Wilkins Peak Member at Firehole Canyon and White Mountain (Kanda, #18 Crossing)*

Although several other lacustrine lithofacies comprise the Wilkins Peak Member, it was the littoral to eulittoral, frequently flooded with shallow saline lake water and subaerially exposed substrates that preserved most of the traces observed (Figs. 6.4.1–2). Two trace suites were identified: 1) littoral to eulittoral full-relief burrows, interpreted as being produced in relatively fresh lacustrine water (hyposaline to mesosaline?; Suite BC1); and 2) evaporitic littoral to eulittoral mammal footprints and simple surficial traces (Suite BC2). The full-relief burrows (Suite BC1) are closely associated stratigraphically with arkosic sediments and the presumably freshwater that was carried within numerous distributary and terminal distributary channels into shallow lake waters or onto probably saline water-influenced mudflats (e.g., SCC, A, m ~1), lower delta-plain (e.g., MFC, A, m ~0.5–2), and beach environments (e.g., FC, D1, m ~30.5). Suite BC3, comprised of vertical burrows, possible earwig nests, and burrow networks produced in subaerially exposed small-channel sands (e.g., SCC, A, m ~1.2), was also associated with lower delta-plain settings where marlstones were deposited. Suite BC1 is also represented in lacustrine carbonate facies present within the arkose beds (discussed below), again at localities showing close association between freshwater fluvial input and the saline lake waters.

D-Bed - Firehole Canyon
FC, D1 - Page 1

*Trace Suites*

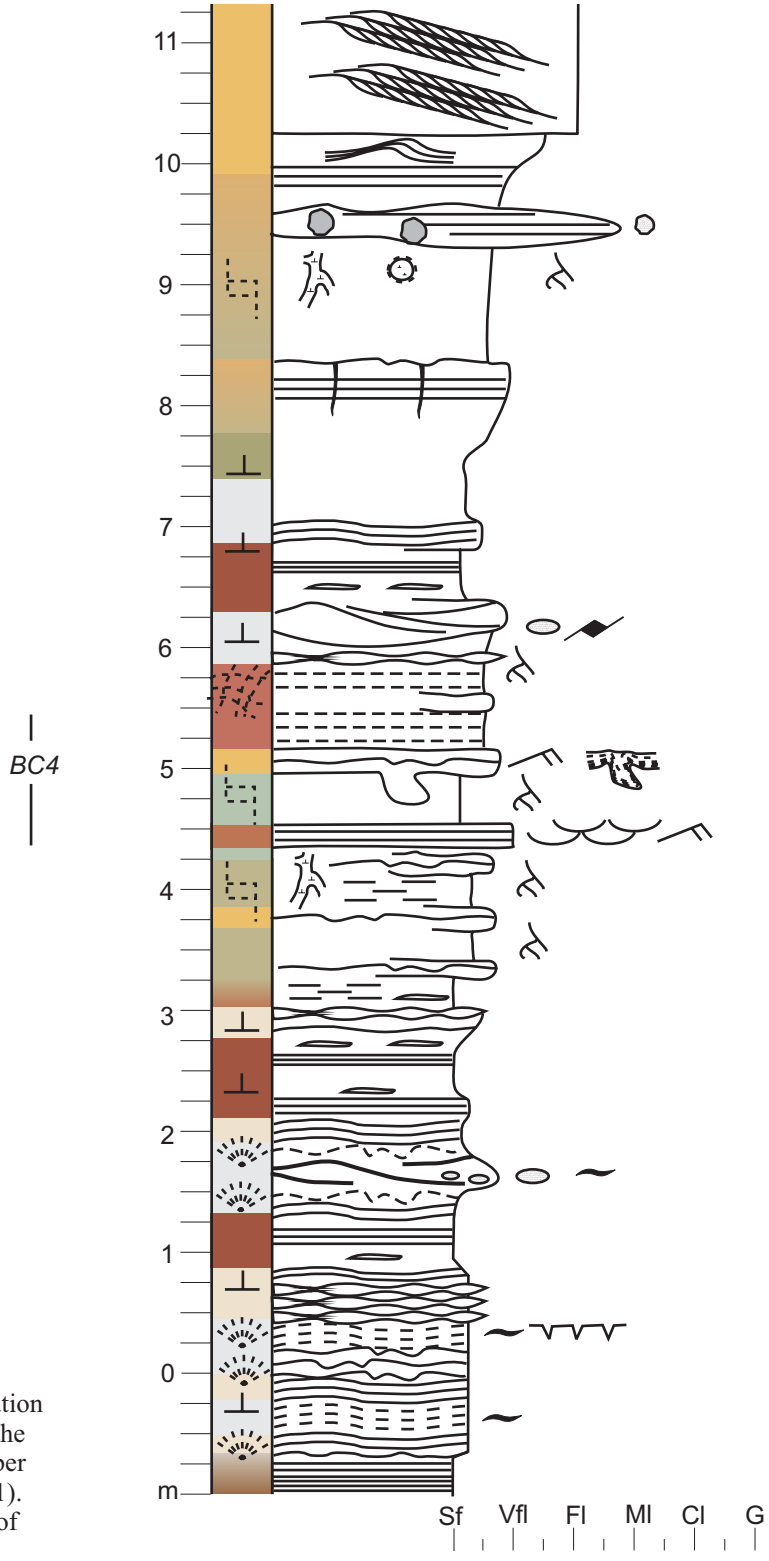


**Fig. 6.4.1.** Vertical distribution of the trace fossil suites in the middle Wilkins Peak Member in Firehole Canyon (FC, D1). Trace suites marked at left of measured section.

D-Bed - Firehole Canyon
FC, D1 - Page 2

*Trace Suites*

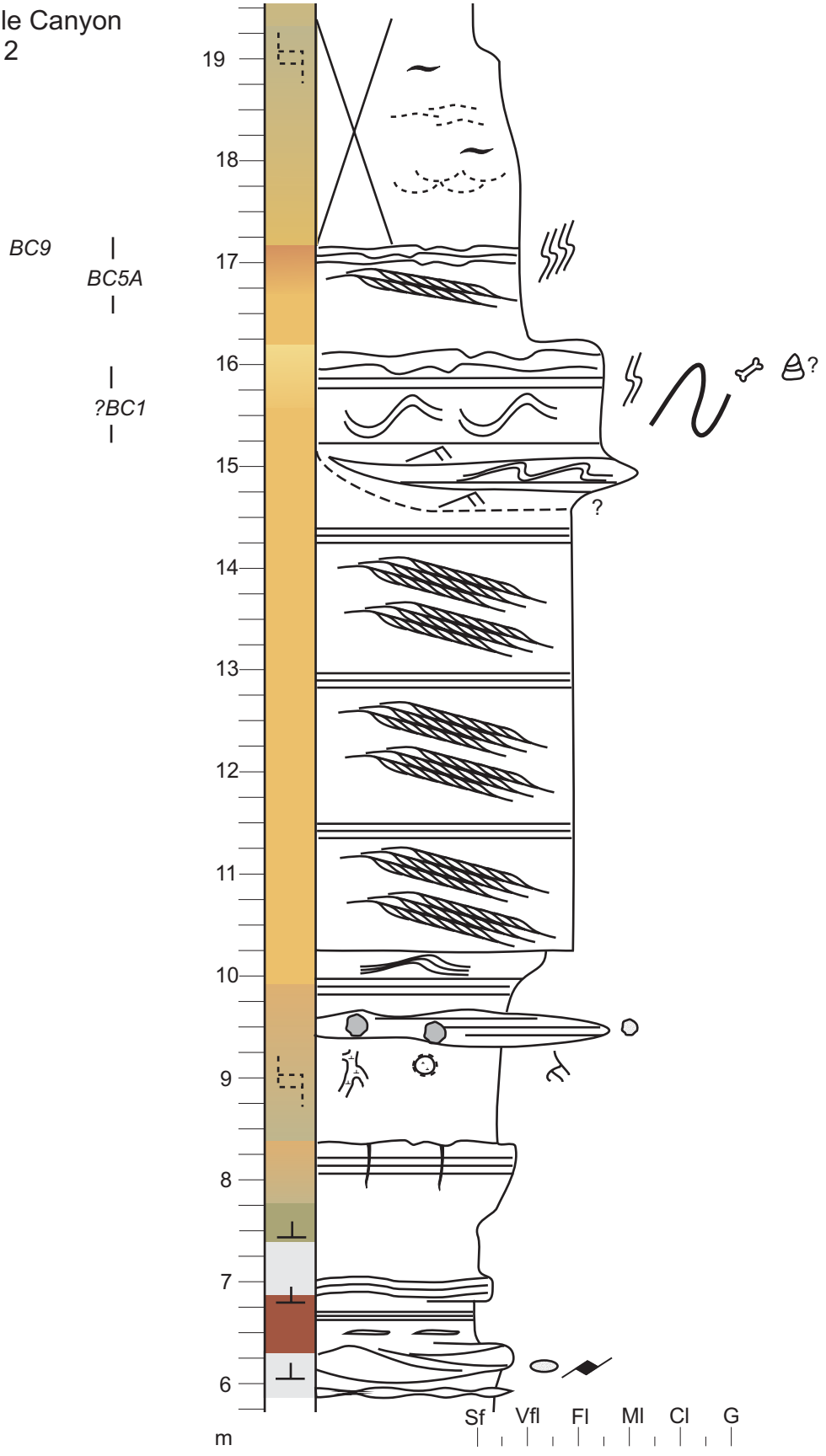


**Fig. 6.4.1.** Page 2.

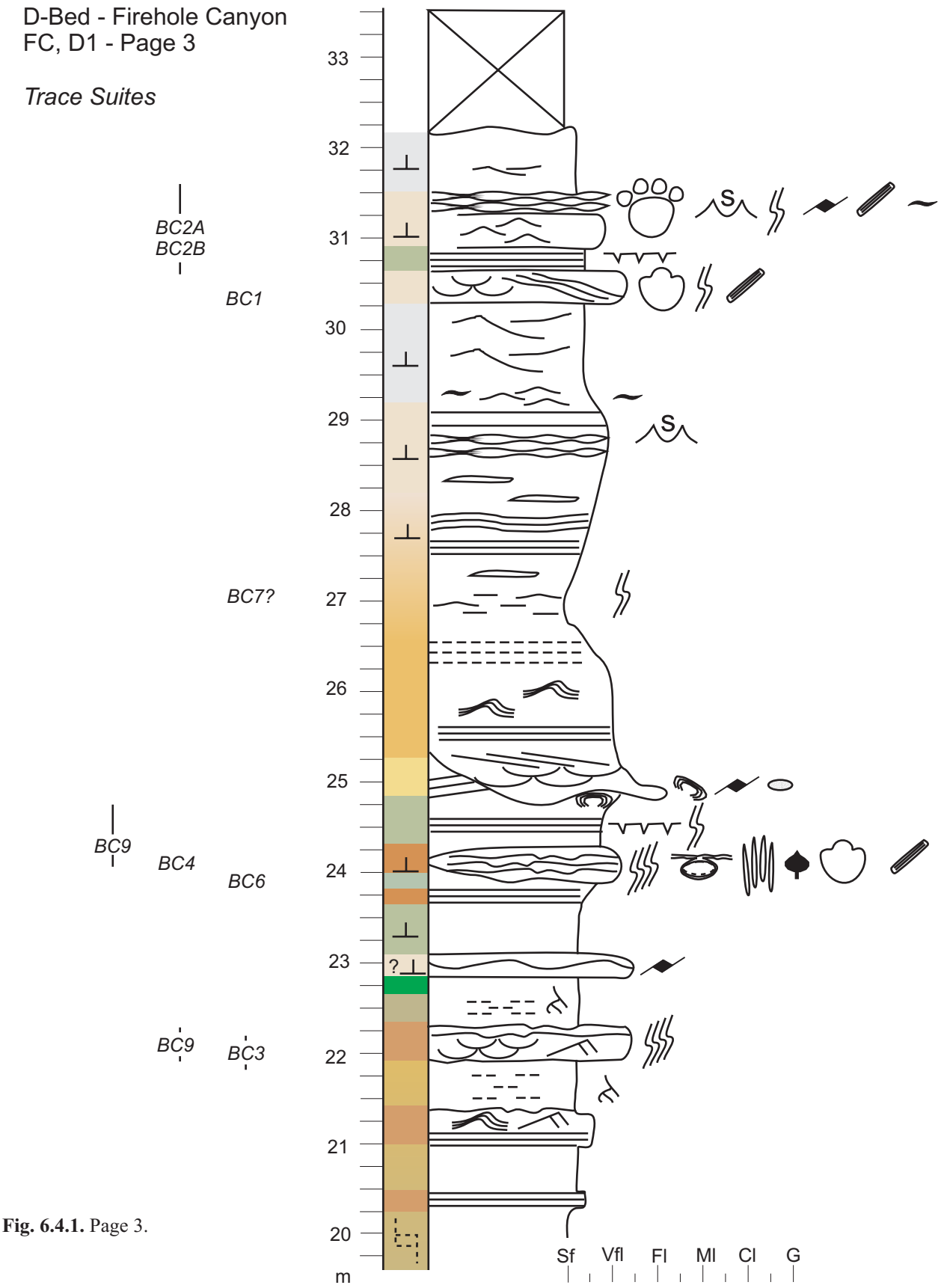


**Fig. 6.4.1.** Page 3.

D-Bed - Firehole Canyon - FC, D2 - Page 1
*Trace Suites*

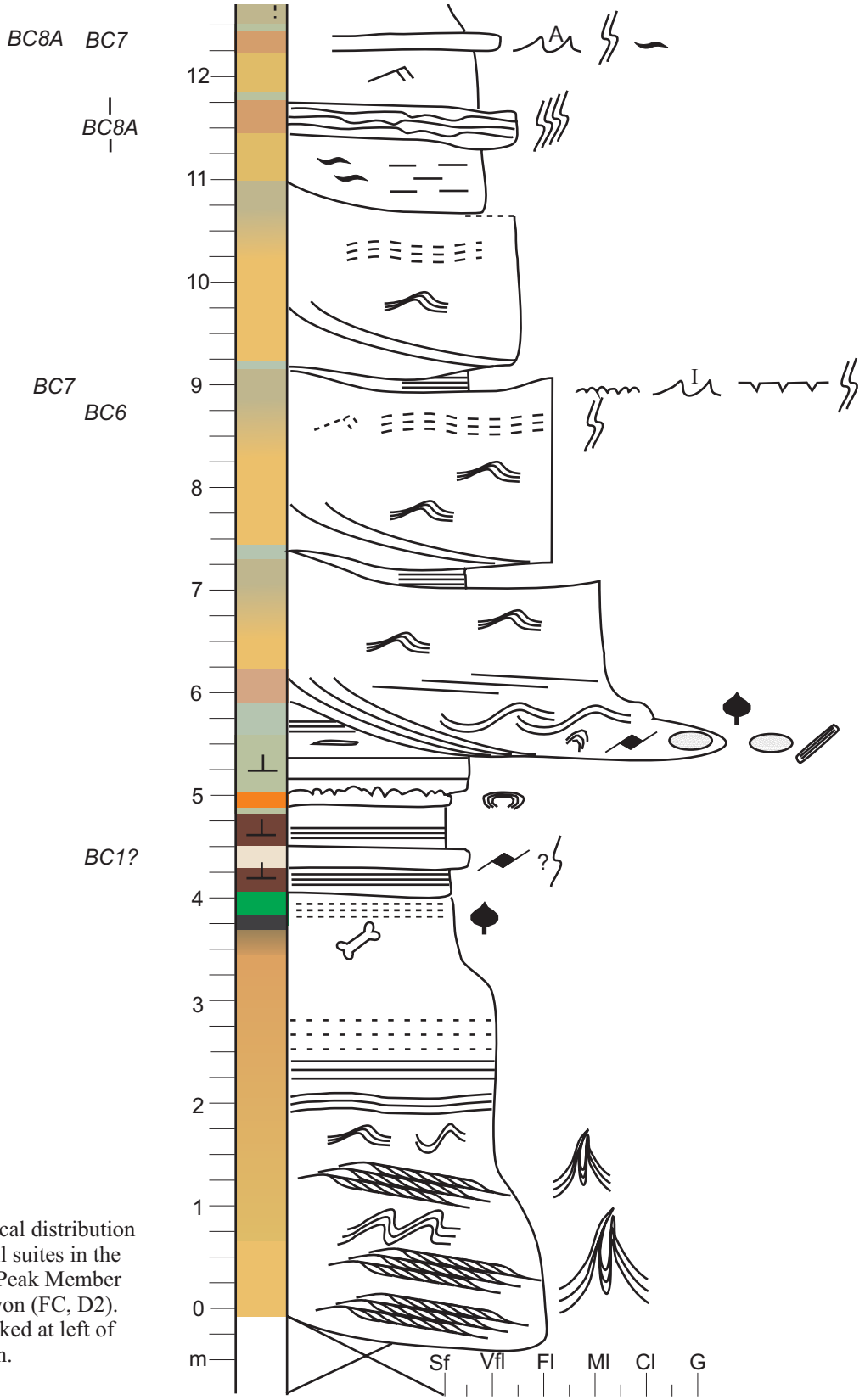


**Fig. 6.4.2.** Vertical distribution of the trace fossil suites in the middle Wilkins Peak Member in Firehole Canyon (FC, D2). Trace suites marked at left of measured section.

D-Bed - Firehole Canyon - FC, D2 - Page 2
*Trace Suites*

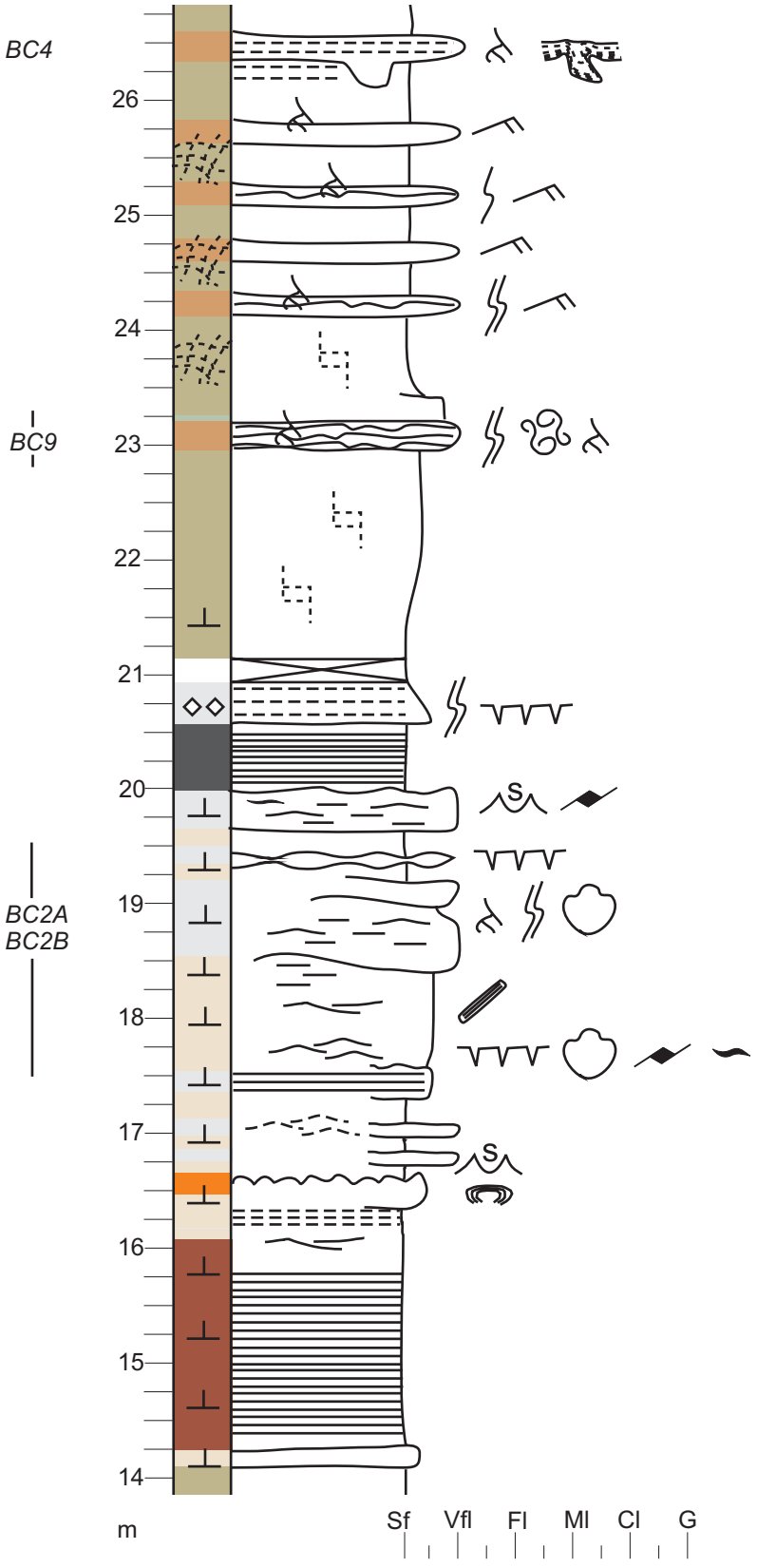


**Fig. 6.4.2.** Page 2.

D-Bed - Firehole Canyon
FC, D2 - Page 3

*Trace Suites*

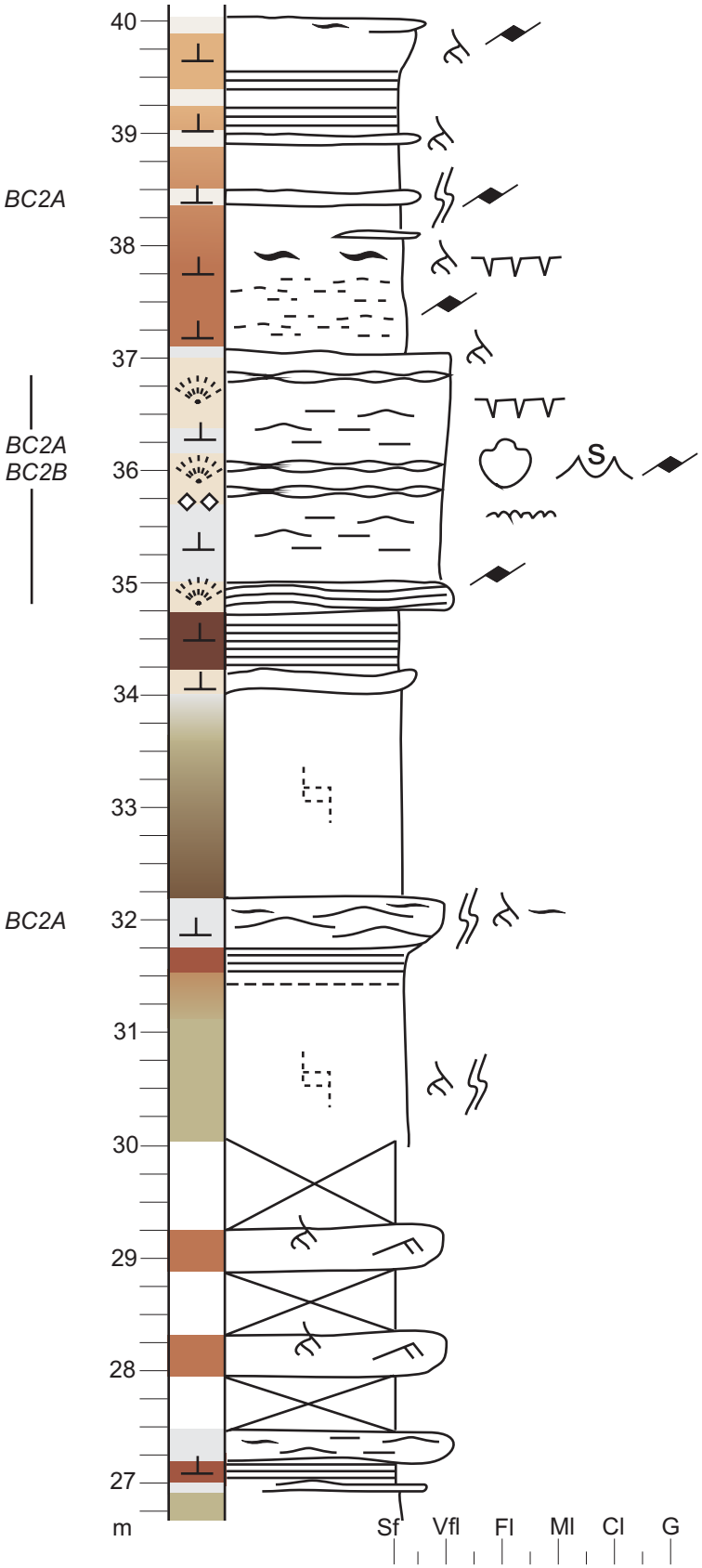


**Fig. 6.4.2.** Page 3.

Suite BC2, however, is preserved in littoral and eulittoral dolomitic mudstones and calciclastic siltstones and sandstones with mudstone drapes. The sediments preserve abundant evidence of desiccation, including carbonate crust intraclast chips formed by the break-up of subaerial exposure of mud-drapes, desiccation cracks, and some evidence of salt efflorescent crusts (e.g., WM, K, below D). Poorly preserved mammal footprints and horizontal branching burrows, probably modified by salt efflorescence and other subaerial processes, were produced in this setting (e.g., Suite BC2B; FC, above D1 and above D2). The very low lake-marginal gradient, perhaps ~1–2°, would have played a role in the depth of the water table, as well as the capillary evaporation of underlying saline groundwater at the exposed lake-plain surface. Although many mammal footprints were preserved in this setting, most examples were isolated on weathered blocks, with no evidence of strongly localized activity across the exposed carbonate flats or mammal-trampled bedding planes.

Simple horizontal trails and tunnels (e.g., *Helminthoidichnites* isp., *Archaeonassa* isp.), preserved in desiccated and non-desiccated mud-drapes on upper bedding planes, were likely formed subaqueously on substrates that were shallowly flooded by lake waters (Suite BC2A). These traces provide evidence of relatively lower salinities of the shoreline areas (?mesosaline: 20–50 g $L^{-1}$) when they were produced. The lack of similar trace fossils on the mud-draped bedding planes associated with bedded evaporite facies (e.g., FC, below D1), which probably formed above a chemocline, suggests that they should not be expected in substrates formed in hypersaline (> 50 g $L^{-1}$) settings. The surface trails and tunnels are especially abundant in carbonate facies above the D-Bed towards northern White Mountain (WM, #18C, above D). This locality is northward of any arkosic channel sandstones in any of the arkose beds (Pietras and Carroll, 2006), but it did preserve south- to southwest-ward directed climbing-rippled very fine-grained sandstones with abundant draped beds which represent sheetfloods. The site is also ~12 km south of the White Mountain Spring mounds, which may or may not have been active during deposition of the middle Wilkins Peak, and possibly provided dilute water to the site (cf. Mayry, 2005). Possible snake locomotion traces and fish swim traces also preserved at White Mountain (#18C) also suggest that this area may have had slightly fresher water than the Firehole Canyon area.

The saline lacustrine and lake-margin carbonate facies of the Wilkins Peak preserve a much less diverse trace fossil assemblage when compared with the arkose beds. The saline facies typically only preserve horizontal traces and mammal tracks (Suite BC2), apparently unless there was influence from a freshwater source. In the latter case, the local dilution of saline lake waters allowed slightly more burrowing activities in the substrate (Suite BC1, Suite BC3). The trace fossils in these settings are attributed to the Scoyenia ichnofacies (e.g., mammal tracks, horizontal burrows, earwig nest-like burrow systems), and possibly with depauperate examples of the Mermia ichnofacies produced in very shallow subaqueous substrates (e.g., surface trails and tunnels, fish swim traces). No examples of cross-cutting, or overprinting, between these suites were found, although there are examples of closely associated Suite BC1 with both Suite BC2 (e.g., FC, above D1, m ~30.5) and Suite BC3 (e.g., SCC, A, m ~1.2; MFC, A, m ~0.5–2). Sedimentation rates were sufficiently high, with the continued aggradation of rapidly cemented carbonate substrates, that trace fossils produced under different environmental conditions (e.g., lower water tables, fresher water conditions) were not overprinted onto Suites BC1, BC2, or BC3 preserved in the basin centre. Similarly, the trace fossils preserved in these suites were produced soon after deposition of the sediments, so that they were closely related with the depositional environments represented by the lithofacies and provide a true view of the conditions during sedimentation.

### *6.4.2. Interpretation of the A-Arkose Bed at Sage Creek Canyon, Firehole Canyon, and Middle Firehole Canyon*

The first of the arkosic sandstone units in the Bridger basin, the A-Arkose Bed overlies laminated carbonate mudstones and siltstones of the Wilkins Peak Member at Middle Firehole Canyon (Fig. 6.4.3), Firehole Canyon (Fig. 6.4.4), and Slate Creek Canyon (Fig. 6.4.5). Near the basin centre, it overlies trona Bed #14 (Culbertson, 1971), which contains the greatest concentration of halite (~25%) of all the trona beds (Wiig et al., 1995). The outcrops investigated were between ~10 km (Sage Creek Canyon) and ~13 km (Middle Firehole Canyon) from the edge of central trona basin, where trona bed thicknesses are more than 2 m (cf. Wiig et al., 1995). If the isopach thickness map of the trona beds of Wiig et al. (1995) can be used to calculate an approximate slope of the basin margin in the Sage Creek to Middle Firehole area, then the lake-margin slope may have been roughly 0.6–1.2 metres per kilometer, or about 1–2°. With such a low gradient, transitional areas (e.g., mudflat) between the lake and lake-margin were likely extensive and the substrates would have frequently experienced shallow flooding from the lake waters, sheetfloods, and/or terminal distributary channels, and subaerial exposure. Saline groundwaters in the lake-margin facies likely persisted for approximately a kilometer eastward of the shoreline, and were likely drawn to the surface by capillary evaporation.

The fluvial system represented by the numerous channel sandstone bodies and lateral accretion surfaces, together with several siltstone and mudstone lithofacies of the A-Arkose Bed, was not separated in time from the underlying carbonate lacustrine facies by an unconformity. Instead, the facies represented in the lower arkosic units of the A-Bed at Sage Creek Canyon, Firehole Canyon, and Middle Firehole Canyon show an interaction between the freshwater-carrying siliciclastic fluvial system and the evaporative carbonate lake. Mudflat facies represented by structureless to horizontally bedded greyish green, brownish green, or tan marl mudstones and siltstones are present in the lower units of the A-Bed in each of the localities, which are separated from one another by ~6.5 km north-south. Each of the measured sections shows a slightly different set of lithofacies, but the interpretations of their deposition and environments are similar. Within the lower ~2 m, structureless and horizontally bedded, fining-upwards marlstones and siltstones give way laterally and vertically to increasing amounts of arkosic sediment, slightly coarser grain sizes, more channelized flow, and more evidence of brief periods of subaerial exposure.

Trace fossils preserved in the finer-grained facies (Suite BC1) include abundant bioturbation by simple full-relief burrows produced in soft-ground substrates (*Planolites* isp.), U-shaped, branched burrows interpreted as prawn burrows (*Thalassinoides* isp. A), and vertical structures in laminated siltstones that represent either escape traces or bird footprints in cross-section. The presence of these traces and their composition imply fresher water conditions (subsaline to hyposaline or mesosaline?) and periods of subaerial exposure of the muddy littoral to eulittoral mudflat, and of the siltstones that filled shallow, scoured channels (e.g., MFC, A, m ~2.3). Adjacent to these lithofacies are sandstones that preserve vertical burrows assigned to Suite BC3. In a small, lenticular cross-laminated sandstone of the lower A-Bed at Sage Creek Canyon (e.g., SCC, A, m ~1.2), for example, these vertical burrows and an earwig nest-like trace (*Thalassinoides* isp. B) are interpreted to signify subaerial exposure and cohesive to firm, wet substrates on the lower delta-plain. Suite BC3 is also preserved at Middle Firehole Canyon (e.g., cf. MFC, A, m ~1–2) in climbing-rippled sandstones that were deposited in a broad shallow channel or by sheetfloods, also interpreted as being on the lower delta-plain.

The lower units continue to coarsen slightly upwards, with progressively larger (wider and slightly deeper) channel bodies cross-cutting smaller channel lenses and horizontally bedded mudflat or muddy littoral facies. The well exposed lower A-Bed in Sage Creek Canyon shows

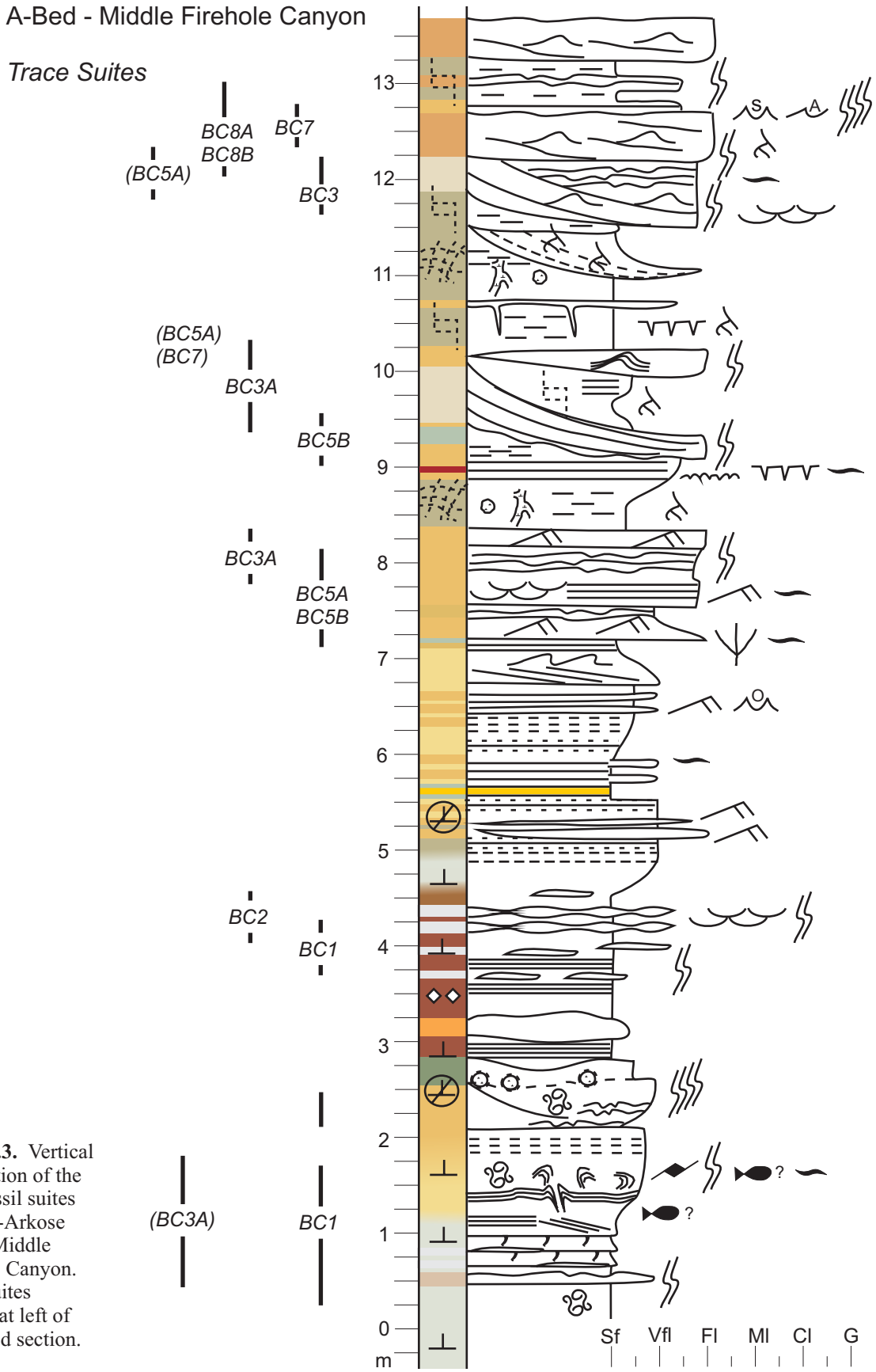


**Fig. 6.4.3.** Vertical distribution of the trace fossil suites in the A-Arkose Bed at Middle Firehole Canyon. Trace suites marked at left of measured section.

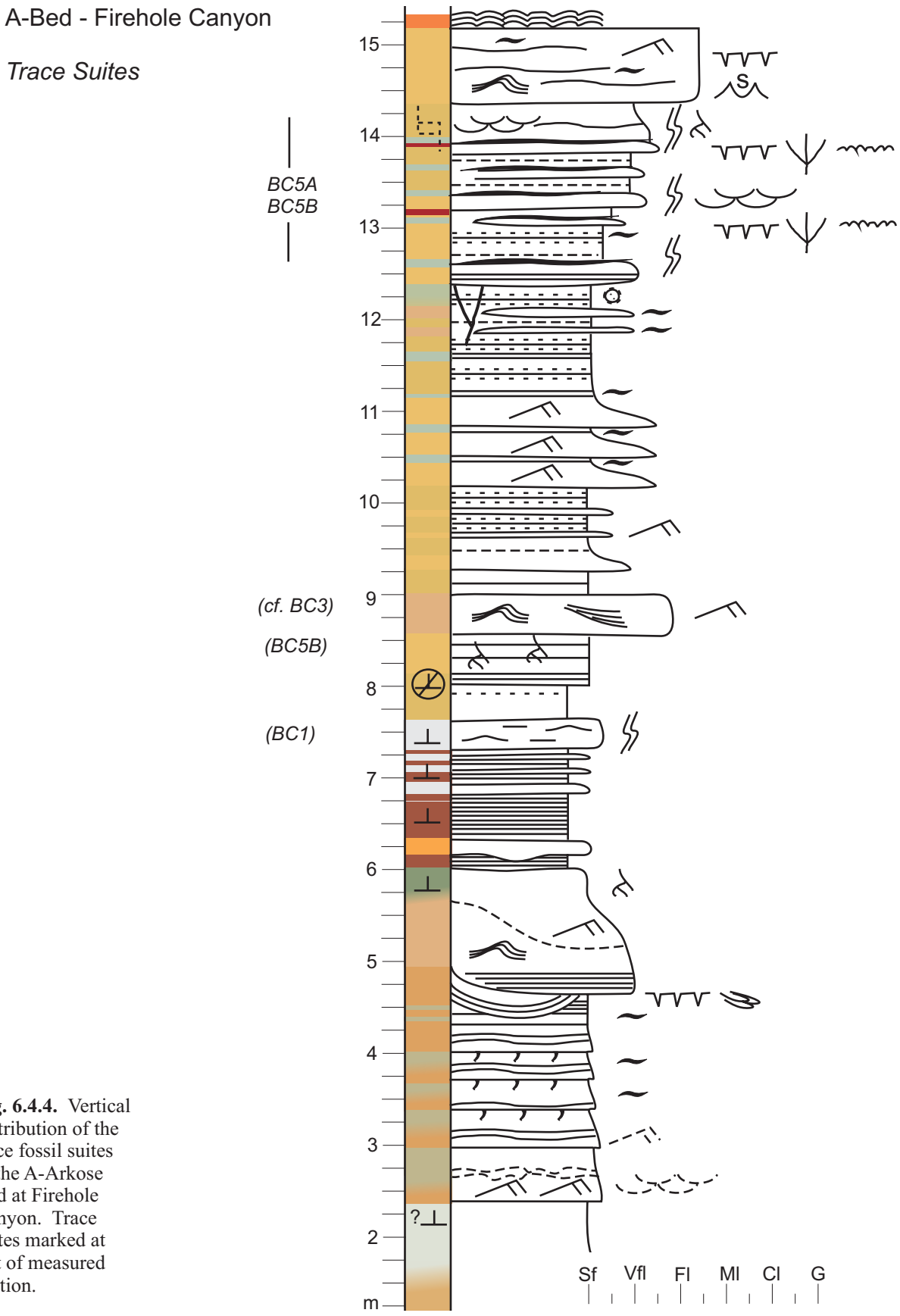


**Fig. 6.4.4.** Vertical distribution of the trace fossil suites in the A-Arkose Bed at Firehole Canyon. Trace suites marked at left of measured section.

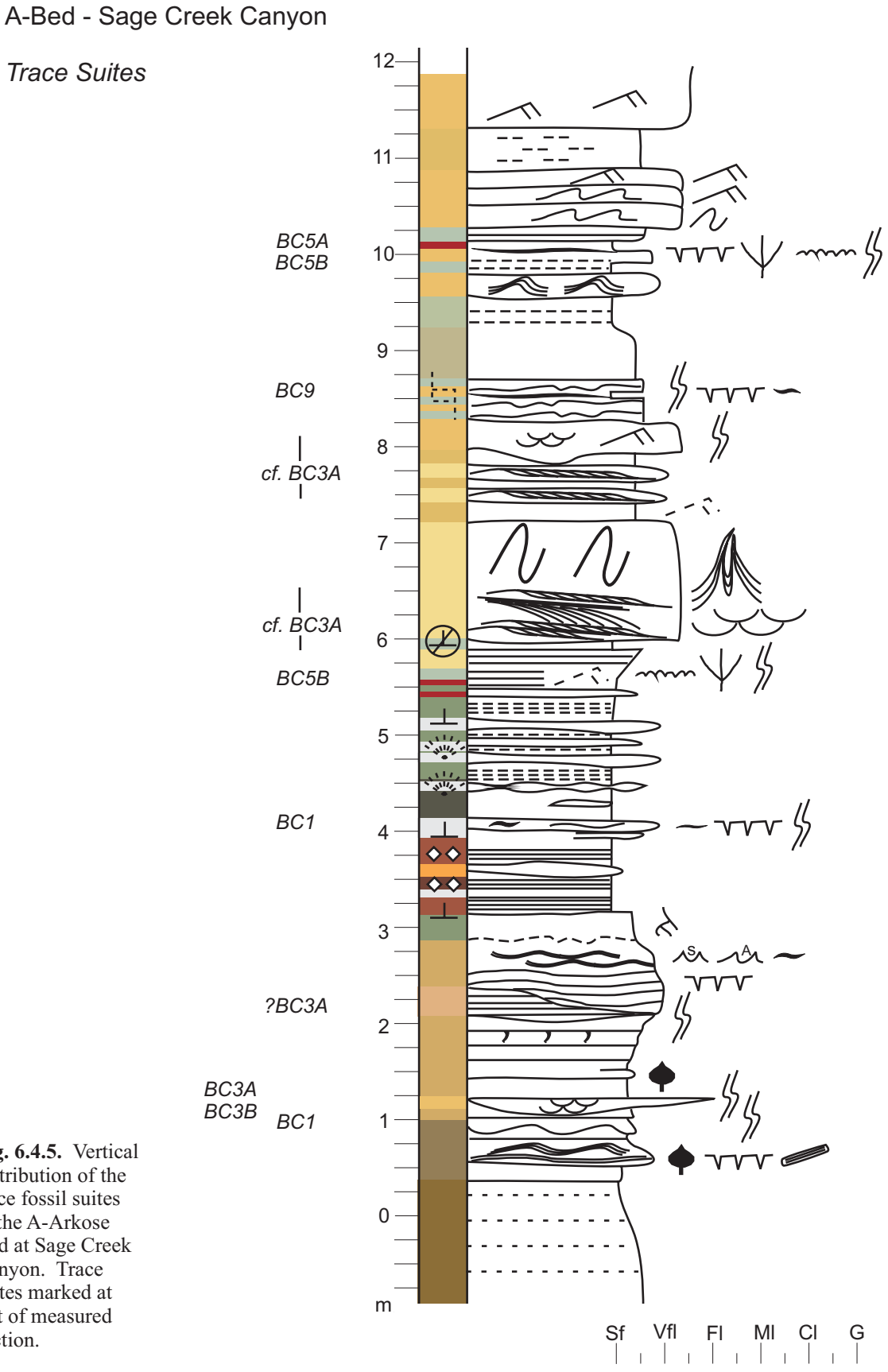


**Fig. 6.4.5.** Vertical distribution of the trace fossil suites in the A-Arkose Bed at Sage Creek Canyon. Trace suites marked at left of measured section.

numerous channels of a variety of sizes. Some channels are revealed by scoured contacts between horizontally bedded siltstones, with minor lateral accretion surfaces or planar cross-bed deposition along the scoured channel-edge. However, the fill of the channels ranges from: 1) horizontal, fining-upwards beds of laminated and structureless marl siltstones and mudstones adjacent to planar cross-beds of silty very fine-grained sandstone; 2) brown silty very fine-grained sandstone in curved, parallel laminae, in which the trace fossil Suite BC3 was observed in one case; to 3) ripple-laminated (unidirectional and combined flow?) and wavy-bedded very fine-grained sandstones. The range of channel-fill sediments, especially the horizontally bedded marl siltstone fill, suggests that these channels record erosion and deposition in the zone of frequent lake-level rise-and-fall in response to storms and minor climate-related changes in precipitation. The Sandai Delta Plain at the mouth of the Sandai River (Lake Bogoria) also shows some of these characteristics, including small sandy point bars formed during seasonal floods that are isolated within widespread silts deposited on the shallow lacustrine delta-front during higher lake levels and reworked on the mudflat during lower lake levels.

In all of the measured sections of the A-Bed, a green to bright green siltstone bed that preserves iron-stained root-marks caps the lower unit. Its colour is interpreted to represent chemical changes in groundwater composition related to the transgressing lake, which is recorded by the succeeding organic-rich lacustrine mudstones of the "white stripe unit". The iron-stained root-marks may have formed in lake-fringing marshes as the water table became shallower. In a slightly lower-lying lens-shaped eroded channel of the uppermost lower A-Bed in Firehole Canyon (N), a thin coal bed directly underlies the laminated carbonate mudstones and supports this interpretation. Transgressive erosion occurred as the lake-level rose, particularly on slightly higher topography of the subaerially exposed lower delta-plain.

Trace fossils are not generally abundant or diverse in the lower unit of the A-Bed, but they provide valuable evidence of subaerial exposure, cohesive to firm subaerially exposed substrates, and areas with relatively freshwater input and soupy to saturated substrates either within the lake or near the shoreline. The *lack* of trace types associated with more terrestrial and fluvial environments, such as meniscate-backfilled burrows and large-sized vertically oriented burrows, also helps to show that the substrates likely did not dry completely and were not well drained. The lower unit represents a shallowing upwards parasequence or lake cycle, and is overlain by the flooding surface of the next parasequence or lake cycle, represented first by the lacustrine facies of the "white stripe" unit, and upwards by the upper, arkosic unit (Figs. 5.3, 5.4, 5.5). Trace fossils, together with pedogenic features provide evidence that helps to: 1) determine the depositional environments of the siltstone and sandstone lithofacies; 2) recognize the major trends in water table depth; 3) recognize changes in sedimentation rates; and 4) recognize brief to prolonged periods of subaerial exposure. These additional lines of evidence help to reconstruct the depositional settings by providing evidence not recorded by sediments alone.

The lower arkosic unit is overlain by fully lacustrine dark brown laminated carbonate mudstones representing the sublittoral to profundal zones. High salinities of the lake waters are indicated by the presence of shortite crystals and trona fan moulds in calciclastic siltstones. No trace fossils were preserved in these sediments. Shallowing of the lake is implied by an upwards transition to lenticular-bedded mudstones with calciclastic siltstone lenses, to interbedded mudstones and calciclastic siltstones and sandstones, to wavy-bedded calciclastic sandstones. Small desiccation cracks are preserved in these interbedded facies at Sage Creek Canyon, and are associated with examples of small (~3 mm diameter), simple full-relief burrows (*Planolites* isp.; Suite BC1) in the mudstones that are filled with calciclastics (e.g., SCC, A, m ~4.0). Similarly, this lithofacies within the A-Bed at Middle Firehole Canyon (e.g., MFC, A, m ~4.1) also preserves small *Planolites* isp. in carbonate mudstones (Suite BC1), as well as indistinct surface

bioturbation on the calciclastic sandstone bedding planes that preserve low-amplitude symmetrical ripple bedforms. This indistinct bioturbation may represent a sub-suite of either Suite BC1, associated with relatively freshwater, or Suite BC2, found in subaerially exposed, saline lake littoral to eulittoral substrates. This trace type shares some features with indistinct bioturbation preserved in freshwater facies preserved at the top of the D-Bed at Kanda and in the upper D-Bed at Firehole Canyon. The presence of full-relief burrows within the saline lacustrine facies (Suite BC1) suggests that for periods the lake waters were relatively fresh (hyposaline to mesosaline?). The upwards transition to lenticular-bedded arkosic mudstones and siltstones with calciclastic lenses also provides evidence that the freshwater supply had been renewed, either by lobe-switching of the delta, or by regression-related basinward movement of the fluvial system. The latter option is preferred because of the lateral extent of the "white stripe" unit, shallowing upwards within the white stripe unit, and similarities between the lower portions of the upper unit at all three localities.

Like the lower unit, the upper unit of the A-Bed preserves a coarsening-upwards succession, although it consists of overall more landward facies, with fluvial sandstones and weakly developed paleosols preserved towards the top. These general features are interpreted as representing progradation, with the lower, and white stripe/upper units representing two progradational parasequences bounded by flooding surfaces (note: the lower flooding surface of the lower unit was not studied). The depth of scoured channels increases upwards, with the deepest channel scours and largest lateral accretion surfaces found at the top of the unit. At Sage Creek Canyon, a shallower channel sandstone (~1.5 m thick) is scoured directly into a much deeper channel sandstone (~3–4 m thick). This example could record the retrogradation of the system in response to increasing lake levels, but more data is required to support this.

The upper units in each of the A-Bed localities appear to contain at least two cycles that coarsen upwards, or become more proximal upwards. The lowermost portions of the upper unit are transitional with the lacustrine and littoral carbonates below, with similar lithofacies as within the lower unit. However, these greyish green to greenish tan marl mudstones and siltstones quickly give way to more landward facies in less than 1 m. At Middle Firehole Canyon and Firehole Canyon, for example, the measured sections both record a rapid transition to interbedded laminated light buff-coloured siltstones and light bluish green mudstones with horizontal, iron-stained horizons. Very thin interbeds of very fine-grained current ripple- to planar-laminated arkosic sandstones may also be iron-stained. This facies association coarsens upwards slightly to thicker beds of planar- and ripple-laminated sandstones with siltstone or mudstone drapes. Due to steep cliff exposures, it was not possible to examine bedding planes for surface traces, however, probable bird footprints produced in bluish green mudstone (Suite BC5B) were preserved as casts within the sandier facies (e.g., MFC, A, m ~7). They were associated with softground bioturbation assigned to the *Planolites* ichnofabric (Suite BC5A) in sandstone beds, as well as vertical burrows and escape traces (Suite BC3) and possible bird footprints in cross section. This succession at Middle Firehole Canyon is interpreted as distal sheetfloods or distal splays into the shallow lake (no traces), onto the lower delta-plain (Suite BC5B), grading upwards to more proximal sheetfloods or splays (Suite BC3A).

The Firehole Canyon section records a similar coarsening upwards succession, but small, lenticular channel sandstones (~20 cm high, ~2–4 m width) were also present within the heterolithic laminated siltstones and mudstones with ripple-laminated sandstone interbeds (e.g., FC, A, m ~9). Together, these features are interpreted to represent the subaerially exposed lower delta-plain, which was buried by lakeward advancing sandy facies with freshwater, fed by the distributary fluvial system. In both cases, the upper sandstones of the successions are capped by discontinuously laminated siltstones and mudstones, interpreted as weakly pedogenically

modified facies, which may either represent sediment bypass in the more proximal portions of the lower delta-plain or of the next coarsening upwards cycle above. The first option is preferred because of the preservation of carbonate root casts with iron-stained rinds (e.g., MFC, A, m ~8.8) that provide evidence of stable sediments.

In contrast, the lower, transitional portion of the upper unit in Sage Creek Canyon (e.g., SCC, A, m ~6–8.2) was scoured and preserves a broad channel sheet sandstone with multiple lateral accretion surfaces. Possible lagoonal facies represented by dark brown to black arkosic mudstones interbedded with planar-laminated very fine-grained sandstones (e.g., SCC, A, m ~5.5–6) are transitional with the underlying marlstones and calciclastic siltstones facies. A bird-trampled surface (Suite BC5B), medium-sized *Planolites* isp. (Suite BC5B), and very small possible open burrows (?cf. Suite BC3A) were preserved, together with black- and red-stained bedding planes with bubbly microbial textures. This facies coarsens upwards slightly to planar-laminated sandstones, then fines to bluish green laminated mudstones before being scoured by the large channel above.

Very small possible open burrows (?cf. Suite BC3A) are present within the trough cross-stratified and ripple-laminated cross-bedded sandstones at the base of the upper unit, in greater densities at the base of the bedset. Alternatively, these structures could by small mudballs that weathered from the outcrop, or dissolved shortite evaporites that formed later from saline pore waters. The channel sandstone bed contains large soft-sediment deformation features that may be due to dewatering of the rapidly deposited sandstone. The overlying ripple-laminated cross-bedded sandstones (e.g., SCC, A, m ~7.2–8.8) are interpreted as channel fill deposits that fine upwards and culminate in mud-draped, desiccated, and bioturbated (Suite BC9) heterolithic facies. Weak pedogenesis and full-relief burrows reworked the ripple-laminated sandstones, suggesting channel abandonment and desiccation of the substrate. Large cf. *Taenidium barretti* burrows were not observed.

The upper portion of the upper unit at Sage Creek Canyon (e.g., SCC, A, m ~8.8–12) consists of a coarsening-upwards cycle, from massive green siltstones, to discontinuously laminated bluish green mudstones, to laminated bluish green mudstones interbedded with climbing-rippled sandstones, to ripple-laminated and convoluted (sheared) beds of very fine-grained sandstones. It is capped by discontinuously laminated siltstones, which may or may not form the upper part of the cycle. Within the heterolithic facies, desiccation cracks, bird footprints, and very small *Taenidium barretti* were preserved, and are included in Suite BC5B. The upper sandstones preserve bioturbation on their base, which may be an example of *Fuersichnus* isp., here included as part of Suite BC5A. This succession, considering the sedimentological and ichnological features, is interpreted as a prograding crevasse splay, initially into standing water, from distal subaqueous facies to desiccated-pond heterolithic facies, to proximal crevasse sandstones. A thick bed (~40 cm thick) of flat-based ripple-laminated sandstones forms the top of the section. This sandstone likely correlates laterally to one of the deeply scoured channels approximately 300 m away. Recessive siltstones continue upwards for ~2 m (unmeasured) below the next lacustrine carbonate mudstone unit. The large-scale geometry of the sandstone channels in the upper unit shows increasing depth and width to the channels upwards, and a lower total number of channels upwards. This is interpreted as representing the progradation of the fluvial system from the lower delta-plain to the upper delta-plain, approaching a more typical set of floodplain facies towards the top

The upper unit of the A-Bed in Firehole Canyon (N) shows a similar succession, with some channel sandstones in the lower portions (e.g., FC (N), A, upper unit) that pinch out to transitional facies from the “white stripe” unit, and which possibly represent the main terminal distributary trunk channels emptying into the shallow lake (e.g., mouth bar deposits). These

sandstones preserve *Vagorichnus* isp. in convex hyporelief (Suite BC5B). Within the measured section, however, four coarsening-upwards cycles interpreted as aggradation of the delta-plain, are represented (e.g., FC, A, m ~8–15). Above the weakly pedogenically modified siltstones that cap the first cycle, another set of heterolithic bluish green mudstones and very fine-grained sandstones persists. Thick mud drapes cover the sandstone beds, preserving abundant desiccation cracks, as well as shorebird footprints and a variety of insect surface tunnels, trails, and trackways (Suite BC5B). Sandstone interbeds are bioturbated by the *Planolites* ichnofabric (Suite BC5A). The top of the section consists of weakly bedded ripple-laminated and desiccated very fine-grained sandstones with iron-stained root-marks and in places, flat-crested, symmetrical ripple bedforms. This succession is interpreted as a prograding crevasse splay or delta-plain 'fan', with facies initially more distal (lateral?) to the main channel that provided freshwater and pulses of sandy sediment. Upwards, sandstones provide evidence of the more landward (upper delta-plain?) or more proximal position relative to the distributary channel. A thin, orange stromatolite-layered carbonate bed marks the sharp change in facies to the overlying carbonate lacustrine unit of the Wilkins Peak Member.

In Middle Firehole Canyon, the upper portions of the upper unit of the A-Bed (e.g., MFC, A, m ~8.5–13.5) preserve weakly developed paleosols that are intercalated with active channel sandstones and an abandoned channel fill by siltstones that were weakly pedogenically modified. A thin bed of planar- to wavy-laminated heterolithic sandstones with mudstone drapes, representing proximal overbank deposits, preserves horizontally oriented *Spongeliomorpha* isp. (cf. *Steinichnus* isp.), with obliquely oriented scratch marks in all directions. The trace type is assigned to Suite BC8A, and represents subaerial exposure of cohesive, moist to wet substrates (e.g., MFC, A, m ~9). Above, the channel sandstones have scoured bases, are mainly small-scale trough cross-laminated and ripple-laminated planar cross-beds, and are interpreted as the lateral accretion of point bars in shallow channels (e.g., MFC, A, m ~9.5–12.5). Vertical burrows (*Skolithos* isp.) and bunch-like root traces were produced from the tops of the cross-laminated bedsets, and were probably produced from point bars during subaerial exposure (Suite BC3B). Possible trace makers of these burrows include spiders or insects (e.g., tiger beetle adults). The vertical burrows are very common in the cross-bedded sandstones at this locality, suggesting that their absence in other examples of similar facies could imply either 1) continuous sedimentation with only very brief pauses in flow; 2) the lack of periods of subaerial exposure; 3) relatively higher energy; or 4) sublacustrine deposition.

Towards the top of the section, overall bioturbation increased (BI= < 4–5), with trace types typically associated with subaerially exposed, more terrestrial settings (Suite BC8). The traces include mainly horizontally oriented, small- to medium-sized backfilled burrows including small *Taenidium barretti*, pellet-backfilled burrows, *Planolites* isp, and an excavated insect (ant?) nest closely associated with *Planolites* burrows. Additionally, bunch-shaped, open vertically to obliquely oriented 'burrow' structure, interpreted as bunch roots of plants, were produced from the upper sandstone surface at m ~12.7. No large cf. *Taenidium barretti* were observed. The trace types and the degree of bioturbation are interpreted to represent a relatively stable, moist, cohesive substrate of a subaerially exposed upper surface of an abandoned channel sandstone on the delta-plain. The degree of bioturbation at the top of the A-Bed in Middle Firehole Canyon represents a period of low sedimentation rates or non-deposition prior to the flooding of that locality by the next transgression of Lake Gosiute. At the three localities investigated, the A-Bed is interpreted either as the coarsening-upwards succession of a basinward-advancing fluvial system or the progradation of a delta into shallow lacustrine areas, with exposed lower and upper delta-plain environments. Fine-grained facies towards the top of the unit are interpreted as pedogenically modified, more landward, terrestrial facies.

### *6.4.3. Interpretation of the D-Arkose Bed at Firehole Canyon (D1 and D2) and White Mountain, Kanda*

Like the A-Arkose Bed, the D-Bed preserves a diverse assemblage of trace fossils that are associated with depositional environments interpreted as freshwater-influenced mudflats, terminal distributary channels, crevasse splays, and relatively freshwater lacustrine deposits from sublittoral, littoral, eulittoral, and delta-plain settings. The D-Bed was investigated in Firehole Canyon (Figs. 5.1, 5.2, 6.4.1–2) and on White Mountain at Kanda. Divided into a lower unit, white stripe unit, second unit, green stripe unit, and an upper unit in Firehole Canyon, the D-Bed in Firehole Canyon is thicker (~25 m) than the A-Bed and probably was deposited during a longer interval before the next major transgression of Lake Gosiute. Trace fossils and lithofacies both record a slightly different succession, with more landward fluvial channel and overbank facies associations when compared to the A-Bed. Like the A-Bed, some overprinting of trace suites was observed in better drained, more terrestrial depositional environments that provide evidence for periods of low sedimentation rates and changing environmental conditions. These changes are recorded mainly by trace fossils, especially towards the top of the unit.

Trace fossil Suites BC1 and BC3 were not preserved in the lower unit of the D-Bed. Instead, the gradual change from carbonate lacustrine mudstones, siltstones, and calciclastic sandstones more closely resembles the upper unit of the A-Bed, with a relatively rapid transition through massive marlstones to subaerially exposed or very shallow water mudflat or lower delta-plain sedimentation in Firehole Canyon (e.g., FC, D1, m ~3–4). Suite BC4, comprised of mammal footprints produced in soupy substrates and preserved in cross-section, are associated with discontinuously laminated bluish green mudstones interbedded with ripple- and planar-laminated very fine-grained arkosic sandstones. The lower unit coarsens slightly upwards in the lower portion, with evidence of longer periods of subaerial exposure at the top of the unit (e.g., weak pedogenic modification, deep desiccation fractures, and carbonate root casts; FC, D1, m ~5–6). The mammal tracks and iron-stained root-marks are intermediate within the unit, and are associated with very shallow water tables. Because of the close association of the lower unit with saline lacustrine sediments below, it is interpreted to have been deposited on the lower delta-plain, with freshwater and sediment input from distal crevasses/levee overbank floods or sheetfloods.

The weakly developed paleosol at the top of the lower unit was scoured slightly during transgression and is sharply overlain by calciclastic sandstones and lacustrine carbonate mudstones (the “white stripe” unit). Massive marlstones and greenish tan arkosic siltstones grade transitionally upwards from the lacustrine carbonate mudstones, and may have been deposited within the lake as suspension-fallout deposits from river-fed low density flows into the saline lake (hypopycnal flows and delta-front to pro-delta deposition). They coarsen upwards to planar-laminated very fine-grained sandstones that were subsequently desiccated. No trace fossils were found within this lowermost portion of the second unit (FC, D1, m ~7–8.5), which may indicate inhospitable soupy substrates with relatively high salinities. Renewed deposition of discontinuously laminated greenish tan arkosic siltstones that also coarsen upwards slightly preserve planar-laminated sandstones with iron-stained root-marks and carbonate root casts, but without evidence of bioturbation (FC, D1, m ~8.5–9.5). These beds are interpreted as being basinward of or lateral to a terminal distributary channel, with sedimentation pulses followed by periods of subaerial exposure.

A thick coset of ripple-laminated fine-grained to very fine-grained arkosic sandstones interpreted as basinward-dipping terminal distributary channel mouth bar deposits (cf. Schomacker et al., 2010) overlies the green and greenish tan siltstone. Within the sandstone units, indistinct ripple-lamination, a lack of draped beds, and a lack of bioturbation (no Suite

BC3) may have been due to high energy flow and continuous sedimentation. The top of this sandstone package (FC, D1, m ~16), however, does preserve bioturbation as large *Planolites* isp. in a fine-grained sandstone with horizontal planar-beds and convolute bedding. This assemblage is interpreted as representing Suite BC1, perhaps a fully freshwater example of this suite, possibly in sandstones deposited as a levee (subaqueous?) of the terminal distributary channel. Above this, a very fine-grained sandstone bedset (FC, D1, m ~17) also preserves escape traces and bioturbation by *Planolites* isp. and *Palaeophycus* isp. (Suite BC1). Unfortunately, this portion of the measured section is poorly exposed and the overlying facies (FC, D1, m ~17–20) are not well described or understood.

The next set of well exposed sediments (FC, D1, m ~20+) preserve structureless greenish tan siltstones intercalated with a coarsening-upwards set of silty very fine-grained sandstones to fine-grained arkosic sandstones that preserve ripple-lamination, climbing ripple-lamination, and small-scale trough cross-lamination. The upper sandstone in this succession preserves abundant trace fossils, produced during deposition (Suite BC3), and is cross-cut by traces produced following the draining of the sandstone bed (Suite BC9). The lithofacies and trace fossil assemblage is interpreted as being deposited on the upper delta-plain, with sedimentation from crevasse-splay sandstones becoming more proximal upwards. The relatively lower water tables evidenced by vertically oriented full-relief burrows of Suite BC9 may have been due to sediment aggradation while lake-levels remained low, or they may simply represent the draining of subaerially exposed sandy sediments above the water table.

The tan siltstones that overlie this bioturbated crevasse sandstone in Section FC, D1 are conformably overlain by green- to bright green-weathering dark brown and black mudstones that form the lower portion of the "green stripe unit". As discussed in Chapter 5, this unit may represent a small lake on the delta-plain or an interdistributary bay of the main lake. The colour change and facies associations are similar to those that cap the lower unit of the A-Bed. A carbonate intraclast conglomerate bed overlies the green stripe, and could represent a transgressive lag of the main lake. Light greyish green mudstones and marlstones were deposited above, without evidence of bioturbation. However, a lenticular-shaped very fine-grained sandstone bed, interpreted as a crevasse splay into standing water, does preserve evidence of bioturbation and trace types that represent relatively freshwater (Suite BC6). Suite BC6 consists of crocodilian footprints and scratch-marks (swimming traces?) together with abundant small *Planolites* isp. that have sharp burrow boundaries, due to their presence in a cohesive, clayey substrate. This assemblage also includes a possible mammal footprint and large reed impressions. In the lenticular sandstone, mammal footprints produced in soupy substrates (Suite BC4) are associated with the deposition of the bed. Full-relief burrows of Suite BC9 (e.g., large, aggregate-filled burrows) overprinted the sandstone from above, suggesting that it was subaerially exposed.

Laminated greyish green mudstones with very small desiccation cracks of the green stripe unit persisted locally following deposition and bioturbation of the crevasse sandstone, upwards to a stromatolitic layered orange carbonate that may represent (continued?) transgression of the lake. Channel sandstones of the upper unit, with large-scale trough cross-stratification, planar-lamination, and cross-lamination, are scoured into the laminated mudstones with an intraclast conglomerate at their base (FC, D1, m ~25). These channel deposits are interpreted as a terminal distributary channel, which was flooded by the advancing lake, leading to the deposition of lenticular bedded marlstones, to wavy-bedded calciclastic sediments, and finally to low-angle planar-laminated calciclastic sandstones bioturbated by Suite BC1 (FC, D1, m ~30.5), and Suite BC2 as the littoral zone lake deposits were subaerially exposed (FC, D1, m ~31).

The channel sandstones here correlated with fine- to coarse-grained channel sandstones and conglomerates of the upper unit preserved in Section FC, D2, about ~500 m west of Section FC, D1. No trace fossils were observed within the planar cross-laminated sandstones. The cross-bedded sandstones fine-upwards to heterolithic facies representing waning flow within the channels, due either to flood deposition and/or avulsion upstream. Simple horizontal trails and burrows, and possibly bird footprints, were observed within the heterolithic facies (Suites BC6, BC7), representing very low energy shallow freshwater unidirectional flows or shallow standing water within the channel. The uppermost portion of the upper unit in Section FC, D2 fines upwards to discontinuously laminated brownish green siltstones intercalated with irregularly bedded and ripple-laminated very fine-grained sandstones. Suite BC8A, with small *Taenidium barretti* and branching, small *Planolites* isp., was preserved in these sandstones, representing subaerial exposure and relatively stable substrates. They are interpreted as overbank deposits on the upper delta-plain, with relatively low sedimentation rates.

The upper unit of the D-Bed on White Mountain at Kanda also preserves large channel sandstones, with ripple-laminated lateral accretion cross-beds associated with planar-laminated sandstones that preserve meniscate horizontal burrows (cf. *Taenidium* isp.: Suite BC7?). The uppermost surfaces of the unit also preserve surface bioturbation, possibly produced by gastropods in quiet standing water following the abandonment of the channel and cessation of active deposition (Suite BC7). Laterally, heterolithic facies either adjacent to the channel or prior to channel incision, preserve mammal footprints of Suite BC4, as well as bird footprints and surface trails and tunnels of Suite BC5B, which provide evidence of high water tables and soupy substrates, as well as desiccation of shallow pools of standing water fed by the fluvial system. These features may simply be present in a setting within close proximity to the freshwater channel, and do not necessarily provide evidence of proximity to the lake.

The D-Bed records a coarsening-upwards succession similar to that of the A-Bed, but preserves a greater proportion of more landward and terrestrial lithofacies (e.g., well drained sandstones, paleosols), especially towards the top of the unit in Firehole Canyon. The brownish green alluvial plain siltstones also comprise most of the E-Bed, with Suites BC9 and BC4 preserved in intercalated very fine-grained sandstones. Unlike the A-Bed, however, the D-Bed in Firehole Canyon (D1) also preserves evidence of an active fluvial system in the upper unit, continuing until flooded by the transgression of the main lake. Lower sedimentation rates and bioturbation by more terrestrial traces (Suite BC8A) towards the top of the D-Bed are preserved in sites adjacent to the terminal distributary channels (e.g., FC, D2, m ~11–14). Overprinting of trace suites was observed in well drained substrates (e.g., crevasse-splay sandstones) that were deposited onto upper delta-plain siltstones, presumably with relatively low water tables (e.g., FC, D1, m ~22.3), as well as sandstones deposited into standing water and then subaerially exposed (e.g., FC, D1, m ~24.5). In general, continued aggradation of the D-Bed permitted the overall vertical separation of trace suites and a lack of intensely bioturbated substrates, except for high densities of *Planolites* isp. of Suite BC6 (FC, D1, m ~24), apparently produced in standing water with little sediment input. Even where some overprinting occurred, environmental conditions had changed little from the original depositional environment of the substrates.

# CHAPTER 7

## 7. DISCUSSION AND CONCLUSIONS

This thesis has presented several case studies from Pleistocene to modern sites in the Kenya Rift Valley and the Eocene Green River Formation of Wyoming, U.S.A. These sites were chosen to allow the direct comparison between modern and ancient biogenic structures in and around lakes of similar hydrochemistry (i.e. saline, alkaline) and with similar trace makers (e.g., Cenozoic birds, mammals, and insects). Several modern localities were investigated so that broad patterns in trace fossil composition and distribution could be recognized, and hypotheses developed and tested by applying the findings to older successions. In each of the localities, importance was placed on understanding the depositional environments first, prior to interpreting the significance of the traces. Detailed descriptions of lithofacies were provided, in order to place any animal and/or plant traces into well-constrained stratigraphic, sedimentological, and paleoecological contexts so that the utility of traces in closed, saline, and alkaline lake basins could be better assessed. Although the existing models for trace fossils in continental environments of Buatois and Mángano (2004, 2007, 2009) were followed as a framework, this study remained exploratory in order to test and refine these models and to develop new concepts for the use of trace fossils in lacustrine sequence stratigraphy. The focus was on the application of traces for paleoecology and stratigraphy. The results of this study provide the basis for several avenues of future research, and were developed into predictive models (Figs. *6.1.6.*1–3, 7.1) from which to compare future studies that analyze the stratigraphic applications of trace fossils in lake-type basins (e.g., underfilled, balanced fill, overfilled). The following sections discuss the findings more broadly (Section 7.1) and summarize the main conclusions of this study (Section 7.2).

### 7.1. Composition and Distribution of Biogenic Structures in Saline Lake Basins

#### *7.1.1. Trace Makers in Saline Lake Basins*

Neoichnological studies that focus on the identification of the organisms that produce the variety of types of burrows, trails, and nests in continental environments, and methods of construction and specific behaviours involved in trace production, has been a field of research undertaken by a small number of workers (e.g., Ratcliffe and Fagerstrom, 1980; Metz, 1987, 1990; Hasiotis and Mitchell, 1993; Lawfield and Pickerill, 2006; Counts and Hasiotis, 2009; Melchor et al., 2010; Halfen and Hasiotis, 2010). Ecological studies by biologists that consider burrow morphology, and the behaviours related to an infaunal lifestyle and specific biogenic structures, can be used for better interpretations of the (paleo)ecology of these trace makers. However, situations where biologists and ichnologists focus on similar problems are rare, and the "translation" of the existing biological data can be difficult. Additionally, most of the well-studied trace-producing organisms inhabit freshwater environments (e.g., oligochaetes, bivalves, decapod crustaceans) (e.g., McCall and Tevesz, 1982), which are not the main focus of this study. Continental neoichnological studies that consider the ecology of more than one group of organisms in one area and how the distribution of different organisms and their traces reflect environmental conditions and species interactions are very rare (e.g., Cohen et al., 1993; Martin, 2009; Hamer and Sheldon, 2010). In some cases, studies that investigated the ecology of modern trace-producing organisms in marginal marine habitats can also be applied in part to continental environments (e.g., Basan and Frey, 1977; Frey and Pemberton, 1986, 1987; Netto and Grangeiro, 2009).

In this thesis, four important trace makers observed at the saline to hypersaline Lakes Bogoria, Magadi, and Nasikie Engida were chosen for the detailed description of their modern traces, together with an analysis of their potential use in paleoecology by reference to the data collected in this study and published biological literature (see Section 4.1.5). The traces of flamingos, earwigs, tiger beetles, and staphylinid beetles and other insects with similar lifestyles (e.g., crickets, carabid beetles, heterocerid beetles) are common in the modern to Pleistocene localities investigated in the Kenya Rift and previously have only rarely been described in ichnological terms (Smith and Hein, 1971; Stanley and Fagerstrom, 1974; Clark and Ratcliffe, 1989; Garcia and Neill, 1991). Termites, ants, spiders, mites, dipteran larvae (e.g., chironomids) and some dipteran adults (e.g., ephydrids), other beetles (e.g., scarabids, tenebrionids, ?dytiscids), and some birds and mammals were also observed to produce biogenic structures at the modern Kenyan sites (see Chapter 4). Crustaceans (e.g., decapods, amphipods, branchiopod anocostracans), bivalves, gastropods, some trace-making insects (e.g., caddisflies: Trichoptera) and oligochaetes were notably lacking from the Kenya sites investigated, but might be present in lacustrine or lake-margin sites with lower salinities (cf. Hammer, 1986). Nematodes were not observed, and no traces attributable to them (e.g., incipient *Cochlichnus*) were found in modern or fossil sediments. Similarly, ostracodes were neither seen in the Kenyan lake deposits investigated nor in modern Lake Bogoria (Harper et al., 2003), but could have produced some of the simple surface trails found in the Green River Formation (cf. De Dekker, 1981; Hammer, 1986). Brine shrimp (Branchiopoda: *Artemia*), although common in North American saline lakes, are rarely reported from the Kenyan lakes (Hammer, 1986; Triantaphyllidis et al., 1998). Bioturbation and the formation of peloidal lacustrine carbonates by brine shrimp may have taken place in Eocene Lake Gosiute, particularly towards the basin margin of the Wilkins Peak Member where peloidal carbonates are common. Trace fossils interpreted as the structures of decapods crustaceans, trichopteran insects, and possibly bivalves and oligochaetes were present in the Green River Formation strata studied, although they were associated with fresher water environments than those presented in detail here. Other potential trace makers of the trace fossils studied in the Green River Formation include snakes, frogs, amphisbaenid and varanid lizards, birds, and other tetrapods such as crocodilians and mammals (see Section 2.4.3).

The important controls on the presence or absence of certain trace makers in a subaqueous lacustrine or lake-margin environment include: 1) hydrochemistry of standing water and pore waters; 2) substrate characteristics, such as drainage, grain size, substrate stability, degree of induration, degree of water saturation, and temperature; 3) lacustrine water depth, turbidity, depth of light penetration, temperature, and stratification; 4) water table depth; and 5) other biological factors such as nutrient supply, food source availability, predation, and competition. Species richness declines with increasing salinity, and species composition changes with salinity (e.g., Hammer, 1986; Williams et al., 1990; Williams, 1998). However, at a higher level of classification (e.g., family or order), many groups of organisms present in continental settings have at least some representatives that are capable of surviving higher salinity conditions (e.g., Williams, 1998). Particularly in the intermediate salinity ranges (hyposaline: 3–20 g $L^{-1}$ to mesosaline: 20–50 g $L^{-1}$), the effect of salinity on species composition and richness cannot be easily distinguished from the effects of other hydrochemical, environmental, and biological factors (Williams et al., 1990; Williams, 1998), even for studies that examine modern environments. For example, the availability of dissolved oxygen, the pH and ionic composition, the degree of permanence of a water body, as well as factors related to species interactions (e.g., competition, predation) and dispersal mechanisms, all affect whether or not an organism is present in a particular environment (e.g., Williams, 1998 and references therein; Schowalter, 2005).

Despite the difficulties in identifying the particular producers of trace fossils and assessing their significance based on modern biological studies, an attempt was made in this study to provide suggestions for possible trace makers where possible (see Chapters 4 and 6). The level of resolution achievable is probably at the familial level at best, depending on the type and simplicity of the trace fossil. Similarly, inferences were made regarding the relative salinity of the substrate or water body for the purpose of identifying variability in trace composition related to changing environments (see Sections 6.2 and 6.4). Nevertheless, the utility of trace fossils as tools in stratigraphy, sedimentology, and paleoecology is not reliant on the accurate identification of the trace makers. For example, the producer of the large, meniscate backfilled burrows preserved in the Green River Formation (large cf. *Taenidium*) is unknown. Despite this, because of their relatively deep tiering nature, abundance in different sedimentary environments at basin margin localities, and dominantly vertical orientation, they appear to be useful for the recognition of relatively deeper water tables and subaerial exposure surfaces (see Sections 5.4, 6.1.2.8, and 6.1.2.9). Their application appears to be similar to that of the termite nests (*Termitichnus* isp.) preserved in the Loboi Silts in the Bogoria basin, which were produced during a period of low lake level (see Sections 4.1.2 and 4.1.6).

### *7.1.2. Composition and Preservation of Trace Fossils in Saline Lake Basins*

Different organisms can make the same types of biogenic structures, particularly if the traces represent simple grazing or deposit-feeding behaviours (e.g., insect larvae, oligochaetes), or are simple, open vertical burrows (e.g., beetles, spiders) (e.g., Bromley, 1996). Conversely, a single organism can produce a variety of trace types, depending on its different behaviours at different times (e.g., staphylinid larvae). For these reasons, the use of formal ichnotaxonomy is essential for communication between ichnologists, and provides the basis for comparisons between different studies. Many ichnotaxa were originally described from marine environments, however, and do not always correspond directly with continental trace types. To illustrate this, the example of *Planolites* and *Palaeophycus* is given here. *Planolites* is unlined and has a fill different from the host material, whereas *Palaeophycus* is lined and has a fill the same as the host material (Pemberton and Frey, 1982). Despite the apparent simplicity of these trace types, it is not always easy to confidently assign continental trace fossils to one of these ichnotaxa because features that correspond to both of the ichnogenera may have been preserved in a single specimen. Keighley and Pickerill (1995) also recognized that this distinction is not always straightforward, and suggested that the presence or absence of a lining is more important than the nature of the fill. The inferred behavioural distinction between these types of traces, or whether the burrows were actively backfilled or passively filled, is the underlying reason for distinguishing between these trace types, and is the important characteristic to try to deduce.

Many of the trace types recognized in this study are not easily assigned to already existing ichnotaxa, and several types probably warrant the erection of new ichnospecies, and possibly new ichnogenera in some cases. Difficulties in assigning ichnotaxa to the material investigated for this study can be largely attributed to similar issues such as the distinction between *Planolites*/*Palaeophycus*, and other potential incongruities between marine and continental ichnotaxa (e.g., *Taenidium*, *Thalassinoides*). It appears that the difficulties may be explained by considering the general characteristics of continental substrates together with the behaviours of continental organisms. For example, the use of unlined burrows as dwelling burrows by some trace makers may be attributed to relatively firm, subaerially exposed substrates that do not require a wall or lining to maintain an open burrow. Additionally, pellet-like infill in burrows may be produced by either the actual defecation of waste in the burrow (true pellets) or by the physical removal and formation of sediment aggregates during burrowing (e.g.,

staphylinid beetles or earwigs; see Sections 4.1.5.3 and 4.1.5.4). These sediment aggregates may be used for the partial plugging of the burrow, which results in a partially backfilled, partly open, unlined/unwalled, dwelling burrow produced in firm substrates. Depending on the particular trace maker (e.g., staphylinid beetles), such burrows may contain a partial lining. Despite these issues, an attempt was made to assign the traces investigated to existing ichnotaxa where possible. If only the ichnotaxonomic references were used for analysis, however, the apparent diversity of trace types preserved in the Green River Formation would be artificially low.

The various trace types recognized in this study were grouped into suites that reflect the typical associations between groups of trace fossils, which were in places closely associated with particular lithofacies or sedimentary characteristics (e.g., soft substrate *Planolites*, bird footprints, 'pock mark' traces). In other cases, mainly with the more terrestrial, basin-margin trace types (e.g., large cf. *Taenidium*), the original environment in which the substrate was deposited did not necessarily affect the distribution of the traces (see Sections 5.4.1, 5.4.3, and 6.2.9). These types of traces can be considered as “facies crossing”, in which the trace makers were responding to environmental conditions that were not necessarily represented by the other features preserved in the substrate (e.g., sedimentary structures). The trace types grouped together into the suites were based on recurrent associations, which were only partly consistent with the existing ichnofacies models for continental environments (see Section 6.3 and Scott et al., 2009 for discussion of this topic). Overall, the Mermia, Scoyenia, Coprinisphaera, Termitichnus, Skolithos, and possibly the Psilonichnus ichnofacies were represented in the examples studied from the Kenya Rift lakes and the Green River Formation. Laterally variable and frequently changing habitats in underfilled basins, from fully lacustrine to subaerially exposed lake-margin to terrestrial settings, contributed to the high diversity of trace types represented.

The composition of trace fossils in saline lake basins is not only affected by the ability to recognize important distinguishing characteristics and assign them to ichnotaxa, or to the variety of sedimentary environments that provide habitat for the trace-making organisms, but also to whether or not they are preserved. Extended periods of subaerial exposure, frequent wetting and drying, and saline pore-waters in substrates may contribute to the low preservation potential of surficial traces and shallow burrows in settings where salt efflorescences can form (i.e. areas with relatively shallow water tables, high evaporation rates, and permeable sediments) (Scott et al., 2010). Conversely, high alkalinities at the lakes investigated can also contribute to the rapid precipitation of authigenic minerals from ions derived from bedrock, previously existing clay minerals and sediments, and spring waters (e.g., Smoot, 1978; Renaut et al., 1986; Renaut, 1993; R.A. Owen et al., 2008). Traces produced in substrates that are quickly indurated by these authigenic minerals (e.g., zeolites, opaline silica, authigenic clays, carbonates), or protected from destruction by subaerial processes (e.g., deflation, break-up of the substrate by efflorescences) by surface 'barriers' (e.g., microbial mats, clay drapes, carbonate and salt crusts) have a better chance of being preserved (Scott et al., 2007, 2010). Animal and plant traces may contribute to the oxygenation of sediments, and to either the break-up of the substrate or to the early cementation of the substrate, depending on the precise conditions. Variability in the composition of trace fossils preserved in different localities may be partly attributable to these factors, especially in saline, alkaline, underfilled lake basins.

Some of these taphonomic factors may also have affected other saline lake trace fossil assemblages reported in the literature (e.g., Gierlowski-Kordesch, 1991; Pickerill, 1992; Rodríguez-Aranda and Calvo, 1998; Metz, 2000). In some examples, preservation in clay-rich substrates of closed, ephemeral water bodies is very good, and they do not appear to have been disrupted by subaerial processes prior to burial (e.g., Zhang et al., 1998; Minter et al., 2007).

Although sub-fossil insect trackways were preserved in sediments near the hot springs of Loburu at Lake Bogoria (Scott et al., 2007; see Section 4.1.4.4), these types of fine, surface features were only rarely observed in the studied localities from Pleistocene Kenya and in the Green River Formation (see Section 6.2.7). Similarities between the examples provided in this study with other saline lake basins are also apparent in the studies by Uchman and Álvaro (2000) and de Gibert et al. (2009), who also recognized the overprinting of terrestrial suites onto lacustrine and/or lake-margin suites under changing environmental conditions. Most assemblages from saline lake and lake-margin environments include typical traces of the Scoyenia and Mermia ichnofacies, including traces such as insect trackways, vertebrate tracks, and meniscate backfilled burrows (Buatois and Mángano, in press, and references therein).

*7.1.3. Diversity and Lateral Variability in Trace Distribution: the Importance of Dilute Inflow*

As stated above (Section 7.1.1), several environmental, hydrochemical, and biological factors determine the species composition and richness in saline lake and lake-margin environments. Lateral heterogeneity in these habitat characteristics is determined by: 1) the structural setting of the basin; 2) climate; 3) tectonically and geomorphologically controlled gradients and basin-shape; 4) depositional subenvironments around a lake; and 5) the input of relatively freshwater to generally saline or hypersaline sites. The effects of salinity on species richness and composition are most clearly recognized when comparing between freshwater and hypersaline settings (Williams et al., 1990; Williams, 1998). By this reasoning, the input of relatively freshwater to saline to hypersaline environments by either point-sourced springs or rivers was predicted to have an oasis-like effect and cause the increase of trace abundance and diversity in these types of settings. Indeed, the results of this study have shown that plant and animal diversity, as well as the traces produced, are much more diverse in areas with hot- and warm-spring input (see Chapter 4) and in areas with relatively stable supply of freshwater in distributary systems (see Chapter 6). At these sites, a diversity of insect burrows and trails dominate the assemblages, and a higher diversity of mammal footprints (at the Kenyan sites) and bird footprints other than flamingos were recorded. In contrast, the trace types observed from settings not influenced by freshwater springs or fluvial input were dominated by mammal footprints, flamingo footprints, simple surface trails produced on subaqueous substrates, and branched burrow systems apparently formed in wet substrates near the shoreline. Flamingo nest mounds in the modern Kenyan sites were mainly observed at sites with fluvial and spring input. Additionally, the quality of preservation for subaerial traces is also higher near spring sites or distributary systems, because substrates are stabilized by microbial mats, the sedimentation rate is higher, clay drapes on subaerial substrates are more abundant, and/or the substrates are less likely to be disrupted by salt efflorescence (Scott et al., 2010).

The lateral variability between habitats contributed to the overall high diversity of modern traces and trace fossil assemblages observed in the underfilled basins investigated, although many of the trace suites from particular sites were of low diversity or even monospecific. Slight changes in environmental conditions, related to lake-level or water-table changes for example, enhanced the diversity of biogenic structures produced at a particular site. When compared with the other lake-types, a higher degree of lateral heterogeneity in habitats and trace fossil assemblages is expected for underfilled lake basins in general, with subaerially produced traces common in basin centre localities. Lateral variability in the preserved trace fossil assemblages of saline lakes may also be attributed to the destruction of surficial traces and shallow burrows by subaerial processes that also vary with similar environmental factors to which the trace makers respond, such as substrate, proximity to shoreline, depth of the water table, temperature and evaporation rates (Scott et al., 2010).

Hot-springs may also contribute to increased trace diversity in underfilled basins formed in tectonically active areas by leading to the development of microbial mats in certain areas, which form the basis of an ecosystem in areas otherwise not conducive to the presence of abundant infaunal and epifaunal life (cf. Mitchell, 1974; Collins et al., 1976). Additionally, certain types of traces in lake basins may be closely related to hot-spring sites and microbial substrates (e.g., 'pock-mark' traces of ephydrid adults; cf. *Labyrintichnus* isp. and cf. *Vagorichnus* isp. of staphylinid beetles; see Section 4.1.5.3). Microbial mats at spring sites or around hypersaline lakes may be especially abundant where there are higher levels of free $CO_2$ (e.g., Wiegert and Fraleigh, 1972), making carbonate and soda lakes, and areas with alkaline springs, especially suitable for ecosystems built on this food source. The high alkalinity of Eocene Lake Gosiute and the possible input from springs, together with high atmospheric concentrations of $CO_2$ at that time (e.g., Zachos et al., 2001), may also have had an effect on the productivity of photosynthesizing microbes. In turn, these conditions may have contributed to the deposition of Na- and Ca-carbonates and the production of oil shale (e.g., Bradley and Eugster, 1969; Smoot, 1978; Bohacs et al., 2000; Carroll and Bohacs, 2001; Lowenstein and Demicco, 2006). These same conditions may have led to the development of food webs based on microbial mats as the primary food source for a variety of trace-making animals (e.g., insect larvae, flamingo-like birds; cf. Collins et al., 1976). These factors may also have contributed to the higher overall diversity in the saline lakes investigated than was originally expected, and the higher diversity of these underfilled basins when compared to the model developed by Buatois and Mángano (2009).

### *7.1.4. Tiering, Overprinting, and the Application of Trace Fossils in Saline Lake Basins*

Trace fossils provide data for paleoenvironmental reconstructions not otherwise evidenced by body-fossil paleontology or the sedimentology of sedimentary successions. Primarily, the composition and distribution of trace fossil assemblages, the degree of bioturbation, and the depths to which the traces penetrate substrates, can be applied in conjunction with sedimentological data to interpret depositional environments. The recognition of archetypal ichnofacies by considering the composition of an assemblage, together with a consideration of the general implications of the ichnofacies, provides a general framework from which to further investigate a particular site (e.g., Buatois and Mángano, 2007). Certain characteristics of the trace fossils, such as their dominant orientation, depth or “tiering” level, and any clues about substrate consistency, can be applied to infer specific information about the sediments being investigated. For example, traces produced in subaerial substrates by terrestrial organisms can provide information about water table depths, and depending on the type of trace, details on moisture conditions within the substrate (e.g., Genise et al., 2000; Hasiotis, 2007). A consideration of the vertical distribution of the trace fossil assemblages is valuable for interpreting the stratigraphic packaging of sedimentary successions, and can be applied using sequence stratigraphic concepts (e.g, stratal packaging, recognition of discontinuity surfaces).

The recognition of changing conditions in a substrate is also possible with trace fossils, particularly if the assemblage can be divided into ichnofacies or smaller-scale groupings (e.g., suites) that are associated with a set of recurrent environmental characteristics (e.g., Metz, 1996; Uchman and Álvaro, 2000; Buatois and Mángano, 2004; de Gibert and Saez, 2009). This application is particularly important in lake-marginal and fluvial successions, and provides an extremely valuable tool for recognizing important stratigraphic surfaces. In sedimentary successions with lower sedimentation rates the different sub-assemblages may be overprinted on one another, showing the response of organisms to the changing conditions. The cross-cutting relationships between the different trace types provide the relative chronology and help to show

the pattern of changes in environmental conditions (e.g., regression, transgression). Typically, these surfaces are palimpsest, subaerially exposed surfaces that show progressively deeper water tables. However, overprinting of terrestrial trace types in exhumed surfaces by lacustrine or lake-margin trace types may also occur during relatively higher lake levels (see Sections 4.1.2, 4.1.3, and 4.1.6). It is in these cases that trace fossils may provide the only indication of lake-level changes, especially if traces typically associated with terrestrial environments are emplaced within lacustrine or lake-margin strata (see Sections 4.1.6, 5.4.1). Similarly, periods of or subenvironments with lower sedimentation rates on delta-plains, such as the abandonment of fluvial channels followed by their bioturbation by terrestrial animals, can be evidenced by the types of traces preserved, as well as their overprinting patterns and degree of bioturbation (e.g., Buatois and Mángano, 2004; Buatois et al., 2007; Section 5.3.2). In aggradational successions without depositional hiatuses, the changing conditions can be deciphered by examining the vertical distribution of lithofacies together with the trace fossils. In this thesis, these concepts have been applied in conjunction with detailed descriptions of outcrop data to develop a depositional and stratigraphic model using trace fossils for the complex and poorly understood arkosic siliciclastic units within the Wilkins Peak Member of the Green River Formation (Sections 5.3 and 6.4).

Sequence stratigraphic concepts have not yet been widely applied in continental basins, although some workers have considered the application of sequence stratigraphic methods to non-marine environments (i.e. fluvial) that are influenced by sea level (Legarreta et al., 1993; Catuneanu et al., 2009). The lake-type model of Carroll and Bohacs (1999) and Bohacs et al. (2000) considers the general stratigraphic packaging of different facies associations. Bohacs et al. (2007b) recognized systems tracts and important stratigraphic surfaces for the Green River Formation in the greater Green River basin, and identified parasequences in stratigraphic units on the scale of 1–5 m thickness (cf. "lake cycles" of Pietras and Carroll, 2006). They interpreted the arkose beds as transgressive systems tracts, placing non-erosional sequence boundaries above the underlying thick trona beds (Bohacs et al., 2007b). The presence of subaerially produced trace fossils in these units (see Chapter 6) questions this interpretation by showing that the accommodation for these siliciclastic units was not always within the lake and that the arkosic units show progradational stacking.

Lake- and base-level fluctuations are controlled by climate, tectonics, and the relationship between the amount of sediment plus water input and the basin-bounding sill height (Carroll and Bohacs, 1999; Bohacs et al., 2000). Climate also causes lake-level fluctuations at several scales, which may be most clearly represented by the "lake cycles" (Pietras and Carroll, 2006) and abrupt changes in facies assemblages (e.g., the arkose beds; M.E. Smith et al., 2010) in underfilled lake-type basins. There is hesitation in applying sequence stratigraphic methods and terminology used for marine strata to lacustrine successions, mainly because of the numerous subaerial exposure surfaces that represent minor fluctuations in lake-level, and do not represent surfaces (i.e. sequence boundaries) that should be used to distinguish between parasequence sets. In this thesis, these types of surfaces were termed "exposure surfaces" to show that subaerial exposure occurred, without suggesting that these periods were major hiatuses or that major changes in the facies assemblages took place above these surfaces. Similarly, Bohacs et al. (2007b) recognized the retrogradational and progradational stacking of shallowing upwards parasequences by focusing on the bounding flooding surfaces. The interpretations presented here differ from those of Bohacs et al. (2007b) in that the upper portions of the arkose beds were deposited in primarily subaerial settings, which are shown by the lithofacies associations that include paleosols (see Chapter 5), and the trace fossils (see Chapter 6). These issues must be better understood in order to characterize the significance of trace fossils for recognizing the

different stratigraphic surfaces in lacustrine successions, especially in underfilled basins, in which subaerial exposure is frequent.

As a summary to this thesis, a schematic model is presented that incorporates the results from the Kenya Rift lakes as well as the Green River Formation in order to show the lateral and vertical distribution of the different trace suites recognized in this study (Figure 7.1). An adapted, sequence stratigraphic representation was chosen to show the positions of the trace types, but also to highlight their usefulness for stratigraphy. Sequence stratigraphic surfaces are generally understood to be diachronous (e.g., Catuneanu et al., 2009), as are the flooding and exposure surfaces recognized in this study. This is also an important consideration for trace fossil distribution, especially in low-gradient non-coincident margins. Depending on the lake-margin gradient in an underfilled lake basin and degree of lake-level change, traces produced subaerially along the shoreline at any one time (e.g., tiger beetle vertical burrows) are predicted to follow the changing substrate conditions as lake-level falls, presenting a diachronous distribution along a subaerially exposed horizon (discussed in Section 4.1.5.2). Mammal footprints, bird footprints, and flamingo nest mounds present a similar scenario, as do other trace types that are present within the zone of typical lake-level rise-and-fall. This adapted, sequence-stratigraphic approach provides a method to show the applicability of trace fossils for stratigraphy in underfilled basins, as well as a way to show the dynamic nature of trace fossil distribution in changing sedimentary environments coupled with the influence of point-sourced oasis-like habitats.

## 7.2. Summary and Conclusions

This study investigated the composition and distribution of modern and fossil animal and plant traces associated with saline, alkaline lakes in underfilled lake-type basins of the Kenya Rift Valley and of the Eocene Green River Formation and its correlative equivalents. The lake basins studied in the Kenya Rift Valley contain numerous hot-spring deposits and modern hot-springs that affect the ecology of the lakes by providing sites of abundant, normally reliable, microbial food sources for animals and relatively freshwater in otherwise saline to hypersaline settings, together with ephemeral streams and rivers. Numerous possible hydrothermal spring deposits were also identified in the greater Green River basin of Wyoming, which may have also impacted the Eocene ecology of the basin. The examples described and discussed from the basin

**Fig. 7.1.** (Next page) Schematic model of the distribution of trace fossil suites in saline, alkaline underfilled lake basins. This model is based on data presented by Culbertson (1961), Pietras and Carroll (2006), Carroll et al. (2008), M.E. Smith et al. (2008b), Scott et al. (2009), and this thesis. Trace suites are numbered according to those used in the text, and shown in their observed and predicted positions in the basins investigated. The basin margin in the diagram is mainly based on the western margin of the Bogoria basin (view would be S to N) and the eastern margin of the Bridger basin (view would be N to S). Arrows represent the basinward movement of certain trace suites along subaerially exposed surfaces. Trace suites observed in the Kenya Rift are clustered around sites associated with faults and springs. Subaerial exposure surfaces are present in all units shown. The numbers 1-9 refer to major events: **(1)** uplift of the basin margin; **(2)** closed lake deposits with closely-sourced deposits at basin margin; cycle terminates in evaporite deposition; **(3)** incision (climate-related?) through basin margin; deposition of an alluvial fan, fan delta, and/or fluvio-lacustrine sediments; input of freshwater to basin; **(4)** transgression of saline lake (due to either autogenic or allogenic mechanisms?); continued sedimentation of fan delta/fluvio-lacustrine sediments; **(5)** basinward progradation of delta-plain and sediment bypass; **(6)** continued subsidence or renewed uplift; transgression (climate-related?) of saline to hypersaline lake; cycle terminates in evaporite deposition; **(7)** incision through uplift or barrier; deposition of alluvial fan, fan delta, and fluvio-lacustrine/delta-plain sediments; interfingering with lacustrine deposits during transgressions; lacustrine deposits freshening upwards; prolonged exposure and incision; **(8)** transgression of saline lake to margin; **(9)** transgression and freshening of lake due to allogenic mechanisms (e.g., climate; change in drainage and/or sill-height).

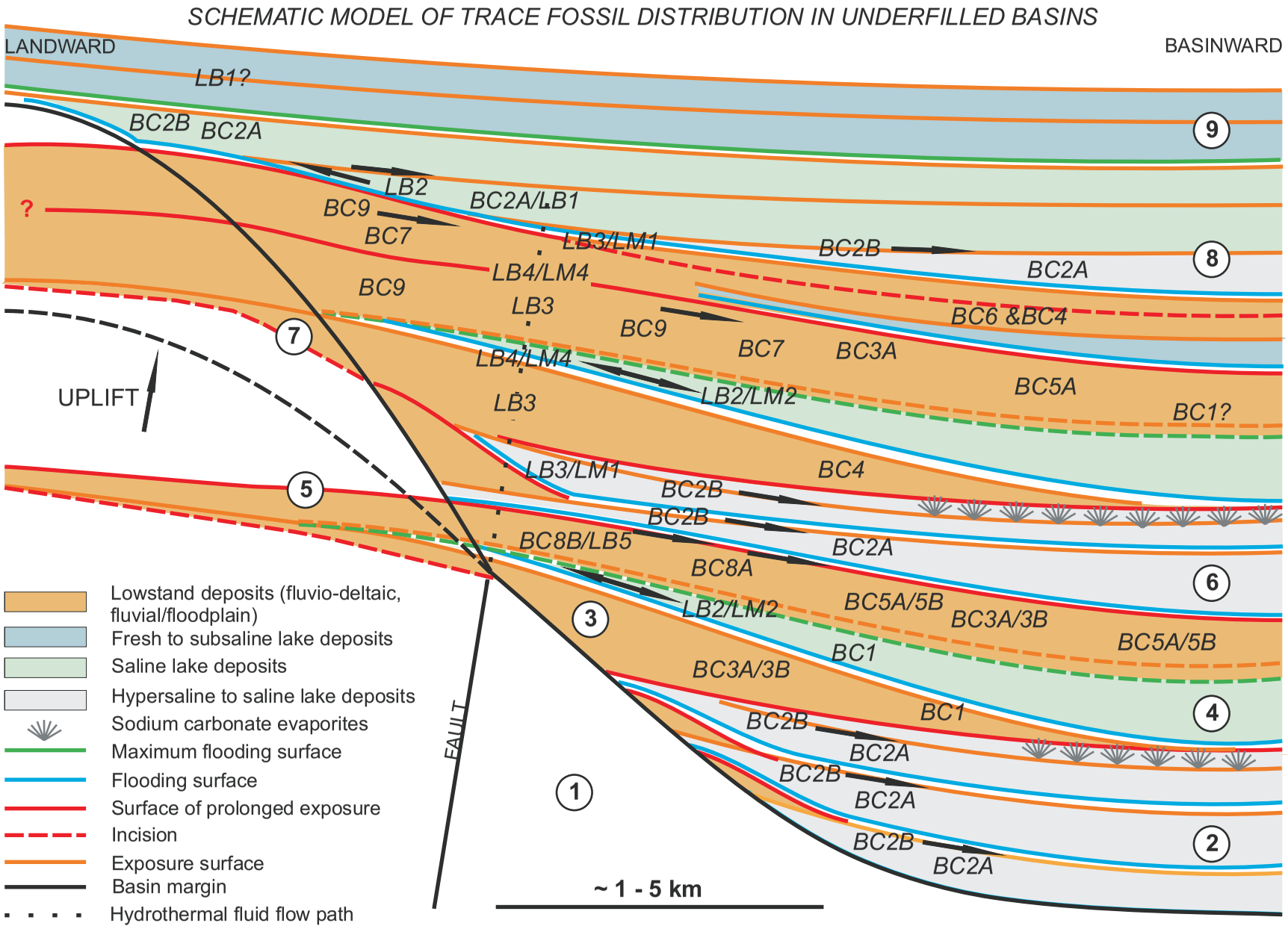
SCHEMATIC MODEL OF TRACE FOSSIL DISTRIBUTION IN UNDERFILLED BASINS
LANDWARD
BASINWARD
LB1?
BC2B
BC2A
LB2
BC9
BC2A/LB1
?
BC7
LB3/LM1
BC2B
BC2A
LB4/LM4
BC9
LB3
BC6 &BC4
BC9
BC7
BC3A
LB4/LM4
BC5A
LB2/LM2
BC1?
UPLIFT
LB3
LB3/LM1
BC4
BC2B
BC2B
BC2A
BC8B/LB5
BC8A
LB2/LM2
BC5A/5B
BC3A/3B
BC5A/5B
BC1
BC3A/3B
BC1
BC2B
BC2A
BC2B
BC2A
BC2B
BC2A
FAULT
9
8
7
6
5
4
3
2
1
~ 1 - 5 km
Lowstand deposits (fluvio-deltaic, fluvial/floodplain)
Fresh to subsaline lake deposits
Saline lake deposits
Hypersaline to saline lake deposits
Sodium carbonate evaporites
Maximum flooding surface
Flooding surface
Surface of prolonged exposure
Incision
Exposure surface
Basin margin
Hydrothermal fluid flow path

centre facies of the Wilkins Peak Member focused on the saline to hypersaline lake deposits and the impact of freshwater input to these sites from rivers on both the lithofacies and trace fossil assemblages.

### *7.2.1. Distribution of Trace Fossils in Underfilled Basins*

Trace fossil distributions in the modern and ancient lakes investigated and the morphologies of traces produced in different substrate conditions were closely associated with the distribution of lithofacies, as well to environmental factors such as salinity. Lithofacies and trace fossils can be used together to reconstruct paleoenvironments and the dynamic histories of lakes (e.g., lake-level changes). In continental settings, the distribution of trace fossil assemblages is strongly influenced by the regional climatic and tectonic settings, which together determine the basin physiography, distribution of drainage systems, amount of water and sediment input into the basin, and the spatial and temporal distribution of sedimentary facies. The distribution of lithofacies, in terms of their geometry, composition, grain size, sorting, early diagenetic cements, and sedimentary structures, is closely linked with the distribution of trace fossil assemblages. However, environmental conditions that also control the distribution and composition of trace assemblages, such as salinity and oxygenation in lacustrine environments, and the depth of the water table and topographic gradient in lake-margin to alluvial environments, remain as important controls that are only indirectly related to the lithofacies.

In summary:

1) The distribution of continental ichnofacies in lake basins, and their subdivided ichnocoenoses, suites, and/or recurrent ichnofabrics, are related to both lithofacies associations (e.g., fluvial channels and overbank deposits), as well as environmental conditions determined by climate and tectonics (e.g., lake salinity).

2) Similar trace fossil suites are found in similar lithofacies in different lake-type basins, thus it is important to consider their distribution when trying to recognize different lake types using traces (e.g., subaerial associations are found in the basin center only for underfilled basins).

3) Trace fossils in underfilled lake-type basins are the most variable in terms of their lateral and vertical distribution when compared with other lake-types (i.e. overfilled, balanced fill), and have frequently changing distribution patterns related to relatively extreme lake level fluctuations.

4) The results of this study generally support the existing model for trace fossils in lake-type basins of Buatois and Mángano (2009), but in the Green River Formation of Wyoming, the underfilled lake-type appears to contain the most diverse trace fossil assemblage. This important finding may be related to periods of changing climate to wetter conditions with more fresh water input to a huge, underfilled lake-type basin.

### *7.2.2. Stratigraphic Application of Trace Fossils in Underfilled Lake Basins*

In saline lake, lake-margin, and alluvial settings in underfilled basins, most animal traces are formed by air-breathing organisms that burrow into subaerially exposed sediments (e.g., Buatois and Mángano, 2004, 2007, 2009; Bohacs et al., 2007a; Hasiotis, 2007). Burrows, nests, and other traces produced by these organisms are not restricted to environments where soils develop, but may also be produced at the shoreline of water bodies, such as saline lakes and around springs. Subaerial exposure is not necessarily equated with soil development, although surficial processes begin to act on subaerially exposed sediments as soon as they are no longer covered by water. Despite the linkage between depositional setting and trace assemblages in continental settings, in many scenarios there may a decoupling between the times of deposition and the burrowing event, which often represents a change in conditions. This decoupling

between the depositional environment and the conditions under which bioturbation occurred can be an extremely valuable tool for the interpretation of changing sedimentary dynamics in paleoenvironmental analyses, and for the recognition of important stratigraphic surfaces not otherwise represented by sediments or by erosional unconformities.

In summary:

1) Overprinting patterns of trace suites that represent regression and/or the lowering of the water table in underfilled basins are common at the basin margin, but are relatively uncommon in aggradational basin center deposits.

2) Trace fossils in the zone of lake-level rise-and-fall within each lake-type basin may provide important clues to recognizing exposure surfaces and combined regressive/flooding surfaces by considering their ichnotaxonomic composition and substrate characteristics.

### *7.2.3. Paleoenvironmental Application of Trace Fossils in Underfilled Lake Basins*

At a variety of scales, the modern and ancient animal traces observed in several depositional settings in the Kenya Rift and Green River Formation were associated with sedimentary lithofacies. The traces may be produced shortly after sedimentation or following a change in conditions after sedimentation. Certain clues provided by the trace morphology, such as the relative water content in the substrate when the traces were made, may help to place the timing of trace formation, and increase the value of the traces for a better understanding of the sedimentary system. It is particularly important when using continental trace fossils to carefully consider the sedimentary environment in conjunction with the composition of trace fossil assemblages. For example, simple vertical burrows (*Skolithos* isp.) can be produced subaerially or subaqueously, depending in part on the life cycle of the particular type of trace maker (e.g., insects). In settings with frequently changing shoreline position for example, it may not always be possible to determine whether a particular trace was formed subaqueously in shallow lake water or subaerially in a wet, but drying, substrate, depending on the available evidence.

The spatial distribution of sedimentary environments and the variety of sedimentary regimes within a particular depositional setting is complex in continental basins. Underfilled basins represent the most variable continental settings because they can contain numerous different subenvironments at the same time and because lake level and lake water chemistry fluctuates frequently. To add to the complexity, the depths to which terrestrial animal traces are produced is also partly controlled by the depth of the water table, which is controlled by the tectonic and climatic setting, as well as the geomorphological characteristics of the terrestrial landscape. Thus, the overprinting of animal traces into previously deposited sediments with an original suite of traces depends on the environmental (and tectonic) changes that have occurred.

The examples provided in this thesis show that trace fossils can be used for paleoenvironmental reconstructions by providing information about substrate conditions, subaerial exposure of the substrate, position relative to the shoreline, the depth of the water table, salinity, food source, sedimentation rate, and the location within a basin. The grouping of traces into suites is useful because it helps the recognition of changing environmental conditions within a particular sedimentary succession. A consideration of the trace fossil assemblage composition together with overprinting patterns and the stratigraphic packaging of the trace-containing sediments can be useful for developing depositional models of the complex and highly laterally variable sedimentary environments in underfilled lake basins.

# REFERENCES


Aanen, D.K., and Eggleton, P., 2005, Fungus-growing termites originated in African rain forest: Current Biology, v. 15, p. 851–855.

Abbassi, N., and Lockley, M.G., 2004, Eocene bird and mammal tracks from the Karaj Formation, Tarom Mountains, Northwestern Iran: Ichnos, v. 11, p. 349–356.

Adamson, D.A., Gasse, F., Street, F.A., and Williams, M.A.J., 1980, Late Quaternary history of the Nile: Nature, v. 288, p. 50–55.

Alcock, J., 1999, Animal Behavior: an Evolutionary Approach, Fifth Edition. Massachussetts: Sinauer Associations Inc. Publishers, 625 p.

Allen, D.J., Darling, W.G., and Burgess, W.G., 1989, Geothermics and hydrogeology of the southern part of the Kenya Rift Valley with emphasis on the Magadi-Nakuru area: British Geological Survey Research Report, SD/89/1, 68 p.

Allen, J.R.L., 1997, Subfossil mammalian tracks (Flandrian) in the Severn Estuary, S. W. Britain: mechanics of formation, preservation and distribution: Philosophical Transactions of the Royal Society of London, B, v. 352, p. 481–518.

Allen, R.P., 1956, The Flamingos: Their Life History and Survival: New York, National Audubon Society, Research Report no. 5, 285 p.

Anderson, G.D., and Herlocker, D.J., 1973, Soil factors affecting the distribution of the vegetation types and their utilization by wild animals in Ngorongoro Crater, Tanzania: Journal of Ecology, v. 61, p. 627–651.

Ashley, G.M., Mworia, J.M., Muasya, A.M., Owen, R.B., Driese, S.G., Hover, V.C., Renaut, R.W., Goman, M.F., Mathai, S., and Blatt, S.H., 2004, Sedimentation and recent history of a freshwater wetland in a semi-arid environment: Loboi Swamp, Kenya, East Africa: Sedimentology, v. 51, p. 1301–1321.

Ataabadi, M.M., 2007, Cenozoic mammal footprints of Iran and their significance, *in* Lucas, S.G., Spielmann, J.A., and Lockley, M.G. (eds.), Cenozoic Vertebrate Tracks and Traces: New Mexico Museum of Natural History and Science Bulletin, v. 42, p. 251–259.

Ataabadi, M.M., and Sarjeant, W.A.S., 2000, Eocene mammal footprints from Eastern Iran: a preliminary study: C.R. Academy of Science Paris, Earth and Planetary Sciences, v. 331, p. 543–547.

Ataabadi, M.M., and Khazaee, A.R., 2004, New Eocene mammal and bird footprints from Birjand area, Eastern Iran: Ichnos, v. 11, p. 363–370.

Bader, J.W., 2008, Stuctural and tectonic evolution of the Cherokee Ridge arch, south-central Wyoming: implications for recurring strike-slip along the Cheyenne Belt suture zone: Rocky Mountain Geology, v. 43, p. 23–40.

Baker, B.H., 1958, Geology of the Magadi Area: Geological Survey of Kenya, Reports, v. 42, 81 p.

Baker, B.H., 1986, Tectonics and volcanism of the southern Kenya Rift Valley and its influence on rift sedimentation, *in* Frostick, L.E., Renaut, R.W., Reid, I, and Tiercelin, J.-J. (eds.), Sedimentation in the African Rifts: Geological Society Special Publication, no. 25, p. 45–57.

Baker, B.H., and Mitchell, J.G., 1976, Volcanic stratigraphy and geochronology of the Kedong–Olorgesailie area and the evolution of the south Kenya rift valley: Journal of the Geological Society, London, v. 132, p. 467–484.

Baker, B.H., and Wohlenberg, J., 1971, Structure and evolution of the Kenya Rift Valley: Nature, v. 229, p. 538–542.

Ballot, A., Krienitz, L., Kotut, K., Wiegand, C., Metcalf, J., Codd, G., and Pflugmacher, S., 2004, Cyanobacteria and cyanobacterial toxins in three alkaline Rift Valley lakes of Kenya–Lakes Bogoria, Nakuru, and Elmenteita: Journal of Plankton Research, v. 26, p. 925–935.

Bankey, V., and Merewether, E.A., 1990, Bouguer gravity anomaly map of southwestern Wyoming, northeastern Utah and northwestern Colorado: U.G. Geological Survey, Geophysical Investigations Map GP-993, scale 1:500,000.

Basan, P.B., and Frey, R.W., 1977, Actual-palaeontology and neoichnology of salt marshes near Sapelo Island, Georgia, *in* Crimes, T.P., and Harper, J.C. (eds.), Trace Fossils 2: Geological Journal, Special Issue, v. 9, p. 41–70.

Baucon, A., 2008, Italy, the cradle of ichnology; the legacy of Aldrovandi and Leondardo: Studi Trentini di Scienze Naturali, Acta Geologica, v. 83, p. 15–29.
Bauer, K.L., 1991, Observations on the developmental biology of *Cicindela arenicola* Rumpp (Coleoptera: Cicindelidae): Great Basin Naturalist, v. 51, p. 226–235.
Bauld, J., 1981, Occurrence of benthic microbial mats in saline lakes: Hydrobiologia, v. 81, p. 87–111.
Becht, R., Mwango, F., and Muno, F.A., 2005, Groundwater links between Kenyan Rift Valley lakes: Proceedings of the 11th World Lakes Conference, Nairobi, 2005, v. 2, p. 7–13.
Becker, T.P., McGroder, M., Rudolph, K.W., Hauge, T.A., and Fan, M., 2010, Paleogene influence of the Moxa Arch on the architecture of the composite Darby-Hogsback-Prospect (DHP) thrust sheet near Labarge, Wyoming, USA: Abstract, AAPG Annual Convention and Exhibition.
Behr, H.-J., 2002, Magadiite and magadi chert: a critical analysis of the silica sediments in the Lake Magadi Basin, Kenya, *in* Renaut, R.W., and Ashley, G.M. (eds.), Sedimentation in Continental Rifts, SEPM Special Publication, no. 73, p. 257–273.
Behr, H.-J., and Röhricht, C., 2000, Record of seismotectonic events in siliceous cyanobacterial sediments (Magadi cherts), Lake Magadi, Kenya: International Journal of Earth Sciences, v. 89, p. 268–283.
Bell, R.H.V., 1982, The effect of soil nutrient availability on community structure in African ecosystems, *in* Huntley, B.J., and Walker, B.J. (eds.), Ecology of Tropical Savannas. New York: Springer-Verlag, Ecological Studies, v. 42, p. 193–216.
Bell, K., Dawson, J.B., and Farquhar, R.M., 1973, Strontium isotope studies of alkali rocks: the active carbonatite volcano Oldoinyo Lengai, Tanzania: Geological Society of America Bulletin, v. 84, p. 1019–1029.
Benner, J.S., Ridge, J.C., And Knecht, R.J., 2009, Timing of post-glacial reinhabitation and ecological development of two New England, USA, drainages based on trace fossil evidence: Palaeogeography, Palaeoclimatology, Palaeoecology, v. 272, p. 212–231.
Bergman, A.N., Laurent, P., Otiang' A-Owiti, G., Bergmand, H.L., Walsh, P.J., Wilson, P., and Wood, C.M., 2003, Physiological adaptations of the gut in the Lake Magadi tilapia, *Alcolapia grahami*, an alkaline- and saline-adapted teleost fish: Comparative Biochemistry and Physiology, Part A, v. 136, p. 701–715.
Berry, H.H., 1971, Flamingo breeding on the Etosha Pan, South West Africa, during 1971: Madoqua, Series I, no. 5, p. 5–31.
Bertling, M., 1999, Taphonomy of trace fossils at omission surfaces (Middle Triassic, East Germany): Palaeogeography, Palaeoclimatology, Palaeoecology, v. 149, p. 27–40.
Bishop, W.W., and Chapman, G.R., 1970, Early Pliocene sediments and fossils from the northern Kenya Rift Valley: Nature, v. 226, p. 914–918.
Bishop, W.W., and Pickford, M.L., 1975, Geology, fauna and palaeoenvironments of the Ngorora Formation, Kenya Rift Valley: Nature, v. 254, p. 185–192.
Bishop, W.W., Chapman, G.R., Hill, A., and Miller, J.A., 1971, Succession of Cainozoic vertebrate assemblages from the northern Kenya Rift Valley: Nature, v. 233, p. 389–394.
Bohacs, K., 2007, Genetic versus contingent controls on subsurface flow properties of lacustrine strata – insights for hydrocarbon exploitation and groundwater conservation: 4th International Limnogeology Congress, Barcelona, Spain, Abstracts, p. 61–62.
Bohacs, K.M., Carroll, A.R., Neal, J.E., and Mankiewicz, P.J., 2000, Lake-basin type, source potential, and hydrocarbon character: an integrated sequence-stratigraphic–geochemical framework, *in* Gierlowski-Kordesch, E.H., and Kelts, K.R. (eds.), Lake Basins through Space and Time: AAPG Studies in Geology, v. 46, p. 3–34.
Bohacs, K.M., Hasiotis, S.T., and Demko, T.M., 2007a, Continental ichnofossils of the Green River and Wasatch Formations, Eocene, Wyoming: a preliminary survey, proposed relation to lake-basin type, and application to integrated paleo-environmental interpretation: The Mountain Geologist, v. 44, p. 79–108.
Bohacs, K.M., Grabowski, G. Jr., and Carroll, A.R., 2007b, Lithofacies architecture and variations in expression of sequence stratigraphy within representative intervals of the Green River Formation, Greater Green River Basin, Wyoming and Colorado: The Mountain Geologist, v. 44, p. 39–60.
Boomer, S.M., Noll, K.L., Geesey, G.G., and Dutton, B.E., 2009, Formation of multilayered photosynthetic biofilms in an alkaline thermal spring in Yellowstone National Park, Wyoming: Applied and Environmental Microbiology, v. 2464–2475.

Bradley, W.H., 1929, The varves and climate of the Green River epoch: U.S. Geological Survey Professional Paper, 158-E, 110 p.
Bradley, W.H., 1964, The geology of the Green River Formation and associated Eocene rocks in southwestern Wyoming and adjacent parts of Colorado and Utah: U.S. Geological Survey Professional Paper, 496-A, 86 p.
Bradley, W.H., and Eugster, H.P., 1969, Geochemistry and paleolimnology of the trona deposits and associated authigenic minerals of the Green River Formation of Wyoming: U.S. Geological Survey Professional Paper, no. 496-B, 71 p.
Brennan, A., and McLachlan, A.J., 1979, Tubes and tube-building in a lotic chironomid (Diptera) community: Hydrobiologia, v. 67, p. 173-178.
Brock, M.L., Wiegert, R.G., and Brock, T.D., 1969, Feeding by *Paracoenia* and *Ephydra* (Diptera: Ephydridae) on the microorganisms of hot springs: Ecology, v. 50, p. 192–200.
Brock, T.D., 1967, Relationship between standing crop and primary productivity along a hot spring thermal gradient: Ecology, v. 48, p. 566–571.
Brock, T.D., 1970, High temperature systems: Annual Reviews, v. 1, p. 191–220.
Bromley, R.G., 1996, Trace Fossils: Biology, Taphonomy and Applications. London: Chapman and Hall, 361 p.
Bromley, R., and Asgaard, U., 1979, Triassic freshwater ichnocoenoses from Carlsberg Fjord, East Greenland: Palaeogeography, Palaeoclimatology, Palaeoecology, v. 28, p. 39–80.
Bromley, R., and Asgaard, U., 1991, Ichnofacies: a mixture of taphofacies and biofacies: Lethaia, v. 24, p. 153–163.
Brown, L.H., 1973, The Mystery of the Flamingos. Nairobi: East African Publishing House, 121 p.
Brown, L.H., and Root, A., 1971, The breeding behaviour of the lesser flamingo *Phoeniconaias minor*: The Ibis, v. 113, p. 147–172.
Brues, C.T., 1924, Animal life in hot springs: Quarterly Review of Biology, v. 2, p. 181–203.
Brust, M.L., Hoback, W.W., Skinner, K.F., and Knisley, C.B., 2006, Movement of *Cicindela hirticollis* Say larvae in response to moisture and flooding: Journal of Insect Behavior, v. 19, p. 251–263.
Buatois, L.A., and Mángano, M.G., 1995, The paleoenvironmental and paleoecological significance of the lacustrine *Mermia* ichnofacies: an archetypical subaqueous nonmarine trace fossil assemblage: Ichnos, v. 4, p. 151–161.
Buatois, L.A., and Mángano, M.G., 1998, Trace fossil analysis of lacustrine facies and basins: Palaeogeography, Palaeoclimatology, Palaeoecology, v. 183, p. 71–86.
Buatois, L.A., and Mángano, M.G., 2004, Animal-substrate interactions in freshwater environments: applications of ichnology in facies and sequence stratigraphic analysis of fluvio-lacustrine successions, *in* McIlroy, D. (ed.), The Application of Ichnology to Palaeoenvironmental and Stratigraphic Analysis: Geological Society, London, Special Publications, v. 228, p. 311–333.
Buatois, L.A., and Mángano, M.G., 2007, Invertebrate ichnology of continental freshwater environments, *in* Miller, W., (ed.), Trace Fossils: Concepts, Problems, Prospects. Amsterdam: Elsevier, p. 285–323.
Buatois, L.A., and Mángano, M.G., 2009, Applications of ichnology in lacustrine sequence stratigraphy: potential and limitations: Palaeogeography, Palaeoclimatology, Palaeoecology, v. 272, p. 127–142.
Buatois, L.A., and Mángano, M.G., in press, Ichnology: Organism-Substrate Interactions in Space and Time. Cambridge: Cambridge University Press.
Buatois, L.A., Netto, R., and Mángano, M.G., 2010, Ichnology of late Paleozoic post-glacial transgressive deposits in Gondwana: Reconstructing salinity conditions in coastal ecosystems affected by strong meltwater discharge, *in* Lopez Gamundi, O., and Buatois, L.A. (eds.), Late Paleozoic glacial events and postglacial transgressions in Gondwana: Geological Society of America Special Paper 468, p. 149-173.
Buatois, L.A., Mángano, M.G., Genise, J.F., and Taylor, T.N., 1998, The ichnologic record of the continental invertebrate invasion: evolutionary trends in environmental expansion, ecospace utilization, and behavioral complexity: Palaios, v. 13, p. 217–240.
Buatois, L.A., Netto, R.G., Mángano, M.G., and Balistieri, P.R.M.N., 2006, Extreme freshwater release during the late Paleozoic Gondwana deglaciation and its impact on coastal ecosystems: Geology, v. 34, p. 1021–1024.
Buatois, L.A., Uba, C.E., Mángano, M.G., Hulka, C., and Heubeck, C., 2007, Deep and intense bioturbation in continental environments: evidence from Miocene fluvial deposits of Bolivia, *in* Bromley, R.G. et al. (eds.): SEPM Special Publication, no. 88, p. 123–136.

Buchheim, H.P., Brand, L.R., and Goodwin, H.T., 2000, Lacustrine to fluvial floodplain deposition in the Eocene Bridger Formation: Palaeogeography, Palaeoclimatology, Palaeoecology, v. 162, p. 191–209.
Butzer, K.W., Isaac, G.L., Richardson, J.L., and Wahbourn-Kamau, C., 1972, Radiocarbon dating of East African lake levels: Science, v. 175, p. 1069–1076.
Cannings, R.A., and Scudder, G.G.E., 1978, The littoral Chironomidae (Diptera) of saline lakes in central British Columbia: Canadian Journal of Zoology, v. 56, p. 1144–1155.
Carroll, A.R., and Bohacs, K.M., 1999, Stratigraphic classification of ancient lakes: balancing tectonic and climatic controls: Geology, v. 27, p. 99–102.
Carroll, A.R., and Bohacs, K.M., 2001, Lake-type controls on petroleum source rock potential in nonmarine basins: AAPG Bulletin, v. 85, p. 1033–1053.
Carroll, A.R., Chetel, L.M., and Smith, M.E., 2006, Feast to famine: sediment supply control on Laramide basin fill: Geology, v. 34, p. 197–200.
Carroll, A.R., Doebbert, A.C., Booth, A.L., Chamberlain, C.P., Rhodes-Carson, M.K., Smith, M.E., Johnson, C.M., and Beard, B.L., 2008, Capture of high-altitude precipitation by a low-altitude Eocene lake, western U.S.: Geology, v. 36, p. 791–794.
Casanova, J., 1986, East African Rift stromatolites, *in* Frostick, L.E., Renaut, R.W., Reid, I, and Tiercelin, J.-J. (eds.), Sedimentation in the African Rifts: Geological Society Special Publication, no. 25, p. 201–210.
Catuneanu, O., Abreu, V., Bhattacharya, J.P., Blum, M.D., Dalrymple, R.W., Eriksson, P.G., Fielding, C.R., Fisher, W.L., Galloway, W.E., Gibling, M.R., Giles, K.A., Holbrook, J.M., Jordan, R., Kendall, C.G.St.C., Macurda, B., Martinsen, O.J., Miall, A.D., Neal, J.E., Nummeal, D., Pomar, L., Posamentier, H.W., Pratt, B.R., Sarg, J.F., Shanley, K.W., Steel, R.J., Strasser, A., Tucker, M.E., and Winker, C., 2009, Towards the standardization of sequence stratigraphy: Earth-Science Reviews, v. 92, p. 1–33.
Caziani, S.M., Olivio, O.R., Ramírez, E.R., Romano, M., Derlindati, E.J., Tálamo, A., Ricalde, D., Quiroga, C., Contreras, J.P., Valqui, M., and Sosa, H., 2007, Seasonal distribution, abundance, and nesting of Puna, Andean, and Chilean flamingos: The Condor, v. 109, p. 276–287.
Chaloner, D.T., and Wotton, R.S., 1996, Tube building by larvae of three species of midge (Diptera: Chironomidae): Journal of the North American Benthological Society, v. 15, p. 300–307.
Chamberlain, C.K., 1975, Recent lebensspuren in nonmarine aquatic environments, *in* Frey, R.W., (ed.), The Study of Trace Fossils: a Synthesis of Principles, Problems, and Procedures in Ichnology. New York: Springer-Verlag, p. 431–458.
Chamberlain, K.R., Frost, C.D., and Frost, B.R., 2003, Early Archean to Mesoproterozoic evolution of the Wyoming Province: Archean origins to modern lithospheric architecture: Canadian Journal of Earth Sciences, v. 40, p. 1357–1374.
Chetel, L.M., and Carroll, A.R., 2010, Terminal infill of Eocene Lake Gosiute, Wyoming, U.S.A.: Journal of Sedimentary Research, v. 80, p. 492–514.
Cioni, R., Fanelli, G., Guidi, M., Kinyariro, J.K., and Marini, L., 1992, Lake Bogoria hot springs (Kenya): geochemical features and geothermal implications: Journal of Volcanology and Geothermal Research, v. 50, p. 231–246.
Clark, G.R., and Ratcliffe, B.C., 1989, Observations on the tunnel morphology of *Heterocerus brunneus* Melsheimer (Coleoptera: Heteroceridae) and its paleoecological significance: Journal of Paleontology, v. 63, p. 228–232.
Claycomb, G.B., 1919, Notes on the habits of *Heterocerus* beetles: Canadian Entomologist, v. 51, p. 25.
Clément, J.-P., Caroff, M., Hémond, C., Tiercelin, J.-J., Bollinger, C., Guillou, H. and Cotton, J., 2003, Pleistocene magmatism in a lithospheric transition area: petrogenesis of alkaline and peralkaline lavas from the Baringo-Bogoria Basin, central Kenya Rift: Canadian Journal of Earth Sciences, v. 40, p. 1239–1257.
Clyde, W.C., Zonneveld, J.-P., Stamatakos, J., Gunnell, G.F., and Bartels, W.S., 1997, Magnetostratigraphy across the Wasatchian/Bridgerian NALMA Boundary (Early to Middle Eocene) in the western Green River basin, Wyoming: Journal of Geology, v. 105, p. 657–669.
Clyde, W.C., Sheldon, N.D., Koch, P.L., Gunnell, G.F., and Bartels, W.S., 2001, Linking the Wasatchian/Bridgerian boundary to the Cenozoic Global Climate Optimum: new magnetostratographic and isotopic results from South Pass, Wyoming: Palaeogeography, Palaeoclimatology, Palaeoecology, v. 167, p. 174–199.
Cohen, A.S., 2003, Paleolimnology. Oxford: Oxford University Press, 500 p.

Cohen, A., Lockley, M., Halfpenny, J., and Michel, A.E., 1991, Modern vertebrate track taphonomy at Lake Manyara, Tanzania: Palaios, v. 6, p. 371–389.
Cohen, A., Halfpenny, J., Lockley, M., and Michel, A.E., 1993, Modern vertebrate tracks from Lake Manyara, Tanzania and their paleobiological implications: Paleobiology, v. 19, p. 433–458.
Collins, N.C., Mitchell, R., and Wiegert, R.G., 1976, Functional analysis of a thermal spring ecosystem, with an evaluation of the role of consumers: Ecology, v. 57, p. 1221–1232.
Collinson, J., Mountney, N., and Thompson, D., 2006, Sedimentary Structures, Third Edition. Harpenden, England: Terra Publishing, 292 p.
Colombini, I., Aloia, A., Fallaci, M., and Chelazzi, L., 1996, Spatial and temporal strategies in the surface activity of some sandy beach arthropods living along the French Atlantic Coast: Marine Biology, v. 127, p. 247–257.
Condie, K.C., Lee, D., and Farmer, G.L., 2001, Tectonic setting and provenance of the Neoproterozoic Uinta Mountain and Big Cottonwood groups, northern Utah: constraints from geochemistry, Nd isotopes, and detrital modes: Sedimentary Geology, v. 141, p. 443–464.
Counts, J.W., and Hasiotis, S.T., 2009, Neoichnological experiments with masked chafer beetles (Coleoptera: Scarabidae): implications for backfilled continental trace fossils: Palaios, v. 24, p. 74–91.
Craig, P.C., 1970, The behavior and distribution of the intertidal sand beetle, *Thinopinus pictus* (Coleoptera: Staphylinidae): Ecology, v. 51, p. 1012–1017.
Criddle, N., 1907, Habits of some Manitoba “tiger beetles” (*Cicindela*): The Canadian Entomologist, v. 39, p. 105–114.
Culbertson, W.C., 1961, Stratigraphy of the Wilkins Peak Member of the Green River Formation, Firehole Basin Quadrangle, Wyoming, *in* Short Papers in the Geologica and Hydrologic Sciences: U.S. Geological Survey Professional Paper 424-D, p. 170–173.
Culbertson, W.C., 1971, Stratigraphy of the trona deposits in the Green River Formation, southwestern Wyoming, *in* Contributions to Geology, Trona Issue: Laramie, University of Wyoming, v. 10, p. 15–24.
Curry, H.D., 1957, Fossil tracks of Eocene vertebrates, southwestern Uintah Basin, Utah: Intermountain Association of Petroleum Geologists, Eighth Annual Field Conference, p. 42–47.
Dadeech, P.K., Krienitz, L., Kotut, K., Ballot, A., and Casper, P., 2009, Molecular detection of uncultured cyanobacteria and animotransferase domains for cyanotoxin production in sediments of different Kenyan lakes: FEMS Microbial Ecology, v. 68, p. 340–350.
D’Alessandro, A., Ekdale, A.A., and Picard, M.D., 1987, Trace fossils in fluvial deposits of the Duchesne River Formation (Eocene), Uinta Basin, Utah: Palaeogeography, Palaeoclimatology, Palaeoecology, v. 61, p. 285–301.
Darling, W.G., Allen, D.J., and Armannsson, H., 1990, Indirect detection of subsurface outflow from a Rift Valley lake: Journal of Hydrology, v. 113, p. 297–305.
Deardorff, D.L., and Mannion, L.E., 1971, Wyoming trona deposits, *in* Contributions to Geology, Trona Issue. Laramie: University of Wyoming, v. 10, p. 25–38.
DeCelles, P.G., 2004, Late Jurassic to Eocene evolution of the Cordilleran thrust belt and foreland basin system, western U.S.A.: American Journal of Science, v. 304, p. 105–168.
DeCelles, P.G., and Mitra, G., 1995, History of the Sevier orogenic wedge in terms of critical taper models, northeast Utah and southwest Wyoming: Geological Society of America Bulletin, v. 107, p. 454–462.
De Dekker, P., 1981, Ostracods of athalassic saline lakes: a review: Hydrobiologia, v. 81, p. 131–144.
DeMenocal, P., Ortiz, J., Guilderson, T., Adkins, J., Sarnthein, M., Baker, L., and Yarusinsky, M., 2000, Abrupt onset and termination of the African Humid Period: rapid climate responses to gradual insolation forcing: Quaternary Science Reviews, v. 19, p. 347–361.
Deocampo, D., 2004, Authigenic clays in East Africa: Regional trends and paleolimnology at the Plio-Pleistocene boundary, Olduvai Gorge, Tanzania: Journal of Paleolimnology, v. 31, p. 1–9.
Des Marais, D.J., 2003, Biogeochemistry of hypersaline microbial mats illustrates the dynamics of modern microbial ecosystems and the early evolution of the biosphere: Biological Bulletin, v. 204, p. 160–167.
Dickinson, W.R., Klute, M.A., Hayes, M.J., Janecke, S.U., Lundin, E.R., Mckittrick, M.A., and Olivares, M.D., 1988, Paleogeographic and paleotectonic setting of Laramide sedimentary basins in the central Rocky Mountain region: Geological Society of America Bulletin, v. 100, p. 1023–1039.

Doebbert, A.C., Carroll, A.R., Mulch, A., Chetel, L.M., and Chamberlain, C.P., 2010, Geomorphic controls on lacustrine isotopic compositions: evidence from the Laney Member, Green River Formation, Wyoming: Geological Society of America Bulletin, v. 122, p. 236–252.
Doemel, W.N., and Brock, T.D., 1974, Bacterial stromatolites: origin of laminations: Science, v. 174, p. 1083–1085.
Dreisig, H., 1980, Daily activity, thermoregulation and water loss in the tiger beetle *Cicindela hybrid*: Oecologia, v. 44, p. 376–389.
Droser, M.L., and Bottjer, D.J., 1986, A semiquantitative field classification of ichnofabric: Journal of Sedimentary Petrology, v. 56, p. 558–559.
Dubinin, A.V., Gerasimenko, L.M., and Zavarzin, G.A., 1995, Ecophysiology and species diversity of cyanobacteria from Lake Magadi: Microbiology, v. 64, p. 717–721.
Duckworth, A.W., Grant, W.D., Jones, B.E., and Van Steenbergen, R., 1996, Phylogenetic diversity of soda lake alkaliphiles: FEMS Microbiology Ecology, v. 19, p. 181–191.
Dyke, G.J., and Walker, C.A., 2008, New records of fossil 'waterbirds' from the Miocene of Kenya: American Museum Novitates, no. 3610, 12 p.
Edgar, W.D., and Meadows, P.S., 1969, Case construction, movement, spatial distribution and substrate selection in the larva of *Chironomus reparius* Meigen: Journal of Experimental Biology, v. 50, p. 247–253.
Ego, J., 1994, Sedimentology and Diagensis of Neogene Sediments in the Central Kenya Rift Valley: Unpublished M.Sc. thesis, University of Saskatchewan.
Ekdale, A.A., Bromley, R.G., and Pemberton, S.G., 1984, Ichnology – The Use of Trace Fossils in Sedimentology and Stratigraphy: SEPM Short Course Publication, no. 15, 317 p.
Ekdale, A.A., Bromley, R.G., and Loope, D.B., 2007, Ichnofacies of an ancient erg: a climatically influenced trace fossil association in the Jurassic Navajo sandstone, Southern Utah, USA, *in* Miller III, W. (ed.), Trace Fossils: Concepts, Problems, Prospects. Amsterdam: Elsevier, p. 562–574.
Erickson, B.R., 1967, Fossil bird tracks from Utah: Science Museum of Minnesota, Museum Observer, v. 5, p. 140–146.
Ericson, P.G.P., 1999, New material of *Juncitarsus* (Phoenicopteriformes), with a guide for differentiating that genus from the Presbyornithidae (Anseriformes): Smithsonsian Contributions to Paleobiology, v. 89, p. 245–251.
Eugster, H.P., 1967, Hydrous sodium silicates from Lake Magadi, Kenya: precursors of bedded chert: Science, v. 157, p. 1177–1180.
Eugster, H.P., 1969, Inorganic bedded cherts from the Magadi area, Kenya: Contributions to Mineralogy and Petrology, v. 22, p. 1–31.
Eugster, H.P., 1980, Lake Magadi, Kenya, and its precursors, *in* Nissenbaum, A. (ed.), Hypersaline Brines and Evaporitic Environments: Developments in Sedimentology, no. 28, p. 195–232.
Eugster, H.P., 1986, Lake Magadi, Kenya: a model for rift valley hydrochemistry and sedimentation?, *in* Frostick, L.E., Renaut, R.W., Reid, I, and Tiercelin, J.-J. (eds.), Sedimentation in the African Rifts: Geological Society Special Publication, no. 25, p. 177–189.
Eugster, H.P., and Jones, B.F., 1968, Gels composed of sodium-aluminium-silicate, Lake Magadi, Kenya: Science, v. 161, p. 160–164.
Eusebi, M.P., Favilli, L., and Lovari, S., 1989, Some abiotic factors affecting the activity and habitat choice of the tiger beetle *Cephalota circumdata lionschaeferi* (Cassola) (Coleoptera, Cicindelidae): Bollettino di Zoologia, v. 56, p. 143–150.
Farrand, W.R., Redding, R.W., Wolpoff, M.H., and Wright, H.T., 1976, An archaeological investigation on the Loboi Plain, Baringo District, Kenya: Museum of Anthropology, University of Michigan, Technical Reports, no. 4, 86 p.
Farrell, K.M., 2001, Geomorphology, facies architecture, and high-resolution, non-marine sequence stratigraphy in avulsion deposits, Cumberland Marshes, Saskatchewan: Sedimentary Geology, v. 139, p. 93–150.
Faure, H,, Walter, R.C., and Grant, D.R., 2002, The coastal oasis: ice age springs on emerged continental shelves: Global and Planetary Change, v. 33, p. 47–56.
Fenster, M.S., Knisley, C.B., and Reed, C.T., 2006, Habitat preference and the effects of beach nourishment on the federally threatened northeastern beach tiger beetle, *Cicindela dorsalis dorsalis*: western shore, Chesapeake Bay, Virginia: Journal of Coastal Research, v. 22, 1133–1144.

Fitzgerald, P.G., and Barrett, P.J., 1986, Skolithos in a Permian braided river deposit, southern Victoria Land, Antarctica: Palaeogeography, Palaeoclimatology, Palaeoecology, v. 52, p. 237–247.
Foster, J.R., 2001, Salamander tracks (*Ambystomichnus*?) from the Cathedral Bluffs Tongue of the Wasatch Formation (Eocene), northeastern Green River basin, Wyoming: Journal of Paleontology, v. 75, p. 901–904.
Foster, W.A., and Treherne, J.E., 1976, Insects of marine saltmarshes: problems and adaptations, *in* Cheng, L. (ed.), Marine Insects: available online from the University of California San Diego, Scripps Institution of Oceanography (http://escholarship.org/uc/item/1pm1485b), p. 5–42.
Frank, J., and Stolz, J.F., 2009, Flat laminated microbial mat communities: Earth-Science Reviews, v. 96, p. 163–172.
Fraser, N.C., Grimaldi, D.A., Olsen, P.E., and Axsmith, B., 1996, A Triassic lagerstätte from eastern North America: Nature, v. 380, p. 615–619.
Frey, R.W., 1975, The Study of Trace Fossils. New York: Springer-Verlag, 562 p.
Frey, R.W., and Pemberton, S.G., 1986, Vertebrate lebensspuren in intertidal and supratidal environments, Holocene Barrier Islands, Georgia: Senckenbergiana Maritima, v. 18, p. 45–95.
Frey, R.W., and Pemberton, S.G., 1987, The *Psilonichnus* ichnocoenose, and its relationship to adjacent marine and nonmarine ichnocoenoses along the Georgia coast: Bulletin of Canadian Petroleum Geology, v. 35, p. 333–357.
Frey, R.W., Pemberton, S.G., and Fagerstrom, J.A., 1984, Morphological, ethological and environmental significance of the ichnogenera *Scoyenia* and *Ancorichnus*: Journal of Paleontology, v. 58, p. 511–528.
Fulton, B.B., 1924, Some habits of earwigs: Annals of the Entomological Society of America, v. 17, p. 357–367.
Gallet, E., 1950, The Flamingos of the Camargue. Oxford: England, Basil Blackwell, 127 p.
Ganeshaiah, K.N., and Belavadi, V.V., 1986, Habitat segregation in four species of adult tiger beetles (Coleoptera: Cicindelidae): Ecological Entomology, v. 11, p. 147–154.
Garcia, C.M., and Niell, F.X., 1991, Burrowing beetles of the genus *Bledius* (Staphylinidae) as agents of bioturbation in the emergent areas and shores of an athalassic inland lake (Fuente de Piedra, southern of Spain): Hydrobiologia, v. 215, p. 163–173.
Garcin, Y., Junginger, A., Melnick, D., Olago, D., and Strecker, M.R., 2009, Late Pleistocene–Holocene rise and collapse of Lake Suguta, northern Kenya Rift: Quaternary Science Reviews, v. 28, p. 911–925.
Gasse, F., 2000, Hydrological changes in the African tropics since the Last Glacial Maximum: Quaternary Science Reviews, v. 19, p. 189–211.
Gasse, F., Chalié, F., Vincens, A., Williams, M.A.J., and Williamson, D., 2008, Climatic patterns in equatorial and southern Africa from 30,000 to 10,000 years ago reconstructed from terrestrial and near-shore proxy data: Quaternary Science Reviews, v. 27, p. 2316–2340.
Genise, J.F., Mángano, G.M., Buatois, L.A., Laza, J.H., and Verde, M., 2000, Insect trace fossil associations in paleosols: the *Coprinisphaera* ichnofacies: Palaios, v. 15, p. 49–64.
Genise, J.F., Melchor, R.N., Bellosia, E.S., and Verde, M., 2010, Invertebrate and vertebrate trace fossils from continental carbonates, *in* Alonso-Zarza, A.M., and Tanner, L.H. (eds.), Carbonates in Continental Settings: Facies, Environments and Processes: Elsevier, Developments in Sedimentology, v. 61, p. 319–362.
Gerdes, G., Spira, J., and Dimentman, C., 1985, The fauna of the Gavish Sabkha and the Solar Lake – a comparative study, *in* Friedman, G.M., and Krumbein, W.E. (eds.), Hypersaline Ecosystems. Berlin: Springer-Verlag, p. 322–345.
Gerdes, G., Claes, M., Dunajtschik-Piewak, K., Riege, H., Krumbein, W.E., and Reinick, H.-E., 1993, Contribution of microbial mats to sedimentary surface structures: Facies, v. 29, p. 11–13.
de Gibert, J.M., and Sáez, A., 2009, Paleohydrological significance of trace fossil distribution in Oligocene fluvial-fan-to-lacustrine systems of the Ebro Basin, Spain: Palaegeography, Palaeoclimatology, Palaeoecology, v. 272, p. 162–175.
Gierlowski-Kordesch, E., 1991, Ichnology of an ephemeral lacustrine/alluvial plain system: Jurassic East Berlin Formation, Hartford Basin, USA: Ichnos, v. 1, p. 221–232.
Gingras, M.K., Pemberton, S.G., Saunders, T., and Clifton, H.E., 1999, The ichnology of brackish water Pleistocene deposits at Willapa Bay, Washington: variability in estuarine settings: Palaios, v. 14, p. 352–374.
Gingras, M.K., Lalond, S.V., Amskold, L., and Konhauser, K., 2007, Wintering chironomids mine oxygen: Palaios, v. 22, p. 433–438.

Goetz, C., and Hillaire-Marcel, C., 1992, U-series disequilibria in early diagenetic minerals from Lake Magadi sediments, Kenya: dating potential: Geochimica et Cosmochimica Acta, v. 56, p. 1331–1341.
Goodwin, J.H., 1973, Analcime and K-feldspar in tuffs of the Green River Formation, Wyoming: American Mineralogist, v. 58, p. 93–105.
Grande, L., 1984, Paleontology of the Green River Formation, with a review of the fish fauna, Second Edition: Geological Survey of Wyoming Bulletin, v. 63, p. 1–333.
Grande, L., and Buchheim, H.P., 1994, Paleontological and sedimentological variation in early Eocene Fossil Lake: Contributions to Geology, University of Wyoming, v. 30, p. 33–56.
Grant, S., Grant, W.D., Jones, B.E., Kato, C., and Li, L., 1999, Novel archaeal phylotypes from an East African alkaline saltern: Extremophiles, v. 3, p. 139–145.
Grant, W.D., and Ross, H.N.M., 1986, The ecology and taxonomy of halobacteria: FEMS Microbiology Reviews, v. 39, p. 9–15.
Grant, W.D., and Tindall, B.J., 1986, The alkaline saline environment, *in* Herbert, R.A. and Codd, G.A. (eds.), Microbes in Extreme Environments: London, Academic Press, p. 25–54.
Greben, R., and Lockley, M., 1992, Vertebrate tracks from the Green River Formation, eastern Utah: implications for paleoecology: Abstracts with Programs, Geological Society of America, Rocky Mountain Section, v. 24, p. 16.
Greenwood, D.R., and Wing, S.L., 1995, Eocene continental climates and latitudinal temperature gradients: Geology, v. 23, p. 1044–1048.
Griffiths, C.L., and Griffiths, R.J., 1983, Biology and distribution of the littoral rove beetle *Psamathobledius punctatissimus* (Le Conte) (Coleoptera: Staphylinidae): Hydrobiologia, v. 101, p. 203–214.
Grimaldi, D., and Engel, M.S., 2005, Evolution of the Insects. Cambridge; New York: Cambridge University Press, 755 p.
Guillet, S., and Vancassel, M., 2001, Dermapteran life-history evolution and phylogeny with special reference to the Forficulidae family: Evolutionary Ecology Research, v. 3, p. 441–447.
Gulas-Wroblewski, B.E., and Wroblewski, A.F.-J., 2003, A crown-group galliform bird from the middle Eocene Bridger Formation of Wyoming: Palaeontology, v. 46, p. 1269–1280.
Gullan, P.J., and Cranston, P.S., 2000, The Insects: an Outline of Entomology. Malden, Massachusetts: Blackwell Science, 470 p.
Gunnell, G.F., and Bartels, W.S., 2001, Basin margins, biodiversity, evolutionary innovation, and the origin of new taxa, *in* Gunnell, G.F. (ed.), Eocene Biodiversity: Unusual Occurrences and Rarely Sampled Habitats. New York: Kluwer Academic/Plenum Publishers, p. 403–432.
Gunnell, G.F., Bartels, W.S., and Zonneveld, J.-P., 2004, A late Wasatchian (late early Eocene) vertebrate assemblage preserved in meandering stream channel deposits, northern Red Desert, Wyoming: Abstracts with Programs, Geological Society of America, v. 36, p. 92.
Guppy, M., Guppy, S., and Hebrard, J., 1983, Behaviour of the riverine tiger beetle *Lophyridia dongalensis imperatrix*: effect of water availability on thermoregulatory strategy: Entomologia Experimentalis et Applicata, v. 33, p. 276–282.
Haas, F., and Kukakova-Peck, J., 2001, Dermaptera hindwing structure and folding: new evidence for familial, ordinal and superordinal relationships within Neoptera (Insecta): European Journal of Entolomology, v. 98, p. 445–509.
Haas, F., Holstein, J., Zahm, A., Häuser, C.L., and Kinuthia, W., 2005, Earwigs (Dermaptera: Insects) of Kenya – Checklist and species new to Kenya, *in* Huber, B.A., Sinclair, B.J., and Lampe, K.-H. (eds.), African Biodiversity. New York: Springer, p. 99–107.
Hadley, N.F., Knisley, C.B., Schultz, T.D., and Pearson, D.L., 1990, Water relations of tiger beetle larvae (*Cicindela marutha*): correlations with habitat microclimate and burrowing activity: Journal of Arid Environments, v. 19, p. 189–197.
Hagadorn, J.W., and Bottjer, D.J., 1997, Wrinkle structures: microbially mediated sedimentary structures common in subtidal siliciclastic settings at the Proterozoic-Phanerozoic transition: Geology, v. 25, p. 1047–1050.
Hagadorn, J.W., and Bottjer, D.J., 1999, Restriction of a Late Neoproterozoic biotope: suspect-microbial structures and trace fossils at the Vendian–Cambrian transition: Palaios, v. 14, p. 73–85.

Halfen, A.F., and Hasiotis, S.T., 2010, Neoichnological study of the traces and burrowing behaviors of the western harvester ant *Pogonomymex occidentalis* (Insecta: Hymenoptera: Formicidae): paleopedogenic and paleoecological implications: Palaios, v. 25, p. 703–720.
Hamblin, A.H., Sarjeant, W.A.S., and Spalding, D.D., 1998, A remarkable mammal trackway in the Uinta Formation (late Eocene) of Utah: Brigham Young University, Geology Studies, v. 43, p. 9–18.
Hamblin, A.H., Sarjeant, W.A.S., and Spalding, D.A.E., 1999, Vertebrate footprints in the Duchesne River and Uinta Formations (middle to late Eocene), Uinta Basin, Utah: Utah Geological Survey, Miscellaneous Publications, v. 99-1, p. 443–454.
Hamer, J.M.M., and Sheldon, N.D., 2010, Neoichnology at lake margins: implications for paleo-lake systems: Sedimentary Geology, v. 228, p. 319–327.
Hamilton, A.C., 1982, Environmental History of East Africa: New York, Academic Press, 328 p.
Hammer, T.U., 1986, Saline Lake Ecosystems of the World. Dordrecht: Dr. W. Junk Publishers, 616 p.
Hanley, J.H., 1976, Paleosynecology of nonmarine Mollusca from the Green River and Wasatch Formations (Eocene), southwestern Wyoming and northwestern Colorado, *in* Scott, R.W. and West R.R. (eds.), Structure and Classification of Paleocommunities. Stroudsburg: Dowden, Hutchinson and Ross, p. 235-261.
Hanley, J.H., 1988, Taphonomy and paleoecology of nonmarine Mollusca in fluvial and lacustrine environments of the Cottonwood Creek Delta, Tipton Tongue of the Green River Formation (Eocene), southeast Washakie Basin, Wyoming: U.S. Geological Survey Bulletin, 1669-B, 19 p.
Hardie, L.A., Smoot, J.P., and Eugster, H.P., 1978, Saline lakes and their deposits: a sedimentological approach, *in* Matter, A., and Tucker, M.E. (eds.), Modern and Ancient Lake Sediments: Special Publication of the International Association of Sedimentologists, no. 2, p. 7–41.
Harper, D.M., Childress, R.B., Harper, M.M., Boar, R.R., Hickley, P., Mills, S.C., Otieno, N., Drane, T., Varschi, E., Nasirwa, O., Mwatha, W.E., Darlington, J.P.E.C., and Escuté-Gasulla, X., 2003, Aquatic biodiversity and saline lakes: Lake Bogoria National Reserve, Kenya: Hydrobiologia, v. 500, p. 259–276.
Hasiotis, S.T., 2003, Complex ichnofossils of solitary and social soil organisms: understanding their evolution and roles in terrestrial paleoecosystems: Palaeogeography, Palaeoclimatology, Palaeoecology, v. 192, p. 259–320.
Hasiotis, S.T., 2007, Continental ichnology: fundamental processes and controls on trace fossil distribution, *in* Miller, W., (ed.), Trace Fossils: Concepts, Problems, Prospects. Amsterdam: Elsevier, p. 268–284.
Hasiotis, S.T., and Mitchell, C.E., 1993, A comparison of crayfish burrow morphologies: Triassic and Holocene fossil, paleo- and neo-ichnological evidence, and the identification of their burrowing signatures: Ichnos, v. 2, p. 291–314.
Hasiotis, S.T., and Honey, J.G., 2000, Paleohydrologic and stratigraphic significance of crayfish burrows in continental deposits: examples from several Paleocene Laramide basins in the Rocky Mountains: Journal of Sedimentary Research, v. 70, p. 127–139.
Hasiotis, S.T., Bohacs, K.M., and Demko, T.M., 2003, Arthropod, plant, and vertebrate ichnofossil evidence for fluctuating groundwater and lake levels, Eocene Green River and Wasatch Formation, Wyoming: Third International Limnogeology Congress, Tucson, AZ, Abstracts, p. 109–110.
Hasiotis, S.T., Ainsworth, B., Amos, K.J., Vakerelov, B.K., Payenberg, T., Krapf, C.B., and Sandstrom, M., 2009, Traces associated with wind-generated tidal deposits formed from the Kalaweerina Creek Terminal Splay Complex, Lake Eyre Basin, Central Australia: sedimentary facies and trace associations that might sway ichnologic interpretations: AAPG Annual Convention and Exhibition.
Hautot, S., Tarits, P., Whaler, K., Le Gall, B., Tiercelin, J.-J., and Le Turdu, C., 2000, Deep structure of the Baringo Rift Basin (central Kenya) from three-dimensional magnetotelluric imaging: implications for rift evolution: Journal of Geophysical Research, v. 105, p. 23,493– 23,518.
Hay, R.L., 1966. Zeolites and zeolitic reactions in sedimentary rocks: Geological Society of America Special Papers, v. 85, 130 p.
Herman, L.H., 1986, Revision of *Bledius*. Part IV. Classification of species groups, phylogeny, natural history, and catalogue (Coleoptera, Staphylinidae, Oxytelinae): Bulletin of the American Museum of Natural History, v. 184, p. 1–368.
Hill, A., Drake, R., Tauxe, L., Monaghan, M., Barry, J.C., Behrensmeyer, A.K., Curtis, G., Jacobs, B. Fine, Jacobs, L., Johnson, N., and Pilbeam, D., 1985, Neogene palaeontology and geochronology of the Baringo basin, Kenya: Journal of Human Evolution, v. 14, p. 759–773.

Hindák, F., 2001, Thermal microorganisms from a hot spring on the coast of Lake Bogoria, Kenya: Nova Hedwigia Beiheft, v. 123, p. 77–93.
Hoback, W.W., Golick, D.A., Svatos, T.M., Spomer, S.M., and Higley, L.G., 2000, Salinity and shade preferences result in ovipositional differences between sympatric tiger beetle species: Ecological Entomology, v. 25, p. 180–187.
Hollnack, D., and Stangel, R., 1998, The seismicity related to the southern part of the Kenya Rift: Journal of African Earth Sciences, v. 26, p. 477–495.
Honey, J.G., 1988, A mammalian fauna from the base of the Eocene Cathedral Bluffs Tongue of the Wasatch Formation, Cottonwood Creek area, southeast Washakie Basin, Wyoming:U.S. Geological Survey Bulletin 1669-C, 14 p.
Hover, V.C., and Ashley, G.M., 2003, Geochemical signatures of paleodepositional and diagenetic environments: a STEM/AEM study of authigenic clay minerals from an arid rift basin, Olduvai Gorge, Tanzania: Clays and Clay Minerals, v. 51, p. 231–251.
Hunt, A.P., and Lucas, S.G., 2007a, Tetrapod ichnofacies: a new paradigm: Ichnos, v. 14, p. 59–68.
Hunt, A.P., and Lucas, S.G., 2007b, Cenozoic vertebrate trace fossils of North America: ichnofaunas, ichnofacies and biochronology, *in* Lucas, S.G., Spielmann, J.A., and Lockley, M.G. (eds.), Cenozoic Vertebrate Tracks and Traces: New Mexico Museum of Natural History and Science Bulletin, v. 42, p. 17–41.
Icole, M., Masse, J.-P., Perinet, G., and Taieb, M., 1990, Pleistocene lacustrine stromatolites, composed of calcium carbonate, fluorite, and dolomite, from Lake Natron, Tanzania: depositional and diagenetic processes and their paleoenvironmental significance: Sedimentary Geology, v. 69, p. 139–155.
Imoff, J.F., Tindall, B.J., Grant, W.D., and Trüper, H.G., 1981, *Ectothiorhodospira vacuolata* sp. nov., a new phototrophic bacterium from soda lakes: Archives of Microbiology, v. 130, p. 238–242.
Ingalls, B.R., and Park, L.E., 2010, Biotic and taphonomic response to lake-level fluctuations in the greater Green River basin (Eocene), Wyoming: Palaios, v. 25, p. 287–298.
James, H.F., 2005, Paleogene fossils and the radiation of modern birds: The Auk, v. 122, p. 1049–1054.
Jennings, D.S., Santucci, V.L., Bucheim, H.P., and Hasiotis, S.T., 2002, A preliminary inventory and assessment of ichnofossils from the Green River Formation: Abstracts with Programs, Geological Society of America, v. 34, p. 556.
Jenkin, P.M., 1957, The filter-feeding and food of flamingoes (Phoenicopteri): Philosophical Transactions of the Royal Society of London, B, v. 240, p. 401–493.
Jobe-Akeley, M.L.J., 1929, Carl Akeley's Africa. New York: Blue Ribbon Books, 321 p.
Johnson, C. Roure, Ashley, G.M., De Wet, C.B., Dvoretsky, R., Park, L., Hover, V.C., Owen, R.B., and McBrearty, S., 2009, Tufa as a record of perennial fresh water in a semi-arid rift basin, Kapthurin Formation, Kenya: Sedimentology, v. 56, p. 1115–1137.
Johnson, E.W., Briggs, D.E.G., Suthren, R.J., Wright, J.L., and Tunncliff, S.P., 1994, Non-marine arthropod traces from the subaerial Ordovician Borrowdale Volcanic Group, English Lake District: Geological Magazine, v. 131, p. 395–406.
Johnson, P.L., and Anderson, D.W., 2009, Concurrent growth of uplifts with dissimilar orientations in the southern Green River Basin, Wyoming: implications for Paleocene–Eocene patterns of foreland shortening: Rocky Mountain Geology, v. 44, p. 1–16.
Johnston, R.E., and Yin, A., 2001, Kinematics of the Uinta Fault System (southern Wyoming and northern Utah) during the Laramide Orogeny: International Geology Review, v. 43, p. 52–68.
Jones, B., and Renaut, R.W., 1998, Origin of platy calcite crystals in hot-spring deposits in the Kenya Rift Valley: Journal of Sedimentary Research, v. 68, p. 913–927.
Jones, B., and Renaut, R.W., 2010, Calcareous spring deposits in continental settings: Chapter 4, *in* Alonso-Zarza, A.M., and Tanner, L.H. (eds.), Carbonates in Continental Settings: Facies, Environments and Processes: Elsevier, Developments in Sedimentology, v. 61, p. 177–224.
Jones, B., Renaut, R.W., and Rosen, M.R., 2005, Taxonomic fidelity of silicified microbes from hot spring systems in the Taupo Volcanic Zone, North Island, New Zealand: Philosophical Transactions of the Royal Society of Edinburgh, Earth Sciences, v. 94, p. 475–484.
Jones, B.E., Grant, W.D., Duckworth, A.W., and Owenson, G.G., 1998, Microbial diversity of soda lakes: Extremophiles, v. 2, p. 191–200.

Jones, B.F., Eugster, H.P., and Rettig, S.L., 1977, Hydrochemistry of the Lake Magadi basin, Kenya: Geochimica et Cosmochimica Acta, v. 41, p. 53–72.
Kear, J., and Duplaix-Hall, N. (eds.), 1975, Flamingos. Berhkhamsted, England: T & A D Poyser, 256 p.
Keighley, D.G., and Pickerill, R.K., 1995, The ichnotaxa *Palaeophycus* and *Planolites*: historical perspectives and recommendations: Ichnos, v. 3, p. 301–309.
Keighley, D.G., and Pickerill, R.K., 1997, Systematic ichnology of the Mabou and Cumberland groups (Carboniferous) of western Cape Breton Island, eastern Canada, 1: burrows, pits, trails, and coprolites: Atlantic Geology, v. 33, p. 181–215.
Keighley, D.G., and Pickerill, R.K., 2003, Ichnocoenoses from the Carboniferous of eastern Canada and their implications for the recognition of ichnofacies in nonmarine strata: Atlantic Geology, v. 39, p. 1–22.
Kevbrin, V.V., Zhilina, T.N., Rainey, F.A., and Zavarzin, G.A., 1998, *Tindallia magadii* gen. nov., sp. nov.: an alkaliphilic anaerobic ammonifier from soda lake deposits: Current Microbiology, v. 37, p. 94–100.
Kim, J.Y., Keighley, D.G., Pickerill, R.K., Hwang, W., and Kim, K.-S., 2005, Trace fossils from marginal lacustrine deposits of the Cretaceous Jinju Formation, southern coast of Korea: Palaeogeography, Palaeoclimatology, Palaeoecology, v. 218, p. 105–124.
Kipkorir, E.C., 2002, Analysis of rainfall climate on the Njemps Flats, Baringo District, Kenya: Journal of Arid Environments, v. 50, p. 445–458.
Kleinwächter, M., and Bürkel, M., 2008, Offspring performance in dynamic habitats: key factors for a riparian carabid beetle: Ecological Entomology, v. 33, p. 286–292.
Knisley, C.B., 1984, Ecological distribution of tiger beetles (Coleoptera: Cicindelidae) in Colfax County, New Mexico: The Southwestern Naturalist, v. 29, p. 93–104.
Knisley, C.B., 1987, Habitats, food resources, and natural enemies of a community of larval *Cicindela* in southeastern Arizona (Coleoptera: Cicindelidae): Canadian Journal of Zoology, v. 65, p. 1191–1200.
Knisley, C.B., and Juliano, S.A., 1988, Survival, development, and size of larval tiger beetles: effects of food and water: Ecology, v. 69, p. 1983–1992.
Knisley, C.B., and Hill, J.M., 2001, Biology and conservation of the Coral Pink Sand Dunes tiger beetle, *Cicindela limbata albissima* Rumpp: Western North American Naturalist, v. 61, p. 381–394.
Kölliker, M., and Vancassel, M., 2007, Maternal attendance and the maintenance of family groups in common earwigs (*Forficula auricularia*): a field experiment: Ecological Entomology, v. 32, p. 24–27.
Kraig, D.H., Wiltschko, D.V., and Spang, J.H., 1987, Interaction of basement uplift and thin-skinned thrusting, Moxa arch and the Western Overthrust Belt, Wyoming: a hypothesis: Geological Society of America Bulletin, v. 99, p. 654–662.
Krapovickas, V., Ciccioli, P.A., Mángano, M.G., Marsicano, and Limarino, C.O., 2009, Paleobiology and paleoecology of an arid-semiarid Miocene South American ichnofauna in anastomosed fluvial deposits: Palaeogeography, Palaeoclimatology, Palaeoecology, v. 284, p. 129–152.
Krienitz, L., Ballot, A., Kotut, K., Wiegand, C., Pütz, S., Metcalf, J.S., Codd, G.A., and Pflugmacher, S., 2003, Contribution of hot spring cyanobacteria to the mysterious deaths of Lesser Flamingos at Lake Bogoria, Kenya: FEMS Microbiology Ecology, v. 43, p. 141–148.
Krivosheina, M.G., 2008, On insect feeding on cyanobacteria: Paleontological Journal, v. 42, p. 596–599.
Kroonenberg, S.B., Rusakov, G.V., and Svitoch, A.A., 1997, The wandering of the Volga Delta: a response to rapid Caspian sea-level change: Sedimentary Geology, v. 107, p. 189–209.
Lamb, R.J., 1975, Effects of dispersion, travel, and environmental heterogeneity on populations of the earwig *Forficula auricularia* L.: Canadian Journal of Zoology, v. 53, p. 1855–1867.
Lamb, R.J., 1976a, Dispersal by nesting earwigs, *Forficula auricularia* (Dermaptera: Forficulidae): Canadian Entomology, v. 108, p. 213–216.
Lamb, R.J., 1976b, Parental behavior in the Dermaptera with special reference to *Forficula auricularia* (Dermaptera: Forficulidae): Canadian Entomology, v. 108, p. 609–619.
Lamberti, G.A., and Resh, V.H., 1983, Distribution of benthic algae and macroinvertebrates along a thermal stream gradient: Hydrobiologia, v. 128, p. 13–21.
Lamond, R.E., and Tapanila, L, 2003, Embedment cavities in lacustrine stromatolites: evidence of animal interactions from Cenozoic carbonates in U.S.A. and Kenya: Palaios, v.18, p. 445–453.
Lawfield, A.M.W., and Pickerill, R.K., 2006, A novel contemporary fluvial ichnocoenose: unionid bivalves and the *Scoyenia–Mermia* transition: Palaios, v. 21, p. 391–396.

Legarreta, L., Uliana, M.A., Larotonda, C.A. and Meconi, G.R., 1993, Approaches to nonmarine sequence stratigraphy: theoretical models and examples from Argentine basins, *in* Eshard, R., and Doliez, B. (eds.), Subsurface Reservoir Characterisation from Outcrop Observations: Editions Technip, Collection Colloques et Seminaires, v. 51, p. 125–145.

Leggitt, V.L., 2007a, Freshwater facies of the saline Wilkins Peak Member of the Green River Formation: 4th International Limnogeology Congress, Barcelona, Spain, Abstracts, p. 115.

Leggitt, V.L., 2007b, Spring deposits in the Wilkins Peak Member of the Eocene Green River Formation: Steed Canyon, Lincoln County, Wyoming: Geological Society of America Abstracts, v. 39, p. 384.

Leggitt, V.L., and Cushman, R.A. Jr., 2001, Complex caddisfly-dominated bioherms from the Eocene Green River Formation: Sedimentary Geology, v. 145, p. 377–396.

Leggitt, V.L., and Cushman, R.A., 2003, Flamingo nest mounds from a crocodilian nesting site in the Eocene Wasatch Formation: Lincoln County, Wyoming: Journal of Vertebrate Paleontology, v. 23, no. 3 supplement, p. 71A.

Leggitt, V.L., and Loewan, M.A., 2002, Eocene Green River Formation "*Oocardium* tufa" reinterpreted as complex arrays of calcified caddisfly (Insecta: Trichoptera) larval cases: Sedimentary Geology, v. 148, p. 139–146.

Leggitt, V.L., Biaggi, R.E., and Buchheim, H.P., 2007, Palaeoenvironments associated with caddisfly-dominated microbial-carbonate mounds from the Tipton Shale Member of the Green River Formation: Eocene Lake Gosiute: Sedimentology, v. 54, p. 661–699.

Le Turdu, C., Coussement, C., Tiercelin, J.-J., Renaut, R.W., Rolet, J., Richert, J.-P., Xavier, J.-P., and Coquelet, D., 1995, Rift basin structure and depositional patterns interpreted using a 3D remote sensing approach: The Baringo and Bogoria basins, central Kenya Rift, East Africa: Centres de Recherches Exploration-Production Elf Aquitaine, Bulletin, v. 19, p. 1–37.

Le Turdu, C., Tiercelin, J.-J., Richert, J.-P., Rolet, J., Xavier, J.-P., Renaut, R.W., Lezzar, K.E., and Coussement, C., 1999, Influence of preexisting oblique discontinuities on the geometry and evolution of extensional fault patterns: Evidence from the Kenya Rift using SPOT Imagery, *in* Morley, C.K. (ed.), Geoscience of Rift Systems–Evolution of East Africa: AAPG Studies in Geology, no. 44, p. 173–191.

Li, C.X., Ivanov, V., Fan, D.D., Korotaev, V., Yang, S.Y., Chalov, R., and Liu, S.G., 2004, Development of the Volga Delta in response to Caspian sea-level fluctuation during last 100 years: Journal of Coastal Research, v. 20, p. 401–414.

Liu, S., and Nummedal, D., 2004, Late Cretaceous subsidence in Wyoming; quantifying the dynamic component: Geology, v. 32, p. 397–400.

Lockley, M., 2007, A tale of two ichnologies: the different goals and potentials of invertebrate and vertebrate (tetrapod) ichnotaxonomy and how they relate to ichnofacies analysis: Ichnos, v. 14, p. 39–57.

Lockley, M.G., Lucas, S.G., and Hunt, A.P., 1994, Vertebrate tracks and the ichnofacies concept: implications for paleoecology and palichnostratigraphy, *in* Donovan, S. (ed.), The Paleobiology of Trace Fossils. New York: Wiley and Sons, p. 241–268.

Lockley, M.G., Ritts, B.D., and Leonardi, G., 1999, Mammal track assemblages from the Early Tertiary of China, Peru, Europe and North America: Palaios, v. 14, p. 398–404.

Love, J.D., and Christiansen, A.C., compilers, 1985, Geological map of Wyoming: U.S. Geological Survey, 3 sheets, scale 1:500,000.

Lövei, G., and Sunderland, K.D., 1996, Ecology and behavior of ground beetles (Coleoptera: Carabidae): Annual Reviews, v. 41, p. 231–256.

Lowenstein, T.K., and Demicco, R.V., 2006, Elevated Eocene atmospheric $CO_2$ and its subsequent decline: Science, v. 313, p. 1928.

Lynds, R., Campbell-Stone, E., Becker, T.P., and Frost, C.D., 2010, Stratigraphic evaluation of reservoir and seal in a natural $CO_2$ field: Lower Paleozoic, Moxa Arch, southwest Wyoming: Rocky Mountain Geology, v. 45, p. 113–132.

MacGinitie, H.D., 1969, The Eocene Green River flora of northwestern Colorado and northeastern Utah: University of California Publications in the Geological Sciences, v. 83, 203 p.

Maitland, D.P., and Maitland, A., 1994, Significance of burrow-opening diameter as a flood-prevention mechanism for air-filled burrows of small intertidal arthropods: Marine Biology, v. 119, p. 221–225.

Markwick, P.J., 1994, “Equability,” continentality, and Tertiary “climate”: the crocodilian perspective: Geology, v. 22, p. 613–616.
Marshak, S., Karlstrom, K., and Timmons, J.M., 2000, Inversion of Proterozoic extensional faults: an explanation for the pattern of Laramide and Ancestral Rockies intracratonic deformation, United States: Geology, v. 28, p. 735–738.
Martin, A.J., 2009, Neoichnology of an Arctic fluvial point bar, North Slope, Alaska (USA): Geological Quarterly, v. 53, p. 383–396.
Martin, A.J., Vazques-Prokopec, G.M., and Page, M., 2010, First known feeding trace of the Eocene bottom-dwelling fish *Notogoneus osculus* and its paleontological significance: Plos One, v. 5, p. 1–8.
Marty, D., Strasser, A., and Meyer, C.A., 2008, Formation and taphonomy of human footprints in microbial mats of present-day tidal flat environments: implications for the study of fossil footprints: Ichnos, v. 16, p. 127–142.
Matagi, S.V., 2004, A biodiversity assessment of the flamingo lakes of eastern Africa: Biodiversity, v. 5, p. 13–26.
Matzke, D., and Klass, K.-D., 2005, Reproductive biology and nymphal development in the basal earwig *Tagalina papua* (Insecta: Dermaptera: Pygidicranidae), with a comparison of brood care in Dermaptera and Embioptera: Entomologische Abhandlungen, v. 62, p. 99–116.
Maughan, E.K., and Perry, W.J. Jr., 1986, Lineaments and their tectonic implications in the Rocky Mountains and adjacent plains region, *in* Peterson, J.A. (ed.), Paleotectonics and Sedimentation in the Rocky Mountain Region, Unites States: AAPG Memoir 41, p. 41–53.
Mawdsley, J.R., 2009, Taxonomy, ecology, and phylogeny of species of *Lophyra* Motschulsky 1859, subgenus *Eriolophyra* Rivalier 1948 (Coleoptera: Cicindelidae): Tropical Zoology, v. 22, p. 57–70.
Mawdsley, J.R., and Sithole, H., 2009, Dry season ecology of riverine tiger beetles in Kruger National Park, South Africa: African Journal of Ecology, v. 46, p. 126–131.
Mawdsley, J.R., and Sithole, H., 2007, Natural history of the African riverine tiger beetle *Chaetodera regalis* (Dejean) (Coleoptera: Cicindelidae): Journal of Natural History, v. 43, p. 1891–1908.
Mayry, M.S., 2007, Geochemistry and sedimentology of spring mounds: Eocene Green River Formation. Unpublished MSc. thesis: Loma Linda University, California.
Mayry, M.S., and Buchheim, H.-P., 2004, Spring mounds within the Tipton and Wilkins Peak Members of the Eocene Green River Formation: geochemical and sedimentological influences on Lake Gosiute: Abstracts with Programs, Geological Society of America, v. 36, p. 288.
Mayry, M.S., and Buchheim, H.-P., 2005, Geochemical and sedimentological records of lacustrine-spring interactions: a large spring mound of the Eocene Green River Formation: Abstracts with Programs, Geological Society of America, v. 37, p. 372–373.
McBrearty, S., 1999, The archaeology of the Kapthurin Formation, *in* Andrews, P., and Banham, P. (eds.), Late Cenozoic Environments and Hominid Evolution: A Tribute to Bill Bishop. London: Geological Society, p. 143–156.
McCall, G.J.H., 1967, Geology of the Nakuru-Thomson’s Falls-Lake Hannington area: Geological Survey of Kenya, Report, no. 78.
McCall, P.L., and Tevesz, M.J.S. (Eds.), 1982, Animal-Sediment Relations: The Biogenic Alteration of Sediments: Topics in Geobiology, v. 2. New York and London: Academic Press, 336 p.
McGrew, P.O., 1980, An Eocene flamingo nesting area, Sweetwater County, Wyoming: National Geographic Society Research Reports, v. 12, p. 473–478.
McGrew, P.O., and Feduccia, A., 1973, A preliminary report on a nesting colony of Eocene birds: Wyoming Geological Association Guidebook, Twenty-Fifth Field Conference, p. 163–164.
McGrew, P.O., and Feduccia, A., 1980, Relationships and evolution of flamingos (Aves: Phoenicopteridae): Smithsonian Contributions to Zoology, v. 316, 73 p.
McIlroy, D., 2008, Ichnological analysis: the common ground between ichnofacies workers and ichnofabric analysts: Palaeogeography, Palaeoclimatology, Palaeoecology, v. 270, p. 332–338.
McLachlan, A.J., Cantrell, M.A., 1976, Sediment development and its influence on the distribution and tube structure of *Chironomus plumosus* L. (Chironomidae, Diptera) in a new impoundment: Freshwater Biology, v. 6, p. 437–443.

Mederos, S., Tikoff, B., and Bankey, V., 2005, Geometry, timing, and continuity of the Rock Springs uplift, Wyoming, and Douglas Creek arch, Colorado: implications for uplift mechanisms in the Rocky Mountain foreland, U.S.A.: Rocky Mountain Geology, v. 40, p. 167–191.
Melchor, R.N., 2004, Trace fossil distribution in lacustrine deltas: examples from the Triassic rift lakes of the Ischigualasto–Villa Unión basin, Argentina, *in* McIlroy, D. (ed.), The Application of Ichnology to Palaeoenvironmental and Stratigraphic Analysis: Geological Society, London, Special Publications, v. 228, p. 335–354.
Melchor, R.N., Bedatou, E., De Valais, S., and Genise, J.F., 2006, Lithofacies distribution of invertebrate and vertebrate trace-fossil assemblages in an Early Mesozoic ephemeral fluvio-lacustrine system from Argentina: implications for the Scoyenia ichnofacies: Palaeogeography, Palaeoclimatology, Palaeoecology, v. 239, p. 253–285.
Melchor, R., N., Genise, J.F., Farina, J.L., Sánchez, M.V., Sarzetti, L., and Visconti, G., 2010, Large striated burrows from fluvial deposits of the Neogene Vinchina Formation, La Rioja, Argentina: a crab origin suggested by neoichnology and sedimentology: Palaeogeography, Palaeoclimatology, Palaeoecology, v. 291, p. 400–418.
Metz, R., 1987, Sinusoidal trail formed by a recent biting midge (Family Ceratopogonidae): trace fossil implications: Journal of Paleontology, v. 61, p. 312–314.
Metz, R., 1990, Tunnels formed by mole crickets (Orthoptera: Gryllotalpidae): paleoecological implications: Ichnos, v. 1, p. 139–141.
Metz, R., 1996, Newark basin ichnology: the Late Triassic Perkasie Member of the Passaic Formation, Sanatoga, Pennsylvania; Northeastern Geology and Environmental Sciences, v. 18, p. 118–129.
Metz, R., 2000, Triassic trace fossils from lacustrine shoreline deposits of the Passaic Formation, Douglasville, Pennsylvania: Ichnos, v. 7, p. 253–266.
M'Gonigle, J.W., and J.H. Dover. 1992, Geologic map of the Kemmerer 30' x 60' Quadrangle, Lincoln and Sweetwater Counties, Wyoming. Reston, VA: U.S. Geological Survey.
Michener, C.D., 1964, Evolution of the nests of bees: American Zoologist, v. 4, p. 227–239.
Michener, C.D., 1974, The Social Behavior of the Bees. Cambridge, Massachusetts: The Belknap Press of Harvard University Press, 404 p.
Mihlbachler, M.C., Lucas, S.G., Emry, R.J., and Bayshashov, B., 2004, A new brontothere (Brontotheriidae, Perissodactyla, Mammalia) from the Eocene of the Ily Basin of Kazakstan and a phylogony of Asian "horned" brontotheres: American Museum Novitates, no. 3439, 43 p.
Mikhodyuk, O.S., Gerasimenko, L.M., Akimov, V.N., Ivanovsky, R.N., and Zavarzin, G.A., 2008, Ecophysiology and polymorphism of the unicellular extremely natronophilic cyanobacterium *Euhalothece* sp. Z-M001 from Lake Magadi: Microbiology, v. 77, p. 717–725.
Miller, M.F., and Smail, S.E., 1997, A semiquantitative field method for evaluating bioturbation on bedding planes: Palaios, v. 12, p. 391–396.
Minter, N.J., Krainer, K., Lucas, S.G., Braddy, S.J., and Hunt, A.P., 2007, Palaeoecology of an Early Permian playa lake trace fossil assemblage from Castle Peak, Texas, USA: Palaeogeography, Palaeoclimatology, Palaeoecology, v. 246, p. 390–423.
Mitchell, R., 1974, The evolution of thermophily in hot springs: Quarterly Review of Biology, v. 49, p. 229–242.
Morley, C.K., 1999, Influence of preexisting fabrics on rift structure, *in* Morley, C.K. (ed.), Geoscience of Rift Systems–Evolution of East Africa: AAPG Studies in Geology, no. 44, p. 151–160.
Morley, C.K., Ngenoh, D.K., and Ego, J.K., 1999, Introduction to the East African Rift System, *in* Morley, C.K. (ed.), Geoscience of Rift Systems–Evolution of East Africa: AAPG Studies in Geology, no. 44, p. 1–18.
Morrill, C., and Koch, P.L., 2002, Elevation or alteration? Evaluation of isotopic constraints on paleoaltitudes surrounding the Eocene Green River Basin: Geology, v. 30, p. 151–154.
Moussa, M.T., 1968, Fossil tracks from the Green River Formation (Eocene) near Soldier Summit, Utah: Journal of Paleontology, v. 42, p. 1433–1438.
Moussa, M.T., 1970, Nematode fossil trails from the Green River Formation (Eocene) in the Uinta Basin, Utah: Journal of Paleontology, v. 44, p. 304–307.
Mustoe, G.E., 2002, Eocene bird, reptile and mammal tracks from the Chuckanut Formation, northwest Washingon: Palaios, v. 17, p. 403–413.

Mwatha, W.E., and Grant, W.D., 1993, *Natronobacterium vacuolata* sp. nov., a haloakaliphilic archaeon isolated from Lake Magadi, Kenya: International Journal of Systematic Bacteriology, v. 43, p. 401–403.
Ndetei, R., and Muhandiki, V.S., 2005, Mortalities of lesser flamingos in Kenyan Rift Valley saline lakes and the implications for sustainable management of the lakes: Lakes and Reservoirs: Research and Management, v. 10, p. 51–58.
Netto, R., 2007, *Skolithos*-dominated piperock in nonmarine environments: an example from the Triassic Caturrita Formation, southern Brazil, *in* Bromley, R.G. et al. (eds.): SEPM Special Publication, no. 88, p. 109–121.
Netto, R.G., and Grangeiro, M.E., 2009, Neoichnology of the seaward side of Peixe Lagoon in Mostardas, southernmost Brazil: the *Psilonichnus* ichnocoenosis revisited: Revista Brasileria de Paleontologia, v. 12, p. 211–224.
Netto, R.G., Balistieri, P.R.M.N., Lavina, E.L.C., and Silveira, D.M., 2009, Ichnological signatures of shallow freshwater lakes in the glacial Itararé Group (Mafra Formation, Upper Carboniferous–Lower Permian of Paraná Basin, S Brazil): Palaeogeography, Palaeoclimatology, Palaeoecology, v. 272, p. 240–255.
Noffke, N., Gerdes, G., Klenke, T., and Krumbein, W., 2001, Microbially induced sedimentary structures–a new category within the classification of primary sedimentary structures: Sedimentary Geology, v. 71, p. 649–656.
Noirot, C., 1970, The nests of termites, *in* Krishna, K., and Weesner, F.M. (eds.), Biology of Termites. New York and London: Academic Press, p. 73–125.
Norris, R.D., Jones, L.S., Corfield, R.M., and Cartlidge, J.E., 1996, Skiing in the Eocene Uinta Mountains? Isotopic evidence in the Green River Formation for snow melt and large mountains: Geology, v. 24, p. 403–406.
North-Lewis, M., 1998, A Guide to Lake Baringo and Lake Bogoria. Nairobi: Horizon Books, 161 p.
Oduor, S.O., and Schagerl, M., 2007, Phytoplankton primary productivity characteristics in response to photosynthetically active radiation in three Kenyan Rift Valley saline–alkaline lakes: Journal of Plankton Research, v. 29, p. 1041–1050.
Ogilvie, M., and Ogilvie, C., 1986, Flamingos. Gloucester, England: Alan Sutton Publishing Limited, 121 p.
Ólafsson, J.S., and Paterson, D.M., 2004, Alteration of biogenic structure and physical properties by tube-building chironomid larvae in cohesive sediments: Aquatic Ecology, v. 38, p. 219-229.
Oliver, D.R., 1971, Life history of the Chironomidae: Annual Reviews, v. 16, p. 211–230.
Olson, S. L., and Feduccia, A., 1980, *Presbyornis* and the origin of the Anseriformes (Aves: Charadriomorphae): Smithsonian Contributions to Zoology, v. 323, p. 1–24.
Olson, S.L., and Matsuoka, H., 2005, New specimens of the early Eocene frigatebird *Limnofregata* (Pelicaniformes: Fregatidae), with the description of a new species: Zootaxa, v. 1046, p. 1–15.
Onkaware, A.O., 2000, Effect of soil salinity on plant distribution and production at Loburu Delta, Lake Bogoria National Reserve, Kenya: Austral Ecology, v. 25, p. 140–149.
Osmond, J.C., 2000, West Willow Creek Field: first productive lacustrine stromatolite mound in the Eocene Green River Formation, Uinta Basin, Utah: The Mountain Geologist, v. 37, p. 157–170.
Overeem, I., Kroonenberg, S.B., Veldkamp, A., Groenesteijn, K., Rusakov, G.V., Svitoch, A.A., 2003, Small-scale stratigraphy in a large ramp delta: recent and Holocene sedimentation in the Volga Delta: Sedimentary Geology, v. 159, p. 133–157.
Owen, R.A., Owen, R.B., Renaut, R.W., Scott, J.J., Jones, B., and Ashley, G.M., 2008, Mineralogy and origin of rhizoliths on the margins of saline, alkaline Lake Bogoria, Kenya Rift Valley: Sedimentary Geology, v. 203, p. 143–163.
Owen, R.B., and Renaut, R.W., 2000, Miocene and Pliocene diatomaceous lacustrine sediments of the Tugen Hills, Baringo District, central Kenya Rift, *in* Gierlowski-Kordesch, E., and Kelts, K. (eds.), Lake Basins Through Space and Time: American Association of Petroleum Geologists, Memoir, no. 46, p. 465–472.
Owen, R.B., Renaut, and Jones, B., 2008, Geothermal diatoms: a comparative study of floras in hot spring systems of Iceland, New Zealand, and Kenya: Hydrobiologia, v. 610, p. 175–192.
Owen, R.B., Renaut, R.W., Hover, V.C., Ashley, G.M., and Muasya, A.M., 2004, Swamps, springs, and diatoms: wetlands of the semi-arid Bogoria-Baringo Rift, Kenya: Hydrobiologia, v. 518, p. 59–78.
Park, L.E., and Gierlowski-Kordesch, E.H., 2007, Paleozoic lake faunas: establishing aquatic life on land: Palaeogeography, Palaeoclimatology, Palaeoecology, v. 249, p. 160–179.

Pazos, P.J., 2002, Palaeoenvironmental framework of the glacial-postglacial transition (late Paleozoic) in the Paganzo-Calingasta Basin (southern South America) and the Great Karoo-Kalahari Basin (southern Africa): ichnological implications: Gondwana Research, v. 5, p. 619–640.
Pearson, D.L., 1988, Biology of tiger beetles: Annual Reviews, v. 33, p. 123–147.
Pearson, D.L., and Knisley, C.B., 1985, Evidence for food as a limiting resource in the life cycle of tiger beetles (Coleoptera: Cicindelidae): Oikos, v. 45, p. 161–168.
Pearson, P.N., van Dongen, B.E., Nicholas, C.J., Pancost, R.D., Schouten, S., Singano, J.M., and Wade, B.S., 2007, Stable warm tropical climate through the Eocene Epoch: Geology, v. 35, p. 211–214.
Pemberton, S.G., and Frey, R.W., 1982, Trace fossil nomenclature and the *Planolites–Palaeophycus* debate: Journal of Paleontology, v. 56, p. 843–881.
Pemberton, S.G., Spila, M.V., Pulham, A.J., Saunders, T., Maceachern, J.A., Robbins, D., and Sinclair, I., 2001, Ichnology and Sedimentology of Shallow and Marginal Marine Systems: Ben Nevis and Avalon Reservoirs, Jeanne D'Arc Basin: Geological Association of Canada, St. John's, Newfoundland, Short Course Notes, no. 15.
Pflüger, F., and Gresse, P.G., 1996, Microbial sand chips–a non-actualistic sedimentary structure: Sedimentary Geology, v. 102, p. 263-274.
Pickerill, R.K., 1992, Carboniferous nonmarine invertebrate ichnocoenoses from southern New Brunswick, eastern Canada: Ichnos, v. 2, p. 21–35.
Pietras, J.T., and Carroll, A.R., 2006, High-resolution stratigraphy of an underfilled lake basin: Wilkins Peak Member, Eocene Green River Formation, Wyoming, U.S.A.: Journal of Sedimentary Research, v. 76, p. 1197–1214.
Pietras, J.T., Carroll, A.R., and Rhodes, M.K., 2003, Lake basin response to tectonic drainage diversion: Eocene Green River Formation, Wyoming: Journal of Paleolimnology, v. 30, p. 115–125.
Pineda, P.M., and Kondratieff, B.C., 2003, Natural history of the Colorado Great Sand Dunes tiger beetle, *Cicindela theatina* Rotger: Transactions of the American Entomological Society, v. 129, p. 333–360.
Popham, E.J., 2000, The geographical distribution of the Dermaptera (Insecta) with reference to continental drift: Journal of Natural History, v. 34, p. 2007–2027.
Porada, H., and Bouougri, E., 2007, "Wrinkle structures" – a critical review, *in* Schieber, J., Bose, P.K., Eriksson, P.G., Sarkar, S., Altermann, W., and Catuneanu, O., (eds.), Atlas of Microbial Mat Features Preserved within the Clastic Rock Record. Amsterdam: Elsevier, p. 135–144.
Prowe, S.G., and Antranikian, G., 2001, *Anaerobranca gottschalkii* sp. nov., a novel thermoalkaliphilic bacterium that grows anaerobically at high pH and temperature: International Journal of Systematic and Evolutionary Microbiology, v. 51, p. 457–465.
Radl, R.C., and Linsenmair, K.E., 1991, Maternal behaviour and nest recognition in the subsocial earwig *Labidura riparia* Pallas (Dermaptera: Labiduridae): Ethology, v. 89, p. 287–296.
Rankin, S.M., Storm, S.K., Pieto, D.L., and Risser, A.L., 1996, Maternal behavior and clutch manipulation in the ring-legged earwig (Dermaptera: Carcinophoridae): Journal of Insect Behavior, v. 9, p. 85–103.
Ratcliffe, B.C., and Fagerstrom, J.A., 1980, Invertebrate lebenspuren of Holocene floodplain: their morphology, origin, and paleoecological significance: Journal of Paleontology, v. 54, p. 614–630.
Reite, O.B., 1974, pH, salinity and temperature tolerance of Lake Magadi *Tilapia*: Nature, v. 247, p. 315.
Renaut, R.W., 1982, Late Quaternary Geology of the Lake Bogoria Fault-trough, Kenya Rift Valley: Unpublished Ph.D. thesis, University of London.
Renaut, R.W., 1993, Zeolitic diagenesis of late Quaternary fluviolacustrine sediments and associated calcrete formation in the Lake Bogoria Basin, Kenya Rift Valley: Sedimentology, v. 40, p. 271–301.
Renaut, R.W., and Owen, R.B., 1988, Opaline cherts associated with sublacustrine hydrothermal springs at Lake Bogoria, Kenya Rift Valley: Geology, v. 16, p. 699–702.
Renaut, R.W., and Owen, R.B., 1991, Shore-zone sedimentation and facies in a closed rift lake: the Holocene beach deposits of Lake Bogoria, Kenya, *in* Anadón, P., Cabrera, L., and Kelts, K. (eds.), Lacustrine Facies Analysis: Special Publication of the International Association of Sedimentologists, no. 13, p. 175–195.
Renaut, R.W., and Tiercelin, J.-J., 1994, Lake Bogoria, Kenya Rift Valley–a sedimentological overview, *in* Renaut, R.W., and Last, W.M., Sedimentology and Geochemistry of Modern and Ancient Saline Lakes: SEPM Special Publication, no. 50, p. 101–123.

Renaut, R.W., and Jones, B., 1997, Controls on aragonite and calcite precipitation in hot spring travertines at Chemurkeu, Lake Bogoria, Kenya: Canadian Journal of Earth Sciences, v. 34, p. 801–818.
Renaut, R.W., and Gierlowski, Kordesch, B., in press, Lakes, *in* James, N. and Dalrymple, R. (eds.), Facies Models, 4th Edition. Toronto: Geological Association of Canada.
Renaut, R.W., Tiercelin, J.-J., and Owen, R.B., 1986, Mineral precipitation and diagenesis in the sediments of the Lake Bogoria basin, Kenya Rift Valley, *in* Frostick, L.E., Renaut, R.W., Reid, I, and Tiercelin, J.-J. (eds.), Sedimentation in the African Rifts: Geological Society Special Publication, no. 25, p. 159–175.
Renaut, R.W., Jones, B., and Tiercelin, J.-J., 1998, Rapid *in situ* silicification of microbes at Loburu hot springs, Lake Bogoria, Kenya Rift Valley: Sedimentology, v. 45, p. 1083–1103.
Renaut, R.W., Tiercelin, J.-J., and Owen, R.B., 2000a, Lake Baringo, Kenya Rift Valley, and its Pleistocene precursors, *in* Gierlowski-Kordesch, E.H., and Kelts, K.R. (eds.), Lake Basins through Space and Time: AAPG Studies in Geology, v. 46, p. 561–568.
Renaut, R.W., Morley, C.K., and Jones, B., 2002a, Fossil hot-spring travertine in the Turkana Basin, northern Kenya: structure, facies, and genesis, *in* Renaut, R.W., and Ashley, G.M. (eds.), Sedimentation in Continental Rifts: SEPM Special Publication, no. 73, p. 123–141.
Renaut, R.W., Owen, R.B., and Ego, J., 2008, Recent changes in geyser activity at Loburu, Lake Bogoria, Kenya Rift Valley: GOSA Transactions, v. 10, p. 4–14.
Renaut, R.W., De Wet, C., Gierlowski-Kordesch, E.H., and Jones, B., 2000b, Recognition and impact of hydrothermal springs in continental rift sedimentation: Geological Society of America, Northeastern Section, 35th Annual Meeting, Abstracts, v. 32, p. 69.
Renaut, R.W., Jones, B., Tiercelin, J.-J., and Tarits, C., 2002b, Sublacustrine precipitation of hydrothermal silica in rift lakes: evidence from Lake Baringo, central Kenya Rift Valley: Sedimentary Geology, v. 148, p. 235–257.
Renaut, R., Owen, R., Scott, J., and Jones, B., 2007, Nasikie Engida: a perennial saline, alkaline lake fed by hot-springs in the Magadi Basin, Kenya Rift Valley: 4th International Limnogeology Congress, Barcelona, Spain, Abstracts, p. 55–56.
Renaut, R.W., Ego, J., Tiercelin, J.-J., Le Turdu, C., and Owen, R.B., 1999, Saline, alkaline paleolakes of the Tugen Hills-Kerio Valley region, Kenya Rift Valley, *in* Andrews, P., and Banham, P. (eds.), Late Cenozoic Environments and Hominid Evolution: A Tribute to Bill Bishop. London: Geological Society, p. 41–58.
Retallack, G.J., and Feakes, C.R., 1987, Trace fossil evidence for Late Ordovician animals on land: Science, v. 235, p. 61–63.
Rhodes, M.K., Carroll, A.R., Pietras, J.T., Beard, B.L., and Johnson, C.M., 2002, Strontium isotope record of paleohydrology and continental weathering, Eocene Green River Formation, Wyoming: Geology, v. 30, p. 167–170.
Richards, L.J., 1983, Feeding and activity patterns of an intertidal beetle: Journal of Experimental Marine Biology and Ecology, v. 73, p. 213–224.
Rodríguez-Aranda, J.P., and Calvo, J.P., 1998, Trace fossils and rhizoliths as a tool for sedimentological and palaeoenvironmental analysis of ancient continental evaporite successions: Palaeogeography, Palaeoclimatology, Palaeoecology, v. 140, p. 383–399.
Roehler, H.W., 1988, Geology of the Cottonwood Creek Delta in the Eocene Tipton Tongue of the Green River Formation, southeast Washakie basin, Wyoming: U.S. Geological Survey Bulletin, 1669-A, 14 p.
Roehler, H.W., 1992a, Introduction to greater Green River basin geology, physiography, and history of investigations: U.S. Geological Survey Professional Paper, 1506A, 14 p.
Roehler, H.W., 1992b, Correlation, composition, areal distribution, and thickness of Eocene stratigraphic units, Greater Green River Basin, Wyoming, Utah, and Colorado: U.S. Geological Survey Professional Paper, 1506E, 49 p.
Roehler, H.W., 1993, Eocene climates, depositional environments, and geography, greater Green River basin, Wyoming, Utah, and Colorado: U.S. Geological Survey Professional Paper, 1506F, 74 p.
Rooijakkers, E.F., and Sommeijer, M.J., 2009, Gender specific brood cells in the solitary bee *Colletes halophilus* (Hymenoptera; Colletidae): Journal of Insect Behavior, v. 22, p. 492–500.
Rothschild, L.J., and Mancinelli, R.L., 2001, Life in extreme environments: Nature, v. 409, p. 1092–1101.

Royse, F. Jr., 1993, An overview of the geologic structure of the thrust belt in Wyoming, northern Utah, and eastern Idaho, *in* Snoke, A. W., Steidtmann, J. R., and Roberts, S. M. (eds.), Geology of Wyoming: Laramie, Wyoming, The Geological Survey of Wyoming Memoir No. 5, p. 273–311.
Rybczynski, D., Dehler, C.M., Link, P.K., and Fanning, M., 2008, A mid-Neoproterozoic Western Interior Seaway; a 766Ma transgression recorded at the Utah-Colorado border, U.S.A.: Abstracts with Programs, Geological Society of America, v. 40, p. 59.
Sands, W.A., 1987, Ichnocoenoses of probable termite origin from Laetoli, *in* Leakey, D.M., Harris, J.M. (eds.), Laetoli: a Pliocene Site in Northern Tanzania. Oxford: Oxford University Press, p. 409–433.
Sarjeant, W.A.S., and Langston, W., Jr., 1994, Vertebrate footprints and invertebrate traces from the Chadronian (late Eocene) of Trans Pecos, Texas: Texas Memorial Museum Bulletin, v. 36, p. 1–86.
Sarjeant, W.A.S., and Wilson, J.A., 1988, Late Eocene (Duchesnean) mammalian footprints from the Skyline Channels of Trans-Pecos, Texas: Texas Journal of Science, v. 40, p. 439–446.
Sarjeant, W.A.S., Reynolds, R.E., and Kissel-Jones, M.M., 2002, Fossil creodont and carnivore footprints from California, Nevada and Wyoming, *in* Reynolds, R.E. (ed.), Between the Basins: Exploring the Western Mojave and Southern Basin and Range Province. Fullerton: California State University, Desert Studies Consortium, p. 37–50.
Satoh, A., and Hori, M., 2005, Microhabitat segregation in larvae of six species of coastal tiger beetles in Japan: Ecological Research, v. 20, p. 143–149.
Satoh, A., Momoshita, H., and Hori, M., 2006, Circatidal rhythmic behaviour in the coastal tiger beetle *Callytron inspecularis* in Japan: Biological Rhythm Research, v. 37, p. 147–155.
Sauphanor, B., and Sureau, F., 1993, Aggregation behaviour and interspecific relationships in Dermaptera: Oecologia, v. 96, p. 360–364.
Schlirf, M., and Uchman, A., 2005, Revision of the ichnogenus *Sabellarifex* Richter, 1921 and its relationship to *Skolithos* Haldeman, 1840 and *Polykladichnus* Fürsich, 1981: Journal of Systematic Palaeontology, v. 3, p. 115–131.
Schlüter, T.G., and Kohring, R.R., 1992, Trace fossils from a saline-alkaline paleoenvironment in northern Tanzania: Berliner Geowissenschaft Abhandlungen, v. 3, p. 295–303.
Schlüter, T.G., and Kohring, R.R., 2002, Palaeopathological fish bones from phosphorites of the Lake Manyara area, northern Tanzania – fossil evidence of a physiological response to survival in an extreme biocenosis: Environmental Geochemistry and Health, v. 24, p. 131–140.
Schomacker, E.R., Kjemperud, A.V., Nystuen, J.P., and Jahren, J.S., 2010, Recognition and significance of sharp-based mouth-bar deposits in the Eocene Green River Formation, Uinta Basin, Utah: Sedimentology, v. 57, p. 1069–1087.
Schowalter, T.D., 2006, Insect Ecology: an Ecosystem Approach. Amsterdam, Boston; Elsevier/Academic Press, 572 p.
Schultz, T.D., 1989, Habitat preferences and seasonal abundances of eight sympatric species of tiger beetle, genus *Cicindela* (Coleoptera: Cicindelidae), in Bastrop State Park, Texas: The Southwestern Naturalist, v. 34, p. 468–477.
Schultz, T.D., and Hadley, N.F., 1987, Microhabitat segregation and physiological differences in co-occuring tiger beetle species, *Cicindela oregona* and *Cicindela tranquebarica*: Oecologia, v. 73, p. 363–370.
Schumm, S.A., 1993, River response to baselevel change: implications for sequence stratigraphy: The Journal of Geology, v. 101, p. 279–294.
Scott, D.J., and Cushman, R.A., 2002, Comparison of plant macro-and microfossil assemblages from the middle Eocene Bitter Creek delta, Wyoming: Abstracts with Programs, Geological Society of America, v. 34, p. 556.
Scott, J.J., 2003, Diagenesis and the paleoecological analysis of a late Pleistocene footprint site in the Baringo-Bogoria Basin, Kenya Rift Valley: Journal of Vertebrate Paleontology, v. 23, p. 95A.
Scott, J.J., 2005, Taphonomy of Modern and Ancient Vertebrate Traces in the Marginal Sediments of Saline, Alkaline and Freshwater Lakes, Baringo-Bogoria Basin, Kenya Rift Valley: Unpublished MSc. thesis, University of Saskatchewan.
Scott, J.J., Renaut, R.W., and Owen, R.B., 2003, Sedimentary structures and surfaces created by flamingos at Lake Bogoria, Kenya Rift Valley: Third International Limnogeology Congress, Tucson, AZ, Abstracts, p. 254.

Scott, J.J., Renaut, R.W., and Owen, R.B., 2008, Preservation and paleoenvironmental significance of a footprinted surface on the Sandai Plain, Lake Bogoria, Kenya Rift Valley: Ichnos, v. 15, p. 208–231.
Scott, J.J., Renaut, R.W., and Owen, R.B., 2010, Taphonomic controls on animal tracks at saline, alkaline Lake Bogoria, Kenya Rift Valley: Impact of salt efflorescence and clay mineralogy: Journal of Sedimentary Research, v. 80, p. 639–665.
Scott, J.J., Renaut, R.W., Owen, R.B., and Sarjeant, W.A.S., 2007, Biogenic activity, trace formation, and trace taphonomy in the marginal sediments of saline, alkaline Lake Bogoria, Kenya Rift Valley, *in* Bromley, R.G. et al. (eds.): SEPM Special Publication, no. 88, p. 311–332.
Scott, J.J., Renaut, R.W., Buatois, L.A., and Owen, R.B., 2009, Biogenic structures in exhumed surfaces around saline lakes: An example from Lake Bogoria, Kenya Rift Valley: Palaeogeography, Palaeoclimatology, Palaeoecology, v. 272, p. 176–198.
Seilacher, A., 1964, Biogenic sedimentary structures, *in* Imbrie, J., and Newell, N.D. (eds.), Approaches to Paleoecology. New York: John Wiley, p. 296–316.
Seilacher, A., 1967, Bathymetry of trace fossils: Marine Geology, v. 5, p. 413–428.
Sewall, J.O., and Sloan, L.C., 2006, Come a little bit closer: a high-resolution climate study of the early Paleogene Laramide foreland: Geology, v. 34, p. 81–84.
Silvey, J.K.G., 1936, An investigation of the burrowing inner-beach insects of some fresh-water lakes: Papers of the Michigan Academy of Science, Arts and Letters, v. 21, p. 655–696.
Simpson, G.B., 1991, Effects of soil type and moisture on development and reproduction of *Nala lividipes* (Dufour) (Dermaptera: Labiduridae): Journal of the Australian Entomology Society, v. 30, p. 281–287.
Simpson, G.B., 1993, Effects of temperature on the development, longevity and fecundity of *Nala lividipes* (Dufour) (Dermaptera: Labiduridae): Journal of the Australian Entomology Society, v. 32, p. 265–272.
Simpson, K.W., 1979, Evolution of life histories in Ephydrini, *in* Deonier, D.L. (ed.), First Symposium on the Systematics and Ecology of Ephydridae (Diptera): The North American Benthological Society, p. 99–109.
Sims, P.K., Finn, C.A., and Rystrom, V.L., 2001, Preliminary Precambrian basement map showing geologic-geophysical domains, Wyoming: U.S. Geological Survey, Open-File Report 01-199, 9 p.
Sitters, J., Heitkönig, I.M.A., Holmgren, M., and Ojwang, G.S.O., 2009, Herded cattle and wild grazers partition water but share forage resources during dry years in East African savannas: Biological Conservation, v. 142, p. 738–750.
Smith, B.J., and McAllister, J.J., 1986, Observations on the occurrence and origins of salt weathering phenomena near Lake Magadi, southern Kenya: Zeitschrift für Geomorphologie, v. 30, p. 445–460.
Smith, J.J., Hasiotis, S.T., Woody, D.T., and Kraus, M.J., 2008, *Naktodemasis bowni*: new ichnogenus and ichnospecies for adhesive meniscate burrows (AMB), and paleoenvironmental implications, Paleogene Willwood Formation, Bighorn Basin, Wyoming: Journal of Paleontology, v. 82, p. 267–278.
Smith, M.E., 2007, Stratigraphy, geochronology, and paleogeography of the Green River Formation, Wyoming, Colorado, and Utah: Unpublished Ph.D. thesis, University of Wisconsin–Madison.
Smith, M.E., Singer, B., and Carroll, A.R., 2003, $^{40}Ar/^{39}Ar$ geochronology of the Eocene Green River Formation, Wyoming: Geological Society of America Bulletin, v. 115, p. 549–565.
Smith, M.E., Carroll, A.R., and Mueller, E.R., 2008a, Elevated weathering rates in the Rocky Mountains during the Early Eocene Climatic Optimum: Nature Geoscience, v. 1, p. 370–374.
Smith, M.E., Carroll, A.R., and Singer, B.S., 2008b, Synoptic reconstruction of a major ancient lake system: Eocene Green River Formation, western United States: Geological Society of America Bulletin, v. 120, p. 54–84.
Smith, M.E., Scott, J.J., and Carroll, A.R., 2009, Weathering, springs, and the origin of Na-evaporites in the early Eocene Green River Formation, Wyoming: Geological Society of America, Abstracts, v. 41, p. 512.
Smith, M.E., Chamberlain, K.R., Singer, B.S., and Carroll, A.R., 2010, Eocene clocks agree: coeval $^{40}Ar/^{39}Ar$, U-Pb, and astronomical ages from the Green River Formation: Geology, v. 38, p. 527–530.
Smith, N.D., and Hein, F.J., 1971, Biogenic reworking of fluvial sediments by staphylinid beetles: Journal of Sedimentary Petrology, v. 41, p. 598–602.
Smith, R.M.H., 1993, Sedimentology and ichnology of floodplain paleosurfaces in the Beaufort Group (Late Permian), Karroo Sequence, South Africa: Palaios, v. 8, p. 339–357.
Smith, R.M.H., and Mason, T.R., 1998, Sedimentary environments and trace fossils of Tertiary oasis deposits in the central Namib desert, Namibia: Palaios, v. 13, p. 547–559.

Smith, R.M.H., Mason, T.R., and Ward, J.D., 1993, Flash-flood sediments and ichnofacies of the Late Pleistocene Homeb Silts, Kuiseb River, Namibia: Sedimentary Geology, v. 85, p. 579–599.

Smoot, J.P., 1978, Origin of the carbonate sediments in the Wilkins Peak Member, Green River formation (Eocene), Wyoming, U.S.A., *in* Matter, A., and Tucker, M.E. (eds.), Modern and Ancient Lake Sediments: Special Publication of the International Association of Sedimentologists, no. 2, p. 109–127.

Smoot, J.P., 1983, Depositional subenvironments in an arid closed basin: the Wilkins Peak Member of the Green River Formation (Eocene), Wyoming, U.S.A.: Sedimentology, v. 30, p. 801–827.

Smoot, J.P., and Castens-Seidell, B., 1994, Sedimentary features produced by efflorescent salt crusts, Saline Valley and Death Valley, California, *in* Renaut, R.W., and Last, W.M. (eds.), Sedimentology and Geochemistry of Modern and Ancient Saline Lakes: SEPM, Special Publication 50, p. 73–90.

Spangler, P.J., and Steiner, W.E., 2003, A new species of water scavenger beetle, Coelostoma (s. str.) tina (Coleoptera: Hydrophilidae: Sphaeridiinae), from Kenya, eastern Africa: Proceedings of the Entomological Society of Washington, v. 105, p. 1–8.

Stal, L.J., 1995, Physiological ecology of cyanobacteria in microbial mats and other communities: New Phytology, v. 131, p. 1–32.

Stal, L.J., Van Gemerden, H., and Krumbein, W.E., 1985, Structure and development of a benthic marine microbial mat: FEMS Microbiology Ecology, v. 31, p. 111–125.

Stanley, K.O., and Fagerstrom, J.A., 1974, Miocene invertebrate trace fossils from a braided river environment, western Nebraska, U.S.A: Palaeogeography, Palaeoclimatology, Palaeoecology, v. 15, p. 63–82.

Steidtman, J.R., and Middleton, L.T., 1991, Fault chronology and uplift history of the southern Wind River Range, Wyoming: implications for Laramide and post-Laramide deformation in the Rocky Mountain foreland: Geological Society of America Bulletin, v. 103, p. 472–485.

Stewart, D.R.M., and Stewart, J., 1963, The distribution of some large mammals in Kenya: Journal of the East Africa Natural History Society and Coryndon Museum, v. 24, no. 3 (107), 52 p.

Stidham, T.A., 2004, Turtle graveyard: a new diverse bird fauna from the early Eocene Wasatch Formation, Wyoming: Abstracts with Programs, Geological Society of America, v. 36, p. 366.

Stidham, T.A., 2005, Birds (Aves) across the Paleocene-Eocene boundary: evidence from Wyoming: Abstracts with Programs, Geological Society of America, v. 37, p.414-415.

Stolz, J.F., 2000, Structure of microbial mats and biofilms, *in* Riding, R.E., and Awramik, (eds.), Microbial Sediments. Berlin: Springer-Verlag, p. 1–8.

Styrski, J.D., and Van Rhein, S., 1999, Forceps size does not determine fighting success in European earwigs: Journal of Insect Behavior, v. 12, p. 475–482.

Surdam, R.C., and Parker, R.D., 1972, Authigenic aluminosilicate minerals in the tuffaceous rocks of the Green River Formation, Wyoming: Geological Society of America Bulletin, v. 83, p. 689–700.

Surdam, R.C., and Eugster, H.P., 1976, Mineral reactions in the sedimentary deposits of the Lake Magadi region, Kenya: Geological Society of America Bulletin, v. 87, p. 1739–1752.

Surdam, R.C., and Stanley, K.O., 1979, Lacustrine sedimentation during the culminating phase of Eocene Lake Gosiute, Wyoming (Green River Formation): Geological Society of America Bulletin, v. 90, p. 93–110.

Surdam, R.C., Eugster, H.P., and Mariner, R.H., 1972, Magadi-type chert in Jurassic and Eocene to Pleistocene rocks, Wyoming: Geological Society of America Bulletin, v. 83, p. 2261–2266.

Svetlitshnyi, V., Rainey, F., and Wiegel, J., 1996, *Thermosyntropha lipolytica* gen. nov., sp. nov., a lipolytic, anaerobic, alkalitolerant, thermophilic bacterium utilizing short- and long-chain fatty acids in syntrophic coculture with a methanogenic archaeum: International Journal of Systematic Bacteriology, v. 46, p. 1131–1137.

Takeuchi, Y., and Hori, M., 2007, Spatial density-dependent survival and development at different larval stages of the tiger beetle *Cicindela japonica* (Thunberg): Population Ecology, v. 49, p. 305–316.

Thornwaite, C.W., 1948, An approach toward a rational classification of climate: Geographical Review, v. 38, p. 55–94.

Tiercelin, J.J., 1981, Rifts continentaux, tectonique, climats, sédiments. Exemples: la sédimentation dans le Nord du Rift Gregory, Kenya, et dans le rift de l'Afar, Ethiopie, depuis le Miocène: Unpublished Ph.D. thesis, Université Aix-Marseille II.

Tiercelin, J.-J., 1990, Rift-basin sedimentation: responses to climate, tectonism and volcanism. Examples of the East African Rift: Journal of African Earth Sciences, v. 10, p. 283–305.
Tiercelin, J.-J., Renaut, R.W., Delibrias, G., Le Fournier, J., and Bieda, S., 1981, Late Pleistocene and Holocene lake level fluctuations in the Lake Bogoria basin, northern Kenya Rift Valley: Palaeoecology of Africa and the Surrounding Islands, v. 13, p. 105–120.
Tiercelin, J.-J., Vincens, A., Barton, C.E., Carbonel, P., Casanova, J., Delibrias, G., Gasse, F., Grosdidier, E., Herbin, J.-P., Huc, A.Y., Jardiné, S., Le Fournier, J., Mélières, F., Owen, R.B., Pagé, P., Palacios, C., Paquet, H., Péniguel, G., Peypouquet, J.-P., Raynaud, J.-F., Renaut, R.W., Renéville, P., Richert, J.-P., Riff, R., Robert, P., Seyve, C., Vandenbrouke, M., and Vidal, G., 1987, Le demi-grabin de Baringo-Bogoria, Rift Gregory, Kenya: 30 000 years of hydrological and sedimentary history: Bulletin de Centres Reserches Exploration-Production Elf Aquitaine, v. 11, p. 249–540.
Tindall, B.J., 1988, Prokaryotic life in the alkaline, saline athalassic environment, *in* Rodriguez-Valera, F. (ed.), Halophilic Bacteria. USA: CRC Press, p. 31–67.
Tindall, B.J., Mills, A.A., and Grant, W.D., 1980, An alkalophilic red halophilic bacterium with a low magnesium requirement from a Kenyan soda lake: Journal of General Microbiology, v. 116, p. 257–260.
Topp, W., and Ring, R.A., 1988, Adaptations of Coleoptera to the marine environment. I. Observations on rove beetles (Staphylinidae) from sandy beaches: Canadian Journal of Zoology, v. 66, p. 2464–2468.
Triantaphyllidis, G.V., Abatzopoulos, T.J., and Sorgeloos, P., 1998, Review of the biogeography of the genus *Artermia* (Crustacea, Anostraca): Journal of Biogeography, v. 25, p. 213–226.
Tryon, C.A., 2006, "Early" Middle Stone Age lithic technology of the Kapthurin Formation (Kenya): Current Anthropology, v. 47, p. 367–375.
Tryon, C.A., and McBrearty, S., 2002, Tephrostratigraphy and the Acheulian to Middle Stone Age transition in the Kapthurin Formation, Kenya: of Human Evolution, v. 42, p. 211–235.
Tryon, C.A., And McBrearty, S., 2006, Tephrostratigraphy of the Bedded Tuff Member (Kapthurin Formation, Kenya) and the nature of archaeological change in the later middle Pleistocene: Quaternary Research, v. 65, p. 492–507.
Tucker, M.E., and Wright, V.P., 1990, Carbonate Sedimentology. Oxford: Blackwell Scientific Publications, 482 p.
Uchman, A., and Álvaro, J.J., 2000, Non-marine invertebrate trace fossils from the Tertiary Calatayud-Teruel Basin, NE Spain: Revista Española de Paleontología, v. 15, p. 203–218.
Uchman, A., Kazakauskas, V., and Gaigalas, A., 2009, Trace fossils from Late Pleistocene varved lacustrine sediments in eastern Lithuania: Palaeogeography, Palaeoclimatology, Palaeoecology, v. 272, p. 199–211.
Uchman, A., Nemec, W., Ilgar, A., and Messina, C., 2007, Lacustrine trace fossils and environmental conditions in the early Miocene Ermenek Basin, southern Turkey: Annales Societatis Geologorum Poloniae, v. 77, p. 123–139.
Vareschi, E., 1978, The ecology of Lake Nakuru (Kenya). I. Abundance and feeding of the Lesser flamingo: Oecologia, v. 32, p. 11–35.
Vincens, A., Casanova, J., and Tiercelin, J.-J., 1986, Palaeolimnology of Lake Bogoria (Kenya) during the 4500 BP high lacustrine phase, *in* Frostick, L.E., Renaut, R.W., Reid, I, and Tiercelin, J.-J. (eds.), Sedimentation in the African Rifts: Geological Society Special Publication, no. 25, p. 323–330.
Voigt, S., and Hoppe, D., 2010, Mass occurrence of penetrative trace fossils in Triassic lake deposits (Krygyzstan, Central Asia): Ichnos, v. 17, p. 1–11.
Walker, K.A., and Fell, R.D., 2001, Courtship roles of male and female European earwigs, *Forficula auricularia* L. (Dermaptera: Forficulidae), and sexual use of forceps: Journal of Insect Behavior, v. 14, p. 1–17.
Ward, D.M., Ferris, M.J., Nold, S.C., and Bateson, M.M., 1998, A natural view of microbial biodiversity within hot spring cyanobacterial mat communities: Microbiology and Molecular Biology Reviews, v. 62, p. 1353–1370.
Werner, K., 1993, Die sandlaufäfer Kenias: Lambillionea, v. 93, p. 51–76.
Wescott, W.A., Morley, C.K., and Karanja, F.M., 1996, Tectonic controls on the development of rift-basin lakes and their sedimentary character: examples from the East African Rift System, *in* Johnson, T.C., and Odada, E.O. (eds.), The Limnology, Climatology and Paleoclimatology of the East African Lakes. Australia: Gordon and Breach Publishers, p. 3–21.

West, M.J., and Alexander, R.D., 1963, Sub-social behavior in a burrowing cricket *Anurogryllus muticus* (De Geer): Ohio Journal of Science, v. 63, p. 19–24.
Wetzel, A., 2008, Recent bioturbation in the deep South China sea: a uniformitarian ichnologic approach: Palaios, v. 23, p. 601–615.
Whaler, K.A., 2006, Magnetotelluric fieldwork adventures in Africa: Astronomy and Geophysics, v. 47, p. 28-37.
Wickstrom, C.E., and Castenholz, R.W., 1985, Dynamics of cyanobacterial and ostracod interactions in an Oregon hot spring: Ecology, v. 66, p. 1024–1041.
Wiegman, R.W., 1964, Late Cretaceous and early Tertiary stratigraphy of the Little Mountain area, Sweetwater County, Wyoming. Upublished MSc. thesis: University of Wyoming, Laramie.
Wiegman, R.W., 1965, Spring deposits: surface expressions of the Henry's Fork fault, Sweetwater County, Wyoming, *in* Sedimentation of Late Cretaceous and Tertiary outcrops, Rock Springs uplift: Wyoming Geological Association, 19th Field Conference Guidebook.
Wiegert, R.G., and Fraleigh, P.C., 1972, Ecology of Yellowstone thermal effluent systems: net primary production and species diversity of a successional blue-green algal mat: Limnology and Oceanography, v. 17, p. 215–228.
Wiegert, R.G., and Mitchell, R., 1973, Ecology of Yellowstone thermal effluent systems: intersects of blue-green algae, grazing flies (*Paracoenia*, Ephydridae) and water mites (*Partnuniella*, Hydrachnellae): Hydrobiologia, v. 41, p. 251–271.
Wiig, S.V., Grundy, W.D., and Dyni, J.R., 1995, Trona resources in the Green River basin, southwest Wyoming: USGS Open-File Report 95-476, 88 p.
Wilf, P., 2000, Late Paleocene–early Eocene climate changes in southwestern Wyoming: paleobotanical analysis: Geological Society of America Bulletin, v. 112, p. 292–307.
Williams, W.D., 1998, Salinity as a determinant of the structure of biological communities in salt lakes: Hydrobiologia, v. 381, p. 191–201.
Williams, W.D., Boulton, A.J., and Taaffe, R.G., 1990, Salinity as a determinant of salt lake fauna: a question of scale: Hydrobiologia, v. 197, p. 257–266.
Willis, H.L., 1967, Bionomics and zoogeography of tiger beetles of saline habitats in the central United States (Coleoptera: Cicindelidae): University of Kansas Science Bulletin, v. 47, p. 145–313.
Wilson, M.V.H., 1978, Paleogene insect faunas of western North America: Quaestiones Entomologicae, v. 14, p. 13–34.
Wing, S.L., 1987, Eocene and Oligocene floras and vegetation of the Rocky Mountains: Annals of the Missouri Botanical Gardens, v. 74, p. 748–784.
Wing, S.L., and Greenwood, D.R., 1993, Fossils and fossil climate: the case for equable continental interiors in the Eocene: Philosophical Transactions of the Royal Society of London, B, v. 341, p. 243–252.
Wirth, W.W., and Mathis, W.N., 1979, A review of the Ephydridae (Diptera) living in thermal springs, *in* Deonier, D.L. (ed.), First Symposium on the Systematics and Ecology of Ephydridae (Diptera): The North American Benthological Society, p. 21–45.
Withjack, M.O., Schlische, R.W., and Olsen, P.E., 2002, Rift-basin structure and its influence on sedimentary systems, *in* Renaut, R.W., and Ashley, G.M. (eds.), Sedimentation in Continental Rifts: SEPM Special Publication, no. 73, p. 57–81.
Wolanski, E., and Gereta, E., 2001, Water quantity and quality as the factors driving the Serengeti ecosystem, Tanzania: Hydrobiologia, v. 458, p. 169–180.
Wolfe, J.A., Forest, C.E., and Molnar, P., 1998, Paleobotanical evidence of Eocene and Oligocene paleoaltitudes in midlatitude western North America: Geological Society of America Bulletin, v. 110, p. 664–678.
Wong, M.H., and Chan, T.D., 1977, The ecology of the marine rove beetle, Bryothinusa spp. (Coleoptera; Staphylinidae) in Hong Kong: Hydrobiologia, v. 53, p. 253–256.
Wood, C.M., Wilson, P., Bergman, H.L., Bergman, A.N., Laurent, P., Otiang' A-Owiti, G., and Walsh, P.J., 2002, Obligatory urea production and the cost of living in the Magadi tilapia revealed by acclimation to reduced salinity and alkalinity: Physiological and Biochemical Zoology, v. 75, p. 111–122.
Wyatt, T.D., 1986, How a subsocial intertidal beetle, *Bledius spectabilis*, prevents flooding and anoxia in its burrow: Behavioral Ecology and Sociobiology, v. 19, p. 323–331.

Wyatt, T.D., and Foster, W.A., 1988, Distribution and abundance of the intertidal saltmarsh beetle, *Bledius spectabilis*: Ecological Entomology, v. 13, p. 453–464.
Wyatt, T.D., and Foster, W.A., 1989, Parental care in the subsocial intertidal beetle, Bledius spectabilis, in relation to parasitism by the ichneumonid wasp, Barycnemis blediator: Behaviour, v. 110, p. 76–92.
Yan-Bin, S., Gallego, O.F., Buchheim, H.P., Biaggi, R.E., 2006, Eocene conchostracans from the Laney Member of the Green River Formation, Wyoming, USA: Journal of Paleontology, v. 80, p. 447–454.
Yang, S.-Y., Lockley, M.G., Greben, R., Erickson, B.R., and Lim, S.-K., 1995, Flamingo and duck-like bird tracks from the Late Cretaceous and Early Tertiary: evidence and implications: Ichnos, v. 4, p. 21–34.
Yonkee, A., and Weil, A.B., 2010, Reconstructing the kinematic evolution of curved mountain belts: internal strain patterns in the Wyoming salient, Sevier thrust belt, U.S.A.; Geological Society of America Bulletin, v. 122, p. 24–49.
Young, J.A.T., and Renaut, R.W., 1979, A radiocarbon date from Lake Bogoria, Kenya Rift Valley: Nature, v. 278, p. 243–245.
Yuretich, R.F., and Ervin, C.R., 2002, Clay minerals as paleoenvironmental indicators in two large lakes of the African Rift Valleys: Lake Malawi and Lake Turkana, *in* Renaut, R.W., and Ashley, G.M. (eds.), Sedimentation in Continental Rifts: SEPM Special Publication, no. 73, p. 221–232.
Zachos, J., Pagani, M., Sloan, L., Thomas, E., and Billups, K., 2001, Trends, rhythms, and aberrations in global climate 65 Ma to present: Science, v. 292, p. 685–693.
Zachos, J.C., Dickens, G.R., and Zeebe, R.E., 2008, An early Cenozoic perspective on greenhouse warming and carbon-cycle dynamics: Nature, v. 451, p. 279–283.
Zerm, M., and Adis, J., 2001, Spatio-temporal distribution of larval and adult tiger beetles (Coleoptera: Cicindelidae) from open areas in central Amazonian floodplains (Brazil): Studies on Neotropical Fauna and Environment, v. 36, p. 185–198.
Zerm, M., and Adis, J., 2003, Exceptional anoxia resistance in larval tiger beetle, *Phaeoxantha klugii* (Coleoptera: Cicindelidae): Physiological Entomology, v. 28, p. 150–153.
Zerm, M., Adis, J., and Krumme, U., 2004, Circulatory responses to submersion in larvae of *Phaeoxantha klugii* (Coleoptera: Cicindelidae) from central Amazonian floodplains: Studies on Neotropical Fauna and Environment, v. 39, p. 91–94.
Zhang, G., Buatois, L.A., Mángano, M.G., and Aceñolaza, F.G., 1998, Sedimentary facies and environmental ichnology of a ?Permian playa-lake complex in western Argentina: Paleogeography, Paleoclimatology, Paleoecology, v. 138, p. 221–243.
Zhilina, T.N., Zavarzin, G.A., Detkova, E.N., and Rainey, F.A., 1996, *Natrionella acetigena* gen. nov. sp. nov., and extremely haloalkaliphilic, homoacetic bacterium: a new member of *Haloanaerobiales*: Current Microbiology, v. 32, p. 320–326.
Zhilina, T.N., Garnova, E.S., Tourova, T.P., Kostrikina, N.A., and Zavarzin, G.A., 2001, *Amphibacillus fermentum* sp. nov. and *Amphibacillus tropicus* sp. nov., new alkaliphilic, faculatively anaerobic, sacchorolytic bacilli from Lake Magadi: Microbiology, v. 70, p. 711–722.
Zhilina, T.N., Zavarzin, G.A., Rainey, F.A., Pikuta, E.N., Osipov, G.A., and Kostrikina, N.A., 1997, *Desulfonatronovibrio hydrogenovorans* gen. nov., sp. nov., an alkaliphilic sulfate-reducing bacterium: International Journal of Systematic Bacteriology, v. 47, p. 144–149.
Zonneveld, J.-P., Gunnell, G.F., and Bartels, W.S., 2000a, Early Eocene fossil vertebrates from the southwestern Green River basin, Lincoln and Uinta counties, Wyoming: Journal of Vertebrate Paleontology, v. 20, p. 369–386.
Zonneveld, J.-P., Lavigne, J.M., and Bartels, W.S., 2000b, Ichnology of an early Eocene meandering fluvial system, Wasatch Formation, Fossil Butte National Monument, Wyoming: Abstracts with Programs, Geological Society of America, v. 32, p. 309.
Zonneveld, J.-P., Lavigne, J.M., Bartels, W.S., and Gunnell, G.F., 2006, *Lunulichnus tuberosus Ichnogen. and Ichnosp. Nov.* from the early Eocene Wasatch Formation, Fossil Butte National Monument, Wyoming: an arthropod-constructed trace fossil associated with alluvial firmgrounds: Ichnos, v. 13, p. 87–94.


**Appendix A.** A legend for the sedimentary features shown in the stratigraphic sections.

**Appendix B.** Microbial taxa known from modern Lakes Bogoria, Magadi, and Nasikie Engida, as well as the Pleistocene Green Beds and High Magadi Beds in the Magadi basin. Note: n.i. = no information provided in reference. References cited in this table are included below.

| Taxa | Type | Description | Preservation; habitat and nutrition | Localities | Reference |
|---|---|---|---|---|---|
| ***LAKE BOGORIA*** | | | | | |
| **Cyanobacteria — Primary producers** | | | | | |
| ***Calothrix*** sp. | filamentous<br>**colour:** forms brownish and brown-green mats | filaments may be sheathed and densely packed; sheaths have external diameter of 15–20 µm and walls < 2 µm thick; (genus known to have heterocysts) | modern; benthic; forms brownish and brownish-green, locally leathery, mats in cooler water (< 40° C); typically form mats with densely packed sheathed trichomes the develop on microtopographic highs | Hot springs, Loburu Delta, Lake Bogoria | Tiercelin et al., 1987; Stal, 1995; Renaut et al., 1998 |
| ***Synechococcus*** cf. *lividus* | coccoid<br>**colour:** green | non-heterocystous | modern; benthic; *Synechococcus* spp. mats are found in very hot waters (> 60° C), commonly with *Phormidium* | Hot springs, Loburu Delta, Lake Bogoria | Tiercelin et al., 1987; Stal, 1995; Renaut et al., 1998 |
| ***Synechococcus*** spp. | coccoid | n.i. | modern; benthic | Loburu Delta, Lake Bogoria | Ballot et al., 2004 |
| ***Synechococcus*** *bigranulatus* | coccoid<br>**colour:** pale to deep blue-green | cells solitary, rod-shaped, straight or slightly curved, 3c long, 1.3–2.4 µm wide; rounded poles; no mucilaginous sheath; non-heterocystous | modern; benthic; genus is common at hot springs worldwide; especially typical at temperatures from 20–75° C; at Bogoria found in mats in waters > 60° C; genus known to fix $N_2$ anaerobically by avoiding oxygen | Microbial mats at hot springs, Loburu Delta; collected in 2001 | Stal, 1995; Renaut et al., 1998; Krienitz et al., 2003 |
| ***Synechocystis*** sp. | coccoid | n.i. | modern; benthic | Loburu Delta, Lake Bogoria | Ballot et al., 2004 |
| ***Spirulina*** *subsalsa* | filamentous<br>**colour:** bright blue-green | filaments solitary; filaments 1.2–1.4 µm in diameter; regularly spiraled; spiral width 3.5–4.5 µm; with or without mucilage envelope | modern; benthic; common at hot springs; have wide ecological distribution; occurs in hot springs and in brackish and marine habitats | Microbial mats at hot springs, Loburu Delta; collected in 2001 | Krienitz et al., 2003 |
| ***Spirulina*** *subtilissima* | filamentous | n.i. | modern; benthic | Loburu Delta, Lake Bogoria | Ballot et al., 2004 |
| ***Oscillatoria*** *willei* | filamentous<br>**colour:** grey-green | filaments solitary, 2–2.5 µm in diameter; may be > 150 µm long; straight with rounded ends; cylindrical cells 2.5–6 µm long | modern; benthic; infrequent occurrence; common at hot springs | Microbial mats at hot springs, Loburu Delta; collected in 2001 | Krienitz et al., 2003 |
| ***Phormidium*** (*Oscillatoria*) *terebriformis* | filamentous<br>**colour:** brown-green | filaments solitary, often very closely attached to each other; 4.5–6 µm in diameter; may be > 100 µm long; slightly undulated; sometimes covered with a sheath; cells nearly cylindrical | modern; benthic; common at hot springs; cosmopolitan member of thermal and sulfur springs | Microbial mats at hot springs, Loburu Delta; collected in 2001 | Krienitz et al., 2003 |
| ***Phormidium*** *incrustratum* | filamentous | filaments in crust are 2–2.5 µm in diameter and grouped into erect bundles; other examples are criss-crossed filaments 4.5–6 µm | Holocene; preserved in microbial laminae in lacustrine stromatolitic encrustations | Lake Bogoria shorelines | Vincens et al., 1986 |

| | | | | | |
|---|---|---|---|---|---|
| ***Arthrospira** fusiformis* | filamentous<br>**colour:** green | helical | modern; lacustrine | Lake water, Lake Bogoria | Tiercelin et al., 1987 |
| ***Microcystis** aeruginosa* | filamentous | n.i. | modern; lacustrine | Lake waters, Lake Bogoria | Dadheech et al., 2009 |
| ***Microcystis** flos-aquae* | filamentous | n.i. | modern; lacustrine | Lake Bogoria | Ndetei and Muhundiki, 2005 |
| ***Anaebaena*** spp. | n.i. | n.i. | modern; lacustrine | Lake Bogoria | Ndetei and Muhundiki, 2005 |
| ***Sphaeroeca*** sp. | n.i. | Note: taxonomic status of genus unknown | modern; lacustrine | Lake waters, Lake Bogoria | Tiercelin et al., 1987 |
| ***Cryptomonas*** sp. | n.i. | Note: taxonomic status of genus unknown | modern; lacustrine | Lake waters, Lake Bogoria | Tiercelin et al., 1987 |
| ***Gomphosphaeria** aponina* | coccoid | Note: taxonomic status of genus unknown | modern; lacustrine | Lake waters, Lake Bogoria | Tiercelin et al., 1987 |
| ***Anabaenopsis** arnoldii* | filamentous | n.i. | modern; lacustrine | Lake waters, Lake Bogoria | Tiercelin et al., 1987 |
| ***Pseudanabaena** catenata* | filamentous | n.i. | modern | Loburu Delta, Lake Bogoria | Tiercelin et al., 1987 |
| ***Pseudanabaena** lonchoides* | filamentous | n.i. | modern | Loburu Delta, Lake Bogoria | Tiercelin et al., 1987 |
| **Note:** Hindák (2001) identified 19 types of cyanobacteria from Lake Bogoria. | | | | | |
| | | | | | |
| **Bacteria — Aerobic Heterotrophs/Organotrophs (use carbohydrates and oxygen, produce sulfide and CO2)** | | | | | |
| ***Chloroflexus*** sp. | aerobic and anaerobic<br>**colour:** orange to dull green in low light, anaerobic conditions | filamentous | modern; thermophilic; alkalitolerant; mat-forming near hot springs; shown from west shore of Lake Bogoria at pH: 9.0 and T: 68° C; chemoheterotroph in aerobic conditions in light or dark; photoheterotroph in anaerobic conditions in light | Hot springs, Lake Bogoria | Grant and Tindall, 1986 |
| ***Bacillus** bogoriensis* (strain LBB3$^T$ of Vargas et al., 2005) | obligate aerobic; gram-positive<br>**colour:** cream–yellow | cells non-motile; spore-forming; cells 0.3–0.4 µm wide by 2.0–3.5 µm long; cells occur singly, in pairs, or in clumps; colonies circular, convex, smooth, opaque cream-yellow | modern; alkaliphilic, halotolerant, heterotrophic; does not reduce nitrate to nitrite<br>**pH:** opt. pH: 10 (range: 8–11)<br>**T:** opt. T: 37° C (range: 10–40° C)<br>**Na:** [Na] tolerance: < 2 M NaCl | Lake water, Lake Bogoria | Vargas et al., 2005 |
| cf. ***Bacillus*** spp. (cf. *B. halodurans*, *B. alcalophilus*, *B. licheniformis*, *B. flavothermus*) (strains LBB2, LBB3, LBC2, LBD1, and LBD3 of Vargas et al., 2004) | obligate aerobic; gram-positive<br>**colour:** white, cream, and yellow | bacilli-shaped cells; cells 0.3–0.8 µm x 0.3–2.8 µm; colonies with rhizoid/filamentous margins | modern; mainly alkalitolerant; halotolerant; lipolytic; heterotrophic<br>**pH:** range: 7–10<br>**T:** opt. T: 37–55° C (range: 25–55° C)<br>**Na:** [Na] tolerance: < 2.5 – < 10% w/v NaCl | Lake water and soil, Lake Bogoria | Vargas et al., 2004 |
| cf. ***Bacillus*** sp. cf. *clarkii* (strain 9B1 of Duckworth et al., 1996) | aerobic; gram-positive | n.i. | modern; alkaliphilic; collected from littoral mud/water with pH: 10.5, T: 36° C, and conductivity: 45 mS cm$^{-1}$ | Lake Bogoria | Duckworth et al., 1996 |

| | | | | | |
|---|---|---|---|---|---|
| cf. ***Bacillus*** sp. cf. *pseudofirmus* (strains 64B and 66B of Duckworth et al., 1996) | aerobic; gram-positive | n.i. | modern; alkaliphilic; collected from a salt crust | Salt crust, Lake Bogoria | Duckworth et al., 1996 |
| cf. ***Pseudomonas*** spp. (e.g., *P. chloritidismutans*) (strains LBA5, LBA14, LBA17, LBA18, LBA19, LBA22, LBA34, LBA36, and LBA38 of Vargas et al., 2004) | aerobic; gram-negative **colour:** white, cream | bacilli- and coccoid-shaped cells; cells 0.3–3.0 µm; colonies with rhizoid/filamentous margins | modern; alkalitolerant; halotolerant; ipolytic; heterotrophic **pH:** range: 7–10 **T:** opt. T: 37–45° C (range: 25–45° C) **Na:** [Na] tolerance: < 2.5 – < 10% w/v NaCl | Lake water and soil, Lake Bogoria | Vargas et al., 2004 |
| cf. ***Halomonas*** *desiderata* (strain LBB1 of Vargas et al., 2004) | aerobic; gram-negative **colour:** white | bacilli-shaped cells; cells 0.3–1.7µm; colonies with rhizoid/filamentous margins | modern; alkalitolerant; halotolerant; lipolytic; heterotrophic **pH:** range: 7–10 **T:** opt. T: 37° C (range: 25–45° C) **Na:** [Na] tolerance: < 2.5 – < 10% w/v NaCl | Lake water and soil, Lake Bogoria | Vargas et al., 2004 |
| ***Bacillus*** *halodurans* | aerobic; gram-positive | rod-shaped; motile; had terminal spores | modern; obligate akaliphilic and halotolerant; heterotrophic on starch; produce extracellular amylases active at pH 10 and 55° C **pH:** opt. pH ~9–10 **T:** opt. T: 55–65° C (range: ~40–75° C) **Na:** [Na] tolerance: < 10% w/v NaCl | Hot springs, Lake Bogoria; collected from hot spring water | Hashim et al., 2004 |
| ***Bacillus*** cf. *flavothermus* (now ***Anoxybacillus*** *flavithermus*) (strain LB3A of Sunna et al., 1997) | aerobic to facultative anaerobic; gram-positive **colour:** yellow | rod-shaped cells; 1.2–1.7 µm long, 0.3–0.5 µm wide; ellipsoidal spore shape | modern; thermophilic; alkalitolerant; heterotrophic; degrades xylanase **pH:** opt. pH: 7 (range: 6–8) **T:** opt. T: 45–62° C (range: 40–70° C) | Sediments, Lake Bogoria | Sunna et al., 1997 |
| ***Bacillus*** *pumilus* | n.i. | n.i. | modern; thermophilic; akaliphilic; gamma-glutamyltranspeptidase enzyme **pH:** opt. pH: 8.9 **T:** opt. T: 62° C | Hot springs, Lake Bogoria | Moallic et al., 2006 |
| ***Paracoccus*** *bogoriensis* | aerobic; gram-negative **colour:** red | motile; has polar flagellum; gram-negative; secretes xanthophylls carotenoid pigments | modern; obligate alkaliphilic; non-methylotrophic | Hot springs, Lake Bogoria; collected from outflow of hot spring | Osanjo et al., 2009 |
| cf. ***Halomonas*** *halodenitrificans* (several strains from Duckworth et al., 1996, 2000: 8B1, 25B1, WB5, WB2, WB4) | faculatively anaerobic; gram-negative **colour:** opaque cream-beige | non-spore forming motile rods 4.0–6.0 µm long x 0.6–0.8 µm wide; colonies are circular, 2–3 mm diameter; low, convex, opaque cream-coloured | modern; alkaliphilic; organotrophic; reduces nitrate and nitrite; no $H_2S$ production **pH:** pH: 9–10 (range: 8.0–11.0) **T:** opt. T: 37° C (range: 20–55° C) **Na:** [Na] tolerance: 0–20% NaCl w/v (opt. [Na]: 0–7%) | Littoral mud, Lake Bogoria; collected from littoral mud/water with pH: 10.5, T: 36° C, and conductivity: 45 mS $cm^{-1}$ | Duckworth et al., 1996, 2000 |
| cf. ***Halomonas*** *pacifica* (strain 65B4 of Duckworth et al., 2000) | obligately aerobic; gram-negative **colour:** opaque cream-beige | non-spore forming motile rods 4.0–6.0 µm long x 0.6–0.8 µm wide; colonies are circular, 2–3 mm diameter; low, convex, opaque cream-coloured | modern; alkaliphilic; organotrophic; reduces nitrate and nitrite; no $H_2S$ production **pH:** pH: 9–10 (range: 8.0–11.0) **T:** opt. T: 37° C (range: 20–50° C) **Na:** [Na] tolerance: 0–20% NaCl w/v (opt. [Na]: 0–7%) | Mud on shoreline, Lake Bogoria | Duckworth et al., 2000 |

| | | | | | |
|---|---|---|---|---|---|
| ***Halomonas*** *magadiensis* (*H. magadii*) (strain 24B1 of Duckworth et al., 1996, 2000) | obligately aerobic; gram-negative<br>**colour:** colonies are opaque cream-beige | non-spore forming motile rods 4.0–6.0 µm long x 0.6–0.8 µm wide; colonies are circular, 2–3 mm diameter; low, convex, opaque cream-coloured | modern; alkaliphilic; organotrophic; reduces nitrate and produces $H_2S$<br>**pH:** opt. pH: 9.5 (range: 7.0–11.0)<br>**T:** opt. T: 37° C (range: 20–50° C)<br>**Na:** [Na] tolerance: 0–20% NaCl w/v (opt. [Na]: 0–7%) | Littoral mud, Lake Bogoria; collected from littoral mud with pH: 10.5, T: 36° C, and conductivity: 45 mS $cm^{-1}$ | Duckworth et al., 1996, 2000 |
| ***Cellulomonas*** *bogoriensis* | aerobic to faculatively anaerobic; gram-positive<br>**colour:** colonies pale yellow to yellow | cells short, straight rods and coccoids; ~ 0.5–0.7 µm diameter; no primary branching; colonies slimy, translucent to opaque, pale yellow, circular and convex, ~2 mm diameter | modern; alkaliphilic; halotolerant; chemo-organotrophic<br>**pH:** opt. pH: 9–10 (range: 6–10.5)<br>**T:** opt. T: 30–37° C (range: 20–37° C)<br>**Na:** [Na] tolerance: 0–8% w/v | Littoral zone, Acacia Camp, Lake Bogoria, 1988; collected at pH: 10.5; T: 33° C; conductivity: 44 mS $cm^{-1}$ | Jones et al., 2005 |
| ***Bogoriella*** *caseilytica* (strain HKI 0088 of Groth et al., 1997) | aerobic to microaerophilic; gram-positive<br>**colour:** colonies are pale to intense yellow | cells are irregular and rod-shaped or coccoid and occur singly, in pairs, or in small irregular clusters; spiky structures over the whole surface of the cell; are 0.5–0.8 µm x 1.0–2.5 µm; non-motile; no endospores formed; occasional filaments < 10 µm long; colonies are round, smooth, slightly convex, 1–3 mm in diameter and pale to intense yellow | modern; alkaliphilic; halotolerant; organotrophic; produces $H_2S$<br>**pH:** opt. pH: 9–10<br>**T:** opt. T: 28–37° C<br>**Na:** [Na] tolerance: 2–18%, poor growth when [Na] > 8% | Soil, Lake Bogoria; collected near Lake Bogoria in soda soil with pH: 10 | Groth et al., 1997 |
| cf. ***Aeromonas*/*Vibrio*** (strain 10B1 of Duckworth et al., 1996) | aerobic; gram-negative | n.i. | modern; alkaliphilic; collected from littoral mud/water with pH: 10.5, T: 36° C, and conductivity: 45 mS $cm^{-1}$ | Littoral mud, Lake Bogoria | Duckworth et al., 1996 |
| cf. ***Arthrobacter*** sp.; cf. ***Terrabacter*** sp. (strains 69B4 and WB3 of Duckworth et al., 1996) | aerobic; gram-positive | n.i. | modern; alkaliphilic; collected from littoral sediment with pH: 10.5, T: 33° C, and conductivity: 44 mS $cm^{-1}$; | Littoral sediment, Lake Bogoria | Duckworth et al., 1996 |
| **Bacteria — Aerobic Sulfur Oxidizers/Chemolithotrophs (use sulfide and oxygen, produce sulfate and CO2)** | | | | | |
| ***Thioalkalivibrio*** *versutus* (strains ALJ 3, ALJ 6, ALJ 7, ALJ 15, ALJ 16, and ALJ 20 of Sorokin et al., 2001) | aerobic<br>**colour:** young colonies white with sulfur; old colonies yellow | cells vibroid to spirilla with one polar flagellum; motile; 0.4–0.6 µm wide and 0.8–3.0 µm long; cell wall usually highly rippled; produce membrane-bound yellow pigment | modern; obligately alkaliphilic; halophilic; thermotolerant; obligately autotrophic; chemolithoautotrophic; sulfur globules accumulate in the periplasmic space outside the cells<br>**pH:** opt. pH: 10.0–10.2 (range: 7.5–10.65)<br>**T:** opt. T: 40° C (range: < 47° C)<br>**Na:** [Na] tolerance: 1.2–4 M (opt. 1–2 M) | Surface sediments with water (pH 10.2–11.0; 60–66 g $L^{-1}$ TDS), Lake Bogoria | Sorokin et al., 2001 |
| ***Thioalkalivibrio*** *denitrificans* (strains ALJ 10 and ALJD$^T$ of Sorokin et al., 2001) | aerobic to faculatively anaerobic and microaerobic<br>**colour:** white to yellow; brownish if anaerobic | cells vibrio to long, thin curved rods; one polar flagellum; motile; 0.4–0.6 µm wide and 0.8–3.0 µm long; cell wall usually highly rippled; produce membrane-bound yellow pigment | modern; obligately alkaliphilic; halotolerant; thermotolerant; obligately autotrophic; chemolithoautotrophic; denitrifier; sulfur globules accumulate in the periplasmic space outside the cells<br>**pH:** opt. pH: 10.0–10.2 (range: 7.5–10.65)<br>**T:** opt. T: 40° C (range: < 47° C)<br>**Na:** [Na] tolerance: 1.2–4 M (opt. 1–2 M) | Surface sediments with water (pH 10.2–11.0; 60–66 g $L^{-1}$ TDS), Lake Bogoria | Sorokin et al., 2001 |

| | | | | | |
|---|---|---|---|---|---|
| ***Thioalkalimicrobium aerophilium*** (strain AL 19 of Sorokin et al., 2001) | obligately aerobic; gram-negative<br>**colour:** reddish pink, without sulfur | cells spirilloid; 0.4–0.6 µm wide and 0.8–1.5 µm long; have 1–3 polar flagella; cell wall undulating; form flat spreading colonies | modern; halotolerant; obligately alkaliphilic; chemolithoautotrophic; oxidizes sulfide and thiosulfate or sulfate, produces sulfate and elemental sulfur<br>**pH:** opt. pH: 9.8–10.0 (range: 7.5–10.6)<br>**T:** max. T: 41° C<br>**Na:** < 1.2–1.5 M [Na] | Sediments (pH 10.2–10.5; 65 g $L^{-1}$ TDS), Lake Bogoria | Sorokin et al., 2001 |
| **Bacteria — Anaerobic Fermenters (Heterotrophic)** | | | | | |
| ***Anaerobranca gottschalkii*** (strain LBS3$^T$ of Prowe and Antrankian, 2001) | obligate anaerobic; gram-positive with atypically thin cell wall<br>**colour:** pale-whitish | cells rod-shaped, motile, flagellated cells (sometimes with Y-type branching); almost no spore formation; cells 0.3–0.5 µm wide 3–5 µm long; occurred singly or in short chains up to four cells; sheath-like structure and surface layer-like structure; colonies lens-shaped with diameters of 3–5 mm | modern; thermophilic; alkaliphilic; halophilic; heterotrophic; grows in presence of sulfate and sulfur and produces sulfide; ferments sugars, produces ethanol<br>**pH:** opt. pH: 9.5 (range: 6.0–10.5)<br>**T:** opt. T: 50–55° C (range: 30–65° C)<br>**Na:** [Na] tolerance: 60–560 mM (opt. [Na]: 230 mM or 1% w/v) | Hot springs, Lake Bogoria; collected from shore of lake and hot spring inlet with T: 50–80° C and pH: 9–10 | Prowe and Antrankian, 2001 |
| ***Thermosyntropha lipolytica*** (strain JW/VS-265$^T$ of Svetlitshnyi et al., 1996) | obligate anaerobic; gram-positive | cells nonmotile; non-spore forming; cells straight or slightly curved rods 0.3–0.4 µm wide by 2.0–3.5 µm long; occurs in pairs or chains | modern; thermophilic; alkalitolerant; organoheterotrophic; lipolytic; utilizes long-chain fatty acids<br>**pH:** opt. pH: 8.1–8.9 (range: 7.15–9.5)<br>**T:** opt. T: 60–66° C (range: 44–73° C) | Hot springs, Lake Bogoria | Svetlitshnyi et al., 1996 |
| cf. ***Fervidobacterium nodosum;*** "*Thermopallium natronophilum*" (strains TG9A and TG7A1 of Duckworth et al., 1996)) | anaerobic | rod-shaped with typical outer sheathlike structure | modern; thermophilic; alkaliphilic; collected from hot spring sediment with pH: 8.5 and T: 96° C and conductivity: 4.8 mS $cm^{-1}$<br>**pH:** opt. pH: 9.5 (range: > 10.5)<br>**T:** opt. T: 70° C (range: < 78° C) | Hot spring sediment, Lake Bogoria | Duckworth et al., 1996; Jones et al., 1998 |
| cf. ***Clostridium*** spp. (strains B7/A, B8/A, B8/C, B8/CFT of Jones et al., 1998) | obligately anaerobic; gram-positive | n.i. | modern; halotolerant; alkaliphilic; chemoorganotrophic; use sugars and produce volatile fatty acids<br>**pH:** range of pH: 8.5– > 10.5<br>**T:**<br>**Na:** [Na] tolerance: 0–12% | Sediment, Lake Bogoria; collected from littoral zone core with pH: 11–11.5, T: 33–34° C, conductivity: 59.6–72.3 mS $cm^{-1}$ | Jones et al., 1998 |
| **Bacteria — Anaerobic Sulfur Oxidizers (Phototrophic, use light, sulfide, carbon, and CO2, produce sulfate and elemental sulfur)** | | | | | |
| ***Ectothiorhodospira vacuolata*** (a.k.a. *E. shaposhnikovii*) | phototrophic, anaerobic sulfide oxidizing phototrophic purple bacteria<br>**colour:** cells are red without presence of elemental sulfur | cells are rod-shaped and possess gas vacuoles under high sulfide concentrations and light intensity; motile, with tufts of polar flagella; cells are ~1.5 µm wide and 2–4 µm long; cells contain intracellular photosynthetic membranes as stacks; pigments are bacteriochlorophyll *a* and spirilloxanthin caronenoids | modern; obligate alkaliphilic; halophilic; phototrophic; chemolithotrophic; oxidizes sulfide and thiosulfate to produce sulfate and forms elemental sulfur, which accumulates outside the cells<br>**pH:** opt. pH: 7.5–8.5 in presence of inorganic reduced sulfur and 8.5–9.5 with organic carbon source<br>**T:** T. range: 30–39° C<br>**Na:** [Na] tolerance: 1–10% (opt. [Na]: 1–7%) | Lake Bogoria | Imhoff et al., 1981 |

| | | | | | |
|---|---|---|---|---|---|
| ***Ectothiorhodospira*** *mobilis* | anaerobic<br>**colour:** purple-red | rod-shaped cells | modern; alkaliphilic, halophilic; deposits sulfur outside the cell | Lake Bogoria | Grant and Tindall, 1986 |
| ***Rhodobaca*** *bogoriensis* (strains LBB1 and LBB2 of Milford et al., 2000) | anoxygenic; gram-negative<br>**colour:** red; anaerobic/light colonies were yellow to yellow-brown, when exposed to air converted to rose–red colour; oxic/dark colonies were pink | cells motile; ovoid to very short rods; distinct from vibrio-shaped cells of *Ectothiorhodospira*; 0.8–1.0 µm x 0.8–1.5 µm | modern; alkaliphilic; halophilic; photoheterotrophic and chemotrophic in darkness; purple non-sulfur bacteria; Na not required for growth; incapable of photoautotrophy and nitrogen fixation (unlike other purple non-sulfur bacteria)<br>**pH:** opt. pH: 9 (range: 7.5–10)<br>**T:** opt. T: 39° C (range: 30–43° C)<br>**Na:** [Na] tolerance: 0–6% (opt.: 1–3%) | Lake water, Lake Bogoria | Milford et al., 2000 |

**Bacteria — Anoxygenic Methanotrophs (use methane, produce carbon)**

Not yet isolated from Lake Bogoria/literature not known

**Bacteria — Anaerobic Methylotrophic Methanogens (use carbon, produce methane)**

Not yet isolated from Lake Bogoria/literature not known

**Bacteria — Anaerobic Sulfate Reducers (use sulfate and organic acids, produce sulfide and CO2)**

Not yet isolated from Lake Bogoria/literature not known

***LAKE MAGADI***

**Green Algae — Primary producers**

| | | | | | |
|---|---|---|---|---|---|
| unidentified green algae | n.i. | n.i. | modern; abundant in spring pools | Lake Magadi | Behr, 2002 |

**Cyanobacteria — Primary producers**

| | | | | | |
|---|---|---|---|---|---|
| ***Anabaenopsis*** *arnoldii* | filamentous | heterocytous | modern | Lake Magadi | Grant and Tindall, 1986 |
| ***Anabaenopsis*** cf. *abijatae* (strain AB2002/25 of Ballot et al., 2008) | filamentous | helical; heterocytous; trichomes straight to irregularly coiled; cells 4.0–7.2 µm long, 7.2–10.4 µm wide; heterocytes 6.4–10.4 µm; akinetes 8.8–15.2; < 19 akinetes in rows forming terminal or intercalary spherical akinetes; filaments encapsulated with mucilage and branching | modern | Lake Magadi | Ballot et al., 2008 |
| ***Euhalothece*** cf. "*natronophila*" (strain Z-M001 of Mikhodyuk et al., 2008) | coccoid<br>**colour:** intense green | unicellular; cells spherical ~2.7–4 µm in diameter; actively growing cells have little mucus, but older cultures had a pronounced pericellular mucus; cells polymorphic depending on [$NaCO_3$] and pH | modern; natronophilic; organotrophic; dependent on $NaCO_3$ for growth and not on $Cl^-$; maximum yield of culture at 180 g $L^{-1}$ of $NaCO_3$ (range: 100–230 g $L^{-1}$ of $NaCO_3$<br>**pH:** opt. pH: 8–11<br>**T:** T. range: no info<br>**Na:** [Na] tolerance: <3 M (opt. [Na]: 1.5–2.4M) | Lake Magadi; collected at the end of the rainy season, 1992 | Mikhodyuk et al., 2008 |

| | | | | | |
|---|---|---|---|---|---|
| ***Anabaenopsis* (*Cyanospira*) *rippkae*** (strain group Mag II 702) | filamentous | helical immotile trichomes 20 µm wide of ovoid or short cylindrical cells devoid of a capsule; cells 4–5 µm in diameter; cells gas-vacuolated with deep constrictions between cells; trichomes have terminal and intercalary heterocysts 8.0–8.5 µm in diameter | modern; obligate photoautotrophs capable of aerobic nitrogen fixation; has protein content (52% dry weight) higher than carbohydrates (16% dry weight)<br>**pH:** opt. pH: 9.5–10.5<br>**T:** opt. T: 25–35° C | Lake water, Lake Magadi; collected in 1981 and 1982 | Florenzano et al., 1985; Ballot et al., 2008 |
| ***Cyanospira capsulata*** (strain group Mag II 504) | filamentous | helical immotile trichomes 20 µm wide; trichomes of gas-vacuolated cells 6.8–7 µm in diameter; trichomes have terminal and intercalary heterocysts 8.0–8.5 µm in diameter; spherical cells possess a thick external capsule; constrictions between cells; produces gelatinous colonies | modern; obligate photoautotrophs capable of aerobic nitrogen fixation; has carbohydrate content (55% dry weight) higher than protein (17% dry weight)<br>**pH:** opt. pH: 9.5–10.5<br>**T:** opt. T: 25–35° C | Lake water, Lake Magadi; collected in 1981 and 1982 | Florenzano et al., 1985 |
| ***Pleurocapsa*** sp. | filamentous | n.i. | modern; non-calcified in recent lake brines and green Holocene lake muds, but calcified in the Pleistocene Green Beds | Lake brine, Lake Magadi; green Holocene lake muds | Behr, 2002 |
| **Note:** Dubinin et al., 1995 reported that more than 10 different cyanobacteria were isolated from Lake Magadi | | | | | |
| **Bacteria and Archaea — Aerobic Heterotrophs/Organotrophs (use carbohydrates and oxygen or nitrate, produce sulfide and CO2)** | | | | | |
| ***Halomonas magadii*** (a.k.a. *H. magadiensis*) (strain 21M1 of Duckworth et al., 1996, 2000) | obligately aerobic; gram-negative<br>**colour:** colonies are opaque cream-beige | non-spore forming motile rods 4.0–6.0 µm long x 0.6–0.8 µm wide; colonies are circular, 2–3 mm diameter; low, convex, opaque cream-coloured | modern; alkaliphilic; halotolerant; reduces nitrate and produces $H_2S$<br>**pH:** opt. pH: 9.5 (range: 7.0–11.0)<br>**T:** opt. T: 37° C (range: 20–50° C)<br>**Na:** [Na] tolerance: 0–20% NaCl w/v (opt. [Na]: 0–7%) | Littoral mud, Lake Magadi; collected from littoral mud with pH: 11.0, T: 36° C, and conductivity: > 100 mS $cm^{-1}$ | Duckworth et al., 1996, 2000 |
| cf. ***Halomonas halodenitrificans*** (strain 27M1 of Duckworth et al., 1996, 2000) | faculatively anaerobic; gram-negative<br>**colour:** colonies are opaque cream-beige | non-spore forming motile rods 4.0–6.0 µm long x 0.6–0.8 µm wide; colonies are circular, 2–3 mm diameter; low, convex, opaque cream-coloured | modern; alkaliphilic; reduces nitrate; no production of $H_2S$<br>**pH:** opt. pH: 9–10 (range: 8.0–11.0)<br>**T:** opt. T: 37° C (range: 20–50° C)<br>**Na:** [Na] tolerance: 0–20% NaCl w/v (opt. [Na]: 0.5–7%) | Littoral mud, Lake Magadi; collected from littoral mud with pH: 11.0, T: 36° C, and conductivity: > 100 mS $cm^{-1}$ | Duckworth et al., 1996, 2000 |
| ***Halomonas campisalis*** (strain Z-7398-2 of Boltyanskaya et al., 2004) | faculatively anaerobic; gram-negative<br>**colour:** colonies light pink | short thick rod-shaped cells 1µm x 1–3 µm; cells occur singly or in pairs; cells with pronounced adhesive properties; motile with flagella; non-spore forming; colonies transparent, light pink, iridescent, with even edges, 1–2 mm diameter | modern; faculatively anaerobic; obligately halophilic and alkaliphilic; requires $Na^+$ and $CO_3^{2+}$ for growth; denitrifying; reduces nitrate and nitrous oxide to produce $N_2$ and $NO_2^-$<br>**pH:** opt. pH: 8.8–9.5 (range: 7.5–10.4)<br>**T:** opt. T: 36–40° C (range: 10–55° C); **Na:** requires 0.16–3.1M [Na], opt. [Na]: 1.0 M [Na] | Sediment in lagoon north of causeway, Lake Magadi; collected from sediment at 30 cm depth in lagoon north of causeway in Sept. 1998, with pH: 10.5, T: 38° C, 260 g $L^{-1}$ | Boltyanskaya et al., 2004 |
| cf. ***Natronococcus*** cf. *occultus* (strain 86M4 of Duckworth et al., 1996) | aerobic<br>**colour:** colonies are pale brown | coccoid-shaped cells; cells occur singly or in pairs only; colonies uniform in size with a diameter of 1 mm | modern; halophilic; obligately alkaliphilic | Alkaline saltern, Lake Magadi; collected from an alkaline saltern with pH: 12.3, T: 56° C, and conductivity: > 100 mS $cm^-$ | McGenity and Grant, 1993; Kanai et al., 1995; Duckworth et al., 1996 |

| | | | | | |
|---|---|---|---|---|---|
| ***Natronococcus*** *amylolyticus* (strain Ah-36$^T$ of Kanai et al., 1995) | obligate aerobic<br>**colour:** colonies are orange-red | cells are non-motile cocci 1–2 µm in diameter; occur singly, in pairs, and mostly as irregular clusters; colonies circular, orange-red, and varied from 1–5 mm | modern; extremely halophilic; alkaliphilic; growth inhibited by $Mg^{2+}$; chemoorganotrophic; requires Na for growth; reduces nitrate and nitrite and hydrolyzes starch<br>**pH:** opt. pH: 9.0 (range: 8.0–10.0)<br>**T:** opt. T: 40–45° C (range: 22–50° C)<br>**Na:** [Na] tolerance: 8–30% NaCl w/v (opt. [Na]: 15–20%) | Lake Magadi | Kanai et al., 1995 |
| cf. ***Natrialba*** *magadiensis* (***Natronobacterium*** *magadii*) (strains 82M4 and 89M4 of Duckworth et al., 1996) | aerobic<br>**colour:** red | rod-shaped cells | modern; halophilic; obligately alkaliphilic; | Lake Magadi; collected from littoral sediment and salt crust with pH: 10.5–12.5, T: 30–48° C, and conductivity: 83–90 mS cm$^-$ | Duckworth et al., 1996 |
| ***Halorubrum*** *vacuolatum* (***Natronobacterium*** *vacuolata*) (strain M24 of Mwatha and Grant, 1993) | strictly aerobic; gram variable<br>**colour:** colonies bright pink | non-motile, short rod-shaped cells; 0.5–0.7 µm wide and 1.5–3.0 µm long; colonies were small (1–2 mm), circular, bright pink, and convex; cells produce large gas vacuoles | modern; obligately haloalkaliphilic; chemoorganotroph; utilizes wide range of amino acids and sugars; requires sodium carbonate for growth<br>**pH:** opt. pH: 9.5 (range: 8.5–10.5)<br>**T:** opt. T: 35–40° C (range: 20–50° C)<br>**Na:** requires 15–30% NaCl w/v, opt. [Na]: 20% (3.5 M NaCl) | Main causeway, Lake Magadi | Mwatha and Grant, 1993 |
| cf. ***Halorubrum*** sp. (strains MSP1, MSP9, MSP11, MSP12, MSP14, MSP16, MSP 17, MSP 22, MSP 23 of Grant et al., 1999) | | n.i. | modern | Brine, Lake Magadi; collected from final evaporating pond in 1996 | Grant et al., 1999 |
| ***Amphibacillus*** *fermentum* (strain Z-7984 of Zhilina et al., 2001a) | faculatively anaerobic; gram-positive<br>**colour:** colonies yellow | cells rod-shaped, thin motile rods; rods short with sharpened ends occurring singly, in pairs, or in short chains up to 6 cells; cells 0.5–0.75 µm wide and 1.5–4.0 µm long; one subterminal flagellum; no spore production; colonies yellowish, circular, with transparent centre, raised denser margins, with 0.5–1.5 mm after 3 days | modern; alkaliphilic; saccharolytic; chemoorganotrophic; requires $Na^+$ and $CO_3^{2-}$, does not require Cl; resistant to heat and drying; heat resistance up to 80° C for 50 min.; anaerobically reduced sodium sulfide and thioglycollate to produce $H_2S$; no nitrogen fixation<br>**pH:** opt. pH: 8.0–9.0 (range 7.0–10.5)<br>**T:** opt. T: 36–38° C (range: 18–56° C)<br>**Na:** [Na] tolerance: 0.17–3.3 M Na/0.98–19.7% (opt. [Na]: 1.87 M Na/10.7%) | Lake Magadi; collected from bottom muds of lagoon during dry period in 1998, with pH: 10.2, T: 39° C, and TDS: 260 g L$^{-1}$ | Zhilina et al., 2001a |
| ***Amphibacillus*** *tropicus* (strain Z-7792 of Zhilina et al., 2001a) | faculatively anaerobic; gram-positive<br>**colour:** colonies white and pink | cells rod-shaped, thin motile rods; cells 0.4–0.5 µm wide and 2–6 µm long; flagellation pritrichous; some spore production (terminal, oval, ~ 1 µm); colonies white with pink, circular, slightly convex, smooth surface, transparent centre, denser uneven margins, ~ 1mm diameter after 3 days | modern; alkaliphilic; saccharolytic; chemoorganotrophic; resistant to heat and drying; could germinate from salt crystal media; requires $Na^+$ and $CO_3^{2-}$, does not require Cl; heat resistance up to 90° C for 10 min.; anaerobically reduced sodium sulfide to produce $H_2S$; no nitrogen fixation<br>**pH:** opt. pH: 9.5–9.7 (range 8.5–11.5)<br>**T:** opt. T: 38° C (range: 18–56° C)<br>**Na:** [Na] tolerance: 0.17–3.6 M Na/0.98–20.9% (opt. [Na]: 1–1.87 M Na/5.4–10.8%) | Lake Magadi; collected from bottom muds of lagoon during wet period in 1992, with pH: 10.2, T: 39° C, and TDS: 160 g L$^{-1}$ | Zhilina et al., 2001a |

| | | | | | |
|---|---|---|---|---|---|
| unnamed Archaea | thermoalkaliphilic Archaea | n.i. | modern; thermoalkaliphilic; collected from warm springs with T: 48° C, pH: 10.5 | Warm springs, Lake Magadi | Jones et al., 1998 |
| **Bacteria — Aerobic Sulfur Oxidizers/Chemolithotrophs (use sulfide and oxygen, produce sulfate and CO2)** | | | | | |
| ***Thioalkalivibrio*** *versutus* (strains ALJ 1 and ALJ 22 of Sorokin et al., 2001) | aerobic **colour:** young colonies white with sulfur; old colonies yellow | cells vibroid to spirilla with one polar flagellum; motile; 0.4–0.6 µm wide and 0.8–3.0 µm long; cell wall usually highly rippled; produce membrane-bound yellow pigment | modern; obligately alkaliphilic; halophilic; thermotolerant; obligately autotrophic; chemolithoautotrophic; sulfur globules accumulate in the periplasmic space outside the cells **pH:** opt. pH: 10.0–10.2 (range: 7.5–10.65) **T:** opt. T: 40° C (range: < 47° C) **Na:** [Na] tolerance: 1.2–4 M (opt. 1–2 M) | Surface sediments with water and salt crust (pH 10.0–10.5; 109 g $L^{-1}$ TDS), Lake Magadi | Sorokin et al., 2001 |
| ***Thioalkalivibrio*** *nitratis* (strain ALJ 18 of Sorokin et al., 2001) | aerobic **colour:** young colonies white with sulfur; old colonies yellow | rod-shaped cells; with one polar flagellum; motile; 0.4–0.6 µm wide and 0.8–3.0 µm long; cell wall usually highly rippled; produce membrane-bound yellow pigment | modern; obligately alkaliphilic; halophilic; thermotolerant; obligately chemolithoautotrophic; can reduce nitrate to nitrite with thiosulfate under oxygen-limiting conditions **pH:** opt. pH: 10.0–10.2 (range: 7.5–10.65) **T:** opt. T: 40° C (range: < 47° C) **Na:** [Na] tolerance: 1.2–4 M (opt. 1–2 M) | Salt crust, Lake Magadi | Sorokin et al., 2001 |
| **Bacteria — Anaerobic Fermenters (Heterotrophic)** | | | | | |
| cf. ***Clostridium*** spp. (strains M12/2, M14/4, M16/4 of Jones et al., 1998) | obligately anaerobic; gram-positive | n.i. | modern; obligately haloalkaliphilic; chemoorganotrophic; use fermenting sugars and amino acids and produce volatile fatty acids **pH:** range of pH: 8.5– >10.5 **Na:** [Na] tolerance: 12–26% | Mud, Lake Magadi; collected from mud under trona beds with pH: 10.5–12, T: 32–34° C, conductivity: 33.8–114.7 mS $cm^{-1}$ | Jones et al., 1998 |
| ***Tindallia*** *magadiensis* (*T. magadii*) (strain Z-7934 of Kevbrin et al., 1998) | obligately anaerobic gram-positive | cells are thin, slightly curved rods with pointed ends; cells 0.5–0.6 µm diameter and 1.2–2.5 < 3.5 µm long; occur singly, in pairs or in chains of 4–6 cells; asporogenous; non-motile, but some cells with flagella; has thin microcapsule | modern; alkaliphilic; obligately halophilic; fermentative; utilizes amino acids and organic acids but not carbohydrates; produces acetate, $H_2$ and ammonium **pH:** opt. pH: 8.5 (range: 7.5–10.7) **T:** opt. T: 37° C (range: 19–47° C) **Na:** [Na] tolerance: 3–10% w/v (opt. [Na]: 4–8%) | Lagoonal mud, Lake Magadi; collected from bottom muds of lagoon during dry season in 1998, with pH: 10.2, T: 39° C, and TDS: 260 g $L^{-1}$ | Kevbrin et al., 1998 |
| ***Spirochaeta*** *alkalica* (strain Z-7491 of Zhilina et al., 1996) | anaerobic, aerotolerant; gram-negative **colour:** colonies are orange | motile; cells helical, 0.4–0.5 µm wide and 9–18 µm long; outermost structure is an outer membrane enclosing the periplasmic flagella and the protoplasmic cylinder; cells have regular, stable primary coils | modern; alkaliphilic; halophilic; fermentative saccharolytic bacteria, decomposes carbohydrates; requires $Na^+$ and $HCO_3^-$ for growth; produces $H_2$ and $CO_2$ **pH:** opt. pH: 8.7–9.6 (range: 8.3–10.8) **T:** opt. T: 33–37° C (range: 15–44° C) **Na:** [Na] tolerance: 3–10% | Cyanobacterial mat in warm spring close to causeway, Lake Magadi | Zhilina et al., 1996b |
| ***Spirochaeta*** *africana* (strain Z-7692 of Zhilina et al., 1996) | anaerobic , aerotolerant; gram-negative **colour:** colonies are orange | motile; cells helical, 0.25–0.3 µm wide and 15–30 µm long; outermost structure is an outer membrane enclosing the periplasmic flagella and the protoplasmic cylinder; cells have regular, stable primary coils | modern; alkaliphilic; halophilic; fermentative saccharolytic bacteria, decomposes carbohydrates; requires $Na^+$ for growth; produces $H_2$, ethanol, and acetate **pH:** opt. pH: 8.8–9.75 (range: 8.0–10.8) **T:** opt. T: 30–37° C (range: 15–47° C) **Na:** [Na] tolerance: 3–10% | Dense bacterial bloom below trona in a shallow lagoon, Lake Magadi; | Zhilina et al., 1996b |

| | | | | | |
|---|---|---|---|---|---|
| ***Natroniella*** *acetigena* (strain Z-7937$^T$ of Zhilina et al., 1996a) | obligately anaerobic; gram-negative | large, motile rod 1.0–1.2 µm diameter and < 12–15 µm long, with rounded ends; peritrichous flagella; cells are singular, in pairs, or short chains; spore-forming, but rare | modern; extremely haloalkaliphilic; chemoorganotrophic; homoacetogenic; requires $Na_2CO_3$ and Cl for growth; utilizes lactate and ethanol for fermentation, produces acetate<br>**pH:** opt. pH: 9.7–10.0 (range: 8.1–10.7)<br>**T:** opt. T: 37° C (range: < 42° C)<br>**Na:** [Na] tolerance: 10–26% (opt. [Na]: 12–15%) | Muddy brine below trona, Lake Magadi; collected from brine below trona in the NW lagoon during dry season | Zhilina et al., 1996a |
| ***Natronincola*** (*Natronoincola*) *histidinovorans* (strains Z-7940 and Z-7939 of Zhilina et al., 1998) | obligate anaerobic; gram-positive | flexible motile rod, 0.7–1.0 µm diameter and 2–6 µm long, sometimes forming long filaments; peritrichous flagella; terminal round mini-cells; gram-positive with no outer membrane; asporogenous or sporogenous | modern; alkaliphilic; obligately halophilic; organotrophic; acetogenic; requires both $Na^+$ and $HCO_3^-$ for growth; ferments amino acids, produces acetate and ammonium; proteolytic<br>**pH:** opt. pH: 9.4 (range: 8.0–10.5)<br>**T:** opt. T: 37° C (range: < 45° C)<br>**Na:** [Na] tolerance: 4–16% (opt. [Na]: 8–10%) | Dried cyanobacterial bloom, Lake Magadi; collected from a desiccated cyanobacterial bloom in the rainy season of 1993 | Zhilina et al., 1998 |
| ***Halonatronum*** *saccharophilum* (strain Z-7986 of Zhilina et al., 2001b) | obligately anaerobic gram-negative<br>**colour:** colonies greenish | cells are long, flexible motile rods with peritrichous flagellation along the entire length of the cell; during growth stage 0.4–0.6 µm diameter and 3.5–3.75 µm long; spore-forming, with spores spherical, ~1.25 µm in diameter and located at one end of the cell; spores heat resistant; cells form curled-up spherolasts at the end of the growth period; colonies were greenish, 0.5–1 mm in diameter with indistinctly shaped smooth edges | modern; obligately halophilic; obligately akaliphilic; thermotolerant; chemoorganotrophic; sacchyrolytic; requires NaCl and $HCO_3^-$ for growth; ferments sugars to produce acetate, ethanol, $H_2$ and $CO_2$; capable of reducing elemental sulfur ($S^0$) to produce $H_2S$; incapable of nitrogen fixation<br>**pH:** opt. pH: 7.7–10.2 (range: 8.0–8.5)<br>**T:** opt. T: 36–55° C (range: 18–60° C)<br>**Na:** [Na] tolerance: 3–17% w/v (opt. [Na]: 7–10%) | Lagoonal mud, Lake Magadi; collected from bottom muds of lagoon during dry period in 1998, with pH: 10.2, T: 39° C, and TDS: 260 g $L^{-1}$ | Zhilina et al., 2001a, b |
| **Bacteria — Anaerobic Sulfur Oxidizers (Phototrophic, use light, sulfide, carbon, and CO2, produce sulfate and elemental sulfur)** | | | | | |
| ***Ectothiorhodospira*** *vacuolata* (a.k.a. *E. shaposhnikovii*) | phototrophic, anaerobic sulfide oxidizing phototrophic purple bacteria<br>**colour:** cells are red without presence of elemental sulfur | cells are rod-shaped and possess gas vacuoles under high sulfide concentrations and light intensity; motile, with tufts of polar flagella; cells are ~1.5 µm wide and 2–4 µm long; cells contain intracellular photosynthetic membranes as stacks; pigments are bacteriochlorophyll *a* and spirilloxanthin caronenoids | modern; obligate alkaliphilic; halophilic; phototrophic; chemolithotrophic; oxidizes sulfide and thiosulfate to produce sulfate and forms elemental sulfur, which accumulates outside the cells<br>**pH:** opt. pH: 7.5–8.5 in presence of inorganic reduced sulfur and 8.5–9.5 with organic carbon source<br>**T:** T. range: 30–39° C<br>**Na:** [Na] tolerance: 1–10% (opt. [Na]: 1–7%) | Lake Magadi | Imhoff et al., 1981 |
| **Bacteria — Anoxygenic Methanotrophs (use methane, produce carbon)** | | | | | |
| Not yet isolated from Lake Magadi/not known from literature | | | | | |

| | | | | | |
|---|---|---|---|---|---|
| **Archaea — Anaerobic Methylotrophic Methanogens (use carbon, produce methane)** | | | | | |
| ***Methanosalsum*** (*Methanohalophilus*) cf. *zhilinaeae* (strain 2-7936 of Kevbrin et al., 1997) | obligately anaerobic | n.i. | modern; obligately alkaliphilic and halophilic; methylotrophic methanogen; requires both $Na^+$ and $HCO_3^-$ for growth; uses methanol and trimethylamine **pH:** opt. pH: 9.0–9.5 for methanogenesis of methanol and 8.5 for methanogenesis of trimethylamine (range: 8.0–10.0) | Lake Magadi; | Kevbrin et al., 1997 |
| **Bacteria — Anaerobic Sulfate Reducers (use sulfate and organic acids, produce sulfide and CO2)** | | | | | |
| ***Desulfonatronovibrio hydrogenovorans*** (strain Z-7935$^T$ of Zhilina et al., 1997) | obligately anaerobic; gram-negative **colour:** yellow | cells are highly motile, non-spore producing, vibrios (curved rod-shaped) with one polar flagellum and filamentous appendages; cells are 0.5 µm wide and 1.5–2.0 µm long; occur singly or in pairs; develop round bodies under suboptimal conditions; colonies yellowish, translucent, lens-shaped, and < 0.2 mm diameter | modern; alkaliphilic; halophilic; lithoheterotrophic; requires $Na^+$ for growth; utilizes $H_2$ or formate and sulfate, thiosulfate, or sulfite to produce oxidized sulfur compounds or acetate (e.g., sulfide); needs organic compounds for growth; sulfur is not reduced **pH:** opt. pH: 9.5–9.7 (range: 7.0–10.2) **T:** opt. T: 37° C (range: 15–43° C) **Na:** [Na] tolerance: 1–12%; opt. [Na]: 3% w/v | Oily-black mud from trench into trona, Lake Magadi; collected from oily-black mud in anoxic brine in dry season of 1991, with pH: 10.2 and T: 50° C | Zhilina et al., 1997 |
| **Note:** Baumgarte (2003, unpublished Ph.D. dissertation) also isolated several types from Lake Magadi, including: cf. *Euhalothece* sp.(Cyanobacteria); cf. *Bacillus alcalophilus*, cf. *B.* cf. *cohnii* (Bacilli); cf. *Thermobrachium* spp. (Clostridia: Clostridiales); cf. *Thermoanaerobacter* spp. (Clostridia: Thermoanaerobacteriales); cf. *Natroniella* sp., cf. *Halocella* sp. (Clostridia: Halanaerobiales); and *Rhodobaca bogoriensis* (Alpha-Proteobacteria). | | | | | |
| ***NASIKIE ENGIDA*** | | | | | |
| **Green Algae — Primary producers** | | | | | |
| unidentified green algae | n.i. | n.i. | modern; abundant | Nasikie Engida | Behr, 2002 |
| **Bacteria and Archaea — Aerobic Heterotrophs/Organotrophs (use carbohydrates and oxygen, produce sulfide and CO2)** | | | | | |
| cf. ***Bacillus*** sp. cf. *clarkii* (strain 95LM4 of Duckworth et al., 1996) | aerobic; gram-positive | n.i. | modern; alkaliphilic; collected from soda crust and brine, with pH: 11.0, T: 37° C, and conductivity: > 100 mS $cm^{-1}$ | Salt crust and brine, Nasikie Engida | Duckworth et al., 1996 |
| cf. ***Natronococcus*** cf. *occultus* (strain 93lLM4 of Duckworth et al., 1996) | aerobic **colour:** colonies are pale brown | n.i | modern; halophilic; alkaliphilic; collected from soda mud | Nasikie Engida | McGenity and Grant, 1993; Kanai et al., 1995; Duckworth et al., 1996 |
| cf. ***Natrialba magadiensis*** (***Natronobacterium magadii***) (strain 93dLM4 of Duckworth et al., 1996) | aerobic **colour:** red | rod-shaped cells | modern; halophilic; alkaliphilic; collected from soda mud | Nasikie Engida | Duckworth et al., 1996 |

| | | | | | |
|---|---|---|---|---|---|
| ***LAKE MAGADI BASIN — CHERTS OF THE PLEISTOCENE GREEN BEDS AND HIGH MAGADI BEDS*** | | | | | |
| **Diatoms — Primary producers** | | | | | |
| ***Navicula*** sp. | diatom | n.i. | Pleistocene; rare in the Green Beds; concentrated in lenses a few mm in diameter | Green Beds | Behr and Röhricht, 2000 |
| **Cyanobacteria — Primary producers** | | | | | |
| ***Pleurocapsa*** sp. a | coccoid | unicellular coccoid; have gliding motility; forms cauliflower-shaped stromatolitic nodules < 20 cm wide that occur in layers; cells encased in polysaccharide capsules held together by mucilaginous slime; number of slime capsules increases < five with the diameter of the spheres; multiple cell fission forms baeocytes, which escape when division is finished and develop into large vegetative cells and repeat the cycle; forms crusts with swarms of baeocytes | Pleistocene; mat-forming; characteristic in hypersaline conditions; irregular cell clusters encrusted by calcite envelopes; not mineralized internally, but remained open; negative structures well preserved; carbonate precipitated in mucilaginous slime; stromatolitic nodules (< 20 cm diameter) widespread as isolated thrombolytic structures and thin bands; calcite is replaced by silica or completely dissolved and hollow spheres and may occur with secondary calcite; internally, the calcite envelopes are intergrown as dense sponge-like structures of decaying mats; may be preserved as magadiite lepispheres (intergrowths of sheet-like crystals with diameters of 10–20 μm | Green Beds; High Magadi Beds: magadiite chert | Behr and Röhricht, 2000<br>Behr, 2002 |
| ***Pleurocapsa*** sp. b | coccoid | smaller species has cell diameter of 1–5 μm including the capsule; capsule less developed, but calcification common; cells are coccoid with disk-shape tendencies; show binary division; form pellet-shaped colonies and spongy thrombolitic crusts; produces mucilaginous extracellular organic slime | Pleistocene; mat-forming; abundant in the Green Beds; preserved by calcite; a minute inclusion may be the only remnant of the central cell chamber; preferentially covers the walls of larger pores or grows on the surfaces of *Pleurocapsa* stromatolites; interpreted to live in deeper water than *Pleurocapsa* sp. or in protected cavities | Green Beds | Behr, 2002 |
| ***Pleurocapsa*** sp. c | coccoid | forms irregular and large globular colonies, several hundred microns in diameter; large amounts of extracellular organic slime; cells are 1–2 μm in diameter; individual cell chambers from 'icicle-shaped' structures on a mat-like substrate | Pleistocene; mat-forming; preserved by calcite and silica | Green Beds | Behr, 2002 |
| ***Gloecocapsa*** *polydermatica* | coccoid | unicellular coccoid; < 6 μm in diameter in the Green Beds cherts; < 20 μm in diameter in the High Magadi Beds (magadiite chert only); possibly enlarged by coatings of magadiite in the High Magadi Beds; resemble coated calcite grains, but "nuclei" are not mineral grains; cells encased in polysaccharide capsules held together by mucilaginous slime; number of slime capsules increases up to five with the | Pleistocene; mat-forming; characteristic in hypersaline conditions; irregular cell clusters encrusted by calcite envelopes forms very compact cell concentrations; not mineralized internally, but remained open; negative structures well preserved; carbonate precipitated in mucilaginous slime; cellular spheres may have been enlarged by calcite; calcite is replaced by silica or completely dissolved as hollow spheres and may occur with secondary calcite; internally, the calcite | Green Beds; High Magadi Beds: magadiite chert | Behr and Röhricht, 2000 |

| | | | | | |
|---|---|---|---|---|---|
| | | diameter of the spheres (suggests low or absent water cover) | envelopes are intergrown as dense sponge-like structures of decaying mats; may be preserved as magadiite lepispheres (intergrowths of sheet-like crystals with diameters of 10–20 µm | | |
| ***Chroococcus minor*** | coccoid | unicellular coccoid; recognized by binary fission; cells encased in polysaccharide capsules held together by mucilaginous slime | Pleistocene; preserved as calcite spheres; calcite is replaced by silica or completely dissolved as hollow spheres and may occur with secondary calcite; in the High Magadi Beds, silicified calcipheres are < 5 mm in diameter; the calcite envelopes are intergrown as dense sponge-like structures of decaying mats | Green Beds | Behr and Röhricht, 2000 |
| ***Entophysalis granulosa*** | coccoid | unicellular coccoid; cells often intergrown in chains, forming club-like aggregates; cells encased in polysaccharide capsules held together by mucilaginous slime | Pleistocene; mat-forming; characteristic in hypersaline conditions; cells often intergrown in chains, forming plug- or club-like aggregates; calcite is replaced by silica or completely dissolved as hollow spheres and may occur with secondary calcite; internally, the calcite envelopes are intergrown as dense sponge-like structures of decaying mats; may be preserved as magadiite lepispheres (intergrowths of sheet-like crystals with diameters of 10–20 µm | Green Beds; High Magadi Beds: magadiite chert | Behr and Röhricht, 2000 |
| ***Synechococcus*** sp. | coccoid | unicellular coccoid; form globular to irregular colonies in all stages of cell division in the High Magadi Beds; colonies ~0.5–5 µm diameter; cells encased in polysaccharide capsules held together by mucilaginous slime | Pleistocene; mat-forming; characteristic in hypersaline conditions; preserved by calcite and magadiite; form globular to irregular colonies in all stages of cell division; calcite is replaced by silica or completely dissolved as hollow spheres and may occur with secondary calcite; in the High Magadi Beds, silicified calcipheres are < 5 mm in diameter; the calcite envelopes are intergrown as dense sponge-like structures of decaying mats | Green Beds; High Magadi Beds – magadiite chert | Behr and Röhricht, 2000 |
| ***Microcystis*** sp. | coccoid | unicellular coccoid; free-floating; form globular to irregular colonies in all stages of cell division; colonies ~0.5–5 µm diameter | Pleistocene; abundant in the High Magadi Beds; preserved by calcite and magadiite | High Magadi Beds: magadiite chert | Behr and Röhricht, 2000; Behr, 2002 |
| ***Microcoleus*** sp. | filamentous | Note: not identified unequivocally; bundles of filaments in carbonaceous sheaths ~3 µm in diameter | Pleistocene; abundant in the bedded chert facies of the Green Beds, rare elsewhere; mat-forming; characteristic in hypersaline conditions; mat-forming; preserved as calcified sheaths forming condensed network structures; sheaths responsible for stabilization of mat fabric | Green Beds | Behr and Röhricht, 2000 |
| ***Phormidium*** sp. | filamentous | Note: not identified uniquivocally | Pleistocene; abundant in the bedded chert facies of the Green Beds, rare elsewhere; mat-forming; characteristic in hypersaline conditions; preserved by calcite | Green Beds | Behr and Röhricht, 2000 |

| | | | | | |
|---|---|---|---|---|---|
| ***Schizothrix*** sp. | filamentous | Note: not identified uniquivocally | Pleistocene; abundant in the bedded chert facies of the Green Beds, rare elsewhere; mat-forming; characteristic in hypersaline conditions; preserved by calcite | Green Beds | Behr and Röhricht, 2000 |
| **Bacteria — Heterotrophs/Organotrophs** | | | | | |
| ***Chloroflexus*** sp. | filamentous (**colour:** orange-pink) | filamentous; gliding | Pleistocene; thermophilic; characteristic in thermal spring environments; (capable of photosynthetic fixation of $CO_2$ or heterotrophic growth; capable of both aerobic and anaerobic growth; oxidize sulfur under anaerobic conditions) | Green Beds; (Yellowstone) | (Doemal and Brock, 1974); Behr, 2002 |
| ***Micrococcus*** sp. | n.i. | have conidiospores; identified by morphology of the mycelium; short hyphae bear only a few sporophores; mycelia may form garlands that hang between chert fragments | Pleistocene; abundant in thin films and laminae of the Green Beds; preserved by calcite | Green Beds | Behr and Röhricht, 2000; Behr, 2002 |
| ***Micromonospora*** sp. | n.i. | have conidiospores; identified by morphology of the mycelium; short hyphae bear only a few sporophores; mycelia may form garlands that hang between chert fragments | Pleistocene; abundant in thin films and laminae of the Green Beds; preserved by calcite | Green Beds | Behr and Röhricht, 2000; Behr, 2002 |
| ***Hyphomicrobium*** sp. | n.i. | n.i. | Pleistocene; abundant in thin films and laminae of the Green Beds; preserved by calcite | Green Beds | Behr and Röhricht, 2000 |
| unidentified bacteria | n.i. | coccoid and rod-like cells; ~1 µ diameter | Pleistocene; many different types that cannot be identified; preserved by calcite | Green Beds | Behr and Röhricht, 2000 |



## REFERENCES CITED IN THIS TABLE


Ballot, A., Krienitz, L., Kotut, K., Wiegand, C., Metcalf, J., Codd, G., and Pflugmacher, S., 2004, Cyanobacteria and cyanobacterial toxins in three alkaline Rift Valley lakes of Kenya–Lakes Bogoria, Nakuru, and Elmenteita: Journal of Plankton Research, v. 26, p. 925–935.

Ballot, A., Dadheech, P.K., Haande, S., and Krienitz, L., 2008, Morphological and phylogenetic analysis of *Anabaenopsis abijatae* and *Anabaenopsis elenkinii* (Nostocales, Cyanobacteria) from tropical inland water bodies: Microbial Ecology, v. 55, p. 608–618.

Behr, H.-J., 2002, Magadiite and magadi chert: a critical analysis of the silica sediments in the Lake Magadi Basin, Kenya, *in* Renaut, R.W., and Ashley, G.M. (eds.), Sedimentation in Continental Rifts, SEPM Special Publication, no. 73, p. 257–273.

Behr, H.-J., and Röhricht, C., 2000, Record of seismotectonic events in siliceous cyanobacterial sediments (Magadi cherts), Lake Magadi, Kenya: International Journal of Earth Sciences, v. 89, p. 268–283.

Boltyanskaya, Y.V., Antipov, A.N., Kolganova, T.V., Lysenko, A.M., Kostrikina, N.A., and Zhilina, T.N., 2004, *Halomonas campisalis*, an obligatory alkaliphilic, nitrous-oxide-reducing denitrifier with a molybdenum cofactor-lacking nitrate reductase: Microbiology, v. 73, p. 271–278.

Dadeech, P.K., Krienitz, L., Kotut, K., Ballot, A., and Casper, P., 2009, Molecular detection of uncultured cyanobacteria and animotransferase domains for cyanotoxin production in sediments of different Kenyan lakes: FEMS Microbial Ecology, v. 68, p. 340–350.

Duckworth, A.W., Grant, W.D., Jones, B.E., and Van Steenbergen, R., 1996, Phylogenetic diversity of soda lake alkaliphiles: FEMS Microbiology Ecology, v. 19, p. 181–191.

Duckworth, A.W., Grant, W.D., Jones, B.E., Meijer, D., Márquez, M.C., and Ventosa, A., 2000, *Halomonas magadii* sp. nov., a new member of the genus *Halomonas*, isolated from a soda lake of the East African Rift Valley: Extremophiles, v. 4, p. 53–60.

Florenzano, G., Sili, C., Pelosi, E., and Vincenzini, M., 1985, *Cyanospira rippkae* and *Cyanospira capsulate* (gen. nov. and spp. nov.): new filamentous heterocystous cyanobacteria from Magadi lake (Kenya): Archives of Microbiology, v. 140, p. 301–306.

Grant, S., Grant, W.D., Jones, B.E., Kato, C., and Li, L., 1999, Novel archaeal phylotypes from an East African alkaline saltern: Extremophiles, v. 3, p. 139–145.

Grant, W.D., and Tindall, B.J., 1986, The alkaline saline environment, *in* Herbert, R.A. and Codd, G.A. (eds.), Microbes in Extreme Environments: London, Academic Press, pp. 25–54.

Groth, I., Schumann, P., Rainey, F.A., Martin, K., Schuetze, B., and Augsten, K., 1997, *Bogoriella caseilytica* gen. nov., sp. nov., a new alkaliphilic actinomycete from a soda lake in Africa: International Journal of Systematic Bacteriology, v. 47, p. 788–794.

Hashim, S.O., Delgado, O., Hatti-Kaul, R., Mulaa, F.J., and Mattiasson, B., 2004, Starch hydrolyzing *Bacillus halodurans* isolates from a Kenyan soda lake: Biotechnology Letters, v. 26, p. 823–828.

Imoff, J.F., Tindall, B.J., Grant, W.D., and Trüper, H.G., 1981, *Ectothiorhodospira vacuolata* sp. nov., a new phototrophic bacterium from soda lakes: Archives of Microbiology, v. 130, p. 238–242.

Jones, B.E., Grant, W.D., Duckworth, A.W., and Owenson, G.G., 1998, Microbial diversity of soda lakes: Extremophiles, v. 2, p. 191–200.

Jones, B.E., Grant, W.D., Duckworth, A.W., Schumann, P., Weiss, N., and Stackebrandt, E., 2005, *Cellulomonas bogoriensis* sp. nov., an alkaliphilic cellulomonad: International Journal of Systematic and Evolutionary Microbiology, v. 55, p. 1711–1714.

Kanai, H., Kobayashi, T., Aono, R., and Kudo, T., 1995, *Natronococcus amylolyticus* sp. nov., a haloalkaliphilic archaeon: International Journal of Systematic Bacteriology, v. 45, p. 762–766.

Kevbrin, V.V., Lysenko, A.M., and Zhilina, T.N., 1997, Physiology of the alkaliphilic methanogen Z-7936, a new strain of *Methanosalsus zhilinaeae* isolated from Lake Magadi: Microbiology, v. 66, p. 261–266.

Kevbrin, V.V., Zhilina, T.N., Rainey, F.A., and Zavarzin, G.A., 1998, *Tindallia magadii* gen. nov., sp. nov.: an alkaliphilic anaerobic ammonifier from soda lake deposits: Current Microbiology, v. 37, p. 94–100.

Krienitz, L., Ballot, A., Kotut, K., Wiegand, C., Pütz, S., Metcalf, J.S., Codd, G.A., and Pflugmacher, S., 2003, Contribution of hot spring cyanobacteria to the mysterious deaths of Lesser Flamingos at Lake Bogoria, Kenya: FEMS Microbiology Ecology, v. 43, p. 141–148.

McGenity, T.J., and Grant, W.D., 1993, The haloalkaliphilic archaeon (archaebacterium) *Natronococcus occultus* represents a distinct lineage within the *Halobacteriales*, most closely related to the other haloalkaliphilic lineage (*Natronobacterium*): Systematic and Applied Microbiology, v. 16, p. 239–243.

Mikhodyuk, O.S., Gerasimenko, L.M., Akimov, V.N., Ivanovsky, R.N., and Zavarzin, G.A., 2008, Ecophysiology and polymorphism of the unicellular extremely natronophilic cyanobacterium *Euhalothece* sp. Z-M001 from Lake Magadi: Microbiology, v. 77, p. 717–725.

Milford, A.D., Achenbach, L.A., Jung, D.O., and Madigan, M.T., 2000, *Rhodobaca bogoriensis* gen. nov. and sp. nov., an alkaliphilic purple nonsulfur bacterium from African Rift Valley soda lakes: Archives of Microbiology, v. 174, p. 18–27.

Moallic, C., Dabonne, S., Colas, B., and Sine, J.-P., 2006, Identification and characterization of a gamma-glutamyl transpeptidase from a thermo-alcalophile strain of *Bacillus pumilus*: Protein Journal, v. 25, p. 391–397.

Mwatha, W.E., and Grant, W.D., 1993, *Natronobacterium vacuolata* sp. nov., a haloakaliphilic archaeon isolated from Lake Magadi, Kenya: International Journal of Systematic Bacteriology, v. 43, p. 401–403.

Ndetei, R., and Muhandiki, V.S., 2005, Mortalities of lesser flamingos in Kenyan Rift Valley saline lakes and the implications for sustainable management of the lakes: Lakes and Reservoirs: Research and Management, v. 10, p. 51–58.

Osanjo, G., Muthike, E.W., Tsuma, L., Okoth, M.W., Bulimo, W.D., Lünsdorf, H., Abraham, W.-R., Dion, M., Timmis, K.N., Golyshin, P.N., and Mulaa, F.J., 2009, A salt lake extremophilie, *Paracoccus bogoriensis* sp. nov., efficiently produces xanthophylls carotenoids: African Journal of Microbiology Research, v. 3, p. 426–433.

Prowe, S.G., and Antranikian, G., 2001, *Anaerobranca gottschalkii* sp. nov., a novel thermoalkaliphilic bacterium that grows anaerobically at high pH and temperature: International Journal of Systematic and Evolutionary Microbiology, v. 51, p. 457–465.

Renaut, R.W., Jones, B., and Tiercelin, J.-J., 1998, Rapid *in situ* silicification of microbes at Loburu hot springs, Lake Bogoria, Kenya Rift Valley: Sedimentology, v. 45, p. 1083–1103.

Sorokin, D.Y., Lysenko, A.M., Mityushina, L.L., Tourova, T.P., Jones, B.E., Rainey, F.A., Robertson, L.A., and Kuenen, G.J., 2001, *Thioalkalimicrobium aerophilum* gen. nov., sp. nov. and *Thioalkalimicrobium sibericum* sp. nov., and *Thioalkalivibrio versatus* gen. nov., sp. nov., *Thioalkalivibrio nitratis* sp. nov. and *Thioalkalivibrio denitrificans* sp. nov., novel obligately alkaliphilic and obligately chemolithoautotrophic sulfur-oxidizing bacteria from soda lakes: International Journal of Systematic and Evolutionary Microbiology, v. 51, p. 565–580.

Stal, L.J., 1995, Physiological ecology of cyanobacteria in microbial mats and other communities: New Phytology, v. 131, p. 1–32.

Sunna, A., Prowe, S.G., Stoffregen, T., and Antranikian, G., 1997, Characterization of the xylanases from the new isolated thermophilic xylan-degrading *Bacillus thermoleovorans* strain K-3d and *Bacillus flavothermus* strain LB3A: FEMS Microbiology Letters, v. 148, p. 209–216.

Svetlitshnyi, V., Rainey, F., and Wiegel, J., 1996, *Thermosyntropha lipolytica* gen. nov., sp. nov., a lipolytic, anaerobic, alkalitolerant, thermophilic bacterium utilizing short- and long-chain fatty acids in syntrophic coculture with a methanogenic archaeum: International Journal of Systematic Bacteriology, v. 46, p. 1131–1137.

Tiercelin, J.-J., Vincens, A., Barton, C.E., Carbonel, P., Casanova, J., Delibrias, G., Gasse, F., Grosdidier, E., Herbin, J.-P., Huc, A.Y., Jardiné, S., Le Fournier, J., Mélières, F., Owen, R.B., Pagé, P., Palacios, C., Paquet, H., Péniguel, G., Peypouquet, J.-P., Raynaud, J.-F., Renaut, R.W., Renéville, P., Richert, J.-P., Riff, R., Robert, P., Seyve, C., Vandenbrouke, M., and Vidal, G., 1987, Le demi-grabin de Baringo-Bogoria, Rift Gregory, Kenya: 30 000 years of hydrological and sedimentary history: Bulletin de Centres Reserches Exploration-Production Elf Aquitaine, v. 11, p. 249–540.

Vargas, V.A., Delgado, O.D., Hatti-Kaul, R., and Mattiasson, B., 2004, Lipase-producing microorganisms from a Kenyan alkaline soda lake: Biotechnology Letters, v. 26, p. 81–86.

Vargas, V.A., Delgado, O.D., Hatti-Kaul, R., and Mattiasson, B., 2005, *Bacillus bogoriensis* sp. nov., a novel alkaliphilic, halotolerant bacterium isolated from a Kenyan soda lake: International Journal of Systematic and Evolutionary Microbiology, v. 55, p. 899–902.

Vincens, A., Casanova, J., and Tiercelin, J.-J., 1986, Palaeolimnology of Lake Bogoria (Kenya) during the 4500 BP high lacustrine phase, *in* Frostick, L.E., Renaut, R.W., Reid, I, and Tiercelin, J.-J. (eds.), Sedimentation in the African Rifts: Geological Society Special Publication, no. 25, p. 323–330.

Zhilina, T.N., Zavarzin, G.A., Detkova, E.N., and Rainey, F.A., 1996a, *Natrionella acetigena* gen. nov. sp. nov., and extremely haloalkaliphilic, homoacetic bacterium: a new member of *Haloanaerobiales*: Current Microbiology, v. 32, p. 320–326.

Zhilina, T.N., Garnova, E.S., Tourova, T.P., Kostrikina, N.A., and Zavarzin, G.A., 2001a, *Amphibacillus fermentum* sp. nov. and *Amphibacillus tropicus* sp. nov., new alkaliphilic, faculatively anaerobic, sacchorolytic bacilli from Lake Magadi: Microbiology, v. 70, p. 711–722.

Zhilina, T.N., Garnova, E.S., Tourova, T.P., Kostrikina, N.A., and Zavarzin, G.A., 2001b, *Halonatronum saccharophilum* gen. nov. sp. nov.: a new haloalkaliphilic bacterium of the Order *Haloanaerobiales* from Lake Magadi: Microbiology, v. 70, p. 64–72.

Zhilina, T.N., Zavarzin, G.A., Rainey, F., Kevbrin, V.V., Kostrikina, N.A., and Lysenko, A.M., 1996b, *Spirochaeta alkalica* sp. nov., *Spirochaeta africana* sp. nov., and *Spirochaeta asiatica* sp. nov., alkaliphilic anaerobes from the continental soda lakes in central Asia and the East African Rift: International Journal of Systematic Bacteriology, v. 46, p. 305–312.

Zhilina, T.N., Zavarzin, G.A., Rainey, F.A., Pikuta, E.N., Osipov, G.A., and Kostrikina, N.A., 1997, *Desulfonatronovibrio hydrogenovorans* gen. nov., sp. nov., an alkaliphilic sulfate-reducing bacterium: International Journal of Systematic Bacteriology, v. 47, p. 144–149.

Zhilina, T.N., Detkova, E.N., Rainey, F.A., Osipov, G.A., Lysenko, A.M., Kostrikina, N.A., and Zavarzin, G.A., 1998, *Natronoincola histidinovorans* gen. nov., sp. nov., a new alkaliphilic acetogenic anaerobe: Current Microbiology, v. 37, p. 177–185.